Aquatic Ecology Series

Tamar Zohary
Assaf Sukenik
Tom Berman
Ami Nishri *Editors*

Lake Kinneret

Ecology and Management

Springer

Aquatic Ecology Series

Volume 6

Editor
Jef Huisman
Ecosystem Dynamics, University Amsterdam Inst. Biodiversity
and Amsterdam, The Netherlands

More information about this series at http://www.springer.com/series/5637

Tamar Zohary • Assaf Sukenik • Tom Berman
Ami Nishri
Editors

Lake Kinneret

Ecology and Management

Springer

Editors
Tamar Zohary
Israel Oceanographic & Limnological Research
Kinneret Limnological laboratory
Migdal
Israel

Tom Berman
Israel Oceanographic & Limnological Research
Kinneret Limnological laboratory
Migdal
Israel

Assaf Sukenik
Israel Oceanographic & Limnological Research
Kinneret Limnological laboratory
Migdal
Israel

Ami Nishri
Israel Oceanographic & Limnological Research
Kinneret Limnological laboratory
Migdal
Israel

ISBN 978-94-017-8943-1 ISBN 978-94-017-8944-8 (eBook)
DOI 10.1007/978-94-017-8944-8
Springer New York Heidelberg Dordrecht London

Library of Congress Control Number: 2014939525

Printed on acid-free paper

Springer is part of Springer Science+Business Media (www.springer.com)

This book is dedicated to the late Prof. Colette Serruya, former Director General of Israel Oceanographic and Limnological Research and director of the Kinneret Limnological Laboratory who paved the way to the exploration and understanding of the limnology of Lake Kinneret

Preface

Lake Kinneret, known also as the Sea of Galilee and Lake Tiberias, has attracted people's attention since ancient times. The lake and its vicinity served as important sites for much of human history in the region, including that associated with the life of Jesus Christ and his ministry. Several of Jesus' disciples were local fishermen and Lake Kinneret plays a prominent role in his teachings. The Northwestern shore of Lake Kinneret at Tabgha is the site of the Miracle of Loaves and Fishes, as described in the *New Testament*. According to the biblical story, five loaves of bread and two small fish that Jesus handed out were sufficient to feed 5,000 people. While this miracle has been explained at times as an act of a higher power, our current understanding of the limnology of Lake Kinneret provides a plausible basis for the story. After the onset of thermal stratification in April or May during years of extremely high spring productivity, the lower water mass (hypolimnion) can become devoid of oxygen relatively early in the season. Internal wave activity, driven primarily by strong westerly winds, can cause strong upwelling of these anoxic waters on the Northwestern shores near Tabgha, trapping and suffocating large schools of bleak ("the Kinneret sardine") and other fish that float to the surface in the thousands. These fish are not poisoned or sick and are fine to eat, even several hours after the upwelling event. As scientists, we can only suspect that the loaves portion of the miracle can be attributed to poetic license.

The modern scientific curiosity about the Sea of Galilee attracted travelers and naturalists such as Fredrik Hasselquist, a student of Charles Linnaeus, who in 1766, provided the first scientific description of the local Tilapia fish species. He was followed by settlers who explored the lake, first for its fishery and later as a reliable source of freshwater for domestic and agricultural uses. The Ministry of National Infrastructures, Energy and Water, and the Israel Water Authority initiated and supported advanced monitoring and research programs aimed at elucidation of physical, geochemical, biological, and ecological processes that affect the lake ecosystem.

Unraveling the mechanisms underlying the functioning of the Lake Kinneret ecosystem is at the heart of this book. The accumulated current knowledge on the structure and functioning of Lake Kinneret as an aquatic ecosystem is comprehensively described, with implications to lake management practices.

Since its establishment in 1967, the Kinneret Limnological Laboratory (KLL) of the Israel Oceanographic and Limnological Research (IOLR) serves as a research center on Lake Kinneret. The contribution of KLL-IOLR scientists and other researchers from Israel and other countries presented in this book demonstrates the interdisciplinary approach taken to unveil this complex ecosystem.

The editors and the contributors are indebted to the professional field and technical crew of KLL that assisted in the field and laboratory work conducted over the last 2–3 decades, including Boaz Avraham, Bonnie Azoulay, Yochi Cahila, Sara Chava, Moti Diamant, James Easton, Eva Feldman, Meir Hatab, Rivka Hershkowitz, Semion Kaganovsky, Bina Kaplan, Mochik Leder, Miki Shlichter, Beny Sulimani, Oz Tzabary-Dar, Shimshon Zakai.

The Israel Water Authority funded the monitoring program on Lake Kinneret right from its beginning in 1969. The team of experts constituting the Lake Kinneret and Watershed Steering Committee of the Israel Water Authority, made substantial contributions toward the constant upgrade and modernization of the Kinneret monitoring program, including support in funding of essential scientific instrumentation. Many granting agencies funded much of the research conducted at the Kinneret Limnological Laboratory, including the research funds of the Israel Water Authority, Israel Ministry of Energy and Water, the Israel Ministry of Science, Technology and Space (MOST), Israel Ministry of Agriculture, the Israel Science Foundation, the USA-Israel binational Science Foundation, the Germany-Israel BMBF, and the Germany Israel Foundation (GIF), the European Community. Lastly, we gratefully acknowledge the long-term financial support and encouragement provided by the North American Friends of IOLR (NAF/IOLR).

The monitoring data presented in this book were collected by several organizations, deposited into a single database, and made available to the interested scientists. In addition to the data collected as part of the Kinneret monitoring program by the Kinneret Limnological Laboratory, the Watershed Unit of Mekorot water company conducted most of the chemical analyses on Kinneret samples and all the analyses on the watershed and salt spring samples. The Hydrological Services of the Israel Water Authority shared discharge data. The Meteorological Services provided meteorological data. The Fisheries Department of the Ministry of Agriculture shared fish harvest and stocking data.

Furthermore, we are greatly indebted to many referees who willingly contributed to the improvement of the contents of the book. These referees were—Amotz Agnon, Jason Antenucci, Yoram Avnimelech, Yuval Bartov, Michael Beyth, Revital Bookman, Patrick Brezonik, Marco Cantonati, Deeksha Narula Katyal, Ray Drenner, Zvi Dubinsky, Yael Duboswsky, Reiner Eckmann, Larell Fabro, Giovanna Flaim, Eran Friedler, Amatzia Genin, Michail Gladishev, Avraham Golik, Noam Greenbaum, Hans Guede, Haim Gvirtzman, Debora Hart, Karl E Havens, Brendan Hicks, Chuck Howard, Danny Ionescu, Alexey Kamishny, Amitai Katz, Avner Kessler, Hanoch Lavee, M Iggi Litaor, Ramon Massana, Tamara Mikeheyeva, Yaacov Nir, Brigitte Nixdorf, Mikko Olin, Adina Paytan, Jarone Pinhassi, Antonio Quaseda, Emil Rydin, Nico Salmaso, Rana Samuels, John Schalles, Amit Segev, Yaela Shaked, Evelyne Sherr, Rhena Schumann, Nadezhda Sushchi, Max Tilzer, Monica

Tolotti, Sasha Turchyn, Michal Ucko, Assaf Vardi, Claudia Weidener, Dalit Wisel-Ohayon, and Priit Zignel.

Finally, a word about Tom Berman, who enthusiastically joined the team of book editors. He died unexpectedly in April 2013 while hiking alone in the Galapagos Islands, at the age of 79. His contribution to the last stages of finalizing this book was greatly missed. Tom was the first director of KLL (1967–1971) and again became its director for the period of 1986–1998. He foresaw the crucial role of long-term records for understanding the functioning of ecosystems, and fostered the close ties between monitoring and research, understanding that this combination forms both, the basis for future research and the basis for recommendations regarding the management of the lake as a main source of drinking water for the State of Israel.

Contents

1 General Background 1
Tom Berman, Tamar Zohary, Ami Nishri and Assaf Sukenik

Part I The Geographical and Geological Setting

2 Structure and Tectonic Development of the Kinneret Basin 19
Zvi Ben-Avraham, Michal Rosenthal, Gideon Tibor, Hila Navon, Hillel Wust-Bloch, Rami Hofstetter and Michael Rybakov

3 Late Quaternary Limnological History 39
Mordechai Stein

4 Lake Bathymetry and Bottom Morphology 59
Gideon Tibor, Ronnie Sade, John K Hall, Zvi Ben-Avraham and Ami Nishri

5 Geomorphology 69
Nurit Shtober-Zisu and Moshe Inbar

Part II The Physical and Chemical Setting

6 Meteorology 81
Baruch Ziv, Elad Shilo, Yury Lechinsky and Alon Rimmer

7 Hydrology 97
Alon Rimmer and Amir Givati

8 Salinity 113
Alon Rimmer and Ami Nishri

9 The Seasonal Hydrodynamic Habitat 133
Jörg Imberger and Clelia Luisa Marti

Part III Pelagic Communities

10 Phytoplankton 161
Tamar Zohary, Yosef Z Yacobi, Alla Alster, Tatiana Fishbein, Shachaf Lippman and Gideon Tibor

11 Peridinium gatunense 191
Tamar Zohary, Assaf Sukenik and Tom Berman

12 Cyanobacteria 213
Assaf Sukenik, Ora Hadas and Aaron Kaplan

13 Metazoan Zooplankton 227
Gideon Gal and K David Hambright

14 Protozoa (Unicellular Zooplankton): Ciliates and Flagellates 247
Ora Hadas, Tom Berman, Nehama Malinsky-Rushansky and Gideon Gal

15 Heterotrophic and Anoxygenic Photosynthetic Bacteria 259
Tom Berman, Yosef Z Yacobi, Werner Eckert and Ilia Ostrovsky

16 Fish Biology and Ecology 273
Ilia Ostrovsky, Menachem Goren, James Shapiro, Gregory Snovsky and Alex Rynskiy

17 The Pelagic Food Web 293
Tamar Zohary, Gideon Gal and K David Hambright

Part IV Nutrient Sources and Biogeochemical Processes

18 Material Loads from the Jordan River 309
Meir Rom, Diego Berger, Benjamin Teltsch and Doron Markel

19 External Sources of Nutrients 329
Ami Nishri and Edit Leibovici

20 The Phosphorus Cycle 347
Werner Eckert and Ami Nishri

21 Quantitative Aspects of the Nitrogen Cycle 365
Ami Nishri

22 Microbial Processes Within the Nitrogen Cycle 381
Ora Hadas

23 Dissolved Inorganic Carbon (DIC) 397
Ami Nishri and Mariana Stiller

24 Primary Production 417
Yosef Z Yacobi, Jonathan Erez and Ora Hadas

25 The Fate of Organic Carbon 439
Tom Berman, Arkadi Parparov, Ora Hadas, Yosef Z Yacobi, Orit Sivan, Ilia Ostrovsky and Werner Eckert

26 Seston and Organic Matter 473
Arkadi Parparov, Tamar Zohary, Tom Berman and Gideon Gal

27 Sedimentation Processes 485
Ilia Ostrovsky, Yosef Z Yacobi and Nir Koren

28 Dynamics of Redox-Sensitive Elements 499
Ami Nishri and Ludwik Halicz

Part V The Littoral

29 The Littoral Zone 517
Tamar Zohary and Avital Gasith

Part VI Integrated Lake-Watershed Management

30 Social and Economic Background 535
Moshe Inbar and Dan Malkinson

31 Operational Management of Lake Kinneret and its Watershed 541
Doron Markel, Uri Shamir and Pinhas Green

32 The Monitoring Program 561
Assaf Sukenik, Tamar Zohary and Doron Markel

33 Water Pollutants 577
Assaf Sukenik, Shmuel Carmeli, Ora Hadas, Edit Leibovici, Nehama Malinsky-Rushansky, Rita Parparov, Rivka Pinkas, Yehudith Viner-Mozzini and David Wynne

34 Water Quality Assessment 607
Arkadi Parparov, K David Hambright and Tom Berman

35 Modeling the Kinneret Ecosystem 617
Gideon Gal, Arkady Parparov and Natasa Atanasova

36 Fisheries Management 635
Ilia Ostrovsky, Tamar Zohary, James Shapiro, Gregory Snovsky and Doron Markel

Part VII Overview

37 Lake Kinneret: Current Understanding and Future Perspectives 657
Tamar Zohary, Assaf Sukenik and Ami Nishri

Index 673

Contributors

Alla Alster The Yigal Allon Kinneret Limnological Laboratory, Israel Oceanographic & Limnological Research, Migdal, Israel

Natasa Atanasova Centre for Marine and Environmental Research (CIMA), Faro, University of Algarve, Algarve, Portugal

Zvi Ben-Avraham Department of Geophysical, Atmospheric and Planetary Sciences, Tel Aviv University, Tel Aviv, Israel

Diego Berger Laboratories and Watershed Unit, Mekorot Water Company, Upper Nazareth, Israel

Tom Berman The Yigal Allon Kinneret Limnological Laboratory, Israel Oceanographic & Limnological Research, Migdal, Israel

Shmuel Carmeli School of Chemistry, Raymond and Beverly Sackler Faculty of Exact Sciences, Tel Aviv University, Tel Aviv, Israel

Werner Eckert The Yigal Allon Kinneret Limnological Laboratory, Israel Oceanographic & Limnological Research, Migdal, Israel

Jonathan Erez Institute of Earth Sciences, The Hebrew University of Jerusalem, Jerusalem, Israel

Tatiana Fishbein The Yigal Allon Kinneret Limnological Laboratory, Israel Oceanographic & Limnological Research, Migdal, Israel

Gideon Gal The Yigal Allon Kinneret Limnological Laboratory, Israel Oceanographic & Limnological Research, Migdal, Israel

Avital Gasith George S. Wise Faculty of Life Sciences, Department of Zoology, Tel-Aviv University, Tel-Aviv, Israel

Menachem Goren Department of Zoology, Tel Aviv University, Tel Aviv, Israel

Pinhas Green Lake Kinneret Administration Unit, Israel Water Authority, Zemah, Jordan Valley, Israel

Ora Hadas The Yigal Allon Kinneret Limnological Laboratory, Israel Oceanographic & Limnological Research, Migdal, Israel

Ludwik Halicz Geological Survey of Israel, Jerusalem, Israel

John K Hall Geological Survey of Israel, Jerusalem, Israel

K David Hambright Department of Biology, University of Oklahoma, Norman, OK, USA

Rami Hofstetter Geophysical Institute of Israel, Lod, Israel

Jörg Imberger Centre for Water Research, The University of Western Australia MO23, Crawley, WA, Australia

Moshe Inbar Department of Geography and Environmental Studies, University of Haifa, Haifa, Israel

Aaron Kaplan Department of Plant and Environmental Sciences, The Hebrew University of Jerusalem, Jerusalem, Israel

Nir Koren The Yigal Allon Kinneret Limnological Laboratory, Israel Oceanographic & Limnological Research, Migdal, Israel

Yury Lechinsky The Yigal Allon Kinneret Limnological Laboratory, Israel Oceanographic & Limnological Research, Migdal, Israel

Edit Leibovici The Yigal Allon Kinneret Limnological Laboratory, Israel Oceanographic & Limnological Research, Migdal, Israel

Shachaf Lippman Charney School of Marine Sciences, University of Haifa, Haifa, Israel

Nehama Malinsky-Rushansky The Yigal Allon Kinneret Limnological Laboratory, Israel Oceanographic & Limnological Research, Migdal, Israel

Dan Malkinson Department of Geography and Environmental Studies and The Golan Research Institute, University of Haifa, Haifa, Israel

Doron Markel Lake Kinneret and Watershed Unit, Israel Water Authority, Rosh Pina, Israel

Clelia Luisa Marti Centre for Water Research, The University of Western Australia MO23, Crawley, WA, Australia

Hila Navon Department of Geophysical, Atmospheric and Planetary Sciences, Tel Aviv University, Tel Aviv, Israel

Ami Nishri The Yigal Allon Kinneret Limnological Laboratory, Israel Oceanographic & Limnological Research, Migdal, Israel

Ilia Ostrovsky The Yigal Allon Kinneret Limnological Laboratory, Israel Oceanographic & Limnological Research, Migdal, Israel

Arkadi Parparov The Yigal Allon Kinneret Limnological Laboratory, Israel Oceanographic & Limnological Research, Migdal, Israel

Rita Parparov The Yigal Allon Kinneret Limnological Laboratory, Israel Oceanographic & Limnological Research, Migdal, Israel

Rivka Pinkas The Yigal Allon Kinneret Limnological Laboratory, Israel Oceanographic & Limnological Research, Migdal, Israel

Alon Rimmer The Yigal Allon Kinneret Limnological Laboratory, Israel Oceanographic & Limnological Research, Migdal, Israel

Meir Rom Laboratories and Watershed Unit, Mekorot Water Company, Upper Nazareth, Israel

Michal Rosenthal Department of Geophysical, Atmospheric and Planetary Sciences, Tel Aviv University, Tel Aviv, Israel

Michael Rybakov Geophysical Institute of Israel, Lod, Israel

Alex Rynskiy The Yigal Allon Kinneret Limnological Laboratory, Israel Oceanographic & Limnological Research, Migdal, Israel

Ronnie Sade Dr. Moses Strauss Department of Marine Geosciences, University of Haifa, Haifa, Israel

Uri Shamir Chair of the Kinneret and Watershed Monitoring Steering Committee Faculty of Civil and Environmental Engineering, Technion—Israel Institute of Technology, Haifa, Israel

James Shapiro Fishery Department, Ministry of Agriculture and Rural Development, Tiberias, Israel

Elad Shilo The Israeli Meteorological Service, Beit Dagan, Israel

Nurit Shtober-Zisu Department of Land of Israel Studies, University of Haifa, Haifa, Israel

Orit Sivan Department of Geological and Environmental Sciences, P.O. Box 653, Ben-Gurion University of the Negev, Beer-Sheva, Israel

Gregory Snovsky Fishery Department, Ministry of Agriculture and Rural Development, Tiberias, Israel

Mordechai Stein Geological Survey of Israel, Jerusalem, 30 Malkhe Israel St., Israel

Mariana Stiller Rishon Leziyyon, Israel

Assaf Sukenik The Yigal Allon Kinneret Limnological Laboratory, Israel Oceanographic & Limnological Research, Migdal, Israel

Benjamin Teltsch Laboratories and Watershed Unit, Mekorot Water Company, Upper Nazareth, Israel

Gideon Tibor Israel Oceanographic & Limnological Research, Haifa, Israel

Yehudith Viner-Mozzini The Yigal Allon Kinneret Limnological Laboratory, Israel Oceanographic & Limnological Research, Migdal, Israel

Hillel Wust-Bloch Department of Geophysical, Atmospheric and Planetary Sciences, Tel Aviv University, Tel Aviv, Israel

David Wynne The Yigal Allon Kinneret Limnological Laboratory, Israel Oceanographic & Limnological Research, Migdal, Israel

Yosef Z Yacobi The Yigal Allon Kinneret Limnological Laboratory, Israel Oceanographic & Limnological Research, Migdal, Israel

Baruch Ziv Department of natural sciences, The Open University of Israel, Raanana, Israel

Tamar Zohary The Yigal Allon Kinneret Limnological Laboratory, Israel Oceanographic & Limnological Research, Migdal, Israel

Chapter 1
General Background

Tom Berman, Tamar Zohary, Ami Nishri and Assaf Sukenik

Abstract The introduction presents a short historical background of the region, including an account of research on Lake Kinneret. An account of recent anthropomorphic changes that have impacted the lake ecosystem and data on morphometric, bathymetric, and other basic limnological characteristics of the lake are given. The main features of the annual cycle of key limnological parameters (temperature, stratification, chlorophyll, pH, dissolved oxygen, nutrients, sulfate, and sulfide) are presented.

Keywords Sea of Galilee · Lake Hula · Kinneret Limnological Laboratory (KLL) · Israel Oceanographic and Limnological Research (IOLR) · Mekorot · National Water Carrier (NWC)

1.1 Historical Background

Human settlement around the shores of Lake Kinneret reaches far back into antiquity and, in fact, predates the modern lake, which has existed in its present form for only some 18,000 years. At Ubadiya, about 2 km southwest of the lake, lies a habitation site which is one of the earliest prehistoric sites yet discovered and which may have been a way station on the migration route of early mankind out of Africa. Surrounded by exotic tropical flora, communities of *Homo erectus* flourished here 1.4 million years ago, as attested by the discovery of fossilized fragments of skull bones and teeth in addition to collections of animal bones and stone artifacts. Subsequent geological upheavals buried these sites and altered the form of the lake. Evidence for later, but still prehistoric settlement, was found in the karst caves of Wadi Amud northwest of the lake where the remains of "Galilee Man," an

T. Zohary (✉) · T. Berman · A. Nishri · A. Sukenik
The Yigal Allon Kinneret Limnological Laboratory, Israel Oceanographic & Limnological Research, P.O. Box 447, 14950 Migdal, Israel
e-mail: tamarz@ocean.org.il

A. Nishri
e-mail: nishri@ocean.org.il

A. Sukenik
e-mail: assaf@ocean.org.il

T. Zohary et al. (eds.), *Lake Kinneret*, *Ecology and Management,* Aquatic Ecology Series 6,
DOI 10.1007/978-94-017-8944-8_1,

early human who lived there 100,000–150,000 years ago, were discovered together with artifacts from the Middle and Upper Paleolithic periods (40,000–100,000 and 20,000–40,000 years ago).

In 1989, during a period of minimum lake level, an Upper Paleolithic "village" of fishermen-hunters was discovered at Ohalo on the southwestern shore (Fig. 1.1). The remains of six charcoal rings where brushwood dwellings had been erected, a grave, and an area that was probably used as a refuse dump were uncovered. This site was probably occupied for only a few generations, but nevertheless its discovery has greatly expanded knowledge of prehistoric hunting and gathering practices.

At Tel Bet Yerach, near Ohalo (Fig. 1.1), 16 identifiable strata of civilization have been revealed, beginning with the Chalcolithic and ending with the Arab. The site was inhabited from the Early Bronze Age (3300–2300 BCE). The Hellenes knew this place as Philoteria, so named after the sister of Ptolemy Philadelphus, the Hellenic king of Egypt; the Romans, in their day, called the town Ariah. After them came the Byzantines and then the Arabs, who named the place Kerak. Close by, in 1909, came a group of seven Jewish settlers to till the lands at Umm Juni and to establish the first kibbutz, Degania. Here, as at many historical sites around the lake, can be found stone testaments to former glories: a second-century synagogue, a fourth-century Roman bathhouse, and a sixth-century Byzantine church.

In ancient times, the natural hot and salty springs around the lakeshores were famous for their healing properties. An Arab folk tale attributes the heat of these springs to a pack of demons assigned to this task by King Solomon. Although this is deemed unlikely by today's hydrologists, the exact sources of the warm, saline waters and the mechanisms responsible for their upwelling within and around the lake have been subject to considerable scientific debate (Chap. 7).

In Greek, Roman, and Byzantine times, a large population, perhaps as many as 50,000–100,000, lived around the lake. The most widely renowned are places mentioned in the New Testament, but these represent only a small portion of the many settlements and towns which flourished in the region. The lake, also known in English as the Sea of Galilee or Lake Tiberias, figures prominently in the life of Jesus and his ministry. Several of his prominent disciples were local fishermen, and many of his activities and miracles took place in the area. During Vespasian's suppression of the Jewish Great Rebellion against the Romans (67–70 CE) in Galilee, the regions around the lake witnessed many bloody events, including a horrendous siege at Gamla and a lake battle off the coast of Migdal (Fig. 1.1).

After the relatively prosperous times of Roman and Byzantine rule came a period of decline, with first Arab, then the Crusader, and again Arab conquests. At the Horns of Hittim, a prominent place about 8 km to the west of Tiberias, a decisive battle was fought on a blazing hot Fourth of July in 1187 between a Saracen army commanded by Saladin and the Crusader knights under King Guy. The defeat of the Crusaders marked the end of the First Kingdom of Jerusalem and destroyed aspirations for Christian sovereignty over the Holy Land.

In the mid-sixteenth century, Tiberias (Fig. 1.1) enjoyed a brief revival when the Ottoman sultan Suleiman the Magnificent granted Doña Gracia and her nephew Joseph Nasi a permit to establish an autonomous Jewish region there. However, by

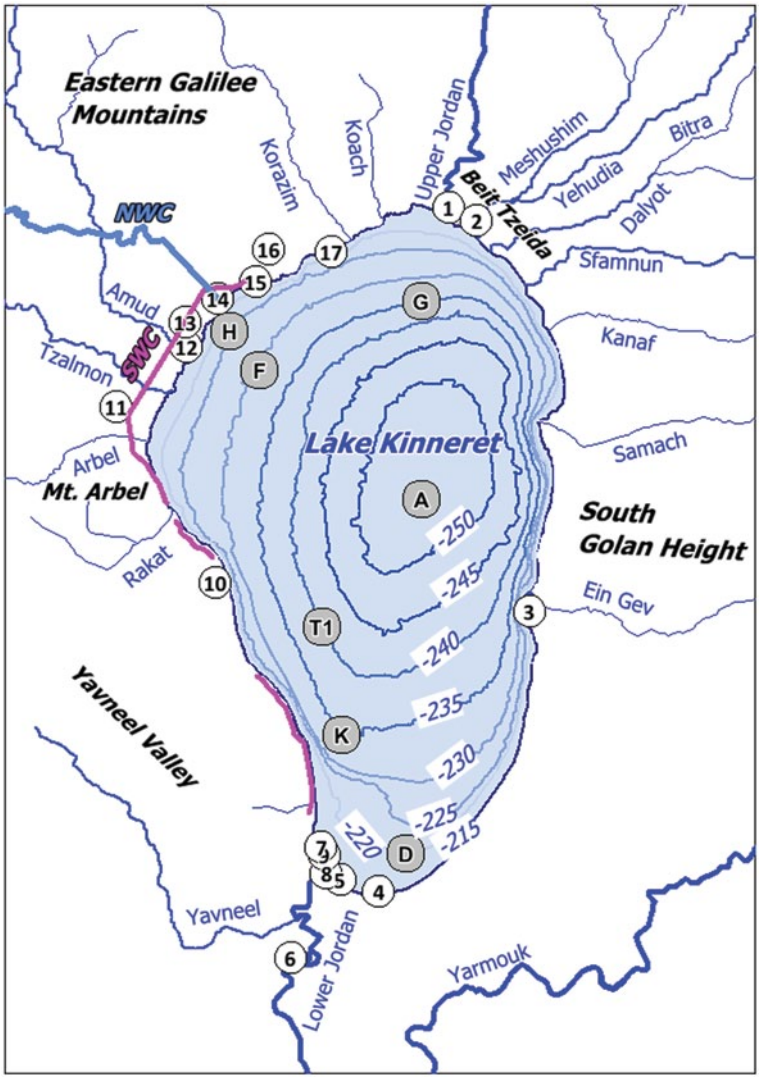

Figure 1.1 Map of Lake Kinneret and its surroundings, showing locations of in-lake sampling stations (*gray circles*) and major archeological and historical sites (numbered *white circles*). Lake bathymetry is shown at 5-m intervals, with absolute altitude (m, amsl) indicated. Sites around the lake (alphabetic order): Bet Yerach—7, Capernaum—17, Degania Dam—9, En Gev—3, Jordan River inflow—1, Jordan River outflow—5, Kinneret Limnological Laboratory and the National Water Carrier pumping station of Mekorot Water Company at Sapir Site—14, Meshushim inflow—2, Migdal—11, Mount of Beatitudes—16, Ohalo—8, salt diversion canal—13, Tabgha—15, Tiberias—10, Ubadiya—6, Wadi Amud—12, Yarmouk diversion inflow—4. *NWC*—National Water Carrier. *SWC*—saltwater diversion canal. (Original, by Alon Rimmer)

1596, Tiberias had declined to a total recorded population of 50 Muslim families and four bachelors. During the eighteenth and the nineteenth centuries, the town and region suffered mixed but mostly ill fortunes, including sieges, sacking and pillage, and a devastating earthquake in 1837.

Throughout the centuries, the Sea of Galilee has attracted visitors, both pious and profane, whose journals chronicle the vagaries of the region's history. These had reached a nadir by the mid-nineteenth century under the Ottoman neglect and misrule. Some modernization came in 1889 with a group of German Catholics who built a hospice and had a relatively large farm at Tabgha, the present-day site of Israel's National Water Carrier (NWC) pumping station and the Kinneret Limnological Laboratory (KLL; Fig. 1.1). Nearby areas surrounding Capernaum and the Mount of Beatitudes were bought by the Franciscans in 1891 and Italian Catholics at the beginning of the twentieth century, respectively. The first clinic in the whole area was opened in Tiberias in 1894 by a Scottish doctor, David Torrance. Even as recently as 100 years ago, the region was without paved roads or telegraph, and rampant with malaria and bandits. An air photograph from ~1912 (Fig. 1.2) provides evidence that not a single tree existed around the southern shores of the lake at that time, with most of the useable timber in the region having gone into the building of the Hejaz railway and fueling its locomotives.

The influx of Jewish settlement around the lake and throughout the Kinneret watershed, beginning with the establishment in 1910 of Degania, the first kibbutz, brought development, increased prosperity (Fig. 1.2), and, subsequently, led to the growing threats of pollution and environmental degradation.

1.2 Research on Lake Kinneret

Scientific curiosity about the Sea of Galilee has been considerable over many centuries. Physical limnology was touched upon, albeit somewhat inaccurately, by Josephus Flavius (37–100 CE), who asserted that the waters of the River Jordan flowed directly along the lake bottom from the inflow in the north to the outflow in the south. He also summarized lake chemistry by simply stating, "Its waters are pure." A limnograph appears on the sixth-century mosaic floor in the Byzantine church at Tabgha, the reputed site of the New Testament miracle of the loaves and the fishes. Among the early travelers to this region were scientists such as Haselquist, a student of Linnaeus, from Sweden, and excellent naturalists like MacGregor (1870) from Scotland, who recorded lively descriptions of the lake and its flora and fauna. For example, we learn from Burckhardt (1822), the Swiss discoverer of Petra, that in the early 1800s the most common fish were the Binnit (*Barbus longiceps*) and St. Peter's fish (*Sarotherodon galilaeus*), species which are still found today. Naturalists such as Tristram (1884), Barrois (1894), and Annandale (1912, 1915) examined and tabulated the flora and the fauna of the lake in the 1860s and in the early years of the twentieth century, respectively. Annandale (1915) also made remarkably detailed and accurate measurements of water temperatures and chemical composition. Somewhat later, from 1914 to 1918, Fr. Schmitz, a German naturalist, ornithologist,

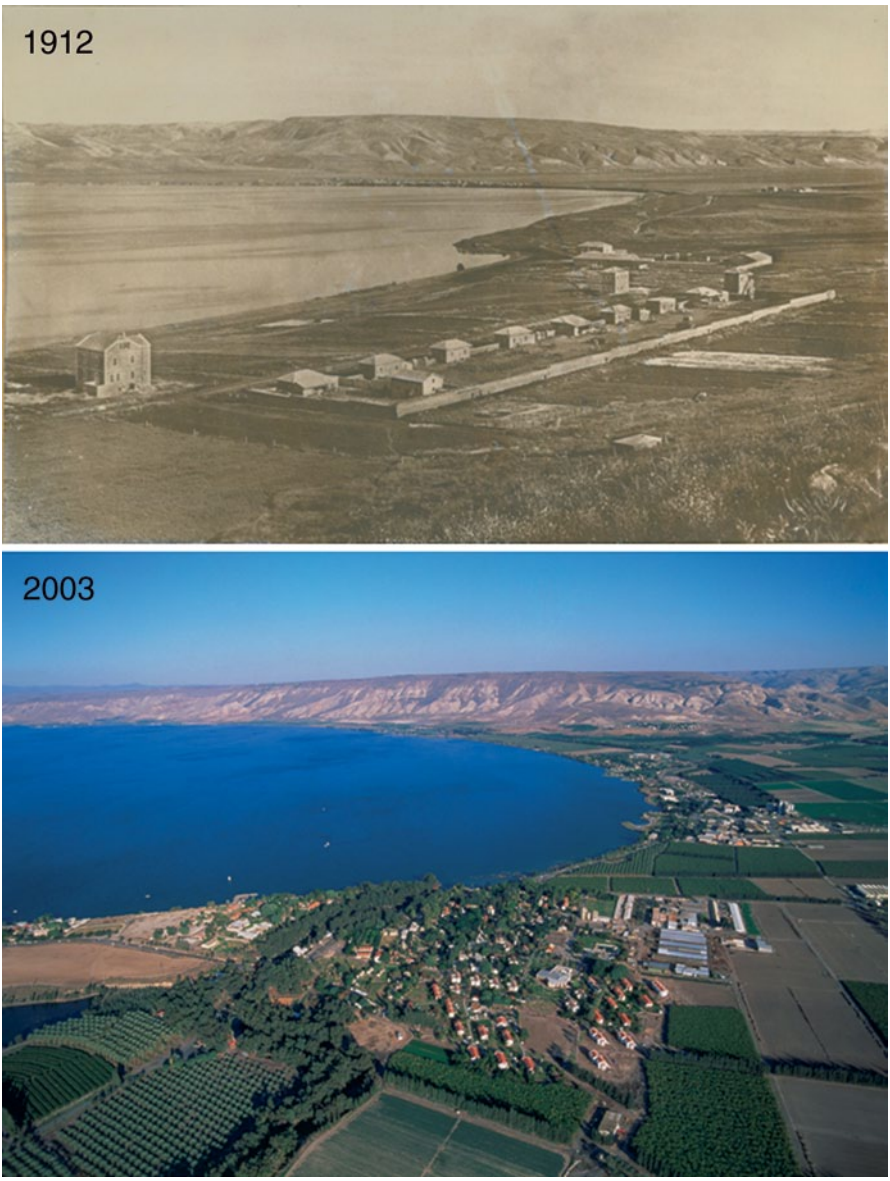

Figure 1.2 Air photos of the southern part of Lake Kinneret and Golan Height: past and present. *Upper* photo taken by the Turkish Air Force circa 1912; note the bare land and lack of trees. (*Lower* photo taken by Albatross Aerial Photography Ltd., in 2001, reproduced with permission)

entomologist, and Roman Catholic priest carried out extensive natural history studies in Palestine, including the shores and waters of Lake Kinneret.

From 1920 to 1950, scientific studies remained mainly of a descriptive nature and were directed principally toward improving the catch of the commercial fishery. In the late 1950s, some careful but limited investigations on the physical and

chemical characteristics of the water (Oren 1957) and the photosynthetic activity of the algae were carried out by Yashouv and Alhounis (1961). Only after 1960, with the decision to use Lake Kinneret as the principal reservoir of the NWC system, was an effort made to encourage more systematic studies of the lake. Mekorot Water Company, which is responsible for most of the water supply in Israel, began to monitor water samples from the lake and catchment area. Scientists from various institutions were funded by Mekorot to carry out research projects, while Tahal (a semipublic company that was at that time responsible for the development of new water sources) undertook to study the hydrology of the saline inputs.

Although well intentioned, these first attempts at a comprehensive research program yielded only fragmented results. Partly, this was because most of the scientists involved spent little time at the lake and thus their work lacked continuity. More important factors were the lack of coordination and understanding of ecological priorities, which caused many independent projects, some of marginal importance, to be funded.

In 1965, Mekorot invited an eminent Swedish limnologist, Wilhelm Rodhe, to appraise the state of the water quality. Somewhat alarmed at seeing a dense bloom of *Peridinium,* Rodhe predicted that a further deterioration of water quality might be expected, and recommended the establishment of a lakeside laboratory for scientific study of the lake. At approximately the same time, the Israeli government set up an organization that became Israel Oceanographic and Limnological Research (IOLR). In turn, this led to the establishment of the KLL in 1968.

With the inception of the KLL, the modern era of closely integrated monitoring and research began. Starting in October 1969, five main sampling stations (Fig. 1.1) were visited weekly or fortnightly to collect water samples for chemical and biological determinations, generating data that today constitute the Lake Kinneret Database. A first monograph entitled "Lake Kinneret," edited by Colette Serruya, was published (Serruya 1978), putting a solid basis to the understanding of the structure and functioning of this warm, monomictic freshwater lake. Since then, more than 1,000 additional scientific papers addressing Lake Kinneret have been published in the peer-reviewed literature. A comprehensive list of research literature up to 1999 was compiled by Hambright. Our objective in the present monograph is to summarize current knowledge on the Kinneret ecosystem, accumulated over four decades of intensive research and monitoring, in a single volume accessible to the professional community.

1.3 Morphometric and Limnological Features of Lake Kinneret

Lake Kinneret is located in the northern Syrian–African Rift Valley, at 32°50′N, 35°35′E. Some main morphometric and limnological features are summarized in Table 1.1. The lake is subject to a Mediterranean climate, with hot, dry summers and cool, wet winters, with rainfall and nutrient inflows limited to 4–6 months of the year (usually from October–November to February–March). Lake bathymetry and also the main sampling stations for the monitoring program are shown in Fig. 1.1. Detailed bathymetric and morphometric data can be found in Chap. 4.

Table 1.1 Morphometric and other characteristics of Lake Kinneret. Morphometric features are measured at a baseline water level of −209 m[a]

Age (modern freshwater lake), years	~20,000
Surface area, km^2	168.7
Mean depth, m	25.6
Maximum depth, m	41.7
Volume, 10^6 m^3	4,325
Maximum length (North–South), km	21
Maximum width (East–West), km	12
Perimeter, km	56
Shoreline development index	1.16
Latitude, °N	32°50′
Longitude, °E	35°35′
Altitude, m a.m.s.l.	−209
Annual Jordan River inflow volume (mean 1971–2010), 10^6 m^3	450
Water residence time, years	7–11
Watershed area, km^2	2,730
Typical thermocline depth in June, m	15
Lower water mass volume, 10^6 m^3	1,600
Epilimnion volume, 10^6 m^3	2,700
Lake floor area covered by hypolimnion, km^2	135

[a] Altitude measurements are given relative to above mean sea level (amsl)

1.4 Seasonal Patterns of some Limnological Parameters

Lake Kinneret is a warm, monomictic meso-eutrophic subtropical lake that is stratified annually from March–April to December–January. During stratification, an aerobic warm (24–30 °C) epilimnion and an anoxic relatively cold (14–16 °C) hypolimnion are formed. Seasonal variations in some characteristic parameters are shown in Fig. 1.3. Multi-annual averages (based on data from 2000 to 2011) for these parameters indicate major differences between epilimnion and hypolimnion with a typical seasonal pattern. The following section gives a brief description of these parameters. Further details on seasonal dynamics and multi-annual variations in physical and chemical driving forces (water flow, nutrient loads, and meteorological parameters) as well as on various biological parameters in Lake Kinneret are presented in the relevant chapters of this book.

Water and air temperatures (Fig. 1.3A). Epilimnetic water temperature shows a gradual rise in accordance with air temperature (*solid line* in Fig. 1.3a) until mid-summer. Subsequently, air temperature drops below epilimnetic temperature inducing the gradual cooling of the upper water column. About a month after the onset of seasonal stratification, the mid-thermocline depth (Fig. 1.3b) begins at 14 m and gradually deepens, typically at 1 ± 0.4 m per month, until October, after which this rate increases. Hypolimnetic temperature (Fig. 1.3a) increases very slowly, only by ~1°C throughout the stratified period.

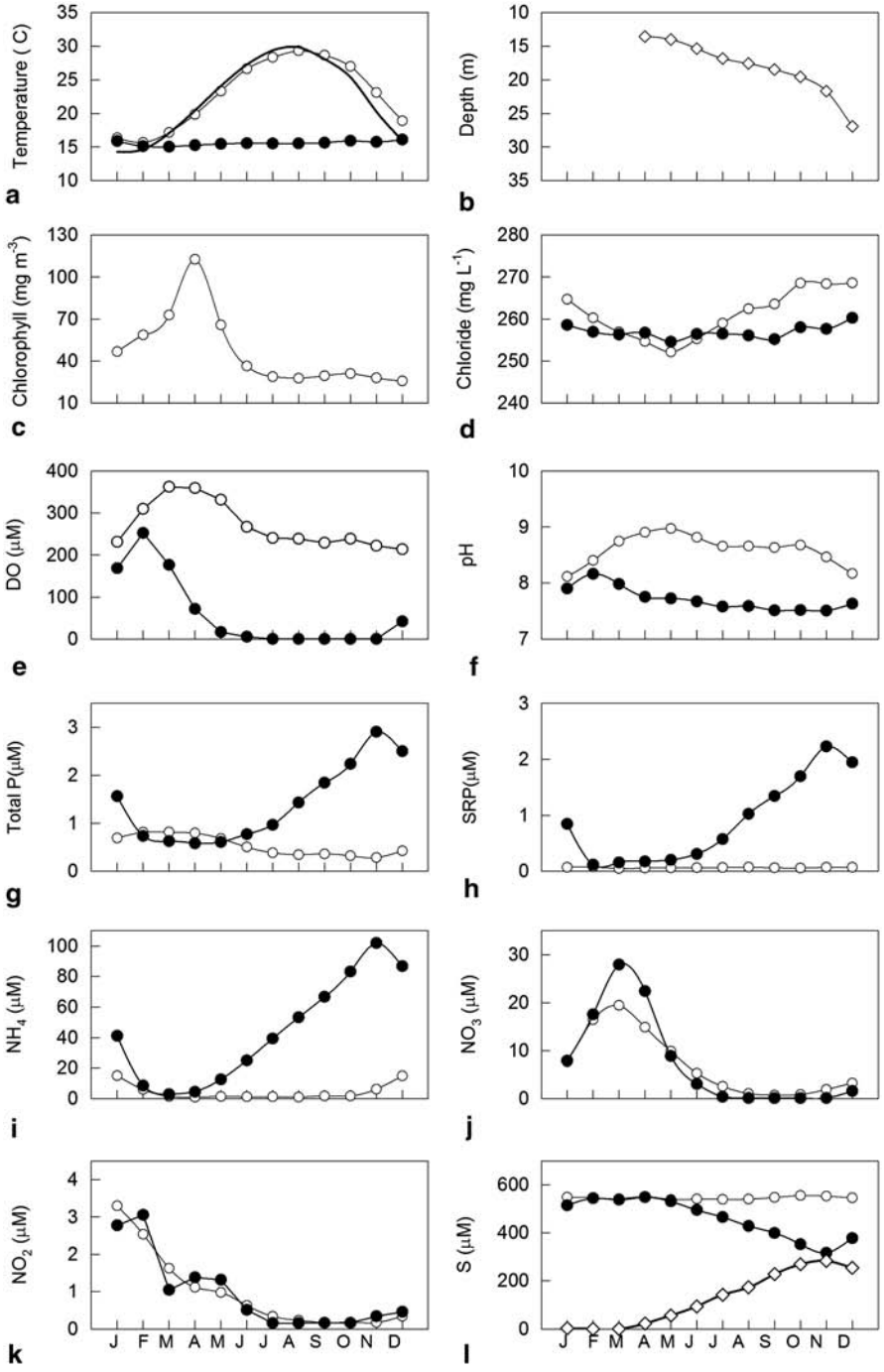

Figure 1.3 Monthly averages of limnological parameters in Lake Kinneret for the decade 2001–2011 in the upper 0–5 m (*empty circles*) and lower >30 m (*solid circles*) water layers at station A. **a** *Solid line* shows air temperature. **b** *Diamonds* represent the depth of the mid-thermocline. **l** *Diamonds* represent the hypolimnetic sulfide concentrations, *empty circles* and *filled circles* refer to sulfate concentrations

Chlorophyll (Fig. 1.3c). Winter–early spring is characterized by a steep rise in chlorophyll (Chl) concentrations to a maximum in April. The crash of the spring bloom in late spring or early summer is indicated by a decline to significantly lower levels of ~120±30 mg Chl m^{-2} that prevail throughout the rest of the year.

Chloride (Fig. 1.3d). Epilimnetic chloride concentration (*empty circles*) decreases during the winter–spring due to freshwater inflows. Starting in May, reduced freshwater inflows combined with the continuous inflows of saline springs and evaporation lead to a rise in epilimnetic Cl^-. Hypolimnetic Cl^- (*filled circles*) remains practically unchanged with a hardly detectable Cl^- raise in October–November, equivalent to ca. 1,000 t. This Cl^- originates from molecular diffusion of pore-water brine underlying the lake pelagic floor.

Oxygen (Fig. 1.3e). The lake surface-water layer is supersaturated with respect to oxygen in spring due to enhanced primary production and weak winds that reduce gas exchange fluxes. Subsequently, the crash of the spring bloom, solar warming of the surface layer, and the incidence of strong westerly winds cause the dissolved oxygen (DO) levels in the near-surface-water layer to be more or less at saturation. In the hypolimnion, DO declines when the lake stratifies and by June, this layer becomes fully anoxic. Anoxia is maintained until turnover in December or January.

pH. In winter–early spring (April), epilimnetic pH (Fig. 1.3f) rises well above 9.0 reflecting high photosynthetic activity and low wind stress that limit CO_2 replenishment from air. In the hypolimnion, pH drops during the stratified period due to CO_2 and H^+ accumulation caused by biodegradation of organic matter.

Particulate phosphorus (Fig. 1.3g). In the epilimnion, particulate phosphorus (PP=total P minus total dissolved P) slowly accumulates in winter–spring. When the spring bloom crashes, PP declines to levels of about one-third of peak spring levels mainly through sedimentation. Hypolimnetic PP begins to decline in late winter–spring probably due to the sedimentation of allochthonous and possibly also due to some autochthonous PP formed during the mixing period.

Soluble reactive phosphorus (SRP) (Fig. 1.4h). Epilimnetic SRP concentrations are mostly at or below the detection limit (~0.2 μM) at all times of the year. Hypolimnetic SRP accumulates gradually, reaching concentrations of ~2.5 μM by the end of the stratification, then gets diluted by mixing with epilimnetic water at turnover.

Ammonium (Fig. 1.3I). Ammonium (NH_4) accumulates in the hypolimnion during the stratified period in summer–fall reaching concentrations of ~110 μM. In the epilimnion, NH_4 concentrations are at or below detection limits. A small peak of NH_4 occurs in winter during the mixed period in both epilimnion and hypolimnion.

Nitrate (Fig. 1.3j). Nitrate (NO_3) accumulates in winter due to riverine inflows and nitrification of NH_4 previously accumulated in the hypolimnion. In March, when stratification usually begins, the NO_3 concentrations in the epilimnion are lower than in the hypolimnion, due to active uptake by phytoplankton. Thereafter, NO_3

concentrations continue to drop in both the epilimnion and hypolimnion due to biological uptake and denitrification, respectively.

Nitrite (Fig. 1.3k). Nitrification–denitrification processes are evident from nitrite (NO_2) peaks in winter in both layers and in spring in the hypolimnion. Nitrite concentrations resulting from nitrification and denitrification processes are highest during the mixed period and close to detection limits for the remainder of the year.

Sulfate and sulfide (Fig. 1.3l). Sulfate (SO_4) in the oxic epilimnion is a conservative ion affected mainly by water evaporation. However, microbial SO_4 reduction in the anoxic hypolimnion, beginning in June, leads to a drop in SO_4 and an accumulation of hydrogen sulfide (HS^-, *empty diamonds*) reaching 0.27 mM in November.

1.5 Man-Induced Changes that Impacted the Lake Kinneret Ecosystem

Until construction of the Degania Dam in 1932, Lake Kinneret could be considered as a natural habitat with only minor influence of human activity. Since then, Lake Kinneret has been subjected to a series of anthropogenic changes that have substantially impacted the lake ecosystem. Today, the lake essentially functions as a regulated large water reservoir, with consideration given to its three main uses: water supply, recreation, and fisheries.

Here, we briefly review the major anthropogenic changes, which have occurred over the past 80 years within the Kinneret watershed, in and around the lake. A chronological listing of these changes is given in Table 1.2. Current demographic and socioeconomic data pertaining to the Kinneret Basin are given in Chap. 30.

Degania Dam: Prior to 1932, there were no major anthropogenic hydrological alterations to Lake Kinneret. Archeological evidence from Biblical-era shore structures as well as modern records from 1926 to 1932 of lake water level indicate that under natural conditions, lake water levels fluctuated annually by ~1.5 m, between a minimum of ~−210.5 m a.m.s.l. in fall and a spring maximum of ~−209.0 m. In 1932, the natural outflow at Bet Yerach was blocked. The new outflow to the southern Jordan River was controlled by a dam that regulated water flow to the Rutenberg Hydroelectric Plant at Naharayim, which operated from 1930 to 1948. The Degania Dam increased the annual fluctuation of water level to 2–3 m. The British Mandatory Authority established permissible limits to these fluctuations with −209 and −212 m as upper and lower levels, respectively. Over the past 44 years, the Degania Dam was opened to release water downstream only on relatively few wet winters (Chap. 7).

Draining of Lake Hula and adjacent wetlands: A drastic change to the Kinneret catchment basin and its hydrology occurred in the 1950s with the draining of Lake Hula and its adjacent wetlands. This major engineering project was undertaken in

Table 1.2 Major anthropogenic changes in Lake Kinneret and its catchment since 1927

Year	Event
1927–1932	The Degania Dam was built on the Jordan River outflow, impounding the lake; outflow deepened to −214 m. Legal maximum and minimum water levels ("*red lines*") were set at −209 and −212 m (based on current altitude measurements)
1932–1948	Hydroelectric production at Naharayim, lake levels were manipulated at larger amplitudes than natural but within −209 and −212 m
1951–1958	Drainage of Lake Hula and surrounding swamps in northern catchment
1952–present	Stocking fingerlings of fish of commercial value, which also contribute to improving water quality (St. Peter's fish, grey mullets, silver carp)
1956–1964	Construction of the National Water Carrier (NWC)
1964–present	Lake Kinneret water is pumped into the NWC from Sapir Site. Since 1973 the NWC operated at full capacity ($300–400 \times 10^6$ m^3 pumped annually, reduced to $\sim 200 \times 10^6$ m^3 with increasing water from desalination since 2012
1967–present	Diversion of offshore saline springs via a salt-water diversion canal to the southern Jordan River
1978–present	Actions to reduce effluents of domestic and agricultural origin, including sewage treatment plants, reduction of fishpond area and recycling of their effluents, and treatment of cowshed effluents. In 1984, the Einan Reservoir was constructed to contain and treat effluents from Kiryat Shmoneh and western Hula basin and recycle them for local agriculture
1981	Legal minimum water level lowered to −213 m
1980s−2000s	Construction of water storage reservoirs in the Golan Heights, storing $\sim 40 \times 10^6$ m^3 of water, for agricultural and domestic use
Early 1990s	Construction of "spurs" at various swimming beaches around the lake, later found to disrupt the natural near-shore flow of water and particles
1994–1999	Hula restoration. Raising the groundwater table; creation of Agmon Wetland, improved drainage and recycling of western Hula Valley water for local use aimed at controlling the flow of water from the Hula Valley to Lake Kinneret
1998–2000	Deepening the Jordan River between Pkak Bridge and Benot Yaacov Bridge for improved drainage control
1995–2006	Subsidized harvest of bleak (Kinneret sardine) to reduce predation on zooplankton and improve water quality
1999–2008	Due to shortage of freshwater, legal minimum water level progressively lowered below −213 m (lower red line). In 2008, the lowest legally permissible water level was declared as −214.87 m. (*Lowest recorded water level, Dec. 2001*)
2012	Local actions to remove shoreline/inundated vegetation and treat mosquito larvae resulting from the 2011/2012 increase in water levels that followed a series of drought years

order to provide arable land for the many settlements that were established in the area and to control the blight of mosquito-borne malaria, which was rampant in those years. Lake Hula was a natural shallow lake, about 25 km upstream of Lake Kinneret, that contained dense macrophyte stands and functioned as a natural pre-impoundment, filtering the inflowing Jordan River water (Dimentman et al. 1992; Hambright and Zohary 1998). The peat-like soils of the drained Hula Valley became a major source of nitrates and sulfates to Lake Kinneret through aerobic decomposition of their organic matter, followed by nitrification (Nishri 2011).

The NWC: Israel's NWC system began operation in May 1964. Subsequently, most of the outflow from Lake Kinneret was pumped into this water delivery system; from the 1970s until the mid-2000s, amounts ranging from 300 to $> 400 \times 10^6$ m^3 were pumped annually from the lake. By contrast, annual outflow via the southern Jordan was limited to 18–20×10^6 m^3. Greater discharge through the Degania Dam only occurred in two winters of high water levels with exceptional precipitation (1968/1969, 1991/1992). The altered pattern of water removal since 1964 resulted in a major change in the timing of maximum water and nutrient removal from the lake (Hambright et al. 2004). Prior to 1964, the discharge volume was greatest during the winter holomixis, when outflowing waters are nutrient rich. Since then, maximum outflows have occurred in summer and fall because of increased pumping needed for agricultural irrigation and domestic supply. In this season, the lake is stratified and surface waters are nutrient depleted. In the long run, the change in outflow regime since 1964 reduced the export of nutrients from the lake.

Local water supplies: In addition to the water pumped from the lake into the NWC, over the past 50 years, numerous small pumping stations were constructed around the shores for local agricultural and domestic needs. The municipal water supply for the town of Tiberias (population ~40,000) is taken directly from the lake. Another large pumping station, situated on the southeastern shore, supplies water to a large rural area south of the lake. In all, these pumping stations supply about 40×10^6 m^3 annually. Since the peace agreement with the Kingdom of Jordan in 1995, an additional 50×10^6 m^3 are pumped annually and transferred to Jordan.

Diversion of saline springs: Concurrently with the construction of the NWC during the 1960s, actions were taken to reduce the salinity of Lake Kinneret so that water provided via the NWC was more suitable for irrigation. A salt water carrier was constructed as a bypass, which channelled ~20×10^6 m^3 annually from saline springs along the northwestern coast into the southern Jordan River. Later, treated sewage from settlements and Tiberias was diverted into this bypass to prevent it from reaching the lake. Operation of the salt water carrier caused a continuous decline in the salinity of Lake Kinneret during the 1970s and 1980s (Nishri et al. 1999). Since the late 1980s, however, salinity levels have gradually increased (for details, see Chap. 8).

Upstream water consumption: After 1967, intensive agriculture was introduced in the Golan Heights and the need for water led to the construction of several reservoirs to retain floodwater. These reservoirs, located within the Kinneret catchment,

have a total storage capacity of 40×10^6 m^3 and hold water that would otherwise reach Lake Kinneret. Expansion of agricultural and municipal and domestic use, including groundwater withdrawal throughout the catchment area, has further contributed significantly to the reduced annual inflow volume when compared with the volume three to four decades ago (more details in Chap. 7).

Einan reservoir: This 5.6×10^6 m^3 operational reservoir was constructed in 1983 to contain and treat high-nutrient and bacteria-containing secondary-treated effluents from Kiryat Shmoneh and the fishponds and cultivated fields of the southwestern Hula Valley, and thus prevent them from flowing into Lake Kinneret. The treated water is used for local agriculture.

Wetland restoration in the Hula Valley: For four decades, the Hula Valley was dry, with various ecological problems, such as aggravated soil erosion by high winds leading to dust storms, underground peat fires, soil subsidence, and loss of endemic species. Large areas of the acid peat soils proved problematic for intensive agriculture. In the early 1990s, a comprehensive plan was initiated to rehabilitate the southern Hula area. In order to raise the water table to prevent fires and soil erosion, a network of connecting canals was dug, and a small (1 km^2) shallow lake, Lake Agmon, was created in 1994. A barrier "curtain" of impervious plastic was placed across the southern end of the valley to prevent Hula groundwater from flowing into the Jordan River (Hambright and Zohary 1998). Lake Agmon and its surroundings have become a major way station for migrating birds (cranes, storks, pelicans, and many others), and ecotourism has supplemented agriculture as an income source. Since the completion of the Hula restoration project in 1998, most of the water draining the western side of the Hula Valley is recirculated locally for agricultural use and no longer reaches Lake Kinneret.

Fisheries management: Fisheries regulations for Lake Kinneret were originally set under the British mandate in the 1930s; most of these regulations are still valid. In order to increase the catch of commercial high value fish, a stocking program of both native and exotic species was initiated in 1952 and is still ongoing. The stocking could impact the balance between species competing for similar resources, and could cause decline in genetic variability of the stocked native species. Overfishing, especially during low-water-level years when the fish have less refuge, was associated with reduced body size of the commercial high value fish species, followed by a collapse of the commercial fishery in 2008. A controversial government-subsidized program that removed from the lake a total of 6,000 t of bleak (Kinneret sardine) over 11 years (1995–2006) was aimed at increasing zooplankton and improving lake water quality (see Chap. 36).

Shoreline development: In addition to being a major source of drinking water, Lake Kinneret is an important site for tourism and recreation which serve as a principal source of local income. This has led to continuous strong pressure for development of the lakeshores and shore properties for hotels, restaurants, and other tourist attractions. Development of swimming beaches and campsites has led to construction of access roads and parking lots, facilities for water sports, boat launching and mooring sites, etc.

In the early 1990s, several artificial embankments, up to 100 m in length and tens of meters wide were built perpendicular to the shoreline with the purpose of creating sites of quiet waters for swimmers. Because of the disruption of shoreline current flows, these structures turned out to be ecologically harmful and are no longer being constructed. From the mid-1990s, some shoreline campsites were constructed with kidney-shaped plans that minimized the disturbance to the current patterns but with vertical outer walls that eliminated the natural shoreline habitat. A more recent approach has been to add to the vertical walls a layer of local basalt rocks sloping into the water thus creating spawning sites and refuge for fish.

By law, a 50-m belt of shoreline around the lake, above the maximum water level of −209 m, belongs to the public. Thus, a public access walking path encircling the lake is being developed not without considerable controversy due to the many buildings that have been illegally constructed within the 50-m zone during the past decades.

Permissible limits for lake water levels: With the growth of Israel's population, the need to supply freshwater increased with time and the volumes of water supplied from Lake Kinneret via the NWC became greater than the annually renewable amounts (i.e., the total inflows minus the loss to evaporation). This demand led to a policy of reducing the permissible minimum water level in order to increase lake storage capacity. As a result, the mandatory minimum permissible level was lowered from −212 to −213 m in 1981 and then again to −215 m in 2001; increasing the potential amplitude of water level fluctuations to 6 m. The lowest-ever water level, −214.87 m, was recorded in November 2001.

New water from desalination: Israel's chronic shortage of freshwater led to a government decision in 2005 to supplement the country's natural supplies by very significant amounts of desalinated water. By 2015, it is envisaged that about 30% of Israel's water requirements will be supplied by desalination. As a result of this policy, the dependence on Lake Kinneret as a supply source of drinking water is decreasing. Since 2012, the stated aim of the Israel Water Authority has been to return the operational water levels of Lake Kinneret to between −209 and −213 m.

References

Annandale TN (1912) The blind prawn of Galilee. Nature 90:25

Annandale TN (1915) A report on the biology of the lake of Tiberias. J Proc Asiatic Soc Bengal 11:435–476

Barrois T (1894) Contribution a l'etude de quelqeus lacs de Syrie. Rev Biol Nord Fr 6:41–46

Burckhardt JL (1822) Travels in Syria and the Holy Land. University of Adelaide, Adelaide. http://ebooks.adelaide.edu.au/b/burckhardt/john_lewis//syria/

Dimentman C, Bromley HJ, Por FD (1992) Lake Hula: reconstruction of the fauna and hydrobiology of a lost lake. Israel Academy of Sciences and Humanities, Jerusalem.

Hambright KD, Zohary T (1998) Lakes Hula and Agmon: destruction and creation of wetland ecosystems in northern Israel. Wetland Ecol Manage 6:83–89

Hambright KD, Eckert W, Leavitt PR, Schelske CL (2004) Effects of historical lake level and land use on sediment and phosphorus accumulation rates in Lake Kinneret. Environ Sci Technol 38:6460–6467

Hasselquist F (1766) Voyages and travels in the Levant. Davis and Reymers, London. http://books.google.co.il/books?id=LkIGAAAAQAAJ&redir_esc=y

MacGregor J (1870) The Rob Roy on the Jordan, Nile, Red Sea, and Gennesareth: a canoe cruise in Palestine and Egypt, and the waters of Damascus. John Murray, Edinburgh. http://books.google.co.il/books/about/The_Rob_Roy_on_the_Jordan_Nile_Red_Sea_G.html?id=kp1CAAAAIAAJ&redir_esc=y

Nishri A (2011) Long-term impacts of draining a watershed wetland on a downstream lake, Lake Kinneret, Israel. Air Soil Wat Res 4:57–70

Nishri A, Stiller M, Rimmer A, Geifman Y, Krom MD (1999) Lake Kinneret (The Sea of Galilee): the effects of diversion of external salinity sources and the probable chemical composition of the internal salinity sources. Chem Geol 158:37–52

Oren OH (1957) The physical and chemical characteristics of Lake Tiberias. Water planning for Israel, Tahal Ltd. Internal Report No. 1445/58

Serruya C (1978) Lake Kinneret. Junk, The Hague

Tristram HB (1884) The fauna and flora of Palestine. Society for promoting Christian knowledge, London

Yashouv A, Alhunis H (1961) The dynamics of biological processes in Lake Tiberias. Bull Res Counc Israel 10B:11–35

Part I
The Geographical and Geological Setting

Chapter 2
Structure and Tectonic Development of the Kinneret Basin

Zvi Ben-Avraham, Michal Rosenthal, Gideon Tibor, Hila Navon, Hillel Wust-Bloch, Rami Hofstetter and Michael Rybakov

Abstract The Sea of Galilee is a freshwater lake in northern Israel, occupying a part of the Lake Kinneret basin along the Dead Sea fault. The basin is located in an area of tectonic complexity, where the main north–south trending segments of the Dead Sea fault intersect with a secondary system of northwest–southeast and east–west trending faults in the Galilee. Plio–Pleistocene basalt flows and intrusions varying in thickness are present around the lake. This tectonic setting produced the complicated sub-bottom structure of the basin. Numerous studies have dealt with this issue using various methods: seismic reflection and refraction, heat flow, bathymetry, magnetics, gravity, and seismicity. This chapter summarizes the findings of the previous and recent studies of the sub-bottom and floor of the lake. The Lake Kinneret basin is composed of two subbasins. The northern subbasin is the most tectonically active zone in the lake and forms the deepest bathymetric part of it. The southern subbasin is the deepest part of the basin, filled with 5–8 km of sediments. Both longitudinal boundary faults and transverse faults are present in the lake; however, their accurate geometry is in dispute. Structural evolution of the

Z. Ben-Avraham (✉) · M. Rosenthal · H. Navon · H. Wust-Bloch
Department of Geophysical, Atmospheric and Planetary Sciences,
Tel Aviv University P.O.B. 39040, 69978 Tel Aviv, Israel
e-mail: zviba@post.tau.ac.il

M. Rosenthal
e-mail: rofemich@post.tau.ac.il

H. Navon
e-mail: hilaweis@post.tau.ac.il

H. Wust-Bloch
e-mail: hillelw@post.tau.ac.il

G. Tibor
Israel Oceanographic & Limnological Research,
P.O.B. 8030, 31080 Haifa, Israel
e-mail: tiborg@ocean.org.il

R. Hofstetter
Geophysical Institute of Israel, P.O.B. 182, 71100 Lod, Israel
e-mail: ramih@gii.co.il

M. Rybakov
e-mail: rybakovmichael6@gmail.com

T. Zohary et al. (eds.), *Lake Kinneret, Ecology and Management,* Aquatic Ecology Series 6,
DOI 10.1007/978-94-017-8944-8_2,

basin is associated with several tectonic processes. The interaction between the two fault systems may have caused rotational opening and transverse normal faulting that formed the northern subbasin. Strike–slip motion along the main segments of the Dead Sea fault is probably responsible for the pull-apart opening of the southern subbasin.

Keywords Active faults · Bathymetry · Dead Sea fault · Gravity · Magnetic · Seismic reflection · Seismic refraction · Volcanism

2.1 Introduction

Lake Kinneret is one of a number of morphotectonic depressions along the Dead Sea fault (Garfunkel 1981; Kashai and Croker 1987; Garfunkel and Ben-Avraham 2001)—a plate boundary of the transform type which connects the Red Sea, where the seafloor spreading occurs, with the Taurus–Zagros zone of continental collision (Fig. 2.1). It is a freshwater lake, 12 km at its widest point and approximately 20 km long. Its surface is approximately 210 m below mean sea level and has a maximum depth of 41.7 m (Chap. 4). Due to high sedimentation rates of 2–7 mm year^{-1} (Serruya 1973; Inbar 1976), the lake floor is relatively flat.

The Lake Kinneret basin is composed of the lake itself and the Kinarot Valley to the south. It forms the northern section of the Kinneret–Beit Shean basin, which began to form during the Neogene (Picard 1943; Schulman 1962; Garfunkel and Ben-Avraham 2001), as a result of the strike–slip motion along the N–S-trending Dead Sea fault. This remains the major fault trend in the basin. However, a secondary NW–SE to W–E-trending fault system composed of branching faults, such as the Carmel fault (Fig. 2.1), exits on the western side of the Dead Sea fault (Saltzman 1964; Freund 1970; Shaliv 1991). This secondary system resulted in reactivation of older systems, creating complicated structures and fault patterns. Braun et al. (2009) suggested a strong coupling of the Carmel fault with the Dead Sea fault, and Sadeh et al. (2012) found that a high fraction of the total slip is being accommodated by the Carmel fault. Farther north, additional faults branch off from the Dead Sea fault (Ron et al. 1984; Heimann 1990) in the region of the Palmyra Range and westward, with the Yammouneh fault being the main branch (Walley 1998).

The structure of Lake Kinneret is complex and results from the intersection of the two fault systems in the area. Superposition of vertical displacements perpendicular or oblique to the N–S transform fault created complicated structures in the area. Because Plio–Pleistocene basalt flows and intrusions vary in thickness, structural interpretation is difficult.

Basalt outcrops are exposed around Lake Kinneret (Fig. 2.2), mainly of the Cover Basalt formation (Picard 1936; Schulman 1962). The maximum thickness of this unit is 175 m (Michelson 1972). K–Ar and Ar–Ar radiometric ages (Siedner and Horowitz 1974; Mor and Steinitz 1982; Mor 1986, 1993; Heimann et al. 1996; Weinstein et al. 2006) indicate that the Cover Basalt is 5.5–3.3 Ma. This age ranges between the Gilbert and the Gauss paleomagnetic eras, each characterized with a different paleomagnetic polarity. Accordingly, the Cover Basalt in the Galilee is

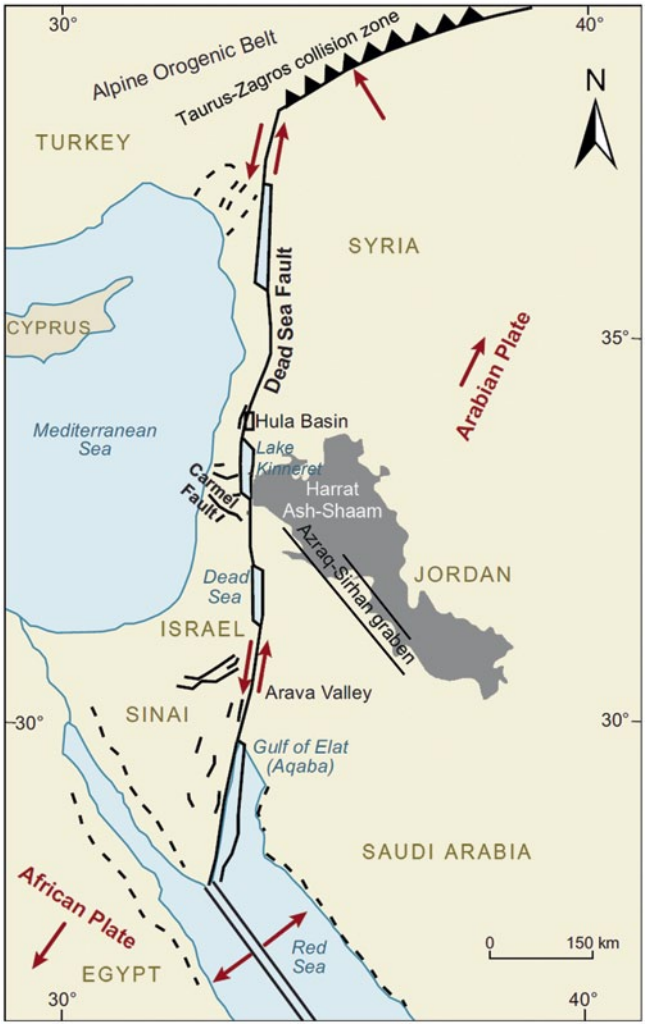

Fig. 2.1 Regional setting of the Dead Sea fault zone and the Carmel fault system (tectonic features are schematic). (Modified with permission after Ben-Avraham et al. 2008)

normally magnetized in the lower part and reversely magnetized in the upper part (Freund et al. 1965). However, in the Golan Heights, the whole Cover Basalt section is reversely magnetized (Ron et al. 1984). Eruptions of the Cover Basalt originated in flat, ellipsoid-shaped, NNW–SSE-trending volcanic cones in the Golan Heights (Mor 1986), at the edge of the large NW-trending Harrat Ash-Shaam volcanic field in Jordan. The location of these cones was probably dictated by the tectonic evolution of the Dead Sea fault (Heimann et al. 1996). Cover Basalt that erupted in the Korazim Heights had not erupted during the Early Pliocene in adjacent areas to the east and west (restoring 25–30 km along the eastern marginal fault), so these basalt flows may have been channeled along active faults (Weinstein 2012).

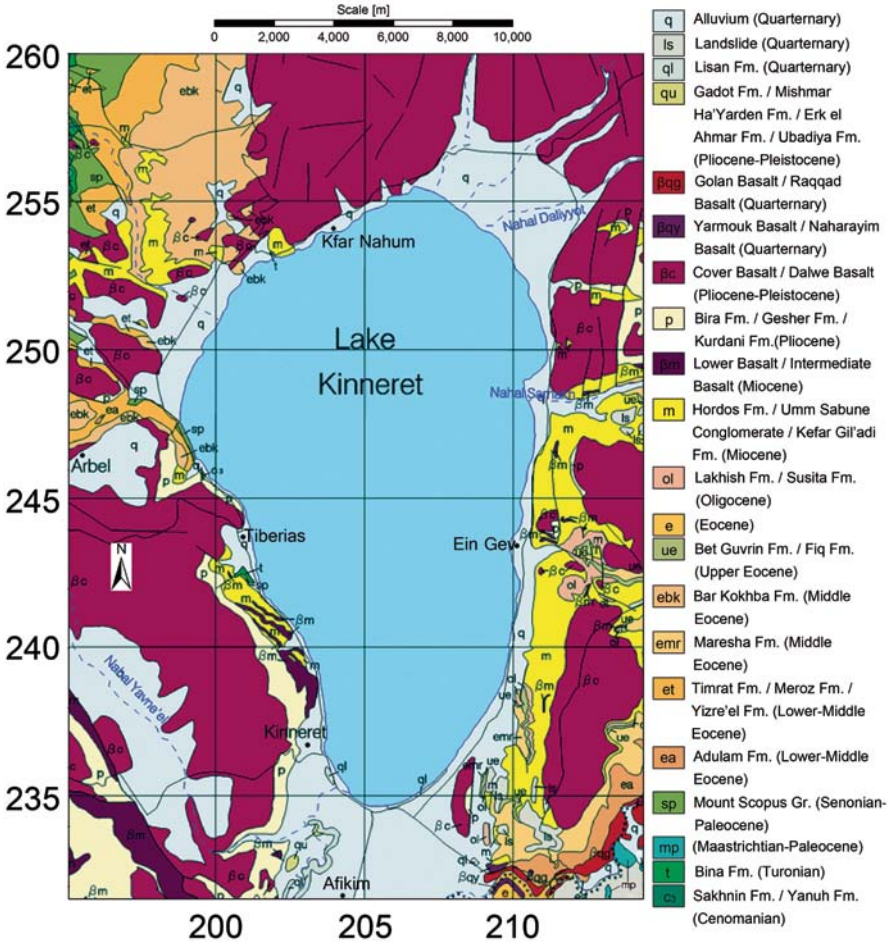

Fig. 2.2 The geology of the surrounding land area of Lake Kinneret. (Modified with permission after the 1:200,000 map of the Geological Survey of Israel; Sneh et al. 1998)

Previous studies of the sub-bottom structure of the lake were carried out using various methods, including seismic reflection and refraction (Ben-Avraham et al. 1981; Ben-Avraham et al. 1986; Ben-Gai and Reznikov 1997; Hurwitz et al. 2002; Reznikov et al. 2004; Ben-Gai 2009), magnetics (Ben-Avraham et al. 1980; Ginzburg and Ben-Avraham 1986), bathymetry (Ben-Avraham et al. 1990), heat flow (Ben-Avraham et al. 1978), and gravity (Ben-Avraham et al. 1996). Although these studies have increased our understanding of the sub-bottom structure of the lake, several key questions remain unsolved: the accurate geometry of the plate boundary in the Lake Kinneret area, the deep sub-bottom structure, the geometry and nature of transverse faulting, and the mechanism controlling the location of submarine springs on the floor of the lake.

Recent studies of the sub-bottom structure of the lake include bathymetry, seismic reflection, magnetics, and seismicity. In these studies, new advanced

instrumentation was used, and the research is ongoing. In this chapter, the main findings of the previous and recent studies will be described and their contribution to the understanding of the structure and evolution of this area will be discussed.

2.2 Bathymetry

The first bathymetric survey of Lake Kinneret was carried out between 1960 and 1970 by TAHAL (Water Planning for Israel). This was followed by a bathymetric survey performed by Ben-Avraham et al. (1990) in 1986 and 1987. The survey was conducted along a grid of N–S and E–W lines with 100-m spacing, and revealed several features. A bathymetric depression, situated >250 m below sea level, occupies the northeastern part of the lake. High gradient slopes are observed mainly along the lake margins, while most of the lake center is associated with a relatively smooth floor. A prominent exception is a steep bathymetric scarp in the southern portion of the lake around latitude 32°45′N (Fig. 2.7). The steep bathymetric slopes might indicate a recent active faulting in the lake that manages to overcome its high sedimentation rates of 2–7 mm year^{-1} (Serruya 1973; Inbar 1976).

The bathymetric data collected by Ben-Avraham et al. (1990) were analyzed in later works (Belitzky and Ben-Avraham 2004; Guitton and Claerbout 2004). In a morphotectonic analysis performed by Belitzky and Ben-Avraham (2004), systematic seafloor disturbances and irregularities were detected and referred to as morpholineaments. Major morpholineaments indicate several kinematic processes: active deformation associated with strike–slip movement along N–S segments of the Dead Sea fault system and normal faulting of the secondary NW–SE to W–E-trending fault system.

A high-resolution bathymetric survey was performed in 2008 with a 4-m grid spacing, using a multibeam system (Tibor and Sade 2009; Sade et al. 2009). Processes of both erosion and accumulation seem to take place in different parts of the lake during the two recent decades, since the previous mapping. Further results based on the recent data are presented and discussed by in Chap. 4.

2.3 Sub-Bottom Structure

2.3.1 Deep Section

2.3.1.1 Magnetic Pattern

A magnetic survey in Lake Kinneret was first carried out by Ben-Avraham et al. (1980). The data were collected with a line spacing interval of 1 km and were analyzed to form a magnetic anomaly map. Its results indicate that the center of the lake is quite smooth in spite of its location at the edge of the large NW-trending Harrat

Ash-Shaam volcanic field in Jordan. Two broad magnetic domains were detected: negative and positive. Both the anomaly domains are trending in E–NE direction, yet the positive anomaly is wider. As opposed to the lake's center, its margins are associated with local anomalies of large amplitude and short wavelength. It is interesting to note that most of the hot salty springs are situated in areas of magnetic anomalies. Apart from basalts, a presence of iron in the surface sediments (Serruya 1971) was suggested as a potential source to the magnetic anomalies (Ben-Avraham et al. 1980). Iron in the form of greigite (Fe_3S_4) was found in sediments of Late Pleistocene age and is thought to affect both the magnetic intensity and the direction of magnetization (Ron et al. 2007).

Magnetic anomalies exist along the northwestern margin of the lake more than in any other part of it (Ben-Avraham et al. 1980). The largest amplitude magnetic anomaly, more than 500 nT, was detected in the northern marginal area near the inflow of the Jordan River into the lake. In the southernmost portion of the lake, there is a significant change in the field pattern, which was later interpreted as a buried basaltic plate dipping from NE to SW at 10° Eppelbaum et al. 2004a; Eppelbaum et al. 2004b; Eppelbaum et al. 2007).

Additional magnetic measurements were performed by Ginzburg and Ben-Avraham (1986), both in the southern part of the lake and farther south on land. The magnetic pattern in these areas revealed that the anomalous zone along the margins of the lake continues onto the land area to the south. Large amplitude anomalies are elongated and aligned along known faults on land, and some of them can be correlated with basalt outcrops. Data interpretation suggests that the main occurrences are of narrow intrusive bodies reaching great depths, such as dykes with associated sills. It seems that several of these bodies form linear features extending southward from the southwestern margin of the lake and then bend to the east, forming the western and southern boundaries of the Kinarot Valley south of the lake.

A recent high-resolution magnetic survey was conducted in 2008 along more than 2,400 km of dense (100 m spacing) grid lines (Tibor and Sade 2009). Analyses of the data produced a new magnetic anomaly map (Fig. 2.3). A comparison between the previous survey and the recent survey revealed general similarities and some new information. Both the magnetic maps show the smooth magnetic domains at the center of the lake: positive in the east (corresponds to normal magnetization) and negative in the north and west (probably corresponds to reverse magnetization). Nevertheless, along the shores of the lake, there are large amplitude anomalies of shorter wavelength, in particular, along the northern shore, where the largest anomalies occur.

2.3.1.2 Gravity

Gravimetric survey was performed in Lake Kinneret by Ben-Avraham et al. (1996). A total of 300 km of continuous marine gravity data were collected in the lake and integrated with land gravity data over 20 km around the lake. The data analysis resulted in gravity anomaly maps and profiles.

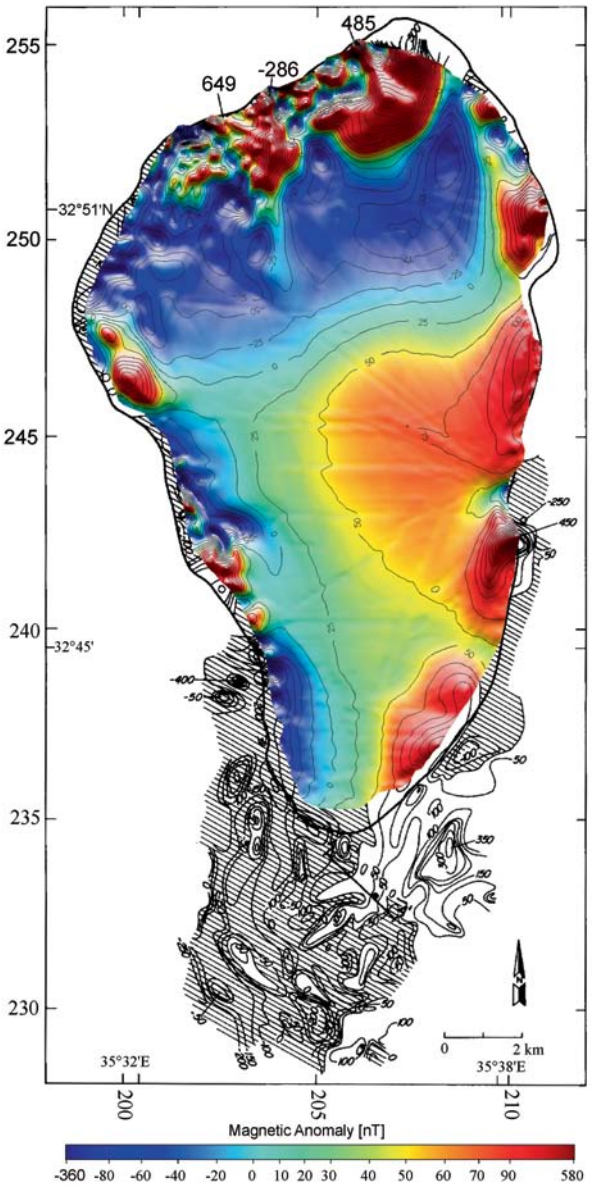

Fig. 2.3 Magnetic anomaly map of Lake Kinneret basin. The marine data are recently obtained (Tibor and Sade 2009) and contoured with an interval of 25 nT. The data on land, south to the lake, with permission after Ginzburg and Ben-Avraham (1986), are contoured with an interval of 50 nT. Areas of negative magnetic anomalies are marked with *diagonal hatching*

The regional and local free-air anomaly maps coincide with the topographic nature of the area: a negative anomaly over the lake itself (−40 mgal) and a positive anomaly (120 mgal) over its surrounding highlands. The negative anomaly is located at the eastern side of the lake, south of the bathymetric depression and along a steep topographic escarpment. In the west, the free-air anomaly drops from the land to the lake margin by about 100 mgal.

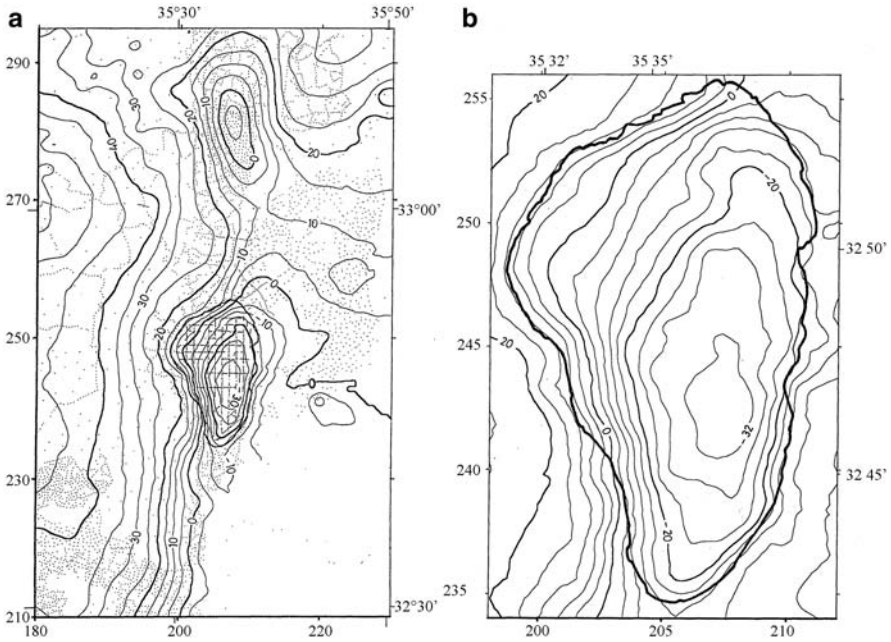

Fig. 2.4 Bouguer gravity anomaly maps of Lake Kinneret (Ben-Avraham et al. 1996): **a** Regional—showing locations of gravity stations (*dots* on land and *lines* in the lake). The gravity values were gridded at 0.65-km square cell size and smoothed. Density used for the Bouguer correction is 2,550 kg m^{-3} above 150 m below sea level (mbsl) and 2,150 kg m^{-3} below 150 mbsl. Reference level for map and lake level during the experiment is 210.2 mbsl. Contour interval is 5 mgal. The Kinneret and Hula basins are clearly expressed on the map. **b** Local—the gravity values were gridded at 0.2-km square cell size and smoothed. Contour interval is 4 mgal. The gravimetric low is located at the southern part of the lake. (Reproduced with permission from Ben Avraham et al. 1996)

Much like the free-air anomaly maps, both the regional and local Bouguer anomaly maps (Fig. 2.4a, b) reveal a prominent gravity low (below −30 mgal) in the southern part of the lake. On the western margin of the Lake Kinneret basin, the values decrease eastward from about 40 mgal to values around 0 mgal. The contour lines do not define clearly the northeastern margin of the lake in any of the maps.

The gravity pattern shown on these maps, together with modeling along E–W gravity profiles, suggests that the Lake Kinneret basin is actually composed of two different structural units, north and south of the latitude 32°49′N. The northern subbasin is asymmetric to the east, and it is wider than the deep southern elongated subbasin. Two N–S boundary faults delimit the southern subbasin: eastern and western. Other geophysical evidence (Fig. 2.5) suggests that these are strike–slip faults (see subsequent discussion).

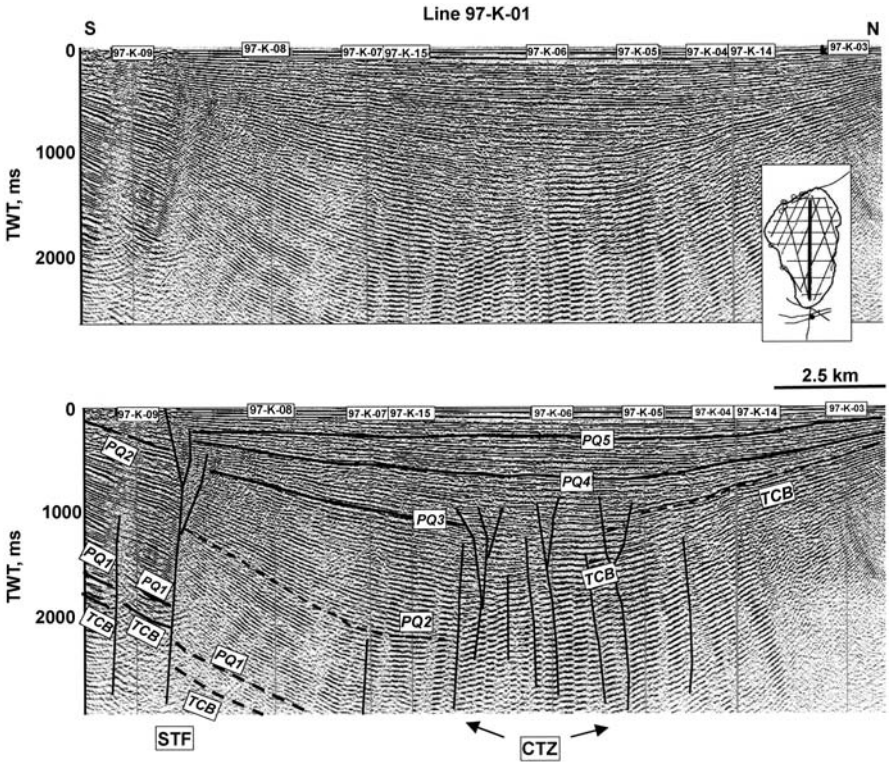

Fig. 2.5 Migrated seismic line 97-K-01 (*top*) and its interpretation (*bottom*) in the Lake Kinneret, reproduced with permission from Reznikov et al. (2004). Southern transverse fault (STF) and central transverse fault zone (CTZ) are southern and central transverse fault zones bordering the deep southern subbasin (Fig. 2.6). *TCB*—top of the Cover Basalt Complex; *PQ*—middle-upper pliocene-quaternary unconformities

2.3.2 Shallow Section

The lake and its surroundings were mapped in previous studies using seismic reflection and refraction surveys (Ben-Avraham et al. 1981; Ben-Avraham et al. 1986; Ben-Gai and Reznikov 1997; Tibor et al. 2004; Reshef et al. 2007). The survey conducted by Ben-Avraham et al. (1981) included several instruments with various frequency bands ranging between few tens to few hundreds of hertz. Despite the poor penetration, evidence of active tectonics, such as folds and faults, was revealed in the uppermost sediments, as well as in the deepest portion of the lake. The next seismic survey was performed with a system of 3.5 kHz (Ben-Avraham et al. 1986). These results showed some bathymetric irregularities, which indicate active tectonic processes that overcome the high sedimentation rate. Using a higher frequency also revealed some zones of increased acoustic penetration: the terrace in the southern part of the lake and areas in the vicinity of hot, salty submarine springs.

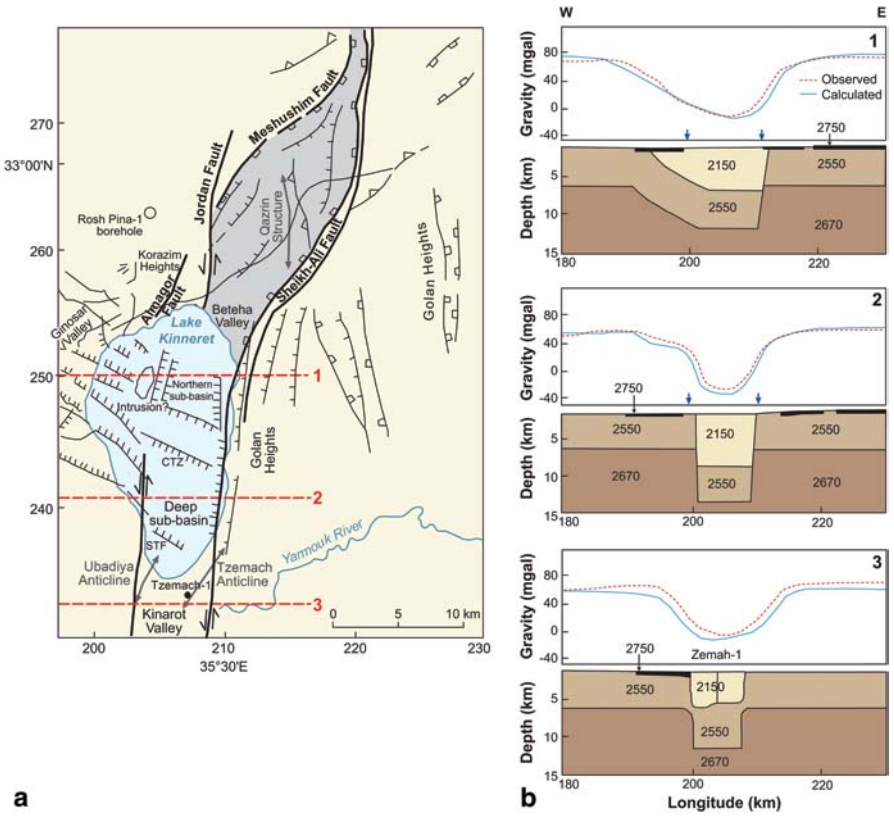

Fig. 2.6 **a** Tectonic map of Lake Kinneret and the Golan Heights based on Ben-Avraham et al. (1996), Hurwitz et al. (2002), Reznikov et al. (2004), and Shulman et al. (2004). *Bold lines* indicate major faults. *Gray area* shows the extent of the Yehudiyya transtensional zone. Major subsurface faults are marked by *squares* and subsurface thrust-faults by *triangles*. *Dashed red lines* (and *numbers*) indicate the location of gravity profiles presented in Fig. 2.6b. STF and CTZ are southern and central transverse fault zones, respectively, bordering the deep southern subbasin. **b** Three E–W gravity profiles (*dashed red lines*) extracted from the free air gravity data, after removal of linear trends, compared with calculated gravity (*solid blue lines*) from two-dimensional density–depth models presented below profiles (based on Ben-Avraham et al. 1996). Location of profiles is shown in Fig. 2.6a. Numbers are densities in kg m^{-3}. *Black layers* represent basalt flows. *Blue arrows* mark the boundaries of the lake. (Modified with permission from Ben-Avraham et al. 2008)

Poor acoustic penetration through most of the lake is caused either by gas presence in the surface sediments (Ben-Avraham et al. 1986) or by homogeneous lithology of fine-grained materials such as silt and clay (Tibor et al. 2004; Reshef et al. 2007).

A multi-channel survey helped in mapping the sub-bottom structure of the lake (Ben-Gai and Reznikov 1997; Hurwitz et al. 2002; Reznikov et al. 2004; Ben-Gai 2009). The presence of dominant N–S-trending longitudinal marginal faults had been suggested by Hurwitz et al. (2002). According to these authors, these steep faults define the boundaries of a large graben that underlies most of the lake. Under

its northwestern part lies another distinct structural zone of pre-rift units at shallow depths. Transverse faults were not observed by Hurwitz et al. (2002), except for the Kfar Nahum fault, which is probably the northern boundary of the Lake Kinneret basin. The eastern marginal fault may be a continuation of the on-land marginal fault in the south (Rotstein et al. 1992). It extends to the northern part of the lake as well, and then continues on land as the Sheikh-Ali fault in the Golan Heights (Fig. 2.6a).

The western marginal fault is also an extension of the on-land fault to the south of the lake, and according to the model proposed by Hurwitz et al. (2002) it crosses its northern part as well. Reznikov et al. (2004) suggested a different model in which the northern continuation of the western marginal fault is a possible part of a large deformation zone under the northwestern part of the lake. The southern part of the lake is occupied by a deep subbasin, which is delimited by the central transverse fault zone (CTZ) and the southern transverse fault (STF) observed in the seismic data (Fig. 2.5). Further features proposed by Reznikov et al. (2004) include a zone of distortion that underlies the central part of the lake, and a possible intrusion in the northwestern part of the lake. Ben-Gai (2009) found no evidence for the southern transverse fault proposed by Reznikov et al. (2004).

2.4 Active Tectonics

The fault geometry in the Lake Kinneret basin includes both longitudinal boundary faults and transverse faults. Steep N–S-trending marginal faults border structural features in the basin (Hurwitz et al. 2002). The eastern marginal fault extends along the northern and southern parts of the lake and continues on land in both directions (Fig. 2.6a): in the north as the Sheikh-Ali fault in the Golan Heights (Shulman et al. 2004) and in the south into the Kinarot Valley (Rotstein et al. 1992; Hurwitz et al. 2002; Reznikov et al. 2004). The western marginal fault extends along the southern part of the lake and continues southward into the Kinarot Valley (Hurwitz et al. 2002; Reznikov et al. 2004). It is unclear whether the western marginal fault extends all the way to the north (Hurwitz et al. 2002) or only up to the point where it meets a complex deformation zone in the northwestern part of the lake (Reznikov et al. 2004). Transverse faults may exist in the northernmost portion of the lake (Hurwitz et al. 2002); however, it is unclear whether they exist in its central and southern parts (Reznikov et al. 2004) or not (Hurwitz et al. 2002; Ben-Gai 2009). Normal faults have been active in the Plio–Pleistocene, keeping up with, and even exceeding sediment accumulation in the Lake Kinneret basin (Marco et al. 2005).

Dramatic variations of the deep sub-bottom structure, based on gravity modeling, occur over different parts of Lake Kinneret (Fig. 2.6b) and explain its unique shape. Based on these variations, the Lake Kinneret basin is divided into two subbasins: northern and southern (Ben-Avraham et al. 1996).

The northern subbasin is a bathymetric depression (Ben-Avraham et al. 1990) occupied by an asymmetric half-graben delimited to the east by the eastern marginal

fault, and to the west by the large deformations suggested by Reznikov et al. (2004). The half-graben structure of a ~6-km sedimentary fill is considered to be an actively subsiding young feature, and it might have been formed due to rotational opening (similar to the one observed in the Korazim Heights and the eastern Galilee by Ron et al. (1984) and Heimann and Ron (1993); see discussion further) and transverse normal faulting, caused by interactions between the two fault systems: the N–S-trending Dead Sea fault and the secondary NW–SE to W–E-trending fault system (Ben-Avraham et al. 1996).

The southern subbasin is a gravimetric depression occupied by a symmetric graben (Ben-Avraham et al. 1996), and it is a deep structure filled with 5–8 km of post-rift sediments with little or no tectonic activity. Sediments of Pleistocene age in the southern subbasin are dipping northward as a result of the active subsidence in the northern subbasin (Ben-Gai 2009). It is unclear whether the graben is delimited in the south by another transverse fault (Reznikov et al. 2004), or whether it extends southward into the Kinarot Valley (Ginzburg and Ben-Avraham 1986; Ben-Avraham et al. 1996; Ben-Gai 2009). The pull-apart graben probably formed as a result of the transform movement along the main strike–slip faults (Freund et al. 1968; Freund 1978; Ginzburg and Ben-Avraham 1986; Hurwitz et al. 2002).

The regional tectonic background in the area can be deciphered (Fig. 2.6a) from features in the vicinity of the Lake Kinneret basin. North to Lake Kinneret, the Korazim Heights is an uplifted block. It may have formed as the block was rotated 11° counterclockwise due to a compressional component that interacted with the geometric relations between the N–S-trending Dead Sea fault and the 20° striking Almagor fault (Heimann and Ron 1993). Therefore, the Korazim Heights is thought to be either a push-up structure (Rotstein and Bartov 1989) or a result of the shortening caused by the compression across the Almagor fault and the uplift of Korazim Heights, which resulted from a block rotation on the inclined Jordan fault (Ben-Avraham et al. 1996). However, the active segment of the Dead Sea fault in this area seems to be along the Jordan fault, rather than the Almagor fault (Marco et al. 2005).

Northeast of Lake Kinneret, the basin continues into the NE–SW Yehudiyya transtensional zone. In its southwestern part, the Beteha Valley is an area of both strike–slip motion along the Jordan fault (Marco et al. 2005) and dip–slip motion towards the deep depression in the northern subbasin of Lake Kinneret (Shulman et al. 2004). The highly faulted Yehudiyya extension zone was formed by the activity of the NE-branching Sheikh-Ali and Meshushim faults from the Dead Sea fault (Fig. 2.6a). This structure probably existed at the time of the Upper Pliocene to Pleistocene basalt eruptions and controlled their flow direction (Shulman et al. 2004).

Paleoseismic studies and archeological sites provide evidence for active tectonics all around Lake Kinneret (Marco 2008; Marco et al. 2005). An active NW–SE fault bisecting the city of Tiberias (Fig. 2.2) was proposed by Marco et al. (2003). Landslides were documented along fault lineaments both east and west of the lake (Katz et al. 2009; Yagoda-Biran et al. 2010).

South of Lake Kinneret, within the Kinarot Valley, the Tzemach−1 (4,249 m) well (Fig. 2.6a), which penetrated a Miocene-to-Late Pleistocene sequence, provides direct evidence for the subsurface composition of the area: limestones, marls, conglomerates, salt, and igneous rocks (Marcus and Slager 1985). These strata filled the Kinarot Valley more than 4 km as it accumulated at rates exceeding 1.5 mm year^{-1} both during the Late Miocene (Horowitz 1987) and between 2.2 and 2 Ma ago (Horowitz 1989; Braun et al. 1991), but at much lower rates ever since (Horowitz 1987, 1989). The subsidence rate since the Pliocene is thought to be 0.12–0.24 mm year^{-1} (Shaliv 1991; Mor 1993). The Kinarot Valley is a possible extension of the southern subbasin (Ben-Avraham et al. 1996; Ginzburg and Ben-Avraham 1986). The NE–SW-trending Tzemach anticline is an uplifted structure in the eastern part of the Kinarot Valley. Rotstein et al. (1992) suggested the presence of a reverse fault that accommodated the Tzemach anticline and acted until the Late Quaternary. According to Ben-Gai (2009), the Tzemach structure is actually a diapir consisting of thick evaporitic section deposited during the Late Miocene and Early Pliocene, when it might have been located in the deepest part of the Kinneret-Beit Shean basin. Upwelling of the Tzemach structure intensifies the dipping of sediments in the southern subbasin as a result of the subsidence in the northern subbasin (Ben-Gai 2009).

2.5 Seismicity

The complex structure of Lake Kinneret basin consists of numerous fault segments in different orientations. The geometry and nature of these faults have not been mapped and deciphered completely. Since the Lake Kinneret basin is part of the seismically active Dead Sea fault, these fault segments generate low-intensity seismicity. The destructive damage that the area has suffered is evident in the local geology and morphology as well as in historical writings and archeological ruins (e.g., Segal et al. 2002; Marco 2008; Wechsler et al. 2009). However, the evident damage was caused by rare strong earthquakes of magnitude greater than $M_S = 7$ (Ambraseys and Barazangi 1989; Ambraseys and Jackson 1998; Ellenblum et al. 1998; Marco et al. 2003, 2005), whose epicenters originated far from the Lake Kinneret basin. Instrumental recording since 1900 shows that the greatest earthquake located within the Lake Kinneret basin was not more than $M_L = 4.5$ (Israeli earthquake catalog from the Geophysical Institute of Israel, GII).

Since Lake Kinneret basin occupies a relatively small area, seismological studies do not refer to it as an independent seismogenic zone but only as part of a greater zone such as the Jordan Valley or the Hula Valley. Previous investigations of the seismicity along segments of the Dead Sea fault reveal that the microearthquakes in the Lake Kinneret basin have a tendency to cluster in space (van Eck and Hofstetter 1990). Focal plane solutions, which were calculated for a number of events within the Lake Kinneret basin, show that the mechanism of the microseismic activity in Lake Kinneret basin is in agreement with the orientation of the transform movement

(van Eck and Hofstetter 1990), but could also have different orientations, which do not always agree with related faults on land (Hofstetter et al. 2007). The calculated *b-value* of the northern segment of the Dead Sea fault fluctuates between 0.8 and 0.86 (Ben-Menahem 1981, 1991; Shapira and Feldman 1987), which is lower than the *b-value* of 0.96 which was calculated for the total Dead Sea fault (Shapira 2002, Appendix C). An interesting observation was made by Kafri and Shapira (1990), who suggested that the recorded seismic activity in the Kinneret region might be related to the water level of the lake and rainfalls. A correlation between the occurrences of felt earthquakes and both the beginning of the rainy season and the annual minimum water level was found. This correlation was explained as a process in which frictional strength along the boundary faults of the Dead Sea fault is reduced by upward flows, triggering an earthquake that would have occurred later due to the tectonic stress.

2.5.1 Microseismic Catalog

In order to characterize the local microseismic events which are generated in the Lake Kinneret basin area, a highly sensitive Seismic Navigation System (SNS) was deployed in the basin area (Navon 2011). During 2010, a cluster of four portable mini-arrays installed in Korazim, Almagor, Ma'ale Gamla, and Ramot (Fig. 2.7) recorded data in a continuous mode at sampling rate of 250 Hz. Within 9 months, the deployment of the SNS has enabled the detection of 121 earthquakes with a magnitude threshold of $M_L = -1.2$. The high sampling rate has enabled to record full signal spectra and to determine their corner frequencies. The results show rather high values of the displacement signals ranging between 7 and 20 Hz.

2.5.2 Implications of Microseismic Data of Different Time Scales

The new catalog, obtained by the SNS, is compared to the local catalog of earthquakes detected over 25 years by the GII (Navon 2011). Both catalogs show that most of the microseismic activity is concentrated in the northern portion of the Lake Kinneret basin (Fig. 2.7). The events in both catalogs are characterized by very low magnitudes, and most of them display shallow hypocentral depths above 12 km deep. The *b-value* that was calculated for the GII catalog was $b = 0.82$, which is in accordance with results achieved in previous studies. The *b-value* calculated for the SNS catalog ($b = 0.65$) is significantly lower and might indicate high stress regime or temporal changes in the stress regime. Both catalogs reveal the tendency to cluster in time and space in the northern subbasin of the Lake Kinneret basin.

Although the data are still too sparse to map the geometry of the Lake Kinneret basin faults with accuracy, the new SNS catalog supplemented by the GII catalog displays seismicity that can be associated with existing tectonic features (Fig. 2.6a). The Jordan fault is presently active, but there is still no evidence showing how its

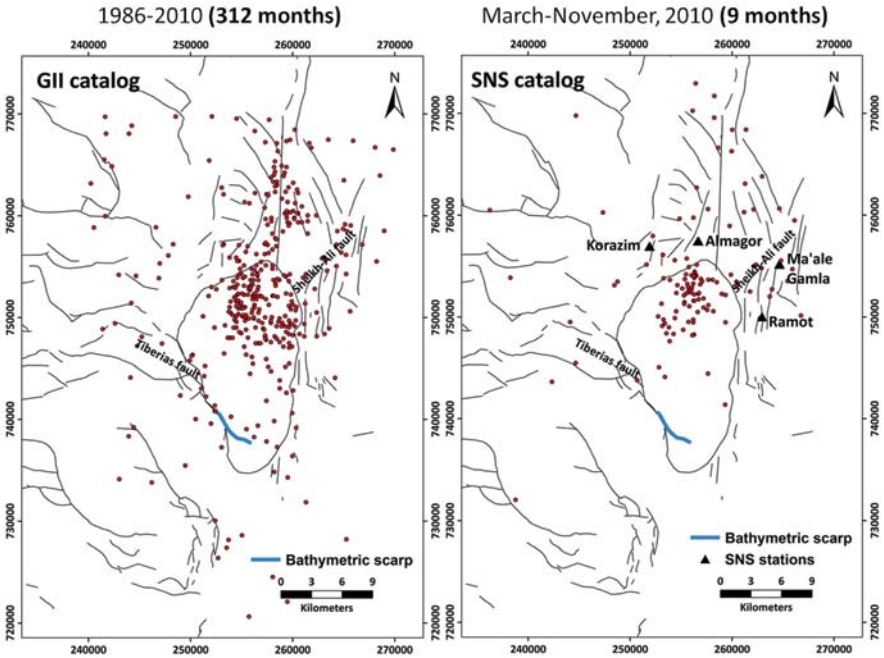

Fig. 2.7 Spatial distribution of seismic activity in the Lake Kinneret basin as observed by the Geophysical Institute of Israel, GII (*left*) and the Seismic Navigation System, SNS (*right*). The deployment of the SNS has enabled the detection of a large amount of earthquakes in a short period of time. Comparing the results of the GII catalog and the SNS catalog displays a rather similar behavior of seismic activity. (Navon 2011)

southern extent connects to the boundary faults of the Dead Sea fault within the Lake Kinneret basin. The northern subbasin is the most seismically active feature, possibly confirming the hypothesis of Ben-Avraham et al. (1996) that it is currently subsiding. The distribution of events in that subbasin also supports the claim that it is highly deformed (Reznikov et al. 2004). Several earthquake clusters, which were observed in the northern subbasin, seem to delimit its borders and indicate that the Lake Kinneret basin functions as a barrier to the movement of the Dead Sea fault in this section (Sibson 1985; van Eck and Hofstetter 1990; Ben-Avraham et al. 1996). The enhanced seismicity along the bathymetric scarp in the southern part of the lake (Fig. 2.7) supports the claim of Ben-Avraham et al. (1990) and Reznikov et al. (2004) that this could be an expression of an active fault line that may be the offshore extension of the active Tiberias fault (Fig. 2.7) The Sheikh-Ali fault (Fig. 2.7) shows moderate seismicity and the absence of seismic activity south of Lake Kinneret suggests that it may be a locked segment of the Dead Sea fault.

2.6 Conclusions

The intricate sub-bottom structure of the Lake Kinneret basin derives from a complex geological history of various tectonic processes that go back to the Neogene. The main tectonic processes are the intersection of the Dead Sea fault system with a NW–SE to W–E-trending fault system crossing the Galilee, combined with the Taurus–Zagros plate collision zone farther north (Fig. 2.1).

The Lake Kinneret basin is divided into two structural units, each associated with a different mechanism of formation. Rotational opening and transverse normal faulting are possibly responsible for the asymmetric half-graben occupying the northern subbasin. The symmetric graben occupying the southern subbasin is the deepest part of the basin, and may have been formed due to pull-apart opening caused by the transform movement along the main segments of the Dead Sea fault.

Active tectonics is taking place across the Lake Kinneret basin and is evident both in morphological features and in recent seismicity. The N–S marginal faults are associated with strike–slip motion, while transverse faults have a main vertical component causing a normal dip–slip motion. The most tectonically active zone is the northern subbasin, which is actively subsiding and forms the bathymetrically deepest part of the lake.

References

Ambraseys NN, Barazangi M (1989) The 1759 earthquake in the Bekaa Valley: implications for earthquake hazard assessment in the Eastern Mediterranean region. J Geophys Res 94(B4):4007–4013. doi:10.1029/JB094iB04p04007

Ambraseys NN, Jackson JA (1998) Faulting associated with historical and recent earthquakes in the Eastern Mediterranean region. Geophys J Int 133(2):390–406. doi:10.1046/j.1365–246X.1998.00508.x

Belitzky S, Ben-Avraham Z (2004) The morphotectonic pattern of Lake Kinneret. Isr J Earth Sci 53(3):121–130. doi:10.1560/YUXY-8DMJ-85B4-GMH7

Ben-Avraham Z, Hänel R, Villinger H (1978) Heat flow through the Dead Sea rift. Mar Geol 28(3–4):253–269. doi:10.1016/0025–3227(78)90021-X

Ben-Avraham Z, Shoham Y, Klein E, Michelson H, Serruya C (1980) Magnetic survey of Lake Kinneret-central Jordan Valley, Israel. Mar Geophys Res 4(3):257–276. doi:10.1007/bf00369102

Ben-Avraham Z, Ginzburg A, Yuval Z (1981) Seismic reflection and refraction investigations of Lake Kinneret-central Jordan Valley, Israel. Tectonophysics 80(1–4):165–181. doi:10.1016/0040–1951(81)90148–7

Ben-Avraham Z, Shaliv G, Nur A (1986) Acoustic reflectivity and shallow sedimentary structure in the Sea of Galilee—Jordan Valley. Mar Geol 70(3–4):175–189. doi:10.1016/0025–3227(86)90001–0

Ben-Avraham Z, Amit G, Golan A, Begin ZB (1990) The bathymetry of Lake Kinneret and its structural significance. Isr J Earth Sci 39(2/4):77–84

Ben-Avraham Z, ten Brink US, Bell R, Reznikov M (1996) Gravity field over the Sea of Galilee: evidence for a composite basin along a transform fault. J Geophys Res 101(B1):533–544. doi:10.1029/95JB03043

Ben-Avraham Z, Garfunkel Z, Lazar M (2008) Geology and evolution of the southern Dead Sea fault with emphasis on subsurface structure. Annu Rev Earth Planet Sci 36:357–387. doi:10.1146/annurevearth.36.031207.124201

Ben-Gai Y (2009) Subsurface geology of the southern Lake Kinneret (Sea of Galilee), Dead Sea transform—evidence from seismic reflection data. Isr J Earth Sci 58(3):163–175. doi:10.1560/ijes.58.3–4.163

Ben-Gai Y, Reznikov M (1997) Multi-channel seismic survey in the Sea of Galilee. Geophysical Institute of Israel, Holon

Ben-Menahem A (1981) Variation of slip and creep along the Levant rift over the past 4500 years. Tectonophysics 80(1–4):183–197. doi:10.1016/0040–1951(81)90149–9

Ben-Menahem A (1991) Four thousand years of seismicity along the Dead Sea rift. J Geophys Res 96(B12):20195–20216. doi:10.1029/91jb01936

Braun D, Ron H, Marco S (1991) Magnetostratigraphy of the hominid tool-bearing Erk el Ahmar formation in the northern Dead Sea rift. Isr J Earth Sci 40:191–197

Braun Y, Kagan E, Bar-Matthews M, Ayalon A, Agnon A (2009) Dating speleoseismites near the Dead Sea transform and the Carmel fault: clues to coupling of a plate boundary and its branch. Isr J Earth Sci 58(3):257–273. doi:10.1560/ijes.58.3–4.257

Ellenblum R, Marco S, Agnon A, Rockwell T, Boas A (1998) Crusader castle torn apart by earthquake at dawn, 20 May 1202. Geology 26(4):303–306. doi:10.1130/0091–7613 (1998) 026<0303:cctabe>2.3.co;2

Eppelbaum L, Ben-Avraham Z, Katz Y (2004a) Integrated analysis of magnetic, paleomagnetic and K–Ar data in a tectonic complex region: an example from the Sea of Galilee. Geophys Res Lett 31(19). doi:10.1029/2004GL021298

Eppelbaum L, Ben-Avraham Z, Katz Y, Marco S (2004b) Sea of Galilee: comprehensive analysis of magnetic anomalies. Isr J Earth Sci 53(3):151–171. doi:10.1560/NQUR-CR5M-AQQX-KX1A

Eppelbaum L, Ben-Avraham Z, Katz Y (2007) Structure of the Sea of Galilee and Kinarot Valley derived from combined geological–geophysical analysis. First Break 25:21–28

Freund R (1970) The geometry of faulting in the Galilee. Isr J Earth Sci 19(3–4):117–140

Freund R (1978) The concept of a sinistral megashear. In: Serruya C (ed) Lake Kinneret. Monographiae biologicae, vol 32. Dr W. Junk bv Publishers, The Hague, pp 27–31

Freund R, Oppenheim MJ, Schulman N (1965) Direction of magnetization of some basalts in the Jordan Valley and Lower Galilee (Israel). Isr J Earth Sci 14(2):37–44

Freund R, Zak I, Garfunkel Z (1968) Age and rate of the sinistral movement along the Dead Sea rift. Nature 220(5164):253–255

Garfunkel Z (1981) Internal structure of the Dead Sea leaky transform (rift) in relation to plate kinematics. Tectonophysics 80(1–4):81–108. doi:10.1016/0040–1951(81)90143–8

Garfunkel Z, Ben-Avraham Z (2001) Basins along the Dead Sea transform. In: Ziegler PA, Cavazza W, Robertson AHF, Crasquin-Soleau S (eds) Peri-Tethyan rift/wrench basins and passive margins, vol 186 (Peri-Tethys Memoir, vol 6). Mémoires du Muséum national d'histoire naturelle, Paris, pp 607–627

Ginzburg A, Ben-Avraham Z (1986) The structure of the Sea of Galilee graben, Israel, from magnetic measurements. Tectonophysics 126(2–4):153–164. doi:10.1016/0040–1951(86)90225–8

Guitton A, Claerbout J (2004) Interpolation of bathymetry data from the Sea of Galilee: a noise attenuation problem. Geophysics 69(2):608–616. doi:10.1190/1.1707081

Heimann A (1990) The development of the Dead Sea rift and its margins in northern Israel during the Pliocene and the Pleistocene, PhD thesis. Hebrew University, Jerusalem

Heimann A, Ron H (1993) Geometric changes of plate boundaries along part of the northern Dead Sea transform: geochronologic and paleomagnetic evidence. Tectonics 12(2):477–491. doi:10.1029/92tc01789

Heimann A, Steinitz G, Mor D, Shaliv G (1996) The cover basalt formation, its age and its regional and tectonic setting: implications from K-Ar and (40)Ar-(39)Ar geochronology. Isr J Earth Sci 45(2):55–71

Hofstetter R, Klinger Y, Amrat A-Q, Rivera L, Dorbath L (2007) Stress tensor and focal mechanisms along the Dead Sea fault and related structural elements based on seismological data. Tectonophysics 429(3–4):165–181. doi:10.1016/j.tecto.2006.03.010

Horowitz A (1987) Palynological evidence for the age and rate of sedimentation along the Dead Sea rift, and structural implications. Tectonophysics 141(1–3):107–115. doi:10.1016/0040–1951(87)90178–8

Horowitz A (1989) Palynological evidence for the quaternary rates of accumulation along the Dead Sea rift, and structural implications. Tectonophysics 164(1):63–71. doi:10.1016/0040–1951(89)90234–5

Hurwitz S, Garfunkel Z, Ben-Gai Y, Reznikov M, Rotstein Y, Gvirtzman H (2002) The tectonic framework of a complex pull-apart basin: seismic reflection observations in the Sea of Galilee, Dead Sea transform. Tectonophysics 359(3–4):289–306. doi:10.1016/S0040–1951(02)00516–4

Inbar M (1976) Contemporary and Holocene denudation rates in the Lake Kinneret watershed. In: Amiran D, Ben-Arieh Y (eds) Geography in Israel: a collection of papers offered to the 23rd International Geographical Congress, USSR, July–August, Jerusalem, 1976. Israel National Committee, International Geographical Union, pp 344–352

Kafri U, Shapira A (1990) A correlation between earthquake occurrence, rainfall and water level in Lake Kinnereth, Israel. Phys Earth Planet Inter 62(3–4):277–283. doi:10.1016/0031–9201(90)90172-t

Kashai EL, Croker PF (1987) Structural geometry and evolution of the Dead Sea–Jordan rift system as deduced from new subsurface data. Tectonophysics 141(1–3):33–60. doi:10.1016/0040–1951(87)90173–9

Katz O, Amit R, Yagoda-Biran G, Hatzor Y, Porat N, Medvedev B (2009) Quaternary earthquakes and landslides in the Sea of Galilee area, the Dead Sea transform: paleoseismic analysis and implication to the current hazard. Isr J Earth Sci 58(3):275–294. doi:10.1560/ijes.58.3–4.275

Marco S (2008) Recognition of earthquake-related damage in archaeological sites: examples from the Dead Sea fault zone. Tectonophysics 453(1–4):148–156. doi:10.1016/j.tecto.2007.04.011

Marco S, Hartal M, Hazan N, Lev L, Stein M (2003) Archaeology, history, and geology of the AD 749 earthquake, Dead Sea transform. Geology 31(8):665–668. doi:10.1130/g19516.1

Marco S, Rockwell TK, Heimann A, Frieslander U, Agnon A (2005) Late Holocene activity of the Dead Sea transform revealed in 3D palaeoseismic trenches on the Jordan Gorge segment. Earth Planet Sci Lett 234(1–2):189–205. doi:10.1016/j.epsl.2005.01.017

Marcus E, Slager J (1985) The sedimentary-magmatic sequence of the Zemah-1 well (Jordan–Dead Sea rift, Israel) and its emplacement in time and space. Isr J Earth Sci 34(1):1–10

Michelson H (1972) The hydrogeology of the southern Golan Heights. Tahal—Water Planning for Israel Ltd., Tel-Aviv

Mor D (1986) The volcanism of the Golan Heights, PhD thesis. Hebrew University, Jerusalem

Mor D (1993) A time-table for the Levant volcanic province, according to K-Ar dating in the Golan Heights, Israel. J Afr Earth Sci (and the Middle East) 16(3):223

Mor D, Steinitz G (1982) K-Ar age of the cover basalts surrounding the Sea of Galilee. Geological Survey of Israel, Jerusalem

Navon H (2011) Microseismic characterization of Lake Kinneret basin, MSc thesis. Tel Aviv University, Tel-Aviv

Picard L (1936) Conditions of underground water in the western Emek (plain of Esdraelon). Bull Geol Dep 1:1–23 (Hebrew University)

Picard L (1943) Structure and evolution of Palestine: with comparative notes on neighboring countries. Bull Geol Dep 4:1–187 (Hebrew University)

Reshef M, Ben-Avraham Z, Tibor G, Marco S (2007) The use of acoustic imaging to reveal fossil fluvial systems—a case study from the southwestern Sea of Galilee. Geomorphology 83(1–2):58–66. doi:10.1016/j.geomorph.2006.05.017

Reznikov M, Ben-Avraham Z, Garfunkel Z, Gvirtzman H, Rotstein Y (2004) Structural and stratigraphic framework of Lake Kinneret. Isr J Earth Sci 53(3):131–149. doi:10.1560/QY1W-VVRM-FLNK-C9M9

Ron H, Freund R, Garfunkel Z, Nur A (1984) Block rotation by strike–slip faulting—structural and paleomagnetic evidence. J Geophys Res 89(NB7):6256–6270. doi:10.1029/JB089iB07p06256

Ron H, Nowaczyk NR, Frank U, Schwab MJ, Naumann R, Striewski B, Agnon A (2007) Greigite detected as dominating remanence carrier in late Pleistocene sediments, Lisan formation, from Lake Kinneret (Sea of Galilee), Israel. Geophys J Int 170(1):117–131. doi:10.1111/j.1365–246X.2007.03425.x

Rotstein Y, Bartov Y (1989) Seismic reflection across a continental transform: an example from a convergent segment of the Dead Sea rift. J Geophys Res 94(B3):2902–2912. doi:10.1029/JB094iB03p02902

Rotstein Y, Bartov Y, Frieslander U (1992) Evidence for local shifting of the main fault and changes in the structural setting, Kinarot basin, Dead Sea transform. Geology 20(3):251–254. doi:10.1130/0091–7613 (1992) 020 <0251:eflsot> 2.3.co;2

Sade AR, Tibor G, Hall JK, Diamant M, Sade H, Hartman G, Amit G, Schulze B, Zohary T, Markel D (2009) High resolution multibeam bathymetry of the Sea of Galilee (Lake Kinneret). Isr J Earth Sci 58(2):121–129. doi:10.1560/IJES.58.2.121

Sadeh M, Hamiel Y, Ziv A, Bock Y, Fang P, Wdowinski S (2012) Crustal deformation along the Dead Sea transform and the Carmel fault inferred from 12 years of GPS measurements. J Geophys Res 117(B8):B08410. doi:10.1029/2012jb009241

Saltzman U (1964) The geology of Tabgha, Hukuk and Migdal area, MSc thesis. Hebrew University, Jerusalem

Schulman N (1962) The geology of the central Jordan Valley, PhD thesis. Hebrew University, Jerusalem

Segal A, Mlynarczyk J, Burdajewicz M, Schuler M (2002) Hippos (Sussita), third season of excavations. Zinman Institute of Archaeology, University of Haifa, Haifa

Serruya C (1971) Lake Kinneret: the nutrient chemistry of the sediments. Limnol Oceanogr 16(3):510–521

Serruya C (1973) Sediments. In: Berman T (ed) Lake Kinneret Data Record. Israel National Council for Research and Development, pp 13–73, 39–45

Shaliv G (1991) Stages in the tectonic and volcanic history of the Neogene basin in the lower Galilee and the valleys, PhD thesis. Hebrew University, Jerusalem

Shapira A (2002) An updated map of peak ground accelerations for the Israel Standard 413. Geophysical Institute of Israel, Lod

Shapira A, Feldman L (1987) Microseismicity of three locations along the Jordan rift. Tectonophysics 141(1–3):89–94. doi:10.1016/0040–1951(87)90176–4

Shulman H, Reshef M, Ben-Avraham Z (2004) The structure of the Golan Heights and its tectonic linkage to the Dead Sea transform and the Palmyrides folding. Isr J Earth Sci 53(3):225–237

Sibson RH (1985) Stopping of earthquake ruptures at dilational fault jogs. Nature 316(6025):248–251. doi:10.1038/316248a0

Siedner G, Horowitz A (1974) Radiometric ages of late Cainozoic basalts from northern Israel: chronostratigraphic implications. Nature 250(5461):23–26

Sneh A., Bartov Y, Rosensaft M (1998) Geological map of Israel 1:200,000, sheet 1. Geological Survey of Israel, Jerusalem

Tibor G, Sade AR (2009) Kinneret seabed mapping at high resolution. Israel Oceanographic and Limnological Research Ltd., Haifa

Tibor G, Ben-Avraham Z, Herut B, Nishri A, Zurieli A (2004) Bottom morphology and shallow structures in the northwestern part of Lake Kinneret. Israel Journal of Earth Sciences 53(3):173–186. doi:10.1560/TE15-KU60–6XV3-XK5U

van Eck T, Hofstetter A (1990) Fault geometry and spatial clustering of microearthquakes along the Dead Sea–Jordan rift fault zone. Tectonophysics 180(1):15–27. doi:10.1016/0040–1951(90)90368-i

Walley CD (1998) Some outstanding issues in the geology of Lebanon and their importance in the tectonic evolution of the Levantine region. Tectonophysics 298(1–3):37–62. doi:10.1016/s0040–1951(98)00177–2

Wechsler N, Katz O, Dray Y, Gonen I, Marco S (2009) Estimating location and size of historical earthquake by combining archaeology and geology in Umm-El-Qanatir, Dead Sea transform. Nat Hazards 50(1):27–43. doi:10.1007/s11069–008-9315–6

Weinstein Y (2012) Transform faults as lithospheric boundaries, an example from the Dead Sea transform. J Geodyn 54:21–28. doi:10.1016/j.jog.2011.09.005

Weinstein Y, Navon O, Altherr R, Stein M (2006) The role of lithospheric mantle heterogeneity in the generation of Plio-Pleistocene alkali basaltic suites from NW Harrat Ash Shaam (Israel). J Petrology 47(5):1017–1050. doi:10.1093/petrology/egl003

Yagoda-Biran G, Hatzor YH, Amit R, Katz O (2010) Constraining regional paleo peak ground acceleration from back analysis of prehistoric landslides: example from Sea of Galilee, Dead Sea transform. Tectonophysics 490(1–2):81–92. doi:10.1016/j.tecto.2010.04.029

Chapter 3
Late Quaternary Limnological History

Mordechai Stein

Abstract Lake Kinneret, occupying the tectonic depression of the Kinnarot basin, has channeled freshwater throughout the late Quaternary times to the terminal lakes in the Dead Sea basin. The history of the water-bodies in the Dead Sea basin commenced with the late Neogene transgression of the Sedom lagoon and was followed by the formation of several saline- to hypersaline lakes. The lakes comprise Ca-chloride brine that was initially formed by the Sedom lagoon. The brines migrated all over the Jordan Rift Valley and are expressed in the compositions of saline springs that are currently discharged into Lake Kinneret. The chapter presents a summary of the limnological history of the lake during the past 40 ka, as reflected in the sedimentary sequences that are exposed around the lake (e.g., Tel Bet Yerach, Tel Qazir) and recovered from trenches and drilled cores (e.g., the Ohalo-II archaeological site). The lake reached its highest stand of ~160 m below mean sea level during the last glacial maximum (~27–24 ka BP) and merged with Lake Lisan. At 24–23 ka BP, it declined below the modern level during the Heinrich (H2) event. Sr/Ca concentration and $^{87}Sr/^{86}Sr$ isotope ratios in modern lake waters and saline springs and in fossil *Melanopsis* shells and ostracods provide constraints on contributions of the fresh and saline waters to the lake during these high- and low-stand periods.

Keywords Brines · Dead Sea rift · Heinrich events · Holocene · Lake level · Lisan · Paleoclimate · Quaternary

3.1 Introduction

During the late Neogene–Quaternary times, the tectonic depressions that were developed along the Dead Sea Transform (DST) were occupied by fresh- to hypersaline water-bodies: e.g., the late Neogene Bira and Gesher water-bodies, the Sedom lagoon, and the Quaternary lakes of Amora, Samra, Lisan, Dead Sea, Hula, and Kinneret (Sea of Galilee; Fig. 3.1). The sediments that were deposited in these water-bodies comprise the "Dead Sea Group" (Zak 1967; Fig. 3.2) that stores the

M. Stein (✉)
Geological Survey of Israel, 30 Malkhe Israel St., 95501 Jerusalem, Israel
e-mail: motistein@gsi.gov.il

T. Zohary et al. (eds.), *Lake Kinneret, Ecology and Management,* Aquatic Ecology Series 6,
DOI 10.1007/978-94-017-8944-8_3,

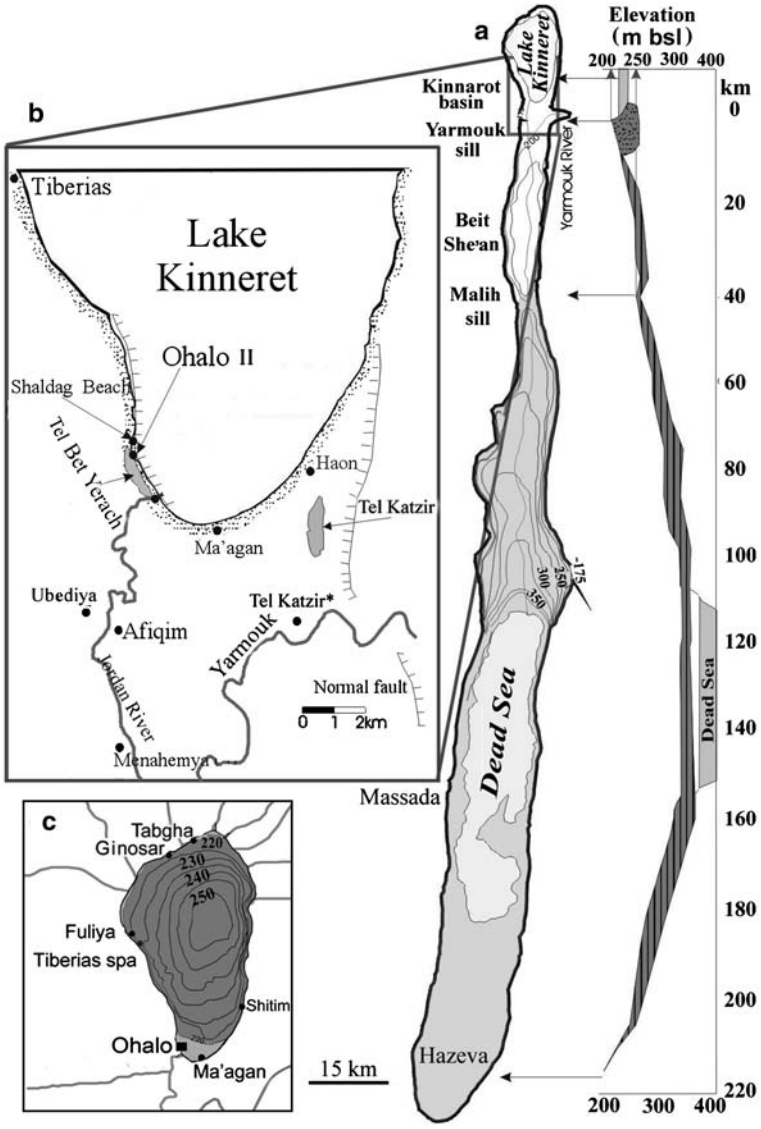

Fig. 3.1 Location map of Lake Kinneret with insets to show specific details. **a** The modern hypersaline Dead Sea and the freshwater Lake Kinneret and the maximum extent of the last glacial Lake Lisan when it reached the elevation of ~160 m b.m.s.l. and merged with Lake Kinneret. The Malih and Yarmouk sills at ~260 and 200 m b.m.s.l. are marked. A north–south section across the tectonic depressions of the Kinnarot basin, Jordan Valley, and the Dead Sea basin is shown on the *right*. **b** Details of the southern part of Lake Kinneret with locations of study sites: Tel Bet Yerach, Shaldag beach, Ohalo-II archaeological site, the Tel Qazir section, Galei Kinneret archeological site, Tiberias Ubeidiya archeological site, and the Menahemya section. The Erq El Ahmer section (site not marked) is located south to Menahemya. **c** The bathymetry of the modern Lake Kinneret and water and *Melanopsis* shells and ostracods sampling sites: Ohalo, Ma'agan, Fuliya (springs) Ginosar, and Tabgha

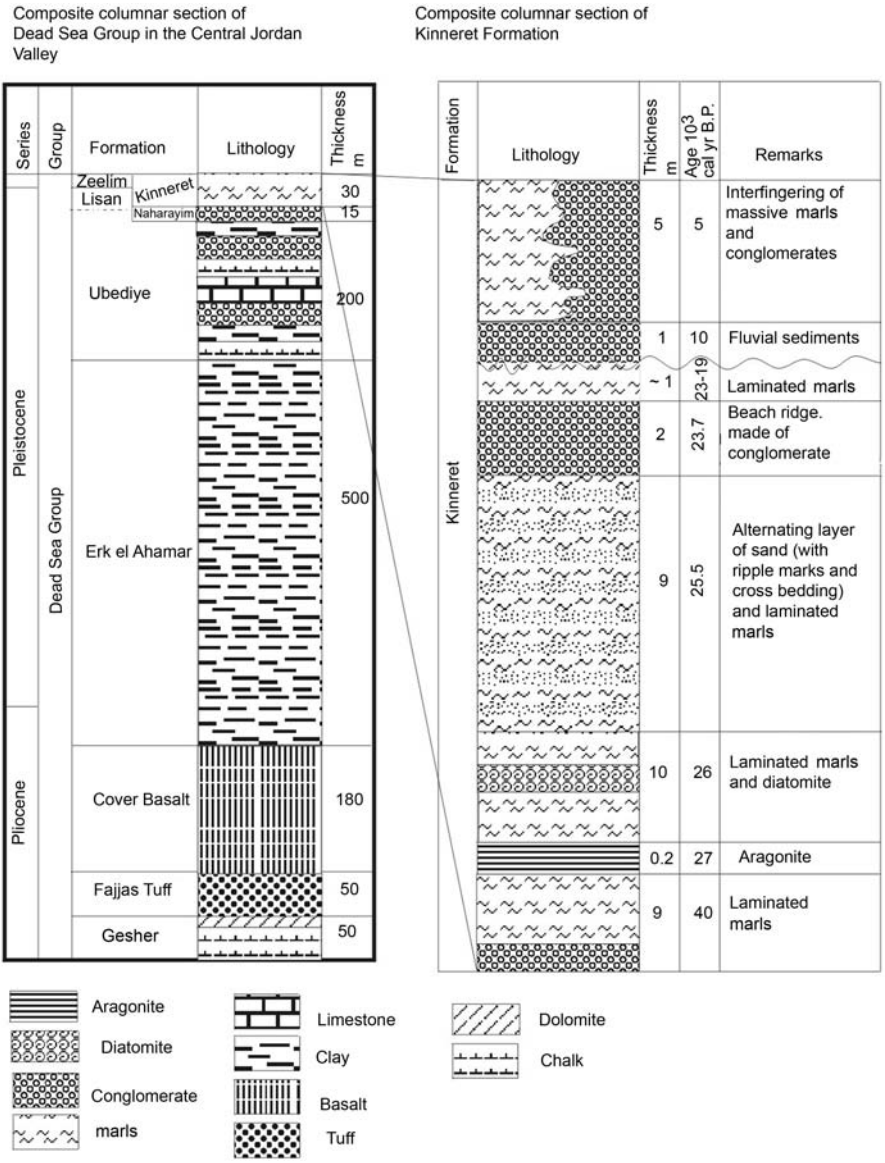

Fig. 3.2 Stratigraphy of the Neogene–Quaternary Dead Sea Group in the Kinnarot basin. The current study focuses mainly on the time interval of the past 40 ka (after Hazan et al. 2005). The main lithological units are laminated marls that contain a significant amount of primary carbonate that deposited from the lake and detrital layers composed mainly of calcite, quartz, and pebbles

environmental–hydrological history of the region (e.g., Neev and Emery 1995; Stein 2001). The water-bodies are located between the current Sahara–Arabia desert belt and the Mediterranean climate zones and their large watershed receives rains and

dust from both regions (Frumkin and Stein 2004; Haliva-Cohen et al. 2012). The waters filling the lakes comprise mixtures of Ca-chloride brine that was originally formed in the late Neogene Sedom lagoon and freshwater from the watershed. The fluxes and mixing between these solutions are dictated by the hydrological regime that in turn reflects regional and global climate. Over the past few decades, extensive efforts have been devoted to establish the geochemical–limnological history of the lakes filling the southern Dead Sea tectonic depression (from the early works of Bentor 1961; Zak 1967; Neev and Emery 1967; Starinsky 1974; Begin et al. 1974; Katz et al. 1977 to more recent works by Stein et al. 1997, 2000; Waldmann et al. 2007; Torfstein et al. 2008, 2009, 2013a, 2013b; see, also review articles in the book "New Frontiers in Dead Sea Paleoenvironmental Research" edited by Enzel et al. 2006).

Here, I focus on the geochemical–limnological history of the late Quaternary Lake Kinneret (Sea of Galilee) that occupies part of the Kinnarot tectonic basin (Fig. 3.1). Unlike the hypersaline terminal Lake Lisan and Dead Sea where water was lost through evaporation and seepage into the adjacent aquifers, Lake Kinneret was for most of its history a fresh, flow-through water-body. Nevertheless, Lake Kinneret's composition is affected by inflows of Ca-chloride brines originated during the late Neogene ingression of the Sedom lagoon (Starinsky 1974). The mechanism of discharge and contribution of the brines to Lake Kinneret has long been a scientifically controversial issue among researchers and is discussed in this chapter in context with its geological history.

3.2 From the Late Neogene Sedom Lagoon to the Modern Dead Sea

The history of the late Neogene–Quaternary water-bodies along the DST commenced with marine ingression into the tectonic depressions of the Yisre'el and Jordan Valleys (e.g., Shaliv 1991; Zak 1967). The late Neogene sedimentary sequences comprise the Bira and Gesher Formations that were deposited between ~10–4 Ma (Shaliv 1991, Heimann et al. 1996; Heimann and Braun 2000) and the Sedom Formation that was deposited in the Dead Sea basin (Zak 1967). The Bira and Gesher Formations consist of marine-lagoonar and lacustrine sequences that are interlayered with volcanic flows and pyroclastic units (Schulman 1962; Shaliv 1991). The Sedom Formation is exposed at the salt diapir of Mount Sedom and was recovered in deep boreholes (Zak 1967). A thick sequence of salts, of marine origin, which may have been deposited in the Kinnarot basin along the same time, was recovered in the Zemah borehole (Marcus and Slager 1985). Other evidence for the sedimentation from the marine lagoon is provided by salt diapirs that were detected in the central Jordan Valley (Belitzky and Mimran 1996; Gardosh and Bruner 1998; Shaliv 1991).

3.2.1 The Sedom Lagoon

The Sedom Formation comprises a sequence of salts, marls, and clastic units (Zak 1967). The extensive thickness of the halite sequences (a few thousand meters) and other geochemical observations led Zak (1967) to suggest that these evaporites precipitated in a marine lagoon, probably connected to the Mediterranean Sea. Most notable of these geochemical indicators is the molar Br/Cl ratio in the halite layers ($0.03–0.18 \times 10^{-3}$) and the $\delta^{34}S$ composition of the Ca-sulfates ($19.8 \pm 0.8‰$: Raab et al. 1997; Stein et al. 2000), which attest to a marine origin of salts, and they are consistent with the sulfur isotope composition of Neogene marine water. Yet, the age of the Sedom lagoon is not well constrained and has been a matter of a long and ongoing debate. Zak (1967) used general stratigraphic and some faunal considerations to suggest a late Pliocene–early Pleistocene age for this lagoon and also estimated that the deposition of salts in this lagoon lasted ~1 Ma. Recently, Belmaker et al. (2013) used atmospheric ^{10}Be decay to date directly the salts of the Sedom Fm. They calculated ages in the range of ~5–3 Ma, consistent with the estimate of Steinitz and Bartov (1991) that relied on general stratigraphic correlation to the Neogene formations at the Yisre'el and Jordan Valleys. Recent efforts to date the Pliocene Erk-El Ahmer Formation, which is exposed in the Jordan Valley south to Lake Kinneret (Fig. 3.1) and considered to comprise freshwater lake deposit (e.g., Braun 1992), yielded ^{10}Be burial age of ~4.3–3.6 Ma (Davis et al. 2011). These ages are comparable to the abovementioned atmospheric ^{10}Be ages of the Sedom salts. If both age estimates were correct, they would infer that during the late Neogene period, freshwater and hypersaline water-bodies coexisted in the Dead Sea–Jordan valley, similar to the present-day configuration. This may imply that the ingression and disconnection of the Sedom lagoon from the open sea was much earlier, perhaps in the mid-Pliocene time (e.g., ~7–6 Ma, Shaliv 1991) before the Messinian salinity crisis.

3.3 Late Quaternary Lakes in the Dead Sea basin

After the disconnection of the Sedom lagoon from the open sea, a series of lakes occupied the Dead Sea basin and the Jordan Valley. The available information on the geochemical and limnological evolution of the early to mid-Pleistocene Lake Amora and the last interglacial Lake Samra is summarized and discussed in Torfstein et al. (2009), Waldmann et al. (2009), respectively. Here, I shortly summarize the histories of the last glacial Lake Lisan and the Holocene Dead Sea that coexisted with Lake Kinneret.

Lake Lisan filled the Dead Sea basin and the Jordan Valley between ~70 and ~14 ka (Haase-Schramm et al. 2004; Torfstein et al. 2013a, 2013b). At its highest stand (~160 m below mean sea level, b.m.s.l.), the lake extended from the Sea of Galilee in the north to the Hazeva area in the south (Fig. 3.1). In the vicinity

of the Dead Sea basin, primary aragonite and gypsum were deposited in this lake (Katz et al. 1977; Stein et al. 1997; Torfstein et al. 2008) together with silt-sized detritus material. The silty detritus material in the lacustrine formations consists of dust grains blown from the North Sahara deserts mainly during the last glacial period (Haliva-Cohen et al. 2012). The aragonite precipitating solution comprised a mixture of freshwaters that contained bicarbonate and the Ca-chloride brine (Stein et al. 1997). Most of the freshwaters originated in the Phanerozoic carbonatic terrains comprising the northern and central parts of the Dead Sea watershed (e.g., Mt. Hermon, Galilee, and Judea Mountains). The freshwaters are primarily supplied by the Mediterranean winter rains that in turn are activated by the Cyprus cyclone (Frumkin and Stein 2004; Ziv et al. 2006; Kushnir and Stein 2010).

At ~17.4 ka BP, Lake Lisan commenced its retreat from its high stand above the marginal terraces and declined to a minimum stand, and below 450 m b.m.s.l. during the Bölling-Allerod period (~14–13 ka BP). Then, during the Younger Dryas (~12–11 ka BP), it rose again and declined at 11–10 ka BP depositing thick sequence of salts (Stein et al. 2010). During the Holocene (the lake is termed the Dead Sea), it stabilized at ~400 ± 30 m b.m.s.l. (Bookman et al. 2004; Migowski et al. 2006; Stein et al. 2010; Fig. 3.3). The lake expansion and retreat coincided with the global cooling/warming that generally imposed more wet/arid conditions in the east Mediterranean–Levant region (Stein 2001; Kushnir and Stein 2010; Torfstein et al. 2013b).

3.4 The Late Pleistocene–Holocene Limnological History of Lake Kinneret

Lake Kinneret, currently at an elevation of ~210 m b.m.s.l., is located in the northern part of the Kinnarot basin, one of the tectonic depressions that were formed along the DST (Fig. 3.1). The surrounding Golan and Galilee mountains comprise Pliocene–Pleistocene basaltic flows, Eocene limestones and chalks, and Neogene sandstones (Heimann and Braun 2000).

Freshwaters are supplied to Lake Kinneret by the Jordan River whose tributaries, the Dan, Banias, and Hazbani, discharge via Jurassic carbonate rocks of Mt. Hermon and rivers and streams draining the basaltic and carbonatic terrains of the Golan Heights and the eastern Galilee.

Saline-waters discharge to Lake Kinneret by several onshore and within-lake springs (i.e., Tabgha, Fuliya, and Tiberias Spa, with 300–18,000 mg Cl L^{-1}; Kolodny et al. 1999 and references therein). The mixing of the saline solutions with the freshwaters dictate the salinity of the lake (e.g., Gat et al. 1969; Goldschmidt et al. 1967; Starinsky 1974). At the beginning of the twentieth century, the chloride concentration was below 300 mg Cl L^{-1} and dropped to ~230 mg Cl L^{-1} after the diversion of the saline springs via the Salinity Diversion Channel (Serruya 1978; Kolodny et al. 1999).

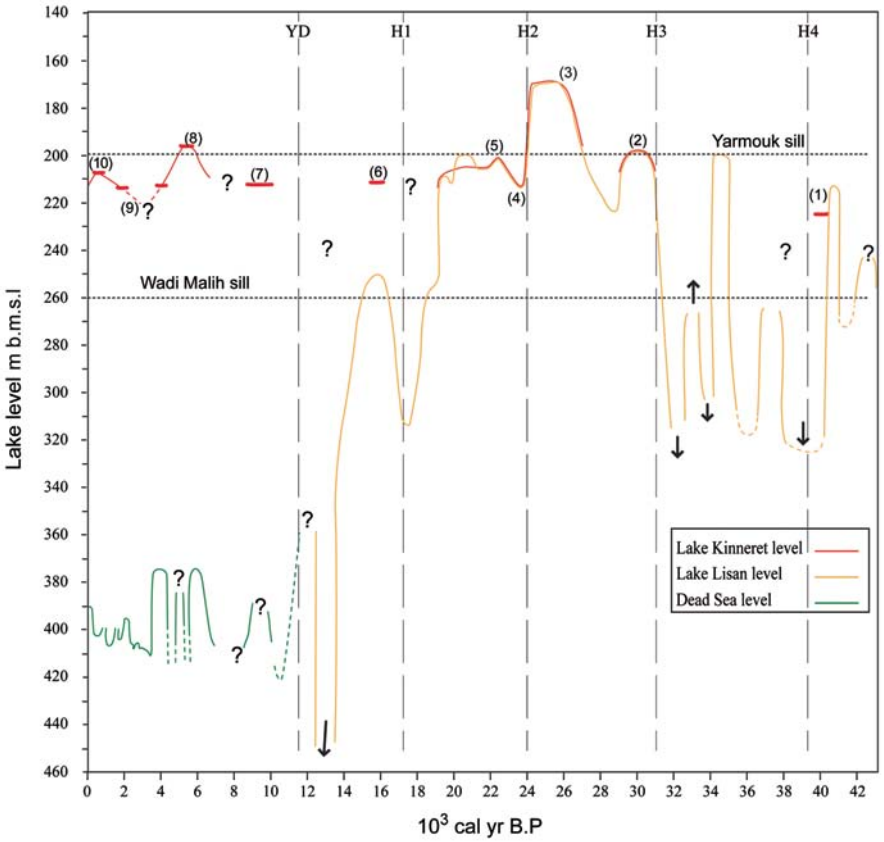

Fig. 3.3 Water level curves for Lake Lisan, Lake Kinneret, and the Dead Sea for the past 40 ka. The curves are based on the works of Bartov et al. (2002, 2003), Bookman et al. 2004, Hazan et al. 2005, Migowski et al. 2006, Stein et al. 2010, Torfstein et al. 2013b). Lake Lisan and Lake Kinneret merged at ~ 27–24 ka BP (during MIS2), and possibly at ~ 30 ka BP when Lake Kinneret water level crossed the Yarmouk sill at ~ 200 m b.m.s.l. Note the simultaneous mid-Holocene rise at both lakes Numbers relate to the sites where paleo- lake levels were determined and dated: (1,2) Kinneret drill at Ohalo-II (KIN2); (3) Tel Katzir; (4,5,6) Ohalo-II and Shaldag beach trenches; (7,8,9) Tel Bet Yerach; (10) Galie Kinneret archeological site

3.4.1 Origin of the Saline Springs

The origin and contributions of saline solutions to Lake Kinneret attracted the attention of many researchers (e.g., Stiller et al. (2009) and references therein). Goldschmidt et al. (1967), Mazor and Mero (1969), Starinsky (1974) classified the saline waters according to their chemistry and geographical locations, where solutions with high Ca/Mg ratios (e.g., Tiberias Spa) are limited to the western side of the lake and those with low Ca/Mg ratios are limited to the lake's eastern and southern side (e.g., Ha'on, Table 3.1).

Table 3.1 Chemical composition and 87Sr/86Sr isotope ratios of fresh and saline waters in the Dead Sea and Lake Kinneret hydrological system

Water source	Conc.	87Sr/86Sr	Sr	Ca	Sr/Ca eq	Mg	Na	K	Cl	SO4	HCO3	TDS	References
	g/L												
Dead Sea		0.70803	0.314	16.7	0.0086	43.8	35.6	7.41	220	0.28	0.20	324	Stein et al. 1997
En Kedem spring		0.70796	0.205	11.5	0.0081	20.8	25.9	4.02	124	0.75	0.09	187	Stein et al. 1997
En Gedi 3 well		0.70798	0.198	8.3	0.0087	12.5	24.6	3.28	90.9	1.19	0.169	140	Stein et al. 1997
Tiberias spa		0.70785	0.06	3.48	0.0079	0.68	6.81	0.35	18	0.69	0.154	30.5	Stein et al. 1997
Fuliya (5-West)		0.70787	0.0015	0.16	0.0043	0.07	0.37	0.012	0.755	0.10	0.313	1.78	Klein-BenDavid et al. 2004; Bergelson et al. 1999
Ha'on			0.0044	0.56	0.0036	0.91	3.69	0.45	8.49	0.77	0.548	15.5	Klein-BenDavid et al. 2004
Rosh Pina deep				27		2.9	33.4	1.16	105	0.7	0.171	171	Klein-BenDavid et al. 2004
	mg/L												
Lake Kinneret[a]		0.70747	0.644	38.9	0.0076	29.6	114	6.2	218	51.8	118.2	577	Stein et al. 1997
Lake Kinneret[b]			0.766	53.5	0.0066	34.8	141	7.44	284	57.4	154	733	Klein-BenDavid et al. 2004
Jordan Arik bridge		0.70669	0.1	43.8	0.0010	9.7	12.2	1.5	18.3	21.3	200	307	Stein et al. 1997
Jordan Yoseph bridge		0.70723	0.05	59.9	0.0004	7.7	6.5	0.98	9.8	25.6	201	312	Stein et al. 1997
Runoff (Darga)		0.70811	0.39	46.2	0.0034	6.5	17.4	4.6	23	54	112	292	Stein et al. 1997

[a] surface water 16/7/1995
[b] mixed lake

The saline spring solutions have salinities similar to that of seawaters; yet, they are depleted in Na (and therefore enriched in Ca + Mg) and enriched in Br relative to seawaters. Based on the isotope composition of oxygen and hydrogen, Gat et al. (1969) concluded that the solutions evolved through a stage with salinity higher than seawater and were later diluted. Several authors suggested that the saline solutions have their roots in the Sedom lagoon that funneled evaporated seawater into the late Neogene rift valley (Goldschmidt et al. 1967; Mazor and Mero 1969; Starinsky 1974). In the vicinity of the Dead Sea basin, the ingressing evaporated seawater interacted with the limestones comprising in the wall rocks of the lagoon (possibly by flowing in the regional aquifers), dolomitized the rocks, and changed their original composition to Ca-chloride brines (Starinsky 1974; Stein et al. 2000). It should be noted that evaporation of seawater alone would produce sulfate-rich brines rather than the observed Ca-chloride brines.

Starinsky (1974) examined the compositions of the modern saline solutions discharged into Lake Kinneret and compared them to the Dead Sea brine and other brines recovered from subsurface drills. The Kinneret saline solutions are diluted in comparison to the modern Dead Sea brine. Waters similar to those of the Kinneret saline springs were recovered from a depth of 2.5 km in the Rosh-Pinah-1 drill hole, located within the rift valley. Brine recovered from the depth of 3.8 km in this borehole shows similarity to the solution recovered from the deep Sedom-2 borehole in the Dead Sea basin attesting to the possible linkage between the subsurface brines at the Dead Sea basin and Lake Kinneret. Starinsky (1974) proposed that the Kinneret saline waters originated at the Sedom lagoon at the Dead Sea basin, where salt was deposited causing the Na/Cl ratio to decrease. Their late dilution with freshwater explains the additional Br contents. The Sedom brines migrated northward in the subsurface aquifers towards the Kinnarot basin. This migration could occur during the existence of the late Neogene Sedom lagoon and later after the disconnection of the lagoon from the open sea and existence of the Dead Sea lakes (e.g., lakes Amora and Lisan). This scenario of temporal migration of the brines could explain the different compositions (Na/Cl, Ca/Mg, Cl/Br) of the saline springs on the western and eastern sides of the modern Lake Kinneret. An alternate scenario invokes the existence of a large hypersaline lake that occupied the entire late Neogene rift valley and its solution infiltrated the mountain aquifers along the western (Judea–Galilee) margins of the rift. Currently, the ancient brines are discharging back into Lake Kinneret and the Dead Sea (e.g., Tiberias Spa and En Kedem, respectively). The evidence for the eastward migration of the ancient Ca-chloride brine can be found in waters drilled in the Yisre'el Valley.

Several mechanisms were proposed to explain the discharge of the saline springs into Lake Kinneret: location along deep faults that enable the upwelling of saline groundwater, tectonic pressure or a geothermal energy-driving mechanism (Mero and Mandel 1963; Mero and Zaltzman 1967), and the hydrological head due to the presence of freshwater aquifers in the Galilee Mountains west of LK (Goldschmidt et al. 1967). The study of the geological–geochemical archives of Lake Kinneret provides important evidence to address this issue.

3.5 The Late Pleistocene and Holocene History of Lake Kinneret

The hydrological history of Lake Kinneret is reflected in its water-level fluctuations. Modern water levels of Lake Kinneret were measured by Torrance (1901–1910) and by the Survey of Palestine (1926–1930, works for the construction of the Degania Dam). In exceptionally rainy years, the lake rose significantly above the average level. For example, in March 1929, the level reached an elevation of 208.5 m b.m.s.l., about 1 m above the normal level of the lake at that time of year. In November 1929, the lake level declined to the minimum stand of 211.7 m b.m.s.l.

The information on the late Pleistocene–Holocene limnological history of Lake Kinneret is inferred from a few exposures at the elevated hills around the lake: Tel Bet Yerach (TBY) and Tel Qazir, sediment profiles recovered from trenches and cores drilled at the Ohalo-II shore and other sites within the lake (Figs. 3.1 and 3.3). The exposures and part of the sediment cores were studied and described by Stiller et al. (1984), Marco et al. (2003), Dubowski et al. (2003), Hazan et al. (2005). The exposed sedimentary sequences were mainly deposited during the last glacial period when the lake level rose above the modern stand. Holocene sequences were mainly recovered from cores drilled in the northern part of Lake Kinneret and from TBY. The recovered sedimentary cores and trenched sequences comprise mainly layers and laminae of primary calcite that was deposited from the lake and detrital calcite, quartz, and clays that were transported to the lake by rivers, runoff, and direct deposition of settled dust. The shore sedimentary sequences, e.g., at the Tel Qazir exposure also contain coarse detritus units that were transported by the Yarmouk River. The sedimentary sequences that were recovered at the modern lake's shores (e.g., at the Ohalo-II archeological site) contain fossil fauna such as *Melanopsis* shells and ostracods that comprise archives of geochemical properties of the lake water (see further). Lev et al. (2007) investigated the potential of using *Melanopsis* shells as radiocarbon chronometers. They applied the radiocarbon contents in living *Melanopsis* and modern water to quantify the radiocarbon reservoir age correction, which is about 800 years. Fossil *Melanopsis* shells of independently known ages (e.g., archeological dates) yielded similar reservoir age. Hazan et al. (2005), Lev et al. (2014) applied Sr/Ca ratios and $^{87}Sr/^{86}Sr$ isotope ratios in *Melanopsis* shells and in ostracods from the last glacial (Lisan time) to trace the water sources and degree of mixing between freshwater and Ca-chloride brines in the lake (see further).

3.5.1 Times of Convergence and Abrupt Drops in Kinneret and Lisan lakes

The freshwater Lake Kinneret and the hypersaline Lake Lisan and the Dead Sea comprise a "chained-lakes system" that are connected by the Jordan River and respond to the regional climatic–hydrological conditions in the watershed. Over the past two decades, extensive efforts were devoted to the reconstruction of lake level

curves for Lake Lisan, the Dead Sea, and Lake Kinneret considering the potential of using these curves as gauges of rains in the watershed (e.g., Neev and Emery 1995, Bartov et al. 2002, 2003; Bookman et al. 2004; Hazan et al. 2005; Migowski et al. 2006. Stein et al. 2010; Torfstein et al. 2013a, 2013b). Enzel et al. (2003) showed that instrumental annual records of rains in the modern Dead Sea watershed indicate rapid response of levels to higher/lower annual precipitation. The last significant manifestation of this behavior was recorded in the extremely rainy winter of 1991/1992, when ca. 800×10^6 m^3 of Lake Kinneret water were released through the southern Jordan River, thus raising the Dead Sea level by 2 m. An interesting related question concerns the long-term behavior of water levels of freshwater Lake Kinneret as compared to the hypersaline Lake Lisan and Dead Sea because the magnitude of evaporation depends on salinity. The level curves for Lake Lisan and Lake Kinneret (Fig. 3.3) were constructed independently, thus allowing an evaluation of their short and long-term behavior, e.g., during different climate periods and in times of abrupt climate changes such as severe regional aridities. The resolution of the Lake Lisan–Dead Sea level curve is much higher than that of Lake Kinneret, reflecting the available shoreline data and the works that were devoted to the lakes. The curves presented in Fig. 3.3 are updated to the most recent reconstruction of Torfstein et al. (2013b).

The lake level diagram indicates the following:

1. Lake Lisan and Lake Kinneret converged between ~27 and 24 ka when their levels reached the maximum elevation of ~160 m b.m.s.l. At this stand, the lakes could rise above the sills formed by the fan deltas of Wadi Malih and Yarmouk Rivers (Fig. 1). It should be emphasized, however, that despite the convergence of lakes during this high-stand period Lake Kinneret was a freshwater lake that precipitated primary calcite while Lake Lisan precipitated primary aragonite.
2. At ~30 ka BP, both lakes approached the elevation of the Yarmouk sill and possibly converged.
3. Both lakes declined simultaneously to low stands during times that coincided with the Heinrich events at the northern Atlantic: at ~40 ka BP, coinciding Heinrich event 4 (H4), Lake Kinneret declined to ~222 m b.m.s.l. significantly below the Yarmouk sill. Lake Lisan declined at that time to ~330 m b.m.s.l. significantly below the Malih sill. At ~24 ka BP, coinciding with Heinrich event H2, both lakes declined below the Yarmouk sill: Lake Kinneret declined to ~214 m b.m.s.l. at the elevation of the Ohalo-II shore where the archeological site was excavated (see further).
4. At ~6 ka BP Lake Kinneret rose above the Yarmouk sill covering TBY. This lake rise coincided with the mid-Holocene rise of the Holocene Dead Sea.

It appears that when data are available and allow direct comparison between the two lakes, their levels display similar behavior—they rose and declined simultaneously, indicating the modulation of hydrological conditions by the same regional and global climatic systems. Nevertheless, independent changes in the limnological behavior of the lakes could occur reflecting the different evaporation properties and the supply of freshwater from the regional drainage. For example, southern Negev

Fig. 3.4 Study sites. **a** Trenching at the Ohalo shore, where the archaeological site Ohalo-II was excavated. Trenching recovered the late glacial section ~24–20 ka BP (Hazan et al. 2005, Lev et al. (2014)). The section comprises laminated and massive marls and silts that were deposited at the shallow lake after its drop from the last glacial (MIS2) highest stand of ~160 m b.m.s.l. Recently, we studied the lithology of the trenched section and analyzed chemical and isotope compositions (e.g.,$\delta^{18}O$, $^{87}Sr/^{86}Sr$, Sr/Ca, Mg/Ca) of ostracods that were recovered from the section (Lev et al. (2014)). **b, c** Tel Bet Yerach, the archeological section overlying the geological section; the sediments comprising the section are laminated calcitic marls that were deposited in the high-stand Lake Kinneret (Hazan et al. 2005)

storms could cause major floods via the Arava–Zin River's drainage into the Dead Sea (e.g., Waldmann et al. 2010; Haliva-Cohen et al. 2012). The floods brought waters and mostly sediments to the southern lakes with no clear documented response in Lake Kinneret.

3.5.2 Geological Studies in Sites Around Lake Kinneret

3.5.2.1 The Ohalo-II Archeological Site and the Menahemya Section

The Ohalo-II shore (Figs. 3.1 and 3.4) located on the southwestern side of Lake Kinneret beneath TBY was exposed during the low lake stand of the late 1990s. Archaeological excavations (termed Ohalo-II archeological site, see location in

Fig. 3.1) conducted by D. Nadel from the Haifa University (Nadel 1995; Nadel et al. 2001; Belitzky and Nadel 2002; Nadel et al. 2004) exposed a well-preserved prehistoric camp covering ~2,000 m^2 at an elevation of 211.5–213.5 m b.m.s.l. Radiocarbon dating of terrestrial organic debris from the camp yielded an age of 19.4 ± 0.8 ka BP (Nadel et al. 2004) that is calibrated to ~21.3 ± 0.8 ka cal BP.

The settlement at the Ohalo shore was possible because of the lake retreated during H2 ~24–23 ka BP, when prehistorical people moved down from their glacial retreats in the Galilee caves.

Geological trenching and drilling that were performed in 1999–2001 at the Ohalo-II shore opened the opportunity to investigate the environmental and hydrological history of Lake Kinneret during the last glacial high stand (~27–24 ka BP) and the time of lake retreat (~24–21 ka BP). The sediments and fossil shells recovered from them were used to infer the types of waters that contributed to the lake during these time intervals (Hazan et al. 2005; Lev et al. (2014). The sedimentary interval of the last glacial lake (~27–24 ka BP) is beautifully laminated indicating a layered and rather stable lake configuration with no activity of boring organisms at the bottom. The laminae mainly comprise primary calcites that were deposited from a relatively freshwater lake. It is important to note that Menahemya, south to the Yarmouk sill, is the northernmost site where aragonitic laminae of similar age (~27 ka BP) to the high-stand section are exposed (see the Menahemya section in Hazan et al. 2005). Thus, it appears that the Ca-chloride brine, which controlled aragonite deposition in the hypersaline Lake Lisan, did not cross the Yarmouk sill during the high-stand period. Lake Kinneret behaved like a large estuary pushing freshwater to the south. The high-stand aragonite sequence at the Menahemya section is topped by black sands with ripple marks indicating a significant lake drop that possibly coincides with the ~24 ka H2 lake drop documented at the Ohalo-II shore. Above the sands, "Kinneret–type" calcitic marls that resemble the sediments described at the Ohalo-II trench (at ages of ~23–21 ka BP) are exposed at Menahemya indicating a moderate lake rise. The lack of aragonite at Menahemya indicates that at this stage, the "Lisan–Dead Sea brine" did not cross the Wadi Malih sill.

Further information on the freshwater brines contribution to Lake Kinneret during the high stand and H2 periods is provided by the $^{87}Sr/^{86}Sr$ and Sr/Ca in fossil *Melanopsis* shells and ostracods from the Ohalo-II sediments and discussed further.

3.5.2.2 Tel Bet Yerach: Sedimentary and Archeological Archive of the Late Pleistocene and Mid-Holocene Lake Kinneret

TBY, one of the important prehistoric sites in the Levant (Bar-Adon 1966; Vinogradov 1992, and references therein; Figs. 3.1 and 3.4), is located on top of the late Pleistocene sedimentary section of Lake Kinneret. The upper part of the Tel comprises archeological layers that are overlain by lacustrine sediments of a mid-Holocene age.

The sedimentary section of the late Pleistocene Lake Kinneret is exposed on the eastern side of TBY. The section comprises alternating sequences of laminated marls and sandy units with ripple marks and cross bedding (Hazan et al.

2004, 2005). A pebble unit that possibly represents beach sediments is exposed at 203.3–204.9 m b.m.s.l. The unit was dated by radiocarbon (on *Melanopsis* shells) to ~19.8–22.3 cal year BP; similar ages were recovered from the Ohalo-II archaeological site that are located at a lower elevation (~213 m b.m.s.l.). This stratigraphic configuration would imply a fast lake rise or vertical displacement of some 7–8 m between the Ohalo II site and TBY over the past 20,000 years.

TBY was inhabited from the early Bronze (EB) Age (5,300–4,300 years ago). Then, it was conquered and destroyed by the EB IV people, who resettled it until 4,200 years ago, and then abandoned it. By that time, most of the rural settlements of the Middle East including TBY were deserted. Migowski et al. (2006) documented a significant drop in Dead Sea level at that time suggesting a regional aridity that could affect the fate of the settlements including TBY. Subsequently, TBY was not resettled until the Hellenistic time, about 2,600 years BP, and later during the Arabic Period (1360–900 years BP). The settlement history of TBY was to a large extent dictated by the climatic lake level changes.

TBY is bounded to the east by the lake and to the south and west by the modern and ancient channels of Jordan River. Flooding of the Tel by the rising lake disrupted the settlements. There are several lines of evidence for rising lake levels that flooded TBY. At the lower part of the Tel at an elevation of −206.5 m, a coarse-sand layer contains numerous *Melanopsis* shells. The shells were dated to ~6000 cal year BP. A drainage channel system of post-EB IV age entrenched across the upper surface of the EB settlement (Bar-Adon 1966). The channels were filled with poorly sorted, cross-bedded sand and small pebbles, lenses, mixed with pottery shreds of EB age, as well as scattered shells of freshwater *Melanopsis* and *Unio* shells that fossils yielded radiocarbon age of ~5.5 ka BP. This flooding of TBY coincides with the mid-Holocene transgression that was documented at the Dead Sea commencing at ~6.5 ka cal BP (Migowski et al. 2006; Bartov et al. 2007).

3.5.2.3 The Late Holocene Lake—The Galei Kinneret Archaeological Site

The Galei Kinneret archeological site at the southern shore of the city of Tiberias (Fig. 3.1) located at 208–212 m b.m.s.l. was excavated in 2002 (by M. Hartal from the Israel Antiquity Authority). The excavation revealed Roman, Byzantine, and early Arabic buildings that were completely buried by alluvium and lake sediments up to an elevation of −208.5 m. The excavation revealed a fault that was attributed to the 749 CE earthquake that hit the Dead Sea–Kinneret basin (Marco et al. 2003). Other Roman and Byzantine maritime installations—jetties and small piers—are known from around the lake at elevations of ~212 m b.m.s.l. The finding of lake sediments, including beach deposits up to 208 m b.m.s.l. in Galei Kinneret, above the Roman to Umayyad structures, is surprising. This may indicate a more complicated structure of the regional hydrological climate regime during the Arabic period that is not revealed by the Dead Sea record, or that local tectonic subsidence (of ~4 m) occurred before the 749 CE earthquake.

3.6 Sr/Ca Ratios and $^{87}Sr/^{86}Sr$ Isotope Ratios Constraints on Sources of Lake Kinneret Waters

Modern Lake Kinneret waters comprise a mixture between freshwater draining the watershed (e.g., north Jordan River water, streams and runoff from the Golan Heights and the Galilee) and saline waters (e.g., Tiberias Spa, Fuliya, Tabgha, Barbutim). Comprehensive discussions of the hydrological–limnological–geochemical conditions in the modern Lake Kinneret and the behavior of the carbonate system are given by Kolodny et al. (1999) and Katz and Nishri (2013). During the high-stand period of the last glacial (~27–24 ka BP), when Lake Lisan converged with Lake Kinneret, the Dead Sea Ca-Chloride brine could migrate northward and mix with Lake Kinneret waters. Yet, as noted above, the section recovered from the Ohalo-II cores revealed laminae of primary calcite indicating that the contribution of the Ca-chloride brine was rather limited. The contribution of brines to Lake Kinneret during the modern, high-, and low-stand periods can be evaluated by using various geochemical properties (e.g., Bergleson et al. (1999). Here, I apply the isotope ratios of $^{87}Sr/^{86}Sr$ combined with the elemental ratios of Sr/Ca in *Melanopsis* shells and ostracods that are recovered from the sedimentary sections and drilled cores to estimate the brine–freshwater relation and identify the types of waters involved (Fig. 3.5). The diagram also displays the compositions of various freshwaters, runoff, saline waters, and brines from Lake Kinneret and the Dead Sea. The Sr/Ca ratios measured in the fossil shells are transformed to Sr/Ca in their supposed habitat water by applying relevant partition coefficient (Rosenthal and Katz 1989; Hazan et al. 2005; Lev et al. (2014). The figure shows that the modern Lake Kinneret and most of the *Melanopsis* shells-habitat waters lie on a possible mixing array between saline springs such as Tiberias Spa or Dead Sea brine and the Jordan River. The *Melanopsis* shells were collected in different stratigraphic units from modern to last glacial (e.g., at the high-stand shoreline at Tel Qazir and TBY). It is interesting that even the *Melanopsis* shell from the Pliocene Erk El Ahmer Formation lies on the same array. This points to an overall long-term "stability" in the contribution of brines and freshwaters to the mixture that makes "Lake Kinneret." The exceptions are early Pleistocene Ubeidiya *Melanopsis* shells that lie off the "Jordan–Dead Sea array" and the late Pleistocene ostracod shells from the Ohalo-II shore that lie away from the "Jordan-brine array" and their habitat waters appear to be affected by the runoff water draining the Galilee Mountains (Lev et al. (2014)). Interestingly, the Fuliya water lies on the low side of the ostracod field and appears to lie on a mixing array between the Tiberias Spa and runoff waters. The contribution of the various water sources to Lake Kinneret during periods of low and high stand requires further consideration and is under current research.

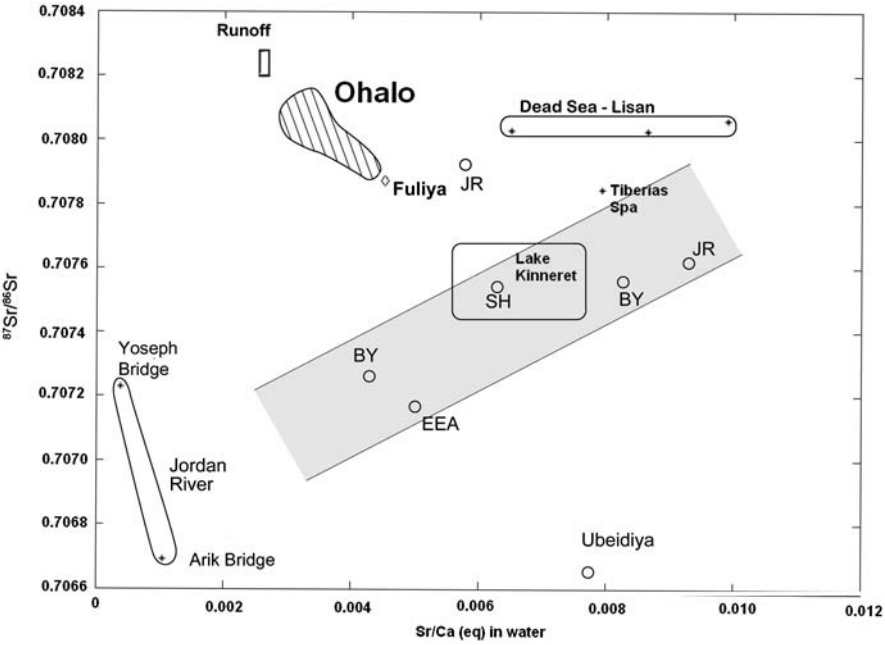

Fig. 3.5 $^{87}Sr/^{86}Sr$ versus Sr/Ca ratios in water from Lake Kinneret, the Dead Sea, Jordan River, and "late Quaternary waters" whose compositions are estimated from the $^{87}Sr/^{86}Sr$ and Sr/Ca ratios measured in *Melanopsis* shells (*open circles*). See locations in Fig. 3.1; BY = Tel Bet Yerach, SH = Shaldag shore a few hundred meters northwest to the Ohalo-II archeological site, EEA = the Pliocene Erk El Ahmer Formation and Ubeidiya of early Pleistocene age, see Fig. 3.2, the exposures are located east of Menahemya). The Dead Sea–Lisan field represents the compositions of primary aragonites deposited in these hypersaline lakes. The modern Lake Kinneret and the habitat waters of the *Melanopsis* shells lie between the compositions of the Jordan River and Tiberias spa or Dead Sea brine. The late glacial ostracods from the Ohalo-II shore show a contribution of runoff from the Galilee Mountains. (Data sources: Rosenthal and Katz 1989; Stein et al. 1997; Hazan 2002; Lev et al. (2014))

3.7 New Studies and Future Perspectives

Recently, several drilling operations were performed in Lake Kinneret opening new possibilities for paleoenvironmental and paleolimnological research. A ~ 20-m long core was drilled at the deepest part of Lake Kinneret (at station A) by a joint German–Israeli group. Preliminary dating of the core indicates that it covers the past 9,000 years. The material is currently studied for the pollen characterization, lithological composition, and geochemistry aiming to reconstruct the paleohydrological and paleoenvironmental conditions in the lake and its watershed during the Holocene (Langgut et al. 2013). A joint US–Israeli group currently works on the geochemistry of live and fossil ostracods in the shallow water environment along the shores of the lake. The ostracods are used for salinity estimation, characterization, and evaluation of the contribution of various fresh and saline water sources to the lake (e.g., by using Sr/Ca and $^{87}Sr/^{86}Sr$ ratios in waters and ostracods, Lev et al.

(2014); see Fig. 3.5). A US–Israeli group investigates the potential of applying the new method of clumped isotopes of oxygen to deduce past water temperature and composition (Zaarur et al. 2012). A Israeli group works on the short-lived U-series isotopes in the lake and the springs (Sharabi et al. 2013), following the early works in this direction (e.g., Moise et al. 2000, and references therein). Another Israeli group investigates the late Neogene transgressions that introduced the marine waters (and brines) to the Kinnarot–Dead Sea basin and are possibly responsible for the deposition of the thick salt units in the Kinnarot basin as recovered by the Zemah borehole (Rosenbaum et al. 2013). These and other studies will certainly lead to better understanding of the history and mechanism of limnological–hydrological—geochemical system of the Lake Kinneret and its parental water-bodies.

Acknowledgments This chapter is based on many studies of colleagues and students who have participated in the exploration of the environmental history of Neogene–Quaternary water-bodies that filled the tectonic depressions along the Dead Sea transform. In particular, I wish mentioning here some of Lake Kinneret researchers who guided me in the field, participated in joint projects and the drilling operations, and composed together scientific papers: David (Bibi) Neev, Jorg Negendank, Amotz Agnon, Nissim Hazan, Shmulik Marco, Thomas Litt, Marcus Schwab, Ahuva Almogi-Labin, Lilach Lev, Emi Ito, Stephen Mischke, Dani Nadel, Ami Nishri, Moshe Hartal, and Yithaki Gal. The chapter benefited from the meticulous review and illuminating conversations with Prof. Amitai Katz. Amitai devoted many years of profound study to the exploration of the geochemistry and limnology of Lake Kinneret, educated and directed students and researchers, where and what to do. The study was supported by the European Research Council under the European Community's Seventh Framework Programme (FP7/2007-2013)/ERC grant agreement 229418 and by the US–Israel Binational Science Foundation (BSF grant 2010347).

I dedicate this chapter to the memory of the late *Prof. Hagai Ron*, an outstanding scientist and a dear friend, with whom I made my first steps at the Ohalo-II shore and had wonderful years of cooperation on the history of the Dead Sea rift lacustrine formations.

References

Bar-Adon P (1966) Zinabery and Bet Yerach in light of origin and the archeological finding, Eretz-Israel vol 4. The Society of Research Israel and Antiquity

Bartov Y, Agnon A, Enzel Y, Reches Z, Stein M (2002) Sequence stratigraphy and reconstruction of Lake Lisan levels. Quat Res 57:9–21. doi:10.1006/qres.2001.2284

Bartov Y, Goldstein SL, Stein M, Enzel Y (2003) Catastrophic arid episodes in the Eastern Mediterranean linked with the North Atlantic Heinrich events. Geology 31:439–442. doi:10.1130/0091–7613(2003)

Bartov Y, Enzel Y, Porat N, Stein M (2007) Evolution of sedimentary deposition in the late Pleistocene and Holocene Dead Sea basin. J Sedim Res 77:680–692. doi:10.2110/jsr.2007.070

Begin ZB, Ehrlich A, Nathan Y (1974) Lake Lisan—the precursor of the Dead Sea. Geol Soc Surv Israel Bull 63:1–30

Belitzky S, Mimran Y (1996) Active salt diapirism at the Zaharat El-Qurei dome, lower Jordan valley (Jordan). Isr J Earth Sci 45:11–18

Belitzky S, Nadel D (2002) Late Pleistocene and recent tectonic deformations at the Oholo II prehistoric site (19K) and the evolution of the Jordan River outlet from the Sea of Galilee. Geoarcheology 17:453–464. doi:10.1002/gea.10022

Belmaker R, Lazar B, Beer J, Christl M, Tepelyakov N, Stein M (2013) ^{10}Be dating of Neogene halite. Geochim Cosmochim Acta 122: 418–429

Bentor YK (1961) Some geochemical aspects of the Dead Sea and the question of its age. Geochim Cosmochim Acta 25:239–260

Bergelson G, Nativ R, Bein A (1999) Salinization and dilution history of ground water discharging into the Sea of Galilee, the Dead Sea Transform, Israel. App Geochem 14:91–118

Bookman R, Enzel Y, Agnon A, Stein M (2004) Late Holocene levels of the Dead Sea. Bull Geol Soc Am 116:555–571. doi:10.1130/B25286.1

Braun D (1992) The geology of the Afiqim region. MSc thesis, Hebrew University, Jerusalem, p. 93 (in Hebrew, English abstract)

Davis M, Matmon A, Fink D, Ron H, Niedermann S (2011) Dating Pliocene lacustrine sediments in the central Jordan Valley, Israel—Implications for cosmogenic burial dating. Earth Planet Sci Lett 305:317–327 doi:org/10.1016/j.epsl.2011.03.003

Dubowski Y, Erez J, Stiller M (2003) Isotopic paleolimnology of Lake Kinneret. Limnol Oceanogr 48:68–78

Enzel Y, Bookman R, Sharon D, Gvirtzman H, Dayan U, Ziv B, Stein M (2003) Late Holocene climates of the Near East deduced from Dead Sea level variations and modem regional winter rainfall. Quat Res 60:263–273. doi:10.1016/j.yqres.2003.07.011

Enzel Y, Agnon A, Stein M (2006) (eds) New Frontiers in Dead Sea paleoenvironmental research. GSA Spec Paper 401

Frumkin A, Stein M (2004) The Sahara-East Mediterranean dust and climate connection revealed by strontium and uranium isotopes in a Jerusalem speleothem. Earth Planet Sci Lett 217:451–464. doi:10.1016/S0012-821X(03)00589-2

Gardosh M, Bruner I (1998) A seismic survey in the Bet Shean region. The Geophysical Institute of Israel, Rep 348/27/98, p. 13.

Gat JR, Mazor E, Tzur Y (1969) The stable isotope composition of mineral waters in the Jordan Rift Valley. Isr J Hydrol 7:334–352

Goldschmidt MJ, Arad A, Neev D (1967) The mechanism of the saline springs in the Lake Tiberias depression. Geol Surv Isr Bull 45, 19

Haase-Schramm A, Goldstein SL, Stein M (2004) U–Th dating of Lake Lisan (late Pleistocene Dead Sea) aragonite and implications for glacial east Mediterranean climate change. Geochim Cosmochim Acta 68:985–1005. doi:10.1016/j.gca.2003.07.016

Haliva-Cohen A, Stein M, Goldstein SL, Sandler A, Starinsky A (2012) Sources and transport routes of fine detritus material to the late Quaternary Dead Sea basin. Quat Sci Rev 49:55–70. doi:org/10.1016/j.quascirev.2012.06.014

Hazan N (2002) Reconstruction of Lake Kinneret levels during the past 40,000 years MSc thesis, The Hebrew University (in Hebrew, English abstract).

Hazan N, Stein M, Marco S (2004) Lake Kinneret late Holocene levels and active faulting in Tiberias. Isr J Earth Sci 53:199–205

Hazan N, Stein M, Agnon A, Marco S, Nadel D, Negendank JFW, Schwab M, Neev D (2005) The late Pleistocene-Holocene limnological history of Lake Kinneret (Sea of Galilee), Israel. Quat Res 63:60–77. doi:10.1016/j.yqres.2004.09.004

Heimann A, Braun D (2000) Quaternary stratigraphy of the Kinnarot Basin, Dead Sea Transform, northeastern Israel. Isr J Earth Sci 49:31–44

Heimann A, Steinitz G, Mor D, Shaliv G (1996) The cover basalt formation, its age and its regional and tectonic setting: implications from K-Ar and ^{40}Ar/^{39}Ar geochronology. Isr J of Earth Sci 45:55–69

Katz A, Nishri A (2013) Calcium, magnesium and strontium cycling in stratified, hardwater lakes: Lake Kinneret (Sea of Galilee), Israel. Geochim Cosmochim Acta 105:372–394. doi:org/10.1016/j.gca.2012.11.045

Katz A, Kolodny Y, Nissenbaum A (1977) The geochemical evolution of the Pleistocene Lake Lisan–Dead Sea system. Geochim Cosmochim Acta 41:1609–1626

Klein-Bendavid O, Sass E, Katz A (2004) The evolution of marine evaporitic brines in inland basins: the Jordan-Dead Sea rift valley. Geochim Cosmochim Acta 68:1763–1775

Kolodny Y, Katz A, Starinsky A, Moise T (1999) Chemical tracing of salinity sources in Lake Kinneret (Sea of Galilee), Israel. Limnol Oceanogr 44:1035–1044

Kushnir Y, Stein M (2010) North Atlantic influence on 19–20th century rainfall in the Dead Sea watershed, teleconnections with the Sahel, and implication for Holocene climate fluctuations, Quat Sci Rev 29:3843–3860. doi:10.1016/j.quascirev.2010.09.004

Langgut D, Stein M, Schiebel V, Litt T, Finkelstein I (2013) Paleoenvironmental conditions during the Bronze and Iron Ages (~5,000–2,500 YBP) in Lake Kinneret area, based on pollen analysis. Annual Meeting of the Geological Society of Israel, Akko

Lev L, Boaretto E., Heller J, Marco S, Stein M (2007) The Feasibility of using Melanopsis Shells as Radiocarbon Chronometers, Lake Kinneret, Israel. Radiocarbon 49:1003–1015

Lev L, Almogi-Labin A, Mishcke S, Ito, E, Ben-Avraham Z, Stein M (2014) Paleohydrology of Lake Kinneret during the Heinrich event H2. Palaeog Palaeoclimat Palaeoecol vol 396, pp. 183–193

Marco S, Hartal M, Hazan N, Lev L, Stein M (2003) Archaeology, history, and geology of the A.D. 749 earthquake, Dead Sea transform. Geology 31:665–668. doi:10.1130/G19516.1

Marcus E, Slager J (1985) The sedimentary-magmatic sequence of the Zemah-1 well (Jordan–Dead Sea Rift, Israel) and its emplacement in time and space. Isr J Earth Sci 34:1–10

Mazor E, Mero F (1969) Geochemical tracing of mineral and fresh water sources in the Lake Tiberias basin, Israel. J Hydrol 7:276–317

Mero F, Mandel S (1963) The hydrological mechanism of the saline springs of the western shore of Lake Kinneret (in Hebrew). TAHAL—Water Planning for Israel Ltd, p. 10

Mero F, Zaltzman U (1967) Some geohydrological observations on the saline springs of Lake Kinneret (in Hebrew). TAHAL—Water Planning for Israel Ltd, p. 10

Migowski C, Stein M, Prasad S, Negendank JFW, Agnon A (2006) Holocene climate variability and cultural evolution in the Near East from the Dead Sea sedimentary record. Quat Res 66:421–431. doi:10.1016/j.yqres.2006.06.010

Moise T, Starinsky A, Katz A, Kolodny Y (2000) Ra isotopes and Rn in brines and ground waters of the Jordan–Dead Sea Rift Valley: Enrichment, retardation, and mixing. Geochim Cosmochim Acta 64:2371–2388

Nadel D (1995) Radiocarbon dating of Ohalo II: archaeological and methodological implications. J Archaeol Sci 22:811–822

Nadel D, Belitzky S, Boaretto E, Carmi I, Heinemeier J, Werker E, Marco S (2001) New dates from submerged late Pleistocene sediments in the southern Sea of Galilee, Israel. Radiocarbon 43:1167–1178

Nadel D, Tsatskin A, Belmaker M, Boaretto E, Kislev ME, Mienis H Rabinovich R, Simchoni O, Simmons T, Weiss E, Zohar I (2004) On the shore of a fluctuating lake: environmental evidence from Ohalo II (19,500 BP). Isr J Earth Sci 53:207–223

Neev D, Emery KO (1967) The Dead Sea. Geol Surv Israel Bull 41:1–147

Neev D, Emery KO (1995) The destruction of Sodom, Gomorrah, and Jericho: geological, climatological and archaeological background. Oxford University Press, New York

Raab M, Friedman GM, Spiro B, Starinsky A, Zak I (1997) The geological history of Messinian (upper Miocene) evaporites in the central Jordan Valley (Israel) and how strontium and sulfur isotopes relate to their origin. Carbonates and Evaporites 12:296–324

Rosenbaum AG, Shaked D, Fursterberg Y, Zilberman E, Sandler A, Starinsky A (2013) Stratigraphy and lithology of Bira and Gesher formations in the Tabor Stream Area. Annual Meeting of the Geological Society of Israel, Akko

Rosenthal Y, Katz A (1989) The applicability of trace elements in freshwater shells for paleogeochemical studies. Chem Geol 78:65–76

Schulman N (1962) The Geology of the central Jordan Valley, PhD thesis. Hebrew University of Jerusalem, p. 103 (in Hebrew, English abstract)

Serruya C (1978) The chemical environment, p. 184–204. In: Serruya C (ed) Lake Kinneret. Junk, The Hague

Shaliv G (1991) Stages in the tectonic and volcanic history of the Neogene basin in the lower Galilee and the Valleys. Geological Survey of Israel Rep GSI/11/91

Sharabi G, Kolodny Y, Halicz L., Nishri A, Lazar B (2013) Redox control on the water column distribution of Ra in a stratified lake—Lake Kinneret, Israel. Goldschmidt meeting, Florence

Starinsky A (1974) Relationship between Ca-chloride brines and sedimentary rocks in Israel, PhD thesis, The Hebrew University, Jerusalem (in Hebrew, English abstract)

Stein M (2001) The history of Neogene-Quaternary water bodies in the Dead Sea Basin. J Paleolimol 26:271–282

Stein M, Starinsky A, Katz A, Goldstein SL, Machlus M, Schramm A (1997) Strontium isotopic, chemical, and sedimentological evidence for the evolution of Lake Lisan and the Dead Sea. Geochim Cosmochim Acta 61:3975–3992

Stein M, Starinsky A, Agnon A, Katz A, Raab M, Spiro B, Zak I (2000) The impact of brine-rock interaction during marine evaporite formation on the isotopic Sr record in the oceans: evidence from Mt Sedom, Israel. Geochim Cosmochim Acta 64:2039–2053

Stein M, Torfstein A, Gavrieli I, Yechieli Y (2010) Abrupt aridities and salt deposition in the post-glacial Dead Sea and their North Atlantic connection. Quat Sci Rev 29:567–575. doi:10.1016/j.quascirev.2009.10.015

Steinitz G, Bartov Y (1991) The Miocene-Pliocene history of the Dead Sea segment of the rift in light of K–Ar ages of basalts. Isr J Earth Sci 40:199–208

Stiller M, Ehrlich A, Pollinger U, Baruch U, Kaufman A (1984) The Late Holocene sediment of Lake Kinneret (Israel). Multidisciplinary study of a five-meter core. Geol Sur Isr Curr Res 4:83–88

Stiller M, Rosenbaum JM, Nishri A (2009) The origin of brines underlying Lake Kinneret. Chem Geol 262:293–309. doi:10.1016/j.chemgeo.2009.01.030

Torfstein A, Gavrieli I, Katz A, Kolodny Y, Stein M (2008) Gypsum as a monitor of the paleolimnological–hydrological conditions in Lake Lisan and the Dead Sea. Geochim Cosmochim Acta. 70:2491–2579. doi:10.1016/j.gca.2008.02.015

Torfstein A, Haase-Schramm A, Waldmann N, Kolodny Y, Stein M (2009) U-series and oxygen isotope chronology of Lake Amora, Dead Sea basin point Geochim Cosmochim Acta 73:2603–2630. doi:10.1016/j.gca.2009.02.010

Torfstein A, Goldstein SL, Kagan E, Stein M (2013a) Multi-site integrated U–Th chronology of the last glacial Lake Lisan. Geochim Cosmochim Acta 104: 210–234. doi:org/10.1016/j.gca.2012.11.003

Torfstein A, Goldstein SL, Enzel Y, Stein M (2013b) Impacts of Abrupt Climate Changes in the Levant from last glacial Dead Sea levels. Quat Sci Rev 69:1–7. doi:org/10.1016/j.quascirev.2013.02.015

Vinogradov Z (1992) “Bet Yerach” Kinneret Book. Ministry of Defense and the Kinneret Administration, p. 354

Waldmann N, Starinsky A, Stein M (2007) Primary carbonates and Ca-chloride brines as monitors of a paleo-hydrological regime in the Dead Sea basin. Quat Sci Rev 26:2219–2228. doi:10.1016/j.quascirev.2007.04.019

Waldmann N, Stein M, Ariztegui D, Starinsky A (2009) Stratigraphy, depositional environments and level reconstruction of the last interglacial Lake Samra in the Dead Sea basin. Quat Res 72:1–15. doi:10.1016/j.yqres.2009.03.005

Waldmann N, Torfstein A, Stein M (2010) Northward intrusions of low- and mid-latitude storms across the Saharo-Arabian belt during past interglacials. Geology 38:567–570. doi: 10.1130/G30654.1

Zaarur S, Stein M, Affek H (2012) Glacial-interglacial paleotemperatures and paleohydrology in the Jordan River Valley from clumped isotopes in fresh water snails. Goldschsmidt Conference, Montréal

Zak I (1967) The geology of Mount Sedom, Ph.D. thesis. Hebrew University of Jerusalem, p. 208 (in Hebrew, English abstract)

Ziv B, Dayan U, Kushnir Y, Roth C, Enzel Y (2006) Regional and global atmospheric patterns governing rainfall in the southern Levant. Int J Climat 26:55–73

Chapter 4
Lake Bathymetry and Bottom Morphology

Gideon Tibor, Ronnie Sade, John K Hall, Zvi Ben-Avraham and Ami Nishri

Abstract The bathymetry and morphology of Lake Kinneret is influenced by its complex tectonic structure and by high annual sedimentation (~100,000 t year^{-1} for the past 50 years). In general, the lake floor has an asymmetric shape with mild bathymetry at its western part and steep bathymetry at the eastern part. Based on a new multibeam bathymetric mapping conducted in 2008, the total surface area of the lake is 168.7 km^2 (at water level −209 m a.m.s.l.) with a maximum depth of 41.7 m (−253.7 m). The water storage capacity ranges from 4,325 to 3,661 × 10^6 m^3 at water levels of −209 to −214 m, respectively. A comparison of the 2008 multibeam bathymetry to echosounder bathymetry of 1986/1987 revealed dramatic changes in the lake bathymetry. The southern basin became significantly shallower; sediment accumulation over the 21 years between the two surveys may have accounted for up to 2 m rise in the lake floor at some places, estimated to represent ~10 × 10^6 t of sediment. The northern basin however does not show evidence for massive sedimentation (< 0.5 m), whereas judging by the −214 m (a.m.s.l.) contour, the littoral perimeter had been eroded significantly. The existence of bathymetric lineaments on the lake floor indicates recent and active processes in the lake. Two main lineament trends were found: a N–S trend, mainly on the eastern and southwestern borders of the lake, probably associated with active traces of the Dead Sea

G. Tibor (✉)
Israel Oceanographic & Limnological Research, P.O.B. 8030, 31080, Haifa, Israel
e-mail: tiborg@ocean.org.il

R. Sade
Dr. Moses Strauss Department of Marine Geosciences, University of Haifa, 31905, Haifa, Israel
e-mail: potolan@zahav.net.il

J. K Hall
Geological Survey of Israel, 30 Malkhe Israel St., 95501, Jerusalem, Israel
e-mail: jkh1@012.net.il

Z. Ben-Avraham
Department of Geophysical, Atmospheric and Planetary Sciences, Tel Aviv University, 69978, Tel Aviv, Israel
e-mail: zviba@post.tau.ac.il

A. Nishri
The Yigal Allon Kinneret Limnological Laboratory, Israel Oceanographic & Limnological Research, P.O. Box 447, 14950, Migdal, Israel
e-mail: nishri@ocean.org.il

T. Zohary et al. (eds.), *Lake Kinneret, Ecology and Management,* Aquatic Ecology Series 6,
DOI 10.1007/978-94-017-8944-8_4,

fault system and a NW–SE trend, which is probably the continuation of the normal faults of the eastern Galilee fault system. The major morpholineament found in the 2008 bathymetry is located in the northwestern deeper parts of the lake (−232 to −242 m) and is N–S oriented. The epicenters of the October 2013 earthquakes are found in the vicinity of this lineament.

Keywords Bathymetry · Bottom morphology · Morpholineaments · Multibeam · Gyres · Lake erosion processes · Sediment transport

4.1 Introduction

The violin shape, "Kinnor" in Hebrew, of Lake Kinneret originated from the tectonic activity along the Dead Sea fault. The narrow southern part of the lake is bordered by N–S trending faults. Its wider northern part was probably formed by the interaction of two sets of faults: the N–S-trending strands of the Dead Sea fault and the NW–SE to E–W trending faults which are part of the eastern Galilee fault system (Ben-Avraham et al. 1981, 1996).

The bathymetry of the lake was first mapped by TAHAL (Water Planning for Israel) in 1961, 1964, and 1969. The second mapping was done in 1986 and 1987 (Ben-Avraham et al. 1990) with a 100 m spacing between survey lines. The latest mapping (Fig. 4.1) was done in 2008 with a high-resolution multibeam system, SeaBeam 1180 from L-3 Elac Nautik GmbH (Sade et al. 2011). The low lake level during the multibeam survey (−212.3 to −212.9 m) enabled mapping from elevations of −214 m and deeper.

The lake is 21 km long and 12 km wide at its widest point (Fig. 4.1). It has a surface area of 168.7 km^2 at water level −209 m, with a maximum depth of 41.7 m (−253.7 m a.m.s.l.). The water storage capacity ranges from $4{,}325 \times 10^6$ to $3{,}499 \times 10^6$ m^3 at water levels of −209 to −214 m, respectively (Sade et al. 2011). The 2008 bathymetric data were used to generate new hypsographic curves, for computing lake volume and surface area versos depth (Fig. 4.2).

The bathymetry and morphology of Lake Kinneret were shaped by its complex tectonic structure, being a part of rhomb-shaped grabens or pull-apart basins along the Dead Sea Transform (Freund et al. 1970), and by high sedimentation rates. For the past 50 years, bulk sediment deposition in the lake is approximately 100,000 t year^{-1}, originating from several sources: (1) riverine allochthonous material (~35,000 t year^{-1} of which the Jordan River contributes ~25,000 t year^{-1} while other streams supply ~10,000 t year^{-1}; Mekorot Water Company database); (2) autochthonous calcite deposition (50–55,000 t year^{-1}; Koren and Klein 2000); and (3) atmospheric dust (~10,000 t year^{-1}; Nishri et al., (2005)). Sedimentation rates vary spatially and in the lake the pelagic rate is the highest, estimated at 2–7 mm year^{-1} by Serruya (1973). Other estimates within this range were made by Stiller (1974). Klein and Koren (1993), Nishri and Koren (1994), Koren and Klein (2000) suggest somewhat smaller rates. Using ^{137}Cs radioisotopes, Stiller (1974) suggested the lowest rates of deposition to be in the south of the lake (Station D in Fig. 1.1, Chap. 1).

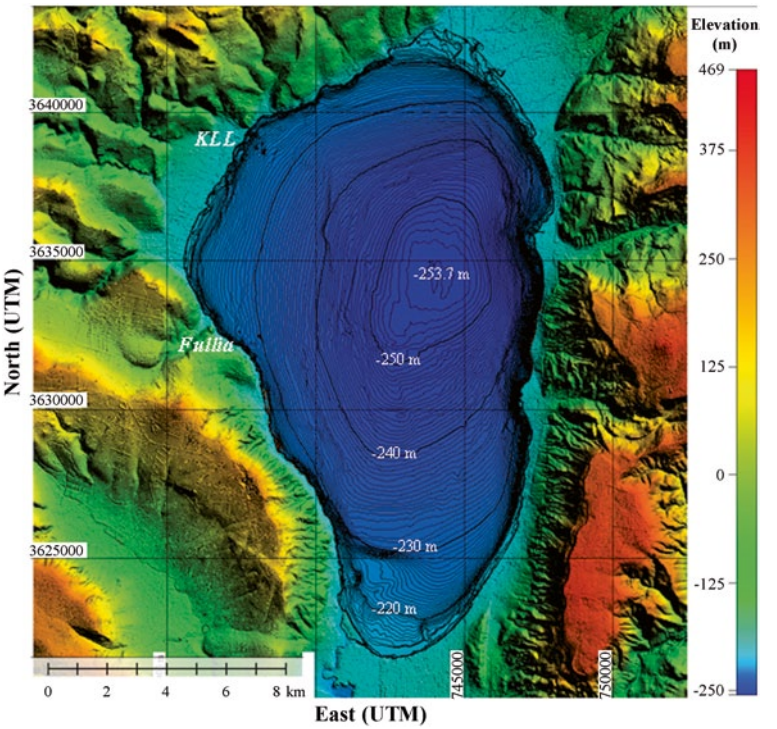

Fig. 4.1 Shaded relief image of the topography and bathymetry of Lake Kinneret. Topographic data are based on a 25 m grid from the Mapping Survey of Israel. Bathymetric data are based on the 5 m multibeam survey grid from 2008. The bathymetric contour interval is 0.5 m and the coordinates are Universal Transverse Mercator (UTM Zone 36). (KLL—Kinneret Limnological Laboratory, Israel Oceanographic & Limnological Research)

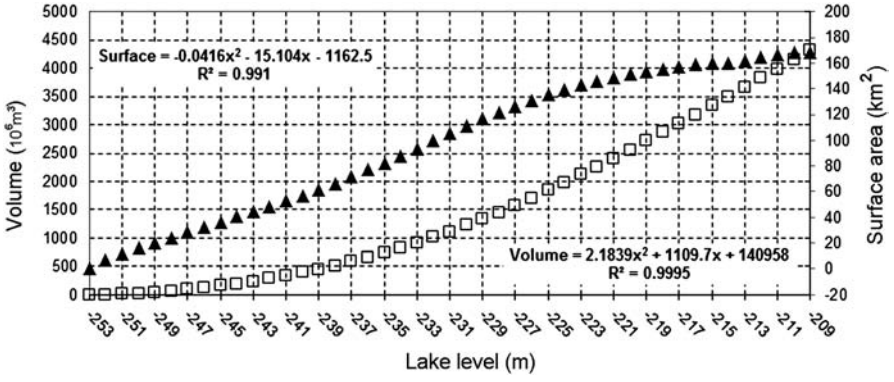

Fig. 4.2 Hypsographic curves for Lake Kinneret based on data from the multibeam bathymetric mapping of 2008. *Empty squares* represent volume and *filled triangles* represent surface area

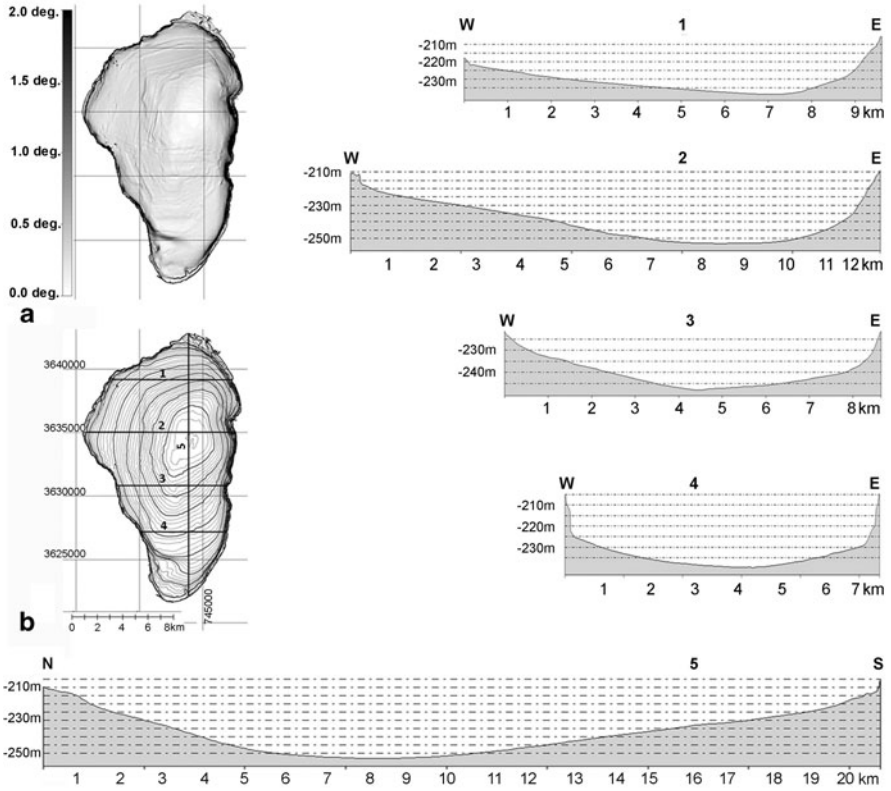

Fig. 4.3 Lake slope and bathymetry based on the 2008 multibeam mapping. **a** Slope map in degrees and **b** location map and five bathymetric transects across and along the lake

4.2 Lake Bathymetry and Bottom Morphology

In general, the lake floor is smooth with gentle slopes that vary from about 0.2° over most of the lake area and up to 2° mainly along its eastern borders (Fig. 4.3a). The lake bottom is asymmetrical. Its deepest part is located ~1.5 km northeast of Station A (Fig. 1.1, Chap. 1). This asymmetry can be seen in a series of E–W transects across the lake, where the deepest parts trend along the NW–SE direction (profiles 1–4 in Fig. 4.3b). In the N–S profile (profile 5 in Fig. 4.3b), the deepest area is in the northern part of the lake.

Like many lakes around the world, gas and fluids escape through the lake floor and produce a variety of morphological crater-like features or so-called pockmarks. Such features and particularly those related to saline submerged water inflows were already mapped in the early 1960s in the vicinity of the Tabgha and Fullia regions (Fig. 4.4a). Some of these craters are still active (e.g., Barbutim salt spring) while others like those of the Ma'agan group (Fig. 4.4b) ceased activity in the 1980s and since then are gradually filled with sediments at an estimated rate of 20 cm year^{-1} between 2003 and 2008. The high-resolution multibeam mapping

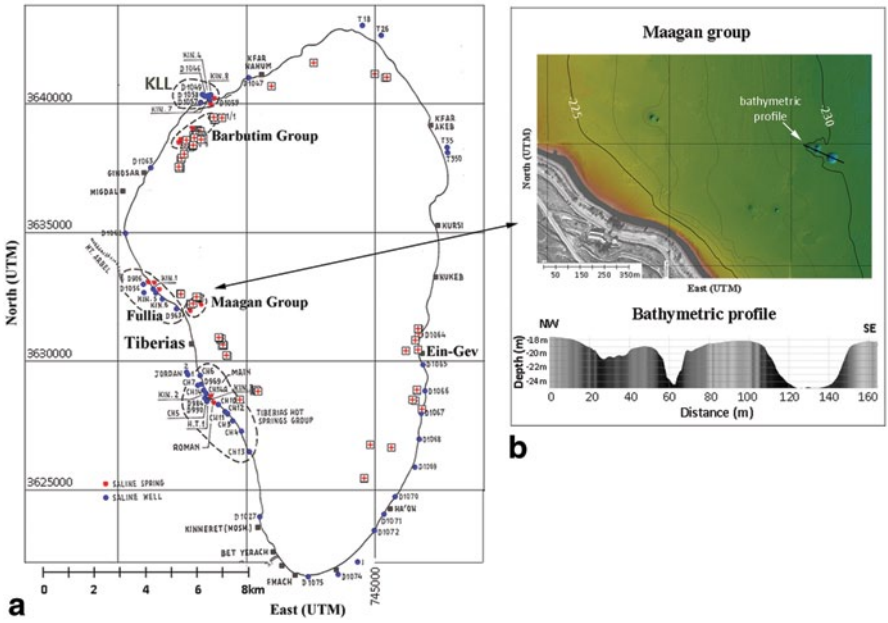

Fig. 4.4 Underwater crater-like features in Lake Kinneret. (a) Location map of saline springs (*red dots*), saline wells (*blue dots*), and settlements (*black squares*) on land and offshore that were mapped in the 1960s (modified from Simon and Mero 1992). The *red pluses* mark the crater-like features that were mapped in the multibeam survey of 2008, (b) high resolution (1×1 m^2) multibeam image of the underwater craters of the Ma'agan group in the Fullia region. The NW–SE bathymetric profile shown is across the largest crater in this group

performed in 2008 revealed the existence of 53 crater-like features (red plus symbols in Fig. 4.4a); some are deep and narrow while the majority are shallow and wide. The shape, depth, and location of these crater-like features suggest different origins. We propose three main mechanisms for their origin (Tibor et al. 2004): (1) salt and fresh underwater springs which are likely to be associated with faults and tectonically active sites (Ben-Avraham et al. 1996), e.g., in the Tabgha and Fullia regions (Fig. 4.3); (2) from gas, mainly methane, that escapes from the lake floor at high rates during low lake levels, especially in the littoral zone; and (3) from man-made or natural objects that settle on the lake floor and strong currents create scour around them.

4.3 Long-Term Changes in Lake Bathymetry

Comparison between the bathymetric map of 1986/1987 and that of 2008 relative to elevation −214 m showed distinct differences in bathymetry (Fig. 4.5), erosion in the littoral parts of the lake (yellow and red colors in Fig. 4.5), and accumulation mainly in the south (green and blue colors in Fig. 4.5). This sediment accumulation

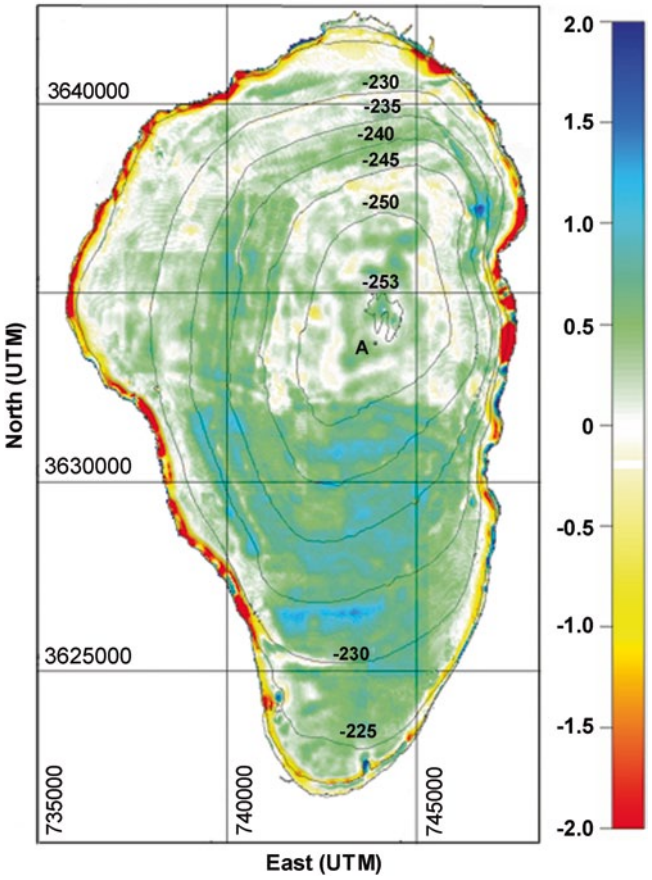

Fig. 4.5 A map showing elevation differences between the 1986/1987 survey and the 2008 survey. Color scale is in meters. *Blue* and *green colors* represent sediment deposition, *red* and *yellow colors* represent erosion. The comparison was made on a grid of 50×50 m^2 and is bounded by lake level of −214 m. The 5 m bathymetric contour intervals are from the 2008 survey. Coordinates are UTM 36

can reach up to 2 m (Tibor and Sade 2009). Accordingly, three zones are distinguished: (1) the northern part of the lake, where during that period the depth did not change significantly except for a "green" strip on the western sub-littoral; (2) the southern basin, where significant sediment accumulation was noted; and (3) the perimeter of the lake, where net erosion was recorded.

Assuming typical porosity of 65–75 % in the upper 1 m of sediments with specific density of 2.5 g cm^{-3}, the mass of sediment accumulated in the southern basin during the 21 years that elapsed between mappings is estimated at ca. 10×10^6 t. For comparison, allochthonous riverine suspended matter inflow loads entering the lake during the same time span was only 1×10^6 t, i.e., one order of magnitude smaller

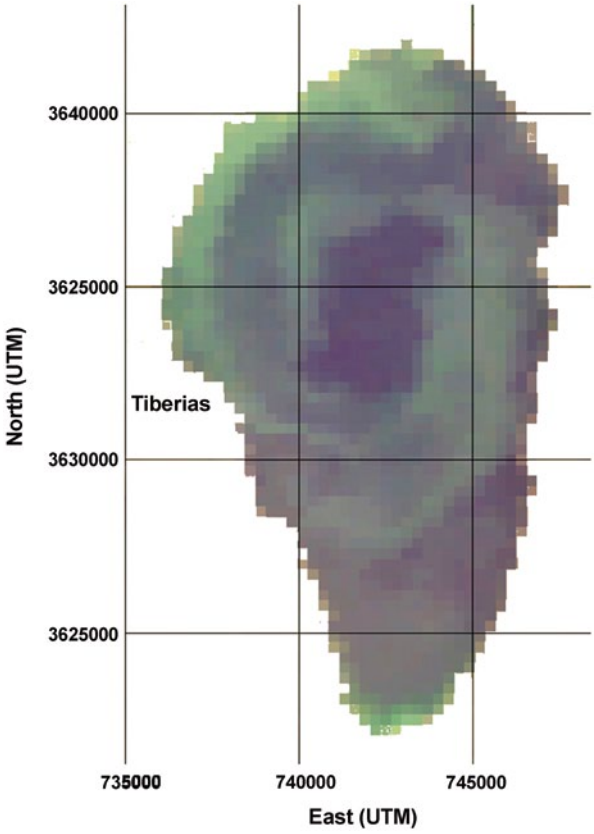

Fig. 4.6 The northern anticlockwise gyre system in the Kinneret as seen in the analysis of MERIS FR satellite image from 25 December 2009

than the net accumulation in the south. This excludes the possibility of external loadings of suspended matter being the reason for the sediment accumulation in the southern basin. Provided that the two bathymetries are comparable then some internal lake process must have been responsible for that phenomenon. Considering the differences in bathymetry shown in Fig. 4.5, this is likely to be erosion from the lake perimeter. Possibly, this erosion was associated with the relatively long periods of lower lake levels during the past two decades, when in some years the level was below −213 m (Fig. 7.5 in Chap. 7).

The question remaining is why would such erosion affect only the southern basin and not affect the northern basin? Our conjecture is that it could be related to the occurrence in Lake Kinneret of two internal gyres characterized by opposing movement directions (Serruya 1975). One is a northern gyre whose deflection is anticlockwise in accordance with the Coriolis effect, while in the southern basin the gyre is clockwise. The counterclockwise northern gyre currents impact alongshore sediment transport from the riverine northern sources, and perhaps also littoral sources within the lake (Herman 1989; Stocker and Imberger 2003). Further support for this conclusion is indicated in Fig. 4.6, which shows the Medium

Resolution Imaging Spectrometer (MERIS) full resolution (FR) satellite image of suspended material taken on 25 December 2009, where the distribution of the suspended matter seems to be controlled by a prominent gyre located in the northern basin. The counterclockwise circular pattern of particle transport with the northern gyre is evident. Littoral sediments eroded in the northern part of the lake may be therefore transported southward and only upon "meeting" with the southern gyre or with water in the southern basin be deflected inward (eastward) to the center of the southern basin. Note that the location of the Ma'agan group of craters (Fig. 4.4b), which have been almost completely filled up with sediments since the 1980s, is along the counterclockwise northern gyre of the lake (Serruya 1975).

After the onset of stratification (Fig. 1.3, Chap. 1), strong summer westerly winds induce intensive wave activity, which affects coastal erosion (Hodges et al. 2000; Gómez-Giraldo et al. 2006). We hypothesize that a drawdown in lake level leads to enhanced wave erosion because fine sediments deposited in mid-depth coastal areas during high lake levels may then become exposed to the higher energy of the waves. Summer is also the season characterized by internal seiche activity, which drives boundary mixing (Chap. 9). However, this type of erosion and transport to the lake center through focusing may be less important because it seems to affect mostly sublittoral (10–16 m depth) bed sediments (Ostrovsky and Yacobi 2010) not included in the yellow–red perimeter in Fig. 4.5.

4.4 Morpholineaments and Their Origin

The existence of bathymetric lineaments in Lake Kinneret, with its high sedimentation rates and smooth bathymetry, indicates recent and active processes in the lake. The first analysis of lineaments was done on the 1986/1987 bathymetric data (Ben-Avraham et al. 1990; Belitzky and Ben-Avraham 2004; Guitton and Claerbout 2004). They revealed systematic relief irregularities and morphological steps that form linear features of various lengths and orientations which they termed morpholineaments (black lines in Fig. 4.7). The analysis of the 2008 multibeam data shows two main lineament trends, N–S and NW–SE (thick black lines in Fig. 4.7). The N–W class are found mainly on the eastern and southwestern borders of the lake and are probably associated with active traces of the Dead Sea fault system. The NW–SE class is hypothesized to be the lake floor expression of normal faults which are extensions of the eastern Galilee fault system (Ben-Avraham et al. 1990).

The major morpholineament found in the 2008 bathymetry is located in the northwestern deeper parts of the lake (−232 to −242 m) and has a N–S trend. This lineament seems to be associated with the southern extension of the active Korazim fault line (KF in Fig. 4.7). In the southwestern part of the lake, a prominent E–W bathymetric step (~6 m) might be associated with the continuation of a NW–SE trending fault near Tiberias and accentuated by the counterclockwise currents.

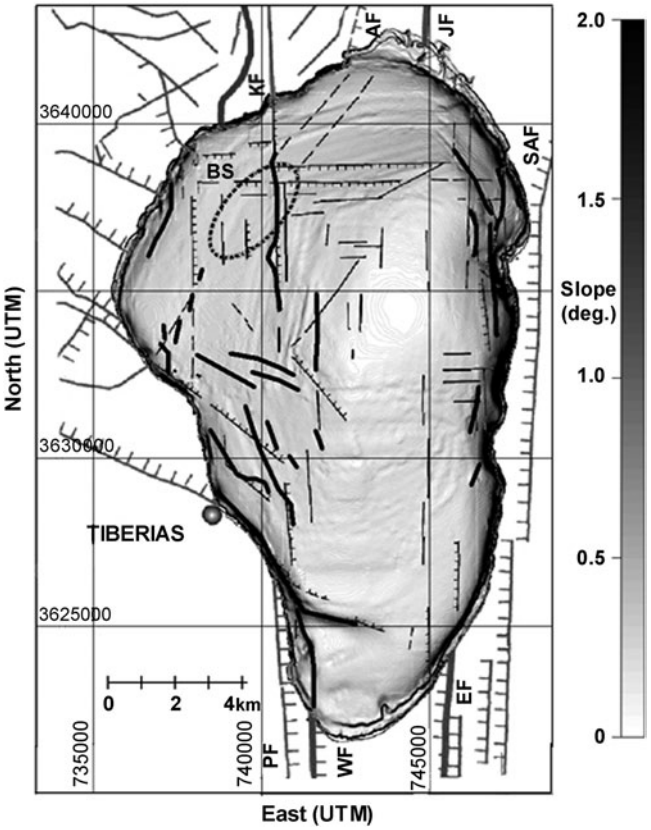

Fig. 4.7 Morpholineaments mapped from bathymetric data. *Thin black and dashed lines* are morpholineaments and faults interpreted from the 1986/1987 bathymetric survey (modified from Belitzky and Ben-Avraham 2004). *Thick black lines* are morpholineaments based on the analysis of the 2008 multibeam survey. Faults on land are from Belitzky and Ben-Avraham, 2004. *KF* Korazim fault, *AF* Almagor fault, *JF* Jordan fault, *SAF* Sheikh-Ali fault, *PF* Poriyya fault, *WF* western marginal fault, *EF* eastern marginal fault, *BS* Barbutim Springs. Note that the *dashed ellipsoid* marks the area of the earthquake epicenters that occurred during October 2013

Additional morpholineaments are found near the margins of the lake. Some of the major morpholineaments are located in areas that were described as structural boundaries on the basis of magnetic and gravity measurements (Ben-Avraham et al. 1981, 1996), and deep seismic profiles (Hurwitz et al. 2002). This may suggest that they are the surface expressions of deep-seated faults.

Acknowledgements The multibeam mapping was funded by the Israel Water Authority (project 4500241642) and a grant from the Margaret Kendrick Blodgett Foundation.

References

Belitzky S, Ben-Avraham Z (2004) The morphotectonic pattern of Lake Kinneret. Isr J Earth Sci 53:121–130

Ben-Avraham Z, Ginzburg A, Yuval Z (1981) Seismic reflection and refraction investigations of Lake Kinneret-central Jordan valley, Israel. Tectonophysics 80:165–181

Ben-Avraham Z, Amit G, Golan A, Begin ZB (1990) The bathymetry of Lake Kinneret and its structural significance. Isr J Earth Sci 39:77–84

Ben-Avraham Z, ten Brink U, Bell R, Reznikov M (1996) Gravity field over the Sea of Galilee: evidence for a composite basin along a transform fault. J Geophys Res 101:533–544

Freund R, Garfunkel Z, Zak I, Goldberg M, Weissbord T, Derin B (1970) The shear along the Dead Sea rift. Phil Trans R Soc Lond Ser A 267:107–130

Gómez-Giraldo A, Imberger J, Antenucci JP (2006) Spatial structure of the dominant basin-scale internal waves in Lake Kinneret. Limnol Oceanogr 51:229–246

Guitton A, Claerbout J (2004) Interpolation of bathymetry data from the Sea of Galilee: a noise attenuation problem. Geophysics 69:608–616

Herman G (1989) The time dependent response of Lake Kinneret to an applied wind stress and hydraulic flow: advection of suspended matter. Arch Hydrobiol 115:41–57

Hodges BR, Imberger J, Saggio A, Winters, KB (2000) Modeling basin-scale internal waves in a stratified lake. Limnol Oceanogr 45:1603–1620

Hurwitz S, Garfunkel Z, Ben-Gai Y, Reznikov M, Rotstein Y, Gvirtzman H (2002) The tectonic framework of a complex pull-apart basin: seismic reflection observations in the Sea of Galilee, Dead Sea transform. Tectonophysics 359:289–306

Klein M, Koren N (1993) The influence of the thermocline on sedimentation in the deeper part of Lake Kinneret, Israel. Limnologica 28:293–299

Koren N, Klein M (2000) Rate of sedimentation in Lake Kinneret, Israel: spatial and temporal variations. Earth Surf Proc Landf 25:895–904

Nishri A, Koren N (1994) Sediment transport in Lake Kinneret. Verh Int Verein Limnol 25:290–292

Nishri A, Koren N, Leibovichi E, Ganor E (2005) Phosphorus deposition in dust in Lake Kinneret. A final research report (in Hebrew) submitted to the Israeli Water Authority

Ostrovsky I, Yacobi YZ (2010) Sedimentation flux in a large subtropical lake: spatio-temporal variations and relation to primary productivity. Limnol Oceanogr 55:1918–1931

Sade AR, Tibor G, Hall JK, Diamant M, Sade H, Hartman G, Amit T, Schulze B, Zohary T, Markel D (2011) High resolution multibeam bathymetry of the Sea of Galilee (Lake Kinneret). Isr J Earth Sci 58:121–129

Serruya C (1973) Sediments. In: Berman T (ed) Lake Kinneret data record. Published by the Israel Council for Research and Development, pp 13–73

Serruya S (1975) Wind, water temperature and motions in Lake Kinneret: general pattern. Verh Int Verein Limnol 19:73–87

Simon E, Mero F, (1992) The salinization mechanism of Lake Kinneret. J Hydrol 138:327–343

Stiller M (1974) Evaluation of sedimentation and transport rates in Lake Kinneret. PhD thesis submitted to the Feinberg Graduate School. Weizmann Institute of Science, p 188 (in Hebrew)

Stocker R, Imberger J (2003) Energy, partitioning and horizontal dispersion in a stratified rotating lake. J Phys Oceanogr 33(3):512–529

TAHAL (1969) Bathymetric map of Lake Kinneret, scale 1:50,000, contour interval 1 m. TAHAL—Water Planning for Israel Ltd., Tel Aviv

Tibor G, Ben-Avraham Z, Herut B, Nishri A, Zurieli A (2004) Bottom morphology and shallow structure in the Northwestern part of Lake Kinneret. Israel J Earth Sci 53:173–186

Tibor G, Sade AR (2009) High resolution mapping of the Kinneret sea floor. IOLR Report H-71/2009 to the Israel Water Authority, 29 p (in Hebrew)

Chapter 5
Geomorphology

Nurit Shtober-Zisu and Moshe Inbar

Abstract The Lake Kinneret watershed covers ten major physiographic units with highly variable geology, geomorphology, soils, climate, vegetation, and land use, characterizing a "mosaic" type of landscapes. This chapter offers an introduction to the physical geography settings of the Lake Kinneret watershed, presenting the characteristics and principal geomorphic processes active in each unit. Human impact on land degradation began with the appearance of humans about 1.5 million years ago, but major effects on landscape modification occurred in historic times. Environmental hazards and natural disasters in the last decade are also discussed in this chapter.

Keywords Erosion · Geomorphology · Lithology · River · Watershed

5.1 Physiographic Units

The Lake Kinneret watershed covers ten major physiographic units with highly variable geology, geomorphology, soils, climate, vegetation, and land use, characterizing a "mosaic" type of landscapes (Fig. 5.1):

1. *Mount Hermon:* The Hermon Mountain is the southern part of the Anti-Lebanon mountain range covering 580 km^2 or 21 % of the total area of the Kinneret basin. The summit, 2,814 m a.m.s.l., is composed mainly of carbonate rocks from the Jurassic period. Karstic processes are dominant and surface features like lapies, dolines, sinkholes, and subsurface caves are common (Fig. 5.2a). Mean annual precipitation is about 1,300 mm.
2. *Jabal al Rarbi–Bir al Dahar:* This unit covers the western flank of the Hermon Mountain and the eastern part of the Jabal al Rarbi and Bir al Dahar anticlinal ranges. Elevation ranges from 770 to 1,200 m a.s.l. and steep slopes of

N. Shtober-Zisu (✉)
Department of Land of Israel Studies, University of Haifa, 31905, Haifa, Israel
e-mail: nshtober@research.haifa.ac.il

M. Inbar
Department of Geography and Environmental Studies, University of Haifa, 31905, Haifa, Israel
e-mail: inbar@geo.haifa.ac.il

T. Zohary et al. (eds.), *Lake Kinneret, Ecology and Management,* Aquatic Ecology Series 6,
DOI 10.1007/978-94-017-8944-8_5,

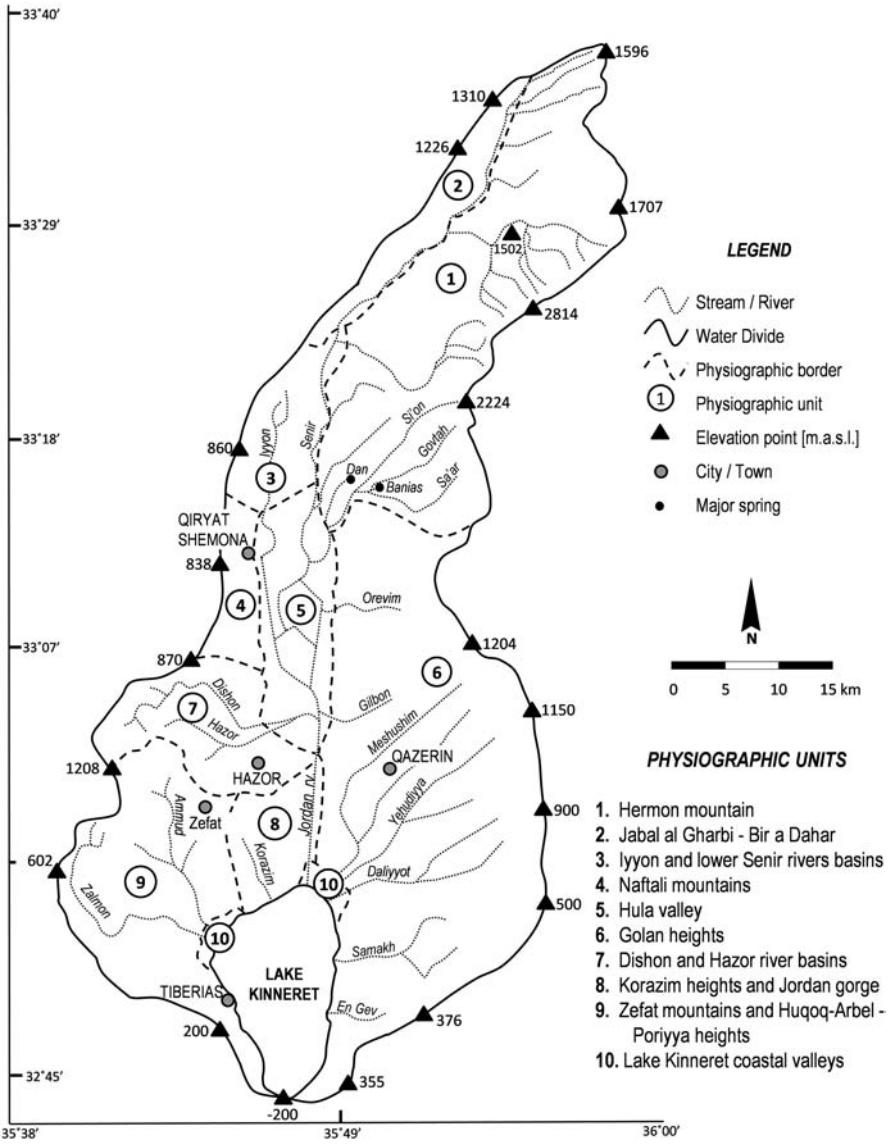

Fig. 5.1 Map of the 10 physiographic units, water divide, elevations, streams, springs, and towns within the Kinneret watershed

carbonate rocks characterize the area. Mean annual precipitation is 900 mm and most of the area drains through the Snir River, mainly after heavy rains with large amounts of sediments (Fig. 5.2b).

3. *Iyyon and Lower Snir Rivers basins:* This unit is a northern extension of the Jordan-Dead Sea Rift. The Iyyon basin includes a polje valley, bounded by

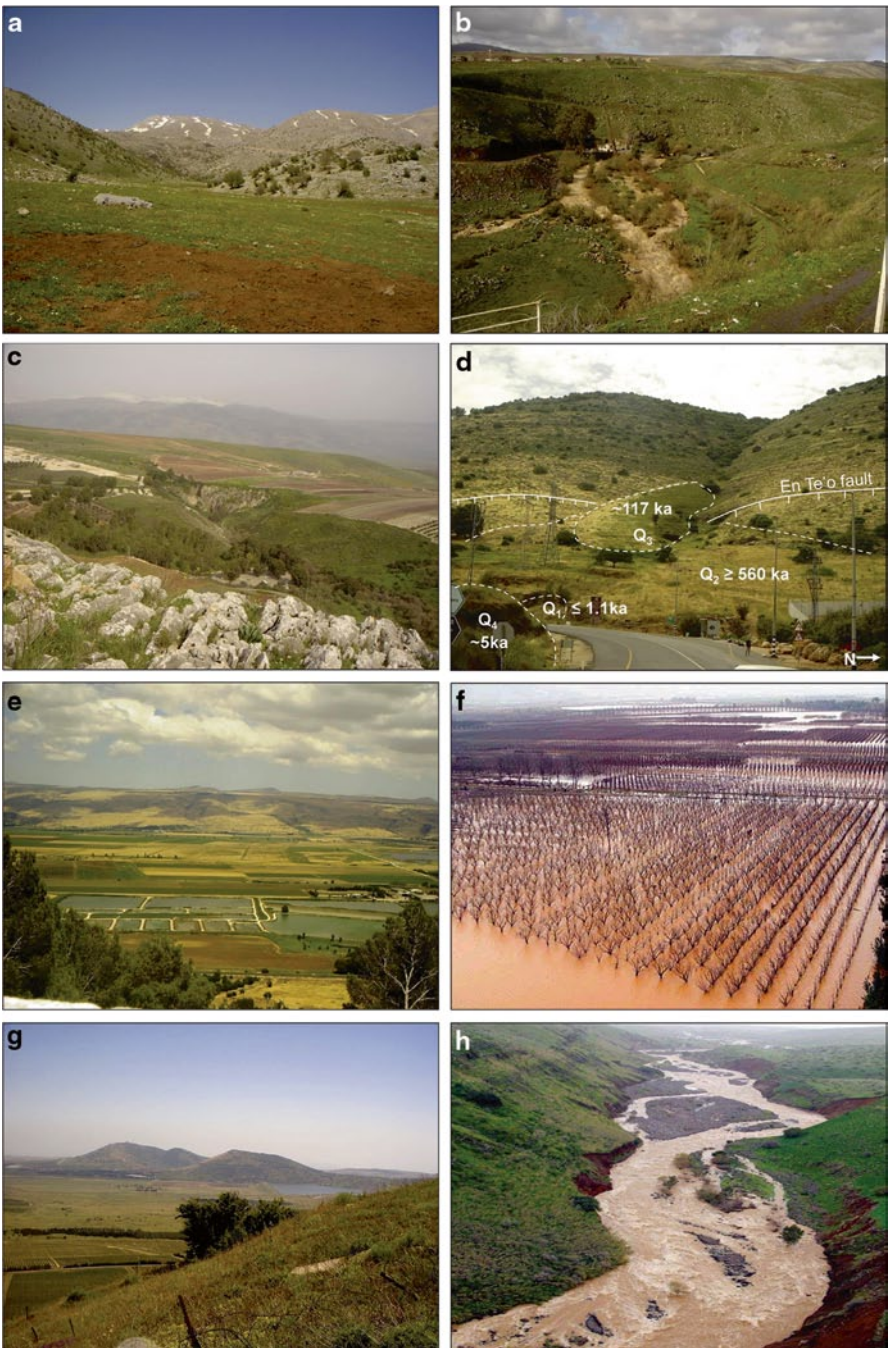

Fig. 5.2 Photographs of various physiographic units in the Kinneret watershed. **a** Nahal Ar'ar filled with deep, clayish soils of Terra Rossa origin. The Hermon Mountain and snow relics are visible in the back; **b** Nahal Snir at Ghajar, incised in a deep basalt canyon; **c** Nahal Iyyon flowing

faults, filled with alluvial soils. Perennial flow from springs is mainly diverted for irrigation during the dry period. The Snir River is deeply incised in Pleistocene basaltic flows (Fig. 5.2c).

4. *Naftali Mountains:* The western margin of the Hula Valley is represented by the Naftali mountain range, a 450–880-m-high escarpment formed by regional faulting. The mountain front is exposed to channel erosion and gravitational debris movements. It is dissected by more than 30 slope channels which are straight, short, ephemeral and developed perpendicular to the piedmont, exhibiting steep gradients (20–60 %) towards the valley. A succession of four generations of fan deposits accumulated during the past one million years, facing the channel mouths (labeled Q1–4 in Fig. 5.2d). The sediments consist of polymictic conglomerates. Carbonate soils and calcrete horizons up to stage V overtops the sediments. These outcrops extend up to an elevation of 300 m above the Hula Valley and their structures imply on depositional pulses followed by periods of quiescence and calcic soil development. The relics were dated from 1.1 to 0.01 ma. Field relationship between the sedimentary units and local faults indicate that no major faulting occurred along the Naftali escarpment during the Upper Pleistocene. The marginal faults displaced a 0.56-ma unit during the mid-Pleistocene, and since then, tectonic activity has shifted from the western marginal faults eastward to younger faults deeply buried in the Hula graben (Shtober-Zisu et al. 2008).

5. *Hula Valley (Fig. 5.2e):* The elongated Hula Valley is 25 km long and 5–8 km wide, covering an area of about 150 km^2. The valley has a gentle slope from 100 m a.s.l. in the north to 65 m a.s.l. in the south. The general outline of the valley is determined by the tectonic features of the Jordan Rift Valley, as their vertical faulting component has evolved since about 4 ma ago. The upper stratigraphic deposits represent a lake occupying the entire basin some 250 ky and a coexisting swamp and lake environment between 250 and 30 ka (Kafri et al. 1983). For the last 2 ma, the average rate of sedimentation is equivalent to the average rate of subsidence in a geological timescale. The annual rainfall ranges from 400 mm in the south to 600 mm in the northern part. Deep hydromorphic, alluvial Grumosol soils cover the valley under intensive agricultural exploitation (Fig. 5.2f). Tributaries of the Jordan River converge within the valley and the flow is perennial due to the large karstic springs draining the Hermon mountain aquifer as well as from Golan margins. The annual contribution of local springs, runoff from the Hula Valley catchment and direct rainwater, equals to the annual water consumption of the Hula Valley, namely about

through Taqiye Fm. marls (Paleocene) toward the Hula Valley; **d** A typical slope channel crossing the Naftali mountain, four generations of fan deposits, labeled Q1–4, have accumulated along the mountain piedmont; **e** The Hula Valley as part of the northern Jordan-Dead Sea Rift. The Golan Heights plateau with several cinder cones is visible in the back; **f** Floods in the Hula Valley cover agriculture plantations; **g** Avital and Bental cinder cones mark the water divide of the Kinneret watershed; **h** Flood in the Jordan River canyon. The slopes are eroded by landslides and sediments are transported towards Lake Kinneret

120×10^6 m^3. Agricultural settlements lie to the north and south of the previous lake and swamp areas.

6. *Golan Heights:* The Golan Heights are a volcanic plateau developed during the Pliocene and Pleistocene epochs (Mor 1993), covering about 900 km^2. Elevations range from more than 1,000–200 m below sea level, but despite this range, the physiography is quite homogeneous. According to the drainage basins, two subbasins were recognized: The first drains to the Hula Valley and the second drains directly to Lake Kinneret. The lithology consists primarily of a sequence of up to 1,000 m of basalt flows, in the middle of the Golan—near Kibbutz Ortal (Meiler et al. 2011). Cinder cones and other volcanic structures are arranged in linear forms, trending from NNW to SSE (Fig. 5.2g). Annual rainfall ranges from 500 to 900 mm, but no major steady sources of water are found in the area. About 75 % of total runoff is created by floods caused by rainstorms. Rivers are deeply incised forming more than 100-m deep canyons. Flow was altered by the construction of channel water dams, changing the natural flow regime (Shtober-Zisu and Inbar 2005).

7. *Dishon and Hazor River basins:* The unit is mountainous with heights ranging from 1,200 m a.s.l. at the summit of Mount Meron to 100 m a.s.l. in the Hula Valley. Faults divide the synclinal area into several blocks consisted of carbonate rocks from the Upper Cenomanian until the Eocene epoch. Pleistocene basalt flows cover the Dalton, Alma, and Dishon blocks. The western part is characterized by tectonic karst depressions. Runoff occurs during heavy rainfall storms.

8. *Korazim Heights and Jordan Gorge:* The Korazim Heights are a volcanic block south of the Hula Valley incised by the Jordan Gorge in its eastern flank. Tel Roman volcano was probably the source of the lava during the Upper Pliocene, but several other small basaltic cones are also present (Heimann and Ron 1993). Shallow basalt soils cover the area and land use is mainly for pasture. The Jordan Gorge is 10-km long and the river flows in a narrow and 200–250-m deep canyon entrenched in the basalt flows (Fig. 5.2h). Along the gorge, active landslides provide boulders and most of the coarse sediment carried by the river to the Beteha Plain. The river channel is composed of gravel and boulders and therefore a high-shear threshold is needed for bedload transport. Almost all bedload sizes, including boulders of more than 1 m in diameter, move during flow events with a 10-year frequency. From the outlet of the canyon to the delta into Lake Kinneret (air distance of 4 km), a planimetric view reveals four different forms of the fluvial system: straight channel within the canyon, with an average slope of 2.5 %, a braided system in the boulder depositional environment, with a channel slope decreasing from 2.5 to 0.5 %, and then a meandering channel with a gradient decreasing to 0.1 %. In the new delta area formed after the 1969 flood, which increased the length of the channel by 750 m, man-made changes created a completely new transfer system, leaving few reaches of the old channel in their natural conditions (Inbar 2002).

9. *Zefat Mountains and Huqoq-Arbel-Poriyya Heights:* Zefat Mountains lie on a monocline structure affected by the main rift valley, forming steep slopes from 900 m a.s.l. in the upper part to about 300 m a.s.l. at the lower parts. The lithology is hard, karstic Eocene limestone with small pockets of Terra Rossa soil exposed mainly between the lapies. The Huqoq block is covered by basaltic layers, whereas the Arbel is an Eocene limestone block covered partially by a basaltic flow. Runoff occurs during rainstorms. Spring water is diverted for consumption and used to maintain a steady baseflow throughout the year. The Poriyya Height is one of the tilted blocks and as a part of the eastern Lower Galilee, is covered with basalt similar to the Arbel block and borders the southwestern area of the lake.
10. *Lake Kinneret Coastal Valleys:* Two major coastal valleys are distinguished: Beteha and Ginosar valleys. The Beteha Valley was formed by the Jordan and Golan river deposits, several tens of meters in depth. The upper 4-m layers are from historical periods. During high lake water levels, coastal lagoons are formed within these valleys. Groundwater level fluctuates according to the lake level. The wetland environment is a protected nature reserve due to the richness in flora and fauna. A recently formed delta at the river mouth increased by 1 km^2 of the valley area. The Ginosar Valley is formed by the Ammud, Zalmon, and Arbel Rivers. During historic periods, the valley served as a fertile agricultural land for the lake coastal settlements.

5.2 Environmental Hazards

In the past 100 years, several natural disasters affected the Kinneret basin:

1927 earthquake in the Dead Sea rift
1934 Tiberias floods
1969 floods in the Jordan and northern rivers (recurrence interval 200 years)

Major historic earthquakes in the past (all A.D.): Bet She'an 749, Benot Yaakov 1202, Zefat 1759 and 1837, and Jerico 1927.

Records of tsunamis in the lake connected to major earthquakes were registered in: 749, 1759, and 1837 (Ben Menahem 1991).

Active landslides are found in the Jordan Gorge, in the river gorges of the Golan Height, and in the Naftali and Zefat mountain escarpments.

5.3 History of Land Degradation

Lake Kinneret lies in the Mediterranean-type climate region, which is an inherently unstable earth surface system.

The human impact in the Lake Kinneret basin began with the appearance of humans about 1.5 million years ago, but major effects on landscape modification occurred in historic times. Since then, human pressure on vulnerable earth resources has increased, driven by an increasing growth of population and land exploitation.

In the past centuries, the degradation processes intensified. These processes included land degradation caused by wild fires and urbanization; increases in the seasonality of stream flow, with higher runoff rates in the winter floods and less percolation into groundwater; decreasing discharge of springs; and lowering exploitable aquifers. The increased vulnerability causes more flood damage and erosion, making water management a more complex and expensive task. Forest fires have increased, and on average 5 % of the forest fires in Israel occur in the Kinneret drainage basin. Urbanization changes the surface to an impervious one, increasing the runoff/rainfall ratio from 2–3 % under natural conditions to more than 30 % in the urbanized areas.

Seven major phases of landscape modification in the Eastern Mediterranean were recognized following Naveh and Dan (1973):

The *first phase* lasted from about 1.4 million years BP to 100,000 years BP, covering the Lower Paleolithic period. The Levant was the main route of dispersal from Africa to Eurasia (Tchernov et al. 1994). During this phase, human activity was hunting and food gathering and the impact on the environment was insignificant.

The *second phase* started with the use of fire. Natural forest fires are rare in the Eastern Mediterranean because lightening events occur only in the winter wet period. The oldest site where the use of fire has been dated is the Benot Yaakov site, south of the Hula Valley, about 760 ka ago (Goren-Inbar et al. 2002).

The *third phase* started with the agricultural revolution, the beginning of agriculture and pastoral livestock husbandry, at the beginning of the Neolithic period around 11,000 years ago. The Kinneret basin was probably the first area that includes sites of cereal cultivation and domestication. The first cereals were wild wheat, the large-grained *Triticum dicoccoides*, the direct ancestor of the emmer wheat *Triticum dicoccum* and the wild ancestor of domesticated barley (*Hordeum spontaneum*) (Butzer 1964).

The *fourth phase* started around 5,000 years ago and lasted until the end of the Byzantine period in the seventh century A.D. It was the period with the greatest development of the agro-pastoral economy in the eastern Mediterranean, with land clearance in the mountainous areas, promoting soil erosion; terraces were built to minimize erosion and gain agricultural land, and Galilee was one of the most populated areas. Deforestation caused the almost complete extinction of the famous cedars of Lebanon, large but slow-growing trees, used in historical times for construction and shipbuilding. Now they exist only in scattered stands, protected as religious places and forest reserves. Deforestation and the resulting land erosion caused a decline in agricultural resources (Conacher and Sala 1998).

The *fifth phase* started with the Muslim conquest of the region in the seventh century and the decline of its economy and agriculture. The pastoral nomadism of the Arab tribes replaced the developed hill lands and irrigation ditches, promoting erosion and creation of swamps in the lower valleys due to the silting of the river channels.

The *sixth phase* covered the twentieth century, with a population increase of 2–10 times in most areas of the Kinneret basin. Mechanization was introduced in agriculture and irrigation schemes were developed. These involved changes in the landscape, as draining of the ancient Hula Lake and the surrounding swamps, diverting spring water and drying of channels, monoculture in agriculture and forests, introduction of exotic plants, and the use of fertilizers and pesticides. For example, the introduction of new tree species, such as *Eucalyptus and Acacia* from Australia and *Pinus radiata* from California, caused major changes in the ecosystem.

The *seventh phase* is the present one. The process of land degradation has been aggravated by population increase, deterioration of water resources, and urbanization of forest and agricultural land. On the other hand, there has been a sharp decline in the use of firewood and the number of grazing animals. Protected areas in nature reserves have been enlarged and reforestation has been conducted on a large scale. In addition, sewage and cowshed effluents are being treated in large proportion; reservoirs were built to store poor quality water, treat it, and use it for agriculture instead of letting it flow to Lake Kinneret; fish ponds were dried and are no longer operational; and a small part of the Hula Valley was re-flooded to reduce erosion and peat fires and to prevent uncontrolled flooding.

A foreseen climate change in the twenty first century is a decrease in rainfall and an increase in temperature in the eastern Mediterranean, meaning a further decrease in vegetation cover and increase in the annual sediment loss.

Human interference in the Mediterranean environment exacerbates the negative natural biophysical processes, and the results are more frequent and more severe geomorphic events, as floods, landslides, and soil erosion.

References

Butzer KW (1964) Environment and archaeology. Aldine Publishing Co., Chicago

Conacher AJ, Sala, M (1998) Land degradation in Mediterranean environments of the world: nature and extent, causes and solutions. Wiley, Chichester

Goren-Inbar N, Werker E, Faibel CS (2002) The Acheulian site of Gesher Benot Yaakov, Israel. The wood assemblage. Oxbow Books, Oxford p 120

Heimann A, Ron H (1993) Geometric changes of plate boundaries along part of the northern Dead Sea Transform—geochronologic and paleomagnetic evidence. Tectonics 12(2):477–491

Inbar M (2002) A geomorphic and environmental evaluation of the Hula Drainage Project, Israel. Aust Geogr Stud 40(2):155–166

Kafri U, Kaufman A, Magaritz M (1983) The rate of Pleistocene subsidence and sedimentation in the Hula basin as compared with those of other time spans in other Israeli tectonic regions. Earth Planet Sci Lett 65:126–132

Meiler M, Reshef M, Shulman H (2011) Seismic depth-domain stratigraphic classification of the Golan Heights, central Dead Sea Fault. Tectonophysics 510(3–4):354–369

Menahem AB (1991) Four thousand years of seismicity along the Dead Sea Rift. J Geophys Res 96:20,196–20,216

Mor D (1993) A time-table for the Levant volcanic province, according to K-Ar dating in the Golan Heights, Israel. J Afr Earth Sci (and the Middle East) 16(3):223–234

Naveh Z, Dan J (1973) The human degradation of Mediterranean landscapes in Israel. In: Di Castri F, Mooney HA (eds) Mediterranean type ecosystems. Springer, New York

Shtober-Zisu N, Inbar M (2005) Downstream effects of river impoundment on hydrological and geomorphological aspects of bedrock rivers (Golan Heights, Israel). IAHS Sp Pub 299: 219–224

Shtober-Zisu N, Greenbaum N, Inbar M, Flexer A (2008) Morphometric and geomorphic approaches for assessment of tectonic activity, Dead Sea Rift, Israel. Geomorphology 102(1):93–104

Tchernov E, Horwitz L, Ronen A, Lister A (1994) The faunal remains from Evron quarry in relation to other Paleolithic hominid sites in the Southern Levant. Quat Rev 42:328–339

Part II
The Physical and Chemical Setting

Chapter 6
Meteorology

Baruch Ziv, Elad Shilo, Yury Lechinsky and Alon Rimmer

Abstract Two key factors in the climate of the Lake Kinneret surrounding affect significantly the physical characteristics of the lake: the relatively high temperatures year round (annual mean of 21 °C) and the wind regime over the lake, attaining a speed of ~10 ms^{-1}, in particular during the afternoon in the months of May–September. Both factors are most important for the determination of the lake's energy balance. The water balance is controlled by the rainfall on the lake watershed. The low annual rainfall on the lake itself (400 mm) with respect to its immediate surroundings (~700 mm) is attributed to the unique topography of the lake, with an elevation of approximately 210 m below sea level, compared to 500 m above sea level of the mountains to the east and >1,000 m to the northwest. Ninety percent of the rainfall over North Israel and Lake Kinneret results from Cyprus lows, low-pressure systems characterizing the mid-latitudes as well as the Mediterranean basin. The Cyprus lows pass the north of Israel and therefore produce the westerly winds, which transport moist air from the Mediterranean into North Israel.

Keywords Energy balance · Rainfall · Sensible heat · Water balance · Westerly winds

B. Ziv (✉)
Department of natural sciences, The Open University of Israel,
P.O. Box 808, 43107 Raanana, Israel
e-mail: baruchz@openu.ac.il

E. Shilo
The Israeli Meteorological Service, P.O. Box 25, 5025001 Beit Dagan, Israel
e-mail: shilo244@gmail.com

Y. Lechinsky · A. Rimmer
The Yigal Allon Kinneret Limnological Laboratory, Israel Oceanographic & Limnological Research, P.O. Box 447, 14950 Migdal, Israel
e-mail: yuryl@ocean.org.il

A. Rimmer
e-mail: alon@ocean.org.il

T. Zohary et al. (eds.), *Lake Kinneret, Ecology and Management,* Aquatic Ecology Series 6,
DOI 10.1007/978-94-017-8944-8_6,

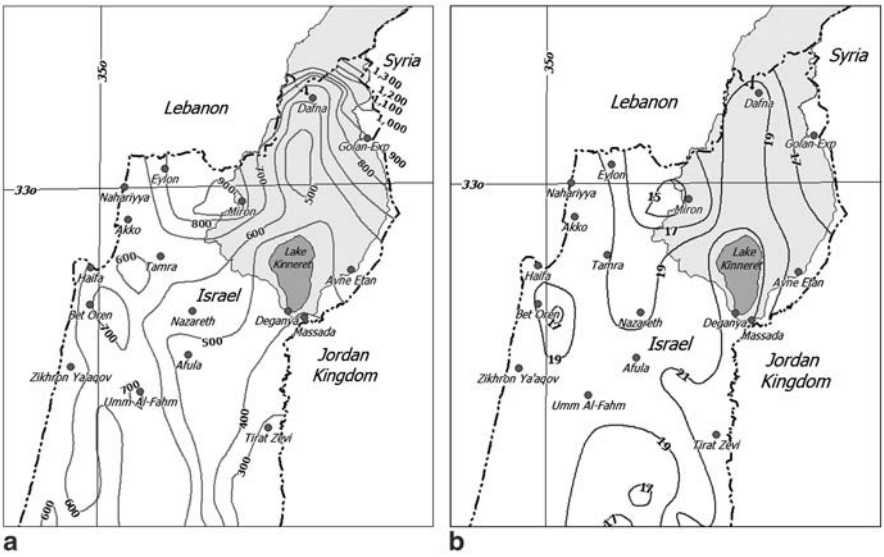

Fig. 6.1 **a** Mean annual rainfall for 1980–2010 (based on the climatological atlas of the Israeli Meteorological Service). **b** Yearly mean air temperature for 1964–1979. (Based on the atlas of Israel 1985, Survey of Israel)

6.1 Climatic Features of Lake Kinneret Watershed

This chapter describes the climatic conditions that prevail over the Lake Kinneret Valley (Fig. 1.1 in Chap. 1). The description also refers to the northernmost quarter of Israel (North Israel, hereafter), extending north of 32°30′N latitude, which includes the Lake Kinneret catchment area.

6.1.1 Climatic Classification of the Lake Kinneret Watershed

A key factor in the regional climate is the annual rainfall and the temperature distributions over North Israel (Fig. 6.1a and 6.1b, respectively). The annual rainfall varies dramatically from one region to another. For instance, the annual rainfall over the northern Golan Heights (northeastern tip of Fig. 6.1a) exceeds 1,200 mm, more than three times the direct rainfall on Lake Kinneret (~400 mm). The temperature map (Fig. 6.1b) indicates that the valleys surrounding Lake Kinneret (hence "the Kinneret Valley") are considerably hotter, by >5 °C, than its surrounding mountains (see the regional topography in Fig. 4.1 of Chap. 4), with an average annual temperature of 21 °C. The reason for the high temperatures and low rainfall in the Kinneret Valley with respect to its surroundings is the unique topography. While the lake elevation is approximately −210 m above mean sea level (a.m.s.l.), that of its surrounding mountains varies between 500 m a.m.s.l. to the immediate east and >1,000 m to the northwest (the Upper Galilee).

Fig. 6.2 Climatic map of North Israel according to Potchter and Saaroni (1998). The notations *Csa*, *Csb*, and *BShs* correspond to Mediterranean hot climate, Mediterranean moderate climate, and semiarid hot climate, respectively

The most common climate classification used among climatologists is the Koppen method (McKnight and Hess 2008) based on the conditions favorable for vegetation types. Koppen differentiates among five major climatic categories entitled A: "tropical," B: "dry," C: "temperate/meso-thermal," D: "temperate/micro-thermal," and E: "polar." The climate map of North Israel (Fig. 6.2) indicates that the majority of this region has what is known as a Mediterranean climate, but the Kinneret Valley is semiarid (belonging to category "B"). The regions categorized as "Mediterranean climate" are those having temperate meso-thermic climate ("C"), with rainfall obtained mainly in the cold season. The majority of North Israel has warm Mediterranean climate (monthly average temperature in at least 1 month exceeds 22 °C). Over the Kinneret Valley, the climate is hot semiarid (average annual temperature above 18 °C). The border between the temperate and dry climates is the rainfall isoline of $20 \times T$ (e.g., Potchter and Saaroni 1998), where T is the annual average temperature. This implies that the Kinneret region has dry climate due to a combined local effect of low rainfall and high temperatures.

6.1.2 Rain

The rainy season in North Israel, including the semiarid part, occurs between October and May. The monthly rainfall distribution of the region is represented here by

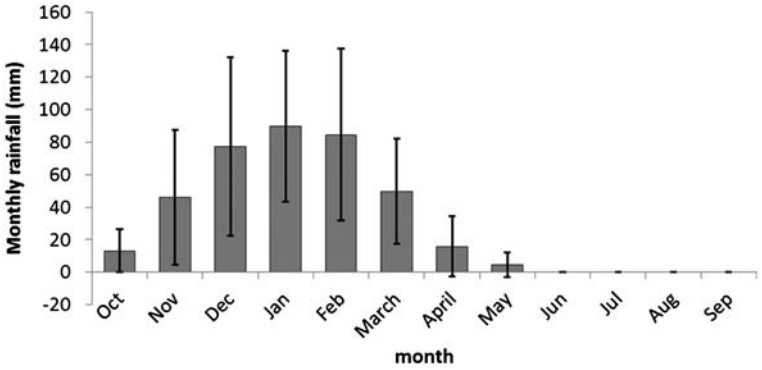

Fig. 6.3 Monthly distribution of average and standard deviations of the rainfall in Degania (near the southern shore of the lake) for the hydrological years 1980–2010 (hydrological year is from October to September)

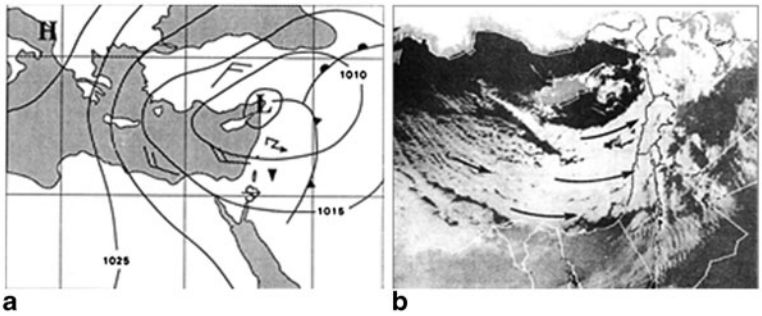

Fig. 6.4 **a** Schematic picture of a typical Cyprus low and **b** satellite image

that of the Degania rain gauge (Fig. 6.3), located near the southwestern shore of the Lake. The annual rainfall is 380 mm, 95 % of which is obtained between November and April and 66 % in the mid-season (December–February, DJF). The interannual variation in the monthly rainfall is extremely high in the transition seasons (> 100 % in October, April, and May) and varies between 50 and 90 % in November–March. The annual relative variation is 31 %.

Ninety percent of the rainfall over North Israel results from Cyprus lows (Goldreich 2003; Saaroni et al. 2010; Lionello 2012), which are low-pressure systems characterizing the mid-latitudes as well as the Mediterranean basin (Ziv et al. 2010). The Cyprus lows, demonstrated in Fig. 6.4, normally move eastward and pass north of Israel (near Cyprus). Therefore, the passage of Cyprus lows is accompanied by westerly winds, which transport moist air into North Israel (see Fig. 6.4a). This moisture transport is the main cause for the high rainfall obtained in this region (comparable to that obtained in western Europe, e.g., Paris and London) in spite of the relatively few rain days (60–70 days in North Israel, compared to ~200 days in western Europe).

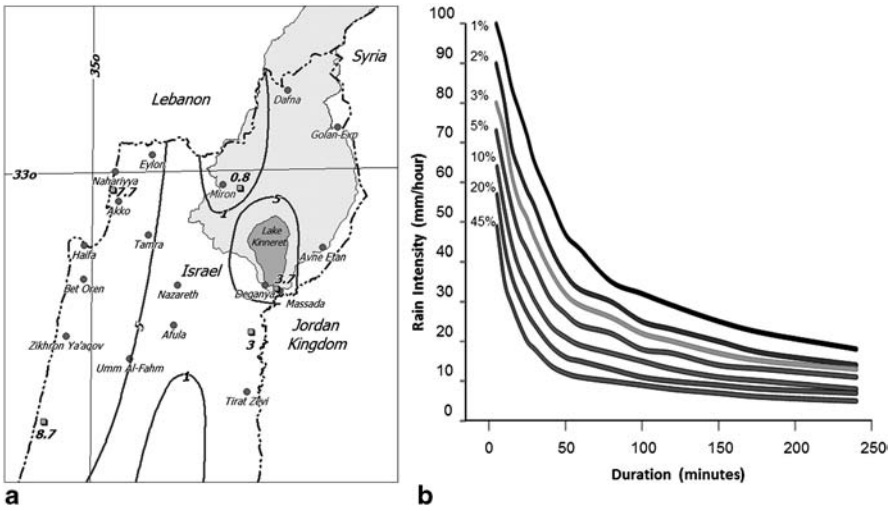

Fig. 6.5 **a** Distribution of the percentage of the total rainfall due to rain with an intensity of >50 mm h^{-1} (based on Kutiel 1978). **b** Intensity–duration–probability (IDP) curves from Degania. (Based on Morin et al. 1998)

The spatial distribution of the rainfall in North Israel (Fig. 6.1a) reflects the interaction of the rain-producing westerly winds with the geographical features (e.g., Shay-El and Alpert 1991; Saaroni et al. 2010). The distribution is shaped by three main factors (Katsnelson 1964; Kutiel 1987; Goldreich 2003). The first is a decrease from north to south due to the increasing distance from the main cyclone track. The second is a decrease from west to east, due to the increased distance from the Mediterranean Sea, the moisture source. The third is an increase in rainfall with elevation due to the orographic effect, which enhances rain formation while the air currents ascend across a topographic obstacle and suppresses it while descending to low elevation. In Israel, the dominance of westerly winds in the rainy days implies that the western slopes of the mountain regions receive more rain than their eastern slopes, resulting in a "rain shadow." The main causes for the low rainfall in the Kinneret Valley are due to it being located in the rain shadow of the mountain regions to its west, and its extremely low elevation. Similar conditions cause the entire Jordan Rift Valley to be dry (see Fig. 6.1a).

In spite of the semiarid climate of the Jordan Rift Valley, this region, including the Lake Kinneret Valley, is prone to torrential rains (Goldreich 2003). These are manifested as localized intense showers, with instantaneous rain rates of >100 mm h^{-1} (Dayan et al. 2001). This tendency is represented by the distribution of percentage of the annual rainfall contributed by torrential rains (more than 50 mm h^{-1}, Fig. 6.5a), which exceeds 5 % along the Israeli coastline of the Mediterranean and around Lake Kinneret. Intensity–duration–probability (IDP) curves from Degania are presented in Fig. 6.5b.

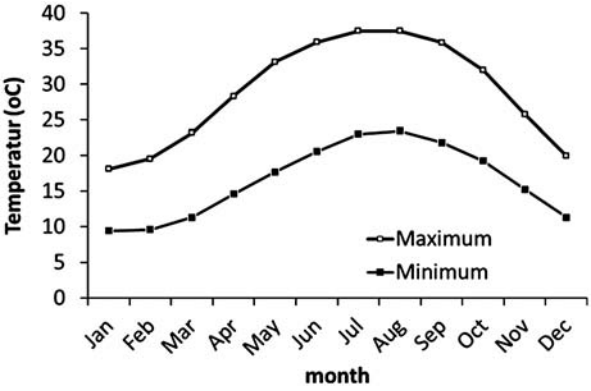

Fig. 6.6 Annual course of the monthly average minimum and maximum temperature in Kibbutz Massada meteorological station for the years 1975–2008

6.1.3 Air Temperature

The high air temperature regime in the Lake Kinneret Valley is reflected by relatively high yearly average temperatures (Fig. 6.1b). Annually (not shown here), the midday temperature in the Kinneret Valley is ~8 °C higher than that at the mountain regions to its northwest and northeast. The maximum temperature in the summer months (Fig. 6.6) exceeds 36 °C. The deviation of the maximum temperatures above specific thresholds at the meteorological station of Kibbutz Massada, located ~3 km south of the lake (Fig. 6.1b), is shown in Table 6.1. It indicates that on average, in 52% of the days between March and November, the temperature exceeds 33 °C, in 33% it exceeds 36 °C, and in 8% (23 days) it exceeds 39 °C.

The Lake Kinneret Valley is a link in the series of valleys comprising the Jordan Rift Valley, characterized by extremely cold winter nights. In spite of the small differences in elevation between these valleys, in the order of 100–200 m, the winter nights in the Lake Kinneret Valley are considerably warmer than those in the neighboring valleys. For instance, the long-term mean minimum temperature for January in Kefar Blum, in the Hula Valley (~40 km north of Lake Kinneret, 70 m a.m.s.l.), is 5.7 °C; at Tirat Zevi, in the Bet She'an Valley (−240 m a.m.s.l., 20 km south of the Kinneret lake) it is 7.0 °C, while the minimum temperature at the station of Kibbutz Massada is only 9.4 °C. The spatial winter nocturnal temperature is demonstrated in Fig. 6.7, based on surface imaging captured by earth-observing satellites on a clear night. The surface temperature at the Hula Valley (denoted HV) is near zero whereas that on the shores of the Lake Kinneret is around 10 °C, and the lake surface water temperature is >13 °C.

The mild nature of the winter nights is manifested also by the occurrences of "cold nights," i.e., nights with minimum temperature <5 °C. According to Avissar and Mahrer (1988), such nights are prone to chill, i.e., the ground surface temperature may reach the freezing level. The long-term mean annual number of "cold nights" in Kibbutz Massada (Fig. 6.8) is 2.5. In 40% of the winters, there is not even one cold night, while in the rest their number varies around five. The cause for the mild winter nights is the ventilation of the region, presumably due to the nocturnal

Table 6.1 Number of days per year in which the maximal temperature in Kibbutz Massada station exceeded specific values, and the long-term positive trend of this number in % per 10 years. (From Ziv et al. 2011)

Temperature threshold (°C)	Average yearly number of days	Increasing trend (%/10 years)
33	145.1	+3.4
36	90.6	+9.7
39	23.1	+5.6
42	2.6	+0.6

Analysis of the months March–November during the period 1975–2010

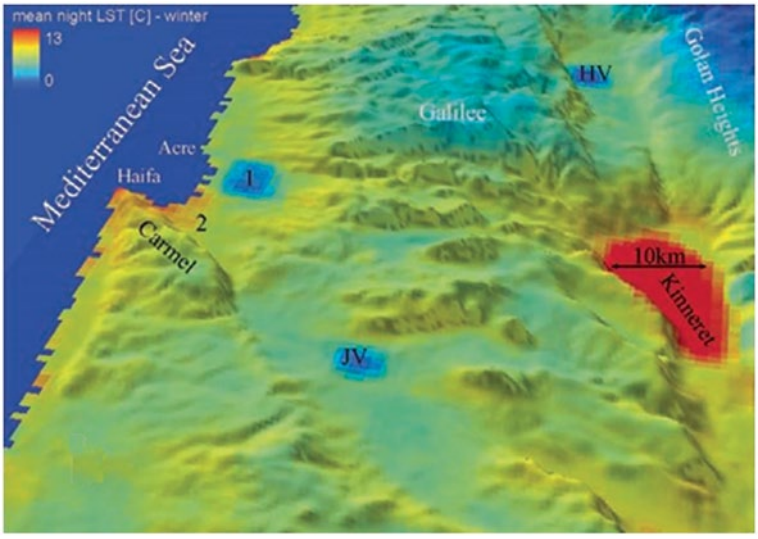

Fig. 6.7 Nocturnal winter temperature distribution at nights with clear sky derived from the TERRA satellite, passing over the surface at 22:30 LST. The notations *JV* and *HV* represent the Yizre'el and Hula valleys. The Mediterranean Sea is masked by *blue color*. (Reprinted from Lensky and Dayan (2011) with permission from the American Meteorological Society)

lake breeze and valley winds induced by the steep slopes toward Lake Kinneret (see next section).

6.1.4 Wind Regime

The wind regime over Lake Kinneret is governed by a combination of various factors at different spatial and temporal scales. In the hot months, in particular May–September, a considerable diel wind cycle is noted. The most prominent feature is the daily wind maximum, attaining a speed of ~10 m s^{-1}, from the west sector (Fig. 6.9). In the summer itself, i.e., June–September, the synoptic situation is relatively weak and highly persistent, and the wind is influenced by mesoscale

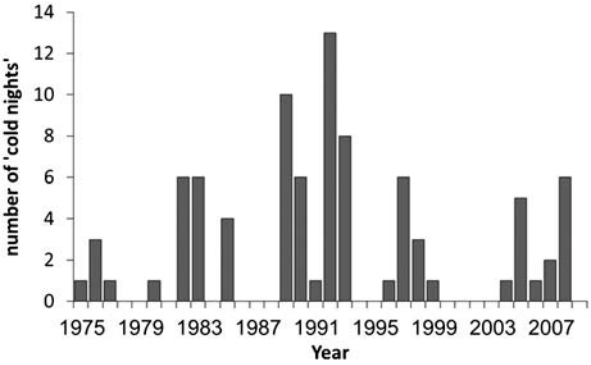

Fig. 6.8 Interannual variation in the number of "cold nights" (nights with minimum temperature < 5 °C) at the Kibbutz Massada meteorological station

and microscale flow patterns, i.e., the local lake breeze and slope winds, on top of which the Mediterranean Sea breeze (MSB) dominates (e.g., Alpert et al. 1982; Bitan 1981; Asculai et al. 1984). This daily maximum is related to the approach of the MSB, supported by the regional prevailing Etesian wind blowing from the west sector (e.g., Ziv et al. 2004). In the hours before the MSB approach, and after its dissipation, the lake is controlled by local winds. During the summer mornings, a lake breeze develops, blowing toward its shores. It ceases at the peak of its development when the westerly wind, originating from the MSB that develops along the Israeli Mediterranean coast, plunges toward the lake (Alpert et al. 1982). This westerly wind is further intensified by negative buoyancy of the relatively cool marine air with respect to the hot air it encounters in the Kinneret Valley. The penetration of the strong MSB is usually observed first near the west coast of the lake, and after a delay of 1–2 h, it reaches the east coast (Assouline and Mahrer 1993). While blowing over the lake, the MSB weakens, and lower wind speeds are usually observed in the eastern shores compared to the western-north shore (Fig. 6.9). In the late hours on summer nights, the lake acts like a thermal low. The wind flows from the land toward the lake, combined with the katabatic winds that are formed along the steep slopes surrounding it (Serruya 1975; Bitan 1981). The lake breezes are observed only below the height of 400–500 m above the lake level (Bitan 1981).

In the winter, the region is dominated by the passage of synoptic-scale (~1,000 km) windstorms, occurring once every few days, followed by several days with weak winds without any dominant direction (Serruya 1975). The resulting average wind vector has a speed in the order of 1 m s^{-1} (Serruya 1975 and the U section in Fig. 6.12). The typical systems that generate strong wind events above the lake can be divided into those producing winds from the western sector and easterly sector. The systems producing wind from the western sectors are the Cyprus lows. Their influence lasts several days, typically. Since this system produces rain above the lake and its catchment area, at times it causes increasing inflows from the Jordan River and other streams. This, in turn, has an effect on both water motions and water quality (Shilo et al. 2007).

Three different systems produce strong easterly winds above the lake, also called "Sharquia." The two relatively frequent systems are anticyclones centered above

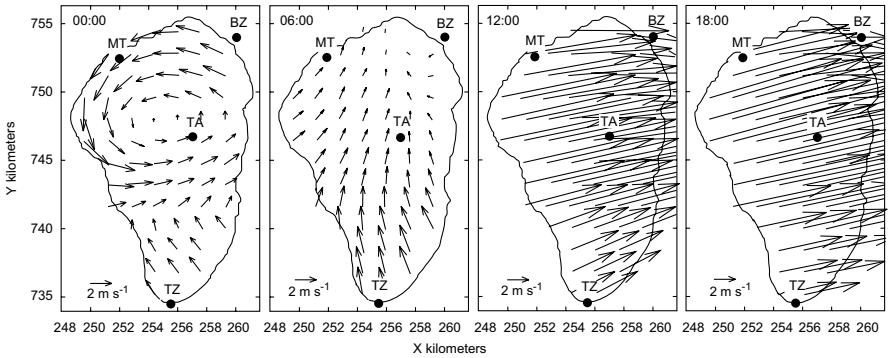

Fig. 6.9 Horizontal distribution of typical summer day winds above the lake surface at 00:00, 06:00, 12:00, and 18:00. Distribution is based on measurements in four meteorological stations in Tabgha, *MT;* Beit Zeida, *BZ;* Station A, *TA;* and Zemach, *TZ*

Turkey and the Red Sea Trough (RST). These systems, described by Saaroni et al. (1998), develop gradually and typically last several days. Another system is the Sharav cyclone (Alpert and Ziv 1989), which is a mesoscale cyclone, typical during the spring season, which enters the region from North Africa and crosses Israel from southwest to northeast. The influence of an individual Sharav cyclone is expressed in strong easterly winds, followed by high temperatures accompanied by dryness, which is broken sharply, and lasts 1 day. The Sharquias tend to be pronounced in the lake valley relative to its surrounding areas and to cause damages to agriculture and infrastructures. In a severe Sharquia event that occurred in March 1992 (Saaroni et al. 1998), the wind pushed the lake water westward. The increased lake level, combined with high waves, destroyed substantially the seaport of Tiberias, located on the west coast of the lake.

6.1.5 Climatic Changes

In the recent decades, since the mid-1970s, the global temperature has experienced a rising trend. Observational research, initiated and supported by the ministry of environmental protection of Israel, was conducted for the period 1975–2010. An analysis of the rate of change of air temperature at the meteorological station of Kibbutz Massada, in degree centigrade per decade, during each one of the four seasons (Fig. 6.10) indicates that air temperature shows rising trends at all times of the year. The rate of increase is considerably higher for the maximum temperature compared to the minimum temperature. The most rapid warming is observed in the summer months of June–August. For the maximum air temperature, the rate of temperature increase is 0.6 °C in 10 years. This warming is manifested by aggravation of the heat stress and increase in the occurrence of extreme high temperatures, as shown in Table 6.1. The general warming in the Upper Jordan Valley is also demonstrated in Fig. 6.11 (following Rimmer et al. 2011).

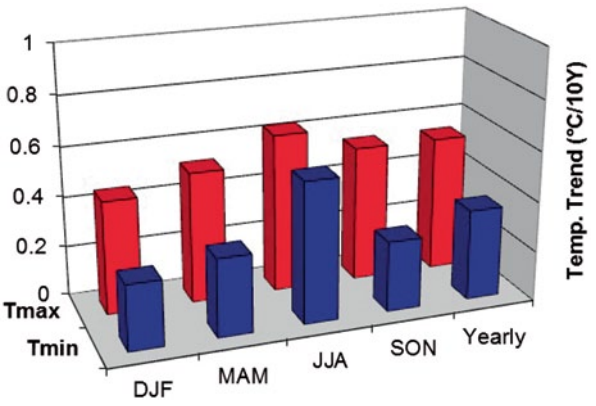

Fig. 6.10 Long-term trend of the maximum (*red*) and minimum (*blue*) air temperature for Kibbutz Massada station. The trend in fall (*SON*), summer (*JJA*), spring (*MAM*), and winter (*DJF*), together with the annual average, was based on data from 1975 to 2010

6.2 Energy Balance and Evaporation from Lake Kinneret Surface

Energy balance of the surface water layer partly belongs in a chapter on the lake physics, partly associated with hydrology and water balance (evaporation), and partly connected to the meteorological conditions over the lake surface. We included this section here, following the lake meteorology chapter because energy balance calculations are mainly associated with the meteorological conditions and measurements.

Reliable methods for the calculation of lake energy balance across different timescales are important for water budget studies, water planning and management, as well as understanding the physical, biological, and limnological processes of the lake. The following section describes the effect of meteorological conditions over the lake surface on the energy and water balance of the lake. To that end, we introduce the physical meteorological measurements above the lake surface, the typical annual and daily patterns of surface fluxes (i.e., net radiation, latent and sensible heat), and the typical patterns of lake heat storage in time.

6.2.1 Meteorological Measurements

Physical meteorological measurements were taken from four stations located around and offshore of Lake Kinneret. The major source of information for this section is the measurements from Tabgha Station (MT) with data available since 1996 (Table 6.2). The station was located above the lake surface, ~700 m offshore (35°33.01 E and 32°51.95 N), at an elevation of approximately −210 a.m.s.l. This station provided meteorological measurements at 10-min intervals. The other three stations (in Beit Zeida, BZ; Station A; and Zemach, TZ; Fig. 1.1 in Chap. 1, Fig. 6.9) provided measurements with similar equipment.

The seasonal and diel course of air temperature, water surface temperature, longwave radiation, shortwave radiation, relative humidity, and wind speed for the years

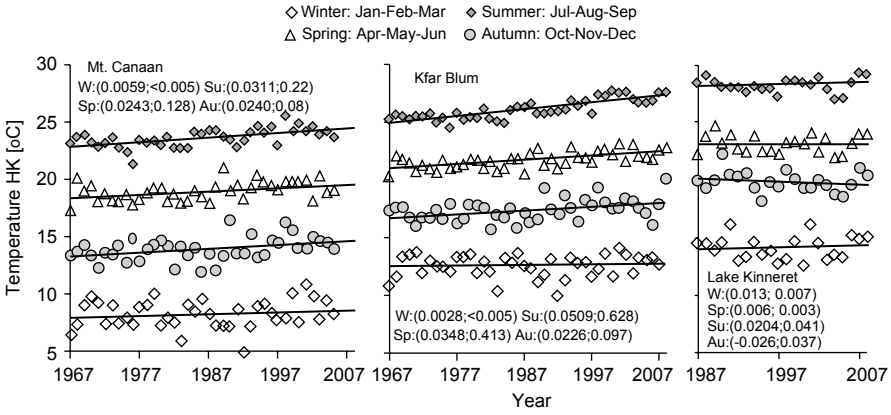

Fig. 6.11 Inter-diel variation (°C year^{-1}) in the yearly air temperature and the long-term trend based on regression in three meteorological stations located in the Lake Kinneret watershed: Mt. Canaan, Kfar Blum, and Lake Kinneret. (Reproduced from Rimmer et al. 2011 with permission from ASLO)

Table 6.2 Meteorological data available since 1996 on the Lake Kinneret surface

Measurement	Equipment	Location
Air temperature (°C) and relative humidity (%)	Young relative humidity and temperature probe model 43372C	~5 m above water level
Global shortwave radiation (305–2,800 nm, Wm^{-2})	Kipp and Zonen Delft BV shortwave radiometer CM11	~5 m above water level
Down-welling longwave radiation (5–25 μm Wm^{-2})	Kipp and Zonen Delft BV longwave radiometer CG1	~5 m above water level
Wind speed (ms^{-1}) and direction (degrees)	Young wind monitor MA−05106	~8 m above sea level
Water surface temperature (°C)	YOUNG platinum floating temperature probe model 41342	Depth of ~0.05 m

1996–2008 at the Tabgha meteorological station are shown in Fig. 6.12. While the diel variations are often masked by longer-term ones, they provide important information for hourly calculations, necessary for understanding the dynamics of the meteorology in the lake area.

According to the measurements, the MSB emerges soon after midday from April to October. It lasts for ~5 h during April, ~10 h in July, and ~5 h during October. At ~8 m above the water surface, it may reach an hourly average speed of 4, 10, and 4 m s^{-1}, during April, July, and October, respectively (U in Fig. 6.12). The relative humidity (RH in Fig. 6.12) is inversely correlated with the wind speed because the wind removes the moist layer above the lake surface, bringing dry air from the adjacent land and reducing RH by ~20% above the lake surface. Air temperature (T_a in Fig. 6.12) fluctuates annually between daily means of 12 and 32 °C. Together with intense shortwave and longwave radiation (R_{SWin} and R_{LWin} in Fig. 6.12, respectively), this makes the lake thermally stratified from about mid-April to late December (Chap. 9). Typical water surface temperature (T_s in Fig. 6.12) varies from

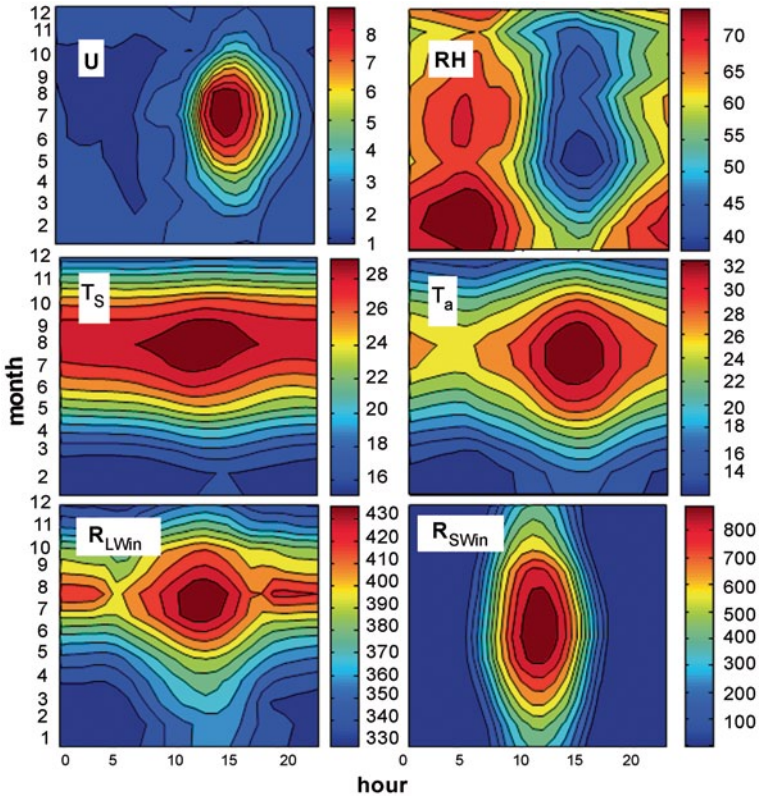

Fig. 6.12 Typical seasonal daily course of wind speed (U, m s^{-1}), relative humidity (RH, %), water surface temperature (T_s, °C), air temperature (T_a, °C), longwave radiation (R_{LWin}, Wm^{-2}), and shortwave radiation (R_{SWin}, Wm^{-2}) for the years 1996–2008 at the Tabgha meteorological station

~15 °C in January to ~30 °C in August. The daily air temperature variations are by far larger than these of the water surface.

6.2.2 The Annual Heat Energy Cycle

The energy budget equation is based on the conservation of energy, which accounts for incoming and outgoing energy, balanced by the amount of energy stored in the system. It does not include terms representing transformations among potential, kinetic, or biological energy, which are orders of magnitude smaller than those of heat energy (Imboden and Wüest 1995). The energy balance equation for an average square meter of the lake and for a certain period of time Δt can be calculated as follows (Rimmer et al. 2009):

$$\frac{\Delta G_L}{A_L} = \left[R_n + \frac{E_{qL}}{A_L} - (LE + H) \right] \Delta t, \tag{6.1}$$

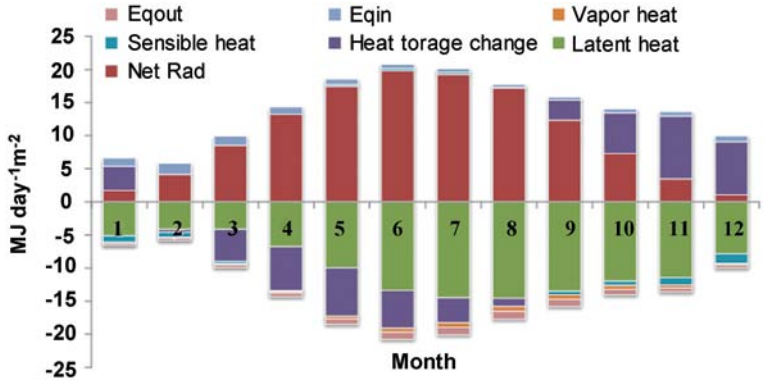

Fig. 6.13 Monthly average of heat balance components (MJ day^{-1} m^{-2}) from the period 1989–2007. Heat storage change, ΔG; net radiation, *Net Rad,* R_n; heat advection from inflows, *Eqin;* heat release from outflows, *Eqout;* latent heat, LE; sensible heat, H; and vapor heat, E_{Qo}

where $\Delta G_L\,(J)$ is the change in heat storage in the lake per unit of time, A_L (m^2) is the lake water surface, R_n (W m^{-2}) is the net radiation at the lake surface, E_{qL} (J s^{-1}) is the total net heat advection from inflows and outflows including withdrawal of evaporated water, LE (W m^{-2}) is the latent heat flux, and H (W m^{-2}) is the sensible heat flux over the surface of the lake.

The monthly heat balance equation was calculated for the entire lake using a slightly modified version of Eq. (6.1), where Δt is 1 month. When coupled with the water and chloride balances (Assouline 1993), this equation enables the calculation of the monthly evaporative loss Q_e and the unknown springs discharge Q_s (in million m^3; Chap. 8) mainly from considerations of water balance rather than energy balance. Using this method, the sensible heat flux H is replaced with $\mathrm{H} = \mathrm{LE} \times \beta$ (Eq. 6.1), where β is the average monthly Bowen Ratio (the ratio of sensible to latent heat fluxes; see also Assouline 1993; Rimmer et al. 2009).

Using the monthly heat balance method, the averaged components of the lake heat balance (1991–2007) are presented in Fig. 6.13. Net radiation and the latent heat flux dominate the changes in heat storage. The sensible heat is negative during winter (the lake contributes heat) and positive during summer. Heat gain from inflows is relatively large during winter and heat loss from outflows is large during summer. In terms of surface fluxes, the latent heat is orders of magnitude larger than the sensible heat flux $(-0.1 < \beta < 0.15)$ and vapor heat flux (a term that takes into account the energy loss from the withdrawal of evaporated water in Eq. 6.1).

6.2.3 The Diel Heat Energy Cycle

While the monthly energy balance method uses the water balance to calculate the evaporation, with aerodynamic methods (Brutsaert 1982), the surface fluxes and the energy balance are calculated using the measured meteorological data directly. This

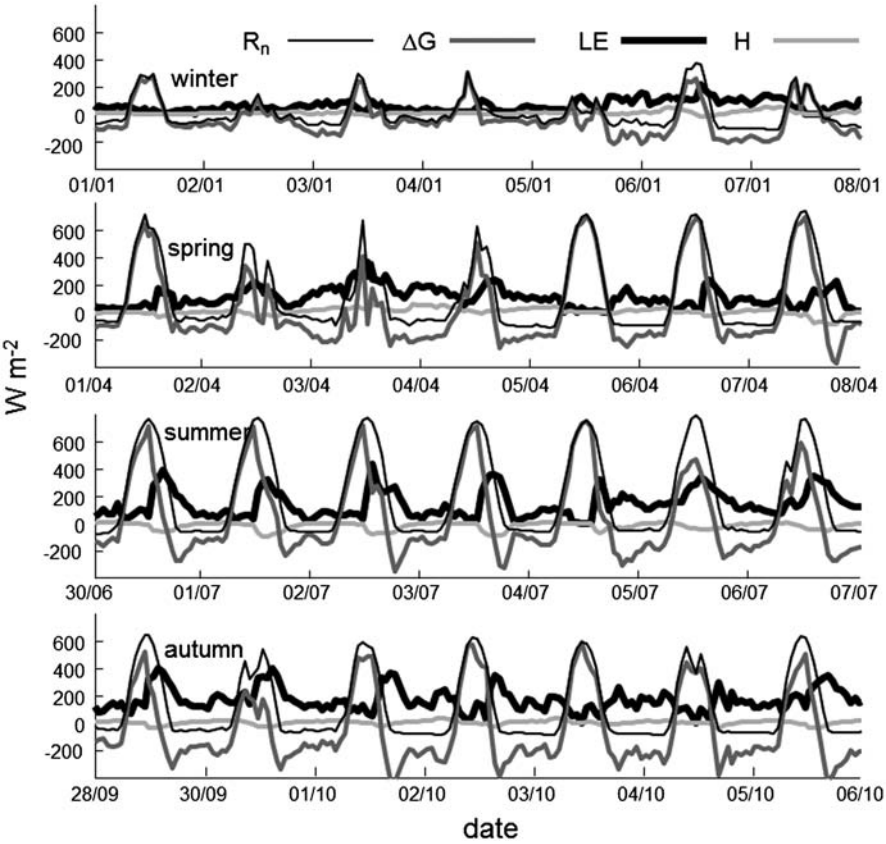

Fig. 6.14 Daily heat balance components (W m^{-2}) for 7 days during the winter, spring, summer, and autumn. R_n net radiation; *LE* latent heat flux; *H* sensible heat flux; ΔG the residual lake heat storage change

calculation is conducted at a single point while Δt is only 10 min. The short timescale in which we conducted this analysis is not suitable for including the energy of inflows and outflows because the travel time of the effect of these components is much larger than 10 min in a lake as large as the Kinneret. Therefore, these components are assumed negligible, and the energy balance (Eq. 6.1) becomes

$$\Delta G \cong \left[R_n - (\mathrm{LE} + H) \right] \Delta t, \tag{6.2}$$

where the right-hand side of Eq. (6.2) is derived from the measured wind speed, global radiation, air humidity, air temperature, and lake surface temperature. In this case, the left-hand side, ΔG, is the residual heat storage change.

Here, the Centre for Water Research (CWR) algorithm, based on Imberger and Patterson (1990), was applied. The algorithm takes into account the atmospheric stability, using the Monin–Obukhov length (Brutsaert 1982 p. 65; Imberger and

Patterson 1990. p. 325). The sensible heat flux H is related to the evaporative heat flux LE through the Bowen Ratio (Rimmer et al. 2009). Net radiation, latent and sensible heat fluxes, and the residual heat storage change were calculated at 60-min intervals describing the diel cycle of the major components of the heat balance. The results demonstrate typical characteristics of the lake surface–atmosphere interaction (Fig. 6.14). During winter, all the surface fluxes are low, and the lake heat storage change is nearly zero if integrated over the entire day. The intense spring and summer radiation heats the upper water column significantly during the daytime, while the strong daily winds cool the lake surface during the afternoon hours through evaporation (latent heat flux). At the same time, the air contributes additional heat to the lake through sensible heat flux. On average, the daily-integrated ΔG at these months (April, July) is positive and the lake keeps warming up during the spring and summer. During the autumn season, the temperature of the air often decreases below the temperature of the water surface, and the integrated ΔG becomes negative, and thus causes the lake to cool.

Estimation of various components of lake energy balance usually requires the use of a variety of methods, all originating from the energy balance equation. Each method is based on different timescales and uses various assumptions, which leads to evaluation of different parts of the equation by measurements, while calculating the parts which are unknowns. In the monthly water-and-energy balance algorithm, the evaporation was calculated as the residual of the water balance. Concurrently, with the 60-min time interval of the aerodynamic method, the heat storage change was calculated as the residual of the energy fluxes on the lake surface. The agreement between the results of various methods (see Rimmer et al. 2009) increases the confidence in our capability to estimate them properly.

References

Alpert P, Cohen A, Neumann J, Doron E (1982) A model simulation of the summer circulation from the Eastern Mediterranean past Lake Kinneret in the Jordan Valley. Mon Wea Rev 110:994–1006

Alpert P, Ziv B (1989): The Sharav Cyclone: observations and some theoretical considerations. J Geophys Res 94:18495–18514

Asculai E, Doron E, Terliuc B (1984) Mesoscale flow over complex terrain—a field study in the Lake Kinneret area. Bound-Lay Meteorol 30(1–4):313–331

Assouline S (1993) Estimation of lake hydrologic budget terms using the simultaneous solution of water, heat and salt balances and a Kalman filtering approach: application to Lake Kinneret. Wat Res Res 29:3041–3048

Assouline S, Mahrer Y (1993) Evaporation from Lake Kinneret: 1. Eddy correlation system measurements and energy budget estimates. Wat Res Res 29:901–910

Avissar R, Mahrer Y (1988) Mapping frost-sensitive areas with a three-dimensional local-scale numerical model. Part II: comparison with observations. J Appl Meteorol 27:414–426

Avissar R, Pan H (2000) Simulation of the summer hydrometeorological processes of Lake Kinneret. J Hydrometeorol 1:95–109

Bitan A (1981) Lake Kinneret (Sea of Galilee) and its exceptional wind system. Bound-Lay Meteorol 21(4):477–487.

Brutsaert, W. (1982) Evaporation into the atmosphere: theory, history, and applications, *D. Dordrecht, the Netherlands. D. Reidel Publ. Company*.
Dayan U, Ziv B, Margalit A, Morin E, Sharon D (2001) A severe autumn storm over the middle-east: synoptic and meso-scale convection analysis. Theor App Clim 69:103–122.
Goldreich Y (2003) The climate of Israel: observation, research and application. Springer, Israel, p 298
Imberger J, Patterson J (1990) Physical Limnology. In: Wu T (ed) Advances in Applied Mechanics, vol 27. Academic Press, New York, pp 303–475
Imboden DM, Wüest A (1995) Mixing mechanisms in lakes. In: Lerman A, Imboden DM, Gat JR (eds) Physics and chemistry of lakes. Springer, Verlag, pp 83–138
Katsnelson J (1964) The variability of annual precipitation in Palestine. Archiv fur Meteorologie, Geophysik und Bioklimatologie 13B:163–172
Kutiel H (1978) Statistical and spatial distribution of rain intensities in Israel, MSc thesis. The Hebrew University of Jerusalem, Israel
Kutiel H (1987) Rainfall variations in the Galilee (Israel). I. Variations in the spatial distribution in the periods 1931–1960 and 1951–1980. J Hydrol 94:331–344
Lensky IM, Dayan U (2011) Detection of finescale climatic features from satellites and implications for agricultural planning. Bull Am Meteorol Soc 92:1131–1136
Lionello P (ed) (2012) The climate of the Mediterranean region, from the past to the future, 1st edn. Elsevier
McKnight TL, Hess D (2008) Physical geography: a landscape appreciation. 9th edn, 622 Prentice Hall, p 720
Morin Y, Sharon D, Rubin S (1998) Rain intensities in Israel—selected station. IMS report 94/1
Potchter O, Saaroni H (1998) Revision of Koppen's climate regions of Israel, Stud Geog Isr 15:179–194
Rimmer A, Samuels R, Lechinsky Y (2009) A comprehensive study across methods and time scales to estimate latent and heat fluxes: the case of Lake Kinneret, Israel. J Hydrol 379:181–192
Rimmer A, Gal G, Opher T, Lechinsky Y, Yacobi YZ (2011) Mechanisms of long-term variations in the thermal structure of a warm lake. Limnol Oceanogr 56(3):974–988
Shay-El Y, Alpert P (1991) A diagnostic study of winter diabatic heating in the Mediterranean in relation with cyclones. Quart. J. R. Meteorol. Soc. 117:715–747
Saaroni H, Bitan A, Alpert P, Ziv B (1998) Continental outbreaks into the Levant and eastern Mediterranean. Int J Clim 16:1–17
Saaroni H, Halfon N, Ziv B, Alpert P, Kutiel H (2010) Links between the rainfall regime in Israel and location and intensity of Cyprus lows, 2009. Int J Clim 30:1014–1025
Serruya S (1975) Wind, water temperature and motions in Lake Kinneret: general pattern. Verh Int Ver Limnol 19:73–87
Shilo E, Ashkenazy Y, Rimmer A, Assouline S, Katsafados P, Mahrer Y (2007) Effect of wind variability on topographic waves: Lake Kinneret case. J Geophys Res Oceans (1978–2012), 112(C12).
Ziv B, Yair Y (1994) Introduction to Meteorology—Volume no. 5: Weather in Israel. The Open University of Israel, Israel (in Hebrew).
Ziv B, Saaroni H, Alpert P (2004) The factors governing the summer regime of the eastern Mediterranean, Int J Clim 24:1859–1871
Ziv B, Saaroni H, Romem M, Heifetz E, Harnik N, Baharad A (2010) Analysis of conveyor belts in winter Mediterranean cyclones. Theor App Clim 99(3–4)441–455
Ziv B, Saaroni H, Alpert P (2011) Temperature, heat–stress and rainfall fluctuations and trends in Israel during the last 30 years: is it an evidence for climatic change? Climatological–synoptic study, report 8–810.

Chapter 7
Hydrology

Alon Rimmer and Amir Givati

Abstract Lake Kinneret watershed, which spans over 2,730 km^2, divided between Israel, Lebanon, and Syria, incorporates four different hydrogeological units: the Jurassic mountainous karst of Mt. Hermon, the basalt plateau of the Golan Heights, the carbonaceous karst of the Eastern Galilee Mountains, and the flat alluvial Hula Valley. This chapter summarizes the hydrology of the lake in four different parts: a description of the hydrological nature of the hydrological units and quantification of their water contribution to the lake; the methods of calculating the annual water balance and their changes during the course of the years; the lake level fluctuations and definitions as a result of historical anthropogenic changes; and an overview of hydrological modeling, both surface water and ground water, of the various hydrogeological units.

Keywords Lake Kinneret watershed · Water–solute–energy balances · Water-level fluctuations · Jordan River · Hula Valley · Golan Height · Mount Hermon

7.1 The Hydrology of Lake Kinneret Watershed

The area of the Lake Kinneret watershed is 2,730 km^2 (Fig. 7.1). The 1,68.7 km^2 lake, located in the central part of the Jordan Rift Valley (Northern Israel), is the most important surface water resource in Israel, currently (year 2012) providing approximately 25–30 % of the annual freshwater consumption. The major water source of the lake is the ~1,600 km^2 of the upper catchments of the Jordan River, of which ~920 km^2 are in Israel, with the remainder located in Syria and Lebanon. The other part of the Lake Kinneret basin is the direct watershed (the section of the watershed that drains directly to the lake) with an area of ~965 km^2, of which 577 km^2

A. Rimmer (✉)
The Yigal Allon Kinneret Limnological Laboratory, Israel Oceanographic & Limnological Research, P.O. Box 447, 14950 Migdal, Israel
e-mail: alon@ocean.org.il

A. Givati
Israeli Hydrological Service, Israel Water Authority, 14 Hamasger Street, 61203 Tel Aviv, Israel
e-mail: amirg@water.gov.il

T. Zohary et al. (eds.), *Lake Kinneret, Ecology and Management,* Aquatic Ecology Series 6,
DOI 10.1007/978-94-017-8944-8_7,

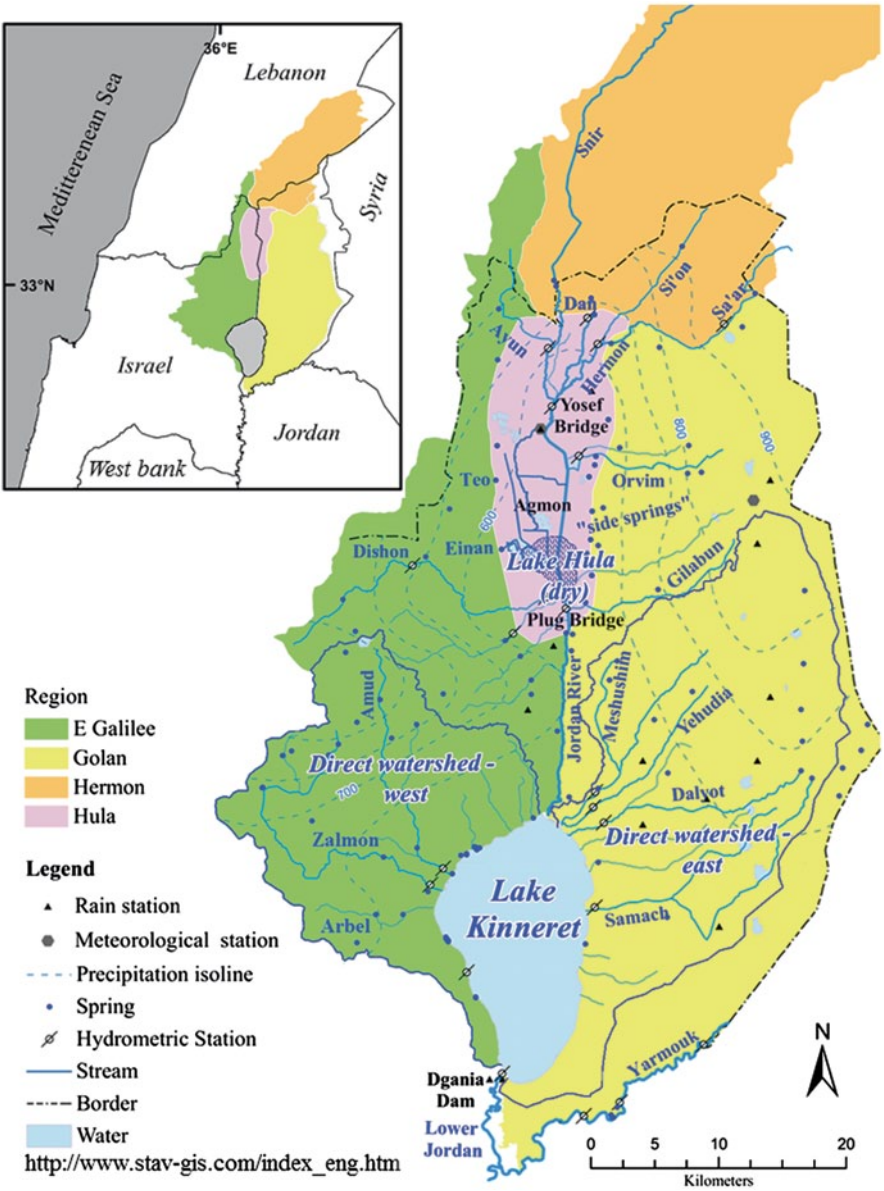

Fig. 7.1 General map of the catchment of Lake Kinneret showing its four hydrographic units

are in the southern part of the Golan Heights in the east, and the other 388 km^2 are part of the Eastern Galilee Mountains to the west of the lake.

The watershed includes four different hydrological units with large differences in their precipitation–stream flow relationships (Fig. 7.1): (1) the Jurassic mountainous karst of Mt. Hermon, (2) the basalt plateau of the Golan Heights, (3) the

Cenomanian–Turonian carbonaceous karst of the Eastern Galilee Mountains, and (4) the flat alluvial Hula Valley.

7.1.1 The Hermon Mountain

The main sources of the Jordan River are located at the south foothill of the Hermon Range, an elongated anticline of mostly karstic limestone of Jurassic age, with thickness > 2,000 m. The Mt. Hermon range is 55 km long and 25 km wide. It is the highest mountain range in Israel. Only 7 % of the range lies at present within Israel while the rest is divided between Syria and Lebanon. The summit, 2,814 m above mean sea level (a.m.s.l.), is located in Syria. The Hermon high regions (above 1,000 m a.m.s.l.) receive the highest annual precipitation in Israel (> 1,400 mm $year^{-1}$), restricted to the wet season from October to April. Snow usually falls on the elevated areas from December to March, and persists on areas 1,400–1,900 m a.m.s.l. until March–June (depending on local conditions). Rainfall and snowmelt of Mt. Hermon recharge the main tributaries of the Jordan River, with the following amount of annual flow (calculated for the years 1985–2010): (1) Dan—255 ± 44 million cubic meters a year (10^6 m^3 $year^{-1}$), (2) Snir (also known as Hazbani)—$107 \pm 66 \times 10^6$ m^3 $year^{-1}$, and (3) Hermon (also known as Banias)—$110 \pm 39 \times 10^6$ m^3 $year^{-1}$.

The Dan stream that immerges from a small topographic catchment of 24 km^2, with ~ 15 km^2 of karst exposures, is the largest spring in the region. Due to small anthropogenic water diversion, its topographic catchment does not contribute stream flow, and therefore it carries only the Dan Spring water. The Snir stream, which exhibits the largest topographic drainage area (612 km^2, with ~ 330 km^2 of karst exposures), is fed mainly by the Wazani and Hazbaya Springs, located near the Israel–Lebanon border and ~ 20 km to the north of the border, respectively. The annual contribution of these springs is 45 and 30×10^6 m^3 $year^{-1}$, respectively (Gilad and Schwartz 1978). The rest of the measured discharge is contributed by surface runoff or quick flow (a term often used in karst hydrology for fast-reacting karstic springs). The Hermon stream (drainage area 153 km^2, and ~ 74 km^2 of karst exposures) receives most of its water from the Banias Spring (~ $69 \pm 19 \times 10^6$ m^3 $year^{-1}$) and the rest from the Sa'ar Spring ($11 \pm 6 \times 10^6$ m^3 $year^{-1}$), Kezinim Spring (15×10^6 m^3 $year^{-1}$), Si'on Spring, and surface runoff. Gilad and Bonne (1990) estimated that the relative contribution of snowfall to the annual water budget of the Hermon aquifer in the period 1983–1987 was 15 to 182×10^6 m^3 $year^{-1}$, with an average of 50×10^6 m^3 $year^{-1}$ (~ 12 %). By using Hydrological Model for Karst Environment (Rimmer and Salingar 2006), Samuels et al. (2010) estimated that snowfall amounts on the Hermon basin for 1970–2000 were 2.4 (1978/1979) to 202.8 (1991/1992) $\times 10^6$ m^3 with an average of $41 \pm 40 \times 10^6$ m^3 $year^{-1}$.

7.1.2 The Hula Valley

The Dan, Hermon, and Snir streams converge near Sede Nehemyha (Yosef Bridge, Fig. 7.1) to form the Jordan River, which for the next 21 km flows through the Hula

Valley (Hula, Fig. 7.1). The valley covers 177 km^2 (25 km long by 6–8 km wide), and serves as a drainage basin to both the streams and groundwater aquifers in the Upper Eastern Galilee Mountains on the west, the Golan Heights on the east, and the Mt. Hermon on the northeast.

Before 1958, the south of the valley was the site of Lake Hula. The lake was 5.3 km long and 4.4 km wide, and about 1.5 m deep in summer and 3 m deep in winter. Basaltic hills of about 200 m altitude, originating from late Pleistocene volcanic activity, define the southern border of the valley. The interception of these hills with the Jordan River is commonly referred to as the basalt "plug" ("Pkak" in Hebrew) because water drainage downstream into Lake Kinneret was greatly restricted, thereby forming the historic Lake Hula and its surrounding wetlands. Completed in 1958, draining of Lake Hula was achieved by deepening and widening the Jordan River at the basalt "plug," which allowed the outflow of larger quantities of water. In the swamp region north of the now dry lake, the Jordan River was diverted into two peripheral canals, the East Canal and the West Canal, which enclosed most of the peat lands. These canals converge near the center of the former lake and then follow the original, but now deepened, course of the Jordan River (see also Hambright and Zohary 1998). Annual rainfall in the valley varies greatly between 400 mm in the south and 650 mm in the north, while the contribution to the flow in the Jordan River is considered as minor.

The valley is filled with sedimentary materials of low permeability. An early study of the Hula groundwater (Neuman and Dasberg 1977) claimed that, due to the surrounding hydraulic heads, there is a significant upwelling groundwater flux in the valley. However, Litaor et al. (2008) and Sade et al. (2010) found that the shallow water table is strongly affected by the water level in the Jordan River canals through significant lateral flow in macrospores. Litaor et al. (2008) suggested that the component of vertical flow upward is fairly mild. The origin of water in the valley is therefore mainly from springs at the margins of the valley and streams that drain the surrounding mountain.

7.1.3 The Golan Heights

The Golan Heights (Golan, Fig. 7.1) is a ~1,160 km^2 upland region in NE Israel. Its boundaries are the slopes of Mt. Hermon in the northwest, the Rokad River in the east, the Hula Valley and the Jordan River in the west, and the Yarmouk River in the south. The total north-to-south length of the Golan Heights is ~80 km, and its width varies between 17 and 23 km. It is a basalt-covered plateau, sliced off by deep canyons at its edges. The plateau slopes gently from north to south, descending from 1,200 m a.m.s.l. on its northern edge to 300 m a.m.s.l. at its southern rim. Average annual rainfall ranges from 1,200 mm at the north to less than 500 mm at the southern part. The Golan area may be divided into two hydrological regions: northern (between Sa'ar-Hermon and Gilabun; Fig. 7.1) and southern (between Meshushim and Yarmouk Valley).

Only ~350 km^2 of the northern Golan area drains into the Jordan River, while the rest flows towards the Rokad basin. The main groundwater contribution from the

Golan to the Jordan River are the so-called Side Springs (Dafny et al. 2003) located on the northwestern slopes of the Golan along the contact line between the main faults and the Hula Valley fill. These springs discharge throughout the entire year yielding $\sim 45 \times 10^6$ m^3 year^{-1}. The rest of the Golan contribution to the Jordan River is 12×10^6 m^3 year^{-1} of surface runoff (IHS 2009).

Nearly 600 km^2 of the central and south Golan drain directly into Lake Kinneret through the Meshushim stream ($\sim 23 \pm 20 \times 10^6$ m^3 year^{-1}), Yehudia ($\sim 16 \pm 16 \times 10^6$ m^3 year^{-1}), Dalyot ($\sim 12 \pm 17 \times 10^6$ m^3 year^{-1}), and Samach ($\sim 6.4 \pm 10 \times 10^6$ m^3 year^{-1}). The remaining area drains to the east and south, into the Rokad and Yarmouk River basins, respectively. The high standard deviations reflect the dramatic difference between flows during dry and extremely wet winters.

7.1.4 The Eastern Galilee Mountains

The water sources originating from this region are the groundwater and stream flows from all subbasins west of the Hula Valley, the Jordan River, and Lake Kinneret. It includes the surface water basins of the Ayun stream ($\sim 6 \times 10^6$ m^3 year^{-1}) in the north, Dishon ($\sim 3.5 \times 10^6$ m^3 year^{-1}), Hatzor ($\sim 0.34 \times 10^6$ m^3 year^{-1}), and down to the Amud ($\sim 1.8 \times 10^6$ m^3 year^{-1}) and Zalmon streams ($\sim 0.32 \times 10^6$ m^3 year^{-1}) that drain directly into Lake Kinneret (Fig. 7.1). The main groundwater resources of this region are the Einan Springs, located southwest of the Hula Valley, and the Teo Spring, about 5 km north of Einan. Prior to 1960, the Einan Spring was the main source of the western region to the Jordan River, with an annual discharge of $\sim 20 \times 10^6$ m^3 (Kidron 1972), and the Teo Spring contributed an annual discharge of $\sim 4.0 \times 10^6$ m^3 (Michelson and Goldshtof 1974). Since 1962, the deployment of the aquifers in this region (Einan Wells) caused a gradual decrease in the natural discharge into the Jordan River. The annual contribution of all the springs in this region today (2012) is only $\sim 6 \times 10^6$ m^3. The system feeding the springs consists of ~600-m-thick Judea Group carbonate aquifers recharged in the East Galilee Mountains. Michelson and Goldshtof (1974) estimated that the recharge area of the Einan Spring is 85 km^2, which includes the Kadesh Valley, and the recharge area of Teo Spring is ~18 km^2. The average annual precipitation in this region is between 400 mm on the Hula Valley (~60 m a.m.s.l.) and 685 mm on Mt. Kna'an (900 m a.m.s.l.).

7.2 Lake Kinneret Water Balance

Calculating periodical water budget is a common procedure applied on a routine basis to sources of water, and especially to lakes, in order to determine rainfall–runoff relationships, evaporation estimation, and lake–groundwater relationship. According to this method, the quantity of water that balances the measured components of the water budget is considered as the contribution of the non-measured components.

When a water balance equation is coupled with energy and solute balances equations (Assouline 1993; Rimmer and Gal 2003), the monthly simultaneous balances can be used to estimate the contribution of water from unmonitored saline springs (through the residual of the water and solute balances) and water losses due to evaporation (through the residual of the water and energy balances; see also Chaps. 6 and 8).

The water balance equation of Lake Kinneret (Assouline, 1993) is based on continuous measurements of inflows, outflows, and changes of lake storage. When measured water quantities are separated from the components, which are not measured directly, the water balance equation is

$$Q_s - Q_e = \Delta V_L + Q_d + Q_p - Q_{gs} - Q_j - Q_y - Q_r - Q_{mr}, \tag{7.1}$$

where the monthly measured quantities (10^6 m^3) at the right hand side of Eq. (7.1) are the change in water volume of the lake (ΔV_L); release of water through the Degania Dam to the southern part of the Jordan River (Q_d); withdrawal of water by pumping to the National Water Carrier (NWC, a canal transporting Lake Kinneret water to consumers at the coastal plain and to the southern parts of Israel since 1964) and by other consumers (Q_p); the Jordan River discharge (Q_j); water diverted into the lake from the Yarmouck River (Q_y); direct rain (Q_r); runoff from the direct watershed (Q_{mr}); and a monitored part of the saline springs that flows into the lake from adjacent aquifers (Q_{gs}). The monthly non-measured quantities (10^6 m^3) at the left hand side of Eq. (7.1) are evaporation loss (Q_e) and the unmonitored saline groundwater contribution from the same aquifers (Q_s).

Water inflows to Lake Kinneret were measured and reported by the British Mandate Hydrological Service (1926–1948), and later by the Israeli Hydrological Service, (IHS, 1948–present). Monthly water, solute, and energy balances of Lake Kinneret have been carried out and reported to the IHS annually by TAHAL (Water Planning for Israel Ltd.) from the 1950s, and more accurately from 1963 to 1986 (TAHAL 1968–1986). Since 1987, this procedure has been carried out by Mekorot (Israel National Water Company; Mekorot, 1987–2011). During the ~50 years of water balance calculations, the locations, methods, and the frequency of monitoring have changed significantly: (a) A small part of the streams that originate from the direct watershed have been measured since the 1940s; however, prior to 1968 discharges of streams from the Golan Heights were estimated rather than directly measured. Since 1986 until today, these discharges have been monitored on a regular basis. (b) The hypsographic curve of Lake Kinneret (Mekorot 2003), which serves as a tool in estimating the monthly difference in water volume (ΔV_L), changed several times through the years with the development of measurements methods. (c) TAHAL (1968–1986) separated the solute from the water and energy calculations; according to the Mekorot method (Assouline 1993), water, solutes, and energy balances were calculated simultaneously every month. (d) TAHAL used a daily balance simulation for direct evaporation calculations, while Mekorot calculated the evaporation on a monthly basis as the residual of the water balance (Eq. 7.1). Taking into account these differences, the results reported in the Annual Water and Solute

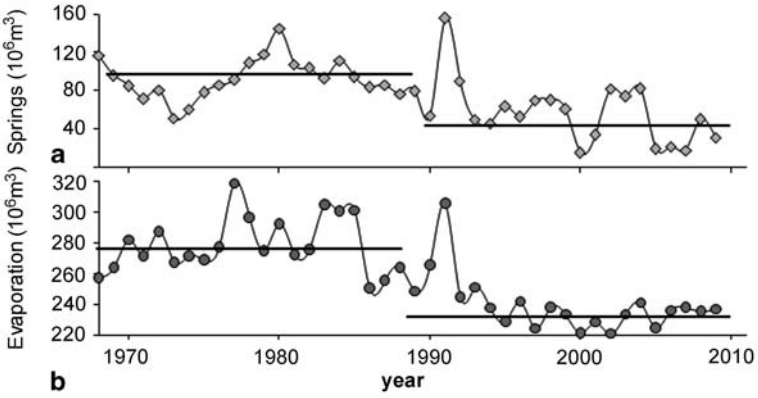

Fig. 7.2 Two components of the Lake Kinneret annual water balance: **a** springs discharge (10^6 m^3) and **b** evaporation (10^6 m^3); TAHAL calculations from 1968 to 1986; Mekorot calculations from 1987 to 2011

Balance (TAHAL 1968–1986; Mekorot 1987–present; IHS 2009) do not constitute a homogeneous time series. With the improved monitoring of water balance components during the last two decades, it can be postulated that the two variables on the left hand side of Eq. (7.1) were probably overestimated before 1987. Data analysis shows that: (1) The reported average annual evaporation between 1969 and 1987 was 282×10^6 m^3 while between 1987 and 2010 it was only 242×10^6 m^3 (Fig. 7.2). (2) The reported average annual spring flow between 1969 and 1987 was 94×10^6 m^3 while between 1987 and 2010 it was only 61×10^6 m^3. Since an error in evaporation estimates must result in a compensating error of the saline spring's contribution (Eq. (7.1)), it is suggested that during 1969–1987 both the evaporation and the saline spring's quantities were overestimated by at least $\sim 30 \times 10^6$ m^3 compared to their actual value. The differences in Fig. 7.2 between the two periods may therefore be attributed to improved monitoring and/or analysis during the years 1987–2010, and not to real hydrological changes.

The water balance of Lake Kinneret for the period 1976–2009 is as follows (Weinberger et al. 2012; Fig. 7.3): On average, the Lake Kinneret watershed produces 811×10^6 m^3 $year^{-1}$. Some 182×10^6 m^3 $year^{-1}$ are used or diverted away from the lake in the upstream areas of the watershed, leaving 629×10^6 m^3 $year^{-1}$ as annual inflows to the lake. An average of 230×10^6 m^3 $year^{-1}$ evaporates from the lake so that the average volume of available water (defined as inflows minus evaporation) is 399×10^6 m^3 $year^{-1}$, from which, 375×10^6 m^3 $year^{-1}$ is consumed and the rest (24×10^6 m^3 $year^{-1}$) flows to the southern part of the Jordan River.

This average amount of outflow is misleading. Actually, according to the policy of the Israeli Water Authority, water release through the Degania Dam is inadvisable. Therefore, in regular years when the lake level remained low, the release was $\sim 10 \times 10^6$ m^3 $year^{-1}$. Only in exceptionally high rainfall years, and in order

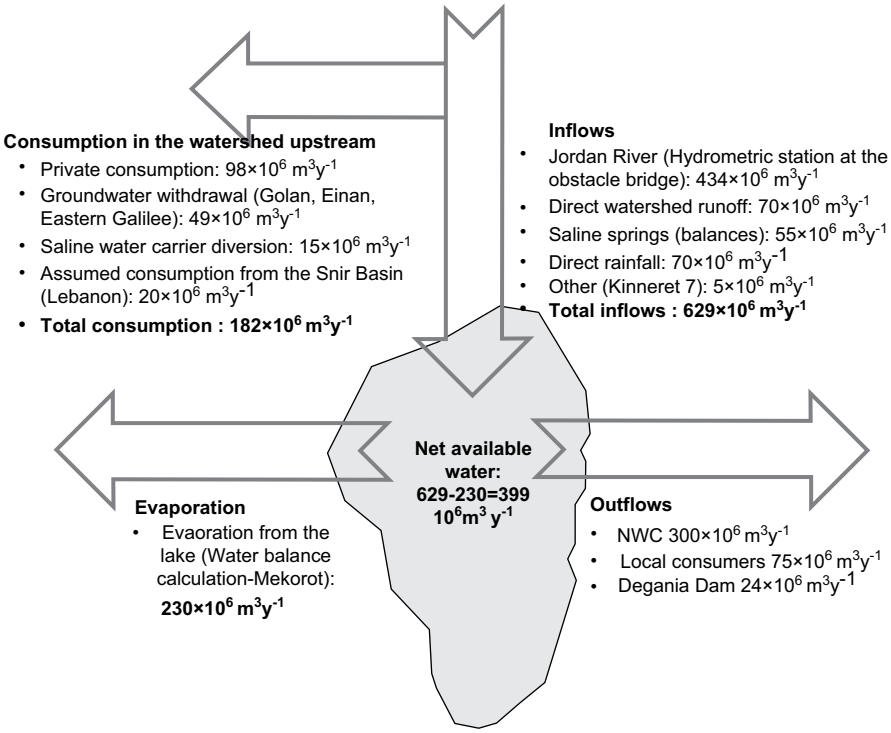

Fig. 7.3 Water balance in the Kinneret basin; average values for the period 1976–2009. (Adapted from Weinberger et al. 2012)

Table 7.1 Amount of water released through the Degania dam during high rainfall years between 1968 and 2012

Hyd year	1968/1969	1969/1970	1970/1971	1977/1978	1979/1980	1980/1981	1987/1988	1991/1992	1992/1993	1994/1995
10^6 m^3	970	261	161	81	102	238	129	258	289	90

From 1995–2012 the dam was not opened

to prevent flooding, the dam was opened and water was released to the southern Jordan River (Table 7.1).

Components of the annual water balance in the Lake Kinneret Watershed are given in Fig. 7.4a. It elaborates the annual available water within the entire Kinneret watershed, which is the sum of available water in the Lake Kinneret itself, and the total consumption in the watershed upstream for the period 1975–2009. A statistically significant decreasing trend in the total annual recharge to the basin is evident during the last 35 years, leading to a decrease in the net available water volumes in the lake (Fig. 7.4b). Since 1975, the available water volumes have decreased by $\sim 6.15 \times 10^6$ m^3 annually (see also Table 7.2). Givati and Rosenfeld (2007) showed that this decreasing trend was escorted by decreasing precipitation

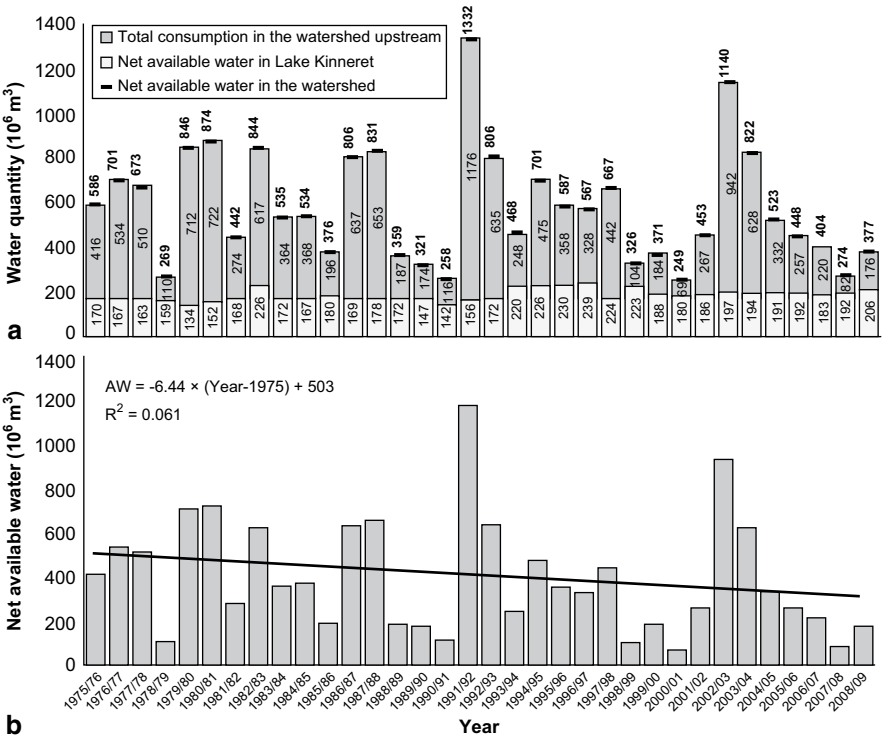

Fig. 7.4 **a** Water balance components in the Kinneret watershed; **b** decreasing long-term trend of available water in Lake Kinneret

Table 7.2 Average water balance components in the Kinneret watershed for 1976–2009 and also divided into two periods: 1976–1992 and 1993–2009

Hydrological year	Net available water in the watershed (10^6 m^3)	Total consumption in the watershed upstream (10^6 m^3)	Net available water in Lake Kinneret (10^6 m^3)
Average 1976–2009	581	182	399
Median 1976–2009	534	180	332
Average 1976–1992	636	166	470
Median 1976–1992	673	167	510
Average 1993–2009	524	204	320
Median 1993–2009	461	196	262

on the Golan Heights from 958 mm for the rainy season in 1975 to 708 mm in 2010. They suggested that the decrease in precipitation caused a decrease of 63 and 14×10^6 m^3 in the annual spring flow of the Dan and Banias, respectively.

Another cause of decrease in the available water at the lake is the increasing water consumption in the lake's watershed (Weinberger et al. 2012) from an average of 153×10^6 m^3 in 1975–1992 to 220×10^6 m^3 in 1993–2009.

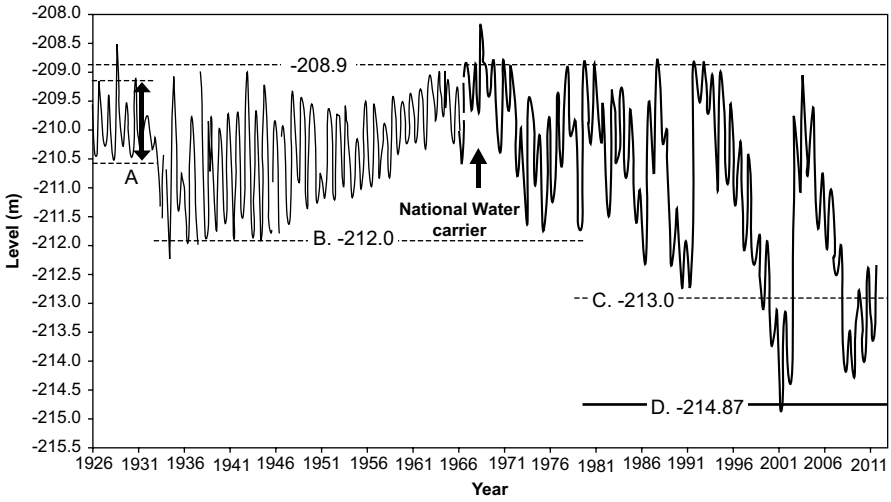

Fig. 7.5 A long-term record of Lake Kinneret monthly mean water levels since the initiation of routine measurements in 1926. **a** The *two-sided arrow* indicates the range of natural water level fluctuations prior to the 1850s based on archeological evidence (Nun 1974). **b** The *upper* and *lower* "*red lines*" at −209 and −212 m a.m.s.l., respectively, as defined by law under the British Mandate. **c** In 1981, the legal *lower red line* was lowered to −213 m by the Israeli government to allow increased pumping during drought years. **d** In November 2011, the lowest-ever water level was reached, −214.87 m. Subsequently, this minimum was declared as a *black line* that should not be crossed

7.3 Natural and Anthropogenic Changes in Water Level

Due to the characteristics of the local Mediterranean climate, with alternations between rainy winters and dry summers, seasonal fluctuations in water levels have been an integral feature of the Kinneret hydrology since the lake formed approximately 20,000 years ago (Serruya 1978). A summary of typical historical/natural water level fluctuations in the lake was brought by Hambright et al. (2008). Based on archaeological evidence, Nun (1974) concluded that natural water levels in Lake Kinneret fluctuated seasonally over a range of ~1.3 m (from −209.5 to −210.8 m a.m.s.l.) between the twelfth and nineteenth centuries (Fig. 7.5). This amplitude, as well as the relatively low maximum water level (−209.5 m a.m.s.l.), were apparently maintained by the presence of two natural outlets at the southern end of the lake: a narrow (30–40 m wide), relatively deep outlet through which small floods were released (the modern-day Lower Jordan River outlet) and a wider (150 m wide) but shallower outlet a few kms northwest of the lower Jordan River outlet (near Moshavat Kinneret), through which large volumes of water were flushed when the lake level rose during heavy floods. Over time, the shallower outlet gradually filled in with sediments and, by the mid-1800s, it closed completely. With only the narrow Jordan River outlet, the maximum water levels in the lake increased by approximately 0.5 m, although, with the exception of the unusual flood years of 1918–1919

and 1928–1929, the amplitude of annual fluctuations remained below 1.3 m through the first quarter of the twentieth century (Hambright et al. 2004).

The natural fluctuations of the water level in the lake may be estimated by taking into account only the natural components of the water balance in Eq. (7.1). It is assumed that under natural conditions: (1) artificial anthropogenic variables (Q_p and Q_y) vanish; (2) the lake level fluctuates between maximal and minimal values from April to December, respectively; and (3) the cumulative outflow during this period is equal to the sum of all inflows. With these assumptions, the water balance equation for April to December remains $\Delta V_L \cong -Q_e$. The calculated average evaporation from the lake from April to December (balances of 1987–2011) results in $Q_e \cong 215 \times 10^6$ m^3 year^{-1}, which is nearly the calculated ΔV_L between the lake's natural level fluctuations from –209.5 to –210.8 m a.m.s.l.

Beginning in the late 1920s, a series of engineered hydrological changes converted Lake Kinneret into a reservoir with two distinct periods of increased water level fluctuations (1932–1948 and 1973–present). During 1927–1932, the lake was impounded and the Jordan River outlet was deepened to supply water for the hydroelectric power station that was constructed ~7 km south of the lake in Naharaim (project completed in June 1932, Serruya 1978). Seasonal water level fluctuated on average 2.1 ± 0.6 m during the period of operation of the hydroelectric station (1932–1948). Water levels gradually returned to natural variability until Lake Hula and its surrounding wetlands (~60 km^2) on the Jordan River in upstream Lake Kinneret were drained in the 1950s (completed in 1957). With the completion of Israel's NWC in 1964, the major outflow of the lake was shifted from the Jordan River outlet at the southern end of the lake to the northwest intake of the NWC, and Lake Kinneret was converted into the primary storage and supply reservoir for the country's freshwater. Since 1973, the NWC has operated at full capacity, minimum legal water levels (see Chap. 31) have been lowered several times (Fig. 7.4), seasonal water level fluctuations have increased to 1.8 ± 0.9 m, seasonal fluctuations reached a maximum of 4.7 m, and the multiannual amplitude of fluctuations reached 6 m.

7.4 Hydrological Modeling in the Lake Kinneret Watershed

Calculating and understanding long-term hydrology (i.e., rainfall, runoff, spring flow, evaporation, reservoirs storage, and consumption) and water balances along the Jordan River and in parts of the Lake Kinneret watershed are essential in order to estimate both the water quantity and quality in the dry climate of the East Mediterranean. In the past, several types of rainfall–runoff analysis, hydrological models, and water balances schemes were proposed for this watershed. Here, we briefly mention part of these studies by dividing them into categories. In this review, we deliberately omit many groundwater models which were developed in order to quantify the direct solute springs' flow into the lake. These models are reviewed in detail in Chap. 8.

Statistical Analysis: Morin et al. (1979) proposed various types of statistical rainfall–runoff relationship attributed to soil types in each sub-basin. Rom (1994), Shentsis and Ben Zvi (1994), Givati and Rozenfeld (2007), and Rimmer et al. (2011) presented a variety of statistical rainfall–runoff correlations, which connected directly rainfall in several gauging stations and the stream flow of the Jordan River. Part of these models was used for several years by the IHS as an efficient tool to predict stream flow based solely on precipitation. In the Jordan River basin, these methods are highly efficient for prediction of annual flow, but efficiencies reduce dramatically for monthly and daily predictions. Other type of statistical analysis is the report of Polak (2005), which focused on estimating frequencies of peak flows in streams within the entire area of the Lake Kinneret basin in Israel.

Linear Reservoir Analysis for the Hermon Springs: In order to physically characterize the major flows to the Jordan River, Michelson (1975), Gilad and Shwartz (1978), Simpson and Carmi (1983), and Gur et al. (2003), attempted to characterize the flow Q_D of the Dan Spring. They calculated the recession coefficient K_D in the curve of the Maillet (1905) exponential equation

$$Q_D = Q_{D_0} \exp(-t / K_D), \tag{7.2}$$

where Q_{D_0} is the spring flow at the end of the rainy season. With this simplified approach, the typical K_D of the Dan Spring was reached with significant deviations, ranging from 300 to 600 days, depending on the seasons that were analyzed.

Physically Based System Analysis: According to Simon (2006), it was Mero (1969) who introduced the first physically based simultaneous hydrometeorological model for the Jordan River sources (Dan, Hermon, and Snir Rivers). Kessler (1999) developed a monthly, long-term streamflow model, taking into account only the Banias and Dan Springs, while Berger (2001) presented a three-linear reservoir model for the entire upper catchment of the Jordan River. Rimmer and Salingar (2005) applied large-scale catchment model (LASCAM; Sivapalan et al. 1996) for the prediction of daily flow in some of the Jordan River tributaries. Later, they developed the daily streamflow Hydrological Model for Karst Environment (HYMKE, Rimmer and Salingar 2006) in order to overcome the unique problems associated with karst hydrology modeling in Mt. Hermon. They found that $K_D \cong 300$ days, independent of the type of rainy season.

Spatially Distributed Groundwater and Surface Water Model: A detailed model for the basalt aquifer of the Golan Height was developed by Dafny et al. (2003), contributing to the understanding of the hydrology of the "Side Springs" in the eastern edges of the Hula Valley and the streams on the east of direct watershed (Fig. 7.1). The rich surface water of the Golan Height was studied in a monthly rainfall–runoff model by Kessler et al. (2005). Spatially distributed groundwater model is less feasible for the Mt. Hermon aquifers. Because of the unique political

situation in the Israel–Lebanon–Syria border, the Mt. Hermon aquifers were not sufficiently investigated, so that the thickness and the borders of the aquifer(s), water-level fluctuations, hydraulic characteristics (i.e., conductivity, porosity), amount of local rainfall distribution, and the amount of annual recharge are not sufficiently revealed (Rimmer and Salingar 2006). Nevertheless, Kunstmann et al. (2006) and Smiatek et al. (2011) applied WASIM (Schulla and Jasper 2000) to parts of the Mt. Hermon catchments, reaching good simulated results for the Hermon and Ayun basins.

Spatially Distributed Water Management Model: Sade et al. (2014) were probably the first to incorporate the main hydrological components of the entire Lake Kinneret watershed and the local consumptions into a single model, using the Water Evaluation and Planning (WEAP; Sieber and Purkey 2002) simulation in order to construct integrated water resources management tool.

7.5 Summary

The Lake Kinneret watershed is one of the most studied hydrological basins in the east Mediterranean. There are, however, several gaps of knowledge which can be attributed to the unique political location of the watershed.

The amount of snow and rainfall on Mt. Hermon, and its contribution to the Jordan River, are not yet fully quantified. This is mainly because the flow of streams and springs in the east and northeast regions of Mt. Hermon is in Syria and Lebanon; thus, no data are available for calculating complete water balance. Moreover, the well-developed karstic landscape increases the complexity of quantitative studies.

Despite the intensive research of water resources in the Kinneret watershed, another unknown aspect is the actual groundwater flow from the Golan Heights to the Hula Valley. In contrast to the considerable lack of information from the Mt. Hermon area, there is an excellent database regarding the hydrology of the Golan Heights and the Hula Valley, but the intensive water consumption, the large flows of the Jordan River, and the lateral flows within the Hula Valley make the calculations of water balances fairly complicated.

To the best knowledge currently available, the expected hydrological changes in the Lake Kinneret basin following the trend of global warming, are significantly smaller than the direct anthropogenic changes affecting the amount of water in the basin (increased pumping, lowering lake levels, etc.; see also Rimmer et al. 2011).

References

Assouline S (1993) Estimation of lake hydrologic budget terms using the simultaneous solution of water, heat, and salt balances and a Kalman filtering approach—application to Lake Kinneret. Water Resour Res 29(9):3041–3048

Berger D (2001) Estimating the natural flow in the upper catchment of the Jordan River. Watershed Unit, Mekorot, Sapir Site, Israel. Volume 393, Issues 1–2, 27 October 2010, pp 133–142 (in Hebrew)

Dafny E, Gvirtzman H, Burg A, Fleischer L (2003) The hydrogeology of the Golan basalt aquifer, Israel. Isr J Earth Sci 52(3):139

Gilad D, Bonne J (1990) Snowmelt of Mt. Hermon and its contribution to the sources of the Jordan River. J Hydrol 114(1/2):1–15

Gilad D, Schwartz S (1978) Hydrogeology of the Jordan sources aquifers. Israel Hydrological Service Report Hydro/5/78, 58 pp (in Hebrew)

Givati A, Rosenfeld D (2007) Possible impacts of anthropogenic aerosols on water resources of the Jordan River and the Sea of Galilee. Water Resour Res 43:1–15

Gur D, Bar-Matthews M, Sass E (2003) Hydrochemistry of the main Jordan River sources: Dan, Banias, and Kezinim springs, north Hula Valley, Israel. Isr J Earth Sci 52(3/4):155–178

Hambright KD, Zohary T (1998) Lakes Hula and Agmon: destruction and creation of wetland ecosystems in northern Israel. Wetlands Ecol Manag 6:83–89

Hambright KD, Eckert W, Leavitt PR, Schelske CL (2004) Effects of historical lake level and land use on sediment and phosphorus accumulation rates in Lake Kinneret. Environ Sci Technol 38:6460–6467

Hambright KD, Zohary T, Eckert W, Schwartz S, Schelske CL, Leavitt PR (2008) Exploitation and destabilization of a warm, freshwater ecosystem through engineered hydrological change. Ecol Appl 18:1591–1603

Israel Hydrological Service (IHS), (2009) Development of water sources exploitation in Israel until autumn 2009, Jerusalem 2011 (in Hebrew)

Kessler A (1999) Hydrologic model of Dan Spring monthly flow using a conic linear reservoir, submitted to the Israeli Water Commission (in Hebrew)

Kessler A, Kessler N, Price E (2005) Calibration of monthly rainfall-runoff model for the Golan Heights, submitted to the Golan's Regional Water Corporation (in Hebrew)

Kidron Y (1972) Einan field—deployment of the Cenomanian aquifer. TAHAL report HR/72/117 (in Hebrew)

Kunstmann H, Heckl A, Rimmer A. (2006) Physically based distributed hydrological modelling of the upper Jordan catchment and investigation of effective model equations. Adv Geosci 9:123–130

Litaor MI, Eshel G, Sade R, Rimmer A, Shenker M (2008) Hydrogeological characterization of an altered wetland. J Hydrol 349:333–34

Maillet E (1905) Essai d'hydraulique souterraine et fluviale: librairie scientifique. Hermann, Paris

Mekorot (2003) Kinneret Lexicon, Mekorot Water Supply Unit. Tel Aviv (In Hebrew)

Mekorot (1987–2011) The annual water-solute-energy balances of Lake Kinneret. Watershed Unit of Mekorot, Sapir Site, Israel (in Hebrew)

Mero F (1969) An approach to daily hydro-meteorological water balance computations for surface and groundwater basins. Proceedings of the ITC–UNESCO seminar for integrated river basin development, Delft. ITC–UNESCO, Delft, 25 pp

Michelson H, Goldshtof Y (1974) Geohydrology of the Cenomanian aquifer in the upper and central Galilee, TAHAL publication 01/74/71. Tel Aviv (in Hebrew)

Michelson H (1975) Geohydrology of the enclave and the southeastern flanks of Mount Hermon, TAHAL 01/75/05 (in Hebrew)

Morin Y, Michaeli A, Agassi M, Atzmon B, Rozentzveig D (1979) The rainfall-runoff-erosion relations in the Lake Kinneret basin. Research report R-42, the Erosion Research Station in Rupin Collage (Israel) (in Hebrew)

Neuman SP, Dasberg S (1977) Peat hydrology in the Hula basin, Israel: II. Subsurface flow regime. J Hydrol 32:241–256
Nun M (1974) Water levels in Lake Kinneret in the historical period. Land Nat 15:212–218 (in Hebrew)
Polak S (2005) Peak flows in streams of the Lake Kinneret watershed. Report to the Lake Kinneret Drainage Authority (in Hebrew)
Rimmer A, Salingar Y (2005) Developing a dynamic river basin model for contaminants transport in the UCJR using GIS. Final researches report submitted to BMBF–MOS cooperation in environmental research—GLOWA. IOLR report T22/2005
Rimmer A, Salingar Y (2006) Modelling precipitation-streamflow processes in Karst basin: the case of the Jordan River sources, Israel. J Hydrol 331(3–4):524–542
Rimmer A, Gal G (2003) The saline springs in the solute and water balance of Lake Kinneret, Israel. J Hydro 284(1–4):228–243
Rimmer A, Givati A, Samuels R, Alpert P (2011) Using ensemble of climate models to evaluate future water and solutes budgets in Lake Kinneret, Israel. J Hydrol 410:248–259
Rom M (1994) Creating synthetic time series of available water for Lake Kinneret, Watershed Unit, Mekorot, Israel (in Hebrew)
Sade R, Litaor MI, Shenker M (2010) Evaluation of groundwater and phosphorus transport in fractured altered wetland soils. J Hydrol 393(1–2) 133–142. doi:10.1016/j.jhydrol.2010.02.032
Sade R, Salingar Y, Denisyuk M, Rimmer A (2014) Water management in complex hydrological basin—application of water evaluation and planning tool (WEAP) to the Lake Kinneret watershed (submitted)
Samuels R, Rimmer A, Hartmann A, Krichak S, Alpert P (2010) Climate change impacts on Jordan River flow: downscaling application from a regional climate model. J Hydrometeorol 11:860–879
Schulla J, Jasper K (2000) Model Description WASIM-ETH (water balance simulation model ETH), ETH-Zurich, Zurich
Serruya C (ed) (1978) Lake Kinneret. Junk, The Hague
Shentsis I, Ben-Tzvi A (1994) Updated model to predict the available water for Lake Kinneret. Israeli Hydrological Service, report, 94/2 (in Hebrew)
Sieber J, Purkey D (2002) WEAP. Water evaluation and planning system user guide for WEAP21. Stockholm Environmental Institute—Boston, and Tellus Institute, user guide for WEAP21, Boston, MA
Simon E (2006) Hydrometeorological model for stream flow calculations. Water Eng 45:14–18 (in Hebrew)
Simpson B, Carmi I (1983) The hydrology of the Jordan tributaries (Israel). Hydrographic and isotopic investigation. J Hydrol 62:225–242
Sivapalan M, Ruprecht JK, Viney NR (1996) Water and salt balance modeling to predict the effects of land-use changes in forested catchments. 1. Small catchment water balance model. Hydrol Process 10:393–411
Smiatek G, Kunstmann H, Heckl A (2011) High resolution climate change simulations for the Jordan River area. J Geophys Res Atmos 116:D16111. http://dx.doi.org/10.1029/2010JD015313
TAHAL (1968–1986) The annual water-solute-energy balances of Lake Kinneret. TAHAL, Tel-Aviv (in Hebrew)
Weinberger G, Givati A, Livshitz Y, Zilberbrand M, Tal A, Weiss M, Zurieli A (2012) The natural water resources between the Mediterranean Sea and the Jordan River, Israeli Hydrological Service, Jerusalem

Chapter 8
Salinity

Alon Rimmer and Ami Nishri

Abstract The salinity of Lake Kinneret, which fluctuates between 190 and 280 mg L^{-1} Cl^-, is significantly higher than the salinity of surface streams that flow to the lake. The high salinity is mainly derived from saline groundwater that emerges through offshore and onshore springs along the coast of the lake. Smaller amounts of solutes are attributed to dispersed seepage and molecular diffusion from the bottom of the lake. This chapter reviews the salinity of Lake Kinneret from the following aspects: the history of salinity measurements, the karst hydrological system of the saline springs that recharge the lake, analysis of the lake solute balance, the chemical composition of the lake as a result of the saline spring's contribution, hydrological conceptual model of the salinization mechanism, and finally, a complete mixing type model to predict the future salinity of the lake is presented.

Keywords Saline springs · Dead Sea Rift (DSR) brines · Solute–water balance · Confined fractured aquifer · Complete mixing model

8.1 Introduction to the Salinity of Lake Kinneret

The salinity of Lake Kinneret (241 ± 25 mg L^{-1} Cl^- during 1987–2010) is significantly higher than the salinity of the water from surface streams (17–30 mg L^{-1} Cl^-) that flow to the lake. It is also higher than the salinity of most fresh groundwater sources in the region. By pumping annually ~300 million cubic meters (10^6 m^3) of water from the lake through the "National Water Carrier" (NWC) to the coastal area of Israel, the lake water is used for drinking, irrigation, and reuse in the populated areas located above the coastal aquifer.

Prior to the operation of major desalination plants in Israel (before the year 2010), Lake Kinneret water was extensively used for agricultural irrigation, both as original Lake Kinneret water and as reused water. Since the salinity of reused Kinneret water

A. Rimmer (✉) · A. Nishri
The Yigal Allon Kinneret Limnological Laboratory, Israel Oceanographic & Limnological Research, P.O. Box 447, 14950, Migdal, Israel
e-mail: alon@ocean.org.il

A. Nishri
e-mail: nishri@ocean.org.il

T. Zohary et al. (eds.), *Lake Kinneret, Ecology and Management,* Aquatic Ecology Series 6, 113
DOI 10.1007/978-94-017-8944-8_8,

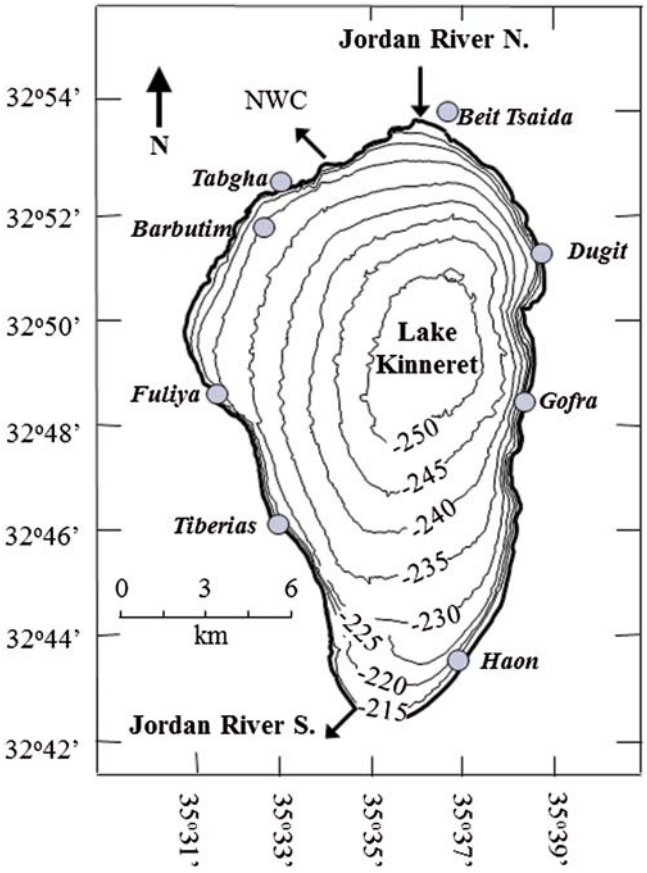

Fig. 8.1 A bathymetric map of Lake Kinneret. Locations of known saline springs are marked

may reach ~400 mg L^{-1} Cl^{-}, a rather problematic concentration for most irrigated crops, this posed a threat to the sustainability of the groundwater and agriculture soils near the coastal areas. Following the connection of desalination plants to the NWC, the chloride concentration was reduced in the water supplied to the coastal area, and the chloride concentrations in the reused effluents are now ranging between 180 and 250 mg L^{-1}. Currently, the problem of water quality associated with the lake salinity is restricted to locations where the lake water is consumed directly.

The salinity of the lake is derived from saline groundwater that emerges mainly through springs along the west coast of the lake (Fuliya (Ful), Tabgha (Tab), and Tiberias (Tib) springs, Fig. 8.1). A smaller contribution of salinity originates from saline seepage at the east coast (Haon, Gofra, Dugit, and Bet Tsaida), and an additional small amount is attributed to seepage from the bottom of the lake (Stiller et al. 1975; Simon and Mero 1992; Stiller 1994). Some of these springs emerge inside the lake (offshore springs) and some on the lake shore (onshore springs).

In this chapter, several aspects of Lake Kinneret salinity are presented in the following order: (1) the history of the lake salinity (~1950–2010), (2) the geohydrological setup, which is directly associated with the Kinneret saline springs, (3) lake solute balance, (4) the geochemical composition of Lake Kinneret, (5) the mechanism of saline springs, and (6) Lake Kinneret long-term salinity model

8.2 The History of Lake Kinneret Salinity

The history of the lake salinity has been documented since the beginning of the twentieth century. The first measurement was reported by the British researcher Annandale in 1913 (Dalinsky 1969) in which Cl^- concentration was 239 mg L^{-1} Cl^-. The British Mandate Hydrological Service (the Israeli Hydrological Service, IHS, since 1948) reported 300 mg L^{-1} Cl^- in 1934. At least seven lake salinity measurements were reported between the years 1945 and 1950 in which lake salinity fluctuated between 260 and 300 mg L^{-1} Cl^-. In 1949, a survey was conducted (Oren 1957) in which Cl^- concentration was measured at various depths of the lake. More regular measurements, conducted by the IHS, Tahal (Israel water planning), Mekorot (Israel water supply company), and KLL-IOLR from 1951 to 2010 created the 60-year time series of salinity elaborated in Fig. 8.2. Since 1964, most of the onshore springs in Tab and Tib were diverted to the "Saline Water Carrier" (SWC) pipe (step 4 in Fig. 8.2, location in Fig. 1.1 of Chap. 1), which carries the brackish water south to the lower Jordan River, thus reducing the lake's potential salinity by ~30%. The potential main contributors of salinity to the lake after the initiation of solute diversion are mainly the offshore springs in Ful, Tab, and Tib.

Rimmer (2007) identified two dominant procedures which caused the salinity of the lake to decrease from an average of ~350 mg L^{-1} Cl^- in the 1960s to ~210 mg L^{-1} Cl^- during the end of the 1980s and then to increase back to ~280 mg L^{-1} in 2010. The major cause, which acted to reduce salinity (step 4 in Fig. 8.2), was the step reduction in solute inflows from $\sim 160 \times 10^6$ to $\sim 105 \times 10^6$ kg Cl^- $year^{-1}$, following the operation of the SWC that started in January 1965. The second procedure, which acts to increase the salinity, was the reduction of inflows from surface runoff (Chap. 7). Analysis of the long-term annual data shows that total water inflow, which was $\sim 780 \times 10^6$ m^3 during the 1960s, was reduced to $\sim 650 \times 10^6$ m^3 in the 2000s, while solutes mass inflows from all sources remained almost the same. This reduction resulted in a change of the leaching ratio (outflows to lake volume) from ~0.12 in 1987 to ~0.09 in 2010 and hence increased the salinity.

An interesting development in the lake salinity occurred prior to the diversion of the saline springs during the years 1954–1962, when lake salinity increased significantly (steps 1–2 in Fig. 8.2). Kolodny et al. (1999) pointed out that less water (and salt) was released from the lake during that period, causing lake level and salinity to increase as well. Indeed, the average annual outflow for these years was $\sim 350 \times 10^6$ m^3 (significantly lower than the known multi-annual discharge), while lake volume increased by $\sim 140 \times 10^6$ m^3. However, water and solute balance

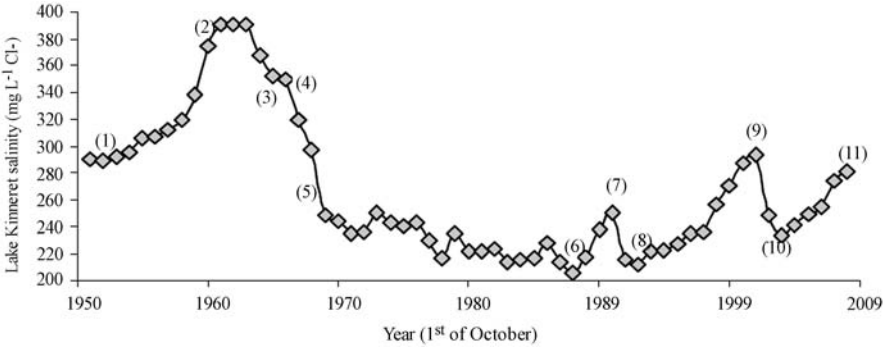

Fig. 8.2 The long-term record of Lake Kinneret salinity from 1951 to 1987 (data: Tahal, Israel water planning) and from 1987 to 2009 (data: Mekorot Water Company). Values presented are annual mean chloride concentration for the entire lake. *1* During the years 1954–1962, a significant increase. *2* Between 1961 and 1963 reaching peak values of ~390 mg L^{-1} Cl^-. *3* In 1964, the NWC became operative, chloride content began to drop. *4* SWC was fully operated in January 1965, preventing an average of ~55,000 t Cl^- from flowing into the lake, salinity decline was enhanced. *5* Lake salinity decline was further enhanced by the exceptionally rainy winter of 1968–1969 (inflows of 200% compared to an average year). *6* The lowest lake salinity, 192 mg L^{-1} Cl^-, was reported in May 1988. *7* Salinity increased to 250 mg L^{-1} Cl^- following three dry winters. *8* Salinity decreased to ~210 mg L^{-1} Cl^- following the exceptionally rainy winter of 1991–1992. *9* Salinity increased to ~290 mg L^{-1} Cl^- from the end of the winter 1993–1994 to the winter of 2001–2002. *10* Following the extreme winter of 2002–2003, the salinity was reduced to ~230 mg L^{-1} Cl^-. *11* From 2004 to 2011, the salinity bounced again to ~280 mg L^{-1} Cl^-

calculations from 1 October 1954 to 1 October 1962 suggest additional solute inflows during this period. From solute balance calculations, it is possible that during this 8-year period, the input of solutes to the lake increased to an annual average of ~168,000 t of Cl^-, i.e., 8,000 t higher than any calculated average measured since 1960 (see details in the solute balance section). The reasons for such an increase remained unexplained for decades, especially because of the exceptional combination of dry years and a large amount of solute inflows.

One explanation for this increased contribution of the saline springs during the years 1954–1962 is a natural cause. However, knowing today the effect of artificial solute removal or addition to the lake, another explanation is suggested. From the experience of lake salinity research during later years, it is known that artificial boreholes, drilled to the depth of ten to several hundred meters in the lake bottom, or very close to the lakeshore, may result in a significant artesian flow with various degrees of salinities. Some of these boreholes perform artesian flow until present, and in one of them (known as Kinneret 7 or "the hidden waterfall" near Tab), the measured solute discharge is nearly 5,000 t annually. During the 1950s, the State of Israel carried out intensive research on the Lake Kinneret salinity, in preparation to develop and operate the NWC. As part of this research effort, at least 60 new boreholes (IHS database) were drilled in the region of the west coast of the lake, from which at least 28 boreholes were drilled offshore in the bottom of the lake. It is suggested that the massive drilling during the 1950s resulted in a temporary distur-

bance to the steady hydrological system of the lake aquifer and a temporary increase in solute flux of the lake (an average of less than 2,000 t Cl^- per offshore borehole). The effect of these boreholes faded throughout the years after they were abandoned, artificially blocked, or clogged by natural sedimentation in the lake.

8.3 Hydrogeological Setup

The saline springs on the west coast discharge into the lake through fractures and faults in the Judea Group carbonate-confined aquifer system (JGA, Gvirtzman et al. 1997). This JGA system overlays deep-seated brines from which a flux of saline water mixes with fresh groundwater. Diluted saline water drains through fractures mainly to the springs, and to a small extent, through the lakebed (Stiller 1994; Hurwitz et al. 1999; Hurwitz et al. 2000a). This hydrological setup was first proposed by Goldschmidt et al. (1967) and modified by Mercado and Mero (1985), Simon and Mero (1992), Gvirtzman et al. (1997), and Rimmer et al. (1999). An illustration of this hydrogeological setup is presented in Fig. 8.3. It includes (a) phreatic upper and lower JGA units recharged by rainfall in the Eastern Galilee Mountains, (b) two confined JGA units near the western Lake Kinneret shoreline, which drain to both onshore and offshore springs through fractured regions, and (c) Lake Kinneret. Hurwitz et al. (2000b) showed that the source of the "Kinneret Brine" (Fig. 8.3) was in a short high-stand phase of the former Lake Lisan (some 18,000 years ago in the late Pleistocene), when saline water of the Lisan percolated into the subsurface (see Chap. 3). Since its recession from the Kinarot basin and the instantaneous formation of the freshwater lake (Kinneret), the previously intruded brine has been flushed backward toward the lake through what is now called the saline springs.

In order to understand the water management problems associated with the salinity of Lake Kinneret, we need to readdress what was commonly known as the lower "Red Line" problem. This line refers to the lowest permitted water level in the lake, set by the Israeli Water Authority. A major motivation for declaring a lower "Red Line" was the concern that declining water levels may lead to increased influx of salt via the saline springs and ground seepage and hence cause severe salinization of Lake Kinneret. On the other hand, given a fixed upper red line, by lowering the lower red line, it was possible to increase the lake's storage capacity.

Two generic conceptual models were proposed to assess the effect of water level on the saline water ascent to the springs, each having an opposing management consequence: Mero and Mandel (1963), Mero and Zaltzman (1967), and Mazor and Mero (1969) hypothesized that overpressure of deep-seated saline water results in their ascent to the surface where they mix with shallow circulating water. According to this "self-potential" model (SPM, see Fig. 8.3), the forces that generate overpressure are independent of the recharge in the Eastern Galilee Mountains, and are created either by compaction of sediments, active tectonic stresses, or a geothermal source. Another mechanism that could produce a similar effect to the SPM is

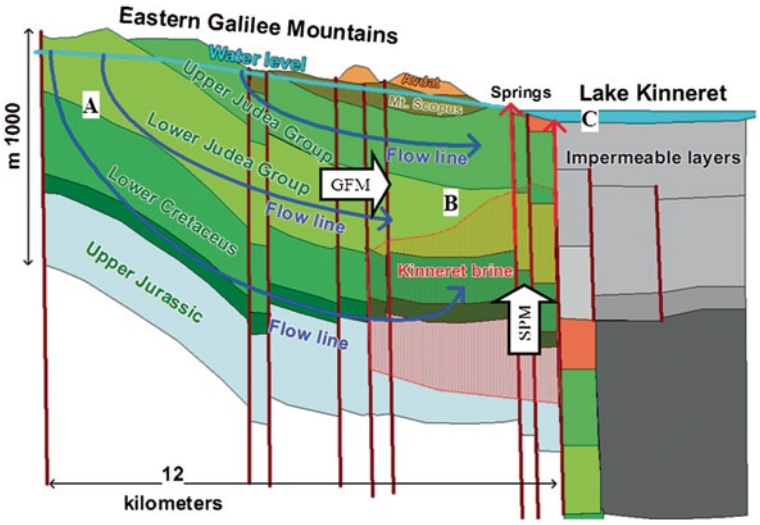

Fig. 8.3 A conceptual structure illustrating the main units of the Lake Kinneret saline aquifers at the west coast. **a** Phreatic upper and lower Judea Group aquifer (JGA) units in the Galilee Mountains. **b** Confined upper and lower JGA units. **c** Lake Kinneret. The *large arrows* indicate the possible mechanisms that cause overpressure: *GFM* gravity driven flow model, *SPM* self-potential model. (Geological structure following Gvirtzman et al. 1997. Modified from Gvirtzman et al. 1997 with permission from Wiley)

the hydraulic pressure in the deep Lower Cretaceous aquifer (Fig. 8.3), which has a relatively very low hydraulic conductivity.

The implications of the SPM hypothesis on managerial decisions were: (1) Fresh groundwater levels in the Eastern Galilee (west of the lake) make a counterbalance to the driving pressure and therefore should not be decreased. Consequently, pumping of groundwater from this area was limited by the Israeli Water Authority for four decades (1960–2000). (2) The lake level should not be reduced below a prescribed "red line," which was posed for many years on −212 m, and later on −213 m a.m.s.l. (Chap. 7). It was claimed that lowering the water levels in both the lake and adjacent aquifers will increase the hydraulic gradient between the saline water and lake, and thus intensive seepage of saline water through the lake sediments will take place.

On the other hand, Goldschmidt et al. (1967), Gvirtzman et al. (1997), and Rimmer et al. (1999) showed that gravity-driven flow (gravity-driven flow model, GFM, Fig. 8.3) plays the major role forcing groundwater and solute emergence at springs along the west shore of Lake Kinneret. According to this model, rainwater that recharges the JGA aquifers in the elevated part of the Galilee Mountains applies pressure on the saline deep-sited groundwater. The upper and lower JGA hydrogeological units to the east and closer to Lake Kinneret become separated by impermeable layers (the Dir Hana formation), thus forming a lower aquifer containing saline water overlain by an upper much fresher aquifer. The hydraulic head acquired in the elevated part of the Galilee Mountains affects both aquifer units. The

consequence of the GFM model on managerial decisions is dual: (1) The flow of saline springs depends on a ~100-m head gradient between aquifers in the Eastern Galilee and Lake Kinneret, and therefore the 1–4 m change in the lake water level has negligible effect on this flow. (2) Reduced hydraulic heads in deep aquifers in the Galilee will lead to reduction of the pressure applied on the deep saline reservoir, and therefore salt flux into the lake will decrease.

A series of studies during the years 1995–2000 (see also Sect. 8.6) came up with an important understanding that the GFM mechanism controls the discharge of the saline springs. These findings resulted in the decision to lower the "red line" during 1999–2001 to lower water levels without fear of enhanced salinization.

However, the mechanism of the saline springs is not yet completely understood. Two large-scale 3D ground water modeling studies focused on the JGA (Abbo et al. 2003; Yechieli et al. 2011). They revealed that the spring's solute originates from a major source of brine in layers deeper than the JGA. Although the full mechanism of this source is still unknown, it can be attributed to one or more of the mechanisms proposed by the SPM.

8.4 The Solute Balance of Lake Kinneret

The water–solute balance of Lake Kinneret is calculated annually by the Mekorot Watershed Unit (1987–2011) and the results are used by the Israeli Water Authority for managerial decisions (Chaps. 7 and 31). When measured variables of the solute balances (Cl^- mass represents salinity) are separated from the unknowns (Assouline 1993), the monthly solute balance equation of Lake Kinneret is:

$$S_{Sp} = \Delta S_L + \sum S_{out} - \sum S_{in}. \tag{8.1}$$

The monthly measured quantities (ton of Cl^-) at the right-hand side of Eq. (8.1) are the change of solute mass in the lake (ΔS_L); the outflows, (S_{out}), including release of solutes to the lower Jordan River through the Degania Dam, withdrawal of solutes by pumping to the NWC and to private consumers; and the inflows (S_{in}) which include solute discharge from: (a) several monitored saline springs, (b) upper Jordan River, (c) solute discharge originated in runoff from the direct watershed, (d) solute diverted to the lake from the Yarmouk River, and (e) solutes from direct rainfall (Mekorot 1987–2011 reports). The monthly unknown quantity (S_{Sp}) at the left-hand side of Eq. (8.1) is the contribution of the unmonitored onshore and offshore saline springs. This unknown encompasses the average salinity (C_{Sp}) multiplied by the discharge (Q_{Sp}) of the unmonitored springs. Rimmer and Gal (2003) showed that there is an unavoidable measurement error of ~11,000 t Cl^- associated with calculating this unknown using the right-hand side of Eq. (8.1). This error, on top of an average ~7,600 t Cl^- that originate from the unmonitored springs on a monthly basis, often results in nonphysical monthly values, such as negative spring discharges and/or negative or extremely high values of spring salinities. In order to minimize

Table 8.1 The annual averages and standard deviations of water and chloride balances for Lake Kinneret during the years 1987–2010

Characteristic	Units	Average	SD
Annual water inflows			
Direct rainfall	10^6 m^3	66.65	18.66
Streams	10^6 m^3	487.59	198.79
Groundwater	10^6 m^3	71.41	31.23
Artificial recharge	10^6 m^3	23.30	11.30
Total	10^6 m^3	648.95	202.41
Annual water outflows			
Evaporation	10^6 m^3	242.16	18.25
Pump and release	10^6 m^3	415.41	142.83
Total	10^6 m^3	657.58	143.99
Annual chloride inflows			
Direct rainfall and fallout	10^3 kg	333.25	93.29
Streams	10^3 kg	9,140.61	5,447.17
Groundwater	10^3 kg	91,712.39	16,976.82
Artificial recharge	10^3 kg	3,145.91	1,524.96
Total	10^3 kg	104,332.16	17,894.64
Annual chloride outflows			
Pump and Release	10^3 kg	98,623.57	33,018.22
Lake			
Cl^- concentration	mg L^{-1}	241.76	24.97
Average chloride mass	10^3 kg	920,693.57	48,728.32
Average residence time	Year	10.50	3.95

SD standard deviation

the effect of these uncertainties, Rimmer and Gal (2003) proposed that the average salinity of the unmonitored saline springs was nearly constant (~1,280 mg L^{-1} Cl^-). Using the lake water and solute balances (Table 8.1), the average annual (1987–2010) mean discharge from the ungauged saline springs was approximated as ~71×10^6 m^3 (only 11 % of the water inflows), and the annual solute discharge was $91{,}712\times10^3$ kg Cl^- ($7{,}642\times10^3$ kg Cl^- monthly, Fig. 8.4), nearly 88 % of the entire solute inflows to the lake.

The long-term calculated record of monthly saline springs discharge and salinity (Rimmer and Gal 2003) were used to clarify issues of the salinization mechanism, which were under debate for several decades. First, a positive relation was found between both water and solute discharges of the saline springs and lake water levels, i.e., lower fluxes of saline groundwater were usually associated with lower water level during dry winters—opposite to what was expected under the SPM mechanism. Second, it was found that the solute discharge to the lake increases with water discharge, in agreement with the GFM and the conclusions of Benoualid and Ben-Zvi (1981), but again in contrast with the expected results from the SPM mechanism.

A study by Tal and Rimmer (2008) was carried out in order to compare the water and solute discharge of the unmonitored springs from Mekorot (1987–2011)

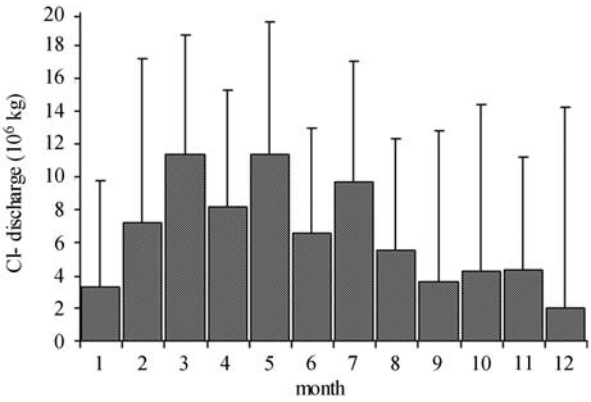

Fig. 8.4 The calculated residual of the Lake Kinneret solute balance (1970–2005) attributed to the Cl^- contribution of the ungauged saline springs: monthly averages and standard deviations. Note the possible large errors associated with monthly calculations

reports and the results of periodic springs discharge and salinity surveys conducted by the IHS. They indicated that most of the unmonitored water inflows can actually be attributed to unmonitored onshore springs, while in the solute mass from the spring's survey there was an annual average of ~22,000 t of Cl^- missing compared to the solute balances of Mekorot. They concluded that in the lake solute balance there is probably an unknown contributing source with small water discharge ($\sim 1–2 \times 10^6$ m^3) having rather large salinity that adds the missing ~22,000 t annally.

8.5 The Chemical Composition of Salinity Sources to Lake Kinneret

A typical chemical composition of Lake Kinneret water, given in mg L^{-1} for winter 2002 (Katz and Nishri 2012), is as follows: Cl^-, 283; Na^+, 141; Mg^{2+}, 34.7; Ca^{2+}, 53; alkalinity (as HCO_3^-), 155.5; SO_4^{2}, 57; K^+, 7.4; Br^-, 2.02; and Sr^{2+}, 0.765. With such chemical composition Lake Kinneret may be considered a relative freshwater lake, affected by salinity which originates from the Dead Sea Rift (DSR) brines. This section discusses only the sources of conservative ions to this lake while others, such as Ca^{2+}, HCO_3^-, and Sr^{2+}, are discussed in Chaps. 23 and 28.

According to Starinsky (1974), the DSR brines were first formed by on-surface evaporation of sea water well within the halite deposition domain, leading to molar ratios of $Na^+/Cl^- < 0.86$ and $Br^-/Cl^- > 3.3 \times 10^{-3}$. The next stage involved seepage into subsurface and subsequent enrichment of the residual brine with Ca^{2+} and loss of Mg^{2+} attained by dolomitization of the surrounding Ca-carbonate rocks. The Ca-chloridic brines ($Ca^{2+} > SO_4^{2-} + HCO_3^-$: concentration in equivalents) that evolved are now emerging from springs in and around Lake Kinneret. The chemical composition of many springs was found (Klein Ben-David et al. 2004) to plot on an almost perfect straight line on a Br^-/Cl^-–Na^+/Cl^- diagram. The model proposed by these authors suggests that the DSR line extends between two points each of which

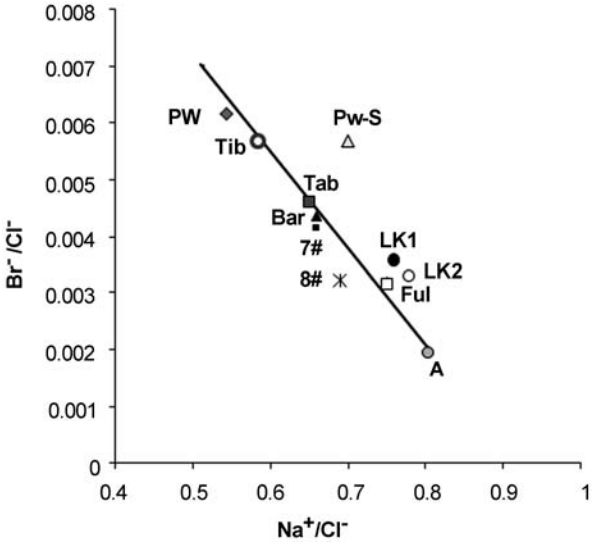

Fig. 8.5 Molar ratios of Na^+/Cl^- versus Br^-/Cl^- measured in brines located nearby Lake Kinneret (labeled points). The *straight line* represents a linear regression of brine compositions measured in the Dead Sea Rift (DSR) by Klein Ben-David et al. (2004). *PW* pore water from Lake Kinneret center at Sta. A, *Pw-S* pore water from Lake Kinneret south at Sta. D, *Tib* Tiberias hot springs, *Tab* Tabgha onshore saline water diverted in 1964, *Bar* Barbutim offshore springs, *7#* Well Kinneret 7 in Tabgha group, *8#* Well Kinneret 8 north of Tabgha group, *LK1* Lake Kinneret at Sta. A in 1960 prior to salt water diversion, *LK2* Lake Kinneret in 1995 at Sta. A, *Ful* Fuliya main offshore springs, *A* a hypothetical brine located at the lower edge of the DSR line

represent hypothetical end member brine, of which one (point **A** in Fig. 8.5) is located at the halite and the other at the bischofite stability fields. The DSR brines are claimed to be mixtures, at various proportions, of these two end members (Klein Ben-David et al. 2004).

In Fig. 8.5, we present part of this DSR line and the potential sources of salinity to Lake Kinneret, with point **A** brine depicted but without the inclusion of the end member located in the bischofite field (which has coordinates of $Na^+/Cl^- = 0.007$ and $Br^-/Cl^- = 0.155$). The composition of Lake Kinneret surface water is given for two periods: LK1 for the early 1960s, prior to the diversion of the onshore Tab and Tib saline springs through the SWC, and LK2 for the mid-1990s, i.e., 35 years after the diversion started. Apparently, this diversion had a significant effect on the chemical composition of Lake Kinneret water (Nishri et al. 1999), which has drifted away from the domain closer to Tab and Tib brines toward higher Na/Cl^- and lower Br^-/Cl^- ratios. Since there are no known brines with higher Na^+/Cl^- and lower Br^-/Cl^- ratios than LK2, and since LK2 has a similar composition to that of the Ful springs, it was concluded that the these springs must be the present major source of Na^+, Cl^-, and Br^- to Lake Kinneret (Nishri et al. 1999; Kolodny et al. 1999; Katz and Nishri 2012).

This conclusion rules out the possibility that Tib and the other western (or eastern) offshore springs play a significant role in Cl^- contribution to Lake Kinneret. Notice, however, that in comparison to Ful type water, the composition of Lake Kinneret water is somewhat shifted to higher Na^+/Cl^- ratios. This can be shown to result from the relatively small but still significant contribution of these solutes from the freshwater streams, including the Jordan River which is characterized by an average Na^+/Cl^- of 0.94. Model calculations by Kolodny et al. (1999) and the Cl^- budgets given in Table 8.1 suggest that ~9% of Cl^- and Br^- loads to Lake Kinneret originate from freshwater streams. The remainder, ~90%, which amounts to ~90,000 t of Cl^-, is then attributed to saline sources. However, the monitoring of the two main offshore springs of Ful reveal that less than half of it enters the lake via these seepages. This may suggest that the remainder inflows from smaller seepages dispersed along the local shore line (Tal and Rimmer 2008).

The molar ratio of Mg/Cl^- in the brines (Klein Ben-David et al. 2004) varies from 0.05 in the Tib springs to 0.08 in the Tab springs and to 0.14 in the Ful springs, as well as in the Lake Kinneret pelagic center pore water (PW) and in Haon and Beit Tsaida brines. Lake Kinneret, however, is characterized by a higher ratio of $Mg/Cl = 0.18$, suggesting the occurrence of another significant source of Mg, beside the Ful springs, with $Mg/Cl > 0.18$. Here again freshwater sources including the Jordan River and the smaller basaltic streams, which are characterized by respective ratios of $Mg/Cl^- >> 0.18$, supply the excess Mg needed to explain the gap between Ful and Lake Kinneret Mg/Cl^- ratios (Katz and Nishri. 2012). Kolodny et al. (1999) attributed ca. 50% of Mg inflows to freshwater streams.

The PW in the sediments underlying the Lake Kinneret pelagic zone has significantly higher salinity than that of the lake (Stiller 1994; Goldman et al. 2004; Stiller et al. 2009). The concentration of conservative major ion solutes (Cl^-, Na^+, Mg, and Br^-) increases linearly with depth approaching Cl^- concentration in PW of 9,060 mg L^{-1} at 18 m depth below the pelagic surface (Nishri, unpublished). The upper 2 m of the PW column is affected by the much fresher boundary with lake water above. Below this depth, $Cl^-/Na^+/Br^-/Mg$ ratios tend to stabilize (Stiller et al. 2009), suggesting that these represent the compositions of the PW brines underlying Lake Kinneret pelagic sediments. The compositions of the PW brine in the lake center and northern part are close to that of the DSR line (Fig. 8.5) but differ from that of the southern basin (Fig. 8.5). Despite the apparent steep concentration gradients prevailing along the PW column, it was estimated (Stiller 1994) that less than 3,000 t Cl^- may annually be released from this source to Lake Kinneret through molecular diffusion. This conclusion is supported by Rimmer et al. (2005) who in their report showed negligible Cl^- accumulation in the relatively isolated hypolimnion during the stratified period. Hypolimnetic Cl^- concentration increases by less than 2 mg L^{-1} over the 8–9 months of the stratification process, which amounts to less than 2,000 t.

The isotopic composition of oxygen and deuterium in the water of Lake Kinneret resembles that of the PW ($\delta H_2{}^{18}O = -0.9 \pm 0.6$‰: $\delta^2H_2O = -3 \pm 4$‰ Stiller et al. 2009). Stiller (1975) detected tritiated (^3H_2O) PW in the upper part of the pelagic PW column. Both types of isotopic data suggest that the water molecules in the bed sediments

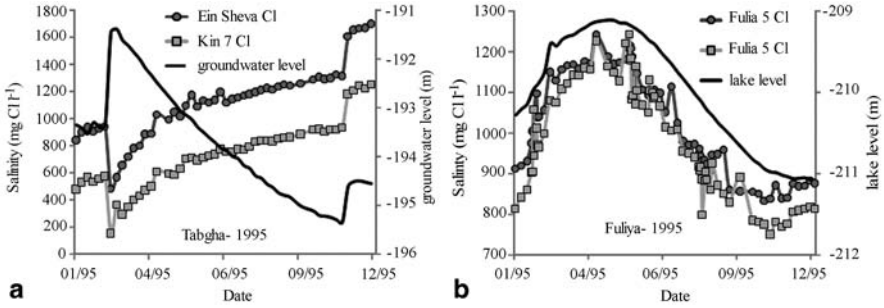

Fig. 8.6 Typical monitoring data of Cl^- concentration and the water level of the driving force during 1995: **a** In Tabgha springs (Ein Sheva and Kin 7 sampling sites), during the dry season groundwater level decreases and salinity increases exponentially with time. **b** In Fuliya springs (two sampling sites), salinity is in correlation with lake level

of Lake Kinneret are affected by diffusion from above whereas chemical data suggest that salinity components diffuse upward from the deep-sited brine (Stiller et al. 2009).

The PW in the pelagic bed sediments may have evolved through a similar mechanism as other saline water sources in the DSR, i.e., through mixing of end brines discussed earlier, but eventually emplaced within the bed sediments of this lake, perhaps during the formation of the Pleistocene precursor of Lake Kinneret, the saline Lisan Lake (Hurwitz et al. 1999). Besides residing on the DSR line, the singular chemical composition of the pelagic PW brine (Fig. 8.5) may also suggest that it is hydraulically disconnected from other saline sources to this lake.

8.6 Saline Springs Mechanism

The saline springs of Tab, Ful, and Tib are the discharge points of a confined carbonate aquifer, interacting with a "discharge lake" (a lake situated downstream of all ground water sources) through fractures and faults (Issar 1993; Gvirtzman et al. 1997; Bergelson et al. 1998; Rimmer et al. 1999; Abbo et al. 2003).

The most interesting and unusual phenomenon regarding these three major groups of springs is that despite the similarity in their general geological setup, they differ significantly from one another in their hydrological characteristics. Discharge and salinity in the Tab springs are strongly correlated with rainfall events and groundwater level. Groundwater levels increase and salinity drops significantly following rainy days, while during the summer dry period groundwater levels and discharge drop, while salinity increases exponentially (Fig. 8.6). At the same time, in the Ful springs, the discharge, groundwater level nearby, and the salinity are strongly positively correlated with lake level (Fig. 8.6) and therefore their general groundwater flow mechanism appears to be different from that operating in the Tab springs. The discharge of the Tib springs is correlated with lake level, while its salinity is very high (~18,000 mg L^{-1} Cl^-) and steady over time, compared to the other two groups of springs.

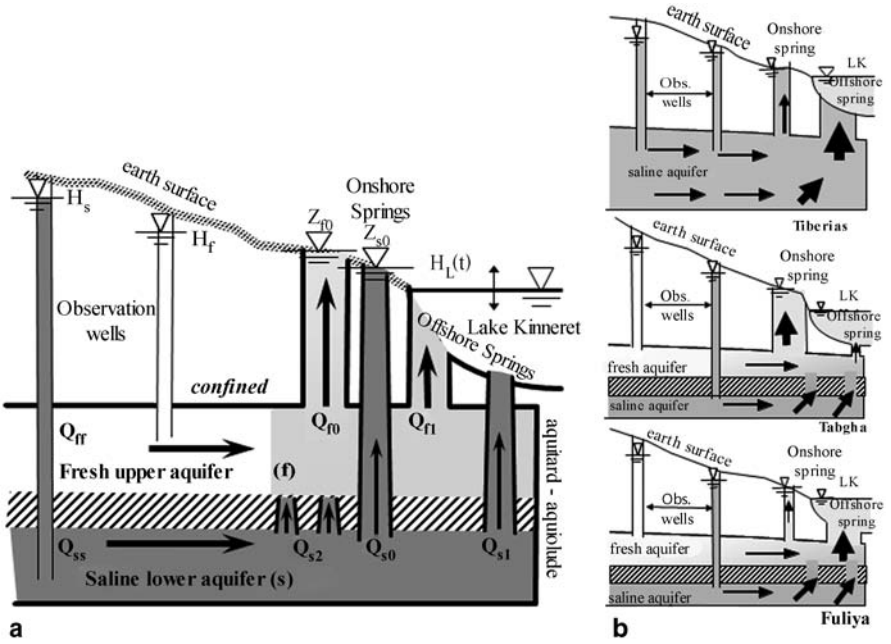

Fig. 8.7 Conceptual model of saline water discharge along the lake's shore: **a** The general structure of the model includes mixing between waters from the saline aquifer (Q_{ss}) and the freshwater aquifer (Q_{ff}). Emergence of saline waters to the mixing zone (Q_{s2}) results from discharge from the higher hydraulic head in the saline water, H_s, to the lower head in the mixed zone H_f. Both the saline water (denoted by *s*) and mixed aquifer (*f*) may leak directly to onshore springs (Q_{s0} and Q_{f0}, respectively) and to the lake bottom (Q_{s1} and Q_{f1}). The saline water and mixed aquifers may drain through a constant head boundary (z_{s0}, z_{f0}), representing onshore springs, and a time varying boundary $H_L(t)$, representing offshore springs. **b** Adaptation of the general concept to Tiberias, Tabgha, and Fuliya springs

The conceptual structure proposed by Rimmer et al. (1999) and modified by Rimmer and Hartmann (2012) was based on the assumption that the spatial distribution of fractured regions, which connect between the aquifer and the lake, is the most important degree of freedom, which distinguishes between the three groups of springs. This conceptual model (Fig. 8.7) consists of two confined aquifers for all three sites (Tab, Ful, and Tib). The lower aquifer corresponds to the lower Judea and Kurnub geological groups and carries saline water, characterized by high chloride concentration in the vicinity of the springs. The upper aquifer includes the top Judea Group and in some cases the Avdat Group aquifer. It carries freshwater characterized by low chloride concentration. In the Galilee, both aquifers have phreatic areas (Fig. 8.7). The lower freshwater aquifer recharged in the Galilee produces hydraulic pressure on the saline water, trapped in a narrow (east-west direction) zone in the vicinity of lake's shore, and pushes them toward emergence points along the western shore line of Lake Kinneret.

The conceptual model shown in Fig. 8.7 describes discharge (Q) between different parts of the system represented by arrows and subscript indices. Mixing between

waters from the two aquifers takes place through fractures in a narrow zone in the vicinity of the lake's shore. Emergence of saline waters to the mixing zone (Q_{s2}) results from discharge from the higher hydraulic head in the saline water, H_s, to the lower head in the mixed zone H_f. According to the unified concept, both the saline water and mixed aquifer may leak directly to onshore springs (Q_{s0} and Q_{f0}, respectively) and to the lake bottom (Q_{s1} and Q_{f1}). The saline water and mixed aquifers are drained through a constant head boundary (z_{s0}, z_{f0}), representing onshore springs, and a time-varying boundary $H_L(t)$, representing offshore springs, respectively. The $H_L(t)$ represents the effect of changing lake level on the discharge from both the onshore and offshore springs. The lateral eastward discharge of freshwater within the lower and upper aquifers are Q_{ss} and Q_{ff}, respectively.

Basic physical considerations can simplify the proposed unified conceptual model for each group of springs. In the Tib springs, the absence of the upper freshwater aquifer (shown in Fig. 8.7a) eliminates Q_{s2}, Q_{f0}, and Q_{f1} from the system (Fig. 8.7b). That is why the saline water in the Tib springs is not mixed with freshwater, leaving the original high salinity of the lower aquifer. In Tab and Ful (Fig. 8.7b), the direct discharge from the saline aquifer to onshore and offshore springs (Q_{s0} and Q_{s1}) was excluded since springs with high chloride concentrations (> 15,000 mg L^{-1} Cl^-) were not found in these groups, and it is not reasonable that emerging saline water will cross a freshwater aquifer without being diluted.

The question which remained open was the reasons for the different temporal characteristics of the Tab and Ful springs. Using the system described in Fig. 8.7, Rimmer et al. (1999) and Rimmer (2000) defined α_0 and α_1 as the conductance between the confined aquifer and the onshore and offshore springs, respectively. When $\alpha_0 >> \alpha_1$, the effect of the lake temporal behavior is negligible and the hydrology of the spring system (i.e., the exponential reduction of discharge and the increased measured salinity in the springs, Fig. 8.7a) is determined by the upstream aquifer (Tab, aquifer-dominated springs). On the other hand, when $\alpha_0 << \alpha_1$, the lake influence is dominant, it curtains the influence of the upstream aquifer levels, and therefore springs discharge and salinity is in correlation with Lake Kinneret level (Ful lake-dominated springs). This approach was later verified by more detailed analytical (Rimmer and Hartmann 2012) and numerical models (Abbo et al. 2003; Kessler and Rimmer 2003; Yechieli et al. 2011).

There are several practical implications for these conclusions. First, due to the variety of observed characteristics of the springs, which is supported by physically based analysis, it is obvious that the measured discharge, head, and salinity in a spring or a group of springs are rarely in agreement with the characteristics of the other groups of springs, and therefore generalization and integration of results should be performed with extra care. Second, the system of the springs proved that the Ful springs site is not sensitive to changes in groundwater levels in the Eastern Galilee, and therefore its monitoring could not provide the right future observations regarding increased pumping at the Eastern Galilee aquifers. On the other hand, monitoring the springs in Tab may provide good evidence for changes in groundwater levels and contribution of solutes from the Eastern Galilee Mountains.

8.7 Lake Kinneret Salinity Model

Operational management, which is based on a reliable hydrological understanding, has the potential to help in controlling Lake Kinneret salinity. Several long-term changes may cause a significant increase or decrease in salinity: (1) solute inflows from the springs to the lake, (2) water inflows from the Jordan River and other streams, (3) evaporation, and (4) outflows and lake-level maintenance. A lake salinity model was developed in order to predict various cases of long-term salinity changes.

The model was verified by comparison of "reconstructed" salinity results with the measured historical data of Lake Kinneret salinity, from 1963 until present (Fig. 8.8). The most significant variable is the solute mass inflow to the Lake Kinneret watershed, which includes: (1) the springs diverted by the SWC ($\sim 55 \times 10^6$ kg year^{-1} where $\sim 38 \times 10^6$ kg year^{-1} from Tab, and $\sim 17 \times 10^6$ kg year^{-1} from Tib), (2) artificial recharge from the Yarmouk River ($\sim 3 \times 10^6$ kg year^{-1}), (3) measured springs that flow to the lake ($\sim 10 \times 10^6$ kg year^{-1}), (4) unknown springs ($\sim 82 \times 10^6$ kg year^{-1}), and (5) surface flow contribution ($\sim 9 \times 10^6$ kg year^{-1}). These annual average solute production ($\sim 159 \times 10^6$ kg year^{-1}) is in agreement with previous estimations (Mero 1978; Benoualid and Ben-Zvi 1981; Simon and Mero 1992; Mero and Simon 1992).

The proposed salinity mechanism (Rimmer 2003, 2007) is a lake-wide model for the solute mass based on the main components of the solute balance and on the understanding of the mechanism of the saline springs. It proposes that lake salinization process can be described by a simple physically based complete mixing (CM) model (Varekamp 1988; Singh 1988) and therefore can be solved analytically.

The theoretical development of the CM model system consists of a simple differential equation for the mass of an inert solute in the lake, as was described in detail by Rimmer (2003):

$$\begin{aligned} &\frac{\mathrm{dS}(t)}{\mathrm{dt}} + q(t)S(t) = S_{\mathrm{in}}(t) \quad S.T.: \quad S\big|_{t=0} = S_0 \\ &q(t) = \frac{Q_{\mathrm{out}}(t)}{V(t)} \quad ; \quad S_{\mathrm{in}}(t) = Q_{\mathrm{in}}(t)\bar{C}_{\mathrm{in}}(t). \end{aligned} \tag{8.2}$$

In this equation, $S = C_{\mathrm{lake}}V$ is the solute mass in the lake (kg), represented by multiplying the average solute concentration in the lake C_{lake} (mg L^{-1} Cl$^-$) by the lake volume V (10^6 m^3), t is a time unit (year), Q_{in} is the inflow discharge (10^6 m^3 year^{-1}) (including direct rainfall), Q_{out} is the outflow from the lake (10^6 m^3 year^{-1}), and S_0 is the initial mass of solute in the lake (kg) at $t=0$, $q(t)$ represents the ratio of outflows to lake volume, which is the reciprocal of water residence time, and $S_{\mathrm{in}}(t)$ stands for variations of annual solute inflows in time. The averaged solute concentration of the incoming solute flux $\bar{C}_{\mathrm{in}}$ (mg L^{-1} Cl$^-$) is an integrated value of all solute contributors from the lake exterior that consist of the lake floor (streams, onshore and offshore springs) and the water surface (direct rainfall and fallout).

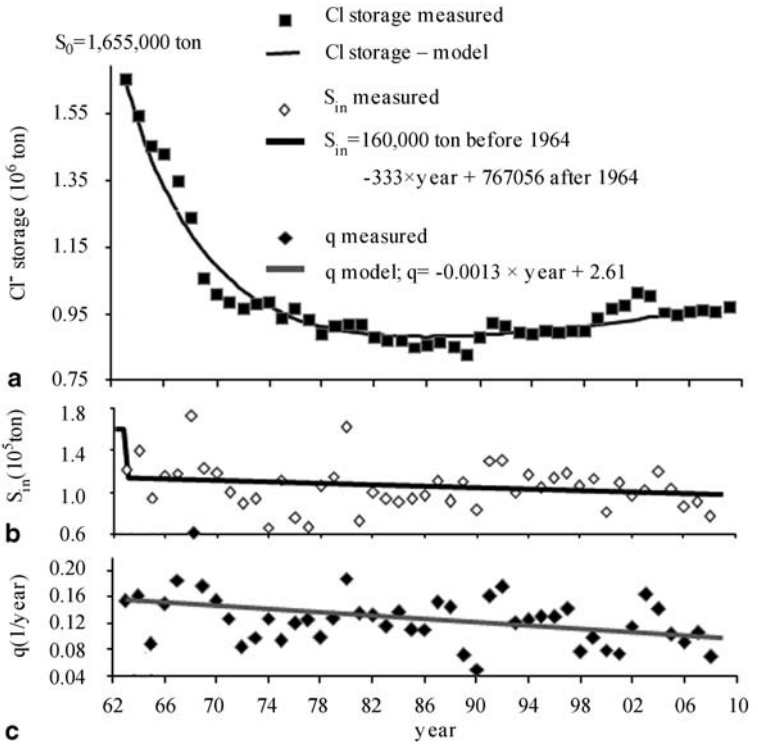

Fig. 8.8 A verification of the solute mass model for Lake Kinneret (**a**), based on annual measured solute inflow, S_{in} (**b**), and the ratio of outflow to lake volume, q (**c**), during 1962–2010 (see Eq. 8.2). **a** The actual Cl^- storage of the lake on 1st of October for each year compared to the model verification as a result of step reduction of S_{in} in 1964 and continuous linear reduction of q. **b** The step reduction in solute inflows from $\sim 160 \times 10^6$ to $\sim 105 \times 10^6$ kg year^{-1}, as a result of the operation of the SWC during January 1965. **c** Gradual decrease in past water inflows were expressed by a linear decrease of q

Equation (8.2) can be solved analytically. The solution shows that the changes of solute mass in the lake are the result of integration in time and space of the solute inflows, outflows, lake volume, and evaporation. The model was verified by comparing it with the measured solute mass from 1963 to 2010. The initial condition is the solute mass in the lake in 1963 ($1{,}655 \times 10^6$ kg Cl^-), while the operational inputs were as follows: (1) step reduction in solute inflows from $\sim 160 \times 10^6$ to $\sim 105 \times 10^6$ kg year^{-1}, as a result of the operation of the SWC during January 1965 (Fig. 8.8a), and (2) assumed linear reduction of inflows from surface runoff, expressed by a linear change of the leaching ratio q (Eq. 8.2) from ~ 0.12 in 1987 to ~ 0.09 in 2010 (Fig. 8.8b). The results of this simplified verification are presented in Fig. 8.8c. Without any need for calibration, the two dominate procedures that caused the major changes in salinity were clearly identified.

The example of the predicted salinity trend with the model (Fig. 8.9) shows the salinity as a result of the following conditions: reduction of 2.6×10^6 m^3 of in-

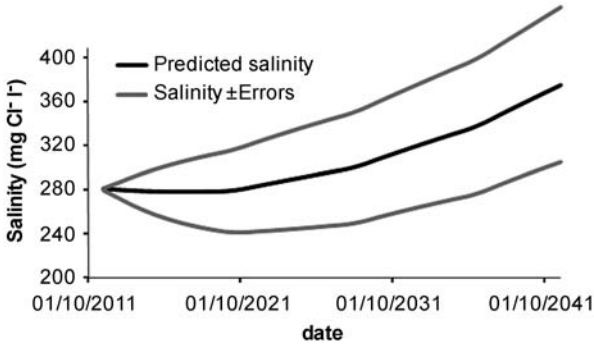

Fig. 8.9 Prediction of future lake salinity, including the stochastic component, under certain conditions (see text)

flows and increase of 0.41×10^6 m^3 in evaporation annually, due to climate change (Rimmer et al. 2011); step reductions of 33 m^3 every 8 years representing human interventions; reduction of ~5,000 t of input Cl^- due to reduced flow of groundwater and steady lake level. Under these conditions, the salinity will increase significantly to ~360 mg L^{-1} Cl^- during the next three decades. The additional stochastic component demonstrates that the single standard deviation of the predicted salinity is ±60 mg L^{-1} Cl^-, depending mainly on the average amount of inflows to the lake. The model enables to calculate each combination of inflows, outflows, evaporation, and solute inflow to predict future lake salinity.

Our predictions are that the future salinity of Lake Kinneret will be higher than today, mainly as a result of the continuous reduction in freshwater input from the Jordan River. The implication of such a change is that without further anthropogenic salinity reduction operations, a decline of lake water quality for both agricultural and domestic use is expected.

References

Abbo H, Shavit U, Markel D, Rimmer A (2003) A numerical study on the influence of fractured regions on lake/groundwater interaction; the Lake Kinneret case. J Hydrol 283(1–4):225–243

Assouline S (1993) Estimation of lake hydrologic budget terms using the simultaneous solution of water, heat, and salt balances and a Kalman filtering approach—application to Lake Kinneret. Water Resour Res 29(9):3041–3048

Benoualid S, Ben-Zvi A (1981) A model to predict the Lake Kinneret salinization and the solutes reservoir. Israel Hydrological Service Report 1981/5, Jerusalem (in Hebrew)

Bergelson G, Nativ R, Bein A (1998) Assessment of hydraulic parameters in the aquifers surrounding and underlying Lake Tiberias. Ground Water 36:409–417

Dalinsky P (1969) The salinization mechanism of Lake Kinneret—a research for the period 1912–1968. No. 746, water planning for Israel (Tahal), Tel-Aviv (In Hebrew)

Goldman M, Gvirtzman H, Hurwitz S (2004) Mapping of saline groundwater beneath the Sea of Gallilee and its vicinity using the Domain electromagnetic (TDEM) geophysical technique. Isr J Earth Sci 53:187–197

Goldschmidt MJ, Arad A, Neev D (1967) The mechanism of the saline springs in the Lake Tiberias depression. Min Dev Geol Surv, Jerusalem, Hydrol. Pap. #11, Bull. 45. 19 pp

Gvirtzman H, Garven G, Gvirtzman G (1997) Hydrogeological modeling of the saline hot springs at the Sea of Galilee, Israel. Water Resour Res 33(5):913–926

Hurwitz S, Goldman M, Ezersky M, Gvirtzman H (1999) Geophysical (time domain electromagnetic model) delineation of a shallow brine beneath a freshwater lake. The Sea of Galilee, Israel. Water Resour Res 35:3631–3638

Hurwitz S, Lyakhovsky V, Gvirtzman H (2000a) Transient salt transport modeling of a shallow brine beneath a fresh water lake, the Sea of Galilee. Water Resour Res 36:101–107

Hurwitz S, Stanislavsky E, Lyakhovsky V, Gvirtzman H (2000b) Transient groundwater-lake interactions in a continental rift: Sea of Galilee, Israel. Geol Soc Am Bull 112:1694–1702

Issar AS (1993) Recharge and salination processes in the carbonate aquifers in Israel. Environ Geol 21:152–159

Katz A, Nishri A (2013) Calcium, magnesium and strontium cycling in stratified, hardwater lakes: Lake Kinneret (Sea of Galilee), Israel. Geochim Cosmochim Acta 105:372–394

Kessler A, Rimmer A (2003) Influence of the Kinneret's water level upon the submerged outflow of Fuliya springs. Report submitted to the Israeli Water Commission (in Hebrew).

Klein Ben-David O, Saas E, Katz A (2004). The evolution of marine evaporitic brines in Inland Basins: the Jordan-Dead Sea Rift valley. Geochim Cosmochim Acta 68:1763–1775

Kolodny Y, Katz A, Starinsky A, Moise T, Simon E (1999). Chemical tracing of salinity sources in Lake Kinneret (Sea of Galilee), Israel. Limnol Oceanogr 44:1035–1044

Mazor E, Mero F (1969) Geochemical tracing of mineral resources in the Lake Tiberias basin, Israel. J Hydrol 7:276–317

Mekorot (1987–2011) The annual water-solute-energy balances of Lake Kinneret. Mekorot, Watershed Unit, Israel. (in Hebrew)

Mercado A, Mero F (1985) The saline discharges to lake Kinneret. Report II. Rep. 01/85/23. Tahal, Tel Aviv, 57 pp (in Hebrew)

Mero F (1978) Hydrology. In: Serruya C (ed) Lake Kinneret, Monographiae Biologicae. Junk, The Hague, pp 88–102

Mero F, Mandel S (1963) The hydrological mechanism of the saline springs of the western shore of Lake Kinneret. Tahal report 2399, Tahal, Tel-Aviv, 10 pp (In Hebrew)

Mero F, Simon E (1992) The simulation of chloride inflows into Lake Kinneret. J Hydrol 138:345–360

Mero F, Zaltzman U (1967) Hydrological observations on the saline springs in Lake Kinneret. TAHAL, Rep. 692, Tahal, Tel-Aviv, 10 pp. (in Hebrew)

Nishri A, Stiller M, Rimmer A, Geifman Y, Krom M (1999) Lake Kinneret, The Sea of Galilee: the effects of diversion of external salinity sources and the probable chemical composition of the internal salinity sources. Chem Geol 158:37–52

Oren OH (1957) Physical and chemical characteristics of Lake Tiberias. Ministry of Agriculture, Division of Fisheries, Sea Fisheries Research Station and TAHAL P.N.9. Tel Aviv

Rimmer A (2000) The influence of lake level on the discharge of the Kinneret saline springs. Adv Limnol 55:55–67

Rimmer A (2003). The mechanism of Lake Kinneret salinization as a linear reservoir. J Hydrol 281(3):177–190

Rimmer A (2007) System approach hydrology tools for the upper catchment of the Jordan river and Lake Kinneret, Israel. Isr J Earth Sci 56:1–17

Rimmer A, Gal G (2003) The saline springs in the solute and water balance of Lake Kinneret, Israel. J Hydrol 284(1–4):228–243

Rimmer A, Hartmann A (2012) Simplified conceptual structures and analytical solutions for groundwater discharge using reservoir equations. Chapter 10 in InTech Open Access book, "Water Resources Management and Modeling", ISBN 978-953-51-0246-5

Rimmer A, Hurwitz S, Gvirtzman H (1999) Spatial and temporal characteristics of saline springs: sea of Galilee, Israel. Ground Water 37(5):663–673

Rimmer A, Aota Y, Kumagai M, Eckert W (2005) Chemical stratification in thermally stratified lakes: a chloride mass balance model. Limnol Oceanogr 50:147–157

Rimmer A, Givati A, Samuels R, Alpert P (2011) Using ensemble of climate models to evaluate future water and solutes budgets in Lake Kinneret, Israel. J Hydrol 410:248–259
Simon E, Mero F (1992) The salinization mechanism of Lake Kinneret. J Hydrol 138:327–343
Singh VP (1988) Hydrologic systems, rainfall-runoff modeling. Prentice Hall, Englewood Cliffs
Starinsky A (1974) Relationships between Ca-chloride brines and the sedimentary rocks in Israel. PhD thesis. The Hebrew University Jerusalem (in Hebrew: English Summary)
Stiller M (1994) The chloride content of pore water of Lake Kinneret sediments. Isr J Earth Sci 43:179–185
Stiller M, Carmi I, Munnich KO (1975) Water transport through Lake Kinneret sediments traced by tritium. Earth Planet Sci Lett 25:297–304
Stiller M, Rosenbaum JM, Nishri A (2009) The origin of brines underlying Lake Kinneret. Chem Geol 262:309–325
Tal A, Rimmer A (2008) Estimation of water and solutes load from Kinneret springs—survey report. Hydrological Service report (in Hebrew)
Varekamp JC (1988) Lake pollution modeling. J Geol Educ 36:4–9
Yechieli Y, Shaliv G, Wallman S, Kessler A, Rozenzpet M, Berger D, Bein A (2011) Three dimensional model for the Kalanit Basin (Fuliya and Tabgha basin). GSI Project report GSI/38/2011

Chapter 9
The Seasonal Hydrodynamic Habitat

Jörg Imberger and Clelia Luisa Marti

Abstract In this chapter, we present a detailed analysis of the annual thermal regime of Lake Kinneret based on high-resolution thermistor chain and meteorological data collected by the Centre for Water Research at the University of Western Australia during the period April 2007–April 2008. Five seasonal regimes of the yearly cycle are defined to illustrate the main physical aspects of the lake hydrodynamics and their effects on ecological processes.

Keywords Benthic boundary layer · Internal wave · Mixing · Metalimnion · Hypolimnion · Surface layer · Thermocline · Turbulent kinetic energy

9.1 Introduction

Lake Kinneret was formed when the Jordan Valley, in which it lies, progressively filled about 120,000 years ago (Hazan et al. 2005). Even though the lake level fluctuated periodically, Dubowski et al. (2003) showed, using isotopic analysis, that primary production over the past 3,000 years or so varied within a similar range as observed currently. This was confirmed, in the recent past, by Rimmer et al. (2011) who presented light extinction coefficient data from 1990 to 2008 that showed a constant value of around 0.5 m^{-1}. These observations would suggest that the thermal structure has also been relatively stationary, varying seasonally with a uniform water column in winter, with a temperature of between 14 and 15 °C and a peak summer stratification when the bottom temperature is typically ~0.4 °C higher than that observed in the previous winter and a surface temperature of between 27 and 28 °C. The thermocline typically resides, during the mid-summer period, at a depth of between 17 and 19 m. A careful analysis by Rimmer et al. (2011) of changes in recent years of the thermal structure showed a small rise of the peak surface temperature and a shallowing and sharpening of the thermocline. These changes

J. Imberger (✉) · C. L. Marti
Centre for Water Research, The University of Western Australia MO23,
35 Stirling Highway, Crawley, WA 6009, Australia
e-mail: jimberger@cwr.uwa.edu.au

C. L. Marti
e-mail: marti@cwr.uwa.edu.au

T. Zohary et al. (eds.), *Lake Kinneret, Ecology and Management,* Aquatic Ecology Series 6, 133
DOI 10.1007/978-94-017-8944-8_9,

were attributed, by these authors, mainly to the lower lake level brought about by a reduction of rainfall and only slightly determined by external influences (Parparov and Gal 2012). The explanation of why a reduced water level leads to an increase in the water column stability of Lake Kinneret becomes clear from Fig. 1.1 in Chap. 1 where it is seen that the 5-m isobaths are most closely spaced near the water level of −210 m a.m.s.l. (above mean sea level), implying that the bottom is more vertical near the lake perimeter, when the lake is full (Chap. 4). Thus, as the lake level drops, the amount of heat captured remains about the same, but the volume of the surface layer decreases so that the surface temperature increases slightly more, as observed by Rimmer et al. (2011). The present authors also measured the thermal structure of Lake Kinneret, with a high-precision thermistor chain, from July 1999 to November 2009. The lake level variations and stratification pattern changes for this period are shown in Fig. 9.1a. Water temperature data were recorded at Station (Sta.) A (~42-m depth, at the deepest part of the lake; see Fig. 1.1 in Chap. 1) using a 30-node thermistor chain sampling at 30-s intervals. Throughout this period, the lake level fluctuated between approximately −209 and −215 m a.m.s.l. The dependence of the surface temperature, metalimnion thickness and surface layer depth on lake water level is shown in Fig. 9.1b–d. As seen, the water surface temperature increased and the thickness of the metalimnion decreased with decreasing water level (Fig. 9.1b, c) in agreement with the independent findings of Rimmer et al. (2011). However, as seen from Fig. 9.1d, the lake water level has a less significant influence of the surface layer depth as characterised by the depth of the 26-ºC isotherm; the surface layer depth was observed to remain nearly constant with lake level. The temperature rise per meter of falling water level was about 0.1 °C m^{-1}. This heating, due to the contraction of the surface layer volume with depth, may be compared to increased water column stability documented due to global warming. Verburg and Hecky (2009) found, for Lake Tanganyika, a long-term heating increase, over the past 100 years, of about 0.4 W m^{-2}. Assuming this to be representative, and with the Lake Kinneret mean surface layer thickness of around 15 m, would imply a temperature increase, due to such global warming, of the water in the surface layer of about 2×10^{-3} °C $year^{-1}$, equivalent to a water level drop of only 0.02 m. Lake Kinneret may thus be seen as a surrogate for the effects of global warming with the water level inducing similar, but stronger, change in the surface layer stability.

A high-resolution image of a 1-year subset of the data, shown in Fig. 9.1, for the period of April 2007–April 2008, is shown in Fig. 9.2 to illustrate the seasonal features of the annual cycle of thermal structure at Sta. A. Serruya (1978) was the first to point out that the biology has evolved in Lake Kinneret to take advantage of this thermal seasonality. Serruya (1978) showed the water column to be cold and uniform in winter with sustained vertical mixing, allowing free communication between the surface and bottom waters (Fig. 9.2a). He hypothesised that the biology is reset with plankton algal cysts being resuspended and then stirred throughout the water column; this winter stirring also mixes oxygen and nutrients and all are homogenized over the depth of the water column by late winter. Sometime in March, the net heat flux at the surface (see Fig. 9.2f) again becomes positive and the water column starts to stratify, the radiation capture taking place in the top 2–3 m (light

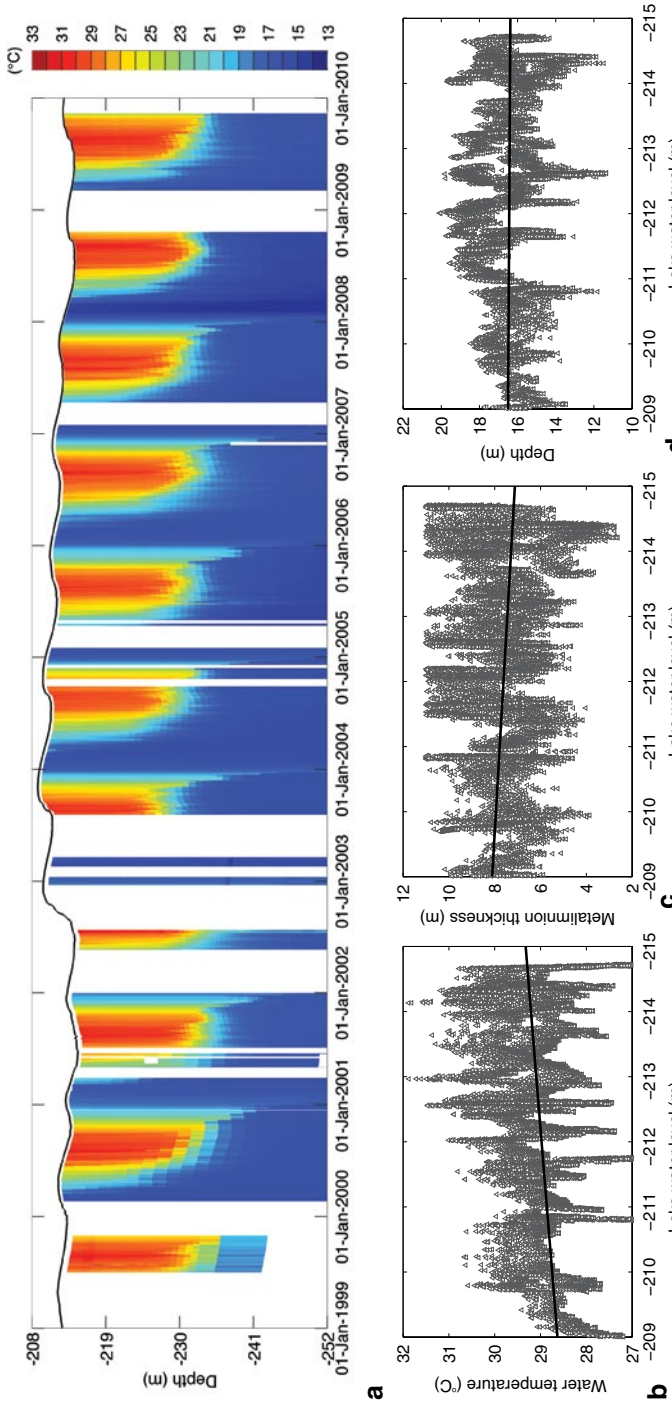

Fig. 9.1 **a** Evolution of the background stratification at Sta. A from July 1999 to November 2009 determined from the average isotherm position over 1-hour interval. *White areas* indicate no data. The depth is indicated in m a.m.s.l. Summary of 1999–2009 summer results (July, August and September) versus lake water level. **b** average water temperature in top 2 m of the surface layer. **c** metalimnion thickness defined as the difference between the depth of the 17 and 27 °C isotherms. **d** the depth of the 26 °C isotherm. Linear regressions (*solid lines*) were fitted to the data shown in **b**, **c** and **d**

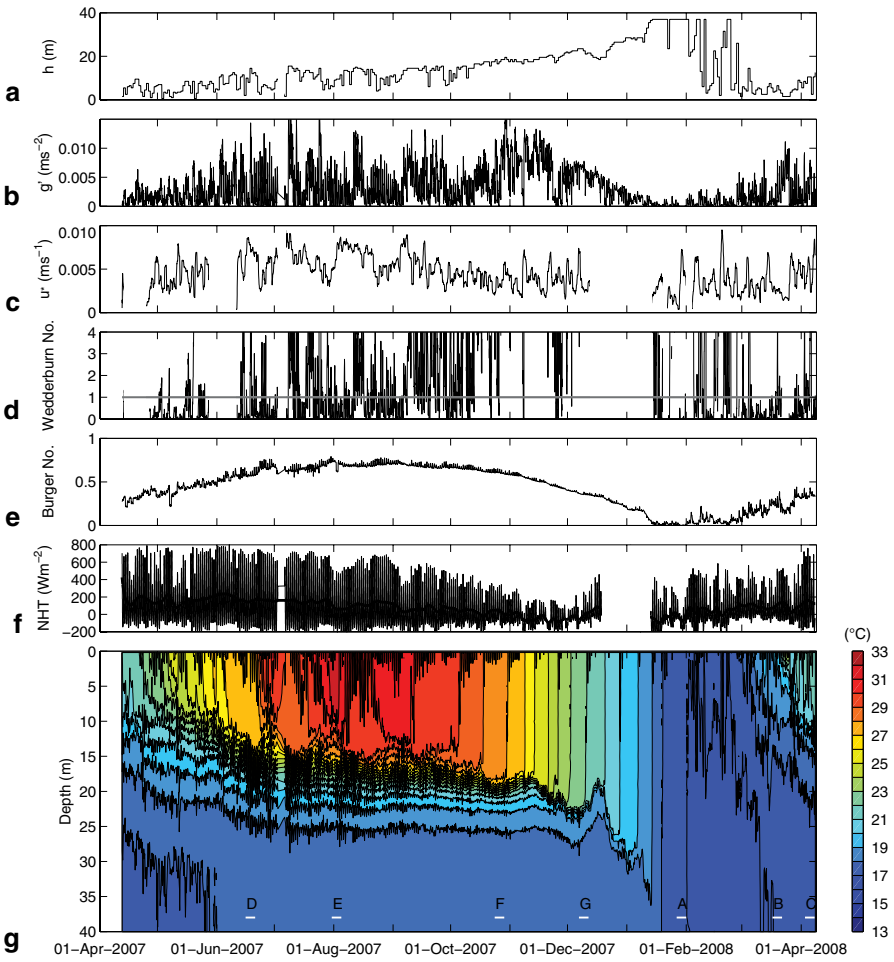

Fig. 9.2 Evolution of **a** the depth of the diurnal thermocline, *h,* **b** reduced gravity, *g'*, **c** daily average surface wind shear velocity, *u*,* **d** Wedderburn number, **e** Burger number, **f** 3-hour and 3-day average (*thick line*) net heat transfer, *NHT,* **g** hourly average isotherm contours derived from the thermistor chain data at Sta. A from April 2007 to April 2008. Sampling every 1 min and containing 30 equally spaced high-precision thermistors over the depth. Contour intervals at 0.5 °C. The marks in the lower panel indicate the times of Figs. 9.3, 9.5, 9.6, 9.8, 9.12, 9.13 and 9.14. Panels **a**, **b**, **d** and **e** were calculated using hourly average data. *White areas* indicate no data

extinction coefficient 0.5 m^{-1}), with the observed deepening of the thermocline in April, May and June, shown in Fig. 9.2g, being the result of wind action at the free surface (Fig. 9.2a, c).

The rate of thermocline deepening over the spring months is, at first, rapid when the water column stability is weak and then slows in June as the surface heating adds stability to the water column (Fig. 9.2b); the wind speeds do not change appreciably (Fig. 9.2c). Over the months from July to September, the surface temperature

is relatively constant with the rate of deepening being almost constant at about 1 m per month; the net incoming heat input approximately balances the heat needed to warm the water that is entrained at the base of the surface layer as deepening proceeds. Then in October, the net surface heat flux becomes negative and the surface water starts to cool (Fig. 9.2f, g). Deepening of the thermocline is observed to accelerate for two reasons; first, the water column progressively loses stability due to surface cooling, making deepening easier and second, the buoyancy flux at the surface adds to the turbulent kinetic energy (TKE) available from the shear production at the base of the surface layer to provide a larger pool of TKE for deepening.

A number of important conclusions may be drawn from the summary by Serruya (1978), the work by Rimmer et al. (2011) and the data displayed in Fig. 9.2. First, as evidenced by the small vertical excursions of the isotherms in the metalimnion, shown in Fig. 9.2g, the stability of the water column, during the stratified period, is much larger than the wind energy available to disturb the water column; from April to December, a 9-month period, Lake Kinneret is made up of two distinct water bodies. First, the surface layer above the thermocline, the home of primary production (Berman et al. 1995), moving horizontally in a combination of gyres and direct wind-induced shear (Laval et al. 2003; Marti and Imberger 2008) and, second, the stagnant, hypolimnetic waters that have an almost constant (< 0.1 °C over 9 months) temperature. To first approximation, the bottom water is sealed from the surface waters by the thermocline and ecologically important chemicals are recycled within the hypolimnion (Imberger 1998; Nishri et al. 2000; Eckert et al. 2002; Chap. 19). This is also confirmed by the value of the Wedderburn number (more details are given in this chapter in 9.4 April, May, June and July: Surface Layer Heating and Mixing and Internal Wave Activity), shown in Fig. 9.2d, that has a few periods of less than one in June and July, but then progressively increases to values greater than one (see Shintani et al. 2010). The transfer between the hypolimnion, where most of the nutrients are recycled, and the surface layer, where the sun supports primary production, is completely controlled by a weak benthic boundary layer (BBL) flux, first documented by Marti and Imberger (2006); vertical mixing transport is absent in Lake Kinneret as evidenced by the constancy of the bottom temperature and the bottom chloride concentration (Rimmer et al. 2005). The stability of the water column in the lake as a whole is further enhanced due to the thermocline being at mid-depth of the water column for much of the stratification period. Horn et al. (2001) showed that when the thermocline is at mid-depth, non-linear steeping of seiches, excited by the wind, is minimum and only simple linear oscillations may be expected in Lake Kinneret; free waves are less common and so boundary breaking (Boegman et al. 2005) is not an important contributor to boundary mixing.

Second, the simple geometric shape of the Lake Kinneret basin (Chap. 4) and the lack of differential deepening (Imberger 1985a) means that horizontal dispersion in the surface layer is relatively small with only the spatial variability of the wind contributing to horizontal dispersion (Stocker and Imberger 2003b; Laval et al. 2003); this explains the patchy nature of the *Peridinium* algae biomass (Ng et al. 2011; Chap. 10). The findings of Rimmer et al. (2011), however, suggest a complication, in that, as the water level decreases, differential heating and cooling

(Imberger 1985a) should be observed to intensify with decreasing water level thus enhancing horizontal dispersion, leading to more uniform algae distributions; this conjecture has, however, not been proven.

Third, the communication between the surface waters and the bottom sediments appears to be a delicate balance between the upward fluxes in the BBL in the 9 months of stratification (Marti and Imberger 2006), the deep mixing in the 3 months of water column overturn (Antenucci and Imberger 2003), possible transport by methane bubbles (Ostrovsky 2003; Meier et al. 2011) and the downward flux of organic carbon particles (Yacobi and Ostrovsky 2008; Chap. 24). What follows is a detailed analysis of the annual cycle of the thermal regime of Lake Kinneret based on high-resolution thermistor chain and meteorological data collected by the authors during the period April 2007–April 2008 at Sta. A and Sta. T1 (see Fig. 1.1 in Chap. 1).

9.2 January: Cold Homogeneous Water Column

We begin the discussion when the lake is cold and homogeneous. The available 1-year data series, shown in Fig. 9.2, starts in April 2007 and finishes in April 2008. For convenience, we start the discussion in the winter of January 2008 (Fig. 9.3), and add the year 2007 to the end of the 2008 data, in that way we obtain a winter-to-winter sequence illustrative of the seasonal transition of processes; data were not available at both chains for a chronological full 1-year sequence.

As seen in Fig. 9.3a, in winter, the winds can be quite strong (>10 m s^{-1}) leading to a well-mixed water column as previously reported by Serruya (1978). As described by Shilo et al. (2007) and in Chap. 6, the winter winds are characterised by eastern Mediterranean weather systems that are noted for storms with a duration of around 1–2 days followed by periods of calm; such a wind event is captured in Fig. 9.3a, b, starting on the morning of 29 January 2008. When the water column is homogeneous, the wind working at the surface introduces TKE that progressively mixes the momentum down into the water column (Imberger and Paterson 1990; Yeates and Imberger 2003) with a characteristic penetration velocity scale given by the surface wind shear velocity:

$$u_* = \left(\frac{\tau_s}{\rho_0}\right)^{1/2} = \left(\frac{C_D \rho_a}{\rho_0}\right)^{1/2} U, \tag{9.1}$$

where τ_s is the wind stress at the air–water interface, C_D ($=1.3\times10^{-3}$) is the water surface drag coefficient, ρ_a ($=1.2$ kg m^{-3}) is the air density, ρ_0 ($=1000$ kg m^{-3}) is the characteristic water density and U is the wind speed (Imberger 2013). From Fig. 9.3a, we may assume a typical wind speed of 10 m s^{-1} leading to a shear velocity of 0.0125 m s^{-1} and given that the water column depth, h, is 40 m, this implies a vertical mixing timescale, h/u^*, of ~0.9 hours. Clearly, the observation by

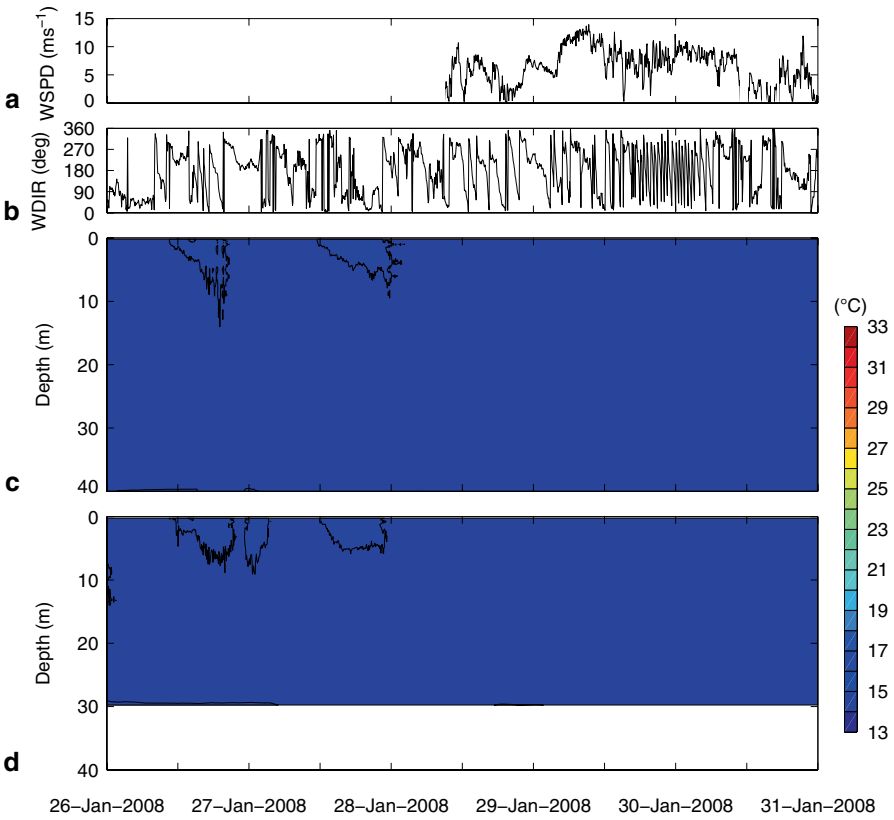

Fig. 9.3 **a** Ten-minute average wind speed, *WSPD*. **b** wind direction, *WDIR*. **c** isotherm contours at Sta. A. **d** isotherm contours at Sta. T1 from 26–31 January 2008. Contour intervals at 0.5˚C. *White areas* indicate no data

Serruya (1978) is correct that the water column is completely mixed in the winter month of January. By comparing the water temperatures in Fig. 9.3c and d, taken at different locations in the lake (see Fig. 1.1 in Chap. 1), we see that the Lake Kinneret was also homogeneous in the horizontal; the water temperatures at Sta. A and Sta. T1 were the same.

Therefore in winter, with the water column being completely homogeneous, the response to a surface wind stress will be confined to surface gravity waves setting up topographic gyres if steady state is established; the earth's rotation will not influence the surface gravity waves as their period, given by $L/(gh)^{1/2}$, is about 20 min, where L (=20,000 m) is the length of the basin and g is the acceleration of gravity. This is very much shorter than the inertial period f^{-1}, of 22.3 hours, where f ($=7.81\times10^{-5}$ rad s^{-1} at 32.5°N) is the inertial frequency at the latitude of Lake Kinneret. However, as pointed out by Shilo et al. (2007), despite the importance of understanding the unsteady wave response occurring during the winter, only the steady state, linear barotropic response of the lake has been examined in any detail.

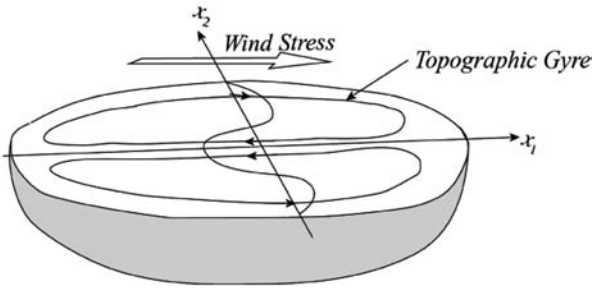

Fig. 9.4 A schematic diagram of Lake Kinneret topographic gyre

The motion arising from a steady wind stress acting on the bowel-shaped Lake Kinneret is best understood by taking a slice of water in the direction of the wind as shown in Fig. 9.4 and assume the flow is dominated by a combination of Couette and Poiseuille flows; the Couette flow being driven by the surface wind stress and the Poiseuille flow being set up to make the net flow zero across the transverse section (Imberger 2013). If it is assumed that the streamlines are approximately parallel and in the direction of the wind, then the water surface slope set up to drive the Poiseuille flow will be independent of the transverse direction. As shown in Imberger (2013), this leads to a net, depth-averaged flow moving with the wind in the shallows and against the wind in the central deeper parts of the lake forming a gyre, as sketched in Fig. 9.4, symmetric about the x_1 axis; this is called a topographic gyre. Shilo et al. (2007) carried out a detailed numerical validation using a realistic wind field and direct field acoustic Doppler current profiler velocity measurements and showed that such gyres do indeed set up in Lake Kinneret, albeit with a large variability in location, size and orientation.

Shilo et al. (2007) added a further observation that the topographic gyres tended to rotate cyclonically once the wind had stopped "consistent with that of a topographic wave". This follows directly from the transport of potential vorticity associated with the topographic gyre (Imberger 2013). Given such gyres transport water, from a shallow region into a deeper region, cyclonic vorticity is strengthened and vice versa, when water moves from deep water into shallow regions, anticyclonic vorticity is strengthened, and this would suggest a cyclonic rotation of the topographic gyres as noted by Shilo et al. (2007).

As already mentioned at the start, during the winter period, Lake Kinneret is fully turbulent over the whole water column; near the surface, the source of the turbulence is the surface wind stress and in the lower part of the lake, the bottom stress associated with the topographic gyres would provide a further source of mixing. Together, the basin mean dissipation of TKE, ε, is of order 10^{-4} m^2s^{-3} (Yeates and Imberger 2003).

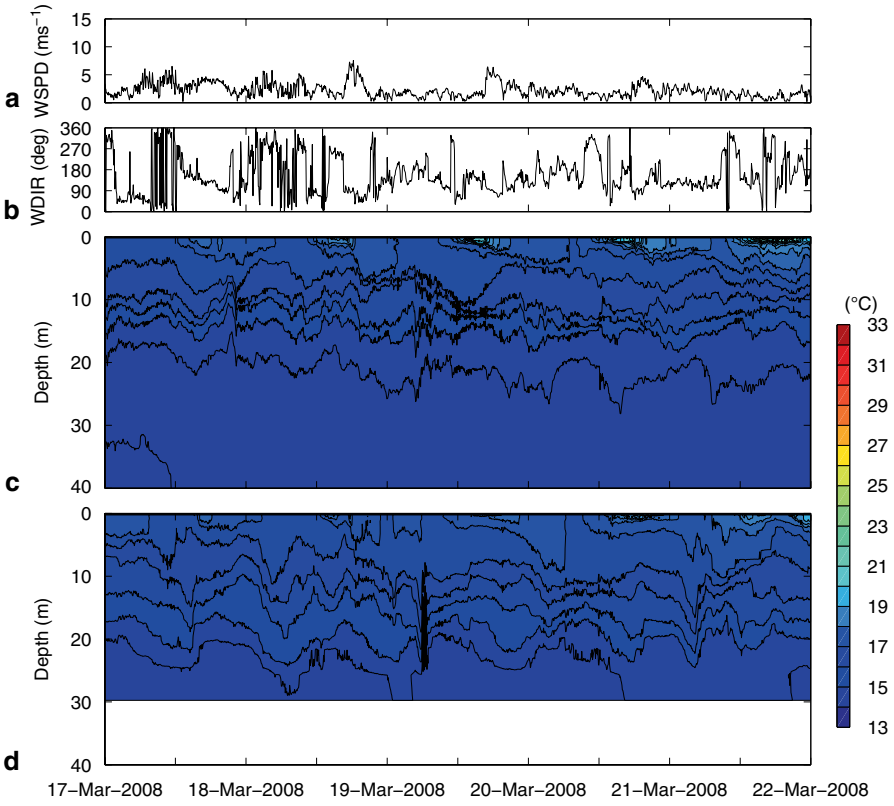

Fig. 9.5 **a** Ten-minute average wind speed. **b** wind direction. **c** isotherm contours at Sta. A. **d** isotherm contours at Sta. T1 from 17–22 March 2008. Contour intervals at 0.5 ˚C

9.3 February and March: Low Wind and Radiative Heating

This period is characterised by relatively weak easterly and southerly winds (Fig. 9.5a, b) and increasing solar radiation (Fig. 9.2f) leading to the build-up of a surface warming decreasing exponentially with depth. The near-surface layer exhibits a 3–5 °C diurnal temperature variation (Fig. 9.5c, d), the thermal energy being mixed vertically into the evolving surface layer by the weak winds and the night cooling. The weak stratification, so formed, is disturbed by the wind stress and free irregular internal waves are observed occassionally (see Fig. 9.5c, d). These disturbances do not appear to be locked to the basin boundaries and there is little correlation between the temperature structure in the centre of the lake, Sta. A (Fig. 9.5c) and that at the southwest boundary at Sta. T1 (Fig. 9.5d). As a consequence of the rather shallow thermocline depth, these internal waves steepen and shoal, as by way of example on the morning of 19 March 2008, forming internal

bores in which mixing may be expected. As is evidenced by the gradual build-up of a smooth, exponential surface temperature gradient, the buoyancy flux supported by the sporadic mixing events is too weak to appreciably change the exponential vertical temperature variation brought about by the radiative heating, observed in Fig. 9.5c, d; in general, the whole water column is relatively quiescent during February and March. In this period, the top part of the water column is stable with only weak vertical mixing. Rising temperatures with time and high transparancy, form ideal conditions for the growth of *Peridinium,* as documented since the mid-1960s as a regular occurrence in Lake Kinneret during February and March until the mid-1990s. However, since 1996, these blooms have become an irregular event (Roelke et al. 2007; Zohary et al. 2012; Chap. 11).

9.4 April, May, June and July: Surface Layer Heating and Mixing and Internal Wave Activity

The end of spring and beginning of summer is marked by a competition between the mechanical working by the wind, mixing the surface layer, and the increasing surface heating adding buoyancy. In April and May, the stronger diurnal winds are normally successful in mixing the diurnal surface layer and an almost two-layer stratification forms at the beginning of April to the end of April as shown in Fig. 9.6 (see also Sherman et al. 1978; Imberger 1985b; Spigel et al. 1986). The motions induced in Lake Kinneret by the surface wind stress during the summer period, when the water column is characterised by a strong two-layer stratification, is best understood by simplifying a cross section of unit width of the lake into a rectangular section containing a two-layer water column as shown in Fig. 9.7 (subindices 1 and 2 refer to the surface layer and deep layer, respectively).

As discussed in detail by Imberger (2013), the wind, initially imparts TKE at the water surface that acts to mix the water column from the surface downwards in a matter of minutes. Krauss and Turner (1967) called this action stirring. At the same time, the surface stress imparted by the wind, transfers some of the momentum in the wind to that part of the water column over which stirring mixes the water, causing the interface to tilt (Spigel et al. 1986; Imberger 2013). For typical conditions, as shown in Fig. 9.6c, d, the tilting time $L/(g'h_1)^{1/2}$ is of order ~13 hours compared to the inertial period due to the earth's rotation of 22.3 hours, where L (= 15,000 m) is the length of the basin at the depth of the thermocline, g'(~1×10^{-2} m s^{-2}) is the reduced gravity and h_1 (= 10 m) the depth of the surface layer (see Fig. 9.2a, b). This time-scale hierarchy shows that, on the commencement of the wind, stirring acts to deepen the diurnal surface layer on a timescale of minutes; the diurnal surface layer tilts on a timescale of about half a day and the velocity field in the surface layer "feels" the earth's rotation in Lake Kinneret on the timescale of the order of a day. Thus, in order to obtain a measure of the upwelling induced by the wind stress, we may neglect Coriolis forces and set up a simple horizontal force balance assuming the motion has come to equilibrium.

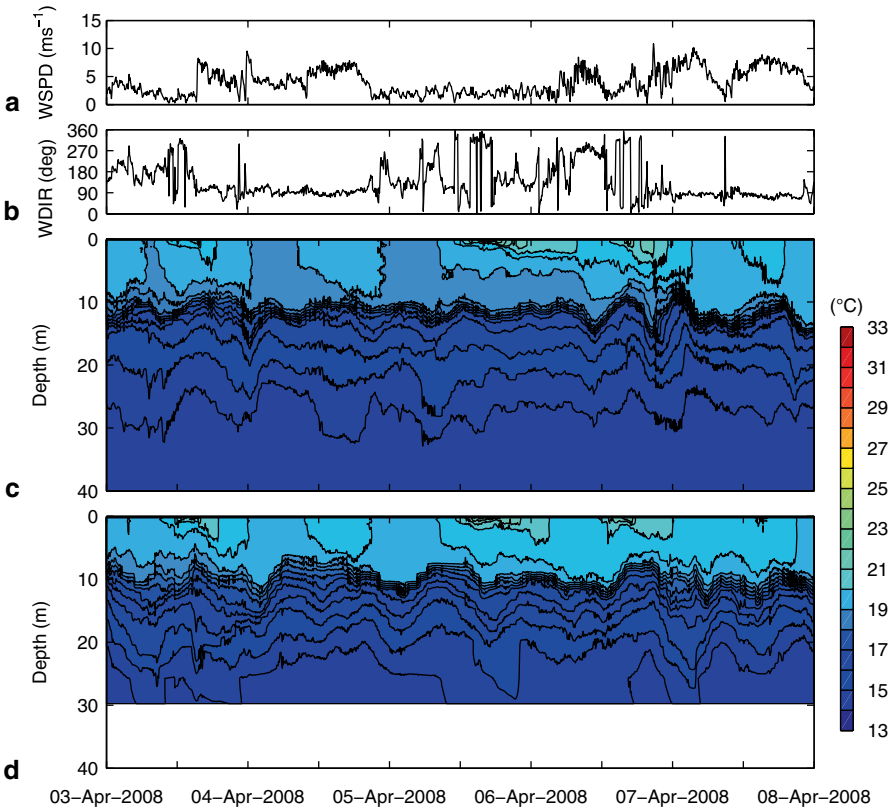

Fig. 9.6 **a** Ten-minute average wind speed. **b** wind direction. **c** isotherm contours at Sta. A. **d** isotherm contours at Sta. T1 from 3–8 April 2008. Contour intervals at 0.5˚C

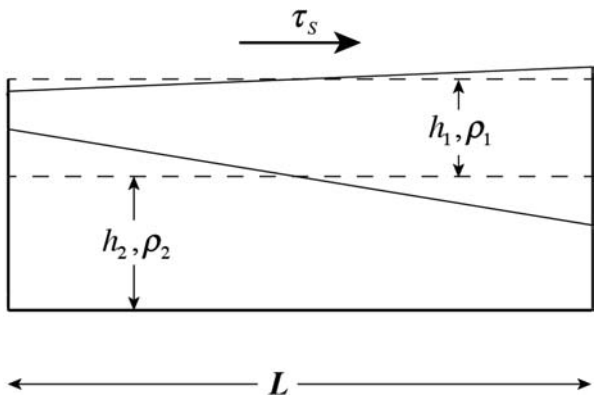

Fig. 9.7 A schematic diagram of a two-layer stratified system

Assuming the pressure is hydrostatic and the pressure in the bottom left corner is equal to the pressure at the bottom right corner (Fig. 9.7) yields:

$$\frac{\Delta}{h_1} = \frac{u_*^2 L}{g' h_1^2} = \frac{1}{W}, \tag{9.2}$$

where W is called the Wedderburn number (see Fig. 9.2d; Thompson and Imberger 1980),

$$W = \frac{g' h_1^2}{u_*^2 L}. \tag{9.3}$$

In deriving Eq. (9.2), we ignored the momentum of the water and any mixing at the interface so the interface vertical excursion Δ, as given by Eq. (9.2), represents only a scale for the excursion; in reality, the interface tilt overshoots this estimate and then oscillates in the form of Kelvin and Poincare waves (Antenucci et al. 2000) and deepens about the estimate given by Eq. (9.2) (Spigel et al. 1986). Substituting typical values from Fig. 9.6 into Eq. (9.2) leads to $\Delta / h_1 = 0.75$ or a peak to trough oscillation of about 7.5 m, which is close to what was observed at Sta. T1, shown in Fig. 9.6d. The concept of the Wedderburn number was recently generalised by Shintani et al. (2010) to allow for sloping side boundaries of a lake, but for Lake Kinneret, this is correction of detail.

The water temperature difference is strong enough to allow coherent basin-scale internal waves to form. At the beginning of this period, the wind stress generated large basin-scale internal waves, as shown in Fig. 9.6c, d, but the extra thermal input from June to July added sufficient buoyancy to the water column so that the induced basin-scale internal waves decreased in amplitude (see Fig. 9.8). The extra stability imparted in May and June, as evidenced by the increased density difference and sharper thermocline, also disengages the surface layer from the hypolimnion, allowing great shear to build up between the two parts of the water column. This leads, as clearly seen in Fig. 9.8c, to frequent generation of high-frequency shear instabilities (Antenucci and Imberger 2001a; Gomez-Giraldo et al. 2008).

For a general stratification, Monismith (1985) vertically subdivided the water column into n horizontal layers and defined separate equations of motion for each layer; as is intuitively plausible, the wind-induced motions in one layer influence the motions in the neighbouring layers and the dynamical equations for the layers are coupled through the pressure term. However, Monismith (1985) showed that there are linear combinations of the layer motions, called normal modes (Imberger 2013), for which the dynamical equations are all independent, of similar form, and equivalent to the equations for the case of a homogeneous lake.

The first class of basin-scale internal waves, observed to propagate parallel to the boundary, are called Kelvin waves. In their simplest form, linear and along a straight lake boundary, the force balance parallel to the wall is simply that of a long gravity wave with unsteady inertia balancing the pressure force due to the free

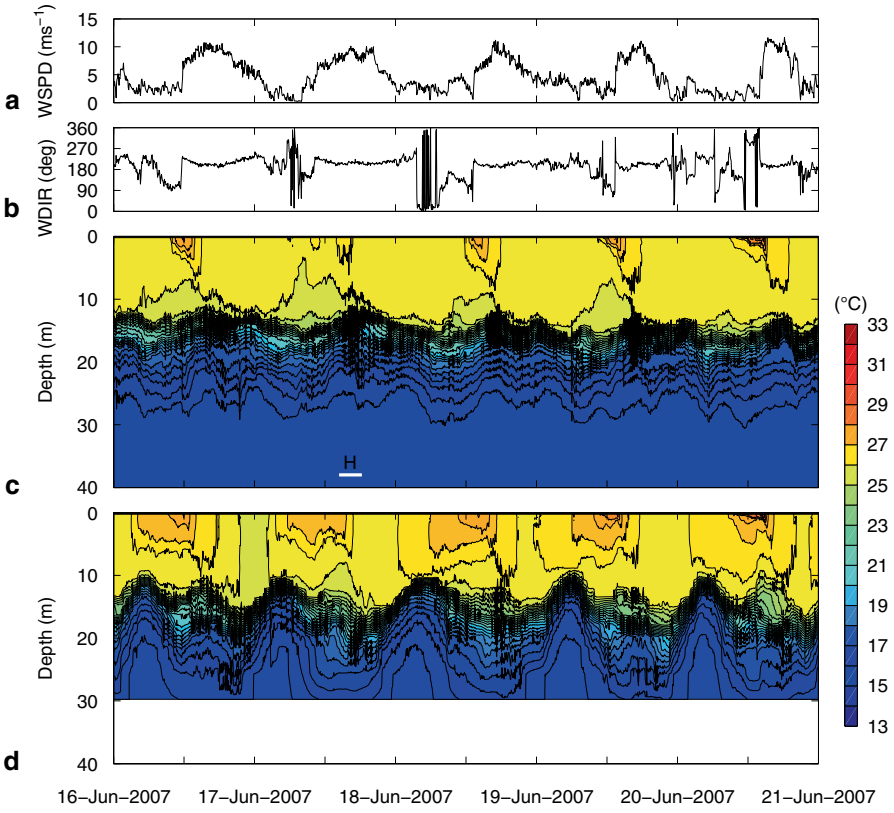

Fig. 9.8 **a** Ten-minute average wind speed. **b** wind direction. **c** isotherm contours at Sta. A. **d** isotherm contours at Sta. T1 from 16–21 June 2007. The mark in the lower panel indicates the time of Fig. 9.9. Contour intervals at 0.5 ˚C

surface or internal density interface deformation; in the transverse direction, this same interface displacement induces a transverse pressure gradient that is balanced by the Coriolis force brought about by the longshore motion of the primary gravity wave. This synchronised force balance constrains Kelvin waves to propagate only cyclonically, in the same direction as the earth's rotation, anticlockwise in the northern hemisphere and clockwise in the southern hemisphere. Kelvin waves are thus simply undulations of the surface or thermocline that propagate as simple long gravity waves in the direction of propagation and have a transverse pressure field that oscillates and transversely decreases exponentially in amplitude. The second type of wave, called a Poincare wave, forms away from the constraints of a wall and so the velocity vector rotates cyclonically with time and the force balance in one direction is between unsteady inertia and the Coriolis force due to the velocity in the other direction. These waves are translational, propagating in a straight line in an unconfined domain.

The ratio of the potential energy PE per unit area to the kinetic energy KE per unit area for a Poincare wave with a frequency of $\omega = 2\pi / T$ (where T is the wave period) is given by (Imberger 2013)

$$\frac{\mathrm{PE}}{\mathrm{KE}} = \frac{\omega^2 - f^2}{\omega^2 + f^2}. \tag{9.4}$$

This is an important result as it shows that, for a given kinetic energy, the potential energy and thus the surface or interface manifestation of the wave goes to zero as the wave frequency ω approaches the inertial frequency f (see also Gill 1982). Thus, low-frequency Poincare waves are simply an oscillation where there is a balance between unsteady inertia and Coriolis forces, with only a minor signature in the free surface for surface Poincare waves or isopycnals for internal modes.

No solutions have been found for a standing Poincare wave in a rectangular basin, but since Poincare waves are linear, two translational waves moving in opposite directions maybe superimposed to yield a standing wave in a duct. Further, Thomson (1879) showed that propagating Poincare wave solutions could be found for a circular basin and Goldstein (1929) derived a mathematical expression for Poincare waves in a flat-bottom elliptical basin (Antenucci and Imberger 2001b).

Internal wave activity was first recorded in Lake Kinneret by Serruya (1975). He related the magnitude of the metalimnetic displacement to the magnitude of the wind and noted that isotherm displacements on opposite sides of the lake were out of phase, with a nodal point in the centre of the lake. The first detailed study of such basin-scale internal waves in Lake Kinneret was reported in a series of papers by Antenucci et al. (2000); Antenucci and Imberger (2001a, 2001b, 2003); Saggio and Imberger (2001); Gomez-Giraldo et al. (2006) and Shimizu and Imberger (2008, 2009, 2010).

Antenucci and Imberger (2001b) applied the theory of normal modes to the study of basin-scale oscillations in Lake Kinneret, by modelling the lake, both as a circular and elliptical flat-bottom basin and the water column stratification as a three-layer structure. They showed that this simplification admitted three vertical modes, the surface oscillation and two internal wave modes, and an infinite array of horizontal modes in the form of Bessel function for the circular geometry and Mathieu functions for the elliptical basin. Antenucci and Imberger (2003) analysed the internal wave behaviour of Lake Kinneret for the year 2000 (see Fig. 9.1a) and Gomez-Giraldo et al. (2006) reported extensions of this work from an analysis of data taken in 2001 (see Fig. 9.1a), a year where the thermal structure was almost identical to that shown in Fig. 9.2g for 2007–2008. By modelling the lake basin as an ellipse, Antenucci and Imberger (2001b) were able to derive the characteristics of the vertical mode-one, mode-two and mode-three waves as a function of the time of the year. The Burger number S_i was computed as:

$$S_\mathrm{i} = \frac{c_\mathrm{i}}{fL}, \tag{9.5}$$

where i indicates the vertical mode and c_i is the baroclinic phase speed. The major axis length of the ellipse $L = 15{,}000$ m and $f = 7.81 \times 10^{-5}$ rad s^{-1} (inertial period of

22.3 hours) resulted in the seasonal evolution of the phase speed c_i leading to the Burger number S_i shown in Fig. 9.2e. The Burger number changes with season as the stratification increases and decreases through the nonrotating phase speed c_i. For a small Burger number, rotation dominates over gravity, and waves approach the oceanic case (known as inertial oscillations) in which the motion is dominated by the kinetic energy signal. For a large Burger number, gravity dominates over rotation, and waves approach the nonrotating case of equal partitioning between potential and kinetic energy. As seen in Fig. 9.2e, during the unstratified period, the Burger number was effectively 0. As the lake heated during spring, S_i gradually increased, reaching a maximum sometime in autumn, before the lake began to cool until again becoming unstratified. Antenucci and Imberger (2003) found that the vertical mode-one Burger number S_1 reached a maximum of 0.8 (see also Fig. 9.2e), whereas the higher vertical-mode Burger numbers reached maxima of <0.3. This implies that rotation will always affect the higher vertical mode waves to a greater extent than the vertical mode-one waves. These authors also confirmed that, for the main stratification period of June to September, the dominant basin-scale internal waves, the Kelvin vertical mode-one wave and vertical mode-two Poincare waves, have periods close to the inertial period and close to the diurnal wind period, the wind forcing thus resonates with these two waves; for these 4 months of the year, Lake Kinneret is kept agitated by the vertical mode-one Kelvin waves and vertical mode-two Poincare waves. When considering the PE/KE ratios (Eq. 9.4), vertical mode-one Kelvin waves have a ratio that is close to unity, whereas vertical mode-one and mode-two Poincare waves have a ratio that ranges from 0 (indicates dominance of rotation over gravity) to unity (indicates importance of gravity increases) as the Burger number increases (Antenucci and Imberger 2003).

High-frequency internal waves in Lake Kinneret were first described by Antenucci and Imberger (2001a). They showed that these waves were generated by shear in the surface layer induced by the wind. Boegman et al. (2003) also showed the existence of high-frequency waves associated with shear in the thermocline generated by high-vertical model basin-scale internal waves. As evidenced by the black patches in Fig. 9.8c, d at the crest of the basin-scale internal waves, the wind-induced shear across the metalimnion combines with the shear of the spectrum of the basin-scale internal waves to trigger shear instabilities. The high-frequency waves resulting from this instability appear whenever the wind above the lake rises to more than about 8 m s^{-1} (Fig. 9.9). Antenucci and Imberger (2001a) and Boegman et al. (2003) showed, also evident from Fig. 9.9, that these oscillations were almost monochromatic with a frequency of around 10^{-2} Hz, just above the maximum buoyancy frequency and the Richardson number fell below the stability limit (Fig. 9.10). Gomez-Giraldo et al. (2008) carried out a detailed investigation of these high-frequency waves and showed that their horizontal geographic coherence was limited to less than 500 m, implying they are locally generated and do not, in general, propagate to the lake boundary to add to the mixing there.

Lake Kinneret is thus in a state of constant gentle agitation for the period from April to July (Antenucci and Imberger 2003; Boegman et al. 2003). As pointed out by Horn et al. (2001), and is evident from Figs. 9.6 and 9.8, the fact that the thermocline is close to mid-depth inhibits non-linear steepening of the basin-scale internal waves generated by the wind; for most of the time, the water in Lake Kinneret

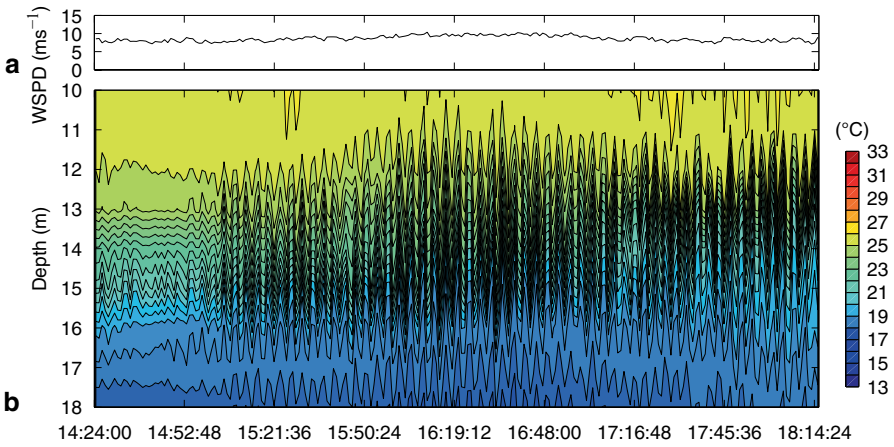

Fig. 9.9 Observations of high-frequency waves, **a** wind speed, and **b** isotherm contours at Sta. A on 17 June 2007 from 14:24:00 to 18:14:24. Contour intervals at 0.5 ˚C

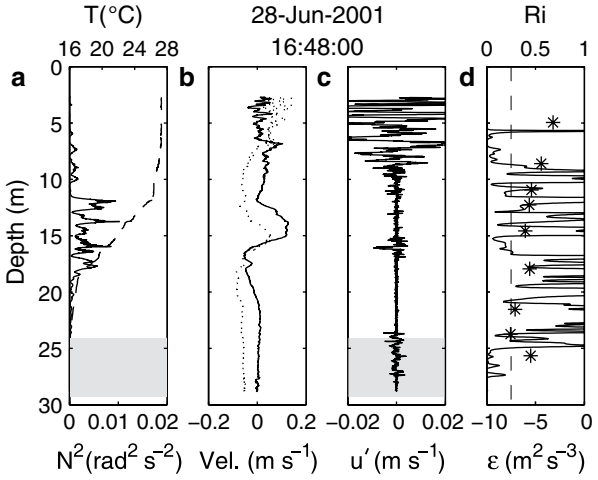

Fig. 9.10 Water column profile from a portable flux profile cast taken on 28 June 2001 in Lake Kinneret near Sta. T1, **a** Temperature, *T*, profile (*dash line*), buoyancy frequency squared N^2 (*solid line*) and mixed BBL thickness (*shaded area*), **b** north–south v (*solid line*) and east–west u (*dotted line*) velocity profiles (velocities are positive to the north and east), **c** fluctuating velocity component *u′* and mixed BBL thickness (*shaded area*), and **d** gradient Richardson number R_i (*solid line*) and dissipation of turbulent kinetic energy ε (*asterisks*)

simply oscillates in the form of Kelvin and Poincare waves. Periodically, in the latter half of this period, high-frequency waves are generated as shown in Fig. 9.9, but there is little evidence that these waves detach from the parent wave and propagate to shore as described by Boegman et al. (2005). The importance of this gentle internal rocking of the water column is that the wind working is transferred to energy

of the basin-scale internal waves that, in turn, are dissipated by bottom friction, generating turbulence that dampens the waves and sustains the BBL and the associated vertical mass flux (Marti and Imberger 2006). A typical 1-day June wind event (see Fig. 9.8) imparts about $E = 4 \times 10^{10}$ J of energy to the total water volume of Lake Kinneret (Antenucci and Imberger 2001b); about 80 % of the wind working goes to dissipation in the surface layer and the remaining energy is dissipated predominantly by bottom friction. The surface area of Lake Kinneret A_s is about 168 km^2 and the bottom is relatively smooth with a bottom drag coefficient C_b of about 2×10^{-3} (Shimizu and Imberger 2008). A velocity scale v_b due to the vertical mode-one Kelvin and Poincare waves (Antenucci et al. 2000) is around 0.1 m s^{-1}. Thus, the bottom average stress

$$\tau_b = C_b \rho_0 v_{b,}^2 \tag{9.6}$$

yields a value of 2×10^{-2} kg m^{-1} s^{-2}; so the rate of working at the bottom is given by

$$W_b = A_s \tau_b v_{b,} \tag{9.7}$$

leads to a value of ~3.4×10^5 W; hence, the spin-down timescale is given by E / W_b of order 1.4 days (see also Shimizu and Imberger 2008). The work done by the bottom stress goes back into the water column (Marti and Imberger 2006) as TKE, which then mostly goes to turbulent dissipation ε_b in the BBL, with a small fraction sustaining the vertical buoyancy flux associated with the BBL circulation (Imberger and Ivey 1993). The thickness of the BBL varies from about 9 m at the deepest point of the lake, Sta. A, to less than a meter near the perimeter of the metaliminion, where the increased density gradient prevents the upward entrainment (Lemckert et al. 2004; Marti and Imberger 2006). Suppose we take an average thickness for the BBL h_b of 2 m and an area for the lake bottom below the thermocline A_b of 90 km^2, then the dissipation in the turbulent BBL sustained by the bottom drag is given by a balance of the rate of working (Eq. 9.7) and the rate of dissipation (the buoyancy flux fraction may be assumed to be small)

$$\varepsilon_b = \frac{W_b}{\rho_0 h_b A_b} \tag{9.8}$$

becomes ~1.9×10^{-6} m^2 s^{-3}. This estimate is very close to what has been measured directly by Marti and Imberger (2006) and later confirmed with an exhaustive set of measurements in Lake Kinneret by Yeates et al. (2013).

The overall energy flux path, during the spring and early summer months, thus consists of the wind energy exciting the basin-scale internal waves, that in turn spin down over 1 or 2 days, energizing the turbulence in the BBL. In this way, given that during this time the wind events are almost always diurnal, the BBL remains continuously energized. The reader is referred to the papers by Antenucci et al. (2000); Antenucci and Imberger (2001b); Lemckert et al. (2004); Shimizu and Imberger (2008) and Shimizu and Imberger (2010) for a detailed description of how

the individual Kelvin and Poincare waves, exited by the wind, are damped by the dissipation in the BBL.

From an ecologist's perspective, there are two important consequences of this energy flux path associated with the basin-scale internal Kelvin and Poincare waves observed in spring and early summer in Lake Kinneret. First, the enhanced, almost steady mixing induced in the BBL by the vertical mode-one basin-scale waves excited by the wind, supports a vertical boundary transport that moves mass from the nutrient-rich hypolimnion to the surface layer for much of the spring and summer months (Imberger and Ivey 1993; Yeates and Imberger 2003; Lemckert et al. 2004; Marti and Imberger 2006, 2008). Second, the basin-scale motions in the surface layer combines with the wind-induced circulation and vertical shear to maintain a steady horizontal dispersion or mixing rate coefficient ε_h of around 10 $m^2\,s^{-1}$ (Stocker and Imberger 2003a, b).

The spring and summer habitats formed by these physical features make Lake Kinneret rather special in that there are few violent vertical mixing events; rather, the surface layer is mixed horizontally on a timescale L^2/ε_h ~66 days or about 2 months, allowing plankton patches to form (Hillmer et al. 2008; Ng et al. 2011), yet mixing the water vertically and sufficiently fast to avoid self-shading. The other physical control is the constraint on summer nutrients offered by the strong thermocline constraining the nutrient flux from the deep water to be through the BBL, so that the supply of nutrients is steady and distributed and at a rate that for thousands of years has supported a stationary seasonal variability with only rare excessive blooms (Berman et al. 1988; Bruce et al. 2006; Roelke et al. 2007; Chap. 10); the location of the thermocline at mid-depth prevents strong upwelling, constraining the exchange to a steady trickle rather than violent episodes.

Marti and Imberger (2006) carried out a very detailed investigation of the properties of the BBL, confirming the dissipation rate in the BBL that had previously been reported by Lemckert et al. (2004). However, Marti and Imberger (2006) then went on to identify the BBL mass and volume flux, and they were the first to provide a quantitative estimate of the volume flux, per unit width, of around $10^{-3}\,m^2s^{-1}$. Given that the lake perimeter at the thermocline depth is around 30,000 m, this implies a discharge of 30 $m^3\,s^{-1}$ of hypolimnetic waters into the base of the surface layer. The path of this discharge and the associated mass flux from the BBL into the metalimnion was documented by Marti and Imberger (2008) with a very detailed CTD–turbidity survey in the northwestern quarter of the lake; they used turbidity that seeded the BBL and this was tracked in the field and with numerical modelling up through the BBL and horizontally out into the metalimnion as an intrusion (Fig. 9.11).

This latter work showed that the above-mentioned mass flux first enters the metalimnion not only as an intrusion that spreads the BBL volume across the lake both as a gravitational intrusion, but also by vertical mode-two waves that progressively occur more and more as the strength of the summer stratification increases and dampens the mode-one oscillations. Such vertical mode-two waves have horizontal velocities in the metalimnion of around 0.2 m s^{-1} (see Fig. 9.10; Marti and Imberger 2008). Given the lake has a horizontal scale of around 15,000 m, this means any

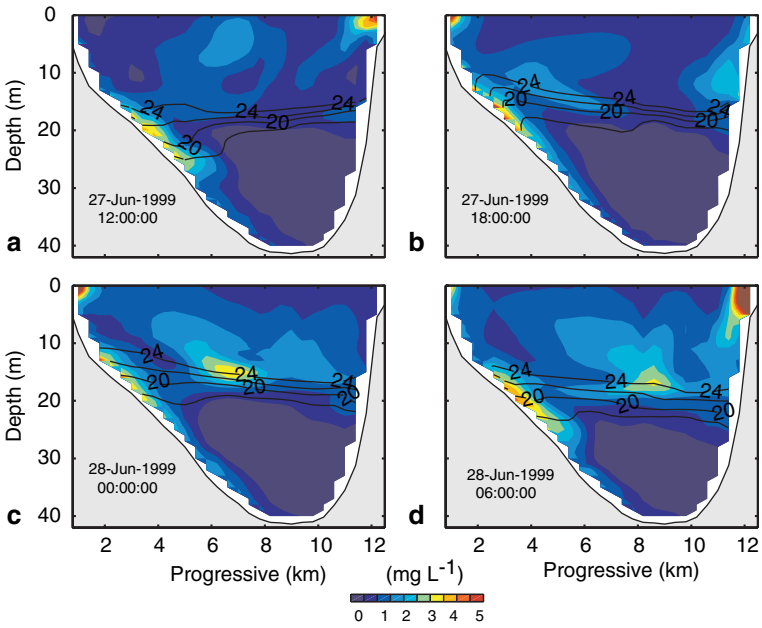

Fig. 9.11 Simulated suspended solids concentrations along the west–east transect in Lake Kinneret at four different times during 27–28 June 1999. The time is noted at the top of each panel

material, such as soluble reactive phosphorus, that is brought up via the BBL is transported across the whole lake at the base of the surface layer in around 21 hours, essentially providing a relatively uniform source of nutrients at the base of the surface layer ready to be injected into the surface layer whenever the wind is sufficient to erode the surface layer a little into the metalimnion.

9.5 August and September: Thermal Equilibrium, Stable Water Column

The 2 months are marked by a constant stratification with the bottom temperature at 16 °C and the surface temperature at 30 °C (Fig. 9.12), the mean Wedderburn number increased to around 2.5 (Fig. 9.2d) and the vertical mode-one waves are observed to decrease in amplitude with only the vertical mode-two and mode-three remaining (Fig. 9.12c, d); these modes, as discussed above, act to homogenize the water in the horizontal within the metalimnion. Non-linear steepening of the vertical mode-two waves is periodically observed sending internal mode-two bores through the metalimnion (see 3 August 2007 in Fig. 9.12d) that intensify as they shoal in the shallows (Boegman et al. 2005).

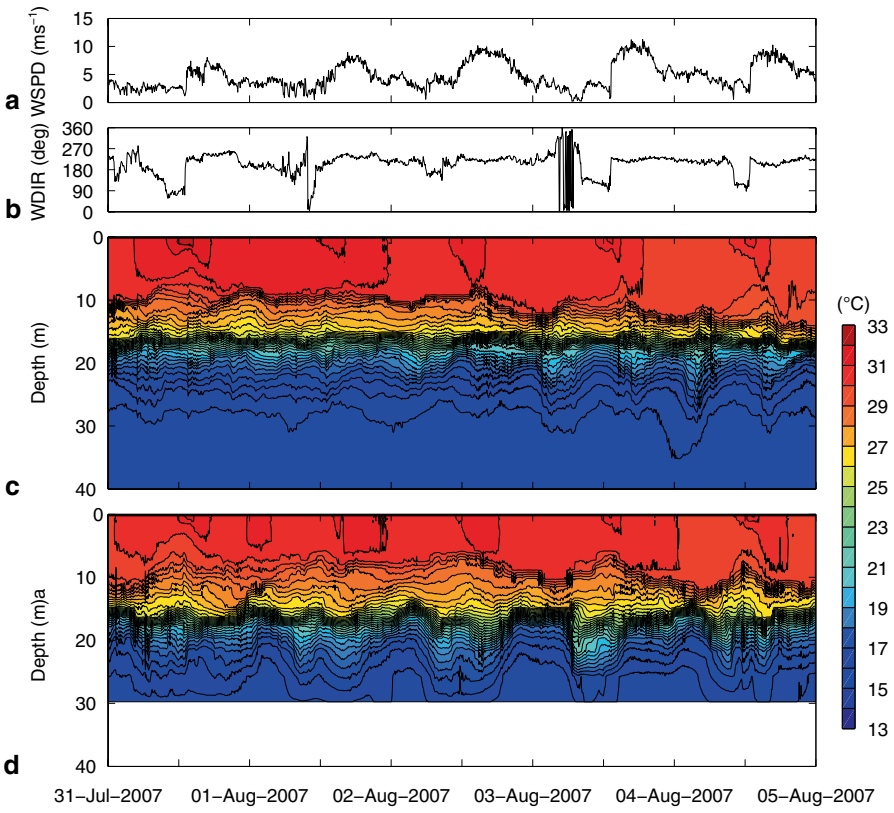

Fig. 9.12 **a** Ten-minute average wind speed. **b** wind direction. **c** isotherm contours at Sta. A. **d** isotherm contours at Sta. T1 from 31 July to 5 August 2007. Contour intervals at 0.5 ˚C

9.6 October, November, December: Convective Deepening and Cooling; Convective cooling, refer to heat flux

The 3 months of autumn are characterised by a strong, sharp thermocline and a net heat loss at the surface of around 100 W m^{-2} (Fig. 9.2f, g). The heat loss at the surface acts to cool the water in the surface layer and the associated buoyancy flux (Imberger 2013) generates TKE at the surface that constantly propagates downwards impinging on the deepening surface layer. This is seen by comparing the isothermal structure in Fig. 9.13 with that shown in Fig. 9.14 and is described accurately by a natural convective cooling (Imberger 2013) of a two-layer thermal stratification. On 1 October 2007 the surface layer temperature was ~28 °C and the bottom temperature was ~15.5 °C with the interface at 18 m. This changed to a two-layer stratification by 31 December 2007 with 17.5 °C at the surface and ~15.5 °C at the bottom with the interface at a depth of 32 m over a period of 7.95×10^6 s of

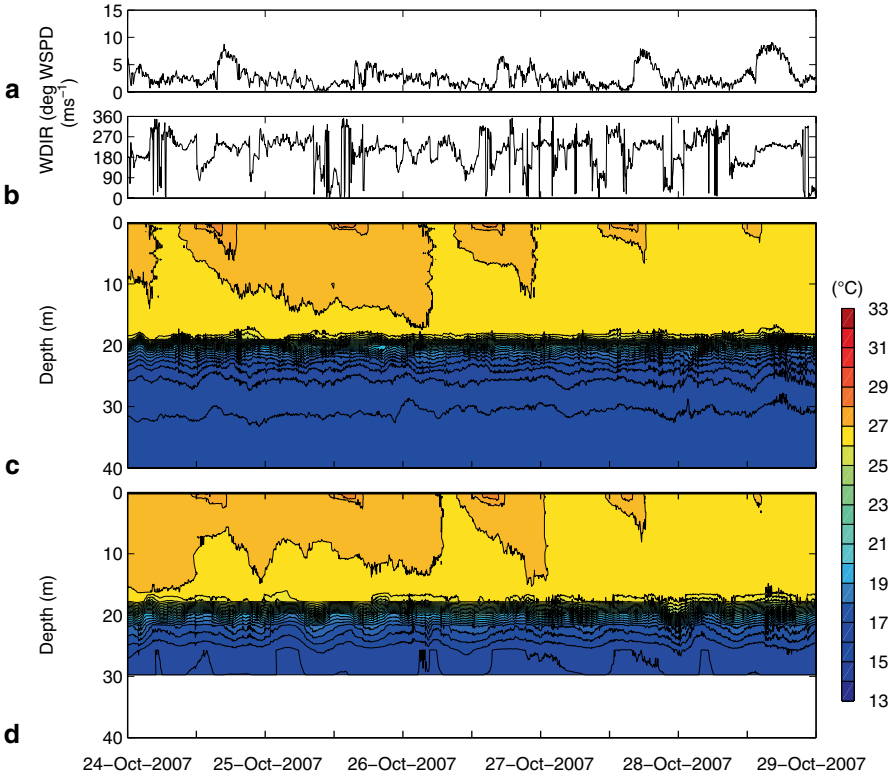

Fig. 9.13 **a** Ten-minute average wind speed. **b** wind direction.**c** isotherm contours at Sta. A. **d** isotherm contours at Sta. T1 from 24–29 October 2007. Contour intervals at 0.5 ˚C

net cooling (see Fig. 9.2g). This implies a net heat loss of around 80 W m^{-2} which compares favourably with the average over the period of the measured heat flux of 75 W m^{-2} (see Fig. 9.2f). The reader may also wish to compare the measured rate of deepening with that given by a simple convective deepening prediction detailed in Imberger (2013); again the two agree well. The autumn period, in Lake Kinneret, is thus represented, very closely, by a general cooling and natural convective deepening of the surface layer; the hypolimnetic water progressively shrinks in volume, remains almost stagnant and is almost constant in temperature, until the mixing reaches the bottom.

9.7 Conclusions

The hydrodynamics of Lake Kinneret is relatively well understood and is marked by five distinct regimes:

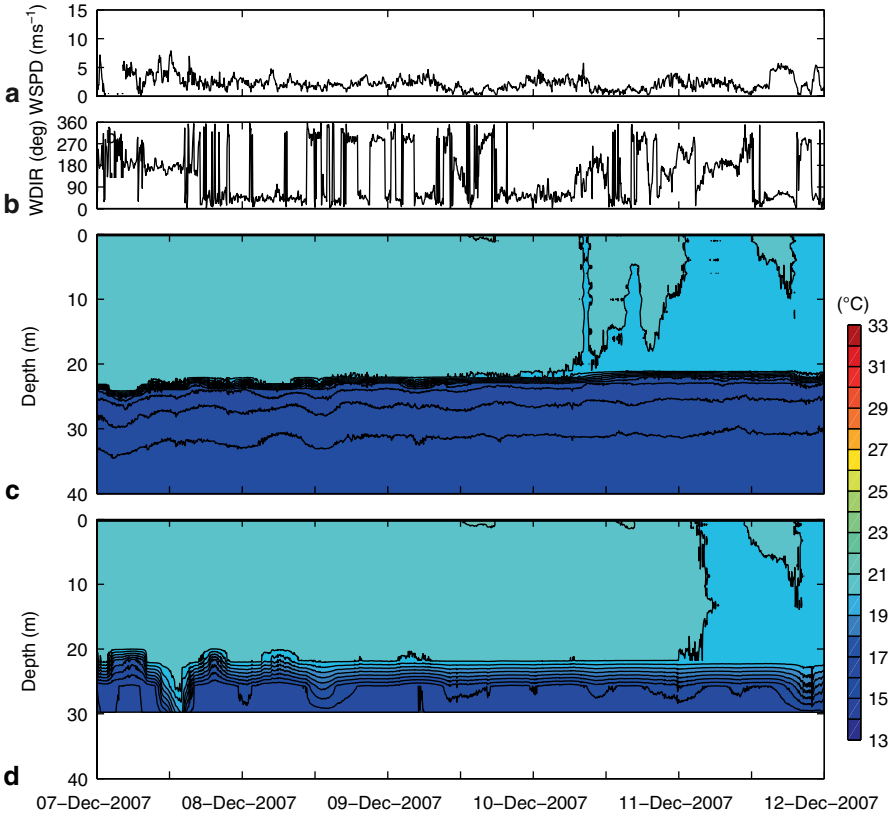

Fig. 9.14 **a** Ten-minute average wind speed. **b** wind direction. **c** isotherm contours at Sta. A. **d** isotherm contours at Sta. T1 from 7–12 December 2007. Contour intervals at 0.5 °C

1. January: mixing over the full depth of the water column and a water temperature around 15 °C. The water column is actively turbulent energized by wind shear, convective mixing and bottom drag due to topographic gyres.
2. February and March: Radiative heating stabilizes the water column and turbulence is weak, an ideal condition for plankton with buoyancy control.
3. April to July: a period of progressive heating and increasing winds; there appears to be a near-perfect balance between Coriolis, buoyancy and wind forces. Basin-scale internal waves persist and are mostly of vertical mode-one linear waves. These waves support both gentle horizontal mixing in the surface layer and a BBL flux that maintains a nutrient supply to the algae in the surface layer established in the February–March period.
4. August and September: a period of thermal equilibrium with vertical mode-two waves homogenizing the nutrients from depth in the previous period and making them available for a further period of 2 months.
5. October–December: Natural convection restores Lake Kinneret to a cold homogeneous water body.

Acknowledgments The authors would like to acknowledge financial support for the Lake Kinneret Research programme from both the Australian Research Council (Projects A00105595, DP0346282 and DP0773823) and the Israeli Water Authority. We also thank Gregory Attwater, Roger Head and Carol Lam for assisting with the field data collection. Both authors are very grateful to Dr Tamar Zohary, and the rest of the KLL team, for their very warm support over the years and especially during the production of this manuscript.

References

Antenucci JP, Imberger J, Saggio A (2000) Seasonal evolution of the basin-scale internal wave field in a large stratified lake. Limnol Oceanogr 45(7):1621–1638

Antenucci JP, Imberger J (2001a) On internal waves near the high-frequency limit in an enclosed basin. J Geophys Res 106(C10):22465–22474

Antenucci JP, Imberger J (2001b) Energetics of long internal gravity waves in large lakes. Limnol Oceanogr 46(7):1760–1773

Antenucci JP, Imberger J (2003) The seasonal evolution of wind/internal wave resonance in Lake Kinneret. Limnol Oceanogr 48(5):2055–2061

Berman T, Yacobi YZ, Pollingher U (1988) Lake Kinneret phytoplankton: stability and variability during twenty years (1970–1989). Aquat Sci 54:104–127.

Berman T, Stone L, Yacobi YZ, Kaplan B, Schlichter M, Nishri A, Pollingher U (1995) Primary Production and Phytoplankton in Lake Kinneret: A Long-Term Record (1972–1993) Limnol Oceanogr 40(6):1064–1076

Boegman L, Imberger J, Ivey GN, Antenucci JP (2003) High-frequency internal waves in large stratified lakes. Limnol Oceanogr 48(2):895–919

Boegman L, Ivey GN, Imberger, J (2005) The degeneration of internal waves in lakes with sloping topography. Limnol Oceanogr 50(5):1620–1637

Bruce LC, Hamilton DP, Imberger J, Gal G, Gophen M, Zohary T, Hambright D (2006) A numerical simulation of the role of zooplankton in C, N and P cycling in Lake Kinneret, Israel. Ecol Model 193 (3–4):412–436

Dubowski Y, Erez J, Stiller M (2003) Isotopic Paleolimnology of Lake Kinneret. Limnol Oceanogr 48(1):68–78

Eckert W, Imberger J, Saggio A (2002) Biogeochemical response to physical forcing in the water column of a warm monomictic lake. Biogeochemistry 61(3):291–307

Gill AE (1982) Atmosphere–ocean dynamics. Academic Press

Goldstein S (1929) Tidal motion in rotating elliptic basins of constant depth. Mon Not R Astron Soc (Geophys. Suppl.) 2:213–231

Gomez-Giraldo EA, Imberger J, Antenucci JP (2006) Spatial structure of the dominant basin-scale internal waves in Lake Kinneret. Limnol Oceanogr 51(1):229–246

Gomez-Giraldo EA, Imberger J, Antenucci JP, Yeates P (2008) Wind-shear generated high frequency internal waves as precursors to mixing in a stratified lake. Limnol Oceanogr 53(1):354–367

Hazan N, Stein M, Agnon A, Marco S, Nadel D, Negendank JFW, Schwab MJ, Neev D (2005) The late quaternary limnological history of Lake Kinneret (Sea of Galilee), Israel. Quaternary Res 63:60–77

Hillmer I, Van Reen P, Imberger J, Zohary T (2008) Phytoplankton patchiness and their role in the modelled productivity of a large, seasonally stratified lake. Ecol Model 218:49–59

Horn DA, Imberger J, Ivey GN (2001) The degeneration of large-scale interfacial gravity waves in lakes. J Fluid Mech 434:181–207

Imberger J (1985a) Thermal characteristics of standing waters: an illustration of dynamic processes. Hydrobiologia 125:7–29

Imberger J (1985b) The diurnal mixed layer Limnol Oceanogr 30:737–770

Imberger J (1998) Flux path in a stratified lake: A review. In: Imberger J (ed) Physical processes in Lakes and Oceans. Vol 54. American Geophysical Union
Imberger J (2013) Environmental Fluid Dynamics. Academic Press
Imberger J, Ivey GN (1993) Boundary mixing in stratified reservoirs. J Fluid Mech 248:477–491
Imberger J, Patterson JC (1990) Physical Limnology. In: Wu T (ed) Advances in Applied Mechanics. Academic Press, The publisher location is Boston
Krauss EB, Turner JS (1967) A one dimensional model of the seasonal thermocline, II The General Theory and its Consequences. Tellus 19:98–106
Laval BE, Imberger J, Hodges BR, Stocker R (2003) Modeling circulation in lakes: Spatial and temporal variations. Limnol Oceanogr 48(3):983–994
Lemckert CJ, Antenucci JP, Saggio A, Imberger J (2004) Physical properties of turbulent benthic boundary layers generated by internal waves. J Hydraul Eng-ASCE 130(1):58–69
Marti CL, Imberger J (2006) Dynamics of the benthic boundary layer in a strongly forced stratified lake. Hydrobiologia 568(1):217–233
Marti CL, Imberger J (2008) Exchange between littoral and pelagic waters in a stratified lake due to wind induced motions: Lake Kinneret, Israel. Hydrobiologia 603(1):25–51
Meier JA, Jewell JS, Brennen CE, Imberger J (2011) Bubbles emerging from a submerged granular bed. J Fluid Mech 666:189–203
Monismith SG (1985) Wind-forced motions in stratified lakes and their effect on mixed-layer shear. Limnol Oceanogr 30:771–783
Ng S, Antenucci JP, Hipsey MR, Tibor G, Zohary T (2011) Physical controls on the spatial evolution of a dinoflagellate bloom in a large lake. Limnol Oceanogr 56(6): 2265–2281
Nishri A, Imberger J, Eckert W, Ostrovosky I, Geifman J (2000) The physical regime and the respective biogeochemical processes in lower water mass of Lake Kinneret. Limnol Oceanogr 45(4):972–981
Ostrovsky I (2003) Methane bubbles in Lake Kinneret: quantification and temporal and spatial heterogeneity. Limnol Oceanogr 48(3):1030–1036
Parparov A, Gal G (2012) Assessment and implementation of a methodological framework for sustainable management: Lake Kinneret as a case study. J Environ Manage 101:111–117. doi:10.1016/j.jenvman.2012.01.030
Rimmer A, Aota Y, Kumagai M, Eckert W (2005) Chemical stratification in thermally stratified lakes: A chloride mass balance model. Limnol Oceanogr 50:147–157
Rimmer A, Gal G, Opher T, Lechinsky Y, Yacobi YZ (2011) Mechanisms of long-term variations of the thermal structure in a warm lake. Limnol Oceanogr 56:974–988
Roelke DL, Zohary T, Hambright KD, Montoya JV (2007) Alternative states in the phytoplankton of Lake Kinneret, Israel (Sea of Galilee). Freshwater Biol 52(3):399–411
Saggio A, Imberger J (2001) Mixing and turbulent fluxes in the metalimnion of a stratified lake. Limnol Oceanogr 46(2):392–409
Serruya C (ed) (1978) Lake Kinneret Monographiae Biologicae. 32: Dr. W. Junk Publishers, The Hague
Serruya S (1975) Wind, water temperature and motions in Lake Kinneret: General pattern. Verh Int Ver Limnol 19:73–87
Sherman FS, Imberger J, Corcos GM (1978) Turbulence and mixing in stably stratified waters. Ann Rev Fluid Mech 10:267–288
Shilo E, Ashkenazy Y, Rimmer A, Assouline S, Katsafados P, Mahrer Y (2007) Effect of wind variability on topographic waves: Lake Kinneret case. J Geophys Res 112 (C12024). doi:10.1029/2007JC004336
Shimizu K, Imberger J (2008) Energetics and damping of basin-scale internal waves in a strongly stratified lake. Limnol Oceanogr 53(4):1574–1588
Shimizu K, Imberger J (2009) Damping mechanisms of internal waves in a continuously stratified rotating basins. J Fluid Mech 637:137–172
Shimizu K, Imberger J (2010) Evolution of damped basin-scale internal waves in a shallow stratified lake. Limnol Oceanogr 55(3):1449–1462

Shintani T, de la Fuente A, Imberger J, Nino Y (2010) Generalizations of the Wedderburn Number: parameterizing upwelling in stratified lakes. Limnol Oceanogr 55(3):1377–1389

Spigel RH, Imberger J, Rayner KN (1986) Modelling the diurnal mixed layer. Limnol Oceanogr 31:533–556

Stocker R, Imberger J (2003a) Energy, partitioning and horizontal dispersion in a stratified rotating lake. J Phys Oceanogr 33(3):512–529

Stocker R, Imberger J (2003b) Horizontal transport and dispersion in the surface layer of a medium size lake. Limnol Oceanogr 48(3):971–982

Thompson RORY, Imberger J (1980) Response of a numerical model of a stratified lake to wind stress. In: Carstens T, McClimans T (eds) Second International Symposium on Stratified Flows, IAHR, Trondheim pp. 562–570

Thomson SIR W (Lord Kelvin) (1879) On gravitational oscillations of rotating water. Proc R Soc Edinb 10:92–100

Verburg P, Hecky RE (2009) The physics of the warming of Lake Tanganyika by climate change. Limnol. Oceanogr 54(6, part 2):2418–2430

Yacobi YZ, Ostrovsky I (2008) Downward flux of organic matter and pigments in Lake Kinneret (Israel): relationships between phytoplankton and the material collected in sediment traps. J Plankton Res 30(10):1189–1202

Yeates PS, Imberger J (2003) Pseudo two-dimensional simulations of internal and boundary fluxes in stratified lakes and reservoirs. International Journal of River Basin Management 1(4):297–319

Yeates PS, Imberger J, Gomez-Giraldo A (2013) Observed relationships between microstructure patches and the gradient Richardson number in a thermally stratified lake. Environ Fluid Mech 13:205–226. doi:10.1007/s10652–013-9269–4

Zohary T, Nishri A, Sukenik A (2012) Present–absent: a chronicle of the dinoflagellate Peridinium gatunense from Lake Kinneret. Hydrobiologia 698:161–174

Part III
Pelagic Communities

Chapter 10
Phytoplankton

Tamar Zohary, Yosef Z Yacobi, Alla Alster, Tatiana Fishbein, Shachaf Lippman and Gideon Tibor

Abstract The phytoplankton assemblage of Lake Kinneret is dominated by dinoflagellates. Secondary phytoplankton biomass contributors are cyanobacteria, chlorophytes, and diatoms, whereas cryptophytes are always present at a low biomass. The main bloom-forming dinoflagellate, *Peridinium gatunense,* bloomed every spring till the mid-1990s, but since then, it bloomed only during high-rainfall years. This change and a suite of additional changes in phytoplankton dynamics since 1994, changes that occurred after more than two decades of recorded constancy, were interpreted as early responses to increasing stress at the ecosystem level. In particular, the loss of the previously predictable annual pattern (spring bloom of *P. gatunense,* summer low-biomass, high-diversity assemblage), the appearance and establishment of toxin-producing cyanobacteria, a major loss in species richness, and a shift to dominance of less grazed species in summer are all manifestations of this change that can be viewed as a regime shift.

Surface and remote sensing of chlorophyll *a* (Chl *a*)—a proxy of algal biomass—indicates that phytoplankton concentration extremes at the lake surface mostly do not surpass a ratio of 1:2. Exceptional is a situation when Lake Kinneret is dominated by *P. gatunense,* and then the spatial heterogeneity of phytoplankton increases to a ratio of 1:50 between extreme concentrations. Chl *a* concentrations were often higher in the northern part of the lake, near the Jordan River inflow, where nutrient enrichment apparently boosts the growth of phytoplankton. The unique Chl *a*

T. Zohary (✉) · Y. Z Yacobi · A. Alster · T. Fishbein
The Yigal Allon Kinneret Limnological Laboratory, Israel Oceanographic & Limnological Research, P.O. Box 447, 14950 Migdal, Israel
e-mail: tamarz@ocean.org.il

Y. Z Yacobi
e-mail: yzy@ocean.org.il

A. Alster
e-mail: alster@ocean.org.il

S. Lippman
Charney School of Marine Sciences, University of Haifa, 31905 Haifa, Israel
e-mail: shachaflippman@yahoo.com

G. Tibor
Israel Oceanographic & Limnological Research, P.O. Box 8030, 31080 Haifa, Israel
e-mail: tiborg@ocean.org.il

T. Zohary et al. (eds.), *Lake Kinneret, Ecology and Management,* Aquatic Ecology Series 6,
DOI 10.1007/978-94-017-8944-8_10,

optical properties enable the identification and quantification of that substance using reflectance spectra emerging from the water surface and are recorded by sensors carried onboard satellites. Since 2006, images derived from optical information acquired by MERIS are utilized for mapping of the spatial distribution of phytoplankton in Lake Kinneret.

Keywords Phytoplankton · Biomass · Ecosystem stability · Dinoflagellates · Cyanobacteria · Chlorophytes · Diatoms · Chlorophyll *a* · Remote sensing · Primary production · Spatial variability

10.1 Species Composition And Abundance:

Tamar Zohary, Alla Alster, Tatiana Fishbein

The phytoplankton is one of the most important components of natural aquatic systems. Being the main primary producers, microscopic algae form the base of the pelagic food web, providing food and energy for higher trophic levels. As in most other lakes, the phytoplankton of Lake Kinneret makes the largest contribution to the total mass of living organisms in the water (Chap. 26). Phytoplankton species composition has a major impact on water quality (Sect. 33.1, Chap. 34). In Lake Kinneret, phytoplankton species composition is a primary indicator of ecosystem stability (see below).

The phytoplankton of Lake Kinneret is impacted dramatically by the presence or absence of *Peridinium gatunense,* a large-celled (~50 μm diameter) dinoflagellate that used to bloom every year during spring—until the mid-1990s. Since then, it blooms only during high-rainfall years (Zohary et al. 2012), whereas in years of its absence, a niche opens for other species.

10.1.1 Methods Employed for Monitoring the Kinneret Phytoplankton

Phytoplankton species composition and wet-weight biomass were followed routinely as part of the Kinneret monitoring program, starting January 1969, as detailed by Zohary (2004). Briefly, phytoplankton microscopic counts (sedimentation chamber technique; Lund et al. 1958) and wet-weight biomass determinations (Hillebrand et al. 1999) were conducted on Lugol-preserved water samples collected weekly or fortnightly from 10 to 13 discrete depths along the water column at the mid-lake Station A (Sta. A; see location in Chap. 1, Fig. 1.1), concurrently with samples collected for chemical analyses. For each sampling date, the discrete-depth biomass estimates were depth integrated to give a water-column value ($g_{wet\ weight}\ m^{-2}$). During stratification, depth integration was to mid-thermocline depth, usually between

15 and 20 m; during holomixis, the integration was over the entire water column. A specialized computer program, PlanktoMetrix, in routine use since 2005, was developed by us to assist the microscope counts and cell size measurements. An Internet photo-catalog of the Kinneret phytoplankton species, viewable at http://kinneret.ocean.org.il/phyt_cat_listView.aspx, was created to assist with species identification. The catalog contains microscope photographs of the Kinneret common species, with text comments highlighting diagnostic taxonomic features. A DNA barcode is now being added to each of the species in the catalog by applying a two-loci molecular system. The sequences of choice are the ribosomal DNA *internal transcribed spacer 1* (*rDNA ITS1*) and a fragment from the chloroplast gene encoding for the ribulose-1,5-bisphosphate carboxylase oxygenase large subunit (*rbcL-a*).

10.1.2 The Long-Term (1969–2012) Phytoplankton Record

10.1.2.1 Main Taxonomic Groups and their Share of Total Biomass

The phytoplankton of Lake Kinneret consists mostly of representatives from five taxonomic groups: dinoflagellates, chlorophytes, diatoms, cyanobacteria, and cryptophytes. Occasionally, representatives from two more groups, chrysophytes and euglenophytes, are also identified (Table 10.1). Until the mid-1990s, dinoflagellates were consistently the main biomass contributors to total phytoplankton biomass, with chlorophytes, diatoms, and cyanobacteria having secondary contributions and cryptophytes having an additional minor share (Pollingher 1986; Berman et al. 1995; Fig. 10.1a). Since the mid-1990s, the proportions have changed, the relative contribution of dinoflagellates has declined, while the shares of diatoms, chlorophytes, and especially cyanobacteria have increased (Fig. 10.1a).

10.1.2.2 Total Phytoplankton Biomass: Annual and Semiannual Means

Annual mean depth-integrated total phytoplankton wet-weight biomass (hence total biomass) ranged from 39.4 g m^{-2} in 1975 (a year with a minor *P. gatunense* bloom) to 156.4 g m^{-2} in 1998 (massive bloom year), with a multiannual mean of 79.2 g m^{-2} (Fig. 10.1b). The year-to-year variability in annual mean total biomass was relatively small in the 1970s and 1980s, but increased substantially since the mid-1990s, with high biomasses in years when *P. gatunense* bloomed ("Peridinium bloom years") and low or medium biomasses in years when it did not bloom ("non-Peridinium years"). Since *P. gatunense* always bloomed in the first half of the year, the pattern of greater year-to-year variability in phytoplankton biomass since the mid-1990s is more pronounced when examining semiannual (January–June) average biomasses (Fig. 10.1c). From 1969 to 1993, the mean January–June biomass was relatively stable. However, since 1994, years of exceptionally high winter–

Table 10.1 The phytoplankton of Lake Kinneret: past (Pollingher's 1978 species list) versus present (2006–2011). Where applicable, the number of the relevant photo (from Figs. 10.2 to 10.6) appears in parentheses after the species name. 1 present in the 1978 list only, 2 present both in the list and currently, 3 present only currently, a identified by Pollingher as "commonly occurring" (an objective measure of "common" was not given), b identified as being currently common (was counted on at least five different sampling dates in each one of the years 2006–2011)

Species (Figure)	Authority	Category
CYANOBACTERIA		
Chroococcales		
Aphanocapsa delicatissima	W & GS West	1
Aphanocapsa elachista	W & GS West	1
Aphanocapsa incerta (Microcystis pulverea var. *incerta)*	(Lemmermann) Cronberg & Komarek	1
Aphanocapsa pulchra	(Kützing) Rabenhorst	1
Aphanocapsa sp.		3
Aphanothece castagnei	(Brebisson) Rabenhorst	1
Aphanothece nidulans	Richter	1
Chroococcus limneticus (Fig. 10.4b)	Lemmermann	2a
Chroococcus minutus	(Kützing) Nageli	2a, b
Chroococcus turgidus (Fig. 10.5a)	(Kützing) Nageli	2a
Coelosphaerium dubium	Grunow	1
Cyanodictyon imperfectum (Fig. 10.4a)	Cronberg & Weibull	3b
Merismopedia angularis (Fig. 10.4c)	Thompson	3
Merismopedia glauca (Fig. 10.4d)	(Ehrenberg) Kützing	2
Merismopedia minima	Beck	2b
Merismopedia punctata (Fig. 10.4e)	Meyen	2
Merismopedia tenuissima	Lemmermann	1
Microcrocis geminata	(Lagerheim) Geiter	1
Microcystis (marginata) novacekii	(Meneghini) Kützing	2
Microcystis aeruginosa (Fig. 10.4f)	(Kützing) Kützing	2a, b
Microcystis botrys (Fig. 10.4g)	Teiling	2a
Microcystis flos-aquae (Fig. 10.4h)	(Wittrock) Kirchner	3b
Microcystis viridis (Fig. 10.4i)	(Braun) Lemmermann	2
Microcystis wesenbergii (Fig. 10.4j, k)	(Komarek) Komarek	2a
Radiocystis geminata	Skuja	2
Oscillatoriales		
Arthrospira maxima (Spirulina platensis)	Setchell & Gardner	1
Phormidium amoenum (Oscillatoria amoena)	(Kützing) Anagnostides & Komarek	1
Phormidium sp.	Kützing ex Gumont	3
Planktolyngbia (Lyngbia) limnetica	(Lemmermann) Komarkova-Legnerova & Cronberg	2b
Planktothrix (Oscillatoria) agardhii	(Gomont) Anagnostidis & Komarek	2
Planktothrix compressa (Oscillatoria mougeotii)	(Utermohl) Anagnostidis & Komarek	2
Pseudanabaena (Phormidium) cf. *mucicola*	(Naumann & Huber Pestalozzi) Schwabe	2
Pseudanabaena catenata	Lauterborn	2
Spirulina albida	Kolkwitz	1
Nostocales		
Anabaena bergii (Fig. 10.3d)	Ostenfeld	3
Anabaena planctonica	Brunnthaler	1a
Anabaena spiroides (Fig. 10.3c)	Klebahn	2a

Table 10.1 (continued)

Species (Figure)	Authority	Category
Anabaenopsis circularis	(GS West) Woloszynska & Miller	1
Aphanizomenon flos-aquae	((Linneus) Ralfs) Bornet & Flahault	1
Aphanizomenon ovalisporum (Fig. 10.3a, b)	Forti	3b
Cylindrospermopsis raciborskii (Fig. 10.3e–g)	Seenayya et Subba Raju	3b
BACILLARIOPHYTA		
Centrales		
Acanthoceras (Attheya) zachariasii	(Brun) Simonsen	1
Aulacoseira (Melosira) granulata (Fig. 10.3h)	(Ehrenberg) Simonsen	2a, b
Aulacoseira (Melosira) granulata var. *angustissima* (Fig. 10.3h)	(Muller) Simonsen	2
Aulacoseira italica ssp. *subarctica*	(Muller) Simonsen	1
Cyclotella meneghiniana (Fig. 10.5b, c)	Kützing	2a
Cyclotella polymorpha (Fig. 10.5d)	Meyer & Hakansson	3b
Cyclotella sp.	(Kützing) Brebisson	3
Discostella stelligera	(Cleve & Grunow) Houk et Klee	2a
Melosira arenaria	(Moore) Ralfs	1
Stephanodiscus hantzschii	Grunow	1a
Pennales		
Achnanthes sp.	Bory	3
Anomoeoneis sphaerophora	(Kutzine) Pfitzer	3b
Epithemia muelleri	Fricke	1
Fragilaria crotonensis	Kitton	2
Gyrosigma acuminatum (Fig. 10.5e)	(Kützing) Rabenhorst	2
Navicula sp. (Fig. 10.5g)	Bory	2a
Nitzschia acicularis	(Kützing) W Smith	2
Nitzschia holstatica	Hustedt	2
Nitzschia sigmoidea (Fig. 10.5f)	(Nitzsch) W Smith	2
Nitzschia stagnorum	Rabenhorst	2
Synedra acus	Kützing	2a
Synedra affinis	Kützing	2
Synedra fasciculata	(Agardh) Kützing	1
Synedra rumpens	Kützing	3b
Synedra ulna	(Nitzsch) Ehrenberg	2
Synedra ulna var. *oxyrhynchus fa. mediocontracta*	(Kützing) Van Heurck	1
Synedra ulna var. *ramesi*	(Heribaud) Hustedt	1
CHRYSOPHYTA		
Dinobryon sp.	Ehrenberg	1
Erkenia subaequiciliata	Skuja	2a, b
Mallomonas sp.	Perty	1
Monas mediovacuolata	Skuja	1
Synura sp.	Ehrenberg	1
DINOPHYTA		
Ceratium hirundinella (Fig. 10.2d, e)	(O.F. Muller) Dujardin	2a, b
Ceratium hirundinella var. *furcoides*	Dujardin	3
Ceratium hirundinella f. *gracile*	Dujardin	2
Ceratium hirundinella var. *robustum*	Dujardin	2
Ceratium hirundinella type *scoticum*	Dujardin	2
Glenodinium (Sphaerodinium) cinctum	(Ehrenberg) Woloszynsca	1

Table 10.1 (continued)

Species (Figure)	Authority	Category
Glenodinium sp.	Klebs	2
Gonyaulax apiculata	(Penard)Entz	1
Gymnodinium lacustre (Fig. 10.2h)	Schiller	2b
Peridiniopsis (Glenodinium) oculatum	(Stein) Bourrelly	2b
Peridiniopsis borgei (Fig. 10.2c)	Lemmermann	3
Peridiniopsis (Peridinium) cunningtoni (Fig. 10.2f)	Lemmermann	2a, b
Peridiniopsis elpatiewskyi (Fig. 10.2g)	(Ostenfeld) Bourrelly	3b
Peridiniopsis penardiformis (Fig. 10.2i)	(Lindemann) Bourrelly	3
Peridiniopsis polonicum (Glenodinium gymnodinium) (Fig. 10.2j)	(Woloszynsca) Bourrelly	2a
Peridinium bipes	Stein	1
Peridinium gatunense (P. cinctum fa. *westii)* (Fig. 10.2a, b)	Nygaard	2a, b
Peridinium inconspicuum	Lemmermann	1a
Peridinium palatinum	Lauterborn	1
Peridinium pseudolaeve	Lefevre	1
Peridinium sp.	Ehrenberg	3
CRYPTOPHYTA		
Chroomonas acuta	Utermohl	1
Cryptomonas erosa	Ehrenberg	2
Cryptomonas ovata	Ehrenberg	2a, b
Cryptomonas reflexa	Skuja	2
Rhodomonas lacustris	Pasher & Ruttner	1
Rhodomonas minuta	Skuja	2a
Plagioselmis nannoplanktica (R. minuta var. *nannoplanktica*	(Skuja) Novarino, Lucas & Morrall	2b
EUGLENOPHYTA		
Euglena acus (Fig. 10.5i)	Ehrenberg	2
Euglena oxyuris	Schmarda	1
Euglena proxima	Dangeard	3
Euglena spathirhyncha	Skuja	1
Euglena texta	(Dujardin) Hubner	1
Euglena tripteris	(Dujardin) Klebs	1
Phacus caudatus	Hubner	2
Phacus longicauda (Fig. 10.5j)	(Ehrenberg) Dujardin	2
Phacus longicauda var. *insecta*	Pochmann	1
Trachelomonas hispida (Fig. 10.5k)	(Perty)Stein	2b
Trachelomonas volvocina	Ehrenberg	2b
CHLOROPHYTA		
Volvocales		
Chlamydomonas sp. 1	Ehrenberg	2
Chlamydomonas sp. 2	Ehrenberg	3
Eudorina elegans (Fig. 10.6e)	Ehrenberg	2
Gonium pectorale	OF Muller	1
Pandorina morum (Fig. 10.6i)	(Muller) Bory	2
Tetrasporales		
Asterococcus superbus	Scherffel	1
Chlamydocapsa (Gloeocystis) ampla (schroeteri)	(Kützing) Fott (Chodat) Lemmermann	1 1

Table 10.1 (continued)

Species (Figure)	Authority	Category
Chlorococcales		
Acanthosphaera zachariasii	Lemmermann	1
Actinastrum hantzschii	Lagerheim	2
Ankistrodesmus falcatus	(Corda) Ralfs	2a
Ankistrodesmus falcatus var. *duplex*	(Kützing) GS West	1
Ankistrodesmus falcatus var. *spirilliformis*	GS West	1
Ankistrodesmus nannoselene	Skuja	1
Ankistrodesmus setigerus	(Schröder) GS West	1
Botryococcus braunii (Fig. 10.4l)	Kützing	2a
Chlorella pyrenoidosa	Chick	1
Chlorella vulgaris	Beijerinck	2a
Chlorococcum infusionum (humicolum)	(Schrank) Meneghini	1
Coelastrum astroideum (Fig. 10.6a)	De-Not	3
Coelastrum cambricum var. *intermedium*	GS West	1
Coelastrum microporum	Nageli	2a, b
Coelastrum reticulatum (Fig. 10.6b)	(PA Dangeard) Senn	2a, b
Coelastrum scabrum var. *torbolense*	Kirchne	1
Coelastrum sphaericum	Nageli	1
Crucigenia emarginata	(W & GS West) Schmidle	1
Crucigenia quadrata (Fig. 10.6c)	C Morren	2
Crucigenia tetrapedia	(Kirchner) W & GS West	2
Crucigeniella pulchra (Tetrastrum pulloideum)	W& GS West	1
Crucigeniella (Crucigenia) rectangularis	(Naegeli) Komarek	2a, b
Dictyosphaerium ehrenbergianum	Nageli	1
Dictyosphaerium elegans	Bachmann	1a
Elakatothrix gelatinosa (Fig. 10.5n)	Wille	2a, b
Franceia ovalis (Fig. 10.5m)	(France) Lemmermann	2b
Golenkinia radiata	(Chodat) Korshikow	2
Hindakia tetrachotoma (=Dictyosphaerium tetrachotomum)	Printz	3
Kirchneriella lunaris	(Kirchner) K. Mobius	2
Kirchneriella obesa (Fig. 10.6f)	(W West) Schmidle	2
Lagerheimia (Chodatella) ciliata	(Laherheim) Chodat	1
Lagerheimia (Chodatella) citriformis (Fig. 10.5l)	(J Snow) Collins	2a, b
Lagerheimia (Chodatella) longiseta	Lemmermann	1
Lagerheimia genevensis	(Chodat) Chodat	2b
Micractinium pusillum (Fig. 10.6g)	Fresenius	2
Monoraphidium arcuatum (=Ankistrodesmus falcatus var. *mirabilis)*	West and West	2
Monoraphidium contortum	(Korshkov) Hindak	3
Monoraphidium komarkovae (=Ankistrodesmus falcatus var. *acicularis)*	(Brebisson) GS West	2
Mucidosphaerium (Dictyosphaerium) pulchellum (Fig. 10.6d)	Wood	2
Nephrochlamys subsolitaria	(G West) Korschikov	2
Nephrocytium agardhianum (Fig. 10.6h)	Nageli	2
Nephrocytium limneticum	(GM Smith) GM Smith	1
Nephrocytium lunatum	West	2
Oocystis elliptica var *minor*	W & GS West	1
Oocystis lacustris (Fig. 10.5o)	Chodat	2a

Table 10.1 (continued)

Species (Figure)	Authority	Category
Oocystis novae-semliae	Wille	1
Oocystis solitaria	Wittrock	2a, b
Oocystis submarina	Lagerheim	1a
Pediastrum boryanum	(Turpin) Meneghini	2a
Pediastrum duplex (Fig. 10.6j)	Meyen	2a
Pediastrum integrum	Nageli	1
Pediastrum simplex (Fig. 10.6l)	Meyen	2a
Pediastrum simplex var. *simplex (P. clathratum)*	(Schröder) Lemmermann	2a
Pediastrum simplex var. *sturmii (P. sturmii)*	(Reinsch) Wolle	2a
Pediastrum tetras (Fig. 10.6m)	(Ehrenberg) Ralfs	2a, b
Planctococcus sphaerocystiformis	Korshikow	1
Quadrigula sp.	Printz	3
Scenedesmus acuminatus (Fig. 10.6n)	(Lagerheim) Chodat	2
Scenedesmus acuminatus var. *tetradesmoides*	G. M. Smith	3
Scenedesmus acuminatus var. *minor*	G. M. Smith	2
Scenedesmus acutiformis	Schröder	2
Scenedesmus acutus	(Lagerheim) Chodat	2
Scenedesmus acutus f. *alternans*	Hortobagyi	2
Scenedesmus arcuatus	Lemmermann (Lemmermann)	1
Scenedesmus armatus	Chodat (Chodat)	2a
Scenedesmus bicellularis	Chodat	2
Scenedesmus bijuga	(Turpin) Lagerheim	2b
Scenedesmus bijuga var. *alternans*	(Reinsch) Hansgirg	2
Scenedesmus bijuga var. *seriatus*	Volk	1
Scenedesmus communis	Hegewald	3
Scenedesmus denticulatus (Fig. 10.6o)	Lagerheim	2
Scenedesmus ecornis	(Ehrenberg) Chodat	2a
Scenedesmus houlensis	Rayss	1
Scenedesmus opoliensis	P Richter	1
Scenedesmus perforatus	Lemmermann	2
Scenedesmus quadricauda (Fig. 10.6p)	(Turpin) Brebisson	2a, b
Scenedesmus quadricauda var. *longispina*	(Chodat) GM Smith	1
Scenedesmus spinosus	Chodat	2
Selenastrum bibraianum (Fig. 10.6q)	Reinsch	2
Selenastrum capricornutum	Printz	1
Selenastrum gracile	Reinsch	2
Selenastrum minutum	(Nagelli) Collins	2
Sphaerocystis planctonica (Fig. 10.6r)	(Korshicov) Bourelly	3
Tetradesmus wisconsinensis f. *wisconsinensis*	GM Smith	3
Tetraedron caudatum	(Corda) Hansgirg	2
Tetraedron minimum (Fig. 10.5q)	(A Braun) Hansgirg	2a, b
Tetraedron quadratum f. *minor-obtusum*	Reinsch	1
Tetraedron regulare fa. minor	Reinsch	1
Tetraedron sp. (Fig. 10.5r)	Kuetzing	3b
Tetraedron triangulare	Korshikov	3b
Tetraedron trigonum var. minor	(Schröder Lemmermann	1a
Tetraedron trigonum	(Nageli.) Hansgirg	1
Tetrastrum glabrum (= Crucigenia triangularis)	(Roll) Ahlstrom and Tiffany	1

Table 10.1 (continued)

Species (Figure)	Authority	Category
Tetrastrum heteracanthum f. *elegans*	Ahlstrom & Tiffany	1
Tetrastrum staurogeniforme (= T. apiculatum)	Shroeder	2
Tetrastrum triangulare (Crucigenia minima)	(Chodat) Komarek	2b
Treubaria setigera (Fig. 10.5s)	(Archer) GM Smith	3b
Treubaria triappendiculata (Fig. 10.5t)	Bernard	2
Zygnematales		
Closterium acerosum	(Shrank) Ehrenberg	1
Closterium aciculare	T West	1
Closterium aciculare var. *subpronum* (Fig. 10.3j)	West et GS West	2a, b
Closterium acutum var. *variabile*	(Lemmermann) Krieger	2b
Closterium gracile	Brebisson	1
Closterium polystictum	Nygaard	2
Closterium pronum	Brebisson	1
Cosmarium sp. 1 (small)	Corda ex Ralfs	3b
Cosmarium sp. 2 (large)	Corda ex Ralfs	3
Cosmarium granatum	Brebisson	1
Cosmarium leave	Rabenhorst	2a
Cosmarium sphagnicolum	W & GS West	1
Euastrum denticulatum	Gay	3
Mougeotia sp. (Fig. 10.3i)	Agardh	3b
Staurastrum gracile	Ralfs	2
Staurastrum longipes	(Nordstedt) Teiling	1
Staurastrum manfeldtii (Fig. 10.5p)	Delponte	3
Staurastrum muticum	Brebisson	1
Staurastrum paradoxum var. *parvum*	W West	2
Staurastrum smithii (S. contortum)	Teiling	3
Staurastrum tetracerum	Ralfs	3b
Staurastrum volans	W & GS West	1
Klebsormidiales		
Koliella sp.	Hindak	3
PRASINOPHYTA		
Tetraselmis (Platimonas; Carteria) cordiformis (Fig. 10.5u)	(HJ Carter) F Stein	2b

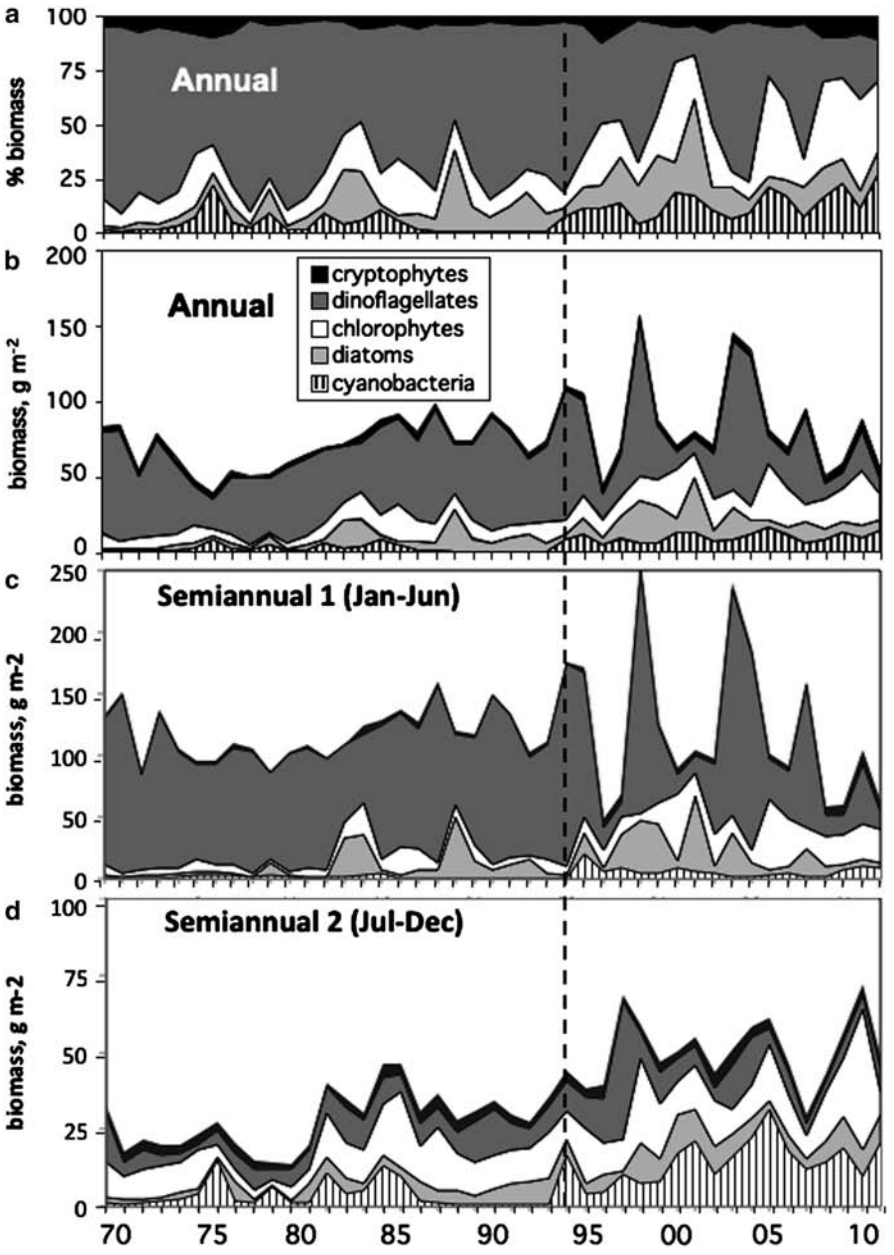

Fig. 10.1 Time series of annual mean and semiannual mean total phytoplankton wet-weight biomass and the contribution of the five main taxonomic groups to the total biomass, 1969–2011. **a** Annual percent contribution of each taxonomic group. **b**–**d** Annual (**b**) or semiannual (**c**, **d**) depth-integrated wet-weight biomass, g m^{-2}; *Thin vertical line* in 1994 denotes the year of the first-ever bloom of *Aphanizomenon ovalisporum* and the onset of a different regime

spring biomass (years with massive *P. gatunense* blooms, 1998, 2003, 2004, and 2012) alternated with non-Peridinium years of considerably lower winter–spring biomass (1996, 1997, 2008, 2009, and 2011).

The summer–fall mean biomass record showed a different long-term pattern, of a continuous increase over time, with semiannual biomass values during 2000–2011 being more than double those of the 1970s (Fig. 10.1d). Until the mid-1990s, the summer–fall biomass was always only a small fraction of the winter–spring biomass; since then, in some non-Peridinium years (1996, 1997, 2008, 2009) it was similar to the winter–spring biomass of the same year. The long-term increase in summer–fall total phytoplankton biomass was accompanied by major changes in species composition and morphological features of those species. The summer–fall assemblage of the 1970s and 1980s was characterized by nanoplanktonic species, mostly unicellular or forming small coenobia and comprising good food for zooplankton (Pollingher 1981, 1986). In contrast, the summer–fall assemblage since the mid-1990s was characterized by filamentous species, such as *Aphanizomenon ovalisporum, Cylindrospermopsis raciborskii, Mougeotia* sp., as well as elongated or spined unicellular species. The diatoms *Synedra ulna* and *Synedra rumpens* and the desmids *Closterium aciculare* and *Staurastrum manfeldtii* belonged to the latter category. Most of these elongated species were newcomers in the lake (Table 10.1) and considered poor food value for zooplankton (Zohary 2004). Thus, lower grazing pressure may explain the gradual long-term increase in the summer phytoplankton biomass notable in Fig. 10.1d.

10.1.2.3 Long-Term Changes at the Species Level

Long-term changes are also apparent at the species level. Of the 205 species (including some varieties) reported from Lake Kinneret by Pollingher (1978), only 118 species appeared in the plankton during 2006–2011 (Table 10.1), while 87 species (42% of the total) are no longer found in the lake. The lost species belonged to all taxonomic groups, with the largest number belonging to the chlorophytes (46), followed by cyanobacteria (15). In parallel, 38 species that were not listed by Pollingher (1978) have appeared in the plankton. The current species list includes 156 species; of those, photographs of 65 species are shown in Figs. 10.2–10.6. The exact numbers of species may be slightly different, due to the change of person identifying the species present, yet an overall severe loss of species is apparent. Such a trend is certainly not desirable in a natural ecosystem and is a cause for concern.

Pollingher (1978) listed 47 species as being "commonly occurring," although objective criteria for this definition were not provided. The current species list has 42 "common" species, defined here as those that were counted on at least five different dates on each one of the years 2006–2011. Eighteen of Pollingher's common species are still common today (Table 10.1) whereas 23 species are no longer common and six of her common species are not seen today at all. At the same time, 14 of the "newcomers," species that were never recorded in the 1970s, are common today.

Dinoflagellates

The dinoflagellates occurring in Lake Kinneret (Table 10.1, Fig. 10.2a–k) are all motile (flagellated) unicellular organisms, most of which are also quite large in size (20–60 μm diamter), and therefore, their contribution to phytoplankton biomass is substantial. Their annual cycle includes a cyst stage for oversummering on the lake bed sediments (Pollingher 1987). Most of the Kinneret species are armored, their protoplast being enveloped by a theca made of polysaccaride plates. *P. gatunense,* the most abundant Kinneret dinoflagellate (Fig. 10.2a, b), is also the most studied species occurring in the lake (see Chap. 11). Until the mid-1990s, *Ps. borgei* (Fig. 10.2c) was the second most abundant dinoflagellate. *Ceratium hirundinella* (Fig. 10.2d, e) is another large dinoflagellate, easily identifiable by its characteristic "horns." This was the first phytoplankton species ever reported from Lake Kinneret by Barrois (1894). Over the past four decades, *Ceratium hirundinella* was usually subdominant to *P. gatunense*; but in the absence of the latter, in spring 2010, a bloom of *C. hirundinella* developed, reaching a peak biomass of 147 g m^{-2} (Zohary et al. 2012).

Other prominent dinoflagellates are additional species of the genus *Peridiniopsis*, including *Ps. cunningtoni, Ps. elpatiewskyi, Ps. penardiformis,* and *Ps. polonicum* (Fig. 10.2f, g, i, j). Since the mid-1990s, *Ps cunningtoni and Ps. elpatiewskyi* (Fig. 10.2f, g) have become particularly abundant and major biomass contributors in non-Peridinium years. A nonpigmented heterotrophic dinoflagellate, *Diplopsalis acuta* (Fig. 10.2k), is also common, as well as the non-thecate, phototrophic *Gymnodinium* sp. (Fig. 10.2h). Further details on the Kinneret dinoflagellates are provided by Pollingher and Hickel (1991).

Cyanobacteria

During the early 1970s, cyanobacteria (Figs. 10.3a–g, 10.4a–k, 10.5a) usually contributed less than 5 g m^{-2} to total phytoplankton biomass (Fig. 10.1). From 1975 to 1985, several years of higher cyanobacterial biomass occurred (usually up to ~20 g m^{-2}), mostly due to peaks in *Microcystis* spp. and *Chroococcus minutus,* with the colonial *Radiocystis geminata* and *Cyanodictyon imperfectum* being common (Pollingher 1986). These years were followed by a sequence of 8 years, from 1986 to 1993, in which cyanobacterial contribution to total biomass declined to barely detectable levels (Fig. 10.1). A prominent feature of the 1969–1993 record is that the Chroococcales species dominated the cyanobacterial assemblage. N_2-fixing cyanobacteria, belonging to the Nostocales, were rare (Pollingher 1991), and although they did occur in the early 1970s, their annual mean contribution to total phytoplankton biomass was only 0.1–1.5 %; in the 1980s and early 1990s their contribution declined to below detection limit (Zohary 2004).

An abrupt change occurred in summer 1994 when the N_2-fixing filamentous cyanobacterium *Aphanizomenon ovalisporum* (Nostocales; Fig. 10.3a, b) appeared and bloomed for the first time (Pollingher et al. 1998; Hadas et al. 2002).

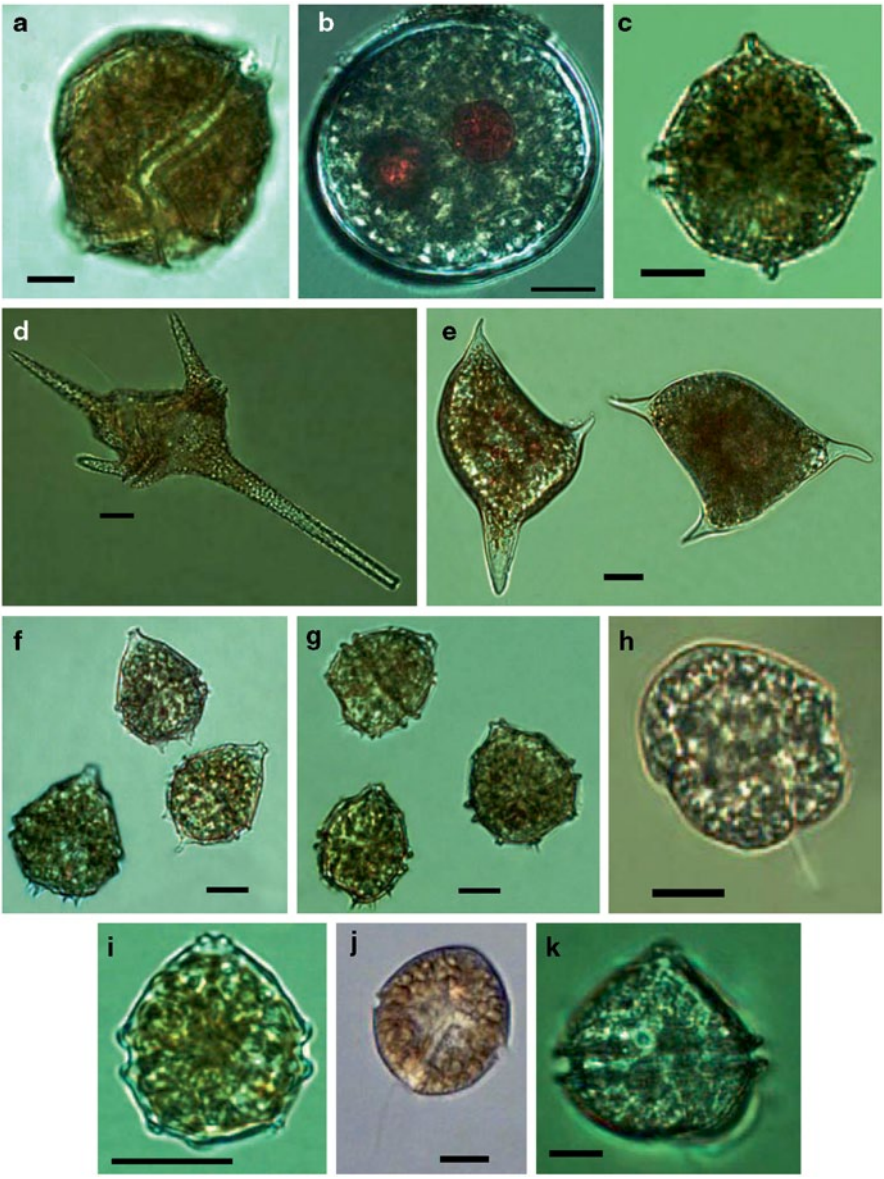

Fig. 10.2 Kinneret dinoflagellates: **a**, **b** *Peridinium gatunense* (**a** vegetative cell, **b** cyst), **c** *Peridiniopsis borgei*, **d**, **e** *Ceratium hirundinella* (**d** vegetative cell, **e** cyst), **f** *Peridiniopsis cunningtoni*, **g** *Peridiniopsis elpatiewskyi*, **h** *Gymnodinium* sp., **i** *Peridiniopsis penardiformis*, **j** *Peridiniopsis polonicum*, **k** *Diplopsalis (Entzia) acuta*. Scale bars, 10 µm. Photographed with an Olympus BX50 light microscope equipped with DIC optics and a PixeLINK camera (×40 or ×100)

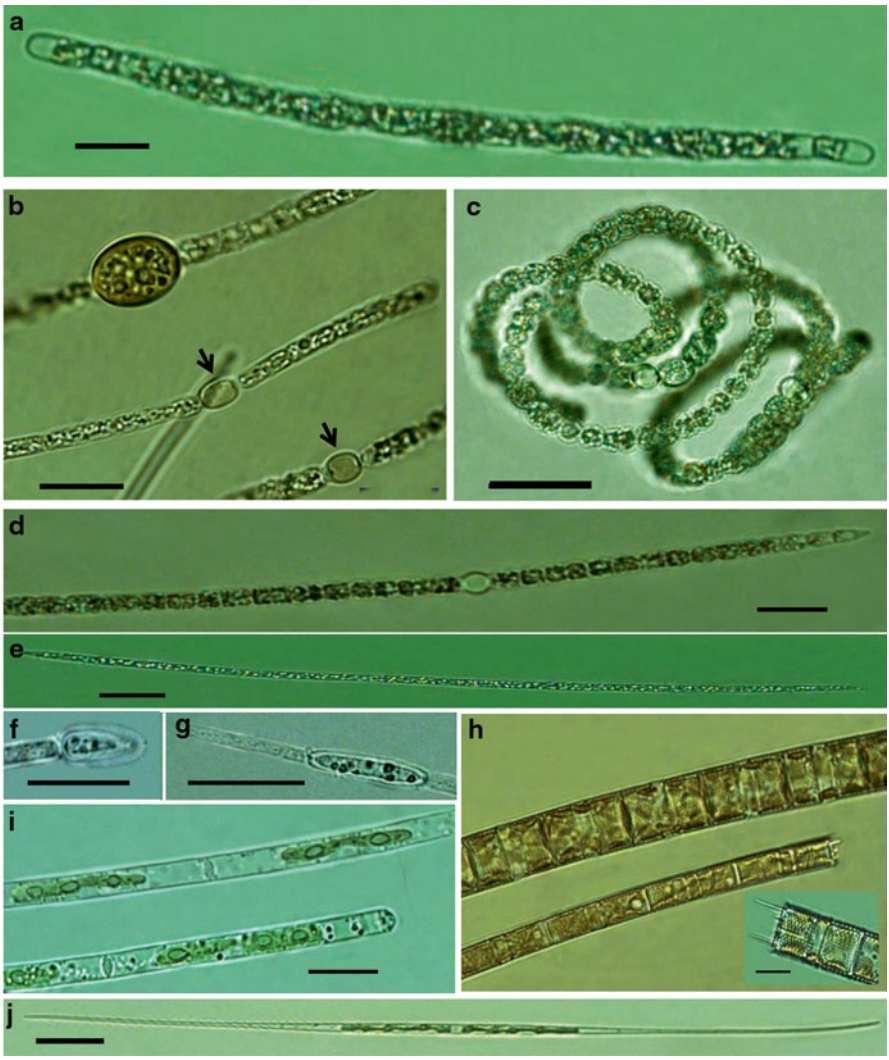

Fig. 10.3 Kinneret filamentous species: **a**–**g** cyanobacteria: **a**, **b** *Aphanizomenon ovalisporum* (**a** filament with hyaline ends, **b** akinete (*largest cell*) and heterocytes (*arrows*)), **c** *Anabaena spiroides*, **d** *Anabaena bergii*, **e**, **f**, **g** *Cylindrospermopsis raciborskii* (**e** filament, **f** akinete, **g** heterocyte), **h** centric diatom: *Aulacoseira granulata* (*thick filament*) and *A. granulata* var. *angustissima* (*thin filament*). *Inset:* end cell with typical spines, **i**, **j** chlorophyta: **i** *Mougeotia* sp., **j** *Closterium aciculare*. Scale bars, 10 µm. Details of photographic equipment as in legend to Fig. 10.2

Recently, this species was assigned to a new genus *Chrysosporum, i.e., Chrysosporum ovalisporum* (Zapomelova et al. 2012), but throughout this book we refer to it as *Aphanizomenon*. This species was shown to produce cyanotoxins (Banker et al. 1997) and as such was considered a main threat to water quality in a lake that is a national source of drinking water (Sect. 33.1). A few years later, around 2000,

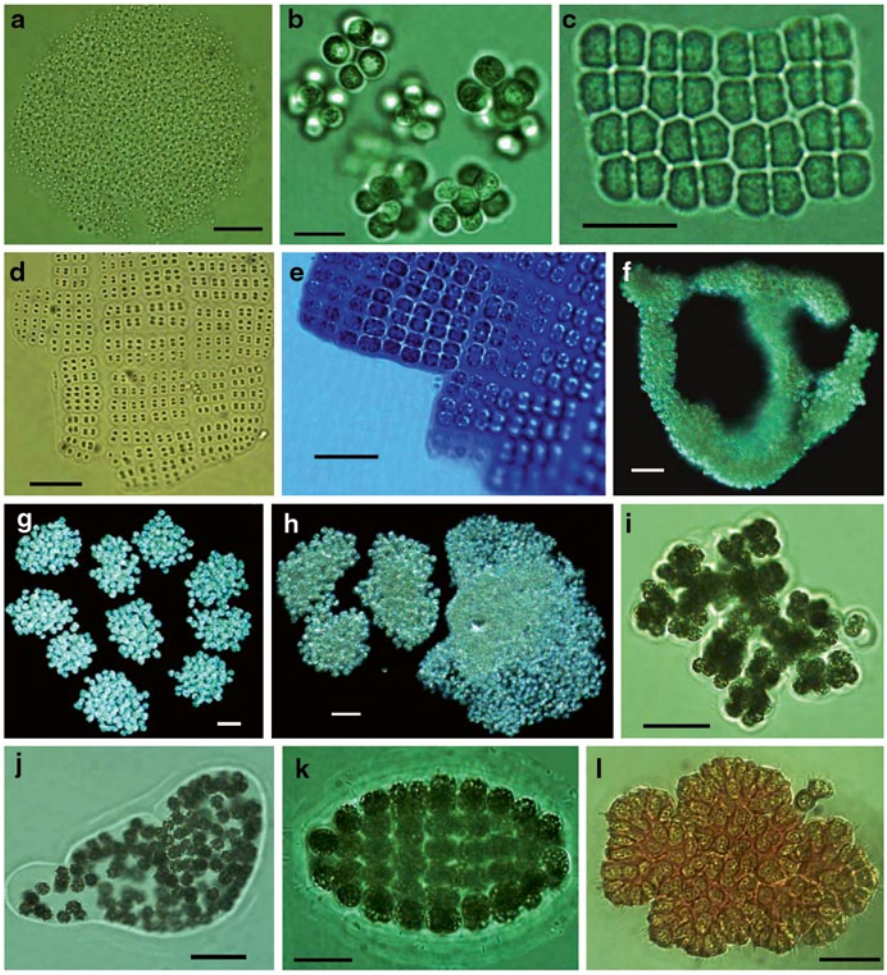

Fig. 10.4 Kinneret colonial species: **a**–**k**, cyanobacteria. **a** Cyanodictyon imperfectum, **b** Chroococcus limneticus, **c** Merismopedia angularis, **d** Merismopedia glauca, **e** Merismopedia punctata (toluidine blue staining), **f** Microcystis aeruginosa, **g** Microcystis botris, **h** Microcystis flos-aquae, **i** Microcystis viridis, **j**, **k** Microcystis wesenbergii (**j** typical colony, **k** young colony), **l** Botryococcus braunii (chlorophyta). Scale bars, 10 mm. Photos **f**–**h** taken in dark field. Details of photographic equipment as in legend to Fig. 10.2

another N_2-fixing filamentous nostocalean species appeared in the lake, *Cylindrospermopsis raciborskii* (Fig. 10.3e–g), forming a major bloom in 2005 (Alster et al. 2010). In 2010, yet another nostocalean species, *Anabaena bergii* (Fig. 10.3d), was found in the lake (Ballot et al. 2011) while *Planktolyngbia limnetica* (hormogonales) has increased in abundance substantially. Since 1994, cyanobacteria have increased in both their relative contribution to total biomass and their absolute biomass (Fig. 10.1). Filamentous forms, some of them toxin producers and N_2 fixers, are now major components of the summer–autumn assemblage. Hadas et al. (2012)

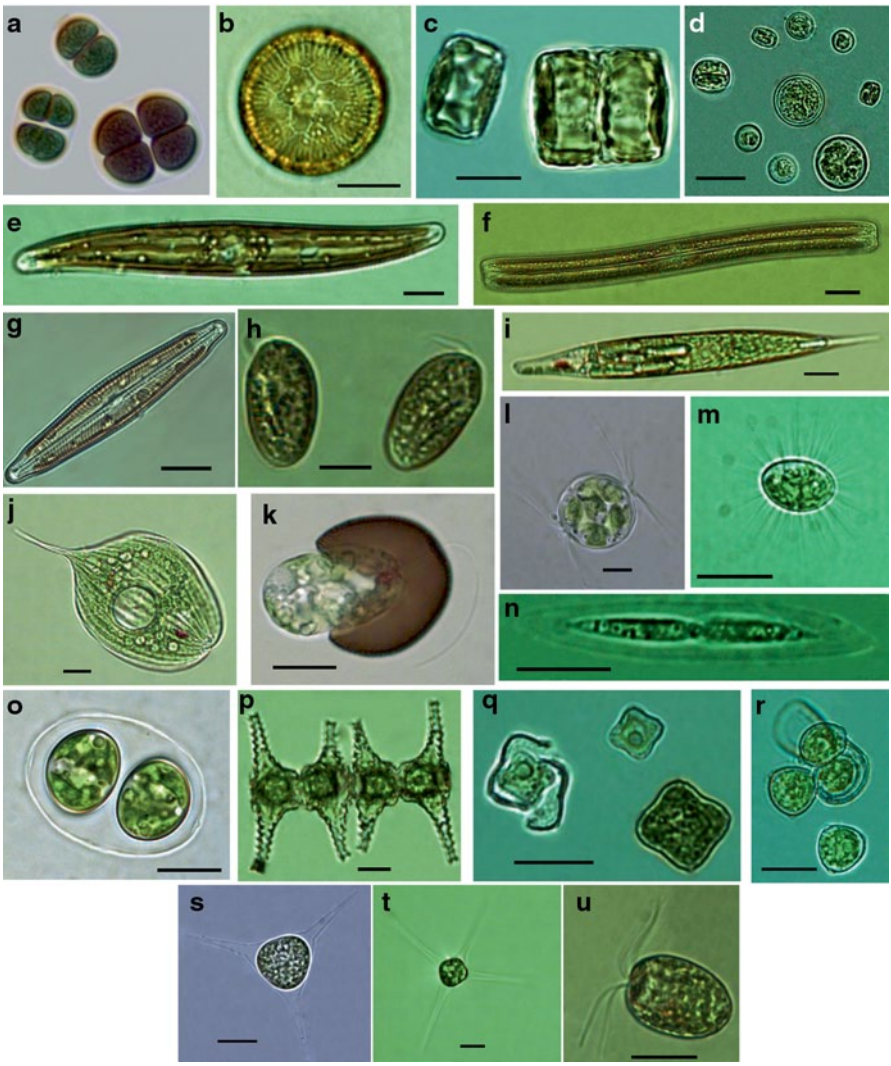

Fig. 10.5 Kinneret unicellular species of various phyla: **a** *Chroococcus turgidus* (cyanobacteria), **b**–**g** diatoms: **b**, **c** *Cyclotella meneghiniana* (**b** valve view, **c** girdle view), **d** *Cyclotella polymorpha*, **e** *Gyrosigma* sp; **f** *Nitzschia sigmoidea*, **g** *Navicula* sp., **h** *Cryptomonas* sp. (cryptophyta), **i**–**k** Euglenophyta: **i** *Euglena acus*, **j** *Phacus longicauda*, **k** *Trachelomonas hispida*, **l**–**u** chlorophyta: **l** *Lagerheimia (Chodatella) citriformis*, **m** *Franceia ovalis*, **n** *Elakatothrix gelatinosa*, **o** *Oocystis lacustris*, **p** *Staurastrum manfeldtii*; **q** *Tetraedron minimum*, **r** Tetraedron sp., **s** *Treubaria setigera*, **t** *Treubaria triappendiculata*, **u** *Tetraselmis cordiformis*. Scale bars, 10 μm. Details of photographic equipment as in legend to Fig. 10.2

attributed the appearance and establishment of the nostocalean cyanobacteria to higher water temperatures and N-depleted conditions. Colonial forms, especially *Cyanodictyon imperfectum* (Fig. 10.4a), and species of the toxin-producing genus *Microcystis* (Fig. 10.4f–k) are also seasonally abundant. Further details on Kinneret cyanobacteria appear in Chap. 12.

Diatoms

Diatoms (Figs. 10.3h, 10.5b–g) comprised only a minor component of the Kinneret phytoplankton in the 1970s (Fig. 10.1a). Their relative biomass has increased in the 1980s, with conspicuous winter (January–February) peaks, exceeding 100 g m^{-2}, occurring in some of the years (Zohary 2004), notably in 1982, 1983, 1988, 1997, 1998, 1999, 2001, 2003, and 2007 (Fig. 10.1c). These winter blooms were attributed to *Aulacoseira* (formerly *Melosira*) *granulata* (Fig. 10.3h), a medium-sized (cell volume, ~3,000 μm^3) filamentous centric diatom. It is relatively heavy due to its silica shell and sinks to the bottom in the absence of turbulence. It blooms when the water column is fully mixed during days of strong wind forcing.

A few other species of diatoms such as the centric *Cyclotella polymorpha* (Fig. 10.5d) and the pennate *Synedra ulna* and *Synedra rumpens* (Table 10.1) are particularly abundant at times (thousands of cells mL^{-1}), usually in the summer. However, due to their small cell size, they never dominate phytoplankton biomass. The high abundance of *Synedra* in summer is a new feature, not recorded during the 1970s and 1980s. Another minute centric diatom, *Discostella* (formerly *Cyclotella*) *stelligera* that forms small chains, appeared in the plankton in 2011. This species was never recorded in the preceding 15 years, but it does appear on Pollingher's list, so possibly it has reappeared in the Kinneret plankton after being gone for many years. Alternatively (and more likely), the more common *Cyclotella polymorpha,* first described and named by Meyer and Hakansson (1996), was referred to in the 1970s as *C. stelligera* whereas *Discostella stelligera* is indeed new to Lake Kinneret.

Chlorophytes

In the 1970s and 1980s, the Kinneret phytoplankton was characterized by a diverse assortment of chlorophytes (Fig. 10.3i, j, 10.4l, 10.5l–u, 10.6a–r) having a relatively modest but significant contribution to total phytoplankton biomass (Fig. 10.1) and no distinct dominant species. Pollingher (1978) listed 110 species and taxonomic varieties of chlorophytes, of which she noted 26 as "commonly occurring" (Table 10.1). These species, of the genera *Ankistrodesmus, Botryococcus, Chodatella, Closterium, Coelastrum, Cosmarium, Crucigenia, Dictyosphaerium, Elakatothrix, Oocystis, Pediastrum, Tetraedron, and Scenedesmus* (Figs. 10.4, 10.5, 10.6), remained common until the mid-1990s. Total chlorophyta biomass has increased since the early 1980s (Fig. 10.1), but the number of species has declined dramatically: 46 of the chlorophyta species in Pollingher's 1978 list are no longer seen in today's plankton, including species that were listed as common (e.g., *Dictyosphaerium elegans, Oocystis submarina*). The increase with time in chlorophyta biomass is due to a few species that have become more abundant than in the past and to new species that have appeared in the lake. Biomass peaks were due to *Closterium aciculare* (November 1998), *Pediastrum tetras* and *Coelastrum microporum* (February 2000), and *Scenedesmus* spp. and *Tetraedron* sp. (January–February 2002; Figs. 10.3i, 10.6m–q, 10.5q, r). Unusually dense but short-lived (few days)

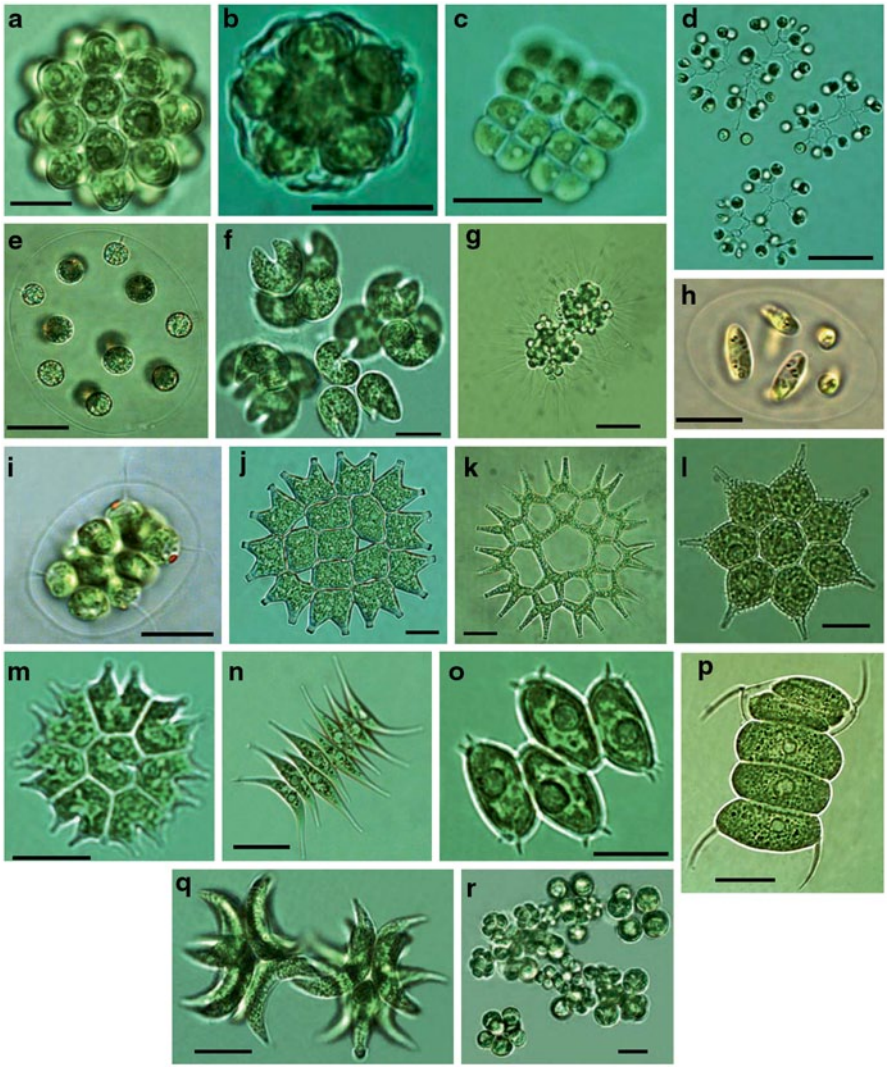

Fig. 10.6 Kinneret coenobial chlorophytes: **a** *Coelastrum astroideum*, **b** *Coelastrum reticulatum*, **c** *Crucigenia quadrata*, **d** Mucidosphaerium *pulchelum*, **e** *Eudorina elegans*, **f** *Kirchneriella obesa*, **g** *Micractinium pussilum*, **h** *Nephrocytium agardhianum*, **i** *Pandorina morum*, **j** *Pediastrum duplex*, **k** *Pediastrum duplex* fa. *gracillimum*, **l** *Pediastrum simplex*, **m** *Pediastrum tetras*, **n** *Scenedesmus acuminatus*, **o** *Scenedesmus denticulatus*, **p** *Scenedesmus quadricauda*, **q** *Selenastrum bibrianum*, **r** *Sphaerocystis planctonica.* Scale bars, 10 µm. Details of photographic equipment as in legend to Fig. 10.2

blooms of *Tetraselmis* (*Carteria) cordiformis* (Fig. 10.5u) and *Botryococcus braunii* (Fig. 10.4l) were recorded in February 1996 and in January 2000, respectively. Both events, recorded by photographs, were missed by our routine sampling, demonstrating that even weekly intervals are insufficient for capturing some of the major events in plankton dynamics in lakes.

Mougeotia sp. (Zygnematales; Fig. 10.3i) appeared in the plankton in May 1998, marking the first-ever record of a filamentous chlorophyte in Lake Kinneret. *Mougeotia* sp. (tentatively identified as *M. gracillima*) is an opportunistic alga that has recently invaded and started forming blooms also in some of the large European lakes, including Lake Maggiore, Lake Garda, and Lake Geneva (Ruggiu et al 1998; Salmaso 2000; Anneville et al. 2002). In Lake Kinneret, it formed a major bloom in spring 2005, a smaller bloom in spring 2006, then bloomed throughout the summer of 2010, and again in the early summer of 2012. While the first three *Mougeotia* bloom events took place in non-Peridinium years, in 2012, *Peridinium* bloomed extensively. Other "newcomer" chlorophytes that were occasionally abundant include *Staurastrum manfeldtii* (Fig. 10.5p), *Staurastrum contortum,* and *Euastrum denticulatum,* all belonging to the Desmidiales.

Cryptophytes

The Kinneret cryptophytes (Fig. 10.5h) are flagellated unicellular species, considered as good food for zooplankton. They are present in the plankton througout the year, with increased abundance in late autumn and winter. Throughout the long-term record, they maintained a stable, relatively small biomass of ~1–5 g m^{-2}, with the winter peaks usually not exceeding 10 g m^{-2}. As such, cryptophytes are the sole group that did not deviate in recent years from their long-term pattern (Fig. 10.1). The main contributors to this group are *Rhodomonas minuta, Plagioselmis nanoplanctica, Cryptomonas erosa,* and *Cryptomonas ovata* (Fig. 10.5h).

Other Photosynthetic Taxa

Phytoplankton belonging to other taxa (Fig. 10.5i–k) also occur in Lake Kinneret but their contribution to total biomass is minor due to either their small cell size or their sporadic occurrence. Of the small-sized taxa, the chrysophyte (also referred to as haptophyte) *Erkenia subaequiciliata* (3–5 µm diameter) is common and at times reaches densities of 5,000 cells mL^{-1}. Picocyanobacteria reach densities of 10^5 cells mL^{-1} in summer–autumn (Malinsky-Rushansky et al. 1995). Of the large but rarely occurring taxa, the euglenophyte genera *Trachelomonas, Euglena,* and *Phacus* (Fig. 10.5i–k) are recorded occasionally, the first more often than the others. Colonial chrysophytes are practically absent, although in May 1998, *Uroglena* colonies were observed. Photosynthetic bacteria, mostly *Chlorobium* spp., produce a dense metalimnetic layer in summer–autumn (Bergstein et al. 1979; Chap. 15.2).

10.1.3 The Annual Cycle of Phytoplankton Biomass and Species Composition

Prior to the mid-1990s, the annual succession of phytoplankton species composition repeated itself from year to year and is well represented by a single, averaged annual pattern for the years 1969–1995 (Fig. 10.7, upper left panel). As previously reported by Pollingher (1986) and Zohary (2004), this pattern consisted of a spring bloom of *P. gatunense* followed by a low-biomass, high-diversity assemblage in the summer and fall. The same overall pattern was observed in the few *Peridinium* bloom years after 1995 (notably in 2004, 2007, 2012). A modified version of this pattern was observed in 1982, 1983, 1988, 1998, 1999, and 2003 when an early winter bloom of *Aulacoseira granulata* preceded the *P. gatunense* bloom. In contrast, phytoplankton succession in non-Peridinium years differed from one year to another (Fig. 10.7); no single species or higher taxonomic group seemed to be able to consistently occupy the niche that opened in the absence of *P. gatunense*. Furthermore, no single species was able to assume and maintain >90% dominance of total phytoplankton biomass as was typical for *P. gatunense*. Instead, several alternative patterns were observed. In 1997 and 2001, an intense bloom of the filamentous diatom *Aulacoseira granulata* developed in January-–February, declining in March. As an unusual event, *P. gatunense* dominated phytoplankton biomass in the second half of 1997. In 2001, no other species took over after *A. granulata* declined. In 2005, 2006, and 2010, the filamentous chlorophyte, *Mougeotia* sp., took over in spring. In 2010, *Mougeotia* remained abundant throughout the summer and fall, attaining its peak biomass in December and declining in early 2011. Another pattern observed was that of increased abundance of dinoflagellates belonging to other genera. *Ceratium hirundinella* dominated in March–April 2010, with peak monthly biomass of 75 g m^{-2}. In the springs of 1996, 2000, 2001, 2005, and 2006, *Ps. elpatiewskyi* and *Ps. cunningtoni,* occurring together, were the major biomass contributors, but the biomass of each never exceeded 35 g m^{-2}. In 2000, a diverse assemblage of chlorophytes dominated the winter–spring biomass, with *Coelastrum microporum, Pediastrum duplex, Pediastrum tetras,* and *Scenedesmus* spp. as main biomass contributors.

As opposed to the many different patterns in species composition in winter–spring, a noticeable summer–fall feature of the phytoplankton assemblage since the mid-1990s was the increased abundance and relative contribution to total biomass of nostocalean cyanobacteria. The summer–fall higher cyanobacterial abundance occurred in both Peridinium bloom years and in non-Peridinium years.

10.1.4 Phytoplankton as Indicators of Lake Stability

The causes for the changes of the Kinneret phytoplankton assemblage, changes that have some profound effects (e.g., water quality is severely affected by the presence of cyanobacterial toxins), are beginning to be unraveled. Zohary et al. (2012) suggested that changes in the hydrology of the catchment, especially the hydrological

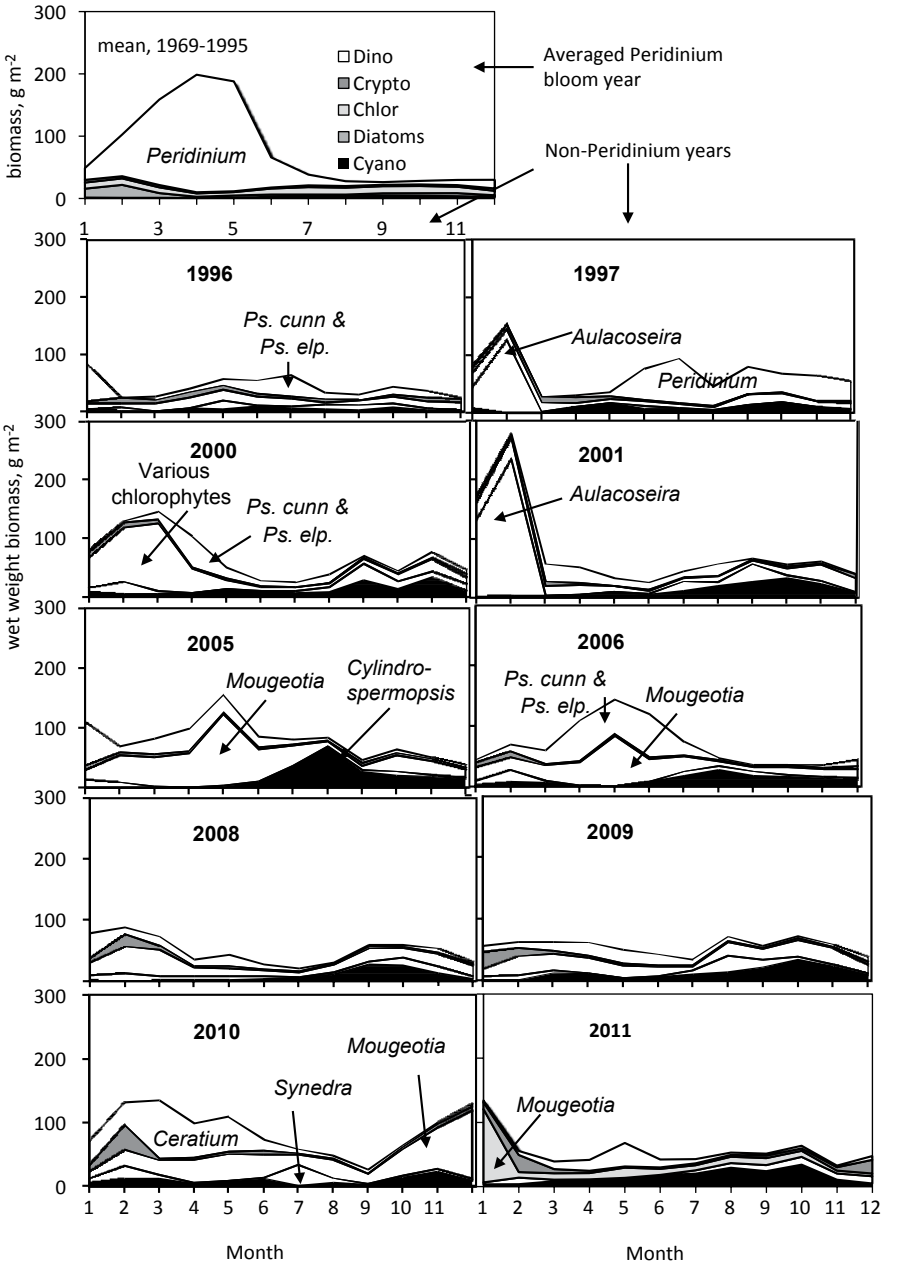

Fig. 10.7 The annual pattern of monthly mean biomass of the main taxonomic groups in Lake Kinneret in an averaged *Peridinium* bloom year (*top left*) and in the ten no-bloom years since 1996 (all other panels). Bloom-forming species are indicated. Ps. cunn., *Peridiniopsis cunningtoni*; Ps. elp., *Peridiniopsis elpatiewskyi*. (Reproduced from Zohary et al. 2012 with permission from Springer)

isolation of the Hula Valley from the Kinneret catchment, prevents critical "growth factors" that are abundant in the peat soils of the Hula Valley from reaching Lake Kinneret on low-rainfall and medium-rainfall years. Only in high-rainfall years, when the Hula Valley gets flooded, excess water from the peats flows into Lake Kinneret, where it sustains a *Peridinium* bloom. Also, only in high-rainfall years, massive biomass of shoreline vegetation gets inundated by the rising water levels; it then decomposes and supplies additional nutrients to support the *Peridinium* bloom after the inflow of nutrients from the catchment has declined, leading to longer bloom seasons.

Schindler (1987) suggested that the earliest responses to increasing stress on lake ecosystems would be changes in species composition of small, rapidly reproducing organisms such as phytoplankton and the disappearance of sensitive organisms. The suite of changes in phytoplankton dynamics in Lake Kinneret since 1994, changes that followed more than two decades of recorded constancy, were interpreted as early responses to increasing stress at the ecosystem level. In particular, the appearance and establishment of toxin-producing species in the country's main drinking water supply is clearly undesirable. In addition, the major loss in species richness (Table 10.1), the appearance of fungal epidemics (Alster and Zohary 2007), the shift to dominance of less-grazed species in summer, and the loss of a previously predictable annual pattern should all be viewed as causes for concern. These negative developments as well as other disturbing events—such as the 2008 collapse of the St. Peter's Fish fishery (see Chap. 36), three incidents of zooplankton biomass collapse (see Chap. 13), an invasive mollusk that took over the snail population (Heller et al. 2014), and leech infestation events (Dolev et al. 2012)—all indicate that the Lake Kinneret ecosystem is no longer as stable as it used to be, at least from the mid-1960s till the mid-1990s. The long-term record of phytoplankton provided the first signs and constituted a primary tool for detecting the above change in ecosystem stability.

10.2 Spatial Distribution

Yosef Z Yacobi, Shachaf Lippman, Gideon Tibor

Spatial and temporal variability is inherent to natural environments; therefore, the information gathered to characterize the distribution of organisms is largely dependent on the temporal and spatial resolution of data acquisition. The issue of temporal variability may be satisfactorily solved by increasing the time resolution of the measurements and is currently feasible using permanently deployed probes and automated recording devices. However, such means are mostly restricted to a few measuring points and in many cases to a single point in any given ecosystem. Even if the deployed instrument stations have profiling capability, the horizontal aspect of variability is deficient.

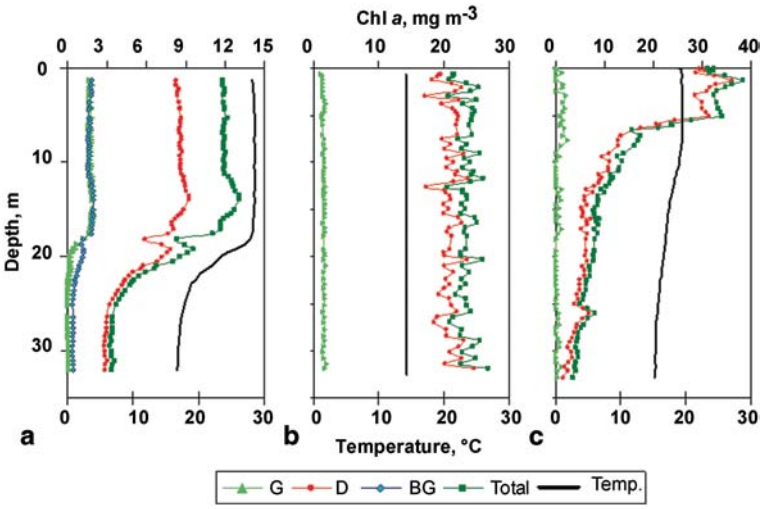

Fig. 10.8 Depth profiles of temperature (*Temp*), total chlorophyll *a* (*Total*), and color group contribution to total chlorophyll *a*: chlorophytes (*G*), diatoms+dinoflagellates (*D*), and cyanobacteria (*BG*) in Lake Kinneret. Measurements were performed on: (**a**) 4 September 2001 (**b**) 30 January 2002, and (**c**) 22 April 2002 by means of a multichannel fluorescence probe (FluoroProbe, bbe Moldaenke, Kiel, Germany). In January, the large filamentous centric diatom *Aulacoseira granulata* was the dominant component of "*D*," while in April it was the dinoflagellate *Peridinium gatunense*

In situ studies In Lake Kinneret, most of the information is gathered at Sta. A (see station location in Chap. 1, Fig. 1.1), located close to the lake geographical center, and close to the deepest point of the lake. At this station, most of the routine sampling for planktonic organisms is done. There is a small-scale sampling scheme at some other stations, but comprehensive attempts to study the spatial distribution of plankton are restricted to sporadic campaigns. An exception is phytoplankton, which may be rapidly estimated quantitatively by the measurement of chlorophyll *a* (Chl *a*), widely used as a proxy for the assessment of total phytoplankton biomass (Evans et al. 1987). Direct determination of algal biomass is a slow, tedious, and expertise-requiring procedure due to the high taxonomic and morphological diversity of all the forms included in the operational term of "algae." But, Chl *a* is common to all oxygen-evolving photosynthetic organisms (higher plants, algae, and cyanobacteria; Rowan 1989), and may be measured by optical instruments either after extraction or in live cells, in laboratory or in situ, using fluorescence, absorption, or reflectance. Within the framework of routine lake sampling, executed at 2-week intervals, the water column at Sta. A is sampled from the surface to the lowest layer just above the bottom sediment. We found that the vertical distribution of Chl *a* is fairly uniform within the euphotic zone, save the periods when the lake phytoplankton is dominated by the large dinoflagellate *P. gatunense* (Yacobi 2006; Sokoletsky and Yacobi 2011). The thermal structure of the water column determines, to a large extent, the degree of homogeneity of Chl *a* vertical distribution, and an abrupt drop in Chl *a* concentrations is observed below the thermocline (Fig. 10.8a). During *Peridinium* dominance, the vertical distribution of Chl *a* is

Table 10.2 Statistical parameters of chlorophyll *a* concentration (mg m^{-3}) in the layer of 4–6 m, and the dominant phytoplankton group in Lake Kinneret during ten lake-wide surveys conducted between June 2001 and April 2002

Date	Min	Max	Avg	SD	Coef. of variation (%)	Dominant phytoplankton
11 June 01	3.9	8.0	5.8	1.00	17.2	Dinoflagellates
19 July 01	5.4	10.2	7.2	1.01	14.6	Cyanobacteria
15 Aug 01	5.2	11.1	6.8	1.41	20.5	Cyanobacteria
04 Sep 01	8.5	14.4	11.3	1.35	11.9	Diatoms
15 Sep 01	4.2	6.7	5.7	0.71	12.4	Cyanobacteria
21 Nov 01	6.4	11.4	9.0	1.14	12.6	Cyanobacteria
30 Jan 02	11.5	25.9	21.9	2.97	13.7	Diatoms
14 Feb 02	13.7	36.0	21.6	5.83	27.0	Chlorophytes
12 Mar 02	9.1	27.1	16.2	4.74	29.2	Chlorophytes
22 Apr 02	7.7	40.4	20.3	7.62	37.6	Dinoflagellates

The measurements of chlorophyll concentration and the contribution of different phytoplankton groups were made with a multichannel fluorescence probe (FluoroProbe, bbe Moldaenke, Kiel, Germany) at 31 sampling stations. The measurement technology was as detailed by Yacobi and Schlichter (2004)
SD standard deviation

conspicuously nonuniform (Fig. 10.8c) and is determined by the diurnal vertical motion of that species (Pollingher 1988). Chl *a* profiles are usually more uniform, from the water surface down to the bottom during holomixis, but it seldom is completely uniform. This finding demonstrates that once algal cells are located below the level where production outcompetes decomposition, phytoplankton concentrations decline. However, Chl *a* profiles may occasionally be uniform during holomixis, indicating high vertical velocities within the water column (Fig. 10.8b).

Studies in Lake Kinneret consistently showed that the lateral distribution of phytoplankton is relatively uniform most of the time, i.e., concentrations do not exceed a ratio of 1:2 between the minimum and maximum at the water surface (Table 10.2). In periods when the lake phytoplankton is dominated by the large dinoflagellate *P. gatunense,* however, the difference between the extreme concentrations usually is as large as an order of magnitude and may be even higher (Berman and Elias 1973; Gitelson et al. 1994; Yacobi et al. 1995; Mayo et al. 1995; Yacobi and Schlichter 2004). That variability is displayed by measurements taken over a small area of Lake Kinneret surface in 2007, when *Peridinium* appeared in massive concentrations (Table 10.3), and also demonstrates the temporal variability typical for *Peridinium,* as much as the spatial variation recorded at each sampling session.

Preliminary short-term investigations suggested that the horizontal distribution of phytoplankton in Lake Kinneret, even throughout periods of relative uniformity, shows higher concentrations in the littoral areas than in deep waters (e.g., Mayo et al. 1995). During the period from July 1999 throughout December 2002, that assumption was tested by monitoring phytoplankton at four pelagic stations, A, D, G, and K, and at three littoral stations, L_N, L_S, and L_W, in the northern, southern, and western areas, accordingly (see station location map in Chap. 32 Fig. 32.1). At

Table 10.3 The chlorophyll *a* concentration (mg m^{-3}) maxima recorded during an intensive survey performed in Lake Kinneret in a small section of approximately 4 km^2 in 2007

Station	T1	T2	T3	T4	T5	T6	T7	Mean	SD
1	162	14	36	799	348	45	417	260	286
2	81	17	113	438	139	137	68	142	137
3	138	195	105	220	73	120	85	134	55
4	92	186	112	116	59	45	86	100	46
5	39	190	94	51	42	29	61	72	56
6	79	54	105	49	38	38	46	58	25
7	49	41	207	352	81	74	39	120	118
8	46	18	156	632	262	110	303	218	210
10	33	15	18	572	217	149	515	217	236
14	63	188	86	80	115	36	71	91	49
17	38	54	91	109	119	63	114	84	32
Mean	74	88	102	311	136	77	164		
SD	42	82	51	265	100	44	167		

Depth profiles of chlorophyll concentrations were determined at 11 stations and seven sampling times (*T1* to *T7*) at each station, from 4:00 p.m. on 26 March to 8:00 a.m. on 28 March 2007. Indicated are the maximum values recorded for each depth profile, means, and standard deviations (*SD*)

each station, water samples were collected for Chl *a* determinations and for primary production measurements in the laboratory under standard light and temperature conditions. Primary productivity was also measured in situ at Sta. A, thus providing a basis to interpret the standard primary productivity data and assess the lake's activities. The overall average Chl *a* concentrations ranged from 10.3 to 15.7 mg m^{-3} and the standard primary productivity from 17.2 to 25.3 mg C m^{-3} h^{-1}. The seasonal dynamics of both variables was similar at all sampling stations; the difference between stations was mainly observed during the winter period when both Chl *a* concentrations and primary productivity had the highest values (Fig. 10.9). The difference between pelagic and littoral stations was low, although we detected somewhat higher averages of both Chl *a* and primary production in the littoral stations (Ostrovsky and Yacobi 2009). Prominently higher values were recorded mainly at the northern littoral station L_N following floods. The basic assumption of the work at these seven stations was that one can pinpoint the initiation of phytoplankton growth in the littoral, prior to it being observed throughout the lake, and particularly at Sta. A, which is the standard biological monitoring site of the lake. Following approximately 3.5 years of measurements, we could state that our assumption was only partially fulfilled because only station L_N was different from other stations, mostly by increased biomass and activity of phytoplankton. Those findings underlined the importance of the northern part of the lake, near the entrance of main tributaries, as an area where changes in phytoplankton development may be expected before they are detected throughout the lake.

Consequently, the next effort for the study of spatial distribution of Chl *a* was concentrated along the northern part of the lake. We sampled at seven stations along the northern shore of the lake and two additional stations in the pelagic for com-

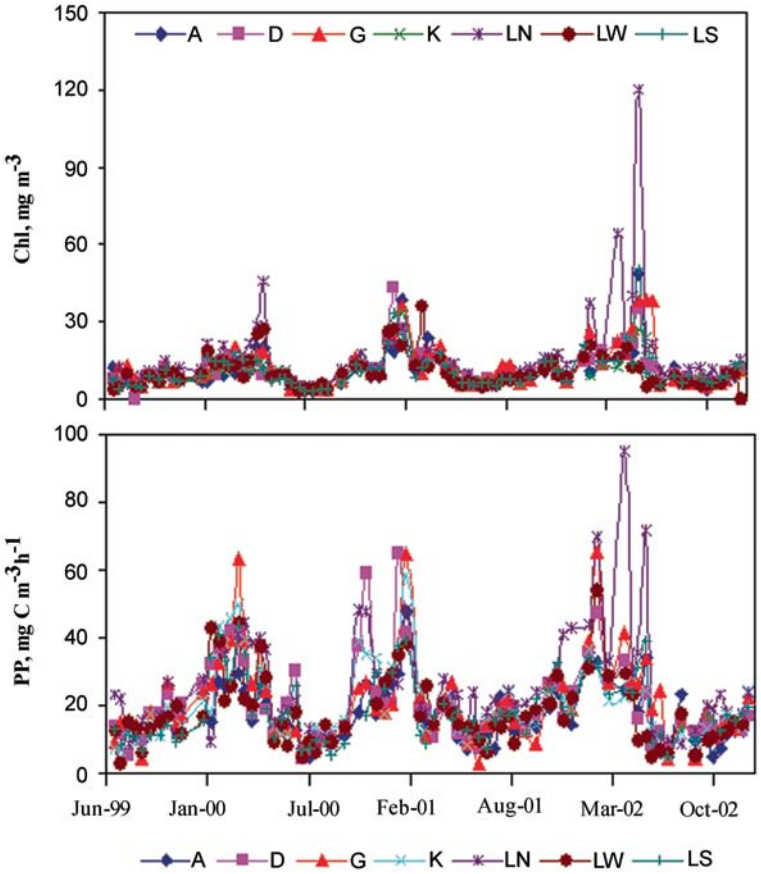

Fig. 10.9 Chlorophyll *a* concentration (*upper*) and primary production (*PP*) at standard conditions (*lower*) at seven stations in Lake Kinneret sampled from July 1999 to December 2002. The measurements were made on composite samples taken from the 0–8 m water layer at the pelagic stations *A*, *D*, *G*, and *K* and from the 0–3 m water column at the littoral stations L_N, L_S, and L_w (station locations in Fig. 32.1 of Chap. 32). Standard conditions (at the laboratory) for primary production measurements were—temperature range: 20–25 °C; light flux: 60 μ mole photon m^{-2} s^{-1}

parison (Sta. A and G). In this 2-year study, we found a prominent signature of river water near the Jordan River entrance (reduced conductivity, increased nitrate concentrations), which persisted along the putative track of the river water entrance to the lake (Serruya 1974). The river nutrient enrichment was not followed by an increase in Chl *a* concentration, but vice versa. It appeared that the river water diluted phytoplankton, as the relationship between nitrate concentration and Chl *a* was negative. That trend is demonstrated for the most prominent species throughout the 2009–2010 monitoring program, the large filamentous chlorophyte *Mougeotia* sp. which showed a clear nonlinear negative correlation between nitrate concentrations and cell number (Fig. 10.10).

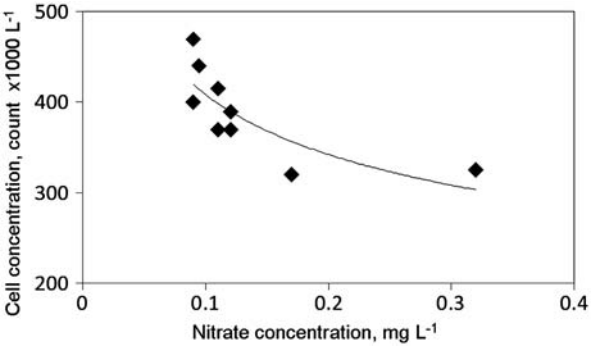

Fig. 10.10 The relationship between nitrate concentration and cell density of the large filamentous chlorophyte *Mougeotia* sp. in Lake Kinneret from April 2009 to September 2010. Each *point* is an average of measurements collected on a particular date at seven sampling stations in the northern part of the lake. Regression line parameters are $r=-0.81$, $p<0.01$, $n=9$

Satellite-based remote sensing studies The unique optical features of Chl *a* makes it an ideal target for observation by remotely operated sensors carried onboard aircrafts and satellites. The reflectance measured by the sensors represents only the uppermost part of the water column, and thus may miss variation when the vertical distribution of Chl *a* is nonuniform. Yet, remote sensing is the only tool for synoptic mapping of the horizontal distribution of Chl *a* and is used in reconnaissance of phytoplankton distribution on local and global scales (Chelton et al. 2011). The first documented attempts to study Chl *a* distribution in Lake Kinneret using satellite-carried sensors were made in the early 1990s, using images acquired by Landsat TM (Mayo et al. 1995; Yacobi et al. 1995). The sensor had fine spatial resolution (30 m), but was deficient for monitoring of phytoplankton dynamics, with a 16-day return interval. Since 2006, spatial mapping of Chl *a* was obtained through SISCAL (Satellite Information System on Coastal area and Lakes). SISCAL was developed during 2004–2006 in the framework of the Fifth IST Program of the European Community. SISCAL (www.siscal.net) provides near-real-time information on ecologically important water quality parameters by combining Earth Observation (EO) images with state-of-the-art algorithms and data integration using a GIS. The sensor used recently for monitoring Chl *a* in Lake Kinneret was the MERIS FR sensor (https://earth.esa.int/web/guest/missions/esa-operational-eo-missions/envisat/instruments/meris), which has 16 spectral bands for mapping optical water quality variables. The image pixel size is 300 m and in effect provides information at 3-day intervals. In the example provided herein (Fig. 10.11), rapid changes in the spatial distribution of surface Chl *a* concentrations is clearly demonstrated, even in periods with a restricted range of concentrations. MERIS activity ceased operation on April 2012, but it would be substituted by another sensor, with similar characteristics, for Chl *a* monitoring in Lake Kinneret. We found that the synoptically acquired information on Chl *a* spatial distribution is useful in attempts to understand the effect of the physical structure of the lake on phytoplankton temporal dynamics (Ng et al. 2011).

Our studies on the spatial distribution of Chl *a* in Lake Kinneret, based on in situ information gathering and on acquisition by satellite-carried sensors, indicate that the distribution of phytoplankton in the lake is mostly within a relatively narrow range. We assume that the apparent heterogeneity of phytoplankton distribution is

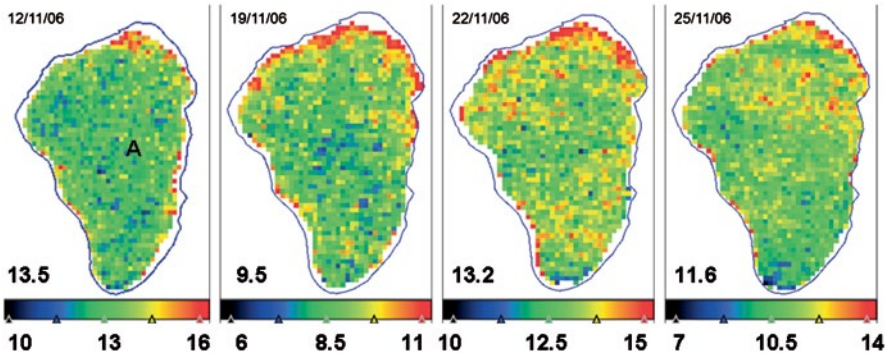

Fig. 10.11 Spatial distribution of chlorophyll *a* (mg m^{-3}) in surface water of Lake Kinneret, November 2006, based on the interpretation of MERIS FR images within the framework of SISCAL (http://isramar.ocean.org.il). Color scales indicate the range of chlorophyll *a* concentrations; *small triangles* are tick marks. The average Chl *a* concentration for each survey is indicated above the respective color scale. The location of Sta. A, used for the routine monitoring, is indicated in the *leftmost panel*

an outcome of the geomorphology and bathymetry of the lake, which facilitate the action of basin-wide, fast water motions (Chap. 9). That vigorous water mass mixing is the factor which prevents the development of large-scale ecological niches in the lake.

References

Alster A, Zohary T (2007) Interactions between the bloom-forming dinoflagellate *Peridinium gatunense* and the chytrid fungus *Phlyctochytrium* sp. Hydrobiologia 578(1):131–139

Alster A, Kaplan-Levy RN, Sukenik A, Zohary T (2010) Morphology and phylogeny of a non-toxic invasive *Cylindrospermopsis raciborskii* from a Mediterranean Lake. Hydrobiologia 639(1):115–128

Anneville O, Ginot V, Druart J-C, Angeli N (2002) Long-term study (1974–1998) of seasonal changes in the phytoplankton in Lake Geneva: a multi-table approach. J Plankton Res 24(10):993–1008

Ballot A, Ramm J, Rundberget T, Kaplan-Levy RN, Hadas O, Sukenik A, Wiedner C (2011) Occurrence of non-cylindrospermopsin-producing *Aphanizomenon ovalisporum* and *Anabaena bergii* in Lake Kinneret (Israel). J Plankton Res 33(11):1736–1746. doi:10.1093/plankt/fbr071

Banker R, Carmeli S, Hadas O, Telsch B, Porat R, Sukenik A (1997) Identification of cylindrospermopsin in the cyanobacterium *Aphanizomenon ovalisporum* (Cyanophyceae) isolated from Lake Kinneret, Israel. J Phycol 33(4):613–616

Barrois T (1894) Contribution a l'etude de quelque lacs de Syrie. Rev Biol Nord Fr 6:224–314

Bergstein T, Henis Y, Cavari BZ (1979) Investigations on the photosynthetic sulfur bacterium *Chlorobium phaeobacteroides* causing seasonal blooms in Lake Kinneret. Can J Microbiol 25(9):999–1007

Berman T, Elias Y (1973) Lake Kinneret: synoptic studies of chlorophyll concentrations. In: Shuval H (ed) Proceedings of the 4th Israel Ecological Society Conference. Balaban F, Rehovot, pp 19–27

Berman T, Stone L, Yacobi YZ, Kaplan B, Schlichter M, Nishri A, Pollingher U (1995) Primary production and phytoplankton in Lake Kinneret: a long-term record (1972–1993). Limnol Oceanogr 40(6):1064–1076

Chelton DB, Gaube P, Schlax MG, Early JJ, Samelson RM (2011) The influence of nonlinear mesoscale eddies on near-surface oceanic chlorophyll. Science 334:328–332

Dolev A, Gal G, Zohary T (2012) Leeches in Lake Kinneret. Eretz HaKinneret 7:36–38 (in Hebrew)

Evans CA, O'Reilly JE, Thomas JP (1987) A handbook for the measurement of chlorophyll *a* and primary production. Texas A & M University, College Station

Gitelson A, Mayo M, Yacobi YZ, Parparov A, Berman T (1994) The use of high-spectral-resolution radiometer data for detection of low chlorophyll concentrations in Lake Kinneret. J Plankton Res 16:993–1002

Hadas O, Pinkas R, Malinsky-Rushansky N, Shalev-Alon G, Delphine E, Berner T, Sukenik A, Kaplan A (2002) Physiological variables determined under laboratory conditions may explain the bloom of *Aphanizomenon ovalisporum* in Lake Kinneret. Eur J Phycol 37:259–267

Hadas O, Pinkas R, Malinsky-Rushansky N, Nishri A, Kaplan A, Rimmer A, Sukenik A (2012) Appearance and establishment of diazotrophic cyanobacteria in Lake Kinneret, Israel. Freshw Biol 57:1214–1227

Heller J, Dolev A, Zohary T, Gal G (2014) Invasion dynamics of the snail *Pseudoplotia scabra* in Lake Kinneret. Biol Invasions 16:7–12

Hillebrand H, Dürselen C-D, Kirschtel D, Pollingher U, Zohary T (1999) Biovolume calculation for pelagic and benthic microalgae. J Phycol 35:403–424

Lund JWG, Kipling C, Le Cren ED (1958) The inverted microscope method of estimating algal numbers and the statistical basis of estimations. Hydrobiologia 11:144–170

Malinsky-Rushansky N, Berman T, Dubinsky Z (1995) Seasonal dynamics of picophytoplankton in Lake Kinneret, Israel. Freshw Biol 34:241–254

Mayo M, Gitelson A, Yacobi YZ, Ben Avraham Z (1995) Chlorophyll distribution in Lake Kinneret determined from LANDSAT thematic mapper data. Int J Remote Sens 16:175–182

Meyer B, Hakansson S (1996) Morphological variation of *Cyclotella polymorpha* sp. Nov. (Bacillariophyceae). Phycologia 35:64–69

Ng SMY, Antenucci JP, Hipsey MR, Tibor G, Zohary T (2011) Physical controls on the spatial evolution of a dinoflagellate bloom in a large lake. Limnol Oceanogr 56:2265–2281

Ostrovsky I, Yacobi YZ (2009) Temporal evolution and spatial heterogeneity of ecosystem parameters in a subtropical lake. In: Ciraolo G, Ferreri GB, Napoli E (eds) Proceedings 13th workshop on physical processes in natural waters, Palermo, Italy, 1–4 September 2009, pp 1–15. ISBN 978-88-903895-0–4

Pollingher U (1978) The phytoplankton of Lake Kinneret. In: Serruya C (ed) Lake Kinneret, Monographiae Biologicae, vol 32. Dr. Junk Publishers, The Hague, pp 229–242

Pollingher U (1981) The structure and dynamics of the phytoplankton assemblages in Lake Kinneret, Israel. J Plank Res 3(1):93–105

Pollingher U (1986) Phytoplankton periodicity in a subtropical lake (Lake Kinneret, Israel). Hydrobiologia 138:127–138

Pollingher U (1987) Ecology of dinoflagellates. B. Freshwater ecosystems. In: Taylor FJR (ed) The biology of dinoflagellates (Botanical monographs 21). Blackwell, Oxford, pp 502–529

Pollingher U (1988) Freshwater armored dinoflagellates: growth, reproductive strategies and population dynamics. In: Sandgren C (ed) Growth and reproduction strategies of freshwater phytoplankton. Cambridge University Press, Cambridge, pp 134–174

Pollingher U (1991) A long term study of *Chroococcus* population in Lake Kinneret (Israel). Algol Stud 64:377–383

Pollingher U, Hickel B (1991) Dinoflagellate associations in a subtropical lake (Lake Kinneret, Israel). Archiv für Hydrobiologie 120(3):267–285

Pollingher U, Hadas O, Yacobi YZ, Zohary T, Berman T (1998) *Aphanizomenon ovalisporum* (Forti) in Lake Kinneret, Israel. J Plankton Res 20:1321–1339

Rowan KS (1989) Photosynthetic pigments of algae. Cambridge University Press, Cambridge

Ruggiu D, Morabito G, Panzani P, Pugnetti A (1998) Trends and relations among basic phytoplankton characteristics in the course of the long-term oligotrophication of Lake Maggiore (Italy). Hydrobiologia 369:243–257

Salmaso N (2000) Factors affecting the seasonality and distribution of cyanobacteria and chlorophytes: a case study from the large lakes south of the Alps, with special reference to Lake Garda. Hydrobiologia 438(1–3):43–63

Schindler DW (1987) Detecting ecosystem responses to anthropogenic stress. Can J Fish Aquat Sci 44:6–25

Serruya S (1974) The mixing patterns of the Jordan River in Lake Kinneret. Limnol Oceanogr 19:175–181

Sokoletsky LG, Yacobi YZ (2011) Comparison of chlorophyll *a* concentration detected by remote sensors and other chlorophyll indices in inhomogeneous turbid waters. Appl Optic 50:5770–5779

Yacobi YZ (2006) Temporal and vertical variation of chlorophyll *a* concentration, phytoplankton photosynthetic activity and light attenuation in Lake Kinneret: possibilities and limitations for simulation by remote-sensing. J Plankton Res 28:725–736

Yacobi YZ, Schlichter M (2004) GIS application for mapping of phytoplankton using a multichannel fluorescence probe derived information. In: Chen Y, Takara K, Cluckie ID, Hilaire De Smedt F (eds) GIS and remote sensing in hydrology, water resources and environment. International Association of Hydrological Sciences Press, Wallinford, pp 301–307 (IHAS Publication 289)

Yacobi YZ, Gitelson A, Mayo M (1995) Remote sensing of chlorophyll in Lake Kinneret using high-spectral-resolution radiometer and Landsat TM: spectral features of reflectance and algorithm development. J Plankton Res 17:2155–2173

Zapomělová E, Skácelová O, Pumann P, Kopp R, Janeček E (2012) Biogeographically interesting planktonic Nostocales (Cyanobacteria) in the Czech Republic and their polyphasic evaluation resulting in taxonomic revisions of *Anabaena bergii* Ostenfeld 1908 (*Chrysosporum* gen. nov.) and *A. tenericaulis* Nygaard 1949 (*Dolichospermum tenericaule* comb. nova). Hydrobiologia 698(1):353–365

Zohary T (2004) Changes to the phytoplankton assemblage of Lake Kinneret after decades of a predictable, repetitive pattern. Freshw Biol 49:1355–1371

Zohary T, Nishri A, Sukenik A (2012) Present-absent: a chronicle of the dinoflagellate *Peridinium gatunense* from Lake Kinneret. Hydrobiologia 698:161–174

Chapter 11
Peridinium gatunense

Tamar Zohary, Assaf Sukenik and Tom Berman

Abstract The armored dinoflagellate *Peridinium gatunense* Nygaard (hence, *Peridinium*) is the best-known and most important bloom-forming phytoplankton species of Lake Kinneret. This chapter provides an overview of the history of its research, its systematics, life cycle and physiological features, spatial and temporal distribution, growth versus loss processes, interspecies interactions, and summarizes its role as a keystone species in the ecology of Lake Kinneret.

Keywords Dinoflagellate · Bloom · Life cycle · Patchiness · Vertical migration

11.1 Background

The armored dinoflagellate *Peridinium gatunense* Nygaard (hence, *Peridinium*) is the best-known and most important phytoplankton species of Lake Kinneret. It forms massive spring blooms, which change the color of the water to coffee brown in distinct patches visible from far away (Fig. 11.1). By "mining" the Lake Kinneret database, we found that those intense blooms impact the entire ecosystem, as evidenced by extreme values reached by a suite of environmental parameters on sampling dates when *Peridinium* biomass exceeded 100 g m^{-2}. At those times, lake water transparency often declined to Secchi depths below 1.5 m (vs. a multiannual mean of 3.25 m), epilimnetic total suspended solid concentrations exceeded 10 mg L^{-1} (compared to a mean of 3.6 mg L^{-1}), and 70 % of all incidences of 0–10 m turbidity greater than 4 NTU (vs. a mean of 2.3 NTU) were associated with blooms of *Peridinium*. In addition, 80 % of all sampling times with epilimnetic pH > 9.1, more than 80 % of the cases of excessive oxygen super-saturation and of 0–10 m total P > 0.05 mg L^{-1}, and more than 60 % of all cases where 0–10 m total N exceeded 1 mg L^{-1} were all associated with those blooms. These numbers demonstrate how

T. Zohary (✉) · A. Sukenik · T. Berman
The Yigal Allon Kinneret Limnological Laboratory, Israel Oceanographic & Limnological Research, P.O. Box 447, 14950, Migdal, Israel
e-mail: tamarz@ocean.org.il

A. Sukenik
e-mail: assaf@ocean.org.il

T. Zohary et al. (eds.), *Lake Kinneret, Ecology and Management,* Aquatic Ecology Series 6,
DOI 10.1007/978-94-017-8944-8_11,

Fig. 11.1 An air-photo showing the patchiness of *Peridinium gatunense*, taken on 24 April 2013 in the north of Lake Kinneret, near Kefar Nahum. The *dark-colored* waters are those with high concentrations of the alga, the lighter-colored waters are those with low concentrations. The border between those two regions is sharp and clear, with a white strip of foam, formed by wave action working on organic matter released from the bloom. (Photo taken by Asaf Dori, Israel Nature and Parks Authority)

a single dominant species can modify the physical and chemical properties of its own environment. As such, *Peridinium* may be viewed as an "ecosystem engineer."

Due to its importance in the ecosystem, monocultures and even axenic cultures of *Peridinium* were obtained in the early years of concerted Lake Kinneret research, creating the possibility for experimental studies of its physiology, behavior, and life cycle. The ongoing long-term record of its abundance and biomass in Lake Kinneret has become another indispensible tool for understanding the ecological role of this organism in the lake. *Peridinium* has become a model organism for studying freshwater dinoflagellate blooms and the focus of many studies. The objective of this section is to review the accumulated knowledge on *P. gatunense*.

11.2 Systematics and Culturing

11.2.1 Species Description

P. gatunense Nygaard 1925 (photo: Chap. 10, Fig. 10.2a, b) is a solitary, motile, large-celled armored (thecate) dinoflagellate. It is one of the two large dinoflagellates

Table 11.1 Morphological parameters for *Peridinium gatunense* based on field measurements (original data)

Morphological parameter	Range (median)	*N*
Cell diameter, μm	44–58 (50)	1,230
Cell height, μm	47–60 (52)	423
Cell volume, μm^3	44,300–99,400 (67,000)	423
Cell wet weight[a], ng	44–99 (67)	423

[a] Specific density of 1.0 is assumed

in Lake Kinneret (the other one being the morphologically different *Ceratium hirundinella*, see Chap. 10, Fig. 10.2d, e). Its shape is a prolate spheroid, on average 50 μm in diameter by 52 μm height, with a median cell biovolume of 67,000 μm^3 (Table 11.1). Based on many measurements, its biovolume (V) can be computed from cell diameter (D) using the equation: $V\,(\mu m^3) = 1.31\ D^{2.7835}$. *Peridinium* mean cell size varies seasonally, with largest sizes recorded in January–February, when nutrients are most plentiful, and smallest sizes in summer, after the bloom crash.

Under the light microscope, the large spheroid cells are distinguished by a thick, colorless shell made of two half-spheres named *thecae,* enveloping the strongly brown-colored living protoplast, and by being larger than the similarly shaped and co-occurring dinoflagellates belonging to the genus *Peridiniopsis*. The *cingulum* (a groove or "girdle" around the cell's "waist") divides the cell into two conical halves of approximately equal size, each covered by one of the two thecae: the *epitheca* (upper half) and *hypotheca* (lower half). During cell division or under stress, the shell splits at the cingulum, the thecae are shed, and a naked protoplast emerges. One of the two flagella, the transverse flagellum, is wound around and within the cingulum. The second, whiplash flagellum, usually the only flagellum seen under the light microscope, is attached at the *sulcus* (a second, longitudinal groove, which defines the ventral side of the cell). A diagnostic characteristic of *P. gatunense* is that the sulcus widens slightly and reaches the posterior-most part of the cell, the *antapex*. Chloroplasts are numerous and parietal. Details of the external and internal cell morphology of *Peridinium* were described based on transmission and scanning electron microscopy (Messer and Ben-Shaul 1969; Pollingher 1978). By using a Parducz fixative followed by critical point drying, Berman and Roth (1979) were able to preserve the flagella and also show the presence of an outer membrane overlying the theca of the *Peridinium* cell.

P. gatunense is known for its cosmopolitan distribution and is reported to occur in all continents except Antarctica; however, Lake Kinneret is the only lake in which it is reported to form regular blooms.

11.2.2 The Recorded History and Identification as P. gatunense

There is no definite information on when regular annual blooms of *Peridinium* began in Lake Kinneret. The dinoflagellate signature pigments, peridinin and dinoxanthin, decompose shortly after cell death and are not preserved in the sediments

(Yacobi et al. 1991). Other cellular material and even resting cysts also do not preserve well. Thus, all the above cannot be used to trace *Peridinium* history in sediment cores. Anecdotal reports indicate that *Peridinium* blooms were occurring at least since the beginning of the twentieth century and certainly before the draining of the Hula wetlands in the 1950s. Rayss (1951) reported finding "huge quantities" of *Peridinium westii* Lemmermann (later renamed *P. gatunense*) in the plankton of Lake Kinneret. Komarovsky (1951, 1959) reported regular spring blooms of *P. westii* in Lake Kinneret, based on monthly samples collected in 1948–1949, and was the first to describe its annual cycle with a spring bloom. *Peridinium* from Lake Kinneret was referred to by various authors as *P. cinctum, P. westii,* or *P. cinctum* fa. *westii* until the 1980s when it was conclusively identified as *P. gatunense* Nygaard (1925) by Boltovskoy (1983) and Hickel and Pollingher (1988).

As documented by routine monitoring since the mid-1960s, the regular late-winter–spring bloom of *Peridinium* was the most salient feature of the Kinneret phytoplankton (Pollingher and Kimor 1970; Pollingher 1986; Berman et al. 1992; Zohary 2004). Those intense blooms could be observed as large patches of coffee-brown-colored water, reaching up to several square kilometers in area. At the bloom peak, *Peridinium* reached mean epilimnion concentrations of 500–1,000 cells mL^{-1} (Fig. 11.2), or 150–250 g m^{-2} of wet weight biomass, and comprised >95 % of total phytoplankton biomass (Pollingher 1986, 1988). The blooms declined sharply in May–June, shortly after the water temperature exceeded 25 °C, thermal stratification was established, and nutrients became scarce, leaving behind resting cysts on the lake sediments. During the summer months, *Peridinium* concentrations in the water column were very low, usually <5 cells mL^{-1} (Fig. 11.2). Autumn turnover caused resuspension of the cysts from the sediments, leading to their excystation and the initiation of the next year's bloom (Fig. 11.3).

After many years of recorded constancy, in the mid-1990s, the regular pattern of late-winter–spring *Peridinium* blooms broke down (Zohary 2004; Roelke et al. 2007). In 1996, for the first time *Peridinium* failed to develop a bloom (bloom defined here as monthly mean wet weight biomass exceeding 100 g m^{-2}, equivalent to ~50–100 cells mL^{-1}; Zohary et al. 2012). Since then, *Peridinium* blooms have become irregular (Zohary and Ostrovsky 2011), occurring only in high-rainfall years (Zohary et al. 2012).

11.2.3 Life Cycle

Throughout the bloom development period, a small proportion of the cells (~1 %) change their morphology to become resting cysts (Pollingher 1988; Alster et al. 2006), which sink to the sediments to remain there as an inoculum for future growth (Fig. 11.3). Unlike dinoflagellates of the temperate zone whose cysts overwinter to avoid harsh winter conditions, in subtropical Lake Kinneret the cysts "over-summer" to overcome the period of elevated water temperatures and low

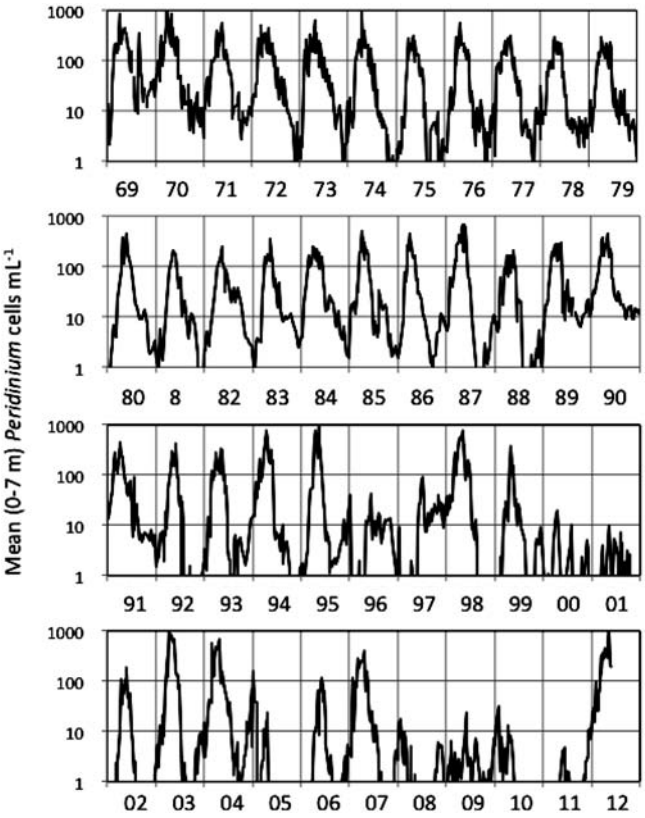

Fig. 11.2 Long-term record (1969–2012) of *Peridinium gatunense* abundance (cells mL^{-1}) at 0–7 m in Lake Kinneret. Data shown are weighted means for samples collected at 0, 1, 2, 3, 5, and 7 m at weekly or fortnightly intervals. The record demonstrates the recurrent bloom event every spring till 1995 but notably no blooms in 1996, 1997, 2000, 2001, 2005, 2006, 2008, 2009, 2010, and 2011. Note log scale on *Y axis*

nutrient availability (Pollingher 1988). The encystation process includes loss of motility, condensation of the protoplasm to form red bodies, and disintegration of the thecae. The cysts are nonmotile, spherical or slightly oval, smaller than the vegetative cells, with a thick and distinct cell wall but no theca, lightly colored, with two red bodies, or "eyespots" (see Chap. 10.1, Fig. 10.2b). Vegetative cells emerging from resting cysts have two distinct red bodies, after cell division each daughter cell keeps one red body; with later divisions the red bodies are diluted out (Eren 1969). The presence of red bodies is an indication of the origin of the cell from a resting cyst. Vegetative cells with one or two red bodies have been observed very rarely, only in littoral water and only between 17:00 and 20:00 h (Pollingher and Serruya 1976).

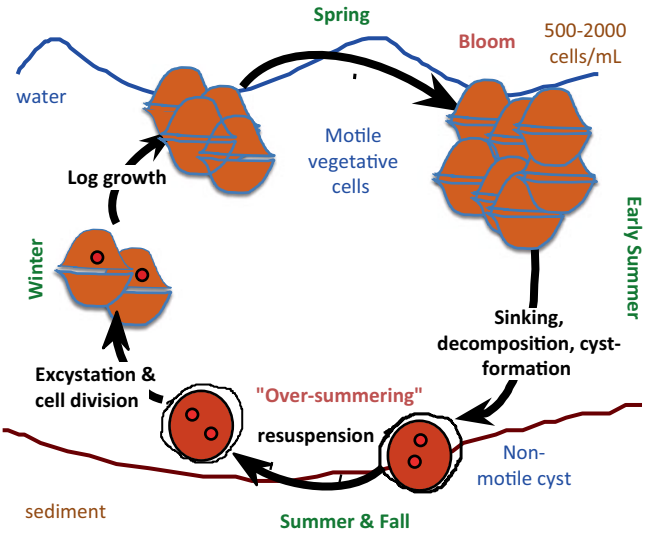

Fig. 11.3 A schematic representation of the annual cycle of *Peridinium gatunense*, showing alternation between a benthic stage of sedentary, nonmotile cysts (resting spores) in summer, and a planktonic stage of motile vegetative cells in winter–spring. A sexual component to this life cycle is not shown as little is known about it

11.2.4 Culturing Peridinium

Culturing *Peridinium* proved to be a challenging task. Rahat (1968) managed to extend the survival of cells collected from the lake during blooms by transferring them into different media, diluted with distilled water, but after three divisions at the most the cells encysted or died. Eren (1969) succeeded in obtaining a culture from cysts, which he maintained in Carefoot medium (Carefoot 1968) diluted with lake water, but the cells failed to grow without addition of lake water. During the late 1960s and 1970s, monocultures of *Peridinium* were maintained for many months at a time at the Kinneret Limnological Laboratory on "Lindström" medium with or without supplements of filtered Lake Kinneret water. Axenic cultures were obtained by Bina Kaplan (Gressel et al. 1975), using antibiotics (gentamicin and Mycostatin) and repeated screening. At the same time, Rodhe and Panders achieved axenic cultures by painstakingly isolating and washing single cells and cysts, which grew out on Lindström media. Lindström and Rhode (1978) made the critical discovery that selenium was a required microelement for *Peridinium,* which led to the formulation of the Lindström L16 medium (Lindström 1991). This medium is characterized by the addition of Se (0.0007 μM), high levels of $NaHCO_3$ (1 meq L^{-1}) and Mo (0.2 μM), but low concentrations of NO_3^-N (150 μM), PO_4^-P (10 μM), Fe (0.4 μM), and Mn (0.2 μM). Lindström L16 remains the medium of choice for culturing *Peridinium*.

11.3 Growth and Physiological Characteristics

11.3.1 Cell Division and Thecae Shedding

Mitotic cellular division in *Peridinium,* by binary fission, occurs mostly in the upper 5 m of the water column, only at night ("phased division") between 00:00 and 07:00 h, peaking between 02:00 and 04:00 h (Pollingher and Serruya 1976). The thecae are shed before or during cell division. The two daughter cells that emerge are smaller in size than the mother cell. Each excretes its own new thecae and grows in size.

Thecae shedding may also occur without cell division, when the cells are subjected to stress, such as nutrient limitation (Criscuolu et al. 1981), long exposure to strong light, or transfer to distilled water (our observations). A naked protoplast emerges which will later secrete new thecae. The bottom of culture flasks in which *Peridinium* are grown under N or P limitation becomes covered with a thick white layer of empty thecae (Criscuolu et al. 1981).

Pollingher and Zemel (1981) noted that in-situ division rates of *Peridinium* were high during extended periods of quiescence, and declined considerably on windy nights, whereas strong winds during the day had no effect on division rates. In laboratory experiments, they elegantly demonstrated that turbulence enhanced cell mortality. Also, turbulence during the dark phase, when nuclear division takes place, prevented cells from dividing. Berman and Shteinman (1998) associated the lack of *Peridinium* bloom in 1996 with extremely high dissipation rates of turbulent kinetic energy, in contrast to high amounts of dinoflagellates in 1994 and 1995 that appeared when dissipation rates were low.

Sexual reproduction is known to occur in *Peridinium* but has rarely been observed in Lake Kinneret, perhaps because it occurs only at night. Pfiester (1977) induced sexual reproduction in *Peridinium* by transferring cultures into N-deficient medium and described the process. The gametes looked just like the vegetative cells but were of smaller size (30–35 μm diameter). Cellular fusion occurred after ~8 h of darkness, forming a motile zygote, ~55 × 60 μm, that excreted new thecae. After 3–5 days, the zygote became nonmotile, the protoplast contracted, and the cell wall thickened and split at the girdle. Meiosis followed producing two daughter cells, each of which divided within 24 h to produce ordinary vegetative cells.

11.3.2 Growth Rates

Because *Peridinium* is a large cell, its growth rate is slow compared with that of other microalgae. Based on the change with time in *Peridinium* cell abundance in Lake Kinneret, Pollingher and Serruya (1976) reported mean in situ (net) growth rates, μ, for the bloom development period of the years 1969–1974 that ranged from 0.017 to 0.040 day^{-1}, equivalent to doubling times ($\ln[2]/\mu$) of 17–41 days. Similar

mean in situ growth rates were reported again in the early 1990s by Zohary et al. (1998): 0.025–0.060 day^{-1} and by Viner-Mozzini et al. (2003): 0.04–0.08 day^{-1}. Pollingher and Serruya (1976) further estimated the actual growth rates from in situ counts of the proportion of dividing cells. Their estimates (Table 11.2) showed a maximum $\mu$of 0.26 day^{-1}, i.e., a doubling time of only 2.7 days. These values are similar to maximum growth rates of ~0.3 day^{-1}, or 2.3 days per doubling for *Peridinium* grown in culture under optimal conditions (Lindström 1984, 1991). Thus, it seems that the maximum potential growth rate of *Peridinium* is 0.25–0.3 day^{-1} or ~2–3 days per doubling.

Rodhe (1978) and Lindström (1984) reported highest biomass development and growth rates in axenic cultures grown at ca. 23 °C and >50 µmol photons m^{-2} s^{-1} of fluorescent light with energy peaks at 440–575 and 665 nm and at a pH of 8.3. Growth rate was reduced at 27 °C and light >90 µmol photons m^{-2} s^{-1}. Similar results were reported by Berman and Dubinsky (1985), who found maximum growth rates at 20 °C under intermittent light (12 h photoperiod) at intensities ranging 50–200 µmol photons m^{-2} s^{-1}. They noted a strong depression of growth at 25 °C in high constant light. At low irradiance (90 µmol photons m^{-2} s^{-1}), growth rates were most rapid at 15 °C. The highest yield after 2 weeks was found at 25 °C under a 12-h photoperiod with high intensity illumination.

11.3.3 Photosynthesis and Respiration

The specific photosynthetic rates (per unit chlorophyll) of *Peridinium* are low in comparison with other phytoplankton prevailing in Lake Kinneret (Yacobi and Pollingher 1993), with mean values of 1.6 ± 0.8 mg C mg Chl^{-1} h^{-1} at the depth of maximum photosynthesis (Table 11.2). However, the strategy of regular diurnal vertical migration (Berman and Rodhe 1971) and daytime accumulation close to the surface water (Berman 1972) enables the population to absorb a relatively large fraction of the incident light (Dubinsky and Berman 1981). With darkness, the motile cells then migrate down the water column perhaps to depths with higher nutrient concentrations. As the bloom progresses, concomitantly with the advancement of spring and increasing ambient solar radiation, *Peridinium* increases its cellular concentrations of photo-protective pigments (Yacobi 2003).

Lindström (1984) reported photosynthetic oxygen production to occur in cultures of *Peridinium* over a wide range of temperatures (5–32 °C) in white fluorescence light from 10 to 105 µE m^{-2} s^{-1}, although below 10 °C photosynthesis rates were very slow. At 33 °C, the cells died. Light saturation values were reached at 500–100 µE m^{-2} s^{-1} with the light saturation index, I_k values at 100–200 µE m^{-2} s^{-1}. Berman-Frank et al. (1994) noted that as the *Peridinium* bloom progressed in Lake Kinneret, dissolved CO_2 concentrations declined to levels limiting the rates of photosynthesis. The dinoflagellates responded to the CO_2 decline with higher levels of external and internal carbonic anhydrase activity and internal storage of inorganic C by means of a C concentrating mechanism. Berman-Frank and Erez (1996)

Table 11.2 Physiological parameters for *Peridinium gatunense* based on field measurements

Characteristic	Average ± SD	*N*	Ref.
Maximum potential growth rate, day^{-1}	0.26	10	1
Turnover time, *d*	7.44 ± 5.05	36	2
C:Chl ratio	55 ± 19	429	2
Assimilation number (at depth of max photosynthesis), mg C mg Chl^{-1} h^{-1}	1.56 ± 0.80	36	2
Chlorophyll content, ng Chl $cell^{-1}$	0.26 ± 0.06	20	3
	0.15 ± 0.05[a]	26	4
Chlorophyll a/peridinin ratio	2.9 ± 0.3	26	4
Dry weight, ng $cell^{-1}$	30 (20–50)	13	5
	34.5 ± 18.9		LKDB[b]
	31.4		
C content, ng C $cell^{-1}$	14.3 ± 0.6	17	3
N content, ng N $cell^{-1}$	1.2	17	3
P content, ng C $cell^{-1}$	0.09 ± 0.03	17	3
C content, % dry weight	45.6 ± 4.7	54	LKDB 3
	47.7 ± 2.1	17	
N Content, % dry weight	4.3 ± 0.6	54	LKDB
	4.0 ± 0.7	17	3
P Content, % dry weight	0.3 ± 0.11	17	3

1 Pollingher and Serruya 1976, *2* Yacobi and Zohary 2010, *3* Wynne et al. 1982, *4* Yacobi et al. 1996, *5* Berman 1978

[a] Computed from Chl content per unit wet weight and cell wet weight from Table 11.1

[b] LKDB-Lake Kinneret database. Mean and standard deviation (SD) computed from *Peridinium* cell abundance and total suspended solids (TSS) data for sampling dates and depths during 1998–2007 when *Peridinium* biomass comprised >95% of total phytoplankton biomass and TSS was determined on the same water sample

followed the presence of the internal C pools, their size and dynamics, demonstrating that the levels of C inside *Peridinium* cells could reach 20–80-fold that of ambient concentrations. Nishri (Chap. 23) proposed that CO_2 released, in the process of calcite precipitation constitutes, an additional source of C for *Peridinium* during bloom development, and computed that this source can explain about half of the C needed for the buildup of the peak bloom biomass.

Lindström (1984) reported that on average, respiration by *Peridinium* in axenic cultures consumed ca. 12% of gross production. The maximum respiration rate recorded was 270×10^{-12} gO_2 $cell^{-1}$ h^{-1} at 31 °C. With the increase in water temperature and solar radiation, the Q_{10} for respiration increased considerably faster than that for photosynthesis.

11.3.4 Chlorophyll and Other Pigments

The long-term (1990–2007) mean chlorophyll content of *Peridinium,* computed from field data for sampling points where this dinoflagellate comprised >90% of total phytoplankton biomass, was 0.22 ± 0.08 ng Chl $cell^{-1}$, similar to values

(0.26 ± 0.06 ng Chl cell^{-1}) determined by Wynne et al. (1982) for the 1976 bloom (Table 11.2). Pigment determination by HPLC showed that in addition to chlorophyll *a, Peridinium* contains chlorophyll *c* and peridinin as accessory pigments (Yacobi et al. 1996). The chlorophyll *a*/peridinin ratio, 2.9 ± 0.34 (Table 11.2), showed high stability throughout the bloom development and decline, such that Yacobi et al. (1996) proposed using peridinin as a surrogate for *Peridinium* abundance.

11.3.5 Motility and Diel Vertical Migration

Peridinium uses its whiplash flagellum, attached at the sulcus, to propel itself forward while its other flagellum causes it to whirl in circles. The cells swim at variable speeds between 50 and 600 μm s^{-1} (Hader et al. 1990). Ultraviolet radiation caused a reduction of the percentage of motile cells and the average individual swimming speed within short (~2 h) exposure times (Hader et al. 1990). *P. gatunense* uses light as a major cue to optimizing its position in its habitat. The cells possess two different phototactic strategies (Liu et al. 1990). At low irradiances, the cells show positive phototaxis: In a culture flask, they swim toward a source of light and in the lake, they migrate upwards toward the light in the early morning hours. At high irradiances, the cells show a prominent transversal phototaxis (diaphototaxis); they tend to become disoriented and stop their upward movement.

Diel vertical migration of *Peridinium* was first studied by Berman and Rhode (1971). Their interpretation was that during daytime, *Peridinium* aggregated at the depth of optimal light intensity. They noted that during calm sunny mornings, a prominent biomass peak formed within the uppermost 1–2-m layer. Between midnight and sunrise, however, no aggregation was visible; *Peridinium* was evenly distributed over the water column. This daily near-surface aggregation was typical of early bloom development stages; as the bloom progressed, the peak appeared deeper in the water column, between 2–4 m before noon and at 5–7 m in the afternoon. By forming dense, self-shading layers, *Peridinium* created its own microclimate, quite different from the regular, large-scale environment. At night, *Peridinium* cells were often concentrated deeper (10–15 m), perhaps in water with higher nutrient levels. During storms, however, *Peridinium* was not able to maintain its position in the water column, resulting with a homogeneous vertical distribution. Pollingher and Hickel (1991) presented data from additional diel studies, correlating the depth distribution of *Peridinium* to the wind regime. They noted that *Peridinium* aggregated above the thermocline when strong winds generated turbulent conditions in the epilimnion. They associated several biotic and abiotic factors with the diel vertical migration, including active movement toward the layer with optimum light intensity (during the light hours) or temperature, settling during the night to depths of higher nutrient concentrations, and wind-created shear mixing (dominant in the evenings) that vertically disperses the accumulated population. Usvyatsov and Zohary (2006) used time-depth chlorophyll data collected at 4–6 h intervals by an automated profiler at a centrally located station in the lake to document the

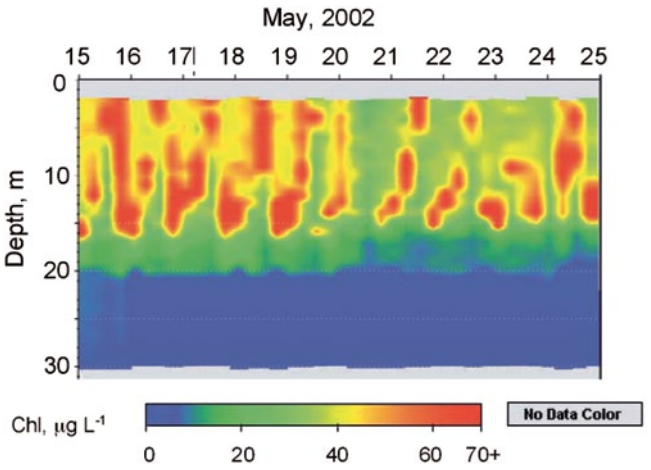

Fig. 11.4 Water column chlorophyll fluorescence data (relative scale) collected by an automatic profiler (RUSS, Apprise Technologies) located at Sta. A in Lake Kinneret, clearly demonstrating diel vertical migration of the algae. Data were collected every 6 h, between May 15 and 26, 2002, during a *Peridinium gatunense* bloom. Date tickmarks indicate 00:00 h. Cells counts confirmed that *Peridinium* constituted >95% of the phytoplankton biomass. (Reproduced with permission from Usvyatsov and Zohary 2006)

evolution of *Peridinium* blooms in 2002, 2003, and 2004. An example of a time-depth chlorophyll record for 15–26 May, 2002 (Fig. 11.4), when *Peridinium* constituted >95% of the phytoplankton biomass, shows a repetitive pattern of diel vertical migrations between 3 and 15 m (unfortunately, the 0–3-m layer could not be covered by our instruments). An interesting feature was that the descent, usually in the late-afternoon hours, was always faster than the ascent that occurred between midnight and midday. A distinct difference was noted between migration depths at the beginning and at the end of the bloom. In March–April, *Peridinium* remained at the upper 2–3 meters during daytime (06:00 until 18:00 h), descending to 10 m by midnight. In May, it remained within the upper 6 m during midday (11:00–14:00 h), reaching depths of up to 20 m by midnight.

11.3.6 Spatial Distribution

The characteristic patchiness in the spatial distribution of *Peridinium* was reported from early on (Komarovsky 1959; Eren 1969; Berman and Rhode 1971). During the bloom, patches scaling hundreds of square meters to several km^2 are often visible from the shore as coffee-brown regions surrounded by bluer water. *Peridinium* cell densities inside a patch usually exceed 1,000 cells mL^{-1}, whereas outside the patch the concentrations are typically an order of magnitude lower.

11.3.7 Cellular C, N, P Content

Peridinium cells contain on average 14.3 ng of C, 1.2 ng of N, and 0.09 ng of P per cell with an average dry weight per cell of 31.4 ng (Table 11.2). This relatively high C content (46 % of dry weight) and low P content (0.3 % of dry weight) lead to unusually high C:P ratios, ranging from 300 to 700 with an average of 464 ± 150 (Wynne et al. 1982). The high C content is due to the thecae that are composed of a polyglucan containing 95 % (by weight) carbohydrates (Nevo and Sharon 1969), with little N and P and make up ~40 % of the cell dry weight. The C:P ratio of isolated thecae is >3,000 (Zohary et al. 1998), making the calculated C:P ratio of the protoplasts ~150, considerably closer to the Redfield ratio of 106. The N content of *Peridinium* is 4 % of dry weight, with a C:N around 14; both parameters remained constant throughout the bloom (Wynne et al. 1982).

11.3.8 Phosphorus Uptake and Metabolism

Not much is known about the in situ P uptake rates of *Peridinium*. Berman and Dubinsky (1985) measured P uptake kinetics of *Peridinium* cells sampled from the lake using 63-μm Nitex nets. After removing most of the nanoplankton by subsequent filtration through 20-μm nets, the concentrated dinoflagellates were diluted into GF/C-filtered lake water to give approximately natural population densities. For each experiment, a series of flasks with increasing amounts of added carrier-free $^{32}PO_4$ was run and incorporation of ^{32}P into the cells was measured at 15, 30, and 60 min. The measured rates of P uptake, normalized to chlorophyll content, ranged 0.017–0.120 μg P μg Chl^{-1} day^{-1}. Maximum uptake (V_{max}) rates ranged from 0.131 to 0.169 μg P μg Chl^{-1} day^{-1}. Parallel experiments indicated that lake nanophytoplankton had greater affinity for inorganic P with at least tenfold more rapid uptake rates. Zohary and Kaplan (2004) conducted similar ^{32}P uptake experiments on *Peridinium* collected from the lake during the 2003 bloom and recorded V_{max} values of 0.04–0.4 μg P μg Chl^{-1} day^{-1}, with indications that the ambient levels of bioavailable P at the time were particularly low, 0.3–0.7 μg P L^{-1}.

Because it was assumed that limitation by available P was a critical factor in determining the growth patterns of *Peridinium,* considerable research attention was focused on various aspects of P metabolism in this organism. Serruya and Berman (1975) measured the ratios of cellular C:P, C:N, chlorophyll *a*:P, chlorophyll *a:*N during blooms of *Peridinium* from 1969 to 1973. Relatively high intracellular P values at the start of the bloom indicated adequate availability of this nutrient and even luxury consumption over a short period of time. Later, *Peridinium* continued to grow despite unusually high C:P ratios (>300:1). These observations, together with supplementary evidence from nutrient addition experiments and determinations of specific alkaline phosphatase levels, indicated that, for most of the growth phase of the bloom, *Peridinium* cells were not directly P limited. The decline of the bloom usually, but not always (e.g., in 1970), was marked by very high C:P ratios.

Thus, a shortage of P may often be a contributory factor to the cessation of the *Peridinium* bloom.

Similar conclusions were reached in studies of the internal P pools of *Peridinium* during blooms and in cultures (Wynne and Berman 1980; Wynne 1981). The hot water extractable P pool contained approximately equal amounts of molybdate reactive phosphorus (MRP) and non-MRP. Short-chain (6–9 units) polyphosphates (MW 630–950) constituted the bulk of the non-MRP pool, which was hydrolyzable by alkaline phosphatase and may serve as a precursor for a more permanent P store. Experiments with *Peridinium* cultures by Elgavish et al. (1980, 1982) indicated that orthophosphate in the hot water extractable fraction was a poor measure of the total intracellular phosphorus storage. These studies showed that decreases in an intracellular P pool, which were not extracted by cold 6% trichloroacetic acid, correlated with a drop in cell yields. This pool always contained the major proportion of intracellular phosphorus. ^{31}P nuclear magnetic resonance revealed that the major constituents of this pool were polyphosphates, organized in rigid aggregates.

In order to clarify the extent to which *Peridinium* were able to exploit organic P substrates, Wynne (1977) isolated both acid and alkaline phosphatases during a dinoflagellate bloom. The acid phosphatase activity was fairly constant over the entire period of the bloom. Alkaline phosphatase activity was very low until a month after the peak of the bloom, when it increased sharply. Polyacrylamide gel electrophoresis revealed one or two bands of alkaline phosphatase that increased in intensity as the bloom progressed. However, the highest activity of the enzyme in the last sample collected corresponded to a new, very intense band on the gels. Both acid and alkaline phosphatases were localized inside the cell. The appearance of the late form of alkaline phosphatase was probably related to the ambient concentrations of available phosphate in the lake and perhaps indicated that the organisms were utilizing organic P sources.

Carpene and Wynne (1986) extracted and purified an alkaline phosphatase (EC 3.1.3.1) from *Peridinium*. The enzyme had a molecular weight of 158,000 ± 5,000, showed a broad pH optimum (in the range pH 8.0–8.5), and was stable to repeated freeze/thawing cycles. It was strongly activated by Mg^{2+} but inhibited by Zn^{2+} and to a lesser extent by Cd^{2+}. Low concentrations of Cu^{2+} activated the enzyme but higher concentrations caused inhibition.

11.3.9 Nitrogen Uptake and Metabolism

Information concerning N nutrition of *Peridinium* is derived mostly from an early study in which the ^{15}N method was used to determine N uptake parameters of Lake Kinneret phytoplankton over a 2-year period (1979–1980). *Peridinium* took up N sources preferentially in order: NH_4 > urea > NO_3. During the annual bloom of *Peridinium* when ambient levels of NH_4 were low and those of NO_3 were high, a considerable portion of the total N uptake attributed mainly to *Peridinium* was derived from NO_3 (McCarthy et al. 1982). A rough calculation based on Fig. 11.3

in Berman et al. (1984) gives approximate NH_4 uptake rates ranging from 170 to 1,630 μgN μg Chl^{-1} day^{-1} and for NO_3 ranging from 100 to 750 μgN μg Chl^{-1} day^{-1}. During the early stages of the bloom (January through mid-March), when the dinoflagellates were growing more actively, *Peridinium* had about the same specific N uptake rates (per chlorophyll) as nanoplankton. Later, when *Peridinium* dominated the algal biomass, the smaller organisms were proportionally much more active in N uptake than the dinoflagellates (Berman et al. 1984). The NO_3 uptake velocity, $V_{NO3,}$ showed a clear diurnal response, decreasing from 7.5×10^{-3} h^{-1} at midday to 2.0×10^{-3} h^{-1} during the night, then increasing again in the morning hours.

The finding that NO_3 is extensively utilized by *Peridinium* raises the question whether the changes in the amounts and timing of NO_3 inputs from the watershed may have been partially responsible for the altered pattern of dinoflagellate blooms in the lake over the past 15 years.

11.3.10 Interspecies Interactions

Laboratory studies revealed allelopathic interactions between *P. gatunense* and a bloom forming toxic cyanobacterium, *Microcystis* sp., which were described by mutual density-dependent relationships (Sukenik et al. 2002; Vardi et al. 2002). *Microcystis* sp. inhibits photosynthesis in *Peridinium* by abolishing its internal carbonic anhydrase activity. Consequently, the availability of CO_2 within the cells is reduced, diverting photosynthetic electrons from CO_2 fixation to O_2, leading to the formation of reactive oxygen species. Furthermore, *Peridinium* responded to the presence of *Microcystis* by a biphasic oxidative burst and activation of certain protein kinases. The addition of MAP-kinase inhibitors prevented the biphasic oxidative burst and affected the fate (death or cell division) of *Peridinium* cells. Exposure to spent *Peridinium* medium induced sedimentation and, subsequently, massive lysis of *Microcystis* cells within 24 h; sedimentation and lysis were concomitant with a large rise in the level of the McyB protein, which is involved in toxin biosynthesis by *Microcystis* (Dittmann et al. 1997). Based on these data, it was proposed that the presence of *Microcystis,* which could induce CO_2 limitation at the beginning of the *Peridinium* growth period, when ample ambient CO_2 is still available, mimics the limiting CO_2 conditions preceding and leading to the collapse of the *Peridinium* bloom. However, if the *Peridinium* population had been previously established in the lake and maintains its patchy distribution it provides an ecological advantage that compensates for the limitation of resources in the patch.

11.4 Loss Processes

Several loss processes contribute to the disappearance of *Peridinium* from the water column. The primary loss of cells is due to death and decomposition in the water column. Second in importance is sinking to bottom sediments, where

decomposition processes prevail but some grazing also takes place. Additional, less important losses are to grazing (see below) and parasitism in the water column. A small proportion of the cells (~1 %) undergo encystation, forming cysts of greater specific gravity than the vegetative cells, these too sink to the bottom sediments to form the inoculum for future blooms. Export with water pumped out of the lake is considered negligible.

11.4.1 Programmed Cell Death

It has been shown that the coordinated collapse of the *Peridinium* population, at the end of its bloom, is mediated by a programmed cell death (PCD)-like process induced by oxidative stress that develops due to CO_2 limitation at the peak of the bloom (Vardi et al. 1999). The oxidative stress-driven death occurs despite a large increase in antioxidant activity per cell, concomitant with increasing cell density toward the peak of the bloom and immediately prior to the collapse of the entire population (Butow et al. 1997a). Studies with laboratory cultures and field-collected samples of *Peridinium* showed that a protease excreted by senescing cells sensitizes younger cells to oxidative stress and consequently triggers synchronized cell death of the population. Induction of specific extracellular protease activity was detected in aging cultures and in lake waters during the *Peridinium* bloom, and was presumably responsible for the higher susceptibility of young cells to oxidative stress. Based on these results, Vardi et al. (2007) proposed that the *Peridinium* population orchestrates a coordinated response to stress, thereby determining the fate of its individuals.

11.4.2 Antioxidative Responses

The antioxidative mechanism found in *Peridinium* exhibited diurnal and seasonal dynamics. Ascorbate was present in the water column throughout the spring bloom period and was responsible, together with catalase, for the elimination of photosynthetically produced H_2O_2 (Butow et al. 1997a). Diurnal changes in antioxidants and their regenerative enzymes were observed. The activities of monodehydroascorbate reductase, glutathione reductase, and ascorbate concentrations showed daily periodicity and were completely in phase throughout the day/night period. Superoxide dismutase (SOD) and catalase activities were generally out of phase during the 24-h period but did show ultradian periodicity (Butow et al. 1997a). SOD activity increased toward the end of the spring bloom simultaneously with maximal photosynthetic activity and elevated ambient stress such as high irradiance, high temperature, and low CO_2 (Butow et al. 1997b). Increased temperature alone caused a slight increase in lipid peroxidation; this was greatly amplified by carbon limitation. Induced carbon limitation increased catalase activity at elevated temperatures but catalase activity declined within 48 h, allowing for the substantial increase in

lipid peroxidation (Butow et al. 1998). A novel insight into *Peridinium* response to oxidative stress was proposed by Murik and Kaplan (2009). Cells that have already experienced oxidative stress, and may therefore be carrying some damage (rise in protein carbonylation or lipid peroxidation), are eliminated via a PCD route thereby enhancing the fitness of the entire population.

11.4.3 Decomposition

Specialized populations of heterotrophic bacteria together with Protista that develop concomitantly with the dinoflagellate bloom are the primary decomposers of *Peridinium* (Hertzig et al. 1981). Sherr et al. (1982) showed that this decomposition was accelerated in the presence of bacterivorous microflagellates that the enhanced bacterial breakdown of the polysaccharide thecae but did not affect the rate of degradation of the protoplasm. The addition of phosphorus instead of microflagellates similarly stimulated the bacterial breakdown of the thecae. This highlights the likely role of microflagellates as P recyclers. Similarly, Zohary et al. (2000) followed the decomposition of freeze-dried whole cells and empty thecae of *Peridinium* under controlled laboratory conditions, with and without nutrient addition. Empty thecae remained intact for 12 days without the addition of external nutrients, but after N and P were added their decomposition was extremely rapid, within 1–2 days they completely disappeared. In contrast, almost no stimulating effect of nutrient addition was observed for the decomposition of whole cells. These findings suggested that external nutrient inputs and/or intensive regenerative nutrient cycling by microflagellates are necessary preconditions for an efficient trophic transfer of the C stored in blooms of thecate dinoflagellates.

11.4.4 Sinking and Sedimentation

Sediment trap studies (Zohary et al. 1998; Viner-Mozzini et al. 2003) revealed a typical seasonal pattern, with relatively low sedimentation rates of *Peridinium* cells during the phase of bloom increase, when thecae released from cell divisions were the main sinking component. Sedimentation rates increased substantially after the peak of the bloom, when the sinking particles were mostly senescent cells, dead cells, and protoplasts. Cysts were trapped in low numbers, usually 1−2 orders of magnitude fewer than live cells, throughout the entire bloom. Interannual variations in total *Peridinium* sedimentation were large and independent of the size of bloom. The proportion of annual *Peridinium* production reaching the sediment traps situated 14 m above the bottom sediments ranged from 6 % in 1994, an exceptionally high-biomass bloom year, to 68 % in 1991, a year with an average-size bloom.

11.4.5 Grazing

Stable isotope and experimental studies by Zohary et al. (1994) and Hambright et al. (2007) confirmed the suggestion of Serruya et al. (1980) that *Peridinium* cells are too large to be grazed by the Kinneret crustacean zooplankton. Spatially and temporally limited grazing on *Peridinium* by the ciliates *Colleps* and *Bursaria* (Rahat 1968; Pollingher 1986) and by the rotifer *Asplanchna* (Zohary et al. 1998) was observed. The native cichlid fish *Sarotherodon galilaeus* was shown to feed primarily on *Peridinium* (Spataru 1976; Zohary et al. 1994). Another native cichlid, *Oreochromis aureus,* fed on *Peridinium* too but to a lesser extent (Zohary et al. 1994). However, fish grazing removes only a total of ~14% of the dinoflagellate standing stock monthly (Pollingher and Serruya 1976) and its impact on the *Peridinium* population is minor. Overall, grazing has a negligible impact on the *Peridinium* population.

11.4.6 Parasitism

In the past, fungal infections of *Peridinium* were a rare event in Lake Kinneret (Pollingher 1988). Epidemic fungal infection of *Peridinium* was reported for the first time by Alster and Zohary (2007). The chytrid fungus *Phlyctochytrium* sp. infecting *Peridinium* cells appeared for the first time in December 2000. Its appearance coincided with a 1,000-fold decline in *Peridinium* abundance within 9 days of the initial observation of the chytrid. In August 2001, a second fungal epidemic occurred, which was again associated with a sharp decline of *Peridinium* concentrations. Initially, it was hypothesized that the fungal epidemics caused the lack of bloom development in some of the nonbloom years. However, laboratory experiments demonstrated that while healthy *Peridinium* cells were not prone to fungal infection, stressed or dead cells were easily infected (Alster and Zohary 2007). In other words, *Phlyctochytrium* was acting as a saprophyte, perhaps a facultative parasite of *Peridinium*. Possibly, another pathogen was responsible for the observed bloom crashes and the saprophytic *Phlyctochytrium* was a secondary parasite, infecting the already moribund cells. The emergence of fungal epidemics in Lake Kinneret has been suggested as an early signal of ecosystem response to increasing anthropogenic stress (Zohary 2004).

11.5 Summary: An Integrated View of *Peridinium* in Lake Kinneret

Destratification and increased turbulence in late fall and early winter cause resuspension of resting cysts, mostly from the northern and northwestern littoral sediments, where *Peridinium* blooms usually begin. Those “over-summering” cysts

have stored excess phosphorus, sufficient for several cell divisions. Organic matter and trace metals entering the lake from the catchment at this time of year and possibly also from decaying shoreline vegetation provide "growth factors" such as selenium needed for development. Photosynthesis and growth rates of *Peridinium* are adapted for developing blooms during winter–spring, when water temperatures are 20–24 °C, solar radiation levels are moderate, and respiratory losses are relatively small. Its large cell size makes *Peridinium* inedible to most of the Kinneret zooplankton, so its grazing mortality is low.

A large, slow-growing cell like *Peridinium* with a relatively small surface to volume ratio might be expected to be a relatively poor competitor for nutrients against the many coexisting nanoplanktonic species. However, this dinoflagellate possesses several attributes that enabled it to compete successfully and dominate phytoplankton biomass year after year. Its motility, phototactic abilities, and diel vertical migration allow it to modify its position in the water column according to light and nutrient availability. The activity of the transverse flagellum leads to increased water flow near the cell surface, making nutrients from the entire water mass more available. *Peridinium* is capable of luxury consumption of P, storing it in polyphosphate bodies. With a cellular C:P molar ratio of 460:1, *Peridinium* has an exceptionally low P requirement—an advantage in the mostly P-limited winter–spring situation. *Peridinium* also has allelopathic abilities at high cell densities, inhibiting the growth of competitors such as *Microcystis*.

As the blooms develop, CO_2 availability becomes growth limiting. To cope, *Peridinium* applies a C-concentrating mechanism and can store inorganic C at concentrations 20–80-fold higher than ambient levels. But eventually the cellular adaptations to declining CO_2 concentrations are insufficient to prevent the decline of photosynthetic rates, contributing to the subsequent collapse of the population in May–June. Other factors may also contribute to the bloom crash: (1) the onset of daily westerly winds (from noon till after midnight) generate turbulence that inhibits cell division; (2) currents that force *Peridinium* to be exposed to damaging intense summer radiation and high temperatures; and (3) limiting N and P concentrations.

Overall, *Peridinium* develops a dense population with low specific productivity and a long generation time. Thus, it immobilizes large amounts of nutrients and slows down the overall recycling of matter within the ecosystem (Serruya et al. 1980).

After many years of recorded constancy, in the mid-1990s, the regular pattern of spring *Peridinium* blooms broke down. In 1996, for the first time since our record begins in 1969, *Peridinium* failed to develop a significant (> 100 g wet weight m^{-2}) spring bloom. Since then, *Peridinium* blooms in Lake Kinneret have become an irregular event, occurring only in high-rainfall years, when the organic soils in the northern catchment are flooded and the excess water is flushed into Lake Kinneret. Field surveys showed that patches of high *Peridinium* densities in Lake Kinneret were associated with inflowing Jordan River water; supplementing laboratory cultures of *Peridinium* with Hula Valley water stimulated its growth relative to unenriched controls (Zohary et al. 2012). A likely explanation to the present irregular appearance of *Peridinium blooms* in Lake Kinneret is hydrological modifications

made in the catchment in the mid-1990s that prevent Hula Valley water from reaching Lake Kinneret except in exceptionally wet years. Zohary et al. (2012) proposed that prior to these hydrological changes, Jordan River water enriched Lake Kinneret with some growth factor/s (a microelement and/or organic compound originating in the Hula Valley) that in recent years arrives in sufficient quantities to support a bloom only in high-rainfall winters.

References

Alster A, Zohary T (2007) Interactions between the bloom-forming dinoflagellate *Peridinium gatunense* and the chytrid fungus *Phlyctochytrium* sp. Hydrobiologia 578:131–139

Alster A, Zohary T, Dubinsky Z (2006) *Peridinium gatunense* cyst type, abundance and germination in Lake Kinneret. Verh Int Ver Limnol 29:2083–2086

Berman T (1972) General biochemical features. In: Serruya C (ed) Lake Kinneret. Monographiae Biologicae, vol 32. Dr. Junk Publishers, The Hague, pp 269–270

Berman T (1978) Profiles of chlorophyll concentrations by *in vivo* fluorescence: some limnological applications. Limnol Oceanogr 17:616–618

Berman T, Dubinsky Z (1985) The autecology of *Peridinium cinctum* fa.*westii* from Lake Kinneret. Verh Int Ver Limnol 22:2850–2854

Berman T, Rodhe W (1971) Distribution and migration of *Peridinium* in Lake Kinneret. In: Mitteilungen Internationale Vereinigung für Theoretische und Angewandte Limnologie, vol 19. pp 266–276

Berman T, Roth IL (1979) The flagella of *Peridinium cinctum* fa *westii*: *in situ* fixation and observation by scanning electron microscopy. Phycologia 18:307–311

Berman T, Sherr BF, Sherr E, Wynne D, McCarthy JJ (1984) The characteristics of ammonium and nitrate uptake by phytoplankton in Lake Kinneret. Limnol Oceanogr 29:287–297

Berman T, Shteinman B (1998) Phytoplankton development and turbulent mixing in Lake Kinneret (1992–1996). J Plankton Res 20:709–726

Berman T, Yacobi YZ, Pollingher U (1992) Lake Kinneret phytoplankton: stability and variability during twenty years (1970–1989). Aquat Sci 54:104–127

Berman-Frank I, Erez J (1996) Inorganic carbon pools in the bloom-forming dinoflagellate *Peridinium gatunense*. Limnol Oceanogr 41:1780–1789

Berman-Frank I, Zohary T, Erez J, Dubinsky Z (1994) CO_2 availability, carbonic anhydrase, and the annual dinoflagellate bloom in Lake Kinneret. Limnol Oceanogr 39:1822–1834

Boltovskoy A (1983) *Peridinium cinctum* f. *westii* del Mar de Galilea, sinonimo de *Peridinium gatunense* (Dinophyceae). Limnobios 2:413–418

Butow BJ, Wynne D, Tel-Or E (1997a) Antioxidative protection of *Peridinium gatunense* in Lake Kinneret: seasonal and daily variation. J Phycol 33:780–786

Butow BJ, Wynne D, Tel-Or E (1997b) Superoxidase dismutase activity in *Peridinium gatunense* in Lake Kinneret: effect of light regime and carbon dioxide concentration. J Phycol 33:787–793

Butow B, Wynne D, Sukenik A, Hadas O, Tel-Or E (1998) The synergistic effect of carbon concentration and high temperature on lipid peroxidation in *Peridinium gatunense*. J Phycol 20:355–369

Carefoot JR (1968) Culture and heterotrophy of the freshwater dinoflagellate, *Peridinium cinctum* fa. *ovaplanum* Lindeman. J Phycol 4:129–131

Carpenè E, Wynne D (1986) Properties of an alkaline phosphatase from the dinoflagellate *Peridinium cinctum*. Comp Biochem Phys B 83:163–167

Criscuolo CM, Dubinsky Z, Aaronson S (1981) Skeleton shedding in *Peridinium cinctum* from Lake Kinneret: a unique phytoplankton response to nutrient imbalance. In: Shuval H (ed) Developments in arid zone ecology and environmental quality. Proceedings of the 12th Scientific

Conference of the Israeli Ecological Society, 1981, Jerusalem. Balaban, Philadelphia, pp 169–176
Dittmann E, Neilan BA, Erhard M, Von Döhren H, Börner T (1997) Insertional mutagenesis of a peptide synthetase gene that is responsible for hepatotoxin production in the cyanobacterium *Microcystis aeruginosa* PCC 7806. Mol Microbiol 26(4):779–787
Dubinsky Z, Berman T (1981) Light utilization by phytoplankton in Lake Kinneret (Israel). Limnol Oceanogr 26:660–670
Elgavish A, Elgavish GA, Halman M, Berman T (1980) Phosphorus utilization and storage in batch cultures of the dinoflagellate *Peridinium cinctum* fa. *westii*. J Phycol 16:626–633
Elgavish A, Halmann M, Berman T (1982) A comparative study of phosphorus utilization and storage in batch cultures of *Peridinium cinctum, Pediastrum duplex* and *Cosmarium* sp. from Lake Kinneret (Israel). Phycologia 21:47–54
Eren J (1969) Studies of development cycle of *Peridinium cinctum* fa. *westii*. Verh Int Ver Limnol 17:1013–1016
Gressel J, Berman T, Cohen N (1975) Dinoflagellate ribosomal RNA—an evolutionary relic? J Mol Evol 5:307–313
Hader D-P, Liu S-M, Hader M, Ullrich W (1990) Photoorientation, motility and pigmentation in a freshwater *Peridinium* affected by ultraviolet radiation. Gen Physiol Biophys 9:361–371
Hambright KD, Zohary T, Gude H (2007) Microzooplankton dominate carbon flow and nutrient cycling in a warm subtropical freshwater lake. Limnol Oceanogr 52(3):1018–1025
Herzig R, Dubinsky Z, Berman T (1981) Breakdown of *Peridinium* biomass in Lake Kinneret. In: Shuval H (ed) Developments in arid zone ecology and environmental quality. Proceedings of the 12th Scientific Conference of the Israeli Ecological Society. Balaban, Philadelphia, pp 179–185
Hickel B, Pollingher U (1988) Identification of the bloom forming *Peridinium* from Lake Kinneret (Israel) as *P. gatunense* (Dinophyceae). Br Phycol J 23:115–119
Komarovsky B (1951) Some characteristic water-blooms in Lake Tiberias and fish ponds in the Jordan Valley. Verh Int Ver Limnol 11:219–223
Komarovsky B (1959) The Plankton of Lake Tiberias. Bull Res Counc Isr B8:65–96
Lindström K (1984) Effect of temperature, light and pH on growth, photosynthesis and respiration of the dinoflagellate *Peridinium cinctum* fa. *westii* in laboratory cultures. J Phycol 20:212–220
Lindström K (1991) Nutrient requirements of the dinoflagellate *Peridinium gatunense*. J Phycol 27:207–219
Lindström KR, Rodhe W (1978) Selenium as a micronutrient for the dinoflagellate *Peridinium cinctum* fa. *westii*. Verh Int Ver Limnol 21:168–173
Liu S-M, Hader D-P, Ullrich W (1990) Photoorientation in the freshwater dinoflagellate, *Peridinium gatunense* Nygaard. FEMS Microbiol Lett 73:91–101
McCarthy JJ, Wynne D, Berman T (1982) The uptake of dissolved nitrogenous nutrients by Lake Kinneret, Israel microplankton. Limnol Oceanogr 27:673–680
Messer G, Ben Shaul Y (1969) Fine structure of *Peridinium westii*, a freshwater dinoflagellate. J Protozool 15:272–280
Murik O, Kaplan A (2009) Paradoxically, prior acquisition of antioxidant activity enhances oxidative stress-induced cell death. Environ Microbiol 11(9):2301–2309
Nevo Z, Sharon N (1969) The cell wall of *Peridinium westii*, a non cellilosic glucan. Biochim Biophys Acta 173:161–175
Pfiester LA (1977) Sexual reproduction of *Peridinium gatunense* (Dinophyceae). J Phycol 13:92–95
Pollingher U (1978) *Peridinium cinctum* fa. *westii* (Lemm.) Lef.: morphology and systematics. In: Serruya C (ed) Lake Kinneret. Monographiae Biologicae, vol 32. Dr. Junk Publishers, The Hague, pp 261–267
Pollingher U (1986) Phytoplankton periodicity in a subtropical lake (Lake Kinneret, Israel). Hydrobiologia 138:127–138
Pollingher U (1988) Freshwater armored dinoflagellates: growth, reproductive strategies and population dynamics. In: Sandgren C (ed) Growth and reproduction strategies of freshwater phytoplankton. Cambridge University Press, Cambridge, pp 134–174

Pollingher U, Hickel B (1991) Dinoflagellate associations in a subtropical lake (Lake Kinneret, Israel). Arch Hydrobiol 120:267–285
Pollingher U, Kimor B (1970) Seasonal and bathymetric changes in the composition of the phytoplankton population of Lake Tiberias based on biomass estimations during the years 1964–1967. Sea Fisheries Research Station, Bulletin No. 55. Sea Fisheries Research Station, Haifa
Pollingher U, Serruya C (1976) Phased division of *Peridinium cinctum* fa. *westii* (Dinophyceae) and development of the Lake Kinneret, Israel bloom. J Phycol 12:162–170
Pollingher U, Zemel E (1981) *In situ* and experimental evidence of the influence of turbulence on cell division processes of *Peridinium cinctum* fa.*westii*. (Lemm.) Lefevre. Br Phycol J 16:281–287
Rahat M (1968) Observations on the life cycle of *Peridinium westii* in a mixed culture. Isr J Bot 17:200–206
Rayss T (1951) Les Algaes des Aeux Continentals. Materiaux Paur la Flore Algologique de la Palestine. Pak J Bot 5:71–95
Rodhe W (1978) *Peridinium cinctum* fa. *westii* (Lemm.) Lef.: growth characteristics. In: Serruya C (ed) Lake Kinneret. Monographiae Biologicae, vol 32. Dr. Junk Publishers, The Hague, pp 275–283
Roelke DL, Zohary T, Hambright KD, Montoya JV (2007) Alternative states in the phytoplankton of Lake Kinneret, Israel (Sea of Galilee). Freshw Biol 52:399–411
Serruya C, Berman T (1975) Phosphorus, nitrogen and the growth of algae in Lake Kinneret. J Phycol 11:155–162
Serruya C, Gophen M, Pollingher U (1980) Lake Kinneret: carbon flow patterns and ecosystems management. Arch Hydrobiol 88:265–302
Sherr B, Sherr E, Berman T (1982) Decomposition of organic detritus: a selective role for microflagellate protozoa. Limnol Oceanogr 27:765–769
Spataru P (1976) The feeding habits of Tilapia galilaea (Artedi) in Lake Kinneret (Israel). Aquaculture 9:47–59
Sukenik A, Eshkol R, Livne A, Hadas O, Rom M, Tchernov D, Vardi A, Kaplan A (2002) Inhibition of growth and photosynthesis of the dinoflagellate *Peridinium gatunense* by *Microcystis* sp.(cyanobacteria): a novel allelopathic mechanism. Limnol Oceanogr 47:1656–1663
Usvyatsov S, Zohary T (2006) Lake Kinneret continuous time-depth chlorophyll record highlights major phytoplankton events. Verh Int Ver Limnol 29:1131–1134
Vardi A, Berman-Frank I, Rozenberg T, Hadas O, Kaplan A, Levine A (1999) Programmed cell death of the dinoflagellate *Peridinium gatunense* is mediated by CO_2 limitation and oxidative stress. Curr Biol 9:1061–1064
Vardi A, Schatz D, Beeri K, Motro U, Sukenik A, Levine A, Kaplan A (2002) Dinoflagellate-cyanobacterium communication may determine the composition of phytoplankton assemblage in a mesotrophic lake. Curr Biol 12:1767–1772
Vardi A, Eisenstadt D, Murik O, Berman-Frank I, Zohary T, Levine A, Kaplan A (2007) Synchronization of cell death in a dinoflagellate population is mediated by an excreted thiol protease. Environ Microbiol 9:360–369
Viner-Mozzini Y, Gasith A, Zohary T (2003) Dinoflagellate bloom development and collapse in Lake Kinneret: a sediment trap study. J Plankton Res 25:591–602
Wynne D (1977) Alterations in activity of phosphatases during the *Peridinium* bloom in Lake Kinneret. Physiol Plant 40:219–224
Wynne D (1981) Phosphorus, phosphatases and the *Peridinium* bloom in Lake Kinneret. Verh Int Ver Limnol 21:523–527
Wynne D, Berman T (1980) Hot water extractable phosphorus: an indicator of nutritional status of *Peridinium cinctum* (Dinophyceae) from Lake Kinneret (Israel)? J Phycol 16:40–46
Wynne D, Patni NJ, Aaronson S, Berman T (1982) The relationship between nutrient status and chemical composition of *Peridinium cinctum* during the bloom in Lake Kinneret. J Plankton Res 4:125–136
Yacobi Y (2003) Seasonal variation of photosynthetic pigments in the dinoflagellate *Peridinium gatunense* (Dinophyceae) in Lake Kinneret Israel. Freshw Biol 48:1850–1858

Yacobi YZ, Mantoura RFC, Llewellyn CA (1991) The distribution of chlorophylls, carotenoids and their breakdown products in Lake Kinneret (Israel) sediments. Freshw Biol 26:1–10

Yacobi YZ, Pollingher U (1993) Phytoplankton composition and activity: response to fluctuation in lake volume and turbulence. Verh Int Ver Limnol 25:796–799

Yacobi YZ, Pollingher U, Gonen Y, Gerhard V, Sukenik A (1996) HPLC analysis of phytoplankton pigments from Lake Kinneret with special reference to the bloom-forming dinoflagellate *Peridinium gatunense* (Diniophyceae) and chlorophyll degradation products. J Plankton Res 18:1781–1796

Yacobi YZ, Zohary T (2010) Carbon:chlorophyll a ratio, assimilation numbers and turnover times of Lake Kinneret phytoplankton. Hydrobiologia 639:185–196

Zohary T (2004) Changes to the phytoplankton assemblage of Lake Kinneret after decades of a predictable, repetitive pattern. Freshw Biol 49:1355–1371

Zohary T, Kaplan B (2004) Phytoplankton phosphorus uptake rates using 33P. Lake Kinneret water quality management and optimization support system—Phase 2: physiological experiments, KLL-IOLR Report # T8/2004. pp 22–30

Zohary T, Ostrovsky I (2011) Ecological impacts of excessive water level fluctuations in stratified freshwater lake. Inland Waters 1:47–59

Zohary T, Erez J, Gophen M, Berman-Frank I, Stiller M (1994) Seasonality of stable carbon isotopes with Lake Kinneret pelagic food web. Limnol Oceanogr 39:1030–1043

Zohary T, Pollingher U, Hadas O, Hambright KD (1998) Bloom dynamics and sedimentation of *Peridinium gatunense* in Lake Kinneret. Limnol Oceanogr 43:175–186

Zohary T, Hadas O, Pollingher U, Kaplan B, Pinkas R, Güde H (2000) The effect of nutrients (N, P) on the decomposition of *Peridinium gatunense* cells and thecae. Limnol Oceanogr 45:123–130

Zohary T, Nishri A, Sukenik A (2012) Present-absent: a chronicle of the dinoflagellate *Peridinium gatunense* from Lake Kinneret. Hydrobiologia 698:161–174

Chapter 12
Cyanobacteria

Assaf Sukenik, Ora Hadas and Aaron Kaplan

Abstract The routine monitoring program of Lake Kinneret, initiated as early as 1969, revealed the presence of many species of cyanobacteria. However, it was only the first bloom of the nostocalean species *Aphanizomenon ovalisporum* in 1994 that attracted special attention to this important division. This chapter describes the abundance of the most important cyanobacterial species in Lake Kinneret and discusses their physiological and biochemical characteristics. Special attention is given to their unique features that contribute to their proliferation and their impact on the lake's water quality.

Keywords Water quality · Cyanotoxins · Nostocales · *Aphanizomenon* · *Cylindrospermopsis* · Chroococcales · *Microcystis*

12.1 Introduction

The division Cyanobacteria belongs to the kingdom Monera, which, together with the Eubacteria ("true" bacteria) and the Archaeobacteria, makes up the prokaryota (Sukenik et al. 2009b). Like all other prokaryotic organisms, cyanobacteria lack cellular organelles; their DNA lies free in the center of the cell and is not enclosed within a nucleus. Cyanobacteria contain chlorophyll *a* and other photosynthetic pigments, which give them blue-green, often strong colors. They acquire their energy through oxygenic (oxygen evolving) photosynthesis, and thus are often referred to as algae (blue-green algae, cyanophyta), although their prokaryotic characteristics are well defined and differentiate them from eukaryotic algae. Cyanobacteria

A. Sukenik (✉) · O. Hadas
The Yigal Allon Kinneret Limnological Laboratory, Israel Oceanographic & Limnological Research, P.O. Box 447, 14950, Migdal, Israel
e-mail: assaf@ocean.org.il

O. Hadas
e-mail: orah@ocean.org.il

A. Kaplan
Department of Plant and Environmental Sciences,
The Hebrew University of Jerusalem, 91904 Jerusalem, Israel
e-mail: aaron.kaplan@mail.huji.ac.il

T. Zohary et al. (eds.), *Lake Kinneret, Ecology and Management,* Aquatic Ecology Series 6,
DOI 10.1007/978-94-017-8944-8_12,

Table 12.1 The most abundant cyanobacteria species in Lake Kinneret and the timing of their appearance

Order	Species	Years of high abundance	Season
Chroococcales			
	Microcystis wesenbergii	1997, 1999–2001	Feb–Apr
	Microcystis botris	2009	Feb–Apr
	Microcystis aeruginosa	1970, 1971, 1974, 1976, 1979, 1983, 1995–2003, 2006, 2009–2010	Feb–Apr
	Chroococcus limneticus	1996–1997	Apr–Jun
	Chroococcus minutus	1978, 1984, 1995, 2001–2003, 2006–2009	Jun–Sep
	Chroococcus turgidis	1975, 1981–1985, 1996, 2000–2001	Sep–Nov
Nostocales			
	Aphanizomenon ovalisporum	1994–1997, 1999–2001, 2001, 2003–2010	Jul–Nov
	Cylindrospermopsis raciborskii	2001, 2003–2006, 2008–2010	Jul–Nov
Pseudanabaenales	*Planktolyngbya limnetica*	1999–2005, 2010	Jul–Nov

Only species with monthly mean areal biomass concentration >5 g w.w. m^{-2} (at least once) are included in the table. Additional cyanobacterial species, not included in the table due to their low contribution to total phytoplankton biomass, are listed in Table 10.1

have relatively simple shapes. These include simple unicells (as in the genera *Synechococcus* and *Chroococcus*), colonies (e.g., *Microcystis*), and filaments, also known as trichomes (e.g., *Oscillatoria, Aphanizomenon*). More complex forms, which are variations of the original simple forms, also occur such as branched filaments (*Calothrix, Fischerella*), filament aggregates (e.g., *Gloeotrichia*), and sheets or mats (*Merismopedia, Hydrococcus*). Some of the filamentous forms evolved to have specialized cells—heterocytes (previously termed heterocysts)—for nitrogen fixation, akinetes as resting stages and motile hormogonia.

This chapter reports on the abundance of various cyanobacterial species in Lake Kinneret over the past 50 years and describes the physiological and biochemical features of the most abundant species and how these features contribute to their proliferation in Lake Kinneret, their role in the ecosystem, and their impact on the lake's water quality.

12.2 The Key Players in Lake Kinneret

The most abundant cyanobacteria in Lake Kinneret belong to two orders: Chroococcales and Nostocales (Table 12.1, see also Sect. 10.1). The dominant species belong to the genera *Microcystis, Aphanizomenon,* and *Cylindrospermopsis*, some of which are known as producers of cyanotoxins (Sect. 33.1) and develop blooms that under certain environmental conditions appear as a thin film on the water surface and in

Fig. 12.1 Floating mats of *Microcystis* in Lake Kinneret. **a** February 2002, Langmuir lines of floating *Microcystis* colonies off shore near Tabgha (original). **b** March 2009, floating scum of *Microcystis* near the northwestern shore (original). **c** February 2010, large patches of floating *Microcystis* mats near Tiberias. (Air photo by Idan Shaked)

extreme cases as thick scums that last several days. Surface mats of *Microcystis* developed in Lake Kinneret on calm days during February and March, when positively buoyant, gas-vesicle-containing *Microcystis* colonies floated to the water surface during the morning hours. The formed thin surface films were pushed by blowing wind and concentrated near shores to form visible scums (Fig. 12.1). The mats were disintegrated by late afternoon, unless the calm conditions persisted. Interestingly, *Microcystis* concentration in the water column during these months was rather low (normally not more than 5 g w.w. m^{-2}), although colonies of variable sizes could be easily observed even by the naked eye.

A study on the genetic diversity of cyanobacterial communities in Lake Kinneret using various molecular techniques revealed the presence of at least 11 different groups of cyanobacteria and significant differences in the cyanobacterial community structure between epilimnetic and hypolimnetic waters. Interestingly, several amplicones showed similarity to sequences from some groups of cyanobacteria so far found in marine habitats (Junier et al. 2007).

While *Microcystis* proliferated and became visible as floating mats or scums, mainly during the winter months (January–April), *Aphanizomenon* and *Cylindrospermopsis* dominated the lake phytoplankton during the summer and autumn. The latter two species never formed scums, although they possess gas vesicles and their concentration in the water column frequently exceeded 10 g w.w. m^{-2} (Hadas et al. 2012). The more homogeneous vertical distribution of Nostocales trichomes in the water column was attributed to low buoyancy potential and high water turbulence imposed by the typical daily afternoon breeze entering the area during the summer and autumn (Berman and Shteinman 1998, Chap. 9).

12.3 Microcystis in Lake Kinneret

The long-term record of Lake Kinneret phytoplankton composition reveals the presence of various *Microcystis* species (*M. aeruginosa, M. botris, M. flos-aquae, M. wesenbergii,* and *M. viridis*; Sect. 10.1). Winter blooms of *Microcystis* spp. were frequently recorded in the 1970s till the mid-1980s and again since 1995 to present

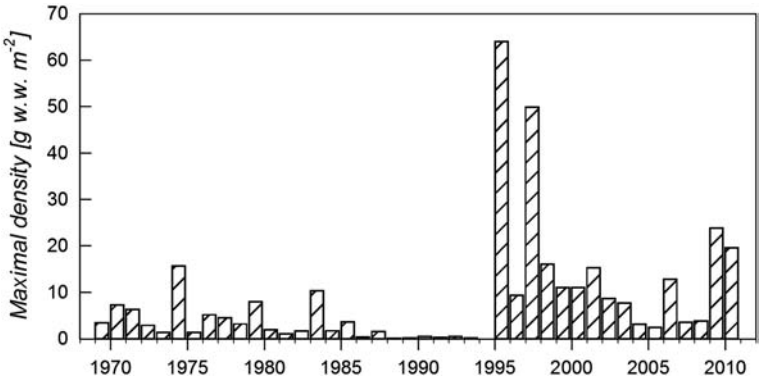

Fig. 12.2 Time series of maximal annual biomass density (g w.w. m^{-2}) of *Microcystis* spp. in Lake Kinneret 1969–2010. (Reproduced with permission from Hadas et al. 2012)

(Fig. 12.2). An exceptional bloom of *Microcystis* sp. was observed in winter 1964 (Pollingher and Kimor 1970; Pollingher 1978) and then once again in 1995. Occasional winter blooms of *Microcystis* sp. (1976, 1978, 1979 and then again in 1995 and 1997) were proposed as the source of disturbance to the annual *Peridinium* spring bloom via allelopathic interactions (Sukenik et al. 2002).

In winter 1995, two *Microcystis* strains (MK-G and MK-B, frequently named also MC-G and MC-B, respectively) were isolated (Hadas unpublished). These strains were clearly distinct from each other by their spectral properties, strain MK-G having a greenish color and strain MK-B a brownish appearance (Masseret and Sukenik 2008), and by the suite of microcystin toxins they produce (Schatz et al. 2005). Furthermore, DNA analysis of 16S rRNA genes of both strains showed high similarity to *M. viridis* or *M. wesenbergii* NIES112 (Schatz et al. 2000).

12.4 The Invasion of Nostocales

The expansion of tropical species of Nostocalean cyanobacteria into lakes in the temperate zone appears to be a worldwide phenomenon (Padisák 1997; Briand et al. 2004; Wiedner et al. 2007; Mehnert et al. 2010; Salmaso et al. 2012; Sukenik et al. 2012a). The invasion was presumably facilitated by human activities or by migrating animals or birds. But reaching a new environment is not sufficient and the invader needs a variety of traits that support its establishment and proliferation. This could be explained by the tolerance of Nostocales to a wide range of environmental conditions and cellular differentiation during their life cycle (Padisak and Reynolds 1998; Vidal and Kruk 2008). One physiological advantage of the Nostocales is their ability to fix atmospheric dinitrogen and thus proliferate in an environment depleted in combined inorganic nitrogen, conditions that prevail in Lake Kinneret during the summer and have become more common since 1994. In addition, Nostocales possess the ability to form dormant cells (akinetes) which stay in the sediment and germinate to produce vegetative cells following improved environmental conditions.

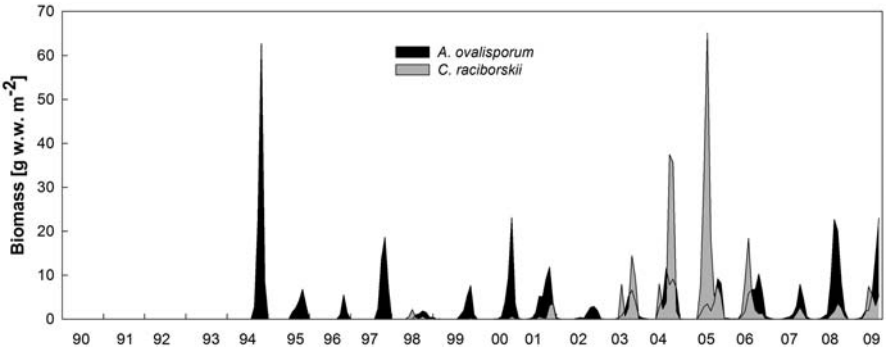

Fig. 12.3 Multi-annual variations in the abundance of two Nostocales species in Lake Kinneret. Note the prompt invasion of *Aphanizomenon ovalisporum* in summer 1994 as compared with a gradual spreading and domination of *Cylindrospermopsis raciborskii*. Data represent monthly average values

The appearance in 1994 and establishment of the Nostocalean species *Aphanizomenon ovalisporum* and *Cylindrospermopsis raciborskii* in Lake Kinneret (Fig. 12.3) could not be advanced without changes in climate conditions such as elevated water temperature, lower summer wind speed, and reduced summer availability of fixed nitrogen (Hadas et al. 2012).

The first appearance of *A. ovalisporum* in Lake Kinneret in August 1994 was apparently boosted by temporary relatively high concentrations of total dissolved phosphorus presumably supported by degradation of the exceptional massive spring bloom of the dinoflagellate *Peridinium gatunense*. In addition, the 1994 bloom was accompanied with exceptionally high alkaline phosphatase (APase) activity (Hadas et al. 1999), which was later attributed to a unique mechanism of phosphate assimilation in *A. ovalisporum* (see below, Bar-Yosef et al. 2010). The N requirement of the summer population of *Aphanizomenon* in1994 was partly provided by nitrogen fixation, as indicated by a high percentage of heterocytes (Pollingher et al. 1998). Since 2001, nitrogen fixation was further demonstrated to take place by *in situ* measurements (Hadas et al. 1999, 2012). For the overall contribution of N_2 fixation by Nostocales to Lake Kinneret's nitrogen balance see Chaps. 19 and 22. The ability of the population to use HCO_3^- as a carbon source under high pH conditions undoubtedly also contributed to its domination (Hadas et al. 1999, as discussed below).

Following the invasion of *A. ovalisporum* in summer 1994, its dormant cells, the akinetes, enabled its establishment as a perennial population. Akinetes were found in the lake's sediments and their distribution in the sediment profile roughly followed the intensity of the bloom in the corresponding year (Ramm et al. 2012; Sukenik et al. 2011). The germination potency of *A. ovalisporum* akinetes and the possible re-proliferation of this cyanobacterium were experimentally demonstrated by incubating lake sediments in nitrogen-depleted BG11 medium, which yielded a dominant population of *A. ovalisporum* (Hadas et al. 1999).

C. raciborskii was first detected in Lake Kinneret in the summer of 1998 and reached a maximum biomass (65 g m^{-2}) in August 2005 (Fig. 12.3), when this sin-

gle species made up 82 % of the phytoplankton biomass. The *C. raciborskii* bloom of summer 2005 collapsed in early September followed by a peak in the *A. ovalisporum* population in November. The long-term record suggests two alternating periods since the 1990s where *A. ovalisporum* dominated the summer–autumn community between 1994 and 2002 and again since 2007, whereas *C. raciborskii* was prominent between 2003 and 2006 (Hadas et al. 2012). The appearance of *A. ovalisporum* and *C. raciborskii* in Lake Kinneret suggests that these species expanded their global distribution as a part of a global invasion process as reported in several lakes in Europe (Sukenik et al. 2012a).

Recently, we reviewed the invasion of Nostocales (cyanobacteria) to subtropical and temperate freshwater lakes and indicated that inappropriate management of watersheds and high pollution triggered the geographic expansion of this group (Sukenik et al. 2012a). But more relevant to Lake Kinneret, these invading species can survive and propagate also under oligotrophic conditions. This is achieved due to their various efficient phosphate acquisition capabilities and nitrogen fixation which seem to be more relevant under oligotrophic than under eutrophic conditions. Thus, in oligotrophic systems, nitrogen cannot be considered as a limiting factor. Phosphate availability controls the development of the N_2-fixing population and its growth. Consequently, management efforts to control eutrophication by reducing N loads, apparently effective in reducing blooms of *Microcystis* and other Chroococcales species, may actually support the growth of Nostocales which easily outcompete native species in such N-limited ecosystems (Schindler et al. 2008).

12.5 Isolation of Toxic and Non-toxic Cyanobacteria Strains from Lake Kinneret

Several species and strains of cyanobacteria were isolated from Lake Kinneret to establish stable cultures of single cyanobacteria species, though none of them was axenic. Two strains of *Microcystis* spp. were isolated, designated MC-G and MC-B, each of which was found to produce different suites of microcystins (see Sect. 24.1) and both lost toxin production capability under laboratory conditions (Schatz et al. 2005). A laboratory culture of *A. ovalisporum* was established from the summer bloom of 1994 (Hadas unpublished). This isolated was identified as a producer of cylindrospermopsin (Banker et al. 1997) and was further studied for its physiological responses to various environmental conditions (Hadas et al. 1999, 2002a). A culture of a non-toxic *C. raciborskii* was established from the 2005 summer bloom (Hadas et al. 2002a) further supporting the reports that the 2005 bloom was non-toxic (Alster et al. 2010). Recently, an additional strain of *A. ovalisporum* and a strain of *Anabaena bergii* were isolated from Lake Kinneret, but neither one was a producer of cylindrospermopsin (Ballot et al. 2011).

Two strains of the pico-planktonic species of the genus *Synechococcus* were isolated from Lake Kinneret and maintained under laboratory conditions (Malinsky-Rushansky et al. 2002). Both strains grew well at high light intensities, but poorly

below 10 μmol photons m^{-2} s^{-1}. Differences in temperature tolerance and photoacclimation suggest that one strain belongs to picocyanobacteria population found in summer below surface waters, while the other stain represents picocyanobacteria found throughout the year at all depths.

12.6 Ecophysiological Properties of Toxic Cyanobacteria from Lake Kinneret

Isolated toxic cyanobacteria species were maintained in laboratory cultures in BG11 medium under continuous low light (10–30 μmol photons m^{-2} s^{-1}). The cultures were studied under controlled environmental conditions to gain a better understanding of the physiological properties that have stimulated their proliferation and bloom formation. The following environmental conditions were examined: temperature, irradiance, phosphate, N:P ratio, $NaHCO_3$, and salinity, indicating that the optimal conditions for *A. ovalisporum* growth under laboratory conditions were close to those observed in the lake in 1994 (Hadas et al. 1999, 2002a, b).

Optimal Light and Temperature for Growth and Photosynthesis– The growth and photosynthetic activity responses of *A. ovalisporum, C. raciborskii,* and *Microcystis* strains (MK-G and MK-B) to different temperatures were studied under laboratory conditions. The optimal temperature for growth varied among these species (Table 12.2). *A. ovalisporum* demonstrated maximal growth rate (0.3 day^{-1}) between 26 and 30 ℃. *Microcystis* strain MK-G demonstrated similarly high growth rates (0.3 day^{-1}) at a wide range of temperatures (20–35 ℃). The MK-B strain had a higher optimal temperature range (30–35 ℃). The optimal temperature for growth of each species or strain verifies its appearance during different seasons in the lake, in agreement with the temperature changes in water column: *A. ovalisporum* and *C. raciborskii* in late summer and autumn, *Microcystis* MK-G (green) in winter and *Microcystis* MK-B (brown) at the beginning of summer.

The saturating light energy for photosynthesis (E_k) was evaluated by running photosynthesis versus irradiance experiments using a photosyntethron, as described by Dubinsky (1980) and Malinsky-Rushansky et al. 2002. All examined strains demonstrated low E_k values (between 12 and 50 μmol photons m^{-2} s^{-1}; Table 12.2), suggesting adaptation to low ambient irradiance. Photoinhibition occurred in *A. ovalisporum* exposed to light intensities higher than 300 μmol photon m^{-2} s^{-1}, but was less obvious in *Microcystis* strains (Hadas et al. 1999, 2002b).

Phosphate Requirement– As in many cyanobacteria, the growth of *A. ovalisporum* was strongly affected by phosphorus availability. In laboratory experiments, maximal growth rate was obtained at inorganic phosphorus (Pi) concentrations above 40 μM. But unlike many members of the Chroococcales, *A. ovalisporum* did not respond to phosphate depletion in the medium by prompt increase in APase activity. This route of phosphate scavenging is efficiently operated only after the internal pool of polyphosphate (polyphosphate bodies, PPB in Fig. 12.4) was utilized. The

Table 12.2 Ecophysiological properties of various cyanobacteria species and strains isolated from Lake Kinneret. (Adopted from Hadas et al. 1999, 2002a, b)

Species	Temperature[a] (℃)	Growth rate (μ) day^{-1}	Light[b] (μmol photons m^{-2} s^{-1})
Aphanizomenon ovalisporum	26–30	0.2–0.3	12–50
Cylindrospermopsis raciborskii	26–32	0.34	12
Microcystis (MK-G)	20–26	0.37	12
Microcystis (MK-B)	30–35	0.26	12–50

[a] Optimal temperature for growth and maximal growth rate
[b] Saturating light for maximal photosynthetic rate

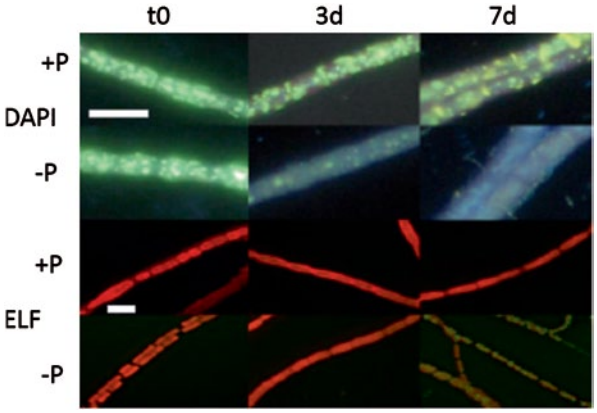

Fig. 12.4 The response of *Aphanizomenon ovalisporum* to inorganic phosphate deprivation is demonstrated by the temporal dynamics in the internal pool of polyphosphate bodies (PPB) and the in situ APase activity in control (+P) and phosphate-deprived (−P) cultures. PPBs are visualized as *greenish granules* using *DAPI* staining, and APase activity is depicted by *green color* using enzyme-labeled fluorescence (*ELF*)–APase protocol (Bar-Yosef et al. 2010). Experimental cultures were sampled at time 0 (*t0*), after 3 (*3d*) and 7 days (*7d*) of growth with or without P. Scale bars indicate 10 μm. (Reproduced with permission from Bar-Yosef et al. 2010)

abundance of PPB in the cells increased fourfold in Pi-rich conditions compared to Pi-limited cultures, but Pi uptake was faster in Pi-depleted compared to Pi-sufficient cells (Hadas et al. 2002a). A unique mechanism of phosphate assimilation was described in *A. ovalisporum* by Bar-Yosef et al (2010). In order to supply its Pi demand, *A. ovalisporum* excretes secondary metabolites, such as the toxic alkaloid cylindrospermopsin, that induce the synthesis and excretion of APase in eukaryotic algae. Pi released by this enzymatic activity is efficiently assimilated by *A. ovalisporum* due to the presence of high efficient Pi transporter (pstS). Only when internal P sources are diminished, the induction of APase occurs in *A. ovalisporum* (Fig. 12.4). This unique mechanism provides an additional advantage to *A. ovalisporum* for its survival and domination in nutrient-depleted environments. During

the course of the 1994 bloom of *A. ovalisporum,* the total dissolved Pi (TDP) level in the epilimnic water column declined from about 0.5 to 0.1 μM (Hadas et al. 1999), suggesting that *A. ovalisporum* may have sequestered significant amounts of the Pi released during the crash of the *Peridinium* bloom. The Pi quota of the natural *A. ovalisporum* population (mainly stored as PPB) declined from 0.21 μmol Pi mg^{-1} dry weight at the beginning of the bloom in July 1994 to 0.08 μmol Pi mg^{-1} dry weight at the peak of the bloom. Therefore, it was suggested that at the beginning of the bloom, growth of *A. ovalisporum* was not Pi-limited, as was also indicated by the relatively low APase activity in *Aphanizomenon* during this time (Bar-Yosef et al. 2012). One month later, at the peak of the bloom, the cells became Pi-limited, as indicated by the significant rise in APase activity (Hadas et al. 1999).

While poly-P granules/bodies of different sizes and shapes are frequently observed in P-replete cultures of *A. ovalisporum*, they were hardly found in mature akinetes. A detailed study of akinete differentiation clearly demonstrated genome multiplication (associated with massive accumulation of nucleic acids) in akinetes. This process is presumably supported by phosphate supplied from inorganic PPB of vegetative cells and was further interpreted in the context of cellular investments for proliferation following long-term dormancy, as the high nucleic acid content would provide the basis for extended survival, rapid resumption of metabolic activity, and cell division upon germination (Sukenik et al. 2009a, 2012b).

Bicarbonate Assimilation and Sodium Requirement– Assimilation numbers as high as 5 μg C μg Chl^{-1} h^{-1} were recorded in Lake Kinneret during the *A. ovalisporum* bloom in late summer and autumn of 1997. These results were verified in laboratory experiments in which the ability of *A. ovalisporum* to acquire bicarbonate was investigated. Maximal photosynthetic rate of 8 μg C μg^{-1} Chl h^{-1} and $K_{1/2}(HCO_3^-)$ of 24 μM were measured at pH 8.2. At pH 7.0, the $K_{1/2}(CO_2)$ was 2.2 and declined to 0.04 μM at pH 9.0. These results strongly indicated that *Aphanizomenon* is a HCO_3^- user and can explain its high photosynthetic rates during the bloom, under high pH and low dissolved CO_2 conditions. Na^+ concentration of about 5 mM was essential for *Aphanizomenon* growth at high pHs, a concentration that is compatible with the values measured in the lake (Hadas et al. 2002a). Na^+ ions are necessary for HCO_3^- uptake by various cyanobacterial species, and the Na^+ concentration required increases with rising pH (Kaplan et al. 1984).

Accessory Pigments– Cyanobacteria maintain relatively higher growth rates than other phytoplankton species under low light conditions. They efficiently acclimate to low light intensities by reorganizing their photosynthetic machinery including chromatic adaptation to different light spectra through their suite of accessory pigments, including phycocyanin and phycoerythrin. Consequently, they may harvest light in the green, yellow, and orange range of the visible light, which is hardly used by other phytoplankton species. Based on the abundance of these accessory pigments, the dominant cyanobacteria species of Lake Kinneret could be divided into two groups: phycoerythrin-less species (*A. ovalisporum, Microcystis* MC-G, and *C. raciborskii*) and phycoerythrin-containing species (*Microcystis* MC-B). Other light-absorbing compounds that are found in cyanobacteria are mycosporin-like

amino acids (MAA). All MAAs absorb UV light that can be destructive to biological molecules (DNA, Proteins, etc). They are effective antioxidants and are able to stabilize free radicals within their ring structure. MAAs were identified in *A. ovalisporum* and *Microcystis* MK-B strains isolated from Lake Kinneret but were not found in *C. raciborskii* and *Microcystis* MK-G.

12.7 Implication of Cyanobacteria to Water Quality and Lake Kinneret Management

It is widely acknowledged that blooms of cyanobacteria in aquatic ecosystems may have impacts on water quality, biological communities, and ecosystem services. Under eutrophic conditions, the potential for cyanobacteria dominance rises rapidly as total phosphorus (TP) increases and the TN:TP ratio decreases (Downing et al. 2001). However, the response pattern in any given system depends also on other factors, such as mean depth, mixing regime, flushing rate, water temperature, wind, and water turbulence. The expansion and establishment of Nostocales as a summer–autumn stable population in Lake Kinneret provides a special example for the hypothesis about cyanobacterial dominance under low N:P ratio (Schindler 2006; Smith 1983). Nostocales appearance was predicted in response to the diminishing dissolved inorganic N (DIN), and the intensity of the bloom was associated with the availability of phosphate (Hadas et al. 2012). It was further suggested that the persistence of the Nostocales population in Lake Kinneret (since 1994) was supported by a combination of their diazotrophic activity and regional climatic and limnological conditions. The latter includes: increased temperatures, changes in wind regime that affect physical mixing processes and water turbulence, and variations in nutrient availability, as well as interactions between various phytoplankton species (Hadas et al. 2012). We doubt whether the winter–spring abundance of *Microcystis* in Lake Kinneret in the past 15–17 years indicates eutrophication of the lake as the monthly averaged density of *Microcystis* exceeded 5 g m^{-2} several times also in the 1970s and 1980s (see 1970–1985 in Fig. 12.1). The exact reasons for the high *Microcystis* biomass in January–March 1995 (~60 g m^{-2}) and in May 1997 (~30 g m^{-2}) are not fully understood. However, we proposed the involvement of allelopathic compounds as mediators that control, among other factors, the abundance and intensity of *Microcystis* populations in Lake Kinneret (Sukenik et al. 2002; Vardi et al. 2002).

Toxin production by certain cyanobacteria (e.g., *A. ovalisporum, C. raciborskii, Microcystis aeruginosa*) may lead to a wide array of biological impacts including: allelopathic effects on other phytoplankton (Sukenik et al. 2002; Leão et al. 2009; Kaplan et al. 2012); suppression of zooplankton grazing leading to reduced growth and reproductive rates and changes in domination (Gilbert 1990; Ghadouani et al. 2004); and hepatotoxic effects on fish (Andersen et al. 1993). Toxins affected survival, growth, and fecundity of snails in laboratory experiments (Gerard and Poullain 2005), and the accumulation of toxins in tissues of freshwater clams has been suggested as a route of toxin transfer to semiaquatic rodents and their preda-

tors (Prepas et al. 1997). In addition to potential toxic effects, cyanobacteria blooms may affect grazing zooplankton by mechanical interference with the filtration apparatus (Gliwicz and Lampert 1990; Hambright et al. 2001) that may indirectly impose changes in zooplankton population structure toward small size species (Havens 2008). Given these biological changes, it is important to consider what effects, if any, frequent or persistent cyanobacterial blooms have on biomass and taxonomic structure of fish. Despite numerous case studies and reports, community-level effects of cyanobacterial blooms are not well understood. Impacts of toxins and changes in food web structure/function in response to cyanobacteria are issues that call for better understanding in the Lake Kinneret ecosystem.

It is expected that bloom events of Nostocales will reoccur in Lake Kinneret in response to management attempts to reduce nutrient loads and forecasting global warming. Further, temperature increase would promote the growth and development of Nostocales species in general. Wiedner et al. (2007) who evaluated a case of an earlier rise in water temperature associated with climate change suggested that earlier warming permits earlier germination of akinetes, thereby shifting the pelagic populations to conditions which advance population establishment and growth. While the possibilities to control and reduce the current trend of global climate change are rather limited, the management of eutrophication processes is feasible. Since a synergistic effect of nutrients and climate was frequently indicated in many sites invaded by Nostocales, it is important that nutrient concentrations in Lake Kinneret be reduced substantially from present values if cyanobacterial dominance is to be controlled. Based on long-term experimental manipulation, Schindler et al. (2008) concluded that N-fixing cyanobacteria cannot be limited by a shortage of dissolved N and instead are competitively favored. Thus, reducing N inputs could actually intensify the dominance of N-fixing cyanobacteria, thus enhancing the expansion of invasive Nostocales. A better approach to control and reduce blooms of Nostocales species and their further expansion in Lake Kinneret is to regulate and reduce external and internal sources of phosphorus, a rather complex task by itself.

Acknowledgments This chapter is based on monitoring and research activities supported by Israel Water Authority, Israel Ministry of Science and Technology (MOST), and German Ministry of Research and Technology (BMBF). A. Sukenik would like to acknowledge knowledge sharing with European experts and researchers via the European Cooperation in Science and Technology, COST Action ES 1105.

References

Alster A, Kaplan-Levy R, Sukenik A, Zohary T (2010) Morphology and phylogeny of a non-toxic invasive *Cylindrospermopsis raciborskii* from a Mediterranean lake. Hydrobiologia 639(1):115–128

Andersen RJ, Luu HA, Chen DZX, Holmes CFB, Kent ML, Le Blanc M, Taylor FJR, Williams DE (1993) Chemical and biological evidence links microcystins to salmon 'netpen liver disease'. Toxicon 31(10):1315–1323

Ballot A, Ramm J, Rundberget T, Kaplan-Levy RN, Hadas O, Sukenik A, Wiedner C (2011) Occurrence of non-cylindrospermopsin-producing *Aphanizomenon ovalisporum* and *Anabaena bergii* in Lake Kinneret (Israel). J Plankton Res 33(11):1736–1746. doi:10.1093/plankt/fbr071

Banker R, Carmeli S, Hadas O, Teltsch B, Porat R, Sukenik A (1997) Identification of cylindrospermopsin in *Aphanizomenon ovalisporum* (cyanophyceae) isolated from Lake Kinneret, Israel. J Phycol 33(4):613–616

Bar-Yosef Y, Sukenik A, Hadas O, Viner-Mozzini Y, Kaplan A (2010) Enslavement in the water body by toxic *Aphanizomenon ovalisporum*, inducing alkaline phosphatase in phytoplanktons. Curr Biol 20(17):1557–1561

Bar-Yosef Y, Murik O, Sukenik A, Hadas O, Kaplan A (2012) Multiannual variations in phytoplankton populations: what distinguished the blooms of *Aphanizomenon ovalisporum* in Lake Kinneret in 2010 from 2009? Enivron Microbiol Rep. doi:10.1111/j.1758–2229.2012.00351.x

Berman T, Shteinman B (1998) Phytoplankton development and turbulent mixing in Lake Kinneret (1992–1996). J Plankton Res 20(4):709–726. doi:10.1093/plankt/20.4.709

Briand J-F, Leboulanger C, Humbert J-F, Bernard C, Dufour P (2004) *Cylindrospermopsis raciborskii* (cyanobacteria) invasion at mid-latitudes: selection, wide physiological tolerance, or global warming? J Phycol 40(2):231–238

Downing JA, Watson SB, McCauley E (2001) Predicting cyanobacteria dominance in lakes. Can J Fish Aquat Sci 58(10):1905–1908

Dubinsky Z (1980) Light utilization efficiency in natural phytoplankton communities. In: Falkowski PG (ed) Primary productivity in the sea. Plenum, New York, pp 83–97

Gerard C, Poullain V (2005) Variation in the response of the invasive species *Potamopyrgus antipodarum* (Smith) to natural (cyanobacterial toxin) and anthropogenic (herbicide atrazine) stressors. Environ Pollut 138(1):28–33

Ghadouani A, Pinel-Alloul B, Plath K, Codd GA, Lampert W (2004) Effects of *Microcystis aeruginosa* and purified microcystin-LR on the feeding behavior of *Daphnia pulicaria*. Limnol Oceanogr 49(3):666–679

Gilbert JJ (1990) Differential effects of *Anabaena affinis* on cladocerans and rotifers: mechanisms and implications. Ecology 71(5):1727–1740

Gliwicz ZM, Lampert W (1990) Food thresholds in *Daphnia* species in the absence and presence of blue-green filaments. Ecology 71(2):691–702

Hadas O, Pinkas R, Delphine E, Vardi A, Kaplan A, Sukenik A (1999) Limnological and ecophysiological aspects of *Aphanizomenon ovalisporum* bloom in Lake Kinneret, Israel. J Plankton Res 21(8):1439–1453

Hadas O, Pinkas R, Malinsky-Rushansky N, Shalev-Alon G, Delphine E, Berner T, Sukenik A, Kaplan A (2002a) Physiological variables determined under laboratory conditions may explain the bloom of *Aphanizomenon ovalisporum* in Lake Kinneret. Eur J Phycol 37(2):259–267. doi:10.1017/S0967026202003645

Hadas O, Pinkas R, Malinsky-Rushansky N, Sukenik A, Kaplan A (2002b) Cyanobacteria in Lake Kinneret: physiological and ecological adaptations. Verh Int Ver Limnol 28:996–1000

Hadas O, Pinkas R, Malinsky-Rushansky N, Nishri A, Kaplan A, Rimmer A, Sukenik A (2012) Appearance and establishment of diazotrophic cyanobacteria in Lake Kinneret, Israel. Freshw Biol 57(6):1214–1227

Hambright KD, Zohary T, Easton J, Azoulay B, Fishbein T (2001) Effects of zooplankton grazing and nutrients on the bloom-forming, N_2-fixing cyanobacterium *Aphanizomenon* in Lake Kinneret. J Plankton Res 23:165–174

Havens KE (2008) Cyanobacteria blooms: effects on aquatic ecosystems. In: Hudnell HK (ed) Cyanobacterial harmful algal blooms: state of the science and research needs. Springer, Berlin, pp 743–748

Junier P, Witzel K, Hadas O (2007) Genetic diversity of cyanobacterial communities in Lake Kinneret (Israel) using 16s rRNA gene, *psbA* and *ntcA* sequence analyses. Aquat Microb Ecol 49(3):233–241. doi:10.3354/ame01161

Kaplan A, Volokita M, Zenvirth D, Reinhold L (1984) An essential role for sodium in the bicarbonate transporting system of the cyanobacterium *Anabaena variabilis*. FEBS Lett 176(1):166–168

Kaplan A, Harel M, Kaplan-Levy RN, Hadas O, Sukenik A and Dittmann E (2012) The languages spoken in the water body (or the biological role of cyanobacterial toxins). Front Microbiol 3:138. doi:10.3389/fmicb.2012.00138

Leão PN, Vasconcelos MTSD, Vasconcelos VM (2009) Allelopathy in freshwater cyanobacteria. Crit Rev Microbiol 35(4):271–282. doi:10.3109/10408410902823705

Malinsky-Rushansky N, Berman T, Berner T, Yacobi YZ, Dubinsky Z (2002) Physiological characteristics of picophytoplankton, isolated from Lake Kinneret: responses to light and temperature. J Plankton Res 24(11):1173–1183. doi:10.1093/plankt/24.11.1173

Masseret E, Sukenik A (2008) Amplified rDNA restriction analysis (ARDRA) for monitoring of potentially toxic cyanobacteria in water samples. Israel J Plant Sci 56:75–82

Mehnert G, Leunert F, Cires S, Johnk KD, Rucker J, Nixdorf B, Wiedner C (2010) Competitiveness of invasive and native cyanobacteria from temperate freshwaters under various light and temperature conditions. J Plankton Res 32(7):1009–1021. doi:10.1093/plankt/fbq033

Padisák J (1997) *Cylindrospermopsis raciborskii* (woloszynska) seenayya et subba raju, an expanding, highly adaptive cyanobacterium: worldwide distribution and review of its ecology. Arch Hydrobiol 107:563–593

Padisak J, Reynolds CS (1998) Selection of phytoplankton associations in Lake Balaton, Hungary, in response to eutrophication and restoration measures, with special reference to the cyanoprokaryotes. Hydrobiologia 384:41–53

Pollingher U (1978) Annual pattern of algal succession. In: Serruya C (ed) Lake kinneret, vol 32. Monographiae Biologicae. Junk, Hague, pp 243–246

Pollingher U, Kimor B (1970) Seasonal and bathymetric changes in the composition of the phytoplankton population of lake tiberias based on biomass estimations during the years 1964–1967. Sea Fisheries Research Station Bulletin No. 55. Sea Fisheries Research Station, Haifa

Pollingher U, Hadas O, Yacobi YZ, Zohary T, Berman T (1998) *Aphanizomenon ovalisporum* (forti) in lake kinneret, Israel. J Plankton Res 20:1321–1339

Prepas EE, Kotak BG, Campbell LM, Evans JC, Hrudey SE, Holmes CF (1997) Accumulation and elimination of cyanobacterial hepatotoxins by the freshwater clam *Anodonta grandis* simpsoniana. Can J Fish Aquat Sci 54(1):41–46

Ramm J, Lupu A, Hadas O, Ballot A, Rücker J, Wiedner C, Sukenik A (2012) A CARD-FISH protocol for the identification and enumeration of cyanobacterial akinetes in lake sediments. FEMS Microbiol Ecol 82:23–36

Salmaso N, Buzzi F, Garibaldi L, Morabito G, Simona M. (2012). Effects of nutrient availability and temperature on phytoplankton development: a case study from the large lakes south of the Alps. Aquat Sci 74:555–570

Schatz D, Eshkol R, Kaplan A, Hadas O, Sukenik A (2000) Molecular monitoring of toxic cyanobacteria. Adv Limnol 55:45–54

Schatz D, Keren Y, Hadas O, Carmeli S, Sukenik A, Kaplan A (2005) Ecological implications of the emergence of non-toxic subcultures from toxic *Microcystis* strains. Environ Microbiol 7(6):798–805

Schindler DW (2006) Recent advances in the understanding and management of eutrophication. Limnol Oceanogr 51:356–363

Schindler DW, Hecky RE, Findlay DL, Stainton MP, Parker BR, Paterson MJ, Beaty KG, Lyng M, Kasian SEM (2008) Eutrophication of lakes cannot be controlled by reducing nitrogen input: results of a 37-year whole-ecosystem experiment. Proc Natl Acad Sci U S A 105(32):11254–11258. doi:10.1073/pnas.0805108105

Smith VH (1983) Low nitrogen to phosphorus ratios favor dominance by blue-green algae in lake phytoplankton. Science 221(4611):669–671

Sukenik A, Eshkol R, Livne A, Hadas A, Rom M, Tchernov D, Vardi A, Kaplan A (2002) Inhibition of growth and photosynthesis of the dinoflagellate *Peridinium gatunense* by *Microcystis* sp. (cyanobacteria): a novel allelopathic mechanism. Limnol Oceanogr 47(6):1656–1663

Sukenik A, Stojkovic S, Malinsky-Rushansky N, Viner-Motzini Y, Beardall J (2009a) Fluorescence approaches reveal variations in cellular composition during formation of akinetes in the cyanobacterium *Aphanizomenon ovalisporum*. Eur J Phycol 44:309–317

Sukenik A, Zohary T, Padisák J (2009b) Cyanoprokaryota and other prokaryotic algae. In: Likens GE (ed) Encyclopedia of inland waters, vol 1. Elsevier, Oxford, pp 138–148

Sukenik A, Gal G, Hadas O (2011) Life cycle of Nostocales—an intrinsic dynamic component essential to predict cyanobacterial blooms in lakes and reservoirs. Final report submitted to Israel Ministry of Science, Technology & Sport. BMBF/MOST program German—Israeli cooperation in water technology research

Sukenik A, Hadas O, Kaplan A, Quesada A (2012a) Invasion of Nostocales (cyanobacteria) to subtropical and temperate freshwater lakes? Physiological, regional and global driving forces. Front Microbiol 3:86. doi:10.3389/fmicb.2012.00086

Sukenik A, Kaplan-Levy RN, Welch JM, Post AF (2012b) Massive multiplication of genome and ribosomes in dormant cells (akinetes) of *Aphanizomenon ovalisporum* (cyanobacteria). ISME J 6:670–679. doi:610.1038/ismej.2011.1128

Vardi A, Schatz D, Beeri K, Motro U, Sukenik A, Levine A, Kaplan A (2002) Dinoflagellate-cyanobacterium communication may determine the composition of phytoplankton assemblage in a mesotrophic lake. Curr Biol 12(20):1767–1772

Vidal L, Kruk C (2008) *Cylindrospermopsis raciborskii* (cyanobacteria) extends its distribution to latitude 34°53′S: taxonomical and ecological features in Uruguayan eutrophic lakes. Pan-Am J Aquat Sci 3(2):142–151

Wiedner C, Rücker J, Brüggemann R, Nixdorf B (2007) Climate change affects timing and size of populations of an invasive cyanobacterium in temperate regions. Oecologia 152:473–484

Chapter 13
Metazoan Zooplankton

Gideon Gal and K David Hambright

Abstract The Lake Kinneret metazoan zooplankton has been monitored since 1969 and currently includes the enumeration of 31 species of cyclopoids, cladocerans, and rotifers in samples collected fortnightly at five stations from around the lake. The zooplankton community has exhibited notable interannual and long-term variation since the start of the monitoring program that have included a decline in community size from the 1970s and 1980s to an extended period of low abundance and biomass in the 1990s followed by an increase during the first decade of the millennium. Along with the increase in abundances since the late 1990s, there has been an increase in interannual variation, which may be related to the unstable phytoplankton population and/or to the large changes in lake level. The introduction of an additional sampling protocol since 2003 has highlighted the highly vertically aggregated nature of some of the rotifer species often found in very high densities near the thermocline. Seasonally, the lowest densities are found during the summer and the highest during the winter–spring. There is no indication of vertical migration by zooplankton in the lake. The zooplankton are patchily distributed and repeated sampling indicates that abundance estimates collected over a period of a year could vary by a factor 2–3 just due to fine-scale patchiness. Zooplankton in the lake play an important role as key nutrient recyclers with microzooplankton accounting for >85 % of the daily mineralization of P and N in the lake.

Keywords Grazing · Herbivorous · Predatory · Vertical migration · Nutrient recycling

G. Gal (✉)
The Yigal Allon Kinneret Limnological Laboratory, Israel Oceanographic & Limnological Research, P.O. Box 447, 14950 Migdal, Israel
e-mail: gal@ocean.org.il

K D. Hambright
Department of Biology, University of Oklahoma, 730 Van Vleet Oval, 304 Sutton Hall, 73019 Norman, OK, USA
e-mail: dhambright@ou.edu

T. Zohary et al. (eds.), *Lake Kinneret, Ecology and Management,* Aquatic Ecology Series 6,
DOI 10.1007/978-94-017-8944-8_13,

13.1 Taxonomic Background

The Lake Kinneret metazoan zooplankton (zooplankton hereafter) species can be divided taxonomically into three major groups: two orders representing the subphylum Crustacea (Copepoda, Cladocera) and the class Monogonata representing the phylum Rotifera. The copepods have been represented in the past by up to 6 species (Gophen and Azoulay 2002), the cladocerans by 8 species, and the number of rotifer species has been reported to range between 10 and 35 (Gophen 2005). Currently, 2 cyclopid species, 8 cladoceran species, and 21 rotifer species are routinely collected as part of the ongoing lake monitoring program (Chap. 32). Zooplankton can also be separated according to two basic functional groups: predators (adult copepods, some rotifers) and grazers. The grazers can be further divided into macro-grazers (cladocerans and juvenile copepods) and micro-grazers (mostly rotifers and copepod nauplii). Note that protozoan zooplankton, i.e., ciliates and flagellates, are excluded from the microzooplankton in this chapter due to a lack of long-term information. Nevertheless, ciliates and flagellates are covered elsewhere (Chap. 14).

Table 13.1 lists the species routinely monitored and their groupings according to functional group.

Sampling The ongoing monitoring of zooplankton in the lake is based on two sampling approaches. The first approach, termed "mix sampling," has undergone only minor changes since the initiation of the monitoring program in 1969 to date, i.e., more than 42 years of a near-consistent sampling protocol, while the second, "profile sampling," was started in 2003. The mix sampling is conducted at five fixed pelagic stations (A, D, G, H, K, see locations in Fig. 32.1, Chap. 32). At each station, 1 L of water is collected using a 5-L Rodhe sampler from each of up to 12 depths, the water samples from the different depths are mixed in a bucket from which 0.8 L is extracted and preserved. Until 2003, all samples were treated, fixed, and preserved in formaldehyde. Since then, however, samples collected are stored on board in sodium bicarbonate-citric acid, transferred at the laboratory to formaldehyde, for fixing, for 24–48 h, and then transferred to 70 % ethanol + 1 % glycerin for preserving.

The mix sampling provides a good overall picture of the zooplankton assemblage but suffers from two main shortcomings. The first is the lack of information on the vertical distribution of the organisms and, the second, is the relative large error associated with species that are either rare or highly aggregated at a certain depth. The small volume of water sampled and analyzed increases the probability of error associated with abundance estimates of rarer species. In order to address these shortcomings, the profile sampling protocol was initiated in 2003 (Hambright and Gal 2004). According to the profile sampling protocol, samples are collected from up to nine depths during the non-stratified periods (1, 3, 5, 7, 10, 15, 20, 25, 33 m). During the stratified periods, samples are collected down to the thermocline with additional samples being collected at 1 m above, within, and 1 m below the thermocline, as with the mix sampling. Moreover, these samples are collected using a 10-L sampler, in which the entire 10 L are filtered through a 63-µm-mesh net, thus reduc-

Table 13.1 List of zooplankton categories (species and life stages or relative size) monitored routinely as part of the Kinneret monitoring program, and associated functional group: predatory (P), and grazers which are separated into macrozooplankton grazers (Ma) and microzooplankton grazers (Mi). Also provided is a list of the mean lengths (and SD) of copepod and cladoceran species based on measurements conducted since 2007 using the Planktometrix software. (Hambright 2008)

Species-developmental stage	Taxonomic grouping	Functional group	Mean length (μm)	SD	Sample size
Cyclops sp. NI–NVI	Copepoda	Mi	145.8	38.6	123,914
Mesocyclops ogunnus CI	Copepoda	Ma	272.1	29.0	8,013
Mesocyclops ogunnus CII	Copepoda	Ma	316.1	17.2	6,108
Mesocyclops ogunnus CIII	Copepoda	Ma	366.8	25.2	9,147
Mesocyclops ogunnus CIV	Copepoda	Ma	447.6	33.7	9,395
Mesocyclops ogunnus CV-male	Copepoda	P	475.3	34.6	667
Mesocyclops ogunnus CV-female	Copepoda	P	565.0	52.0	6,304
Mesocyclops ogunnus CVI-male	Copepoda	P	545.0	48.7	4,547
Mesocyclops ogunnus CVI-female	Copepoda	P	723.9	78.5	2,762
Mesocyclops ogunnus CVI-female with eggs	Copepoda	P	752.8	96.9	321
Thermocyclops dybowski CI	Copepoda	Ma	268.5	26.6	6,694
Thermocyclops dybowski CII	Copepoda	Ma	313.8	17.0	4,057
Thermocyclops dybowski CIII	Copepoda	Ma	364.9	23.5	7,564
Thermocyclops dybowski CIV	Copepoda	Ma	434.2	32.7	6,809
Thermocyclops dybowski CV-male	Copepoda	P	447.2	29.1	2,623
Thermocyclops dybowski CV-female	Copepoda	P	494.2	42.7	2,284
Thermocyclops dybowski CVI-male	Copepoda	P	498.4	34.5	4,591
Thermocyclops dybowski CVI-female	Copepoda	P	571.2	46.8	4,308
Thermocyclops dybowski CVI-female with eggs	Copepoda	P	567.6	40.6	851
Diaphanosoma brachyurum-small	Cladocera	Ma	331.7	58.9	1,593
Diaphanosoma brachyurum-large	Cladocera	Ma	602.3	135.6	5,585
Bosmina longirostris typica-small	Cladocera	Ma	251.5	28.7	5,007
Bosmina longirostris typica-large	Cladocera	Ma	338.3	40.0	3,642
Bosmina longirostris cornuta-small	Cladocera	Ma	262.7	29.8	369

Table 13.1 (continued)

Species-developmental stage	Taxonomic grouping	Functional group	Mean length (μm)	SD	Sample size
Bosmina longirostris cornuta-large	Cladocera	Ma	350.8	38.5	2,662
Ceriodaphnia reticulata-small	Cladocera	Ma	260.3	34.2	5,130
Ceriodaphnia reticulata-large	Cladocera	Ma	373.4	57.3	8,216
Ceriodaphnia rigaudi-small	Cladocera	Ma	253.4	26.1	1,296
Ceriodaphnia rigaudi-large	Cladocera	Ma	386.9	62.4	3,578
Ceriodaphnia pulchella-large	Cladocera	Ma	145.0	239.6	3
Chydorus sphaericus-small	Cladocera	Ma	219.8	18.0	538
Chydorus sphaericus-large	Cladocera	Ma	293.0	36.3	996
Moina rectirostris-small	Cladocera	Ma	339.1	45.7	191
Moina rectirostris-large	Cladocera	Ma	536.7	99.5	656
Asplanchna brightwelli	Rotifera	P	–	–	–
Asplanchna priodonta	Rotifera	P	–	–	–
Synchaeta oblong	Rotifera	Mi	–	–	–
Synchaeta pectinata	Rotifera	Mi	–	–	–
Polyarthra remata	Rotifera	Mi	–	–	–
Hexarthra sp	Rotifera	Mi	–	–	–
Brachionus sp1	Rotifera	Mi	–	–	–
Trichocerca stylata	Rotifera	Mi	–	–	–
Collotheca sp.	Rotifera	Mi	–	–	–
Anuraeopsis fissa	Rotifera	Mi	–	–	–

NI–NVI represent nauplii stages 1–6 and CI–CVI represent copepodid stages 1–6
P predatory, *Ma* macrozooplankton grazers, *Mi* microzooplankton grazers, *SD* standard deviation

ing the error associated with rarer species. Species-specific densities typically range from tens and up to hundreds of individuals per liter. Furthermore, most, or even the entire sample is counted, reducing error even further, especially for the rare species in the sample. Nevertheless, species occurring at densities of 1–2 individuals per 10 L or less are likely to be underrepresented, resulting in a bias in our description of the species assemblage but having no effect on zooplankton biomass estimates.

Zooplankton enumeration and biomass estimation on both "mix" and "profile" samples are conducted as described by Gophen (2005) and by Gal and Anderson (2010). Since the start of the profile sampling in 2003, only station A mix samples have been analyzed routinely. Zooplankton biomass is estimated based on the application of species-specific conversion factors to wet weight (Gophen 1978; Gophen 2005).

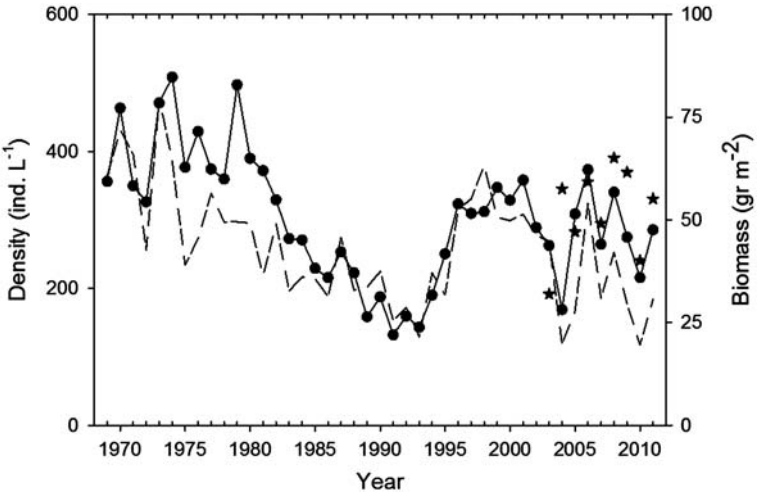

Fig. 13.1 Long-term record of annual mean total zooplankton biomass (*dashed line*) and density based on mix (*black circles, solid line,* 1969–2011) and profile (*stars,* 2003–2011) sampling from station A

13.2 Temporal Dynamics: Interannual Patterns

The Lake Kinneret zooplankton have exhibited large interannual variation since 1969 (Gophen 2003; Hambright 2008; Gal and Anderson 2010), and the total zooplankton density can be divided into three distinct periods (Fig. 13.1). Total densities were stable through to 1980 with mean annual values ranging between 326 and 508 ind. L^{-1} and a multiannual mean of 408 ind. L^{-1}. Between 1980 and 1993, there was a marked decrease in zooplankton density in the lake reaching a minimum of 132 ind. L^{-1} in 1991. Since 1996, however, the zooplankton have maintained a relatively moderate mean density (295 ind. L^{-1}) with a high degree of variability with >2× difference between the minimum (2004) and maximum (2006) mean annual values. The wet weight biomass dynamics largely mirrors the changes in abundances except for the period 1975–1982, during which the biomass did not demonstrate a period of elevated values. As the biomass is not directly measured as part of the monitoring program but rather estimated via constant species-specific conversion factors, we predominantly use abundance in the remainder of this chapter. Further information on the relative changes in biomass and density during 1970–2002 can be found in Hambright (2008).

The long-term dynamics in the zooplankton density was accompanied by changes to the relative contribution of the various groups (Fig. 13.2). Copepod contribution to the total zooplankton abundance declined from a mean value of 61% (1969–1979) to 55% during 1980–1999 and has maintained a similar level over the past 6 years (2006–2011). During 2001–2003, copepod contribution was at the highest level since 1969 (71–74% of total abundance); however, these values were

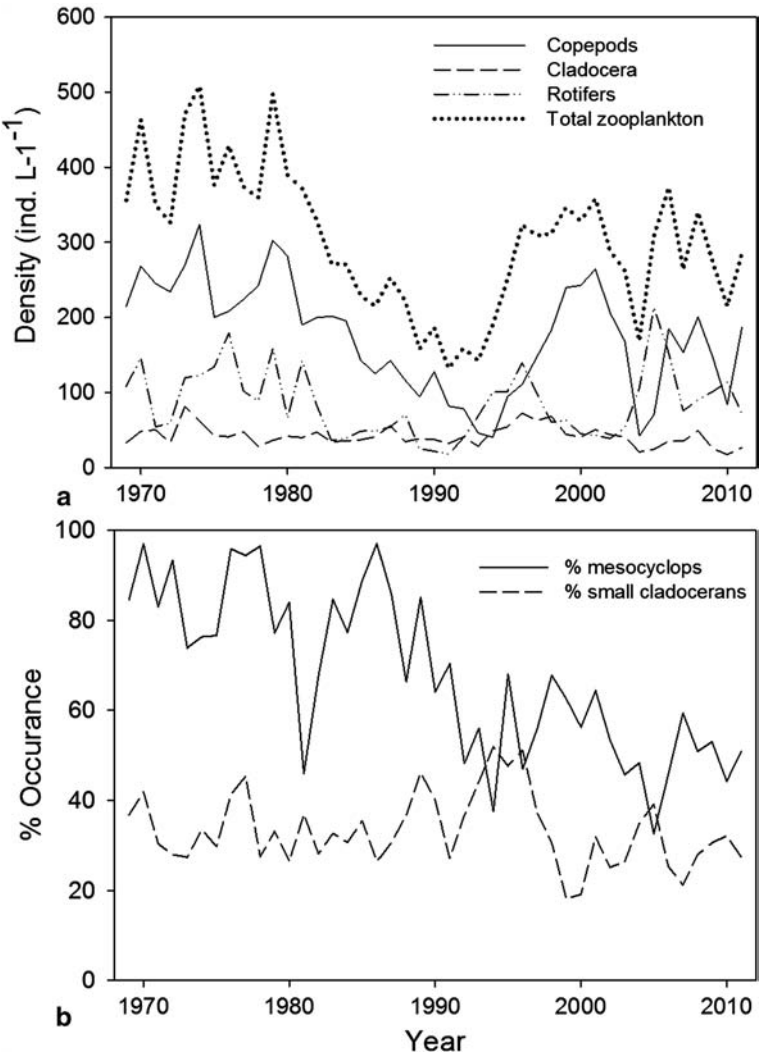

Fig. 13.2 **a** The annual mean contribution of the three taxonomic groups to total zooplankton density for the period 1969–2011 based on the mix sampling. **b** The annual mean proportion of adult *M. ogunnus* of the total copepod adult density (*solid line*) and of small cladoceran species to total cladocerans (*dashed line*)

followed by the lowest ever (23–25 %) during 2004–2005. These values followed a regime shift that occurred in the copepod population resulting in a significant change to the population characteristics (Gal and Anderson 2010). According to Gal and Anderson (2010), using tools taken from the world of statistics and econometrics, the copepod population shifted, with high probability, to a different regime in 1993 indicated by the major decline in predatory zooplankton in the lake. This observation is in line with additional reports of changes that occurred to the ecosystem

during that period. For example, Roelke et al. (2007) reported the phytoplankton changes in the lake during the mid-1990s as a shift to an alternate state and Zohary (2004) described the large shift away from a very stable and predictable phytoplankton succession pattern to one characterized by large variations in composition and biomass.

Long-term changes in zooplankton species composition, biomass, and other parameters have often been linked to changes in fish predation pressure on the zooplankton (Brooks and Dodson 1965; Carpenter et al. 1987; Galbraith Jr 1967). Body size has frequently been used as an indicator of changes in predation pressure (Mills et al. 1987) and it is therefore insightful to examine long-term changes in density or biomass in the context of composition and body size. And indeed, the decrease in zooplankton abundance and biomass from 1980 to 1993 has been linked to intensified fish predation pressure which led to a decrease in the relative contribution of the larger species and the overall biomass (Hambright 2008). During the period 1980–1999, the copepod contribution to the total zooplankton biomass declined to a mean of 29 % from a mean of 35 % (1969–1975), but has increased since 2006 and averaged 45 % over the past 6 years (2006–2011).

Gophen (1978) reported that during 1969–1975, 90 % of the total copepod biomass consisted of *Mesocyclops ogunnus,* the large body size species. It is therefore interesting to note the consistent decrease in contribution of *M. ogunnus* adults to the total adult cyclopoid population, while the contribution of the smaller species, *Thermocyclops dybowski* increased (Fig. 13.2b, see also, Hambright 2008). The decline of the contribution of the large species was evident even during the period of moderate levels of abundance of zooplankton between 1996 and 2001 reaching a mean value below 50 % in recent years (2006–2011). The lowest value was found in 2005 during which copepods contributed on average only 33 % of the total zooplankton density.

The decrease in copepod contribution to the total zooplankton density has been linked to an extreme increase in the bleak (*Mirogrex terraesanctae*) population resulting in excessive predation pressure on the predatory and herbivorous zooplankton (Gal and Anderson 2010; Ostrovsky and Walline 2000; Zohary and Ostrovsky 2011). Alternatively, Hambright (2008) argues that overharvest of the bleak population resulted in a decrease in mean bleak body sizes (see Hambright and Shapiro 1997), which through allometric scaling of body size and metabolism, resulted in an increase in predation pressure on zooplankton. While both hypotheses have support in the form of indirect evidence, they remain untested and confounded by possible roles of resource availability and competition. Nevertheless, there is little evidence pointing to changes in the resources as a possible explanation for the changes in the zooplankton community. While large changes to the phytoplankton community in the lake have occurred since the mid-1990s (Chap. 10.1), a large portion of the phytoplankton biomass in the lake remain inedible for herbivorous zooplankton (Zohary 2004; Hambright et al. 2007).

The relative annual contribution of small species to the total cladoceran assemblage also changed over time with a marked shift in the interannual variation prior to, and following, 1995 (Fig. 13.2b, see also Hambright 2008). Through to 1995,

the relative mean (standard deviation, SD) contribution of the small cladoceran *Bosmina longirostris* was 35% (22%) with a coefficient of variation (CV) of 63%. Following a large increase during 1994–1996, the contribution of this species decreased to a lower mean level of 31% but with larger variations and a resulting CV of 78%. The larger variation since the mid-1990s was also reflected in the total cladoceran abundance (Fig. 13.2a). Peak annual mean cladoceran abundance occurred in 1996 (72.5 ind. L^{-1}) declining to minimum values in 2004 (20.9 ind. L^{-1}) and 2010 (17.3 ind. L^{-1}). Mean annual rotifer contribution to the total zooplankton biomass, for the period 1969–2011, was 9%, up from the previously reported 7% (Gophen 1978), though the mean annual values ranged between 2 and 23%, with peak values occurring during periods of low adult copepod density (Fig. 13.3).

The observed temporal pattern reflected in the profile-based sampling coincides with the trend observed in the mix sampling (Fig. 13.1). Throughout the 9 years of profile sampling, with the exception of only 1 year (2004), there is an overlap in the trends seen in the two sampling protocols. However, in most cases, the profile sampling provides higher estimates of zooplankton density than mix sample-based estimates. This is expected, in part, due to the improved representation of species that tend to congregate at confined depths like rotifers (see below) and rare species. Indeed there is a consistent difference between the two methods which tends to relate to species composition and distribution. Therefore, on dates during which there are large congregations of certain species such as the rotifer *Anuraeopsis fissa* that occurs along the thermocline in extreme densities (thousands per liter) during the fall, there will be large differences between the two methods. In addition, the sampling of a larger volume of water (10 L at each depth vs. 1 L for all depths) reduces some of the effect of variability in the water column (see Sect. 13.4).

Separation of the zooplankton into functional groups can provide additional insight into the assemblage from a food-web perspective. The predatory zooplankton, composed of the adult stages of the two cyclopoid species in the lake, have varied between 8 and 38 ind. L^{-1} with a mean annual value of 21 ind. L^{-1} (Fig. 13.3a). The herbivores, comprised of the cladoceran species and copepodid stages of the cyclopoids, varied in density between 31 and 117 ind. L^{-1} while the mean annual density was 78 ind. L^{-1}. The microzooplankton, consisting of the majority of the rotifers along with the naupliar stages of the cyclopoids, exhibited large variation with densities ranging between 56 and 365 ind. L^{-1}, with a mean annual density over the 43 years, of 190 ind. L^{-1}. Part of the large variation in abundances can be linked to the dramatic decline in predatory zooplankton and the shift from a stable *Peridinium*-dominated phytoplankton community to an unstable cyanobacteria-abundant community that occurred during the mid-1990s (see Chap. 10.1, Gal and Anderson 2010; Zohary 2004) which may have affected some of the foodweb interactions. For example, from 1969 through to the mid-1990s, there was a positive correlation ($r = 0.53$) between the copepods and rotifer densities, but from the mid-1990s through to 2011 the correlation was negative ($r = -0.67$, Fig. 13.2). The negative correlation suggests predator–prey interactions between the copepods and rotifers. This may be an outcome of the decreasing contribution of the relatively large adult *M. ogunnus* to the total adult cyclopoid assemblage.

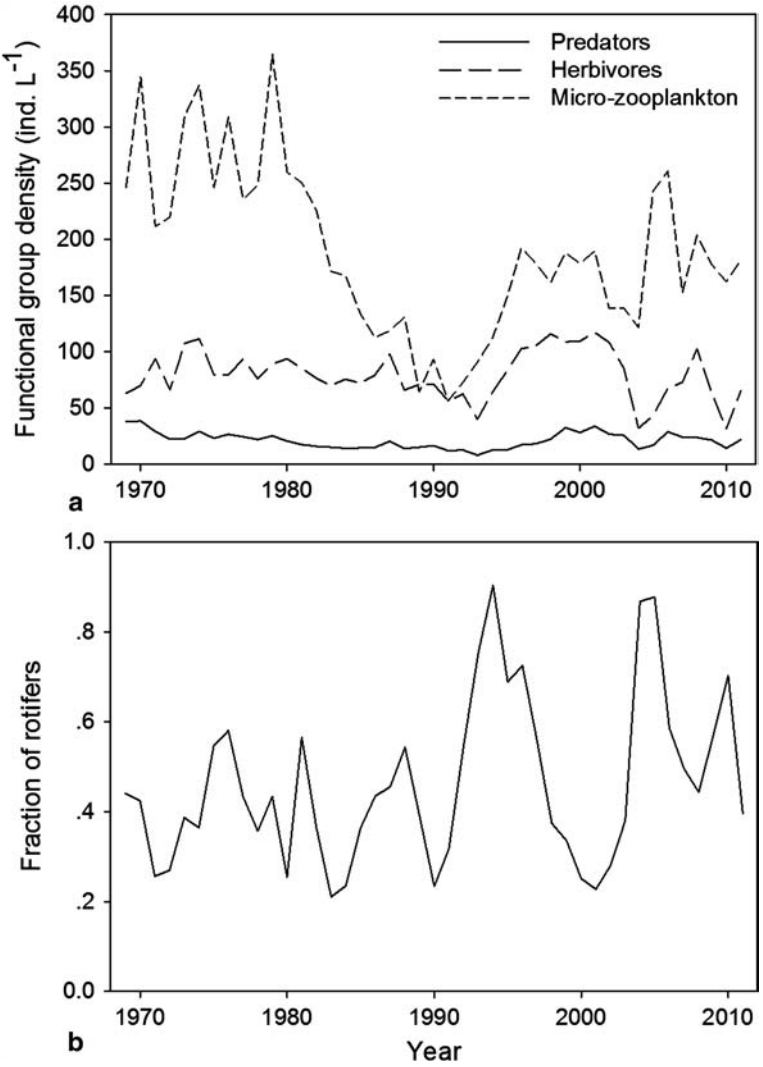

Fig. 13.3 The annual mean contribution of the three functional groups for the period 1969–2011 based on the mix sampling (**a**) and the annual mean relative portion of rotifers of the total micro-zooplankton (rotifers + nauplii) group (**b**)

13.3 Temporal Dynamics: Seasonal Patterns

There are seasonal differences in the distribution of the three taxonomic groups of zooplankton in the lake. Gophen (1978) reported that there was little seasonal variation in the copepod biomass but that cladoceran and rotifer biomass peaked during the winter–spring and was lowest during the summer. Gophen (2005) further

reported that rotifer biomass was typically at its highest during spring (April–May) and was lowest between July and December, with intermediate values in the winter (January–March). The results of the profile sampling conducted between 2003 and 2011 indicate a large degree of variation across the various months for all three groups. While the variation hinders detection of any statistically significant seasonal patterns, it is possible to visually identify a number of trends emerging from the data (Fig. 13.4). The copepod abundance reflected trends of higher values during the winter–spring decreasing toward the summer and intermediate values during the fall. Indeed, during the first half of the year (January–June) the copepod abundance was significantly higher than in the second half of the year ($p<0.05$, $n=53$, Mann–Whitney U test). The summer months were also characterized by larger variability than the other months. The cladocerans exhibited a smaller degree of variability with a similar trend, and though not as predominant, of lower values during the summer. The rotifers also exhibited large variations, but there was a clear trend of significantly ($p<0.001$, $n=53$, Mann–Whitney U test) higher abundances during January–June with the lowest values occurring during August–November.

13.4 Temporal Dynamics: Fine-Scale Patterns

One of the main characteristic traits of zooplankton communities is their patchy distribution over a wide range of spatial scales (Haury et al. 1978; Pinel-Alloul et al. 1988). Patchy distributions greatly affect the required sampling resources and as a consequence will have implications on the results and conclusions. Only limited information on the patchy distribution of zooplankton in the lake has been reported. Pinel-Alloul et al. (2004) reported variability ranging between 16 and 63 % between triplicates of samples collected at a number of depths on one occasion. Kalikhman et al. (1992) detailed spatial relationships between fish, zooplankton, and abiotic conditions, on a single date, and linked the variability in zooplankton spatial distribution to fish predation pressure. They showed high zooplankton biomass at the center and southeast part of the lake and low biomass in the western and northern parts.

In order to provide additional information on the fine-scale patchiness in the zooplankton distribution in the lake, we conducted a “patchiness study” in which we collected a series of repeated samples over 9 months (Gal and Easton, unpublished data). The sampling included five replicate samples of 10 L collected, from a depth of 5 m at station A, 11 times over a period from March to December 2004. The replicates were collected within minutes of each other between 9:00–10:00 on the day of sampling. Samples were collected using the protocol for “profile” sampling (see above). In the laboratory, the entire sample was counted when possible. Subsampling was used when samples included large quantities of phytoplankton. Samples were enumerated under a dissecting scope and organisms were grouped into four gross taxonomic categories: nauplii, copepods, cladocerans, and rotifers.

Results of the analysis indicate the existence of a large variation in zooplankton density estimates between the replicate samples. There was no relation between

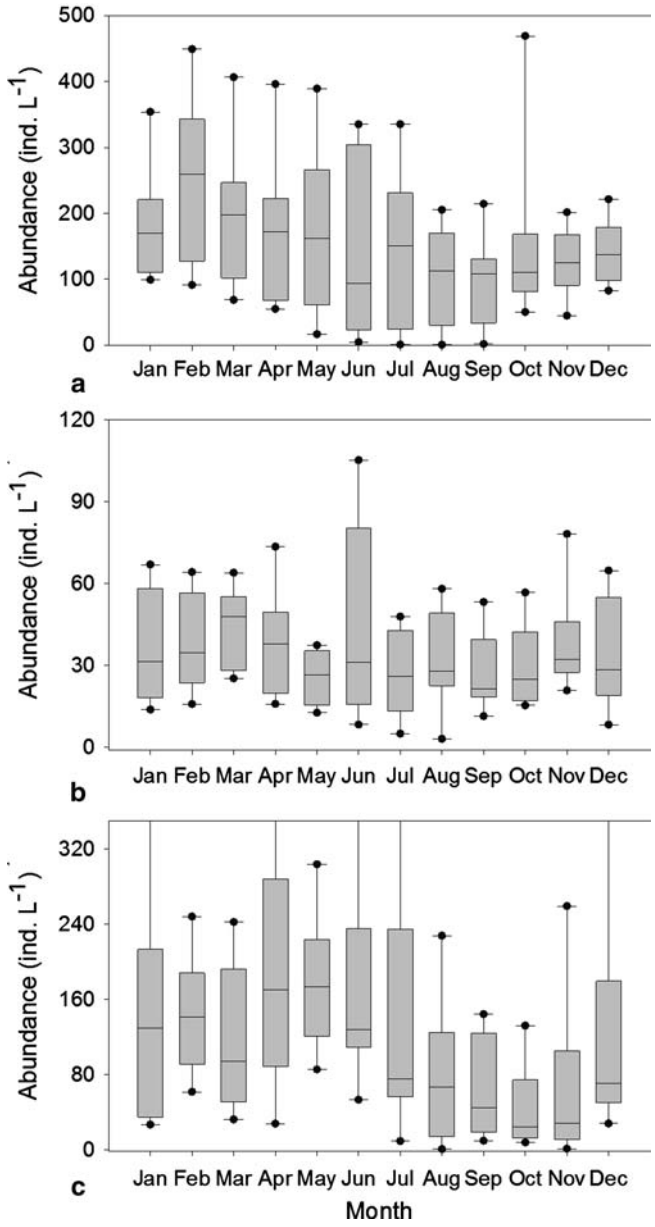

Fig. 13.4 Box plot presentation of monthly abundances of copepods (**a**), cladocerans (**b**), and rotifers (**c**) over a 9-year period (2003–2011) based on profile sampling

the number of individuals counted and the variability. For example, the differences between the standard deviations for samples collected on March 30 and December 21 were small, while the average density on March 30 was lower by nearly an order of magnitude than the density on December 21. For densities of each separate taxonomic group (copepods, cladocera, and rotifers), and the total zooplankton density, we examined the differences between replicates, on a given date, by calculating the coefficient of variation (CV, Fig. 13.5) and also the ratio between the highest and lowest densities over the five replicates. Finally, for each group, we determined the range of ratios (highest to lowest densities per date) found over the entire year (Table 13.2) thus providing a range of error associated with the density estimates. The rotifers, and then cladocerans, displayed the largest differences between the minimum and maximum density over the five replicates. The mean variation over all samples ranged between 1.9 (total zooplankton density) and 3.3 (rotifers) suggesting that abundance estimates collected over a period of a year could vary by a factor of 2–3 just due to fine-scale patchiness. CV values were relatively high for all groups but especially for rotifers, where the values approached 80 on two occasions and values of approximately 40 (37–45) on six additional sampling dates. The calculated CV values did not differ greatly, however, among the other groups.

The relatively large variation in density estimates, especially for rotifers, between samples collected over a short period of time highlight the difficulty in accurately estimating zooplankton abundance for a given date based on a single sample. As a consequence, conclusions should not be drawn based on a single date or limited number of sampling dates. The fine-scale variation also limits our ability to fully understand the interactions between zooplankton and phytoplankton at fine scales. Given the fine-scale variability, trends over extended periods of time should be examined in order to study changes to zooplankton in the lake and efforts should be made to introduce replicate sampling thereby increasing certainty in the estimated abundances.

13.5 Spatial Dynamics: Vertical Patterns

To date, only a limited number of studies have reported on the vertical distribution of zooplankton in the lake and have focused on either one specific date (Easton and Gophen 2003; Pinel-Alloul et al. 2004) or a limited number of seasonal cycles (Gophen 1978). While these studies have provided information on the vertical distribution, they have at times missed significant characteristics that may result in a bias against species with high densities at specific depths. The samples collected since 2003, as part of the profile sampling, generally reinforce the seasonal and taxonomic specific distributions previously reported (Gophen 1978). Nevertheless, results of the profile sampling, conducted since 2003 (Fig. 13.6), provided additional information, supporting the continued need for the profile sampling protocol.

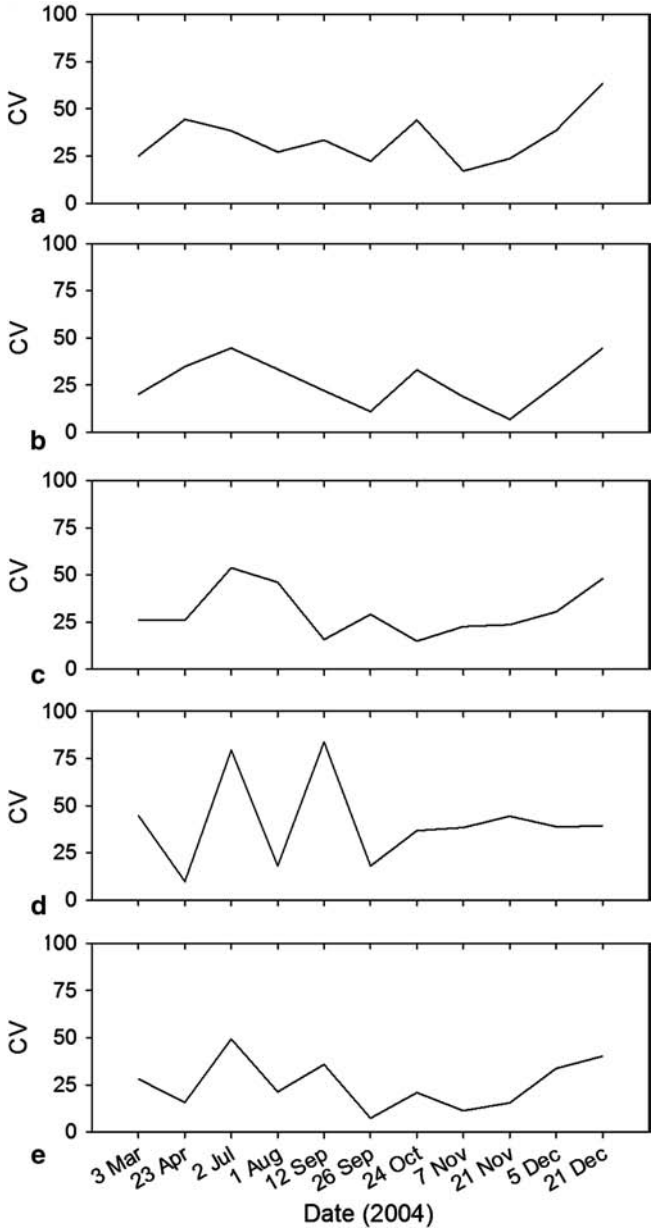

Fig. 13.5 The calculated CV values for each sampling date in 2004 for **a** Nauplii, **b** copepods, **c** cladocerans, **d** rotifers, and e total zooplankton. (Data based on the patchiness study)

Table 13.2 The minimum and maximum values of the *ratio* between the highest and lowest density estimates for a given sampling date, per group, over the entire sampling period and the range of CV values found over the course of the year. (Data collected as part of the patchiness study conducted March–December 2004; see text)

Group	Minimum	Maximum	Min–Max CV
Nauplii	1.4	4.1	17.1–63.5
Copepods	1.2	4.3	6.8–44.7
Cladocerans	1.4	5.7	14.9–53.8
Rotifers	1.2	12.8	9.8–83.8
Total density	1.2	4.1	7.3–49.4

CV coefficient of variation

There were seasonal differences in the vertical distribution of zooplankton in the lake with noticeable variation in the densities, especially in the rotifer distribution. During the winter–early spring, prior to the onset of stratification, the zooplankton were distributed relatively homogenously over the water column with the exception of the top 1 m which exhibited lower densities and a deep peak in rotifers found at the top of the thermocline in 2006. With the onset of stratification in the spring, however, we found larger portions of the assemblage concentrated at approximately 5-m depth (cladocera and Rotifera) with a slightly deeper peak in the copepod distribution which coincided with the lower boundary of the thermocline in 2005. The shallow rotifer peak resulted, at times, in large densities as found, for example, in April 2011 when the rotifer *Keratella cochlearis* densities ranged between 1,602 and 2,200 ind. L^{-1} at depths of 3–7 m. During the summer, the zooplankton were confined to the layer delimited by the metalimnion, with peak rotifer densities occurring, during both in 2005 and 2006, in proximity to the mid-upper metalimnion, typically at 15 m, often reaching large densities (>1,000 ind. L^{-1}). Peak values of 1,400 and 1,800 ind. L^{-1}were found, for example, on June 16 and 30, 2008, respectively, and 1,500 ind. L^{-1}on July 19, 2009. Copepods and cladocerans also exhibited a peak distribution in the metalimnion in 2005 but not in 2006 during which they exhibited shallower peaks. Indeed, Pinel-Alloul et al. (2004) similarly reported peak densities at 5 and 15 m during the summer. During the fall, with the deepening of the thermocline, but prior to overturn, we typically found a relatively homogenous distribution of copepods and cladocerans from the surface down to the thermocline. The rotifers, however, were usually found congregating near the lower boundary of the thermocline. To date, the highest rotifer density recorded was found during this period with the species *Anuraeopsis fissa* reaching a density of 7,131 ind. L^{-1} on Dec. 24, 2005 in the thermocline (depth of 24 m).

Diel vertical migration which often characterizes zooplankton in lakes with high fish predation pressure and large-bodied zooplankton has been studied, to a limited degree, in Lake Kinneret. The result, however, has been somewhat contradictory, though it is clear that no major vertical migration takes place in the lake. Gophen (1978) mentioned vertical migration and later Gophen (1979) reported that the vertical migration was predominantly by copepods and cladocerans. He linked the migration to light conditions and *Peridinium* densities with most of the migration

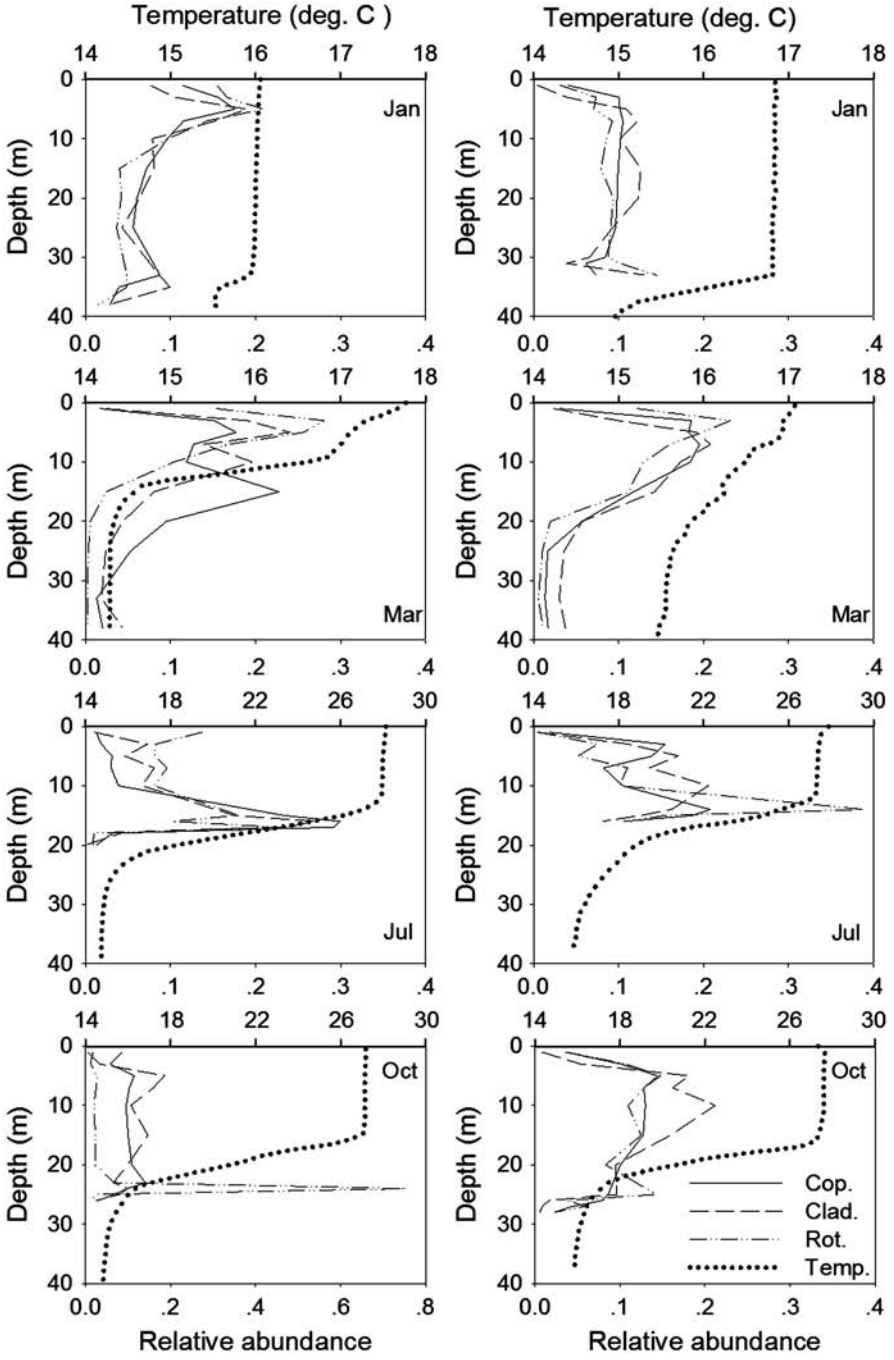

Fig. 13.6 Monthly mean relative vertical distribution (shown as fraction of group-specific density) of the three taxonomic groups, and temperature profiles, for four dates during 2005 (*left panels*) and 2006 (*right panels*) representing the distinct seasons. (Data based on profile sampling)

occurring during sunrise and sunset. More recently, Easton and Gophen (2003) reported that only limited vertical movement was observed during a 24-h study. The vertical movement exhibited by the cyclopoids, according to their observations, mimicked seiche movement. Thus, it is likely that the observed change in vertical placement is not an active form of vertical migration, but rather a passive form of movement with the water.

13.6 Grazing and Nutrient Mineralization

Crustacean zooplankton are considered not only as the main link between primary producers and upper trophic levels but also as important sources of mineralized nutrients for producers (Sterner and Elser 2002). A number of modeling studies of the Lake Kinneret ecosystem support the role of zooplankton as nutrient recyclers in the ecosystem. Based on the model they constructed of the carbon flows in the Lake Kinneret ecosystem, Stone et al. (1993) calculated that microbial grazers provided 40 and 46 % of herbivore zooplankton and copepod carbon requirements, respectively, during the spring and 36 % of the copepod demand during the summer. Furthermore, some 45 % of total bacterial production was consumed by zooplankton in the summer. In a separate model of the carbon flow in the lake, Hart et al. (2000) showed that more than 40 % of the carbon fixed by phytoplankton is grazed by zooplankton of which cladocerans accounted for 63 % of the herbivory. Microzooplankton and cladocerans proved to be the main bacteria grazers while copepods were the main microzooplankton consumers. These links result in an efficient pathway and increased utilization of bacterial productions bypassing the protozoan portion of the microbial loop. Hambright et al. (2007) experimentally tested this model and showed that mass-specific carbon ingestion rates by microzooplankton (there defined as all grazers passing through 150-µm mesh, and consisting of rotifers, nauplii, ciliates, and flagellates) were 20 times higher than ingestion rates of crustaceans, with most carbon ingested by microzooplankton in the form of bacteria. Nevertheless, microzooplankton ingestion rates on pico- and nanophytoplankton were substantially higher than crustacean ingestion rates, and more phytoplankton taxa were grazed by microzooplankton. Even when correcting for differing biomass between the two grazer groups, microzooplankton grazing inflicted up to ten times higher mortalities on both phytoplankton and bacteria than did crustaceans.

Zooplankton grazing is translated not only into carbon flow through the system but also into remineralization of nitrogen and phosphorous into biological available forms. Bruce et al. (2006), in their application of the ecosystem model DYRESM-CAEDYM, estimated that, during 1997–1998, zooplankton remineralization provided 3–46 % and 5–55 % of the P and N uptake by phytoplankton, respectively. Furthermore, they calculated that zooplankton excretion provided approximately 60 % of the total nutrient fluxes in the photic zone of the lake during stratification. The role of nutrient recycling by zooplankton has also been experimentally documented

(Hambright et al. 2007). Hambright et al. (2007) measured crustacean mineralization rates of 0.04 and 0.36 μg μgC_{zoop}^{-1} day^{-1} of P and N, respectively, while microzooplankton rates were 2.8 μgP μgC_{zoop}^{-1} day^{-1} and 20 μgN μgC_{zoop}^{-1} day^{-1}. According to their results, the Lake Kinneret microzooplankton, with mineralization rates 55–70 times higher than crustacean rates, accounted for >85 % of the daily mineralization of P and N in the lake, with turnover rates of 0.36 and 1.1 days, respectively.

13.7 Summary

We have characterized the Lake Kinneret zooplankton on a number of temporal and spatial scales and have reported on the seasonal patterns along with a strikingly patchy distribution observed in the various zooplankton taxonomic groups. The zooplankton in the lake has exhibited interannual variation in abundance and biomass over the past four decades along with changes in the relative contributions of the various taxonomic groups and the larger species. Some of the changes coincided with the shifts observed in the lake ecosystem, especially since the mid-1990s, such as the changes in phytoplankton succession in the lake including the increasing dominance of cyanobacteria species and unpredictable occurrence of *Peridinium*. While the underlying processes leading to those changes are yet to be fully uncovered, the impact of abiotic changes, namely changes to lake level, on the ecosystem, in general, and on the zooplankton, in particular, have been hypothesized. Indeed, recently, a data-driven modeling study linked between the rate of change in lake level and zooplankton abundance in the lake (Gal et al. 2013). The changes have also affected the interactions between the various zooplankton taxonomic groups. This was most obvious in the relationship between the copepods and rotifers with a clear negative correlation between their abundances since the mid-1990s (Fig. 13.2). It remains unclear whether the zooplankton community is stabilizing following decades of change or if it will continue to fluctuate in reaction to the ongoing changes to the biotic and abiotic components of the ecosystem. The changes to the zooplankton community in the lake have wide implications due to their role as nutrient recyclers. Given the large differences in excretion rates between crustacean zooplankton and microzooplankton, major declines or increases in either of these groups will change the amount of nutrients available to primary producers in the lake. This in turn could potentially influence the phytoplankton assemblage in the lake.

Acknowledgments The authors acknowledge the dedication and efforts of the current and past zooplankton technicians, especially Sara Chava and Bonnie Azoluay who spent endless hours carefully analyzing the thousands of zooplankton samples collected from the lake since 1969. We also thank James Easton who contributed to the patchiness work described in this chapter.

References

Brooks JL, Dodson SI (1965) Predation, body size, and composition of plankton. Science 150:28–35

Bruce LC, Hamilton D, Imberger J, Gal G, Gophen M, Zohary T, Hambright KD (2006) A numerical simulation of the role of zooplankton in C, N and P cycling in Lake Kinneret, Israel. Ecol Model 193:412–436

Carpenter SR, Kitchell JF, Hodgson JR, Cochran PA, Elser JJ, Elser MM, Lodge DM, Kretchemer D, He X (1987) Regulation of lake primary productivity by food web structure. Ecology 68(6):1863–1876

Easton J, Gophen M (2003) Diel variation in the vertical distribution of fish and plankton in Lake Kinneret: a 24-h study of ecological overlap. Hydrobiologia 491(1–3):91–100

Gal G, Anderson W (2010) A novel approach to detecting a regime shift in a lake ecosystem. Methods Ecol Evol 1:45–52

Gal G, Skerjanec M, Atanasova N (2013) Fluctuations in water level and the dynamics of zooplankton: a data-driven modelling approach. Freshw Biol 58:800–816. doi:10.1111/fwb.12087

Galbraith MG Jr (1967) Size-selective predation on *Daphnia* by rainbow trout and yellow perch. Trans Am Fish Soc 96(1):1–10

Gophen M (1978) Zooplankton of Lake Kinneret. In: Serruya C (ed) Lake Kinneret, Monographie Biologicae, vol 32. Junk Publishers, The Hague, pp 297–310

Gophen M (1979) Bathymetrical distribution and diurnal migrations of zooplankton in Lake Kinneret (Israel) with particular emphasis on *Mesocyclops leuckarti* (claus). Hydrobiologia 64:199–208

Gophen M (2003) Water quality management in Lake Kinneret (Israel): hydrological and food web perspectives. J Limnol 62(suppl 1):91–101

Gophen M (2005) Seasonal rotifer dynamics in the long-term (1969–2002) record from Lake Kinneret. Hydrobiologia 546:443–450

Gophen M, Azoulay B (2002) The trophic status of zooplankton communities in Lake Kinneret (Israel). Verh Int Ver Limnol 28:836–839

Hambright KD (2008) Long-term zooplankton body size and species changes in a subtropical lake: implications for lake management. Fund Appl Limnol 173(1):1–13

Hambright KD, Gal G (2004) Renovation of the Lake Kinneret zooplankton monitoring program. Kinneret Limnological Laboratory, IOLR Report T4/2004

Hambright KD, Shapiro J (1997) The 1993 collapse of the Lake Kinneret bleak fishery. Fish Manag Ecol 4:275–283

Hambright KD, Zohary T, Gude H (2007) Microzooplankton dominate carbon flow and nutrient cycling in a warm subtropical freshwater lake. Limnol Oceanogr 52:1018–1025

Hart DR, Stone L, Berman T (2000) Seasonal dynamics of the Lake Kinneret food web: the importance of the microbial loop. Limnol Oceanogr 45(2):350–361

Haury LR, McGowan JA, Wiebe PH (1978) Patterns and processes in the time-space scales of plankton distributions. In: Steele JH (ed) Spatial pattern in plankton. Plenaum Press, NY, pp 277–327

Kalikhman I, Walline P, Gophen M (1992) Simultaneous patterns of temperature, oxygen, zooplankton and fish distribution in Lake Kinneret, Israel. Freshw Biol 28:337–347

Mills EL, Green DM, Schiavone AJ (1987) Use of zooplankton size to assess the community structure of fish populations in freshwater lakes. N Am J Fish Manag 7(3):369–378

Ostrovsky I, Walline PD (2000) Multiannual changes in population structure and body condition of the pelagic fish *Acanthobrama terraesanctae* in Lake Kinneret (Israel) in relation to food sources. Verh Int Ver Limnol 27:2090–2094

Pinel-Alloul B, Downing JA, Perusse M, Codin-Blumer G (1988) Spatial heterogeneity in freshwater zooplankton: variation with body size, depth, and scale. Ecology 69(5):1393–1400

Pinel-Alloul B, Methot G, Malinsky-Rushansky NZ (2004) A short-term study of vertical and horizontal distribution of zooplankton during thermal strati cation in Lake Kinneret, Israel. Hydrobiologia 526:85–98

Roelke DL, Zohary T, Hambright KD, Montoya JV (2007) Alternative states in the phytoplankton of Lake Kinneret, Israel (Sea of Galilee). Freshw Biol 52(3):399–411. doi:10.1111/j.1365-2427.2006.01703.x

Sterner RW, Elser JJ (2002) Ecological stoichiometry: the biology of elements from molecules to the biosphere, 1st edn. Princeton University, Princeton

Stone L, Berman T, Bonner R, Barry S, Weeks SW (1993) Lake Kinneret: a seasonal model for carbon flux through the planktonic biota. Limnol Oceanogr 38(8):1680–1695

Zohary T (2004) Changes to the phytoplankton assemblage of Lake Kinneret after decades of a predictable, repetitive pattern. Freshw Biol 49:1355–1371

Zohary T, Ostrovsky I (2011) Ecological impacts of excessive water level fluctuations in stratified freshwater lake. Inland Water 1:47–59

Chapter 14
Protozoa (Unicellular Zooplankton): Ciliates and Flagellates

Ora Hadas, Tom Berman, Nehama Malinsky-Rushansky and Gideon Gal

Abstract Heterotrophic and mixotrophic protozoa have been recognized as important constituents of aquatic microbial food webs since the 1990s. Much less is known about the ecosystem roles of these organisms than about bacteria and archaea. Several pioneering studies in Lake Kinneret made in the 1980s clearly indicated that heterotrophic and mixotrophic ciliates and flagellates were of great significance in the mineralization of organic matter and cycling of carbon, nitrogen, and phosphorus. Modeling studies suggested that the protozoa, especially ciliates, appeared to be a critical food source for copepods. However, only after many years there was renewed research on protozoa as drivers of carbon flux and nutrient cycling. Routine monitoring of the lake ciliate populations was begun in 2006.

Keywords Clearance · Grazing · Nutrient cycling · Protozoa · Remineralization · Uptake

14.1 Introduction

Since the 1980s, the idea that a considerable portion of photosynthetically fixed carbon in aquatic systems passes through a microbial food web, where nutrients and energy are recycled via organisms in the size range of ~1–20 μm, has been proved in numerous environmental and laboratory experiments (Azam et al. 1983; Sherr and Sherr 1988; Berman 1990a). The microbial food web consists of bacteria, archaea, picophytoplankton, and protozoa (flagellates and ciliates) and the abundance and distribution of each component within the microbial loop is controlled by nutrient supply (bottom up) and grazing (top down) regulation in addition to environment variables (thermocline/oxycline).

O. Hadas (✉) · T. Berman · N. Malinsky-Rushansky · G. Gal
The Yigal Allon Kinneret Limnological Laboratory, Israel Oceanographic & Limnological Research, P.O. Box 447, 14950, Migdal, Israel
e-mail: orah@ocean.org.il

N. Malinsky-Rushansky
e-mail: Hami@ocean.org.il

G. Gal
e-mail: gal@ocean.org.il

T. Zohary et al. (eds.), *Lake Kinneret, Ecology and Management,* Aquatic Ecology Series 6,
DOI 10.1007/978-94-017-8944-8_14,

Several pioneering studies on heterotrophic and mixotrophic flagellates and ciliates in Lake Kinneret were conducted in the 1980s (Sherr et al. 1982, 1983, 1991; Hadas et al. 1990). These clearly indicated that ciliates and flagellates were of great significance in the mineralization of organic matter and recycling of carbon, nitrogen, and phosphorus in the lake. Modeling studies (Stone et al. 1993; Hart et al. 2000) suggested that the protozoa, especially ciliates, appeared to be a critical food source for copepods. However, only after many years was there renewed research on protozoa as drivers of carbon flux and nutrient cycling (Hambright et al. 2007). Routine monitoring of the lake ciliate populations began in 2006.

14.2 Heterotrophic Nanoflagellates

There is a definite seasonal pattern of protozoan distribution in Lake Kinneret resulting from a combination of physical conditions, biological factors, and top down predation pressures. Hadas et al. (1990) showed that small monads (2–5 μm) were the most abundant forms of heterotrophic nanoflagellates (HNAN) in the lake. From January to June, HNAN dominated the water column, reaching maximum numbers of 3×10^6 cells L^{-1} and a biovolume of 146 mm^3 wet weight m^{-3}; in autumn, minimum numbers (6.6×10^5 cells L^{-1}) of HNAN were observed. Although HNAN were distributed throughout the water column including the anaerobic hypolimnion during the entire year, the maximum numbers of HNAN were always found in the epilimnion. Peak numbers coincided with the bloom of *Peridinium gatunense*. For example, in July, maximum HNAN biomass was found at the thermocline where, sinking, partly decomposed *Peridinium* cells and high numbers of bacteria were present (Hadas and Berman 1998).

HNAN numbers depended in a complex manner on those of bacteria. In January, after lake overturn, low bacteria and high HNAN numbers were observed. The decrease in bacterial numbers may have been partially due to relatively low temperatures but more probably high grazing pressure of HNAN on bacteria led to an increase in HNAN at the expense of bacteria. This was confirmed in laboratory experiments when 8-μm filtered lake water with addition of dissolved substrates extracted from *Peridinium* cells were incubated for 2 weeks (Hadas et al. 1990). Initially, the experimental samples showed an increase in bacterial numbers followed after 1–3 days by a rise in HNAN. Subsequently, with intensification of HNAN grazing pressure, bacterial numbers declined. The bacterial population changed in size and shape, with small spherical bacteria observed toward the end of incubation, suggesting preferential feeding and selection of larger bacteria by HNAN.

Sherr et al. (1982) had shown that the decomposition of *Peridinium* cells was accelerated in the presence of bacterivorous HNAN. The microflagellates enhanced bacterial breakdown of the polysaccharide cell wall (theca) but did not increase the rate of degradation of the cell protoplasm. Hydrolytic bacteria which preferentially attacked the theca were stimulated by protozoan grazing and by the addition of inorganic phosphorus. These authors proposed that an important role of

HNAN in aquatic ecosystems was therefore to selectively facilitate the breakdown of detritus with a high structural carbohydrate/low mineral content. These findings were later experimentally corroborated showing that external addition of N and P resulted in the decomposition of isolated thecae in 1–2 days, due to the intensive heterotrophic activity of both bacteria and HNAN, but with almost no effect on the decomposition of the protoplasts (Zohary et al. 2000). The high nutrient demand during the degradation processes of the *Peridinium* bloom, and the competition for nutrients between heterotrophs (degradation) and autotrophs (production), with stronger competitive ability of heterotrophic bacteria, results in less carbon transfer to higher trophic levels.

Heterotrophic protozoa are effective processors of particulate organic matter because of their high weight-specific clearance rates and rapid digestion of bacteria and other food (Fenchel 1982; Sherr and Sherr 1984). Flagellates are typically capable of clearing food particles from a water volume about 10^5 fold their own cell volume per hour (i.e., 2×10^{-6} to 2×10^{-5} ml h^{-1}) depending on size (Berman 1990b). Growth rates and metabolism of HNAN are often as rapid as those of bacteria in optimal conditions. Sherr et al. (1983) studied aspects of the population growth of a *Monas* sp., isolated from Lake Kinneret, feeding on four species of bacteria. Growth rates, rates of ingestion of bacteria, and final population yields generally increased with increasing bacterial concentrations, although the exact relationship varied, depending on the species of bacteria used as food. Grazing rates decreased hyperbolically with increasing food density. Gross growth efficiencies and ammonia excretion rates were similar over a range of food densities among the four species of bacteria. Under optimum conditions (18–24° C), *Monas* had average population doubling times of 5.0–7.8 h, average growth efficiencies of 23.7–48.7 %, and average ammonia excretion rates of 0.76–01.23 μmol N (mg dry wt)$^{-1}$ h^{-1}. HNAN growing in filtered lake water supplemented with *Peridinium* extract had remineralization rates of 0.46–0.6 μmol N (mg dry wt)$^{-1}$ h^{-1} and 0.01–0.03 μmol P (mg dry wt)$^{-1}$ h^{-1} for nitrogen and phosphorus, respectively (Hadas et al. 1990). By comparison, NH_4 mineralization rates for Kinneret copepods and cladocerans were considerably slower and ranged from 0.02 to 0.09 μmol N (mg dry wt)$^{-1}$ h^{-1} (Gophen 1978). Hambright et al. (2007) reported N remineralization rates of 0.36 and 20.0 μgN μgC^{-1} day^{-1} for crustaceans and microzooplankton, respectively, and 0.04 and 2.8 μgP μgC^{-1} day^{-1} for P. Evidence of the major role HNAN play in recycling of nitrogen and phosphorus has also been reported by others (Goldman and Caron 1985; Caron 1989).

14.3 Mixotrophic Nanoflagellates

Although mixotrophic protozoa are now recognized to be significant in many aquatic ecosystems, little is known about these organisms in Lake Kinneret. Paran et al. (1991) reported on experiments with a small (3–5 μm) mixotrophic flagellate feeding on bacteria. The flagellate, isolated from the lake, was identified as a

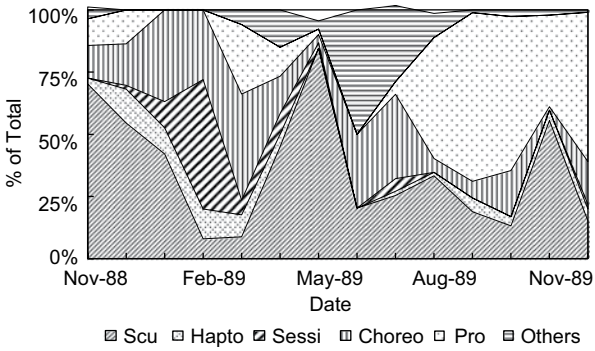

Fig. 14.1 Proportional abundance (based on cell counts) of major ciliate orders in the water column of Lake Kinneret, November 1988 to December 1989. Scuticociliatida (*Scu*), Choreotnchida (*Choreo*), Haptorida (*Hapto*), Prorodontida (*Pro*), Sessilida (*Sessi*). Others include *Saprodinium, Caenomorpha, Colpoda*

chrysophyte but not an *Ochromonas*. TEM sections showed a single chloroplast structure which was visible as a large red spot under epifluorescence microscopy. In the dark, this flagellate grew only with additions of bacteria. In the light (200 μE m^{-2} s^{-1}) with few bacteria, the flagellate grew out only after a lag of several weeks. However, when additional bacteria were given to the flagellates at the start of the experiment in the light, protozoan growth responded immediately suggesting a kind of symbiotic relationship between the flagellates and their accompanying bacteria in the light.

14.4 Ciliates

The major classes of ciliates in Lake Kinneret are the Oligohymenophorea and Spirotrichea (Madoni 1990). The annual pattern of relative abundance of ciliate classes in the lake (as measured in 1988–1989) is shown in Fig. 14.1. Within the Oligohymenophorea, the order Scuticociliatida (*Cyclidium* sp., *Dexiotricha* sp., and *Pleuronema* sp.) is abundant in autumn (5–180 cells ml^{-1}). *Cyclidium* was observed mainly in the epilimnion, whereas *Dexiotricha* was abundant in the hypolimnion. The order Sessilida (*Vorticella mayerii*) reached highest densities in February (13 cells ml^{-1}). Within the class of Spirotrichea, the orders Choreotrichida and Oligotrochida were abundant all year; additionally, *Tintinidium* appeared every year in February to early March after lake overturn. Representatives of the order Haptorida, *Didinium* sp., *Mesodinium* sp., and *Askensia* sp., carnivores that feed on other ciliates (Bick 1972), were found throughout winter, spring, and autumn but were rare in summer (Fig. 14.1).

In 1989, cell numbers and carbon biomass ranged from 3 to 99 cells ml^{-1} and 1.4 to 61 mg C m^{-3}. The greatest numbers of ciliates were found in autumn and in spring whereas relatively low numbers were recorded in February. In April, a peak of 64 cells ml^{-1} with a biovolume of 433 mm^3 m^{-3} (61 mg C m^{-3}) was recorded at 40-m depth, near the bottom sediments, during the formation of the chemocline. These were mainly anaerobic and facultative ciliates (*Saprodinium dentatum,*

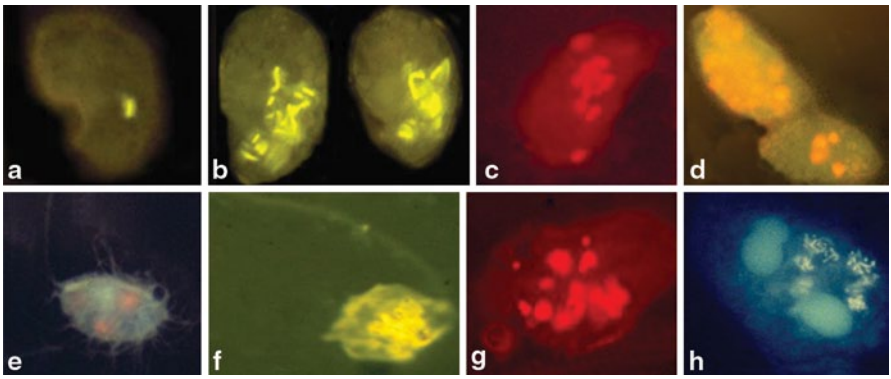

Fig. 14.2 Epiflouorescent microscope photos of heterotrophic nanoflagellates (*HNAN*) and ciliates from Lake Kinneret that had fed on fluorescently labeled bacteria or on autofluorescing phytoplankton. **a–b** *Colpoda steinii* that fed on fluorescently labeled bacteria: **a** at time 0 and **b** after 30 min of feeding. **c** *Colpoda steinii* that fed on *Synechococcus* sp. **d** Ciliates that fed on picoeukaryotes. **e** *Cyclidium* sp. that fed on *Synechococcus* sp. **f** HNAN that fed on fluorescently labeled bacteria. **g–h** *Stylonichia* sp. that fed on **g** *Synechococcus* sp. and **h** fluorescently labeled bacteria

Plagiopyla), which were feeding on sulfur cycle bacteria. After the onset of thermal stratification (May–June), high densities of ciliates were found in the thermocline and hypolimnion, probably grazing on bacteria growing on *Peridinium* derived detritus. With the deepening of the chemocline/thermocline below the euphotic zone in October, there was an increase in ciliate numbers and biovolume (99 cells ml^{-1} and 275 mm^3 m^{-3}). In December 1996, at the chemocline/thermocline (32.5 m) a "monoculture" of *Coleps hirtus* was observed (180 *Coleps* ml^{-1}), most likely feeding on very active (high dark carbon fixation ~40 mg C m^{-3} h^{-1}) chemoautotrophic bacteria at that depth. $\delta^{13}C$ of particulate organic carbon from this depth showed a low $\delta^{13}C$ value of −31.59‰ characteristic of chemoautotrophic bacteria. $\delta^{13}C$ analysis of the microbial populations (Hadas et al. 2001) indicated that ciliates were feeding not only on the chemoautotrophic bacteria but also on nano- and pico-sized algae, flagellates, and even small ciliates. This feeding behavior was also confirmed by microscopic observations (Fig. 14.2).

Since 2006, ciliates have been sampled monthly at three depths at St. A in order to represent surface (1 m), metalimnion (typically 20 m but varies and can be as shallow as 13 m), and the bottom layer (between 34 and 40 m, depending on the lake's water level). Biomass data were converted to carbon using a factor of 0.14 pg C μm^{-3} (Putt and Stoecker 1989). During the period 2006–2011, ciliate abundances were highest in the surface and metalimnion layers with little differences between them (Fig. 14.3). Only 2006 was exceptional with notably higher abundances in the metalimnion than at the surface. During all seasons, spherical- and prolate spheroid-shaped ciliates have dominated the samples collected from the lake (Fig. 14.4). Overall annual mean density and carbon content has not varied greatly with the exception of 2007 (Fig. 14.5) when the estimated abundance of ciliates was only ~30% of that in other years. Since 2007, there has been a steady increase in ciliate carbon biomass.

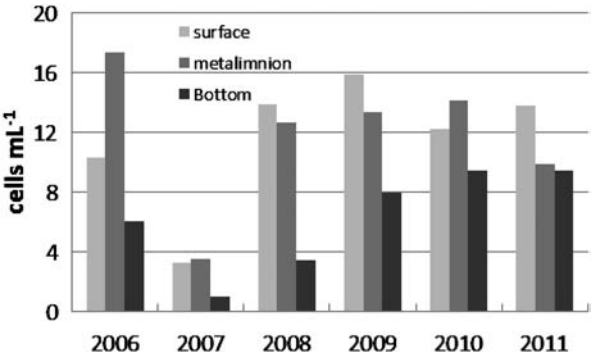

Fig. 14.3 The mean annual ciliate density in the surface layer (1 m), metalimnion (approx. 20 m), and near bottom (34–40 m) at Sta. A for the period 2006–2011

The predominant ciliate species in the lake was the raptorial predator *C. hirtus* which was abundant throughout the whole water column during all seasons, reaching highest numbers at the chemocline during autumn. *C. hirtus* contain fluorescent bodies (Sherr et al. 1991) which may be symbiotic algae (Esteve et al. 1989) supplying oxygen at the metalimnic and hypolimnic layers where there were anaerobic or low oxygen conditions.

During the stratified period, the major ciliate genera in the anaerobic hypolimnion (sulfide concentrations ranging from 1 to 12 mg L^{-1}) were *Metopus, Caenomorpha, Epalxella, Plagiopyla, Brachonella, and Saprodinium,* known to tolerate anaerobic and high sulfide conditions (Fenchel et al. 1990).

14.5 Grazing, Food Selection, and Nutrient Regeneration by Ciliates

Ciliates are a diverse group with regard to their feeding behavior. They can consume heterotrophic and autotrophic picoplankton, nanophytoplankton, cyanobacteria, bacteria, flagellates, and small ciliates (Sherr et al. 1991). Grazing rates of ciliates on bacteria and cyanobacteria were studied by direct uptake of bacteria (Madoni et al. 1990), or by the uptake of fluorescently labeled bacteria (FLB) and cyanobacteria (FLC) following the method of Sherr et al. (1987). Bacterial concentrations were determined by DAPI staining (Porter and Feig 1980), while autotrophic picoplankton were counted using their autofluorescence. Labeled bacteria were added in concentrations of 3–7 % of total bacteria. Time course uptake experiments were performed for 60 min with 10-ml subsamples being collected at different time intervals for the examination of consumption of the variety of food sources per specific ciliate. The cell ingestion rate was determined by counting the number of FLBs or autotrophic picoplankton within the protoplast of 100 protozoans using an epifluorescence microscope (Zeiss Axioscope). Five-milliliter portions of the time series subsamples were filtered through 0.8-μm polycarbonate (Poretics) black filters stained with the fluorochrome Primuline according to Bloem et al. (1986). No staining of protozoa was necessary in grazing experiments using *Synechococcus*

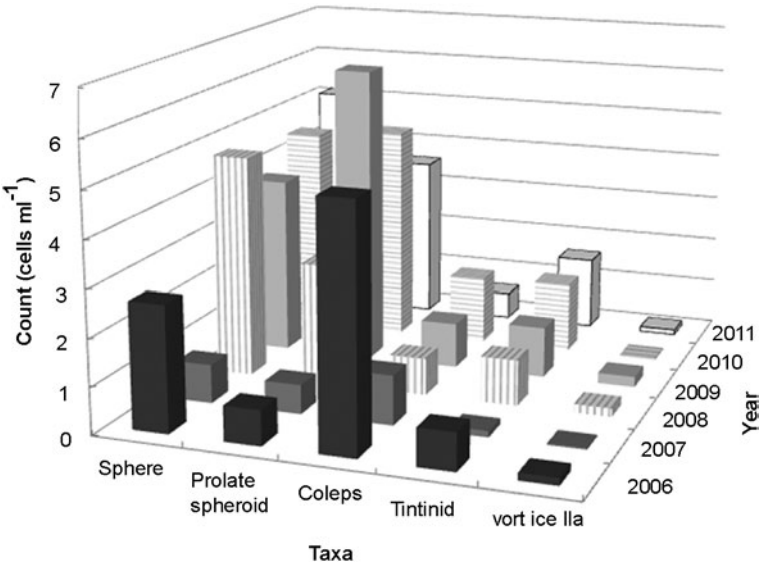

Fig. 14.4 Changes in the mean annual density of the various ciliate taxonomic and morphologic groups, in the water column, based on samples from Sta. A at 1, 20, and 34–40 m, from 2006 to 2011. *Sphere* and *Prolate spheroid* are unidentified ciliate taxa, grouped based on cell shape

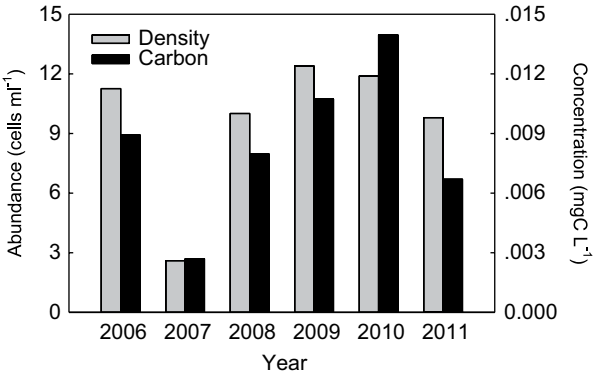

Fig. 14.5 The mean annual ciliate water column density (*left axis*) and carbon concentration (*right axis*). Mean water column values are based on sampling conducted at 1, 20, and 34–40 m on a monthly basis (2006–2011) at Sta. A

and picoeukaryotes since their pigments and the contour of the ciliate cells were clearly seen under the epifluorescence microscope. Clearance rates and growth parameters for ciliates fed on the different food sources were calculated from the linear portion of the uptake curve (Table 14.1).

Madoni et al. (1990) tested the growth of *C. hirtus* isolated from the lake in response to 12 species of planktonic algae and seven species of cultured bacteria from lake isolates, which were offered as food. Eight species of algae (one Cryptophyceae and seven Chlorophyceae) and four bacteria supported good to excellent growth of *C. hirtus*. Growth rates (μ) and doubling times ranged from 0.008 to 0.029 h^{-1} and from 23.9 to 90.8 h, respectively. *C. hirtus* was able to grow on

Table 14.1 Ciliate growth parameters: growth rate μ (h^{-1}), doubling time *dT* (h); uptake rates (pico cil^{-1} h^{-1}) and clearance rates (nl cil^{-1} h^{-1}) of Lake Kinneret ciliates fed on picoplankton. (Based on grazing experiments)

Species	Food source	μ (h^{-1})	*dT* (h)	Uptake rate pico cil^{-1} h^{-1}[a]	Clearance rate (nl cil^{-1} h^{-1})	Reference
Ciliate species epilimnion (November–December)	Coccoid cyanobacteria	0.036–0.072	9.6–19.4		62–78	Sherr et al. 1991
	Bacterioplankton				86	
Coleps hirtus	*Rhodopsedomonas palustris*	0.08–0.029	23.9–90.8			Madoni et al. 1990
	Bacteria (T_{10})					
	Tetraedron minimum					
	Chlamydomonas					
	Cryptomonas					
Colpoda sp.	*Synechococcus* sp.	0.154	4.5			Sherr et al. 1991
	Synechococcus (P)[a]	0.091	7.6	5–53	53	
						Hadas et al. 1998
	Synechococcus (CN)[a]	0.047	15	6–29	27–62	
	Pico euk			0.7–3	3	
	Bacteria (T_{10})[a]	0.14	5	930–1054	31–405[b]	
Cyclidium	Bacteria (T_{10})	0.05	14	35	4	Hadas et al. 1998
	Synechococcus (P)			3	16	
Stylonichia sp.	Bacteria	0.028	24.4	1210	67	Hadas et al. 1998
	Synechococcus (P)			22–36	36–124	
	Synechococcus (CN)			27.8	28.2	
	Picoeukaryotes			55		

[a] P, CN, and T_{10} refer to different strains

[b] Depends on food concentrations

bacteria at concentration levels as low as 2 to 8×10^5 cells ml^{-1}. In laboratory experiments, *Peridinium* cells in the exponential phase did not support *Coleps* growth, but during the decline of the *Peridinium* bloom, *Coleps* were attached to dead or moribund *Peridinium* cells feeding on the protoplast components (Hadas, unpublished). *Colpoda steinii* had a high growth efficiency on bacteria with growth rates of 0.14 h^{-1} and doubling times of 5 h (Hadas et al. 1998).

Grazing by phagotrophic protozoa is also a major factor controlling biomass and production of autotrophic and heterotrophic picoplankton in both marine and freshwater systems (Fenchel 1980; Irriberri et al. 1993; Simek et al. 1996). During the years 1988–1992, ciliate abundance in Lake Kinneret was found to be maximal at the thermocline/chemocline region in autumn when picocyanobacteria reached abundances of 6×10^5 cells ml^{-1} (Malinsky-Rushansky et al. 1995; Hadas and Berman 1998). When the lake was strongly stratified during late autumn (November), ciliates were important consumers of picoplankton in the epilimnion with doubling times of 8–24 h and grazing rates ranging from 62 to 86 nl $cell^{-1}$ h^{-1} (Sherr et al. 1991). *Colpoda steinii,* isolated from the lake, grew on a cultured freshwater *Synechococcus* sp. with a doubling time of 4.5 h and a gross growth efficiency of 48 %. At this time, the estimated daily requirements of ciliates for growth approximately equaled total phytoplankton production and ciliates in the epilimnion were clearing ~4–10 % of the bacterioplankton and cyanobacterial standing stocks per day. Because this appeared to be insufficient food consumption to meet the daily carbon requirement of the ciliates, Sherr et al. (1991) proposed that these organisms were also grazing significant amounts of autotrophic and heterotrophic eukaryotic cells.

14.6 Regeneration of Nutrients

Ciliates fed on bacteria and *Synechococcus* are capable of regenerating nutrients (N, P), which can be used by bacteria and autotrophs, resulting in an inverse oscillation pattern between the two populations (Hadas et al. 1990). *Colpoda steinii* and *Stylonichia* sp. grown on bacteria or *Synechococcus* sp. exhibited nitrate reductase activity that increased in the presence of nitrate. *Colpoda steinii* showed a dependence on initial nitrate concentrations for growth. Ammonium excretion was observed mostly as the outcome of N remineralization from the food supply, but also partially due to dissimilatory nitrate reduction. Thus, ciliates may play an important role in nutrient recycling in the lake and some species could use nitrate respiration in anoxic regions in the water column (Hadas et al. 1992). Protozoa located near the oxic–anoxic boundaries (metalimnion) may use either aerobic or anaerobic respiration. These ciliates would also be able to escape from potential predators (rotifers, microcrustaceans), which are dependent on oxygen, by moving to the anaerobic part of the water column (Beaver and Crisman 1989).

14.7 Carbon Cycling by Flagellates and Ciliates

Stone et al. (1993) incorporated both flagellates and ciliates in their carbon flux model for Lake Kinneret. They based their estimates of protozoan carbon uptake, release, and respiration on measured biomass and doubling times for these organisms. This model inferred that ciliates were of great importance as a carbon source for copepods, especially in summer when >40 % of the copepod carbon intake could derive from ciliates. Hart et al. (2000) modified the previous model by adding a flux from nanophytoplankton to ciliates and increasing the time resolution to all four seasons. Their model suggested that flagellates (both heterotrophic and mixotrophic), ciliates, and cladocerans were all important consumers of bacteria. Flagellates were especially important in the winter when they accounted for about 60 % of all grazing on bacteria. Ciliates were the major summer bacterial grazers and were the major source of carbon for copepods in summer, but much less at other seasons. Overall, these models indicate that even in eutrophic environments, protozoa can supply significant amounts of carbon to metazoan zooplankton. As yet we have no idea of the extent of carbon supply to the system by phage lysis as a competing fate to protozoan grazing of bacteria.

Some confirmation of these models was provided by an experimental study by Hambright et al. (2007) who showed that microzooplankton (in this case, ciliates, flagellates, as well as rotifers and naupliar stages of copepods) could dominate both the grazing of phytoplankton and bacteria and the mineralization of phosphorus and nitrogen in Lake Kinneret. The microzooplankton were also important components of omnivorous copepod diets in Lake Kinneret (Blumenshine and Hambright 2003). Today, the crucial role of the protozoa (unicellular zooplankton) in the Kinneret food web is greatly appreciated, as reflected in the revised scheme of the Kinneret food web (Fig. 17.2 in Chap. 17).

References

Azam F, Fenchel T, Field JG, Meyer-Reil LA, Thingstad T (1983) The ecological role of water column microbes in the sea. Mar Ecol Prog Ser 10:257–263

Beaver JR, Crisman TL (1989) The role of ciliated protozoa in pelagic freshwater ecosystems. Microb Ecol 17:11–136

Berman T (1990a) Microbial food webs and nutrient cycling in lakes: changing perspectives. In: Tilzer M, Serruya C (eds) Large lakes. Springer, Berlin

Berman T (1990b) Protozoans as agents in aquatic nutrient cycling. In: Reid PC, Turley CM, Burkhill PH (eds) Protozoa and their role in marine processes. Springer, New York

Bick H (1972) Ciliated protozoa. World Health Organization, Geneva

Blumenshine S, Hambright KD (2003) Top-down control in Lake Kinneret: a role for invertebrate predation. Hydrobiologia 491:347–356

Bloem J, Bar-Gillissen MJB, Cappenberg T (1986) Fixation, counting and manipulation of heterotrophic nanoflagellates. Appl Environ Microbiol 52:1266–1272

Caron DA (1989) Evolving role of protozoa in aquatic nutrient cycles. In: Proc NATO-ASI Workshop, Plymouth, pp 387–415

Esteve I, Gaju JMN, McKhann H, Margulis L (1989) Green endosymbiont of *Coleps* from lake Cisco identified as *Chlorella vulgaris*. Symbiosis (Balaban), Rehovoth
Fenchel T (1980) Suspension feeding in ciliated protozoa: feeding rates and their ecological significance. Microb Ecol 6:13–25
Fenchel T (1982) Ecology of heterotrophic microflagellates. IV. Quantitative occurrence and importance as bacterial consumers. Mar Ecol Prog Ser 9:35–42
Fenchel T, Kristensen LD, Rasmussen L (1990) Water column anoxia: vertical zonation of planktonic protozoa. Mar Ecol Prog Ser 62:1–10
Goldman JC, Caron DA (1985) Experimental studies on an omnivorous flagellate: implications for grazing and nutrient regeneration in the marine microbial food chain. Deep-Sea Res 32:899–915
Gophen M (1978) Zooplankton. In: Serruya C (ed) Lake Kinneret. Junk, The Hague, pp 297–311
Hadas O, Berman T (1998) Seasonal abundance and vertical distribution of protozoa (flagellates, ciliates) and bacteria in Lake Kinneret, Israel. Aquat Microb Ecol 141:161–170
Hadas O, Pinkas R, Albert-Diez C, Bloem J, Cappenberg T, Berman T (1990) The effect of detrital addition on the development of nanoflagellates and bacteria in Lake Kinneret. J Plankton Res 12: 185–199
Hadas O, Pinkas R, Wynne D (1992) Nitrate reductase activity, ammonium regeneration and orthophosphate uptake in protozoa isolated from Lake Kinneret, Israel. Microb Ecol 23:107–115
Hadas O, Malinsky-Rushansky N, Pinkas R, Cappenberg TE (1998) Grazing on autotrophic and heterotrophic picoplankton by ciliates isolated from Lake Kinneret, Israel. J Plankton Res 20:1435–1448
Hadas O, Pinkas R, Erez J (2001) High chemoautotrophic primary production in Lake Kinneret, Israel—a neglected link in the C cycle of the lake. Limnol Oceanogr 46:1968–1976
Hambright KD, Zohary T, Gude H (2007) Microzooplankton dominate carbon flow and nutrient cycling in a warm subtropical freshwater lake. Limnol Oceanogr 52:1018–1025
Hart DR, Berman T, Stone L (2000) Seasonal dynamics of the Lake Kinneret food web: the importance of the microbial loop. Limnol Oceanogr 45:350–361
Iriberri J, Begona A, Unanue M, Barcina I, Egea L (1993) Channelling of bacterioplankton production toward phagotrophic flagellates and ciliates under different seasonal conditions in a river. Microb Ecol 26:111–124
Madoni P (1990) The ciliated protozoa of the monomictic Lake Kinneret (Israel). Species composition and distribution during stratification. Hydrobiologia 190:111–120
Madoni P, Berman T, Hadas O, Pinkas R (1990) Food selection and growth of the planktonic ciliate *Coleps hirtus* isolated from a monomictic subtropical lake. J Plankton Res 12:735–741
Malinsky-Rushansky N, Berman T, Dubinsky Z (1995) Seasonal dynamics of picophytoplankton in Lake Kinneret, Israel. Freshw Biol 34:241–254
Paran N, Dubinsky Z, Berman T (1991) Interactions between mixotrophic flagellates and bacteria in aquatic systems. Symbiosis 10:219–231
Porter KG, Feig YS (1980) The use of DAPI for identifying and counting aquatic microflora. Limnol Oceanogr 25:943–948
Putt M, Stoecker DK (1989) An experimentally determined carbon: volume ratio for marine "oligotrichous" ciliates from estuarine and coastal waters. Limnol Oceanogr 34:1097–1103
Sherr EB, Sherr BF (1984) Role of heterotrophic protozoa in carbon and energy flow in aquatic ecosystems. In: Klug MJ, Reddy CA (eds) Current perspectives in microbial ecology. American Society of Microbiology, Washington, DC
Sherr EB, Sherr BF (1988) Role of microbes in pelagic food webs: a revised concept. Limnol Oceanogr 33:1225–1227
Sherr BF, Sherr EB, Berman T (1982) Decomposition of organic detritus: a selective role for microflagellate protozoa. Limnol Oceanogr 27:765–769
Sherr BF, Sherr EB, Berman T (1983) Grazing, growth, and ammonium excretion rates of a heterotrophic microflagellate fed with four species of bacteria. Appl Environ Microbiol 45:1196–1201

Sherr BF, Sherr EB, Fallon RD (1987) Use of monodispersed, fluorescently labelled bacteria to estimate *in situ* protozoan bacterivory. Appl Environ Microbiol 53:958–965

Sherr EB, Sherr BF, Berman T, Hadas O (1991) High abundance of picoplanktivorous ciliates during late fall in Lake Kinneret, Israel. Limnol Oceanogr 34:1202–1213

Simek K, Macek M, Pernthaler J, Straskrabova V, Psenner R (1996) Can freshwater planktonic ciliates survive on a diet of picoplankton? J Plankton Res 18:597–613

Stone L, Berman T, Bonner R, Barry S, Weeks SW (1993) Lake Kinneret: a seasonal model for carbon flux through the planktonic biota. Limnol Oceanogr 38:1680–1695

Zohary T, Güde H, Pollingher U, Kaplan B, Pinkas R, Hadas O (2000) The role of nutrients in decomposition of a thecate dinoflagellate. Limnol Oceanogr 45:123–130

Chapter 15
Heterotrophic and Anoxygenic Photosynthetic Bacteria

Tom Berman, Yosef Z Yacobi, Werner Eckert and Ilia Ostrovsky

Abstract This chapter reviews the current knowledge of the heterotrophic and anoxygenic photosynthetic bacteria in Lake Kinneret. Morphological and phylogenetic diversity of bacteria and archaea as well as data from routine total bacterial cell counts are summarized. From 2001 to 2011, there was a definite, significant trend to lower the annual average cell counts that coincided with a significant decrease in bacterial productivity. Additional information is provided on anoxygenic phototrophic bacteria prevailing in Lake Kinneret. The most abundant of these phototrophs is the green sulfur bacterium (GSB) *Chlorobium phaeobacteroides* Pfennig. It forms (almost consistently) a prominent layer in the metalimnion from June through October. The spatial distribution of BChl *e,* an indicator of *C. phaeobacteroides,* was fairly heterogeneous, and its peak values often exceeded the record of chlorophyll *a* peaks. *C. phaeobacteroides* was identified as a major contributor to the sedimenting material in the lake in the summer, making up on average 27% of the carbon settling towards the bottom.

Keywords Bacteria · Archaea · Bacterial morphology · Phylogenetic diversity · Bacterial abundance · Metalimnion · *Chlorobium phaeobacteroides* · Bacteriochlorophyll *e* · Sedimentation

The bacterial community of Lake Kinneret was recently unveiled due to advanced molecular techniques and improved analytical procedures. Here, we present the current knowledge of the bacterial community, their abundance, and temporal dynamics in the lake. A special attention is given to anoxygenic photosynthetic bacteria, due to their unique pigment signal that serves as an indicator for their abundance, distribution, and sedimentation.

Y. Z Yacobi (✉) · T. Berman · W. Eckert · I. Ostrovsky
The Yigal Allon Kinneret Limnological Laboratory, Israel Oceanographic & Limnological Research, P.O. Box 447, 14950 Migdal, Israel
e-mail: yzy@ocean.org.il

W. Eckert
e-mail: werner@ocean.org.il

I. Ostrovsky
e-mail: ostrovsky@ocean.org.il

T. Zohary et al. (eds.), *Lake Kinneret, Ecology and Management,* Aquatic Ecology Series 6,
DOI 10.1007/978-94-017-8944-8_15,

15.1 Bacteria and Archaea: Phylogeny, Morphology, and Abundance

Tom Berman

Relatively little is known about the phylogenetic diversity of bacteria in the lake. Even less is known about the archaea, although representatives of the latter kingdom, such as the methanogens active in the anaerobic hypolimnion and sediments and aerobic ammonia oxidizing archaea, are undoubtedly present. As yet, only two lists of bacterial species based on denaturing gradient gel electrophoresis (DGGE) and 16S rRNA gene amplification of epilimnetic lake water samples have been published and more powerful techniques to delineate the diversity of archaeal and bacterial populations in Lake Kinneret have not yet been applied.

In a study made in 1999–2000, Pinhassi and Berman (2003) noted that α-proteobacteria constituted a majority of the colonies found in lake dilution cultures during the year; *Sphingomonas* species were found in all unenriched dilution cultures. Other frequently abundant species were *Brevundimonas aurantiaca* (strain K1) and *Asticcacaulis* sp. (strain K48). γ-Proteobacteria such as *Acinetobacter* sp. (strain K93), *Pseudomonas anguilliseptica* (strain K116), and *Rheinheimera* sp. (strain K89) were occasionally abundant in these cultures. Both β- and γ-proteobacteria were dominant on one occasion shortly after high inflows from the Jordan River caused by heavy rainfall. (*Note: Nothing is known about the bacterial populations of the Jordan River.*) When nutrients were added to natural lake water, mainly β- and γ-proteobacteria grew out. The γ-proteobacteria *Aeromonas veronii* (strain K103) and *Rheinheimera* sp. (strains K35 and K89) were dominant throughout the year. Other repeatedly occurring species were *Shewanella putrefaciens* (strain K80), *Pseudomonas pavonanceae* (strain K90), a β-proteobacterium (strain K109), a *Cytophaga* sp. strain (strain K30), and the α-proteobacteria *B. aurantiaca* (strain K1) and *Caulobacter* sp. (strain K137).

Baltar et al. (2012) used DGGE analysis to follow the variability of prokaryotic community structure during long-term (10–20 days) dark bottle incubations of near-surface Lake Kinneret water. During the first 24 h of incubation, there were only minor changes in the composition of the bacterial community. Thereafter, there were marked shifts in the prokaryotic community structure (see Baltar et al. 2012 for details). The major bacterial phylotypes identified in this study are listed in Table 15.1.

Schwartz et al. (2007) analyzed the structure, species composition, and relative abundance of microbial community composition of the anoxic, profundal sediment of Lake Kinneret, using culture-independent molecular methods. Pairwise comparison of archaeal and bacterial ribosomal RNA (rRNA) genes terminal restriction fragment length polymorphism (T-RFLP) profiles obtained from samples taken in January 2003, July 2003, and October 2004 indicated seasonal stability of the microbial community. The numbers of archaea and bacteria, quantified by real-time polymerase chain reaction (RT-PCR), amounted to ~10^8 and 10^{10} rRNA gene copies per cubic centimeter sediment, respectively, suggesting that archaea accounted

Table 15.1 Bacteria identified in surface waters of Lake Kinneret based on phylogenetic affiliation of 16S rRNA gene sequences as described by Baltar et al. (2012)

Closest cultured relative in GenBank	%	Closest relative in GenBank	%	Class	Phylum
Cryomorphaceae bacterium Haldis-1	90	*Uncultured bacterium*	99	*Flavobacteria*	*Bacteroidetes*
Trojanella thessalonices	85	*Uncultured SAR11*	100	*Alphaproteobacteria*	*Proteobacteria*
Arcicella aquatica strain NO-502	99	*Arcicella* sp. *NSW-5*	99	*Cytophagia*	*Bacteroidetes*
Mucilaginibacter daejeonensis	91	*Uncultured Bacteroidetes CL1H6*	99	*Sphingobacteria*	*Bacteroidetes*
Fluviicola taffensis strain RW262	92	*Uncultured Fluviicola* sp.	99	*Flavobacteria*	*Bacteroidetes*
Sphingobacterium sp.*35*	84	*Uncultured Bacteroidetes 2K51*	94	*Sphingobacteria*	*Bacteroidetes*
Christensenella minuta	81	*Uncultured Fibrobacter* sp.	99	*Fibrobacteres*	*Fibrobacteres*
Emticicia oligotrophica	91	*Uncultured Emticicia* sp.	93	*Cytophagia*	*Bacteroidetes*
Owenweeksia hongkongensis	82	*Uncultured bacterium DP7.4.20*	87	*Flavobacteria*	*Bacteroidetes*
Owenweeksia hongkongensis	87	*Unidentified bacterium K2-30-6*	96	*Flavobacteria*	*Bacteroidetes*
Owenweeksia hongkongensis	89	*Uncultured bacterium*	99	*Flavobacteria*	*Bacteroidetes*
Desulfonatronum cooperativum	81	*Uncultured bacterium*	100	*Fibrobacteres*	*Fibrobacteres*
Herbaspirillum aquaticum	90	*Uncultured proteobacterium WR 124*	92	*Betaproteobacteria*	*Proteobacteria*
Propionivibrio limicola	93	*Uncultured bacterium K2NMV-30-B39*	99	*Betaproteobacteria*	*Proteobacteria*
Sphingobium xenophagum	84	*Uncultured Sphingomonas* sp.	86	*Alphaproteobacteria*	*Proteobacteria*
Hyphomicrobium sulfonivorans	81	*Uncultured SAR11*	97	*Alphaproteobacteria*	*Proteobacteria*
Chryseobacterium sp.	99	*Chryseobacterium* sp. *PanRB005*	99	*Flavobacteria*	*Bacteroidetes*
Chryseobacterium sp.	88	*Uncultured Bacteroidetes MEf05b11A2*	98	*Flavobacteria*	*Bacteroidetes*
Sphingobacterium sp. *35*	88	*Uncultured bacterium*	99	*Sphingobacteria*	*Bacteroidetes*
Pedobacter sp. *A12*	81	*Uncultured Haliscomenobacter* sp	87	*Sphingobacteria*	*Bacteroidetes*
Burkholderia bryophila	94	*Uncultured proteobacterium*	100	*Betaproteobacteria*	*Proteobacteria*
Pedobacter lentus strain DS-40	85	*Uncultured BacteroidetesTK-NE8*	95	*Sphingobacteria*	*Bacteroidetes*
Modestobacter sp. *SSW1-42*	91	*Uncultured bacterium THBP.09.12.68*	99	*Actinobacteria*	*Actinobacteria*

For each phylotype, closest relative GenBank and closest cultured relative are shown together with the sequence similarity (%) designated class and phylum

for only about 1 % of the total prokaryotic sediment community. Hydrogenotrophic *Methanomicrobiales* and acetoclastic *Methanosaeta* spp. were prominent among the archaea while *δ-proteobacteria,* sulfate reducers, and syntrophs dominated the bacterial community. The *Bacteroidetes–Chlorobi* group was also abundant. Only one group, affiliated with halorespiring bacteria of subphylum II of the *Chloroflexi,* showed variation in abundance within the sediment samples investigated. This study highlighted the particular importance of sulfate reducers, syntrophs, bacteroidetes, halorespirers, and methanogens in the profundal sediment of Lake Kinneret.

Morphology of Kinneret Bacteria Generally, bacteria are considered rather boring morphologically, usually appearing as coccoid, rod, or spiral-shaped objects. Some years before the takeover of bacterial taxonomy by molecular techniques, a scanning electron and epifluorescence microscope study of natural populations in Lake Kinneret made by Schmaljohann et al. (1987) indicated some of the variety of morphological forms that could be observed in this lake. An example of the wide assortment of bacterial morphologies found in a near-surface (3 m) sample taken at station A in August 1982 is shown in Fig. 15.1a. Unexpected cell forms were frequent. For example, in a sample from 3-m depth in October 1981, abundant budding bacteria were observed (Fig. 15.1b). These had a large spindle-shaped mother cell (4.0 × 1.0 μm) that formed one to three hyphae at both cell poles. Usually, only a single hypha extended from one cell pole while at the other pole two or three hyphae were located, one of which formed a bud at its end.

Other unusual cells, not shown here, that were observed in these samples included: (a) numerous star-shaped bacteria resembling *Ancalomicrobium* sp., with two or more bacteria connected by an appendage 0.4–0.5 μm thick. Each of these cells carried another two to four straight appendages up to 10 μm long. (b) A large, double-S-shaped bacterium with a diameter of 0.5 μm and a length up to 40 μm with tapering ends. (c) Long straight filaments with diameters of 0.4 μm and lengths up to 30 μm.

Bacterial populations in the metalimnion (Fig. 15.1c) were dominated by numerous straight or slightly curved large rods (0.8–1.0 μm thick and 3–7 μm long) probably *Chlorobium phaeobacteroides,* a photosynthetic green sulfur bacterium (GSB) known to form dense layers in the metalimnion of Lake Kinneret (Bergstein et al. 1979). Also observed in these samples were long, thin, and slightly curved bacteria (1.2–1.5 μm thick and 15–20 μm long) and S-shaped cells with tapering ends (0.6–1 μm thick and 3–5 μm long). Similar cells were also common in deep hypolimnion samples (40 m), which contained many other types of anaerobic microflora.

During a *Peridinium* bloom in May 1984, many, very small semicircular and even circular *Microcyclus aquaticus* were observed (thickness ~0.2 μm, outer diameter of the cells < 1.0 μm, Fig. 15.1d). When the lake was homothermic, *Planktomyces bekefii* (Fig. 15.1e) and *Vibrio*-like bacteria were prominent.

Lake Kinneret is a potentially fruitful site for microbiologists working on budding and appendaged bacteria, which appear to be present in large numbers especially in autumn and winter. Detailed phylogenetic studies of the bacteria and archaea with up-to-date methods are lacking, but would probably yield a wealth of important insights about the microbial communities inhabiting the many and varied ecological niches of Lake Kinneret.

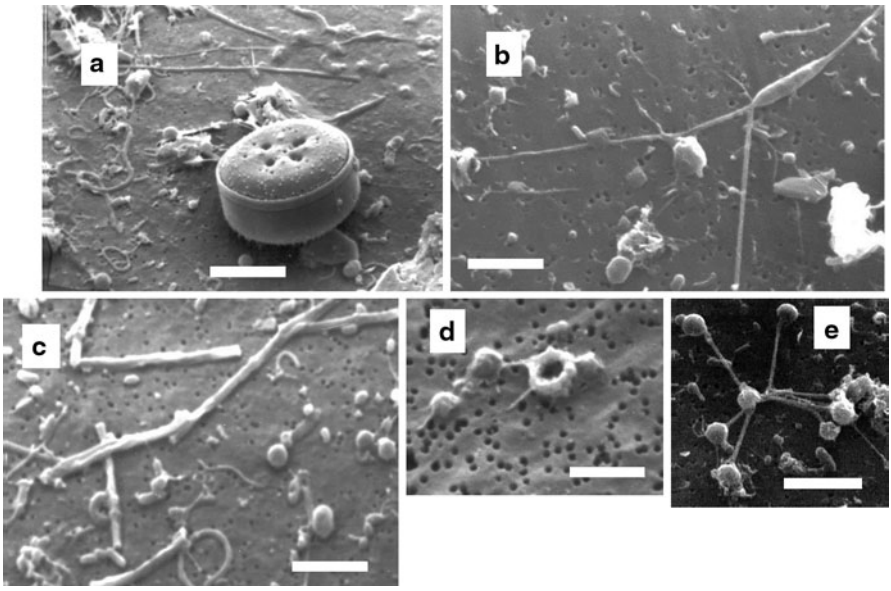

Fig. 15.1 SEM micrographs of Lake Kinneret bacteria sampled at station A. **a** 3 m deep, with algal cell, *Cyclotella* sp. Aug 1982, Bar = 5 µm. **b** 3 m, budding bacterium, Oct. 1981, Bar = 3 µm. **c** 18 m, sample from metalimnion with *Chlorobium phaeobacteroides,* Oct. 1981, Bar = 5 µm. **d** 3 m, *Microcylus*-like bacterium, May 1984, Bar = 2 µm. **e** 3 m, Mar. 1983, *Planktomyces bekefii,* Bar = 5 µm. (See also Schmaljohann et al. 1987)

Bacterial Abundance Bacterial counting using 4′,6-diamidino-2-phenylindole (DAPI) staining and epifluorescence microscopy at 3-m depth at station A in the lake began in March 1988. Subsequently, from January 1995, routine bacterial counts were made monthly at 5–6-m depths. Since January 2001, bacterial biomass production (BP, as milligrams of carbon per liter per day) in these samples has also been determined (Sect. 25.1). The annual averages and standard deviations of bacterial abundance in the epilimnetic waters (0–10 m and 0–15 m averaged from 1988 to 2000 and from 2001 to 2011, respectively) are shown in Fig. 15.2a and b. Overall averages and standard deviations during the first and second periods were very similar, $3.8 \pm 0.8 \times 10^6$ and $3.2 \pm 1.2 \times 10^6$ cells mL^{-1}, respectively. Although there was some annual variability over the first period (1989 being exceptionally low), from 2001 to 2011 there was a definite, significant trend to lower the annual average cell counts that coincided with a significant ($p = 0.011$) decrease in BP (Sect. 25.1). The decline in the annual averages of both bacterial abundance and BP in the epilimnic water does not appear to be correlated to any change in annual averages of phytoplankton biomass, primary production, or chlorophyll.

The seasonal patterns, as reflected by monthly averages for the periods 1988 to 2000 and 2001 to 2011, are shown in Fig. 15.2c, d. During the first period, maximum bacterial counts were recorded in April, May, and June, during and slightly after the late-winter and early spring blooms of *Peridinium gatunense* that occurred

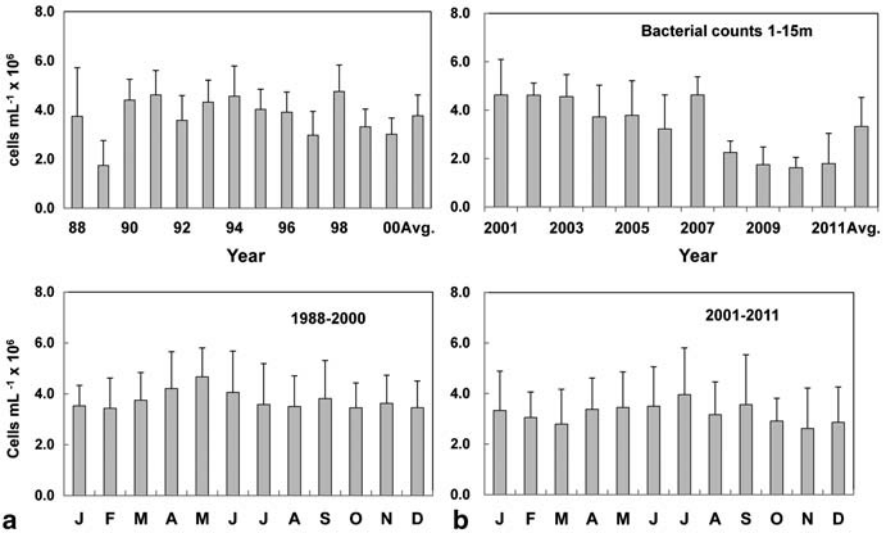

Fig. 15.2 Bacterial abundance in Lake Kinneret (cells per milliliter, averaged from 0 to 15 m depth). Annual average, multiannual average (*Avg.*), and standard deviation from 1988 to 2000 (**a**) and from 2001 to 2011 (**b**). Monthly averages for the period 1988 to 2000 (**c**) and from 2001 to 2011 (**d**)

regularly. Possibly, these maxima reflected increased bacterial growth on the large input of organic matter released when the dense dinoflagellate blooms crashed. This pattern of seasonal abundance did not appear during the period from 2000 to 2011, when large *Peridinium* blooms occurred only in 2003, 2004, and, briefly, in 2007.

15.2 Anoxygenic Photosynthetic Bacteria

Yosef Z Yacobi, Werner Eckert, Ilia Ostrovsky

Isolation and Identification of Anoxygenic Phototrophs Several anoxygenic phototrophs have been isolated from Lake Kinneret, with the GSB *C. phaeobacteroides* Pfennig being the most abundant. Although *C. phaeobacteroides* was detected throughout the entire anoxic part of the water column during the stratified season (Bergstein et al. 1979; Eckert et al. 1990; Butow and Bergstein-Ben Dan 1992), its cell density peaked in the metalimnion, forming intense blooms from July until November nearly every year. Other anoxygenic phototrophs isolated from Lake Kinneret are *Prosthecochloris aestuaris, Thiocapsa roseopersicina* (Eckert et al. 1986), *Rhodopseudomonas palustris* (Butow and Bergstein-Ben Dan 1992), and *C. limicola* (Wynne and Bergstein-Ben Dan 1995).

Molecular analysis based on *bchY* primer set (Yutin et al. 2009) showed that the genetic variability of anoxygenic photosynthetic bacteria is far larger than realized by culturing efforts and/or photosynthetic pigment analysis. The *bchY* primer set successfully amplified genes from both sediment and metalimnetic samples from Lake Kinneret. While the signal from the sediments was restricted to *Chlorobium*-like *bchY* sequences, the metalimnetic samples yielded both *Chlorobium*-like and proteobacteria-like *bchY* sequences and displayed variability in both groups (Fig. 15.3). The variability of genotypes in the sediment is expected, as we know from past records that Lake Kinneret hosts several species (and an unknown number of strains) of anoxygenic phototrophs, which surface occasionally. More surprising was the variability observed in the metalimnion. The molecular analysis indicated that various genotypes of both green sulfur and purple sulfur phototrophic populations exist in the water column although probably only one genotype rises to the position of overwhelming domination, as documented by pigment analysis. In contrast to GSB that are strict anaerobes, purple sulfur bacteria are tolerant to low oxygen concentrations (Imhoff 1995) and may persist in the water column year-round and develop relatively dense populations, given certain environmental conditions are fulfilled (Butow and Bergstein-Ben Dan 1992).

The Green Sulfur Bacterium (GSB) C. phaeobacteroides *C. phaeobacteroides* is an obligatory anoxic organism occurring in many water bodies throughout the world (Trüper and Imhoff 1999) using reduced sulfur compounds as electron donors (Imhoff 1995). *C. phaeobacteroides* contains bacteriochlorophyll *e* (BChl *e*) as its main antenna pigment, as well as isorenieratene as the main carotenoid (Imhoff 1995; Hirabayashi et al. 2004). Antenna BChl *e* consisting of several homologues is specific to GSB (Smith 1994) and, therefore, may be used for identification and quantification of this group of organisms (Yacobi et al. 1990; Hurley and Watras 1991). Depth profiles of the BChl *e* along with physicochemical variables determined at a central station in Lake Kinneret (station A, see location in Fig. 1.1 of Chap. 1) showed that the *C. phaeobacteroides* population had its maximum abundance at a narrow water layer in the metalimnion right below the chemocline (Eckert et al. 1990), delineated by the sharp drop in the Eh profile (Fig. 15.4). This maximum, located at a depth of approximately 19 m on the specific day displayed in Fig. 15.4, is an outcome of the physiological requirements of light and hydrogen sulfide by *C. phaeobacteroides*.

Most of the early field studies on *C. phaeobacteroides* in Lake Kinneret were conducted at station A (e.g., Bergstein et al. 1979; Butow and Bergstein-Ben Dan 1992). A clear-cut proof for a lake-wide distribution of a photosynthetic bacterial layer was more recently provided when a multichannel chlorophyll fluorescence detector was deployed in Lake Kinneret (Fig. 15.5). The instrument was originally developed for the measurement of chlorophyll *a* and for the determination of the contribution of different phytoplankton groups to the bulk of the photosynthesizing community (Beutler et al. 2002). However, we realized that the instrument measures the signal of BChl *e,* the signature pigment of *C. phaeobacteroides* (Imhoff 1995), and can be used for mapping the abundance of that bacterium along transects across the lake (Yacobi and Eckert 2002). BChl *e* absorption maxima (in vivo) are at 460,

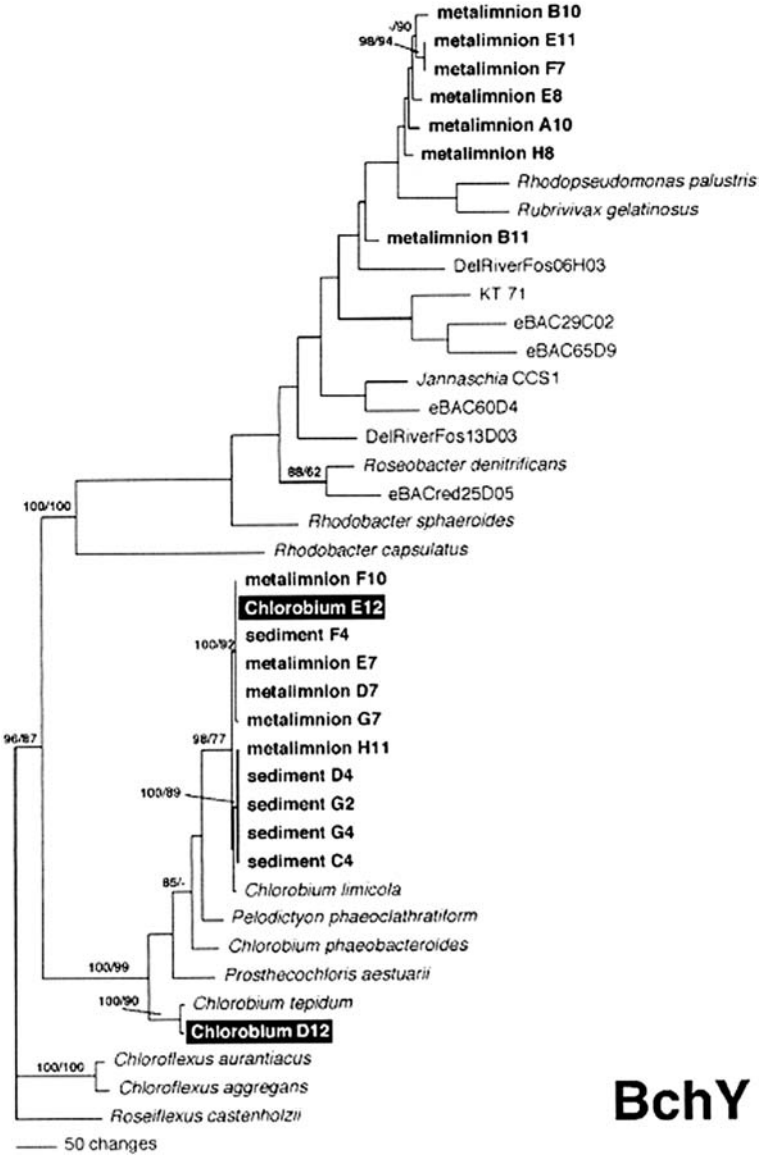

Fig. 15.3 Phylogenetic parsimony tree of bchY protein sequences. *Black background* denotes sequences retrieved from *Chlorobium* cultures kept in the Lake Kinneret collection; *bold lettering* indicates cultures based on inoculums derived either from the metalimnion or sediments from Lake Kinneret. (For methodological details, see Yutin et al. 2009)

526, and 722 nm. The first two peaks overlap the absorption maxima of chlorophyll *c* and of carotenoids from algae that harbor chlorophyll *c* (diatoms, dinoflagellates). Nevertheless, we found a good agreement between BChl *e* concentrations estimated by an in situ probe and those quantified by high-performance liquid chromatography

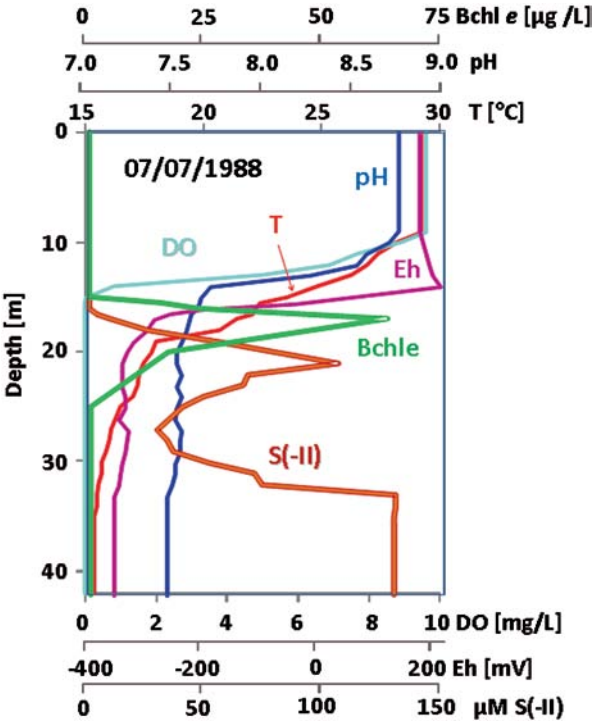

Fig. 15.4 Depth profiles of temperature (*T*), total sulfide (*S[-II]*), redox (*Eh*), dissolved oxygen (*DO*), and bacteriochlorophyll *e* (*BChl e*) measured along the water column at a central station of Lake Kinneret on 7 July 1988. (From Eckert et al. 1990)

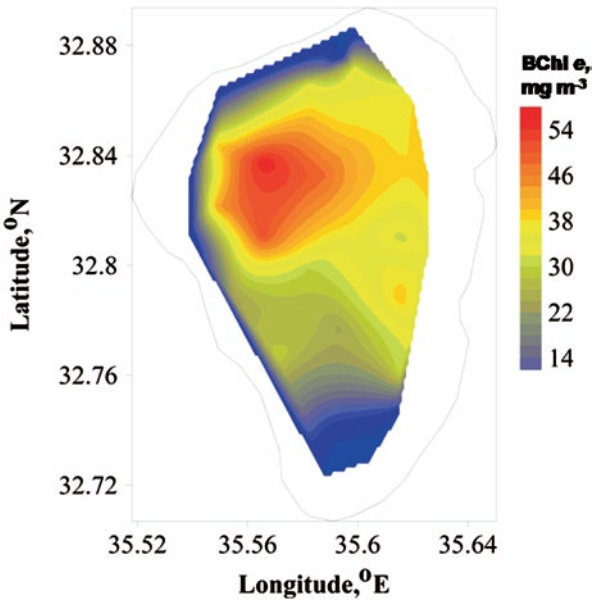

Fig. 15.5 Spatial distribution of BChl *e* concentration in micrograms per liter, in Lake Kinneret, 27 September 2005. The lake was surveyed by profiling at 31 stations using a fluoresce-based probe (Yacobi and Schlichter 2004). The data presented were taken from the depth where the maximum value of BChl *e* was measured. This depth varied between sampling locations and ranged from 15.62 to 19.60 m

(HPLC; Rimmer et al. 2008). We found that the spatial distribution of BChl *e* is heterogeneous (Fig. 15.5). In locations of highest concentrations, BChl *e* reaches values of tens of microgram per liter, several times higher than the concentrations of algal chlorophyll *a* found in the epilimnion, at the same time. A standing stock of 200 mg m^{-2} BChl *e* is not unusual in the anoxic part of the water column of Lake Kinneret when *C. phaeobacteroides* thrives in the lake. To calculate the contribution of *C. phaeobacteroides* to the carbon budget, we assumed a conversion factor of 20:1 (C-to-BChl *e* ratio). This conversion factor is based on the ratio between bacteriochlorophyll and protein in GSB (van Gemerden 1980; Oelze and Golecki 1988), and is used only as a rough estimate of the potential contribution of *C. phaeobacteroides* to the carbon budget. Using that ratio, we conclude that 4 g C m^{-2} accumulated in *C. phaeobacteroides* at the location where it peaks. Consequently, we estimate that the upper limit for *C. phaeobacteroides'* contribution to carbon budget is approximately 50 % of the carbon contained in phytoplankton in the epilimnion.

The light prevailing at the depth of 15.5 m in Lake Kinneret, i.e., at the top of the metalimnion in the lake center, is on average (± standard deviation) 1.59 (± 1.59) µmol photon m^{-2} s^{-1} (Yacobi unpublished). This is below the light required by *C. phaeobacteroides* to reach its maximal photosynthetic activity, which ranges from 5 to 30 µmol photon m^{-2} s^{-1} (Bergstein et al. 1979). We assume that the high concentrations of BChl *e* observed in the metalimnion are the result of increased light flux onto the layer where *C. phaeobacteroides* is found. This happens in Lake Kinneret when anoxic water layers are elevated towards the surface close to the littoral due to internal seiching (Rimmer et al. 2008).

The metalimnetic *C. phaeobacteroides* blooms represent important carbon sources, attracting crustacean zooplankton (Gophen et al. 1974) and probably ciliates, which concentrate in its upper oxygenated layer (Hadas and Berman 1998, Chap. 14), and graze on this bacterial pool. It is possible that organic material produced by these bacteria cascades through the food web and eventually become food for fish, which are numerous at the top of the thermocline (Chap. 16).

Pigment analysis of the particulate material has shown that high concentrations of BChl *e* are found also in sedimenting seston collected in sediment traps and in the uppermost layer of bottom sediments (Ostrovsky and Yacobi 1999, 2010). The sedimentation flux of BChl *e* was temporally variable, as was the percentage contribution of BChl *e* to the total sedimentation flux of phytoplankton (as chlorophyll *a*; (Fig. 15.6). Owing to the dense metalimnic biomass, *C. phaeobacteroides* forms all over the lake from July to October; its direct contribution to the flux of settling organic particles was high in summer, although extremely variable between years (Table 15.2). *C. phaeobacteroides* was apparently the single most important organism in terms of direct contribution to sedimenting material in the lake throughout the summers from 2006 through 2010, despite its apparently low photosynthetic rate in situ, in Lake Kinneret (Bergstein et al. 1979). The combination shown by *C. phaeobacteroides,* of low photosynthetic rate and high contribution to overall biomass, is not unique to Lake Kinneret and has been recognized in other ecosystems (Manske et al. 2005). High contribution of photosynthetic bacteria to the carbon sedimentation flux during the bloom period is also related to the fact that the majori-

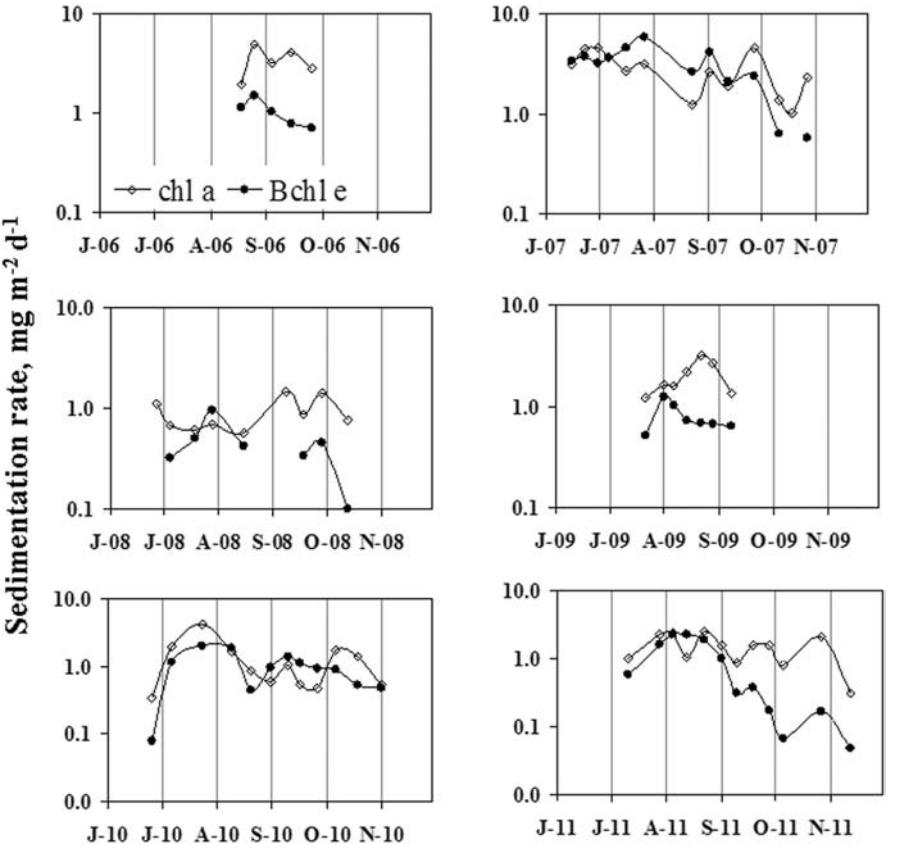

Fig. 15.6 Temporal variation of sedimentation rate of Chl *a* and BChl *e* (in milligrams per square meter per day) in seston collected in sedimentation traps located in Lake Kinneret center (station A), positioned 1.5 m above the bottom sediments. Data shown are for the period from June through November each year, 2006–2011

Table 15.2 Estimated *Chlorobium phaeobacteroides* contribution to carbon sedimenting flux in Lake Kinneret, 2006–2010

Year	Pigment sedimentation rate, mg m^{-2} d^{-1}			Carbon equivalent sedimentation rate[a], mg m^{-2} d^{-1}			*Chlorobium* contribution to sedimenting C, %	
	July–September		Year-round	July–September		Year-round	July–September	Year-round
	BChl *e*	Chl *a*	Chl *a*	BChl *e*	Chl *a*	Chl *a*		
2006	1.02	3.34	3.86	20.4	183.6	849.8	11.1	2.4
2007	3.03	2.80	4.02	60.6	153.7	884.5	39.4	6.9
2008	0.44	0.90	6.59	8.8	49.6	1,450.8	17.8	0.6
2009	0.78	1.96	2.16	15.7	107.7	475.4	14.5	3.3
2010	1.06	1.34	1.61	21.2	73.8	354.3	28.8	6.0
Average	*1.47*	*1.99*	*3.67*	*29.4*	*109.5*	*807.4*	*26.8*	*3.6*

[a] Assuming C-to-BChl *e* ratio = 20:1 (see text), and C-to-Chl *a* ratio = 55:1

ty of organic carbon is recycled within the upper productive layer while only ~20% of primary production is exported to the hypolimnion (Ostrovsky and Yacobi 2010).

References

Baltar F, Lindh MV, Parparov A, Berman T, Pinhassi J (2012) Prokaryotic community structure and respiration during long-term incubations. Microbiology open 1:214–224. doi:10.1002/mbo3.25

Bergstein T, Henis Y, Cavari B-Z (1979) Investigations on the photosynthetic sulfur bacterium *Chlorobium phaeobacteroides* causing seasonal blooms in Lake Kinneret. Can J Microbiol 25:999–1007

Beutler M, Wiltshire KH, Meyer B, Moldaenke C, Lüring C, Meyerhöfer M, Hansen U-P, Dau H (2002) A fluorometric method for the differentiation of algal populations in vivo and in situ. Photosynth Res 72:39–53

Butow B, Bergstein-Ben Dan T (1992) Occurrence of *Rhodopseudomonas palustris* and *Chlorobium phaeobacteroides* blooms in Lake Kinneret. Hydrobiologia 232:193–200

Eckert W, Frevert T, Bergstein-Ben Dan T, Cavari B-Z (1986) Competitive development of *Thiocapsa roseopersicina* and *Chlorobium phaeobacteroides* in Lake Kinneret. Can J Microbiol 32:917–921

Eckert W, Yacobi YZ, Trüper HG (1990) A bloom of a brown phototrophic sulfur bacterium in Lake Kinneret: hydrochemical aspects. Microb Ecol 20:273–282

Gophen M, Cavari B-Z, Berman T (1974) Zooplankton feeding on differentially labelled algae and bacteria. Nature 247:393–394

Hadas O, Berman T (1998) Seasonal abundance and vertical distribution of protozoa (flagellates, ciliates), and bacteria in Lake Kinneret, Israel. Aquat Microb Ecol 141:161–170

Hirabayashi H, Takasada I, Takaichi S, Inoue K, Uehara K (2004) The role of carotenoids in the photoadaptation of the brown-colored sulfur bacterium *Chlorobium phaeobacteroides*. Photochem Photobiol 79:280–285

Hurley JP, Watras CJ (1991) Identification of bacteriochlorophylls in lakes via reverse-phase HPLC. Limnol Oceanogr 36:307–315

Imhoff JF (1995) Taxonomy and physiology of phototrophic purple and green sulfur bacteria. In: Blankenship RE, Madigan MT, Bauer CE (eds) Anoxygenic photosynthetic bacteria. Kluwer Academic, Dordrecht, pp 1–15

Manske AK, Glaeser J, Kuypers MMM, Overmann J (2005) Physiology and phylogeny of green sulfur bacteria forming a monospecific phototrophic assemblage at the depth of 100 m in the Black Sea. Appl Environ Microbiol 71:8049–8060

Oelze J, Golecki JR (1988) Growth rate and the control of development of the photosynthetic apparatus in *Chloroflexus aurantiacus* as studied on the basis of cytoplasmatic membrane structure and chlorosome size. In: Olson JM, Ormerod JG, Amesz J (eds) Green photosynthetic bacteria. EMBO Workshop, Nyborg, pp 35–42

Ostrovsky I, Yacobi YZ (1999) Organic matter and pigments in surface sediments: possible mechanisms of their horizontal distribution in a stratified lake. Can J Fish Aquat Sci 56:1001–1010

Ostrovsky I, Yacobi YZ (2010) Sedimentation flux in a large subtropical lake: Spatio-temporal variations and relation to primary productivity. Limnol Oceanogr 55:1918–1931

Pinhassi J, Berman T (2003) Differential growth response of colony-forming α- and γ-proteobacteria in dilution culture and nutrient addition experiments in Lake Kinneret, eastern Mediterranean and Gulf of Eilat. Appl Environ Microbiol 69:199–211

Rimmer A, Ostrovsky I, Yacobi YZ (2008) Light availability for *Chlorobium phaeobacteroides* development in Lake Kinneret. J Plankton Res 30:765–776

Schmaljohann J, Pollingher U, Berman T (1987) Natural population of bacteria in Lake Kinneret: Observations with scanning electron and epifluorescence microscopy. Microb Ecol 13:1–12

Schwartz JIK, Eckert W, Conrad R (2007) Community structure of archaea and bacteria in a profundal lake sediment Lake Kinneret (Israel). Syst Appl Microbiol 30:239–254

Smith KM (1994) Nomenclature of the bacteriochlorophylls *c*, *d* and *e*. Photosynth Res 41:23–26

Trüper HG, Imhoff JF (1999) International Committee on Systematic Bacteriology—Subcommittee on the taxonomy of phototrophic bacteria. Int J Syst Bacteriol 49:925–926

van Gemerden H (1980) Survival of *Chromatium vinosum* at low light intensities. Arch Microbiol 125:115–121

Wynne D, Bergstein-Ben Dan T (1995) The effect of light and phosphate concentrations on phosphatase activities of the photosynthetic bacterium *Chlorobium* spp. Can J Microbiol 41:278–283

Yacobi YZ, Eckert W (2002) Determination of spatial distribution of *Chlorobium phaeobacteroides* with the aid of a submersible multi-channel fluorometer. 8th Symposium on Aquatic Microbial Ecology, October 25–30, 2002, Taormina (Messina), Italy, p 54

Yacobi YZ, Schlichter M (2004) GIS application for mapping of phytoplankton using a multichannel fluorescence probe derived information. In: Chen Y, Takara K, Cluckie ID, Hilaire De Smedt F (eds) GIS and remote sensing in hydrology, Water Resources and Environment, IHAS Publication 289: 301–307, International Association of Hydrological Sciences Press, Wallinford, UK

Yacobi YZ, Eckert W, Truper HG, Berman T (1990) High performance liquid chromatography detection of phototrophic bacterial pigments in aquatic environments. Microb Ecol 19:127–136

Yutin N, Suzuki M, Rosenberg M, Rotem D, Madigan MT, Sülling J, Imhoff JF, Béja O (2009) *BchY*-based degenerate primers target all types of anoxygenic photosynthetic bacteria in a single PCR. Appl Environ Mirobiol 75:7556–7559

Chapter 16
Fish Biology and Ecology

Ilia Ostrovsky, Menachem Goren, James Shapiro, Gregory Snovsky and Alex Rynskiy

Abstract The chapter summarizes current knowledge on fish biology in Lake Kinneret. Nineteen native fish species belonging to six families populate the lake. Three of these species are endemic to the lake and four other species are endemic to the Jordan Valley system. Eight alien species are found in the lake. Four of them are breeding in nature, three cannot breed but are regularly stocked, and one is a hitchhiker that cannot breed. Growth rate equations and weight-length relationships are presented for the dominant cyprinids (*Mirogrex terraesanctae, Hypophthalmichthysmolitrix, Cyprinus carpio, Barbuslongiceps, Capoetadamascina, Carasobarbuscanis*), cichlids (*Oreochromisaureus, Sarotherodon galilaeus, Tilapiazillii, Tristramellasimonis*), grey mullets (*Lizaramada, Mugilcephalus*), and catfish (Clariasgariepinus). The long-term changes in fish community composition in the lakewere associated with introduction and invasion of fishes; changes in fishing intensity; modifications of the littoral, and changes of the lake ecological regime. Temporal dynamics, spatial distribution, total abundance and biomass of fish in the lake were studied based on long-term hydroacoustic monitoring. The size structure and abundance of fish in the pelagic zone of the lakedisplay explicitseasonal changes associated with fish spawning migrations and winter-spring recruitment of the dominant bleak M. terraesanctae. Water level fluctuations beyond natural have modified the littoral habitats, which are of specific importance during different life

I. Ostrovsky (✉) · A. Rynskiy
The Yigal Allon Kinneret Limnological Laboratory, Israel Oceanographic & Limnological Research, P.O. Box 447, 14950 Migdal, Israel
e-mail: ostrovsky@ocean.org.il

A. Rynskiy
e-mail: rynskiy@ocean.org.il

M. Goren
Department of Zoology, Tel Aviv University, 69778 Tel Aviv, Israel
e-mail: gorenm@tauex.tau.ac.il

J. Shapiro · G. Snovsky
Fishery Department, Ministry of Agriculture and Rural Development, 14100 Tiberias, Israel
e-mail: Jamess@moag.gov.il

G. Snovsky
e-mail: gregorys@moag.gov.il

T. Zohary et al. (eds.), *Lake Kinneret, Ecology and Management,* Aquatic Ecology Series 6,
DOI 10.1007/978-94-017-8944-8_16,

stages of fish. Water level has an immense impact on fishreproduction, survival, recruitment, population dynamics, and eventually determines the catches of commercially important species.

Keywords Cichlids · Mugilids · Cyprinids · Water-level fluctuations

16.1 Introduction

Interest in the fishes of Lake Kinneret goes back to the dawn of human history, when hunter-gatherer peoples fished in the lake (Zohar 2003). As evident from the New Testament (Luke 5:1–11), fishing was a common practice among the inhabitants of the Galilee. The first modern scientist to study the fishes of the lake was the Swedish naturalist Hasselquist[1] (1757), who collected the St. Peter's fish *Sarotherodon galilaeus,* which was described by Linnaeus (1758) as *Sparus galilaeus*. The last of the lake fish species to be described as new to science is the most common fish in the lake—*Mirogrex terraesanctae* (Steinitz 1952), referred to in some publications as *Acanthobrama terraesanctae*. In the mid-nineteenth century, the Holy Land became a fashionable target for European scientists, who have published since then articles on the fishes of the Jordan Valley and Lake Kinneret (Cuvier and Valenciennes 1840, 1842; Heckel 1843; Günther 1865, 1866; Lortet 1875, 1876, 1883; Tristram 1884; Pellegrin 1911, 1923, 1933; Tortonese 1938, 1952; Trewavas 1942, 1965; Ricardo-Bertram 1944; Kosswig 1950, 1961, 1967; Komarovsky 1952; Banarescu et al. 1982; Krupp 1987; Krupp and Schneider 1989). The first Israeli scientist to study the Jordan Valley fishes was Bodenheimer (1935). He was followed by Steinitz (1952, 1953, 1954, 1959), Ben-Tuvia (1959), Steinitz and Ben-Tuvia (1957, 1960), Fishelson (1962, 1966, 1967), Goren (1972, 1975, 1983), and Goren et al. (1973).

Nineteen native fish species belonging to six families have been reported from Lake Kinneret (Table 16.1). Three of these species are endemic to the lake and four species are endemic to the Jordan Valley system. One species that was identified as *Paracobitis tigris* is probably an undescribed one. Eight alien species are common in the lake. Four of them are breeding in nature (*Cyprinus carpio, Gambusia affinis, Oreochromis aureus* hybrids*, Xiphophorus hellerii*), three of them do not breed in the lake but are regularly stocked (*Hypophthalmichthys molitrix, Mugil cephalus, Liza ramada* = *Mugil capito*; Cuvier 1829), and one is a hitchhiker (*Anguilla anguilla*) that arrived with the stocked *Mugil* but does not reproduce in the lake (Goren and Ortal 1999; Roll et al. 2007).

[1] *Fredrik Hasselqvist (1722–1752) died while touring the Middle East. His notes were edited and published by Linnaeus.*

Table 16.1 The fishes of Lake Kinneret, their habitat, food and biogeographic affiliation (numbers in parentheses represent the references listed in the table footnotes)

Family	Species	Common name	Hebrew name	Habitat	Food (in Lake Kinneret)	Origin
	Native species					
Blenniidae	*Salaria fluviatilis* (Asso, 181)	Blenny	Karnun naharoni	Shallow waters among stones (3, 8)	Benthic invertebrates (3)	Mediterranean
Cichlidae	*Astatotilapia flaviijosephi* (Lortet, 1883)[a]		Amnunit yosef	In shallow water among rocks and stones (8)	Benthic invertebrates (16)	Africa
Cichlidae	*Oreochromis aureus* (Stiendachner 1864)	Blue tilapia	Amnun ha'yarden	Throughout the lake (8)	Adults: filter feeders, herbivorous, detritus, zooplankton (15, 19)	Africa
Cichlidae	*Sarotherodon galilaeus* (Linnaeus, 1758)	Mango tilapia, St. Peter's fish	Amnun ha'galil	Pelagic schools in winter, littoral in couples in spring and summer	Young: visual feeding, mostly zooplankton; adults and young (>50 mm): filter feeding, large algae, mostly *Peridinium* (5, 13, 19)	Africa
Cichlidae	*Tilapia zillii* (Gervais 1848)	Common St. Peter's fish	Amnun matsuy	Throughout the lake (20)	Omnivorous: zooplankton, zoobenthos, and higher plants (14)	Africa
Cichlidae	*Tristamella sacra* (Günther 1864)[b]		Tvarnun listani	Among immersed vegetation around the lake (8)	Fish, crustaceans, insects (2)	Africa
Cichlidae	*Tristramella simonis* (Günther 1864)[b]		Tvarnun hakinneret	Throughout the lake (8)	Plankton, benthic plants, invertebrates, zooplankton, small fish (2)	Africa
Clariidae	*Clarias gariepinus* (Burchell 1822)	Catfish	Sfamnun	Benthic, littoral, during winter concentrates near hot springs in winter (8, 9)	Omnivorous: invertebrates, fish, plants, seeds, mollusks (9, 20)	Africa
Cyprinidae	*Barbus longiceps* (Valenciennes 1842)[a]	Barbel	Binit arukat rosh	Benthic, littoral, adults descend in winter to deeper waters (8)	Zoobenthos and young fish (2, 9)	Asia

Table 16.1 (continued)

Family	Species	Common name	Hebrew name	Habitat	Food (in Lake Kinneret)	Origin
Cyprinidae	*Mirogrex terraesanctae* (Steinitz 1952)[b]	Kinneret bleak	Lavnun ha'kinneret	Pelagic (8)	Zooplankton: prefer cladocera in winter feed from bottom: musquito larvae, nematods (1, 2, 6, 7, 10, 19)	Middle East
Cyprinidae	*Acanthobrama lissneri* Tortonese 1952[a]		Lavnun lisner	Vegetated and stony habitats around the lake (8)	Zoobenthos and algae (9)	Middle East
Cyprinidae	*Carasobarbus canis* (Valenciennes, 1842)[a]		Binit gdolat kaskas	Benthic and pelagic (8)	Juvenile fish (Lavnun) and pelagic and benthic invertebrates (16)	Asia–Africa
Cyprinidae	*Capoeta damascina* (Valenciennes, 1842)		Hafaf	Benthic (8)	Algae, detritus, benthic invertebrates (8)	Middle East
Cyprinidae	*Garra rufa* (Heckel 1843)	Reddish log sucker, Levantine sucker	Agulest	Benthic, on stones in littoral and thermal sprigs (8)	Scratching algae and detritus from surface of rocks, benthic invertebrates (9)	Asia
Cyprinidae	*Hemigrammocapoeta nana* (Heckel 1843)		Yableset	Vegetated and stony habitats around the lake (8)	Zoobenthos and algae (8)	Middle East
Cyprinidae	*Pseudophoxinus kervillei* (Pellegrin 1911)		Lavnunit ha'galil	Stony habitats around the lake (8)	Zoobenthos and algae (8)	Asia–Europe
Cyprinodontidae	*Aphanius mento* (Heckel 1843)	Pupfishes	Na'avit kahula	Vegetated habitats around the lake (8)	Zooplankton, zoobenthos, and filamentous algae (8)	Asia
Balitoridae	*Oxynoemacheilus tigris* (Heckel 1843)[c]		Binun kinnarti	Stony habitats around the lake (8)		Asia–Europe
	Alien species					
Cichlidae	*Oreochromis aureus hybrids*		Amnun ha'yarden	Throughout the lake (8)	Zooplankton benthic organisms and detritus (15)	Oreochromis niloticus X O. aureus
Cyprinidae	*C. carpio Linnaeus* 1758	Common carp	Karpion matsui	Inshore throughout the lake (8)	Bottom invertebrates and detritus (20)	Asia

Table 16.1 (continued)

Family	Species	Common name	Hebrew name	Habitat	Food (in Lake Kinneret)	Origin
Poeciliidae	*Gambusia affinis* (Baird and Girard 1853)	Mosquito fish	Gambusia metsuya	Littoral, protected bays in shallow water among plants (20)	Crustaceans, insects, fish larvae, and algae (8)	North America
Poeciliidae	*Xiphophorus hellerii* Heckel 1848	Green swordtail	Saifan	Rare, vegetated areas (20)	Aquatic insects, zoobenthos, and fish larvae (18)	North America
	Regularly stocked species (alien)					
Cyprinidae	*Hypophthalmichthys molitrix* Valenciennes, 1844	Silver carp	Kasif	Pelagic (20)	Filter feeder, phytoplankton (Peridinium bloom), and zooplankton (11, 16)	China
Mugilidae	*Mugil cephalus* Linnaeus 1758	Flathead grey mullet	Kipon gdol rosh	Inshore pelagic (20)	Planktonic and benthic organisms and detritus (2, 18)	Mediterranean Sea
Mugilidae	*Liza ramada* (Risso, 1827) (=*Mugil capito* Cuvier 1829)	Thinlip grey mullet	Kipon tober	Inshore pelagic, in small schools (18)	Planktonic and benthic organisms and detritus (12)	Mediterranean Sea
	Hitchhiker species (alien)					
Anguillidae	*Anguilla anguilla* Linnaeus 1758	European eel	Tslofach	Benthic (18)	Piscivore (4)	Atlantic Ocean, Mediterranean, and Black Sea

1 Azouly and Gophen 1992, *2* Ben-Tuvia 1978, *3* Gasith and Goren 2009, *4* Golani et al. 1988, *5* Gophen 1980, *6* Gophen and Landau 1977, *7* Gophen and Scharf 1981, *8* Goren 1983, *9* Goren and Gasith 1999, *10* Landau et al. 1988, *11* Shapiro 1985, *12* Shapiro 1998, *13* Spataru 1976, *14* Spataru 1978, *15* Spataru and Zorn 1978, *16* Spataru and Gophen 1985b, *17* Spataru et al. 1987, *18* Zismann 1976, *19* Zohary et al. 1994, *20* Personal unpublished data

[a] Endemic to the Jordan Valley system

[b] Endemic to Lake Kinneret

[c] Taxonomic status needs clarification

Table 16.2 The weight–length and von Bertalanffy growth equations of dominant fish species in Lake Kinneret

Species	Weight–length relationship $W = a\,L^b$			von Bertalanffy growth equation $L_t = L_\infty\,(1\text{-}e^{-kt})$		
	a	b	Reference	L_∞	k	Reference
S. galilaeus	0.0177	3.07	1	35.0	0.495	3
O. aureus	0.0958	2.47	1	31.3	0.598	3
T. simonis	0.0148	3.12	1	20.0	0.635	3
T. zillii	0.0179	3.06	1	20.7	0.480	1
M. terraesanctae[*]	0.0047	3.24	2	34.2	0.173	4
Male	–	–	–	22.4	0.326	4
Female	–	–	–	29.2	0.247	4
C. carpio	0.0074	3.22	1	105.8	0.390	1
H. molitrix	0.0106	3.04	1	133.0	0.267	5
B. longiceps	0.0171	2.86	1	–	–	–
C. canis	0.0254	2.77	1	–	–	–
C. damascina	0.114	2.31	1	–	–	–
C. gariepinus	0.0204	2.75	1	125.0	0.444	1
M. cephalus	0.0088	3.04	1	89.1	0.194	6
L. ramada	0.0078	3.03	1	57.6	0.237	6

L is total length in cm, W is weight in g, L_t is the total fish length in cm at age t(yr), k is growth coefficient in yr^{-1}, Fish age is counted from the moment of time when $L = 0$

1 author's original data, 2 Ostrovsky and Walline 2001, 3 recalculated from Ben-Tuvia 1959, 4 recalculated from Ostrovsky and Walline 1999, 5 recalculated from Snovsky 2000, 6 recalculated from Snovsky 1993

[*]Growth rates of *M. terrascantae* males and females are different. For practical reasons a "mixed" von Bertalanffy equation was computed taking into consideration the difference in growth rate of males and females and decrease in proportion of males with length. The "mixed" equation allows calculating reasonably well size-specific growth rate of the bleak; however, the coefficients of such a "mixed" equation are unrealistic

16.2 Fish Biology

The biology of Lake Kinneret fish was reviewed by Ben-Tuvia (1978), Reich (1978), Goren (1975), and Ben-Tuvia et al. (1992). A summary of the available information on habitat and food preferences of the Kinneret fishes and their geographical region of origin are presented in Table 16.1. Information on body growth and weight–length relationships of the dominant fish species is summarized in Table 16.2. Additional information regarding the most abundant species is presented hereafter.

Cichlidae Four out of the six Kinneret cichlids have commercial value (*O. aureus, S. galilaeus, Tristramella simonis,* and *Tilapia zillii*), and another two are either too small (*Astatotilapia flaviijosephi*) or too rare (*Tristramella sacra*). All cichlids in the lake are fish of African origin. Two species of this group (*Tilapia sacra, T. simonis*) are endemic to the lake, one (*A. flaviijosephi*) is endemic to the central Jordan River basin, while the other three cichlids (*O. aureus, S. galilaeus,* and *T. zillii*) are widely distributed in Israel and Africa. The presence of these two groups of cichlids in the Jordan Valley may reflect at least two waves of biogeographical migration

from the coastal system (Goren and Ortal 1999). As these fishes are of tropical and subtropical origin, they are sensitive to low temperatures and show poor growth and high mass mortality during winter (Chervinski and Lahav 1976). Due to their affiliation to warm water, some of Kinneret cichlids concentrate near the warm salt springs in the western side of the lake when water temperature drops below 14–16 °C in winter. In extremely cold winters (e.g., 1991–1992), when temperature dropped below 12–13 °C, high mortality of these fish was reported (Shapiro and Snovsky 1997).

S. galilaeus is a biparental mouthbrooder fish spawning up to five times from April to August, with each progressive spawn containing smaller numbers of eggs (Ben-Tuvia 1978; Balshine-Earn 1994). During the nesting season, these fish show territorial behavior. The most intensive reproduction occurs in April–May. During this period adults inhabit shallow (< 1.5 m) areas protected from the wind and waves by either lagoons or inundated vegetation that has developed around the lake at low water levels over the past two decades (Gasith and Gafny 1990). During most of the year, adult *S. galilaeus* move in schools of various sizes in open waters, while breeding adults and juveniles inhabit the littoral. *S. galilaeus* is the most commercially valuable cichlid species in Lake Kinneret (Chap. 36).

The other cichlid species (except *T. zillii*) are female mouthbrooders. During the breeding season (spring and summer), males possess territories in shallow water and court females that enter their territory. After spawning, the females take the fertile eggs into their mouth cavity and leave the area. Females of *T. zillii* spawn in nests or burrows, dug by the males. Both parents guard the brood and later the school of juveniles for a few days (Ben-Tuvia 1959; Goren 1983; Bruton and Gophen 1992).

Juveniles of all cichlids live in rocky or vegetated areas in the littoral, while adults of *T. simonis* and *O. aureus* are found during most of the year forming schools in the open water. *T. sacra* was found among reeds near the shore and in springs around the lake. Multiannual decrease in water level caused disappearance of its habitat and *T. sacra* have been listed as extinct since 1990 (Goren 2003).

Clariidae The African catfish *Clarias gariepinus* is the largest native freshwater fish in Israel (up to 1.5 m in length and 20 kg body weight). The fish is an omnivore and feeds on invertebrates and fish (Spataru et al. 1987; Goren and Gasith 1999). Being a scavenger (in addition to being a predator), the catfish plays a "sanitary" role in the lake as it preys on carrion of fish and birds. Its breeding season starts in March–April when the catfish migrate into the lagoons and remain there until June. The number of eggs ranges between 150,000 and 200,000 per kg of body weight (Goren and Gasith 1999).

Cyprinids Four out of the eight native lake cyprinids are objects of fisheries. The most important cyprinid from both, ecological and economical aspects is the Kinneret bleak *M. terraesanctae* (Hebrew name: lavnun ha'kinneret). This is the dominant fish in Lake Kinneret by abundance (> 80 %) and biomass (> 50 %; Walline et al. 1992). *M. terraesanctae* spawns from November to March when water levels rise. The bleak eggs are adhered to freshly inundated, epiphyton-free stones in very shallow water (< 30 cm; Gafny et al. 1992). The emerged larvae stay for some time in shallow area, but usually they are dispersed by currents to the pelagic zone and

inhabit the upper part of the water column during winter and early spring; then the young-of-the-year fish form schools that live in the open water. Due to its high abundance and feeding on zooplankton (Gophen and Landau 1977; Gophen and Scharf 1981; Landau et al. 1988; Azoulay and Gophen 1992), the bleak has a significant impact in the food web of the lake (Walline et al. 2000; Ostrovsky et al. 2013). The dependence of *M. terraesanctae* reproduction success on the availability of freshly inundated stones in the shallow littoral causes the population dynamics of this species to be sensitive to large fluctuations in water level taking place in Lake Kinneret over the past two decades, as discussed below.

The three barbel species (*Carasobarbus canis, Barbus longiceps,* and *Capoeta damascina*) inhabit mainly the shallow water. *C. canis* and *B. longiceps* are frequently observed together with *M. terraesanctae* fry, which is one of the barbel's food components (G Snovsky and J Shapiro, unpublished data). Barbels spawn from November to March. *B. longiceps, and C. damascina* migrate in autumn upstream the surrounding rivers, where they spawn. A hybrid of these two species has been often observed in the lake and surrounding rivers (Stoumboudi et al. 1992; Fishelson et al. 1996).

The carp, *C. carpio,* was stocked only at the end of the 1940s with the scaled carp variety. Stocking was not repeated, but since then the population was bolstered by escapees (mirror carp variety) from the surrounding fishponds. Since the late 1980s, conditions for the natural reproduction of carp in the lake became favorable due to the formation of large littoral areas with flooded vegetation, and the catch of carps has increased considerably (see Chap. 36). At the same time, the mirror carp variety, which was abundant in the 1960s–1980s, was replaced by the wild-type-scaled carp, such that in the late 1990s the all-scaled fish already accounted for >96% of the entire population (Shapiro and Snovsky, unpublished data). This reflects a decrease in abundance of escapees (mirror carps) and possibly more advantageous conditions for scaled carp reproduction in the lake.

The silver carp *H. molitrix,* which was stocked periodically since 1969, grows in the lake as fast as in ponds (Shefler and Reich 1977) and achieves a weight of 20–30 kg in 5–8 years (Snovsky 2000). Leventer and Teltsch (1990) reported that in the Netofa reservoirs *H. molitrix* achieves a weight of 6–15 kg in 6–8 years. Silver carp is stocked in an attempt to reduce the amount of phytoplankton and improve water quality (Shapiro 1985; Spataru and Gophen 1985a; Snovsky and Pizanty 2002; Chap. 36).

Mugilildae The grey mullets *L. ramada* and *M. cephalus* have been stocked in the lake since 1963 in order to make use of benthic resources while supporting the commercial fishery (Bar-Ilan 1975; Reich 1978; Shapiro 1998). About 28% of stocked grey mullets are landed. The mean natural mortality rates were 0.39 yr_{-1} and 0.30 yr_{-1} for L. *ramada*, M. *cephalus*, respectively (Snovsky and Ostrovsky 2014). *L. ramada* is the more abundant (>75%) grey mullet species in the lake. In November–January, *L. ramada* forms large schools, which become an easy target for fishermen, leading to winter catch maxima. In contrast, *M. cephalus* does not form large schools and its catches are distributed more uniformly throughout the year. Since the decline of the harvest of cichlids and bleak in recent years, grey mul-

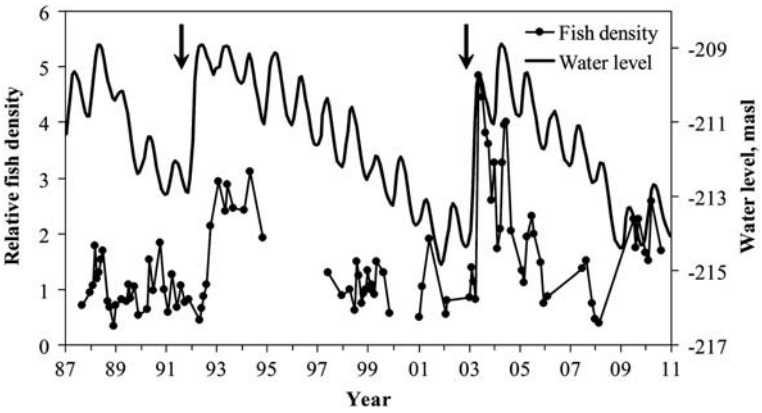

Fig. 16.1 Time series of water level and fish abundance in Lake Kinneret. *Arrows* mark the two events of 4 m (winter 1991–1992) and 4.7 m (winter 2002–2003) rise in water level. Fish density (mainly *M. terraesanctae*) was determinated based on hydroacoustic surveys. The relative density of fish in a given date was computed as a ratio of the estimated density of fish (acoustic targets >-60 dB) to the mean density prior to the rapid rise in water level, computed for two periods of averaging: 1987–1991 and 1997–2002. The fish abundance data were collected with a 70-kHz Simrad single-beam echo sounder (model EY-M) during 1987–1994, 120-kHz Biosonics dual-beam echo sounder (model 102) during 1997–1999, and 120-kHz Biosonics dual-beam echo sounder (model DE5000) after 2001. For more details on the acoustic surveys see Walline et al. (1992). (Adapted from Ostrovsky et al. 2013 with permission of Wiley)

lets have become the most valuable commercial fish in the lake and account for up to 65 % of the value of the total catch (Snovsky et al. 2010).

16.3 Effect of Water Level Fluctuation on Fish

Since the early 1990s, high rates of water consumption relative to water supply led to three distinct long-term periods of gradual decrease in water level and to a general increase in the amplitude of water-level fluctuations (Fig. 16.1). These changes affect the availability of spawning habitats in the littoral (Chap. 29). At high water levels, the proportion of hard substrates (gravel, boulders, and rocks) in the littoral zone is much higher than at low water levels, when sand and silt become the dominant substrate. Hard-substrate habitats are favorable for the development of diverse periphytic and invertebrate communities, and provide good feeding conditions for herbivore, planktivore, and benthivore fishes and their fingerlings (Gasith and Gafny 1990). The hard substrates also provide refuge and breeding sites for different fishes (Gafny et al. 1992; Chap. 36). Therefore, at high water levels the density of fish and the diversity of their communities in the littoral zone are notably larger than at low water levels (Gasith et al. 1996, 2000; Gasith and Goren 2009).

The long-term decreases in water levels and enlarged seasonal fluctuations favored the development of another ecologically important fish habitat in the litto-

ral—inundated terrestrial plants. These plants proliferated in the exposed shores at the lake circumference when water level dropped below −212 m above mean sea level, i.e., about 3 m below the lake's maximal water level (−209 m; Gasith and Gafny 1990); then, these plants were inundated after subsequent winter–spring floods (Gafny and Gasith 2000). Especially wide areas of inundated plants were observed over 2–3 years following the extreme water level rises of 1991–1992 and 2002–2003. Such well-protected littoral areas served as preferred refuge and spawning habitat for the cichlids and cyprinids, where they could also find plenty of periphyton and invertebrate food. The flooded vegetation also provided protected nursing grounds for fish fry and fingerlings, increasing their survival (Gasith and Gafny 1998; Chap. 29) and eventually leading to increased catches of the commercially valuable species (*S. galilaeus, C. carpio*) after 1–2 years lag time (Chap. 36).

Another species apparently benefits the increased abundance of inundated vegetation was *H. molithrix,* an introduced species whose catch, despite a decline in the rate of its stocking, was greatly increased 2–3 years after the development of the inundated vegetation areas (Chap. 36). This suggests improved survival of the stocked fingerlings, which probably also use the inundated vegetation for feeding and refuge.

Large water-level fluctuations also affect the population dynamics of the bleak *M. terraesanctae*. Gradual declines in the annual mean water level from 1988 to 1991 and again from 1995 to 2002 resulted in reduced availability of suitable spawning substrates (freshly inundated rocks and stones). These gradual water level declines were followed by two extremely rainy winters (1991–1992 and 2002–2003) resulting in a 4–5-m rise in water level within a single season and large increases in the availability of spawning sites for *M. terraesanctae*. These water level rises were highly favorable for bleak reproduction and fingerlings survival (Ostrovsky and Walline 1999; Gafny and Gasith 2000; Zohary and Ostrovsky 2011). Consequently, the density of *M. terraesanctae* fingerlings increased sharply following the years with exceptional water level rise (Fig. 16.1).

The rapid increases in *M. terraesanctae* abundance were followed by increases in fish biomass with 1–2 years lag time (Ostrovsky and Walline 1999, 2001). A misbalance between food requirements of these zooplanktivorous fish and zooplankton productivity (Ostrovsky and Walline 2001; Zohary and Ostrovsky 2011) can explain the collapses of the zooplankton (mainly copepods) observed in 1993–1994 and again in 2004–2005 (Gal and Anderson 2010, Chap. 13). These collapses led to food shortage that affected mainly the post-spawning *M. terraesanctae,* as indicated by lowered body condition index (BCI) in larger-size fish in 1994–1995 (Fig. 16.2) and 2004–2005 (unpublished data) and by increased fish mortality. A huge decline in the proportion of fish with body size exceeding the minimal required for commercial harvest caused a collapse of the bleak fishery in 1994 and again in 2005 (Ostrovsky et al 2013, Chap. 36).

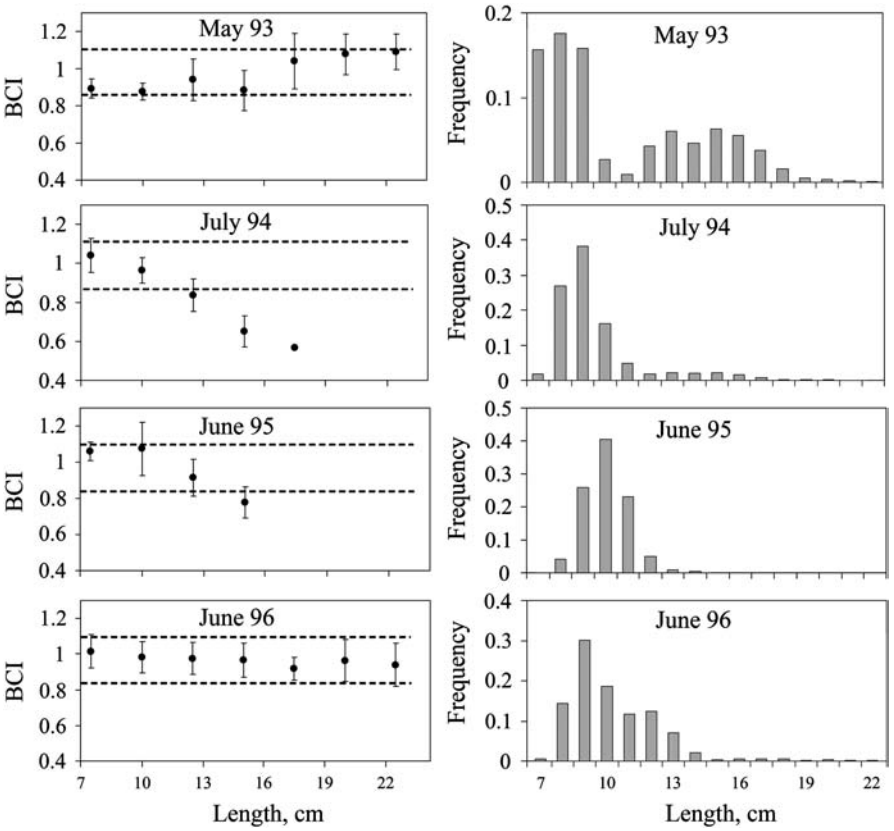

Fig. 16.2 Changes in body condition index (BCI) and length–frequency distribution of Lake Kinneret bleak *M. terraesanctae* in 1993–1996. Sharp decline in the BCI occurred in larger-size (>12 cm) fish in 1994 and 1995, 2–3 years after an unusual increase in abundance of these zooplanktivorous fish and 1–2 years after the lowest-ever record of zooplankton abundance (1993). Disappearance of larger fish from the population co-occurred with the poor BCI of adult individuals, affecting high mortality

16.4 Spatial Variability and Abundance of Pelagic Fish

The abundance and spatial distribution of pelagic fish in Lake Kinneret are being monitored routinely since the late 1980s, along 14 transects, using scientific echo sounders (Walline et al. 1992; 2000; Ostrovsky et al. 2013). Those acoustic surveys indicate that the spatial distribution of fish is highly heterogeneous (Fig. 16.3). In winter and early spring, fish larvae concentrate in the north, where lake productivity is higher than in other areas (Ostrovsky and Sukenik 2008; Ostrovsky and Yacobi 2009) and newly born fish (predominantly *M. terraesanctae*) may have better feeding conditions for growth and survival. During that time, the larvae populate the upper 5–10-m stratum in the pelagic zone (Fig. 16.4a). In summer and fall, when

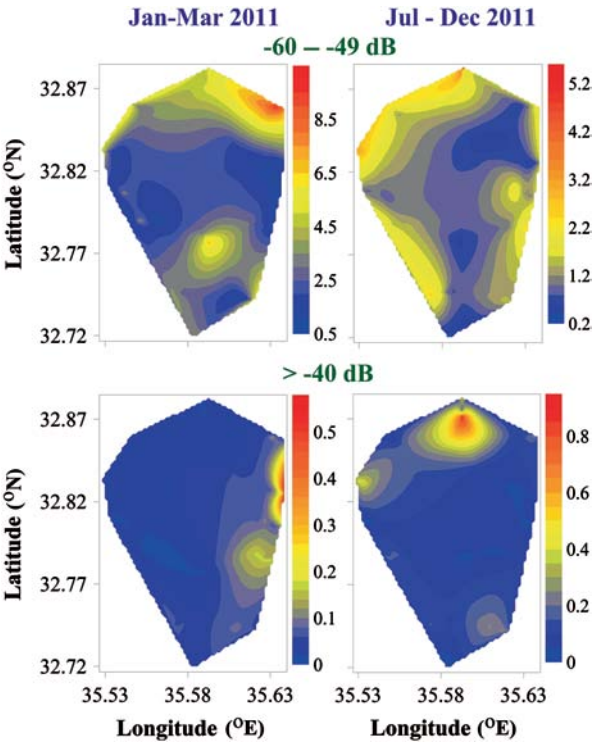

Fig. 16.3 Spatial distribution of depth-integrated fish density in 2011. *Upper panels:* small fish (−60 to −40 dB, mainly *M. terraesanctae)*; *lower panels:* large fish (>−40 dB, mainly commercially valuable species); *left panels:* distributions during the holomixis (averaged from three surveys from January to March), *right panels:* distributions during the stratified period (averaged from five surveys from July to December). *Color bars* show the fish density in ind m^{-2}. Small fish concentrate in the northern section of the lake during holomixis and at the sublittoral areas around the lake during the stratified period. Larger fish migrate all over the lake, but the higher mean density is usually observed near the Jordan inlet zone (northern tip)

the metalimnion and hypolimnion are anoxic, fish are usually concentrated at the lake periphery (Fig. 16.3), where boundary-mixing processes induce sediment resuspension (Ostrovsky and Yacobi 2010), increase local productivity (Ostrovsky et al. 1996), and thus may improve local feeding conditions. During that time, larger fish (possibly mullets, barbells, carps) concentrated at the upper part of the metalimnion (Fig. 16.4b), where cooler water could be a thermal refuge for these fish as surface water temperatures in Lake Kinneret exceed 30 °C in summer. It is also possible that higher concentration of resuspended particulate matter, sinking detrital particles, and some planktonic organisms in such locations may, in turn, attract the benthos- and plankton-feeding fish. It was shown that the lateral heterogeneity in the distribution of the zooplanktivore *M. terraesanctae* can be associated with the lateral distribution of their prey (Kalikhman et al. 1995). Specifically, these authors found "patchy correlation zones," i.e., zones where strong positive and/or negative correlations occurred between distribution fields of the fish and the zooplankton in the lake. The formation of such zones can be attributed to *M. terraesanctae*'s foraging behavior and feeding migrations.

The large majority of the total number of fish in the lakes is due to small individuals, mostly fish larvae, which have acoustic size (target strength, TS) of less than −60 dB (<3 cm length). These small fish exhibit highest abundance in winter and early spring, when *M. terraesanctae* larvae are dispersed by currents and appear

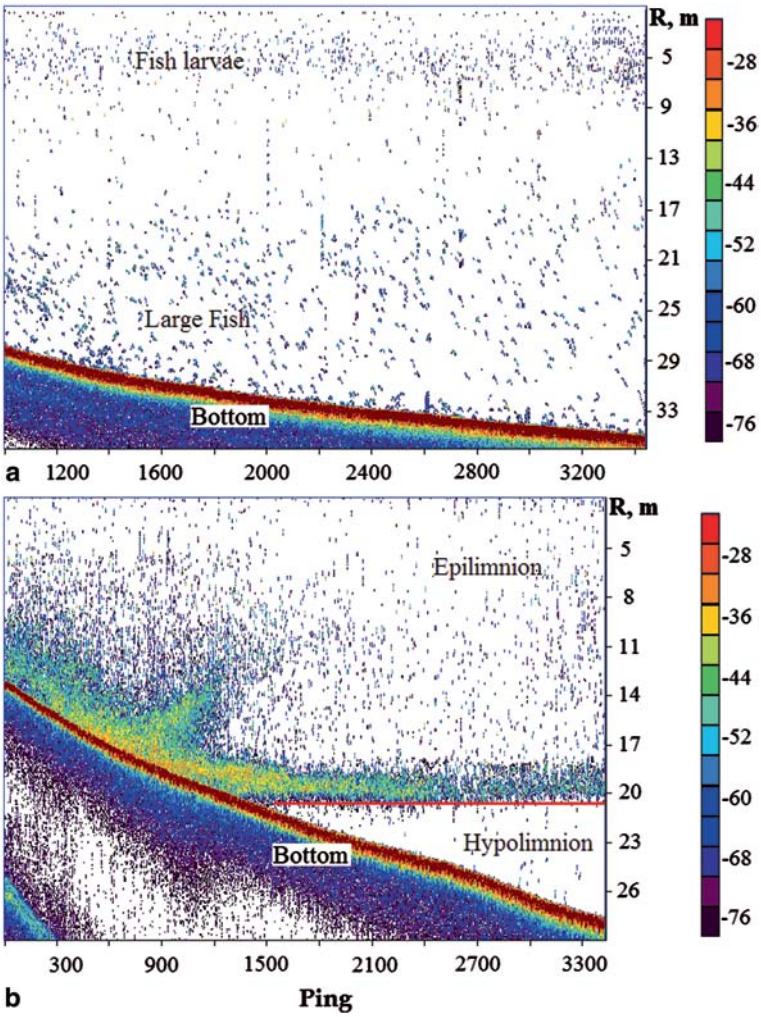

Fig. 16.4 Echograms of fish distributions along two transects. **a** A transect taken during holomixis (February 2011, Gofra). Scattered fish are seen in the entire water column. Clouds of *M. terraesanctae* larvae (< −60 dB) inhabit the upper part of the lake, while larger fish are more dispersed and inhabit the deeper part of the water column. **b** A transect taken during lake stratification (September 2011, Akeb), when anoxia prevailed in the hypolimnion (> 18 m water depth). The majority of fish (*reddish, yellow,* and *green* structures) were concentrated at the thermocline-bottom interface, at the top of the sublittoral bottom, and at the top of the metalimnion (16–18 m), while the dispersed fish were seen in the upper and mid-epilimnion. *Horizontal red line* shows the location of the mid-metalimnion. Below this line, targets seen refer to methane bubbles rising from the bottom; bubbles are commonly abundant at low water levels (for more details see Ostrovsky 2009a, b). The data were collected at a rate of five pings per second. Range (*R*) shows the distance from the transducer, which was mounted 0.8 m below the water surface. A legend relates the color of pixels on the echogram to volume backscattering strength (dB re 1 m^{-1})

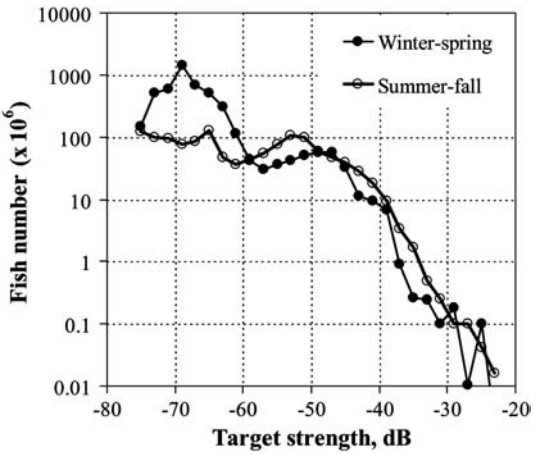

Fig. 16.5 Abundance of fish of different acoustic sizes (target strength, TS) in 2012. Fish abundance was evaluated in the pelagic zonefor winter-spring (February-March) and summer-fall (July-October). The fish abundance data were collected with a 120-kHz Simrad scientific split-beam echo sounder (model EK60). Peripheralareaswith bottom depth < 7–10 m depth were not acoustically surveyed.

in the pelagic zone (Fig. 16.5). Fast growth of the young-of-the-year explains an increase of fingerling (−59 to −49 dB, or 3–5 cm) abundance from winter to summer. In the pelagic zone, the number of larger fish (>−45 dB) also increases from winter to summer. Such an increase can be attributed mainly to seasonal migration of *M. terraesanctae* from the littoral, where these fish are concentrated during the spawning season, to deeper waters.

For assessment of total fish abundance, the minimal TS limit was usually set to −60 dB to disregard the larvae—a highly variable and the most abundant part of the population. Our evaluations of fish number in summer–fall time when most of the fish stay in the pelagic zone and can be accurately quantified with an echo sounder show that the total number of fish in the pelagic zone in 2011 and 2012 was 270 and 590 million, respectively. The last number is higher than the maximal value of 280 million reported for the period of 1987–1994 (Ostrovsky and Walline 2001), which may reflect an increase in the *M. terraesanctae* stock due to a decrease in its landing (cf. Chap. 36).

To approximate fish biomass using the acoustic surveys, we computed the following average TS–length (*L,* cm) relationship, based on the published data for various freshwater fish species (Horn et al. 2000; Rudstam et al. 2003; Mehner et al. 2010):

$$TS = 22.7 \log L - 70.3 \tag{16.1}$$

To evaluate fish biomass, a combined weight (*W,* g)–length (*L,* cm) relationship was calculated for the three most abundant fishes in Lake Kinneret (*M. terraesanctae, L. ramada,* and *M. cephalus*):

$$W = 0.00604 \cdot L^{3.11}. \tag{16.2}$$

The contributions of different size groups to the total fish abundance and biomass are illustrated in Fig. 16.6. The fish of the intermediate-size group of −47 to −33 dB

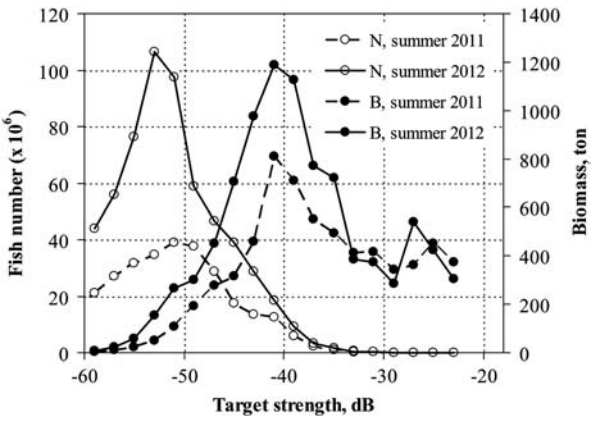

Fig. 16.6 Abundance (*N*) and biomass (*B*) of fish of different acoustic sizes (target strength, TS) in summerfall of 2011 and 2012. Acoustic surveys carried out in that time better represent the abundance and biomass of fish in the lake, because in summer and fall the dominant fish species inhabit the pelagic areas and thus can be properly sampled by the echo sounder. Other explanations as in Fig. 16.5

play an important role in formation of the total fish biomass, while fish smaller than −47 dB largely contribute to the total fish number. The estimated total biomass of pelagic fish in Lake Kinneret was 6,400 and 9,100 t in the summer of 2011 and 2012, respectively. Implementation of the Walline's TS–*L* relationship of bleak (Horne et al. 2000) would lessen the assessed biomass by ~30% and be closer to the previous estimates of 3,500–6,000 t (Walline et al. 1992; Ostrovsky and Walline 1999). Still, the accuracy of the presented values can be considered after detailed experimental measurements of TS–*L* relationships of dominant fishes in Lake Kinneret.

Extreme overfishing of large commercially important fish species (Ostrovsky 2005; Ostrovsky et al. 2013) caused a decrease in their biomass in the lake over the past decade. Concurrently, *M. terraesanctae* biomass increased due to reduced fishing pressure (Chap. 36). Combined, these two trends could substantially shift the fish community in favor of the zooplanktivore bleak. Because *M. terraesanctae* has gained the ability to control zooplankton abundance under some circumstances (see above), these changes could make the pelagic community more vulnerable to external disturbances and extreme events (e.g., water-level fluctuations). One can speculate that the bleak-driven shifts between top-down and bottom-up regulation of zooplankton grazers may also have contributed to destabilization of the phytoplankton community since 1993 (Zohary and Ostrovsky 2011), and thus affect ecosystem integrity.

Overall, the long-term changes in fish community composition in Lake Kinneret were associated with introduction, invasion, and continuous stocking of fishes; changes in fishing intensity; modifications of the littoral; and changes of the lake ecological regime. Water-level fluctuations beyond natural have modified the littoral habitats, which are of specific importance during different life stages of fish (Chap. 29, Ostrovsky et al. 2013), and affected fish reproduction, survival, and recruitment. The destabilization of lake ecological state modified the trophic relationships in the pelagic zone (Zohary and Ostrovsky 2011). Overexploitation of main fishery resources modified the fish community and has led to collapse of certain fisheries (Chap. 36). To protect fish resources and mitigate the negative im-

pact of rapidly altering environmental conditions in the ecosystem, special efforts should be focused on conservation of the native fish species and the lake's natural ecological regime to which the food web components have adapted evolutionarily (Ostrovsky et al. 2013).

References

Azoulay B, Gophen M (1992) Feeding habits of larval *Mirogrex terraesanctae* (Steinitz, 1952) in Lake Kinneret (Israel) I. Field study. Hydrobiologia 246(3):243–249

Balshine-Earn S (1994) The evolution of parental care in cichlid fishes. University of Cambridge, Cambridge, p 196

Banarescu PM, Nalbant TT, Goren M (1982) The noemacheiline loaches from Israel (Pisces: Cobitidae: Noemacheilinae). Isr J Zool 31(1–2):1–25

Bar-Ilan M (1975) Stocking of *Mugil capito* and *Mugil cephalus* and their commercial catch in Lake Kinneret. Aquaculture 5(1):85–89

Ben-Tuvia A (1959) The biology of the cichlid fishes of Lake Tiberias and Hulah. Bull Res Counc Isr 8B(4):153–188

Ben-Tuvia A (1978) Fishes. In: Serruya C (ed) Lake Kinneret, Monographiae Biologicae, vol 32. Dr W Junk Publishers, The Hague, pp 407–430

Ben-Tuvia A, Davidoff EB, Shapiro J, Shefler D (1992) Biology and management of Lake Kinneret fisheries. Isr J Aquac Bamidgeh 44(2):48–65 (in Hebrew)

Bodenheimer FS (1935) Animal life in Palestine: an introduction to the problems of animal ecology and zoogeography. L. Mayer, Jerusalem, p 506

Bruton MN, Gophen M (1992) The effect of environmental factors on the nesting and courtship behaviour of *Tilapia zillii* in Lake Kinneret, Israel. Hydrobiologia 239(3):171–178

Chervinski J, Lahav M (1976) The effect of exposure to low temperature on fingerlings of local tilapia (*Tilapia aurea*) (Steindacher) and imported tilapia (*Tilapia vulcani*) (Trewavas) and *Tilapia nilotica* (Linne).Israel. Isr J Aquac Bamidgeh 28:25–29 (in Hebrew)

Cuvier G (1829) Le Règne Animal, distribuéd'après son organisation, pour servir de base à l'histoirenaturelle des animaux et d'introduction à l'anatomiecomparée. (edition 2), vol 2. Pitois, Paris, pp i-xv + 1–406.

Cuvier G, Valenciennes A (1840) Histoire naturelle des poissons. Tome quinzième. Suite du livre dix-septième. Siluroïdes, vol 15. Pitois, Paris, pp i–xxxi + 1–540. (Pls. 421–455)

Cuvier G, Valenciennes A (1842) Histoire naturelle des poissons. Tome seizième. Livre dix-huitième. Les Cyprinoïdes, vol 16. Pitois, Paris, pp i–xx + 1–472. (Pls. 456–487)

Fishelson L (1962) Hybrid of two species of fishes of the genus *Tilapia* (Cichlidae, Teleostei). Fishermen Bull Haifa 4(2):14–19 (in Hebrew)

Flshelson L (1966) Untersuchungen zur vergleichenden Entwicklungsgeschichte der Gattung *Tilapia* (Cichlidae, Teleostei). Zoologische Jahrbücher. Abteilung für Anatomie und Ontogenie der Tiere 83:571–656

Flshelson L (1967) Cichlidae of the genus *Tilapia* in Israel. Bull Fish Cult Isr Bamidgeh 18:67–80 (in Hebrew)

Fishelson L, Goren M, Van Vuren J, Manelis R (1996) Some aspects of the reproductive biology of *Barbus* spp, *Capoeta damascia* and their hybrids, Cyprinidae, Teleostei, in Israel. Hydrobiologia 317(1):79–88

Gafny S, Gasith A (2000) Spatial and temporal variation in the standing biomass of emergent macrophytes: effect of water level fluctuation. Ergeb Limnol 55:301–316

Gafny S, Gasith A, Goren M (1992) Effect of water level fluctuation on shore spawning of *Mirogrex terraesanctae* (Steinitz), (Cyprinidae*)* in Lake Kinneret, Israel. J Fish Biol 41:863–871

Gal G, Anderson W (2010) A novel approach to detecting a regime shift in a lake ecosystem. Method Ecol Evol 1:45–52

Gasith A, Gafny S (1990) Effects of water level fluctuation on the structure and function of the littoral zone. In: Tilzer MM, Serruya C (eds) Large lakes, ecological structure and function. Springer, Berlin, pp 156–171

Gasith A, Gafny S (1998) Importance of physical structures in lakes: the case of Lake Kinneret and general implications. In: Jeppesen E, Sondergaard M, Sondegaard M, Christoffersen K (eds) Structuring role of submerged macrophytes in lakes. Springer, Berlin, pp 331–338

Gasith A, Goren M (2009) Habitat availability, reproduction and population dynamics of the fresh water blenny *Salaria fluviatilis* (Asso, 1801) in Lake Kinneret, Israel. Electron J Ichthyol 2:34–46

Gasith A, Goren M, Gafny S (1996) Ecological consequences of lowering Lake Kinneret water level: effect on breeding success of the Kinneret sardine. In: Steiuberger Y (ed) Preservation of our world in the wake of change, vol VI. ISEEQS, Jerusalem, pp 569–573

Gasith A, Gafny S, Goren M (2000) Response of the fish assemblage of rocky habitats to lake level fluctuation: possible effect of varying habitat choice. Archiv fur Hydrobiologie: Special Issues in Advanced Limnology 55:317–331

Golani D, Shefler D, Gelman A (1988) Aspects of growth and feeding habits of the adult European Eel **(***Anguilla Anguilla***)** in Lake Kinneret (Lake Tiberias), Israel. Aquaculture 74(3–4):349–354

Gophen M (1980) Food sources, feeding behaviour and growth rates of *Sarotherodon galilaeum* (Linnaeus) fingerlings. Aquaculture 20(2):101–115

Gophen M, Landau R (1977) Trophic interactions between zooplankton and sardine *Mirogrex terraesanctae* populations in Lake Kinneret, Israel. Oikos 29:166–174

Gophen M, Scharf A (1981) Food and feeding habits of Mirogrex fingerlings in Lake Kinneret (Israel). Hydrobiologia 78:3–9

Goren M (1972) The populations of *Pseudophoxinus zeregi* (Heckel) in Israel and Syria and the status of *Pseudophoxinus (Pararhodeus) drusensis* (Pellegrin) (Pisces: Cyprinidae). Zool J Linn Soc 51(2):141–145

Goren M (1975) The freshwater fishes in Israel. Isr J Zool 23(2):67–118

Goren M (1983) The freshwater fishes of Israel. Kibbutz Ha'Muhad Publishing House, Tel Aviv, p 102 (Hebrew)

Goren M (2003) Fishes. In Dolev A, Pervelozky A (eds.) Endangered species in Israel—Red list of threatened animals. Keter, Jerusalem, pp 39–54

Goren M, Gasith A (1999) The biology of the catfish *Clarias gariepinus* in Lake Kinneret (Israel). Dayig Umidge 31:1–14 (in Hebrew)

Goren M, Ortal R (1999) Biodiversity of the inland water fishes of Israel. Biol Conserv 89:1–9

Goren M, Fishelson L, Trewavas E (1973) The Cyprinid fishes of *Acanthobrama* Heckel and related genera. Bull Br Mus 24(6):293–315

Günther A (1865) Report on a collection of reptiles and fishes from Palestine. Proc Zool Soc Lond 1864:488–493

Günther A (1866) Catalogue of fishes in the British Museum. Catalogue of the Physostomi, containing the families Salmonidae, Percopsidae, Galaxidae, Mormyridae, Gymnarchidae, Esocidae, Umbridae, Scombresocidae, Cyprinodontidae, in the collection of the British Museum. Cat fish Br Mus 6:I–XV + 1–368

Hasselquist F (1757) Iter Palestinum, eller vesa til Heliga Landet, förättad ifrån ar 1749 til 1752, Stockholm

Heckel JJ (1843) Ichthyologie [von Syrien]. In: von Russegger J (ed) Reisen in Europa, Asien und Africa, mit besonderer Rücksicht auf die naturwissenschaftlichen Verhältnisse der betreffenden Länder unternommen in den Jahren 1835 bis 1841, etc. Stuttgart. Ichthyologie [von Syrien] 1(2):990–1099

Horne JK, Walline PD, Jech JM (2000) Comparing acoustic model predictions to in situ backscatter measurements of fish with dual-chambered swimbladders. J Fish Biol 57:1105–1121

Kalikhman Y, Ostrovsky I, Walline P, Gophen M, Yacobi YZ (1995) Distribution fields for aquatic ecosystem components: method of identification of correlation zones. Freshw Biol 34:317–328

Komarovsky B (1952) An analysis of the stomach content of *Acanthobrama terraesanctae* from Lake Tiberias. Bull Sea Fish Res Stn Caesarea 4:1–8

Kosswig C (1950) Die Gattung *Tylognathus* in Vorderasien. Zool Anz 145:406–415
Kosswig C (1961) Speciation in the earlier Central Anatolian lake basin. In: Blair WF (ed) Vertebrate speciation. University of Texas, Austin, pp 561–593
Kosswig C (1967) Tethys and its relation to the Perimediterranean faunas of freshwater fishes. In: Adams CG, Ager DV (eds) Aspects of Tethyan biogeography. Systematics Association, London, pp 313–321
Krupp F (1987) Freshwater ichthyogeography of the Levant. In: Krupp F, Schneider W, Kinzelbach R (eds) Proceeding and symposium on the fauna and zoogeography of the Middle East, Mainz, 1985. Beihefte zum Tübinger Atlas des Vorderen Orients, Reihe A (Naturwissenschaften) 28, Dr. Ludwig Reichert, Wiesbaden, pp 229–237
Krupp F, Schneider W (1989) The fishes of the Jordan River drainage basin and Azraq Oasis. Fauna Saudi Arab 10:347–416
Landau R, Gophen M, Walline P (1988) Larval *Mirogrex terraesanctae* (Cyprinidae) of Lake Kinneret (Israel): growth rate, plankton selectivities, consumption rates and interaction with rotifers. Hydrobiologia 169(1):91–106
Leventer H, Teltsch B (1990) The contribution of silver carp (*Hypophthalmichthys molitrix*) to the biological control of Netofa reservoirs. Hydrobiologia 191(1):47–55
Linnaeus C (1758) Systema Naturae, Ed. X. (Systema naturae per regna tria naturae, secundum classes, ordines, genera, species, cum characteribus, differentiis, synonymis, locis. Tomus I. Editio decima, reformata.), vol 1. Holmiae, pp i–ii + 1–824
Lortet L (1875) Sur un poissons du Lac de Tiberade le Chromis paterfamilias, qui incube ses oeufes dans la cavite buccale. Comptes rendus hebdomadaires des Séances de l'Académie des Sciences, Paris 81(1875):1196–1198
Lortet L (1876) Sur un poisson du lac de Tibériade, le Chromis paterfamilias, qui incube ses oeufs dans la cavité buccale. Comptes rendus hebdomadaires des séances de l'Académie des Sciences, Paris 81:1196–1198
Lortet L (1883) Études zoologiques sur la faune du lac de Tibériade, suivies d'un aperçu sur la faune des lacs d'Antioche et de Homs. I. Poissons et reptiles du lac de Tibériade et de quelques autres parties de la Syrie. Arch Mus Hist Nat Lyon 3:99–189. (Pls. 6–18)
Mehner T, Busch S, Helland IP, Emmrich M, Freyhof J (2010) Temperature-related nocturnal vertical segregation of coexisting coregonids. Ecol Freshw Fish 19:408–419
Ostrovsky I (2005) Assessing mortality changes from size-frequency curves. J Fish Biol 66(6):1624–1632
Ostrovsky I (2009a) Hydroacoustic assessment of fish abundance in the presence of gas bubbles. Limnol Oceanogr Method 7:309–318
Ostrovsky I (2009b) The acoustic quantification of fish in the presence of methane bubbles in the stratified Lake Kinneret, Israel. ICES J Mar Sci 66(6):1043–1047
Ostrovsky I, Sukenik A (2008) Spatial heterogeneity of biogeochemical parameters in a subtropical lake. In: Mohanty PK (ed) Monitoring and modeling lakes and coastal environments. Springer, Berlin, pp 79–90
Ostrovsky I, Walline P (1999) Growth and production of the dominant pelagic fish, *Acanthobrama terraesanctae* (Cyprinidae), in subtropical Lake Kinneret (Israel). J Fish Biol 54:18–32
Ostrovsky I, Walline P (2001) Multiannual changes in the pelagic fish *Acanthobrama terraesanctae* in Lake Kinneret (Israel) in relation to food sources. Verh Int Ver Theor Angew Limnol 27:2090–2094
Ostrovsky I, Yacobi YZ (2009) Temporal evolution and spatial heterogeneity of ecosystem parameters in a subtropical lake. In: Ciraolo G., Ferreri GB, Napoli E (eds) Proceedings of the13th International workshop physical processes in natural waters, Palermo, Italy, 1–4 Sep 2009, University of Palermo, on CD, ISBN 978-88-903895-0-4, pp 1–15
Ostrovsky I, Yacobi YZ (2010) Sedimentation flux in a large subtropical lake: spatiotemporal variations and relation to primary productivity. Limnol Oceanogr 55:1918–1931
Ostrovsky I, Yacobi YZ, Walline P, Kalikhman Y (1996) Seiche-induced water mixing: its impact on lake productivity. Limnol Oceanogr 41:323–332
Ostrovsky I, Rimmer A, Yacobi YZ, Nishri A, Sukenik A, Hadas O, Zohary T (2013) Long-term changes in the Lake Kinneret ecosystem: the effects of climate change and anthropogenic

factors. In: Goldman CR, Kumagai M, Robarts RD (eds) Climate change and inland waters. Impacts and mitigation approaches for ecosystems and society. Wiley-Blackwell, Hoboken, pp 271–293
Pellegrin J (1911) Poisson de Syrie recueillis par M. Henri Gadeau de Kerville. Bull Soc Zool Fr 36:107–111
Pellegrin J (1923) Etude sur les poissons rapportes par M. Henri Gadeau de Kerville de son voyage zoologique en Syrie. Gadeau de Kerville H en Syrie. Voyag Zool 4:1–39
Pellegrin J (1933) Description du poisson nouveau de la Syrie meridionale apparetenant au genera *Phoxinellus*. Bull Mus Hist Nat 5:368–369
Reich K (1978) Lake Kinneret fishing in its development. Isr J Aquac Bamidgeh 30:37–64 (in Hebrew)
Ricardo-Bertram LK (1944) Abridged report on the fish and fishery of Lake Tiberias, Department of Agriculture and Fisheries, Palestine, pp 1–14
Roll U, Dayan T, Simberloff D, Goren M (2007) Characteristics of the introduced fish fauna of Israel. Biol Invasion 9:813–824
Rudstam LG, Parker SL, Einhouse DW, Witzel LD, Warner DM, Stritzel JL, Parrish DL, Sullivan PJ (2003) Application of in situ target strength estimations in lakes: examples from rainbow smelt surveys in Lakes Erie and Champlain. ICES J Mar Sci 60:500–507
Shapiro J (1985) Food and intestinal contents of the silver carp, *Hypothalmichthys molitrix* (Val), in Lake Kinneret between 1982–1984. Isr J Aquac Bamidgeh 37(1):3–18 (in Hebrew)
Shapiro J (1998) Food of the thin-lipped grey mullet (*Liza ramada*) in Lake Kinneret. Isr J Aquac Bamidgeh 50:3–11 (in Hebrew)
Shapiro J, Snovsky G (1997) The effect of the 1991/1992 winter upon the fishing industry of Lake Kinneret, Israel. Fish Manag Ecol 4(3):249–252
Shefler D, Reich K (1977) Growth of silver carp (*Hypophtalmichthys molitrix*) in Lake Kinneret in 1969-1975. Isr J Aquac Bamidgeh 29:3–16 (in Hebrew)
Snovsky G (1993) Biological aspects and fishery of grey mullets in Lake Kinneret. Fish Aquac Isr 1:33–50 (in Hebrew)
Snovsky G (2000) Biology and fishery of the silver carp. Fish Aquac Isr 1:108–117 (in Hebrew)
Snovsky G, Ostrovsky I (2014) The grey mullets in Lake Kinneret: the success of introduction and possible effect on water quality. Water and Irrigation 533:32–35 (in Hebrew)
Snovsky G, Pizanty S (2002) The silver carp fishery and effectiveness of stocking. Fish Aquac Isr 1:349–355 (in Hebrew)
Snovsky G, Sonin O, Shapiro J (2010) Commercial fishing of mullets in the Sea of Galilee in recent years. Fish Fishbreed Isr 41:1414–1422 (in Hebrew)
Spataru P (1976) The feeding habits of *Tilapia galilaea* (Artedi) in Lake Kinneret (Israel). Aquaculture 9:47–59
Spataru P (1978) Food and feeding habits of *Tilapiu zillii* (Gervais) (Cichlidae) in Lake Kinneret (Israel). Aquaculture 14:327–338
Spataru P, Gophen M (1985a) Feeding behaviour of silver carp *Hypophthalmichthys molitrix* Val. and its impact on the food web in Lake Kinneret, Israel. Hydrobiologia 120(1):53–61
Spataru P, Gophen M (1985b) Food composition of the barbel *Tor canis* (Cyprinidae) and its role in the Lake Kinneret ecosystem. Environ Biol Fish 14:295–301
Spataru P, Zorn M (1978) Food and feeding habits of *Tilapia aurea* (Steindachner) (Cichlidae) in Lake Kinneret (Israel). Aquaculture 13:67–69
Spataru P, Viveen WJAR, Gophen M (1987) Food Composition of *Clarias gariepinus* (= *C. lazera*) (Cypriniformes, Clariidae) in Lake Kinneret (Israel). Hydrobiologia 144(1):77–82
Steinitz H (1952) *Acanthobrama terrae-sanctae* sp. n. from Lake Tiberias, Israel. Ann Mag Nat Hist 12(5):293–298
Steinitz H (1953) The freshwater fishes of Palestine. Bull Res Counc Isr 3B:207–227
Steinitz H (1954) The distribution and evolution of the freshwater fishes of Palestine. Publication of the Hydrobiological Research Institute, Faculty of Science, University of Istanbul, B1:225–275
Steinitz H (1959) Dr. H. Lissner's study of the biology of *Acanthobrama terrae-sanctae* in Lake Tiberias. Bull Sea Fish Res Stn Isr B8:43–64

Steinitz H, Ben-Tuvia A (1957) The hybrid of *Barbus longiceps* C. V. and *Varicorhinus damascinus* C. V. (Cyprinidae, Teleostei). Bull Res Counc Isr 6B:176–188

Steinitz H, Ben-Tuvia A (1960) The Cichlid fishes of the genus *Tristramella* Trewavas. Ann Mag Nat Hist 3:161–175

Stoumboudi MT, Abraham M, Villwock W, Ben-Tuvia A, Economidis PS, Shapiro J (1992) Gonad development and somatic growth in an intergeneric cyprinid hybrid from Lake Kinneret, Israel. J Appl Ichthyol 8(1–4):110–121

Tortonese E (1938) Viaggio del Enrico Festa in Palestina e in Siria (1893), Pesci. Bullettino del Museo di Zoologia dell'Universita di Torino 3:15–20

Tortonese E (1952) On a new cyprinoid fish of the genus *Acanthobrama* from Palestine. Ann Mag Nat Hist 5(12):271–272

Trewavas E (1942) The cichlid fishes of Syria and Palestine. Ann Mag Nat Hist 9(11):526–536

Trewavas E (1965) *Tilapia aurea* (Steindachner) and the status of *Tilapia nilotica exul, T. monadi* and *T. lemassoni* (Pisces, Cichlidae). Isr J Zool 14:258–276

Tristram HB (1884) The survey of western Palestine. The fauna and flora of Palestine. The Committee of the Palestine Exploration Fund, London

Walline PD, Pisanty S, Lindem T (1992) Acoustic assessment of the number of pelagic fish in Lake Kinneret, Israel. Hydrobiologie 231:153–163

Walline PD, Tyler JA, Brandt SB, Ostrovsky I, Jech JM (2000) Lavnun abundance: how changes may affect consumption of Lake Kinneret zooplankton. Arh Hydrobiol 55:493–511

Zismann L (1976) Food and feeding of young grey mullets. Progress Report of Israel Oceanographic and Limnological Research, Haifa, Israel, pp 1–5

Zohar I (2003) Fish exploitation at the Sea of Galilee (Israel) by early fisher-hunter-gatherers (23,000 B.P.): ecological, economical, and cultural implications. PhD Dissertation, Tel Aviv University

Zohary T, Ostrovsky I (2011) Ecological impacts of excessive water level fluctuations in stratified freshwater lake. Inland Water 1:47–59

Zohary T, Erez J, Gophen M, Berman-Frank I, Stiller M (1994) Seasonality of stable carbon isotopes with Lake Kinneret pelagic food web. Limnol Oceanogr 39:1030–1043

Chapter 17
The Pelagic Food Web

Tamar Zohary, Gideon Gal and K David Hambright

Abstract Our current understanding of the food web of Lake Kinneret has developed over four decades of intensive research employing diverse methodologies such as gut content analyses, feeding experiments, stable isotopes, and modeling. The food web includes 12 major interconnected functional groups of organisms (=compartments), all contributing to a common pool of organic, inorganic, and detrital nutrients, but at differing flux rates. A schematic drawing of this food web highlights the central role of micrograzers (ciliates, heterotrophic flagellates, rotifers, copepod nauplii) in both transferring nutrients up the food web and recycling them. The evolution of our current understanding of the Kinneret food web reflects in many ways developments in the fields of ecology and limnology over the last three to four decades.

Keywords Microbial loop · Microzooplankton · Zooplanktivore · Herbivore · Heterotrophic · Dissolved organic C

In the previous chapters, the different biological components thriving in the pelagic waters of Lake Kinneret are addressed: eukaryotic phytoplankton and cyanobacteria, heterotrophic bacteria (hB), bacteria of other physiological strategies, microzooplankton (μZ) and macrozooplankton, and fish. In this chapter, we examine the interrelationships between those components, and between the different members within each group of organisms. Specifically, we address the issues of how the different organisms merge into a complex web of producers and consumers. The evolution of our

T. Zohary (✉)
The Yigal Allon Kinneret Limnological Laboratory, Israel Oceanographic & Limnological Research, P.O. Box 447, Migdal 14950, Israel
e-mail: tamarz@ocean.org.il

G. Gal
e-mail: gal@ocean.org.il

K D. Hambright
Department of Biology, University of Oklahoma, 730 Van Vleet Oval, 304 Sutton Hall, Norman, OK 73019, USA
e-mail: dhambright@ou.edu

T. Zohary et al. (eds.), *Lake Kinneret*, *Ecology and Management,* Aquatic Ecology Series 6,
DOI 10.1007/978-94-017-8944-8_17,

current understanding of the Kinneret complex food web reflects in many ways developments in the fields of ecology and limnology over the last three to four decades.

17.1 Methods Employed for Studying the Kinneret Food Web

A diversity of tools and methods were used in studies of grazing, predation, and nutrient remineralization in Lake Kinneret. These included:

1. *Gut content analyses,* mostly for studying the diets of fish (e.g., Spataru 1976, 1978; Spataru and Zorn 1976, 1978; Spataru and Gophen 1985, 1986, 1987; Shapiro 1985,1998; Azoulay and Gophen 1992a; Easton and Gophen 2002; Ofek 2010) but also of zooplankton (Gophen 1977; Gophen and Scharf 1981)
2. *Feeding experiments with different food types* to study fish feeding preferences (Gophen 1980; Drenner et al. 1987; Vinyard et al. 1988; Azoulay and Gophen 1992b) or ciliate feeding (Madoni et al. 1990)
3. *Feeding experiments with radioactively or fluorescently labeled food***.** Such experiments were employed to study zooplankton feeding on bacteria and algae (Gophen et al. 1974) and ciliate feeding on bacteria (Hadas et al. 1998)
4. *Serial dilution/concentration experiments* to study zooplankton feeding and nutrient remineralization (Hambright et al. 2001, 2007)
5. *Stable isotopes:* $\delta^{13}C$ was determined on members of the food web to track pathways of C though the main food web components from phytoplankton to fish (Zohary et al. 1994). Later, $\delta^{13}C$ and $\delta^{15}N$ were determined to investigate the fate of chemosynthetic bacteria (Hadas et al. 2001) and to assess zooplankton food sources in the absence of *Peridinium* (Goodwin 2010)
6. *Bioenergetics modeling* to estimate growth and food consumption for various zooplanktons and fishes (Ostrovsky and Walline 1999; Hambright et al. 2002; Blumenshine and Hambright 2003; Makler-Pick et al. 2011)
7. *Ecosystem and data-driven models* were used to describe and predict various paths and interaction strengths within the Kinneret pelagic food web (Serruya et al. 1980; Stone et al. 1993; Walline et al. 1993; Hart et al. 2000; Bruce et al. 2006; Atanasova et al. 2011; Makler-Pick et al. 2011; Gal et al. 2013)

17.2 The Early Two-Food-Chain View

The current understanding of the Lake Kinneret pelagic food web has evolved over more than four decades of intensive research and monitoring programs. In the late 1970s, the generalized two-food-chain view of Serruya et al. (1980) prevailed: the "nanoplankton food chain" and the "*Peridinium* food chain" (Fig. 17.1). In the nanoplankton food chain, the nano-sized phytoplankton at the base of the food

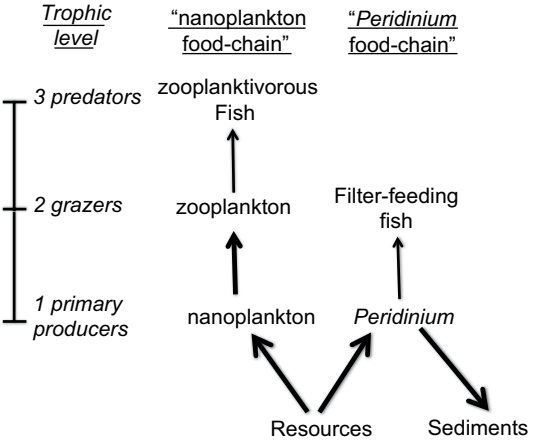

Fig. 17.1 A simplified two-chain and three-trophic-level view of the Lake Kinneret food web, as perceived in the 1970s. The "nanoplankton food chain" was comprised of a diverse assemblage of nanophytoplankton as primary producers, crustacean zooplankton as grazers, and the bleak as the main zooplanktivorous fish. The "*Peridinium* food chain" included dinoflagellates as primary producers and filter-feeding fish, mostly tilapia, as their grazers. It was acknowledged that grazing was a minor pathway in this chain; the major pathway for *Peridinium* biomass was sinking to the sediments where it decomposed. *Arrow* thickness is proportional to the extent of C flow

chain, including nearly all non-*Peridinium* phytoplankton species, are grazed by crustacean zooplankton, the primary food source for the presumed most abundant fish in the lake, *Mirogrex terraesanctae* (syn. *Acanthobrama terraesanctae,* the Kinneret Bleak, or locally, *lavnun*). It was characterized as a highly active, fast-turnover food chain, with rapid transfer of energy and matter between trophic levels.

In the second, much less active, food chain, *Peridinium gatunense* was the main primary producer (Fig. 17.1). It was assumed that due to its large cell size, this species was not grazed by crustacean zooplankton. Thus, its biomass accumulated in the water column, diverting a substantial fraction of the photosynthetically fixed C into a temporarily inactive pathway. The ultimate fate of *Peridinium* was either decomposition in the water column or sinking to the bottom sediments where it became food for microbial decomposers and bottom-feeding fish and invertebrates. Another less important fate of *Peridinium* was grazing by fish, mostly the Kinneret tilapia species, *Sarotherodon galilaeus* and *Oreochromis aureus,* and by some rotifers, such as *Asplanchna* spp. and *Bursaria* spp.

17.3 Key Findings Since 1980

Several key findings contributed to our revised perception of the Lake Kinneret ecosystem as a complex food web (Fig. 17.2), which includes the microbial loop, bacterial anoxygenic photosynthesis and chemosynthesis, an abundance of

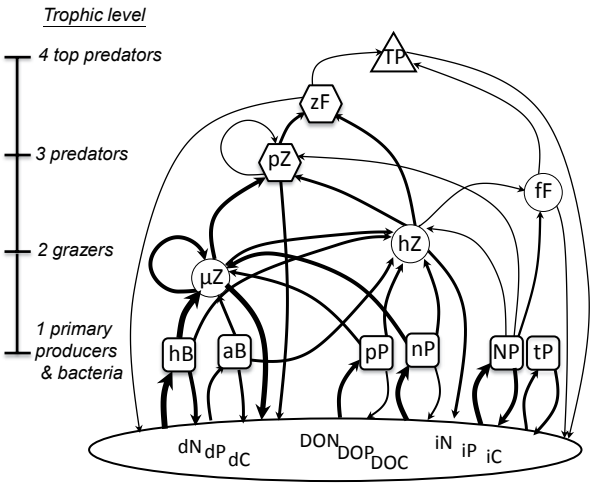

Fig. 17.2 A revised simplified view of the Lake Kinneret food web, as perceived today. The *ruler* on the left indicates trophic levels. *Squares* indicate osmotrophs (primary producers, heterotrophic bacteria), *circles* represent grazers, *hexagons* represent level 1 predators, and the *triangle* represents top predators. Abbreviations used (in trophic level order): *TP* top predators; *zF, fF* zooplanktivorous and filter-feeding fish, respectively; *pZ, hZ,* µ*Z* predatory, herbivorous, and microzooplankton, respectively; *pP, nP, NP, tP* picophytoplankton, nanophytoplankton, net-phytoplankton, and toxic phytoplankton, respectively; *hB, aB* heterotropic and anoxygenic autotrophic bacteria, respectively; *dN, dP, dC* detrital N, P, C, respectively; *DON, DOP, DOC* dissolved organic N, P, C, respectively; *iN, iP, iC* inorganic N, P, C, respectively. Note that some components are located at intermediate trophic levels (e.g., zooplanktivorous fish, filter-feeding fish). *Arrows* between compartments indicate flow of C, N, and P; their thickness is proportional to the extent of the flow. *Cyclical arrows* within a compartment indicate cannibalism and feeding within the compartment, e.g., for the µZ compartment: rotifers feeding on microflagellates and ciliates; for the fF compartment: fish eating their young. *Arrows* going down to the "resources disk" indicate excretion/release of nutrients in their organic or inorganic forms as well as losses as detrital material

picophytoplankton and micrograzers. Furthermore, the trophic interactions are further complicated by cannibalism and intra-guild predation. Following is a brief account of the key findings since 1980:

1. *The microbial loop*

The microbial loop (Azam et al. 1983) describes a previously unappreciated trophic pathway by which dissolved organic carbon (DOC) is returned to higher trophic levels via its incorporation into heterotrophic bacterial biomass, followed by grazing on the bacteria by heterotrophic eukaryotes and larger zooplankton. Autochthonous DOC is introduced into Lake Kinneret by diverse mechanisms such as leakage and exudation of fixed C from phytoplankton, by lysis of plankton cells, sloppy feeding by zooplankton and fish, excretion of waste materials by aquatic animals, and breakdown and dissolution of organic matter. Additional DOC is allochthonous, arriving from the catchment via runoff and river inflows.

Heterotrophic bacteria (hB) and heterotrophic unicellular eukaryotic grazers were not even mentioned in the 1978 Lake Kinneret monograph (Serruya 1978), as they were unexplored food web components at the time. Not much later, Sherr et al. (1982) reported that bacterial decomposition of dead *Peridinium* cells was accelerated in the presence of bacterivorous microflagellates. The addition of microflagellates enhanced the bacterial breakdown of the polysaccharide cell wall (thecae) but did not increase the rate of degradation of the protoplast. The breakdown of the thecae was likewise stimulated by the addition of phosphorus. The authors hypothesized that protozoan grazing increased the availability of mineral nutrients to bacteria degrading the mineral-poor thecae, demonstrating a key feedback pathway of the microbial loop. Zohary et al. (2000) studied the decomposition of freeze-dried *Peridinium* whole cells and empty thecae under controlled laboratory conditions. They found that thecae did not decompose at all, unless N and P were added, in which case the thecae vanished completely within 24 h. Whole-cell decomposition took place without nutrient addition. The results suggested that intensive regenerative nutrient cycling or external nutrient inputs are a necessary precondition for an efficient trophic transfer of the energy stored in blooms of thecate dinoflagellates. The high nutrient demands of microbial degradation imply furthermore a competition for nutrients between heterotrophic degradative and phototrophic productive processes.

Using a balanced C flowchart approach, Stone et al. (1993) further demonstrated the key role of the microbial loop in cycling C. Their charts suggested that 40 % of C requirement of copepods in the summer was supplied by ciliates that fed on bacteria and heterotrophic nanoflagellates. Using a mass-balanced carbon flux model and network analysis, Hart et al. (2000) examined the role of bacteria and protozoa in the food web of Lake Kinneret over a 4-year period (1989–1992). They concluded that these microorganisms supplied nearly half of the C requirements of metazoan zooplankton grazers during *Peridinium* blooms, when the lake was in its most eutrophic phase. Bacterial production was transferred to metazoans in a relatively efficient one- or two-step process. Hambright et al. (2007) confirmed experimentally that a substantial fraction of bacterial carbon could be transferred to higher trophic levels within the food web by both μZ (heterotrophic flagellates, ciliates, and rotifers) and small crustacean zooplankton.

2. *Picophytoplankton*

In the late 1980s, abundant phytoplankton cells <2 μm in diameter, or picophytoplankton, were discovered in Lake Kinneret (Malinsky-Rushansky and Berman 1991), following the discovery of *Procholorococcus* and the dominance of picoplanktonic cells in oligotrophic oceans. Both picocyanobacteria (*Synechococcus* type, but not prochlorophytes) and picoeukaryotes were found in Lake Kinneret at all depths and times of the year, at concentrations ranging from $<10^3$ to 10^5 cells mL^{-1}, with picocyanobacteria being much more abundant than picoeukaryotes (Malinsky-Rushansky et al. 1995). The relative contribution of those minute photosynthetic organisms to total phytoplankton photosynthesis was small, but occasionally, at seasons and depths where picocyanobacteria were abundant, it could account

for >50% of the photosynthetic activity (Malinsky-Rushansky et al. 1997). Picocyanobacteria contributed to the DOC pool by higher rates of extracellular release of dissolved organic compounds than larger algal cells (Malinsky-Rushansky and Legrand 1996). In addition, picophytoplankton comprised an important food source for heterotrophic nanoflagellates and ciliates (Sherr et al. 1991; Hadas et al. 1998).

3. *Anoxygenic photosynthetic bacteria*

Already in the early 1970s, layers of high turbidity and pigment content were noticed within the metalimnion during summer, when the thermocline was at about 15 m depth. Those were shown to be due to abundant sulfur photosynthetic bacteria, at the aerobic–anaerobic interphase (Bergstein et al. 1979; Eckert et al. 1986; Sect. 15.2). Those photosynthetic bacteria provided an additional source of fixed carbon, previously unaccounted for, and an additional food for zooplankton and ciliates (Hadas and Berman 1998). Gophen et al. (1974) reported preferential assimilation by zooplankton of the anoxygenic photosynthetic bacterium *Chlorobium* over *Chlorella* or *Chlamydomonas,* both isolated from Lake Kinneret, suggesting it was a preferred food source.

4. *Chemoautotrophic bacteria*

Chemosynthesis was another unexplored process in Lake Kinneret until a stable isotope study (Zohary et al. 1994) suggested that during winter, the zooplankton apparently fed on some yet unknown C source, with a particularly low $\delta^{13}C$ signature. They proposed that this source could perhaps be chemosynthetic bacteria. Hadas et al. (2001) were the first to conclusively demonstrate that intensive chemosynthetic microbial activity fueled by H_2S oxidation with dissolved O_2 was occurring in Lake Kinneret at sites and times of the year where oxygen and H_2S coexisted. This activity was measured as ^{14}C fixation in the dark and in the light in the presence of 3-(3,4-dichlorophenyl)-1,1-dimethylurea (DCMU), blocking bacterial photosynthesis. They computed that when conditions suitable for chemosynthesis exist, depth-integrated chemoautotrophic primary production contributed on average ~20% of the daily photosynthetic primary production (see Sect. 24.2). The particularly low $\delta^{13}C$ of particulate organic matter at the chemocline associated with intensive chemosynthesis suggested that indeed, those bacteria comprised the previously unknown food for zooplankton in winter, either directly or indirectly through the microbial loop.

5. *Heterotrophic nanoflagellates and ciliates*

With the understanding of the importance of the microbial loop, in the late 1980s, a search for unicellular micrograzers began, and indeed, they were plentiful. Madoni (1990) identified and listed the key ciliate species. Hadas and Berman (1998) quantified the seasonal abundances and vertical distributions of heterotrophic nanoflagellates and ciliates. The highest numbers of ciliates were recorded in autumn at the thermocline, at the time that chemosynthetic bacteria were abundant at the same layer. Hadas et al. (1998) fed three ciliate species isolated from Lake Kinneret with fluorescently labeled bacteria and picoplankton and computed their growth rates and water clearance rates. They concluded that picophytoplankton alone

was not sufficient to support ciliate growth and that supplementing with bacteria or nanoplankton was necessary. A summary of the knowledge on this group of microorganisms is given in Chap. 14.

6. *The role of μZ as primary grazers and recyclers of nutrients*

Until the early 1980s, the primary consumer trophic level (i.e., the herbivores) in Lake Kinneret was seen as being dominated by crustacean zooplankton. Rotifers were also acknowledged and their abundance followed routinely together with that of crustacean zooplankton, but due to their small contribution to total zooplankton biomass (~7%, Gophen 1978), they were considered less important and received minimal scientific attention. Following changes in the zooplankton sampling design, however, the highly heterogeneous vertical distribution of rotifers became evident with extreme concentrations occurring at the thermocline during the spring and fall seasons (see Chap. 13). The findings later on, regarding the role of the microbial loop and the abundant presence and activity of small-sized microorganisms (heterotrophic, photosynthetic, and chemosynthetic bacteria; picophytoplankton; and heterotrophic and mixotrophic nanoflagellates), made it necessary to reassess the relative importance of protist versus crustacean zooplankton. Hart et al. (2000) examined this theoretically using a mass-balanced C flux model, which generated hypotheses that were later tested experimentally by Hambright et al. (2007). Using serial dilution/concentration microcosm experiments, they demonstrated that μZ (defined as zooplankton passing through a 150 μm mesh net, mostly flagellates, ciliates, rotifers, and copepod nauplii), not macrozooplankton (mostly cladocerans and adult copepods), were the primary grazers of bacteria, picophytoplankton, and nanophytoplankton, as well as recyclers of nutrients. While macrozooplanktons consumed their body weight in carbon daily (~1 μgC (μgC grazer)$^{-1}$ day^{-1}; see also, Cyr 1998), mass-specific μZ grazing rates were ~20 times higher. Similarly, mass-specific excretion rates of N and P were ~50-fold and 70-fold higher for the μZ, respectively, compared with the crustacean zooplankton. While μZ grazing and nutrient remineralization rates were determined in the absence of potential predation by larger zooplankton, such as cyclopoid copepods, which obtain ~16% of their food in the form of μZ (Blumenshine and Hambright 2003), these rates are within the range expected from the consideration of ecological metabolic theory (Brown et al. 2004), and are consistent with findings from other studies (see for example, Sanders et al. 1989, Müller 1991, Kenter et al. 1996). Like these studies, the results of Hambright et al. (2007) indicate that μZ grazing and nutrient mineralization are indeed driving forces affecting bacteria and phytoplankton dynamics, playing important roles in carbon and nutrient transfer to higher trophic levels.

7. *Herbivorous zooplankton versus planktivorous zooplankton and intra-guild predation*

Another factor complicating the Kinneret food web is that not all crustacean zooplankters are herbivorous, many are omnivorous or planktivorous (Gophen 1978). The main Kinneret predator of crustacean zooplankton, the fish *M. terraesanctae* (Cyprinidae), feeds on all types of zooplankton, with preference to planktivorous copepods (Easton and Gophen 2002; Ofek 2010). This creates a trophic triangle, referred

to as intra-guild predation (IGP, Holt and Polis 1997), with *M. terraesanctae* and predatory zooplankton (copepods, the IG-predators) both feeding on herbivorous zooplankton (hZ; cladocerans and juvenile copepods, the IG-prey), but at the same time, *M. terraesanctae* also feeds on predatory zooplankton. A theoretical analysis led Hart (2002) to claim that IGP can dampen or even reverse the top-down effects predicted by the food-chain theory. During typical conditions, predatory zooplanktons were the main planktivores in the lake. During extreme conditions, however, fish (*M. terraesanctae*) could become the dominant planktivores (Ostrovsky and Walline 2000; Gal and Anderson 2010; Makler-Pick 2010). Blumenshein and Hambright (2003) used bioenergetics models to compare potential predation pressure on Lake Kinneret hZ by *M. terraesanctae* and cyclopoid copepods. They too found that, despite having much lower biomass, cyclopoid copepods accounted for a greater portion of the predation mortality on hZ than fish. Their results suggested that reductions in *M. terraesanctae* predation pressure (by subsidized harvest) may allow for increases in cyclopoid copepod abundance and thereby a net increase in predation pressure on hZ. This was later supported by modeling work using the Lake Kinneret ecosystem model in which the impact of different levels of *M. terraesanctae* biomass in the lake was examined (Makler-Pick 2010).

8. *Top predators*

While the lake ecosystem was considered in the past to be with practically no top predators (TP) except humans (fishermen), we now realize that there is at least a moderate level of top predation on both the zooplanktivorous fish *M. terraesanctae* and the filter-feeding cichlids by migrating Great Cormorants and the catfish *Clarias gariepinus*. A large increase in the European population of Great Cormorants since the 1980s has led to a significant increase in the number of cormorants overwintering in Israel (Shy et al. 2003). Being chased away from feeding in fishponds, these cormorants have shifted their major feeding site to Lake Kinneret, where they feed mostly on small individuals of *M. terraesanctae* and tilapia (Artzi 2011). Their impact on the populations and catch of *S. galilaeus* in Lake Kinneret is being debated and is currently under investigation. Studies of cormorant effects on fishes elsewhere (e.g., Fielder 2008) indicate that these predators deserve attention. There are anecdotal reports by fishermen about a considerable increase in the number of catfish and observations reporting that they consume juvenile *S. galilaeus* at the time of stocking of their fingerlings. Preliminary studies (Goren and Gasith 1999) suggest that indeed fish comprise a substantial portion of the diet of this omnivorous species. Further studies on these two TP are currently underway.

17.4 Changes in Phytoplankton Species Composition and Food Web Implications

In addition to those new findings, the phytoplankton of Lake Kinneret has exhibited major changes in species composition since the mid-1990s (Zohary 2004; Sect. 10.1), with considerable implications for interactions within the food web. In

particular, filamentous cyanobacteria and other elongated needle-shaped or chain-forming species dominate the summer assemblage, replacing the previously dominant nanoplanktonic forms (Zohary 2004). These new elongated forms are less palatable to zooplankton (e.g., Hambright et al. 2001), and possibly do not enter the "nanoplankton food chain." Furthermore, some of those filamentous cyanobacteria are toxigenic, comprising lower-quality food for zooplankton (Chap. 12).

Furthermore, the dinoflagellate *P. gatunense* no longer dominates phytoplankton biomass. Since routine monitoring began in the 1960s and until the mid-1990s, this key species bloomed in winter–spring each year, forming a massive bloom that fueled most of the microbial activity in the lake, as well as providing abundant high-quality food for cichlids. However, since 1996, significant *Peridinium* blooms developed in only 6 out of 16 years. In years when *Peridinium* did not bloom, the phytoplankton assemblage was unpredictable and differed from year to year (Zohary et al. 2012), leading to different foods, both in terms of quantity and quality, for higher trophic levels. These new food sources included toxigenic forms or species of lower nutritional value compared with *Peridinium,* the latter being an important source of amino acids, fatty acids, and vitamins such as B_1 and B_{12}.

In 2008, the flagship Kinneret fishery of the cichlid *S. galilaeus* (St. Peter's Fish) collapsed (Chap. 36). *Peridinium* comprised the main food source of this species, accounting for 80% of its C biomass (Zohary et al. 1994). The loss of *Peridinium* alone was not enough to explain this collapse: *S. galilaeus* can efficiently filter most particles greater than 10 μm (Drenner et al. 1987), and thrives in other natural water bodies in Israel, where there is no *Peridinium*. Overfishing and lack of enforcement of regulations to protect the spawning areas during the spawning season (Chap. 36), toxic food, poor-quality food, loss of suitable spawning grounds, and loss of refuge for the fingerlings at low water levels (Chap. 29), and predation by cormorant and catfish, all combined, most likely explain the collapse.

17.5 A Revised View of the Lake Kinneret Pelagic Food Web

Based on all the above findings, our revised understanding of the Lake Kinneret pelagic food web is summarized in Fig. 17.2. The geometric shapes stand for the food web compartments, with each shape representative of a trophic level; the connecting arrows indicate pathways of C, N, and P through the food web; and their thickness is indicatory of the rate of flow. Although this food web is much more complex than the two food chains depicted in Fig. 17.1, it too is simplified, showing only the more important components and flowchart arrows. Factors relating to taxonomic identity, ontogeny, and omnivory, for example, render countless other food web compartments and arrows that, if depicted, would obscure the primary interactions.

The osmotrophs (squares), at the base of the food web, include bacteria and phytoplankton. They rely on C, N, and P in the form of inorganic nutrients, dissolved organic nutrients, or as particulate matter, mostly as detritus. Bacteria belong to two main functional groups: hB and anoxygenic autotrophic bacteria

(aB), including chemosynthetic and anoxygenic photosynthetic bacteria. The phytoplankton are subdivided into four main functional groups, of which the first three are split by size (pico-sized, nano-sized, and net-sized phytoplankton; pP, nP, and NP, respectively) whereas the forth group contains toxin-producing species (tP; mostly cyanobacteria of the genus *Microcystis* and the filamentous *Aphanizomenon ovalisporum*). The pP and nP groups include the small-celled prokaryotic and eukaryotic species that are heavily grazed by μZ and hZ zooplankton groups. The NP group includes in some years only dinoflagellates (usually only *P. gatunense*), but in other years it contains large filamentous species such as the diatom *Aulacoseira granulata,* the chlorophyte *Mougeotia* sp., the cyanobacterium *Cylindrospermopsis raciborskii,* and other needle-shaped or complex-shaped species that are poorly grazed by zooplankton, such as the desmids *Closterium aciculare* and *Staurastrum manfeldtii*.

The zooplanktons are split into three main functional groups based on size and food types. The μZ is a diverse group of organisms, which includes a variety of small grazers: heterotrophic flagellates, ciliates, rotifers, and copepod nauplii. These organisms feed on the small osmotrophs, mostly hB and aB, pP and nP, and also on other taxa within the same group (e.g., ciliates feed on heterotrophic flagellates), hence the cyclic arrow from this compartment and back into the same compartment. The hZ compartment includes mostly cladocera and copepodites. These too feed on the osmotrophs but at reduced rates compared with the smaller μZ. Predatory zooplankton (pZ), mostly adult copepods, prey on the two other groups of zooplankton.

Two main fish groups occur in the pelagic waters: (1) zooplanktivorous fish (zF)—mostly bleak (*M. terraesanctae*), the main zooplanktivore among the Kinneret fish; (2) filter-feeding fish (fF) that mostly eat phytoplankton, but also zooplankton and detritus. The latter include mostly the native St. Peter's fish (*S. galilaeus*) and three other cichlid species, as well as the stocked silver carp and grey mullets.

Although we have only anecdotal evidence, we suggest that cormorants and possibly catfish function as TP of the pelagic system, feeding on zF and the various fF, especially on small individuals. Based on years of commercial development and well-recognized impacts of overfishing on multiple fishes, the ultimate TP in Lake Kinneret of at least some of the fish species are fishermen.

There are several additional interesting points to note in Fig. 17.2:

- The thick arrows all concentrate around the smaller components of the food web, representing the much greater (orders of magnitude) rates of C, N, and P flow through those compartments.
- Each compartment contributes nutrients to the overall C, N, and P resource pool (recycling or remineralization); again, the rates of these contributions vary by orders of magnitude, with considerably higher rates for the smaller organisms.
- The IGP triangle of hZ, pZ, and zF is evident.
- Toxic phytoplankton, tP, practically do not enter the food web.

17.6 A View to the Future

The upper levels of the Lake Kinneret food web are those that received considerably less research attention over the last two decades and should be the focus of future food-web research. The role of cormorants and catfish as potentially important TP requires overall investigation, especially relating to feeding habits and population dynamics. We need to learn more about the diets of the different species of the fF group, as well as any possible implications of the lack of *Peridinium* for fF species. The spawning practices and survival and recruitment rates of the different fish species should be investigated, given the recent greater-than-natural water-level fluctuations. Grazing by zooplankton and fish on the larger phytoplankton species that invaded the lake since the mid-1990s, including species that are toxigenic, requires further attention.

References

Artzi Y (2011) Greater Cormorant feeding in Lake Kinneret, Winter 2010–11. Nature & Parks Board Report (in Hebrew)

Atanasova N, Džeroski S, Todorovski L, Kompare B, Gal G (2011) Automated discovery of a model for dinoflagellate dynamics. Environ Model Softw 26:658–668

Azam F, Fenchel T, Field JG, Gray JS, Meyer-Reil LA, Thingstad TF (1983) The ecological role of water-column microbes in the sea. Mar Ecol Prog Ser 10:257–263

Azoulay B, Gophen M (1992a) Feeding habits of larval *Mirogrex terraesanctae* (Steinitz 1952) in Lake Kinneret (Israel). I. Field study. Hydrobiologia 246(3):243–249

Azoulay B, Gophen M (1992b) Feeding habits of larval *Mirogrex terraesanctae* (Steinitz 1952) in Lake Kinneret (Israel). II. Experimental study. Hydrobiologia 246(3):251–258

Bergstein T, Henis Y, Cavari BZ (1979) Investigations on the photosynthetic sulfur bacterium *Chlorobium phaeobacteroides* causing seasonal blooms in Lake Kinneret. Can J Microbiol 25(9):999–1007

Blumenshine SC, Hambright KD (2003) Top-down control in pelagic systems: a role for invertebrate predation. Hydrobiologia 491:347–356

Brown J, Gillooly JFH, Allen AP, Savage VM, West GB (2004) Toward a metabolic theory of ecology. Ecology 85:1771–1789

Bruce LC, Hamilton D, Imberger J, Gal G, Gophen M, Zohary T, Hambright KD (2006) A numerical simulation of the role of zooplankton in C, N and P cycling in Lake Kinneret, Israel. Ecol Model 193(3-4):412–436

Cyr H (1998) Cladoceran- and copepod-dominated zooplankton communities graze at similar rates in low-productivity lakes. Can J Fish Aquat Sci 55:414–422

Drenner RW, Hambright KD, Vinyard GL, Gophen M, Pollingher U (1987) Experimental study of size-selective phytoplankton grazing by a filter-feeding cichlid and the cichlid's effects on plankton community structure. Limnol Oceanogr 32(5):1138–1144

Easton J, Gophen M (2002) Trophic relations between zooplankton and bleaks (*Acanthobrama* spp.) in Lake Kinneret (Israel). Int Ver Theor Angew Limnol 28(3):1258–1261

Eckert W, Frevert T, Bergstein-Ben Dan T, Cavari BZ (1986) Competitive development of *Thiocapsa roseopersicina* and *Chlorobium phaeobacteroides* in Lake Kinneret. Can J Microbiol 32:917–921

Fielder DG (2008) Examination of factors contributing to the decline of the yellow perch population and fishery in Les Cheneaux Islands, Lake Huron, with emphasis on the role of Double-crested Cormorants. J Great Lakes Res 34:506–523

Gal G, Anderson W (2010) A novel approach to detecting a regime shift in a lake ecosystem. Method Ecol Evol 1:45–52
Gal G, Skerjanec M, Atanasova N (2013) Fluctuations in water level and the dynamics of zooplankton: a data-driven modelling approach. Freshw Biol 58:800–816
Goodwin A (2010) Stable carbon and nitrogen isotopes in Lake Kinneret food web (Msc Thesis). Hebrew University of Jerusalem, Israel
Gophen M (1977) Food and feeding habits of *Mesocyclopsleuckarti* (Claus) in Lake Kinneret (Israel). Freshw Biol 7:513–518
Gophen M (1978) Zooplankton. In: Serruya C (ed) Lake Kinneret (Monographiae Biologicae), vol 32. Dr. Junk Publishers, The Hague, pp 297–311
Gophen M (1980) Food sources, feeding behaviour and growth rates of *Sarotherodon galilaeum* (Linnaeus) fingerlings. Aquaculture 20:101–115
Gophen M, Scharf A (1981) Food and feeding habits of *Mirogrex* fingerlings in Lake Kinneret (Israel). Hydrobiologia 78(1):3–9
Gophen M, Cavari BZ, Berman T (1974) Zooplankton feeding on differentially labeled algae and bacteria. Nature 247(5440):393–394
Goren M, Gasith A (1999) Biological aspects of the fish *Clarias gariepinus* in Lake Kinneret. Dayig Umidge 31:1–14 (in Hebrew)
Hadas O, Berman T (1998) Seasonal abundance and vertical distribution of Protozoa (flagellates, ciliates) and bacteria in Lake Kinneret, Israel. Aquat Microb Ecol 14:161–170
Hadas O, Malinsky-Rushansky N, Pinkas R, Cappenberg TE (1998) Grazing on autotrophic and heterotrophic picoplankton by ciliates isolated from Lake Kinneret, Israel. J Plankton Res 20:1435–1448
Hadas O, Pinkas R, Erez J (2001) High chemoautotrophic primary production in Lake Kinneret, Israel: a neglected link in the C cycle of the lake. Limnol Oceanogr 46:1968–1976
Hambright KD, Zohary T, Easton J, Azoulay B, Fishbein T (2001) Effects of zooplankton grazing and nutrients on the bloom-forming, N_2-fixing cyanobacterium *Aphanizomenon* in Lake Kinneret. J Plankton Res 23:165–174
Hambright KD, Blumenshine C, Shapiro J (2002) Can filter-feeding fishes improve water quality in lakes? Freshw Biol 47:1173–1182
Hambright KD, Zohary T, Güde H (2007) Microzooplankton dominate carbon flow and nutrient cycling in a warm subtropical freshwater lake. Limnol Oceanogr 52(3):1018–1025
Hart DR (2002) Intraguild predation, invertebrate predators and trophic cascades in lake food webs. J Theor Biol 218:111–128
Hart DR, Stone L, Berman T (2000) Seasonal dynamics of the Lake Kinneret food web: the importance of the microbial loop. Limnol Oceanogr 45(2):350–361
Holt RD, Polis GA (1997) A theoretical framework for intraguild predation. Am Nat 149(4):745–764
Kenter U, Zimmermann H, Müller H (1996) Grazing rates of the freshwater ciliate *Balanion planctonicum* determined by flow cytometry. J Plankton Res 18:1047–1053
Makler-Pick V (2010) A computer ecosystem model applied for studying the food web and water quality of Lake Kinneret, with emphasis on top-down control. PhD thesis. The Technion-Israel Institute of Technology
Makler-Pick V, Gal G, Shapiro J, Hipsey MR (2011) Exploring the role of fish in a lake ecosystem (Lake Kinneret, Israel) by coupling an individual-based fish population model to a dynamic ecosystem model. Can J Fish Aquat Sci 68:1265–1284
Madoni P (1990) The ciliated protozoa of the monomictic Lake Kinneret (Israel): species composition and distribution during stratification. Hydrobiologia 190:111–120
Madoni P, Berman T, Hadas O, Pinkas R (1990) Food selection and growth of planktonic ciliate *Coleps hirtus* in a monomictic sub-tropical lake. J Plankton Res 12(4):735–741
Malinsky-Rushansky N, Berman T (1991) Picocyanobacteria and bacteria in Lake Kinneret. Int Rev Gesamten Hydrobiol 76(4):555–564
Malinsky-Rushansky NZ, Legrand C (1996) Excretion of dissolved organic carbon by phytoplankton of different sizes and subsequent bacterial uptake. Mar Ecol Prog Ser 132(1–3):249–255

Malinsky-Rushansky N, Berman T, Dubinsky Z (1995) Seasonal dynamics of picophytoplankton in Lake Kinneret, Israel. Freshw Biol 34:241–254
Malinsky-Rushansky NZ, Berman T, Dubinsky Z (1997) Seasonal photosynthetic activity of autotrophic picoplankton in Lake Kinneret, Israel. J Plankton Res 19(8):979–993
Müller H (1991) *Pseudobalanion planctonicum* (Ciliophora, Prostomatida): ecological significance of an algivorous nanociliate in a deep mesoeutrophic lake. J Plankton Res 13:247–262
Ofek T (2010) Checking the relationship between the bleak (*Acanthobrama terraesanctae*) and zooplankton, and its implication on the dilution of the bleak in Lake Kinneret (in Hebrew). Dept. Evolutionary and Environmental Biology. Haifa, Haifa University. M.Sc.: 43
Ostrovsky I, Walline P (1999) Growth and production of the dominant pelagic fish *Acanthobrama terraesanctae* in subtropical Lake Kinneret, Israel. J Fish Biol 54:18–32
Ostrovsky I, Walline P (2000) Multiannual changes in the pelagic fish Acanthobrama terraesanctae in Lake Kinneret (Israel) in relation to food sources. Int Ver Theor Angew Limnol 27:2090–2094
Sanders RW, Porter KG, Bennett SJ, DeBiase AE (1989) Seasonal patterns of bacterivory by flagellates, ciliates, rotifers, and cladocerans in a freshwater planktonic community. Limnol Oceanogr 34:673–687
Serruya C (ed) (1978) Lake Kinneret (Monographiae Biologicae) vol 32. Dr. Junk Publishers, The Hague
Serruya C, Gophen M, Pollingher U (1980) Lake Kinneret: carbon flow patterns and ecosystems management. Arch Hydrobiol 88(3):265–302
Shapiro J (1985) Food and intestinal contents of the silver carp, *Hypothalmichthys molitrix* (Val), in Lake Kinneret between 1982–1984. Bamidgeh–Isr J Aquac 37(1):3–18
Shapiro J (1998) Food of the thin-lipped grey mullet (*Liza ramada*) in Lake Kinneret, Israel. Bamidgeh–Isr J Aquac 50:3–11
Sherr B, Sherr E, Berman T (1982) Decomposition of organic detritus: a selective role for microflagellate protozoa. Limnol Oceanogr 27:765–769
Sherr EB, Sherr BF, Berman T, Hadas O (1991) High abundance of picoplanktivorous ciliates during late fall in Lake Kinneret, Israel. J Plankton Res 13(4):789–799
Shy E, Geva A, Goren M (2003) Resolving the conflict between Great Cormorant *Phalactrocorax carbo* and aquaculture in Israel: efficiency and cost-benefit analysis of methods, use of alternative feeding sites and presumed Cormorant impact on water quality of the national reservoir. Vogelwelt 124(Suppl.):355–367
Spataru P (1976) The feeding habits of *Tilapia galilaea* (Artedi) in Lake Kinneret (Israel). Aquaculture 9:47–59
Spataru P (1978) Food and feeding habits of *Tilapia zilli* (Gervais) (Cichlidae) in Lake Kinneret (Israel). Aquaculture 14:327–338
Spataru P, Gophen M (1985) Feeding behaviour of silver carp *Hypophthalmichthys molitrix* Val. and its impact on the food web in Lake Kinneret, Israel. Hydrobiologia 120(1):53–61
Spataru P, Gophen M (1986) Food and feeding habits of *Capoeta damascina* (Cyprinidae) in Lake Kinneret, Israel. J Aquac Trop 1:147–153
Spataru P, Gophen M (1987) The food and benthophagous feeding habits of *Barbus longiceps* (Cyprinidae) in Lake Kinneret (Israel). Arch Hydrobiol 110(3):331–337
Spataru P, Zorn M (1976) Some aspects of natural food and feeding habits of *Tilapia galilaea* (Artedi) and *Tiplapia aurea* (Steindachner) in Lake Kinneret. Bamidgeh–Isr J Aquac 28:12–17
Spataru P, Zorn M (1978) Food and feeding habits of *Tilapia aurea* (Steindachner) (Cichlidae) in Lake Kinneret (Israel). Aquaculture 13:67–79
Stone L, Berman T, Bonner R, Barry S, Weeks SW (1993) Lake Kinneret: a seasonal model for carbon flux through the planktonic biota. Limnol Oceanogr 38(8):1680–1695
Vinyard GL, Drenner RW, Gophen M, Pollingher U, Winkelman DL, Hambright KD (1988) An experimental study of the plankton community impacts of two omnivorous filter-feeding cichlids, *Tilapia galilaea* and *Tilapia aurea*. Can J Fish Aquat Sci 45(4):685–690
Walline PD, Pisanty S, Gophen M, Berman T (1993) The ecosystem of Lake Kinneret. In: Christansen V, Pauly D (eds) Trophic models of aquatic ecosystems, International Center for Living Resources Management conference proceedings, Manila, 1993. ICLARM, International Council for Exploration of the Sea, and Danish International Development Agency, eds, pp 103–109

Zohary T (2004) Changes to the phytoplankton assemblage of Lake Kinneret after decades of a predictable, repetitive pattern. Freshw Biol 49:1355–1371
Zohary T, Erez J, Gophen M, Berman-Frank I, Stiller M (1994) Seasonality of stable carbon isotopes with Lake Kinneret pelagic food web. Limnol Oceanogr 39(5):1030–1043
Zohary T, Hadas O, Pollingher U, Kaplan B, Pinkas R, Güde H (2000) The effect of nutrients (N, P) on the decomposition of *Peridinium gatunense* cells and thecae. Limnol Oceanogr 45:123–130
Zohary T, Nishri A, Sukenik A (2012) Present-absent: a chronicle of the dinoflagellate *Peridinium gatunense* from Lake Kinneret. Hydrobiologia 698:161–174

Part IV
Nutrient Sources and Biogeochemical Processes

Chapter 18
Material Loads from the Jordan River

Meir Rom, Diego Berger, Benjamin Teltsch and Doron Markel

Abstract The Jordan River is a major source of water, solutes, and allochthonous particles to Lake Kinneret contributed by the river tributaries as well as through leaching and erosion of soils and leakage of effluents. Those external nutrient loads impact the Lake Kinneret ecosystem. The current chapter presents a processed time series of material loads for 1971–2012 based on discharge measurements at the "Pkak Bridge", located on the Jordan River downstream of all tributaries and the Hula Valley. Also presented are chemical analyses performed on water samples collected at the same place. During the early 1990s, water sampling was gradually changed from being manual to an automatic sampling method, with an overlap period from 1991 to 1996 during which both methods were widely applied. Discrepancies between the two sets of parallel data obtained during the years of overlap were analyzed, with conclusions used to produce a single coherent corrected long-term record. Robust trend analysis performed on the corrected time series revealed significant long-term declines in the loads of nitrogen and phosphorus compounds, and suspended matter, while total nitrogen to total phosphorus ratio remained unchanged. The time series also reflects a wide range of anthropogenic activities in the watershed, such as increasing population and effluents in the 1970s, the peat area reclamation by the "Hula Project" since 1994, and the various watershed management actions implemented to vigorously eliminate pollution sources in the Lake Kinneret watershed.

Keywords Watershed management · Material loads · Monitoring stations · Sampling · Robust statistics · Nonparametric statistics · Trend analysis

M. Rom (✉) · D. Berger · B. Teltsch
Laboratories and Watershed Unit, Mekorot Water Company, P.O. Box 610,
17105, Upper Nazareth, Israel
e-mail: merom@mekorot.co.il

D. Berger
e-mail: dberger@mekorot.co.il

B. Teltsch
e-mail: bteltsch@gmail.com

D. Markel
Lake Kinneret and Watershed Unit, Israel Water Authority, Z.H.R. Industrial Park,
P.O. Box 623, 12000 Rosh Pina, Israel
e-mail: Doronm10@water.gov.il

T. Zohary et al. (eds.), *Lake Kinneret, Ecology and Management,* Aquatic Ecology Series 6,
DOI 10.1007/978-94-017-8944-8_18,

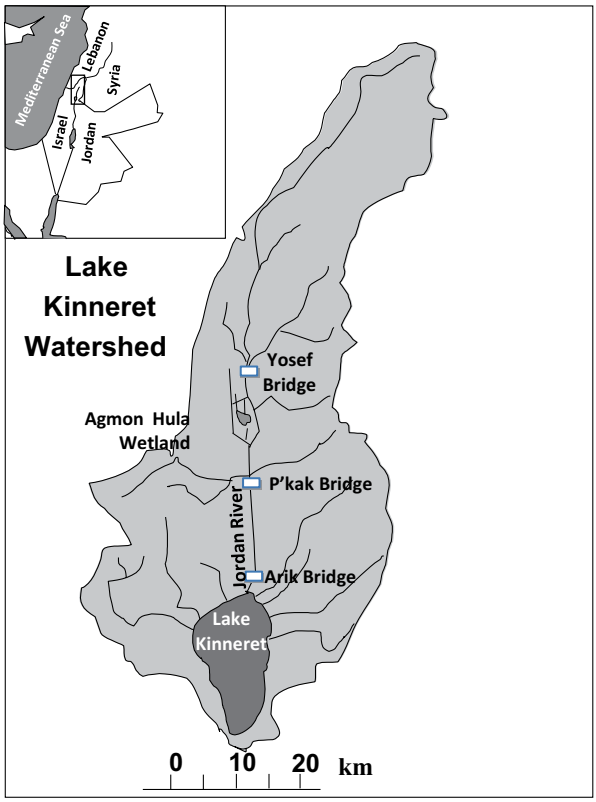

Fig. 18.1 Lake Kinneret watershed map showing the locations of the monitoring stations on the Jordan River at the Pkak Bridge, Yosef Bridge, and Arik Bridge

18.1 Introduction

Effective lake and watershed management depends on understanding the relationship between a lake and its watershed (Novotny 2003). Aquatic ecosystems are susceptible to external loads of nutrients and suspended solids (Wetzel 1983; Horne and Goldman 1994). These may either originate from point or nonpoint sources that can be of anthropogenic, agricultural, industrial, or natural origin.

In the case of Lake Kinneret, the Jordan River drains ~60% of the watershed area and brings ~70% of the recorded inflows (Chap. 7). The Jordan River also transfers with the water more than 80 and 90%, respectively, of the phosphorus and nitrogen load (Water Authority, unpublished data). It is therefore possible to consider the recorded load transfers by the Jordan River as a reasonable representation of the load from the entire watershed.

A continuous record of discharge and loading data, based on monitoring at the Pkak Bridge (located south of the Hula Valley, see Fig. 18.1) performed since 1971, represents fairly well the long-term loadings from the Jordan River to Lake Kinneret. Between 1971 and 2012, sampling at this station was performed manually, at 1–3 days intervals between 1971 and 1996 but thereafter only at weekly intervals.

Since 1990, an automatic high-frequency sampler is being operated at this station in parallel with manual sampling.

The extensive multi-annual data set of the Pkak Bridge Station enabled us to analyze quantitatively, long-term changes and trends in the materials load transfer from the Jordan River to Lake Kinneret, as it was analyzed in the past by Geifman and Rom (1995) and Rom (1999). It is anticipated that the annual (hydrological year) loads from the Jordan River are strongly affected by the annual discharge and also by anthropogenic activity in the watershed, including watershed management activity.

In the following sections we describe: (1) the different schemes of load quantification for the manual and automatic sampling methods; (2) the corrected load data over the course of the past 40 years; (3) the performance of robust trend analyses made for the loads time series, and (4) general interpretation of these trends with regard to major natural events (e.g., floods), anthropogenic activity, and different management activities in the watershed.

18.2 Evaluation of Material Loads

18.2.1 Definition and Estimation of Riverine Loads

We define the riverine load, *L,* of some material over period *T* as a time-integrated product of discharge volume by the concentration of this material at the point of discharge measurement. Mathematically, *L* can be expressed as

$$L \equiv L(T) = \int_T C(t)R(t)\mathrm{d}t \tag{18.1}$$

where $C(t)R(t)$ denotes the multiplication of the associate material concentration *C* with river discharge *R* at point of time *t*. Accordingly, let $\tilde{L}$ denote an estimator of *L* (in tons) based on the sample data,

$$\tilde{L} \equiv \tilde{L}(T) = \sum \tilde{C}(\Delta t)\tilde{R}(\Delta t) \tag{18.2}$$

where $\tilde{C}(\Delta t)$ denotes the material mean concentration (mg L^{-1}) over some small time interval Δt and $\tilde{R}(\Delta t)$ denotes the total river discharge (10^6 m^3) over that same interval. The summation in Eq. 18.2 is over all distinct time periods Δt for which $\sum \Delta t = T$. Note that Eq. 18.2 can be expressed as

$$\tilde{L} \equiv \tilde{L}(T) = \tilde{R}^* \sum \tilde{C}(\Delta t)\left[\frac{\tilde{R}(\Delta t)}{\tilde{R}^*}\right] = \tilde{R}^* \sum \tilde{C}(\Delta t)w(\Delta t) \tag{18.3}$$

where $\tilde{R}^* = \sum \tilde{R}(\Delta t)$ denotes the total water discharge over time period *T* and $w(\Delta t) = \dfrac{\tilde{R}(\Delta t)}{\tilde{R}^*}$ is the fraction of water discharge over Δt out of the total discharge.

Note that the summation in Eq. 18.3 is a *weighted average* of concentration values with weights defined by $w(\Delta t)$. Simple averaging of the concentration values may apply only if all the corresponding discharge values $\tilde{R}(\Delta t)$ are identical, i.e., constant flow. In this case, the loads over period T can be calculated by multiplication of the total water discharge by the mean concentration for the period.

Here, T often denotes a basic time period of 1 month, and Δt represents a 24 h day period; however, sometimes we may refer to winter, summer, or even annual loads. In which case, simple summation of appropriate monthly loads would be sufficient.

18.2.2 Quantification of Loads During the Period 1971–2012

The quantification of all material loading presented in this chapter is based on data from a single water quality monitoring station (WQMS) located on the Jordan River at the Pkak Bridge (Fig. 18.1). As explained above, data collected at this station are considered good estimates of the riverine loads entering Lake Kinneret via the Jordan River. Material concentration values from other neighboring sampling sites were used here for treating outliers.

18.2.2.1 Discharge Measurement and Sampling

Water discharge was assessed through continuous measurement of water level with a hydrometric station, where each water level represents a defined discharge. These stations generally have a precision error of 5–10 % (Pelletier 1988). The continuous water level data are then translated to continuous discharge data and then to daily, monthly, and annual volumes of water. The hydrometric gauge installed at the Pkak Bridge has a precision error of 2 % during the summer which may rise to 10 % in winter (Israeli Hydrological Service, internal report). Since this gauge was not changed during the monitoring period, those seasonal errors are applicable to the entire data set.

Water quality measurements were made on water samples taken next to the hydrometric gauge. Until 1990, only manual samples were taken; since 1990, an automatic sampler operates in parallel to the manual sampling at this station. The new sampling technology amplified the time resolution of sampling for water quality parameters from a single time point (via manual sampling) into multiple time points every 30 min, 7 days a week, while keeping running costs as low as the former method. In the automatic sampler, water is pumped via a 30 m long, 2-inch diameter propylene pipe into a polyvinyl chloride (PVC) bath located in an air-conditioned shed. Water is recycled continuously back to the river in order to keep the water in the bath as fresh as possible. Every 30 min, water is pumped from the bath into a bottle—one of a set of refrigerated bottles in a carousel (Fig. 18.2). The receiving bottle is replaced automatically every 6 h. Twice a week, the bottles are replaced by

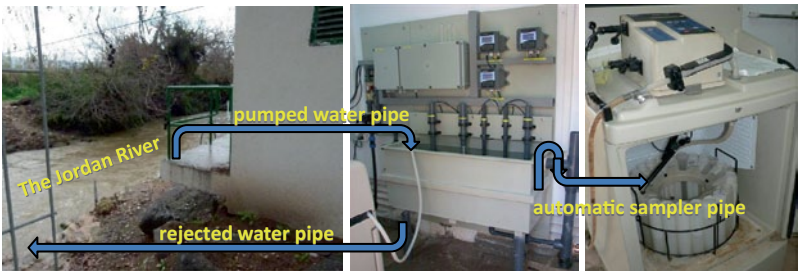

Fig. 18.2 A schematic diagram of the water quality monitoring station (WQMS) at the Pkak Bridge. River water is pumped through a polypropylene pipe into a PVC bath inside an air-conditioned shed, from which it is continuously recirculated to the river. Electrodes dipped in the bath provide a continuous record of temperature, pH, conductivity, oxidation–reduction potential, ammonium, and turbidity. Every 30 min, water from the bath is pumped into one bottle in a rotating carousel placed inside a refrigerator; every 6 h, the bottle is changed automatically. Twice a week the bottles are taken to the laboratory for chemical analyses

empty ones and taken to the laboratory, where water from four successive bottles are combined to give a time-integrated water sample representing a day. A series of chemical analyses is then conducted on those daily-integrated samples, as well as on the manually collected samples. Laboratory measurements of all chemical constituents (including phosphorus species, nitrogen species, major elements, and total suspended solids) are made according to the most updated standard methods (APHA 2005).

Manual sampling at the Pkak Bridge as well as at other watershed stations has been conducted since the Kinneret watershed monitoring program began in 1970. Sampling location was aimed towards the midstream of the river. Samples were taken by throwing a bucket from a bridge or from the riverbank. In order to sample representatively, the bucket was allowed to sink below the top layer (Rutherford 1994).

Manual sampling frequency at the Pkak Bridge during the period 1971–1997 (Fig. 18.3) was adjusted to accurately quantify loads from flood events. During heavy flood events, when material concentrations typically change rapidly over time, sampling frequencies were increased to several times a day. Daily loads were then calculated by multiplying the daily discharge by the mean daily concentration, derived by simple averaging (Harmel et al. 2010).

An overlap study period (shaded rectangle in Fig. 18.3) is chosen here during the first 6 years, 1991–1996, of the automated sampling. During those years, the manual sampling scheme was maintained with a background sampling frequency of ten times a month in summer, which was increased to 15–20 times per month in winter (Fig. 18.3). Comparisons of the monthly loads determined, based on the two sampling methods, revealed important properties of the loads calculated via automatic sampling, as detailed in the following sections.

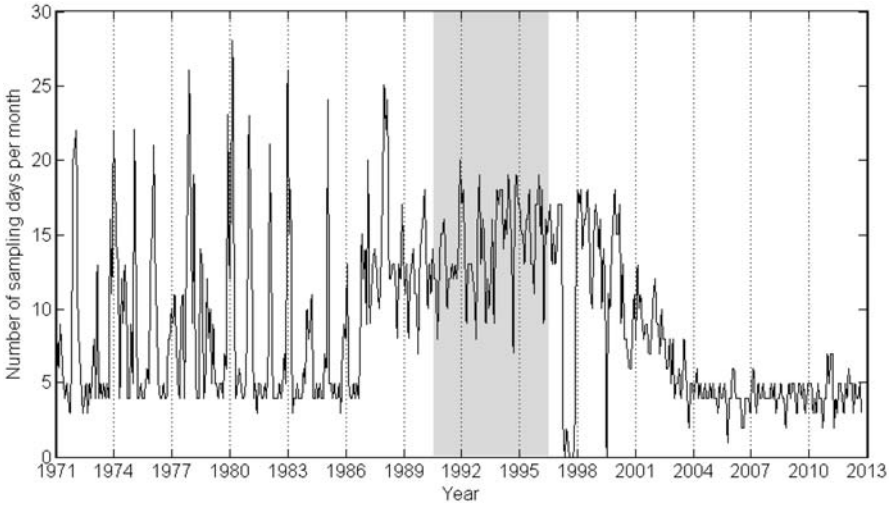

Fig. 18.3 The number of manual sampling days per month for 1971–2012. *Shaded area* corresponds to the period of overlap between manual and automatic sampling used for our method comparison analysis

18.2.2.2 Outlier Detection and Data Restoration at the Pkak Bridge Station

Water quality data collected in situ may include occasional extreme values, which reflect uncontrollable sampling deficiencies rather than fluctuations in the natural system (Novotny 2003). In manual sampling, if the bucket is used on shallow water, it may hit the riverbed and collect sediments; thus, extreme values may be recorded suggesting a pollution event. In automatic sampling at WQMS, extreme values may be recorded during heavy flooding events, when resuspended sediments accumulate at the bottom of the PVC bath from which the water is pumped into the refrigerated bottles. Since the particulate pollutants may sink and remain in the bath even after the flooding ends (actually, until the bath is manually cleaned), those records are easily detected (Rom et al. 2002–2012). Furthermore, since those high nutrient concentration values are important and cannot be omitted, they are carefully reconstructed. Reconstruction of data values from the Pkak Bridge is made by synchronizing and comparing water discharge and concentration values, associated with manual sampling from the nearest southern and northern stations: Arik Bridge or Yosef Bridge, respectively (Fig. 18.1). Occasionally, the procedure involves subjective decisions based on the high values to be restored; hence, subjective data reconstruction is performed by a panel of experts (Rom et al. 2002–2012). Using nonparametric statistical techniques in the analyses of the next section guarantees that the exact nominal values of the restored data have no impact on our analysis.

18.2.2.3 Monthly Load Calculations

Manual sampling provides single observation (concentration) for each constituent at a given time. In most cases, only one observation represents a daily outcome; however, in flooding events, more water samples may be taken from the river on the same day. A common estimator of daily load is given by the mean concentration values multiplied by the total water discharge of the same day. When only a single concentration value is involved, this value is taken as the mean; when no value exists (no sampling on that day), linear interpolation is used to fill in missing daily concentration values, then Eq. 18.2 is used to estimate the corresponding monthly load derived from the manual sampling data (MSL) by summing the daily load values of a given month.

The automatic sampling generates a complete set of daily concentration values. The calculation of daily and monthly loads derived from the automatic sampling data (ASL) is then straightforward using Eq. 18.2.

18.2.2.4 Comparison of Monthly Loads Based on Manual Versus Automatic Sampling

Comparison of the synchronized monthly ASL values with the corresponding MSL values during the overlap period 1991–1996 suggests severe bias for some nutrients, especially during the summer months (Fig. 18.4). The ratios of the manual to automatic loading values, MSL/ASL, are presented as box plots, enabling simultaneous side-by-side comparisons of many distributions (Tukey 1977; Benjamini 1988). It is clear that concentration values of the particulate constituents, TSS, total phosphorus (TP), and organic nitrogen (N_{org}), as well as that of ammonium (NH_4) associated with manual sampling have higher values than the corresponding values from the automatic sampler. The opposite occurs with some of the dissolved materials such as total dissolved P (TDP).

18.2.2.5 The Bias Associated with ASL

The average and median residence time of water samples in the refrigerated carousel, before being taken to the laboratory for chemical analyses, is 60 h with a maximal value of 120 h. This relatively long residence time allows for geochemical processes in the open sampling bottles to occur, such as sedimentation, dissolution, gas emission, or calcite precipitation. Furthermore, although refrigeration reduces the rates of microbial activity it does not stop it completely. These processes should cause lower NH_4, N_{org}, Ca, TSS, PP, and TP in the ASL relative to the MSL (MSL/ASL ratio higher than 1; Fig. 18.4) and higher TDP and NO_3 (MSL/ASL ratio lower than 1; Fig. 18.4). While residence time in the sample bottles seems to be a major bias factor in calculations from the ASL, the corresponding residence time associated with manual sampling (until water samples reach the laboratory) is no

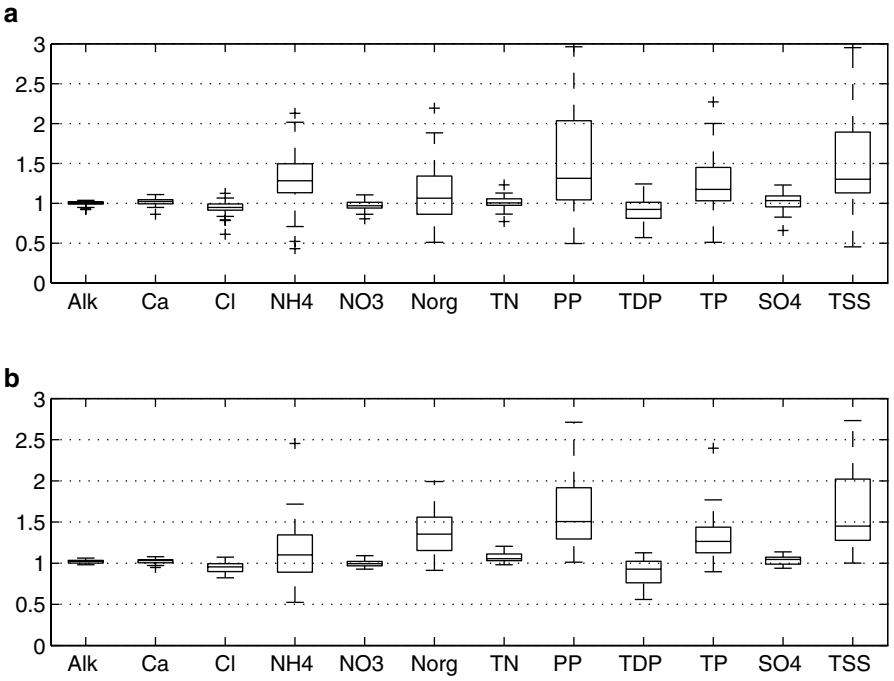

Fig. 18.4 Box plots of the distribution of values of monthly MSL/ASL ratios during the overlap study period 1991–1996: winter (**a**) summer (**b**). *Boxes* include 50 % of the data between the 25th and 75th percentiles, *horizontal line* shows the median, whiskers extend either to the maximal (minimal) value or up to 1.5 of the interquartile range (IQR), *pluses* show outliers which fall beyond the whisker length

longer than 7 h; thus, MSL reflect fresh river water and have considerably smaller bias caused by storage effects.

Another possible bias associated with the ASL is the long-distance pipeline (ca. 30 m) between the river and the bath in the monitoring station, which may cause less efficient transfer of particles compared to solutes. Moreover, the pipe (ca. 3 m) in which water flows from the bath to the refrigerated bottles may develop biofilms, those biofilms may further reduce the number of particles transferred to the sampling bottle. In addition, the location of the pipe's inlet is fixed at about 3 m from the riverbank and 1 m below the surface, while the location of the manual sampler is usually set at midstream in the river where the current is strongest, sampling the surface water. All the above contribute to the discrepancies between the loads estimated from automatic versus manual sampling.

This bias phenomenon of automatic sampling is well documented (Eads and Thomas 1983; Gray et al. 2000; Roseen et al. 2011). Roseen et al. (2011) concluded that "automatic samplers are under-representing sediment loads." Therefore, one should expect lower concentration of all particle-associated parameters (namely TSS, TP, and PP) in the ASL compared to the MSL (MSL/ASL ratio higher than 1 in Fig. 18.4).

Table18.1 Seasonal factors (unitless) for modifying ASL values

	ALK	CA	CL	NH_4	NO_3	N_{org}	TN	SRP	DP	TP	SO_4	TSS
Winter	1.003	1.002	0.948	1.282	0.969	1.063	1.005	0.977	0.923	1.174	1.033	1.302
Summer	1.023	1.033	0.955	1.101	0.994	1.352	1.054	0.918	0.927	1.264	1.045	1.451

Values in the table are medians of MSL/ASL ratios during the overlap study period of 1991–1996

18.2.2.6 Forming Homogeneous Series of Material Loads

In order to construct a continuous time series of monthly material loads for the period 1971–2012, it is essential to control the bias inherent in the ASL values by modifying the loads associated with the automatic sampling during the time period 1991–2012. Such a modification is done by multiplying the ASL values by the respective seasonal factors for each material and season listed in Table 18.1. These factors are the median of the MSL/ASL ratios (horizontal lines of each box in Fig. 18.4) for 1991–1996. The resulting modified series are shifted in such a way that the median of the modified MSL/ASL ratios tend to one in the overlap period and the bias of the ASL values is clearly decreased over the next years. Concatenating the MSL 1971–1990 values with the modified ASL 1991–2012 values forms a new corrected time series of material loads at the Pkak Bridge (Table 18.2), to be analyzed in the following sections.

18.2.2.7 Trend Analysis

Since environmental data are often characterized by high fluctuations and large outliers, classical statistical analysis do not apply; hence, nonparametric statistical techniques and Kendall-based trend tests are used to filter out the noise inherent in the data (Hirsch et al. 1982; Hirsch and Slack 1984; Conover 1999). *Robust* regression lines (Rousseeuw 2003) and running median smoothed curves are used here for presentation of the temporal dynamics of loads. These curves replace the commonly used regression line (Velleman 1980). By using such techniques, no assumption is made concerning the distribution of the noise and no minimization procedure is required. In addition, slopes are estimated using a Theil–Sen estimator, which is the median of all the slopes computed from pairing all data points in the sample (Wilcox 2001). This estimator is strongly resistant to outliers and is highly efficient in cases where the distribution of the noise is non-normal and highly skewed.

For smoothing curves, we use here a running median (instead of running mean) with a 3-year window size. This window size was subjectively and visually chosen (as most smoothers do) to filter out short variation and keep mid-term visual dynamics of the loadings. A robust regression line may be regarded too as a special smoother with maximal window size; thus, in fact, we apply two robust smoothers which differ by their window size.

Table 18.2 The corrected annual (hydrological year) loads of different materials from the Jordan River to Lake Kinneret as sampled at the Pkak Bridge and calculated in the current work. Vol – Discharge, TSS – Total Suspended Solids, TP- Total P, TDP – Total Dissolved P, TN- Total N; Units are in tons yr^{-1} except discharge (Vol): 10^6 m^3 yr^{-1} and TN/TP (unitless).

Year	Vol	TSS	TP	DP	TDP	PP	TN	TN/TP	NH_4	NO_3	N_{org}	SO_4	Alk	Ca	Cl
1970/71	645	68,588	113.6	7.5	13.9	99.7	1,701	15.0	34.8	1,183	483	26,783	103,367	42,841	9,887
1971/72	491	29,028	72.6	6.7	10.2	62.5	1,137	15.6	41.8	698	397	19,964	83,739	31,753	7,382
1972/73	270	18,079	53.6	5.6	10.8	42.9	677	12.6	24.1	416	236	10,272	48,012	18,215	3,908
1973/74	479	42,210	105.6	12.1	16.1	89.5	2,168	20.5	60.4	1,621	489	25,552	82,862	35,876	8,566
1974/75	376	33,046	85.0	7.3	17.1	67.9	1,069	12.6	29.7	508	532	11,723	64,069	24,363	6,233
1975/76	479	42,980	115.2	11.5	21.7	93.5	1,256	10.9	43.0	614	600	13,281	76,199	28,065	7,888
1976/77	557	48,190	121.4	14.1	25.4	96.1	1,560	12.8	60.6	807	690	16,553	90,985	35,209	9,446
1977/78	575	66,604	167.8	15.6	26.5	141.3	1,477	8.8	64.4	827	587	14,011	93,089	34,694	8,236
1978/79	276	17,641	58.7	9.4	12.7	46.0	674	11.5	46.0	367	264	7,368	46,493	16,861	3,951
1979/80	569	58,269	143.5	20.6	26.4	117.1	2,169	15.1	94.1	1,464	611	21,419	93,431	36,418	11,424
1980/81	633	46,507	133.7	21.1	29.6	104.1	2,260	16.9	83.0	1,594	583	24,856	107,406	44,281	14,839
1981/82	380	25,274	89.0	12.1	17.9	71.1	950	10.7	72.4	630	254	11,396	65,886	24,427	7,198
1982/83	559	41,818	114.7	24.4	26.4	88.3	2,055	17.9	107.2	1,741	281	28,527	93,445	40,222	12,696
1983/84	466	42,134	93.4	13.4	22.2	71.3	1,170	12.5	93.0	684	393	14,184	77,708	31,304	8,026
1984/85	433	34,902	90.6	17.1	20.7	69.9	1,094	12.1	87.0	812	194	14,576	74,836	31,610	8,459
1985/86	291	18,918	57.0	12.0	9.6	47.4	681	11.9	67.2	482	131	10,401	51,183	20,798	4,606
1986/87	639	74,213	163.6	19.6	23.5	140.1	1,707	10.4	55.8	1,331	328	20,626	109,280	44,251	11,590
1987/88	659	39,822	106.0	20.5	25.9	80.1	2,059	19.4	82.1	1,723	261	24,963	111,544	46,001	13,446
1988/89	306	16,690	45.4	8.5	10.5	34.9	664	14.6	30.6	496	137	8,056	54,417	20,142	5,280
1989/90	214	12,288	34.9	6.4	8.3	26.6	484	13.9	37.2	355	93	6,878	38,817	14,181	4,082
1990/91	251	15,730	39.5	6.8	9.0	30.5	499	12.6	15.5	364	122	6,844	42,963	16,498	3,920
1991/92	842	102,468	271.7	43.3	52.0	219.7	4,960	18.3	96.8	3,945	1,123	51,257	145,228	66,995	22,714
1992/93	589	47,411	131.2	22.4	26.2	105.0	1,758	13.4	54.7	1,357	352	21,482	102,536	41,537	12,272
1993/94	380	23,515	67.0	13.5	17.5	49.5	876	13.1	39.1	656	177	8,919	64,599	24,585	6,271

Table 18.2 (contuinued)

Year	Vol	TSS	TP	DP	TDP	PP	TN	TN/TP	NH_4	NO_3	N_{org}	SO_4	Alk	Ca	Cl
1994/95	521	38,856	118.3	20.7	27.4	90.9	2,058	17.4	42.1	1,552	459	24,457	90,797	40,013	10,794
1995/96	409	13,003	52.4	16.8	19.0	33.4	893	17.1	30.7	705	156	14,531	71,136	29,030	7,381
1996/97	400	20,673	68.0	18.9	21.2	46.8	1,208	17.8	21.2	877	311	17,400	70,089	29,707	7,798
1997/98	467	32,717	82.1	17.3	19.2	62.9	1,309	15.9	27.2	1,004	265	21,566	81,695	34,731	9,242
1998/99	215	14,512	35.8	7.3	7.9	27.9	491	13.7	10.3	346	133	5,962	36,992	15,017	3,538
1999/2000	254	16,398	57.2	12.9	14.6	42.6	687	12.0	21.0	528	134	8,492	44,123	17,450	5,382
2000/01	199	7,685	25.4	5.9	7.0	18.3	409	16.1	12.7	317	78	5,598	34,560	12,305	3,210
2001/02	326	22,041	58.0	12.1	17.0	41.0	826	14.3	18.7	656	140	12,123	55,976	22,226	6,353
2002/03	714	121,392	277.0	29.8	32.1	245.0	3,013	10.9	27.9	2,462	458	27,461	124,228	50,305	17,197
2003/04	546	58,166	115.5	16.1	19.3	96.2	1,725	14.9	17.0	1,448	197	19,544	93,941	39,178	11,151
2004/05	442	42,265	98.2	12.2	13.7	84.5	1,095	11.1	21.4	883	174	13,837	75,532	30,484	7,227
2005/06	372	19,695	50.0	9.5	10.7	39.3	846	16.9	17.1	689	135	11,584	66,203	26,574	6,520
2006/07	357	36,537	87.0	12.2	13.1	74.0	808	9.3	10.9	651	144	10,414	64,973	25,674	6,535
2007/08	230	9,970	29.0	5.1	5.5	23.6	486	16.7	12.6	392	91	6,259	41,179	15,788	3,573
2008/09	263	15,447	41.5	3.9	4.7	36.8	593	14.3	8.2	425	164	7,304	48,734	18,184	4,251
2009/10	424	50,344	132.9	10.9	16.5	116.5	1,131	8.5	14.7	908	192	14,280	84,253	30,556	8,298
2010/11	426	28,706	79.7	10.8	11.4	68.3	1,113	14.0	6.0	972	126	17,393	80,227	32,186	8,022
2011/12	518	28,662	70.2	13.1	13.9	56.3	1,501	21.4	7.3	1,298	166	19,094	93,214	38,221	9,648
Average	439	36,747	94.1	14.0	17.9	76.2	1,317	14.2	41.6	971	306	16,124	75,713	30,446	8,296
Median	430	32,881	86.0	12.2	17.1	69.1	1,122	13.9	32.7	756	245	14,232	75,866	30,520	7,843

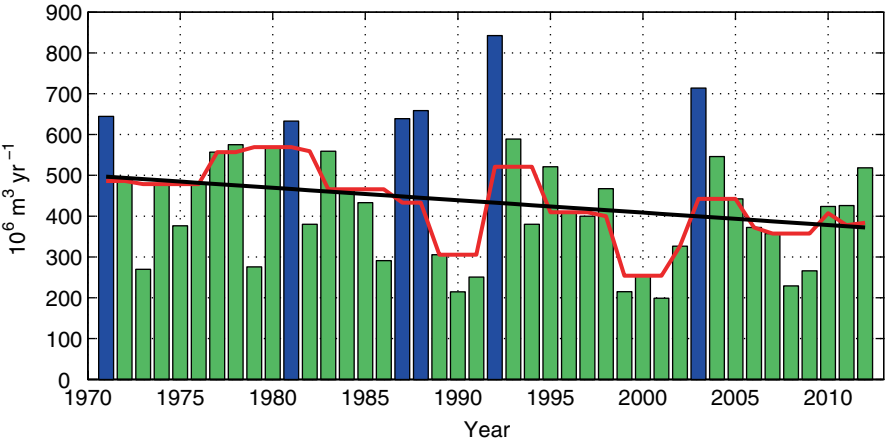

Fig. 18.5 Annual (hydrological year) discharge of the Jordan River (10^6 m^3 year^{-1}) as measured by the Hydrological Survey of Israel at Pkak Bridge Station. The rainy years with discharge >600 10^6 m^3 year^{-1} are in *blue*. The *red curve* is the moving median smoother with a window size of 3 years. The *black line* is the robust regression line with a slope of −3.2 10^6 m^3 year^{-1}. This value corresponds to the Theil–Sen slope estimator with *P* value of 0.061, derived by the Kendal test

18.3 Results

18.3.1 Long-Term Changes of the Jordan River Discharge Volumes

The annual (hydrological year between October in a given year and September in the following one) discharge of the Jordan River, as measured by the Hydrological Service of Israel at Pkak Bridge Station, decreased from ca. 500 10^6 m^3 year^{-1} in the 1970s to ca. 400 10^6 m^3 year^{-1} in the 2010s (Fig. 18.5). This 20% decrease is probably a combined effect of two processes, namely decrease in effective rain at the northern part of the watershed and increase in water consumption in the watershed (Givati and Rosenfeld 2004; Chaps. 7 and 31). This change should affect all material loads and it is anticipated that if there were no anthropogenic and management effects, the loads would have followed this 20% decrease. Figure 18.5 also demonstrates the importance of the rainy hydrological years of 1971 (October 1970 to September 1971), 1981, 1987, 1988, 1992, and 2003 that had discharge peaks of 645, 633, 639, 659, 842, and 714 10^6 m^3 year^{-1}, respectively (Table 18.2).

18.3.2 Corrected Annual Material Loads from the Jordan River to Lake Kinneret

The time series of corrected annual (hydrological year from October in a given year to September in the following one) loads of different materials transported via the Jordan River to Lake Kinneret from 1971 to 2012 (Fig. 18.6) suggests that the load of most materials decreased during these years, following the long-term trend of the discharge. However, for most of the constituents the periodical trends represented by the moving median smoother varied among the years, suggesting short- and mid-term changes, which may be a consequence of anthropogenic activity as well as the watershed management actions that were applied in the watershed since the 1970s.

TSS load values decreased from ca. 40,000 t year^{-1} in the 1970s to ca. 25,000 t year^{-1} in the 2010s (Fig. 18.6). The running median reveals that the load was relatively stable until the hydrological year of 1988 (and then began to decrease until it increased again in 2003). Although there was a higher discharge in 1992 as compared to 2003, the TSS load in 2003 was almost 20% higher than the load of 1992 (121,360 and 102,441 t, respectively, Table 18.2).

All phosphorus fractions, TP, total dissolved phosphorus (TDP), and particulate phosphorus (PP, which is simply the difference between the former two) decreased from ca. 100, 20, and 80 t year^{-1}, respectively, in the 1970s to ca. 65, 15, and 50 t year^{-1}, respectively, in the 2010s (Fig. 18.6). A careful examination of the periodic changes reveals a dramatic increase in TDP in the 1970s to the mid-1980s, and then shows a significant decrease to the present with two exceptions in the early 1990s and the early 2000s. Despite the higher discharge in 1992 compared to 2003, the TP load in 2003 was higher than the load of 1992 (277 and 271.7 t, respectively, Table 18.2). The difference in PP is even higher (245 and 219.7 t, respectively, Table 18.2), most probably due to the same drainage enhancing effect like the one that affected the TSS. Unlike the PP load, the TDP load was higher in 1992 than in 2003 (52 and 32.1 t, respectively, Table 18.2).

The annul load of nitrogen compounds, nitrate (NO_3), ammonium (NH_4), N_{org}, and total nitrogen (TN), shows a different pattern than does the phosphorus. NH_4 and N_{org}loads increased in the 1970s, reaching peak levels of 107.2 and 689.8 t year^{-1} in 1983 and 1977, respectively (Fig. 18.6 and Table 18.2). In later years, NH_4 and N_{org} load decreased gradually to 10 and 150 t year^{-1}, respectively, in the 2010s. The NO_3 load exhibits small changes over time which follow the short-term changes in discharge. In the long term, there is a slight decrease from ca. 900 t year^{-1} in the 1970s to ca. 800 t year^{-1} in the 2010s. Since nitrate is the main contributor of N to total nitrogen, the relatively constant pattern of the NO_3 load masked the changes in NH_4 and N_{org} in the TN pattern, which decreased constantly from ca. 1500 t year^{-1} in the 1970s to ca. 1,000 t year^{-1} in the 2010s (Fig. 18.6). This constant decrease is similar to the constant decrease in the TP load mentioned above; hence, the TN/TP ratio has no significant long-term trend, but is rather stable over time at a value of 14–15. Still, low annual mean levels of TN/TP of 12, 10.9, 11.2, 9.3, and 8.5 were recorded in the hydrological years 2000, 2003, 2005, 2007, and 2010, respectively.

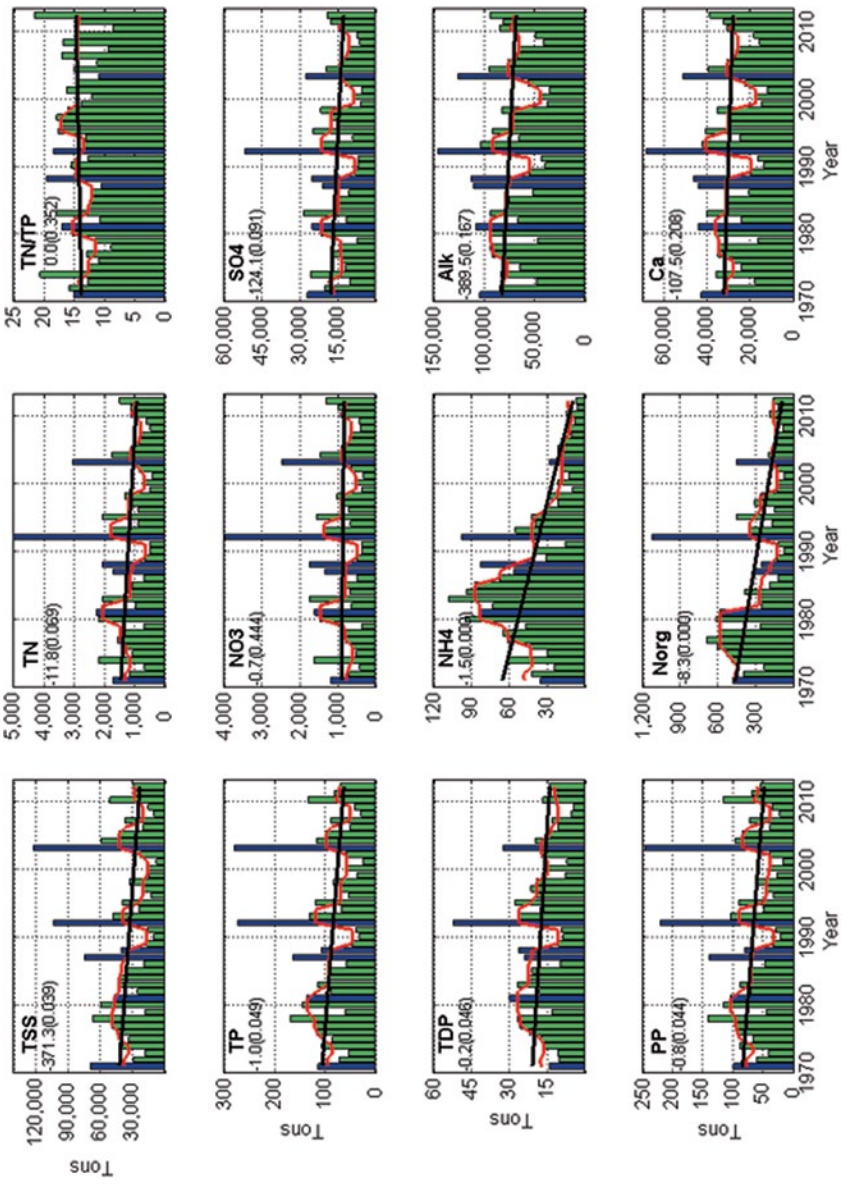

Fig. 18.6 Corrected annual loads (ton year^{-1}) of different materials at Pkak Bridge Station as calculated by the current study. The unitless ratio TN/TP is also shown. The rainy years with discharge > 600 10^6 m^3 year^{-1} are in *blue*. The *red curve* corresponds to the moving median smoother with a window size of 3 years. The *black line* corresponds to a robust regression line. Slope value (ton year^{-1}) and *P*-value in parentheses are calculated via Theil–Sen estimator and Kendal test, accordingly

The annual load of sulfate (SO_4), alkalinity (Alk), and calcium (Ca) decreased from ca. 18,000, 80,000, and 32,000 t year^{-1}, respectively, in the 1970s to ca. 13,000, 75,000 and 29,000 t year^{-1}, respectively, in the 2010s. A noticeable decrease of SO_4, Alk, and Ca loads occurred since 1994, followed by an increase since 2006.

18.4 Discussion

The first important achievement of this chapter is the creation of a new corrected data set of the monthly and annual material load from the Jordan River to Lake Kinneret. The former reports of Geifman and Rom (1995) and Rom (1999) used the manual sampling period (1971–1990) and automatic sampling period (since 1991) as a continuous record, without any correction. It is now clear that, although providing a much better sampling frequency which is important for evaluating nutrient loads (Cassidy and Jordan 2011), the automatic sampling load has to be corrected due to a systematic bias causing lower concentrations of the particulate constituents (mainly TSS, TP, PP, and N_{org}), as well as NH_4 concentration. As discussed earlier, the causing for this bias has to do mainly with the long pump pipe for the particulate matter and volatilization of gas in the open bottles for ammonium. The new data set of material loads to Lake Kinneret for the past 40 years will serve as a new reference for any future work on the lake and its watershed. This current contribution will also guide future data treatment needed in order to create a reliable combined data set based on manual and automatic sampling at the same location.

The long-term dynamics of the material load transferred from the Jordan River to Lake Kinneret between 1971 and 2012 are a consequence of changes in river discharge volumes as well as changes in anthropogenic activities and management actions that were taken. Typically, the Jordan River discharge and loads are highly variable; their values during storm events can be an order of magnitude higher than their median values (Chap. 7). Moreover, the difference between the annual discharge in rainy years and that of drought years may be of several hundred million m^3 year^{-1} while the median value is 430×10^6 m^3 year^{-1} (Fig. 18.5 and Table 18.2). These changes as well as the long-term reduction of discharge mentioned above directly affect the annual loads, simply because the load is a product of discharge and concentration. This discharge effect on material loads in the Jordan River is evident by the very high loads of TSS, phosphorus species, and nitrogen species during the rainy years of 1971, 1981, 1987, 1992, and 2003 and by the long-term reduction of most material loads (Fig. 18.6).

Anthropogenic development and management actions in the watershed (that were detailed in Table 31.3 of Chap. 31) can also explain some of the variability observed in the annual material loads (Fig. 18.6). However, the impact of these actions on the annual material loads is sometimes masked by the variability of the discharge. Therefore, we analyzed the material load data using unmasking methods that are not presented here, giving the insight to understand the impact of anthropogenic development and management actions.

In the 1970s, an increase in TDP, N_{org}, and NH_4loads was recorded. It is suggested that this increase occurred due to the rapid population increase in the Kinneret watershed at these years, followed by a rapid increase in the number of dairy farms. The sewage and cow manure was treated poorly in the 1970s, mainly by decentralized septic systems. It is well documented that such a poor treatment results in leakage of dissolved phosphorus, organic nitrogen, and ammonium to the environment (Edmonson 1970; Bailey et al. 2002).

In the mid-1980s, a decrease in the loads of TP, TDP, PP, N_{org}, and NH_4 was observed (Fig. 18.6), possibly as a consequence of the operation of the Einan Reservoir and other reservoirs to treat and contain effluents from Qiryat Shemona and the northern Hula basin, to be recycled for local agriculture. Generally, the operation of reservoirs for treated sewage with residence time of 2–6 months causes the dissolved phosphorus to be absorbed and precipitated as PP which sinks to the reservoir bottom (Bailey et al. 2002; Neal et al. 2010). It also leads to the oxidation of N_{org} and $NH_4$to NO_3. Novotny (2003) describes the nitrogen oxidation process as follows:

$$N_{org} \rightarrow NH_4^+ + O_2 \rightarrow NO_2^- + O_2 \rightarrow NO_3^-.$$

According to this sequence, N_{org} is likely to decompose to NH_4, which is oxidized to NO_2, which rapidly oxidizes to NO_3 through bacterial nitrification processes (Novotny 2003). Once treated effluents are used for irrigation, phosphorus and nitrate are utilized by the plants and the excess load that drains from the fields is significantly lower than the load that was introduced to the field (Novotny 2003). Another possible explanation for the decline of the N_{org} load since the late 1970s is the change in wind erosion of the drained Hula peat soils due to the introduction of sprinkler irrigation (Yatom S and Yasur E, pers comm; Avnimelech et al. 1978; Chap. 17). Since the 1980s, groundwater level at the Hula peat decreased, leading to more oxidation of organic nitrogen to nitrate according to the above sequence, resulting in excess NO_3 leaching from the Hula peats. The combination of decreasing NO_3 load in the 1980s due to the utilization of treated sewage for irrigation and the increasing NO_3 leaching from the Hula Valley may explain the observation that while N_{org} and NH_4 loads decreased during the 1980s, NO_3 load was more or less stable over time.

The creation of the Agmon wetland in the Hula Valley as part of the "Hula Project" initiated in 1994 is one of the most important management actions taken in the Lake Kinneret watershed (Chap. 31). The project included the re-flooding part of the drained Hula peat soils and stabilizing the surrounding peat soils by increasing groundwater levels, in order to decrease their decomposition, reclaim the agricultural value of the soils, develop ecotourism attractions and decrease nutrient loads to Lake Kinneret (Shaham 1994; Hambright and Zohary 1998; Markel 2000). This project decelerated the peat decomposition process, resulting in a slight decrease in the NO_3 load between 1994 and 2009, although hard to detect due to the masking of the load data by the variability in discharge, as explained above. Since 2010, the Hula project is managed in a new manner, by directing winter drainage of the peat

to Lake Kinneret in order to increase the NO_3 load (Barnea et al. 2012). As can be seen in Fig. 18.6, this policy actually affected the NO_3 loads since 2010, when the annual NO_3 load started to increase. It is also possible that this new management is responsible for the observed increases in SO_4, Alk, and Ca loads since 2010 (Fig. 18.6 and Table 18.2).

Flood protection and improved drainage measures were installed in 1998–2000, including deepening the Jordan River channel in the 3-km stretch between the Pkak and Benot Yaacov bridges (Chap. 31). These drainage works increased the slope of the Jordan River and resulted in higher flow velocity leading to more erosion and soil loss from the drained soils and from the riverbanks and increased TSS loads (Markel 2004). Similar phenomena were reported elsewhere (Goldman et al. 1986; Novotny 2003). Moreover, Markel et al. (2006) used a load transport model, AVGWLF, to simulate TSS and TP loads at the Pkak Bridge Station and concluded that the transport characteristics of the Jordan River at Pkak Bridge were modified in 2000 due to these drainage works. It is therefore suggested that this action caused the increase in particulate material load, mainly TSS and PP observed since 2000 (Fig. 18.6). Probably, this is also the reason for the observation that in 1992, the highest rainfall year in the entire 40-year record, the loads of particulate constituents like TSS and PP (102,441 and 220 t, respectively) were lower than in 2003 (121,360 and 245 t, respectively, Table 18.2). In contrast, dissolved constituents like TDP and NO_3 in 1992 (52 and 3,945 t, respectively) were higher than in 2003 (32 and 2,462 t, respectively), supporting the explanation for the observed changes in particles transport change explained above.

The combination of decreasing NO_3 load as a result of the "Hula Project" and increasing PP as a consequence of the enhanced drainage in 1998–2000 led to less stable values of TN/TP ratio since 2000 (Fig. 18.6). This ratio is purported to be important as a limiting factor for nitrogen-fixing cyanobacterial blooms in general (Novotny 2003) and particularly in Lake Kinneret (Zohary 2004; Hadas et al. 2012). In this respect, the change in the Hula project operation to directing winter flows from the Hula peat to Lake Kinneret rather than to Einan Reservoir (Chap. 31) was important for increasing the nitrogen load and the TN/TP ratio, which increased to 14.1 and 21.4 in 2011 and 2012, respectively (Table 18.2).

Acknowledgments The authors would like to thank the reviewers and editors for their insightful remarks which helped improve this manuscript. The authors are grateful for the efforts and dutiful contributions of Mekorot's Laboratory and Field staff at the Sapir site: David Maman, Avraham Bachar, Asher Afengar, Eran Dahan, Yacov Lavi, Rafi Cohen, Gali Nadir, Florette Sarusi, Oshrat Levi, Dora Levi, Malvina Yael Shwartz, Carmit Udi-Zilha, Pavel Raines, Ashley Davidson, Dr. Liliya Simkhovich, and Dr. Ram Porat. Special thanks to Dr. Bonnie Azoulay for assistance in the preparation of this manuscript.

References

APHA (2005) Standard methods for the examination of water and wastewater, 21st edn. American Public Health Association, Washington, DC

Avnimelech Y, Dasberg S, Harpaz A, Levin I (1978) Prevention of nitrate leakage from the Hula Basin, Israel: a case study in watershed management. Soil Sci 125:233–239

Bailey RA, Clark HM, Ferris JP, Krouse S, Strong RL (2002) Chemistry of the environment, 2nd edn. Academic, Waltham, 835 pp

Barnea I, Markel D, Bar Ilan I, Natanson T, Milard H (2012) Hydro-chemical monitoring of the surface water in the Hula project. Water Eng 80:38–43 (in Hebrew)

Benjamini Y (1988) Opening the box of a boxplot. Am Stat 42(4):257–262

Cassidy R, Jordan P (2011) Limitations of instantaneous water quality sampling in surface-water catchments: comparison with near-continuous phosphorus time-series data. J Hydrol 405:182–193

Conover JW (1999) Practical nonparametric statistics. Wiley, Hoboken

Eads RE, Thomas RB (1983) Evaluation of a depth proportional intake device for automatic pumping samplers. J Am Water Resour Assoc 19(2):289–292

Edmondson WT (1970) Phosphorus, nitrogen and algae in Lake Washington after diversion of sewage. Science 169(3946):690–691

Geifman Y, Rom M (1995) Material loads transfer from the watershed into Lake Kinneret. Mekorot Watershed Unit Report (in Hebrew)

Givati A, Rosenfeld D (2004) Quantifying precipitation suppression due to air pollution. J Appl Meteorol 43:1038–1056

Goldman SJ, Jackson K, Bursztynsky TA (1986) Erosion and sediment control handbook. McGraw-Hill, New York

Gray JG, Glysson D, Turcious LM, Schwarz GE (2000) Comparability of suspended-sediments concentrations and total suspended solids data. Water Resources Investigations Rep. No. 00-4191, USGS, Reston, VA

Hadas O, Pinkas R, Malinsky-Rushansky N, Nishri A, Kaplan A, Rimmer A, Sukenik A (2012) Appearance and establishment of diazotrophic cyanobacteria in Lake Kinneret, Israel. Freshw Biol 57(6):1214–1227

Hambright KD, Zohary T (1998) Lakes Hula and Agmon: destruction and creation of wetland ecosystems in northern Israel. Wetl Ecol Manag 6:83–89

Harmel RD, Slade RM, Haney RL (2010) Impact of sampling techniques on measured stormwater quality data for small streams. J Environ Qual 39(5):1734–1742

Hirsch RM, Slack JR (1984) A nonparametric trend test for seasonal data with serial dependence. Water Resour Res 20(6):727–732

Hirsch RM, Slack JR, Smith RA (1982) Techniques of trend analysis for monthly water quality data. Water Resour Res 18(1):107–121

Horne AJ, Goldman CR (1994) Limnology, 2nd edn. McGraw-Hill, New York, 576 pp, pp 20–21

Markel D (2000) Biogeochemical processes in a re-flooded wetland: sulfur and iron cycles in Lake Agmon, Hula Valley, northern Israel. Report GSI/1/2000, 135 pp (in Hebrew)

Markel D (2004) Pollutants transfer from the Jordan River to Lake Kinneret during the winter of 2002/2003. Water Irrig 448:14–17, 35 (in Hebrew)

Markel D, Somma F, Evans MB (2006) Using a GIS transfer model (AVGWLF) to evaluate pollutant loads in the Lake Kinneret watershed, Israel. Water Sci Technol 53(10):75–82

Neal C, Williams R, Jarvie HP, Love AL, Neal M, Wickham H, Harman S, Armstrong L (2010) Declines in phosphorus concentration in the upper River Thames (UK): links to sewage effluent cleanup and extended end-member mixing analysis. Sci Total Environ 408(6):1315–1330

Novotny V (2003) Water quality: diffuse pollution and watershed management, 2nd edn. Wiley, New Jersey 864 pp

Pelletier PM (1988) Uncertainties in the single determination of river discharge: a literature review. Can J Civ Eng 15(5):834–850. doi:10.1139/l88-109

Rom M (1999) Kinneret watershed: trends and changes in material load 1970–1998. Mekorot Watershed Unit (in Hebrew)
Rom M, Berger D, Sarusi F, Teltsch B (2002/2012) Annual winter reports, Mekorot Watershed Unit (in Hebrew)
Roseen RM, Ballestero TP, Fowler GD, Qizhong G, Houle J (2011) Sediment monitoring bias by automatic sampler in comparison with large volume sampling for parking lot runoff. J Irrig Drain Eng 137(4):251–257
Rousseeuw PJ, Annick ML (2003) Robust regression and outlier detection. Wiley Series in Probability and Mathematical Statistics, 516. Wiley, Hoboken, p 67. ISBN: 978-0-471-48855-2
Rutherford JC (1994) River mixing. Wiley, New York, 362 pp
Shaham G (1994) The Hula project—a dynamic intervention of human in nature. Ecol Environ 1–4:221–228 (in Hebrew)
Tukey JW (1977) Exploratory data analysis. Addison-Wesley, London
Velleman PF (1980) Definition and comparison of robust nonlinear data smoothing algorithms. J Am Stat Assoc 75(371):609–615
Wetzel RG (1983) Limnology, 2nd edn. Saunders College Publishing, Philadelphia, 767 pp
Wilcox RR (2001) Theil–Sen estimator, fundamentals of modern statistical methods: substantially improving power and accuracy. Springer, Berlin, pp 207–210. ISBN: 978-0-387-95157-7
Zohary T (2004) Changes to the phytoplankton assemblage of Lake Kinneret after decades of a predictable, repetitive pattern. Freshw Biol 49(10):1355–1371

Chapter 19
External Sources of Nutrients

Ami Nishri and Edit Leibovici

Abstract The primary source of nitrogen to Lake Kinneret drainage basin is dissolved inorganic N originating in southern Europe and being carried over the Mediterranean Sea by the rain clouds. Evidence is presented that this nitrogen is cycled within the mountainous aquifers eventually outflowing to the Jordan River and later to Lake Kinneret as nitrate. Within the watershed, there are additional sources of nitrogen that add almost half of the total annual riverine load. These include "old" N previously buried in peat within the historic Hula Lake and marshes as well as N in fertilizers and N resulting from cattle excretion. The drying out of the Hula Valley water bodies some 60 years ago resulted in the oxic degradation of this peat and the conversion of organic N to NH_4^+ which is later nitrified and the NO_3 product is transported in the watershed waterways. At some stage, particularly during the 1970s, peat dust was spread over all of the drainage basin, including Lake Kinneret, through aeolian transport. This is indicated by high levels of organic C and N in the northern tributaries and in the Jordan River itself as well as in Lake Kinneret. As a result of the additional respiratory processes induced by the large amounts of this allochthanous organic matter, those waterways and Lake Kinneret surface water showed lower pH and dissolved oxygen (DO) levels than in the following decades.

The two main external sources of phosphorus to Lake Kinneret are riverine and dust. In accordance with water discharge, the riverine source predominates in winter, while the dust source is more important in the dry season that follows. Isotopic (oxygen) evidence suggests that most of the P in dust originates from P fertilization of cultivated soils. Notice that in this relatively dry climate, aeolian transport of nutrients plays an important role, particularly in summer.

Keywords Nutrients · DIN · Peat · Aeolian transport · Phosphorus in dust · Oxygen isotopes in nitrate

A. Nishri (✉) · E. Leibovici
The Yigal Allon Kinneret Limnological Laboratory, Israel Oceanographic & Limnological Research, P.O. Box 447, 14950 Migdal, Israel
e-mail: nishri@ocean.org.il

E. Leibovici
e-mail: edit@ocean.org.il

T. Zohary et al. (eds.), *Lake Kinneret, Ecology and Management,* Aquatic Ecology Series 6,
DOI 10.1007/978-94-017-8944-8_19,

19.1 Background

The prevailing climate in the Lake Kinneret watershed has significant impacts on riverine nutrient loads to the lake. Precipitation is characterized by a seasonal typical Mediterranean pattern falling mostly in winter while the summer–fall is dry. Annual precipitation varies greatly between the different parts of the watershed, ranging between ~400 mm in the south (over the lake) and 500–800 mm in the center of the basin and to >1,000 mm on Mount Hermon in the north (Fig. 7.1 in Chap. 7). The main source of water in the watershed is the mountainous aquifer in the north. It feeds the Jordan River through two major groundwater springs, the Dan and the Banias. Typically, more than half of the riverine loads of N and P to Lake Kinneret occur during the 3–4 months of rainy season (December–March), while the following drier season is characterized by diminishing riverine nutrient loads, in accordance with their respective water discharge.

In spring, the monomictic Lake Kinneret becomes stratified, such that the lower water mass (LWM) is to a large extent separated from the overlying photic layer. Consequently, organic matter produced in the epilimnion settles through the seasonal thermocline and accumulates in the LWM where it decomposes. Mineralization products of this decomposition are mostly retained in the LWM and to a large extent are excluded from supporting phytoplankton activity in the epilimnion. Thus, in the dry season, not only do the external riverine sources decline but also the internal cycling between layers is restricted. This combination leads to below detection levels of soluble P and dissolved inorganic nitrogen (DIN) species in the lake epilimnion.

Over the past six decades, Lake Kinneret has undergone significant biological changes (Chap. 10). Some of these were attributed to alterations in riverine nutrient loads which resulted in a decline in N:P ratios in the lake (Gophen et al. 1999) as well as to a decline in riverine loads of selenium and dissolved organic matter (Zohary et al. 2012). The routine monitoring of external sources of nutrients to the lake was, until a few years ago, focused on riverine sources only. This monitoring did not yield satisfactory explanations for the long-term biological changes documented in the lake. Neither did it offer appropriate explanations for shorter-term effects such as what supports biological activity in the lake during summer, when riverine water discharge declines. Or else, what maintained the unexpected relatively high biological activity during sequences of drought years (three times over the past 40 years). It was often assumed that long residence time of the nutrients facilitated through release from bed sediments supported activity during prolonged droughts. Recent monitoring activity, which includes P contribution through dust deposition, added valuable information to our understanding of this system.

In addition to the short-term (seasonal and annual) variability in riverine loads, long-term changes in the supply of nutrients were noticed. Over the past century, the watershed has undergone major anthropogenic impacts (Table 1.2 in Chap. 1). Notable among these is the draining of Lake Hula and its surrounding swamps (total area estimated at ~63 km^2) in the 1950s (Karmon 1960 and Fig. 19.1). Lake Hula was a shallow natural lake located in the central low-lying part of the watershed. It functioned as a natural settling pond for particles and as a site of assimilation of soluble nutrients by its massive submerged and emergent macrophyte flora.

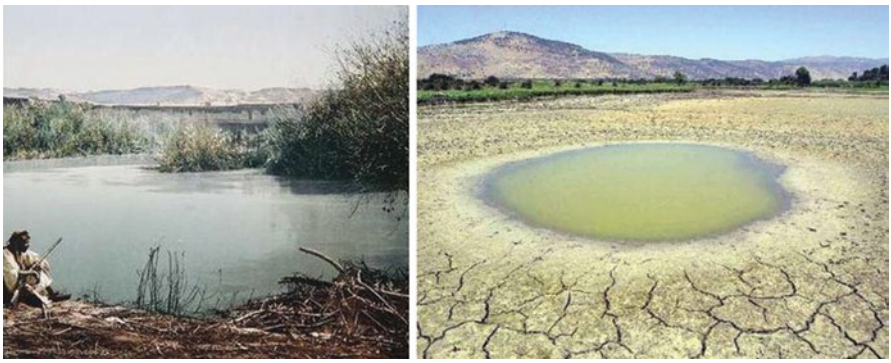

Fig. 19.1 Landscape scenes of Lake Hula before (1890) and during (1957) its drainage. (Source: Internet)

The high macrophyte productivity of Lake Hula and its associated marshes led to the accumulation over time of thick peat deposits interlayered with marls (Cowgill 1969; Dimentman et al. 1992). After its drainage, the Hula Valley was cultivated and became a potential source of new nutrients to the downstream lake, Lake Kinneret. Not only freshly added fertilizers but also "old" nutrients were released from the peat to the waterways as a direct consequence of biogeochemical processes that followed the drying. The exposure of the peat to air resulted in enhanced aerobic decomposition, which impacted nutrient release (Nishri 2011).

The aims of this chapter are to gain an overall view of external sources of N and P (to some extent also selenium) to Lake Kinneret at present and in the past. According to differences between the modes of supply, this chapter is divided into nitrogen and phosphorus sources.

19.2 Sources of Nitrogen

19.2.1 General Lake Budget

In the riverine sources to Lake Kinneret, nitrogen exists mainly as nitrate (NO_3^-) and to a lesser extent as organic nitrogen (Norg) while ammonium is negligible (<3%). Since routine monitoring started in 1970 nitrate loads did not show a distinct long-term trend, although large interannual variability was recorded. Typical riverine loads of NO_3 are 1,000±700 t N year^{-1}, but the interannual variability is large, mainly due to large variability in precipitation and discharge. In the extremely rainy year of 1992, riverine NO_3 was almost 4,000 t, whereas in relatively dry years (1979, 1989, 1990, 1991, 1999, 2000, 2001) the respective load was an order of magnitude smaller (see Fig. 18.6 in Chap. 18). Organic nitrogen (mostly DON), however, shows a prominent long-term decline from 500–600 t N year^{-1} in the mid-1970s to a respective recent average of ~150 t N year^{-1}.

At present, more than half of the nitrogen input to Lake Kinneret originates in the northern Jordan River tributaries, which are fed by the Dan and Banias groundwater springs. An additional major source of nitrogen to the Jordan River is the flushing of peat soils in the Hula Valley as well as flushing of agricultural and pastoral land on the mountain slopes to the east of the valley (see Fig. 5.2e, g in Chap. 5).

The amounts of nitrogen removed from Lake Kinneret through pumping and through burial in the lake bed sediments were estimated as being much smaller than riverine inflows and the difference, of 60–80%, was attributed to denitrification (Serruya 1978; Smith et al. 1989).

19.3 Mount Hermon Sources of Nitrogen

Mount Hermon (>2,000 m) located in the northern edge of the watershed (Fig. 7.1 in Chap. 7) is mainly composed of a carboniferous Jurassic sequence. It hosts a thick and highly porous phreatic aquifer. Water emerging from its two major springs is nearly oxygen-saturated (>97%), while NO_3^- constitutes more than 97% of DIN in this water. The larger and most pristine water source to the Jordan River is the Dan Spring, with discharge of $\sim 240 \times 10^6$ m^3 $year^{-1}$ characterized by a relatively steady concentration of NO_3, at ~1.15 mg N L^{-1} (Fig. 19.2a) (Mekorot data base). The Banias Stream has, however, somewhat higher levels, at 1.38 mg N–NO_3 L^{-1} (Fig. 19.2a) attributed to effluents originating from villages in the north of the Golan Heights (D Markel, pers. com.). The anthropogenic origin of this excess NO_3 in the Banias may be indicated by its slightly heavier $\delta^{15}N$–NO_3, as compared to that of the Dan Stream (Fig. 19.2b).

The Mount Hermon catchment for the Dan Aquifer is covered by natural vegetation. Local precipitation, either as rain or snow, seems to be the only potential source of water and of DIN to the underlying groundwater that feed the Dan spring. Regional rain clouds migrate eastward over the Mediterranean and the mountains of Galilee (see Chap. 6, Fig. 6.4b), picking up a variety of particles and solutes from various sources on the way. The Na:Cl molar ratio in local rain (~0.81) which resembles that of the Mediterranean Sea, provides evidence that the Dan Stream has a sea spray source. DIN concentration in rain varies over the watershed between ~0.1 mg N L^{-1} and up to 2.5 mg N L^{-1} (see the sum of NH_4^+ and NO_3 concentrations in Fig. 19.3), with a basin average of 1.32 mg N L^{-1}. There is a distinct spatial variability in DIN concentrations in rain (Fig. 19.3); in the northern mountainous region, DIN is lowest, with an average of 0.5 mg N L^{-1}, while in the central and southern parts of the basin it is somewhat higher than the basin average. Thus, DIN concentrations in rain in the Dan region, 0.5 mg N L^{-1}, are only ~40% of nitrate concentrations in the groundwater spring that is presumably fed by this rain (~1.2 mg N L^{-1}). The reasons for this discrepancy are related to the different fates of nitrogen and of water in this system. Regional typical ratios between overall precipitation and groundwater discharge are estimated at roughly 2.5:1 (Yechielly, pers. com.). About 60% of the precipitation is actually evapotranspirated or is

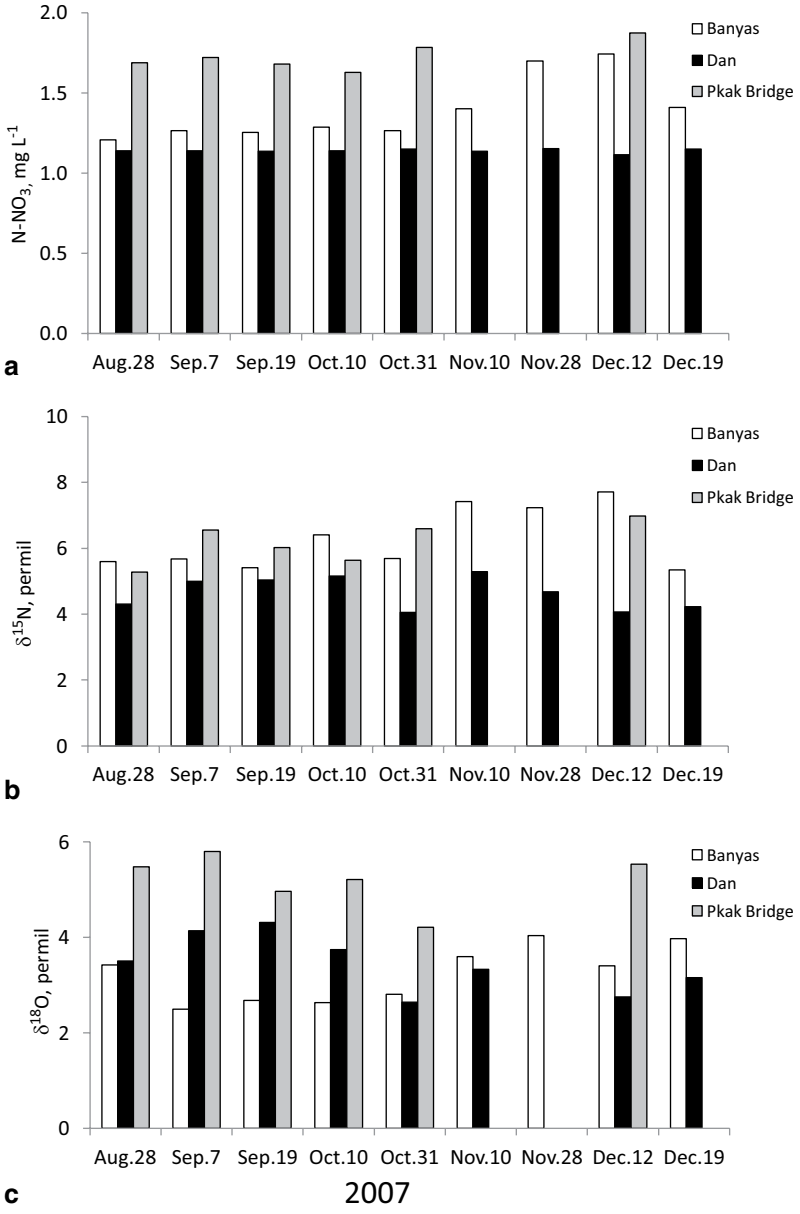

Fig. 19.2 **a** NO3 concentrations, **b** $\delta 1^5N–NO_3$, and c $\delta^{18}O–NO_3$ in the Dan stream, the Banias stream, and the Jordan River at Pkak Bridge during summer–autumn 2007

transported by subsurface almost horizontal flow facilitated by the highly permeable soil layers. The remaining 40 % infiltrate into the aquifer. As for DIN, we assume that all of DIN content of the rain is assimilated by the flora, hence retained

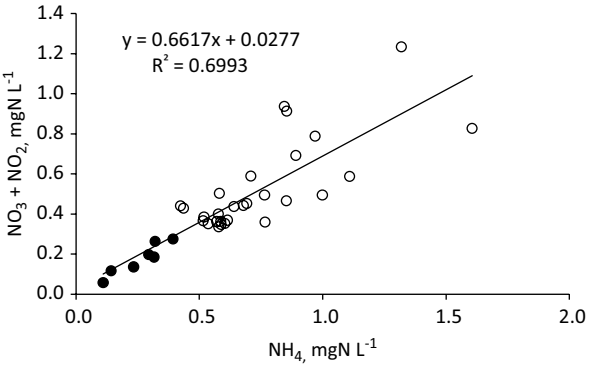

Fig. 19.3 NH_4–N versus (NO_2 N ve$_3$–N) in samples of rain and snow collected during the winters of 2005, 2007, and 2011–2012 in the Lake Kinneret watershed. *Filled circles* represent samples taken on Mount Hermon (snow and rain) and nearby mountains. *Empty circles* represent samples taken mostly near Lake Kinneret. Note the higher concentrations of DIN in precipitation falling in the southern part of the basin as compared to the northern basin (Mount Hermon). The *regression line* indicates the strong correlation between NH_4 and NO_3 and NO_2

locally. At a later stage, the decomposition of this flora (often in summer) yields NH_4 which is momentarily adsorbed onto local soil layers. Through adsorption–desorption equilibrium the next winter rains infiltrating downward acquire this NH_4 which then undergoes nitrification to form NO_3. Thus, unlike the fate of water, all of the N from rain is assumed to infiltrate the aquifer. Therefore, under steady state, the ratio between the concentrations of NO_3 in the underlying aquifer and its concentration in rain is inversely proportional to the ratio between the amount of water outflowing from the spring over the amount falling on the mountain as rain and snow. In support of this hypothesis, a similar case seems to exist also in an Eocene aquifer exposed in the hilly area north of Lake Kinneret. This chalky phreatic shallow aquifer is covered by mostly uncultivated soils and has groundwater DIN levels (here also mostly as NO_3), three times higher (~4 mg N L^{-1}) than the DIN content of the local rain, at ~1.2 mg N L^{-1}.

There are other differences in the chemical composition between the Dan region rain and the Dan spring water. First, unlike the predominance of NO_3 species in the Dan spring water, in rain DIN is made of a mixture of about two-thirds of NH_4 and one-third of NO_3+NO_2. Overall basin rain data show a positive correlation ($R^2=0.68$) between NH_4 and (NO_2+NO_3) with a slope of 0.64 (Fig. 19.3), suggesting some sort of equilibrium between these forms of DIN. Rain samples (~25) were collected during winter 2010–2011 on the Mediterranean coast (on top of the building of Israel Oceanographic and Limnological Research in Haifa: courtesy of B Herut), ~50 km west of Lake Kinneret. DIN determination on these samples showed a positive correlation ($R^2=0.47$) between NH_4 and (NO_3+NO_2) with a slope of 0.55 and an average DIN of 0.9 mg N L^{-1}. The most likely source of the rain sampled is west of the coastline in the Mediterranean or in southern Europe

(including Turkey). Another rain sample, taken on February 2012 at Eshkol Reservoir, midway between Lake Kinneret and the Mediterranean coast, had NH_4:NO_3 ratio that also falls on the regional regression line of Fig. 19.3. Taking into account (1) the predominant direction of movement of rain clouds, and (2) that inland rain samples and Mediterranean cost rain samples show a rather similar DIN species distribution pattern, then, DIN in the rain falling over the watershed was likely to have originated from southern Europe.

An additional difference that exists between the Dan spring water and the local rain is in their oxygen isotopic composition of nitrate, $\delta^{18}O_{(NO3)}$. In the rain, $\delta^{18}O_{(NO3)}$ is equal to $+69 \pm 5$‰ while in the Dan (and Banias) spring it is much lighter, at 3.25 ± 0.6‰ (Fig. 19.2c). Such $\delta^{18}O_{(NO3)}$ in rain is most probably acquired through tropospheric interactions with ozone (Mayer et al. 2001), while that of the groundwater springs is acquired through in situ nitrification. This nitrification, of the NH_4 degradation products delivered from the cover soil flora above, takes place within the oxic aquifer. During nitrification, ammonium acquires two oxygen atoms per molecule from the ambient water and one from air (Mayer et al. 2001). The oxygen isotope composition of the groundwater of the Hermon aquifers, $\delta^{18}O_{(H2O)}$, is -7.45‰ (Gat 1970; Gat and Dansgaard 1972). Considering that atmospheric O_2 has $\delta^{18}O$ of $+23.5$‰ (Kroopnick and Craig 1972) the expected $\delta^{18}O_{(NO3)}$ in the Dan and Banias streams should be $+2.9$‰, which is close to the spring value of 3.25‰ reported above. Hence, isotopic data seem to support an idea that total nitrogen (TN = DIN + Norg) is conservative within this almost fully oxidized Dan aquifer system; only the forms of N change. Eventually, the NH_4, NO_3, and NO_2 from rain entering the Dan aquifer system, exit via the groundwater spring mostly as NO_3. This NO_3 acquires its oxygen isotopic signature from the ambient groundwater and the air, irrespective of whether it was primarily precipitated in rain as NH_4 or as NO_3.

19.3.1 Hula Valley Sources of Nitrogen

A prominent hydrological function of the historic Lake Hula was slowing the rate of flow of the Jordan River downstream the Hula Valley. The drainage of Lake Hula and its adjacent swamps in the 1950s was achieved by widening the Jordan River channel at the outflow from Lake Hula. This resulted in a drawdown of the phreatic soil water table in the valley (Fig. 19.1 right panel) exposing peat soils to air. Soil cultivation required to keep the ground water table at ~1-m depth and to introduce suitable irrigation methods. A drainage system was constructed to maintain this water table and thus to lower the release of nutrients and organic matter from deeper peat soils to the Jordan River (Avnimelech et al. 1978). However, the invasion of air into the previously anoxic peat could not be fully prevented and extensive oxidative degradation of the peat followed (Shoham and Levin 1968). The ammonium degradation product released was then adsorbed into the soil, which was then flushed and desorbed by flood or irrigation water deficient in NH_4. The situation worsened

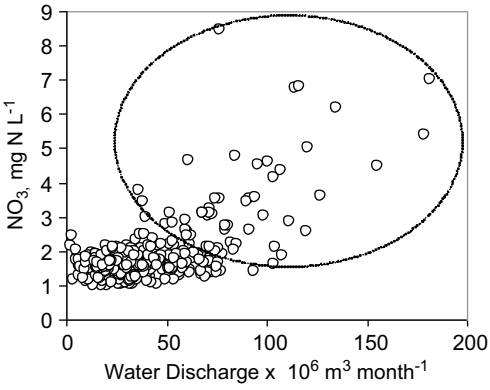

Fig. 19.4 Monthly average water discharge against NO_3–N concentration in Jordan River (Pkak Bridge), 1970–2011. The *circle* highlights the points of high discharge and high nitrate

during the 1970s, when poor management resulted in further lowering of soil water table, which led to enhanced oxidative degradation. Three modes of nitrogen export from this valley are identified after its drainage. One mode was through flushing of the peat soils with the freshwater discussed above, the second mode was through surface erosion and aeolian transport of peat in dust, and the third mode was of leaching of nitrogen originated from agricultural activities.

The oxidative degradation of the peat and destruction of soil structure (Brachyau 1958; Avnimelech et al. 1978; Hambright and Zohary 1998 and references therein) led to additional biogeochemical consequences. Among these was the accumulation of selenium (Se) in the peat soil water at concentrations of up to 10 μg L^{-1} (Nishri et al. 1999). Selenium is considered to be an essential micronutrient for growth of the bloom-forming dinoflagellate *Peridinium gatunense* (Lindstrom 1980; Chap. 11, 24). Another drainage-induced process was the diagenetic formation of gypsum ($CaSO_4$*$2H_2O$), which accumulated in the subsoil layers (Bein and Nielsen 1988; Markel et al. 1998; Bein 1986).

The uncontrolled drawdown of the water table in the Hula Valley in the 1970s allowed flood and irrigation water to infiltrate the peat soils and interact with the solid phase causing: (1) desorption of NH_4, (2) accumulation of Se(IV) in the anoxic peat soil water, and (3) dissolution of sedimentary gypsum (Markel et al. 1998) and therefore a buildup in SO_4 and Ca^{+2} levels in the soil water. These processes continue today. Upon flushing and emergence to the fully oxidized drainage canals, fast nitrification (within few hours) occurs as well as the appearance of more oxidized Se species, mostly Se(VI) (Nishri et al. 1999; Nishri and Sukenik 2012). A few days after each rainstorm, the flushed peat water enters the Jordan River at the southern part of the valley, via drainage canals. Concomitantly, river water concentrations of NO_3^-, SO_4, and Se (VI plus IV) increase. There is an apparent relationship between the magnitude of flood events and NO_3^- concentrations in the river. When discharge exceeds ~50×10^6 m^3 $month^{-1}$ then monthly average concentrations of NO_3 at Pkak Bridge (south of the valley) may exceed (marked by an ellipse in Fig. 19.4) the "normal" range of 1.1–2.2 mg N L^{-1}. In extreme singular floods, river nitrate con-

centrations may even rise up to >10 mg N L^{-1}, with a concomitant increase in concentrations of SO_4 and soluble Se up to 110 mg L^{-1} and 1 μg L^{-1}, respectively (data not shown). In such events, river water at the Pkak Bridge may contain up to 3–4% of flushed peat soil water.

However, floods are not the only cause for Hula Valley contribution of NO_3 to Lake Kinneret. Agricultural irrigation using Jordan River water may lead to a similar result because here again NH_4-depleted river water interact with NH_4-enriched peat water. This may be indicated from data (Mekorot Water Company Database) that even in the dry seasons nitrate concentrations at the Pkak Bridge are higher by almost 50% than the respective concentrations in the two major northern tributaries, Dan and Banias (Fig. 19.2).

Another mode of nitrogen delivery from the valley, particularly during the mid-1970s and early 1980s, is through aeolian erosion and transport. Aeolian erosion in the Hula Valley was negligible before the draining of Lake Hula and remained relatively low also after drainage in the 1960s when the groundwater table was maintained at relatively shallow depth. However, in the 1970s the erosion of peat soils intensified, generating dark-colored dust that was carried by winds and deposited onto the surrounding water bodies (Nishri 2011). This process had a pronounced effect on long-term records of Norg levels in the Jordan River, in its northern tributaries and in Lake Kinneret itself. In the 1970s, Norg loads were almost twice as high as in the following decades (Chap. 18). Moreover, the dark dust concomitantly contributed to higher levels of organic carbon (Corg) and suspended particles in the river (Nishri 2011). In the 1980s, the extent of aeolian erosion of the peat soils has declined due to partial cessation of peat soil cultivation and development of dense natural vegetation, which may have prevented surface erosion. In addition, the 1980s were characterized by a further drop in the soil water table; thus, the arena for exothermic peat oxidation was transferred into deeper soil layers, as was indicated by frequent occurrence of underground fires. The transition between the 1970s and the 1980s was not only marked by a significant decline in external loads of Norg (and Corg) to Lake Kinneret but also by elevated levels of pH and dissolved oxygen (DO) in Lake Kinneret surface water and of pH of the Jordan River (Nishri 2011). These inverse temporal patterns (almost mirror image profiles) between pH and organics were attributed to elevated bacterial respiration stimulated by high levels of biodegradable allochthanous organic matter in the 1970s and less so in the 1980s. Significant amounts of Hula peat had also been shown to accumulate in Lake Kinneret pelagic bed sediments, dated to deposit during the 1950s (Dubowski 1996; Nishri 2011).

In the mid-1970s, allochthanous (mostly aeolian) peat resources were so high, that they could potentially support about half of the zooplankton activity in Lake Kinneret (Nishri 2011). This may have been the reason for the similar temporal pattern between lake levels of Norg (in this case a surrogate of allochthanous organics) and zooplankton biomass. The latter being high in the 1970s and was characterized by a twofold decline during the 1980s (Gophen et al. 1990), without having a concomitant decline in the lake's primary productivity.

19.3.2 Isotopic Considerations

The two major sources of nitrate in the watershed are expected to have different oxygen isotopic signatures. Nitrate formed within the Hula Valley, which contributes almost half of the NO_3^- in the Jordan River, is expected to have a heavier oxygen isotopic composition than nitrate from the northern tributaries because $\delta^{18}O_{(H2O)}$ in the Hula Valley water is isotopically heavier. This has two reasons. First, due to altitudinal differences the rain falling on the Hula Valley is ~2‰ heavier than the rain falling on Mount Hermon. Second, river water used in the Hula Valley for irrigation becomes isotopically heavier due to evaporation. Few samples of water extracted from Hula Valley soils revealed $\delta^{18}O_{(H2O)}$ of -4 ± 0.5‰. Accordingly it is predicted that $\delta^{18}O_{(NO3)}$ formed through nitrification within the valley would have $\delta^{18}O_{(NO3)}$ equal to ~+5.5‰. Under the assumption that half of the nitrate at Pkak Bridge, south of this valley, originates from the valley and half from the northern springs, the predicted $\delta^{18}O_{(NO3)}$ value in this bridge should be ~+4.1‰. This predicted value is somewhat lower than the measured values of $+5 \pm 0.5$‰ (Fig. 19.2c).

Further down, in Lake Kinneret $\delta^{18}O_{(H2O)}$ varies between −0.5 and +1.5‰ (Gat and Dansgaard 1972), hence $\delta^{18}O_{(NO3)}$ of the NO_3^- formed through nitrification within the lake is predicted to be ~+7.8‰, considerably heavier than in riverine sources. This makes the oxygen isotopic composition a potentially powerful tool to distinguish between riverine and in-lake sources of nitrate (T. Zilberman, pers. com.). A schematic presentation of nitrogen fluxes and transformations in the watershed, based on isotopic and chemical considerations, is given in Fig. 19.5, which summarizes the processes shown in the above sections.

19.3.3 Historical View of Nitrogen Loading

The conclusion that nitrogen in the Lake Kinneret drainage basin originates from rain coming from Europe, implies that much of the natural vegetation in this basin and perhaps also in other parts of Israel was (and still is) supported by this remote source. The long-term accumulation of thick layers of peat in the Hula Valley represents net accumulation over time of nitrogen, probably of European origin, in buried flora. Thus, prior to the drainage of Lake Hula, only that part of the N from rain which was not incorporated into macrophytic and other vegetation within the Hula Valley, was transported to Lake Kinneret, i.e., less nitrogen was inflowing into Lake Kinneret.

19.4 Sources of Phosphorus

19.4.1 Riverine Sources

Two analytically defined species of phosphorus are regularly measured in the Jordan River: total phosphorus (TP) and total dissolved phosphorus (TDP). The

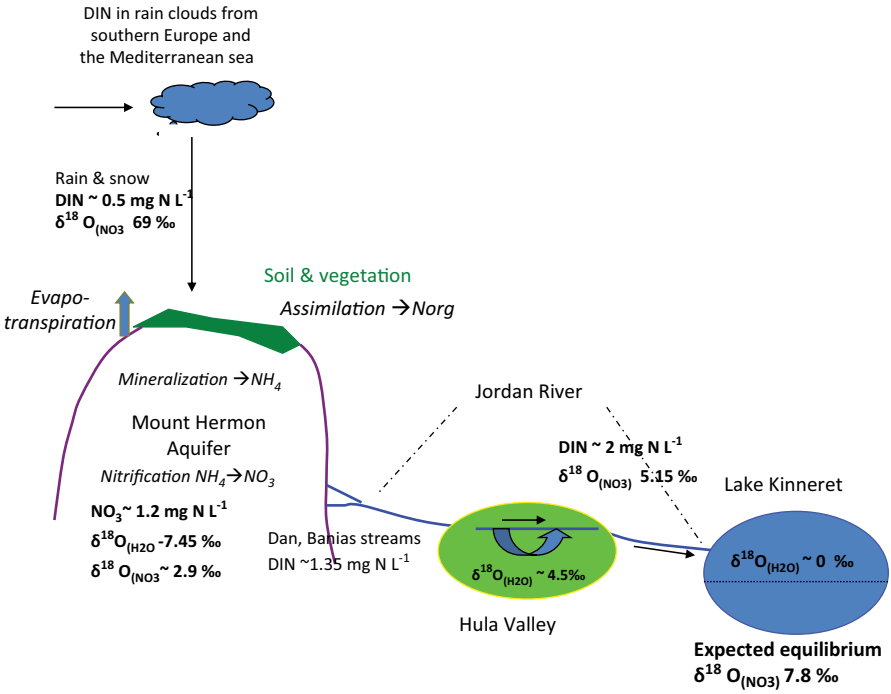

Fig. 19.5 Schematic view of the major nitrogen fluxes, DIN concentrations, $\delta^{18}O_{(NO3)}$ and $\delta^{18}O_{(H2O)}$ in the different water bodies of the Lake Kinneret watershed

calculated difference between them represents particulate phosphorus (PP). The multiannual (1972–2011) average TP load from the Jordan River is 87 t year^{-1} (Chap. 18) with a typical annual pattern shown in Fig. 19.6. About 70% of the riverine TP load is made of PP (see Chaps. 18 and 20), most of which appears as calcium-bound phosphorus, presumably apatite or calcium carbonate phosphate (Salingar et al. 1993), and is therefore assumed to be of limited availability for biotic uptake in Lake Kinneret. The remainder 30% of TP appears as TDP (mostly SRP), assumed to be bioavailable. In the river, PP concentration is positively and significantly correlated ($R^2 = 0.86$) with total suspended solids (TSSs), having an average content of 0.176% phosphorus. This resembles the concentrations of phosphorus in Lake Kinneret northern littoral bed sediments, of ~0.16% (see Chap. 20). Both TSS and PP are also positively correlated with water discharge, with higher loads of PP to Lake Kinneret in rainy winters. TDP concentrations are also positively correlated with river discharge ($R^2 = 0.50$). Most of this dissolved P originates from the dissolution of fertilizers or desorption from clay minerals and iron oxides (Nishri 2010) as well as degradation of fecal products of cattle (Oren Reichman pers. Com).

The large multi-annual and seasonal variability in rainfall affects riverine phosphorus loads, which decrease considerably during dry years and in the summer months. As an example, in the moderately rainy winter of 2011 the annual riverine load of TP was only 51 t (Table 18.2, Chap. 18). The concurrent riverine TDP loads

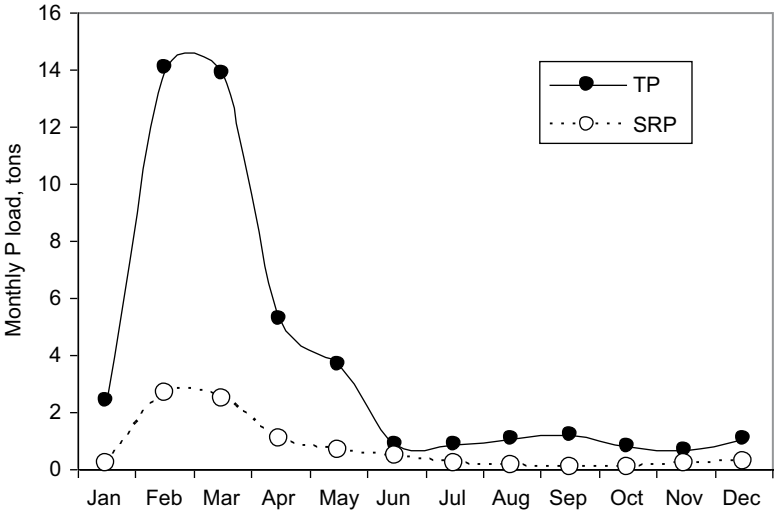

Fig. 19.6 Monthly loads of TP and TDP in the Jordan River (Pkak Bridge) during the moderate rainfall year of 2011. (Data courtesy of Mekorot Water Company)

were extremely low, ranging between 3 t month^{-1} in winter to ~0.2 t month^{-1} in summer (Fig. 19.6). Based on the assumption that 70% of the PP is Ca-bound (see Chap. 20) total bioavailable riverine P inflows, which includes 30% of the PP and all of the TDP load in 2011, were ~26 t with an average of 0.7 t month^{-1} in the 7 months of the summer period and ~4–5 t month^{-1} in winter.

The following is an attempt to make a P budget for Lake Kinneret by estimating the P removal flux. Approximately 100,000 t of sediment is deposited in Lake Kinneret (Chap. 23) each year. Out of this, between 50 and 60% is relatively P-depleted autochthonous calcite (between 100 and 150 μg P g^{-1}) and the remainder is made of allochthanous material (riverine plus dust) as well as buried organic matter. TP concentrations in the lake bed sediments vary between 1,000 μg g^{-1} in the pelagic zone and ~1,600 μg g^{-1} in the littoral zone (Chap. 20). Thus, it is estimated that P burial in the bed sediments obtained by multiplying its concentration by bulk sedimentation, amounts to 130 ± 30 t year^{-1}. Removal of P through water outflow, mostly by pumping, exports ~10 t P annually. Additional 10 t P are removed annually by fishing. This amount is obtained by multiplying the average P content of fish (0.63%) by a mean annual catch of ~1,500 t wet weight (Chap. 36, Fig. 36.2). Hence, a total P removal amounts to 150 ± 30 t year^{-1}. Removal therefore exceeds the multiannual riverine inflow P load of 63 ± 30 t year^{-1} given above. The only possible mechanism to balance the phosphorus budget is through atmospheric wet and/or dry deposition.

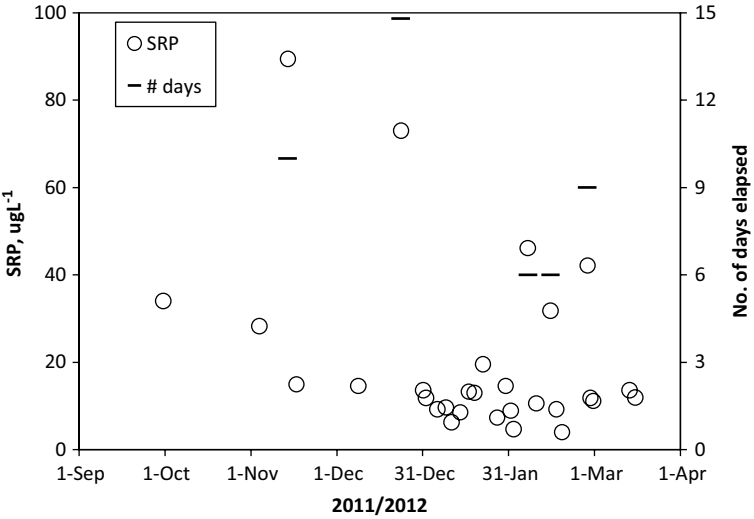

Fig. 19.7 Soluble reactive phosphorus (*SRP*) concentrations in rain samples (*left y axis*) collected between 1 October 2011 and 26 March 2012 on the roof of the Kinneret Limnological Laboratory. The *right y-axis* indicates the number of days elapsed since the previous rain event

19.4.2 Atmospheric Sources: Wet Deposition

A detailed study of phosphorus in wet deposition was made during the rainy winter between 1 Oct 2011 and 26 Mar 2012. Out of the 38 rainy days, we collected 29 daily rain samples and analyzed soluble reactive phosphorus (SRP), TP, and nitrogen species. Mean SRP concentration was ~14 μg P L^{-1} and the mean number of days elapsed between rain events was 4.2 days. However, in five samples, SRP concentrations were significantly above the mean (Fig. 19.7) and these 5 days were characterized by having longer (mean of 9 days) intermittent dry periods before the rain event. Moreover, these 5 peak SRP days were also characterized by exceptionally high PP levels (100–200 μg L^{-1}) as compared to the remaining days with only few tens of micrograms of PP L^{-1}. This suggests that longer dry intermissions between rain events allowed for the accumulation in the air of particles containing phosphorus, part of which was leachable by moisture. Local rainfall on Lake Kinneret itself is ~70×10^6 m^3 $year^{-1}$ and therefore annual wet deposition may supply only ~1 t P (as SRP) $year^{-1}$ to the lake, the equivalent of only 2–4% of riverine phosphorus inflow loads.

19.4.3 Atmospheric Sources: Dry Deposition (Dust)

In a previous study, Ganor et al. (2003) have shown that dust deposited on Lake Kinneret may be an important source of P to the lake. To verify this, two procedures

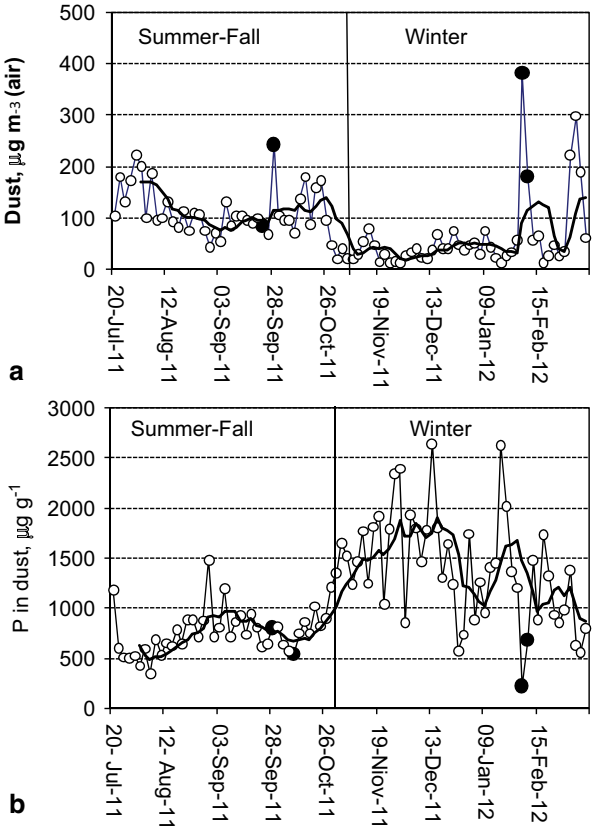

Fig. 19.8 **a** Dust concentration in air sampled by an active dust collector on the roof of the Kinneret Limnological Laboratory, from 19 July 2011 to 19 March 2012 every 2–3 days. **b** Phosphorus concentration in this dust. *Filled large circles* represent desert dust events of which the one occurring on 8 Feb 2012 was the largest

were used by us for dry dust collection: (1) actively pumping air at 40 cubic feet h^{-1} through a filtration system fitted with a dust collector and (2) passive collection with four large (18 L, diameter of 0.34 m) plastic buckets filled with deionized water and sodium azide added to eliminate biological activity during collection. The buckets were covered by course mesh net to eliminate birds, filled to 1 cm below their rim, and refilled biweekly to compensate for evaporation. Here, the underlying assumption was that the dust particles trapped in the buckets would simulate the mode of particles entrapment in the lake surface. Both systems were deployed simultaneously on the roof of the Lake Kinneret Laboratory located on the northwestern coastline of this lake.

Active dust collection The concentration of dust particles in air obtained by pumping air through a filter, had a clear seasonal pattern with ~110 µg dust m^{-3} in summer and ~40 µg m^{-3} in winter (Fig. 19.8a). The concentration of phosphorus in dust (Fig. 19.8b) showed an opposite seasonal trend, with concentrations that were about two times greater in winter than in summer. Of note is that desert dust events associated with winds from the east ("Sharkia," mostly originating in the Arabic Peninsula) raise dust concentration in air but are characterized very low P concentrations,

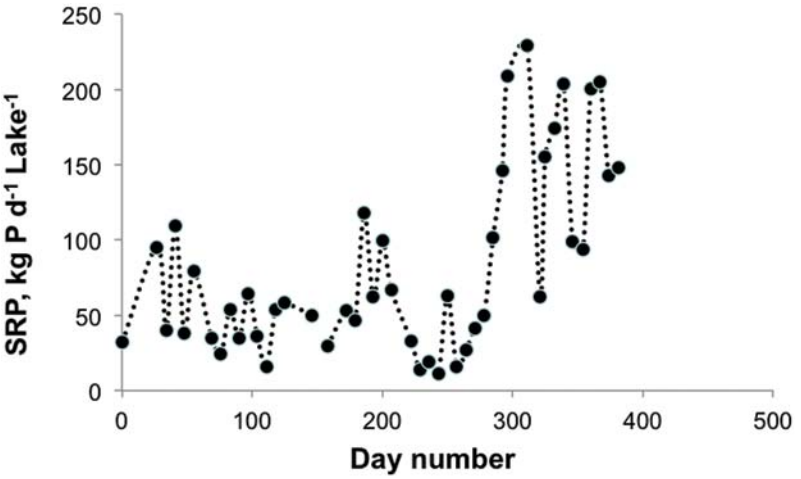

Fig. 19.9 Deposition fluxes of soluble reactive P (*SRP*) in dust, obtained with passive traps deployed from 6 June 2011 (day ayn dust, obtained witday ayn dust, obtained with paKinneret Limnological Laboratory. SRP represents the part of P in dust, which was solubilized in the deionized water contained in the experimental buckets used for dust collection

200–600 μg P g(DW)$^{-1}$ (Fig. 19.8). Mean particulate P concentrations in the air were estimated at 75 ng m^{-3} in summer and 55 ng m^{-3} in winter. By assuming steady settling velocities, the phosphorus sedimentation flux in winter should be ~50% less than in summer. The commonly used literature value of settling velocity of dust P in air, is 1.8 cm s^{-1} (Duce et al. 2001; Prospero et al. 1996). Accordingly, the calculated lake-wide sedimentation flux through dry dust deposition would be ~0.6 t P month^{-1}, i.e., only 7.5 t year^{-1}. This flux is much smaller than the flux of 63 ± 30 t year^{-1} estimated above through mass balance of P in the lake. The obvious problem is whether the settling velocity selected here is realistic.

Passive dust collection Data obtained by use of passive traps included soluble P and of TP concentrations, measured on the water samples from the bucket. The dry weight of the bulk dust was obtained by filtration of the bucket content and drying of the filters. The advantages of passive traps are that they may well represent the lake surface capacity for trapping dust particles and that there is no need to make assumptions regarding settling velocities. Another advantage is that the leaching of P from the particles is due to inorganic reactions only. The apparent disadvantage of this system is poorer reproducibility obtained between buckets deployed at the same place. Two active dust collectors deployed at a distance of ~5 m apart would show deviations of bulk dust and P in dust of less than 5% whereas buckets deployed at the same site would show a respective difference of ~15%. The annual flux of TP in dust measured with the buckets (June 2011–June 2012) was 37.6 ± 6 t of which 86% was solubilized and appeared as SRP. This makes a monthly average flux of SRP in dust of 2.7 t deposited on Lake Kinneret (Fig. 19.9), which is several times larger than the flux based on active pumping discussed above. The difference

between data collected by the two types of traps may be attributed to an incorrect assumption on settling velocities used in the active pumping procedure. Thus, the annual flux obtained from the passive traps is closer to the 63 ± 30 t missing from the Lake Kinneret phosphorus multiannual budget discussed above. Notice also that in summer–fall phosphorus in dust flux is considerably larger than riverine TP inflows. We therefore advocate for this manual passive method, rather than the more commonly used active dust collector methods, at list in the case of the Lake Kinneret watershed.

19.4.4 Sources of Phosphorus in Dust

Atmospheric deposition on Lake Kinneret, therefore, appears to be the major source of phosphorus in the summer of wet years, and at all seasons in dry years. The questions that arise are, "What is the source of the phosphorus associated with dust?" and "Is this source manageable?" An attempt to resolve these issues was made by Gross et al. (2013) through comparison of the isotopic composition of the oxygen in inorganic phosphate (δ^{18}Op) leached by water from local soils and from the filtered material collected with the dust collectors. This study showed that it was possible to isotopically distinguish between phosphorus originating from fertilized soils (δ^{18}Op values ranging between 19.3 and 22.1‰) to phosphorus originating from uncultivated soils with natural vegetation (17.4–18.2‰). The P fertilizers used for agriculture in this area have δ^{18}Op values of ~+22.5‰. The δ^{18}Op values in dust, collected continuously over Lake Kinneret during June 2011–March 2012, were in the same range found for agricultural soils.

An additional source of phosphorus in dust was identified during desert dust events generally emanating from southeast of the lake. This source contained extremely high concentrations of yellowish dust with a high content of $CaCO_3$(s) but a low phosphorus content (~200 μg gr^{-1} Fig. 19.8b).

The conclusion drawn from this study was that for most of the year, the source of phosphorus in dust to Lake Kinneret is fertilized soils. This may also explain the extremely high concentrations (in some cases even 0.5% of the dry weight) of leachable phosphorus detected in the active traps.

19.5 Summary

The primary source of nitrogen to Lake Kinneret drainage basin is DIN originating in southern Europe which is carried over the Mediterranean Sea by rain clouds. Evidence is presented that this nitrogen is cycled within the mountainous aquifers eventually outflowing as nitrate to the Jordan River and Lake Kinneret. Riverine loads of nitrogen are not the sole sources. Other sources include "old" N previously buried in peat within the historic Hula Lake and marshes as well as N in fertilizers and N resulting from cattle excretion. The drying out of the Hula Valley water

bodies some 60 years ago resulted in oxic degradation of this peat and the conversion of Norg to NH_4 which is later nitrified and the NO_3 product is transported in the watershed waterways. At some stage, particularly during the 1970s, peat dust was spread over all of the drainage basin, including also Lake Kinneret, mainly through Aeolian transport. This is indicated by high levels of organic C and N in the Jordan River, Meshushim stream, and other tributaries as well as in Lake Kinneret itself. As a result of decomposition of this allochthanous organic matter, those waterways and Lake Kinneret surface water showed lower pH and DO levels in the 1970s than in the following decades.

The two sources of phosphorus to Lake Kinneret are riverine and dust. In accordance with water discharge, the riverine source predominates in winter, while the dust source is more important in summer. Isotopic (oxygen) evidence suggests that most of the P in dust originates from P fertilization of cultivated soils.

Acknowledgment I greatly acknowledge Wendy Paul, Tamar Zohary and Assaf Sukenik in assisting the editing of this chapter.

References

Avnimelech Y, Dasberg S, Harpaz A, Levin I (1978) Prevention of nitrate leakage from the Hula Basin, Israel. A case study in watershed management. Soil Sci 125:233–239

Bein A (1986) Early evolution and transformation of organic matter in the active continental Jordan Rift valley. Org Geochem 10:751–757

Bein A, Nielsen H (1988) Sulfur diagenesis in freshwater lignites (Hula Basin Israel). Implications for S-C relationships in organic sediments. J Geol Soc 145:133–136

Brachyau A (1958) Aspects of draining the Huleh. Eng Archit 16:186–190

Cowgill UM (1969) The water of Merom: a study of Lake Huleh, I. Introduction and general stratigraphy of a 54 m core. Arch Hydrobiol 66(3):249–272

Dimentman C, Broomly HJ, Por FD (1992) Lake Hula reconstruction of the fauna and hydrobiology of a lost lake. Israel Academy of Sciences and Humanities, Jerusalem, p 170

Dubowski Y (1996) Stable isotopes paleolimnology of Lake Kinneret. MSc thesis submitted to the Hebrew University Jerusalem, The faculty of Earth Sciences (In Hebrew, English abstract)

Duce RA, Liss PS, Merrill JT, Atlas EL, Buat-Menard P, Hicks BB, Miller JM, Prospero JM, Arimoto R, Church TM, Ellis W, Galloway JN, Hansen L, Jickells TD, Knap AH, Reinhardt KH, Schneider B, Soudine A, Tokos JJ, Tsunogai S, Wollast R, Zhou M (2001) The atmospheric input of trace species to the world ocean. Global Biogeochem Cycle 5:193–259

Ganor E, Foner HA, Gravenhorst G (2003) The amount and nature of the dust fall on Lake Kinneret (the Sea of Galilee, Israel), flux and fractionation. Atmos Environ 37(30):4301–4315

Gat JR (1970) Environmental isotope balance of Lake Tiberias. Summary of a symposium on the use of isotopes in hydrology. IAEA (SM-129/8), Vienna, pp 109–127

Gat JR, Dansgaard W (1972) Stable isotope survey of the fresh water occurrences in Israel and the Northern Jordan Rift Valley. J Hydrol 16:177–211

Gophen M, Serruya S, Spataru P (1990) Long-term patterns in nutrients, phytoplankton and zooplankton of Lake Kinneret (Israel) during 1969–1985. Hydrobiologia 191:39–46

Gophen M, Smith VA, Nishri A, Threlkeld ST (1999) Nitrogen deficiency, phosphorus sufficiency, and invasion of Lake Kinneret, Israel, by the N_2 fixing cyanobacterium *Aphanizomenon ovalisporum*. Aquat Sci 61:01–14

Gross A, Nishri A, Angert A (2013). Use of phosphate oxygen isotopes for identifying atmospheric-P sources: a case study at Lake Kinneret. Environ Sci Technol 47:2721−2727

Hambright KD, Zohary T (1998) Lakes Hula and Agmon: destruction and creation of wetland ecosystems in northern Israel. Wetl Ecol Manag 6:83–89
Karmon Y (1960) The drainage of the Hula swamps. Geog Rev 50:169–193
Kroopnick P, Craig H (1972) Atmospheric oxygen: isotopic composition and solubility fractionation. Science 175(4017):54–55
Lindstrom K (1980) *Peridinium cinctum* bioassays of Se in Lake Arken. Arch Hydrobiol 89:110–117
Markel D, Saas E, Lazar B, Bein A (1998) Biogeochemical evolution of sulfur rich aquatic system in a re-flooded wetland environment (Lake Agmon, Northern Israel). Wetl Ecol Manag 6:103–120
Mayer B, Bollwerk SM, Mansfeldt T, Hutter B, Veizer I (2001) The oxygen isotope composition of nitrate generated by nitrification in forest floors. Geochem Cosmochem Acta 65:2743–2756
Nishri A (2010) Phosphorus and nitrogen transport mechanisms from the Hula Valley to the Jordan River. Isr J Earth Sci 58:1–14
Nishri A (2011) Long-term impacts of draining a watershed wetland on a downstream lake, Lake Kinneret, Israel. Air Soil Water Res 4:57–70
Nishri A, Sukenik A (2012) Monitoring of selenium species in Lake Kinneret and in its drainage basin. IOLR report # T23/2012 (in Hebrew)
Nishri A, Brenner IB, Hall GEM, Taylor HE (1999) Temporal variation in dissolved selenium in Lake Kinneret (Israel). Aquat Sci 61(3):215–233
Prospero JM, Barret K, Church T, Dentner F, Duce RA, Galolloway JN, Levy H, Moody J, Quinn P (1996) Atmospheric deposition of nutrients to the North Atlantic Basin. Biogeochemistry 35:27–73
Salingar Y, Geifman Y, Aronowitch M (1993) Orthophosphate and calcium carbonate solubility in the upper Jordan Watershed Basin. J Environ Qual 22:672–677
Serruya C (1978) Lake Kinneret. Junk Publishers, The Netherlands, p 501
Shoham D, Levine I (1968) Subsidence in the reclaimed Hula swamp area of Israel. Isr J Agri Res 18:15–18
Smith SV, Serruya S, Geifman Y, Berman T (1989) Internal sources and sinks of water, P, N, Ca and Cl in Lake Kinneret, Israel. Limnol Oceanogr 34(7):1202–1213
Zohary T, Sukenik A, Nishri A (2012) Present–absent: a chronicle of the dinoflagellate *Peridinium gatunense* from Lake Kinneret. Hydrobiologia 698:161–174

Chapter 20
The Phosphorus Cycle

Werner Eckert and Ami Nishri

Abstract The chapter on the phosphorous (P) cycle of Lake Kinneret presents an overview of more than 40 years of research and monitoring while following up earlier published assessments on P partitioning, sedimentation, and diagenesis. The P evolution in the water column is described based on the understanding of physical forcing processes and their role in internal P loading. Our results point towards a novel transport mechanism that is responsible for the depletion of soluble reactive phosphorus in the hypolimnion. A whole-lake mass balance model, based on data from the 1970s, is updated according to the annual P fluxes measured later on while taking into consideration previously neglected components such as P export due to commercial fisheries and aeolian P inputs. At present, the annual load of bioavailable P from dust exceeds that of the riverine load. Our long-term trends indicate dramatic changes in the total P (TP)-inventory. Between the early 1980s and the early 2000s, the TP content of Lake Kinneret dropped by 30 %. The observed drop is linked to man-made perturbations in the watershed that led to a gradual reduction of allochthonous inputs and internal P loads. The relationship between the observed changes in P loading rates and changes observed in the Lake Kinneret ecosystem is discussed.

Keywords Phosphorus cycle · P partition · Internal loading · Allochthonous P · Benthic boundary layer

20.1 Introduction

The phosphorus (P) cycle is the most intensively studied biogeochemical cycle in freshwaters (Wetzel 2001, p. 239). While P is the 11th most abundant element in the Earth's crust, of all macronutrients that are essential for the biota it is least abundant in the hydrosphere and most commonly limits biological productivity in aquatic

W. Eckert (✉) · A. Nishri
The Yigal Allon Kinneret Limnological Laboratory, Israel Oceanographic & Limnological Research, P.O. Box 447, 14950 Migdal, Israel
e-mail: werner@ocean.org.il

A. Nishri
e-mail: nishri@ocean.org.il

T. Zohary et al. (eds.), *Lake Kinneret, Ecology and Management,* Aquatic Ecology Series 6,
DOI 10.1007/978-94-017-8944-8_20,

systems (e.g., Istvánovics 2008). P is chemically reactive but does not participate in oxidation–reduction reactions as is the case with carbon, nitrogen, and sulfur compounds. P is released as phosphate into the hydrosphere by the weathering of phosphate-mineral rich rocks—primarily apatite—but dissolved phosphate is present in relatively small quantities because it tends to reprecipitate as secondary minerals of low solubility, to sorb onto surfaces, and form complexes with metal ions (Stumm and Leckie 1971). The scarceness of free phosphate in surface waters has always been a major challenge for the biota where P is universally needed by every organism for storing and controlling chemical energy (ATP) and genetic information (DNA and RNA), for the construction of phospholipid membranes, and for coordinating metabolic processes (Istvánovics 2008). In response, aquatic organisms have developed uptake strategies that allow them to concentrate P in their biomass compared to the abundance of available P in the water (Currie 1990). Challenged by the low ambient P concentrations, biotic communities efficiently recycle most of the P that is lost from the living biomass in dissolved or particulates forms (Lenton and Watson 2004) and one of the most characteristic features of the P cycle is its fast dynamics. The research of the P cycle increased dramatically in the late 1960s due to a worldwide deterioration of water quality of freshwater lakes caused by eutrophication. After P was perceived as the driving force for eutrophication (e.g., Vollenweider 1968; Schindler 1977), attempts were made to reverse the eutrophication process. However, initial remedial measures to improve water quality by reducing external nutrient loading did not meet the expectations because of resilience due to the accumulation of P in bed sediments (e.g., Marsden 1989). In many cases, in-lake P concentrations remained high due to internal loading and effective recycling within the photic zone (Prepas and Burke 1997).

Here, we present a synopsis of the P cycle of Lake Kinneret based on 40 years of monitoring and research. Our goals are (1) to interpret new and historical data sets on loading, partition, sedimentation, and diagenesis of P in terms of recent findings concerning the roles of physical forcing and microbial activity and (2) to analyze temporal variations in the P inventories in the context of changing loading rates with special emphasis on a whole-lake mass balance approach. In order to achieve these goals, we applied the following strategies:

- Analysis of the long-term trends in P inventories and allochthonous P load
- Estimating the relative portion of bioavailable P in the external load
- Incorporating new insights on P fluxes into an existing mass balance model

20.1.1 The Annual and Multiannual P Cycle in the Water Column

The study of the P cycle of Lake Kinneret goes back to 1969 when a weekly monitoring program was launched aimed at elucidating the spatiotemporal dynamics of water quality parameters in the water column. One of the first P-related discoveries was that free phosphate, commonly referred to as soluble reactive phosphorus

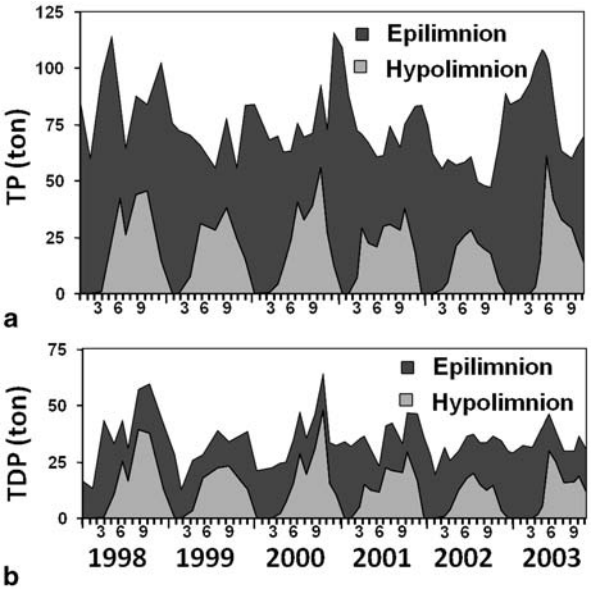

Fig. 20.1 Seasonal changes in the monthly inventories of total phosphorus (*TP,* **a**) and total dissolved phosphorus (*TDP,* **b**) in the epilimnion and hypolimnion of Lake Kinneret between 1998 and 2003. (analysis is based on the data from Lake Kinneret Data Base, LKDB)

(SRP), is present in the photic zone at concentrations close to or below the detection limit of 0.05 µM and comprises the limiting nutrient for phytoplankton development (Berman 1969, 1970). Serruya et al. (1975) showed that during the spring dinoflagellate bloom, close to 100 % of the total P (TP) can be found in the algal biomass. For further information concerning the role of P for phytoplankton development and diversity in Lake Kinneret, we refer the reader to Zohary (2004) and Chap. 10. First TP data from this program were published by Serruya (1975) and Serruya et al. (1975) who used a whole-lake mass balance approach to follow monthly changes in the lake's P inventory as a function of loading, sedimentation, and biological uptake.

A prominent feature of Lake Kinneret is its regular seasonal pattern of the vertical P distribution in the water column as exemplified by six consecutive annual cycles from 1998 until 2003, with TP inventories varying between 50 and 120 t (Fig. 20.1a). Water column TP typically increases during the flood season (winter) followed by a decline during summer and fall when hypolimnetic P reaches its maximum. Hereby, the annual increase of hypolimnetic P is mainly the result of internal loading with total dissolved P (TDP) being the dominant fraction (Fig. 20.1b).

Contrary to that, in the epilimnion TDP represents only a minor fraction of the TP. Figure 20.2 displays a set of depth profiles of particulate P (PP), TDP, SRP, and ammonium in relation to the physical structure of the water column of Lake Kinneret during the stratified period. The absence of phosphate and generally low TDP concentrations in the epilimnion are obvious signs of P limitation of the Lake Kinneret ecosystem. Less obvious is the continuation of this trend throughout the hypolimnion until a depth of ~30 m—the upper limit of the benthic boundary layer (BBL, see Fig. 20.2). SRP is the dominant P fraction in the BBL where it accumulates

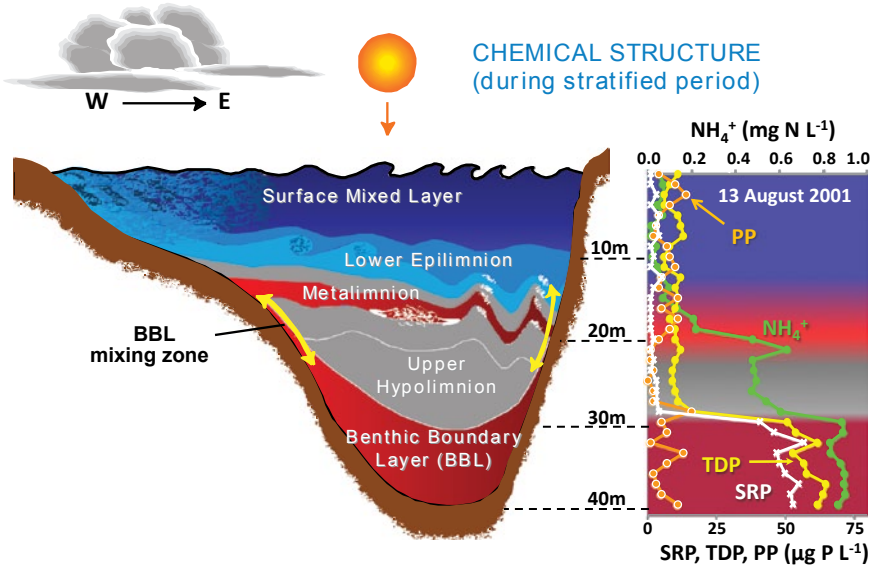

Fig. 20.2 A schematic presentation of the thermal stratification pattern in the water column of Lake Kinneret during summer, illustrating the presence of five distinct layers of water. The vertical distribution of particulate P (*PP*), soluble reactive phosphorus (*SRP*), total dissolved phosphorus (*TDP*), and NH_4^+ across those layers are shown on the *right*. *Yellow arrows* indicate the zone of boundary mixing. (Modified from Eckert et al. 2002; reproduced with permission of Springer)

similar to NH_4^+. The role of the BBL for nutrient enrichment was shown previously (Nishri et al. 2000). Apparently, the selective increase of SRP in the BBL is causing the hypolimnetic accumulation of TDP seen in Fig. 20.1b. However, unlike NH_4^+, concentrations of dissolved P do not increase in the hypolimnetic layer that is overlaying the BBL. Furthermore, this layer is characterized by PP concentrations below detection. One of our goals in this chapter is to find an answer to this paradox that could play a critical role for the mass balance of P in Lake Kinneret.

During the time period of monitoring, annually averaged TP and TDP inventories in the water column of Lake Kinneret have varied between 44 to 113 t and from 18 to 68 t, respectively (Fig. 20.3). Until the early 1980s, both P fractions exhibited an increasing trend that, according to Smith et al. (1989), was related to allochthonous P loading. The all-time maxima with 115 t TP and 70 t TDP were recorded in 1981. Following that record year, the P inventories of both fractions began to gradually decline until the present at a rate of about 1 t per year. A further central topic of this chapter addresses the question of how this decline in P inventory is related to changing external loads and/or internal processes.

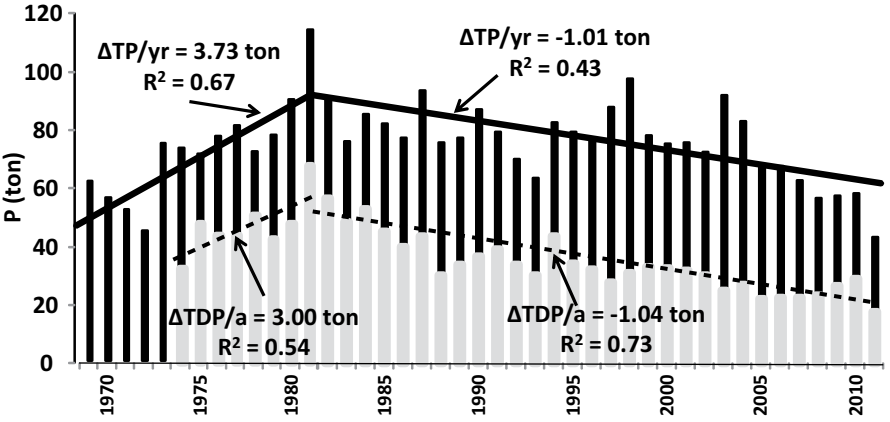

Fig. 20.3 Temporal changes in average annual total phosphorus (*TP, black*) and total dissolved phosphorus (*TDP, grey*) inventories in the water of Lake Kinneret during 1969–2011 (data from LKDB). Linear regression lines were drawn for the period 1969–1981 and 1982–2011, from which the annual rates of change in the P inventory were computed

20.1.2 The Role of External Loading for the P Cycle of Lake Kinneret

The Jordan River brings ~85% of the total annual inflow and most of the nutrient loading to Lake Kinneret. Since the implementation of the Jordan River monitoring program by the Mekorot Water Company in 1972, the Jordan River discharge has varied greatly between 240×10^6 and 890×10^6 m^3 $year^{-1}$. Concurrently, the annual load of allochthonous P varies by an order of magnitude, between 20 and 220 t, with 75% ± 10% of the TP being in particulate form (based on data from Lake Kinneret Data Base, LKDB). As shown by Markel et al. (1994), particle size distribution of Lake Kinneret sediments is a function of the distance from the Jordan River inflow, with sand as the dominant fraction of the suspended matter settling out rapidly upon entering the lake. In the latter study carried out on sediments sampled along a 7.8 km transect from the Jordan River inflow to the central lake station, sand comprised 60% of the bulk sediment at Sta. J, some 600 m away from the inflow. Nevertheless, 2.9 km from the Jordan inflow, sand was absent. Shteinman and Kamenir (1998) and Shteinman et al. (2000) provided further evidence for the fast sedimentation of coarse particles in the Jordan delta. They estimated that 70–80% of the load of suspended particulate matter (SPM) precipitates within the first 500 m after being flushed into the lake.

Two critical issues regarding the allochthonous load of PP are the proportion that is bioavailable and the fate of the particles upon entering the lake. Addressing these issues requires knowledge on: (a) the sedimentation pattern of the SPM and (b) the partitioning of PP into different fractions. The latter can be distinguished operationally via sequential P extraction as loosely bound, metal-bound, calcium-bound PP (Ca-PP), and particulate organic PP (Hieltjes and Lijklema 1980; Eckert and Nishri

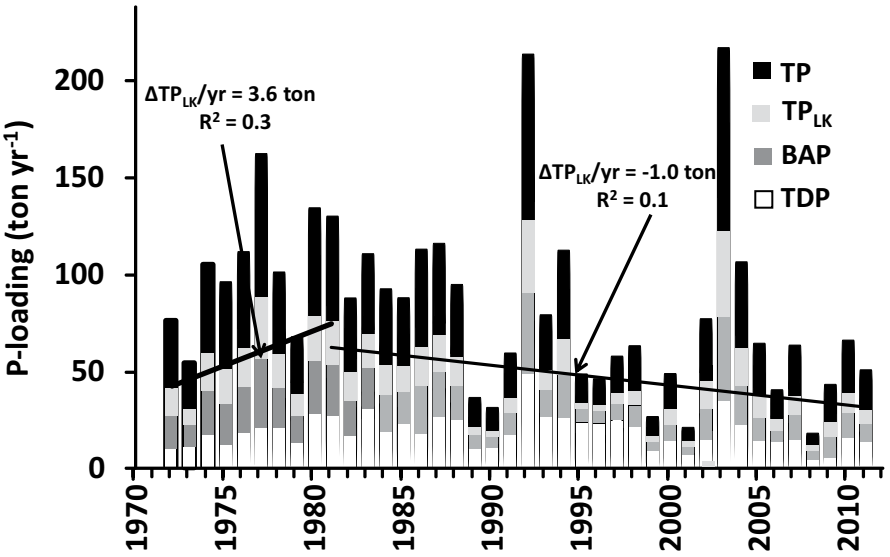

Fig. 20.4 Annual allochthonous phosphorous loads in the Jordan River between 1972 and 2011 (data from LKDB as available in June 2012, prior to the modifications presented in Chap. 18). Total phosphorus (*TP*) and total dissolved phosphorus (*TDP*) = sum of daily loads, TP_{LK} = Lake Kinneret-relevant *TP* load estimated as: *TDP* + PP in fine fraction of SPM, bioavailable P (*BAP*) = *TDP* + BAPP in fine fraction of SPM. Linear regression lines were drawn for the period 1969–1981 and 1982–2011, from which the annual rates of change in the TP_{LK} loading

2000). Of these, Ca-PP that includes for instance apatite, can be regarded as biologically inert, while the other fractions represent potential P sources for the biota (Eckert et al. 2003), referred to below as bioavailable PP or BAPP. Size fractionation of SPM sampled in the Jordan River during 2007–2009 showed a 51–49 % (± 12 %) distribution between fast- (sand) and slow-settling (fine = silt + clay) particles (Eckert unpublished data).

The sand fraction was characterized by stable total PP (TPP) concentrations (1.59 ± 0.13 mg P gDW^{-1}) and a uniform pattern of P partitioning (Table 20.1) while fine particles (1.88 ± 0.27 mg P gDW^{-1}) showed a higher variability due to changes in the BAPP fraction. With the coarse SPM fraction settling in the Jordan delta, only the BAPP fraction with 22 % of the allochthonous PP should be regarded as an ecosystem variable for Lake Kinneret. We applied this assumption to correct historical annual TP and TDP loads in the Jordan River: (a) for the P fraction likely to reach the lake ($TP_{LK} = TP - PP_{Sand}$) and (b) for the ecosystem relevant BAP, where BAP = $TDP + BAPP_{silt + clay}$ (Fig. 20.4).

Based on the time series of the allochthonous P load, between 1972 and 1981, TP_{LK} estimates increased annually by 3.6 t ($r^2 = 0.3$, $p < 0.05$) followed by a declining trend of ca. 1 t per year ($r^2 = 0.1$, $p < 0.05$). Despite the extremely high variability due to record floods and draught years, these trends match closely those of the annual TP inventories (Fig. 20.3) and point at a close dependency of the Lake Kinneret ecosystem on riverine P loading. This hypothesis is further substantiated by the

Table 20.1 Mean ± SD concentrations of the three major fractions of particulate P: bioavailable (BAPP), Ca-bound (Ca-PP), and total (TPP) in the load of suspended matter (SPM) from the Jordan River, 2007–2009. (Eckert unpublished data)

$n=35$	SPM (mg P gDW^{-1})	Sand (mg P gDW^{-1})	Percent of TPP load	Fine material (mg P gDW^{-1})	Percent of TPP load
BAPP	0.73 ± 0.16	0.61 ± 0.10	20	0.84 ± 0.11	22
Ca-PP	0.99 ± 0.09	0.98 ± 0.08	32	1.02 ± 0.11	26
TPP	1.72 ± 0.20	1.59 ± 0.13	52	1.88 ± 0.27	48

Based on samples collected at monthly intervals ($N=35$)

mean P concentration in surface sediments of the Jordan delta, of 1.52 mg P gDW^{-1}, which is similar to that of the fast-settling coarse SPM (1.59 mg P gDW^{-1}, Table 20.1). At the same time, the long-term decline of the TDP content of Kinneret water by 1 t P $year^{-1}$ (Fig. 20.3) is only partially explained by changes in the allochthonous BAP load. The later decreased at a rate of 0.7 t $year^{-1}$ (regression line not shown in Fig. 20.4). This discrepancy could either be due to changes in the internal P loading or other allochthonous sources of BAP, such as dust that was shown recently to play a substantial, yet long-forgotten, role in the lake's P cycle (Chap. 19).

20.1.3 Sedimentary P and P Precipitation

First investigations on sediment P in Lake Kinneret were carried out during the early 1970s to investigate the spatial variability of PP in surface sediments on a lake-wide scale. Results showed that the greater part of the lake had a relative uniform PP distribution in surface sediments with concentrations between 1.0 and 1.2 mg P gDW^{-1}. Elevated concentrations, 2.4 and 4.5 mg P gDW^{-1}, were recorded near the Jordan River inflow and in the southern part, respectively (Serruya et al. 1974). The results obtained in surface sediments from the central station were very similar to those measured in sediment cores collected in the early 1990s by Markel et al. (1994) and Eckert et al. (1997). Using the oxygen isotope signature of phosphates as a tracer for P sources in Lake Kinneret, Markel et al. (1994) attributed the elevated PP concentrations in the sediments of the Jordan delta to fast-settling apatite-enriched particles in the total suspended solids (TSS) load of the Jordan River. They further mentioned the possible role of a P calcite-surface complex in the lake's P cycle. According to Avnimelech (1983) and Staudinger et al. (1990), this complex is stable under the hypolimnetic conditions of Lake Kinneret.

The fate of allochthonous PP was investigated in a study that compared the P partitioning in the TSS of the Jordan River to that of sediment from the Jordan delta (Sta. J, Fig. 20.5) and other sites of Lake Kinneret using the sequential P extraction method (Eckert et al. 2003). From the above-mentioned observation of the similarity between the TPP content measured in the sediments of Sta. J and that of the coarse material (Fig. 20.5, Eckert, unpublished data), we hypothesize that only the P in the fine fraction ought to be treated as potentially ecologically relevant for

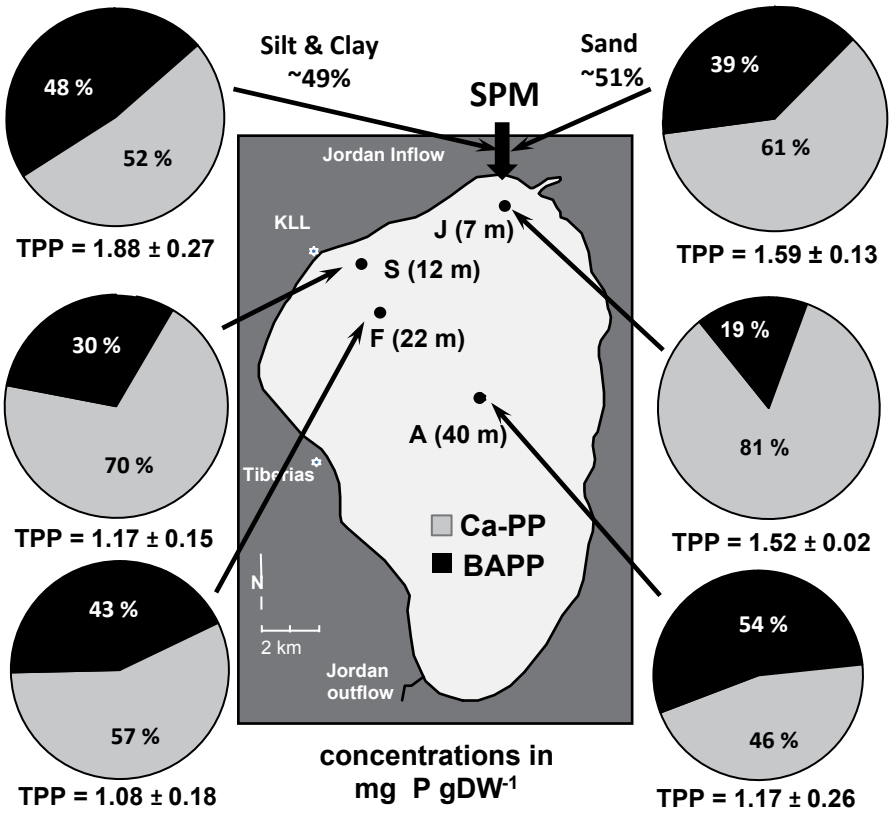

Fig. 20.5 Phosphorus partitioning between Ca-bound (*Ca-PP*) and bioavailable particulate P (*BAPP*) in particulate matter from surface sediments of Lake Kinneret from Sta. S, F, and A (n=75, 1998–2007), Sta. J (n=3, 2007–2009) and in suspended matter from the Jordan River (n=35, 2007–2009) with further explanations in text. The maximum depth at each station is indicated next to its name. *SPM* suspended particulate matter, *TPP* total particulate P. (Eckert et al. 2003; Eckert unpublished data)

Lake Kinneret, whereas the P in the course fraction is most likely retained in the sediments of the Jordan delta. Moreover, the apparent increase of Ca-PP in the sediments of Sta. J (81 % of TPP) is an indication for early diagenesis that is responsible for reshuffling the PP fractions without affecting the overall TPP content. During this process, phosphate is first released from organic material via microbial mineralization and/or from P-containing inorganic particles via desorption and dissolution before reprecipitating as Ca-PP (Berner 1980; Hupfer et al. 1995).

Compared to surface sediments in the Jordan delta, the PP concentration in surface sediments of Lake Kinneret is lower, averaging around 1.1–1.2 mg P gDW^{-1} (Fig. 20.5) a discrepancy that can be explained by a dilution effect due to a massive formation of authigenic carbonate that represents more than 50 % of the settling matter (Serruya 1974). The topic of calcite precipitation in Lake Kinneret is detailed in Chap. 23.

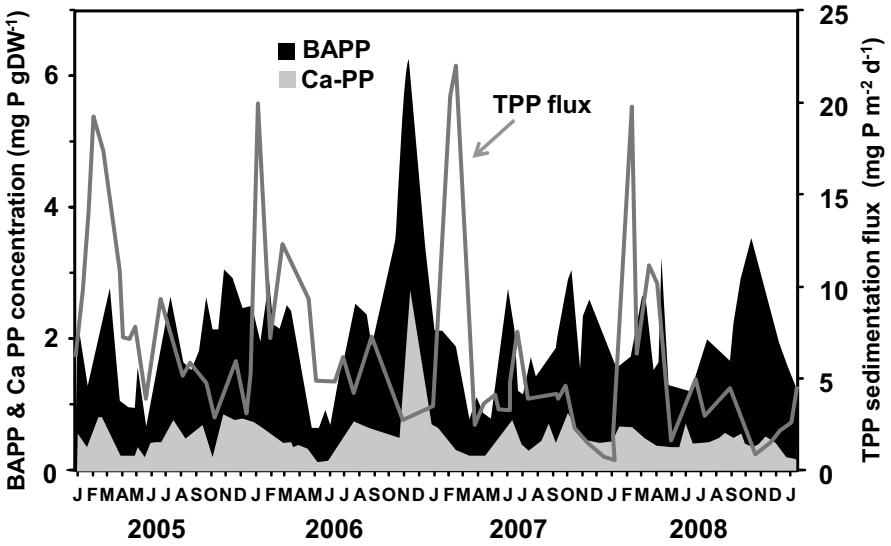

Fig. 20.6 Temporal variations in total particulate P (*TPP*) sedimentation flux and in the fractions of bioavailable particulate P (*BAPP*; Ca-bound PP, *Ca-PP*) in seston material collected in near-bottom sediment traps at Sta. A between January 2005 and January 2009. (Eckert unpublished data)

While average TPP concentrations were stable among sites, surface sediments sampled along a transect from the littoral to the lake's center (Sta. S to A in Fig. 20.5) differed in their P fractions and in the variability of their TPP concentrations. For instance, the BAPP portion increased from 30 % at Sta. S to 54 % at Sta. A, an observation that is typical for sediments from accumulation zones—in contrast to erosion zones—and a higher content of P-enriched organic material (Weyhenmeyer and Bloesch 2001). Early measurements of P sedimentation rates during the period October 1972–October 1973 revealed an annual PP sedimentation flux of 1.4 gP m^{-2} for the central lake station while the average PP concentration in the tripton was 2.2 mg P gDW^{-1} (Serruya 1977).

The high variability in TPP at Sta. A (Fig. 20.5) can be seen as the result of seasonal changes in the composition of the settling matter (Fig. 20.6). Eckert et al. (2003) showed that TPP concentrations were maximum when sedimentation fluxes were lowest—i.e., summer and fall—and vice versa *in* winter and spring. The observed trends were confirmed by recent sedimentation trap deployments sampled in weekly to biweekly intervals. The TPP content of the seston material varied largely between 0.7 and 6.0 mg P gDW^{-1} and the TPP settling flux between 1 and 20 mg P m^{-2} day^{-1} (Fig. 20.6). In the seston material from the near bottom trap at Sta. A, BAPP was generally the dominant fraction confirming previous findings for pelagic and sublittoral sampling locations in Lake Kinneret (Eckert et al. 2003).

Integration of our time series data on sedimentation fluxes and P partitioning revealed for the near-bottom trap at the lake center (A40) BAPP and Ca-PP sedimentation fluxes of 1.6 ± 0.3 and 0.6 ± 0.2 g P m^{-2} $year^{-1}$, respectively (Table 20.2).

Table 20.2 Annual averages of TPP concentrations and P partitioning into bioavailable (BAPP) and Ca-bound (CA-PP) fractions in seston collected in sediment traps from Sta. A (25 m, 40 m), F, S, and J together with annual settling fluxes for particulate matter (Bulk Sed.), Ca-PP, and BAPP

Sta.	TPP (mg P DW^{-1})	BAPP (%)	Ca-PP (%)	Sedimentation flux			No. of samples
				Bulk Sed. (kg m^{-2} $year^{-1}$)	Ca-PP (g P m^{-2} $year^{-1}$)	BAPP (g P m^{-2} $year^{-1}$)	
A25	1.6±0.3	69	31	0.9±0.1	0.4±0.1	0.8±0.1	106
A40	2.0±0.8	73	27	1.3±0.3	0.6±0.2	1.6±0.3	142
F	2.0±0.8	73	27	2.8±0.1	1.6±0.1	3.3±0.1	39
S	1.6±0.4	39	61	5.6±0.4	4.9±0.5	3.9±0.6	66
J	1.7±0.2	34	66	21.2±5.0	23.2±5.6	11.4±2.5	76

Data are based on biweekly to monthly determinations over the years 1999–2008

The material collected in the lower trap, deployed within the BBL indicated a significantly larger sedimentation flux compared to the upper trap, deployed in the upper hypolimnion at 25 m. Based on Ostrovsky and Yacobi (2010), the hypolimnetic trap is representative of the settling flux of authigenic material since this zone was shown to be unaffected by turbulent mixing processes throughout the stratified period (Eckert et al. 2002). The lower trap that is suspended in the turbulent BBL (Fig. 20.2) collects as well material that originates from the internal wave-induced resuspension and mixing processes. This hypothesis is supported by the similarity of the TPP concentration and P partitioning of the two near-bottom traps at stations A40 and F (Table 20.2). The traps at Sta. F were located at 20-m depth, within the zone of internal wave braking characterized by intensive resuspension (Ostrovsky and Yacobi 2010). The greater portion of the resuspended material resettles at the site leading to the relatively higher bulk sedimentation flux at F in comparison to Sta. A. Some portion will be transported within the BBL to finally settle within the accumulation zone of the lake. In the P flux model below, these findings turned out to be a useful means to verify mass balance considerations.

The littoral sites in Table 20.2 (S and J) are characterized by elevated sedimentation fluxes and relatively high proportion of Ca-PP in the trap material. These observations are indicative of frequent resuspension–resettling cycles as they typically occur in erosion zones (Eckert et al. 2003). This conclusion is substantiated by the high Ca-PP content of the underlying sediments (Fig. 20.5). The opposite conditions are found at the sublittoral (F) and profundal (A) sites, in which BAPP dominates the trap material. The difference between PP concentrations of settling particles and that in the uppermost sediment is indicative for intensive P mineralization at the sediment–water interface (SWI) as one of the critical processes for internal P loading (Eckert and Nishri 2000; Eckert et al. 2003).

Targeting P diagenesis in the sedimentary column as well as historical changes in the P loading of Lake Kinneret, Hambright et al. (2004) used a combination of analytical and palaeolimnological methods to estimate P sedimentation fluxes and changes in P partitioning prior to the time period covered by the LKDB (Fig. 20.7).

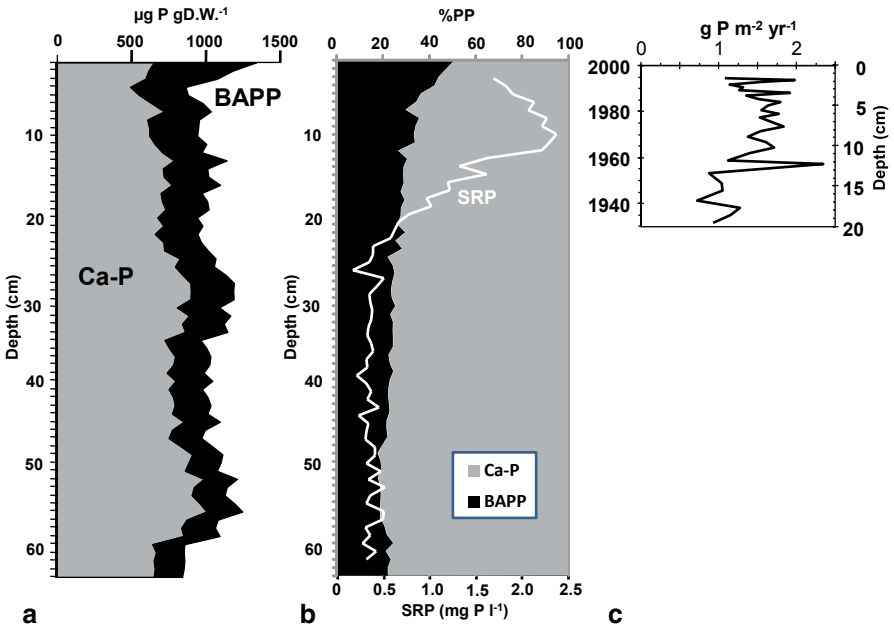

Fig. 20.7 Phosphorus diagenesis in the sediments and historical P fluxes at Sta. A. **a** Vertical variation in the concentrations of the Ca-bound P (*Ca-P*) and BAP fractions of particulate-P. **b** Depth profiles of pore water soluble reactive phosphorus (*SRP*) and the proportions of bioavailable particulate P (*BAPP*) and Ca-PP. **c** Estimates of historical changes in PP precipitation. (Modified from Hambright et al. 2004; reproduced with permission of ACS Publications)

Apart from the P-enriched uppermost layer, sedimentary TPP concentrations varied little with depth (1.05 ± 0.10 mg P gDW^{-1}). BAPP declined in the upper 10 cm accompanied by a concomitant pore water peak in SRP and an increasing Ca-PP fraction (Fig. 20.7a, b). This distribution is likely the result of P diagenesis and is representative for calcareous freshwater lakes in general (Hupfer et al. 1995). P diagenesis describes the process of phosphate being released during the ongoing mineralization of organic material followed by the formation of authigenic Ca-PP minerals (Berner 1980). Regarding the estimates of historical loading rates, P fluxes were about 1 g m^{-2} $year^{-1}$ until the late 1950s, when a prominent peak of >2.5 g m^{-2} $year^{-1}$ is observed. This peak coincides with time of draining of the Hula swamps (Fig. 20.7c). The time period in the aftermath of the drainage is characterized by increasing PP accumulation from the pre-draining values to 1.8 g m^{-2} $year^{-1}$ in the beginning of the 1980s. The declining trend during the following decade matches the gradual decrease in allochthonous P loading during the same time period (Fig. 20.4). This trend reflects the efforts to reduce external nutrient loading via point sources including the construction of the "Einan" reservoir during the early 1980s aimed at diverting drainage water from the Hula Valley and the effluents of the Qiryat Shemona sewage plant out of the watershed. In addition, Lake Agmon was created in 1994 as part of a re-flooding project aimed at controlling soil erosion in the former swamp area (Chap. 31).

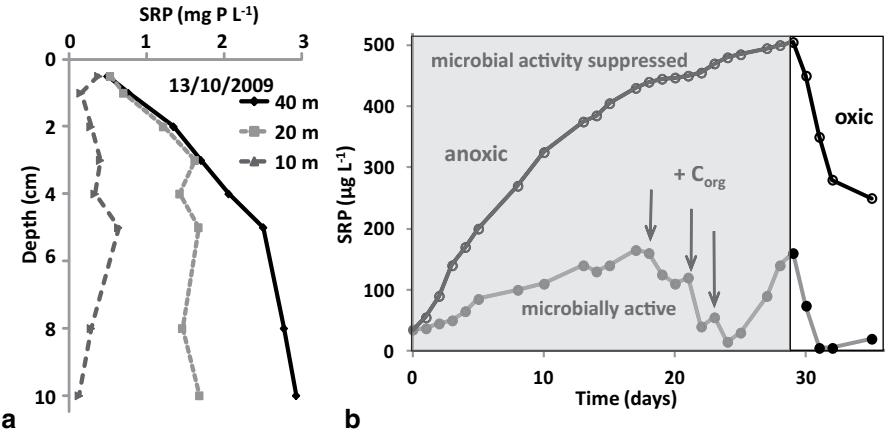

Fig. 20.8 **a** Representative depth profiles of soluble reactive phosphorus (*SRP*) concentrations in Lake Kinneret sediments at Sta. S (10 m), F (20 m), and A (40 m); Eckert, unpublished data. **b** *SRP* release to the overlaying water of incubated sediment cores, with and without microbial activity, under anoxic (first 29 days) conditions followed by oxic conditions. *Arrows* indicate addition of glucose. (Modified from Eckert et al. 1997, reproduced with permission of Springer)

20.1.4 Internal P Loading: The Role of the Benthic Boundary Layer

As mentioned above, the difference between the TPP concentration in the seston and that in the sediments can only be explained by intensive microbial mineralization at the SWI. As a consequence, the upper 5 cm of the organic matter-enriched sublittoral sediments (depth ≥20 m) are characterized by steep pore water gradients of SRP with concentrations increasing with depth to 2–3 mg P L^{-1} (Fig. 20.8a). Note the relatively lower SRP concentration in the littoral sediment! The governing role of microbial activity for the P exchange at the SWI of Lake Kinneret was shown by Eckert et al. (1997) who compared the P flux to the overlaying water of intact and poisoned sediment cores under both, aerobic and anaerobic conditions (Fig. 20.8b). They demonstrated that based on the availability of organic carbon microbial uptake, the SRP flux to the overlaying water can be effectively reduced. These findings contradict earlier conclusions by Serruya et al. (1974) who claimed that P exchange across the SWI is strictly regulated by abiotic processes with sediments acting as a P sink.

With the combined knowledge on P dynamics at the SWI and on particle settling flux, we can now explain the ambiguity of the vertical distribution of P in Lake Kinneret (see Fig. 20.2). The key to understanding is a selective enrichment in the BBL and a more-or-less P-depleted upper hypolimnion. Based on the ammonium profile in Fig. 20.2 that is included as a tracer for solute release at the SWI, one would expect a very similar profile for SRP due to vertical diffusion processes from the NH_4^+ and SRP-enriched BBL into the laminar upper hypolimnion (Rimmer et al. 2006). Possible explanations for the absence of SRP are removal by either biotic or abiotic

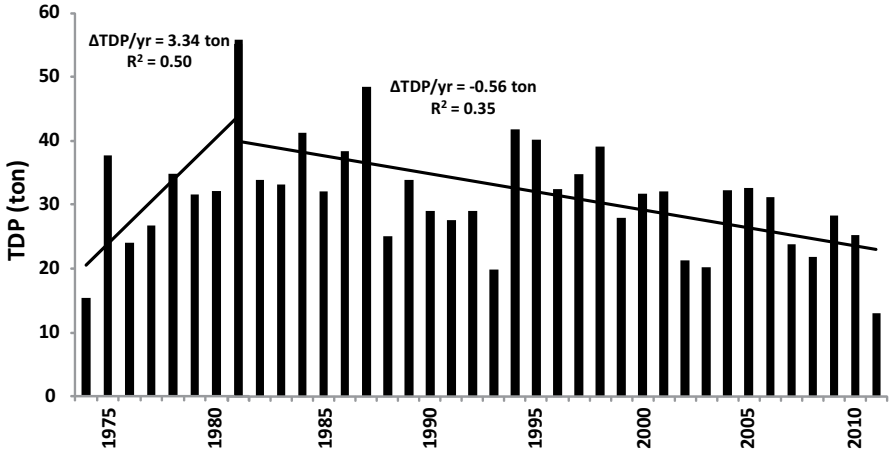

Fig. 20.9 Annual internal loading of total dissolved phosphorus (*TDP*) in Lake Kinneret, 1974–2011 (data from LKDB). Linear regression lines were drawn for the period 1969–1981 and 1981–2011, from which the annual rates of change in the *TDP* inventory were computed

processes. However, what complicates things further is the concomitant deficiency of PP in the upper hypolimnion. Supported by our findings on sedimentary P fluxes showing a relative increase in the BAPP fraction of the A40 trap compared to A25 (Table 20.2) and previous work (Gächter et al. 1988), we can conclude that upwards diffusing SRP is scavenged by bacteria populating settling particles and as such effectively removed from the hypolimnion.

In summary, internal P loading in Lake Kinneret is linked closely to the timing of the onset of thermal stratification, to the rate of hypolimnetic oxygen depletion—as a function of the organic carbon availability (Eckert and Hambright 1996) and the length of the stratified period.

Estimation of the total amount of TDP that accumulates annually in the hypolimnion of Lake Kinneret via extrapolation of the TDP profiles renders annual figures for internal P loading between 15 and 55 t for the time period 1974 until 2011 (Fig. 20.9). Compared to the long-term pattern observed with the P inventories of Lake Kinneret (Fig. 20.3) and that of external P load by the Jordan River (Fig. 20.4), the change in time of the internal P load (Fig. 20.9) follows similar trends as they were increasing until the beginning of the 1980s followed by a gradual decrease until present. The rate of decline is 0.56 t year^{-1}, similar to the drop observed in the BAP load in the Jordan River (Fig. 20.4) that declined annually by 0.66 t year^{-1} during the same period. As shown above in the case of annual TP inventories (Fig. 20.3), the long-term record of the internal loading seems to be linked to the riverine inputs by the Jordan River and as such can be interpreted as a secondary effect caused by the management activities in the watershed (Chap. 18).

20.1.5 A P Mass Balance Model for Lake Kinneret

A first attempt to estimate TP fluxes in Lake Kinneret was published by Serruya (1975) to test the applicability of the Vollenweider model (Vollenweider 1968) by means of a whole-lake mass balance approach. This article provides first estimates about monthly changes in the TP inventory of Lake Kinneret ranging between 43 and 96 t as a function of loading, sedimentation, and biological uptake. The TP fluxes were further detailed by Smith et al. (1989) based on calculations from the datasets that had been collected in the LKDB until 1984. They estimated that from an average allochthonous TP load of 120 t year^{-1}, 109 are buried in the sediments. One of their conclusions had been that the TP inventory of Lake Kinneret increased gradually during the investigated time period as a result of increased P inflows. However, two critical factors were not included in their mass balance calculations:

1. The P input by dust (Chap. 19) accounts annually for ~38 ± 5 t P. Nearly all of the phosphorus in dust is bioavailable, in comparison with the riverine phosphorus which is mostly unavailable to the biota. Thus, in comparison to the annual riverine BAP loads, this BAP-dominated aeolian P source exceeds the BAPP load of the Jordan River (26 ± 18 t year^{-1}). Furthermore, its negligence in the past suggests that previous estimates underestimated the external P fluxes considerably.
2. The P export by commercial fisheries during the time period covered by Smith et al. (1989) was 1,800 t fish year^{-1} (Chap. 16). While this figure varied little until the end of the 1990s, during the past 10 years the annual catch has decreased to about 1,000 t. In terms of P removal, this change corresponds to a drop from 9 to 5 t P year^{-1} (Griffiths 2006).

Based on the observed changes in loading rates and new data on P partitioning, we have updated the existing P mass balance model for Lake Kinneret to include fluxes due to dust and fisheries (Fig. 20.10). Apart from the TP inventory (in tons for the entire lake), the numbers in the model represent estimates of annual fluxes (ton P year^{-1}) with those in brackets delineating the earlier estimates by Smith et al. (1989).

In this model that averages the annual P fluxes from the past decade, we have corrected the external P load (70 ± 55 t P year^{-1}) for the fraction that likely plays a role in the Kinneret ecosystem (TP_{LK} in Fig. 20.4) by subtracting the fast-settling sand fraction (29 ± 25 t P). Taking into consideration the P input from dust, Lake Kinneret receives annually 64 ± 18 t of BAP a figure that is close to the TP inventory of 67 ± 14 t. Together with the 15 t of Ca-PP in the fine fraction of the allochthonous load, this renders a total external P flux of 79 t that can be regarded as being relevant for the TP inventory of Lake Kinneret.

The sedimentation flux of 93 t P year^{-1} was calculated as the difference between the P import (79 t) and export (11 t) plus the internal loading (25 t) as the latter was shown to originate mainly from freshly settled particles. The burial flux (68 t P) represents the difference between sedimentation and internal loading. We compared these calculated sedimentation data with our sediment trap measurements

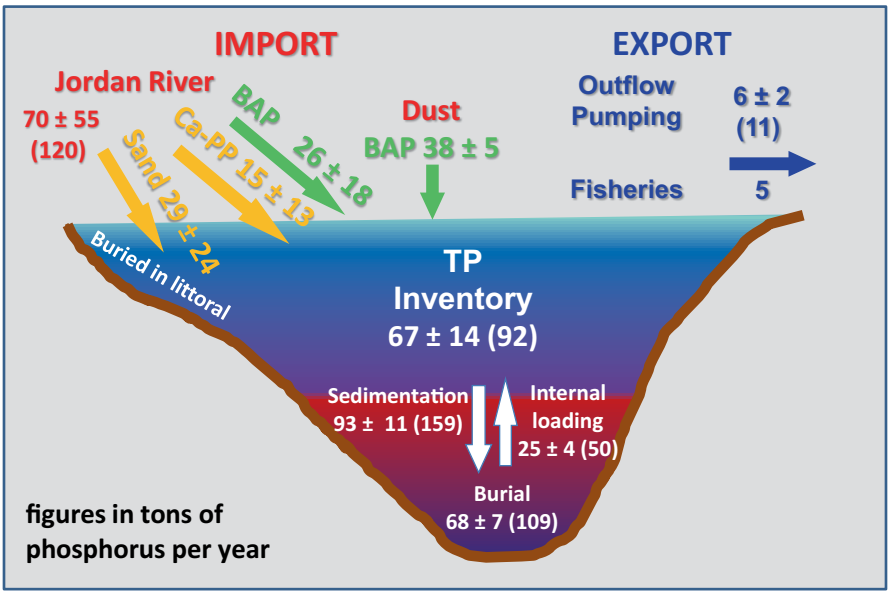

Fig. 20.10 A model of P mass balance in Lake Kinneret, based on annual average fluxes of P during the time period 2001–2011. Numbers are mean annual fluxes (ton P year^{-1} ± SD), except the total phosphorus (*TP*) inventory, which is in tons, based on data for 2000–2010 from Lake Kinneret Data Base, LKDB, and Eckert (unpublished data). Data in brackets represent fluxes calculated by Smith et al. (1989)

(Table 20.2) by extrapolating the averaged annual P fluxes (2.2 gP m^{-2} year^{-1}) from our A40 site to that part of the lake bottom where sediment accumulation is expected to occur. Supported by the findings of Eckert et al. (2002) and Ostrovsky and Yacobi (2010), the relevant area is that underlying the BBL (39–43 km^2). The resulting figures (86–95 t P year^{-1}) correspond well to the average settling flux of 93 t P year^{-1} in Fig. 20.10. This is critical as P sedimentation and P burial are the only fluxes in our mass balance model that are not measured directly and as such the confirmation of one of them renders the confirmation of the model as a whole.

As indicated already in Figs. 20.3, 20.4, and 20.9, the P cycle of Lake Kinneret underwent some dramatic changes during the 40 years of monitoring, changes that seem to be linked closely to differences in the P loading rates. For example, the drop in the TP inventory by 25 t from the early 1980s until 2011 was accompanied by a similar drop in the internal P load (Fig. 20.9). This drop also corresponded well with the decreasing trend observed in the annual riverine load (Fig. 20.4). While man-made perturbations in the watershed certainly play a critical role in the reduction of the allochthonous P load by nearly 50 % at this stage, we cannot say that the observed changes in the Lake Kinneret ecosystem (Chap. 31) are a direct consequence of the change in P loading. How far the observed trends will hold in the future? This is one of the questions to be solved by our ongoing sampling and analytical program for the various P fractions in the water column, seston, and sediments of Lake Kinneret.

References

Avnimelech Y (1983) Phosphorus and calcium-carbonate solubilities in Lake Kinneret. Limnol Oceanogr 28:640–645

Berman T (1969) Phosphatase release of inorganic phosphorus in Lake Kinneret. Nature 224:1231–1232

Berman T (1970) Alkaline phosphatase and phosphorus availability in Lake Kinneret. Limnol Oceanogr 15(5):663–674

Berner RA (1980) Early diagenesis: a theoretical approach (Princeton Series in geochemistry). Princeton University Press, NY

Currie DJ (1990) Large-scale variability and interactions among phytoplankton, bacterioplankton, and phosphorus. Limnol Oceanogr 35:1437–1455

Eckert W, Hambright KD (1996) Seasonal and vertical distributions of temperature, pH, oxygen and sulfide in Lake Kinneret. Limnologica 26:345–351

Eckert W, Nishri A (2000) Sedimentary phosphorus flux in Lake Kinneret: precipitation vs. release. Adv Limnol 55:397–411

Eckert W, Nishri A, Parparova R (1997) Factors regulating the flux of phosphate at the sediment-water interface of a subtropical calcareous lake: a simulation study with intact sediment cores. Water Air Soil Pollut 99:401–409

Eckert W, Imberger J, Saggio A (2002) Biogeochemical evolution in response to physical forcing in the water column of a warm monomictic lake. Biogeochemistry 61:291–307

Eckert W, Didenko J, Uri E, Eldar D (2003) Spatial and temporal variability of particulate phosphorus fractions in seston and sediments of Lake Kinneret under changing loading scenario. Hydrobiologia 494(1–3):223–229

Gachter R, Meyer JS, Mares A (1988) Contribution of bacteria to release and fixation of phosphorus in lake sediments. Limnol Oceanogr 33:1542–1558

Griffiths D (2006) The direct contribution of fish to lake phosphorus cycles. Ecol Freshw Fish 15:86–95

Hambright KD, Eckert W, Leavitt PR, Schelske CL (2004) Effects of historical lake level and land use on sediment and phosphorus accumulation rates in Lake Kinneret. Sci Total Environ 38:6460–6467

Hieltjes AHM, Lijklema L (1980) Fractionation of inorganic phosphates in calcareous sediments. J Environ Qual 9:405–407

Hupfer M, Gachter R, Giovanoli R (1995) Transformation of phosphorus species in settling seston and during early sediment diagenesis. Aquat Sci 57:305–324

Istvánovics V (2008) The role of biota in shaping the phosphorus cycle in lakes. Freshw Rev 1:143–174

Lenton TM, Watson AJ (2004) Biotic enhancement of weathering atmospheric oxygen and carbon dioxide in the Neoproterozoic. Geophys Res Lett 31(5):L05202

Markel D, Kolodny Y, Luz B, Nishri A (1994) Phosphorus cycling and phosphorus sources in Lake Kinneret: tracing by oxygen isotopes in phosphate. Isr J Earth Sci 43:165–178

Marsden AW (1989) Lake restoration by reducing external phosphorus loading: the influence of sediment phosphorus release. Freshw Biol 21:139–162

Nishri A, Imberger J, Eckert W, Ostrovsky I, Geifman Y (2000) The physical regime and the respective biogeochemical processes in the lower water mass of Lake Kinneret. Limnol Oceanogr 45(4):972–981

Ostrovsky I, Yacobi YZ (2010) Sedimentation flux in a large subtropical lake: spatiotemporal variations and relation to primary productivity. Limnol Oceanogr 55(5):1918–1931

Prepas EE, Burke JM (1971) Effects of hypolimnetic oxygenation on water quality in Amisk Lake, Alberta, a deep, eutrophic lake with high internal phosphorus loading rates. Can J Fish Aquat Sci 54: 2111–2120

Rimmer A, Eckert W, Nishri A, Agnon Y (2006) Evaluating hypolimnetic diffusion parameters in thermally stratified lakes. Limnol Oceanogr 51:1906–1914

Schindler DW (1977) Evolution of phosphorus limitation in lakes. Science 195:260–262
Serruya C (1975) Nitrogen and phosphorus balances and load-biomass relationship in Lake Kinneret (Israel). Verh Int Ver Limnol 19:1357–1369
Serruya C (1977) Rates of sedimentation and resuspension in Lake Kinneret. In: Interactions between sediments and freshwater. Proceeding of an International Symposium, Dr W Junk Publishers, The Hague, pp 48–56
Serruya C, Edelstein A, Pollingher U, Serruya S (1974) Lake Kinneret sediments: nutrient composition of the pore water and mud water exchanges. Limnol Oceanogr 19:489–508
Serruya C, Pollingher U, Gophen M (1975) N and P distribution in Lake Kinneret (Israel) with emphasis on dissolved organic nitrogen. Oikos 26:1–8
Smith SV, Serruya S, Geifman Y, Berman T (1989) Internal sources and sinks of water, P, N, Ca, and Cl in Lake Kinneret, Israel. Limnol Oceanogr 34:1202–1213
Staudinger B, Peiffer S, Avnimelech Y, Berman T (1990) Phosphorus mobility in interstitial waters of sediments in Lake Kinneret, Israel. Hydsrobiologia 207:167–177
Shteinman B, Kamenir Y (1998) Decrease in suspended matter concentration with distance from the Jordan River mouth, Lake Kinneret: hydrodynamical aspects. Adv Hydro-Sci Eng III:122–136
Shteinman B, Wynne D, Kamenir Y (2000) Study of sediment dynamics in the Jordan River-Lake Kinneret contact zone using tracer methods. IAHS Publ 261:275–284
Stumm W, Leckie JO (1971) Phosphate exchange with sediments: its role in productivity in surface waters. Adv Water Pollut Res Conf III Art 16, 16 pp
Vollenweider RA (1968) Scientific fundamentals of the eutrophication of lakes and flowing waters, with particular reference to nitrogen and phosphorus as factors in eutrophication. Water Management Research. Water Management Research OECD Paris DAS/CSI/68.27. p 192
Wetzel RG (2001) Limnology, lake and river ecosystems. Academic, San Diego
Weyhenmeyer GA, Bloesch J (2001) The pattern of particle flux variability in Swedish and Swiss lakes. Sci Total Environ 266(1–3):69–78
Zohary T (2004) Changes to the phytoplankton assemblage of Lake Kinneret after decades of a predictable, repetitive pattern. Freshw Biol 49:1355–1371

Chapter 21
Quantitative Aspects of the Nitrogen Cycle

Ami Nishri

Abstract This chapter discusses the quantitative aspects of the nitrogen cycle in Lake Kinneret including its sources and sinks. A thorough discussion is devoted to the internal flux of NH_4^+ from the lower water mass (LWM) to the epilimnion during the stratified period. Also, it is shown that most nitrogen removal from this lake occurs by emitting N_2(g) through a combined process of presumably dissimilatory nitrate reduction to nitrite (DNRN) which is followed by anaerobic ammonium oxidation (anammox). In these processes, NO_3 locked in the LWM at the onset of stratification is claimed to be converted to NO_2 through DNRN heterotrophic activity, while the NH_4^+ is contributed through degradation of organic matter settling from the epilimnion, thus facilitating the occurrence of anammox. Both biotic processes which occur in the sub-oxic LWM account for the removal of approximately 70 % of the annual riverine N inflows to this lake. This leaves only about one third of the N introduced from riverine sources to be used in the following annual cycle.

Keywords Anammox · Ammonium diffusion · DNRN · N_2 fixation nitrogen cycling · N_2 fixation

21.1 External Sources of Nitrogen

The largest external source of nitrogen to Lake Kinneret is the Jordan River. Sources of nitrogen to the river are primarily the headwater springs emerging from the Hermon mountainous aquifer and to a lesser extent N leached from the soils of the central part of the watershed in the Hula Valley. Combined riverine sources supply annually approximate loads of ~1,100 t N as NO_3 and ~200 t N as organic N (Norg; Chap. 18). The seasonal pattern of riverine nitrogen inflows resembles that of riverine water discharge, of which over 60 % is in winter. Throughout the remainder of the year, N inflow loads decline gradually in accordance with water discharge, which is typically at its seasonal minimum in October.

A. Nishri (✉)
The Yigal Allon Kinneret Limnological Laboratory, Israel Oceanographic & Limnological Research, P.O. Box 447, 14950 Migdal, Israel
e-mail: nishri@ocean.org.il

T. Zohary et al. (eds.), *Lake Kinneret, Ecology and Management,* Aquatic Ecology Series 6,
DOI 10.1007/978-94-017-8944-8_21,

Table 21.1 Mass balance of nitrogen in Lake Kinneret

1. Whole lake typical annual fluxes of nitrogen					
In			*Out*		
Type of flux	*Form of N*	*Tons year*$^{-1}$	*Type of flux*	*Form of N*	*Tons year*$^{-1}$
Riverine	NO_3, Norg	1,300	Outflow	DIN, Norg	300
Atmospheric	DIN	200	N_2(g) removal	[NO_3 + NH_4^+]	1,100
N-fixation	N_2	50	Burial	PON	150
Total influx		1,550	Total outflux		1,550
2. N fluxes in the *epilimnion*					
In			*Out*		
Type of flux	*Form of N*	*Tons year*$^{-1}$	*Type of flux*	*Form of N*	*Tons year*$^{-1}$
Riverine	NO_3, Norg	400	Outflow	DIN, Norg	200
Atmospheric	DIN	50	Sedimentation	PON	1,100
N-fixation	N_2	50			
Transfer from LWM	NH_4	800			
Total influx		1,300	Total outflux		1,300

1 for the whole lake on an annual basis, *2* for the epilimnion only during stratification (including the phase of destratification in fall/early winter), *DIN* dissolved inorganic N includes: ammonium (NH_4^+), + nitrate (NO_3), and + nitrite (NO_2), *Norg* organic N, *PON* particulate organic N, *LWM* lower water mass

Additional, though smaller, external sources of N to the lake are wet and dry atmospheric depositions. Rain falling directly on the lake surface is characterized by a typical concentration of ~1.3 mg L^{-1} of dissolved inorganic N (DIN; Chap. 19) and multiannual average precipitation of 70×10^6 m^3 $year^{-1}$. Hence, direct wet deposition amounts to ca. 100 t DIN $year^{-1}$. Dry deposition is also estimated at ca. 100 t N $year^{-1}$ (Nishri unpublished).

N fixation provides an additional source of N in the summer–fall (Gophen et al. 1999). Since 1994, when nitrogen-fixing cyanobacteria first appeared in the lake, this source contributes roughly 50 t N $year^{-1}$ (Chap. 22, Table 21.1). Thus, the combined external sources of nitrogen to Lake Kinneret add up to a multiannual mean of roughly 1,550 t N $year^{-1}$. However, this load is highly variable. For example, in the draught year of 1991, riverine sources of N amounted to ~800 t whereas in the following unusually wet year of 1992 the corresponding load was almost 5,000 t, of which ~80 % was nitrate.

21.2 Internal Sources of Nitrogen

Internal sources of nitrogen to the biota in the epilimnion include recycling of organic matter within the epilimnion, upward transport of NH_4^+ from the lower water mass (LWM) of this monomictic lake, and N originating from the decomposition of shoreline vegetation that in some years may constitute a significant source (Chap. 29).

Recycling of organic matter within the epilimnion—this process is mostly a result of microbial decomposition, grazing, and excretion, and remineralization by

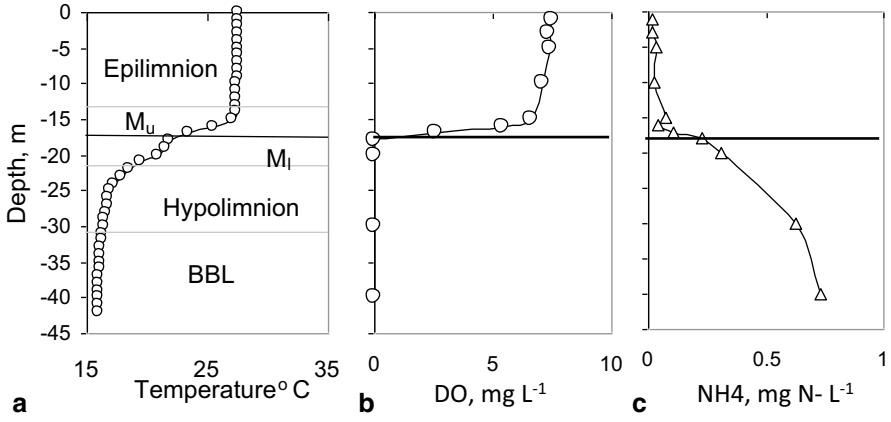

Fig. 21.1 Depth profiles of **a** temperature, **b** dissolved oxygen (*DO*), and **c** ammonium taken on 24 July 1994, at Sta. A at the deepest part of Lake Kinneret. The mid-thermocline depth is marked by a solid line at 18-m depth. M_u upper part of metalimnion, M_l lower part of metalimnion, *BBL* benthic boundary layer

bacteria and zooplankton, issues that are addressed elsewhere (Chaps. 13, 14, 17, and Sect. 25.1).

21.2.1 Upward Transport of NH_4 from the LWM

Various processes lead to transport of N from the ammonium-enriched LWM, across the temperature-gradient barrier in the metalimnion, to the N-depleted epilimnion where most of the biological activity takes place. The seasonal thermocline is located at the middle of the metalimnion, a sub-layer characterized by a steep temperature gradient (Fig. 21.1a). The thermocline usually also marks the oxic–anoxic interface along the water column (Fig. 21.1b). Contrary to the well-oxygenated epilimnion, the upper part of the metalimnion (M_u) is characterized by declining dissolved oxygen (DO) concentrations that reach zero at the oxycline, separating M_u from the anoxic lower part of the metalimnion M_l. During the stratified season, ammonium accumulates in the LWM, including also in the M_l sub-layer; while in the M_u, it rarely accumulates (Fig. 21.1c). Thus, depth profiles of ammonium concentration across the metalimnion show steep gradients and are often truncated by the thermocline–oxycline (Fig. 21.1c). Despite the steep gradient, ammonium diffusion upward toward the impoverished M_u in the lake pelagic is relatively small due the prevalence of a small respective eddy diffusion coefficient. Most of the mixing of LWM water in the epilimnion occurs in littoral zones through boundary mixing (Chap. 9).

The LWM can be divided between two hydrodynamically distinct strata (Nishri et al. 2000): the quiescent hypolimnion (Lemckert and Imberger 1998; Lemckert et al. 2004), lying just below the lower part of the metalimnion, and the more dynamic and turbulent benthic boundary layer (BBL) in the deeper part of the LWM

(Fig. 21.1a, see also Fig. 20.2 in Chap. 20). In summer, the hypolimnion typically extends between ~18- and ~30-m depth while the thickness of the BBL is variable and depends on the intensity of the seiche-induced vertical turbulence (Nishri et al. 2000). At its maximum intensity, the BBL in the pelagic may reach up to the ~30-m depth horizon (i.e., it is about 10 m thick). A major source of ammonium accumulated in the LWM is that which is formed in the BBL, thereafter diffusing upward across the hypolimnion (Rimmer et al. 2006). Boundary mixing is considered to be the major process that causes the introduction of LWM water into the base of the epilimnion. Imberger and Marty (Chap. 9) have estimated this flow to be 30 $m^3\ s^{-1}$ which implies a daily inflow to the photic layer of $\sim 2.5 \times 10^6\ m^3$. In comparison, typical daily riverine discharge of water to this lake in the summer months is only $0.7 \times 10^6\ m^3$.

The BBL layer in sublittoral zones is much thinner than in the lake pelagic, only ~2 m thick (Eckert et al. 2002). Typical NH_4^+ concentrations in the sublittoral BBL is only ~0.4 mg N L^{-1} (Nishri and Ostrovsky 2012) as compared to double this concentration in the pelagic BBL. Assuming that this type of sublittoral BBL water is mixed within the epilimnion, it was possible to estimate typical monthly fluxes of 30 t between the LWM and the epilimnion. In comparison, external riverine sources (~2 mg $N\text{-}NO_3L^{-1}$) in summer would also have about the same monthly load.

The late autumn (mid-October–December) is characterized by fast deepening of the thermocline due to convective buoyancy mixing induced by heat loss from the surface water due to the cooling of the air. This vertical mixing results with a relatively fast introduction of NH_4^+ from the pelagic-enriched LWM into the overlying oxic layers (Chap. 9). Eventually, in the fully mixed lake, NH_4 is evenly distributed along the entire water column having concentrations of several hundred μg $(N\text{-}NH_4)\ L^{-1}$. Typically, the final stage of mixing, whereby the BBL is mixed vertically, lasts less than 2 weeks during which between 600 and 1,100 t of $N\text{-}NH_4$ are internally injected into the mixed lake. Here, the exact value depends on how much NH_4^+ accumulated in the LWM during that year. Another internal lake source of nitrogen in winter, which shows very large interannual variability, is that of N released through the decomposition of inundated shoreline vegetation (Chap. 29).

21.3 Seasonal Patterns of DIN Species in Surface Water

To illustrate the seasonal pattern of N species in surface water we selected the year of 1994 because this year was characterized by a large bloom of *Peridinium gatunense* in spring and by a bloom of N_2-fixing cyanobacteria in summer–fall. Both have significant impacts on the seasonal pattern.

As discussed above, there are two major sources of DIN to the lake photic zone in winter: (1) NH_4 injected from the ammonium-enriched LWM due to mixing that leads to destratification and (2) riverine nitrate inflows. While the timing of both fluxes often overlap, in some winters, it is possible to distinguish between their contributions. In less rainy winters, such as that of 1994, when riverine nitrate loads

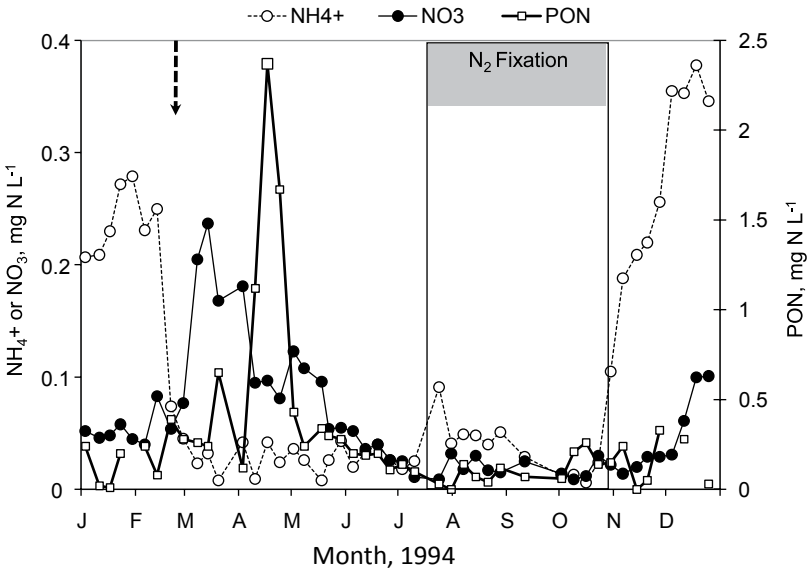

Fig. 21.2 Surface water (1-m depth, Sta. A) weekly concentrations of NH_4, NO_3, and particulate organic N (*PON*) in 1994. That year, a *Peridinium* bloom started in the end of March peaking on 17 April (designed by a *large empty square*) while the crash of the bloom occurred in early May. *Dashed arrow* marks the timing of NO_2 peak, although NO_2 concentrations are not plotted. The period of N fixation in summer by nostocalean cyanobacteria is indicated by a *rectangle* between 20 July and 30 October

are small, DIN sources through mixing of NH_4 originating from the LWM may predominate. Following destratification in January 1994, the predominant DIN species in the surface water was NH_4 at ~270 μgN L^{-1} (Fig. 21.2). Between 14 February and 21 February of that year, NH_4 in surface water declined below 80 μgN L^{-1} and was replaced by a peak in NO_2 of ~225 μgN L^{-1}. A week later, NO_2 disappeared and was replaced by a similar peak of NO_3, ~250 μgN L^{-1}. This sequence of appearance and disappearance of DIN species had already been noticed (Cavari and Phelps 1977; Smith et al. 1989) and taken to indicate the occurrence of the multistage nitrification (Chap. 22). The unusual large accumulation of the intermediate NO_2 species suggests the occurrence of uncoupling between the bacterially mediated stages of the nitrification process and that the rate-limiting step for this sequence is $NO_2 \rightarrow NO_3$.

The bloom-forming dinoflagellate *P. gatunense* frequently occupies the late winter–spring niche (Chap. 11) and is known (McCarthy et al. 1982) to assimilate NO_3 as a source of N. This dinoflagellate has a patchy distribution, which on 17 April 1994 was indicated by an exceptionally high peak of particulate organic nitrogen (PON; Fig. 21.2). The crash of the spring bloom in May–June is indicated by an abrupt decline in epilimnetic PON followed by a relatively small rise in dissolved organic nitrogen (not shown). During and after the spring bloom, nitrate levels in the surface water decline gradually. Often in mid-July, levels approach the detection

limit of ca. 5 µg N L^{-1}. Therefore, in summer and more so early autumn (Aug–Oct), the phytoplankton is prone to nitrogen limitation. This may explain why N_2-fixing cyanobacteria, such as *Aphanizomenon ovalisporum,* usually appear in late summer. In July–October 1994, the amount of N_2(g) fixed by *Aphanizomenon* was exceptionally high and estimated at 315 t N (Gophen et al. 1999). Thus, in 1994, the seasonal flux of N_2(g) fixed was in the same order of magnitude as the sum of the autumnal riverine load and the transfer from the LWM to the photic layer. However, in the following years, N_2 fixation was several fold smaller (Chap. 22) than the other sources. The prevalence of N_2-fixing cyanobacteria was not associated with any increase in surface water levels of PON (Fig. 21.2). In mid-October 1994, concomitant with the crash of the N-fixing cyanobacteria, fast buoyancy mixing (Chap. 9) resulted in the entrainment of NH_4-enriched LWM water within the epilimnion, eventually elevating epilimnetic levels to 0.37 mg (N-NH_4) L^{-1}. It is therefore possible that the crash of the N_2fixers is stimulated by increased availability of ammonium at that time.

21.3.1 Factors Affecting Epilimnetic DIN Levels in Summer–Fall when N_2 Fixers Appear

The difference between outflows and inflows from and to the epilimnion accounts for the gradual drop in epilimnetic NO_3 levels during the spring and summer. In typical years, combined internal and external fluxes of N to the photic layer in summer are estimated between 60 and 150 t per month, with higher loads in higher rainfall years. Export of nitrogen from this layer through pumping in late spring and summer ($\sim 40 \times 10^6$ m^3 $month^{-1}$) amounts to roughly 30 t N $month^{-1}$. However, the largest removal flux from the epilimnion is through the sedimentation of PON which is later mineralized in the LWM and is discussed below.

21.4 Nitrogen Removal Processes from the Whole Lake

Nitrogen removal from the lake water may occur through three pathways: (1) epilimnetic water withdrawal, (2) sedimentation which is followed by burial of PON in the bed sediments, and (3) N_2(g) evasion.

The amount of N removed through water pumping (or natural outflow) can be estimated by assuming an average epilimnetic concentration and using available data on the volume of water pumped or released downstream. Typical annual removal of N through outflow/pumping is estimated at ~300 t $year^{-1}$ (Table 21.1) which in the summer would be ~30 t $month^{-1}$.

Smith et al. (1989) estimated the burial of PON indirectly according to typical ratios between sedimentary N and P in the lake pelagic. Ostrovsky et al. (1997) attempted to estimate this flux by studying total organic N (Norg; both labile and nonlabile) concentrations in surface bed sediments (upper 1 cm) along transects made across the lake. Norg concentration was found to vary between <0.1% of the bulk dry-sediment weight in the littoral and 0.4% in the lake center. Mass bal-

ance considerations show that the annual bulk sedimentation in this lake is in the order of magnitude of 100,000 t dry weight year^{-1} (Chap. 23). N removal through sedimentation is therefore estimated at approximately 300 t N year^{-1}. However, this represents a flux which may be larger than the actual burial flux, because part of this organic N may later be mineralized through diagenetic processes and return as NH_4 to the overlying lake water. At this stage, we may therefore only set an upper limit for N burial at 300 t year^{-1}. Thus, less than 500 t N year^{-1} may be attributed to the processes of outflow/pumping and burial combined (Table 21.1).

Considering average annual inflow loads of 1,550 t year^{-1} (Table 21.1), this leaves an unaccounted removal of ca. 1,000-t N year^{-1}, i.e., between 60 and 70% of the annual inflow load. Cavari and Phelps (1977), Serruya (1978), and Smith et al. (1989) attributed this unaccounted loss of N to denitrification, referring to this process as the multistage conversion of NO_3 to N_2(g) under sub-oxic conditions. In Lake Kinneret, these conditions are found in the LWM during transition to anoxia in April through June. However, the total inventory of NO_3 locked in the LWM upon the onset of stratification in early spring rarely exceeds 500 t N-NO_3 and it is therefore clear that the so-called denitrification process cannot be the sole sink for N annually removed from the lake. This discrepancy was attributed by Cavari and Phelps (1977) and Paerl and Pinckney (1996) to the occurrence of N_2(g) removal through denitrification in microenvironments devoid of oxygen within epilimnetic seston or at the sediment–water interface where the underlying pore water are anoxic (Seitzinger 1988).

The following stoichiometry was commonly applied to link NO_3^-disappearance with N_2 production (Richards 1965):

$$\left(CH_2O\right)_{106}\left(NH_3\right)_{16}H_3PO_4 + 94.4\ HNO_3 = 106\ CO_2 + 55.2\ N_2 + 177.2\ H_2O + H_3PO_4. \quad (21.1)$$

Equation 21.1 implies that the 110.4 mol of N_2 (in N units) produced are made of 16 mol of organic N and 94.4 mol of NO_3. However, recent studies have challenged canonical views of the marine nitrogen cycle (e.g., Codispoti et al. 2001). While denitrification remains acknowledged as the predominant sink, questions have been raised regarding stoichiometry between NO_3 deficits and N_2 production, the importance of alternative pathways such as anaerobic ammonium oxidation (anammox) have been discovered (Dalsgaard et al. 2003; Kuypers et al. 2003). The anammox pathway is carried out by specialized, obligate chemo-autotrophs, slow-growing organisms that oxidize NH_4^+ with NO_2^- to produce N_2 as follows**:**

$$NO_2^- + NH_4^+ \Rightarrow N_2(g) + 2H_2O. \quad (21.2)$$

The biogeochemical implications of anammox include strong deviations from Richard's stoichiometry (Eq. 21.1), particularly where a large pool of NH_4 is available. At its upper limit, there is a 1:2 relationship between NO_3^- consumed and N_2 produced (in N units). This could be obtained if every NO_2^- ion (produced from NO_3 reduction) was reduced by NH_4 as a consequence of anammox. Codispoti et al. (2001), using N_2/Ar mass spectrometric data, showed that in the Arabian Sea,

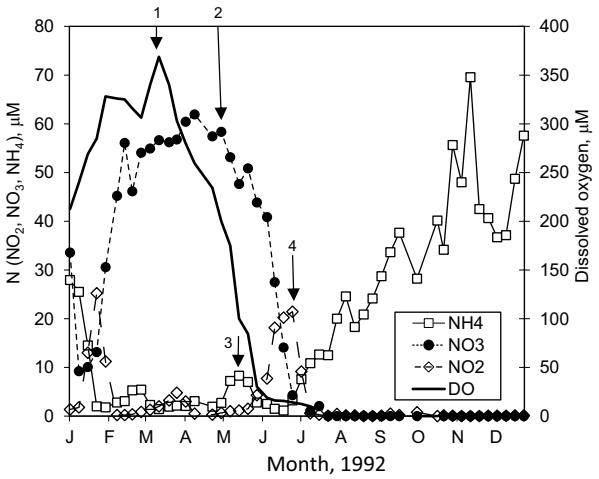

Fig. 21.3 Time series (weekly measurements) of NH_4, NO_2, NO_3, and dissolved oxygen (*DO*; secondary Y-axis) concentrations in the benthic boundary layer (at 40-m depth, Sta. A) during 1992. The onset of stratification is marked by *arrow 1,* the start of NO_3 removal is marked by *arrow 2,* short-term accumulation of NH_4 is marked by *arrow 3,* and peak NO_2 ~20 μmol L^{-1} by *arrow 4*

biogenic N_2 was up to twice that predicted from NO_3 deficits given in Eq. 2.11. It was suggested that water-column denitrification has been seriously underestimated and that perhaps the assumed stoichiometries were incorrect due to previously overlooked processes such as anammox.

For the demonstration of N-related removal processes in Lake Kinneret LWM, we have selected time series data for samples taken from Sta. A at 40-m depth during 1992 (Fig. 21.3). Winter 1991–1992 was extremely rainy and cold, characterized by exceptionally large inflow volumes and high riverine loads of nitrogen. However, due to the cold temperatures, a spring bloom developed later than usually and the concentrations of organic nitrogen species (both dissolved and particulate) remained low, in the order of only 10 μM. This was a significantly lower concentration than that of DIN, which allowed us to treat DIN mass balances exclusively while ignoring temporal variability in organic N species. Upon the onset of stratification, indicated from the initiation of DO decline in the LWM, on 15 March 1992 (Fig. 21.3), oxygen declined from a peak of 369 μM (arrow #1) until this layer became anoxic on July 10. However, in between, on 2 May (arrow #2), while DO declined to 198 μM (ca. 75% saturation), the beginning of NO_3 removal started to be noticed. Thereafter, there was a small peak in NH_4 on 15 May (ca. 8.5 μM arrow #3) with a concomitant drop in NO_3 of about 10 μM (from 57 to 47 μM). After 17 May, ammonium dropped again to below detection limit (~0.3 μM) concomitantly with a buildup of NO_2 to a peak value of ~20 μM on May 30 (arrow #4). Irrespective of the oxygen regime, between 1 Jan and 12 July, NH_4^+ and NO_2 show mirror image profiles; whenever one of these species increases the other one decreases. Thus, NO_2 *does not coexist* with NH_4^+ in this layer and NH_4^+ accumulation in summer starts only after DO, NO_3, and NO_2 removal is completed. If only for oxidative

degradation of organic matter, characterized by a Redfield stoichiometry, assuming an oxygen:nitrogen ratio of 135:16, then a total DO depletion of 369 μM is expected to result with an accumulation of 43.5 μM of N-NH_4^+. However, no NH_4^+ was detected on 4 July and it is therefore assumed to be removed by some process. Preliminary molecular studies of samples taken in May 2004 and January 2005 using a combination of primers specific to *Planctomycetes* and/or anammox (Pla 46F/Amx 820R; Chap. 22) resulted in few clones of uncultured *Planctomycetes,* anaerobic ammonia oxidizers. Thus, in Lake Kinneret, the process of *anammox* participates in NO_3 removal from the LWM due to the following lines of evidence: (1) Due to mass balance estimates, the amount of annual N removal (probably through N_2(g)) is double the amount of NO_3 locked in the LWM at the onset of stratification; (2) the absence of NH_4^+ accumulation in the LWM during DO decline, i.e., during the sub-oxic stages; and (3) the lack of coexistence of NO_2 and NH_4^+ in the LWM.

Based on the DO decay profile, it may be assumed that the source of NH_4^+ needed for anammox to proceed is through the supply of PON which settles from above and is mineralized in the LWM. However, anammox may proceed only if NO_2 is also available; hence, a preliminary process of converting NO_3 to NO_2 is expected. Notice that both processes combined must also fulfill the condition obtained from nitrogen mass balances that the total amount of nitrogen removed annually as N_2(g) would be about twice the amount of NO_3 locked in the LWM upon the onset of stratification. Among the known bacterial processes, heterotrophic dissimilatory nitrate reduction to nitrite (DNRN) has two consequences (Koeve and Khaler 2010): (1) It converts NO_3 to NO_2 and (2) due to its heterotrophic nature, it mineralizes organic nitrogen to NH_4^+. Hadas (Chap. 22) detected nitrate reductase activity in this layer.

According to Koeve and Khaler (2010), DNRN is described by

$$\mathrm{C}_a\mathrm{H}_b\mathrm{O}_c\mathrm{N}_d\mathrm{P}_e\mathrm{S}_f + x\mathrm{HNO}_3 \rightarrow a\mathrm{CO}_2 + d\mathrm{NH}_3 + e\mathrm{H}_3\mathrm{PO}_4 + f\mathrm{H}_2\mathrm{SO}_4 + y\mathrm{NO}_2 + z\mathrm{H}_2\mathrm{O}, \quad (21.3)$$

Whereby in the stochiometric efficient $x=y$ and $d = (2a + 0.5b - c + 2.5e + 3f) / (1.5)$. In other words, in DNRN, NO_3 is fully converted to NO_2 ($x=y$) while some NH_3 ($=d$) originates from the heterotrophic activity associated with it.

As in winter, when the water column in the lake is fully mixed and nitrification occurs (Fig. 21.2), it looks as if immediately after the onset of stratification, between 14 March and 12 April (indicated from the beginning of decline in DO), the rise in NO_3 from 56 up to 65.5 μM in the BBL (Fig. 21.3, Table 21.1) may also be attributed to nitrification because DO is still above 259 μM (~100% saturation). The most probable source of ammonium for this nitrification is the mineralization of organic matter settling from above.

The period between 12 April, when NO_3 ceases to rise, and 17 July may be subdivided into three distinct stages: stage I until the first days of June (Fig. 21.3b), stage II until 5 July when the NO_3 is completely removed and which leads to the accumulation of some NO_2, and stage III when the decay of the residual NO_2 occurs under anoxic conditions. Stage I is characterized by a steep decline of DO to ca. 10% saturation and by a mild decline in NO_3 levels from 61.4 to 42 μM

Table 21.2 Concentrations of dissolved oxygen (DO) and dissolved inorganic species of N below 35-m depth during Jan–Jun 1992. Typical daily removal fluxes of nitrate [$\Delta NO_3/\Delta t$] in May–Jun 1992

Date, 1992	DO, μM	NO_3, μM	NO_2, μM	NH_4, μM	ΣDIN, μM	$\Delta NO_3/\Delta t$ μmol L^{-1} d^{-1}
Jan 5	240.0	33.6	1.4	27.9	62.9	
Jan 26	285.0	13.1	25.8	2.0	40.9	
Mar 1	306.3	54.1	0.9	5.4	60.4	
Mar 15	368.8	56.2	2.0	2.0	60.2	
Mar 29	303.1	56.8	4.8	2.1	63.7	
Apr 12	259.4	61.9	0.5	3.1	65.5	
May 17	100.0	50.0	1.1	8.3	59.4	0.31
May 31	25.0	44.0	4.2	2.8	51.0	0.43
Jun 21	15.6	14.1	20.2	1.1	35.4	1.43
Jun 28	14	4.3	21.4	3.7	29.4	1.43
Later	0	0	0	Increase	Increase	

DIN dissolved inorganic N

(a rate of ~0.4 μmol L^{-1} d^{-1}), while stage II is characterized by a mild decline in DO (<0.9 μmol L^{-1} d^{-1}) but a steep decline in NO_3 (1.43 μmol L^{-1} d^{-1}; Fig. 21.3b, Table 21.2). The difference between stages I and II is obvious, as in the first stage most biodegradation occurs through an oxic process where the nitrogenous product expected is NH_4^+, while in the second stage it mostly occurs through nitrate reduction where the end product expected is N_2(g). For the first stage, the drop in DO is equal to 255 μM and the respective decline for NO_3 is 20 μM. Assuming a 135:16 DO:N ratio (=8.44) during oxic respiration, 29.6 μM of NH_4^+ is expected to be released. This is almost 10 μM more than the respective drop in NO_3(from 29.6 to 20 μM). About 3 μM of this difference may be attributed to the small rise in NH_4^+ (at the end of the first stage) and approximately 7 μM to the presumably DNRN heterotrophic process (29.6−20−3=7). Or in other words, in terms of the stoichiometric coefficients presented in Eq. 21.3, x/d ≈3. For the second stage, the drop in DO is equal only to ~25 μM L^{-1}; hence, that ~3 μM of NH_4^+ may be attributed to oxic degradation. The drop in NO_3 is equal to 42 μM but the parallel rise in NO_2 is smaller and only ca. 20 μM (Table 21.2). Assuming the occurrence of anammox, it means that concomitant supply of NH_4 from all sources must have been 22 μM (42–20) of which only ca. 3 μM may be attributed to oxic degradation (=25 μM/8.44) and another 2 μM to NH_4^+ removed during the transition from stage I. Hence, ca. 17 μM NH_4^+ may have been released due to DNRN activity (Eq. 21.3) and in this case, the ratio x/d ≈2.5 (42/17), which is not very different from the ratio obtained in the first stage. The rather similar x/d ratios obtained in both oxic and sub-oxic stages supports the idea of a coupling between DNRN and anammox in Lake Kinneret LWM. The last anoxic stage until July 17 is assumed to be completed in the presence of other oxidizing agents such as Fe oxides or even SO_4.

Regardless of whether the DNRN suggested here prevails or not, just by assuming that anammox causes the removal of NO_2 and that the source of NH_4^+ for this process is the biodegradation of organic matter settling from above, it is possible to quantify N removal as N_2(g) from the LWM by multiplying the inventory of NO_3

locked in this layer ($NO_{3(LWM-i)}$) upon the onset of stratification. In other words, [$N_2(g)^* = 2\ NO_{3(LWM-i)}$]. The overall amount of nitrogen that is associated with the biodegradation and mineralization of organic matter in the LWM includes also the amount of ammonium which is accumulated throughout the stratification period after the completion of $N_2(g)$ production, referred to as NH_4^*. Between 5 July and December, NH_4^* accumulated amounted to 50 μM, a value that resembles the multiannual average annual concentration in this lake. At the onset of stratification in 1992, the volume of the LWM was ~$1{,}650 \times 10^6$ m^3, suggesting that $N_2(g)^*$ equals ca. 2,900 t. In comparison in 1992, the amount of epilimnetic water released to the southern Jordan River and pumped out of the lake was 850×10^6 m^3 $year^{-1}$ resulting in an outflow of ca. 500 t N. Considering also few hundred tons burial in the lake floor, the budget shows that in 1992 only 23 % of the N riverine load on that rainy year accumulated as NH_4 in the LWM.

Having such an extensive removal of nitrogen through anammox has significant ecological implications. First, it implies that the nitrogen stored in the LWM in one summer and then supplied to the mixed water column of the following winter is only about one-third or even less of the inflow loads during the first year. Second, it implies that larger riverine winter-inflow loads lead to larger N-removal flux, not only because more NO_3 is locked in the LWM at the onset of stratification but also because more PON is mineralized to NH_4 in the LWM as is required to "titrate" it through anammox. Thus, the occurrence of anammox is shown to satisfy the nitrogen budget in the lake without having to claim the occurrence of extensive "denitrification within epilimnetic seston" or in mixed pore water (Seitzinger 1988; Paerl and Pinckney 1996).

It is therefore possible to estimate how much PON settles from the epilimnion downward to the LWM during the stratified period and decomposes. This amount is equal to NO_3 removal as $N_2(g)$ from the LWM during the sub-oxic stages and to NH_4^+ buildup thereafter. Combined with the known inflows of DIN to the euphotic layer allows for budgeting nitrogen fluxes in the epilimnion.

21.4.1 Vertical heterogeneity in rates of NO_3 removal along the LWM water column

Chemical stratification in Lake Kinneret evolves seasonally in response to the annual cycle in temperature-dependent density stratification. This is illustrated by the temporal evolution of O_2 versus depth, as registered by an autonomic profiler set in Sta. A (Wagner et al. 2005, Nishri et al. 2011) from 21 May to 27 June 2003 (Fig. 21.4). The epilimnion (in this case, above 12-m depth) was then characterized by DO saturation ($\%DO_{sat}$) levels of between 50 and 110 %; the metalimnion (12–20-m depth, starting in 24 May) with $DO_{sat} < 15\%$; the hypolimnion (21–30-m depth) with $\%DO_{sat}$ between 16 and 35 %; and the BBL (>30 m) was anoxic throughout the entire period. The distinct oxygen minimum in the metalimnion and the lack of oxygen in the BBL are associated with intensive respiration following the crash of the spring bloom of *P. gatunense*. The occurrence of relatively high levels of

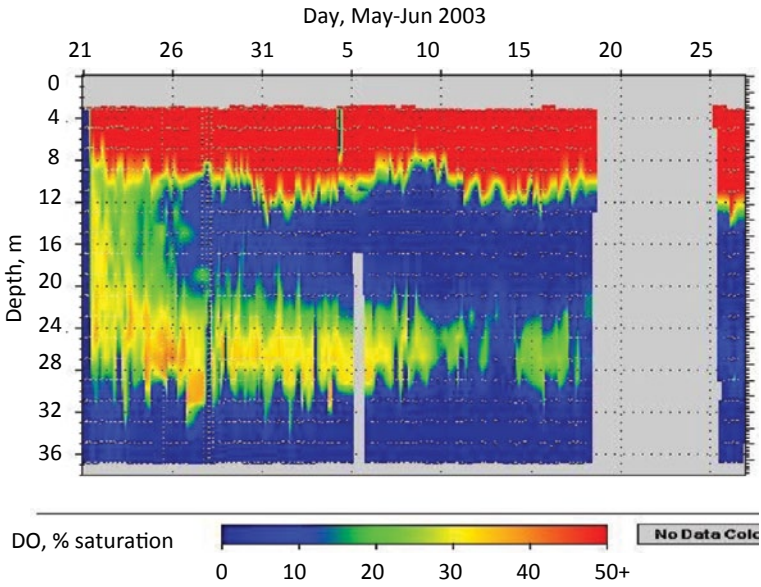

Fig. 21.4 Time–depth color-coded map of percent oxygen saturation based on data collected by an automatic profiler (RUSS) equipped with depth and oxygen sensors, situated at Sta. A. Depth profiles were taken every 4 h, 21 May to 27 June 2003. The uppermost and lowest 3-m layers were not sampled. The epilimnion is well oxygenated (>50 % saturation) whereas the benthic boundary layer (>32 m) is anoxic throughout this period. At the beginning of this period, the metalimnion (12–20 m) shows a decline in dissolved oxygen (*DO*) saturation level from ~30 % on 21 May to <10 % on 26 May. Deeper, between 22 and 28 m, oxygen in the hypolimnion fades slowly to its complete elimination by ~18 June. Thereafter, the entire lower water mass is anoxic

oxygen in the hypolimnion (21–30-m depth) late in June 2003, was attributed to the lower decomposition activity in this sub-layer due to it being poor in organic matter relative to the water above and below it. This is due to the absence of a temperature gradient in this layer such that particles sink right through it (Nishri et al. 2011). The gradual decline in DO in the hypolimnion was attributed to slow diffusion upwards and downwards to adjacent anoxic layers. Notice that compared to other water layers, the 21–30-m layer is characterized by having the smallest vertical eddy diffusion coefficient which explains the slow diffusion to both boundaries (Nishri et al. 2011).

Considering that DNRN is a heterotrophic process, the low effective concentrations of biodegradable material in the hypolimnion would also inhibit the conversion $NO_3 \rightarrow NO_2$. Indeed during June 2003, NO_3 levels in the hypolimnion remained relatively stable until mid-June, i.e., ca. 3 months after the onset of stratification (Fig. 21.5). Only later, during the past 2 weeks of June, concomitantly with O_2 decline was there also a gradual decrease in NO_3 levels in this sub-layer (the middle of which was at 25-m depth); but unlike the case presented above for the BBL in 1992, it occurred without a parallel rise in NO_2. In 2003, rates of NO_3 removal were fastest in the BBL and relatively fast in the metalimnion. Hence, similarly to the case of dissolved oxygen, the delayed decline of NO_3 in the hypolimnion (25 m) is attrib-

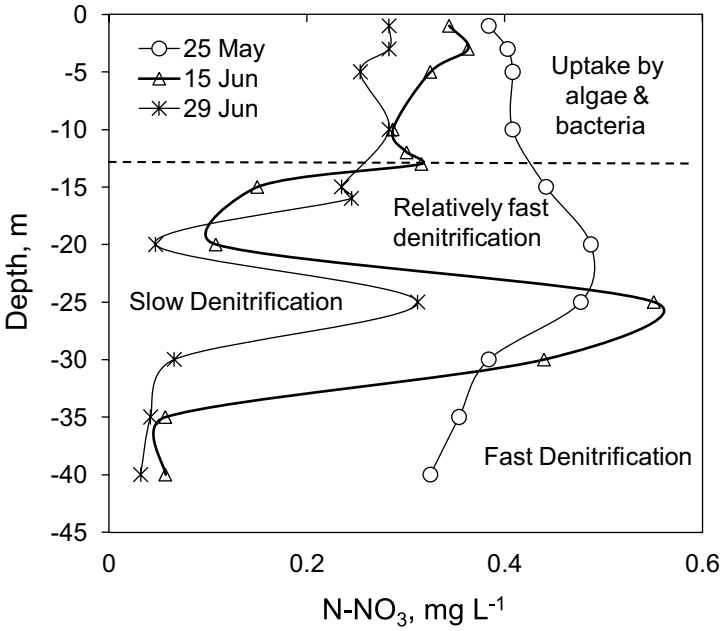

Fig. 21.5 Depth profiles of nitrate concentration at Sta. A on 25 May, 15 June, and 29 June 2003. The main N-cycle processes taking place at each layer are marked. Note the peaks of NO_3 concentration in the hypolimnion, at or near 25-m depth. *Dotted line* marks the depth of the seasonal thermocline

uted to inhibition of heterotrophic DNRN activity due to the lack of biodegradable organic matter. The eventual slow decline in NO_3 is attributed to its slow vertical diffusion to the already NO_3-deficient adjacent sub-oxic layers (BBL below and metalimnion above) rather than to in situ removal through heterotrophic activity. Thus, the physical dimensions and regime in Lake Kinneret LWM (Chap. 9) allow for a distinction between three sub-layers, which are characterized by different rates of DO and NO_3 depletion: the metalimnion, hypolimnion, and BBL.

21.5 Summary

A schematic presentation of nitrogen cycling in Lake Kinneret is illustrated in Fig. 21.6. In winter (Fig. 21.6a), turnover enriches the epilimnion with NH_4 that was previously locked in the LWM and this induces nitrification, converting the ammonium to nitrite first and later to nitrate. Concomitantly and thereafter, riverine inflows rich in nitrates commence. Upon the onset of stratification in early spring, the existing pool of nitrate is divided between the epilimnion and the LWM, according to the relative water volumes in each layer. Nitrate in the epilimnion supports the biological activity in this layer, producing PON that later settles to the LWM where

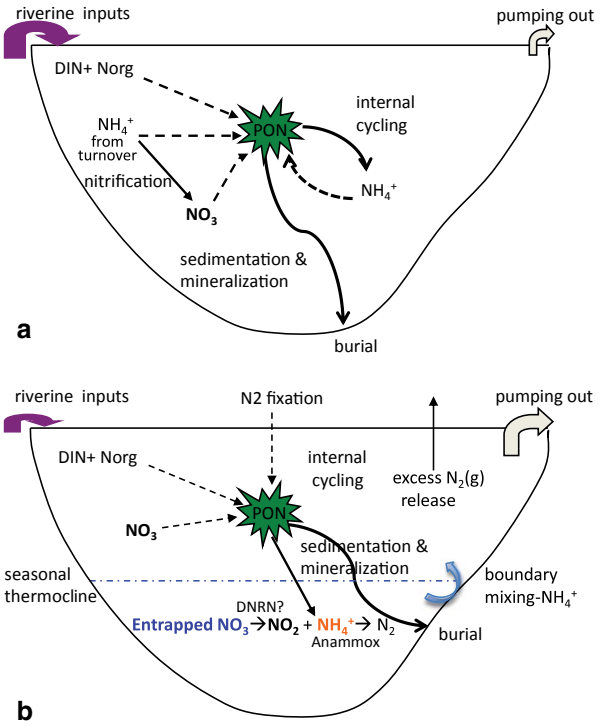

Fig. 21.6 A schematic presentation of the main processes in the nitrogen cycle of Lake Kinneret **a** in winter and **b** in summer. See details in text. *DIN* dissolved inorganic N, *Norg* (organic N), *PON* particulate organic nitrogen, *DNRN* dissimilatory nitrate reduction to nitrite

it is mineralized to form NH_4. There is no other way to explain the lack of NH_4 accumulation in the BBL during the stages of DO and NO_3 plus NO_2 depletion in this layer but to assume the prevalence of an anammox process. The NO_3 entrapped in the LWM is assumed to be removed through a combination of DNRN with anammox activity. Thus, N removed as N_2(g) amounts to double the amount of N-NO_3 entrapped in the LWM upon the onset of stratification. This satisfies previous and recent observations that the amount of N removed from this lake annually is more or less double the amount of NO_3entrapped in the LWM. On a multiannual scale, out of ~1,550 t N in external inflows, ~500 t N are buried in the bed sediments or withdrawn through water pumping and ~1,050 t are removed by a combination of presumably DNRN and anammox.

In summer (Fig. 21.6b), biological activity in the epilimnion is supported by NO_3 remaining from the spring and by the scarce summer sources of DIN. Among these is NH_4 which is transported upward to the photic layer through lake boundary mixing. Later in fall, this flux is larger and is maintained through the erosion of the top of the LWM induced by buoyancy mixing. Other summer sources are riverine inflow, dust, and N_2 fixation. At some stage in summer, epilimnetic DIN levels become extremely low due to the imbalance between sources and sinks, enabling the appearance of N_2-fixing cyanobacteria. This contributes a considerable amount of external N to the epilimnion estimated at ~50 t within 3 months, during the low epilimnetic DIN season.

References

Cavari BZ, Phelps G (1977) Denitrification in Lake Kinneret in the presence of oxygen. Freshw Biol 7:385–391

Codispoti L, et al (2001) The oceanic fixed nitrogen and nitrous oxide budgets: moving targets as we enter the anthropocene? In: Gili J, Pretus J, Packard T (eds) A marine science Odyssey into the 21st century, p 85–105. Sci Mar 65:85–105

Dalsgaard T, Canfield DE, Petersen JB, Thamdrup B, Acuna-Gonzalez J (2003) N_2 production by the anammox reaction in the anoxic water column of Golfo Dulce, Costa Rica. Nature 422:606–608

Eckert W, Imberger J, Saggio A (2002) Biogeochemical evolution in response to physical forcing in the water column of a warm monomictic lake. Biogeochemistry 61:291–307

Gophen M, Smith VH, Nishri A, Threlkeld ST (1999) Nitrogen deficiency and invasion of Lake Kinneret, Israel, by the N_2-fixing cyanobacterium *Aphanizomenon ovalisporum*. Aquat Sci 61:293–306

Koeve W, Kahler P (2010) Heterotrophic denitrification vs. autotrophic anammox-quantifying collateral effects on the oceanic carbon cycle. Biogeosciences 7:2327–2337

Kuypers MMM, et al (2003) Anaerobic ammonium oxidation by anammox bacteria in the Black Sea. Nature 422:608–611

Lemckert C, Imberger J (1998) Turbulent benthic boundary layer mixing events in freshwater lakes. In: Imberger J (ed) Physical processes in lakes and oceans, Coastal and Estuarine studies. Am Geophys Union 54:503–516

Lemckert C, Antenucci J, Saggio A, Imberger J (2004) Physical properties of turbulent benthic boundary layers generated by internal waves. J Hydraul Eng 130(1):58–69

McCarthy JJ, Wynne D, Berman T (1982) The uptake of dissolved nitrogenous nutrients by Lake Kinneret, Israel microplankton. Limnol Oceanogr 27:673–680

Nishri A, Ostrovsky I (2012) Nutrient contribution from the LWM to Lake Kinneret photic layer. IOLR Report T24/2012 (in Hebrew)

Nishri A, Imberger J, Eckert W, Ostrovosky I, Geifman J (2000) The physical regime and the respective biogeochemical processes in the lower water mass of Lake Kinneret. Limnol Oceanogr 45(4):972–981

Nishri A, Rimmer A, Wagner U, Rosentraub Z, Yeats P (2011) Physical controls on the spatial variability in decomposition of organic matter in Lake Kinneret. Aquat Geochem 17(3):195–207

Ostrovsky I, Wynne D, Bergstein-Ben Dan T, Nishri A, Yacobi YZ, Koren N, Parparova R (1997) Spatial distributions of biogeochemical parameters in Lake Kinneret bed sediments. Water Air Soil Pollut 62(4):497–505

Paerl HW, Pinckney JL (1996) A minireview of microbial consortia: their role in aquatic production and biogeochemical cycling. Microb Ecol 31:225–247

Richards FA (1965) Anoxic basins and fjords. In: Riley JP, Skirrow G (eds) Chemical oceanography, vol 1. Academic Press, London, pp 611–645

Rimmer A, Eckert W, Nishri A, Agnon Y (2006) Evaluating hypolimnetic diffusion parameters in thermally stratified lakes. Limnol Oceanogr 51(4):1906–1914

Seitzinger SP (1988) Denitrification in freshwater and coastal marine systems: ecological and geochemical significance. Limnol Oceanogr 33:702–724

Serruya C (ed) (1978) Lake Kinneret. Dr. W Junk Publishers, The Hague

Smith S, Serruya SV, Geifman J, Berman T (1989) Annual mass balance of P, N, Ca and Cl in Lake Kinneret, Israel. Limnol Oceanogr 34:1202–1213

Wagner U, Nishri A, Zohary T, Sukenik A (2005) The Ecoraft: a remote controlled monitoring station in Lake Kinneret. SIL News 46:7–8

Chapter 22
Microbial Processes Within the Nitrogen Cycle

Ora Hadas

Abstract Biological processes within the nitrogen cycle in Lake Kinneret are mediated by microbial populations and seasonally and spatially divided. Changes in stratification, dissolved inorganic nitrogen (DIN), and O_2 concentration in the epilimnion and hypolimnion of the lake (internal factors), in addition to external sources such as input of nitrate and organic N via the Jordan River and atmospheric deposition, all have an impact on microbial diversity and activity. Assimilation, nitrification, denitrification, ammonification, and N_2 fixation are the main processes mediated by microbial populations in Lake Kinneret. Large temporal variations in the nitrogen isotopic composition ($\delta^{15}N$) of particulate organic matter (POM) and DIN species in Lake Kinneret occurred in response to the dominant nitrogen cycle processes.

Keywords Assimilation · Nitrification · Denitrification · Nitrogen fixation · Anammox · Chemoautotrophy · Lake Kinneret

Biological processes within the nitrogen cycle in Lake Kinneret are seasonally and spatially divided. Changes in stratification, dissolved inorganic nitrogen (DIN), and O_2 concentration in the epilimnion and hypolimnion of the lake (internal factors), in addition to external sources such as input of nitrate and organic N via the Jordan River and atmospheric deposition, all have an impact on microbial diversity and activity. Assimilation, nitrification, denitrification, ammonification, and N_2 fixation are the main processes mediated by microbial populations in the lake (Figs. 22.1 and 22.2). Regeneration of N-nutrients via the microbial loop and higher trophic levels are addressed in Chaps. 13 and 14. The microbial processes within the nitrogen cycle in the lake are described according to the temporal sequence of their occurrence, by analyzing data for two consecutive years, 2004 and 2005.

O. Hadas (✉)
The Yigal Allon Kinneret Limnological Laboratory, Israel Oceanographic & Limnological Research, P.O. Box 447, 14950 Migdal, Israel
e-mail: orah@ocean.org.il

T. Zohary et al. (eds.), *Lake Kinneret, Ecology and Management,* Aquatic Ecology Series 6,
DOI 10.1007/978-94-017-8944-8_22,

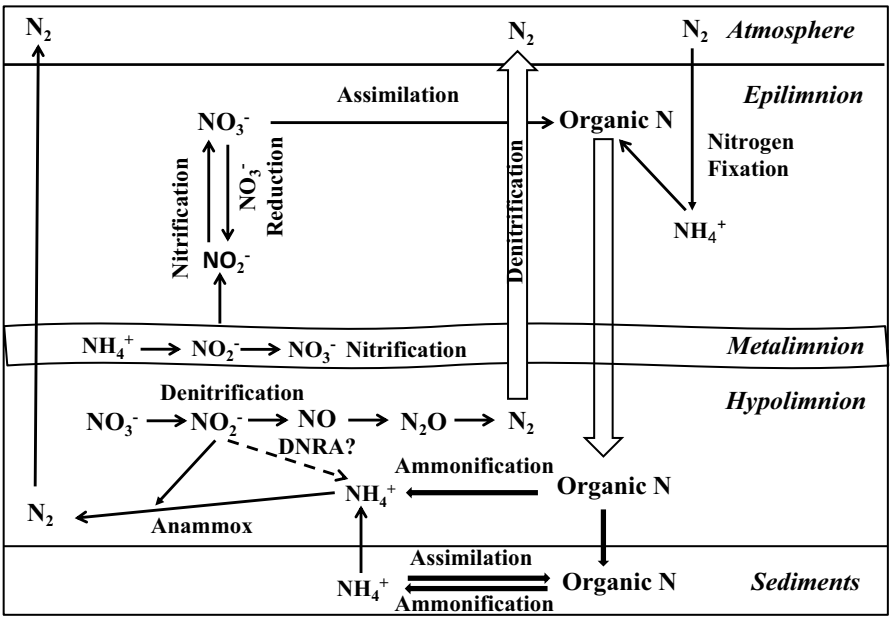

Fig. 22.1 Schematic representation of the spatial distribution of the main microbial processes within the nitrogen cycle in the water column of Lake Kinneret. *DNRA* dissimilatory **n**itrate **r**eduction to **a**mmonia

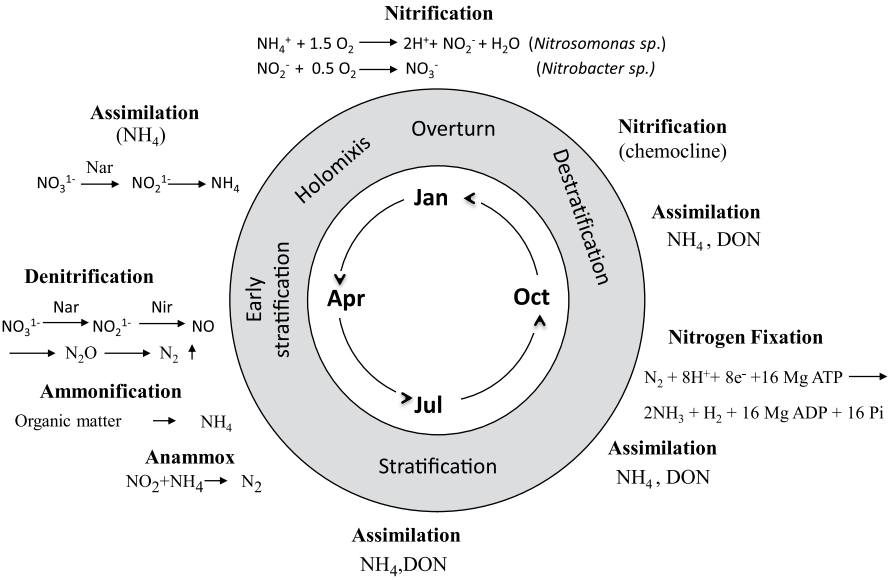

Fig. 22.2 Schematic representation of the annual pattern of the main microbial processes within the nitrogen cycle in the water column of Lake Kinneret. *Nar* nitrate reductase, *Nir* nitrite reductase

22.1 Overturn and Holomixis (Winter–Spring)

Nitrification (ammonia oxidation)—is the dominant process in the lake in winter when ammonia is oxidized to nitrate by nitrifying bacteria.

Ammonia oxidation is an autotrophic process carried out by three groups of microorganisms; aerobic ammonia-oxidizing bacteria (AOB) and archaea (AOA), and anaerobic AOB (anammox) which oxidize ammonia using nitrite as an electron acceptor and producing atmospheric dinitrogen. All have slow growth rates and poor growth yields.

In AOB, the first step of the process is the conversion of ammonia to nitrite; at first, ammonia is oxidized to hydroxylamine by the membrane-bound enzyme ammonia monooxygenase (AMO), followed by the oxidation of hydroxylamine to nitrite (NO_2^-) by hydroxylamine oxidoreductase (HAO), which is the energy-producing step. The second step is the oxidation of nitrite to nitrate (NO_3^-). Within the bacteria *Nitrosomonas, Nitrosospira*, *Nitrosococcus* produce nitrite which is then converted to nitrate by the *Nitrobacter* bacteria. Most nitrifying bacteria are autotrophic, with carbon dioxide serving as their carbon source. The nitrification processes are dependent on environmental factors; substrate and oxygen concentration, temperature, and pH.

In Lake Kinneret, overturn in winter (late December–January) brings NH_4^+ (concentrations of about 120 μmol L^{-1}) trapped in the hypolimnion into the isothermal and oxygenated water column, conducive to nitrification. Usually, NO_3^- accumulated simultaneously with NH_4^+ decreases due to similar rates of NH_4^+ and NO_2^- oxidation (Cavari 1977).

Two seasonal NO_2^- maxima typically occur, one during the nitrification period in January, about 10–15 μmol L^{-1} and another during denitrification in May. The concentration of NO_2^- is usually low and it is present for a short period of ~1 week. The year 2005 was unique, with an exceptionally high peak in NO_2^- (18 μmol L^{-1}) and NO_2^- presence for 2 weeks in January, which cooccurred with NH_4^+ disappearance, indicative of the first stage of nitrification. By the end of January, no NO_2^- and very low NH_4^+ concentrations were observed indicating nitrification had almost reached completion. NO_3^- concentration reached 33 and 27 μmol L^{-1} at 1-m depth in 2004 and 2005, respectively (Fig. 22.3a).

On an annual basis, NO_3^- concentrations varied from 0 to 50 μmol L^{-1}, in response to inputs from the watershed via Jordan River flood events and NH_4^+ oxidation in winter, and removal by algal uptake or denitrification.

Molecular characterization of the bacteria in the water column in winter, using 16S ribosomal RNA (rRNA) cloning, revealed that 90% of the 16S rRNA clone library was related to *Nitrosomonas* sp. (National Center for Biotechnology Information Gene Bank accession numbers: DQ154782–DQ154799), a bacterium responsible for the oxidation of ammonium to nitrite.

Assimilation, NH_4^+ and NO_3^- uptake: The winter–spring period in Lake Kinneret is characterized by massive phytoplankton blooms. Until 1994 and in few years since then, the bloom of the dinoflagellate, *Peridinium gatunense* dominated.

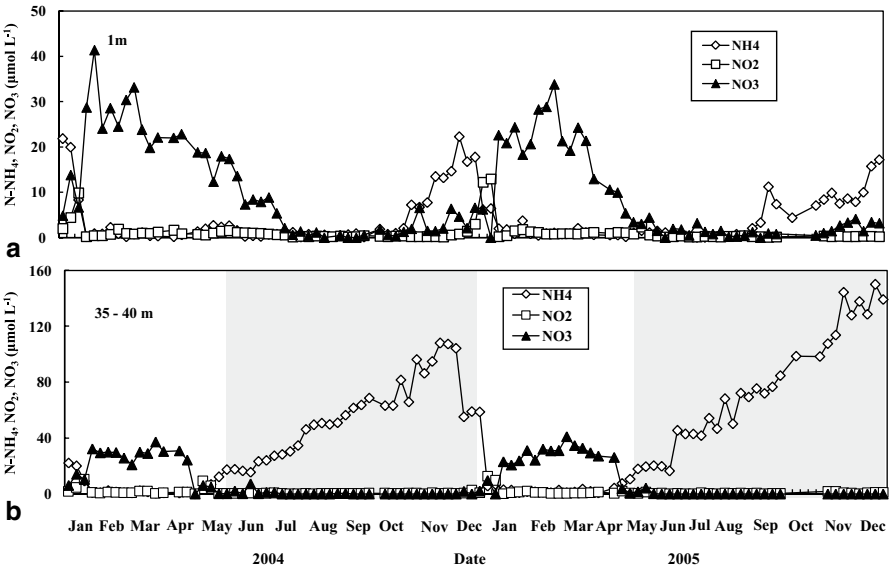

Fig. 22.3 Dissolved inorganic nitrogen concentrations in the **a** epilimnion at 1-m depth and **b** hypolimnion 35–40-m depth. N-NH_4^+ µmol L^{-1} (◊), N-NO_2^- µmol L^{-1} (□), N-NO_3^- µmol L^{-1} (▲). *Shaded area* corresponds to stratification period. (Reprinted from Hadas et al. 2009, Copyright 2014 by the Association for the Sciences of Limnology and Oceanography, Inc.)

Since 1994, other species took over (i.e., *Mougeotia* sp. in 2005, *Ceratium hirundinella* in 2010), demanding N sources for growth and bloom development. Due to the completion of nitrification at the end of January, almost no ammonium is left in the water column; the main nitrogen source is nitrate (>90% ΣN as NO_3^-). The actual uptake rate from any specific N source will be a function of the availability of that source and the potential for its incorporation into the cells. Although ammonium is the preferred nitrogen source for phytoplankton in the lake (McCarthy et al. 1982), in all seasons and depths, it can only boost the beginning of the blooms in January. The development and peaking of the blooms (February–May) have to use nitrate or other nitrogen sources (DON, or regenerated NH_4^+) to supply their nitrogen demands.

Using the ^{15}N tracer method, a measured average nitrogen uptake rate of 2.4 µmol N L^{-1} day^{-1} or 86 t $lake^{-1}$ day^{-1}, for nitrogen was recorded during the *Peridinium* bloom season, for a euphotic zone of 15 m over a lake area of 170 km^2. The *Peridinium* bloom periods were characterized by the highest specific uptake and transport rates for NH_4^+. The NH_4^+ uptake rates, V_{NH4} were generally higher than the corresponding V_{NO3}^- or V_{urea} rates. Maximum rate of uptake (V_{max}) was about 4×10^{-3} h^{-1}, with (K_S) between 0.1 and 0.6 µmol NH_4^+-N L^{-1}. Turnover times ranged from 1 to 630 h for NH_4^+, 21 to ~7,000 h for NO_3^-, and 5 to >560 h for urea-N (McCarthy et al. 1982; Berman et al. 1984). Although nitrate was the dominant N-species during the bloom season, the uptake rates were slow and turnover times long. Still, the highest V_{max} values for nitrate were recorded at the peak of the

Peridinium bloom and flux of NO_3^- constituted a considerable proportion of the total N uptake from February to April (Berman et al. 1984). In addition to *Peridinium,* the uptake of nitrate by nanoplankton was responsible for the assimilation of NO_3^-. Nanoplankton generally had higher nitrogen uptake activities than net phytoplankton but during the early stages of *Peridinium* development it was as active (per unit of chlorophyll) as the smaller algae (McCarthy et al. 1982; Sherr et al. 1982). Later in the bloom period, *Peridinium* had lower specific rates for both NH_4^+ and NO_3^- than the nanoplankton present at the same time. Thus, high relative activities are depending also on the physiological state of the cells (Sherr et al. 1982).

The activity of nitrate reductase has been used as an indicator of ongoing nitrate uptake by phytoplankton and reflects the utilization of nitrate rather than ammonium as the source of algal nitrogen nutrition. Significant enzyme activities (5–25 nmol NO_2^- formed per mg protein h^{-1}) were found in *Peridinium* taken from the lake in March through May (Hochman 1982). Near-surface water samples of natural phytoplankton from Lake Kinneret, as well as axenic cultures of *Chlamydomonas* sp., *Chlorella* sp., *Scenedesmus minuta, Selenastrum* sp., and *Pediastrum duplex,* grown on NO_3^- showed high activities of nitrate reductase indicating nitrate uptake by Lake Kinneret phytoplankton (Hochman et al. 1986). Highest nitrate reductase activities were found in water samples during the *Peridinium* bloom, proportional to chlorophyll concentrations (Wynne and Berman 1990).

The assimilated NH_4^+ or NO_3^- moved rapidly into proteins and nucleic acids and little N remained in low-molecular-weight compounds (Berman et al. 1984). Since the *Peridinium* is hardly grazed and mostly decomposed, NO_3^- that was incorporated directly into the dinoflagellate biomass would return to the water by heterotrophic activity as NH_4^+ or DON (Serruya et al. 1980; Sherr et al. 1983; Hadas et al. 1990; Zohary et al. 2000).

22.2 Beginning of Stratification (Late Spring–Early Summer)

Denitrification is the conversion (reduction) of nitrate by microbially mediated processes, finally resulting in the production of dinitrogen (N_2) gas, which is then released into the atmosphere. Intermediate gaseous nitrogen oxide products are involved in this process:

$$\text{nitrate}\left(NO_3^-\right) \rightarrow \text{nitrite}\left(NO_2^-\right) \rightarrow \text{nitric oxide (NO)} \rightarrow \text{nitrous oxide}\left(N_2O \rightarrow N_2\right).$$

Denitrification is a respiratory process dependent on nitrate concentrations, availability of labile organic matter, oxygen concentrations (redox), and temperature. The process is performed by heterotrophic bacteria (such as *Paracoccus denitrificans* and various pseudomonads), although autotrophic denitrifiers have also been identified (e.g., *Thiobacillus denitrificans*).

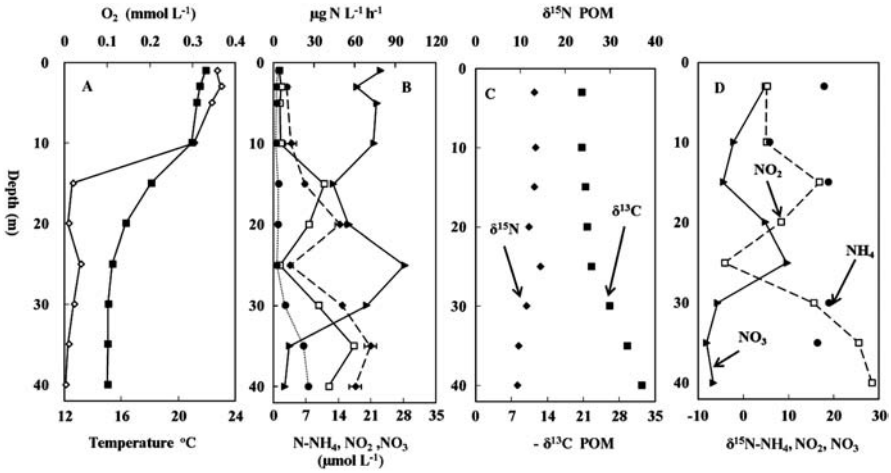

Fig. 22.4 Depth profiles of various parameters relevant to denitrification in Lake Kinneret, beginning of May 2004. **a** Oxygen concentration (◊), temperature °C (■). **b** Concentrations of NO_3^- (▲), NO_2^- (□),NH_4^+ (●). **c** $\delta^{15}N$—POM (♦), $\delta^{13}C$—POM (■). **d** $\delta^{15}N$-NH_4^+ (●), $\delta^{15}N$ NO_2^- (□), $\delta^{15}N$ NO_3^- (▲)

In Lake Kinneret, denitrification begins at the sediment–water interface in late March. Intense denitrification typically takes place in late April and May when the spring bloom biomass decomposes and heterotrophic microbial degradation of organic matter consumes available O_2 and then uses NO_3^- as an electron acceptor (Fig. 22.4a). For example, between March and June 2004, when low hypolimnic O_2 concentrations were established, NO_3^- concentrations decreased in the hypolimnion from 37 to 0 µmol L^{-1}, respectively (Fig. 22.3b). Correspondingly, high nitrate reductase activity was measured at the beginning of May at 30–40-m depth, indicating to the first step of denitrification, i.e., reduction of nitrate to nitrite (Fig. 22.2). At this time, NH_4^+ began to accumulate in the lower part of the hypolimnion due to the continuing degradation of organic matter derived from sinking *Peridinium gatunense* cells and supply from the sediments (Figs. 22.3b and 22.4b).

Denitrification in the sediments probably occurs throughout the whole year (Cavari and Phelps 1977) since the necessary anoxic conditions are found in the sediments generally at a depth of a few millimeters, when appropriate electron donors (organic matter) and acceptors are present. At the chemoclines (oxic–anoxic interfaces), denitrification is probably coupled to nitrification processes. In some years, the denitrification begins in the metalimnion; this is due to an early stratification and accumulation of organic matter at the metalimnic layer. Lake Kinneret nitrogen balance reveals that 60 % of the nitrogen entering the lake is denitrified; thus, denitrification is probably the main process regulating the DIN inventory preventing the accumulation of nitrate (Serruya 1978).

We characterized the bacterial community of denitrifiers present in the water column during the denitrification process using specific primers for the functional genes *nirS* and *nirK* encoding the enzyme nitrite reductase (reduction of nitrite to

nitric oxide by nitrite reductase is the first step that distinguishes denitrifiers from nitrate-respiring bacteria, which do not reduce nitrite to gas). Denitrifying bacteria in Lake Kinneret consist of the species *Paracoccus, Thauera, Pseudomonas, Alcaligenes* (National Center for Biotechnology Information Gene Bank; accession numbers: AMO 71455–71487).

Although denitrification is the dominant N loss process in lakes, two additional pathways of N removal should be considered, anaerobic ammonia oxidation (anammox) and dissimilatory nitrate reduction (DNRA).

Anammox (anaerobic ammonia oxidation): The conversion of nitrate to N_2 by heterotrophic bacteria (denitrification) was believed to be the only important sink for fixed inorganic nitrogen in the ocean. Anaerobic ammonium oxidation (anammox) bacteria, which were discovered in waste water sludge in the early 1990s, have the unique metabolic ability to combine ammonium and nitrite or nitrate to form nitrogen gas, according to the equation:

$$NH_4^+ + NO_2^- \rightarrow N_2 + 2H_2O.$$

During the past two decades, evidence for bacteria that anaerobically oxidize ammonium with nitrite to N_2 was accumulated in marine environments (Dalsgaard et al. 2003; Kuenen 2008; Kuypers et al. 2003) and is probably widespread in aquatic systems. In stratified lakes, chemoclines, sediment–water interfaces, and benthic boundary layers (BBL), where ammonia, nitrite, and nitrate coexist are potential sites to anammox reactions besides denitrification, especially during bloom collapse and oxygen decrease. Anammox processes occurred in the suboxic water column of Lake Tanganyika (Shubert et al. 2006) and in the Thames sediment (Trimmer et al. 2003). The presence and distribution of anammox 16S rRNA gene sequences in freshwater sediments from Wintergreen Lake and from wetlands in Florida Everglades were demonstrated using specific primers targeted to anammox bacteria. This suggests that anammox bacteria are agents of nitrogen removal from freshwater lakes besides denitrification (Penton et al. 2006).

In Lake Kinneret, there are two periods in which NH_4 and NO_2 coexist: (1) during turnover (January, probably at anaerobic niches) and (2) during the collapse of the phytoplankton bloom in late April–May, concomitantly with the denitrification process (Fig. 22.3).

Preliminary molecular studies of samples taken in May 2004 and January 2005, using a combination of primers specific to *Planctomycetes* and/or anammox (Pla 46F/Amx 820R), resulted in few clones of uncultured *Planctomycetes,* anaerobic ammonia oxidizers. Two clones showed as closest relative to *Candidatus Brocadia* and *Candidatus Kuenenia,* indicative of anammox bacteria presence in Lake Kinneret.

The pitfall of the process is the slow growth of the anammox bacteria. The rates of the anammox process, as compared to denitrification, should be studied in the future. Recent findings suggest that anammox bacteria could be mediating DNRA to ammonium in natural ecosystems (Kartal et al. 2007).

DNRA is the direct reduction of nitrate to ammonium. The relative partitioning between denitrification, in which N (as N_2) is lost from the system, and DNRA, in which N (as NH_4) is conserved in the system and may be available to the organisms in the lake, will have an impact on the N budget in Lake Kinneret, and should be studied in the future.

Sulfate reduction is the major mineralization process in Lake Kinneret and sulfide has been accumulating in the hypolimnion of the lake since May. Sulfide is toxic to many bacterial processes, including denitrification, but chemolithoautotrophic bacteria that use reduced sulfur compounds as an electron donor and reduce NO_3^- to NH_4^+ (i.e., coupling of NO_3^- and sulfide) may contribute to preserve N in the lake via the DNRA process (An and Gardner 2002).

22.3 Stratification (Summer–Autumn)

N-assimilation: During the dry summer and autumn, when Lake Kinneret is strongly stratified, nutrient inputs from the watershed are low, and so are hypolimnion contributions of inorganic nitrogen to the epilimnion (Serruya 1978, Chap. 21). From about mid-May–June until December, the nitrogen utilized by phytoplankton is in the form of NH_4^+ or DON, much of which is regenerated, and as atmospheric dinitrogen fixed by filamentous nitrogen-fixing cyanobacteria.

Nitrogen Fixation: It is a process by which nitrogen (N_2) in the atmosphere is assimilated into organic compounds. Microorganisms that can fix nitrogen are prokaryotes (bacteria and archaea) called diazotrophs.

Until 1994, rates of nitrogen fixation in Lake Kinneret were negligible (Bergstein et al. 1981; Cavari 1978). In 1994, the characteristic pattern of phytoplankton assemblage in Lake Kinneret changed when an exceptional bloom of a filamentous nitrogen-fixing cyanobacterium, identified as *Aphanizomenon ovalisporum* (Nostocales), occurred in the lake (Pollingher et al. 1998, Hadas et al. 1999, Sukenik et al. 2012). Another nostocalean species, *Cylindrospermopsis raciborskii,* was observed in the lake for the first time in the summer of 1998 (Zohary 2004; Alster et al. 2010), forming a major summer bloom in 2005 and, since then, co-dominating the summer biota with *A. ovalisporum,* contributing in some years between 60–80 % of the monthly phytoplankton biomass. This shift in the phytoplankton composition since 1994 toward enhanced diazotrophic activity in summer could be linked to changes in climate conditions, and nitrogen availability during the summer cumulatively, supporting the persistence of nitrogen-fixing cyanobacteria (Hadas et al. 2002, 2012; Sukenik et al. 2012; Chap. 12).

In summer and early autumn, low DIN concentrations measured in the epilimnion (Fig. 22.3a) concomitantly with phosphate pulses may be responsible for the stimulation of N_2-fixing cyanobacteria. Specialized cells, heterocysts, capable of fixing atmospheric dinitrogen into combined nitrogen were abundant at the early stages of the bloom, enabling the development of the population under N-limited conditions. The abundance of *A. ovalisporum* heterocysts was severalfold higher

than that of *C. raciborskii*. The ratio of heterocyst biomass to *Aphanizomenon* total biomass was in most cases 2- to 20-fold higher than the ratio in *C. raciborskii. A. ovalisporum* appears later in summer, which may suggest that *A. ovalisporum* is more dependent on N_2 fixation than *C. raciborskii.*

Rates of N_2 fixation in the water column have been monitored since 2001. Fixation usually started in June and reached maximum rates in August or September. Depth profiles of fixation rates during the autumn of 2001 and the summer of 2005 (Fig. 22.5) present the case for *A. ovalisporum* and *C. raciborskii*. Hourly N_2 fixation rates were expressed per unit of chlorophyll and also per heterocyst. Nitrogen fixation occurred in the upper 7 m, with maximal rates ranging between the water surface and 3-m depth. Maximal N_2 fixation equivalent to 2.4 nmol C_2H_4 μg^{-1} chl h^{-1} and 73 fmol C_2H_4 Het^{-1} h^{-1} were measured during the *Aphanizomenon* bloom in 2001, as compared with 3.3 nmol C_2H_4 μg^{-1} chl h^{-1} and 26 fmol C_2H_4 het^{-1} h^{-1} during the *Cylindrospermopsis* bloom in 2005 (Fig. 22.5). These data correspond to maximal N_2 fixation rates of 15.3 and 21.7 mg N_2 m^{-2} day^{-1} in 2001 and 2005, respectively. The threefold higher N_2 fixation by *Aphanizomenon* heterocysts compared with *Cylindrospermopsis* heterocysts may be due to a more efficient supply of carbon substrates by neighboring vegetative cells, from both sides, whereas the terminally located heterocysts of *Cylindrospermopsis* may be substrate limited. Maximal fixation rates of about 2.5 t per lake day^{-1} were recorded in August 2005, whereas in 2001, 2004, and 2009 the highest rates observed in September were about 1.81, 1.66, and 1.05 t per lake day^{-1}, respectively. The contribution of nitrogen fixation to the lake N budget during the summer–autumn period was as little as 0.5 t in 2003 and as much as 123 t in 2005 (Table 22.1, Hadas et al. 2012). During the summer–autumn months of 2001, 2004, 2005, and 2009, Lake Kinneret was provided with "new N," which during these years was between 63 and 150% of summer DIN inflows from the watershed via the Jordan River.

DON uptake: The DON pool is a heterogeneous mixture of compounds that varies widely in space and time within the aquatic environment. DON includes proteins (such as enzymes, modified bacterial wall proteins, dissolved combined and free amino acids, nucleic acids, and humic-like materials (Berman and Bronk 2003). In Lake Constance, dissolved free amino acids and proteins supported 58% of bacterial C and 80% of bacterial N demands (Rosenstock and Simon 2001). In Lake Kinneret, urea was found to be a potential N source for phytoplankton during the *Peridinium* bloom period when ammonium concentrations were low. Several non-axenic Lake Kinneret algal cultures grew successfully on guanine, hypoxanthine, glucosamine, and urea as a sole N source. These DON compounds were rapidly degraded to urea and/or NH_4^+ and could be easily used by phytoplankton and bacteria (Berman and Chava 1999). Urea was proposed as a major N source for freshwater *Synechococcus* as well as for *A. ovalisporum* isolated from Lake Kinneret and grown in non-axenic cultures (Berman and Chava 1999). Although urea was the sole N source for *A. ovalisporum* in these experiments, the cleavage of urea to ammonium by the bacteria present in the experimental flasks could not be excluded.

The capacity of some algal species to exploit DON compounds as sources of N suggested that specific organic N substrates available in any given environment

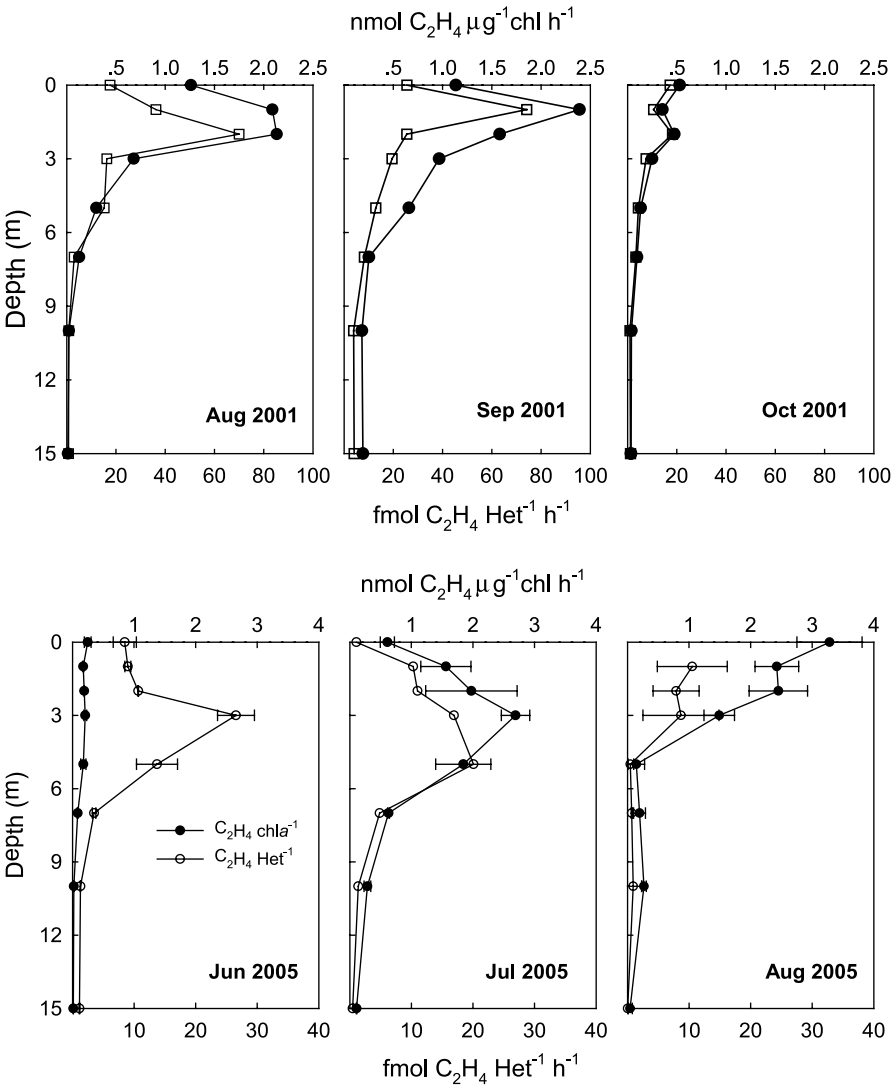

Fig. 22.5 Depth profiles of rates of N_2 fixation measured in Lake Kinneret during summer bloom events in 2001 (*upper panels*) and 2005 (*lower panels*). Hourly N_2 fixation rates are presented as C_2H_4 reduction rates per unit of chlorophyll and per heterocyst. (Reproduced from Hadas et al. 2012, with permission from Wiley Publ.)

could influence the species composition of the phytoplankton community (Paerl 1997; Seitzinger and Sanders 1999; Berman and Chava 1999). Sources of DON in Lake Kinneret could be both allochthonous and autochthonous. The former includes the Jordan River and atmospheric deposition. Autochthonous sources came from phytoplankton and bacteria exudation, from bloom decomposition, micro- and

Table 22.1 The contributions of nitrogen fixation (tons per lake) to the Lake Kinneret budget during summer–autumn (June–October) 2001–2012

Year	2001	2002	2003	2004	2005	2006	2007	2008	2009	2010	2011	2012
N_2 fixed, tons lake^{-1}	97.5	12.5	0.5	83.4	123	35.1	1.6	59	81.1	21	6.9	79

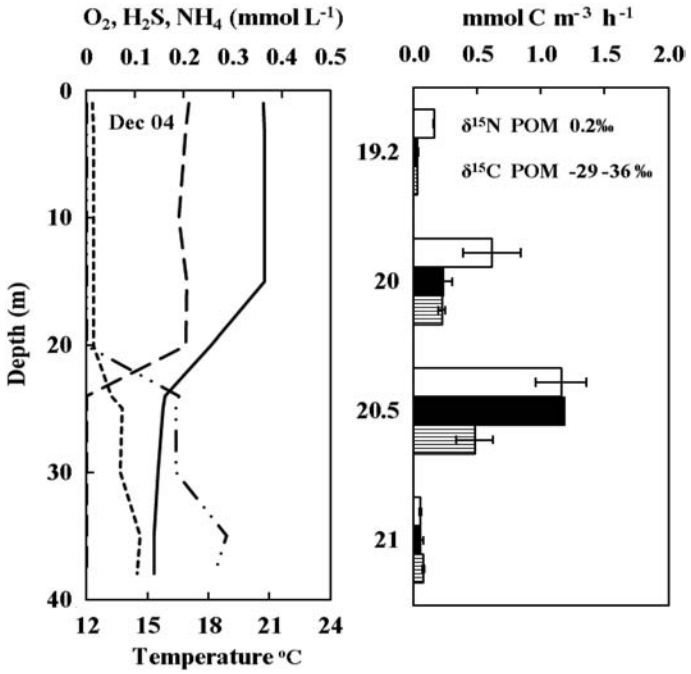

Fig. 22.6 Rates of photosynthetic (□), dark chemosynthetic carbon fixation (■), dark chemosynthetic carbon fixation with the addition of the inhibitor N-serve(▤) (*right panel*), and depth profiles of temperature (——), dissolved oxygen (– – –), sulfide (–··–) and ammonia (·····) (*left panel*) in Lake Kinneret, December 2004

macrozooplankton grazing and excretion, and from viral lysis. In many freshwater systems, anthropogenic sources are responsible for significant inputs of DON (Seitzinger and Sanders 1997, 1999). DON can be also adsorbed to very small particles such as transparent exopolymer particles (TEP) (Alldredge et al. 1993) and be utilized by particle-associated bacteria and protists.

Nitrification at the chemocline in the pelagic waters in autumn: Strong thermal stratification during autumn forms a metalimnic layer characterized by steep gradients of temperature, sulfide, ammonium, and oxygen, below the euphotic zone, enabling the proliferation of chemoautotrophic bacteria (Fig. 22.6). Intensive chemosynthetic carbon fixation due to sulfide oxidizers was measured. Using inhibitors like N-serve which blocks the first step of the nitrification process, i.e., AOB,

Table 22.2 Carbon fixation (mmol C m^{-3} h^{-1}) at the sediment–water interface, along a transect from the Kinneret Limnological Laboratory to Sta. F (locations in Fig. 1.1, Chap. 1), Lake Kinneret, October 2004

Station maximal depth (m)	Light fixation	Dark fixation	Dark + N-serve
15	1.62	0.72	0.22
17	0.96	0.74	0.2
18.8	–	1.96	1.96

one can differentiate between the two groups of sulfide and ammonia oxidizers. Because of sampling limitations, we could not record chemosynthetic activity of AOB's in the past (Hadas et al. 2001). Improving sampling procedures revealed that the upper part of the metalimnetic layer is inhabited by AOB. Chemosynthetic dark carbon fixation dropped from 1.2 to 0.48 mmol C m^{-3} h^{-1} after N-serve addition in December 2004, indicating nitrification processes (Fig. 22.6). *Nitrosospira* strains were identified in samples taken from the metalimnetic layer during the stable stratification period in autumn (Junier et al. 2008).

Metalimnetic Deepening The rise of epilimnetic NH_4^+ concentrations in November–December was mainly due to input from the hypolimnion and sediments as the thermocline deepens. With overturn, in late December or early January, surface water NH_4^+ concentrations reach their annual peak. At about the same time or shortly afterwards, winter flooding from the watershed lead to a dramatic rise in NO_3^- levels (Fig. 22.3).

Nitrification (ammonium oxidation) at the sediment water interface: Although the major part of the ammonia oxidation occurs during overturn in winter (December–January), chemosynthetic activity due to the activity of AOB was recorded at all defined chemoclines in the lake, year-round. Besides the upper metalimnion in the pelagic water column in autumn (see above), ammonia oxidation (nitrification) activity was recorded at the sediment–water interface in the littoral zone at all times of the year.

Overlying water from sediment cores (10 cm of the water above the sediments), were taken along a transect (15, 17, and 18.8 m maximal depth). Chemoautotrophic fixation in the overlying water reached rates of 0.72 and 0.74 mmol C m^{-3} h^{-1} at 15 and 17 m, respectively (Table 22.2). The rate of carbon fixation was inhibited by about 70 % as result of N-serve addition, indicating ammonia oxidizers activity. At the deeper station (18.8 m), which had an anaerobic hypolimnion rich in ammonium and H_2S, no nitrification was observed. Although some oxygen reached this layer, due to turbulence, the presence of H_2S excluded ammonia oxidation since sulfide is toxic to the process. Nevertheless, high dark carbon fixation (1.96 mmol C m^{-3} h^{-1}) was recorded at this depth due to sulfide oxidation (Table 22.2).

Ammonia oxidizers play a minor role in the carbon cycle at these regions and are restricted to the interface layers where oxygen and ammonium coexist and sulfide presence is excluded.

22.4 Seasonal Variations in $\delta^{15}N$ of Particulate Organic Matter

The nitrogen and carbon isotopic composition of particulate organic matter (POM) in aquatic environments reflects and integrates the influence of biogeochemical processes in the water column and sediments including primary production, redox-sensitive nitrogen transformations, and carbonate chemistry. Measurements of the natural distribution of stable isotopes are valuable in situ indicators of N and C elemental cycling in the ecosystems (Bernasconi et al. 1997; Kendall et al. 2001; Altabet 2006). The nitrogen isotopic composition ($\delta^{15}N$) of POM is influenced by the isotopic composition of DIN sources for phytoplankton, isotopic fractionation during partial utilization of these sources, as well as transfer to higher trophic levels.

Large temporal variations in the $\delta^{15}N$ of POM and of DIN species in Lake Kinneret occurred in response to dominant nitrogen cycle processes. The lowest $\delta^{15}N$ POM values (−5.5‰) were observed in early winter, a consequence of isotopic fractionation by chemoautotrophic microbial NH_4^+ assimilation and during the first phase of the nitrification period, by NH_4^+ oxidizers. Nitrification itself was strongly fractionating, producing ^{15}N-depleted NO_3^- and enriching the water column with ^{15}N NH_4^+. The phytoplankton bloom period in later winter and early spring resulted in a 15–30‰ jump in $\delta^{15}N$ POM due to assimilation of high $\delta^{15}N$ NH_4^+. Maximal $\delta^{15}N$ POM values were measured during the algal blooms of *Peridinium gatunense* in 2004 and *Mougeotia* sp. *and Microcystis* sp. in 2005 (Fig. 22.7). Toward the end of the blooms in mid-to-late spring, $\delta^{15}N$ POM values decreased to values similar to $\delta^{15}N$ for NO_3^- (8–12‰), indicating a switch to this DIN source. NO_3^- assimilation into POM appeared to occur without isotopic fractionation. The $\delta^{15}N$ POM at 3-m depth in 2005 was 9.9‰ as compared to the isolated *Mougeotia* $\delta^{15}N$ of 10.6‰. In 2004 when *Peridinium gatunense* bloomed, a similar switch from NH_4^+ to NO_3^- utilization occurred as *Peridinium* is capable of nitrate uptake when ammonia is limiting (McCarthy et al. 1982; Sherr et al. 1982; Berman et al. 1984). The denitrification period with NO_3^- removal in the newly suboxic hypolimnion in late spring showed increased $\delta^{15}NO_3^-$ values in the residual NO_3^-, i.e., NO_3^- has become ^{15}N-enriched due to denitrification. Complete consumption of NO_3^- by denitrification was reflected by a lack of increase in $\delta^{15}N$ POM in the epilimnion at this time, since the thermocline was an effective barrier to the upward transport of hypolimnion enriched NO_3^-. The suboxic hypolimnion, with chemoautotrophic activity of sulfide-oxidizing bacteria, resulted in decreased $\delta^{15}N$ POM, opposite to the expected effect of POM degradation (Figs. 22.4c and 22.7).

In late summer and early autumn during the bloom of the filamentous N_2-fixing cyanobacteria, *A. ovalisporum* and *C. raciborskii,* low $\delta^{15}N$ POM was found (3.3‰) in the epilimnion, indicative of atmospheric N_2 fixation. The $\delta^{15}N$-DON isotopic signature at this time was significantly higher, 8–12‰, suggesting a phytoplankton source from earlier in the seasonal cycle. C: N ratios dropped during the blooms of *Aphanizomenon and Cylindrospermopsis* indicating release from N stress due to N_2 fixation. N_2 fixation was thus the most likely cause for decreasing

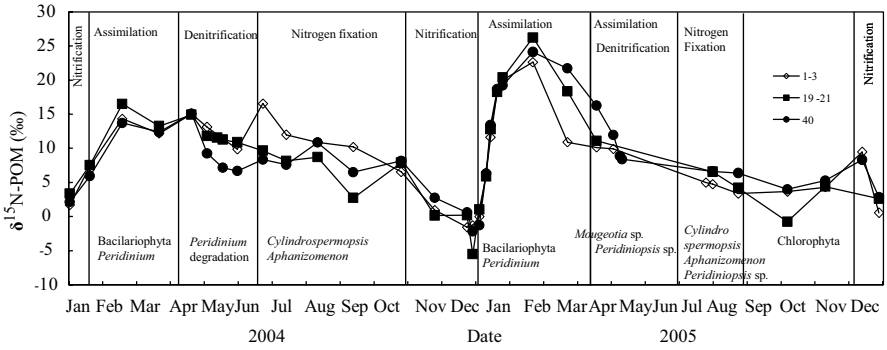

Fig. 22.7 Time series of $\delta^{15}N$ POM at different depths (1–3 m, 19–21 m, 38–40 m) at Sta. A, Lake Kinneret, 2004–2005. (Reprinted from Hadas et al. 2009, Copyright 2014 by the Association for the Sciences of Limnology and Oceanography, Inc.)

of $\delta^{15}N$-POM in later summer and autumn in Lake Kinneret. In addition, *A. ovalisporum* isolated from the first bloom in autumn 1994 had an average $\delta^{15}N$ value of 0.3 ‰, indicating N_2 fixation.

During autumn when the chemocline was sharp and deepened below the euphotic zone, a drop of 6 ‰ in $\delta^{15}N$ POM could be observed within the chemocline, probably due to isotopic fractionation during NH_4^+ uptake and chemoautotrophic H_2S oxidation.

Low $\delta^{15}N$ POM as well as $\delta^{13}C$ POM values were measured at all chemolines, at the pelagic oxycline/thermocline and at the sediment–water interface, indicative of nitrification and sulfide oxidation processes (Sect. 24.2 and above).

In conclusion, the microbial processes involved in the nitrogen cycle in Lake Kinneret are influenced and linked to climate changes and nitrogen availability. Since 1994, an increase in the temperature of the epilimnetic water column in summer, and to some extent a greater frequency of lower summer wind speed events affected water turbulence and water column stratification, thus providing better physical conditions favorable for cyanobacteria.

Due to consecutive dry years and less water entering Lake Kinneret via the Jordan River, less nitrate entered the lake in winter, with possible impact on the development and character of phytoplankton blooms in the lake. The early decrease in DIN sources at the beginning of summer shifts the system to nitrogen fixation with blooms of nitrogen-fixing cyanobacteria.

The isotopic composition of $\delta^{15}N$ POM reflects the biogeochemical processes within the nitrogen cycle.

References

Alldredge AL, Passow U, Logan BE (1993) The abundance and significance of a class of large, transparent organic particles in the ocean. Deep Sea Res 40:1131–1140

Altabet MA (2006) Isotopic tracers of the marine nitrogen cycle. In: Volkman J (ed) Marine organic matter: chemical and biological markers. The handbook of environmental chemistry. Springer, Berlin

Alster A, Kaplan-Levy R, Sukenik A, Zohary T (2010) Morphology and phylogeny of a non-toxic invasive *Cylindrospermopsis raciborskii* from a Mediterranean Lake. Hydrobiologia 639:115–128

An S, Gardner WS (2002) Dissimilatory nitrate reduction to ammonium (DNRA) as a nitrogen link, versus denitrification as a sink in a shallow estuary (Laguna Madre/Baffin Bay, Texas). Mar Ecol Prog Ser 237:41–50

Bergstein T, Henis Y, Cavari BZ (1981) Nitrogen fixation by the photosynthetic bacterium *Chlorobium phaeobacteroides* from Lake Kinneret. Appl Environ Microbiol 41:542–544

Berman T, Bronk D (2003) Dissolved organic nitrogen: a dynamic participant in aquatic ecosystems. Aquat Microb Ecol 31:279–305

Berman T, Chava S (1999) Algal growth on organic compounds as nitrogen sources. J Plankton Res 21:1423–1437

Berman T, Sherr BF, Sherr E, Wynne D, McCarthy JJ (1984) The characteristics of ammonium and nitrate uptake by phytoplankton in Lake Kinneret. Limnol Oceanogr 29:287–297

Bernasconi SM, Barbiri A, Simona M (1997) Carbon and nitrogen isotope variations in sedimenting organic matter in Lake Lugano. Limnol Oceanogr 42:1755–1765

Cavari BZ (1977) Nitrification potential and factors governing the rate of nitrification in Lake Kinneret. Oikos 28:285–290

Cavari BZ (1978) Bacteria of the nitrogen cycle. In: Serruya C (ed) Lake Kinneret monographiae, Junk, The Hague, pp 314–317

Cavari BZ, Phelps G (1977) Denitrification in Lake Kinneret in the presence of oxygen. Freshw Biol 7:385–391

Dalsgaard T, Canfield DE, Petersen J, Thamdrup B, Acuna-Gonzalez J (2003) N2 production by the anammox reaction in the anoxic water column of Golfo Dulce, Costa Rica. Nature 422:606–608

Hadas O, Pinkas R, Albert-Diez C, Bloem J, Cappenberg T, Berman T (1990) The effect of detrital addition on the development of nanoflagellates and bacteria in Lake Kinneret. J Plankton Res 12:185–199

Hadas O, Pinkas R, Delphine E, Vardi A, Kaplan A, Sukenik A (1999) Limnological and ecophysiological aspects of *Aphanizomenon ovalisporum* bloom in Lake Kinneret, Israel. J Plankton Res 21:1439–1453

Hadas O, Pinkas R, Erez J (2001) High chemoautotrophic primary production in Lake Kinneret, Israel-a neglected link in the C cycle of the lake. Limnol Oceanogr 46:1968–1976

Hadas O, Pinkas R, Malinsky-Rushansky N, Shalev-Alon G, Delphine E, Berner , Sukenik A, Kaplan A (2002) Physiological variables determined under laboratory conditions may explain the bloom of *Aphanizomenon ovalisporum* in Lake Kinneret. Eur J Phycol 37:259–267

Hadas O, Altabet MA, Agnihotri R (2009) Seasonally varying nitrogen isotope biogeochemistry of particulate organic matter (POM) in Lake Kinneret, Israel. Limnol Oceanogr 54:75–85

Hadas O, Pinkas R, Malinsky-Rushansky N, Nishri A, Kaplan A, Rimmer A, Sukenik A (2012) Appearance and establishment of diazotrophic cyanobacteria in Lake Kinneret, Israel. Freshw Biol 57:1214–1227

Hochman A (1982) Studies of nitrate reductase in the fresh water dinoflagellate *Peridinium cinctum*. Arch Microbiol 133:62–65

Hochman A, Nissany A, Wynne D, Kaplan B, Berman T (1986) Nitrate reductase: an improved assay method for phytoplankton. J Plankton Res 8:385–392

Junier P, Kim O, Hadas O, Imhoff JF, Witzel K-P (2008) PCR primer selectivity and phylogenetic specificity evaluated using amplification of 16S rRNA genes from beta proteobacterial ammonia-oxidizing bacteria (AOB) in environmental samples. Appl Environ Microbiol 74:5231–5236

Kartal B, Kuypers MM, Lavik G, Shalk J, Op denCHJ, Jetten MS, Strous M (2007) Anammox bacteria disguised as denitrifiers: nitrate reduction to dinitrogen gas via nitrite and ammonium. Environ Microbiol 9:635–642

Kendall C, Silva SR, Kelly VJ (2001) Carbon and nitrogen isotopic compositions of particulate organic matter in four large river systems across the United States. Hydrol Process 15:1301–1346

Kuenen JG (2008) Anammox bacteria: from discovery to application. Nat Rev Microbiol 6:320–326

Kuypers MM, Sliekers AO, Lavik G et al (2003) Anaerobic ammonium oxidation by anammox bacteria in the Black Sea. Nature 422:608–611

McCarthy JJ, Wynne D, Berman T (1982) The uptake of nitrogenous nutrients by Lake Kinneret microplankton. Limnol Oceanogr 27:673–680

Penton CR, Devol AH, Tiedje JM (2006) Molecular evidence for the broad distribution of anaerobic ammonium-oxidizing bacteria in freshwater and marine sediments. Appl Environ Microbiol 72:6829–6832

Paerl HW (1997) Coastal eutrophication and harmful algal blooms: importance of atmospheric deposition and groundwater as 'new' nitrogen and other nutrient sources. Limnol Oceanogr 42:1154–1165

Pollingher U, Hadas O, Yacobi YZ, Zohary T, Berman T (1998) *Aphanizomenon ovalisporum* (Forti) in Lake Kinneret (Israel). J Plankton Res 20:1321–1339

Rosenstock B, Simon M (2001) Sources and sinks of dissolved free amino acids and protein in a large and deep mesotrophic lake. Limnol Oceanogr 46:644–654

Schubert CJ, Durisch-Kaiser E, Wehrli B, Thamdrup B, Lam P, Kuypers MM (2006) Anaerobic ammonium oxidation in a tropical freshwater system (Lake Tanganyika). Environ Microbiol 8:1857–1863

Seitzinger SP, Sanders R (1997) Contribution of dissolved organic nitrogen from rivers to estuarine eutrophication. Mar Ecol Prog Ser 159:1–12

Seitzinger SP, Sanders R (1999) Atmospheric inputs of dissolved organic nitrogen stimulate estuarine bacteria and phytoplankton. Limnol Oceanogr 44:721–730

Serruya C (1978) Water chemistry. In: Serruya C (ed) Lake Kinneret, Junk, The Hague, pp 185–204

Serruya C, Gophen M, Pollingher U (1980) Lake Kinneret: carbon flow patterns and ecosystem management. Arch Hydrobiol 88:265–302

Sherr BF, Sherr EB, Berman T (1983) Grazing, growth, and ammonium excretion rates of a heterotrophic microflagellate fed with four species of bacteria. Appl Environ Microbiol 45:1196–1201

Sherr BF, Sherr EB, Berman T, McCarthy JJ (1982) Differences in nitrate and ammonia uptake among components of a phytoplankton population. J Plankton Res 4:961–965

Sukenik A, Hadas O, Kaplan A, Quesada A (2012) Invasion of Nostocales (cyanobacteria) to subtropical and temperate freshwater lakes-physiological, regional, and global driving forces. Front Microbiol 3:86

Trimmer M, Nicholls JC, Deflandre B (2003) Anaerobic ammonium oxidation measured in sediments along the Thames Estuary, United Kingdom. Appl Environ Microbiol 69:6447–6454

Wynne D, Berman T (1990) The influence of environmental factors on nitrate reductase activity in freshwater phytoplankton. Hydrobiologia 194:235–245

Zohary T (2004) Changes to the phytoplankton assemblage of Lake Kinneret after decades of a predictable, repetitive pattern. Freshw Biol 49:1355–1371

Zohary T, Gude H, Pollingher U, Kaplan B, Pinkas R, Hadas O (2000) The role of nutrients in decomposition of a *Thecate dinoflagellate*. Limnol Oceanogr 45:123–130

Chapter 23
Dissolved Inorganic Carbon (DIC)

Ami Nishri and Mariana Stiller

Abstract Various factors control the seasonal succession of the phytoplankton community in Lake Kinneret. One such factor is whether they are CO_2 or HCO_3^- users. In spring, CO_2-only users such as the dinoflagellate *Peridinium gatunense* often predominate and develop a bloom despite of extremely low levels of ambient aqueous CO_2 and its rather poor carbon-concentrating mechanism. Based on seasonal dynamics of calcium and carbonate concentrations, mass balance considerations, and the relationships between planktonic $\delta^{13}C$ and aqueous CO_2 ($\delta^{13}C$), we claim that massive precipitation of calcite which occurs concomitant with the bloom supplies the $CO_{2(aq)}$ needed for the algae to develop and maintain the bloom. Besides riverine inflows that supply most HCO_3^-, Ca^{2+}, P, N, Se(IV), and perhaps also picoplankton (that seem to serve as nuclei for calcite crystal growth) in the spring, the prevalence of relatively high temperatures and low winds also supports the bloom. The low wind restricts gas exchange and facilitates the gradual accumulated deficiency in $CO_{2(aq)}$ in surface water leading to higher pH and a raise in $\Omega_{calcite}$ to an extent that induces massive calcite precipitation. By the end of this season, the capacity of the lake surface water to precipitate calcite is almost exhausted and bicarbonate users take over.

About one third of the autochthonous calcite precipitating from the epilimnion dissolves in the lower water mass (LWM), which is undersaturated with respect to this mineral. However, only 22.5 % of the seasonal accumulation of dissolved inorganic carbon (DIC; ~90 % HCO_3^-) in the LWM originates from calcite dissolution while 77.5 % originates through direct biodegradation processes under initially oxic and eventually anoxic conditions (mediated mostly by bacterial SO_4 reduction) and from the underlying bed sediments through methanogenesis. A potential sink of CO_2 and perhaps also of isotopic fractionation in the LWM may be its uptake by anammox organisms during the sub-oxic stage (Chap. 20). The almost steady $\delta^{13}C_{(DIC)}$ of approximately between 8 and 9 ‰ in the LWM approached in the anoxic

A. Nishri (✉)
The Yigal Allon Kinneret Limnological Laboratory, Israel Oceanographic & Limnological Research, P.O. Box 447, 14950 Migdal, Israel
e-mail: nishri@ocean.org.il

M. Stiller
Ha'em 3 St., 7524014, Rishon Leziyyon, Israel
e-mail: stiller@netvision.net.il

T. Zohary et al. (eds.), *Lake Kinneret, Ecology and Management,* Aquatic Ecology Series 6,
DOI 10.1007/978-94-017-8944-8_23,

stage represents the relative contribution of each of these pools as well as of the primary DIC pool in this layer before stratification commences.

Keywords Calcite · Dissolved inorganic carbon · CO_2 user · *Peridinium gatunense* · $\delta^{13}C$ · Isotopic fractionation

23.1 Introduction

Various aspects of dissolved inorganic carbon (DIC) in Lake Kinneret have been studied over the past 40 years. Perhaps the primary motivation for these studies originated from the question: What are the sources of inorganic C that support the high primary production during the spring bloom? Typically in the spring, the pH of the surface water in this hard water lake increases above 9.0 and concomitantly there is a decline in $CO_{2(aq)}$ to low levels (range of 1–3 μM) that seemed insufficient to support the respective seasonally high primary production. In the case of the predominant bloom species *Peridinium gatunense* (hence *Peridinium*), active transport of bicarbonate can be ruled out because this dinoflagellate is known to be a CO_2 rather than a HCO_3^- consumer (Berman-Frank et al. 1994). Moreover, Vardi et al. (1999) showed experimentally that CO_2 limitation causes the collapse of the *Peridinium* bloom. A relative advantage of this dinoflagellate with respect to the low ambient CO_2 levels might be its carbon-concentrating mechanism (CCM) of which the activity is induced by the low external $CO_{2(aq)}$. The CCM facilitates the maintenance of an internal carbon pool (C_i- which is made of both HCO_3^- and CO_2) 60 to 80 times higher than that of external $CO_{2(aq)}$ concentration, thus allowing for some photosynthesis to proceed despite low external $CO_{2(aq)}$ levels (Berman et al. 1998). The still unresolved issue of the identification of the primary source of carbon for algal photosynthesis in Lake Kinneret during the spring is discussed in the present chapter. Once identified, we further make an attempt to define what controls the size of the spring bloom biomass in the lake. Finally, the somewhat scientifically neglected issue of DIC cycling in the lake's lower water mass (LWM) is also presented.

23.2 Potential Sources of Carbon to the Euphotic Layer

Several processes affect DIC concentrations in the trophogenic layer of Lake Kinneret. In addition to the well-known impacts of photosynthesis (leads to higher pH and lower $CO_{2(aq)}$) and respiration (the opposite), other processes include partial mixing with the CO_2-rich LWM water, CO_2 gas exchange with the atmosphere, and calcite precipitation and dissolution. The impacts of the latter three processes are addressed below.

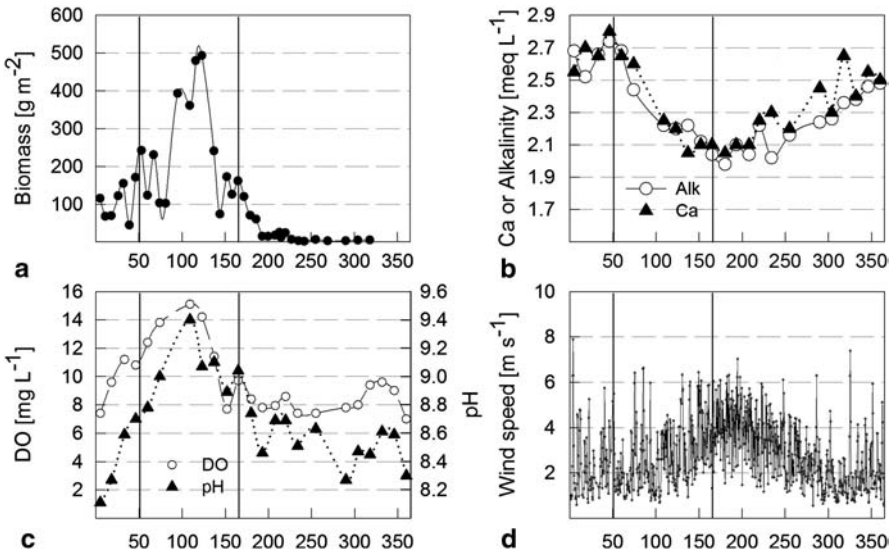

Fig. 23.1 The annual pattern of Lake Kinneret parameters measured during 1998 at the pelagic Sta. A (source: Lake Kinneret Date Base). **a** Weekly or fortnightly measured depth-integrated phytoplankton wet weight biomass (g m^{-2}). **b** Fortnightly measured alkalinity and Ca^{2+} at 1-m depth. **c** Weekly pH and dissolved oxygen at 1-m depth. **d** Wind speed (6-h averages based on 10-min measurements) measured at 3.5 m above the water surface on a pole ~1 km offshore from the Kinneret Limnological Laboratory. The two *vertical lines* mark the bloom period, spanning between day 50 and day 170. The peak of the bloom appears on day 110. Note that the seasonal rise in wind speed from daily average of ~2.8 m s^{-1} occurs also at day 110. The bloom ends when wind velocity acquires typical summer daily averages of ~6 m s^{-1} (peak afternoon wind velocities may then be >12 m s^{-1}) and when calcite precipitation (if any) is insignificant

23.2.1 Seasonal Stratification and the LWM

The main two layers identified in Lake Kinneret during the stratified period are the oxic, relatively warm epilimnion and the layer below the thermocline, referred to as the LWM, which is colder and most of the time anoxic. The onset of stratification typically occurs in mid-March; from then on, the seasonal thermocline–chemocline deepens gradually from ~13 m in spring to ~19 m in September and further to ~22 m in November. At the onset of stratification, winds are usually mild (Fig. 23.1d), and the activity of internal waves (seiches) is weak. The bloom of *Peridinium* in Lake Kinneret often starts to develop prior to the onset of thermal stratification, but most of its growth takes place when stratification is already established and therefore CO_2 transfer from the LWM to the euphotic layer is restricted (Fig. 23.1a). Later in summer, strong westerly winds induce extensive internal seiching (Chap. 9), which leads to some mixing between layers in the littoral zones. This process may supply the epilimnion with some CO_2 from the relatively enriched LWM layer. In autumn, when the wind weakens again, the seasonal drop in air temperature induces buoy-

ancy mixing and therefore fast deepening of the thermocline and consequently a flux of CO_2 from the LWM to the euphotic layer.

The LWM may be subdivided into two sub-layers: the benthic boundary layer (BBL) extending between the pelagic lake floor (~40-m depth) to ~30-m depth and the hypolimnion which overlies the BBL and is sandwiched between it and the seasonal thermocline (Chaps. 9, 20, 21). These two sub-layers are distinguished by a weak but still detectable temperature difference (Lemckert et al. 2004). In summer, the BBL is characterized by significant vertical turbulence induced by seiche activity (Chap. 9), which leads to vertical homogenization of its properties, including its temperature and solute concentrations (Nishri et al. 2000). In contrast, the hypolimnion above, between ~29- and ~15-m depth, is characterized by significantly smaller vertical turbulence, as indicated by exponentially shaped vertical profiles of temperature and solutes such as NH_4^{2+}. Thus, the hypolimnion is a relatively quiescent sub-layer characterized by a laminar flow regime, which is governed by *horizontal mixing* (Lamckert et al. 2004). These two sub-layers also differ in the intensity of decomposition of organic matter taking place within each of them. As indicated by the rate of removal of dissolved oxygen (DO) and by the rate of denitrification (Chap. 21), the BBL is the major site for biodegradation (Nishri et al. 2000; Rimmer et al. 2006) while the hypolimnion water sub-layer exhibits little evidence for biodegradation (Nishri et al. 2011).

23.2.2 CO_2 Gas Exchange Fluxes Through the Water–Air Interface

A potential primary source of CO_2 to algae is through gas exchange when atmospheric partial pressure of CO_2 (pCO_2) is larger than pCO_2 in water. Physicochemical equilibrium implies that $pCO_{2(air)} = pCO_{2(aq)}$ in the water and isotopic equilibrium implies that $\delta^{13}_{CO2(air)} \approx \delta^{13}_{CO2(aq)}$. Stiller and Nissenbaum (1999) have examined the gas exchange flux in Lake Kinneret in two ways. First, by gaining a rough idea on flux direction by examining seasonal deviations of Lake Kinneret surface water from equilibrium with CO_2 in air. They found that thermodynamic equilibrium was rarely attained and in most cases $pCO_{2(aq)}$ was either much smaller (in spring) or much higher (in winter) than pCO_2 in air. They estimated the CO_2 gas exchange flux by using a conventional stagnant boundary layer model in which its thickness (in μm) is affected by wind velocity and which includes a chemical enhancement factor for CO_2. They estimated that in spring, despite the high pH (Fig. 23.1c), which is expected to raise chemical enhancement, the CO_2 gas *invasion* (adsorption by the lake) was rather low at ~6.7 mmol CO_2 m^{-2} day^{-1}. In winter, however, pCO_2 in the mixed water column is relatively high due to the introduction of CO_2-enriched hypolimnetic water during the mixing process. Wind velocity is then sufficient for gas *evasion* (release from the lake) to be an order of magnitude higher. Stiller and Nissenbaum's (1999) conclusion regarding the sluggish gas exchange in spring is supported by the observation of low wind speeds in that season, restricting wind

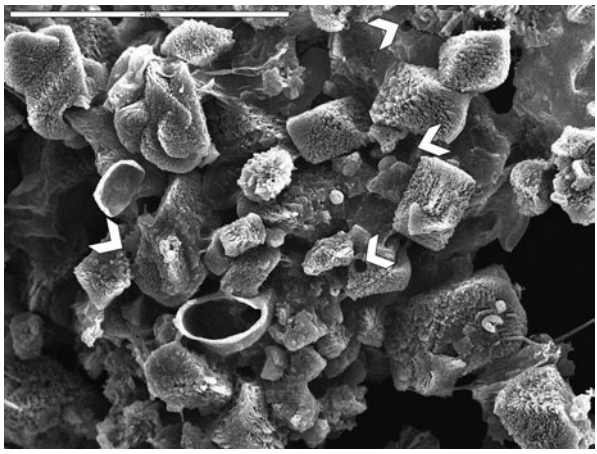

Fig. 23.2 Scanning electron microscope photo of calcite crystals collected in spring 2002 by a sediment trap deployed at Sta. A in the LWM of Lake Kinneret. Crystal sizes vary between 10 and 25 μm. Note the dissolution pits that cover the surface of the crystals as well as rounded cavities (1–2 μm: *white arrows*) in the middle of some crystals, possibly representing degraded picoplankton cells

induced exchange. Further support is derived from the similarity between surface water and air temperature at that time (Fig. 1.3 in Chap. 1) that reduces surface water convective exchange. Moreover, in this season, surface water DO saturation levels (Fig. 23.1c) may remain over 200% for relatively lengthy durations of up to a few weeks, having day–night variations of less than 15%. Assuming typical primary production (^{14}C method) during the spring period of 230 mmol C m^{-2} day^{-1} (Sect. 24.1), it is estimated that CO_2 invasion in spring may provide only ~3% of the daily photosynthetic C requirement. Thus, for strict CO_2-only users such as *Peridinium,* other processes probably control carbon availability.

23.2.3 Calcite Precipitation

Between 50 and 60% of Lake Kinneret pelagic bed sediments, and even a higher percentage of the sediments in the littoral zone, consist of calcite (Serruya 1978; Dubowski et al. 2003). This mineral is mostly autochthonous, as indicated from Sr/Ca content of carbonates in the pelagic bed sediments (Katz and Nishri 2013; Nishri unpublished). In spring, calcite crystals were identified microscopically in sediment trap material (Fig. 23.2), and their sedimentation fluxes ranged between 10 and 20 g m^{-2} day^{-1} (Koren 1994; Koren and Ostrovsky 2009). These spring fluxes are five to tenfold larger than the respective fluxes measured between June and December (~2 g m^{-2} day^{-1}).

The multiannual (2001–2011) averaged seasonal concentration of Ca^{2+} and alkalinity in the epilimnion and in the BBL (Fig. 23.3a, b) shows a simultaneous and practically identical drop in epilimnetic levels of both solutes between February and June, of ~0.7 meq L^{-1}. This again suggests massive calcite precipitation, which is estimated at ~80,000 t of $CaCO_3$(s), lake wide. Summer and fall are however characterized by an increase in the surface water concentration of alkalinity and Ca^{2+}.

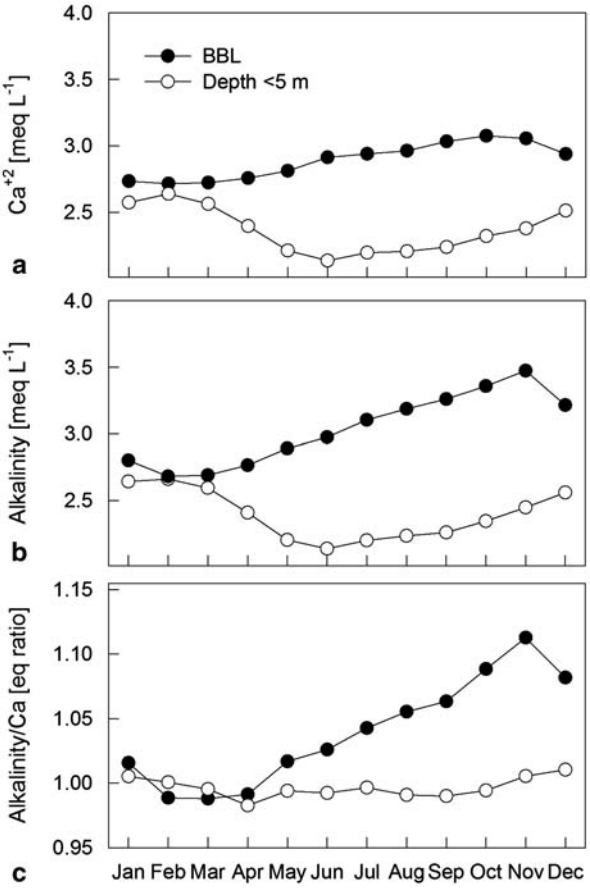

Fig. 23.3 Multiannual (2001–2011) monthly averages of **a** Ca^{2+} and **b** alkalinity for the upper 0–10-m layer (*empty circles*) and the lower > 30-m layer (Benthic Boundary Layer (*BBL*): *filled circles*), and **c** the equivalent ratio Alk/Ca for those layers

Even if some autochthonous calcite is formed during these seasons, its potential impact on epilimnetic levels of both solutes is negligible and masked by the seasonal prominent rise. This summer rise in alkalinity and Ca^{2+} in the growing epilimnion is due to: (1) enhanced seasonal evaporation; (2) continuous inflow of $CaCl_2$ brines from submerged littoral sources, which are characterized by a high Ca/HCO_3 molar ratio > 1 (Kolodni et al. 1999); and (3) mixing of HCO_3^- and Ca^{2+}-enriched LWM water with Ca/HCO_3^- molar ratio < 1 (see for instance, the November epilimnetic value in Fig. 23.3 c). Despite Koren's (1994) finding that some calcite accumulates in sediment traps deployed at the LWM during summer–fall, it is unclear whether it was formed at that time or whether it was resuspended from littoral areas or possibly its origin was calcite in dust (Nishri et al 2005). Considering these arguments, our results further support the conclusion given by Katz and Nishri (2013) that calcite either does not form in summer–fall or that its precipitation rates are very low.

In the LWM, however, we have clear evidence from solute chemical data that calcite dissolves over most of the stratified period (March–November) as the con-

centration of Ca^{2+} increases over time (Fig. 23.3). Multiplying the rise in Ca^{2+} in the LWM by its volume, the dissolution flux is estimated at ~25,000 t $CaCO_3$(s) $year^{-1}$. The difference of ~55,000 t between the spring time autochthonous calcite precipitation and annual dissolution in the LWM is assumed to represent the annual burial of calcite, which forms between 50 and 60 % of the dry weight of pelagic bed sediments. The percentage of $CaCO_3$ in the bed sediments and water column budgets of Ca^{2+} and alkalinity are basically the reason for claiming that bulk sediment sedimentation in this lake is about 100,000 t $year^{-1}$.

From a purely physicochemical perspective, calcite should precipitate from solution only when the degree of solution saturation with respect to this mineral $\Omega_{calcite} \geq 1$, and dissolve only when $\Omega_{calcite} < 1.0$. $\Omega_{calcite} = \mathbf{IAP}_{calcite} / Ksp_{(calcite)}$, where **IAP** represents the ion activity product of Ca^{2+} and CO_3^{-2} and $Ksp_{(calcite)}$ is the thermodynamic solubility constant. $Ksp_{(calcite)}$ is temperature dependent and decreases at higher temperatures. Hence, if only for the seasonal temperature rise of surface water, calcite precipitation is more likely to occur in spring and summer than in winter. In Lake Kinneret during the spring–early summer, both calcite precipitation and enhanced primary production co-occur (Fig. 23.1a, b). Primary producers, through the assimilation of $CO_{2(aq)}$, induce a shift in carbonate equilibrium towards raising the pH (Kelts and Hsui 1978) and this in turn raises $\mathbf{\Omega}_{(calcite)}$, thus increasing the probability for calcite precipitation. However, besides the prerequisite that $\mathbf{\Omega}_{calcite}$ should be ≥ 1.0, there are additional factors that may control calcite precipitation. Some studies discuss the necessity of having calcite seed crystals in the solution before the initiation of crystallization. Furthermore, crystallization will begin only at some critical value of supersaturation, because the formation energy must be exceeded before new-phase calcite precipitates (Raidt and Koschel 1988). The nature of efficient nuclei of crystallization is still unclear. Rounded holes at the center of lacustrine calcite crystals were suggested by Dittrich et al. (2004) and Dittrich and Obst (2004) to have previously contained picocyanobacterial cells, which may have induced crystallization. Similar rounded cavities with a diameter of ~2 μm are observed in the partially dissolved Lake Kinneret calcite crystals examined by a scanning electron microscope (Fig. 23.2). In Lake Kinneret during the winter, the predominant picophytoplankton ($\sim 3.5 \times 10^5$ cells ml^{-1}) are typically 2 μm in cell diameter (Malinsky-Rushansky et al. 1995) and have a spheroid or ovoid shape (Hanagata et al. 1999). These may serve as nuclei for calcite crystallization in Lake Kinneret.

23.3 Synchronous Chemical–Biological Changes in the Lake Surface Water

Photosynthetic CO_2 fixation that results with the formation of organic matter (CH_2O) is presented in a simplified Eq. (23.1) as following

$$CO_2 + H_2O \rightarrow CH_2O + O_2, \tag{23.1}$$

while calcite precipitation in alkaline water may be represented by

$$2HCO_3^- + Ca^{+2} \rightarrow CaCO_3(s) + CO_2 + H_2O. \quad (23.2)$$

When both processes occur simultaneously, CO_2 emitted through reaction (23.2) may be consumed in photosynthesis.

23.3.1 Seasonal Variability

The data presented in Fig. 23.1 represents an annual cycle of a series of relevant parameters taken in the lake surface water during 1998, a year characterized by a massive spring bloom of *Peridinium* that was maintained at high levels over more than a month. The bloom started to be noticed in February (day ~50), reached a maximum on day 110 (mid-April), and crashed in mid-June, day 175 (Fig. 23.1a). During the growth period, the rise in *Peridinium* wet weight biomass (Fig. 23.1a) was from ~150 to >500 g m^{-2}, i.e., a net increase in biomass of ~350 g m^{-2}. *Peridinium* is characterized by a patchy distribution that leads to highly variable biomass when measured only at one pelagic station. The fact that in 1998 the size of this bloom was relatively stable over more than a month implies that the assessment of the biomass is truly representative for the lake. Assuming that carbon constitutes 16% of this biomass (Yacobi and Zohary 2010) and multiplying the C content of the biomass (350×0.16) by a lake surface area of 168 km^2, the respective amount of particulate organic carbon (POC) accumulated lake wide is therefore estimated at ~9,400 t. The concomitant seasonal decline in Ca^{2+} and alkalinity in surface layers, which is indicative of calcite precipitation, was ca. 0.7 meq L^{-1} (Fig. 23.1b). In terms of carbon released as CO_2 (Eq. 23.2), it is estimated that lake-wide (epilimnetic volume of $\sim 2.5 \times 10^9$ m^3) contribution of C-CO_2 through calcite precipitation is approximately 10,000 t.

The observations presented above suggest that a major source of carbon for photosynthetic production during the bloom of *Peridinium* in Lake Kinneret is CO_2 released through calcite precipitation. Thus, the following equation that combines calcite precipitation and photosynthesis is proposed:

$$2HCO_3^- + Ca^{+2} \rightarrow CaCO_3(s) + CH_2O + O_2. \quad (23.3)$$

Another issue associated with the spring bloom is the seasonal patterns of pH and DO (Fig. 23.1c). The winter of 1998, until day ~110, was characterized by mostly mild winds (Fig. 23.1d); thereafter in summer, strong winds prevailed until the end of August, during which in the afternoon westerly winds often exceeded 10 m s^{-1} (Chap. 6). The bloom development and mild winds are linked to a gradual rise in both pH and DO in surface water (Fig. 23.1c) while the decline of the bloom started at about the same time that winds became stronger and concomitantly with the decline in DO and pH (day ~110). As stated above, other than some calcite accumulated in sediment traps deployed in the LWM, we do not have indications

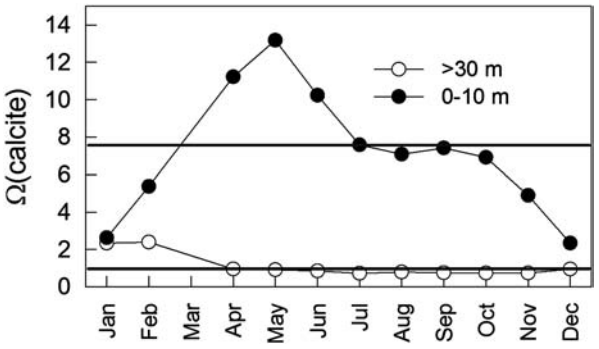

Fig. 23.4 The calculated degree of saturation for calcite, $\Omega_{calcite}$, in the epilimnion (0–10 m) and in the BBL (>30 m) during 2002. The *horizontal line* at $\Omega_{calcite} = 1$ represents thermodynamic saturation; the *line* at $\Omega_{calcite} = 7.6$ represents the level of supersaturation needed to achieve crystallization of calcite in Lake Kinneret

for autochthonous calcite precipitation in summer–fall. During the time of massive calcite precipitation in spring, $\mathbf{\Omega}_{calcite}$ may be >15 while in typical summer months (July through October) $\mathbf{\Omega}_{calcite}$ varies between 7 and 7.6 (Fig. 23.4). Therefore, an $\mathbf{\Omega}_{calcite}$ value of ~7.6 was selected as a threshold (Fig. 23.4, horizontal grey line). Below that threshold, calcite precipitation in Lake Kinneret declines significantly and it cannot serve as a major source of CO_2 to support algal blooms. The connection between $\mathbf{\Omega}_{calcite}$ and forcing factors such as wind is clear; stronger winds in summer reduce the chances for buildup of CO_2 deficiency in the surface water, as is the case in spring, and CO_2 levels may be significantly affected by gas exchange, tending to approach atmospheric pCO_2. In this case, lower pH levels are expected to lead to lower activity of the carbonate ion, $\mathbf{a}_{CO3}^{=}$, and therefore lower $\mathbf{\Omega}_{calcite}$. Under such conditions, as long as there is no other limiting nutrient, algal species that are CO_2-only users may exist but their productivity may depend on the gas exchange flux. To our best knowledge, in summer–fall, bicarbonate users such as the dinoflagellates *Peridiniopsis* spp. and the cyanobacterium *Aphanizomenon ovalisporum* (Sukenik et al. 2002) are common and in terms of biomass may even form minor blooms, which are less dependent on gas invasion rates in this alkaline lake.

23.3.2 Short-Term Variability

In spring, there is so much calcite precipitating that it is often possible to follow the quantitative issues discussed above even on a semi-daily time scale. For instance, on 7 May 2002, most primary production, mainly by *Peridinium,* occurred above the diel thermocline, which around 10:00 h was identified at 5.5 m depth. Depth-integrated ^{14}C primary production that day amounted to ~1.7 g C m^{-2} day^{-1} (Fig. 23.5a). At noon, the concentrations of Ca^{2+} and alkalinity in the upper 5.5 m layer became smaller by ~60 μeq than the respective concentrations in the deeper 5–10 m layer (Fig. 23.5b). Assuming that the deeper (5–10 m) layer represents surface water concentration of these solutes before sunrise (~05:30 h), the difference between these epilimnetic sub-layers may be attributed to ~6 h of calcite precipitation during which surface water DIC was also affected by the balance between pho-

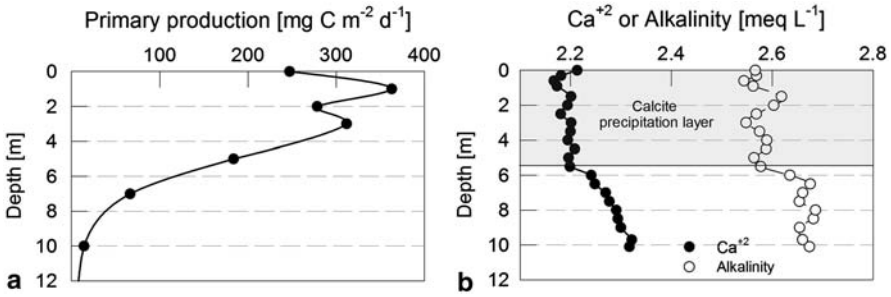

Fig. 23.5 Depth profiles (0–10 m) of ^{14}C-measured primary production, **a** and Ca^{2+} and alkalinity, **b** on 7 May 2002, at Sta. A. (Primary production data courtesy of YZ Yacobi; Ca^{2+} and alkalinity data: courtesy of A Katz)

tosynthesis and respiration (note that photosynthesis should not affect alkalinity). If only for calcite precipitation, during these 6 h, the pH of the surface layer would be expected to decline. In contrast, if only for primary production (which in this layer at that time is probably much larger than respiration), the pH would be expected to rise. In our measurements, the pH rose by less than 0.1 pH units, indicating that primary production may have been slightly more effective than calcite precipitation. The calculated respective drop in surface water $CO_{2(aq)}$ was estimated at ~1 μm which is only ~3 % of the daily ^{14}C carbon assimilation (Fig. 23.5a).

On that day of 7 May 2002, calcite precipitation from the surface 5.5-m thick layer was ~16.5 g $CaCO_3$(s) m^{-2} per 6 h, during which ~2 g C (as CO_2) m^{-2} (Eq. 23.2) was released to the ambient water. Thus, on a semi-daily scale, measured ^{14}C uptake (1.7 g m^2 day^{-1}) and the mass of C-CO_2 converted from ambient water HCO_3^- due to calcite precipitation (Eq. 23.2) were rather similar. Our high-resolution data also allows exploring how the pH and $\mathbf{\Omega}_{calcite}$ responded to this chemical–biological activity. The morning hour's shift in surface layer pH was from 9.25 to 9.33 resulting in a decline of $\mathbf{\Omega}_{calcite}$ from 20 to 18.2 (Fig. 23.6), while the deeper epilimnetic sublayer (5.5–10 m) showed an opposite trend in pH, decreasing from 9.14 to 9.05. The negative shift in pH in the deeper epilimnetic layer most probably results from having a larger respiratory than photosynthetic flux.

23.4 Inorganic Carbon Cycling in the Lower Water Mass

Following the onset of stratification, there are three main sources of DIC in the LWM, in addition to the DIC that got trapped there: (1) DIC originating initially through oxic and later through sub-oxic and anoxic (including sulfate reduction) decomposition of organic matter; (2) DIC added through calcite dissolution, where for each mole of Ca^{2+} released from calcite one mole of DIC is released; and (3) DIC originating from methanogenesis of which the products presumably diffuse from the underlying bed sediments and pore water (Sect. 25.4). Loss processes for CO_2 are: (1) uptake by chemosynthetic autotrophic organisms (Chap. 21, Sect. 24.2) in spring and early summer and (2) hypolimnetic–epilimnetic fluxes.

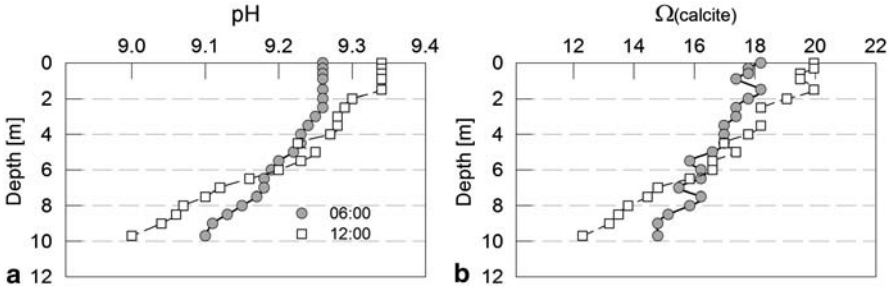

Fig. 23.6 Depth profiles (0–10 m) of **a** pH and **b** $\Omega_{calcite}$ at Sta. A on 7 May 2002, at 06:00 and at 12:00. pH was recorded by a RUSS profiler (Wagner et al. 2005); $\Omega_{calcite}$ was calculated from temperature, alkalinity and pH by PHREEQE-C using the chemical dataset of Katz and Nishri (2013)

The dissolution of calcite crystals in the LWM is evident from the co-occurrence of several phenomena: (1) deep dissolution pits that litter the calcite crystal faces collected in this layer (Fig. 23.2); (2) undersaturation with respect to calcite (Fig. 23.4), as of April ($\Omega_{calcite} \sim 1$) through October–November 2002 ($\Omega_{calcite} = 0.72$); and (3) coeval, but not identical, increasing concentrations of Ca^{2+} and HCO_3 (Fig. 23.3a, b; Fig. 23.7) in the LWM water. This concentration increase is characterized by HCO_3^-/Ca^{2+} equivalent ratios >1 (Fig. 23.3c) indicating that beside calcite dissolution there are other sources for the raise in alkalinity. The seasonal multiannual pattern of this ratio reveals a rise from ~0.98 in March to 1.12 in November (Fig. 23.3c).

Organic matter settling through the seasonal thermocline degrades first by oxidation, which in the LWM results in the complete removal of oxygen. During this stage, oxidation of one mole of Redfield-type organic matter would yield 124 and 106 moles of H^+ and HCO_3^- respectively, with subsequent production of some carbonic acid (H_2CO_3) via carbonate equilibrium. During this stage, both H^+ and H_2CO_3 are capable of dissolving calcite.

The oxic stage is followed by N_2(g) production on account of dissolved inorganic nitrogen through the heterotrophic dissimilatory nitrate reduction to nitrite (DNRN) which is followed by anammox and which lasts for a relatively short period of ca. 6 weeks (Chap. 21).

When both DO and NO_3 reservoirs are exhausted, bacterial sulfate reduction is initiated forming a major pathway for anoxic biodegradation in the lake (Hadas and Pinkas 1995). In comparison to oxic biodegradation, anaerobic processes are characterized by relatively low yield of H^+ (Müller et al. 2003, 2006). For instance, per one mole of organic matter (=106 moles of C; 256 moles of H) undergoing degradation, in sulfate reduction (Eq. 23.4), only 39 moles of H^+ released remain as such, while 53 and 64 moles of H^+ become associated with HS− and NH_4^+, respectively. Thus, unlike the case of oxic degradation, the sulfate-reduction pathway allows for more HCO_3^- to remain in solution as such, without further interacting with H^+ to form carbonic acid:

$$C_{106}H_{263}O_{110}N_{16}P + 53SO_4^{2-} \rightarrow 106HCO_3^- + 16NH_4^+ + HPO_4^{2-} + 39H^+. \qquad (23.4)$$

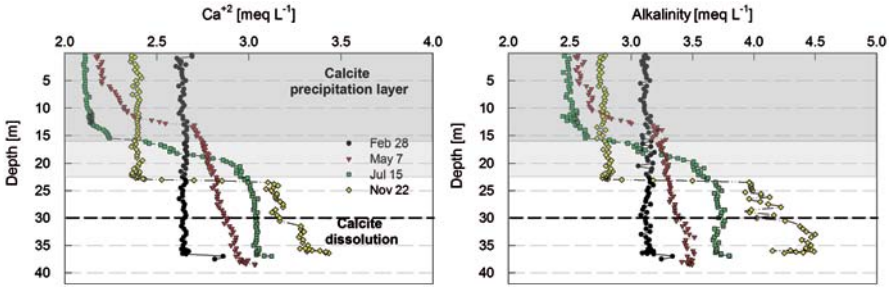

Fig. 23.7 Seasonal high-resolution depth profiles (0.2-m intervals) of Ca^{2+} (*left*) and alkalinity (*right*) in Lake Kinneret during 2002. The *horizontal dashed line* marked the boundary between the hypolimnion and BBL in summer. The *dark grey shading* represents the epilimnion in summer, the *lighter grey* the metalimnion in summer. Note the difference in concentrations between the hypolimnion and the BBL in the November profiles. (Data from Katz and Nishri 2013)

Under oxic conditions, whereby more H_2CO_3 and H^+ form during organic matter degradation, calcite dissolution is more efficient than under the anoxic stage that follows. However, in reality, since the LWM is a relatively closed system, there is a continuous accumulation of biodegradation products such as H^+ in this layer. This is indicated by a gradual decline in the pH of this anoxic environment and consequently by a gradual decline in $\Omega_{calcite}$ (Fig. 23.4) and rise of $CO_{2(aq)}$, both causing this water layer to be even more hostile to the calcite crystals than in the oxic stage.

While calcite dissolution in the LWM proceeds throughout the stratified period, the Ca^{2+} concentration-time slope during the "oxic–sub-oxic stages" in spring (March–June) is steeper than that characterizing later summer and fall anoxic stage (Figs. 23.3a and 23.7a). It is significant that the steep slope found for the changes in (Ca^{2+}) with time (Fig. 23.3a) coincides with an elevated calcite sedimentation flux through the thermocline (Koren and Ostrovsky 2009). Since biodegradation in the LWM leads to $\boldsymbol{\Omega}_{calcite}$ values < 1.0, it is possible that this correlation between the Ca^{2+} concentration-time slope and calcite sedimentation flux means that the extent of calcite dissolution in the LWM is affected by the availability of calcite surface area rather than the exact state of undersaturation. The slowing down of calcite precipitation later in summer and in fall left the calcite-rich sediment–water interface to take over as the main dissolution site (Katz and Nishri 2013) as is indicated by the preferential rise in Ca^{2+} (and alkalinity) in the BBL (Fig. 23.7a). For instance, between July and November, the rise in the hypolimnion was from ~3 to 3.15 meq Ca^{2+} L^{-1} while in the BBL the respective rise was twice as large, from ~3 to ~3.3 meq L^{-1}. The respective changes in alkalinity were from ~3.7 to 4.1 meq $L^{-1}$and from ~3.7 to ~4.5 meq L^{-1}. The larger rise for alkalinity is obviously caused by the additional sources of DIC to this layer discussed above as expected from direct breakdown of organic matter mediated by bacterial sulfate reduction.

The effect of methanogenesis is indicated by the occurrence of isotopically heavy $\delta^{13}C_{(DIC)}$ in pore water of ~+12 ‰ (Stiller and Magaritz 1974). In the pelagic bed sediments of Lake Kinneret, methanogenesis was identified (Sect. 25.4) below ~7-cm depth. Based on CH_4 and HS^- concentration profiles in the LWM, Eckert and

Conrad (2007) determined a typical HS^-:CH_4 concentration ratio of ~3:2 during the stratified period. Hence, based on available HS− data, it is possible to estimate the magnitude of CH_4 diffusion from below and by assuming that methanogenesis yields CO_2:CH_4 of 1:1 it becomes possible to estimate methanogenetic contribution of DIC (which does not include CH_4) to the LWM (Sect. 25.4).

Taking advantage of the monthly depth-profile data collected in 2002 (Fig. 23.7), the calculated DIC concentration in the BBL varied between 2.583 mM at the beginning of the stratified period (mid-March, pH = 8.3, T = 15.5°C) and 2.885 at the end of the oxic stage (7 May, pH = 7.7, T = 15.9°C) and 4.896 mM in November before monomixis (pH = 7.3, T = 16.2°C, HS− ~0.28 mM). The respective changes in Ca^{2+} were from 1.39 to 1.46 and to 1.65 mM. The final DIC in November is therefore calculated to originate from the following sources: 52.6% (=2.583/4.896) from the preliminary pool of DIC that prevailed upon the onset of stratification. Of the additional pool, 22.5% originates from calcite dissolution while the remainder 77.5% of this pool originates through the degradation of organic matter. The overall ratio between these two sources of DIC is therefore equal to 3.45 (=77.5/22.5). These proportions differ from the proportions during the oxic stage in which about half of the DIC accumulation in the LWM is due to calcite dissolution and the other half from mineralization of organic matter.

The relative size of each of these sources is supported also by $\delta^{13}C_{(DIC)}$ isotopic data. The $\delta^{13}C$ of the pre-stratification DIC is ~−5‰ (Stiller and Nissenbaum 1999), and that of total plankton during stratification is ~−21.5‰ (Stiller 1977), CO_2 arising from methanogenesis is isotopically heavy at +12‰ whereas the DIC originating from calcite dissolution is about +0.5‰ (Dubowski et al. 2003). The predicted final $\delta^{13}C_{(DIC)}$ obtained by multiplying the relative contribution to total DIC of each of these sources by its typical isotopic composition should be −8.57‰ which is close to measured values (Stiller and Nissenbaum 1999) of −8‰ and even more to our recent October 2013 unpublished data of −8.39 ± 0.05‰. Hence, our evaluation of the relative contribution by each source seems to be realistic. Based on calculations with PHREEQ-C (a computer program for low-temperature aqueous geochemistry calculations), the November 2002 data indicated that almost 9% of the DIC in the LWM was $CO_{2(aq)}$ while the remaining ~91% was HCO_3^-.

23.5 Isotopic Evidence for the Carbon Cycling in the Epilimnion

The isotopic composition of newly formed organic matter $\delta^{13}C_{(plk)}$ is determined by factors that revolve around primary productivity. Generally, $\delta^{13}C_{(plk)}$ increases when $CO_{2(aq)}$ becomes less available (Stiller 1977; Hollander and Mckenzie 1991; Erez et al. 1998), as well as when algal-specific growth rates increase (Stiller and Nissenbaum 1999; Gervais et al. 2002). The canonic view is that the universal carboxylating enzyme, which incorporates CO_2 into a carbohydrate in photosynthetic cells,

the Rubisco, fractionates carbon isotopes. It incorporates $^{12}CO_2$ faster than $^{13}CO_2$ (Raven 1997) and this is why the majority of organic matter is depleted in ^{13}C, i.e., showing *more negative* $\delta^{13}C_{(plk)}$ values than $\delta^{13}C_{(CO2\ aq)}$. Fractionation by Rubisco may occur only if in addition to CO_2 uptake there is also leakage of CO_2 out of the cell ("open diffusion model"). Otherwise, where the entire flux of CO_2 entering the cell is incorporated by Rubisco, no isotopic fractionation occurs and $\delta^{13}C_{(plk)}$ is expected to be equal to $\delta^{13}C_{(CO2)}$ which enters the cell or, in the case of active uptake of bicarbonate, to $\delta^{13}C_{(HCO3)}$ which is considerably heavier. It should be mentioned that CO_2 diffusion across the cell membrane involves some kinetic fractionation whereby $\delta^{13}CO_2$ crossing the cell is lighter by ~4‰ than $CO_{2(aq)}$. Thus, the overall fractionation involves both fractionations due to the crossing of the cell membrane combined with that of Rubisco. In a closed system where fractionation by Rubisco may be ignored, the kinetic fractionation is expected to be relatively important. However, this may not be the case for larger molecules of HCO_3 where the mass difference between ^{13}C and ^{12}C affects mass fractionation to a lesser extent. The occurrence of fractionation affects the ambient water by enriching $\delta^{13}CO_{2(aq)}$.

The difference between the $\delta^{13}C$ values in different carbon compartments is commonly expressed in Δ terms, in ‰ (PDB) values. Traditionally and until the development of membrane inlet mass-spectrometer (MIMS) systems, the isotopic composition of DIC was measured indirectly by first converting all of it (through acidification) to $CO_{2(g)}$ which can then be measured by the mass spectrometer. By measuring pH, temperature, and alkalinity and by assuming equilibrium (both chemical and isotopic) between DIC species, it becomes possible to calculate $\delta^{13}C$ of each of the different DIC species. This is done in two stages: First evaluating through thermodynamic modeling the relative fraction of each DIC species ($CO_{2(aq)}$, HCO_3^-, $CO_3^=$) in the ambient water by using pH, temperature, and alkalinity data. Second, evaluating the isotopic composition of each species by using the measured $\delta^{13}C_{(DIC)}$ and experimentally derived isotopic equilibrium values, which are temperature dependent (Mook et al. 1974). In typical Lake Kinneret epilimnetic water, $\delta^{13}C_{(DIC)}$ is −3.5‰ (Stiller and Nissenbaum 1999), ranging seasonally within the narrow range of between −2.4 and −5‰. Using conversion tables of Mook et al. (1974) we estimated that at a typical spring-time temperature of 23°C, $\Delta\delta\ ^{13}C_{(HCO_3-CO_{2(aq)})}$ is equal to ~9‰. Since in the lake surface water HCO_3 typically constitutes ~97% of the DIC pool, $\delta^{13}C_{(CO2)aq}$ is calculated to be ≈−12.5‰. This means that when $CO_{2(aq)}$ rather than HCO_3^- is taken up by algae, than in an hypothetical case that isotopic discrimination by Rubisco does not occur (closed system), $\delta^{13}C_{(plk)}$ should also be equal to ≈−12.5‰.

However, based on $\delta^{13}C_{(DIC)}$ data from two lakes, isotopic discrimination seems to occur even when $CO_{2(aq)}$ concentration is extremely small. For instance, Hollander and Mckenzie (1991) noticed that in Lake Greifen (Switzerland) there was a large seasonal variability in $\delta^{13}C_{(plk)}$, ranging between −27‰ during the summer bloom and −38‰ in winter, while $\delta^{13}C_{(DIC)}$ was characterized by much smaller seasonal variability. $\Delta\delta\ ^{13}C_{(DIC-plk)}$ was minimal during the summer bloom at ca. 18‰ while in fall and winter it became larger and up to 29‰. In general, their data showed a good linear correlation between both parameters; when the concentration of $CO_{2(aq)}$ declined, $\Delta\delta\ ^{13}C_{(CO_2-Plk)}$ also declined.

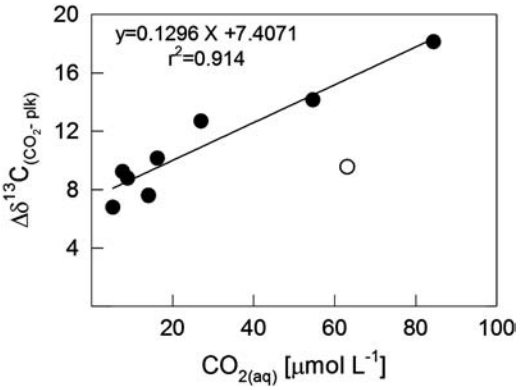

Fig. 23.8 $\Delta\delta\ ^{13}C_{(CO_2 - plk)}$ vs. $CO_{2(aq)}$ concentration between September 1974 and June 1975 in Lake Kinneret surface water (0–5-m depth). The *linear fit* excludes the February 1975 data point (*empty circle*). (Based on data from Stiller and Nissenbaum 1999)

Using the raw data collected by Stiller and Nissenbaum (1999) in 1974 and 1975, we have calculated the seasonal variability of $\Delta\delta\ ^{13}C_{(CO_2 - plk)}$ in Lake Kinneret and presented it against the concentration of $CO_{2(aq)}$, expressed in µmol L^{-1} (Fig. 23.8). Here also, we found a linear correlation between $\Delta\delta\ ^{13}C_{(CO_2 - plk)}$ and $CO_{2(aq)}$ concentrations. When $CO_{2(aq)}$ concentration was high, the difference in $\Delta\delta\ ^{13}C_{(CO_2 - plk)}$ was large regardless of the different species of algae that prevailed during 1974–1975. The conventional view of such dependency between both parameters (Kaplan pers.com) is that when the CO_2 concentration is high, the cells are working in an "open diffusion" mode and vice versa when it is low the system tends to be working in a more closed mode. However, when ambient CO_2 concentration is low, a CCM is activated and the Rubisco is working in a more closed environment and thereby forced to use the heavier isotope as well, leading to a less negative $\delta^{13}C$ in the organic product. This has been shown in all the modes of CCM such as C4, crassulacean acid metabolism (CAM), and algal CCMs (Kaplan pers.com). Here, we show that even when CO_2 in the water is approaching zero concentration, as is the case of the spring bloom of *Peridinium,* there is a distinct, though small, isotopic discrimination of 7.4‰ (Fig. 23.8). One would expect that Rubisco discrimination will be between 20 and 30‰ (Yakir 2003). This suggests that even in a relatively "closed mode," some isotopic fractionation does occur. Furthermore, by adding this minimum isotopic discrimination of 7.4‰ to the calculated $\delta^{13}C_{(CO2aq)}$ in spring, of −12.5‰, the expected $\delta^{13}C_{(plk)}$ should be about −19.9‰. This value is within the range of $\delta^{13}C_{(plk)}$ measured in Lake Kinneret by Stiller (1977) in plankton during the spring bloom, and by Zohary et al. (1994) in *Peridinium* cells. The latter were found to have $\delta^{13}C_{(Peridinium)}$ values which varied between −23.2‰ in January 1991 and −17.9‰ in May 1991. Another possibility is that *Peridinium* actually works in a "closed system" and that $\Delta(\delta^{13}{}_{CO2}{}^{-}\delta^{13}{}_{Peridinium})$ of 7.4‰ is somewhat shifted from the real kinetic isotopic effect. It should be noticed that Hollender and Mckenzie (1991) did not relate CO_2 supply in Lake Greifen to the occurrence of calcite precipitation but claimed that shortage in CO_2 drives algal succession to the dominance of species that are capable of exploiting the isotopically heavy HCO_3^-.

We would like to also raise the peculiar issue that during most of the *Peridinium* growth period, oxygen concentration in Lake Kinneret surface water is extremely

high and may exceed 200% saturation. This presumably would lead to high intracellular oxygen content next to the Rubisco apparatus in *Peridinium* cells and thus perhaps support a contemporary oxygenase activity on the account of carboxilating processes (Raven et al. 2008), thereby reducing primary production.

23.6 Synopsis

The relatively small atmospheric invasion of CO_2 gas and the high consumption of CO_2 by the bloom-forming *P. gatunense,* a CO_2-only user, leaves one major potential source of carbon for this alga, the CO_2 released through autochthonous calcite precipitation. Mass accumulation of POC in the lake during spring shows that the amount of CO_2 released by calcite precipitation and the net C accumulated in algae are similar. Moreover, the periods of the spring bloom and of massive calcite precipitation overlap. The C-isotope signature of *Peridinium* is in accordance with the expected isotopic value at low $CO_{2(aq)}$ concentrations.

These findings allow for an evaluation of the maximum possible biomass of *Peridinium* under the conditions that C is the limiting nutrient. Autochthonous calcite precipitation is not unlimited and it occurs mostly when $\Omega_{calcite} \geq 7.6$, i.e., in spring–early summer. In the more windy late summer, which does not allow for pH increases above ~9.0, $\Omega_{calcite}$ cannot rise above 7.6, calcite precipitation stops or is minimal, and thus the supply of $CO_{2(aq)}$ is severely restricted. At that time, low $CO_{2(aq)}$ availability limits the growth of CO_2 users. Summer algae must either be bicarbonate users or else rely on the relatively small gas invasion flux of CO_2. For the spring bloom, we propose a model whereby CO_2 is originating from the conversion of HCO_3^- through interaction with Ca^{2+} and crystallization of calcite, acquiring $\delta^{13}C_{CO2(aq)}$ of ~−12.5‰. Thereafter, the $CO_{2(aq)}$ is consumed by *Peridinium* where internal cell isotopic C fractionation or kinetic fractionation due to diffusion through the cell membrane of ~7.4‰ occurs. After the crash of the bloom, calcite precipitation proceeds but in a much slower rate, shifting the source of carbon to algae to be HCO_3^-, an almost unlimited source of C for bicarbonate users. In Lake Kinneret, this shift occurs around June, when bicarbonate-using dinoflagellates of the genus *Peridiniopsis* become abundant (Zohary et al. 1994; Chap. 11). In September, the wind ceases but $CaCO_3$ precipitation does not seem to increase and another bicarbonate user may take over. During the past two decades, this niche became often occupied by the cyanobacteria *A. ovalisporum* (Chap. 12). This cyanobacteria seems to be a bicarbonate user (Hadas et al. 1999) not only because of the relatively high ambient pH and predominance of HCO_3 in Lake Kinneret water but also because the lake contains >5mM Na^+ which facilitates the active transport of this DIC species across the cell membrane. In addition to being a HCO_3^- user, *A. ovalisporum* also has an efficient CCM, and can store phosphorus in polyphosphate bodies (Kaplan et al. 1998).

Being relatively isolated from the epilimnion, the accumulation of biodegradation products in the LWM induces calcite dissolution during all of the stratified

period, due to the cumulative increases in H^+ and $CO_{2(aq)}$ levels. The rate of these processes is however faster during the initial oxic stage, namely in spring, mainly because there is a much larger flux of autochthonous calcite settling from the photic layer. In summer–fall, the dissolution process shifts to deeper water layers and occurs mainly in the near bottom layers, dissolving Ca-carbonate in the bed sediments. Typically, about 30 % of the annual amount of calcite formed in the surface layer undergoes dissolution in the LWM. This implies that the flux of calcite buried in the sedimentary column (approximately 55,000 t $year^{-1}$) may be larger if both riverine inflows and epilimnetic productivity in spring are larger. However, since the burial flux is affected by the extent of calcite dissolution in the LWM, it is also expected to rise if productivity and autochthonous precipitation become larger. As of the concentration of calcite in the bed sediments, this picture becomes even more complicated because large riverine inflows in winter are associated with higher loads of allochthonous material, often made of clay minerals, thus diluting sediment calcite concentration (Dubowski et al. 2003).

References

Berman-Frank I, Kaplan A (1998) Changes in inorganic carbon uptake during the progression of a dinoflagellate bloom in a lake ecosystem. Can J Bot 76:1043–1051

Berman Frank I, Zohary T, Erez J, Dubinsky Z (1994) CO_2 availability, carbonic anhydrase, and the annual dinoflagellate bloom in Lake Kinneret. Limnol Oceanogr 39(8):1822–1834

Dittrich M, Obst M (2004) Are picoplankton responsible for calcite precipitation in lakes Ambio 33: 559–564

Dittrich M, Kurz PH, Wehrli B (2004) The role of autotrophic pico-cyanobacteria in calcite precipitation in an oligotrophic lake. Geomicrobiol J 21:45–53

Dubowski Y, Erez J, Stiller M (2003) Isotopic paleo-limnology of Lake Kinneret. Limnol Oceanogr 48(1):68–78

Eckert W, Conrad R (2007) Sulfide and methane evolution in the hypolimnion of a subtropical lake: a three-year study. Biogeochemistry 82:67–76

Erez J, Bouevitch A, Kaplan A (1998) Carbon isotope fractionation by photosynthetic aquatic microorganisms: experiments with Synechococcus PCC 7942 and simple carbon flux model. Can J Bot 76:1109–1118

Gervais F, Riebesell U, Gorbunov MY (2002) Changes in primary productivity and chlorophyll a in response to iron fertilization in the Southern Polar Frontal Zone. Limnol Oceanogr 47(5):1324–1335

Hadas O, Pinkas R (1995) Sulfate reduction processes in the hypolimnion and sediments of Lake Kinneret, Israel. Freshw Biol 33(1):63–72

Hadas O, Pinkas R, Dellphine E, Vardi A, Kaplan A, Sukenik A (1999) Limnological and ecophysiological aspects of *Aphanizomenon ovalisporum* bloom in Lake Kinneret, Israel. J Plankton Res 21(8):1439–1453

Hanagata NA, Malinsky-Rushansky N, Dubinsky Z (1999) Eukariotic picoplankton, *Mychonastes homosphaera* in Lake Kinneret, Israel. Phycol Res 47:263–269

Hertzig R, Dubinsky Z, Berman T (1981) Breakdown of *Peridinium* biomass in Lake Kinneret. In: Shuval H (ed) Developments in zone ecology and environmental quality. Balaban ISS, Philadelphia, pp 179–185

Hollander DJ, Mckenzie JA (1991) CO_2 control on carbon isotope fractionation during aqueous photosynthesis: a paleo pCO_2 barometer. Geology 19:929–932

Katz A, Nishri A (2013) Calcium, magnesium and strontium cycling in stratified, hardwater lakes: Lake Kinneret (Sea of Galilee), Israel. Geochim Cosmochim Acta 105:372–394

Kaplan A, Ronen-Tarazi M, Tchernov D, Bonfil DJ, Zer H, Schatz D, Vardi A, Hassidim M, Reinhold L (1998) The inorganic carbon-concentrating mechanism of cyanobacteria: genes and ecological significance. In: Peschek GA, Loeffelhardt W, Schmetterer G (eds) The phototrophic prokaryotes. Kluwer Academic, New York, pp 561–571

Kelts K, Hsui J (1978) Freshwater carbonate sedimentation. In: Lerman A (ed) Lakes: chemistry, geology, physics. Springer, Heidelberg, pp 295–323

Kolodny Y, Katz A, Starinsky A, Moise T, Simon E (1999) Chemical tracing of salinity sources in Lake Kinneret (Sea of Galilee), Israel. Limnol Oceanogr 44:1035–1044

Koren N (1994) Rates of sedimentation in Lake Kinneret. MSc thesis, Haifa University, Israel (in Hebrew)

Koren N, Ostrovsky I (2009) Sedimentation in a stratified subtropical lake. Verh Int Ver Limnol 27:2636–2639

Lemckert C, Antenucci J, Saggio A, Imberger J (2004) Physical properties of turbulent benthic boundary layers generated by internal waves. J Hydraul Eng 130:58–69

Malinsky-Rushansky N, Berman T, Dubinsky Z (1995) Seasonal dynamics of picophytoplankton in Lake Kinneret, Israel. Freshw Biol 34:241–254

Mook WG, Bomerson JC, Staverman WH (1974) Carbon isotope fractionation between dissolved bicarbonate and aqueous carbon dioxide. Earth Planet Sci Let 22:169–176

Müller B, Wang Y, Dittrich M, Wherli B (2003) Influence of organic carbon decomposition on calcite dissolution in surficial sediments of a freshwater lake. Water Res 37:4524–4532

Müller B, Wang Y, Wehrli B (2006) Cycling of calcite in hard water lakes of different trophic states. Limnol Oceanogr 51:1678–1688

Nishri A, Imberger J, Eckert W, Ostrovsky I, Geifman Y (2000) The physical regime and the respective biogeochemical processes in the lower water mass of Lake Kinneret. Limnol Oceanogr 45:972–981

Nishri A, Koren N, Leibovici E (2005) Deposition of P in dust on Lake Kinneret. KLL-IOLR report T15/2005 (In Hebrew)

Nishri A, Rimmer A, Wagner U, Rosentraub Z, Yeates P (2011) Physical controls on the spatial variability of the decomposition of organic matter in Lake Kinneret. Aquat Geochem 17(3):195–207

Pollingher U, Serruya C (1976) Phased division of *Peridinium cinctum* fa. *westii* and the development of the bloom in Lake Kinneret (Israel). J Phycol 12: 162–170

Raidt H, Koschel R (1988) Morphology of calcite crystals in hardwater lakes. Limnologica 19:3–12

Raven JA (1997) CO_2 concentrating mechanisms: a direct role for thylakoid lumen acidification? Plant Cell Environ 20(2):147–154

Raven JA, Cokell CS, De-La Rocha CL (2008) The evolution of inorganic carbon concentrating mechanisms in photosynthesis. Phil Trans R Soc Lond B Biol Sci 365(1504):2641–2650. doi:10.1098/rstb.2008.0020

Rimmer A, Eckert W, Nishri A, Agnon Y (2006) Evaluating hypolimnetic diffusion parameters in thermally stratified lakes. Limnol Oceanogr 51:1906–1914

Serruya C (ed) (1978) Lake Kinneret, Monographiae Biologicae. Junk, The Hague

Stiller M (1977) Origin of sedimentation in Lake Kinneret traced by their isotopic composition. In: Golterman HL (ed) Interactions between sediments and freshwater. Junk, The Hague, pp 57–64

Stiller M, Magaritz M (1974) Carbon-13 enriched carbonate in interstitial waters of Lake Kinneret sediments. Limnol Oceanogr 19(5):849–853

Stiller M, Nissenbaum A (1999) A stable isotope carbon study of dissolved inorganic carbon in hard water Lake Kinneret (Sea of Galilee). S Afr J Sci 95:166–170

Sukenik A, Eshkol R, Livne A, Hadas O, Kaplan A, Tchernov D, Vardi A, Rom M (2002) Inhibition of growth and photosynthesis of the dinoflagellate *Peridinium gatunense* by Microcystis sp. (cyanobacteria): a novel allelopathic mechanism. Limnol Oceanogr 47:1656–1663

Tchernov D, Hassidim M, Luz B, Sukenik A, Reinhold L, Kaplan A (1997) Sustained net CO_2 evolution during photosynthesis by marine microorganisms. Curr Biol 7(10):723–728

Vardi A, Berman-Frank I, Rozenberg T, Hadas O, Kaplan A, Levine A (1999) Programmed cell death of the bloom-forming dinoflagellate *Peridinium gatunense* is mediated by CO_2 limitation and oxidative stress. Curr Biol 9:1061–1064

Web-PHREEQC program (on line) Aqueous Geochemical modeling, Dept. Geosciences, North Dakota State University. http://www.ndsu.nodak.edu/webphreeq.

Wagner U, Nishri A, Sukenik A, Zohary T (2005) The ECORAFT in Lake Kinneret. SIL News: 46–47

Wynne D, Panti NJ, Aaronson S, Berman T (1982) The relationship between nutrient status and chemical composition of *Peridinium Cinctum* during the bloom of Lake Kinneret. J Plankton Res 4:125–134

Yacobi YZ, Zohary T (2010) Carbon:chlorophyll a ratio, assimilation numbers and turnover times in Lake Kinneret phytoplankton. Hydrobiologia 639:185–196

Yakir, D. (2003) The Stable Isotopic Composition of Atmospheric CO_2. Treatise on Geochemistry, Volume 4. Editor: Ralph F. Keeling. Executive Editors: Heinrich D. Holland and Karl K. Turekian. pp. 347. ISBN 0-08-043751-6. Elsevier, 2003., p.175–212

Zohary T, Erez J, Gophen M, Berman-Frank I, Stiller M (1994) Seasonality of stable isotopes within the pelagic food web of Lake Kinneret. Limnol Oceanogr 39(5):1030–1043

Zohary T, Pollingher U, Hadas O, Hambright KD (1998) Bloom dynamics and sedimentation of *Peridinium gatunense* in Lake Kinneret. Limnol Oceanogr 43:175–186

Chapter 24
Primary Production

Yosef Z Yacobi, Jonathan Erez and Ora Hadas

Abstract The synthesis of organic compounds from aqueous carbon dioxide, the aquatic primary production, principally occurs through the process of photosynthesis, which uses light as its source of energy, but it also occurs through chemosynthesis, which uses the oxidation or reduction of chemical compounds as its source of energy. Here, we present both pathways and their contribution to the primary production in Lake Kinneret. Phytoplankton density, measured as chlorophyll *a* (Chl *a*), and photosynthetic primary productivity (PP), measured as radiocarbon isotope uptake, have been monitored in the lake for more than four decades. The average Chl *a* areal concentration in the lake is 208 mg m^{-2} and the PP is 1.66 g C m^{-2} day^{-1}. Both parameters displayed marked seasonal patterns, with highest values occurring in April and May. From July to December, Chl *a* and PP values were on average only 24 and 64 %, respectively, of the spring maxima. However, since the mid-1990s, a definite weakening of the seasonal periodicity of Chl *a* and PP was observed.

Intensive chemosynthetic microbial activity, fueled by H_2S oxidation, was measured at the chemoclines during its deepening below the photic zone in late autumn, and close to the sediment–water interface in May when the chemocline starts to form. Averaged depth-integrated chemoautotrophic primary production at the chemocline was 16 and 24 % of the photosynthetic primary production in May and during autumn, respectively. The $\delta^{13}C$ of particulate organic matter at the chemocline ranged between −27 and −39 ‰, suggesting the involvement of intensive chemosynthesis. Mass and isotopic balance of carbon and H_2S suggest that chemosynthetic production contributes between 20 and 30 % of the total primary production in Lake Kinneret annually. This component should be considered when the lake's carbon budgets and food webs are assessed.

Y. Z Yacobi (✉) · O. Hadas
The Yigal Allon Kinneret Limnological Laboratory, Israel Oceanographic & Limnological Research, P.O. Box 447, 14950, Migdal, Israel
e-mail: yzy@ocean.org.il

J. Erez
Institute of Earth Sciences, The Hebrew University of Jerusalem, 91904, Jerusalem, Israel
e-mail: erez@vms.huji.ac.il

O. Hadas
e-mail: orah@ocean.org.il

T. Zohary et al. (eds.), *Lake Kinneret, Ecology and Management,* Aquatic Ecology Series 6,
DOI 10.1007/978-94-017-8944-8_24,

Keywords Carbon fixation · Chemoautotrophy · Chemocline · Chlorophyll · H_2S oxidation · Light attenuation · Light penetration · Primary production · Oxic–anoxic interface · Sediment–water interface

For many years, the primary production in Lake Kinneret was solely assessed from in situ measurement of photosynthetic carbon assimilation. Phytoplankton abundance (in terms of chlorophyll *a* concentration) and photosynthetic primary production have been systematically measured for more than four decades within the framework of the Lake Kinneret monitoring program. The contribution of chemosynthetic bacteria was only occasionally measured and indicated the role and contribution of chemosynthesis to the overall primary production and to the carbon cycle in the lake. This chapter summarizes the observed trends of intra- and interannual variation in key phytoplankton variables, chlorophyll abundance, photosynthetic primary production rates, as well as the contribution of chemotrophic bacteria to the production.

24.1 Photosynthetic Primary Production

Yosef Z Yacobi

24.1.1 A Short Historical Account

The first systematic measurement of primary productivity (PP) in Lake Kinneret was made from June 1956 to July 1957 at a single offshore station located at the southwestern side of the lake (Yashouv and Alhunis 1961). The measurements were based on the oxygen light and dark bottle method. Using the same methodology, Hepher and Langer (1970) extended the work in 1964–1965 to six stations distributed over the lake; they were also the first to systematically measure chlorophyll *a* (Chl *a*) as a crude estimate of phytoplankton biomass. Both studies revealed typical seasonality of phytoplankton abundance and PP, with a substantial peak in spring, when the dinoflagellate *Peridinium gatunense* bloomed. Thus, Chl *a* and photosynthetic rates reached maximum values before solar input and temperatures reached their annual maxima. In 1969, the ^{14}C-tracer method (Steemann-Neilsen 1952) was introduced by Rohde (1972) and was soon established as the routine method for the assessment of PP in Lake Kinneret. Multiannual summaries of chlorophyll *a* and primary production dynamics in Lake Kinneret have been published on several occasions (Berman and Pollingher 1974; Pollingher and Berman 1977, 1982; Berman et al. 1992, 1995; Yacobi and Pollingher 1993; Yacobi 2006). The methodologies used for measurement of Chl *a* (Holm-Hansen et al. 1965) and PP (Steemann-Nielsen 1952) have remained unchanged throughout the entire period, enabling direct comparison of measurements in the multiannual record.

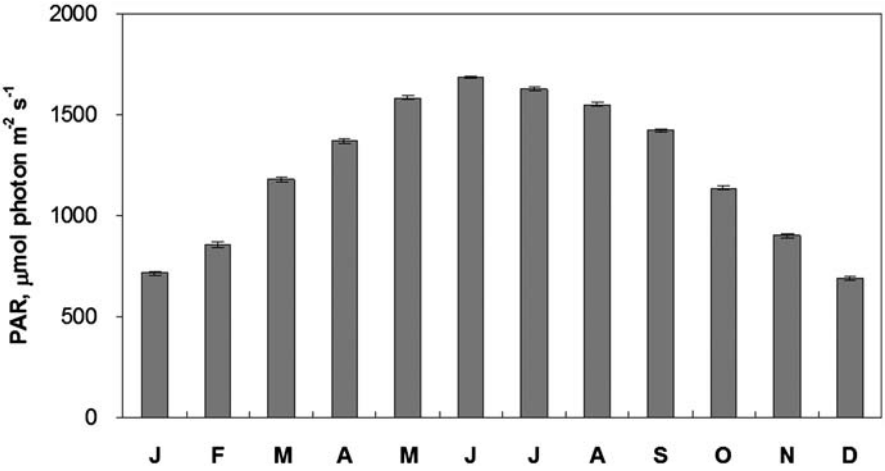

Fig. 24.1 Monthly averages (±standard error) of incident photosynthetically active radiation (*PAR*) in Lake Kinneret (1995–2011)

24.1.2 Light Characteristics

Photosynthetically active radiation (PAR) input has been measured systematically in Lake Kinneret since 1994, using a quantum sensor LI−190 (Licor, Lincoln, NE, USA). The average (±SD) PAR measured at the Lake Kinneret water surface during 1995–2011 was 1,232 (±472) µmol photon m^{-2} s^{-1}. Maximum values were usually recorded in June and minimum values in December (Fig. 24.1). The early PAR measurements within the water column of the lake were restricted to four wavelength bands (Rohde 1972; Berman 1976a) and 19 wavelength bands (Dubinsky and Berman 1976, 1979). The result of these studies showed: (a) seasonal changes in PAR penetration in the lake and suggested a two-way relationship between light penetration and phytoplankton density (phytoplankton affected light penetration, and limited its own light availability); (b) the dense crop formed by *P. gatunense* dramatically shifted the spectral properties of the underwater light field, from green being the most penetrating wavelength at the beginning of the bloom towards red prior to its collapse; (c) light utilization efficiency in the water column increased with depth. The integrated value for light utilization efficiency in the trophogenic layer ranged from 0.33 to 4.01 %, with lowest values associated with domination of *P. gatunense*.

From 1970 until the present, in-water PAR measurements, based on a broadband (400–700 nm) sensor, were used for routine calculation of the light attenuation coefficient, K_d. The vertical distribution of particles was mostly fairly uniform and the value of K_d varied only slightly with depth in the euphotic zone, except when massive blooms of *P. gatunense* occurred. However, when *P. gatunense* dominated the lake phytoplankton, with a dense crop in the uppermost layers of the water column, K_d changed conspicuously with depth (Dubinsky and Berman 1979). In order to

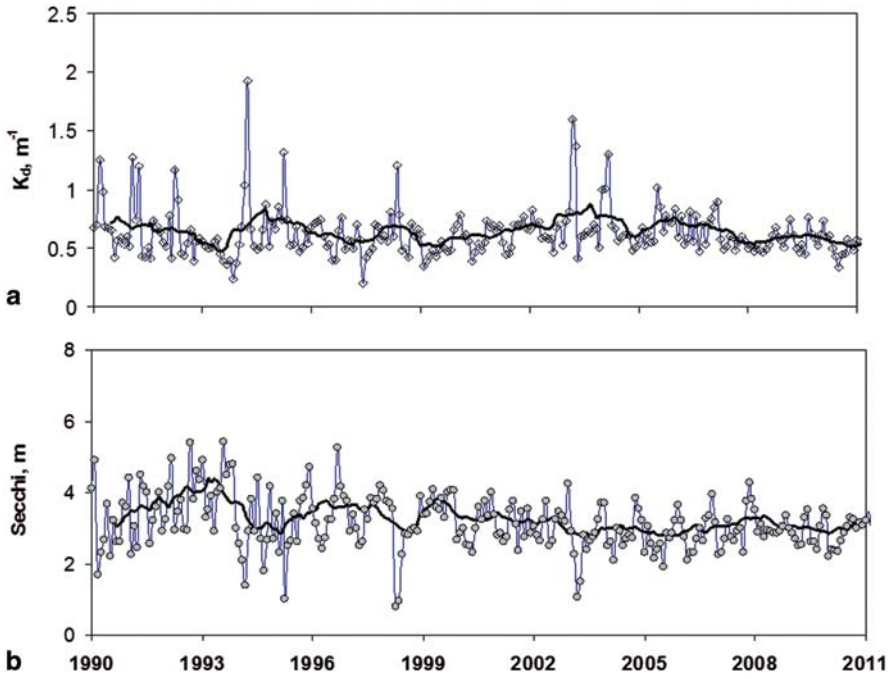

Fig. 24.2 Time series and 12-month (13 point) smoothed averages (*solid line*) of all monthly averages of in-water light characteristics of Lake Kinneret (1990–2011). **a** Broadband (400–700 nm) light attenuation coefficient (K_d from 0.5 to 2.5 m) and **b** Secchi depth

circumvent the issue of heterogeneous vertical distribution of particles during *P. gatunense* blooms, a depth interval of 0.5–2.5 m was used to calculate K_d (Yacobi 2006). From 1990 through 2011, the average K_d in the 0.5–2.5-m water layer ranged by almost an order of magnitude (Fig. 24.2a, Table 24.1), with the highest values in April and the lowest in July and August (Fig. 24.3). Over the period from 1990 to 2011, there was a nonsignificant trend of decrease in K_d (Fig. 24.2a). A more extensive data set based on measurements from 1970 to 2008 also showed a very slight time-dependent increase of K_d (Rimmer et al. 2011). Thus, it appears that the average in-water light penetration in Lake Kinneret has remained essentially unchanged over the past four decades.

The slope of the regression of K_d versus Chl *a* concentration yields the value of the partial attenuation attributed to Chl (K_c). For the period 1990 to 2011, K_c was 0.0033 mg^{-1} Chl *a* m^{-2}. Elimination of entries where Chl *a* was >60 mg m^{-3}, i.e., when *P. gatunense* dominated the phytoplankton community, brought the K_c value to 0.007 mg^{-1} Chl *a* m^{-2}.

The Secchi depth showed a significant decreasing trend from 1990 to 2011 (Fig. 24.2b), suggesting that in-water light scattering increased in that time interval. By contrast, in the period from 1970 to 1990, no significant trend for the Secchi depth was observed. Increase in scattering may be the result of increase in

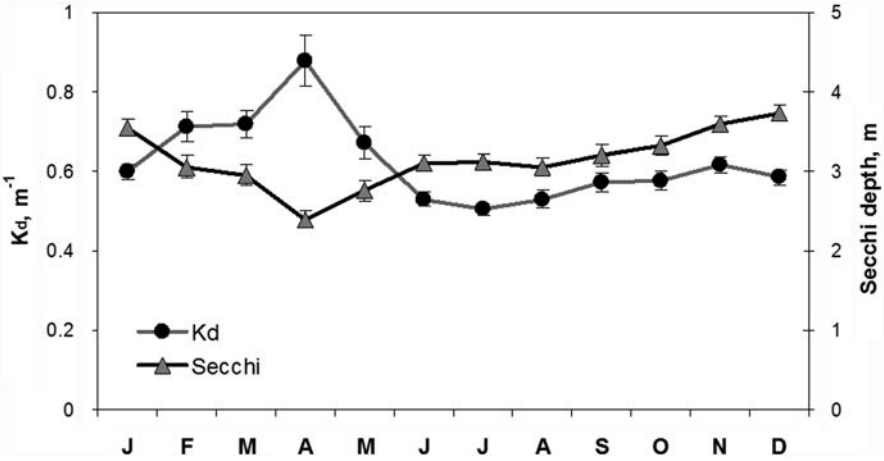

Fig. 24.3 Monthly averages (±standard error) of downwelling attenuation coefficient K_d and Secchi depth from 1990 to 2011. K_d calculated for the water layer from 0.5 to 2.5 m

the concentration of particles or in light scattering per particle. Data on particle concentrations in the lake do not indicate a consistent time-dependent increase since 1998 (Chap. 26). Thus, it appears more likely that the decrease in the Secchi depth reflects changes in the taxonomic composition of the phytoplankton (Chap. 10) and in the size and/or composition of detrital and inorganic particles (Chap. 26).

The reciprocal of Secchi depth and K_d were positively correlated for all data points from 1990 to 2011 ($r^2=0.31$, $p<0.001$, $n=495$). Both optical parameters were moderately correlated with the average Chl *a* density in the 0–15-m water column or in the uppermost (0–1 m) layer of the lake, with the strongest correlation between Chl *a* concentration in the uppermost layer and the reciprocal of Secchi depth ($r^2=0.52$, $p<0.001$, $n=495$). When Chl *a* values >20 mg m^{-3} were excluded, a much weaker correlation resulted ($r^2=0.06$, $p<0.001$ $n=393$) suggesting that in periods when *P. gatunense* was not dominant, phytoplankton was not the major factor determining the light climate in the water column. The levels of colored dissolved organic matter in the epilimnion were extremely low; consequently, particulate detritus was probably the major modifier of water optical characteristics.

24.1.3 Chl a and Primary Production: 1970–2011

Mean (±SD) Chl *a* in the epilimnion (0 to 15 m) of the lake from 1970 to 2011 was 208 (±186) mg m^{-2} and mean (±SD) daily PP 1.67 (±0.70) g C m^{-2} day^{-1} (Table 24.1). Monthly averages of Chl *a* were positively correlated with microscopically determined phytoplankton wet weight biomass ($r^2=0.67$, $p<0.001$, $n=504$,). For all sampling dates from 1972 until 2011, Chl *a* and phytoplankton wet weight biomass were significantly positively correlated with PP, but with relatively

Table 24.1 Lake Kinneret: chlorophyll *a* (Chl *a*), primary production (PP), assimilation number (A.N., calculated for optimal depth, sensu Kirk 1994), light attenuation coefficient (K_d), and Secchi depth

	Mean	SD	Median	Min.	Max.	*n*
Areal[a]						
Chl *a,* mg m^{-2}	208	186	144	40	1,436	503
PP, mg C m^{-2} day^{-1}	1,665	697	1,569	308	4,339	440
Volumetric[b]						
Chl *a,* mg m^{-3}	16.9	22.8	10.5	1.0	650	4,448
PP, mg C m^{-3} day^{-1}	183	243	131	0.1	4,741	4,408
At optimal depth[c]						
Chl *a,* mg m^{-3}	21.2	45.6	10.7	2.3	650	518
PP, mg C m^{-3} day^{-1}	411	431	298	59	4,741	518
A.N., mg C Chl a^{-1}, h^{-1}	2.97	1.43	2.73	0.25	8.85	518
K_d[d], 0.5–2.5 m	0.623	0.221	0.580	0.203	1.954	495
Secchi depth[b], m	3.15	0.82	3.00	0.70	6.30	495

SD standard deviation

[a] Areal Chl *a* and PP were calculated by depth-integrating data based on samples taken biweekly at eight depths from 0 to 15 m. Measurements from 1970 (Chl *a*) or 1972 (PP) to 2011

[b] Volumetric variables and Secchi depth are based on measurements from 1990 to 2011

[c] Optimal depth is the depth in the water column "at which the light intensity is optimal for photosynthesis" (Kirk 1994). Variables at optimal depth are based on measurements from 1990 to 2011

[d] K_d is based on measurements from 1994 to 2011

low coefficients of correlation ($r^2 = 0.19$ and 0.16, respectively, $p < 0.001$, $n = 441$). Primary production per unit of Chl *a* changed conspicuously with phytoplankton taxonomic identity (Yacobi and Zohary 2010) as well as temporally, indicating variation in light climate in the water column and probably the availability of nutrients.

The monthly averages of Chl *a* (Fig. 24.4a) and PP (Fig. 24.4b) displayed a seasonal pattern of phytoplankton density and photosynthetic activity, with a clear Chl *a* peak in April and somewhat less prominent peaks of PP in April and May. The high spring peaks were caused by the development of dense populations of *P. gatunense,* a highly regular phenomenon until the early 1990s (Zohary 2004; Chap. 10). Overall, the monthly averages of Chl *a* showed greater variability than those of PP, as shown by the ratio between maximum and minimum monthly averages (4.5 and 2.2 for Chl *a* and PP, respectively). Similarly, a comparison of all measurements showed that integrated Chl *a* varied more widely than PP (Table 24.1).

The seasonality of Chl *a* and PP is shown in Fig. 24.5 from 1970 to 2011. Changes in the seasonal pattern occurred after the mid-1990s due to the absence of *P. gatunense* blooms in some years (1996–1997, 2001–2002, 2005, 2008–2011) but very dense *P. gatunense* populations in 1994, 1995, 1998, 2003, and 2007, with a ratio of >10 between the highest and lowest monthly averages. Judging by the running average (Fig. 24.5), it seems that overall, from 1970 to 2011, Chl *a* concentrations and PP rates have not changed dramatically. On the other hand, the pattern of intra-annual variation of phytoplankton parameters did change.

Lake Kinneret data have often been presented in terms of semiannual averages, representative of the winter–spring (January–June) and the summer–autumn

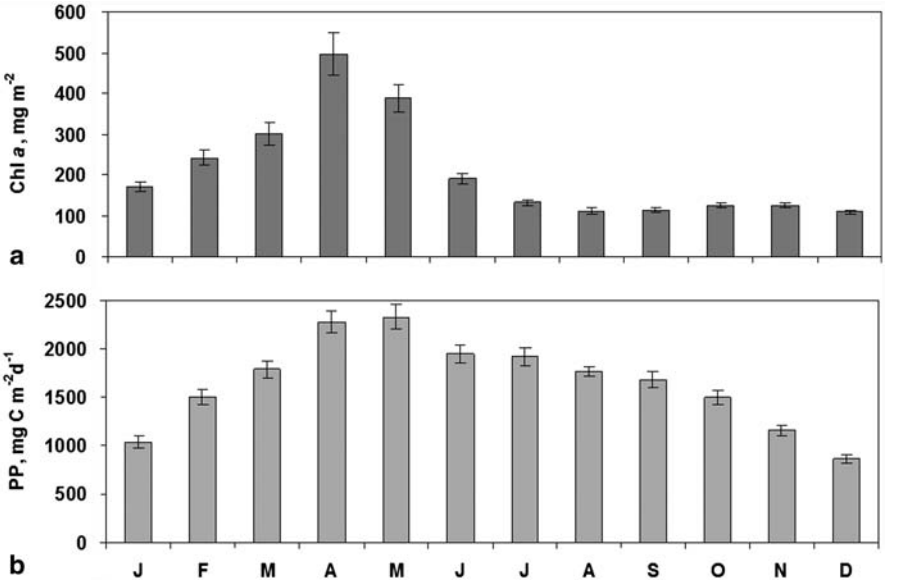

Fig. 24.4 Monthly average (±standard error) of **a** *Chl a* content and **b** daily primary production (*PP*) calculated for depth-integrated profiles from 1970 (*Chl a*) or 1972 (*PP*) through 2011

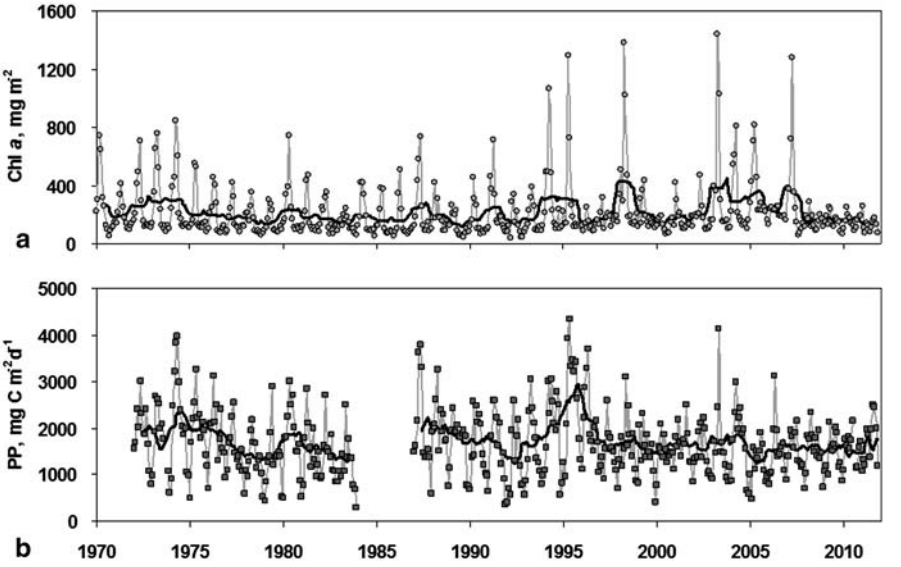

Fig. 24.5 Time series and 12-month (13 point) smoothed averages (*solid line*) of all monthly averages of **a** *Chl a* (mg m^{-2}) and **b** primary production (*PP*, mg C m^{-2} day^{-1}) calculated for depth-integrated profiles from 1970 (*Chl a*) or 1972 (*PP*) through 2011

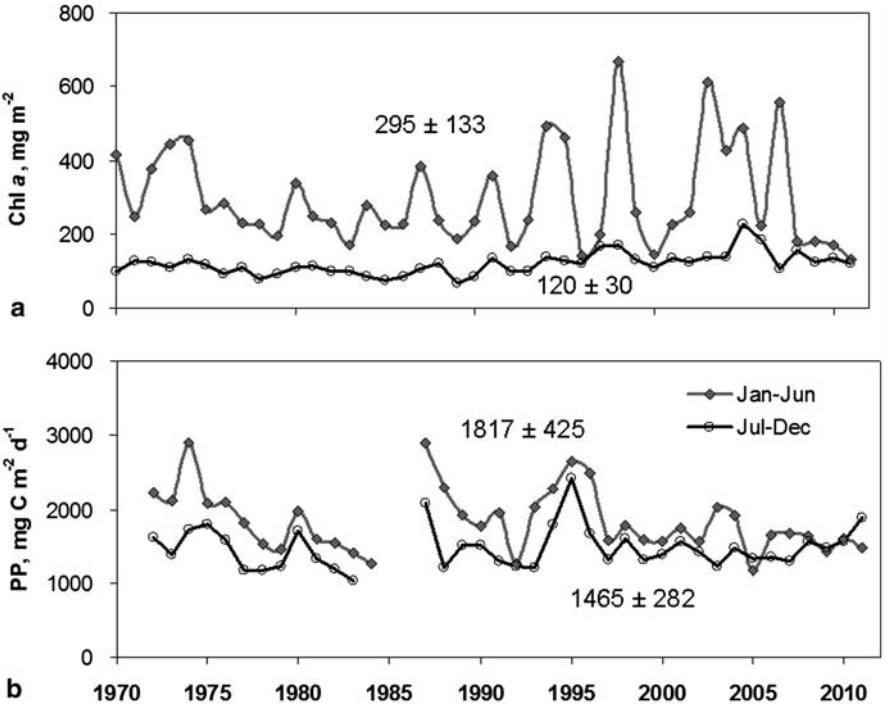

Fig. 24.6 Semiannual averages of depth-integrated **a** *Chl a* (mg m^{-2}) and **b** primary production (*PP,* mg C m^{-2} day^{-1}), from 1970 (*Chl a*) or 1972 (*PP*) through 2011. The multiannual average (± standard deviation) for each variable is indicated, *upper:* winter–spring, *lower:* summer–autumn

(July–December) conditions (e.g., Berman et al. 1995). Both Chl *a* concentrations and PP rates were higher in winter–spring than in summer–autumn, although only the former differed significantly. The semiannual averages of Chl *a* varied within a restricted range from 1970 to 1994 (Fig. 24.6a); since then, a sharp increase occurred in the variability of the semiannual Chl *a* averages. Comparison of the Chl *a* averages for the winter–spring season from 1970 to 1994 with the Chl *a* averages from 1995 to 2011 showed no significant difference. By contrast, in the summer–autumn season, average Chl *a* concentrations from 1995 to 2011 were significantly higher than from 1970 to 1994. The overall variability of PP declined from 1997 to 2011 (Fig. 24.6b).

24.1.4 Primary Production at Optimal Depth

Optimal depth is the depth in the water column "at which the light intensity is optimal for photosynthesis" (Kirk 1994). The very definition of optimal depth indicates that it fluctuates diurnally with the solar energy input. The data used for the current analysis were derived from biweekly measurements made from 09.00 to 12.00 as

Table 24.2 Average assimilation number (mg C mg Chl a^{-1} h^{-1}) and downwelling photosynthetically active radiation (PAR; μmol photon m^{-2} s^{-1}) at optimal depth in Lake Kinneret from 1990 through 2011

Depth, m	A.N. average	PAR	*n*
0	2.26 ± 1.29^{a}	570^{a}	102
1	3.05 ± 1.43^{b}	404^{b}	194
2	3.23 ± 1.36^{b}	294^{c}	170
3	3.23 ± 1.36^{b}	206^{d}	49
5	2.85 ± 0.85^{ab}	71^{e}	3

Averages of each variable followed by different letters were significantly different ($p < 0.001$, using Dunn's test)

part of the routine PP monitoring program. From 1990 to 2011, mean optimal depth was 1.34 (±0.94) m with a mean assimilation number (A.N.) of 2.97 (±1.43) mgC mg Chl a^{-1} h^{-1} ($n = 518$). A.N. values at 1-, 2-, and 3-m depth were comparable, but significantly different from those at 0 m (Table 24.2). The highest A.N. in Lake Kinneret were recorded when cyanobacteria were the most abundant phytoplankton, followed by diatoms and chlorophytes; the lowest A.N. were calculated when dinoflagellates were the dominant phytoplankton (Yacobi and Zohary 2010). The mean A.N. of samples dominated by *P. gatunense,* from 1990 to 2011, was 1.43 (±0.73) mg C mg Chl $a^{-1}h^{-1}$ ($n = 48$). The relatively low A.N. values at 0-m depth resulted from the tendency of *P. gatunense* to concentrate close to the water surface and to reduce the light available near the surface as well as in deeper strata. In addition, *P. gatunense* dominated when solar input was often below the value enabling maximum photosynthetic activity. Consequently, *P. gatunense* in Lake Kinneret was seldom photo-inhibited, although it does not lack the genetic potential destined for coping with excessive radiation (Yacobi 2003). The highest A.N. were recorded in August and September and the lowest from March to May (Fig. 24.7), when *P. gatunense* reached maximum densities. Optimal depth was relatively shallow from December to February and deepest throughout the summer months (Fig. 24.7), corresponding to the intensity of solar input (Fig. 24.1). A.N. varied widely from 1990 to 2011 (Fig. 24.8), although it was fairly stable from 1970 to 1990 (Ostrovsky et al. 2013; Table 24.3).

24.1.5 Phytoplankton Characteristics Driven by the Physicochemical Environment

The differences in phytoplankton community structure and metabolic activity during the winter–spring and the summer–autumn were basically driven by the changes in thermal structure of the lake, i.e., full mixing at about the beginning of January to March, followed by stratification and, finally, stable stratification in June. The lake layers remain stratified throughout the summer. From September, the thermocline deepens until the overturn in the last third of December or early January. Nutrient supply, either by release from bottom sediments (Nishri et al. 2000) or from inflows from the watershed, is relatively high during winter–spring (Nishri 2010). This may explain the higher PP rates and Chl *a* concentrations that occurred in months when

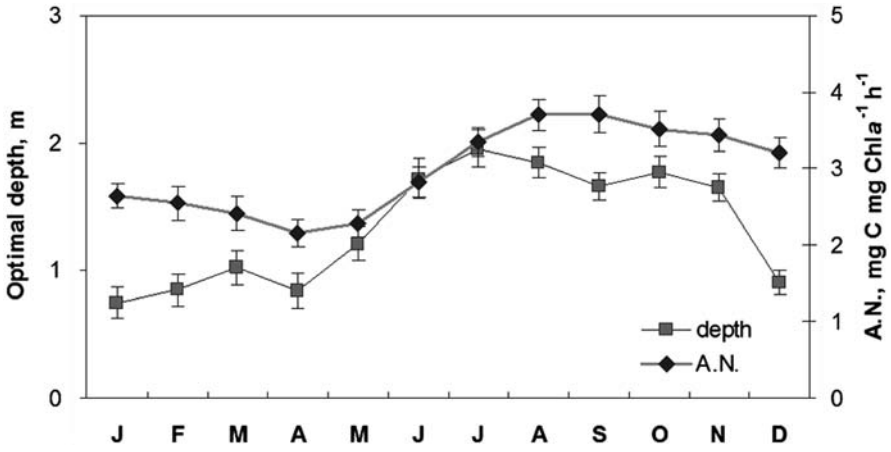

Fig. 24.7 Monthly averages (± standard error) of optimal depth (m) and assimilation number (*A.N.*) at the optimal depth from 1990 to 2011

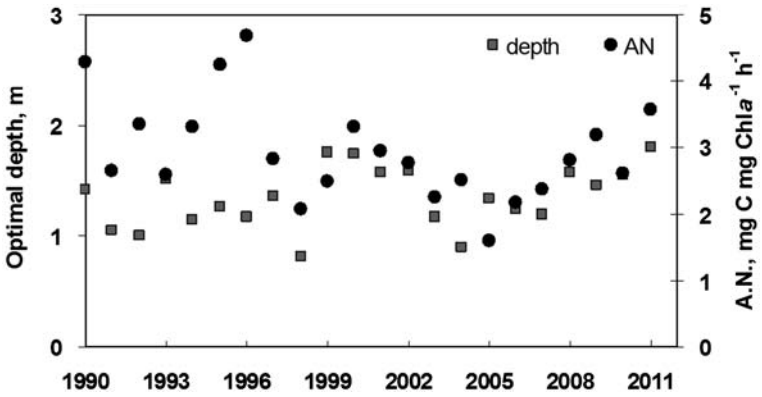

Fig. 24.8 Annual average of assimilation number (*A.N.*) at optimal depth (*OD*) and the location of optimal depth (m) from 1990 to 2011

water temperatures, insolation, and PAR within the water column were low as compared to summer–autumn. When the lake became strongly stratified, part of this nutrient supply was retained within the plankton biomass in the epilimnion. During the stratification period, this store of nutrients was actively recycled within the epilimnion and provided the main nutrient source for phytoplankton in the upper, productive water layers in summer. This was probably the reason for the significant correlations between the average rates of PP in winter–spring and those in the following summer–autumn period (Fig. 24.9a). A positive correlation between the average Chl *a* in winter–spring and Chl *a* in the subsequent summer–autumn period was also observed (Fig. 24.9b).

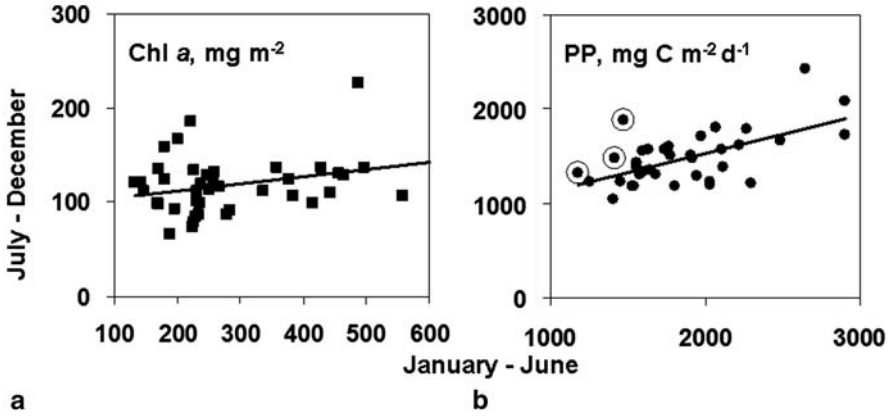

Fig. 24.9 Pair-wise comparison of semiannual averages of **a** *Chl a* and **b** *PP*. Years with a higher summer–autumn *PP* than winter–spring average are circled. Regression lines: (a) $r^2 = 0.12$, $p < 0.029$, $n = 42$; (b) $r^2 = 0.37$, $p < 0.001$, $n = 37$

The fluxes of particles and solutes, which strongly affect nutrient availability for phytoplankton, depend on the thermal structure of the lake. The long-term continuous change in the thermal structure of Lake Kinneret reported for the period 1969–2008 was reflected by a decrease in epilimnion thickness of ~3 cm year^{-1} and an average epilimnion temperature increase of ~0.028°C year^{-1} (Rimmer et al. 2011). The increased range of annual water-level fluctuations together with the trend of decreasing lake levels was most probably the trigger for these slight, but detectable modifications in the thermal structure and may have impacted the entire lake ecosystem. Serruya and Pollingher (1977) and Hambright et al. (1997) proposed the following cascade of events for a situation of declining lake levels: (1) a decrease in hypolimnion volume, (2) enhanced nutrient concentrations in the hypolimnion, (3) increased nutrient concentrations in the epilimnion following lake mixing, and (4) changes in phytoplankton population composition and reduction of total algal biomass. As predicted, N and P concentrations in the hypolimnion have indeed increased with the water level lowering (Zohary and Ostrovsky 2011). However, the observed response of phytoplankton after lake overturn and holomixis only partially followed the predicted sequence of events. Changes in phytoplankton community composition have occurred (Zohary 2004), but total phytoplankton biomass, determined as Chl *a,* did not decline but, on the contrary, increased in summer (Fig. 24.5).

In summary, four decades of monitoring Chl *a* and PP in Lake Kinneret have showed wide ranges of variability (Fig. 24.5). Seasonal patterns of Chl *a* and PP that characterized the lake from 1970 until the mid-1990s have changed dramatically. The regular appearance of the late-winter–spring bloom of *P. gatunense* has become erratic. In years without blooms, maximum values of Chl *a* and PP were not observed in April or May, but either earlier or in summer, in sharp contrast to the typical pattern found until the mid-1990s (Fig. 24.10).

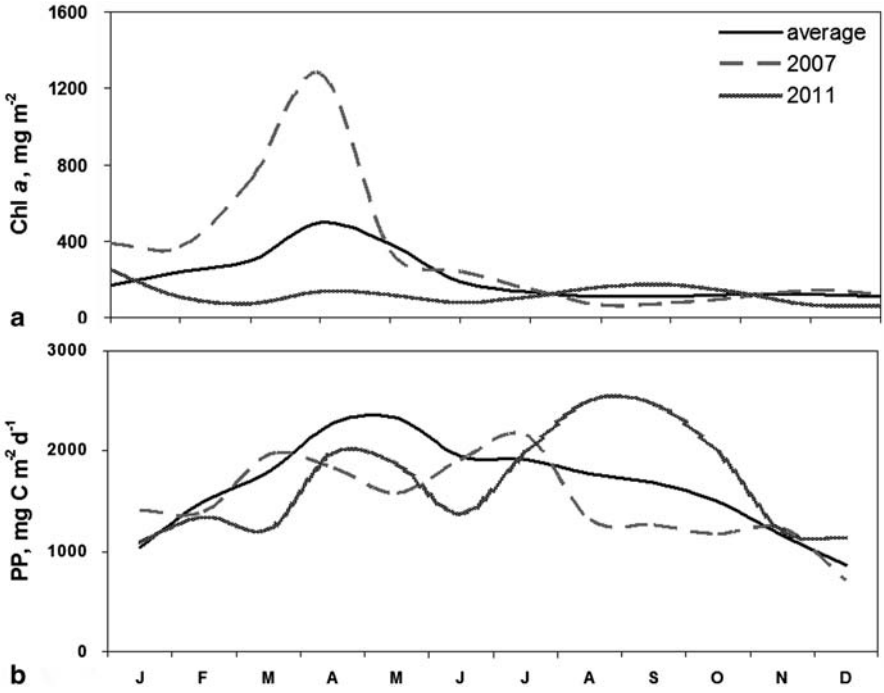

Fig. 24.10 Monthly averages of **a** *Chl a* and **b** *PP* calculated for depth-integrated profiles. Averages for 2007, a "Peridinium year," are compared with averages for 2011, a "non-Peridinium year" and with the multiannual average

24.1.6 Primary Production in the Carbon Balance of Lake Kinneret

The standard ^{14}C method used since 1972 in Lake Kinneret for measurement of PP is based on the uptake of radiolabeled carbon and yields a result between gross primary production (GPP) and net primary production (NPP). The ^{14}C method may even underestimate NPP (based on oxygen metabolism measurements), if the uptake of the radioisotope is hindered by intracellular or environmental factors (Ostrom et al. 2005; Yacobi et al. 2007). Part of the fixed carbon is readily respired or lost in exudates (Berman 1976b); therefore, the amount of ^{14}C retained in the particulate matter underestimates the total carbon uptake or GPP (Berman and Pollingher 1974; Williams and Robertson 1991; Marra 2009). GPP, however, is a critical parameter in any estimation of ecosystem carbon flux (Häkanson and Peters 1995).

A recent study by Parparov and Yacobi (unpublished) compared ^{14}C to ΔO_2 methods for measuring primary production. GPP was measured by ΔO_2 concentration in light and dark bottles incubated for 24 h in situ in the lake, together with ^{14}C uptake in separate, parallel samples. A close relationship was found between

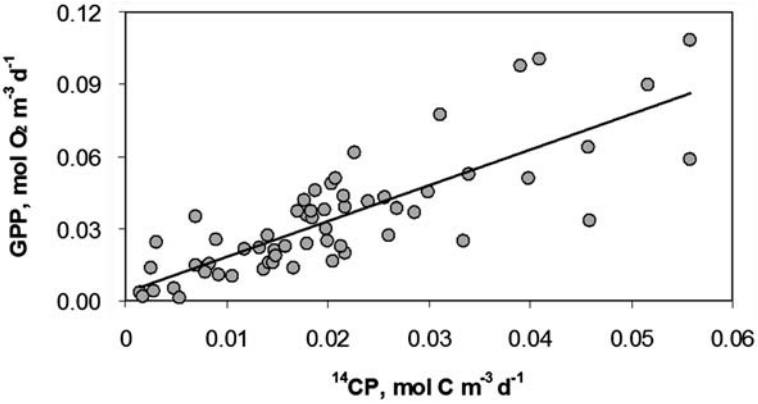

Fig. 24.11 Comparison of primary production measurements based on the ^{14}C method (^{14}CP) versus gross primary production (*GPP*). *GPP* is based on the measurement of ΔO_2 in light and dark bottles incubated for 24 h in situ from 0 to 5 m in Lake Kinneret. The experiments were carried out from October 2005 to June 2006. The regression equation is given by GPP = 1.48* ^{14}CP + 0.003 ($r^2 = 0.44$, $n = 64$, $p < 0.001$). The line represents a 1:1 ratio

these two variables ($r^2 = 0.44$, $p < 0.0001$, $n = 64$), with an O_2:C molar ratio of ~1.5 (Fig. 24.11). Thus, it appears that the PP values obtained by the ^{14}C method that has been routinely used in Lake Kinneret since 1972 are close to NPP (Berman and Pollingher 1974; Figs. 24.12 and 24.13).

Throughout most of the year, GPP measured by the uptake of $^{18}O_2$ (supplied to the medium as $H_2{}^{18}O_2$) was higher by a factor of approximately 2 than PP measured by the ^{14}C method. However, when there were dense crops of *P. gatunense* in the lake, PP measured with $^{18}O_2$ was sevenfold higher than PP measured with ^{14}C; far higher than the limits found in other aquatic systems. This extremely high ratio between $^{18}O_2$ and ^{14}C-based PP estimates was explained as resulting, at least in part, from oxygen uptake by the Mehler reaction and from the recycling of the ^{14}C tracer by dark respiration and the alternative oxidase (AOX) pathway (Luz et al. 2002).

Primary production is the major source for organic carbon in Lake Kinneret, fixing approximately 608 g m^{-2} $year^{-1}$, or when extrapolated to the entire lake area, ~1.02×10^5 ton C $year^{-1}$ (based on ^{14}C uptake values). External inputs of organic carbon are much lower; the average annual input from the Jordan River is 1.8×10^3 ton organic C $year^{-1}$ (Lake Kinneret database). The major sinks of organic carbon, respiration (Berman et al. 2009; Sect. 25.1), and sedimentation (Ostrovsky and Yacobi 2010; Chap. 27) taken together are approximately equal to the organic carbon provided to the system by primary production. Lake Kinneret is thus net autotrophic (Sect. 25.5). Net autotrophy may be rather the rule than the exception for lakes such as Lake Kinneret, located in arid and semiarid zones, where the water supply is limited and seasonally restricted with low levels of soil organic matter-content in the surrounding watershed.

24.2 Chemosynthetic Primary Production: A Missing Input into the Carbon Cycle

Ora Hadas, Jonathan Erez

24.2.1 Introduction

All organisms require carbon and energy sources to drive cellular maintenance, growth, biosynthesis, and function. The carbon source can be obtained by the conversion of CO_2 to organic carbon (autotrophy) or by consuming fixed organic material (heterotrophy). Energy can come from light (radiant) and be converted to chemical energy via the process of photosynthesis or from oxidation–reduction processes using inorganic or organic molecules. Organisms that use CO_2 as their carbon source and get their energy by oxidizing inorganic reduced chemicals are defined as chemolithoautotrophs or chemoautotrophs (Konhauser 2007).

Chemoautotrophs use inorganic energy sources, such as hydrogen sulfide, elemental sulfur, thiosulfate, tetrathionate, ferrous iron, molecular hydrogen, methane, and ammonia. Most are bacteria or archaea that utilize the chemical energy released when those reduced compounds are oxidized for CO_2 fixation. They generally fall into several groups: sulfur oxidizers and reducers, methanogens, nitrifiers, anammox bacteria, and thermoacidophiles.

Oxic–anoxic interfaces (chemoclines) are favorable for growth of chemoautotrophic bacteria, which oxidize H_2S and other reducing substances to obtain energy for CO_2 fixation. The microscale mixing patterns within the chemocline will control the temporal and spatial distribution of the various sulfide-oxidizing, ammonium-oxidizing, and other oxidizing microorganisms.

H_2S and NH_4^+ are the most important electron donors for chemosynthesis in Lake Kinneret. Chemoautotrophic bacteria, which oxidize H_2S (*Thiobacillus*, *Thiomicrospira,* and *Beggiatoa*), require the concomitant presence of both suitable electron acceptors and suitable electron donors. Oxygen is the preferred electron acceptor for all sulfide oxidizers, but nitrate and oxidized iron may serve as alternative acceptors. Furthermore, denitrification processes in the lake may be driven by sulfide-oxidizing bacteria (Sect. 25.3). Ammonium and nitrite (via nitrification), hydrogen gas (utilized by some sulfate-reducing bacteria), and methane (used by methanotrophs) are other reduced compounds used by chemoautotrophs in Lake Kinneret. This chapter describes spatial and temporal variations in chemosynthetic primary production due to H_2S oxidation, and its relative importance in the carbon cycle in Lake Kinneret. Ammonium oxidation is addressed in Chap. 22)

24.2.2 Oxic–Anoxic Interfaces (Chemoclines)

In Lake Kinneret, oxic–anoxic interfaces are found at different locations at different times of the year. In the pelagic water, such interfaces are found within the

metalimnic layer, during stable stratification (June–December). A chemocline with a steep gradient of sulfide (H_2S), ammonium (NH_4), and dissolved oxygen (DO) is formed and creates unique chemical conditions for various groups of microbial communities. During summer, when the oxic–anoxic (O_2–H_2S) interface is between 14 and 20 m, where some light is still available (~0.1 to 1 % of the incident light), the development of photosynthetic bacteria performing anoxygenic photosynthesis is observed, contributing about 1 % to primary production of the lake (Butow and Bergstein-Ben Dan 1992; Sect. 15.2). In October, this thermocline/oxycline deepens below the euphotic zone, excluding photosynthetic but not chemoautotrophic carbon fixation.

Chemoclines are also formed in the deeper part of the water column in late spring when fresh organic matter is supplied to the hypolimnion, benthic boundary layer, and sediments due to degradation of phytoplankton blooms (such as *P. gatunense* and *Mougeotia* sp.). There is a decrease and depletion in oxygen and, due to intensive sulfate-reduction processes in the hypolimnion, H_2S is released near to "pockets" and layers of the still oxygenated water column, forming local chemoclines suitable for chemosynthetic activity (Chap. 21). In addition, a chemocline is formed near the bottom sediments, where H_2S and ammonium are released to the overlying water in late spring–early summer. *Beggiatoa* sp. mats are observed at the sediment–water interface during this period all over the lake (Hadas and Pinkas 1995a).

In the littoral and sublittoral zones, where physical processes such as "wave break" and resuspension of the sediments provide a continuous supply of H_2S from the sediments to the oxygenated water column, an oxic–anoxic interface exists year-round with intensive chemoautotrophic activity. For details on physical processes and thermocline/chemocline structure, see Chap. 9.

24.2.3 Methods

Chemosynthetic carbon fixation was measured by the ^{14}C method in parallel light and dark bottles, with and without the addition of 5 μM 3-(3, 4-dichlorophenyl)-1, 1-dimethylurea (DCMU), an inhibitor of photosystem II. This approach enabled distinguishing between photosynthetic (in the light) and chemosynthetic (dark) carbon fixation (Hadas et al. 2001).

24.2.4 Chemosynthesis in the Lower Water Mass and Sediment–Water Interface During the Formation of the Chemocline (May)

In early summer, when the thermocline and chemocline begin to develop, they are at different depths. The thermocline forms by warming of epilimnic surface water while the chemocline starts to develop at the sediment–water interface as the result of anaerobic mineralization processes. Oxic–anoxic interfaces can be found throughout the entire lower water mass, where sulfide and DO coexist at low concentrations,

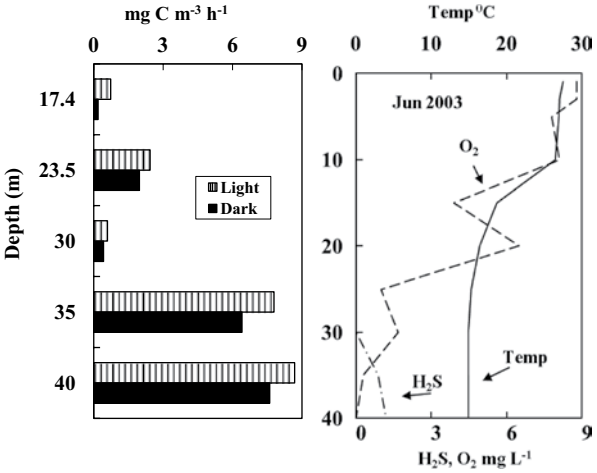

Fig. 24.12 **a** Photosynthetic and chemosynthetic carbon fixation rates at the time of chemocline formation at Sta. A, June 2003. **b** Depth profiles of temperature, dissolved oxygen, and sulfide concentrations at the time of sampling. Due to the cold and rainy winter of 2003, the beginning of stratification shifted from May to June

favoring mainly H_2S-based bacterial chemosynthesis (Fig. 24.12). Chemosynthetic carbon fixation ranged from 0.42 ± 0.01 to 16.9 ± 1.24 mg C m^{-3} h^{-1} at depths of 30 and 40 m in 2003 and 2004, respectively. The low carbon fixation rate measured at 30 m in 2003 was the result of the DO concentrations at this depth (Fig. 24.12 and Chap. 21), conditions which were not favorable for chemosynthetic sulfide oxidation. In May 1995, a 4-m-thick chemocline region, at the benthic boundary layer, at 38–42 m, showed chemosynthetic activity ranging from 9.83 ± 0.15 to 12 ± 0.15 mg C m^{-3} h^{-1} (Hadas et al. 2001).

24.2.5 Chemosynthesis in the Metalimnion in Autumn, the Time of Chemocline Deepening

Chemosynthesis was measured as dark $^{14}CO_2$ fixation in the metalimnion of Lake Kinneret at Station A (Sta. A), from October, when the chemocline declines below the euphotic zone, until a turnover in December or January. At that time, the chemocline was characterized by steep gradients of H_2S and DO and a thin layer of 0.5–2.0 m thickness, where the two coexisted (up to 0.4 mg L^{-1} of oxygen and 0.2 mg L^{-1} of H_2S). As the thermocline deepened, the temperature gradient was smaller, but the steep gradients of O_2 and H_2S at the chemocline were maintained or even increased. Measured rates of dark $^{14}CO_2$ fixation were in the range of 0.4–40 mg C m^{-3} h^{-1} with the highest value recorded at 32.5-m depth at Sta. A in December 1996, when the activity was restricted to a 0.5-m-thick chemocline. The thickness and depth of the interface layer in the pelagic waters in the lake varied as a result of internal waves. The amplitude of the thermocline/chemocline tilt due to seiche oscillations can reach 10 m over 24 h, causing mixing and displacement of water layers within the metalimnion (Serruya 1975; Chap. 9). These daily mixing events can enhance the chemosynthetic process by mixing DO and H_2S within the

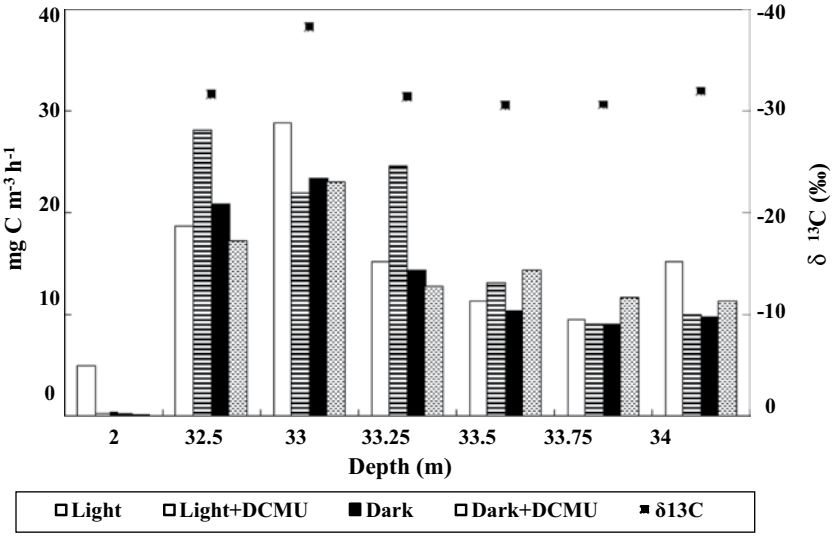

Fig. 24.13 Carbon fixation rates (mg C m^{-3} h^{-1}) in the dark and in the light, with and without the addition of DCMU (*bars*), and the isotopic composition of the total particulate organic matter (™^{13}C, ‰, symbols) at 2 m depth and at various depths within the chemocline at Sta. A, 12 December 1994

chemocline. For example, during 2 days between 15 and 17 December 1996, the chemocline shifted upwards by 8 m (from 32 to 24 m), with chemoautotrophic dark CO_2 fixation of 40 and 29 mg C m^{-3} h^{-1}, respectively. In December 1994, a ~2-m-thick chemocline was located at a depth of 32–34 m (Fig. 24.13) in which much higher chemosynthetic carbon fixation was measured (23.4 ± 2.2 mg C m^{-3} h^{-1}) than photosynthetic carbon fixation (5 ± 0.9 mg C m^{-3} h^{-1}) at 2 m in the euphotic zone. In water, from 2-m depth, carbon fixation was totally inhibited in the dark or in the presence of DCMU, whereas dark carbon fixation in the sample from the chemocline was entirely due to bacteria and was DCMU-resistant (Hadas et al. 2001).

Photosynthetic primary production in the euphotic zone (0–15 m) from October to December averaged 1,300 ± 686 mg C m^{-2} day^{-1} during the years 1992–1996. Chemoautotrophic primary production at the chemocline (below the euphotic zone) over the same period averaged 314 ± 172 mg C m^{-2} day^{-1}, i.e., ~24% of the photosynthetic primary production during that period. The maximal monthly value for chemosynthesis was observed in December 1992 when it reached 92% of the photosynthetic production fixation. In May 1992, photosynthetic and chemosynthetic primary production values averaged 3,276 ± 972 and 533 ± 453 mg C m^{-2} day^{-1}, respectively, i.e., chemosynthetic production was 16% of photosynthetic production (Table 24.3). Similar values were measured at Sta. A in June 1997. The difference in primary production between the two periods was due to the characteristic yearly bloom of *P. gatunense* in winter/spring with 7–10 times higher biomass than that of nanophytoplankton in summer/autumn (Berman et al. 1995). It should be stressed that these values were measured during the 1990s based on integrated values of che-

Table 24.3 Chemosynthetic (chemo) and photosynthetic (photo) carbon fixation (PP) at Sta. A. (Data represent depth-integrated values[a] for three characteristic seasons in Lake Kinneret). (Reproduced from Hadas et al. 2001 with permission from ASLO)

Period	Photo PP (mg C m^{-2} day^{-1})	Chemo PP (mg C m^{-2} day^{-1})	Chemo/Photo (%)
Early summer (May)	3,276 ± 972	533 ± 453	16 % range (9–28)
Summer (June)	1,883	305.7	16 % range (11–16)
Autumn–Winter (October–December)	1,300 ± 686	314 ± 172	24 % range (8–92)

[a] Integrated depths for photosynthetic primary production 1–15 m and chemosynthetic production at the chemocline ranging from 20 to 35.5 m

mosynthesis of 4 m above the sediments. Recent studies indicated that chemosynthesis may also occur at O_2 and H_2S interfaces within the hypolimnion (Fig. 24.12), and its contribution to the carbon fixation during this period may be much higher, depending on the extent of sulfide and oxygen coexistence, which differs from year to year.

24.2.6 Bacterial Carbon Fixation at the Shallow Areas of the Lake

During the period of the *Peridinium* bloom, the littoral zone is characterized by the highest PP and biomass, providing the sediments with fresh organic matter after the degradation and decomposition of the bloom. This supply of decomposed organic matter results in intensive sulfate reduction within the sediments and H_2S production (Hadas and Pinkas 1995b; Hadas et al. 2000). Wind and resuspension processes induce mixing at this area, and reduced materials, mostly H_2S and NH_4, are released from the sediments to meet oxic waters and form chemoclines. The appearance of white filamentous bacterial mats of *Beggiatoa* on sulfide-rich sediments indicates high organic load and oxygen depletion (Sweerts et al. 1990).

In the euphotic littoral and sublittoral zones, where light reached the chemocline, the continuous supply of sulfide supported bacterial photosynthetic carbon fixation as well. Photosynthetic bacteria contributed 40 % of the bacterial carbon fixation in this region (Hadas et al. 2000). In addition, in the sublittoral of the lake, fish avoided the zone of 1–2 m from the bottom sediments, implying that this layer with reduced compounds (H_2S) is toxic (Ostrovsky et al. 1996).

24.2.7 Chemoautotrophic Activity and Carbon Isotopes

Carbon flow between different trophic levels in marine and freshwater ecosystems can be traced by stable carbon isotope ratios of various components in the food web (e.g., Fry and Sherr 1984; Rau et al. 1990; Kelley et al. 1998; Fry 2006). In Lake Kinneret, two phenomena were observed, i.e., (1) in late autumn–early winter, low

standing stocks of phytoplankton and (2) low Chl *a* concentrations were observed in the water column (Chap. 10). At this time, the zooplankton was characterized by very low $\delta^{13}C$ values (ca. −34‰; Zohary et al. 1994). These negative $\delta^{13}C$ values did not correspond to those expected if the zooplankton had been feeding on nanoplanktonic algae which have 6–10‰ more positive $\delta^{13}C$ values. This raised the question of what food source zooplankton were using during this period. Because chemoautotrophic bacteria have highly negative $\delta^{13}C$ signatures (Ruby et al. 1987), it was proposed that these bacteria served as the major carbon source for zooplankton during this season, either directly or via the microbial food web.

The $\delta^{13}C$ values of total particulate carbon in the chemocline of Lake Kinneret ranged from −27 to −39‰. Particulate organic matter from water layers in the lake with high bacterial chemosynthetic activity was found to have low $\delta^{13}C$ (Zohary et al. 1994), typical of chemosynthetic bacteria (Cavanaugh et al. 1981). The total particulate carbon of pelagic waters in Lake Kinneret had lighter carbon composition as compared to the littoral stations. The relatively higher abundance of photosynthetic bacteria, characterized by heavy carbon composition, may have contributed to the heavier carbon composition in the shallow area of the lake.

There are two main possibilities to explain the low $\delta^{13}C$ values displayed by the chemosynthetic bacteria. First, the $\delta^{13}C$ of the hypolimnetic inorganic carbon is low, in the range of −6 to −8‰ (Stiller and Nissenbaum 1999). Second, the pH in these waters is 7.8, and hence the $CO_{2(aq)}$ concentrations are high, well above 100 µM, so that the bacteria can fractionate carbon isotopes at their maximum capacity. With the deepening of the thermocline and oxycline below the euphotic zone in October and during the formation of the chemocline (April–May), there was an increase in both numbers and biovolumes of ciliates in this region. In December 1996, at 32.5-m depth, an almost pure culture of *Coleps hirtus* was observed (180 *Coleps* ml^{-1}), corresponding to high dark carbon fixation (~40 mg C m^{-3} h^{-1}) and low $\delta^{13}C$ value of −31.59‰, suggesting that *Coleps* was feeding on chemoautotrophic bacteria. Other protozoa present were the ciliates *Cyclidium, Vorticella mayeri,* and small flagellates. High numbers of anaerobic or facultative ciliates (*Saprodinium dentatum, Plagiopyla*) were observed near the bottom sediments in April–May, feeding on sulfur cycle bacteria. Zooplankton may feed on these ciliates (Chaps. 14 and 17) and this way acquires the observed low $\delta^{13}C$ isotopic signatures in winter.

24.2.8 Conclusions

Bacterial chemosynthetic production in Lake Kinneret is significant and should be taken into account in the carbon budgets calculated for the lake as well as in food web carbon fluxes. It should be stressed that this production was energetically derived from organic carbon, which at an earlier stage was fixed by photosynthesis. The use of reduced compounds (sulfide, ammonium, and methane) originating from anaerobic metabolism, which is energetically inefficient, can be partly compensated by utilization of these compounds. In this way, at least part of the photosynthetic energy, potentially convertible to biomass under aerobic conditions, can be gained

back by chemosynthesis; otherwise, this energy would be completely lost to the system. The phylogenetic lineages of the microbial populations involved in chemoautotrophic processes in the lake should be elucidated in the future using molecular biology tools.

Acknowledgments This chapter is based on data collected mainly by KLL supporting staff. YZY thanks Ms. Sara Chava and Mr. Semion Kaganovsky for their skilled and devoted work on the lake and in the laboratory. Skippers Mr. Moti Diamant and Mr. Oz Tsabari-Dar were essential and reliable partners in the execution of the lake work. The Israeli Water Commission and the Israeli Ministry of Science (MOS) grant no. 0033-GR01421 via DISUM-BMFT program supported the chemosynthetic production study.

References

Berman T (1976a) Light penetrance in Lake Kinneret. Hydrobiologia 49:41–48

Berman T (1976b) Release of dissolved organic matter by photosynthesizing algae in Lake Kinneret, Israel. Freshw Biol 6:13–18

Berman T, Pollingher U (1974) Annual and seasonal variations of phytoplankton, chlorophyll and photosynthesis in Lake Kinneret. Limnol Oceanogr 19:31–54

Berman T, Yacobi YZ, Pollingher U (1992) Lake Kinneret phytoplankton: stability and variability during twenty years (1970–1989). Aquat Sci 54:104–127

Berman T, Stone L, Yacobi YZ, Kaplan B, Schlichter M, Nishri A, Pollingher U (1995) Primary production and phytoplankton in Lake Kinneret: a long-term record (1972–1993). Limnol Oceanogr 40:1064–1076

Berman T, Yacobi YZ, Parparov A, Gal G (2009) Estimation of long-term bacterial respiration and growth efficiency in Lake Kinneret. FEMS Microbiol Ecol 71:351–363

Butow B, Bergstein-Ben Dan T (1992) Occurrence of *Rhodopseudomonas palustris* and *Chlorobium phaeobacteroides* blooms in Lake Kinneret. Hydrobiologia 232:193–200

Cavanaugh CM, Gardiner SL, Jones ML, Jannasch HW, Waterbury JB (1981) Prokaryotic cells in the hydrothermal vent tube worm *Riftia pachyptila Jones*: a possible chemosynthetic symbiont. Science 213:340–342

Dubinsky Z, Berman T (1976) Light utilization efficiencies of phytoplankton in Lake Kinneret (Sea of Galilee). Limnol Oceanogr 21:226–230

Dubinsky Z, Berman T (1979) Seasonal changes in the spectral composition of downwelling irradiance in Lake Kinneret (Israel). Limnol Oceanogr 24:652–663

Erez J, Bouevitch A, Kaplan A (1998) Carbon isotope fractionation by photosynthetic aquatic microorganisms: experiments with *Synechococcus* PCC 7942 and simple carbon flux model. Can J Bot 76:1109–1118

Fry B (2006) Stable isotope ecology. Springer, Heidelberg

Fry B, Sherr E (1984) $\delta^{13}C$ measurements as indicators of carbon flow in marine and fresh waters ecosystems. Contrib Mar Sci 27:13–47

Hadas O, Pinkas R (1995a) Sulfate reduction in the hypolimnion and sediments of Lake Kinneret, Israel. Freshw Biol 33:63–72

Hadas O, Pinkas R (1995b) Sulfate reduction processes in sediments at different sites in Lake Kinneret, Israel. Microb Ecol 30:55–66

Hadas O, Rushansky-Malinsky N, Pinkas R, Halicz E, Erez J (2000) High chemoautotrophic primary production across a transect in Lake Kinneret, Israel. Arch Hydrobiol Spec Issues Adv Limnol 55:413–420

Hadas O, Pinkas R, Erez J (2001) High chemoautotrophic primary production in Lake Kinneret, Israel—a neglected link in the C cycle of the lake. Limnol Oceanogr 46:1968–1976

Hakanson L, Peters RH (1995) Predictive limnology: methods for predictive modelling. SPB Academic, Amsterdam
Hambright KD, Zohary T, Eckert W (1997) Potential influence of low water levels on Lake Kinneret: re-appraisal and modification of an early hypothesis. Limnologica 27:149–155
Hepher B, Langer J (1970) On the primary production by phytoplankton in Lake Kinneret (Tiberias). Sea Fish Res Stn Haifa Bull 55:21–61
Holm-Hansen O, Lorenzen CJ, Holmes RW, Strickland JDH (1965) Fluorometric determination of chlorophyll. J Cons Cons Int Explor Mer 30:3–15
Imberger J (1994) Transport processes in lakes. In: Margalef R (ed) Limnology now, a paradigm of planetary problems. Elsevier, Oxford
Kelley CA, Coffin RB, Cifuentes LA (1998) Stable isotope evidence for alternative bacterial carbon sources in the Gulf of Mexico. Limnol Oceanogr 43:1962–1969
Kirk JTO (1994) Light and photosynthesis in aquatic ecosystems. Cambridge University, Cambridge
Konhauser K (2007) Introduction to geomicrobiology. Blackwell, London
Luz B, Barkan E, Sagi Y, Yacobi YZ (2002) Evaluation of community respiratory mechanisms with oxygen isotopes: a case study in Lake Kinneret. Limnol Oceanogr 47:33–42
Marra J (2009) Net and gross productivity: weighing in with 14C. Aquat Microb Ecol 56:123–131
Nishri A (2010) Phosphorus and nitrogen transport mechanisms from the Hula Valley to the Jordan River. Isr J Earth Sci 58:87–98
Nishri A, Imberger J, Eckert W, Ostrovsky I, Geifman Y (2000) The physical regime and the respective biogeochemical processes in the lower water mass of Lake Kinneret. Limnol Oceanogr 45:972–981
Ostrom NE, Carrick HJ, Twiss MR, Pieinsky L (2005) Evaluation of primary production in Lake Erie by multiple proxies. Oecologia 144:115–124
Ostrovsky I, Yacobi YZ (2010) Sedimentation flux in a large subtropical lake: spatio-temporal variations and relation to primary productivity. Limnol Oceanogr 55:1918–1931
Ostrovsky I, Yacobi YZ, Walline P, Kalikhman I (1996) Seiche induced mixing: its impact on lake productivity. Limnol Oceanogr 41:323–332
Ostrovsky I, Rimmer A, Yacobi YZ, Nishri A, Sukenik A, Hadas O, Zohary T (2013) Long-term changes in the Lake Kinneret ecosystem: the effects of climate change and anthropogenic factors. In: Goldman CR, Kumagai M, Robarts RD (eds) Climatic change and global warming of inland waters: impacts and mitigation for ecosystems and societies. Wiley, pp 271–293. ISBN:9781118470596. doi:10.1002/9781118470596.ch16
Pollingher U, Berman T (1977) Quantitative and qualitative changes in the phytoplankton of Lake Kinneret, Israel, 1972–1975. Oikos 29:418–428
Pollingher U, Berman T (1982) Relative contributions of net and nanno phytoplankton to primary production in Lake Kinneret (Israel). Arch Hydrobiol 96:33–46
Rimmer A, Gal G, Opher T, Lechinsky Y, Yacobi YZ (2011) Causes for long-term variations of thermal structure in a warm lake. Limnol Oceanogr 56:974–988
Rau GH, Teyssie JL, Rassoulzadegan F, Fowler SW (1990) $^{13}C/^{12}C$ and $^{15}N/^{14}N$ variations among size-fractionated marine particles: implications for their origin and trophic relationships. Mar Ecol Prog Ser 59:33–38
Rohde W (1972) Evaluation of primary production parameters in Lake Kinneret (Israel). Verh Int Ver Limnol 18:93–104
Ruby EG, Jannasch HW, Deuser WG (1987) Fractionation of stable carbon isotopes during chemoautotrophic growth of sulfur-oxidizing bacteria. Appl Environ Microbiol 53:1940–1943
Serruya C (1972) Metalimnic layer in Lake Kinneret, Israel. Hydrobiologia 40:355–359
Serruya S (1975) Wind, water temperature and motion in Lake Kinneret: general pattern. Int Ver Theor Angew Limnol Verh 19:73–87
Serruya C, Pollingher U (1977) Lowering of water level and algal biomass in Lake Kinneret. Hydrobiologia 54:73–80
Steemann-Neilsen E (1952) The use of radioactive carbon (^{14}C) for measuring organic production in the sea. J Cons Cons Int Explor Mer 18:117–140

Stiller M, Nissenbaum A (1999) A stable carbon isotope study of dissolved in organic carbon in hardwater Lake Kinneret (Sea of Galilee). S Afr J Sci 95:166–170

Sweerts JP, De Beer RA, Nielsen LP, Verdouw H, Van Den Heuvel JC, Cohen Y, Capenberg TE (1990) Denitrification of sulfur oxidizing *Beggiatoa* spp. mats on freshwater sediments. Nature 344:762–763

Williams PJ leB, Robertson JE (1991) Overall planktonic oxygen and carbon dioxide metabolisms: the problem of reconciling observations and calculations of photosynthetic quotients. J Plankton Res 13(Suppl):153–169

Yacobi YZ (2003) Seasonal variation of photosynthetic pigments in the dinoflagellate *Peridinium gatunense* (Dinophyceae) in Lake Kinneret Israel. Freshw Biol 48:1850–1858

Yacobi YZ (2006) Temporal and vertical variation of chlorophyll *a* concentration, phytoplankton photosynthetic activity and light attenuation in Lake Kinneret: possibilities and limitations for simulation by remote-sensing. J Plankton Res 28:725–736

Yacobi YZ, Ostrovsky I (2008) Downward flux of organic matter and pigments in Lake Kinneret (Israel): relationships between phytoplankton and the material collected in sediment traps. J Plankton Res 30:1189–1202

Yacobi YZ, Pollingher U (1993) Phytoplankton composition and activity: response to fluctuations in lake volume and turbulence. Verh Int Ver Limnol 25:796–799

Yacobi YZ, Zohary T (2010) Carbon: chlorophyll *a* ratio, assimilation numbers and turnover times in Lake Kinneret phytoplankton. Hydrobiologia 639:185–196

Yacobi YZ, Perel N, Barkan E, Luz B (2007) Unexpected underestimation of primary productivity by ^{18}O and ^{14}C methods in a lake: implications for slow diffusion of isotope tracers in and out of cells. Limnol Oceanogr 52:329–337

Yashouv A, Alhunis M (1961) The dynamics of biological processes in Lake Tiberias. Bull Res Counc Isr (B) 10:12–35

Zohary T (2004) Changes to the phytoplankton assemblage of Lake Kinneret after decades of a predictable, repetitive pattern. Freshw Biol 49:1355–1371

Zohary T, Ostrovsky I (2011) Ecological impacts of excessive water level fluctuations in stratified freshwater lakes. Inland Waters 1:47–59

Zohary T, Erez J, Gophen M, Berman-Frank I, Stiller M (1994) Seasonality of stable carbon isotopes within the pelagic food web of Lake Kinneret. Limnol Oceanogr 39:1030–1043

Chapter 25
The Fate of Organic Carbon

Tom Berman, Arkadi Parparov, Ora Hadas, Yosef Z Yacobi, Orit Sivan, Ilia Ostrovsky and Werner Eckert

Abstract In Lake Kinneret, the majority of photosyntetically produced organic carbon (OC) is cycled through the microbial loop. Taken together, bacterial production (BP) and bacterial respiration (BR), i.e., bacterial carbon demand (BCD), accounted for about 65 % of gross primary production (GPP), measured biweekly and averaging 2.3 g C m^{-2} day^{-1} during the last decade (2001–2011). Community respiration (CR) was 2.1 g C m^{-2} day^{-1}. The major contributors to total CR were bacterial and phytoplankton respiration (~80%) while zooplankton respiration accounted for the reminder. Most (~ 83 %) of the OC input were eventually respired, ~3 % lost to outflows, while ~15 % of the total OC input were transferred annually to the sediments. Here oxic mineralization is gradually replaced by anoxic processes as a function of the availability of suitable electron acceptors. After the depletion of oxygen in the hypolimnion, sulfate (500 μM) becomes the dominant oxidant. Depending on the settling flux of OC sedimentary sulfate reduction (SR) rates were measured from 0.01 to 1.67 μmol cm^{-3} day^{-1} in December and July, respectively. SR is the dominant anaerobic terminal decomposition process in Lake Kinneret and is responsible for the accumulation of sulfide in the hypolimnion to concentrations up to 400 μM. Methanogenesis is restricted to those sediment layers that are depleted of sulfate (below 3–5 cm). Seasonal profiles and 13C signatures of dissolved methane in the

W. Eckert (✉) · T. Berman · A. Parparov · O. Hadas · Y. Z Yacobi · I. Ostrovsky
The Yigal Allon Kinneret Limnological Laboratory, Israel Oceanographic & Limnological Research, P.O. Box 447, 14950 Migdal, Israel
e-mail: werner@ocean.org.il

O. Hadas
e-mail: orah@ocean.org.il

Y. Z Yacobi
e-mail: yzy@ocean.org.il

I. Ostrovsky
e-mail: ostrovsky@ocean.org.il

A. Parparov
e-mail: parpar@ocean.org.il

O. Sivan
Department of Geological and Environmental Sciences, Ben-Gurion University of the Negev, P.O. Box 653, 8410501 Beer-Sheva, Israel
e-mail: oritsivan@gmail.com

T. Zohary et al. (eds.), *Lake Kinneret, Ecology and Management,* Aquatic Ecology Series 6,
DOI 10.1007/978-94-017-8944-8_25,

sediment pore water of Lake Kinneret have indicated anaerobic methane oxidation in the deeper sediments (below 20 cm), with Fe(III) as electron acceptor. Lake Kinneret resembles the first aquatic ecosystem where the existence of this process could be verified. Changes in the watershed and lake environment are suggested as possible causes for the apparently significant declines in bacterial numbers, BP, and BCD that have taken place over the last decade in Lake Kinneret.

Keywords Heterotrophic bacteria · Respiration · Bacterial production · Growth efficiency · Sulfate reduction · Sediments · Methanogenesis · Methanotrophy · Benthic boundary layer · Net heterotrophic · Net autotrophic

25.1 Heterotrophic Bacterial Production, Respiration, and Growth Efficiency

Tom Berman, Arkadi Parparov, and Yosef Z Yacobi

25.1.1 Heterotrophic Bacteria in Organic Carbon Processing

As in most lakes, so too in Lake Kinneret, the metabolic activities of aerobic heterotrophic bacteria are major drivers of organic carbon (OC) cycling (Cole et al. 1988; del Giorgio and Williams 2005a). In Sect. 15.1, the patterns of bacterial abundance (BA) based on 4′,6-diamidino-2-phenylindole (DAPI) counts and some phylogenic and morphological data relating to Lake Kinneret bacteria are presented. Here, we shall show data concerning various aspects of bacterial metabolic activity and their far-reaching impacts on OC cycling of the lake.

25.1.2 Bacterial Production

The first set of monthly bacterial production (BP) measurements were made using the ^{3}H-thymidine method (Riemann et al. 1982) from June 1988 through May 1993 at five depths at Station A (location in Fig. 1.1 of Chap. 1). Routine measurements, using ^{14}C-leucine (Kirchman et al. 1985) were resumed only in 2001 on samples collected at Sta. A from 1, 5, 10, 20, 30, and 40 m and mid-thermocline depth. (For the ^{3}H-thymidine method, empirical conversion factors were used; literature values were used for the ^{14}C-leucine method.) The annual means for the two data sets (1988–1993 and 2001–2011) are shown in Fig. 25.1. Although the mean annual BP values for both periods appear to be very similar, it should be noted that during the first period sampling was much less frequent or complete than in 2001–2011. The former data set was used for the first models of carbon cycling in Lake Kinneret that emphasized and quantified the central role of the bacteria in carbon flux in this ecosystem (Stone et al. 1993; Berman and Stone 1994; Hart et al. 2000).

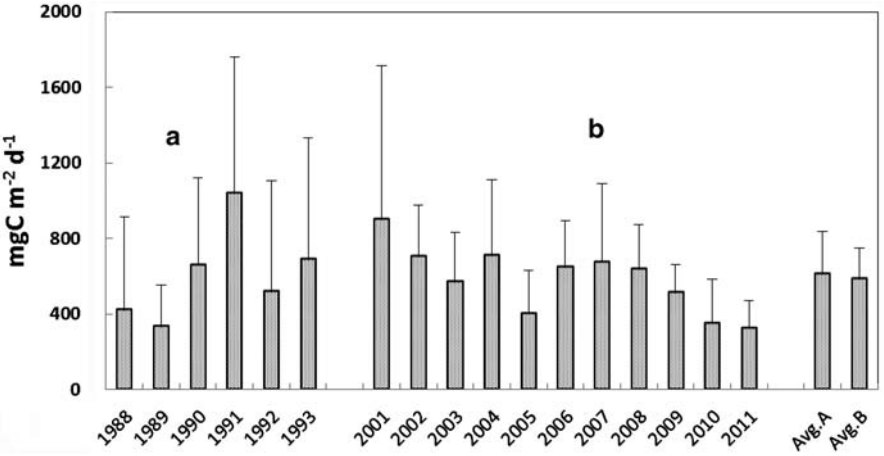

Fig. 25.1 Annual means (mg C m^{-2} d^{-1}) and standard deviations of bacterial production (*BP*) in the euphotic zone, 0–15 m at Sta. A. **a** From 1988 to 1993, measured with ^{3}H-thymidine. **b** From 2001 to 2011 measured with ^{14}C-leucine

From 2001 to 2011, the mean annual BP in the lake epilimnion was 558 ± 179 mg C m^{-2} day^{-1} with annual values ranging from 902 to 1,320 mg C m^{-2} day^{-1} in 2011 and 2001, respectively. Semiannual means of BP are given in Table 25.1. On a semiannual basis, BP ranged from 12 to 38 % (mean 25 %) and from 18 to 57 % (mean 38 %) of gross primary production (GPP) and net primary production (NPP), respectively. Until 2008, mean semiannual BP was always greater in January–June as compared to July–December, a pattern that also corresponded with PP levels. However, from 2009 through 2011, this pattern reversed, as has also been reported for primary production (see Chap. 24). Furthermore, as noted in Chap. 15, in the years from 2001 to 2011, there was a significant trend ($r^2 = 0.93$, $p < 0.0001$, $n = 11$) to lower annual average BA that coincided with a significant decrease ($r^2 = 0.57$, $p = 0.004$, $n = 11$) in BP; the annual means of BA and BP were also significantly correlated ($r^2 = 0.43$, $p = 0.028$, $n = 11$). The marked drop in BP has had a significant impact on OC flows within the lake system (see below).

The declines in the annual averages of both BA and BP in the epilimnic water do not appear to be correlated to any change in annual averages of phytoplankton biomass, primary production, or chlorophyll. Nevertheless, the apparently real and significant declining trend in BP and the changes in semiannual patterns of primary production and BP (Table 25.1; Fig. 25.1) appear to reflect a definite slowing down in the rate of OC cycling in the lake over the last decade. This trend may be a further indication of the profound ecosystem shift that has occurred (and is probably still ongoing) since the mid-1990s (Zohary and Ostrovsky 2011).

As previously reported for the period 2001–2007 (Berman et al. 2010), strong correlations were obtained from 2001 to 2010 between semiannual BP and total community respiration (CR; $r^2 = 0.67$, $p = < 0.0001$, $n = 22$). A rather weaker, but still significant correlation was observed between semiannual BP and GPP ($r^2 = 0.22$, $p = 0.03$, $n = 22$) from 2001 to 2011.

Table 25.1 Semiannual means of gross primary productivity (GPP, calculated as 1.5 *14C-measured primary productivity (see Chap. 24)), phytoplankton respiration (*PR*), community respiration (*CR*), bacterial productivity (*BP*), bacterial respiration (*BR*), and zooplankton respiration (*ZR*) from 2001 to 2011

	January–June						July–December					
	GPP	PR	CR	BP	BR	ZR	GPP	PR	CR	BP	BR	ZR
2001	2,610	780	2,460	990	1,120	560	2,350	710	2,150	810	970	480
2002	2,350	700	2,310	740	1,070	530	2,150	640	1,710	660	710	360
2003	3,050	910	3,190	720	1,520	760	1,850	550	1,560	420	670	340
2004	2,870	910	3,370	870	1,640	820	2,210	680	1,660	550	650	330
2005	1,770	530	1,940	400	940	470	1,990	600	1,450	400	570	280
2006	2,470	740	2,080	660	890	450	2,030	610	1,700	630	730	360
2007	2,520	760	2,920	840	1,440	720	1,960	590	2,090	510	1,000	500
2008	2,450	650	1,500	700	570	290	2,360	680	1,550	560	580	290
2009	2,130	670	1,420	510	500	250	2,220	630	1,720	510	730	360
2010	2,390	730	1,970	310	820	410	2,340	710	1,840	390	750	380
2011	1,980	590	1,410	300	540	270	2,850	860	nd	350	nd	nd
Average	2,420	725	2,234	640	1,005	503	2,210	660	1,743	526	736	368
SD	350	112	660	221	380	189	260	80	215	131	137	68

All values are in mg C m^{-2} day^{-1}
SD standard deviation, *nd* not defined

25.1.3 Bacterial Growth Rates and Turnover Times

The estimation of cell-specific C incorporation rates (expressed as fg C $cell^{-1}$ day^{-1} and calculated as BP/BA from samples taken monthly at five depths in Sta. A) from 2001 through 2011 falls within the expected ranges. Overall mean cell-specific carbon uptake for epilimnic depths (0–15 m) was 18.0 ± 1.2 fg C $cell^{-1}$ day^{-1}. Assuming a mean bacterial cell content of 30 fg C bacterial $cell^{-1}$ (Stone et al. 1993; Hart et al. 2000), this would give a mean carbon turnover (doubling) time of 3.1 ± 0.4 days. Note that despite the large decreasing trends observed in both the annual mean BA and BP, the ratio BP:BA (i.e., cell-specific carbon uptake) showed no significant trend and remained more or less constant throughout the period 2001–2011.

For hypolimnic depths (samples taken close to 40 m), mean cell-specific carbon uptake was distinctly slower with much higher variability (13.4 ± 5.8 fg C $cell^{-1}$ day^{-1}), and with longer turnover times (7.3 ± 10.9 days). These values for samples from the anaerobic hypolimnion should be viewed with caution since the actual BP measurements were not made under strictly anaerobic conditions. Nevertheless, because metabolic efficiency would be expected to be lower in anaerobic than aerobic environments (Fenchel and Finlay 1995), it is reasonable that bacteria in the hypolimnion would have considerably slower C uptake rates and turnover times than epilimnic bacteria.

The above values for cell-specific carbon uptake and turnover times were based on the assumption that all DAPI-counted bacterial cells (Chap. 15) were metabolically active. Berman et al. (2001) used three different staining techniques,

each of which detected different aspects of cellular state or metabolic activity to assess the proportion of active bacteria within the total counted population. Their data indicated that in Lake Kinneret, usually only a small fraction (probably < 20 %) of the entire bacterial assemblage was metabolically active at any given time. In this case, the active bacterial population would have cell-specific carbon uptake rates of ~ 90 fg C $cell^{-1}$ day^{-1} and turnover times of about 14–15 h. Unfortunately, no studies have been made in Lake Kinneret of the impact on bacterial cell turnover of lysis by bacteriophage (Suttle 2007).

Berman et al. (2001) also observed that even apparently inactive bacteria could become highly active under appropriate conditions (Choi et al. 1999). This "switching on" might occur as a result of nutrient inputs caused by upwelling events, or on a more localized scale, because of inputs from protistan or zooplankton excretion or sloppy feeding (Jumars et al. 1989) or from algal cell lysis (Berman and Wynne 2005). Thus, the bacterial populations in the lake should be regarded as a dynamic mixture with various components functioning at different degrees of activity at any given moment, constantly modulating their physiological activities to changes in their localized environment.

25.1.4 Bacterial Respiration, a Major Fraction of Total Community Respiration

Bacterial respiration (BR) was estimated using the method suggested by Berman et al. (2004, 2010) as follows:

$$BR = CR - PR - ZR \quad (1)$$

where CR is community respiration, PR is phytoplankton respiration, and ZR is zooplankton respiration. CR was directly measured by the ΔO_2 method (Sect. 25.2). PR was calculated as 0.3* GPP derived as 1.5* primary production (PP) determined by routine ^{14}C measurements of PP (Sect. 24.1). Based on previous studies (Berman and Pollingher 1974; Berman et al. 1995), these PP values were assumed to be close to NPP.

Some explanation of the ZR term is required. Historically, crustaceans (cladocera and copepods) together with the rotifers were included in the category of "zooplankton" (Gophen 1978). Hambright et al. (2007) used the term "microzooplankton" to describe the assemblage of rotifers, numerous ciliated and flagellated protists, and nupliar stages of copepods. In their previous work, Berman et al. (2010) used ZR values based on routine monitoring measurements of the crustacean and rotifer biomasses multiplied by experimentally determined group-specific respiration rates (Gophen 1981) to obtain BR (Eq. 1 above); however, similar ZR values were calculated by assuming that ZR ranged from 0.33 to 0.5 BR (for details, see Berman et al. 2010). There are no data available on ciliate or flagellate respiration in the lake and no explicit mention of protist respiration has been made in previous studies. In

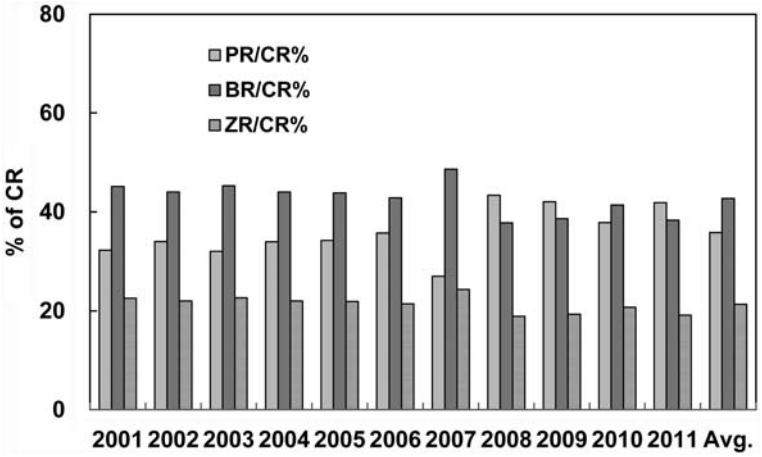

Fig. 25.2 Relative contribution to total community respiration (*CR*) by phytoplankton (*PR*), bacteria (*BR*), and zooplankton (*ZR*), based on annual means from 2001 to 2011 (Table 25.2), Sta. A. (Note: 2011 values are based on January–June data only)

the present study, ZR was taken to include both crustacean and microzooplankton respiration and assigned a value of 0.5 BR; therefore

$$\mathrm{BR} = (\mathrm{CR\text{-}PR})/1.5 \tag{2}$$

This implies that the directly measured values for crustacean ZR in Berman et al. (2010) were overestimated and that the ZR values used in their study included respiration of the protists as well as crustaceans and rotifers. (Note: Fish respiration, based on biomass, has been estimated at between 3 and 5% of CR (Stone et al. 1993), which is below the sensitivity of this method; therefore, this source of respiration has been omitted.)

The semiannual means of BR (Eq. 2) from 2001 to 2011 are given in Table 25.1. There was a strong, positive correlation between BR and BP ($r^2=0.41$, $p=0.0018$, $n=21$), although the decrease in BR during this period was only weakly significant ($r^2=0.20$, $p=0.0412$, $n=21$). Generally, with the exception of 2009 and 2010, BP levels were higher in January–June than in July–December as might be expected because of the higher levels of phytoplankton biomass and GPP at this season (see Sect. 24.1).

The relative proportions contributed annually by PR, BR, and ZR to total CR are shown in Fig. 25.2. The 10-year averages of PR, BR, and ZR as percentages of CR were 36, 43, and 21%, respectively. With the exception of 2008 and 2009, BR was always the major component of CR. As previously observed (Hart et al. 2000; Berman et al. 2004, 2010), ZR was consistently the smallest contributor to CR ranging from 14 to 24% on an annual basis and showing no clear trend during these years.

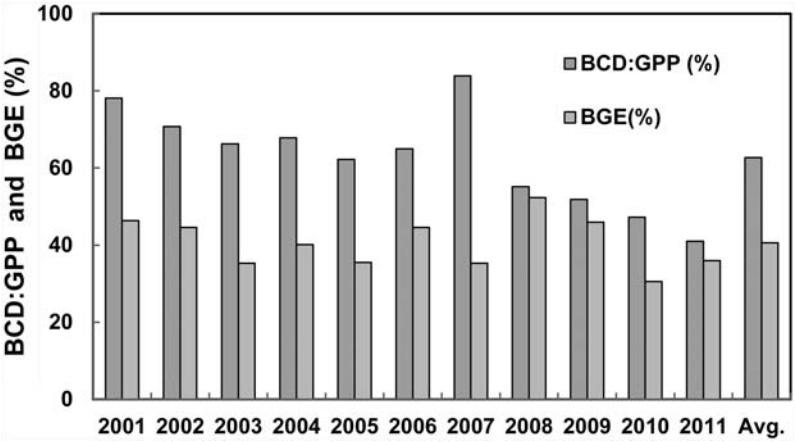

Fig. 25.3 Annual means of bacterial carbon demand: gross primary production (*BCD:GPP*) and bacterial growth efficiency (*BGE*) from 2001 to 2011, Sta. A. (Note: 2011 values are based on January–June data only)

25.1.5 Bacterial Carbon Demand and Bacterial Growth Efficiencies

Previous studies (Berman et al. 2004, 2010) had shown high levels of bacterial carbon demand (BCD; defined as BP+BR) in Lake Kinneret, consistent with the generally high levels of BP and BR. As shown in Table 25.1 and Fig. 25.3, a large proportion of GPP was cycled through the epilimnic bacterial community. These are high, but by no means impossible levels for BCD:GPP (Table 25.2). Even in the absence of external inputs, the total bacterial carbon uptake by heterotrophic bacteria and by secondary and tertiary consumers can sometimes exceed GPP because of recycling within the system (Strayer 1988), as was shown to be the case for Lake Michigan (Scavia 1988). For the years 2001–2007, Berman et al. (2010) reported annual mean BCD:GPP% of 75 ± 17% for the entire period 2001–2010; however, BCD:GPP% decreased to 65 ± 13% as a result of the sharp drop in BCD since 2007. There was an overall slight but significant decrease ($r^2 = 0.46$, $p = 0.029$, $n = 10$) in BCD from 2001 to 2010.

BCD levels tended to be somewhat higher during the first half of the year (average 66 ± 14%) than in the second half (60 ± 10%) with the notable exception of 2009 and 2010. In these years, BCD fluxes were only about half of those measured in peak years, although GPP levels did not show a similar drop. BCD reached a maximum of 84% during the *P. gatunense* bloom of 2007 (Table 25.2). It is reasonable to assume that this seasonal pattern reflects the increased cycling by heterotrophic bacteria of dissolved organic carbon (DOC) derived directly or indirectly from the larger biomasses of phytoplankton usually present in winter–spring than in summer–fall. Sherr et al. (1982) demonstrated that bacterivorous

Table 25.2 Semiannual means of bacterial carbon demand (*BCD*), bacterial growth efficiency (*BGE*), bacterial production: gross primary production (*BP:GPP*) and *BCD:GPP*, 2001–2011 at Sta. A

	January–June				July–December			
	BCD mg C m^{-2} day^{-1}	BP:GPP (%)	BCD:GPP (%)	BGE (%)	BCD mg C m^{-2} day^{-1}	BP:GPP (%)	BCD:GPP (%)	BGE (%)
2001	2,110	38	81	47	1,780	34	76	46
2002	1,810	32	77	41	1,380	31	64	48
2003	2,240	24	73	32	1,090	23	59	38
2004	2,510	30	87	35	1,200	25	54	46
2005	1,340	23	76	30	970	20	49	41
2006	1,560	27	63	43	1,360	31	67	47
2007	2,290	34	91	37	1,510	26	77	34
2008	1,290	29	53	56	1,140	24	48	49
2009	1,010	24	47	51	1,240	23	56	41
2010	1,130	13	47	27	1,140	16	49	34
2011	810	15	41	36	nd	12	nd	nd
Average	1,645	26	67	39	1,281	24	60	42
SD	552	7	17	8	223	6	10	5

SD standard deviation, *nd* not defined

flagellates increased the decomposition rate of the dinoflagellate carbohydrate thecae by increasing the rate of recycling of nutrients, which stimulated bacterial activity. Thus, the heterotrophic flagellates could be a driver for the increased bacterial (i.e., microbial loop) carbon demand during dinoflagellate blooms in the lake.

Over the period 2001–2010, there was a significant trend of decreasing BCD:GPP measured in winter–spring but not in summer–fall. The drop in both the absolute amounts of BCD and the ratio of BCD:GPP in the winter–spring season may have resulted from the trend to fewer *Peridinium* years. In any event, the decrease in the flux of OC via the microbial loop may be connected with lower levels of BP and BA (see above and Chap. 15).

In contrast to BCD, annual mean bacterial growth efficiencies (BGE; defined as BP/(BP+BR)) showed no consistent, significant change over the period 2001–2011 (Fig. 25.3). The overall, average annual BGE (41 ± 6 %) was very similar to that reported for the years 2001–2007 (Berman et al. 2010). In general, estimates for BGE levels in this lake tend to be higher than in most reported freshwater systems. However, it is presently unclear whether these high BGE estimates are accurate or reflect some inherent difference between various methods used for estimating BGE. In the present study, we have assumed that the respiration of protists is included in the ZR term; thus, BR refers to bacterial respiration only. The indirect method of calculating BR (and hence BGE) used here has not been widely used. Most BR measurements reported in the literature to date have utilized experimental data from 1-μm filtered water to directly estimate BR; this approach also has some limitations (see Berman et al. 2010). Future research should compare results obtained with both the above approaches to estimate BR and BGE.

25.1.6 What Caused the Significant Drop in BP, BA, and BCD From 2001 Through 2010?

As documented elsewhere (Chaps. 10 and 11), the most visible evidence of ecosystem change in Lake Kinneret has been the disruption of the regular seasonal pattern of phytoplankton development (as typified by late winter–early spring blooms of *P. gatunense* with dominance of small chlorophytes in summer–fall) to highly erratic dinoflagellate blooms and the increasing dominance of N_2-fixing cyanobacteria especially in summer–fall. Here, we have shown that dramatic changes have also occurred both in the abundance (Chap. 15) and in the metabolic activity of the bacterial populations from 2001 to 2011.

Not much is known about limiting factors for the bacterial populations in this lake. Zohary et al. (2000) found that P addition enhanced bacterial degradation of dinoflagellate thecae in Lake Kinneret water. Pinhassi and Berman (2003), working with samples taken from near-surface lake waters, found that P appeared to be limiting BP and growth at most times. Additionally, similarly to previous research (Berman et al. 1993), they found that the availability of Fe or chelators could play an important role in regulating bacterial metabolism and growth even in Lake Kinneret where ambient concentrations of total Fe are relatively high. These observations might suggest two possible causes for the significant continuous decreases in BP, BA, and BCD levels from 2001 to 2011 documented here: (1) From the mid-1990s, major hydrological changes in the catchment area have altered the amounts and characteristics of organic chelators and/or Fe and other trace metal ions flowing into the lake. (2) Prolonged periods of low lake levels and low volume winter inflows may have been responsible for the increasing abundance of N_2-fixing cyanobacteria (Chap. 12). These cyanobacteria would be expected to compete more effectively with the heterotrophic bacteria for relatively scarce available nutrients, especially P and Fe, than the previously dominant chlorophytes and dinoflagellates. In any event, there appears to be little doubt that a profound shift in carbon cycling has taken place over the last decade in Lake Kinneret.

25.2 Community Respiration

Arkadi Parparov and Tom Berman

25.2.1 Background

Dark pelagic respiration (hereafter, CR) is a major flux in biogeochemical cycles, being the largest sink for organic matter and oxygen in freshwater lakes (del Giorgio and Williams 2005b; Pace and Prairie 2005). Traditionally, CR has been measured as oxygen depletion (ΔO_2) in dark bottles ("dark respiration"). A basic assumption

Table 25.3 Community respiration (*CR*) in Lake Kinneret measured at different periods

Period	Method	CR		Reference
		g O_2 m^{-2} day^{-1}	g C m^{-2} day^{-1}	
1964–1965	ΔO_2	7.6	2.28	Hepher and Langer 1969
1972	Carbon budget	6.27	1.88	Serruya et al. 1980
1970–1990	Oxygen budget	3.18	0.95	Nishri et al. 1998
1996–1998	$^{18}[O_2]$	19.4	5.82	Luz et al. 2002
2001–2010	ΔO_2	6.86	2.06	This study

of the oxygen method is that CR rates in the light and dark are similar. Although this assumption has been controversial (Pringault et al. 2007, 2009), in most ecological situations, differences between light and dark CR appear to be insignificant (Winberg 1960; Aristegui et al. 1996; Gazeau et al. 2007).

The first systematic determinations of CR in Lake Kinneret were made by Hepher and Langer (1969), who used the ΔO_2 method. Subsequently, lake CR has been estimated from the budget of OC (Serruya et al. 1980), from daily changes in the pool of dissolved oxygen (Nishri et al. 1998) and using $^{18}O_2$ (Luz et al. 2002). From 2001, CR was monitored biweekly at the central pelagic Sta. A (see location in Chap. 1, Fig. 1.1), using the ΔO_2 method. This involved in situ incubations of water from five depths (0, 1, 5, 10, and 15 m) in dark bottles over 24 h. A factor of 0.3 was used to convert mg O_2 L^{-1} to mg C L^{-1} (i.e., Respiration Quotient, RQ = 0.8). In natural aquatic environments, an RQ of 0.8 may be more accurate than the often used RQ = 1 for CR because the respiration of organic matter includes proteins and lipids in addition to carbohydrates (Winberg 1960; Geider 1997; Robinson 2008).

25.2.1.1 Community Respiration in Lake Kinneret (1964–2010)

Estimates of CR in the lake, based on measurements made by a variety of methods, are shown in Table 25.3. The annual average value of CR for the period from 2001 to 2010, when the most detailed monitoring of this parameter was carried out, is surprisingly close to early estimates obtained in 1964–1965 (Hepher and Langer 1969) and in 1972 (Serruya et al. 1980). Although it is tempting to suggest that this similarity of CRs attests to a relative stability in the rates of aerobic decomposition of organic matter over the decades, we note that the early data are based on relatively few actual measurements. Much lower CR values (3.18 g O_2 m^{-2} day^{-1} or 0.95 g C m^{-2} day^{-1}) were calculated by Nishri et al. (1998) for the period 1970–1990, based on oxygen mass balance calculations. It seems probable that these CR values were considerably underestimated because they are much lower than values for average daily primary production (1.54 g C m^{-2} day^{-1}) measured by the ^{14}C method for the same period (Berman et al. 1995; Yacobi 2006). Furthermore, it seems unlikely that lower CR would occur during a period of overall higher standing stock algal biomass. In contrast, extremely high CR values were reported by Luz et al. (2002) for the years 1996–1998 using the $^{18}O_2$ method (Table 25.3).

25.2.1.2 Community Respiration from 2001 to 2010

Berman et al. (2010) reported that from 2001 to 2007, annual CR averaged 7.28 g O_2 m^{-2} day^{-1}. Community respiration was consistently higher in winter–spring than in summer–fall by an average factor of 1.48 (±0.37). It was also correlated closely with BP as well as with parameters of phytoplankton biomass (Chl) and photosynthetic activity.

The average annual values for CR for the period 2001 to 2010 (Fig. 25.4a) averaged 6.86±1.91 g O_2 m^{-2} day^{-1} and ranged from 4.93±2.53 g O_2 m^{-2} day^{-1} in 2009 to 9.91±6.18 g O_2 m^{-2} day^{-1} in 2007. Daily levels of CR varied very widely from 0.61 to 31.7 g O_2 m^{-2} day^{-1}. The highest CR values (>15 g O_2 m^{-2} day^{-1}) were recorded in spring during intense dinoflagellate blooms ("*Peridinium* years," when maximum phytoplankton biomass exceeded 100 g m^{-2}; Zohary et al. 2012) that occurred in 2003, 2004, and 2007; in years without such blooms ("non-*Peridinium* years"), the spring maxima of CR were smaller or even absent. The discrepancy between these two annual patterns of CR is most clearly shown by comparing the monthly CR recorded in 2004 and 2009 (Fig. 25.4b). Community respiration was much higher during the first half of 2004 than in 2009; subsequent monthly differences between these years were minimal. It seems reasonable to assume that the greater input of OC that occurred as a result of the *Peridinium* blooms provided the substrate for enhanced respiration rates recorded during these years. During dense dinoflagellate blooms, high CR values were measured even when the upper water layer (0–15 m) was supersaturated (up to 130%) with oxygen. On these occasions, GPP should be higher than the corresponding measured CR values which ranged from 4.50 to 31.7 g O_2 m^{-2} day^{-1} (1.35–9.51 g C m^{-2} day^{-1}) assuming no significant allochthonous inputs of OC. Such high values for GPP greatly exceed primary production rates measured with the ^{14}C method during *Peridinium* blooms. In general, the ^{14}C method as used in the long-term studies in Lake Kinneret gives values close to NPP (Berman and Pollingher 1974); during dense *Peridinium* blooms, the ratio of GPP:NPP was close to 2 (see Chap. 24.1).

The mean monthly CR (averaged for the period 2001–2010) is shown in Fig. 25.4c. Despite the large variability shown in these measurements, there was nevertheless a clear trend of higher CR in the late winter–spring months (April, May). Overall, CR was consistently higher in winter–spring than in summer–fall by a factor of 1.44, consistent with the generally higher levels of phytoplankton biomass measured during the former season.

25.2.2 Contributions of Major Biological Groups to CR

Phytoplankton, heterotrophic bacteria, and zooplankton (including protista) all contribute to the total measured CR in the epilimnic waters of Lake Kinneret. Some attempts have been made to measure directly respiration rates for heterotrophic bacteria (Berman et al. 1979), phytoplankton (Berman and Gerber 1980; Berman and Kaplan 1984a, 1984b), and zooplankton (Gophen 1981). The first estimates

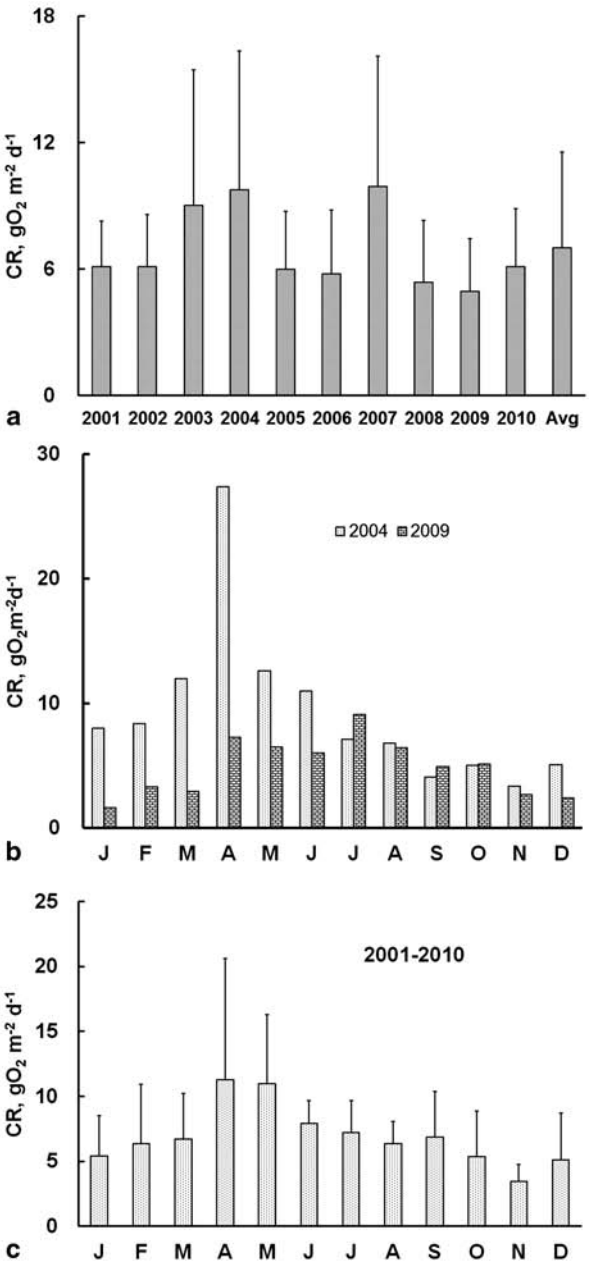

Fig. 25.4 Lake Kinneret community respiration (*CR,* g O_2 m^{-2} d^{-1}) recorded at Sta. A, 2001–2010. **a** Annual averages and overall average (*Avg*). **b** Monthly *CR* for a "*Peridinium* year" (2004) and "non-*Peridinium* year" (2009). The annual mean contributions of dinoflagellates to total phytoplankton biomass were 65.5% in 2004 and 38.4% in 2009. **c** Multi-annually averaged monthly *CR* for the period 2001–2010. Whiskers in **a** and **c** indicate standard deviation (*SD*)

for the specific contribution of the major planktonic biological groups to overall lake CR were derived from carbon mass balances measured from 1989 to 1992 (Hart et al. 2000). These indicated (Fig. 25.5) that heterotrophic bacterial and PF

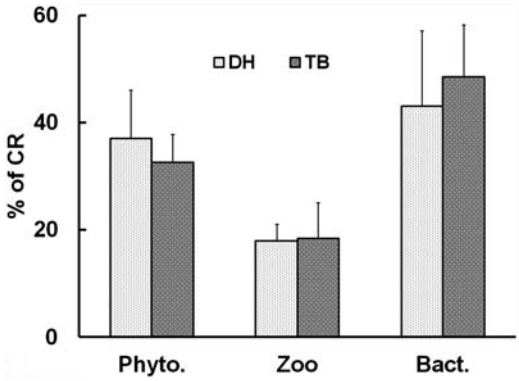

Fig. 25.5 The relative contributions of three groups of planktonic organisms to total community respiration (*CR*). DH (D. Hart): estimates based on Hart et al. (2000) for the years 1989–1992; TB (T. Berman): estimates based on Berman et al. (2010) for the years 2001–2010. Whiskers indicate standard deviation (*SD*)

contributed about equally (~40 % each) to total CR, with only ~20 % contributed by zooplankton (cladocera, copepoda, rotifers) and protozoa (ciliates and flagellates). The contribution of fish respiration was at most only a few percent of total CR.

The data on dry weight-specific respiration (mg O_2 $mgTSS^{-1}$ day^{-1}) associated with seston dominated by different algal groups are presented in Table 26.3 of Chap. 26.

Berman et al. (2004, 2010) introduced a method of estimating the relative amounts of respiration contributed annually by PR, BR, and ZR to total CR. Using this approach, the calculated, overall, 10-year (2001–2011) averages of PR, BR, and ZR of CR were 36, 43, and 21 % of CR, respectively (details in Fig. 25.2, Sect. 25.1). With the exception of 2008 and 2009, BR was always the major component of CR, slightly higher than PR. As previously estimated (Hart et al. 2000; Berman et al. 2004, 2010), ZR was consistently the smallest contributor to CR, ranging from 14 to 24 % on an annual basis and showing no clear trend during these years. Note, the contribution of fish respiration to total CR was excluded here because it was assumed to be too low to be within the resolution of this method.

25.3 Sulfate Reduction

Ora Hadas and Riki Pinkas

25.3.1 Introduction

Anaerobic mineralization of organic matter is mediated by a series of bacterial metabolic pathways such as nitrate reduction and manganese and iron reduction with sulfate reduction and methanogenesis being the terminal processes in the anaero-

bic decomposition of organic matter (Oremland and Polcin 1982; Ingvorsen and Jorgensen 1984; Capone and Kiene 1988). Sulfate-reducing bacteria (SRB) play a key role in the mineralization processes in marine sediments, but significant sulfate reduction rates have also been reported for freshwater sediments, despite low sulfate concentrations in the pore water (King and Klug 1982; Landers and Mitchell 1988). This finding suggests that SRB in freshwater have acquired high-affinity sulfate uptake systems to cope with the low sulfate concentrations (Smith and Klug 1981; Ingvorsen and Jorgensen 1984). High substrate affinities of SRBs for acetate, H_2, and other electron donors can account for the inhibition of methanogenesis in sulfate-rich environments (Lovley and Klug 1986; Skyring 1988), although syntrophism in methanogenic environments is not excluded (Plugge et al. 2011). Although until recently sulfate reduction was considered a strict anaerobic process (Postgate 1984), we know today that SRBs may thrive under oxidizing conditions in which they respire with nitrate or even oxygen (Canfield and Des Marais 1991; Frund and Cohen 1992; Cypionka 2000).

Sulfate reduction is one of the major driving forces in the maintenance of deep water anoxia in Lake Kinneret. As in other sites, sulfate reduction forms the basis of the biological sulfur cycle in this lake. The factors controlling the rate of sulfate reduction are: (1) availability of organic matter from decomposing material, mostly planktonic carbon in the water column; (2) ambient SO_4^{2-} concentration; (3) redox potential; (4) temperature; and (5) pH (Westrich and Brenner 1988).

The conditions in Lake Kinneret hypolimnion and sediments regarding those controlling factors were followed closely at Sta. A (station location map in Fig. 1.1 of Chap. 1) during 1988–1989. Two other stations Sta. G and the shallow Sta. S were studied during different seasons in 1991 and 1992. The findings are summarized below.

25.3.2 Sources of Organic Matter

The annual average of total phytoplankton biomass was similar in 1988 and 1989 (73 g wet wt m^{-2} in 1988 and 74 g wet wt m^{-2} in 1989). In 1988, the highest biomass (225 g wet wt m^{-2}) was observed in February due to a bloom of the filamentous diatom *Aulacoseira granulata* (182 g wet wt m^{-2}) whereas the *Peridinium* peak appeared in May (124.7 g wet wt m^{-2}). In 1989, the *Peridinium* peak was in March–April (166, 184 g wet wt m^{-2}), contributing more than 90 % of the total phytoplankton biomass; no significant biomass of *Aulacoseira* was observed in 1989 (Table 25.4).

The heavy filaments of *A. granulata* appear in the water column in times of high turbulence, and at the end of the turbulent period, they sink toward the sediments (mixed water column), supplying fresh organic material to the sediments. These blooms supplied the organic matter for sulfate reduction by SRBs in the hypolimnion and sediments, where anoxia existed, sulfate was available, and temperature and pH were also suitable, as discussed below.

Table 25.4 Monthly mean total, *Peridinium gatunense* and *Aulacoseira granulata* biomass (g w.w. m^{-2}) at the trophogenic layer at Sta. A, and sulfate reduction rates (mmol m^{-2} $month^{-1}$)

Month	Total biomass		*Peridinium*		*Aulacoseira*		SO_4^{-2} reduced	
	1988	1989	1988	1989	1988	1989	1988	1989
January	91.7	97.2	11.2	21.3	58.5	NS	152	100
February	225	99	24.8	43.2	182	NS	260	115
March	126.7	166.4	61	157.2	54.8	NS	–	137
April	91.5	183.9	83.4	177.7	NS	NS	229	148
May	134.2	108	124.7	97.9	NS	NS	216	–
June	58.2	35.4	40.7	14.6	NS	NS	527	193
July	35.4	44.7	23.6	24	NS	NS	880	580
August	18.3	31.2	1.7	11.5	NS	NS	421	305
September	25	28.5	2.6	5.6	NS	NS	416	169
October	36.7	24.2	3.8	7.3	NS	NS	207	224
November	23.6	28.6	3.4	15	NS	NS	146	239
December	27.7	28.5	6.8	16.6	NS	NS	119	46

NS not significant

25.3.3 Sulfate and Sulfide Concentrations

Hypolimnion: Strong seasonal variations in sulfate and sulfide concentrations in the hypolimnion of Lake Kinneret were found. Levels of sulfate ranged from 531 to 547 μM during holomixis and dropped to minima of 198–219 μM in December, at the end of the stratification period. An inverse pattern was observed for sulfide concentrations, 0 during the mixing period and reaching maxima of 309 and 366 in 1988 and 1989, respectively, just before overturn (Fig. 25.6). The decrease in sulfate concentrations corresponded stoichiometrically to the increase in that of sulfide, suggesting that intensive sulfate reduction was occurring in the hypolimnion of the lake, with sulfide accumulating as a result of sulfate reduction. The higher sulfide concentrations in 1989 compared with 1988 were probably due to a smaller hypolimnion volume, due to lower water levels (1,555 and 1,296 million m^3 in 1988 and 1989, respectively).

Sediments: The highest sediment pore water sulfate concentrations were found during the mixing period in February, 438 μM at 0.3 cm depth in 1988 and 781 μM at 0.6 cm depth in 1989 due to turbulence, oxygen diffusion into the first few millimeters and bioturbation by transitory dwellers (e.g., *Leydigia* sp., Cladocera), and some copepods and chironomids. Minimum values were detected toward the end of the stratification period, 8–20 μM, of sulfate in November–December 1988 (Fig. 25.7). In some years, no sulfate is detected in December below 1.5 cm.

25.3.4 Arylsulfatase

When sulfate concentrations are low, the enzymatic activity of arylsulfatases may supply part of the sulfate demands of SRB in the sediments. In Lake Kinneret, the activity of arylsulfatase varied with depth and season (Hadas and Pinkas 1992,

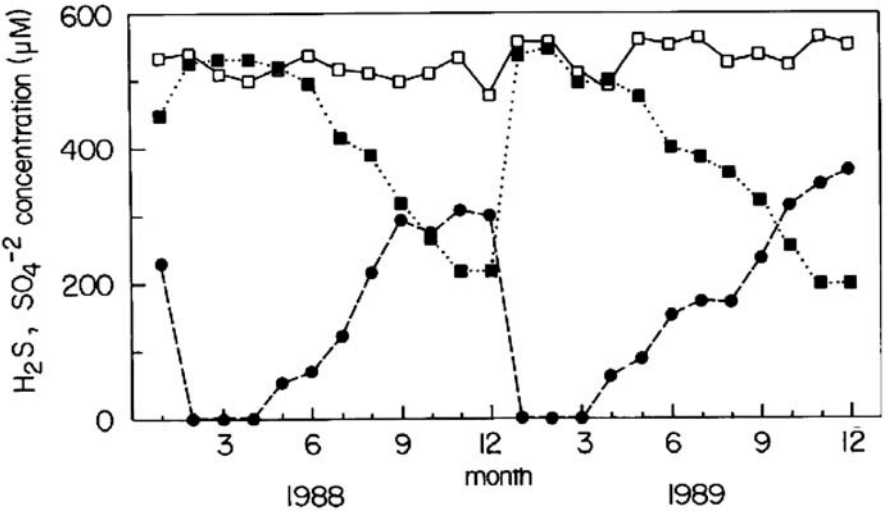

Fig. 25.6 Monthly average concentrations (µM) of sulfate at 10-m depth (*empty squares*) and sulfate (*full squares*) and sulfide (*circles*) at 40-m depth at Sta. A in Lake Kinneret, 1988–1989. (Reproduced from Hadas and Pinkas 1995a with permission from Wiley)

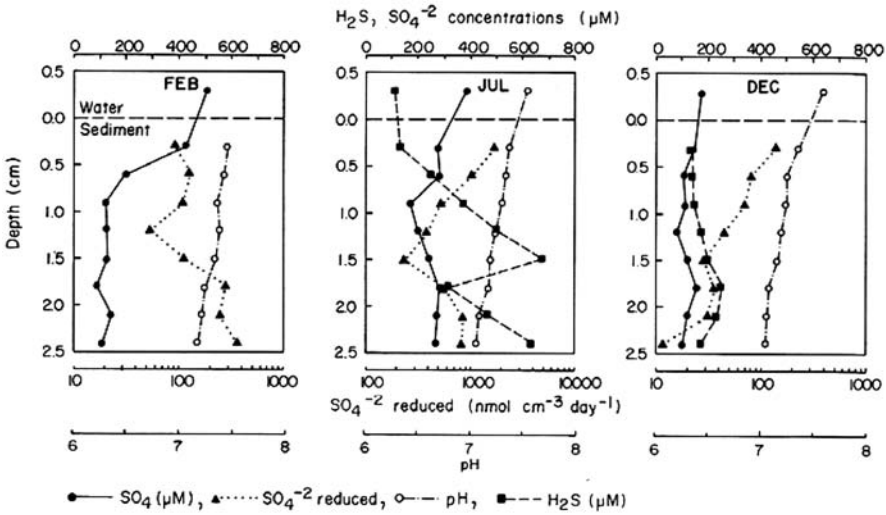

Fig. 25.7 Depth profiles of H_2S and SO_4 concentrations and pH and sulfate reduction rates in different seasons in Lake Kinneret sediments and overlying water. (Reproduced from Hadas and Pinkas 1995a with permission from Wiley)

1997). Maximum activity was found in the sediments in July (670 nmol *p*-nitrophenol, PNP, g w.w.$^{-1}$ h^{-1}) and December, and minimum in February. The lower activity in February was correlated with high SO_4^{-2} available. During the stratified period,

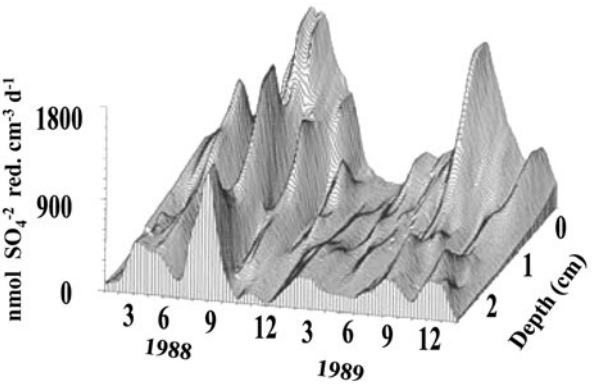

Fig. 25.8 Time–depth distribution of rates of sulfate reduction in Lake Kinneret sediments in 1988–1989. (Reproduced from Hadas and Pinkas 1995a with permission from Wiley)

intensive sulfate reduction resulted in decrease in SO_4^{-2} concentrations and increase in arylsulfatase activity. At the decline of the *Peridinium* bloom, supplying organic matter and sulfate esters, high arylsulfatase activity was induced (Hadas and Pinkas 1992, 1997).

25.3.5 Redox, Temperature, and pH

The pH in the sediment cores decreased with depth and ranged between 7.45 and 7.05 with no seasonal variation (Fig. 25.7). The temperature of the hypolimnion at Sta. A is in the range of 14–16 °C and does not vary during the year, with interannual variations averaging 2 °C. There is a drop in redox potential in the sediment due to availability of organic matter, high microbial activity, and depletion of oxygen at the beginning of summer. These conditions enabled intense sulfate reduction activity (Figs. 25.7 and 25.8).

25.3.6 Sulfate Reduction Rates

Sediment cores were taken with a Tessenow gravity sampler (Tessenow et al. 1977) at Sta. A (Central, 42 m depth) during 1988–1989 and at Sta. G (Northern, 22 m) influenced by the Jordan River, and Sta. S (shallow, 10 m) representing sediments covered with oxic water the whole year. Sampling was carried out at different seasons of the year, corresponding to the thermal stratification and *Peridinium* bloom: (1) in February during full mixing at the beginning of the *Peridinium* bloom, (2) in July after the crash of the bloom, and (3) in December during stable stratification. Sulfate reduction rates were measured by the method of Jorgensen (1978) using $Na_2{}^{35}SO_4$ as described previously (Hadas and Pinkas 1992, 1995a, 1995b).

25.3.6.1 Hypolimnion

According to the stoichiometric equation:

$$2(CH_2O)_n + SO_4^{-2} \rightarrow 2HCO_3^- + H_2S \quad (3)$$

2 mol of OC are oxidized per mole of sulfate reduced. The accumulation of H_2S in the hypolimnion was accompanied by a decrease in SO_4^{-2} concentrations of 0.31 and 0.35 mM in 1988 and 1989, respectively (Fig. 25.6). The average hypolimnion volume of the lake was 1,555 and 1,296 million m^3 in 1988 and 1989, respectively. Accordingly, 964×10^6 and 907×10^6 mol C could have been oxidized in 1988 and 1989 via sulfate reduction. The total accumulated yearly phytoplankton biomass was about 150,000 t wet weight. Since most of it was *Peridinium* with 20% C content, about 36 and 39% of the phytoplankton biomass could have been oxidized via sulfate reduction in the hypolimnion in 1989 and 1988, respectively. This is in agreement with the reports that 50% of the primary production may be decomposed by SRB in the hypolimnion (Smith and Oremland 1987; Canfield 1989).

25.3.6.2 Sediments

The rate of sulfate reduction in Lake Kinneret sediments varied seasonally (Figs. 25.7, 25.3) and was dependent on both the availability of sulfate in the pore water and organic matter supplied from the epilimnion and reaching the sediments. The relative fraction of organic matter reaching the sediments depends on the timing of the algal bloom and the shape of the isotherms. An early bloom of *Peridinium* (or other species) and a long mixing period would usually increase the amount of organic matter reaching the sediments (Serruya et al. 1974). At the beginning of summer, the crash of the *Peridinium* bloom resulted in an increased input of fresh organic matter.

During thermal stratification, the phytoplankton is mostly decomposed in the epilimnion and the supply of organic matter reaching the sediments is low resulting in lower sulfate reduction rates in autumn (Fig. 25.3). During the mixing period, although sulfate concentrations are high, the limited supply of organic matter resulted in low sulfate reduction rates. An exception was February 1988, in which a second peak of sulfate reduction occurred due to the *A. granulata* bloom sinking toward the sediments (no thermal barrier) and providing fresh organic matter (Fig. 25.3).

High sulfate reduction rates were observed in July 1988 throughout the whole 2.4-cm depth sediment core, reaching a maximum of 1,699 nmol SO_4^{-2} reduced cm^{-3} day^{-1} at 0.3-cm depth (Figs. 25.7 and 25.8). These high rates were also observed in June and August at the upper layers of the sediments. In November and December, due to the strong thermal stratification, depletion of organic matter, and of sulfate, lower rates were measured (14 and 80 nmol SO_4^{-2} reduced cm^{-3} day^{-1}). In 1989, the sulfate reduction peak occurred in July at 0.3-cm depth and, at least at this depth, was as high as in 1988 (Figs. 25.7 and 25.8). Lower rates were observed

Table 25.5 Semiannual and annual monthly average carbon oxidized through sulfate reduction (mmol C m^{-2} $month^{-1}$) and carbon supplied by primary production (mmol C m^{-2} $month^{-1}$) in the sediments at Sta. A

Month	Carbon oxidized through sulfate reduction (mmol C m^{-2} $month^{-1}$)[a]		Carbon supplied by primary production (mmol C m^{-2} $month^{-1}$)	
	1988	1989	1988	1989
January–July	754±557	424±366	575±150	496±53
August–December	524±293	393±194	370±170	361±152
January–December	650±451	410±287	493±183	440±122

[a] Based on the assumption that 2 mol of carbon are oxidized per mol of sulfate reduced

in December, just before the overturn (12 nmol SO_4^{-2} reduced cm^{-3} day^{-1} at 2.4-cm depth; Hadas and Pinkas 1995a).

The integrated values of sulfate reduction in the sediments in 1989 were only 63% of those in 1988. The difference in the phytoplankton composition and the higher productivity during the first half of the year (January–June), 2,300 and 2,000 mg C m^{-2} day^{-1} in 1988 and 1989, respectively, could probably account for part of the difference in sulfate reduction rates between those years (Table 25.5). Furthermore, the mixing period of the lake was a month longer in 1988 than in 1989, resulting in higher amounts of organic matter reaching the sediments. Only 10% of the carbon fixed by photosynthesis reaches the sediments (Serruya 1978). Based on this value, the phytoplankton primary production reaching the bottom could account for most or all the potential sulfate reduction in the sediments at Sta. A (Table 25.5). $\delta^{13}C$ of the organic matter in the sediments have shown values lower by 4‰ as compared to the organic matter sinking from lake water indicating diagenetic processes in the sediments (Stiller and Magaritz 1974).

25.3.7 Sulfate Reduction Rates at Stations G and S as Compared to Station A (Based on the Years 1990–1992)

Station G, located in the northern part of the lake, is mostly influenced by the inflow of the Jordan River. The Jordan and its tributaries bring relatively high amounts of particulate organic matter. The sediments at station G are rich in detrital elements (Fe, P, Mn) as the result of deposition of suspended matter associated with the early floods. High sulfate reduction rates were observed immediately after the first heavy rainfalls in December 1991. Another peak (1,350 nmol SO_4^{-2} reduced cm^{-3} day^{-1}) was recorded in July at the crash of the *Peridinium* bloom when organic matter and sulfate were available. During drought years when the contribution of the Jordan River was small, low sulfate reduction rates were recorded (Hadas and Pinkas 1995b).

Station S (10 m depth, in the littoral at the western side of the lake) is exposed to an oxygenated water column during the whole year; however, the sediments at Station S are anoxic and oxygen penetrates to less than 0.6 mm. At low lake levels, if less organic matter was available, low sulfate reduction rates were recorded

(6–48 nmol SO_4^{-2} reduced cm^{-3} day^{-1} in February, 1991). During periods of low water levels (e.g., 1990–1991) shoreline vegetation (*Tamarix jordanis* and *Phragmites australis*) developed on the exposed shores. This vegetation decomposed after being covered by the rising water (like in 1992), supplying fresh organic material that resulted in high sulfate reduction rates.

25.3.8 Prospective

The main trigger for the sulfate reduction process in Lake Kinneret was the decline and decomposition of the *Peridinium* bloom. In years of low water levels, the bloom started early (February), peaked in April, and declined in May–June supplying fresh organic material to the hypolimnion and sediments. At high water levels (usually correlated with cold and rainy winters), the bloom of *A. granulata* added to the organic fraction supplied to the sediments. During the past 2 decades, the characteristic annual bloom of *Peridinium* does not appear every year, and in some years other species (e.g., *Mougeotia*) are the main phytoplankton contributing to the primary production. Sulfate reduction rates calculated from sulfate concentration profiles using a numerical model and based on profiles in 2008 ("non-*Peridinium* year," Adler et al. 2011) showed values in the range of the rates measured by Hadas and Pinkas (1995a) without the peaks measured in July after the degradation of the *Peridinium* bloom. The changes in the phytoplankton composition pattern of the lake and invasion of new species with different seasonal distribution patterns and bloom timing may have an impact on sulfate reduction in the hypolimnion and sediments and on the mineralization processes of organic matter in the lake.

25.4 Methanogenesis

Werner Eckert and Orit Sivan

Methanogenesis is a key terminal process in the anaerobic decomposition of organic matter that dominates in the absence of other electron acceptors such as nitrate, ferric iron, and sulfate. It is meditated by methanogenic bacteria (MB), a diverse group of microorganisms, all belonging to the Archaea. They are responsible for ~70% of the globally produced methane estimated at 500–600 Tg CH_4 per year (Conrad 2009). This biologically produced methane derives mainly from the reduction of CO_2 with hydrogen (hydrogenetic methanogenesis), or from the fermentation of acetate (acetoclastic methanogenesis), which is split into CH_4 and CO_2 and, to a lesser extent, from other C −1 compounds (Whitman et al. 1991). In aquatic environments, methanogenesis is primarily a sedimentary process controlled by the prevailing sulfate concentrations due to the competition between MB and SRB for

common substrates. Even in freshwater sediments that are relatively poor in sulfate, SRB can outcompete MB (Lovley and Klug 1983) restricting the process of methanogenesis to the deeper sediment layers that are depleted of SO_4^{2-}. Nevertheless, methanogenesis was repeatedly confirmed as the dominant process in the final mineralization of organic matter (Kuivila et al. 1989; Sinke et al. 1992). On a global scale, the contribution of aquatic ecosystems to the atmospheric methane budget is relatively small (3 %)—a fact that seems to disagree with the well-established importance of methanogenesis in carbon cycling (e.g., Rudd and Taylor 1980). This apparent contradiction is the result of the activity of methane-oxidizing prokaryotes, or methanothrophs, that in aquatic environments effectively attenuate the sedimentary CH_4 flux by oxidizing upward diffusing methane in the presence of suitable electron acceptors (Conrad 2009). For a long time, methanotrophy was regarded as a strictly aerobic process performed by gamma- or alpha-proteobacteria (e.g., Trotsenko and Murrell 2008). However, increasing evidence suggests the existence of a group of Archaea capable of anaerobic oxidation of methane (AOM). AOM was estimated to consume the methane equivalent to 20 ± 5 % of the present atmospheric methane flux (Valentine and Reeburgh 2000).

In Lake Kinneret, both methanogenesis and methanotrophy were unexplored processes until 1998. At that time, a scientific program was launched aimed at learning about methane evolution in the water column, its role in the lake's carbon cycle, and physiological aspects of methanogenesis. The study of hypolimnetic methane accumulation together with that of sulfide during several annual lake cycles showed that the biogeochemical processes in the lake are tightly linked to the physical forcing of the water column (Eckert et al. 2002). During the stratified period, strong daily westerly winds lead to the formation of a benthic boundary layer (BBL) that is characterized by enhanced microbial activity. As such, oxygen and nitrate are depleted first in this ~ 10 m thick BBL delineated by a sharp drop of the oxygen-reduction potential, as exemplified by the April profile in Fig. 25.9. Only when the upper hypolimnion, with its significantly lower microbial activity (e.g., rate of oxygen consumption was shown to be ca. four times lower in this layer; Eckert et al. 2002), has turned anoxic as well, does the chemocline rise to the depth of the thermocline (August profile in Fig. 25.9). In the absence of suitable electron acceptors, sedimentary release causes the continuous increase of CH_4 into the hypolimnion with near-bottom concentrations reaching up to 400 µmol L^{-1} (Eckert and Conrad 2007). The peaks of both solutes in the upper hypolimnion are likely the result of BBL mixing due to internal wave braking followed by advection across the laminar hypolimnion (Eckert et al. 2002; Chap. 9, physics). Compared to other freshwater systems, this concentration is relatively high. Similar quantities measured in the hypolimnion of some temperate lakes in the northern USA (L. Paul: 250 µmol L^{-1}; L. Peter: 600 µmol L^{-1}, and L. Hummingbird: 300 µmol L^{-1}, Bastviken et al. 2008) could be attributed to low sulfate (< 60 µmol L^{-1}) and high DOC concentrations (> 500 µmol L^{-1}; Houser et al. 2003). But Lake Kinneret generates such concentrations at a tenfold higher sulfate and five times lower DOC. Conditions are similar for Lakes Konstanz and Lugano where CH_4 concentrations in the anaerobic zone remain significantly lower at 120 µmol L^{-1} (Schmidt and Conrad 1993) and 80 µmol L^{-1} (Liu et al. 1996),

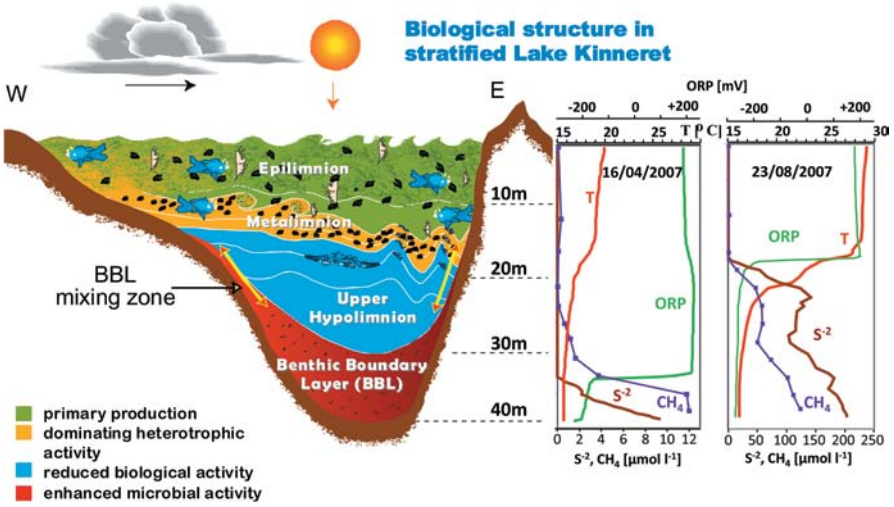

Fig. 25.9 Biological stratification in Lake Kinneret during summer in response to physical forcing. Microbial activity is highest in the benthic boundary layer and the metalimnion, and lowest in the laminar "upper hypolimnion." The effect of the stratification on the evolution of biochemical processes in the water column is indicated in the right panel by the sulfide (S^{2-}), CH_4, oxidation reduction potential (*ORP*), and temperature (*T*) profiles from April and August. (Reproduced from Eckert et al. 2002 with permission from Springer)

respectively. The only environmental parameter that may explain the relative high methane concentrations in Lake Kinneret is the elevated temperature in comparison to temperate lakes (Thebrath et al. 1993).

During the stratified period, the accumulation pattern of methane in the hypolimnion of Lake Kinneret follows closely that of sulfide (Fig. 25.10), with annual average concentrations around 3 and 6 mol m^{-2}, respectively. The relative impact of both processes on the mineralization of OC was elaborated further by Eckert and Conrad (2007), who established a carbon budget for Lake Kinneret. Sulfate reduction was identified as the dominant process in the decomposition of organic matter that seasonally settles into the hypolimnion (~20 mol C m^{-2} $year^{-1}$), accounting for 60 % of the C input. Methane release represented 30–40 % including that of methane gas ebullition. The latter constituted approximately 25 % of the sedimentary methane flux (Eckert and Conrad 2007), a figure that was confirmed by echosounder measurements (Ostrovsky 2003; Ostrovsky et al. 2008; Ostrovsky and Tegowski 2010).

Physiological studies targeting methanogenesis in the sediment of Lake Kinneret have indicated extreme substrate limitation, with methane production from acetate being partly due to syntrophic oxidation coupled with hydrogenotrophic methanogenesis rather than direct acetoclastic cleavage (Nüsslein et al. 2001, 2003; Schwarz et al. 2008). Molecular analysis of the microbial community structure in the upper 10 cm of profundal sediments revealed that the numbers of archaea and bacteria,

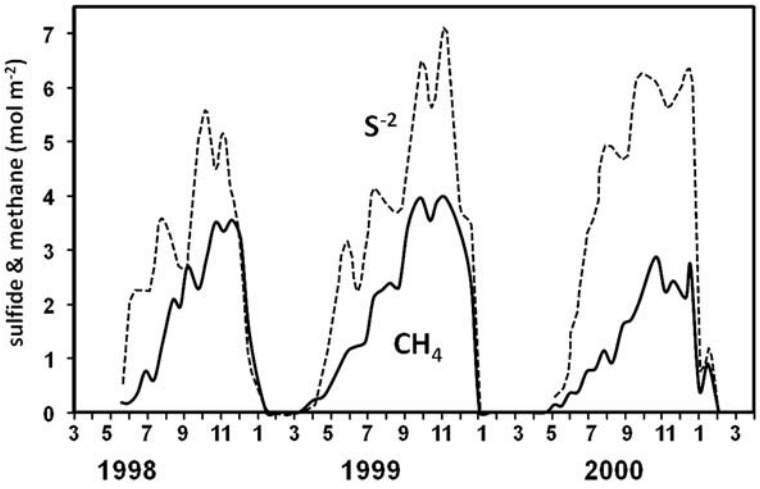

Fig. 25.10 Seasonal patterns of near-bottom dissolved methane and total sulfide concentrations in the hypolimnion of Lake Kinneret during the years 1998–2000. (Reproduced from Eckert and Conrad 2007 with permission from Springer)

quantified by real-time polymerase chain reaction (PCR), amounted to about 10^8 and 10^{10} 16S rRNA gene copies cm^{-3} sediment, respectively, suggesting that Archaea account for only a minor fraction (approximately 1 %) of the total prokaryotic community (Schwarz et al. 2007a, 2007b). Since methanogenesis is carried out by Archaea only, this observation supports the overall assumption that methanogenesis plays only a minor role in the carbon cycle of the Lake Kinneret.

Seasonal profiles of dissolved methane in the pore water of intact sediment cores from the centrally located Sta. A (see location in Fig. 1.1a, Chap. 1) typically show a prominent increase in sediment depth with a maximum around 10 cm (Fig. 25.11a, redrawn from Adler et al. 2011). Below the peak zone, dissolved methane decreases again to concentrations similar to those measured in the upper sediment layers. Model results (Adler et al. 2011) as well as incubation experiments suggest that this decline is the result of a methane sink in the deeper lake sediments. Apparently, methanogenesis is not substrate limited in this zone, based on the DOC profile that is characterized by increasing concentrations with depth (Fig. 25.11a). Thus, the hypothesis evolved that methane production may be balanced by methane consumption.

The assumption of AOM could be further manifested by means of the $\delta^{13}C$ signatures measured within the zone of deep methane decrease (Fig. 25.11b, modified from Sivan et al. 2011). The $\delta^{13}C$-CH_4 profile shows a decrease from −60 ‰ at 1-cm depth to about −65 ‰ at 7-cm depth and then an increase to a maximum of −53.5 ‰ at 24 cm, an increase that can only be explained by methanotrophy, in which the residual methane becomes isotopically heavier. Besides this geochemical evidence for AOM in deep Kinneret sediments, Sivan et al. (2011) suggested

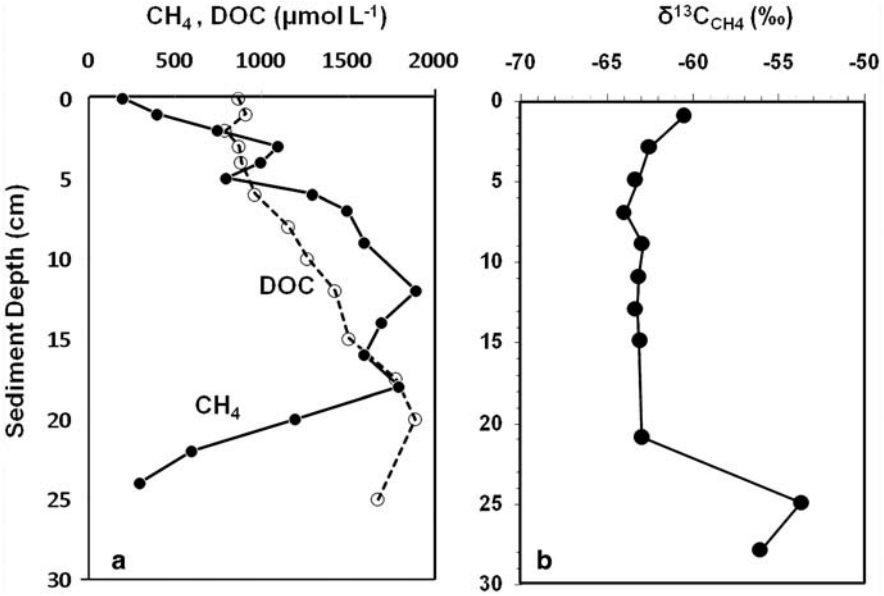

Fig. 25.11 Sediment pore water depth profiles of **a** dissolved methane and dissolved organic C (*DOC*) and **b** $\delta^{13}C$–CH_4 signature measured in intact sediment cores sampled in August 2009 at Sta. A at the center of Lake Kinneret (location in Fig. 1.1 of Chap. 1). (The *DOC* profile represents unpublished data of Bar Or and Eckert; CH_4 and $\delta^{13}C$ profiles are redrawn from Sivan et al. 2011—Copyright 2014 by the Association for the Sciences of Limnology and Oceanography, Inc.)

that AOM is likely driven by iron (Fe) reduction, a hypothesis that was verified by dissolved iron concentration and isotopic profiles measured in the pore water of intact sediment cores and by Fe(III)-amended mesocosm studies.

Analysis of seasonal sediment cores from Sta. A revealed that below the sediment water interface sulfate reduction is the dominant process throughout the year with rates peaking at around 1.5×10^{-12} mol cm^{-3} s^{-1} and declining exponentially with depth (Fig. 25.12). Methanogenesis starts at ~3 cm depth with maximum rates of 4×10^{-13} mol cm^{-3} s^{-1} at 5–12 cm depth, followed by decreasing methane concentrations below the maximum methane production zone. Apparently, this decline is caused by AOM taking place at a rate of about 5×10^{-14} mol cm^{-3} s^{-1} (Adler et al. 2011). To explain the average annual hypolimnetic CH_4 accumulation of 3 mol m^{-2} (Fig. 25.10) with the reported rates of methanogenesis requires a 20–25 cm-thick sedimentary zone of methane production—a presumption that matches well our measured profiles (Fig. 25.12).

In summary, the study of methane cycling in Lake Kinneret revealed some unique features in comparison to other freshwater lakes. Besides the relatively high concentrations of dissolved CH_4 in spite of high sulfate and low DOC concentrations, there is the important discovery of sedimentary AOM with ferrous iron, shown for the first time ever in a natural aquatic system.

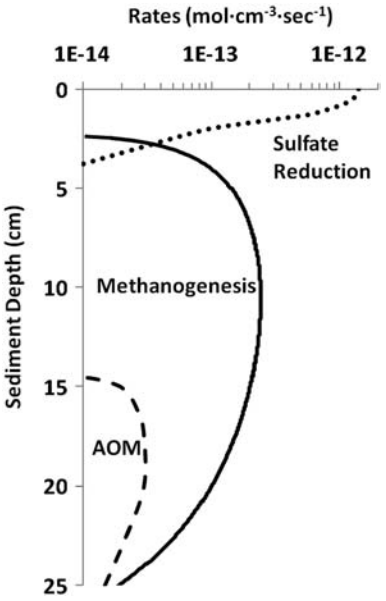

Fig. 25.12 Geochemical model output of the changes with sediment depth of rates of sulfate reduction (*dotted line*), methanogenesis (*full line*), and anaerobic methane oxidation (*AOM, dashed line*) in Lake Kinneret. (Drawn from data published by Adler et al. 2011 and Sivan et al. 2011)

25.5 Fluxes of Organic Carbon in the Epilimnion

Tom Berman, Arkadi Parparov, Yosef Z Yacobi, and Ilia Ostrovsky

25.5.1 Organic Carbon Sources and Sinks in Lake Kinneret

The first delineation of carbon flows in the Lake Kinneret system was by Serruya et al. (1980) who emphasized the different patterns observed during the "*Peridinium* season" and during the summer–fall. In winter–spring, the major OC input was from primary production during the regular annual dinoflagellate bloom by large *Peridinium* cells that were mostly not grazed by zooplankton but broken down in the water column by heterotrophic bacteria. By contrast, in summer–fall, primary production was carried out by smaller phytoplankton, mostly chlorophyta, that were readily grazed by the resident cladocerans, which in turn provided sustenance for copepods and fish. Later studies provided more detailed quantitative descriptions of carbon fluxes in the lake ecosystem, based on more extensive data including bacterial and protozoan (ciliates and flagellates) participation in OC cycling (Stone et al. 1993; Hart et al. 2000). Here, we present an overview of OC fluxes in the lake, based on data from 2001 to 2010.

Table 25.6 Lake Kinneret: Annual, averaged, daily organic carbon fluxes in the epilimnion (0–15 m) for the years 2001 through 2010

Year	Input	Sink		Ratio	Balance
	GPP	CR	SED	SED/GPP (%)	GPP-CR-SED
2001	2,480	2,310	540	22	−370
2002	2,240	2,010	*nd*	*nd*	*nd*
2003	2,450	2,370	*nd*	*nd*	*nd*
2004	2,540	2,520	360	14	−340
2005	1,880	1,700	300	16	−120
2006	2,250	1,890	300	13	60
2007	2,240	2,500	400	18	−660
2008	2,400	1,530	380	16	490
2009	2,170	1,570	340	16	260
2010	2,360	1,900	280	12	180
Average	2,301	2,030	360	16	−63
SD	200	350	80	3	

GPP calculated as $1.5 \times {}^{14}$C-measured primary production, except for years when *Peridinium* bloomed (shown in bold) when the GPP for January–June was calculated as $2 \times {}^{14}$C-measured primary production; CR measured by ΔO_2 method; and SED measured in sediment traps positioned 11 m above the bottom to avoid the impact of resuspension (Ostrovsky and Yacobi 2010). Allochthonous organic C inputs are generally ~1 % of GPP. Ratios of SED:GPP are given as percentages, *nd* not defined

GPP Gross primary production, *CR* community respiration, *SED* sedimentation are given in mg C m^{-2} day^{-1}

In Table 25.6, we show the major, annual, averaged daily OC fluxes for the years 2001–2010; during this period, *Peridinium* blooms occurred only in 2003, 2004, and 2007. Table 25.6 shows only the major autochthonous OC input, GPP (calculated from routine measurements of ^{14}C primary production, see Sect. 24.1), and sinks (CR, measured with ΔO_2, see Sect. 25.2 and sedimentation, SED, determined from direct measurements with sediment traps). These fluxes are also shown separately for the winter–spring and summer–fall seasons in Table 25.7.

By far, the major input of OC into Lake Kinneret was from GPP by phytoplankton (Sect. 24.1), with GPP estimated as $1.5 \times {}^{14}$C-measured primary production, except for January–June 2003, 2004, and 2007, when, during *Peridinium* blooms, GPP was calculated as $2.0 \times {}^{14}$C-measured primary production. Minor additional inputs were from chemoautotrophic bacteria (Sect. 24.2), watershed inflows, direct rainfall, benthos, littoral vegetation, and dust. The major loss of OC derived from community respiration (Sect. 25.2), followed by losses from sedimentation (Fig. 25.13). Other losses through outflows via the National Water Carrier, local water consumption (including water to the Kingdom of Jordan), and to the southern Jordan River were very small.

Note that the data (given as mg C m^{-2} day^{-1}) in Tables 25.6 and 25.7 were derived from measurements made in the epilimnion (here, taken as the water layer from 0 to 15 m) and show only the major OC fluxes in this system. Neither OC production nor OC losses have been quantified in the deeper waters of the lake (average lake depth ~24 m). In addition, we have not included in these tables autochthonous

Table 25.7 Lake Kinneret: Semiannual, averaged, daily organic carbon fluxes (January–June and July–December) in the epilimnion (0–15 m) for the years 2001 through 2010

Year	January–June						July–December					
	Input	Sink		Ratio	Sink	Ratio	Input	Sink		Ratio	Sink	Ratio
	GPP	CR	SED	SED:GPP (%)	BCD	BCD:GPP (%)	GPP	CR	SED	SED:GPP (%)	BCD	BCD:GPP (%)
2001	2,610	2,460	850	33	2,110	81	2,350	2,150	220	9	1,770	75
2002	2,350	2,310	*nd*	*nd*	1,810	77	2,140	1,710	*nd*	*nd*	1,380	64
2003	3,050	3,190	*nd*	*nd*	2,240	73	1,840	1,560	*nd*	*nd*	1,090	59
2004	2,870	3,370	470	16	2,510	87	2,210	1,660	250	11	1,200	54
2005	1,770	1,940	400	23	1,340	76	1,990	1,450	190	10	970	49
2006	2,470	2,080	390	16	1,560	63	2,030	1,700	200	10	1,360	67
2007	2,520	2,920	500	20	2,280	90	1,960	2,090	300	15	1,510	77
2008	2,450	1,500	440	18	1,280	52	2,360	1,550	330	14	1,140	48
2009	2,130	1,420	450	21	1,010	47	2,220	1,720	240	11	1,240	56
2010	2,390	1,960	310	13	1,130	47	2,340	1,840	240	10	1,140	49
Average	2,460	2,320	480	20	1,730	70	2,140	1,740	250	11	1,280	60
SD	340	640	150	6	510	15	170	220	40	2	220	10

GPP, CR, SED (defined in legend for Table 25.6), and BCD (bacterial C demand = bacterial production + bacterial respiration) are given in mg C m^{-2} day^{-1}. GPP was calculated as explained in the legend of Fig. 25.1; CR measured by ΔO_2 method; and SED measured in sediment traps positioned 11 m above the bottom to avoid the impact of resuspension (Ostrovsky and Yacobi 2010). Ratios of SED:GPP and BCD:GPP are given as percentages. Years when *Peridinium* bloomed are shown in bold

SD standard deviation, *nd* not defined

inputs of OC resulting from chemoautotrophic activity. Chemoautotrophic inputs may add somewhere between ~5 and 10% OC on an annual basis, but these have not been consistently monitored and occur only in aerobic/anaerobic interfaces such as in the metalimnion and sediment–water interface (Sect. 24.2). Additional inputs of allochtonous OC into Lake Kinneret brought by river inflows from the watershed (Chap. 18), direct rainfall, benthos, littoral vegetation, and dust constitute a very small percentage (~1–2%) of the GPP and have not been included in Tables 25.6 and 25.7. Other losses that occur but are not shown in these tables include OC removed in fish biomass by commercial fishing and birds, and in the water outflows to the National Water Carrier, to the southern Jordan River, to local water consumers, and to the Kingdom of Jordan (Chap. 31). In total, these OC losses are estimated to be not greater than ~1–5% of GPP.

The major sink for OC was always CR; annual losses by SED averaged 16% varying from 12 to 22% of GPP (Table 25.6). Note that CR data in Table 25.6 were based on measurements that did not include respiration by fish, estimated to be <3% of CR (Hart et al. 2000). Overall, the 10-year record of the difference "Inputs-Sinks" indicated that some further inputs and sinks not shown in Table 25.6 could be required to better balance the OC budget; however, these "missing" components were quantitatively minor. Also, inherent problems in the measurements of GPP, CR and SED add a measure of uncertainty to the data.

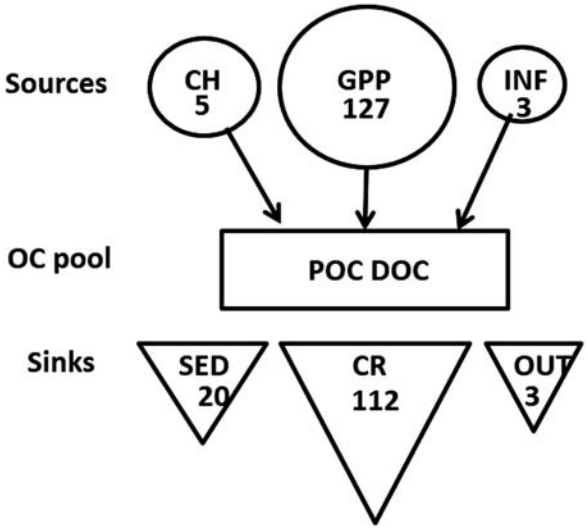

Fig. 25.13 Organic carbon (*OC*) fluxes for the epilimnic waters of Lake Kinneret based on averaged annual rates from 2001 to 2010. Sources of *OC* are gross primary production (*GPP*), chemosynthesis (*CH*), and inputs (*INF*) from watershed inflows and dust. Sinks of *OC* are community respiration (*CR*), sedimentation (*SED*), and outflows (*OUT*) via the National Water Carrier, southern Jordan River, and pumping for local water consumption and to the Kingdom of Jordan. The *OC* pool in the lake is comprised of particulate and dissolved *OC* (*POC* and *DOC*). The numbers represent annual *OC* fluxes as tons C lake$^{-1} \times 1{,}000$, based on lake surface area = 151 km^2 measured for an average lake depth of 24 m

Clear differences in OC semiannual flux patterns over the period 2001–2010 were observed (Table 25.7). With few exceptions, the relative amounts of GPP, CR, and SED were usually greater in the first half of the year in comparison with the second half of the year, resulting from the higher levels of primary production and nutrient inputs in winter–spring (Table 25.8). This was particularly evident with respect to GPP and CR in 2003, 2004, and 2007 when dense blooms of *Peridinium* occurred. In winter–spring season of these years, measured rates of CR exceeded those of GPP, presumably due to the high intrinsic respiration of the dinoflagellate bloom and subsequently to elevated rates of bacterial respiration linked to the breakdown of the phytoplankton biomass.

The ratio between GPP (winter–spring) and GPP (summer–fall) in any given year ranged from 0.9 to 1.7 (average 1.2 ± 0.2) whereas the ratio between SED (winter–spring) and SED (summer–fall) was always higher, ranging from 1.3 to 3.9 (average 2.0 ± 0.8). This suggests that the main reason for the lower average percentage of summer–fall SED:GPP (11 ± 2 %) compared to winter–spring SED:GPP (20 ± 6 %) was because more of the autochthonous particulate organic carbon (POC) generated by GPP was lost by respiration or transformation to DOC in the second half of the year. This observation implies that the POC formed in the latter half of

Table 25.8 Ratios of winter–spring to summer–fall averages of gross primary production (*GPP*), community respiration (*CR*), sedimentation (*SED*), and bacterial C demand (*BCD*) measured in Lake Kinneret, 2001–2010, and the multiannual average and standard deviation (*SD*), (*nd*: not defined)

	GPP	CR	SED	BCD
2001	1.1	1.1	3.9	1.2
2002	1.1	1.4	nd	1.3
2003	1.7	2.1	nd	2.0
2004	1.3	2.1	1.9	2.1
2005	0.9	1.3	2.1	1.4
2006	1.2	1.2	2.0	1.1
2007	1.3	1.4	1.7	1.5
2008	1.0	1.0	1.3	1.1
2009	1.1	0.8	1.9	0.8
2010	1.0	1.1	1.3	1.0
Average	1.2	1.3	2.0	1.4
SD	0.2	0.4	0.8	0.4

the year was relatively more labile (i.e., less POC reached the lake bottom) than the POC formed in winter–spring. Another possible reason for the observed difference in SED: GPP is a more efficient recycling of POC within the epilimnion in summer and fall (see Chap. 27).

The annual averages of CR (Table 25.6) were weakly correlated to GPP ($r^2 = 0.47$; $p = 0.028$; $n = 10$); a much stronger correlation ($r^2 = 0.67$; $p = 0.004$; $n = 10$) was found between CR and GPP measured for the January–June season only (Table 25.7). No significant relationship was observed for CR and GPP in the latter half of the year. Curiously, no correlations were found between GPP and SED or, less surprisingly, between CR and SED.

25.5.2 Net Autotrophic and Heterotrophic States of the Lake

In view of the unexpectedly high potential of lakes to act as sources or sinks of greenhouse gasses and to function as significant regulators of climate change on a global scale (Williamson et al. 2009), considerable interest has focused on their overall net autotrophic or heterotrophic status. Given the low OC external inputs, it is not surprising that the euphotic zone of Lake Kinneret is generally net autotrophic. However, when examined on a semiannual basis, measured CR was higher than GPP in the winter–spring (January to June in 2003, 2004, 2005, and 2007), indicative of net heterotrophic conditions. As noted, 2003, 2004, and 2007 were years with large *Peridinium* blooms with intrinsically high levels of respiration. Additionally, after the rapid die-off of the bloom, the dense phytoplankton biomass would be expected to undergo extensive degradation by heterotrophic bacteria, giving rise to heightened CR. In spring 2005, there was an unusual bloom of the filamentous green alga *Mougeotia* sp. (Zohary et al. 2012) which may have resulted in a net heterotrophic situation where CR > GPP (Table 25.7). Overall, however, despite relatively short, occasional periods of net heterotrophy, Lake Kinneret is clearly net autotrophic (see below).

25.5.3 Organic Carbon Flux Through the Microbial Loop

In early studies of OC cycling in Lake Kinneret (Serruya et al. 1980), the role of microorganisms was scarcely considered. However, later modeling studies of carbon fluxes in the lake indicated the central function of bacteria and protista in cycling of OC (Stone et al. 1993; Hart et al. 2000); this was subsequently confirmed by experimental measurements (Berman et al. 2004, 2010). As can be seen in Table 25.7, BCD (calculated as the sum of BP plus BR), a measure of the OC flux through the heterotrophic bacteria, was always a relatively high proportion of the total autochthonous OC inputs, ranging from 45 to 91 % of GPP in winter–spring and 48 to 77 % of GPP in summer–fall (for more details on BCD, see Sect. 25.1).

25.5.4 Generalized Organic C Budget for Epilimnic Waters of Lake Kinneret

We show a generalized diagram quantifying annual OC fluxes for the epilimnic waters of Lake Kinneret based on averaged annual rates from 2001 to 2010 in Fig. 25.13. Here, we have included estimates for minor inputs such as chemosynthetic primary production, OC in river inflows from the watershed, direct rainfall on the lake, benthos, littoral vegetation and dust, as well as minor OC sinks such as OC in outflows to the National Water Carrier, local water consumers, southern Jordan River outflow, and water supply to the Kingdom of Jordan.

The decade-long summary shown in Fig. 25.13 would imply that over this period, ~94 % of OC input derived from autochthonous, photosynthetic carbon fixation by lake phytoplankton. Possibly, this underestimates the contribution of chemosynthetically fixed OC (Sect. 24.2), albeit most chemosynthetic activity would not occur within the epilimnic waters of the lake. Most (~83 %) of the OC input was eventually respired. A considerable portion of the OC pool was taken up, recycled, and respired through the microbial communities; BCD accounted for ~65 % of GPP annually (Table 25.7). Reflecting the net autotrophic status of Lake Kinneret, about ~20,000 t C (~15 % of the total OC input) was transferred to the sediments annually.

References

Adler M, Eckert W, Sivan O (2011) Quantifying rates of methanogenesis and methanotrophy in Lake Kinneret sediments (Israel) using pore-water profiles. Limnol Oceanogr 56:1525–1535

Aristegui J, Montero MF, Ballesteros S, Basterretxea G, van Lenning K (1996) Planktonic primary production and microbial respiration measured by ^{14}C assimilation and dissolved oxygen changes in coastal waters of the Antarctic Peninsula during austral summer: implications for carbon flux studies. Mar Ecol Prog Ser 132:191–201

Bastviken D, Cole JJ, Pace ML, Van de Bogert MC (2008) Fates of methane from different lake habitats: connecting whole-lake budgets and CH4 emissions. J Geophys Res 113:G02024

Berman T, Gerber C (1980) Differential filtration studies of carbon flux from living algae to microheterotrophs, microplankton size distribution and respiration in Lake Kinneret. Microb Ecol 6:189–198
Berman T, Kaplan B (1984a) Diffusion chamber studies of carbon flux from living algae to heterotrophic bacteria. Hydrobiologia 108:127–135
Berman T, Kaplan B (1984b) Respiration of Lake Kinneret microplankton measured by carbon loss in the dark. Arch Hydrobiol Beih Ergeb Limnol 19:157–162
Berman T, Pollingher U (1974) Annual and seasonal variations of phytoplankton, chlorophyll and photosynthesis in Lake Kinneret. Limnol Oceanogr 19:31–54
Berman T, Stone L (1994) Musings on the microbial loop: twenty years after. Microbial Ecol 28:251–253
Berman T, Wynne D (2005) Assessing phytoplankton lysis in Lake Kinneret. Limnol Oceanogr 50:526–537
Berman T, Hadas O, Marchaim U (1979) Heterotrophic glucose uptake and respiration in Lake Kinneret. Hydrobiologia 62:275–282
Berman T, Kaplan B, Chava S, Parparova R, Nishri A (1993) Effects of iron and chelation on Lake Kinneret bacteria. Microb Ecol 26:1–8
Berman T, Stone L, Yacobi YZ, Kaplan B, Schlichter M, Nishri A, Pollingher U (1995) Primary production and phytoplankton in Lake Kinneret: a long-term record (1972–1993). Limnol Oceanogr 40:1064–1076
Berman T, Kaplan B, Chava S, Viner Y, Sherr BF, Sherr E (2001) Metabolically active bacteria in Lake Kinneret. Aquatic Microb Ecol 23:213–224
Berman T, Parparov A, Yacobi YZ (2004) Planktonic community production and respiration and the impact of bacteria on carbon cycling in the photic zone of Lake Kinneret. Aquat Microb Ecol 34:43–55
Berman T, Yacobi YZ, Parparov A, Gal G (2010) Estimation of long-term bacterial respiration and growth efficiency in Lake Kinneret. FEMS Microbiol Ecol 71:351–363
Canfield DE (1989) Sulfate reduction and oxic respiration in marine sediments: implications for organic carbon preservation in euxenic environments. Deep Sea Sci 36:121–138
Canfield DE, Des Marais DJ (1991) Aerobic sulfate reduction in microbial mats. Science 251:1471–1473
Capone DG, Kiene RP (1988) Comparison of microbial dynamics in marine and freshwater sediments: contrasts in anaerobic carbon catabolism. Limnol Oceanogr 33:725–749
Choi JW, Sherr EB, Sherr BS (1999) Dead or alive? A large fraction of ETS-inactive marine bacterioplankton cells, as assessed by reduction of CTC, can become ETS-active with incubation and substrate addition. Aquat Microb Ecol 18:105–115
Cole JJ, Findlay SEG, Pace ML (1988) Bacterial production in fresh and saltwater ecosystems: a cross-system overview. Mar Ecol Prog Ser 43:1–10
Conrad R (2009) The global methane cycle: recent advances in understanding the microbial processes involved. Environ Microbiol Rep 1(5):285–292
Cypionka H (2000) Oxygen respiration in *Desulfovibrio* species. Ann Rev Microbiol 54:827–848
del Giorgio P, Williams P (2005a) Respiration in aquatic ecosystems. Oxford University Press, Oxford, 324 pp
del Giorgio P, Williams P (2005b) The global significance of respiration in aquatic ecosystems: from single cells to the biosphere. In: del Giorgio P, Williams P (eds) Respiration in aquatic ecosystems. Oxford University Press, Oxford, pp. 267–303
Eckert W, Conrad R (2007) Sulfide and methane evolution in the hypolimnion of a subtropical lake: a three-year study. Biogeochemistry 82:67–76
Eckert W, Imberger J, Saggio A (2002) Biogeochemical evolution in response to physical forcing in the water column of a warm monomictic lake. Biogeochemistry 61:291–307
Fenchel T, Finlay BJ (1995) Ecology and evolution in anoxic worlds. Oxford University Press, Oxford
Frund C, Cohen Y (1992) Diurnal cycles of sulfate reduction under oxic conditions in cyanobacterial mats. Appl Environ Ecol 58:70–77

Gazeau FJ, Middelburg JM, Loijens JP et al (2007) Planktonic primary production in estuaries: a comparison of the ^{14}C, O_2 and ^{18}O methods. Aquat Microb Ecol 46:95–106
Geider RJ (1997) Photosynthesis or planktonic respiration? Nature 388:132
Gophen M (1978) Zooplankton. In: Serruya C (ed) Lake Kinneret. W Junk, The Hague
Gophen M (1981) Metabolic activity of herbivorous zooplankton in Lake Kinneret (Israel) during 1972–1977. J Plankton Res 3(1):15–24
Hadas O, Pinkas R (1992) Sulfate reduction process in sediments of Lake Kinneret, Israel. Hydrobiologia 235:295–301
Hadas O, Pinkas R (1995a) Sulfate reduction in the hypolimnion and sediments of Lake Kinneret, Israel. Freshw Biol 33:63–72
Hadas O, Pinkas R (1995b) Sulfate reduction processes in sediments at different sites in Lake Kinneret, Israel. Microb Ecol 30:55–66
Hadas O, Pinkas R (1997) Arylsulfatase and alkaline phosphatase (Apase) activity in sediments of Lake Kinneret, Israel. Water Air Soil Pollut 99:671–679
Hambright KD, Zohary T, Gude H (2007) Microzooplankton dominate carbon flow and nutrient cycling in a warm subtropical freshwater lake. Limnol Oceanogr 52:1018–1025
Hart DR, Berman T, Stone L (2000) Seasonal dynamics of the Lake Kinneret food web: the importance of the microbial loop. Limnol Oceanogr 45:350–361
Hepher B, Langer J (1969) Summary of the final research on the primary production in Lake Kinneret. Alon Techni (Mekorot) 4(2):32–35 (in Hebrew)
Houser JN, Bade DL, Cole JJ, Pace ML (2003) The dual influences of dissolved organic carbon on hypolimnetic metabolism: organic substrate and photosynthetic reduction. Biogeochemistry 64:247–269
Ingvorsen K, Jorgensen B (1984) Kinetics of sulfate uptake by freshwater and marine species of *Desulfovibrio*. Arch Microbiol 139:61–66
Jorgensen BB (1978) A comparison of methods for the quantification of bacterial sulfate-reduction in coastal marine sediments. Geomicrobiol J 1:11–27
Jumars PA, Penry DA, Baross JA, Perry MJ, Frost W (1989) Closing the microbial loop: dissolved carbon pathway to heterotrophic bacteria from incomplete ingestion, digestion and absorption in animals. Deep-Sea Res 36:483–495
King GM, Klug MJ (1982) Comparative aspects of sulfur mineralization in sediments of eutrophic lake basin. Appl Environ Microbiol 43:1406–1412
Kirchman DL, Knees E, Hodson RE (1985). Leucine incorporation and its potential as a measure of protein synthesis by bacteria in natural aquatic systems. App Environ Microbiol 49:599–607
Kuivila KM, Murray JW, Devol AH (1989) Methane production, sulfate reduction and competition for substrates in the sediments of Lake Washington. Geochim Cosmochim Acta 53:409–416
Landers DH, Mitchell MJ (1988) Incorporation of $^{35}SO_4$ into sediments of three New-York lakes. Hydrobiologia 160:85–95
Liu R, Hofmann A, Gulacer FO, Favarger PY, Dominik J (1996) Methane concentration profiles in a lake with permanently anoxic hypolimnion (Lake Lugano, Switzerland-Italy). Chem Geol 133:201–209
Lovley DR, Klug MJ (1983) Sulfate reducers can outcompete methanogens at freshwater sulfate levels. Appl Environ Microbiol 45:187–192
Lovley DR, Klug MJ (1986) Model for the distribution of sulfate reduction and methanogenesis in freshwater sediments. Geochim Cosmochim Acta 50:11–18
Luz B, Barkan E, Sagi Y, Yacobi YZ (2002) Evaluation of community respiratory mechanisms with oxygen isotopes: a case study in Lake Kinneret. Limnol Oceanogr 47(1):33–42
Nishri A, Zohary T, Gophen M, Wynne D (1998) Lake Kinneret dissolved oxygen regime reflects long term changes in ecosystem functioning. Biogeochemistry 42:253–283
Nüsslein B, Chin KJ, Eckert W, Conrad R (2001) Evidence for anaerobic synthrophic acetate oxidation during methane production in the profundal sediment of subtropical Lake Kinneret (Israel). Environ Microbiol 3:460–470
Nüsslein B, Eckert W, Conrad R (2003) Stable isotope biogeochemistry of methane formation in profundal sediments of Lake Kinneret (Israel). Limnol Oceanogr 48(4):1439–1446

Oremland RS, Polcin S (1982) Methanogenesis and sulfate reduction: competitive and noncompetitive substrates in estuarine sediments. Appl Environ Microbiol 44:1270–1276
Ostrovsky I (2003) Methane bubbles in Lake Kinneret: quantification, temporal, and spatial heterogeneity. Limnol Oceanogr 48:1030–1036
Ostrovsky I, McGinnis DF, Lapidus L, Eckert W (2008) Quantifying gas ebullition with echo sounder: the role of methane transport with bubbles in a medium-sized lake. Limnol Oceanogr Method 6:105–118
Ostrovsky I, Tegowski J (2010) Hydroacoustic analysis of spatial and temporal variability of bottom sediment characteristics in Lake Kinneret in relation to water level fluctuations. Geo-Mar Lett 30:261–269
Ostrovsky I, Yacobi YZ (2010) Sedimentation flux in a large subtropical lake: spatiotemporal variations and relation to primary productivity. Limnol Oceanogr 55(5):1918–1931
Pace ML, Prairie YT (2005) Respiration in lakes. In: del Giorgio P, Williams P (eds) Respiration in aquatic ecosystems. Oxford University Press, Oxford, pp 103–121, (324 pp)
Pinhassi J, Berman T (2003) Differential growth ersponse of colony-forming α- and γ-proteobacteria in dilution culture and nutrient addition experiments in Lake Kinneret, eastern Mediterranean and Gulf of Eilat. Appl Environ Microbiol 69:199–211
Plugge CM, Zhang W, Sholten JCM, Stams AJM (2011) Metabolic flexibility of sulfate-reducing bacteria. Front Microbiol. doi:10.3389/fmicb.2011.00081
Postgate JR (1984) The sulphate reducing bacteria, 2nd edn. Cambridge University Press, Cambridge
Pringault O, Tassas V, Rochelle-Newall E (2007) Consequences of light respiration on the determination of production in pelagic systems. Biogeosciences 4:105–114
Pringault O, Tesson S, Rochelle-Newall E (2009) Respiration in the light and bacteriophytoplankton coupling in a coastal environment. Microb Ecol 57:321–334
Riemann B, Fuhrman J, Azam F (1982) Bacterial secondary production in freshwater measured by 3 H-thymidine incorporation method. Microb Ecol 8:101–114
Robinson C (2008) Heterotrophic bacterial respiration. In: Kirchman DL (ed) Microbial ecology of the oceans, 2nd edn. Wiley, New York, pp 299–334
Rudd JWM, Taylor CD (1980) Methane cycling in aquatic environments. Adv Aquat Microbiol 2:77–150
Scavia D, Lang GA, Kitchel JF (1988) Dynamics of Lake Michigan plankton: a model evaluation of nutrient loading, competition, and predation. Can J Fish Aquat Sci 45(1):165–177
Schmidt U, Conrad R (1993) Hydrogen, carbon monoxide, and methane dynamics in lake constance. Limnol Oceanogr 38:1214–1226
Schwarz JIK, Eckert W, Conrad R (2007a) Community structure of Archaea and Bacteria in a profundal lake sediment, Lake Kinneret (Israel). Syst Appl Microbiol 30(3):239–254
Schwarz JIK, Lueders T, Eckert W, Conrad R (2007b) Identification of acetate-utilizing Bacteria and Archaea in methanogenic profundal sediments of Lake Kinneret (Israel) by stable-isotope probing of rRNA. Environ Microbiol 9:223–237
Schwarz JIK, Eckert W, Conrad R (2008) Response of the methanogenic microbial community of a profundal lake sediment (Lake Kinneret, Israel) to algal deposition. Limnol Oceanogr 53:113–121
Serruya C (1978) Water chemistry. In: Serruya C (ed) Lake Kinneret. W Junk, The Hague
Serruya C, Edelstein M, Pollingher U, Serruya S (1974) Lake Kinneret sediments: nutrient composition of the pore water and mud water exchanges. Limnol Oceanogr 19:489–508
Serruya C, Gophen M, Pollingher U (1980) Lake Kinneret: carbon flow patterns and ecosystem management. Arch Hydrobiol 88(3):265–302
Sherr BF, Sherr EB, Berman T (1982) Decomposition of organic detritus: a selective role for microflagellate protozoa. Limnol Oceanogr 27:765–769
Sinke AJC, Cornelese AA, Cappenberg TC, Zehnder AJB (1992) Seasonal variation in sulfate reduction and methanogenesis in peaty sediments of eutrophic Lake Loosdrecht, The Netherlands. Biogeochemistry 16:43–61

Sivan O, Adler M, Pearson A, Gelman F, Bar-Or I, John SG, Eckert W (2011) Geochemical evidence for iron-mediated anaerobic oxidation of methane. Limnol Oceanogr 56:1536–1544
Skyring GW (1988) Acetate as the main energy substrate for the sulfate reducing bacteria in Lake Eliza (South Australia) hypersaline sediments. FEMS Microbiol Lett 53:87–94
Smith RL, Klug MJ (1981) Electron donors utilized by sulfate reducing bacteria in eutrophic lake sediments. Appl Environ Microbiol 42:116–121
Smith RL, Oremland RS (1987) Big Soda Lake (Nevada) 2. Pelagic sulfate reduction. Limnol Oceanogr 32:794–803
Stiller M, Magaritz M (1974) Carbon-13 enriched carbonate in interstitial waters of Lake Kinneret. Limnol Oceanogr 19:849–853
Stone L, Berman T, Bonner R, Barry S, Weeks SW (1993) Lake Kinneret: a seasonal model for carbon flux through the planktonic biota. Limnol Oceanogr 38:1680–1695
Strayer D (1988) On the limits to secondary production. Limnol Oceanogr 33(5):1217–1220
Suttle CA (2007) Marine viruses—major players in the global ecosystem. Nat Rev Microbiol 5:801–812
Tessenow U, Frevert W, Hofgastner W, Moser A (1997) Ein simultanschliesender serienwasser-schopfer fur sedimentkontaktwasser mit fotoelektrischer selbstauslosung und fakultativem sedimentstecher. Arch Hydrobiol Suppl 48:438–452
Thebrath B, Rothfuss F, Whiticar MJ, Conrad R (1993) Methane production in littoral sediment of Lake Constance. FEMS Microbiol Lett 102:279–289
Trotsenko YA, Murrell JC (2008) Methabolic aspects of aerobic obligate methanotrophy. Adv Appl Microbiol 63:183–229
Valentine DL, Reeburgh WS (2000) New perspectives on anaerobic methane oxidation. Environ Microbiol 2(5):477–484
Westrich JT, Berner RA (1988) The effect of temperature on rates of sulfate reduction in marine sediments. Geomicrobiol J 6:99–117
Whitman WB, Bowen TL, Boone DR (1992) The methanogenic bacteria. In: Balowes A, Truper HG, Dwarkin M, Harder W, Schliefer KH (eds.) The Prokaryotes, 2nd edn. Springer, New York, pp 719–767
Williamson CE, Saros JE, Vincent WF, Smold JP (2009) Lakes and reservoirs as sentinels, integrators, and regulators of climate change. Limnol Oceanogr 54:2273–2282
Winberg GG (1960) Primary production of water bodies. The Academy of Sciences of BSSR, Minsk, 328 pp (in Russian)
Yacobi YZ (2006) Temporal and vertical variation of chlorophyll a concentration, phytoplankton photosynthetic activity and light attenuation in Lake Kinneret: possibilities and limitations for simulations by remote sensing. J Plankton Res 28:725–736
Zohary T, Hadas O, Pollingher U, Kaplan B, Pinkas R, Güde H (2000) The effect of nutrients (N, P) on the decomposition of *Peridinium gatunense* cells and thecae. Limnol Oceanogr 45:123–130
Zohary T, Ostrovsky I (2011) Ecological impacts of excessive water level fluctuations in stratified freshwater lake. Inland Waters 1:47–59
Zohary T, Nishri A, Sukenik A (2012) Present-absent: a chronicle of the dinoflagellate *Peridinium gatunense* from Lake Kinneret. Hydrobiologia 698:161–174

Chapter 26
Seston and Organic Matter

Arkadi Parparov, Tamar Zohary, Tom Berman and Gideon Gal

Abstract Studies carried out during 2000–2010 allowed us to estimate the temporal and spatial dynamics of structural and functional characteristics of seston and organic matter in Lake Kinneret: seston mass (total suspended solids, TSS), and particulate, dissolved, and total organic carbon (POC, DOC, and TOC = POC + DOC). Similar characteristics were determined for the Jordan River. On average, TSS, POC, DOC/POC, and TOC declined with water depth, indicating relative increase of seston decomposition. Phytoplankton was the largest component of the living part of seston in Lake Kinneret, comprising on average 24.7 % of the seston dry weight. During intense dinoflagellate blooms, phytoplankton comprised up to 90 % of the seston mass. Despite significant variability of the living compartments and drastic changes in the phytoplankton structure, the nonliving component was, on average, the largest component of Lake Kinneret seston, comprising about 60 % of seston mass. Metabolic activity associated with seston dominated by specific algal taxa was also estimated. The potential ecosystem importance of transparent exopolymer particles (TEP), a previously unrecognized, major component of the seston, is described. Major fluxes within the seston cycle were estimated directly, allowing the compilation of a seston budget. Sources and sinks of seston appeared to be approximately balanced which is in good agreement with the observed long-term stability of seston dynamics.

Keywords Organic carbon · Total suspended solids · Seston · Community respiration

A. Parparov (✉) · T. Zohary · T. Berman · G. Gal
The Yigal Allon Kinneret Limnological Laboratory, Israel Oceanographic & Limnological Research, P.O. Box 447, 14950, Migdal, Israel
e-mail: parpar@ocean.org.il

T. Zohary
e-mail: tamarz@ocean.org.il

G. Gal
e-mail: gal@ocean.org.il

T. Zohary et al. (eds.), *Lake Kinneret, Ecology and Management,* Aquatic Ecology Series 6,
DOI 10.1007/978-94-017-8944-8_26,

26.1 Introduction

Seston is a collective term for all particulate materials present in the free water, including both living (plankton and nekton) and nonliving particles (Wetzel 2001). Conceptually, seston is "a united structural and functional compartment of aquatic ecosystems, which participates as a united whole in production and destruction of organic matter, recycling of nutrients, sedimentation, and meeting the trophic requirements of filtrators" (Ostapenia 1989). The organic fraction of the seston together with the dissolved organic matter fraction forms the pool of organic matter in the water column. Here, we summarize the results of our studies on the structural (e.g., concentrations) and functional (time dependent, e.g., losses due to respiration) characteristics of seston and organic matter in Lake Kinneret.

26.2 Methodology

Several parameters of seston and organic matter in Lake Kinneret water were determined routinely during 2000–2010, as a part of the lake monitoring program. In order to estimate the impact of the inflows from the tributaries on cycling of seston and organic matter, similar determinations were carried out during 2003–2005 on Jordan River water. The concentration of seston dry weight (measured as total suspended solids, TSS) was estimated gravimetrically after filtration of water samples through pre-weighed Whatman GF/F filters and drying to a constant weight at 105 °C (APHA 2002). Particulate organic carbon (POC) was estimated as 50 % of the particulate organic matter, the latter assumed to be equal to loss on ignition (LI) at 550 °C of dried seston collected on GF/F filters. Recent determinations of POC with a CHN analyzer gave good agreement between these two methods (W. Eckert, unpublished). Concentrations of dissolved organic carbon (DOC) were measured on GF/F-filtered water samples by the wet combustion method with the 1010 model OC Analyzer (OI-Analytical, TX, USA). Total organic carbon (TOC) was calculated as TOC = POC + DOC. Water samples for determination of TSS, POC, and DOC were collected at Sta. A from 0-, 10-, and 20-m depth, and from 1 m above bottom sediments ("35 m" thereafter). Particle size distribution was determined on samples from depths 0 m, middle of metalimnion, and 35 m in 2003–2005 with a MET ONE WGS267 liquid particle counter (Hach, CO, USA). The instrument counts particles in the following average size fractions: 3.5, 7.5, 15, 35, 60, and > 150 µm. The average size of particles in the water sample was calculated as follows:

$$\text{Average size} = \frac{(\Sigma N_i \times S_i)}{\text{Tot. No.}}, \tag{1}$$

where N_i is the number of particles of size fraction *i,* S_i is the average size of the respective size fraction *i,* and Tot. No. is the total number of particles in all size fractions.

Water samples for determinations of the wet weight biomass of the living planktonic components (bacteria, phytoplankton, zooplankton) and the concentrations of TSS were collected fortnightly (monthly for bacteria) from the uppermost water layer (0–1 m) at Sta. A from January 2001 till August 2010. Water samples from the Jordan River were collected monthly at Arik Bridge. It was assumed that the Jordan River discharge comprises 70 % of total tributary inflow (Gal et al. 2003).

Dry weight of the living part of seston (LiveDW) was calculated as the sum of the dry weights of phytoplankton (PhytoDW), bacterioplankton (BactDW), and zooplankton (ZooDW):

$$\text{LiveDW} = \text{PhytoDW} + \text{BactDW} + \text{ZooDW}. \tag{2}$$

Other live components such as fungi and protozoa were considered to have negligible to very small contribution to LiveDW and were excluded. The wet weight of phytoplankton was determined using the sedimentation chamber and inverted microscope method as described by Zohary (2004). Zooplankton counts were converted to biomass using values of mean wet weight per individual assuming a constant size within each taxonomic or life-history group. Carbon content was estimated as 5 % of wet weight (Gal et al. 2009). The bacterial biomass was calculated (Sherr et al. 1991) as a product of the cell count on cell-specific weight (0.05 pg cell^{-1}). The following conversion factors from biomass wet weight to dry weight (mg mg^{-1}) of the planktonic organisms were chosen based on literature values (Ostapenia 1989; Coma 2001; Hessen et al. 2003): phytoplankton, 0.20; bacterioplankton and zooplankton, 0.15.

The concentration of the nonliving particles (Non-LiveDW) was calculated as:

$$\text{Non-LiveDW} = \text{TSS} - \text{LiveDW}. \tag{3}$$

The dynamics of these parameters were followed as semiannual average values: winter–spring (WS, January–June) and summer–autumn (SA, July–December). These periods have significantly different ecological features related to the dominance of dinoflagellates in the first half of the year (Berman et al. 2004) and of cyanobacteria in the second half (Zohary 2004).

Dry-weight-specific respiration was obtained by calculating the regression of measured values of community respiration, CR (measured as ΔO_2 in the dark over 24 h), versus TSS sampled in surface lake water and in a series of experiments in which seston was added at increasing concentrations to lake water samples. Dry-weight-specific respiration was also estimated by analyzing the regressions obtained from a series of experiments based on measurements of CR and TSS at different times and locations (see Parparov et al. 1998).

Oxygen demand kinetics was measured in order to estimate organic matter lability. First-order kinetics was approximated by the following equation:

$$\text{BOD}_t = \text{BOD}_{ult}(1 - e^{-kt}), \tag{4}$$

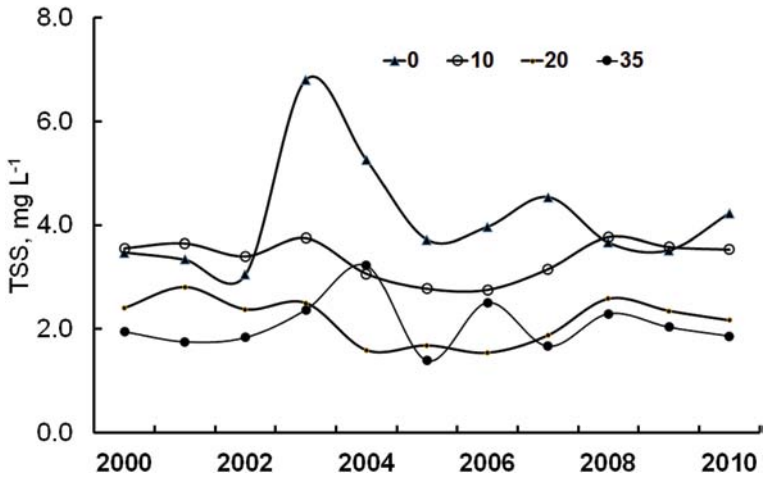

Fig. 26.1 Temporal variations in the annual average of seston (TSS) concentration at several water depths (m) in Lake Kinneret, 2000–2010

where BOD_t (mg O_2 L^{-1}) is the biological oxygen demand at time t (days); BOD_{ult} is the ultimate or total BOD, asymptotic at $t \rightarrow \infty$; and k (d^{-1}) is the reaction constant. The parameters of Eq. (4) have a clear interpretation: BOD_{ult} provides an estimate of the total labile organic carbon pool (OC_L), while k represents an estimate of lability per se, i.e., a larger k implies a more rapid breakdown of OC. The reciprocal of k is a measure of the turnover time of OC_L. In this study, we ran BOD incubations for 20–25 days (see Ostapenya et al. 2009 for more details).

26.3 Structural Characteristics of the Seston and Organic Matter in Lake Kinneret

The seston of Lake Kinneret was dominated by small particles, < 10 μm in diameter, with the largest number of particles in the metalimnion. Overall mean particle size was larger in the surface water (~8 μm) and smaller in the metalimnion and near-bottom water (~6.5 and ~6 μm, respectively).

From 2000 to 2010, TSS in the surface water layer ranged from 0.7 to 52.7 mg L^{-1}, with peak values observed during spring *Peridinium* blooms in 2003, 2004, and 2007. TSS variability in the deeper water layers was lower: from 0.3 to 7.3 mg L^{-1}. Long-term average TSS values (Table 26.1) showed a gradual decline with water depth: from 4.16 mg L^{-1} at the surface to 2.06 mg L^{-1} near the bottom. There were no distinct temporal trends in the TSS dynamics during 2000–2010, for either annual or semiannual concentrations in each water stratum (Fig. 26.1).

The organic content of the seston (i.e., % of particulate organic matter, estimated as loss on ignition, LI) varied from 29 to 99% of TSS, with maxima observed dur-

Table 26.1 Concentrations of seston and organic matter components (mg L^{-1}) at Sta. A

Depth, m	TSS	POC	DOC	TOC = POC + DOC	DOC/POC
0	4.16	1.65	3.91	5.56	2.37
10	3.35	1.24	3.76	5.00	3.03
20	2.17	0.74	3.76	4.50	5.08
35	2.06	0.64	3.87	4.51	6.05

Data are averages for 2000–2010
TSS total suspended solids, *TOC* particulate organic carbon, *DOC* dissolved organic carbon, *TOC* total organic carbon

ing the spring blooms. Average values were fairly similar with depth, ranging from 77 % in the surface water to 73 % near bottom. The concentration of POC ranged from 0.3 to 25.2 mgC L^{-1}, with average concentrations decreasing from 1.65 to 0.64 mg L^{-1} at 0 and 35 m, respectively (Table 26.1). The percentage of POC content of the seston dropped, on average, from 40 % in the surface water to 31 % near the bottom (Table 26.1). In contrast with POC, DOC varied insignificantly with water depth; therefore, the DOC/POC ratio increased with depth almost threefold, from 2.37 at 0 m to 6.05 near the bottom (Table 26.1). The increase of the DOC/POC ratio with depth (Table 26.1) is indicative of increasing losses of POC by microbial decomposition and dissolution (Parparov and Berman 2000). Apparently, this process also explains the drop of TOC from 5.56 mg L^{-1} near the surface to 4.50 mg L^{-1} in deeper water layers (Table 26.1). During *Peridinium* blooms, in the surface water, POC significantly exceeded DOC (DOC/POC = 0.3).

26.4 Sediments and Organic Matter Transported in the Jordan River

The characteristics of particulate matter (sediments) transported in the Jordan River differed from those of the lake seston and were highly variable. The average particle size of transported particulates in the Jordan River water was 12.6 ± 2.4 μm, considerably larger than that of lake sestonic particles (6–8 μm). Dry weight concentration of the transported particulates was correlated with water discharge ($r^2 = 0.59$; $P < 0.01$), indicating that riverine transfer of suspended matter was influenced by hydrological conditions. During the period studied (2002–2004), water discharge varied within an order of magnitude from 0.62 to 5.70×10^6 m^3 d^{-1} causing significant variability in the measured parameters (Table 26.2). The organic content of the transported sediments was much lower than that of lake seston (18 and 77 %, respectively). Relatively low levels of biologically available organic matter were found in the river water: BOD_5 varied within relatively narrow limits (0.72–2.24 mg O_2 L^{-1}) and never exceeded 3.0 mg O_2 L^{-1}, considered as an upper limit for sources of drinking water. Jordan River inflow water had a DOC/POC = 0.43 compared to DOC/POC = 2.4 for Lake Kinneret surface water (Table 26.1).

Table 26.2 Parameters of transported sediments and organic matter in Jordan River water (average and range of variability of monthly determinations carried out during 2002–2004)

	TSS, mg L^{-1}	LI	POC, mg L^{-1}	DOC, mg L^{-1}	TOC, mg L^{-1}	BOD_5, mgO_2L^{-1}
Average	62.0	0.18	4.83	2.10	6.93	1.59
Min–Max	18.8–360	0.06–0.27	0.77–25.0	0.45–4.33	1.22–29.3	0.72–6.73

LI loss on ignition, *TSS* total suspended solids, *POC* particulate organic carbon, *DOC* dissolved organic carbon, *TOC* total organic carbon, BOD_5 biological oxygen demand for 5 days

Table 26.3 Ranges of measured values for dry-weight-specific respiration rates (mgO_2 $mgTSS^{-1}d^{-1}$) associated with seston dominated by different algal groups

Dominant phytoplankton	Dry-weight-specific respiration	No. of cases
Dinoflagellates	0.09–0.18	7
Aulacoseira granulata	0.026–0.048	6
Microcystis spp.	0.032–0.074	6
Mougeotia sp.	0.088	1
Mixed seston[a]	0.091 ± 0.04	

[a] Calculated from regression between CR and TSS measured for samples collected at water surface

26.5 Metabolic Activity of the Seston and Organic Matter in Lake Kinneret

Estimates of dry-weight-specific CR of Lake Kinneret seston (Parparov et al. 1998; Berman et al. 2004; Ostapenia et al. 2009) and dominating phytoplankton groups indicated that the metabolism of seston is strongly affected by the metabolic properties of the phytoplankton (Table 26.3). Seston dominated by dinoflagellates had the highest dry-weight-specific respiration: on average, 0.125 mgO_2 $mgTSS^{-1}day^{-1}$. Lower values (0.032 – 0.074 mgO_2 $mgTSS^{-1}day^{-1}$) were obtained for seston associated with *Microcystis*, the species dominating the Kinneret cyanobacteria in winter–spring. The specific respiration value obtained for "mixed" seston, 0.091 mgO_2 $mgTSS^{-1}day^{-1}$, could be applied to express estimates of CR based on averaged values of seston concentration. Seston deriving from different sources exhibited very different rates of respiration. Thus, the estimated turnover rates for *Peridinium*- and *Microcystis*-dominated seston were 0.115 ± 0.005 and 0.77 ± 0.023 day^{-1}, respectively (Parparov and Berman 2000)

There was no clear seasonal trend in labile OC concentration (estimated as BOD_{ult}) which ranged from 0.70 to 6.39 mg C L^{-1}, with an average value of 1.37 mg C L^{-1}, while the decomposition constant k varied from 0.02 to 0.13 day^{-1} (0.058 day^{-1} on average). The labile fraction of OC in Lake Kinneret water comprised on average 27 % of the total OC pool.

Table 26.4 Concentrations (mg DW L^{-1}) of the living: phytoplankton (PhytoDW), zooplankton (ZooDW), bacterioplankton (BactDW), and nonliving components of the seston (Non-LiveDW)

Statistic	PhytoDW[a]	BactDW	ZooDW	Non-LiveDW[b]
Average	1.27	0.16	0.21	2.53
SD		0.09	0.11	1.86
Min–Max	0.15–39.2	0.02–0.62	0.01–0.81	0.01–19.8

Data for the uppermost water layer (0–1 m), from 2000 to 2010
[a] The variables were not normally distributed; therefore, SD values were not estimated
[b] Calculated according to Eq. (3)

26.6 Living and Nonliving Components of Seston in Lake Kinneret

The concentrations of seston and its living components varied widely during the period of observation (Table 26.4). On average, phytoplankton biomass was six to eight times higher than bacterial or zooplankton biomass but only about 30% of TSS.

The relative contribution of phytoplankton to total seston (PhytoDW/TSS, %) varied widely in individual samples: from 4.1 (December 2008) to 90% (intense *Peridinium* bloom in spring 2004). Bacterioplankton and zooplankton made a smaller contribution to total seston abundance, each comprising on average < 10% of seston mass. The semiannual average of the percentage of zooplankton in TSS varied from 3.6 to 10.5%. The bacterial component of seston varied from 2.0 to 10.0% of TSS, showing a clear tendency to decrease over time, an obvious consequence of the long-term trend of declining bacterioplankton biomass (Chap. 15).

There was a strong correlation between PhytoDW and LiveDW ($r^2 = 0.99$, $p < 0.001$, not shown), and also between the PhytoDW/TSS and LiveDW/TSS ($r^2 = 0.88$, $p < 0.01$). Phytoplankton dry weight was significantly correlated with TSS ($r^2 = 0.59$, $p < 0.01$). The relative contribution of total living and nonliving compartments to total seston (obtained from Eqns. 2 and 3, respectively) was on average 37.4 ± 6.1 and 62.6 ± 6.2% of TSS, respectively. Note that such relatively small variability (coefficient of variance for Non-LiveDW/TSS ranged from 8 to 12%) was recorded during a period that included years of intense *Peridinium* blooms (2003, 2004, and 2007), and "non-bloom" years when the dinoflagellates were at a minimum (2001, 2005, 2006, 2008, 2009; see Chaps. 10 and 11). Over the entire period of observations, the nonliving fraction was always the largest component of seston (Fig. 26.2).

Comparison of data from Lake Kinneret with those from the Naroch Lakes in Belarus (Table 26.5), where seston partitioning was extensively investigated (Ostapenia 1989), revealed some common features of seston partitioning in these lakes; (1) phytoplankton dominated the living part of seston and (2) the nonliving fraction was always the largest component of the seston.

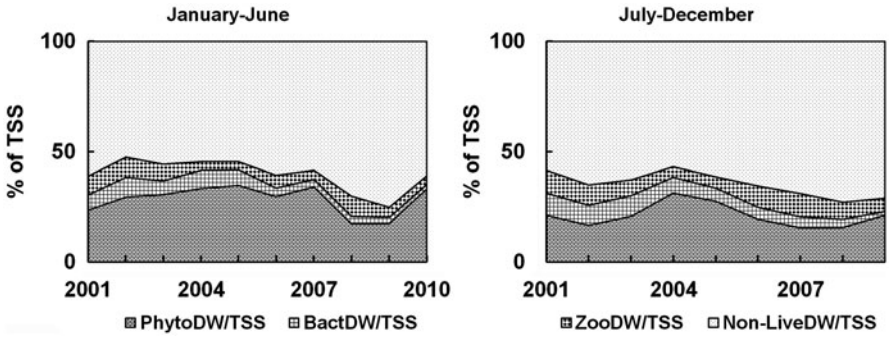

Fig. 26.2 Semiannual average values of the relative contents of the nonliving and living components of seston (as % of TSS) in winter–spring (*left panel*) and summer–autumn (*right panel*) in Lake Kinneret, 2001–2010

The organic fraction dominates in entire seston (77 % of TSS) and is close to the organic content of the living fraction (≈ 85 % of LiveDW). Consequently, the organic component (i.e., detritus) prevails also in the nonliving part (≈ 70 % of Non-LiveDW).

26.7 Transparent Polysaccharide and Proteinaceous Particles as a Major Seston Fraction

A generally unrecognized fraction of seston consists of organic transparent gel-like particles with sizes ranging from > 0.4 to > 300 μm. Since their discovery by Alldredge et al. (1993), extensive research has shown that these transparent exopolymer particles (TEP) play extremely important roles in the ecosystem functioning of both marine and freshwater environments, especially with respect to the cycling and transportation of OC and other materials, in the formation of macroaggregates (lake snow), as "hot spots" (Azam 1998) of intense microbial metabolism leading to nutrient recyling, as a food source for micrograzers, and as sites for adsorption of trace metals (Passow 2004; Bar Zeev et al. 2011). Sedimenting TEP-rich aggregates generated in near-surface waters have been imputed to effectively transport organic matter, microorganisms, nutrients, and metals such as Fe down through the water column (Passow et al. 1994; Bar Zeev et al. 2009).

The first account of TEP in Lake Kinneret appeared in Grossart et al. (1998) who observed high abundance of these particles shortly after the decline of a bloom of *A. ovalisporum* filaments. During the late summer and fall, filamentous cyanobacteria were the main producers of TEP. They observed that these aggregates with their associated microorganisms were centers of rapid recycling of particulate and dissolved organic matter; additionally, TEP and large "lake snow" particles could serve as potentially important food source for higher trophic levels such as larval, even juvenile, fish.

Table 26.5 Percentage of living and nonliving components of seston dry weight (annual average) in three Naroch Lakes (Belarus; Ostapenia 1989) and in Lake Kinneret (this study)

Lake	Living components			Nonliving component
	Phyto-plankton	Bacterio-plankton	Zooplank-ton	
Naroch (oligotro-phic)	13.4	4.6	5.2	77.5
Miastro (mesotro-phic)	23.3	3.9	3.9	67.9
Batorino (eutro-phic)	18.2	3.6	2.8	73.3
Kinneret (meso-eutrophic)	24.7	5.9	6.9	62.5

A study by Berman and Viner (2001) reported on two kinds of transparent particles in Lake Kinneret: TEP (stained with Alcian Blue for polysaccharide) and Coomassie Blue-stained proteinaceous particles (CSP). A large proportion of TEP and CSP appeared to be derived from previously particulate, detrital material. Although highly variable in abundance and characteristics, both kinds of particles were ubiquitously present throughout the year. CSP tended to be larger than TEP but were generally about threefold fewer in abundance. In contrast to TEP, significant linear correlations were found between CSP and either chlorophyll concentration or phytoplankton biomass measured at the same date. Higher densities (approximately three to tenfold) of attached bacteria were observed on CSP than on TEP which may suggest that proteinaceous particles provide a more nutritious substrate than those composed mainly of polysaccharide. Some examples of TEP from the lake are shown in Fig. 26.3. Quantitative measurements of TEP and CSP in the lake indicated that the total volume and surface area of these gel particles were much greater than that of phytoplankton, although their specific density would be expected to be much lower than that of algal cells. The high concentrations of TEP and CSP found in Lake Kinneret suggest that these microgel particles together with their associated microflora constitute a substantial amount of the lake seston.

In Lake Kinneret, where the autochthonous production of organic matter is predominant, TEP microgels are likely to be major players in the cycling of seston. This has been documented in both marine (Bar Zeev et al. 2011) and freshwater environments (de Vicente et al. 2009). TEP, formed in the upper euphotic zone from dissolved or particulate matter released by phytoplankton and bacteria or by aggregation of detrital material, may become active sites of intense microbial activity ("hot spots"). As these particles sink, they will transport organic and inorganic matter (dust), attached metals, and microorganisms down the water column; microbial metabolism and exoenzymes will cause them to partially or wholly degrade during sedimentation. The above topics will be studied in a new research project beginning in 2013.

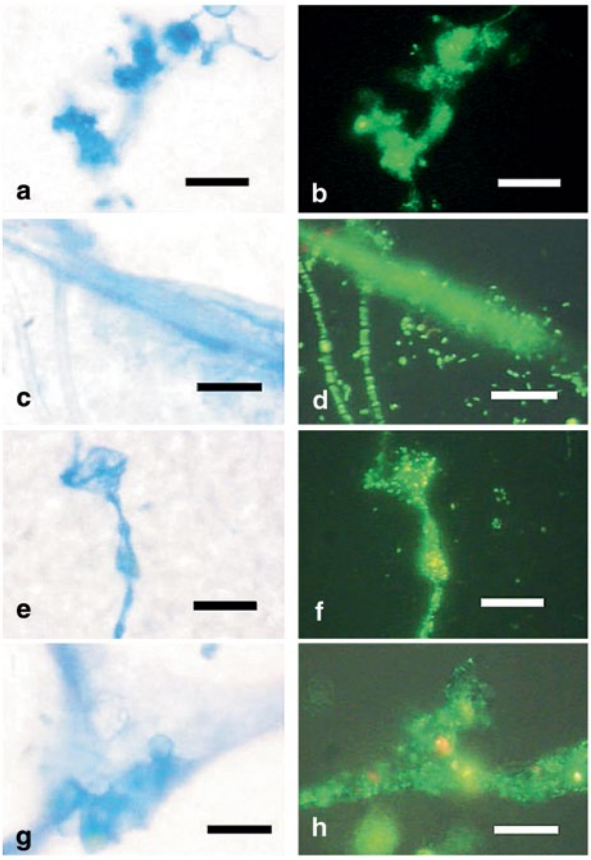

Fig. 26.3 TEP in Lake Kinneret. TEP particles stained with Alcian blue and observed under light microscope (*left panels*). SYBR green-stained TEP (*right panels*); bacteria appear as bright *green* spots or rods. The faint *green* staining of some, but not all, TEP is probably due to nucleic acids adsorbed to these particles. *Red* staining objects are chlorophyll-containing algal cells. Scale bars = 10 μm. (Reproduced with permission from Berman and Parparova 2010)

26.8 Major Fluxes of Seston in Lake Kinneret

Some of the seston within a lake may be derived from allochthonous particles transported by inflows or by winds, or by resuspension from bottom sediments. However, the bulk of seston in the pelagic waters of relatively deep lakes is formed in situ as a result of primary and secondary production or by non-photosynthetic formation (e.g., co-precipitation, aggregation, TEP formation, and biomass production by attached bacteria, see Berman et al. 1999; Parparov and Berman 2000). Here, we assumed that the non-photosynthetic formation of seston is balanced by its dissolution. Seston losses are due to sedimentation and in-lake processes such as respiration and solubilization.

Studies carried out within the past decade have led to overall estimates of the major fluxes of the seston cycle in Lake Kinneret (Table 26.6). Photosynthetic production was the largest source of seston, while community respiration was the principal sink. Sediments transported from the lake watershed comprised about 20 % of total seston input; during floods, the impact of this flux may be more significant. Given

Table 26.6 Major fluxes of seston in Lake Kinneret (gTSS m^{-2} $year^{-1}$)

Sources		Sinks	
Tributaries[a]	385	Net sedimentation[b]	305
Photosynthesis (PP)[b]	1,524	Community respiration[c]	1,880
Dust[d]	60	Outflow	7.6
Total	*1,969*	*Total*	*2,193*

[a] Assuming that water discharge from the Jordan River comprises 70% of total tributaries discharge
[b] Assuming that net sedimentation, corrected for resuspension, comprises 20% of PP (Ostrovsky and Yacobi 2010), and PP = 1.67 g Cm^{-2} d^{-1} (Sect. 24.1)
[c] Based on data presented in Sect. 25.2
[d] Based on data presented in Chap. 19

the uncertainties of the estimates for individual fluxes, the totals of the sources and sinks from Table 26.6 are approximately equal, and therefore the seston budget in Lake Kinneret is approximately balanced. This is in good agreement with the absence of any clear trend in TSS dynamics over the past decade (Fig. 26.1).

References

Alldredge AL, Passow U, Logan BE (1993) The abundance and significance of a class of large, transparent organic particles in the ocean. Deep Sea Res 40:1131–1140

APHA (2002) Standard methods for the examination of water and wastewater, 22nd edn. 2540B. Total Solids Dried at 103°–105° C, American Public Health Association. Greenberg AE, Clescerl LS, Eaton AD [eds]

Azam F (1998) Microbial control of oceanic carbon flux; the plot thickens. Science 280:694–695

Bar-Zeev E, Berman-Frank I, Stambler N, Dominguez EV, Zohary T, Capuzzo E, Meeder E, Suggett DJ, Iluz D, Dishon G et al (2009) Transparent exopolymer particles (TEP) link phytoplankton and bacterial production in the Gulf of Aqaba. Aquat Microb Ecol 56:217–225

Bar-Zeev E, Berman T, Rahav E, Dishon G, Herut B, Kress N, Berman-Frank I (2011) Transparent exopolymer particles (TEP) dynamics in the eastern Mediterranean Sea. Mar Ecol Prog Ser 431:107–118

Berman T, Parparova R (2010) Visualization of transparent exopolymer particles (TEP) in various source waters. Desalin Water Treat 21(1–3):382–389

Berman T, Parparov A, Simon M (1999) Carbon fluxes in limnetic seston: relative significance of respiration, solubilization and non-photosynthetic formation. Arch Hydrobiol Spec Issues Advanc Limnol 54:77–90

Berman T, Parparov A, Yacobi YZ (2004) Planktonic community production and respiration and the impact of bacteria on carbon cycling in the photic zone of Lake Kinneret. Aquat Microb Ecol 34:43–55

Berman T, Viner-Mozzini Y (2001) Abundance and characteristics of polysaccharide and proteinaceous particles in Lake Kinneret. Aquat Microb Ecol 24:255–264

Coma R, Ribes M, Gili JM, Hughes RN (2001) The ultimate opportunists: consumers of seston. Mar Ecol Prog Ser 219:305–308

de Vicente I, Ortega-Retuerta E, Romera O et al (2009) Contribution of transparent exopolymer particles to carbon sinking flux in an oligotrophic reservoir. Biogeochemistry 96:13–23

Gal G, Imberger I, Zohary T, Antenucci J, Anis A, Rosenberg T (2003) Simulating the thermal dynamics of Lake Kinneret. Ecol Model 162:69–86

Gal G, Hipsey M, Parparov A, Wagner U, Makler V, Zohary T (2009) Implementation of ecological modeling as an effective management and investigation tool: Lake Kinneret as a case study. Ecol Model 220:1697–1718.

Grossart HP, Berman T, Simon M, Pohlmann K (1998) Occurrence and microbial dynamics of macroscopic organic aggregates (lake snow) in Lake Kinneret in fall. Aquat Microbial Ecol 14:59–67

Hessen DO, Andersen T, Brettum P, Faafeng BA (2003) Phytoplankton contribution to sestonic mass and elemental ratios in lakes: implications for zooplankton nutrition. Limnol Oceanogr 48(3):1289–1296

Ostapenia AP (1989) Seston and detritus as structural and functional components of water ecosystems. Ref Diss Zoological Institute, Minsk, 42 pp. (in Russian)

Ostapenia A, Parparov A, Berman T (2009) Lability of organic carbon in lakes of different trophic status. Freshw Biol 54:1312–1323

Ostrovsky I, Yacobi YZ (2010) Sedimentation flux in a large subtropical lake: spatiotemporal variations and relation to primary productivity. Limnol Oceanogr 55(5):1918–1931

Parparov AS, Berman T, Grossart HP, Simon M (1998) The metabolic activity associated with seston in Lake Kinneret. Aquat Microb Ecol 15:77–87

Parparov AS, Berman T (2000) Turnover rates of freshwater seston and their experimental estimates. Arch Hydrobiol Spec Issues Advanc Limnol 55:376–395

Passow U (2004) Switching perspectives: do mineral fluxes determine particulate organic carbon fluxes or vice versa. Geochem Geophys Geosyst 5(4):Q04002

Passow U, Alldredge AL, Logan BE (1994) The role of particulate carbohydrate exudates in the flocculation of diatom blooms. Deep Sea Res Part I: Oceanogr Res Pap 41(2):335–357

Sherr EF, Sherr BF, Berman T, Hadas O (1991) High abundance of picoplankton-ingesting ciliates during late fall in Lake Kinneret, Israel. J Plankton Res 13:789–799

Wetzel RG (2001) Limnology. Lake and river ecosystems, 3rd edn. Academic, San Diego, 1006 pp

Zohary T (2004) Changes to the phytoplankton assemblage of Lake Kinneret after decades of a predictable, repetitive pattern. Freshw Biol 49:1355–1371

Chapter 27
Sedimentation Processes

Ilia Ostrovsky, Yosef Z Yacobi and Nir Koren

Abstract Sedimentation is a major process for removal of particulate material from the water column and an important determinant accounting for the stability of aquatic ecosystems. Gross sedimentation rates (GSRs) in Lake Kinneret (Israel), regularly monitored from 1999 up to date with sedimentation traps, showed salient temporal and spatial variability. In the lake center, the annual mean GSR ranged from 1.9 to 6.0 g m^{-2} day^{-1}. The accumulation rate of sediments at the lake centrum during the study averaged from 2.6 to 4.3 mm $year^{-1}$, in agreement with values obtained by sediment core dating. Organic matter (OM) content comprised 33–42 % of the sinking particulate matter in sediment traps located in the lake center and was 1.5–2 times lesser in peripheral stations. The highest seasonal values of OM content in traps were associated with collapse of algal blooms. Algae and their debris are the main components of OM and their fate in the water column can be well traced by photosynthetic pigments. Chlorophyte signature pigments display much lower degradability in the water column than those of diatoms and dinoflagellates and leave a relatively persistent residue in the buried sediments. Analysis of seasonal changes of algal signature pigments in the upper euphotic zone and those in sedimentation traps allow us to follow the fate of dominant algal phyla in the water column. We argue thatlarge individual algal cells may have better ability to survive in the deep non-stratified water column with limited light, while the ability to retain and recycle in the euphotic epilimnion under conditions of nutrient limitation may well confer an evolutionary advantage to small or buoyant algal populations. Despite large variation in algal community composition, the ratio of OM sedimentation flux to primary production (i.e., the export ratio) alters only slightly throughout the stratified period. Approximately 20 % of the OM supplied to the lake by primary production found its way to the traps. A large decline of water level in recent years affected the processes of particle resuspension and offshore translocation, which caused prominent site-specific impacts on the sedimentation regime. We argue that changes in sedimentation rates observed in the lake are related to fluctuations of loads from the watershed and prominent water-level fluctuations.

I. Ostrovsky (✉) · Y. Z Yacobi · N. Koren
The Yigal Allon Kinneret Limnological Laboratory, Israel Oceanographic & Limnological Research, P.O. Box 447, 14950 Migdal, Israel
e-mail: ostrovsky@ocean.org.il

Y. Z Yacobi
e-mail: yzy@ocean.org.il

T. Zohary et al. (eds.), *Lake Kinneret, Ecology and Management,* Aquatic Ecology Series 6,
DOI 10.1007/978-94-017-8944-8_27,

Keywords Sedimentation rate · Phytoplankton pigments · Suspended particles · Primary production · Resuspension

Sedimentation is a major process by which particulate material is removed from the water column and an important determinant accounting for the stability of aquatic ecosystems (Håkanson and Jansson 1983; Bloesch 2004). Sedimenting organic particles fuel biogeochemical processes in the hypolimnion and bottom sediments, and determine the burial rate of nutrients and pollutants. Understanding the fate of newly produced particulate organic material (POM) in the water column is one of the fundamental questions in limnology. In the context of organic carbon (OC) cycling, a foremost issue is the proportion of primary production recycled within the upper productive stratum versus the part of this material that is exported to deeper strata, buried in sediments, or removed by other means from the ecosystem (Ostrovsky et al. 1996; Wassmann 2004).

27.1 Gross Sedimentation Rate

Since 1999, gross sedimentation rate (GSR) is regularly monitored in Lake Kinneret with sedimentation traps, moored at stations A, F, and M (for station location see Fig. 32.1 in Chap. 32). GSR has a high spatial and temporal variability (Fig. 27.1).

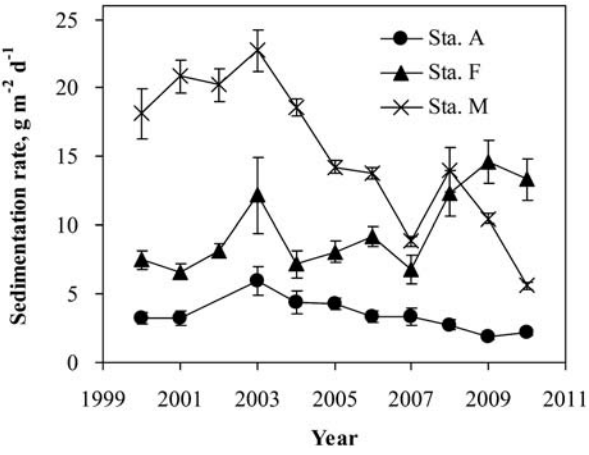

Fig. 27.1 Multiannual variations of the mean (± standard error) gross sedimentation rates in sediment traps positioned ~ 1.5–2.5 m above the lake bottom ("low traps") at three stations. *Sta. A* is a pelagic station located in the lake center (ca 40-m depth), *Sta. F* is a deep peripheral station (20-m depth), and *Sta. M* is a littoral station (ca 10-m depth). Station locations are indicated in Fig. 32.1, Chap. 32; method details are given in Ostrovsky and Yacobi (2010). In winter 2002–2003 a rapid rise of the water level occurred

Between 2003 and 2010, a 3- to 4-fold decrease in the annual GSR was observed at the lake center (Sta. A, depth 40 m) and at the littoral (Sta. M, 10 m), while an opposite trend was observed at a sublittoral station (Sta. F, 20 m). Since primary production in Lake Kinneret is quite stable (Chap. 24), the decrease in GSR at Sta. A, where resuspension is usually insignificant (Ostrovsky and Yacobi 1999, 2010), suggests notable changes in the rate of POM export from the epilimnion downwards. The observed strong positive correlation between GSR and the maximal annual water level ($r=0.81$, $P<0.01$) or with annual water inflow ($r=0.75$, $P<0.01$) implies that allochthonous particles, imported from the watershed and remaining long term in the water column, affect the sedimentation processes. Another important factor strengthening the correlation between inflows and particle concentration is the external load of nutrients and associated winter–spring dinoflagellate blooms. Over the past two decades, dinoflagellate blooms have been highly correlated with riverine nutrient loads (Zohary and Ostrovsky 2011) and their fluctuations could affect the GSR.

Resuspended materials may contribute up to 80–90 % of the measured GSR at the shallower stations M and F (Ostrovsky and Yacobi 1999, 2010). Therefore, changes in resuspension strongly affect the sedimentation regime at peripheral locations. Since 2001, a conspicuous decrease in GSR has been recorded at the littoral Sta. M ($r=-0.96$, $P<0.001$). This change could be associated with large water-level fluctuations. A progressive decrease in water level exposes large areas of the bottom sediments to energetic surface wave activity, which removes fine particles and redeposits them at deeper locations. As a result, much coarser particles, which are harder to resuspend, become dominant in the littoral. These changes in bottom sediment particle size distribution eventually reduced the contribution of resuspended particles to GSR measured in the shallowest location.

GSR measured at Sta. F was influenced by material transport driven by a combined effect of a fast-deepening thermocline and internal seiching that cause resuspension and redeposition of recently settled fine particles from the shallower area toward the lake center (Ostrovsky and Yacobi 2010). A temporal increase in the annual sedimentation rate at Sta. F ($r=0.73$, $P<0.01$) over the last decade could be associated with processes causing sediment redeposition and focusing in the lake. We suppose that gradual decrease in the mean water level together with enlarged water-level fluctuations were the main driving factors responsible for intensive relocation of finer particles from the littoral and sublittoral areas. One can also speculate that the observed increase in the ratio between lake surface and the epilimnion volume with the decrease in mean water level (Rimmer et al. 2011) leads to more effective transfer of wind energy to the lake boundaries, which should enhance sediment resuspension (Ostrovsky et al. 2006).

Comparison of recent sedimentation trap measurements with previously published data on GSR expressed in units of dry weight (DW) m^{-2} day^{-1} shows conspicuous changes over time (Table 27.1). Most of the data compiled in Table 27.1 are based on measurements made with sedimentation traps placed at Sta. A, 1–2.5 m above the bottom sediments. However, the data for 1990–1996 were collected with traps placed 15.5 and 26 m above the bottom (cf. Nishri and Koren 1993; Koren and Klein 2000). Such positioning is expected to lead to notably lower GSRs than those obtained with near-bottom traps (Ostrovsky and Yacobi 2010). At Sta. A, high

Table 27.1 Mean annual gross sedimentation rate measured with sedimentation traps

Location	Sedimentation rate, g DW m^{-2} day^{-1}	Trap location, m above bottom	Period	Reference
Sta. A	1.8–2.2	1	1972–1973	Serruya et al. (1974); Serruya (1978)
PS	2.5–7.3	1		
Sta. A	3.9–5.6	26	1990–1992	Nishri and Koren (1993)
Sta. A	3.8–5.1	15.5 and 26	1995–1996	Koren and Klein (2000)
PS	4.8–15.2	1.5–2		
Sta. J	22–25	1.5–2		
Sta. A	3.8–6.4	2.5	1999–2000	Eckert et al. (2003)
Sta. A	2.7–6.0	2.5	1999–2008	Present study
Sta. A	1.9–2.2	2.5	2009–2011	Present study
PS	5.2–21.6	1.5	1999–2011	Present study

Sta. A station at the deepest part of the lake (bottom depth of 38–44 m depending on water level), *PS* peripheral stations excluding Sta. J (depth <25 m), *Sta. J* station located south of the Jordan River inlet (depth <10 m)
Station locations are indicated in Fig. 32.1 of Chap. 32

GSRs (4–6 g DW m^{-2} day^{-1}) were observed from the early 1990s to the mid-2000s. The GSRs for 1990–1996, collected for near-bottom locations, could be even larger than numbers presented in Table 27.1. Much lower values of ~2 g DW m^{-2} day^{-1} were reported in 1972–1973 (Serruya et al. 1974; Serruya 1978) and in 2009–2011 (present study). We suggest that the enlarged GSR in the 1990s and earlier 2000s were triggered by exceptionally high water-level fluctuations, which caused massive redeposition of the historically settled particulate material to reach a new equilibrium with external forcing.

At peripheral locations, the measured GSRs were usually much higher and more variable than at Sta. A. The highest GSRs were recorded near the Jordan River inflow (Sta. J), where the contribution of allochthonous material delivered from the watershed is high. Shteinman et al. (2000) indicated that larger particles settle close to the river inflow and form a bar, while smaller particles are transported further into the lake. Vertical profiles of turbidity measured in spring along a transect from the Jordan River inflow to the lake center showed the presence of a thin (a few tens of centimeters) turbid water layer above the bottom (Ostrovsky unpublished). This suggests spreading of the fluvial material along the sloping bottom all the way down to the deepest part of the lake by gravity flow, following the model suggested for the dispersion of cold riverine water at the top of the thermocline or near the bottom (Serruya 1974).

27.2 Sedimentation of Particulate Inorganic Matter

Precipitation of $CaCO_3$ is the major sedimentation component of particulate inorganic material in Lake Kinneret. Spring decrease of alkalinity in the epilimnetic water indicates that the annual mean $CaCO_3$ sedimentation all over the lake ranges

Table 27.2 Comparison of published estimates of external loads of particulate matter

Source	Average load, t year^{-1}	Sedimentation rate[a], g DW m^2 day^{-1}	Method	Period	Reference
Jordan River inflow	74,000	1.2	Loads	1968–1970	Serruya (1971)
Jordan River inflow	70,000	1.2	Sediment traps	1971–1978	Inbar (1982)
Jordan River inflow	35,500	0.60	Loads	1970–1987	Authors' assessment
	14,500	0.25	Loads	1987–2011	
Atmospheric deposition	10,000–16,000	0.16–0.26	Dust traps	1993–1996	Ganor et al. (2003)
Atmospheric deposition	10,000	0.17	Dust traps	2005	Chap. 19

[a] Average annual sedimentation rates of material exported from the Jordan River or as atmospheric deposits were calculated assuming equal distribution of loaded material over the whole lake area

from 0.7 to 1.4 g m^{-2} day^{-1}, which comprises 20–70 % of the sedimentation flux of inorganic particles measured at the center of the lake. Two allochthonous sources of inorganic particulate material should also be considered: (1) loads of suspended solids provided by rivers and creeks (the Jordan River is the dominant source of inorganic particles supplied from the watershed) and (2) dust (Table 27.2). Assuming a uniform distribution of the autochthonous and allochthonous particles over the lake bottom—the rates of particle contribution by the Jordan River, $CaCO_3$ precipitation, and dust settling were −0.52, 1.09, and 0.17 g m^{-2} day^{-1}, respectively, over the period from 1999 to 2011. Taking into account that the average sedimentation rate of inorganic material at Sta. A was 2.15 g m^{-2} day^{-1}, the three mentioned sources of inorganic material combined accounted for 83 % of the annual sedimentation flux of inorganic components. Taking into account uncertainties in appraisal of these components (e.g., part of fluvial particles is deposited near the river inlet zone; fine particles may be focused in the deeper part of the lake), this rough balance well portrays the main sources of sedimented material.

Previous studies suggested that material deposited at Sta. A contains, on average, about 50–60 % of $CaCO_3$, 23–36 % of silicates, and 14–25 % of POM (Serruya 1978; Klein and Koren 1998). The measurements carried out in 1999–2011 resulted in a higher proportion of POM of 33–42 %. The higher values may be partly explained by lesser diagenesis of organic particles in traps over a generally shorter time of their exposure (1–2 weeks in 1999–2011 vs. 2–4 weeks in earlier studies). Seasonal variations of trap material composition are event specific. A large proportion of POM in trap material is characteristic of the time of algal bloom collapse, while the inorganic fraction is usually high during a period of flood, which supplies particles from the watershed, and during spring precipitation of $CaCO_3$ (Koren and Ostrovsky 2002). Particles collected at shallower (peripheral) stations are characterized by 1.5–2 times lower percentage of POM than that at Sta. A. This is associated with wind- and internal wave-induced resuspension, which, on the one hand, washes the lighter particles out of the shallower areas and, on the other hand,

delivers the organic-depleted resuspended particles to the traps (Ostrovsky et al. 1996; Ostrovsky and Yacobi 2010).

27.3 Sedimentation of Particulate Organic Matter

Organic matter sedimentation rates (OMSR), measured in the lake interior (Sta. A) by means of sediment traps positioned within the quiescent part of the hypolimnion, provide the most reliable assessments of POM fluxes from the upper productive layer into the deeper layers (Ostrovsky and Yacobi 2010). The POM sedimentation flux gradually declines from February until October (Fig. 27.2a). The ratio of this flux to primary production, called the export ratio (ER), shows the proportion of primary production settled from the upper productive layer. This ratio displays clear seasonality (Fig. 27.2b) that is related to the composition of the phytoplankton and

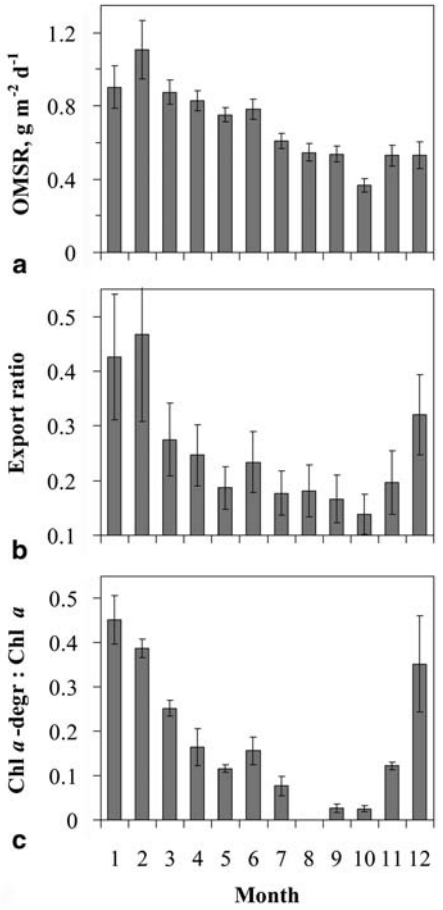

Fig. 27.2 The annual pattern of sedimentation parameters in Lake Kinneret. Means for 2005–2008: (**a**) organic matter sedimentation rate (*OMSR*), (**b**) export ratio, calculated as the ratio between the monthly averages of *OMSR* and primary production at Sta. A, and (**c**) mass ratio of chlorophyll degradation product sedimentation rate to chlorophyll *a* sedimentation rate (Chl *a*–degr: Chl *a*). Traps were positioned at ~11 m above the bottom to avoid oversampling of particulate material under turbulent conditions in the benthic boundary layer (Ostrovsky and Yacobi 2010). For details of primary production measurements, see elsewhere (Yacobi 2006). *Vertical bars* show ± standard error

to the physical regime in the lake. During holomixis (January–March), large-celled algae (e.g., the diatom *Aulacoseira granulata,* and the dinoflagellate *Peridinium gatunense*) dominate the phytoplankton and are hardly consumed by zooplankton (Zohary 2004). The high sinking velocity of such cells is an apparent reason why a high proportion of the phytoplankton reaches the lake bottom during warm winter days with low wind speeds when turbulent mixing is subtle. We assume that the temporal lag between algal production and sedimentation explains the highest proportion of POM in the settling material in February. Increased turbulence that prevails throughout the well-mixed water column entrains large algal cells and circulates them between the euphotic zone and the trap locations. The latter is apparently the reason for the overestimation of sedimentation flux of negatively buoyant particles in the non-stratified water column (Buesseler et al. 2007; Yacobi and Ostrovsky 2012). Loading of large amount of clay particles from the watershed and resuspension of particles from the bottom (specifically at the lake periphery) caused by surface waves on windy days explains the occurrence of organic-poor particles in the traps, and higher OMSR in winter and early spring. All these factors could account for the enlarged ER during complete (January–February) or partial holomixis (December). A prominent drop in ER occurs promptly after thermal stratification has established and the lower part of the water column becomes physically separated from the upper productive layer. Following the establishment of stable stratification, the ER declines from 27 to 18 % (Fig. 27.2b) and is explained by a shift in dominance in algal community from large to small slow-sinking phytoplankton species throughout the development of strong thermal stratification (Zohary 2004; Yacobi and Ostrovsky 2012). Development of buoyant filamentous cyanobacteria (e.g., *Aphanizomenon, Cylindrospermopsis*) in summer–fall since 1994 could also contribute to the seasonal decrease in the ER due to the floating capacity of these species (Walsby 1994). High turnover rates characteristic of small algal species also enhance nutrient recycling within the euphotic zone and may be the reason for the lowest rate of phosphorous loss from the epilimnion between July and November (Ostrovsky and Yacobi 2010). The seasonal timing of minimal ER and the greatest retention of limiting nutrients in the upper productive layer could be an outcome of universal adaptation of planktonic communities to stratification, when nutrient losses could not be replenished from internal or external sources. During the period of rapid thermocline deepening in late fall–early winter, large areas of the lake bottom, which were previously below the hypolimnion and where fresh organic particles had accumulated, now become overlain by the metalimnion or even the epilimnion. The interaction between internal waves, which are continuously presented in the metalimnion, with the exposed sediments cause massive resuspension of deposited fine particles and their lateral transportation toward the deepest part of the lake (Ostrovsky and Yacobi 1999; Ostrovsky 2000; Ostrovsky and Sukenik 2008). Such focusing of POM may explain high values of the ER computed for the end of the stratified period (Fig. 27.2b). The average ER of ~20 % apprised for the large part of the stratified period (March–October) when OMSR is the least biased at Sta. A is the best estimate for the export flux of the newly produced POM from the upper mixed layer. This value is typical for many productive lakes and the open

ocean (Tilzer 1984; Baines et al. 1994; Bloesch and Uherlinger 1986; Laws et al. 2000; Ostrovsky and Yacobi 2010) and it probably reflects the adaptability of algal communities to varying ambient conditions.

27.4 Sedimentation and the Fate of Phytoplankton Pigments in the Water Column

A substantial component of POM is planktonic algae and their debris. The fate of this material can be traced by the examination of photosynthetic pigments in particles prevailing in water, traps, and bottom sediments (Hurley and Armstrong 1990; Leavitt and Hodgson 2003). Chlorophyll *a* (Chl *a*) is a pigment found universally in all oxygenic photosynthesizers (algae, cyanobacteria, and higher plants) and is usually used for quantification of phytoplankton biomass. Upon degradation, Chl *a* yields an array of degradation products, which reflect diagenetic processing of phytoplankton (Matile et al. 1999). Analysis of the seasonal variation of the ratio between Chl *a*-degraded products and intact Chl *a* in sediment traps helps to elucidate the trophic efficiency by which algal material in the water column is utilized (Ostrovsky and Yacobi 2010). This unitless ratio displayed similar seasonal dynamics in all traps, irrespective of their location, with maximum values of 0.4–0.6 during holomixis. The ratio had near-zero values from August to October (Fig. 27.2c), when the algal community consisted of small or buoyant species that possess low settling velocity (ca. tens of centimeters per day, Reynolds 2006) and are easily consumed by zooplankton, and thus can be readily recycled within the epilimnion (cf. low ER). The maximum values of the ratio during the holomixis are related to dominance of large algae, too big for consumption by zooplankton. These algae populate the entire water column such that a high proportion of their fragments may be maintained in the well-mixed turbulent water for a long time.

To better understand the fate of specific algal groups in the lake, a trap-to-water ratio (TWR) was developed (Yacobi and Ostrovsky 2008, 2012; Ostrovsky and Yacobi 2010). It compares pigment indices in the trap (PI_{trap}) and in the water of the upper productive stratum (PI_{water}), as follows

$$TWR = \frac{PI_{trap}}{PI_{water}} = \frac{F_i / F_{ref}}{C_i / C_{ref}}, \tag{27.1}$$

where F_i, F_{ref} are the fluxes (in mg m^2 day^{-1}) of the *i*th signature pigment and common reference pigment in trap, respectively; C_i, C_{ref} are the concentrations (in mg m^{-3}) of the *i*th signature pigment and reference common pigment in the upper productive stratum, respectively. Like Chl *a*, *β*-carotene (*β*-car) is found in all phytoplankton (save cryptophytes) and is thus suitable as a signature of total vegetative biomass. We preferred using *β*-car as a reference pigment, as this compound is the most stable algal pigment (Leavitt and Hodgson 2003). The TWR calculated on the

Table 27.3 Trap-to-water ratio (TWR) for different signature pigments in 2006

Pigment	Signature for	Jan–Mar (holomixis, oxic water)	Apr–Jun (stratified, suboxic hypolimnion)	Sep–Oct (stratified, anoxic hypolimnion)
Chl *a*	All algal groups	1.3	0.9	0.7
Chl *b*	Chlorophytes	*2.6*	*1.4*	*0.9*
Lutein + zeaxanthin	Chlorophytes (mainly)[a]	*2.6*	0.9	0.8
Fucoxanthin	Diatoms	*2.4*	0.3	0.4
Echineneone	Cyanobacteria	<1	<1	*0.5*
Peridinin	Dinoflagellates	0.5	*0.7*	Not in traps
Chl *c*	Dinoflagellates, diatoms	0.3	0.3	Not in traps

Ratios were calculated by Eq. (27.1) using β-carotene as a reference pigment (modified from Yacobi and Ostrovsky 2008). Numbers in italics refer to dominant algal groups

[a] In this study, lutein (a signature pigment of chlorophytes) could not be analytically separated from zeaxanthin (a signature pigment of cyanobacteria). From January to June the mixture of these pigments reflect primarily chlorophytes since cyanobacteria were presented only in minor quantities (Yacobi and Ostrovsky 2008). This was also supported by a high correlation ($r^2 > 0.9$) between concentrations of lutein + zeaxanthin and Chl *b* (indicatory of chlorophytes) in the samples

basis of *β*-car reflects the "freshness" of the newly settled algal material relative to that in the euphotic zone.

We calculated the TWR for pigments that are signatures of phytoplankton groups (Table 27.3). Although TWR changed in the three defined periods, the stability of phytopigments appears as follows: β-carotene > lutein > Chlorophyll *b* (Chl *b*) > Chl *a* > fucoxanthin > echinenone > Chlorophyll *c* (Chl *c*) > peridinin (Yacobi and Ostrovsky 2008). This pattern agrees with results reported earlier (e.g., Hurley and Armstrong 1990; Leavitt and Hodgson 2003) and suggests the following order of algal preservation: chlorophytes > diatoms > cyanobacteria > dinoflagellates. Chl *c* displayed the same pattern of degradability as peridinin reflecting a fast decomposition of dinoflagellates in the water column although sometimes dinoflagellates reach traps intact (Zohary et al. 1998). Fucoxanthin was harbored mainly by diatoms, which formed high concentrations in February, in June–July, and in September–November. Abrupt appearance and disappearance of the large centric diatom *Aulacoseira granulata* is typical in winter. The species sinks massively, such that a large part of the sinking population includes intact cells and determines high TWR for fucoxanthin. In contrast, low TWR values for fucoxanthin in the summer and autumn were associated with the dominance of small pennate diatoms (Zohary 2004) which have low thinking velocity; they are consumed by zooplankton and decompose mainly within the epilimnion. Chl *b* and lutein showed a prominent peak in March–April, when relatively dense population of chlorophytes were eliminated from the euphotic zone. The high TWR of Chl *b* and lutein indicates that chlorophyte, or debris originating in chlorophyte cells, accumulated in the traps in higher rates than other algae that prevailed simultaneously in the epilimnion (Yacobi and Ostrovsky 2012). During the stratified period, the TWR for Chl *b* and lutein are slightly below 1, indicating better preservation of chlorophyte cells comparatively to other phytoplankton groups. Echinenone TWR was mostly <1 during the ho-

lomixis and consistently low when the lake was stratified (Yacobi and Ostrovsky 2008). This indicates that echinenone is less stable than the signature pigments of the chlorophytes and suggests that cyanobacteria recycle mainly in the upper part of the water column. Thus, TWR > 1 is characteristic for most pigments during holomixis when algal cells settle down intact, while TWR < 1 is characteristic of pigments in a stratified lake and suggests that cells mostly decompose in the epilimnion before reaching the bottom (Yacobi and Ostrovsky 2008, 2012). These temporal changes in TWR concur with the above described dynamics of Chl *a*-degraded products and ER, as large individual cells may have better ability to survive in the deep non-stratified water column with limited light, while the ability to retain and recycle in the upper euphotic layer under conditions of nutrient limitation may well confer an evolutionary advantage to small or buoyant algal populations.

27.5 The Burial of Sedimented Particles

Sediment accumulation (= burial) rate, SAR, can be most reliably assessed from sedimentation flux estimates at Sta. A, because recurrently resuspended material have minimal influence on trap measurements at this deep station (Ostrovsky and Yacobi 2010). The computed SAR indicated twofold variations over the last decade: from 2.5–3 mm year^{-1} during the drought of 2008–2011 to 5.7 mm year^{-1} in the rainy 2003. The mean SARs based on trap measurements for the 1990s and early 2000s (4–5 mm year^{-1}) well agree with sediment core dating (Table 27.4). Sobek et al. (2011) found that SAR near the Jordan inlet (Sta. J) is ~1.5 times higher than at the lake center. On the other hand, at peripheral stations, SARs are 1.5–2 times lower than that at Sta. A. The latter corroborates our conclusion about relocation of sedimented particles from shallow areas toward the lake center (Ostrovsky and Yacobi 1999, 2010). Gradual increase in organic matter content in the uppermost (few millimeters) layer of bottom sediments from the littoral to the lake center (Ostrovsky and Yacobi 1999; Yacobi and Ostrovsky 2000) supports the notion of focusing of lighter organic-rich particles in the deep part of the lake. At the same time, much lower content of organic material in the uppermost layer during holomixis in comparison with the stratified period suggests seasonal dissimilarity in chemical and physical processes influencing the fate of settling and decomposition of organic and inorganic particles in the water column. In particular, internal seiching strongly influences the sedimentation regime during the stratified period (Ostrovsky et al. 1996, 1997; Ostrovsky and Yacobi 2010).

Overall, the dynamic sedimentation processes ultimately affect the amount of suspended organic and inorganic material, concentrations of nutrients and pollutants in the upper productive stratum by means of their export to lower strata and bottom sediments. The anthropogenic increase in water demands and reduction of precipitation in the region during the past decades altered the hydrological regimes and material load from the watershed to Lake Kinneret (Ostrovsky et al. 2013; Chaps. 7 and 18). Such changes concurrently with the increase beyond natural in

Table 27.4 Sediment accumulation rates

Location	Accumulation rate, mm year^{-1}	Method	Layer location in sediments	Period	Reference
Sta. A	2.8	^{137}Cs profiles	Surface layer	–	Stiller and Assaf (1973)
PS	2.0–5.1	^{137}Cs profiles	Surface layer		Stiller and Assaf (1973)
Sta. A	3.5	Sediment trap	Surface layer	1990–1992	Nishri and Koren (1993)
Sta. A	4	^{137}Cs profiles	Surface layer	Recent	Nishri and Koren (1993)
KINU8	4.7	^{210}Pb dating	0–5 cm	1982–1993	Erel et al. (2001)
	5.0	and $\delta^{13}C_{org}$ ED	5–12 cm	1959–1982	Erel et al. (2001)
	7.1		12–33 cm	1953–1959	Erel et al. (2001)
KINU8	4.3	$\delta^{13}C_{org}$ ED	0–11 cm	1975–1993	Dubowski et al. (2003)
	5.6	and	11–25 cm	1950–1975	Dubowski et al. (2003)
	6.1	C_{org} content	25–59 cm	1872–1950	Dubowski et al. (2003)
Sta. A	3.6	^{210}Pb	0–40 cm	1890–2002	Hambright et al. (2004)
Sta. A	4.5	Mixed	0–10 cm	Recent	Sobek et al. (2011)
PS	2.0–2.8	^{210}Pb and ^{137}Cs	0–10 cm	Recent	Sobek et al. (2011)
Sta. J	6.1		0–10 cm	Recent	Sobek et al. (2011)
Sta. A	4.3 ± 0.7[a]	Sediment trap	Surface layer	1999–2007	Present study
Sta. A	2.6 ± 0.3[a]	Sediment trap	Surface layer	2008–2011	Present study

Accumulation rates are presented as means and ranges, or means ± SD
KINU8 is a sampling station located ~2 km northwest of Sta. A, *PS* are peripheral stations, $\delta^{13}C_{org}$ *ED* is event dating using δ^{13}C. Locations of Sta. A and Sta. J are indicated in Fig. 32.1, Chap. 32
[a] Calculations are based on specific gravity of ash fraction = 2.65 g cm^{-3} and organic matter fraction = 1 g cm^{-3}; porosity in the upper 10-cm layer = 87% (Sobek et al. 2011)

the amplitude of water-level fluctuations as well as long-term water-level decline influenced the algal community and modified the GSRs and material redeposition in the lake.

References

Baines SB, Pace ML, Karl DM (1994) Why does the relationship between sinking flux and planktonic primary production differ between lakes and oceans? Limnol Oceanogr 39:213–226

Bloesch J (2004) Sedimentation and lake sediment formation. In: O'Sullivan PE, Reynolds CS (eds) The lakes handbook, vol 2: lake restoration and rehabilitation. Blackwell, Malden, pp 197–229

Bloesch J, Uehlinger U (1986) Horizontal sedimentation differences in a eutrophic Swiss lake. Limnol Oceanogr 31:1094–1109

Buesseler KO, Lamborg CH, Boyd PW, Lam PJ, Trull T, Bidigare RR, Bishop JKB, Casciotti KL, Dehairs F, Elskens M, Honda M, Karl DM, Siegel DA, Silver MW, Steinberg DK, Valdes J, VanMooy B, Wilson S (2007) Revisiting carbon flux through the ocean's twilight zone. Science 316:567–570

Dubowski Y, Erez J, Stiller M (2003) Isotopic paleolimnology of Lake Kinneret. Limnol Oceanogr 48:68–78

Eckert W, Didenko J, Uri E, Eldar D (2003) Spatial and temporal variability of particulate phosphorus fractions in seston and sediments of Lake Kinneret under changing loading scenario. Hydrobiologia 494:223–229

Erel Y, Dubowski Y, Halicz L, Erez J, Kaufman A (2001) Lead concentrations and isotopic ratios in the sediments of the Sea of Galilee. Environ Sci Technol 35(2):292–299
Ganor E, Foner HA, Gravenhorst G (2003) The amount and nature of the dustfall on Lake Kinneret (the Sea of Galilee), Israel: flux and fractionation. Atmos Environ 37:4301–4315
Håkanson L, Jansson M (1983) Principles of lake sedimentology. Springer, Berlin
Hambright KD, Eckert W, Leavitt PR, Schelske CL (2004) Effects of historical lake level and land use on sediment and phosphorus accumulation rates in Lake Kinneret. Environ Sci Technol 38:6460–6467
Hurley JP, Armstrong DE (1990) Fluxes and transformations of aquatic pigments in Lake Mendota, Wisconsin. Limnol Oceanogr 35:384–398
Inbar M (1982) Measurement of fluvial sediment transport compared with lacustrine sedimentation rates: the flow of the River Jordan into Lake Kinneret. Hydrol Sci J 27(4):439–449
Klein M, Koren N (1998) The influence of the thermocline on sedimentation in the deeper part of Lake Kinneret, Israel. Limnologica 28:293–299
Koren N, Klein M (2000) Rate of sedimentation in Lake Kinneret, Israel: spatial and temporal variations. Earth Surf Proc Landf 25:895–904
Koren N, Ostrovsky I (2002) Sedimentation in a stratified subtropical lake. Verh Int Ver Theor Angew Limnol 27:2636–2639
Laws EA, Falkowski PG, Smith WO, Ducklow H, McCarthy JJ (2000) Temperature effects on export production in the open ocean. Global Biogeochem Cycle 14(4):1231–1246
Leavitt PR, Hodgson DA (2003) Sedimentary pigments. In: Smol JP, Birks HJB, Last WM (eds) Tracking environmental changes using lake sediments, vol 3: terrestrial, algal, and siliceous indicators. Kluwer, Dordrecht, pp 295–325
Matile P, Hörtensteiner S, Thomas H (1999) Chlorophyll degradation. Annu Rev Plant Physiol Plant Mol Biol 50:67–95
Nishri A, Koren N (1993) Sediment transport in Lake Kinneret. Verh Int Ver Theor Angew Limnol 25:290–292
Ostrovsky I (2000) The upper most layer of bottom sediments: sampling and artifacts. Ergeb Limnol 55:243–256
Ostrovsky I, Sukenik A (2008) Spatial heterogeneity of biogeochemical parameters in a subtropical lake. In: Mohanty PK (ed) Monitoring and modeling lakes and coastal environments. Springer, Dordrecht, The Netherland, pp 79–90
Ostrovsky I, Yacobi YZ (1999) Organic matter and pigments in surface sediments: possible mechanisms of their horizontal distributions in a stratified lake. Can J Fish Aquat Sci 56:1001–1010
Ostrovsky I, Yacobi YZ (2010) Sedimentation flux in a large subtropical lake: spatio-temporal variations and relation to primary productivity. Limnol Oceanogr 55:1918–1931
Ostrovsky I, Yacobi YZ, Walline P, Kalikhman I (1996) Seiche induced mixing: its impact on lake productivity. Limnol Oceanogr 41:323–332
Ostrovsky I, Wynne D, Bergstein-Ben Dan T, Nishri A, Li H, Yacobi YZ, Koren N, Parparova R (1997) Spatial distributions of biogeochemical parameters in surface sediments at the beginning of the stratified period in a subtropical lake. Water Air Soil Pollut 99:497–505
Ostrovsky I, Rimmer A, Agnon Y, Koren N (2006) Sediment resuspension in the hypolimnion of Lake Kinneret (Israel): the impact of water level fluctuation. Verh Int Ver Theor Angew Limnol 29:1625–1629
Ostrovsky I, Rimmer A, Yacobi YZ, Nishri A, Sukenik A, Hadas O, Zohary T (2013) Long-term changes in the Lake Kinneret ecosystem: the effects of climate change and anthropogenic factors. In: Goldman CR, Kumagai M, Robarts RD (eds) Climate change and inland waters: impacts and mitigation approaches for ecosystems and society. Wiley-Blackwell, Oxford, UK, pp 271–293
Reynolds CS (2006) Ecology of phytoplankton. Cambridge University Press, Cambridge
Rimmer A, Gal G, Opher T, Lechinsky Y, Yacobi YZ (2011) Causes for long-term variations of thermal structure in a warm lake. Limnol Oceanogr 56:974–988
Serruya C (1971) Lake Kinneret: the nutrient chemistry of the sediments. Limnol Oceanogr 16:510–521

Serruya S (1974) The mixing patterns of the Jordan River in Lake Kinneret. Limnol Oceanogr 19:175–181

Serruya C (1978) Sediment chemistry. In: Serruya C (ed) Lake Kinneret, momographiae biologicae. Junk, Amsterdam, pp 205–215

Serruya C, Edelstein M, Pollingher U, Serruya S (1974) Lake Kinneret sediments: nutrient composition of the pore water and mud water exchanges. Limnol Oceanogr 19:489–508

Shteinman B, Wynne D, Kamenir Y (2000) Study of sediment dynamics in the Jordan River-Lake Kinneret contact zone using tracer methods. The hydrology–geomorphology interface: rainfall, floods, sedimentation, land use. Proceedings of the Jerusalem Conference, May 1999. IAHS Publ. 261, pp 275–284

Sobek S, Zurbrügg R, Ostrovsky I (2011) The burial efficiency of organic carbon in the sediments of Lake Kinneret. Aquat Sci 73:355–364

Stiller M, Assaf G (1973) Sedimentation and transport in Lake Kinneret traced by ^{137}Cs. In: Hydrology of lakes. Proceedings Helsinki Symposium, July 1973. IAHS Publ. 109, pp 397–403

Tilzer MM (1984). Estimation of phytoplankton loss rates from daily photosynthetic rates and observed biomass changes in Lake Constance. J Plankton Res 6:309–324

Walsby AE (1994) Gas vesicles. Microbiol Rev 58:94–144

Wassmann P (2004) Eutrophication, primary production and vertical export. In: Wassmann P, Olli K (eds) Drainage basin nutrient inputs and eutrophication: an integrated approach. University of Tromsø, Norway, pp 126–138 (available at http://hdl.handle.net/10037/2389)

Yacobi YZ (2006) Temporal and vertical variation of chlorophyll a concentration, phytoplankton photosynthetic activity and light attenuation in Lake Kinneret: possibilities and limitations for simulation by remote-sensing. J Plankton Res 28:725–736

Yacobi YZ, Ostrovsky I (2000) Lake Kinneret sediments: spatial distribution of chloropigments during holomixes. Arch Hydrobiol 55:457–469

Yacobi YZ, Ostrovsky I (2008) Downward flux of organic matter and pigments in Lake Kinneret (Israel): relationships between phytoplankton and the material collected in sediment traps. J Plankton Res 30:1189–1202

Yacobi YZ, Ostrovsky I (2012) Sedimentation of phytoplankton: role of ambient conditions and life strategies of algae. Hydrobiologia 698:111–120

Zohary T (2004) Changes to the phytoplankton assemblage of Lake Kinneret after decades of predictable repetitive pattern. Freshw Biol 49:1355–1371

Zohary T, Ostrovsky I (2011) Ecological impacts of excessive water level fluctuations in stratified freshwater lake. Inland Waters 1:47–59

Zohary T, Pollingher U, Hadas O., Hambright KD (1998) Bloom dynamics and sedimentation of *Peridinium gatunense* in Lake Kinneret. Limnol Oceanogr 43:175–186

Chapter 28
Dynamics of Redox-Sensitive Elements

Ami Nishri and Ludwik Halicz

Abstract Following the onset of stratification in spring, the interaction between the oxy-anions of Mo, U, and Sb with reduced solutes in Lake Kinneret lower water mass (LWM) causes the removal of part of these redox-sensitive elements. However, the removal is shown here to occur also during the de-stratification stage in autumn in both the top of the HS^-, Fe oxide, and Fe(II) enriched LWM and a thin partially mixed layer above it. This process is shown to be associated with the fast thermocline deepening and induced by enhanced sedimentation of organic matter and Fe–Mn oxides. The primary source of this matter is hypothesized to be the resuspension of sediments deposited at those lake floor areas which become exposed to the intensive water motions in the upper layers due to thermocline deepening. The present chapter describes the effect of physical and biogeochemical regime across the mid-water temperature transition layer on the removal of redox-sensitive elements such as Mo, U, Sb, and Se.

Keywords Buoyancy mixing · Redox · Lower water mass · Manganese · Molybdenum · Selenium · Antimony

28.1 Introduction

For many years, the research on geochemical processes of trace elements in Lake Kinneret was focused on elements which were shown to affect biological processes in the euphotic layer. Notably of these were iron (Berman et al 1993; Sivan et al 1998; Shaked 2002), copper (Frevert et al. 1982; Wynne and Pieterse 2000), and selenium (Lindström and Rhode 1978; Lindström 1982, 1983; Nishri et al. 1999).

A. Nishri (✉)
The Yigal Allon Kinneret Limnological Laboratory,
Israel Oceanographic & Limnological Research,
P.O. Box 447, 14950 Migdal, Israel
e-mail: nishri@ocean.org.il

L. Halicz
Geological Survey of Israel, 30 Malkhe Israel St.,
95501 Jerusalem, Israel
e-mail: ludwik@gsi.gov.il

T. Zohary et al. (eds.), *Lake Kinneret, Ecology and Management,* Aquatic Ecology Series 6,
DOI 10.1007/978-94-017-8944-8_28,

Table 28.1 Typical concentrations of soluble trace elements in Lake Kinneret surface water (0–10 m) and benthic boundary layer (BBL > 30-m depth) during the stratified period, and in the Jordan River (Pkak Bridge). The question mark implies that the result is below detection limit

	Fe	*Mn*	**Ba**	Zn	**Li**	**B**
Surface	*2.26*	*0.5*	**52**	0.34	**11.35**	**98**
BBL	*15.3*	*62.6*	**70.8**	0.9	**11.5**	**100**
Jordan R.	*2*	*1*	**14**	0.5	**0.70**	**22**
	Cd	Pb	*Al*	*Sb*	Th	**Rb**
Surface	*0.004*	*0.02*	*1.34*	0.07	0.02	**3.19**
BBL	0.005	*0.02*	*1.15*	0.04	0.01	**3.23**
Jordan R.	0.042	*0.01*	*8*	0.01	0.005	**1.3**
	Ni	*Co*	*Mo*	Cu	*U*	V
Surface	0.27	0.014	0.92	0.15	0.61	2.37
BBL	0.39	0.031	0.65	0.15	0.52	1.58
Jordan R.	0.35	0.1	0.75	0.8	0.4	5
	As	Cr	*Ti*	*Se*	Ag	–
Surface	0.66	1.55	*0.003*	0.1	0.004	–
BBL	0.67	1.78	*0.002*	0.1	0.007	–
Jordan R.	0.5	18	*0.001*	0.45	?	–

Obtained from multi-annual averages of data extracted from the Lake Kinneret database. Concentrations (determinations by ICP-MS) are given in μg L^{-1}. The data are coded between three different types of sources of the elements: regular font letters (such as Zn, Cd, Sb)—elements from riverine sources that enter the lake in their soluble form; in italics—elements originating from riverine sources mostly in the particulate form (such as Fe, Mn, Al); and in bold—elements originating from submerged saline sources in soluble form (Ba, Li, B, Rb)

It is interesting to note that the concentrations of many soluble trace elements are lower in the lake's sulfide-rich lower water mass (LWM) than in the surface water (Table 28.1). This phenomenon was attributed to the development of anoxia in the spring–summer period that leads to the removal of these redox-sensitive elements. The present chapter is devoted to biogeochemical processes that occur during destratification in autumn, a physical process which is associated with abundant supply of organic matter through sedimentation to the LWM and which also leads to the removal of redox-sensitive trace elements. We present depth distribution data from a multielement high-resolution sampling scheme across the redox transition layer at the thermocline, conducted at various occasions during the deepening process of the thermocline. Results are presented in two consecutive methodological steps. First, establishing the physical and biogeochemical settings of the thermocline layer and for that purpose, we use temperature, chloride (Cl), ammonium (NH_4^+), alkalinity, and oxygen data. Second, demonstrating depth-related variations in the concentrations of redox-sensitive elements: cobalt (Co), iron (Fe), molybdenum (Mo), antimony (Sb), uranium (U), and selenium (Se).

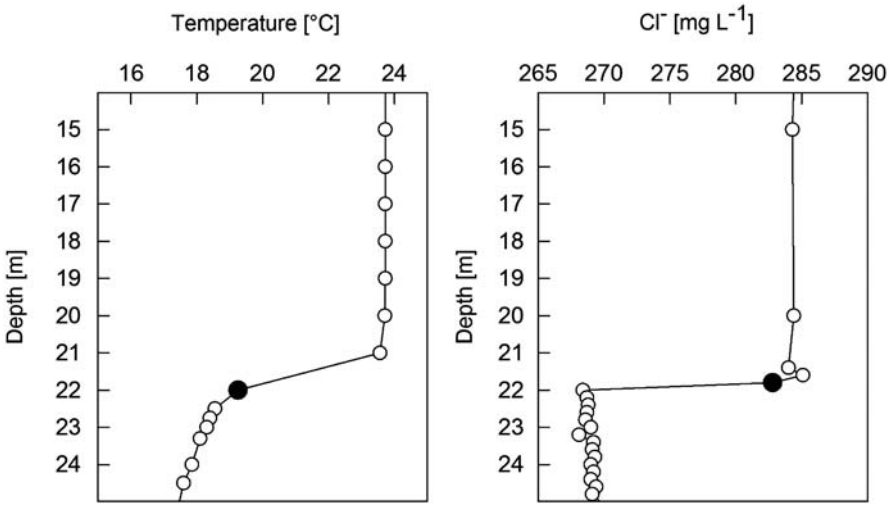

Fig. 28.1 Depth profiles of temperature (*left*) and chloride (*right*) on 21 November 2010 at mid-lake Sta A. The *filled circles* mark the 21.8-m depth horizon

28.2 The Physical and Geochemical Gradients in the Thermocline/Metalimnion

Typical profiles of temperature and chloride recorded during the spring in Lake Kinneret are presented in Fig. 28.1. Water temperature in the lower epilimnion (between 14- and 21-m depth) was fairly constant at 23.7 ℃, indicating a well-mixed water layer. Two temperature zones were noticed below 21-m depth: between ~21 and 24 m, the temperature decreased sharply from 23.7 to 18 ℃ forming a temperature transition layer. Below that sharp gradient, the temperature declined slowly approaching 16.7 ℃ at 31 m, which marks the top of the BBL. Chloride concentrations were constant in each of the lake's major layers; above 21.6-m depth it was 286 ± 1.4 mg L^{-1} and below 22-m depth it was 269 ± 1.3 mg L^{-1} (Fig. 28.1). Chloride concentrations in each major layer stem from the conservative behavior of Cl^{-}, while the differences between these two layers reflect the effects of saline sources and evaporation in the epilimnion. The chloride concentration at 21.8-m depth (indicated by black dots in Fig. 28.1) reflects an intermediate value between the two major water masses with chloride concentration of 284 mg L^{-1}. Assuming that the 21.8-m layer represents a mixture between the epilimnetic water and the LWM, a mixing ratio of ~9:1 between the two layers, respectively, reflects a gradual erosion of LWM water within the growing epilimnion. We hereby refer to this layer as the freshly "eroded layer" which, in accordance with our sampling resolution, may have a thickness of less than 40 cm, between >21.6 and <22 m.

The deepening of the thermocline is an annual process that ends when full water column mixing occurs. The rate of thermocline deepening in 2010 is represented in

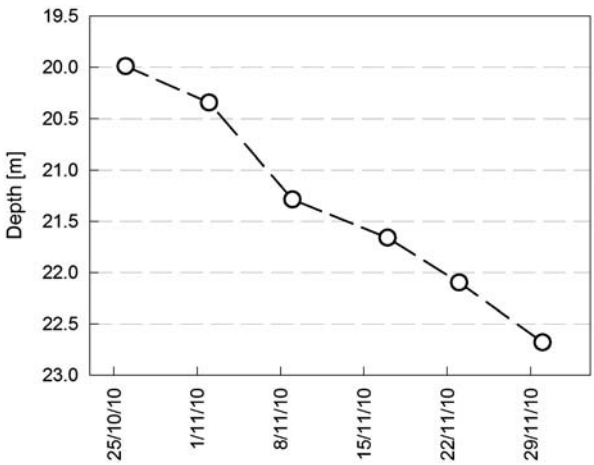

Fig. 28.2 Mid-thermocline depth calculated from weekly temperature profiles measured from 24 October through 28 November 2010 at Sta. A. (Data courtesy of A. Rimmer)

Fig. 28.2. The mid-thermocline depth was calculated as the first derivative (dT/dZ) of weekly temperature profiles acquired by a conductivity, temperature, and depth (CTD) profiler. The mid-thermocline depth on 21 November 2010 was at 22.06 m. A relatively stable deepening rate of ca. 7.3 cm day^{-1} was calculated for the period between the 7th and the 28th of November. Using this deepening rate, we calculated that the time required for complete mixing of a freshly eroded layer between the <22 and >21.6 water layer defined in Fig. 28.1 is less than 5.5 days.

Oxygen concentration along the water column was not measured at the same resolution as the other parameters presented here, but at 21-m depth it was equal to 190 μM while the 22-m depth layer was evidently (see below) anoxic. Considering the mixing ratio obtained from the Cl profile of 9:1, dissolved oxygen (DO) at 21.8-m depth should have been equal to ca. 170 μM. But, as will be shown below, this layer contains high levels of Mn(II) and Fe(II) which originate through the reduction of their respective oxides and therefore is devoid of oxygen, suggesting the occurrence of extensive oxic respiration processes within the freshly eroded layer before the Mn–Fe oxides were reduced.

The data presented below indicate that extensive biodegradation and mineralization occurs also in the anoxic metalimnion, below the freshly eroded layer. The magnitude of degradation in anoxic HS^--containing water can be traced by following NH_4^+ and alkalinity accumulation, as both are proxies for biodegradation in this water (Chap. 23). Typical June to early October profiles of NH_4^+ in the LWM are characterized by high concentrations in the deeper part of the lake (BBL) that decrease linearly upward toward the thermocline.

As an example of such a profile, see the 2 October 2011 low-resolution (every 5 m) profile (Fig. 28.3). This type of LWM profile was attributed by Rimmer et al. (2006) to be shaped by extensive biodegradation in the sediment–water interface, followed by upward diffusion of the NH_4^+ mineralization product. However, 3 weeks later, on 23 October 2011 the shape of this profile is modified considerably

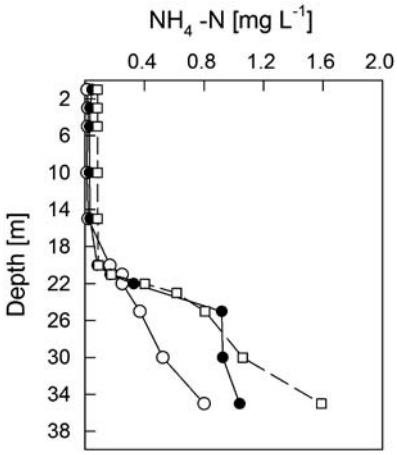

Fig. 28.3 N–NH_4^+ depth profiles taken on 2 October (*empty circles*), 23 October (*full circles*), and 6 November (*empty squares*) 2011 at Sta. A

(Fig. 28.3), showing not only higher BBL levels but also a peak at ca. 24-m depth. The high-resolution data through the metalimnion recorded in the preceding autumn (November 2010, Fig. 28.4) reveal the fine details of such an autumn profile whereby an additional major source of NH_4^+ can be identified in the upper part of the LWM. Notice here the concave shape extending between 21.6 and 23.8 m, with peak concentration at 22-m depth (Fig. 28.4). This concave profile appears only within a temperature/buoyancy gradient zone where the accumulation of fine particles settling from above is expected. Below this zone and down to the BBL, there is no prominent peak in NH_4^+.

Below 21.8 m, the predominant oxidizing agent is sulfate (SO_4) and most biodegradation is mediated by the activity of sulfate-reducing bacteria (SRB, see Sect. 25.3) which leads to the accumulation of sulfide on the account of SO_4. Sulfate levels in the overturned winter water column of Lake Kinneret are relatively high, ~0.6 mM, and toward the end of the stratified period, the concentration in the BBL drops to ca. 0.3 mM. Biodegradation of organic matter mediated by SRB results in the production of carbonate alkalinity rather than of CO_2 (Chap. 23) while when occurring under oxic or sub-oxic conditions the expected carbon product is CO_2. Thus, below 21.8-m depth (indicated by filled circle in Fig. 28.4), NH_4 and alkalinity profiles have a similar concave shape that indicates the occurrence of relatively intensive SRB activity peaked at 22-m depth. This similarity is expressed by a positive correlation, of $R^2 = 0.95$ ($n = 10$), between both solutes. Unfortunately, sulfide concentration was not measured at the same resolution as other parameters but only at 25-, 30-, and 35-m depth. These three samples showed a good positive correlation between NH_4^+ and HS^- ($R^2 = 0.998$; $HS^- = 2.21 \times NH_4^+ + 0.017$; molar units). Assuming that this correlation holds also for the 22–24-m depth layers, it becomes possible to reconstruct an HS^- profile in this transition layer.

Above 22-m depth in the sub-oxic freshly eroded layer, NH_4 and alkalinity profiles become uncoupled (Fig. 28.4) because different processes affect these solutes. At the freshly "eroded" 21.8-m depth layer, alkalinity reveals a conservative

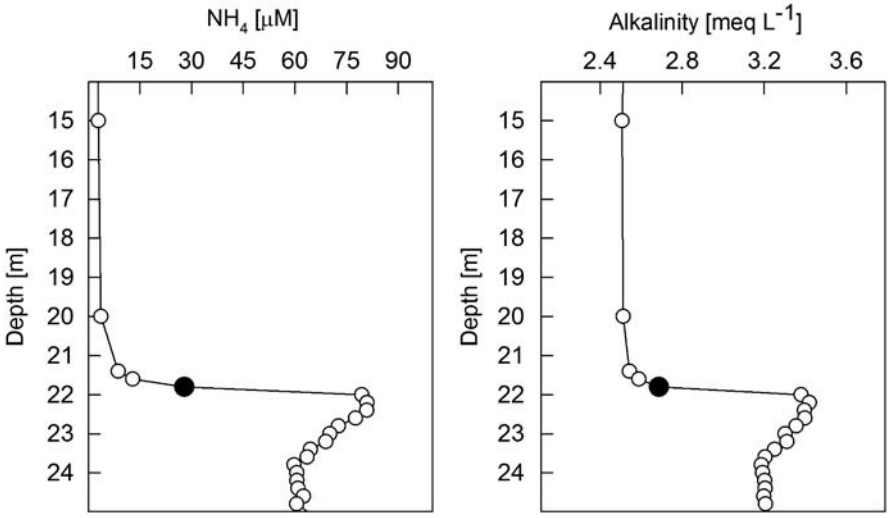

Fig. 28.4 High depth-resolution profiles of NH_4 (*left*) and alkalinity (*right*) between 20- and 25-m depth at mid-lake Sta. A on 21 November 2010. The *filled circle* marks the 21.8-m depth horizon

behavior because its concentration indicates a mixing ratio between epilimnetic and LWM contribution similar to that obtained by Cl^-, of approximately 9:1. Ammonium, however, shows a respective ratio of 0.35:0.65, hence a much higher concentration than the level expected due to a 9:1 mixing ratio. This suggests a non-conservative behavior of NH_4^+ that is affected by a variety of biological processes, including its addition through in situ biodegradation, a conclusion supported by the respective substantial removal of oxygen mentioned above.

28.2.1 Redox/Oxidation State of Trace Elements

28.2.1.1 Cobalt (Co) and Iron (Fe)

Cobalt is often associated with Mn across redox gradients due to its adsorption on Mn hydrous oxides (Singh et al. 1984) and the redox-driven interconversion between dissolved Mn and particulate Mn-oxide species (Leinemann et al. 1997). In Lake Kinneret water column, except for at mid-water layers, soluble Co (Co_s) concentration was below detection limit (20 ng L^{-1} by inductively coupled plasma mass spectrometry, ICP-MS). Significant peaks in Co_s and particulate (Co_p) were observed at 21.8-m depth (Fig. 28.5a, filled large circle), where an extremely large Mn(II) peak (4.8 μM) was also found (G Scharabi, pers. com.). Therefore, we hypothesize that above this layer, Co was scavenged uniquely by hydrous manganese oxides, and that at this depth both Co and Mn were simultaneously released to the

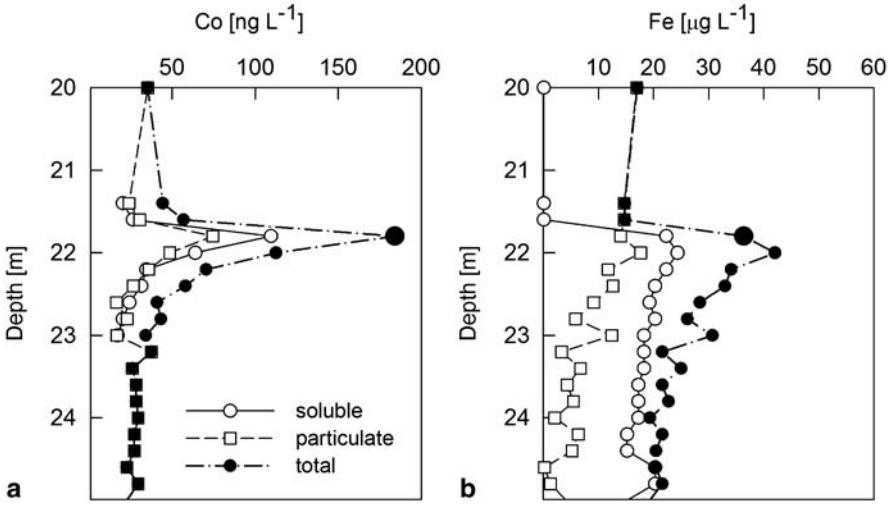

Fig. 28.5 Depth distribution of cobalt (**a**) and iron (**b**) species across the thermocline between 20- and 25-m depth at mid-lake Sta. A on 21 November 2010. The *enlarged symbols* refer to the 21.8-m depth horizon

ambient water during reductive dissolution of the oxides. The Co_s:Mn_s molar ratio at 21.8-m depth was 3.2×10^{-3}, not much different than the ratio of 2.6×10^{-3} in the water column of Lake Paul, Michigan (Leinmann et al. 1997). The similarity in ratios suggests the possibility that in both cases, the manganese oxides that formed had reached adsorption saturation with respect to Co. The importance of identifying the depth of this peak is that redox conditions at the 21.8-m peak must have been intermediate between those in the oxic layer above and in the SRB-active zone below. The peak of Co_p identified at 21.8 m (Fig. 28.5a) may represent a solid cobalt phase that was formed after Co_s was released to the ambient water.

Soluble iron ($Fe_s \approx Fe(II)$) was absent from the oxic epilimnion. At this stratum, Fe appeared only as particulate (Fe_p) at concentrations ranging between 5 and 20 µg L^{-1} (Fig. 28.5b), presumably as Fe(III) oxi-hydroxides. These oxides originate from external and internal lake sources such as riverine, dust, resuspension of littoral bed sediments, and perhaps also some oxides formed through oxidation of Fe(II) above the redox cline. Notice that the general concave shape of Fe_s (and Fe_t) profile resembled that of NH_4^+ (and of alkalinity) and therefore is assumed to resemble the preceding pattern of the biodegradable organic particle accumulation. Having such similarity in vertical distribution is an expected consequence of an effective retention for both types of particles, within the buoyancy transition layer.

Based on the Fe_p profile in the LWM (Fig. 28.5b), we suggest that most of it is comprised of unreduced Fe oxides rather than $FeS_{x(s)}$. Below 22-m depth and down to the sediment–water interface, Fe_p gradually decreased from ca. 20 µg L^{-1} to low levels of ca. 2–4 µg L^{-1} in the BBL. Such a pattern would not be expected if Fe_p is made of $FeS_x(s)$ which may have been formed in this water through interaction

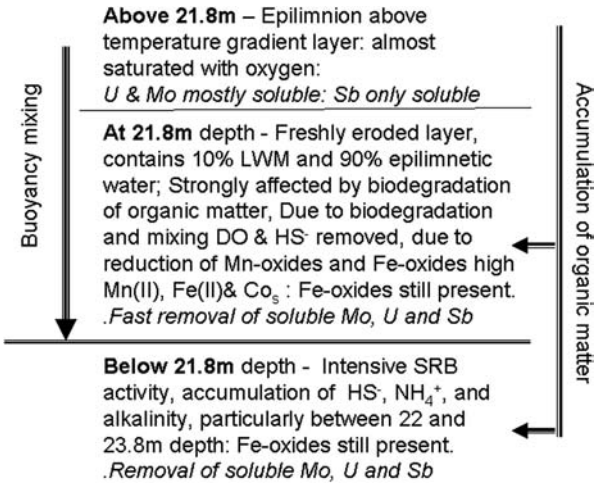

Fig. 28.6 Schematic presentation of the physical and biogeochemical regime, across the temperature transition layer, as depicted on 21 November 2010

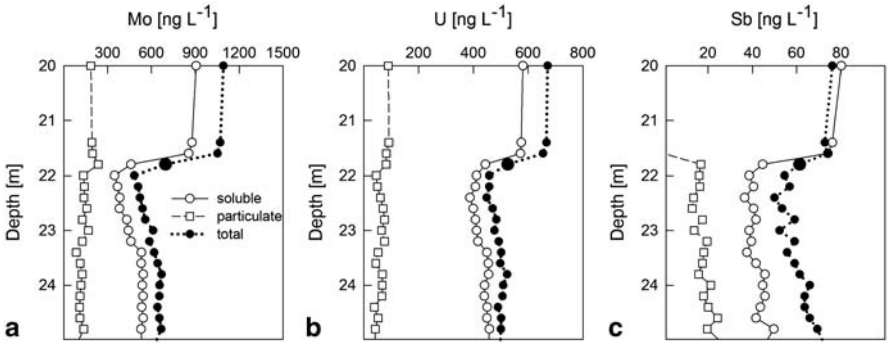

Fig. 28.7 Depth distribution of molybdenum (**a**), uranium (**b**), and antimony (**c**) species across the thermocline between 20- and 25-m depth, measured at mid-lake Sta. A on 21 November 2010. *Enlarged symbols* mark the 21.8-m depth horizon

between Fe oxides or Fe(II) and HS^-. For the sake of the following discussion and clarity, a schematic view of the physical and biogeochemical setting that prevails across the mid-water temperature transition layer is presented in Fig. 28.6.

28.2.1.2 Molybdenum (Mo), Uranium (U), and Antimony (Sb)

The vertical profiles of the different forms of Mo, U, and Sb are shown in Fig. 28.7. The soluble and therefore the total concentration of all three elements show convex

mirror-image profiles to the concave profiles of NH_4^+, alkalinity Fe-II, Fe oxides, and HS^-, suggesting that in the transient SRB-active layer (between 22- and 23.8-m depth) extensive biodegradation is linked to larger removal from water of the soluble forms of these metals. However, this observation does not elucidate on the exact mechanism of removal of these oxy-anions. Notice also that in this transient layer, there is no parallel increase in the concentration of the particulate forms of these metals, implying that removal through sedimentation of the newly formed particles is fast.

Molybdenum may have an important role in nitrate uptake by algae and thus affect photosynthesis whereas biological functions of uranium and antimony are less known. The onset of stratification in Lake Kinneret and subsequent anoxia in the LWM lead to significant decline in the concentrations of Mo, U, and Sb in this layer whereas epilimnetic concentration of the soluble forms of these elements remain relatively high. As demonstrated in Fig. 28.7, additional removal occurs in autumn when the thermocline deepens. Below 21.8 m, the similarity in profiles between uranium and molybdenum is expressed by a good correlation ($r^2 = 0.97$; $U = 0.347 \times Mo + 0.27$). Since oxygen is absent in this layer, the removal of the soluble species of Mo and U must be due to a process which is unrelated to the ambient oxygen concentration. It is therefore hypothesized that either the occurrence of Fe oxide reduction or local accumulation of HS^- induces the removal of the metals.

Metal removal seems to occur also in the freshly eroded layer above, where SRB activity probably does not occur but into which some HS^- contributed from the LWM end member may have been introduced during mixis. Accepting the 9:1 mixing ratio model suggests that following the deepening of the thermocline over 50% of the Mo_s and U_s, originating from epilimnetic water, is removed through fast sedimentation because the local concentration of these solutes is much smaller (enlarged symbols) than expected from a 9:1 mixing ratio. The obvious questions are therefore what are the mechanisms involved in the conversion of the soluble species to particulate phases and what facilitates the fast removal of the particulate products.

Mo(VI) is the stable oxidation state in oxygenated water and appears as the oxy-anion of MoO_4^{-2} which tends to sorb onto Mn oxi-hydroxides (Bertine and Turekian 1973). In oxidized water, soluble uranium also appears as an oxy-anion of U(VI). Barnes and Cochran (1991) showed experimentally that U is released from Fe–Mn oxides as they are reduced. It is therefore expected that under oxic conditions both elements may either appear in the soluble form, as oxy-anions, or be associated with oxides. Upon reducing conditions, these adsorbed elements will be released to the ambient water. However, no buildup of Mo_s and U_s can be shown at the freshly eroded layer where Mn and Fe oxide reduction occurs. The mass balance summarized above points only to the possibility that soluble species of these metals partially disappeared from the water. Additional data that can be shown are that particulate Mo (Mo_p) decreased gradually from epilimnetic values of ca. 0.18 μg L^{-1} to ~0.1 μg L^{-1} in the BBL (Fig. 28.7a) but it did not appear to bear any relationship with (Mo_s).

Crusius et al. 1996 claimed that under sulfidic conditions the reduction of Mo(VI) to Mo(V) and enrichment in sediments is expected. Heltz et al. (1996) hypothesized that in the presence of HS^-, a sulfur atom replaces an oxygen on MoO_4^{-2}, creating a complex that makes the Mo compound more likely to bind to iron sulfides or humic SH complexes. This mechanism reduces the importance of Mo reduction as the initial step in Mo precipitation under reducing conditions. Thus, it may explain the removal of Mo_s from the water solely due to the presence of HS^-. Soluble Mo (Mo_s) and soluble U (U_s) concentrations were minimal at 22-m depth and slightly increased downward to the 23.8-m depth. Within this depth range, they were negatively correlated with the calculated HS^- (For Mo: $r^2 = 0.96$; slope -5.8×10^4, in molar concentrations). This supports the notion of a link between Mo_s (or U_s) removal and the presence of HS^-. An additional option is that molybdenum is an essential trace element required by anaerobic SRB and the activity of these bacteria leads to the formation of poorly crystalline Mo sulfides (Shukor et al. 2008). However, on the larger scale, across the whole LWM water column, there is no such inverse correlation between HS^- and Mo_s (or of U_s). In the BBL, despite the significantly higher HS^- (0.2–0.3 mM) Mo_s (not shown) was only 0.41 μg L^{-1}, hence similar to the concentration at 22-m depth. This implies that only having higher HS^- does not necessarily lead to lower Mo_s (or U_s) and that metal removal may depend on other factors as well.

Reduction of the soluble form to insoluble U(IV) is an important mechanism for the immobilization of uranium in aquatic sediments and for the formation of some uranium ores. U(VI) reduction has generally been regarded as a biological reaction in which sulfide, molecular hydrogen, or organic compounds function as reducing agents. Another option of biotic reduction of U(VI) was proposed by Lovely et al. (1991) who reported that dissimilatory Fe(III)-reducing microorganisms can obtain energy for growth by electron transport to U(VI) and furthermore that this form of microbial metabolism may be much faster than commonly cited biological mechanisms for U(VI) reduction. Despite the evidence gathered on a link between HS^- and uranium removal, Anderson et al. (1989) suggested that in the Black Sea, soluble U(VI) was neither reduced to the thermodynamically favored U(IV) nor scavenged from the water column by particulates.

Typical concentrations of Sb in natural freshwater range from 0.03 to 10 ng L^{-1} while the respective levels measured in Lake Kinneret and in the Jordan River were tenfold higher (40–100 ng L^{-1}: Table 28.1). A prominent difference between the profiles of Sb to Mo and U (Fig. 28.7) is that only soluble Sb (Sb_s) was detected in the epilimnion while the particulate form (Sb_p) was below detection, whereas in the case of Mo and U both soluble and particulate forms were detected in this layer.

The prevalent oxidation states of Sb in the environment are Sb(III) and Sb(V). In most epilimnic waters, the oxidation of Sb(III) to Sb(V) by O_2 is extremely slow (time scale of years, Leuz 2002). Under oxidizing conditions, Sb (III) is found at relatively low concentrations because it tends to sorb onto oxi-hydroxides of Al, Mn, and Fe. Following adsorption, some Sb(III) may be oxidized by Fe to form Sb(V), a process which is much faster than oxidation by O_2 (Belzile et al 2001; Filella et al. 2002; Leuz 2002, 2006). This leads to soluble Sb(V) release to the

ambient water and under oxidized conditions it appears mainly as $Sb(OH_6)^-$. Accordingly, we assume that in the oxic epilimnion of Lake Kinneret Sb appears exclusively as Sb(V) and that this explains the relatively high Sb_s and absence of Sb_p in this layer (Fig. 28.7c).

In the freshly eroded layer (enlarged symbols in Fig. 28.7c), Sb_p was similar to the level below 22-m depth whereas (Sb_s) was somewhat larger and somewhere between the layers. Considering that $Sb_t = Sb_s + Sb_p$, the drop in Sb_t (-0.02 µg L^{-1}) equals the drop in $\sim Sb_s$ (-0.04 µg L^{-1}; from 0.08 to 0.04 µg L^{-1}) plus the rise in Sb_p ($+0.02$ µg L^{-1}). Accepting the 9:1 mixing model for this layer implies that following the erosion of the LWM, Sb_s and Sb_t should have become momentarily higher, at almost epilimnetic levels, but later about half of the Sb_s was converted to Sb_p, of which a portion sedimented out, leaving in water Sb_p which is similar to the layer below.

Depending on pH, Fe may act as a reducing or as an oxidizing agent. In anaerobic alkaline solutions, Leuz (2006) reported that Fe(II) reduced Sb(V) to Sb(III). Moreover, within a pH range of 2–12, thermodynamic considerations posit the reduction of Sb(V) to Sb(III) by S^{-2}. Thus, both the occurrence of Fe(II) and of S^{-2} in the SRB activity zone, below 22 m, and in the freshly eroded layer (HS^- introduced upon mixing) favor the appearance of Sb (III). Li et al. (1984) claim that affinity of Sb for natural particles in oxic systems is weak as compared to higher affinity in H_2S water.

28.2.1.3 Selenium

Selenium is a redox-sensitive element, which serves as a micronutrient for the growth of the bloom-forming dinoflagellate *Peridinium gatunense* in Lake Kinneret. In batch cultures, optimal growth was obtained with 50 ng Se (IV) L^{-1} (Lindström 1983). In Lake Kinneret, we have identified the soluble species of Se(IV) and Se(VI) and a residual fraction obtained as the difference between measured total and soluble selenium. This fraction is assumed to consist of elemental Se^o and Se^{-2}, and is referred to here as Se_{org}. In oxic water, Se(VI) is the thermodynamically stable phase (Séby et al. 2001). The presence of Se(IV) in oxidized water is not well understood, although Se(IV) is commonly assumed to be the species preferred for algal consumption. Cycling of the Se_{org} fraction may also provide biologically available Se. Lindström (1983) suggested that Se(VI) was also utilized by algae. Se_T (total Se) concentration in Lake Kinneret is ca.150 ng L^{-1}.

The major source of Se to Lake Kinneret is from the Hula Valley peat soils (Chap. 19). In winter, Se_T in the River Jordan varies between 300 and 700 ng L^{-1} of which ~75% appears as Se(VI), ~10% as Se(IV), and the remainder as Se_{org} (Nishri and Sukenik 2012). There is a potential link between man-made changes in the Lake Kinneret watershed and the frequency of appearances of *Peridinium gatunense* blooms in the lake. In 1994, a new drainage system was constructed in the Hula Valley aimed to restrict flushing of water through peat soils but in following decades the frequency of spring-forming blooms of *Peridinium gatunense* in Lake Kinneret changed (Chap. 11). Zohary et al. (2012) suggested that shortage of Se in Lake Kinneret may have caused this change.

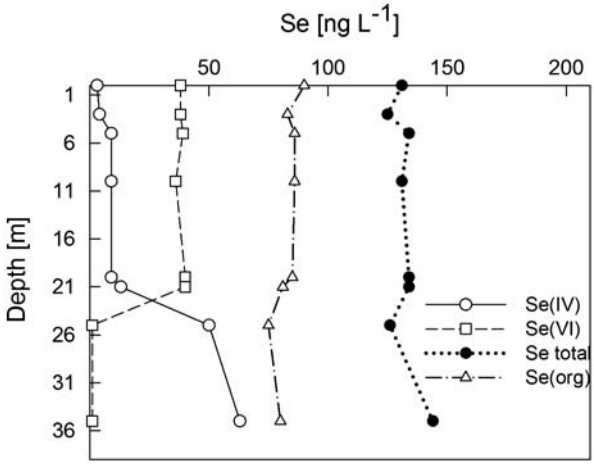

Fig. 28.8 Depth distribution of selenium species between 0- and 35-m depth in the pelagic zone in November 2011

Depth profiles of Se concentrations in Lake Kinneret were measured from 1993 to 1995 and in 2011 (Fig. 28.8). The following seasonal patterns were observed: (1) During the mixed period, Se(IV) concentrations were ~50 ng L^{-1}. When the spring bloom crashed, i.e., 1–3 months after the onset of stratification, the epilimnetic concentration decreased below detection limit (to ca. 3–5 ng L^{-1}). At this time, concentrations of Se(VI) in the epilimnion decreased only slightly. (2) During the stratified period, epilimnetic Se_{org} increased. In the hypolimnion, Se(VI) decreased, practically disappearing from this layer (Fig. 28.8); by contrast, Se(IV) increased, most probably as a result of Se(VI) reduction. (3) The ongoing deepening of the thermocline during autumn led to the transfer of Se(IV) into the euphotic layer.

The levels of biologically available forms of Se in late winter and spring may be critical for the development of *Peridinium* in the lake. If we assume that Se(IV) is more labile than Se_{org} and that both these forms are more available for algal uptake than Se(VI), the fact that most (~75%) of the external riverine Se input is in the form of Se(VI) implies the potential for Se limitation of the spring bloom in Lake Kinneret in years of low rainfall. Contrary to the trace metals discussed above, we do not have indications that soluble species of Se form a particulate phase in the HS^--containing hypolimnion where only the reduction of soluble Se(VI) to soluble Se(IV) had been identified.

28.3 Summary

In Lake Kinneret, the autumn is characterized by buoyancy mixing due to the cooling of the air to temperatures lower than the surface water (Imberger 2012; Chap. 9). During this season, Ostrovsky and Yacobi (2010) reported on enhanced sedimentation of organic matter to the LWM despite relatively low chlorophyll levels in the epilimnion. They also showed that in October–December the ratio between organic

matter sedimentation (measured in sediment traps) and primary production has been seasonally high. Hence, this represents a case where the seasonal pattern in organic matter sedimentation is unrelated to contemporaneous epilimnetic biological activity. In support of these conclusions, notice that during the 34 days elapsed between 2 October and 5 November 2011 (Fig. 28.3) NH_4^+ concentration in the BBL almost *doubled,* as compared to the 2 October level, which represents several summer stratification months (May–October) of accumulation. The source of this biodegradable organic matter is suggested to be the resuspension and focusing toward the lake pelagic of partially decomposed organic particles due to the deepening of the thermocline. These partially decomposed particles are assumed to have primarily settled in the depth zone between 22- and 28-m depth which in fall, concomitantly with thermocline deepening, becomes exposed to the higher turbulent energy of the growing epilimnion.

Moreover, we speculate that in autumn sedimentation of organic particles is not controlled by their "free fall" along the epilimnetic water column but rather by occlusion within the so-called water parcels sinking from the lake surface. This may be one of the reasons for the poor levels of epilimnetic chlorophyll in autumn despite the intensive introduction of nutrient (NH_4^+ and soluble P)-enriched LWM water into the epilimnion. We hypothesize the finer organic fraction is entrapped in the mid-water buoyancy transition zone, eventually forming, through biodegradation, the concave shape profiles of the direct and indirect degradation products, namely, of NH_4^+, alkalinity, and HS^-. The coarser organic particles settle directly to the pelagic sediment–water interface forming the largest mineralization peak in the BBL. As with the fine organic particles, we also assume that turbulent convection sweeps down epilimnetic Fe and Mn oxides forming an assemblage of both reducing and oxidizing agents in the metalimnion.

Across the metalimnion which is defined by its steep temperature gradient, the biodegradation and mineralization of these particles form a redox gradient zone in which three sub-layers are distinguished: an upper well-mixed oxygenic epilimnion, a lower metalimnetic anoxic HS^--enriched layer, which constitute the upper part of the LWM, and in between a thin freshly eroded sub-oxic transition layer where mixing between layers is apparent. This thin layer represents a transitory stage during thermocline deepening of LWM water not yet fully mixed within the epilimnion. As such, it is characterized by having intermediate composition of various LWM and epilimnetic constituents. Processes associated with enhanced biodegradation such as DO depletion and Mn and Fe oxide reduction are shown to occur within the freshly eroded sub-oxic layer shortly (less than few days) after the erosion of LWM water commences. The SRB-active layer that stretches below is also characterized by Fe-oxide reduction. In both sub-oxic and anoxic layers, there are indications for the removal of soluble Mo, U, and Sb, which is followed by fast sedimentation of particulates. The overall removal process seems to include the transformation of the soluble oxy-anionic forms of all of the three metals that prevail in the oxidizedlimnetic water into species that may interact with solutes present in the ambient water to form particles, which are removed through fast sedimentation to the lake floor.

References

Anderson RF, Fleisher MQ, Hurry AP (1989) Concentration, oxidation state and particulate flux of uranium in the Black Sea. Geochim Cosmochim Acta 53:2215–2224

Barnes CE, Cosharan JK (1991) Geochemistry of uranium in the Black Sea sediments and the oceanic U balance. Earth Planet Sci Lett 97:94–101

Belzile N, Chen UW, Wang Z (2001) Oxidation of antimony (III) by amorphous iron and manganese oxyhydroxides. Chem Geol 174(4):379–387

Berman T, Kaplan B, Chava S, Parparova R, Nishri A (1993) Effects of iron and chelation on Lake Kinneret bacteria. Microb Ecol 26(1):1–8

Bertine K, Turekian K (1973) Molybdenum in marine deposits. Geochim Cosmochim Acta 37(6):1415–1434

Crusius J, Calvert S, Pedersen T, Sage D (1996) Rhenium and molybdenum enrichments in sediments as indicators of oxic, suboxic, and sulfidic conditions of deposition. Earth Planet Sci Lett 145:65–78

Filella M, Nelson B, Chen YW (2002) Antimony in the environment: a review focused on natural waters II. Relevant solution chemistry. Earth Sci Rev 59:265–285

Frevert T, Pollingher U, Berman T (1982) Why do River Jordan algae not grow in Lake Kinneret. In: Hemphill (ed) Trace Subst Environ Health Proc Univ Mo Annu Conf 16:174–186

Heltz CR, Miller CV, Charnock JM, Mosselmans JFW, Patrick RAD, Garner CD, Voughan DJ (1996) Mechanisms of molybdenum removal from the sea and its concentration in black shales: EXAF evidence. Geochim Cosmochim Acta 60:3631–3642.

Imberger J (2012) Environmental fluid dynamics. Academic, Waltham

Leinemann CP, Taillefert M, Perret D, Galliard JF (1997) Association of cobalt and manganese in aquatic systems: chemical and microscopic evidence. Geochim Cosmochim Acta 61(7):1437–1446

Leuz AK (2002) Redox chemistry of antimony in aquatic systems: e.g. lakes. Diploma thesis, Carl von Ossietzky University, Oldenburg

Leuz AK (2006) Redox reactions of antimony in the aquatic and terrestrial environment. Dissertation no. 16582, submitted to ETH, The Swiss Federal Institute of Technology, Zurich

Li YH, Burkhardt L, Buchholtz M, O'hara P, Santchi PH (1984) Partition of radiotracers between suspended particles and sea water. Geochim Cosmochim Acta 48:2011–2019

Lindström K (1982) Environmental requirements of the dinoflagelate *Peridinium Cinctum* fa. *westii*. PhD thesis, University of Upsala, Sweden

Lindström K (1983) Selenium as a growth factor for plankton algae in laboratory experiments and in some Swedish lakes. Dev hydrobiol 13:31–47

Lindström K, Rodhe W (1978) Selenium as a micronutrient for the dinoflagellate *Peridinium cinctum* fa. *westii*. Mitt int Ver Theor Angew Limnol 21:168–173

Lovely DR, Phililps EPJ, Gorby YA, Landa ER (1991) Microbial reduction of uranium. Nature 350:413–416

Nishri A, Sukenik A (2012). Examination of selenium species in Lake Kinneret and in the Hula Valley. KLL-IOLR report T20/2012, (in Hebrew) submitted to the Israel water Authority

Nishri A, Brenner IB, Hall GEM, Taylor HE (1999). Temporal variations in dissolved selenium in Lake Kinneret (Israel). Aquat Sci 61:215–233

Ostrovsky I, Yacobi YZ (2010) Sedimentation flux in a large subtropical lake: spatiotemporal variations and relation to primary productivity. Limnol Oceanogr 55(5):1918–1931

Rimmer A, Eckert A, Nishri A, Agnon Y (2006) Evaluating hypolimnetic diffusion parameters in thermally stratified lakes. Limnol Oceanogr 51(4):1906–1914

Séby F, Potin-Goutier M, Giffaut E, Borge G, Donard OFX (2001) A critical review of thermodynamic data for selenium species at 25℃. Chem Geol 171:173–194

Shaked Y (2002) Iron redox dynamics and biogeochemical cycling in the epilimnion of Lake Kinneret. PhD dissertation, The Hebrew University Jerusalem, 190 pp

Shukor MY, Rahman FA, Shamaan NA, Lee CH, Karim MI, Said MA (2008) An improved enzyme assay for molybdenum reducing activity in bacteria. Appl Biochem Biotechnol 144:293–300

Singh SK, Subramanian V, Gibbs RJ (1984) Hydrous Fe and Mn oxides, scavengers of heavy metals in the aquatic environment. Crit Rev Environ Control 14(1):33–90

Sivan O, Erel Y, Mandler D, Nishri A (1998) The dynamic redox chemistry of iron in the epilimnion of Lake Kinneret. Geochim Comochim Acta 62(4):565–576

Wynne D, Pieterse AJH (2000) The effect of copper on photosynthesis, nitrate reductase and phosphatase activities in Lake Kinneret phytoplankton. Arch Hydrobiol Beih Ergebn Limnol 55:581–593

Zohary T, Sukenik A, Nishri A (2012) Present–absent: a chronicle of the dinoflagellate *Peridinium gatunense* from Lake Kinneret. Hydrobiologia 698:161–174

Part V
The Littoral

Chapter 29
The Littoral Zone

Tamar Zohary and Avital Gasith

Abstract The littoral zone of Lake Kinneret is characterized by high diversity of both abiotic (sand, stone) and biotic (vegetation) substrates, forming habitats of varying complexity that change markedly on both spatial and temporal scales. Most Kinneret fish and macro-invertebrates use littoral habitats for at least part of their life cycle. Many use littoral resources (substrate for attachment, refuge, food) for reproduction and growth. Higher species diversity and fish abundance and biomass are associated with higher degree of habitat complexity. Water level fluctuations (WLFs) influence the availability of littoral resources, with impacts not only on the littoral fauna and flora but indirectly also on the pelagic populations. Consecutive years of drought and a negative water balance for Lake Kinneret result in low lake levels and exposure of continuously increasing shore areas on which shore vegetation develops. The shore vegetation is inundated in high-rainfall winters, presenting a window of opportunity for the littoral zone biota that takes advantage of the temporarily augmented vegetative resources (e.g., enhanced reproduction of cichlids; refuge for young of the year of many fish species). Upon drawdown of the lake water levels, the proportion of rocky littoral declines, limiting the biota that dwell in this habitat. Correspondingly, littoral biota flourish on years of high water levels when rocky habitats are abundant. For example, fluctuation of population size of the endemic cyprinid *Mirogrex* (syn: *Acanthobrama*) *terraesanctae,* a major planktivore, was directly influenced by the availability of freshly inundated rocky substrate used for spawning. In a cascading effect, the pelagic zooplankton populations were impacted by the resulting fluctuations in *Mirogrex* population size and in their predation pressure. The case of Lake Kinneret underscores the importance of WLFs that can act as a major environmental factor influencing littoral habitat structure and resources, and resulting populations dynamic. Intensification of these fluctuations beyond their natural amplitude is likely to markedly impact the lake ecosystem structure and function.

T. Zohary (✉)
The Yigal Allon Kinneret Limnological Laboratory, Israel Oceanographic & Limnological Research, P.O. Box 447, 14950 Migdal, Israel
e-mail: tamarz@ocean.org.il

A. Gasith
George S. Wise Faculty of Life Sciences, Department of Zoology, Tel-Aviv University, 69978 Tel-Aviv, Israel
e-mail: avitalg@tauex.tau.ac.il

T. Zohary et al. (eds.), *Lake Kinneret, Ecology and Management,* Aquatic Ecology Series 6,
DOI 10.1007/978-94-017-8944-8_29,

Keywords Habitat complexity · Littoral · Macrophytes · Refuge · Spawning · Water level fluctuations

29.1 Littoral Zones: General Overview

Lake shores are transitional zones, or ecotones, that provide habitats for both terrestrial and aquatic organisms. The littoral zone is the shallow-water, near-shore region of the lake, interfacing between land and water, extending to the lower limit of the euphotic zone, where light reaching the bottom is sufficient to support plant growth (Wetzel 2001). The littoral zone depth varies from one lake to another, often extending 1–5 m. Habitat diversity in the littoral zone is higher than that found in the pelagic zone. It emanates from the variety of bottom substrates and the mosaic of macrophytes, as well as the diverse biotic conditions resulting from the interaction between substrate and water and between water and air in this shallow-water environment (Schmieder 2004).

Littoral zones tend to be more productive than pelagic zones (Wetzel 2001), and have richer species diversity of both micro- and macro-organisms. The microbiota of the littoral zone includes bacteria, algae, fungi, and small invertebrates. The macrobiota includes macroinvertebrates, fish, birds, and submerged, floating and emergent plants. The structured substrate, whether abiotic (e.g., rocks) or biotic (e.g., plants), provides surface for attachment for algae and invertebrates, refuge for prey organisms, sites for fish spawning, and nursery grounds for young fish (Gafny et al. 1992; Schmieder 2004). Most fish in lakes inhabit the littoral zone and use its resources during at least part of their life cycle.

Gasith and Gafny (1990) pointed out the importance of littoral habitat complexity. Niche availability increases with "particle" size: Small particles such as sand and silt provide relatively low structural complexity, suitable only for small organisms, whereas larger particles such as stones and boulders provide refuge for both small and large organisms. Macrophytes, tree stems, and roots further increase habitat complexity (Gasith and Gafny 1998; Gasith and Hoyer 1998; Meerhoff et al. 2007; Brauns et al. 2008). Different macrophyte species provide habitats varying in food, cover, and structure for the aquatic biota (Wilcox and Meeker 1992). In contrast, man-made structures along lakeshores, such as walls, piers, and paved surfaces, usually reduce habitat complexity.

Littoral zones shift their position with changes in water level that exposes or inundates shore areas. Correspondingly, habitat complexity (physical structure provided by rocks and vegetation) varies with the regime of water level fluctuations (WLFs) and lake bathymetry. Wave action is another factor influencing structure and habitat conditions in the littoral zone. Wave action in interaction with changing water levels facilitates transport of small particles to deeper water, leaving rocks at higher water level marks (Hofmann et al. 2008). While rocky substrates are stable over time, the physical structure provided by plants is often seasonal, with large interannual variability; both types of substrates change with water depth and are influenced by WLFs (Gasith and Hoyer 1998).

Shallow lakes have extensive littoral area. In contrast, the littoral of deep lakes is limited to a narrow belt around the lake perimeter, often occupying <10% of the lake surface area (Gasith 1991; Beauchamp et al. 1994). As the size and depth of the lake increase, the source of autochthonous organic matter shifts from that of macrophytes in the littoral zone to that of phytoplankton in the pelagic zone. Concomitantly, non-metabolic littoral structural resources such as stones or macrophytes, used by the biota for colonization, refuge, and spawning, become increasingly scarce. Based on this consideration, Gasith (1991) hypothesized that littoral resources become increasingly limiting with increasing lake size and depth. In deep lakes, macrophytes are restricted to near shore areas of the littoral zone; therefore, the structure and food that they provide may result in short supply (Gasith 1991; Beauchamp et al. 1994; Gasith and Gafny 1998).

Species inhabiting lakes undergoing natural WLFs are adapted to the seasonal changes in habitat structure and conditions. However, accentuated WLFs produced by man can reduce species survival as their resilience is surpassed (Smith et al. 1987). As a result, the diversity of the littoral fauna and flora declines; in extreme cases, macrophytes are lost altogether and the fauna consists of only short-lived ephemeral species (e.g., insect larvae).

29.2 The Littoral Zone of Lake Kinneret

The following section will address the diversity of littoral habitats, the factors impacting the characteristics of those habitats, the biota that inhabit them, and the interactions between habitat type and the biota.

29.2.1 Physical Factors

Physical factors such as wave action, WLFs , and substrate particle size are important drivers that determine the nature and conditions (including lake bathymetry as reflected in shoreline development and basin slope) of littoral habitats in Lake Kinneret.

Bathymetry of the littoral zone: The 56-km-long shoreline of Lake Kinneret is mostly regular, with a shoreline development index of 1.14; it includes only one region of natural lagoons, in the north of the lake (Beteha lagoons). This region is dry during periods of low water levels (below ~−213 m). The slope of the Kinneret shoreline ranges from being gentle (1–2%) in the Beteha lagoons in the south (Tzemach) and in the Ginnosar Valley on the west, and to being much steeper (>5%) in the vicinity of Tiberias, at the north-east shore of the lake (Amnun, Kefar Nahum), and along much of the eastern side of the lake (details in Chap. 4). As water levels fluctuate between −214 and −209 m, the position of the littoral area of gentle-sloping shores is shifted by hundreds of meters whereas in steep-sloping shores it may shift only a few tens of meters. Correspondingly, the extent

of shoreline vegetation that gets inundated varies markedly between gentle-sloping and steep-sloping shores (see below).

Wave action: In summer, westerly winds blow nearly every afternoon, causing strong wave action along the eastern shores. The winter period is less windy but with occasional exceptionally high-velocity easterly winds, known as "Sharakiya," causing strong waves action on the western shores (details in Chap. 6). The absence of continuous growth of macrophytic vegetation in the littoral zone of Lake Kinneret may be attributed in part to the strong wave action that is capable of uprooting young shoots.

WLFs: Natural WLFs in Lake Kinneret are ~1.5 m, fluctuating between a maximum in spring (March–May) and a minimum in autumn (November–December). However, since the late 1960s, the lake supplies 25–30% of the country's demand of potable water, which increased the multiannual amplitude of Kinneret WLFs up to 6 m, substantially impacting littoral zone habitats and resources (Zohary and Ostrovsky 2011).

Abiotic substrates: The lake bottom in the littoral zone is made of particles of variable sizes, ranging from fine clays, silt, and sand to gravel, pebbles, stones, and boulders. Rocky substrate including boulders is more prevalent in shores with a steep slope, whereas the gentle slopes tend to be sandy or silty.

The proportion of shores with fine substrates increases with declining water levels, whereas that of rocky substrate respectively declines. Gasith and Gafny (1990) reported that the overall percent of littoral bottom covered by fine substrates increased from 6% at −209.5 m to 49% when the water level was 3 m lower (−212.5 m). The change in the proportion of rocky littoral area in a selected site in a year of low lake level followed by high lake levels is demonstrated for example in Fig. 29.1. Using fluorescently dyed Kinneret sand particles, Shteinman and Parparov (1997) demonstrated that wave action transports small-grain sediments, and that the extent of the transport was correlated with the strength of the wave action. Currents transport the sediment along the shoreline. The sediment particles segregate by size, moving towards or away from the shore, depending on basin slope.

29.2.2 Biotic Substrates: Macrophytic Vegetation

Inundated emergent vegetation provides biotic substrates that contribute to habitat complexity of the littoral zone. Submerged macrophytes (*Myriophyllum spicatum* and *Potamogeton pectinatus*) were sporadically abundant in the past (Gophen 1982) but have become extremely rare in Lake Kinneret of recent years, both spatially and temporally (Gafny and Gasith 1999b; Gasith, unpublished data). Waisel (1967) attributed the limited growth of submerged vegetation to an increase in the magnitude of the lake's WLFs and to unfavorable light conditions. An additional contributing factor operating in Lake Kinneret may be the destructive effect of high wave action, which uproots germinating rooted plants. For the same reasons, emergent macrophytes do not germinate and develop in the littoral zone. Emergent macrophytes seen in the lake are plants that germinated and started to develop

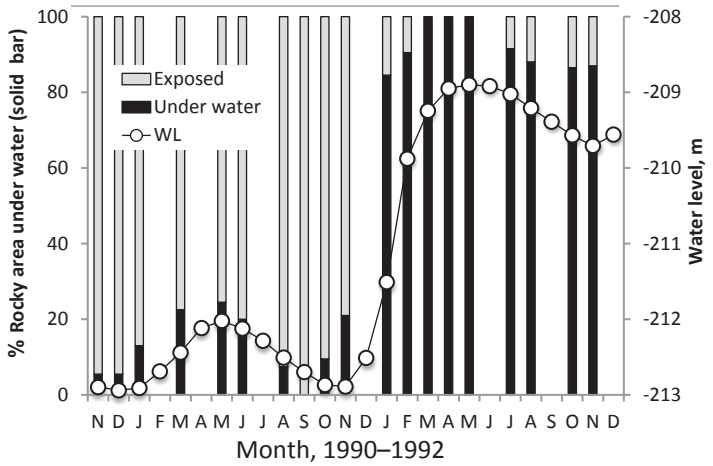

Fig. 29.1 Temporal changes in the availability of rocky area in the littoral zone of Lake Kinneret in an eastern beach on a dry year (1991) followed by a rainy year (1992). *Solid line* indicates changes in water level. *Solid* and *open bars* indicate the proportion of rocky area under and above the water level, respectively. (Reproduced from Gasith and Gafny (1998) with permission from Springer)

on shores, and become part of the littoral zone when inundated by the rising lake level (Fig. 29.2a). The community of emergent macrophytes is composed mostly of *Phragmites australis* (common reed), *Typha angustata* (cattail or bulrush), *Cyperus alopecuroides* (sedge), and the tree *Tamarix jordanis* (tamarisk). When inundated, this vegetation contributes structure and reduces wave action and the strength of currents among the plants.

Plant growth on exposed shores responds positively to declining basin slope (highest growth rates and biomass attained on gentle slopes) and inversely to sediment particle size (lowest on rocky shores). Moreover, the extent of growth of the shore vegetation is positively influenced by the duration of shore exposure (Gafny and Gasith 2000). Following three consecutive years of low lake levels (1984–1986), when the upper region of the littoral zone (altitude −209 to −210 m) was exposed, Gafny and Gasith (2000) estimated the total standing biomass of the shore vegetation around the lake in fall, 1986, at 4,000 t wet weight (ranging from <0.01 to 1.8 kg dry weight m^{-2}). *Cyperus alopecuroides* and *Tamarix jordanis* contributed about 60 % of the biomass. Similar estimates were made in other years of low water levels (e.g., 1990/1991). In years of high lake levels (e.g., 1987–1989), the estimated standing biomass of shore vegetation was <2 % of that recorded on years of low lake level, mostly because the belt of exposed shores was narrower, leaving smaller areas suitable for plant germination and growth.

In years of low water level, typically with massive shore vegetation, the littoral zone is mostly devoid of inundated vegetation, whereas in years of high water levels that follow years of low lake level, the extent of inundated vegetation can be massive (Fig. 29.2b). Thus, the extent of vegetative cover in the littoral zone varies spatially and temporally, depending on the extent of WLFs and the recent history

Fig. 29.2 **a** Recently inundated young *Phragmites* reeds that germinated and grew when the same site was exposed due to lower water levels (photo: Gasith A). **b** Dense shoreline vegetation (mostly tamarisk trees) that developed during consecutive years of below-average rainfall and low water levels, Ginnosar region (photo: Gasith A). **c** Periphyton-covered stones in the shallow water of Lake Kinneret (photo: Gasith A). **d** Shore aggregation of Kinneret snail shells. Native species: *Melanopsis costata; Melanoides tuberculata*; invasive species: *Pseudoplotia scabra* (photo: Zohary T)

of those fluctuations. An analysis of a series of >300 air photographs of the lake perimeter taken in May 2009 when lake level was low (−213.37 m) shows that >90% of the littoral zone had no emergent macrophytes (Fig. 29.3a). In contrast, in May 2012, following a rise in water level by 2.35 m in a single winter (−211.32 m; i.e., ~2 m higher than in May 2009), only 39% of the littoral zone had no vegetation, the rest was covered by either dense (45%) or sparse (16%) inundated vegetation (e.g., Fig. 29.3b).

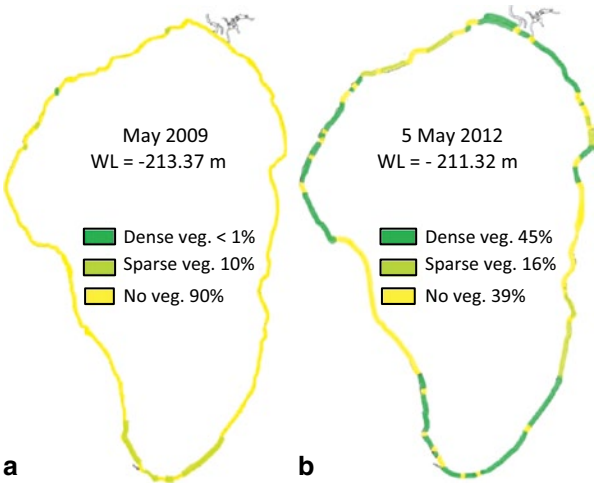

Fig. 29.3 Maps showing the locations of inundated vegetation in the littoral zone in May, the time of the year when water level is at or near its annual maximum. **a** In 2009, a low-water-level year that followed three drought years with declining water levels. **b** In 2012, a year of a major water level rise that followed six consecutive below-average rainfall years. Areas of thick, sparse, or no vegetation are indicated. The hand-drawn maps (by David Cummings) are each based on a series of >300 aerial photographs, on 1 May 2009, by Idan Shaked and on 5 May, 2012, by Asaf Dori, Israel Nature Parks Authority. Only inundated vegetation was mapped, shore vegetation outside the water was ignored

Following six consecutive years of below-average rainfall starting in 2005, dense shore vegetation developed, covering not only the sandy shores but also rocky regions. Moreover, we observed that when the shores were exposed continuously for more than 3–4 years, the tree *Tamarix jordanensis* replaced the common reed *Phragmites australis* as the dominant plant, forming dense, forest-like vegetation (Fig. 29.2b). In certain shore areas, alien invasive trees including *Acacia saligna, Eucalyptus* sp., *Parkinsonia aculeate,* and *Washingtonia* palms also got established. However, after inundation by the rising water levels, most of the vegetation died or was uprooted by wave action and decomposed within several months. Exceptional were large *Tamarix* trees with much of their canopy extending above the water; these trees may apparently survive long periods of inundation (possibly years).

The rise of the lake level is associated with periodic high accumulation of organic debris. In years of massive accumulation of plant litter (at times of shore inundation after several years of continuous low lake levels), puddles within piles of debris may be formed on the shore with potential development of short-term nuisances of foul smell and mosquitoes. In 2011/2012, such nuisances raised a debate whether the vegetation should be massively removed to alleviate related inconveniences but at the same time risking the integrity of the lake ecosystem. Most scientists argued that the nuisances can be treated and their effect can be drastically reduced which was proved true. Until relevant information will be obtained, the precautionary principle should be followed. Accordingly, vegetation will be completely removed from bathing beaches; partly removed (up to 30%) from nearby shores and fronts of the local kibbutzim; and removed elsewhere to form access corridors, where needed.

29.2.3 Benthic Algae and Heterotrophic Bacteria

Phytobenthos: The benthic algae of the littoral zone (Fig. 29.2c) comprise an important food source for higher trophic levels inhabiting this region. Nevertheless, so far the phytobenthos was studied only sporadically. Dor (1971, 1974) reported that benthic diatoms comprised a low-diversity, high-abundance assemblage, whereas benthic cyanobacteria were highly diverse but of low abundance. According to Round (1978), the phytobenthos is richly developed on all available substrates in the littoral zone, extending to the limit of light penetration. Diatoms dominate, often covering the substratum by a brown mucilaginous "blanket" and contribute most (~90 %) of the primary production. Filamentous and coccoid cyanobacteria, filamentous green algae, and occasionally euglenoids, cryptomonds, and some desmids, are also abundant. Unlike the pattern typical of temperate lakes, highest biomass and species richness of epilithon in the littoral zone of Lake Kinneret was recorded in winter, and was lowest in the summer (Gafny and Gasith 1999a). As the water level rises in winter and spring, newly inundated rocky areas are colonized by epilithon. The organic matter produced by the epilithon is more labile than that produced by macrophytes, and is probably a better quality food for the littoral biota. According to Gafny and Gasith (1999a, 2000), benthic primary production may amount to only a fraction of 1 % of the annual phytoplankton production in the lake, but is higher by an order of magnitude than that of inundated vegetation. They further showed that epilithon production declines drastically with falling water levels, and warned that if the water level is further reduced, littoral benthic grazers may be deprived of an important food source. Yehoshua et al. (2008) showed that epilithon growth rates in the Kinneret littoral were higher on limestone than on basalt and flint, and that different assemblages inhabited the different kinds of stones.

Heterotrophic bacteria: Little is known on heterotrophic bacteria and their activity in the littoral zone of Lake Kinneret. Ora Hadas (unpublished) recorded considerably higher rates of microbial production and glucose uptake rates in the littoral zone compared with that measured in the pelagic waters of Lake Kinneret. Similarly, Sala and Güde (2006) concluded that the overall contribution of the littoral zone to degradation of organic matter in Lake Constance was comparable to that of the total pelagic water body although the littoral comprised less than 10 % of the lake surface area.

Sukenik and Parparov (2008) conducted laboratory experiments and showed that *Phragmites australis* and *Tamarix jordanensis* decomposed rapidly in Kinneret water, with loss rates of 2–3 % of dry weight per day. The loss rates of nitrogen and phosphorus were twice as high (6.0 and 5.3 % day^{-1}, respectively). However, Gafny and Gasith (2000) recorded much slower rates of in situ decomposition rates, of ~0.6 % day^{-1} for *P. australis,* and half of that rate for *T. jordanensis*. Part of the difference in the rates recorded in these two studies may be attributed to the lower temperatures in the in situ experiments.

29.2.4 Invertebrates

The first encompassing report on the benthic invertebrates in the littoral zone of Lake Kinneret was that of Por (1968) and Por and Eitan (1970). An additional study of the invertebrates in the shallow littoral zone (<2 m) was conducted by Tamir and Gasith during 1999–2001 (Tamir 2002). Taxa richness in rocky and soft sediment substrates was similar (19 and 17 species, respectively) but species composition was different. On rocky substrates, the amphipod *Echinogammarus veneris* was dominant (64–75 % of total organisms) whereas on soft sediments chironomid larvae and oligochaetes were most prevalent. Seven taxa were found exclusively on rocks (sponges, bryophytes, leeches, mayflies, and three species of caddisflies; Trichoptera; Gasith 1969) as well as the invasive snail *Radix natalensis*. Four taxa were found exclusively in soft sediment (oligochaetes, bivalves). Native gastropods had representatives on both types of substrate. A seasonal succession was apparent with dominance of mollusca in the summer and that of *Echinogammarus* and the snail *Bithynia phialensis* in winter.

The native snail fauna of Lake Kinneret consists of three main freshwater species, *Melanopsis costata, Melanoides tuberculata*, and *Theodoxus jordani,* species that were reported to occur in the Jordan Valley for the last 1.5 million years (Heller 2010), long before Lake Kinneret existed in its current form. The abundance of the native molluscs declined dramatically after an unusually large water level rise of winter 2002/2003. This decline coincided with the establishment of an invasive snail *Pseudoplotia scabra,* first reported in the lake (as *Thiara scabra*) in 2007 by Mienis and Mienis (2008). By summer 2010 and throughout 2011, *P. scabra* was the dominant mollusc around the entire lake, with all the native species seen only rarely (Fig. 29.2d; Heller et al. 2014). However, by December 2012, the abundance of *P. scabra* has declined and that of the native species increased. The consequences of this recent invasion for the fauna and flora of Lake Kinneret and the impact on the functioning of the ecosystem are still unknown.

Three native species of bivalve molluscs are known in Lake Kinneret, two unionid mussels *Unio terminalis terminalis* and *Potamida (previously Unio) semirugatus* and a clam *Corbicula fluminalis*. Of those, *U. t. terminalis* is the most abundant species, *C. fluminais* is common, and *P. semirugatus* is rare. Cohen (1993) found high density of *U.t. terminalis* on relatively steep-sloping, sandy bottom on the east side of the lake where relatively strong lateral currents prevail. Ostrovsky et al. (1993) reported highest densities of *Unio t. terminalis* in muddy sands at 0.3–6-m depth, and especially near the Jordan River inflow. They concluded that this bivalve plays a substantial role in removing particulate matter from the water in the shallow inshore area, supplying suspended organic matter to the benthic community and regenerating nutrients. Its larval stage (glochidium) is an obligatory parasite on fish and was recorded on the Kinneret bleak (*Acanthobrama terraesanctae*; Cohen 1993). Like the snails, the abundance of *U. t. terminalis* has declined dramatically over the last decade, but no studies were conducted to highlight any aspects of this decline.

Fig. 29.4 **a** Leeches (*Helobdella stagnalis*) attached to foot after standing for 3 min in the shallow water, May 2012 (photo Beny Sulimany). **b** A regular nest of tilapia (*Oreochromis aureus*) among inundated plants (photo: David Cummings). **c** A single nest of *Oreochromis aureus,* found in a wide sandy area bare of vegetation. It was dug next to the only physical structure present (photo A Gasith)

The stony shores of Lake Kinneret are inhabited by three species of leeches, *Helobdella stagnalis, Dina lineata,* and *Batracobdelloides tricarinatus* (Bromley 1994). They are usually found, in low numbers, adhering to the bottom side of pebbles or stones in shallow waters. Dolev et al. (2012) examined these three species in the field and in the laboratory and reported that *B. tricarinatus* fed on small fish, sucking their blood, *H. stagnalis* fed on snails, and *D. lineata* fed on snails, with preference for the invasive snail *Pseudoplotia scabra.* Gasith (unpublished) recorded that *D. lineata* fed also on chironomid larvae. Several outbreak events of *Helobdella stagnalis,* in summer 2005 and again in summer 2012, attracted attention to this group of invertebrates. Swimmers complained that after standing in the shallow water for a few minutes their feet got covered by tens of leeches (Fig. 29.4a). The leeches do not suck human blood, and are not pathogenic to humans; however, finding them stuck to one's feet was a cause for public complaints. The leech outbreaks were limited in time (few days to weeks) and space (focal

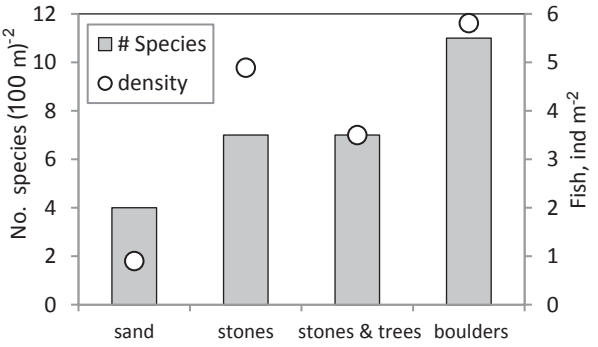

Fig. 29.5 Relationship between fish species richness and abundance and habitat type in the littoral zone of Lake Kinneret. (Source of data: Gafny 1992)

points of several tens of square meters). They occurred at a few man-modified sites, where the bottom substrate was covered by gravel to make wading in the water easier for vacationers.

29.2.5 Fish

Nineteen native fish are present in Lake Kinneret, including an endemic species (the Kinneret bleak, *Mirogrex* (syn. *Acanthobrama*) *terraesanctae,* cyprinidae; Goren and Ortal 1999) and additional alien species (Chap. 16). Most of the fish of Lake Kinneret spend at least part of their life in the littoral zone (Gasith et al. 2000). As shown by Gafny (1992) and Gasith et al. (2000), the nature of the littoral substrate affects fish distribution, richness, density, and biomass. These attributes of the fish community increase with increasing habitat complexity that is influenced by substrate size. Higher richness, density, and biomass (including larger fish) were recorded in littoral zone areas with large stone and boulders than in sandy areas (Fig. 29.5). Thus, WLFs that influence littoral zone structure and habitat complexity have an indirect effect on the fish community. In the following sections, we address some of the fish species individually.

The Kinneret bleak is the most abundant fish in Lake Kinneret, comprising more than 80% of all pelagic fish (Chap. 16). Being a zooplanktivore, this fish plays a central role in the lake's food–web interactions. This fish depends on littoral resources to complete its life cycle. It spawns in winter when the water level rises and inundates rocky areas, where the fish sheds its eggs that adhere to the freshly inundated (i.e., epiphyton-free) stones, in shallow (< 50 cm) water (Fig. 29.6; Gafny et al. 1992; Gasith et al. 1996). As the water level rises, there is a short window of opportunity of several days for the bleak to successfully spawn on the algae-free stony surface. Algae may completely cover the stones within a week. Once the algae (e.g., diatoms such as *Navicula* and *Gomphonema*) cover the stone surface, they prevent the eggs from adhering to the stone's surface; the eggs fall to the ground and are infested by the fungus *Saprolegnia* (Gasith, unpublished). Preference of epiphyton-free substrates for adhering eggs was reported for other fish species in other

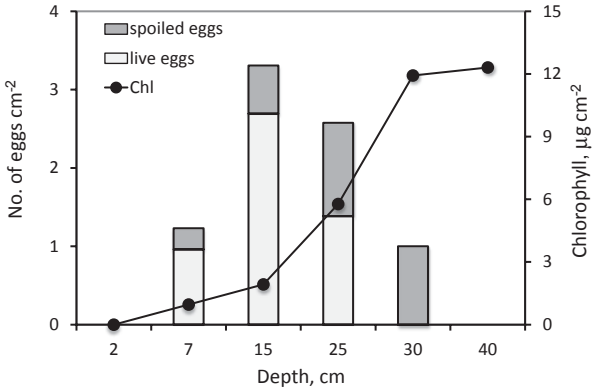

Fig. 29.6 The relationship between water depth, epilithon development (Chlorophyll-a concentration, Chl) and egg density on stones of the Kinneret bleak (*Mirogrex terraesanctae*) in the Kinneret littoral zone. (Reproduced from Gafny et al. 1992, with permission from John Wiley and Sons)

lakes, e.g., *Abramis brama* (cyprinid), (Probst et al. 2009), yellow perch (Fisher et al. 1996), and American smelt (Rupp 1965).

Gafny et al. (1992) and Gasith et al. (1996) showed that the availability of stony substrate suitable for spawning of *M. terraesanctae* increases with increasing rise of the lake level and vice versa. They therefore hypothesized that reproductive success of the bleak is directly influenced by the extent and rate of change of the lake level. Ostrovsky and Walline (2000) and Zohary and Ostrovsky (2011) later corroborated this hypothesis: Based on data from hydroacoustic fish surveys, they showed that indeed years of exceptional rise of the water level were followed by population explosion of *M. terraesanctae*. They too attributed the marked population increase to the increase in the availability of suitable spawning substrate relative to years of natural WLFs. Furthermore, Gasith and Gafny (1998) and Zohary and Ostrovsky (2011) argued that the newly inundated vegetation in years of high water level provide the young of the year with ample food, shelter from predators, and refuge from strong currents thus increasing their survivorship.

Among the fish species that require littoral habitats stands out a small blenny *Salaria fluviatillis* that besides a short pelagic larval stage spends the rest of its life in the shallow water in rocky habitats. It spawns under rocks with preference of rocks of a certain size (Aidlin et al. 1994); therefore, its breeding success is predicted to be affected by WLFs that determine the availability of rocky habitats (Gasith and Goren 2009). Another strictly littoral species is the small cichlid *Astatotilapia (Haplochromis) flaviijosephi* (Spataru and Gophen 1985).

The native cichlids of Lake Kinneret, and particularly *Sarotherodon galilaeus, Tilapia zilli,* and *Oreochromis aureus,* utilize sandy littoral habitats for nesting and spawning, preferably near or among inundated vegetation (Gasith and Goren, unpublished; Fig. 29.4b). Some cichlids may also spawn in sandy areas with no vegetation (Gophen and Bruton 1989). The preference of nesting in sheltered sites is demonstrated, for example, in choosing to nest by a single rock that was available and not nearby in barren sandy area (Fig. 29.4c). Gasith and Goren (unpublished) found that when inundated vegetation is available, *Oreochromis aureus* and *Tilapia zilli* favor the vegetation over bare sand substrate for nesting (Fig. 29.4b). This

was corroborated in a recent survey of cichlid reproduction (spring–summer 2012), which clearly indicated that cichlids used the window of opportunity when structured habitat was available, and favored nesting near or among the inundated vegetation. Between mid-April and mid-September 2012, 11 different sites around the lake were visited regularly and nesting of cichlids was recorded along transects perpendicular to the shoreline. Nesting activity was recorded at all but one site (Gofra) where the substrate is rocky. Of the total of ~6,000 squares of 1 m^2 each surveyed, about 50 % were covered by inundated vegetation and 50 % were without vegetation (although plants may have been close by, even in the adjacent square). The density of nests in the vegetated sites was on average 28 nests per 100 m^2, double the density of nests in areas with no vegetation (14 nests per 100 m^2). Most of the nests were of *Tilapia zilli* and *Oreochromis aureus,* those of *S. galilaeus* were seen infrequently. The latter was seen breeding in shallow littoral sites near vegetation after only minimal nest-building activity.

The common carp *Cyprinus carpio* as well as the catfish *Clarias gariepinus* also reproduce in the spring, among inundated vegetation. Furthermore, the littoral zone is the main nursing ground for fingerlings of most fish species. Fingerlings of the Kinneret bleak and other cyprinids and of cichlids were observed in the littoral zone during spring and summer, mostly among inundated vegetation (Gasith and Goren, unpublished).

29.3 Impacts of Processes in the Littoral Zone on Ecosystem Functioning and Services

Processes occurring in the littoral zone may have a cascading impact on the entire ecosystem and the services it provides. Some examples are given here:

a. The Kinneret bleak reproduces in the littoral but lives most of its life and feeds on zooplankton in the pelagic zone. Its reproduction success has direct impact on the zooplankton populations. Years of exceptional reproduction success of the bleak (e.g., 1992 and 2003, years of high rise of the water level) were followed by the bleak's population explosion and a collapse of the zooplankton—that is attributed to high predation pressure (Gal and Anderson 2010; Zohary and Ostrovsky 2011).
b. Sukenik and Parparov (2008) estimated that the maximal nutrient addition due to inundated macrophyte decomposition occurred in April and May, comprising 17 % of the externally loaded total phosphorus during these months. They concluded that there is a potential for enhanced biological activity (extended bloom) during the spring and early summer following a flooding event of massive shoreline vegetation areas, but that the impact would not extend further in time. Their conclusion was supported in spring 2012 that followed a wet winter with 2.35-m rise in water level and inundation of massive areas with dense shoreline vegetation. An intensive bloom of the dinoflagellate *Peridinium gatunense* developed

that spring, a bloom that persisted longer and reached higher peak biomass than in most other years (see Chap. 11). Thus, the lake's major pelagic foodweb structure was impacted.

c. Following consecutive years of low lake levels, rising of the water levels in 2012 with improved conditions for cichlid reproduction and survivorship, the commercial harvest of *S. galilaeus* has also improved, from an all-time minimum of 8 t in 2008 to 166 t in 2012 (Jamie Shapiro, Dept. of Fisheries, pers. comm.).

29.4 Conclusions

Littoral zones of large lakes naturally occupy relatively small proportion of the lake surface area (<10%) but have a disproportionately important role, by providing resources that are available nowhere else in the lacustrine ecosystem (Gasith 1991; Gasith and Gafny 1998; Wantzen et al. 2008).

Shoreline vegetation is an integral part of the lake ecosystem and when inundated provides a "window of opportunity" for the fish to reproduce, feed, and find refuge.

Changes in the structure of the littoral zone and its resource availability are expected to cascade to the pelagic zone, eventually influencing ecosystem processes and water quality (Gasith 1991; Gal and Anderson 2010; Zohary and Ostrovsky 2011).

Management of the lake's hydrology in a way that reduces extreme WLFs will prevent excessive growth of shoreline vegetation and associated short-term environmental nuisances when inundated. Less variable amplitude of WLFs is also expected to support a healthier Lake Kinneret ecosystem.

Acknowledgements We acknowledge the contribution of our partners Menachem Goren (Dept. of Zoology, Tel-Aviv University) and Sarig Gafny (presently Ruppin Academic Center) to Lake Kinneret littoral research and to graduate students for their pivotal role in various littoral studies.

References

Aidlin M, Gasith A, Goren M (1994) Selected aspects in the biology and ecology of *Salaria fluviatilis* (Blenniidae) in the littoral zone of Lake Kinneret. Isr J Zool 40:91

Brauns M, Garcia XF, Pusch MT (2008) Potential effects of water-level fluctuations on littoral invertebrates in lowland lakes. Hydrobiologia 613:5–12

Bromley HJ (1994) The freshwater leeches (Annelida, Hirudinea) of Israel and adjacent areas. Isr J Zool 40:1–24

Beauchamp DA, Byron ER, Wurtsbauch WA (1994) Summer habitat use by littoral-zone fishes in Lake Tahoe and effects of shoreline structures. N Am J Fish Manage 14:385–394

Cohen N (1993) Selected aspects in the biology and ecology of the bivalve *Unio terminalis terminalis* in Lake Kinneret. MSc thesis, Tel Aviv University, 73 p (in Hebrew, with English abstract)

Dolev A, Gal G, Zohary T (2012) Leeches in Lake Kinneret. Eretz HaKinneret 7:36–38 (in Hebrew)

Dor I (1971) Benthic algae of Lake Tiberias and surrounding springs. PhD thesis, the Hebrew University of Jerusalem, Israel
Dor I (1974) Considerations about the composition of benthic algal flora in Lake Kinneret. Hydrobiologia 44:255–264
Fisher SJ, Pope KL, Templeton LJ, Willis DW (1996) Yellow perch spawning habitats in Pickerel Lake, south Dakota. Prairie Nat 28:65–75
Gafny S (1992). The influence of substrate on the structure of the littoral zone in Lake Kinneret PhD thesis, Tel-Aviv University, Israel, 122 p (in Hebrew, with English abstract)
Gafny S, Gasith A (1999a) Spatial distribution and temporal dynamics of the epilithic community in the littoral zone of Lake Kinneret, Israel. Verh Int Ver Limnol 27:1–7
Gafny S, Gasith A (1999b) Spatially and temporally sporadic appearance of macrophytes in the littoral zone of Lake Kinneret, Israel: taking advantage of a window of opportunity. Aquat Bot 62:249–267
Gafny S, Gasith A (2000) Spatial and temporal variation in the standing biomass of emergent macrophytes: effect of water level fluctuations. Adv Limnol 55:301–316
Gafny S, Gasith A, Goren M (1992) Effect of water level fluctuation on shore spawning of *Mirogrex terraesanctae* (Steinitz), (Cyprinidae) in Lake Kinneret, Israel. J Fish Biol 41:863–871
Gal G, Anderson W (2010) A novel approach to detecting a regime shift in a lake ecosystem. Methods Ecol Evol 1:45–52
Gasith A (1969) The caddisflies (Trichoptera) of Israel. MSc thesis, Tel Aviv University, 82 p (in Hebrew, with English abstract)
Gasith A (1991) Can littoral resources influence ecosystem processes in large, deep lakes? Verh Int Ver Limnol 24:1073–1076
Gasith A, Gafny S (1990) Effects of water level fluctuation on the structure and function of the littoral zone. In: Tilzer MM, Serruya C (eds) Large lakes: ecological structure and function. Springer, Berlin, pp 156–171
Gasith A, Gafny S (1998) Importance of physical structures in lakes: the case of Lake Kinneret and general implications. In: Jeppesen E, Sondergaard M, Sondergaard M, Christoffersen K (eds) Structuring role of submerged macrophytes in lakes. Springer, Berlin, pp 331–338
Gasith A, Goren M (2009) Habitat availability, reproduction and population dynamics of the fresh water blenny *Salaria fluviatilis* (Asso 1801) in Lake Kinneret, Israel. Electron J Ichthyol 2:34–46
Gasith A, Hoyer MV (1998) Structuring role of macrophytes in lakes: changing influence along lake size and depth gradients. In: Jeppesen E, Sondergaard M, Sondergaard M, Christoffersen K (eds) Structuring role of submerged macrophytes in lakes. Springer, Berlin, pp 381–392
Gasith A, Goren M, Gafny S (1996) Ecological consequences of lowering Lake Kinneret water level: effect on breeding success of the Kinneret Sardine. In: Steinberger Y (ed) Preservation of our world in the wake of change. Proceedings of the 6th International Conference of the Israeli Society for Ecology and Environmental Quality Sciences, Vol VI A/B. IEEQS, Jerusalem, pp 569–573
Gasith A, Gafny S, Goren M (2000) Response of the fish assemblage of rocky habitats to lake level fluctuations: possible effect of varying habitat choice. Arch Hydrobiol Spec Issues Adv Limnol 55:317–331
Gophen M (1982) Unusually dense water milfoil (*Myriophyllum spicatum* L.) vegetation in the Southern Basin of Lake Kinneret (Israel) in 1979. Aquat Bot 13:307–315
Gophen M, Bruton M (1989) Slaughter in the Beteha: fish reproduction in the Beteha lagoons in the northeast of Lake Kinneret. Land Nat 31:51–55 (in Hebrew)
Goren M, Ortal R (1999) Biogeography, diversity and conservation of the inland water fish communities in Israel. Biol Conserv 89:1–9
Heller J (2010) Land snails of the land of Israel. Pensoft, Sofia & Moscow (English)
Heller J, Dolev A, Zohary T, Gal G (2014) Invasion dynamics of the snail *Thiara scabra* in Lake Kinneret. Biol Invasions 16:7–12
Hofmann H, Lorke A, Peeters F (2008) Temporal scales of water-level fluctuations in lakes and their ecological implications. Hydrobiologia 613:85–96
Meerhoff M, Iglesias C, De Mello FT, Clemente JM, Jensen E, Lauridsen TL, Jeppesen E (2007) Effects of habitat complexity on community structure and predator avoidance behavior of littoral zooplankton in temperate versus subtropical shallow lakes. Freshw Biol 52:1009–1021

Mienis HK, Mienis D (2008) *Thiara scabra*, a tropical snail, has invaded the Sea of Galilee, Israel. Triton 18:35–36

Ostrovsky I, Walline P (2000) Multiannual changes in the pelagic fish *Acanthobrama terraesanctae* in Lake Kinneret (Israel) in relation to food sources. Verh Int Ver Limnol 27:2090–2094

Ostrovsky I, Gophen M, Kalikhman I (1993) Distribution, growth, production, and ecological significance of the clam *Unio terminalis* in Lake Kinneret, Israel. Hydrobiologia 271:49–63

Por FD (1968) The invertebrate zoobenthos of Lake Tiberias: I. Qualitative aspects. Isr J Zool 17:31–50

Por FD, Eitan G (1970) The invertebrate zoobenthos of Lake Tiberias: II. Quantitative data (level bottoms). Isr J Zool 19(2):125–134

Probst WN, Stoll S, Peters L, Fischer P, Eckmann R (2009) Lake water level increase during spring affects the breeding success of bream *Abramis brama* (L.). Hydrobiologia 632:211–224. doi: 10.1007/S10750-009-9842-5

Round FE (1978) The benthic algae. In: Serruya C (ed) Lake Kinneret. Junk, the Hague, pp 323–328

Rupp RS (1965) Shore-spawning and survival of eggs of American Smelt. Trans Am Fish Soc 94:160–168

Sala MM, Güde H (2006) Seasonal dynamics of pelagic and benthic (littoral and profundal) bacterial abundances and activities in a deep prealpine lake (L. Constance). Arch Hydrobiol 167:351–369

Schmieder K (2004) European lake shores in danger — concepts for a sustainable development. Limnologica 34:3–14

Shteinman B, Parparov A (1997) An approach to particulate matter transfer studies in littoral zones of lakes with changing morphometry. Water Sci Technol 36:199–205

Smith BD, Maitland PS, Pennock SM (1987) A comparative-study of water level regimes and littoral benthic communities in Scottish lochs. Biol Conserv 39:291–316

Spataru P, Gophen M (1985) Food composition and feeding habits of *Astatotilapia flaviijosephi* (Lortet) in Lake Kinneret (Israel). J Fish Biol 26(5):503–507

Sukenik A, Parparov A (2008) Nutrient release from inundated shoreline vegetation in Lake Kinneret. In: The response of Lake Kinneret ecosystem to low water levels and to amplitudes of fluctuation greater than natural, pp 42–45. KLL-IOLR Report T17/2008 (in Hebrew)

Tamir E (2002) Impact of low lake levels on the littoral zoobenthos and phytobenthos community in Lake Kinneret. MSc thesis, Tel Aviv University, 77 p (in Hebrew, with English abstract)

Waisel Y (1967) A contribution to the knowledge of phanerogamous vegetation of Lake Tiberias. Bull Sea Res Stn Haifa 44:3–16

Wantzen KM, Rothhaupt KO, Mortl M, Cantonati M, Toth LG, Fischer P (2008) Ecological effects of water-level fluctuations in lakes: an urgent issue. Hydrobiologia 613:1–4

Wetzel RG (2001) Limnology: lake and river ecosystems. Academic, London, p 1006

Wilcox DA, Meeker JE (1992) Implications for faunal habitat related to altered macrophyte structure in regulated lakes in Northern Minnesota. Wetlands 12:192–203

Yehoshua Y, Dubinsky Z, Gasith A, Berman T, Alster A, Iluz D (2008) The epilithic algal assemblages of Lake Kinneret, Israel. Isr J Plant Sci 56:83–90

Zohary T, Ostrovsky I (2011) Ecological impacts of excessive water level fluctuations in stratified freshwater lake. Inland Waters 1:47–59

Part VI
Integrated Lake-Watershed Management

Chapter 30
Social and Economic Background

Moshe Inbar and Dan Malkinson

Abstract This chapter gives a brief overview of the present population and social and economic characteristics of the Kinneret watershed area as the setting for subsequent chapters dealing with aspects of lake and watershed management. Some projections for future development are also given.

Keywords Agriculture · Forestry · Land use · Population · Tourism · Watershed

30.1 Introduction

This chapter is intended to give a brief overview of the present population and social and economic characteristics of the Kinneret watershed area as the setting for subsequent chapters dealing with aspects of lake and watershed management. Some projections for future development are also given.

30.2 Population

At the end of 2011, the population for the entire Kinneret watershed basin (area 2,730 km^2) was about 360,000. This includes 252,000 inhabitants in Israel (including the Golan) and an estimated population of 110,000 in the Lebanese area of the basin. Changes in population over the past 60 years are shown in Table 30.1. The mean annual rate of population growth in the Israeli area was 2% from 1995 to 2010, compared with 1.8% for overall population growth in Israel. The average population densities are 120 and 169 persons km^{-2} for the Israeli and Lebanese

M. Inbar (✉)
Department of Geography and Environmental Studies,
University of Haifa, 31905, Haifa, Israel
e-mail: inbar@geo.haifa.ac.il

D. Malkinson
Department of Geography and Environmental Studies and The Golan Research Institute,
University of Haifa, 31905, Haifa, Israel
e-mail: dmalk@geo.haifa.ac.il

T. Zohary et al. (eds.), *Lake Kinneret, Ecology and Management,* Aquatic Ecology Series 6,
DOI 10.1007/978-94-017-8944-8_30,

Table 30.1 Population (in thousands of individuals) in the Kinneret drainage basin (Israel), 1948–2010. (Source: Israel Central Bureau of Statistics (2011))

Year	1948	1961	1972	1983	1995	2008	2010
Population	30.3[a]	88.9[a]	100	140	194	246	252

[a] Not including the Golan

parts of the drainage basin, respectively. In the Israeli area, there are five towns with predominantly Jewish inhabitants, Tiberias (population in 2008: 41,734), Zefat (30,398), Qiryat Shemona (23,326), Hazor (8,673), and Qatzrin (6,712), as well as small towns with Arab and Druse populations; these include Tuba-Zangariyye, Maghar, Majdal Shams, and Gush Halav. The percentage of urban population in the basin is 44 %. We have no access to similar information for the Lebanese part of the catchment.

30.3 Agriculture

Cultivated Area Total cultivated area in the Israeli basin, most of which is irrigated, is about 390 km^2 (Table 30.2). The hilly and upper elevations in the basin are dominated by grazing pastures and forested land cover. Deciduous fruit orchards (e.g., apples, apricots, cherries, plums) are the dominant income crops of the northern region. The Hula valley is the major agricultural area; land use by various crops is shown in Table 30.3. In the Golan Heights, agricultural development has increased in recent years to a total irrigated area of 91.1 km^2 with 60 % in fruit orchards and vineyards and 40 % in field crops. Fruit crops such as bananas, mango, and dates are grown around the shores of Lake Kinneret while avocado, citrus, olives, kiwi, and lychee are cultivated in the hills west and north of the lake.

Pasture The total area of uncultivated pasture is 1,250 km^2, about half on the Golan Heights and half in the Galilee, sustaining about 60,000 head of cattle. Livestock (mainly sheep) in the Lebanese region is estimated to have the grazing equivalent impact of about 20,000 head of cattle.

Forestry The Israel Forest Authority (Keren Kayemet L'Israel) is in charge of 94 km^2 in the basin. More than half of this area, 54 km^2, is planted with conifers; the rest is under eucalyptus and natural forest. The total forested area is ~150 km^2, about 8 % of the total basin area. Due to intensive deforestation and overgrazing, few natural forests remain in the Lebanese area of the basin.

Table 30.2 Land use (km^2) in the Kinneret basin (Israel) in 2010. (Original data based on geographic information system, GIS, mapping)

Field crops	Fruit orchards	Forest	Pasture	Built area	Other	Total
164	230	146	1,254	85	19	1,898

Table 30.3 Land use in the Hula valley in 2010. (Original data based on GIS mapping)

Land use	km^2	%
Public land	0.1	0.05
Forest	7.4	3.9
Agriculture	85.7	45.8
Orchards/citrus	63	33.6
Open land	19.7	10.5
Built area	7.3	3.9
Roads	4.0	2.2
Total area	187.2	100

30.4 Manufacturing and Services

There are several industrial parks in the basin: Qiryat Shemona, Tzachar, near Rosh Pinna, Qazrin, Zefat, and Tiberias. Factories and some high-tech enterprises are also found in many of the kibbutzim (collective settlements); some of these are of medium size with several hundred employees. There are no heavy manufacturing or chemical plants; two food processing plants are connected to modern sewage and water treatment systems. Commercial and shopping centers are found in all towns and have multiplied rapidly in recent years.

30.5 Tourism

Domestic and foreign tourism has increased markedly during the past decade and is a major driver of development in the Kinneret basin. In the past decade, there has been a considerable development of tourist infrastructure, with many hotels and bed and breakfast facilities throughout the area. The surroundings of Lake Kinneret, Upper Galilee, and the Golan are rich in sites of natural, archaeological, geological, historical, and religious significance. About 20 nature reserves and parks are found around the lake and another 50 in the northern basin. In 2010, tourist volume around the lake and in the Kinneret basin was estimated at 2,650,000.

30.6 Education, Health, and Sport

The educational system covers all levels, from kindergarten to higher education. Academic colleges at Tel Hai, Emek Hayarden, Zefat, and Qazrin offer degree courses in many fields of science, arts, and education. In 2011, the Bar-Ilan University Medical School was inaugurated in Zefat. In addition, there are two scientific institutes, the Kinneret Limnological Laboratory affiliated with Israel Oceanographic and Limnological Research, located at the northwestern area of the lake shore and the Galilee Technology Center (MIGAL) at Qiryat Shemona. The region is served by two major hospitals at Zefat and Poriyya; community clinics are found in all towns and most rural communities. There are several large sport and recreation centers; the Canada Center in Metula even has one of the few ice rinks in Israel.

30.7 Environment

The total solid waste produced in the basin is about 200,000 t year^{-1}, most of it from the Israel basin. Solid waste is buried at the Te'enim site near Hazor for the northern areas and at the southern Talia site in the Jordan Valley, outside the lake drainage basin, for Tiberias and the southern basin. Over the past decades, intense efforts have been made to treat all sewage sources at least to the secondary level locally and eliminate their flow to Lake Kinneret in order to minimize pollution pressures on the lake.

30.8 Transport Infrastructure

A dense network of roads, totaling 800 km, connects all settlements of the area. The main highway (Route 90) runs from the south of the lake northwards along the western edge of the Hula valley to Qiryat Shemona and Metula. Fairly extensive and frequent local and intercity bus services connect the main urban centers to Haifa, Jerusalem, and the Tel Aviv region. A local airport at Rosh Pinna provides twice-daily flights to Tel Aviv.

30.9 Projected Development

By 2030, the population for the entire Kinneret basin is projected to increase by ~50% to reach about 550,000 (Paltiel et al. 2012). The rise in population implies higher domestic water consumption and will require the expansion of infrastructure for sewage treatment and a new disposal site for solid waste. No major industrial

development is foreseen, but the tourist industry may increase several fold, necessitating the building of hotels and the expansion and further development of nature reserves and parks as well as archeological, pilgrimage, and historical sites. The total area of land under cultivation will probably remain unchanged, but a shift may occur from field crops to fruit orchards or vineyards which may require higher amounts of irrigation water. Additionally, ensuring adequate water flow in the region's nature reserves will require the annual diversion of several million cubic meters of water from the inflows to Lake Kinneret.

References

Israel Central Bureau of Statistics (2011) Statistical abstract of Israel, 2011. http://www.cbs.gov.il. Accessed 24 Apr 2014

Paltiel A, Sepulcre M, Kornilenko I, Maldonado M (2012) Long range population projections for Israel, 2009–2059. Demographic and Census Development, Israel Central Bureau of Statistics. http://www.cbs.gov.il. Accessed 24 Apr 2014

Chapter 31
Operational Management of Lake Kinneret and its Watershed

Doron Markel, Uri Shamir and Pinhas Green

Abstract This chapter places Lake Kinneret in the framework of the Israeli national water sector as one of its principal water sources and an important storage reservoir that provides about 20–30 % of the country's freshwater supply. The lake is Israel's only surface freshwater source and reservoir. It resides within a 2,730 km^2 watershed, 25 % of which is outside Israel's borders. The watershed is populated and contains urban, agricultural, and minor industrial activities, which produce a variety of nutrient and pollution loads that endanger water quality in the lake. The 2012 Long-Term Master Plan for the National Water Sector states the dual role that the lake is to play in the national water policy: to be a source of freshwater supply and to provide environmental services, noting that ecological health of the lake is an essential condition for both. This chapter outlines the policy, decision-making process, monitoring program, the organizational structure, and the management frameworks of Lake Kinneret and its watershed that sustain these roles of the lake. The major lake and watershed management actions implemented during the last 4 decades are detailed with their possible impact on the lake's water quality. It is concluded that ongoing and expanded lake and watershed management are promising means for maintaining a healthy ecological system and improved water quality in Lake Kinneret.

Keywords National Water Sector · Decision-making process · Monitoring program · Watershed · Water quality · Lake management · Watershed management

D. Markel (✉)
Lake Kinneret and Watershed Unit, Israel Water Authority,
Z.H.R. Industrial Park, P.O. Box 623, 12000 Rosh Pina, Israel
e-mail: doronm10@water.gov.il

U. Shamir
Chair of the Kinneret and Watershed Monitoring Steering Committee,
Faculty of Civil and Environmental Engineering,
Technion—Israel Institute of Technology, 32000 Haifa, Israel
e-mail: shamir@technion.ac.il

P. Green
Lake Kinneret Administration Unit, Israel Water Authority Zemah, 15132 Jordan Valley, Israel
e-mail: pinhasg@water.gov.il

T. Zohary et al. (eds.), *Lake Kinneret, Ecology and Management,* Aquatic Ecology Series 6,
DOI 10.1007/978-94-017-8944-8_31,

31.1 Lake Kinneret in the National Water Balance

For several decades, Israel has been using its entire natural potential of freshwater (defined as water that can be supplied for urban use with minimal conventional treatment) to meet with high reliability the rising demands of an increasing population and maintain the segments of agriculture and industry that must have high-quality water. The Palestinian Authority is served by some of the same sources, and their needs are also rising.

Table 31.1 is taken from the "Long-Term Master Plan for the Water Sector—Part A: Policy Document Version 4, August 2012" (IWA 2012) and represents a base scenario for the coming decades. The total annual consumption of freshwater in Israel in 2010 was $1{,}354 \times 10^6$ m^3, of which the domestic consumption was 764×10^6 m^3 (56%), industry consumption of freshwater was 90×10^6 m^3, agricultural consumption of freshwater was 500×10^6 m^3 (37%), 50×10^6 m^3 were transferred from the Israeli system to the Hashemite Kingdom of Jordan, and 46×10^6 m^3 to the Palestinian Authority. The water balance in 2010 also includes 644×10^6 m^3 of reclaimed wastewater and saline ground water supplied to agriculture. These figures change somewhat from year to year as a result of freshwater availability and in response to pricing and allocation policies. This total is forecasted to grow to reach $3{,}570 \times 10^6$ m^3 year^{-1} by 2050, of which $2{,}090 \times 10^6$ m^3 year^{-1} will be freshwater, including $1{,}421 \times 10^6$ m^3 year^{-1} desalinated sea and brackish waters (IWA 2012).

As urban demands have grown, the allocation of freshwater to agriculture in Israel was reduced from $1{,}100 \times 10^6$ m^3 year^{-1} only 2 decades ago to less than 500×10^6 m^3 year^{-1} in recent years, and is declining further. To maintain the desired level of agriculture, increasing quantities of treated wastewater effluents, saline groundwater, and floodwaters (IWA 2012) are used, so that the total used by agriculture is forecasted to increase from $1{,}044 \times 10^6$ m^3 year^{-1} in 2011 to 1,450 m^3 year^{-1} in 2050. At the same time, water efficiency in agriculture has improved dramatically largely due to advanced irrigation techniques.

Lake Kinneret is the only natural surface freshwater reservoir among the major water resources between the Jordan River and the Mediterranean Sea (see Fig. 18.1 in Chap. 18). The other sources are: Western Galilee Aquifer, Carmel Aquifer, Coastal Aquifer (excluding the Gaza Strip), three basins of the Mountain Aquifer (West, East, Northeast), and Negev and Arava Aquifers.

The 2012 master plan includes the following long-term policy elements that relate to Lake Kinneret:

- Integrated management: The water authority will manage the natural and desalinated sources of water as a single integrated national system.
- Lake Kinneret will be designated as a source of water mainly to the north of Israel, but will remain connected to the national water system.
- The natural water sources whose quality has declined in recent years, to a level considered inappropriate for public consumption, will be restored to drinking water quality, subject to cost–benefit analysis.

Table 31.1 The national water balance for 2010–2050. (IWA 2012, p. 13–15, with explanatory comments on p. 15)

Population and per capita consumption			Water sources (10^6 m^3 $year^{-1}$)							
Year	National population (10^6)	Per capita consumption (m^3/capita/year)	Year	Natural freshwater[a]	Saline (direct consumption)	Treated wastewater (including Dan region STP*)	Desalination of saline waters	Desalination of seawater[b]	Required supplement[c]	Total supply
2010	7.6	100	2010	1,200	174	450	23	280	4	2,131
2020	9.1	99	2020	1,140	150	573	50	750	9	2,672
2030	10.9	98	2030	1,080	140	685	60	750	50	2,765
2050	15.6	95	2050	1,020	130	930	70	750	671	3,571

[a] Total net average replenishment of natural freshwater (after losses) of freshwater with salinity less than 400 mg Cl L^{-1}

[b] Desalination of seawater: according to the currently approved government decision

[c] Required supplement: the difference between total consumption of freshwater (bottom table) and total sources of freshwater

Year	Urban	Water consumption (10^6 m^3 $year^{-1}$)												
		Industry			Agriculture				Regional[b]	Reservoir storage recovery	Nature and landscape[c]		Unexpected[d]	Total consumption
		Freshwater	Saline	Total	Freshwater[a]	Saline	Treated wastewater (including Dan region STP)	Total			Fresh	Total		
2010	764	90	30	120	500	144	400	1,044	143	0	10	60	0	2,131
2020	902	95	30	124	490	120	528	1,138	143	200	50	95	70	2,672
2030	1,064	99	30	129	470	110	645	1,225	143	0	50	90	114	2,765
2050	1,482	108	30	138	450	100	900	1,450	143	0	50	80	278	3,571

[a] The planned reduction in consumption of freshwater for agriculture is contingent upon conversion to high-quality treated wastewater

[b] Regional consumption includes supply to the Palestinian Authority and to Jordan

[c] The total includes treated wastewater that flows in riverbeds

[d] Unexpected = in preparation for possible future scenarios (e.g., geopolitical agreements, increase in immigration)

* STP = Sewage Treatment Plant

- In addition to quantitative goals for rehabilitation of national reservoirs, qualitative goals will also be set for the natural sources of water, as well as criteria for the quality of the water supply to all consumption sectors.

In the second half of the twentieth and into the twenty-first century, extraction from the natural sources exceeded the annual replenishment and water levels in the sources declined to the "lower red lines," creating an assessed deficit (relative to desired operational levels) of some 1.5–2 billion m^3 of water. Water quality in the sources declined due to incursion of lower-quality waters from adjacent water bodies and infiltration of pollution from surface sources. During these years, construction of seawater desalination plants was postponed for a variety of reasons; the first desalination plant in Ashqelon came on line only in 2005. Thus, the natural sources, including Lake Kinneret, had to "wait" for the occasional wet years to recover from the accumulated deficit. By 2010, three large seawater desalination plants (Ashqelon, Palmahim, and Hadera) produced close to 300×10^6 m^3 $year^{-1}$. Two additional seawater desalination plants, at Soreq and Ashdod, are coming on line so that by the end of 2014, the total installed capacity of desalinated sea and brackish water will reach 640×10^6 m^3 $year^{-1}$. The stable production of desalinated water, which does not depend on climate, is a major asset, as is its excellent quality, which allows blending with waters of lower quality from other sources and rendering these waters usable. The total amount of desalination capacity already approved by the government is to reach 750×10^6 m^3 $year^{-1}$ by 2020, and then go beyond, while the timing of development will be assessed periodically to ensure that there is no under- or overcapacity.

While the balance between natural and desalinated water shifts toward more desalination, the natural sources, among them Lake Kinneret, remain a strategic national asset for sustained water supply that will remain protected and managed with the greatest care. The "Policy Document" of the "Long-Term Master Plan for the National Water Sector" (IWA 2012) designates Lake Kinneret as "…primarily a source of supply for the northern sections of the country." This Policy Document also states that further actions will be taken to improve and maintain the water quality in Lake Kinneret. It further stipulates that the lake will be operated between the upper and lower "red lines" (a high level of −208.80 m above mean sea level (a.m.s.l.) above which there are overflows and potential flood damages, and a low level of −213.00 m a.m.s.l. below which serious negative ecological consequences may occur). The range between −213.00 and −208.80 m corresponds to an operational volume of about 700×10^6 m^3 (below which the remaining water volume of the lake is about $3{,}500 \times 10^6$ m^3).

Lake Kinneret and the upper sources of the Jordan River will quite certainly play a role in any further regional arrangements of water management with Israel's neighbors, and its operational mode may therefore be affected by such agreements.

Table 31.2 Mean and standard deviation (SD) of the annual natural replenishment into all natural sources of water between the Mediterranean Sea and the Jordan River, presented for three time periods and divided into three categories: (1) all sources, (2) the yield of the Kinneret watershed (including the lake), and (3) Lake Kinneret alone. (Source: Weinberger et al. 2012)

Annual replenishment (10^6 m^3 year^{-1})						
	Total, all sources		Kinneret watershed		Lake Kinneret	
Period	Mean	SD	Mean	SD	Mean	SD
1976–1992	1,848	684	636	283	470	284
1993–2009	1,643	465	524	231	320	219
1976–2009	1,748	584	581	258	399	262

31.2 Annual Replenishment of Lake Kinneret and its Watershed

Table 31.2 contains the mean and standard deviation of the annual replenishment of all water sources between the Mediterranean Sea and the Jordan River combined, of the Kinneret watershed (including the lake), and of Lake Kinneret alone. The last two columns in Table 31.2 are the means and standard deviations of the annual net replenishment (termed "available water") to Lake Kinneret itself, and computed as (inflow) + (rainfall on the lake) − (evaporation from the lake). The numbers in the "Kinneret watershed" columns include water consumed in the watershed (where evapotranspiration can only be estimated), and are therefore an estimate of the total natural yield of the watershed.

The data in Table 31.2 indicate that Lake Kinneret accounts for 20–25 % of the total replenishment of all sources, and that its contribution has declined with time. The standard deviation of the total amounts in Table 31.2 is 28–37 % of the mean, and in the Lake Kinneret watershed, it is 43–45 %. Both numbers are high, and indicate large unpredictable variability in inflows from year to year as seen in the long-term sequence of annual amounts of available water (Fig. 31.1). Even more important are the sequences of dry years, which created accumulated deficits in the volume of water stored in the lake when the extraction was not adjusted to the replenishment sequence. The result has been a decadal reduction in minimum lake water level, as seen in Fig. 31.2. The decline in mean replenishment volumes from the first period (1976–1992) to the second (1993–2009) is 11 % for the total replenishment and 13 % for the Lake Kinneret watershed, while for the lake itself it is 32 % due to increased upstream uses. There are indications that the amounts are declining further, due to various causes, potentially including climate change.

Figure 31.1 follows the historical sequence, 1975/1976 to 2010/2011, of annual net replenishment to Lake Kinneret as published by the Hydrological Service of Israel (Weinberger et al. 2012). It shows a decline in the net replenishment to the lake of ca.150×10^6 m^3 year^{-1} over 36 years. Sixty percent of this reduction is attributed to decreased precipitation and a change in the rain pattern (Givati and Rosenfeld 2007). The remaining 40 % is attributed to increased water consumption in the watershed, including in Lebanon.

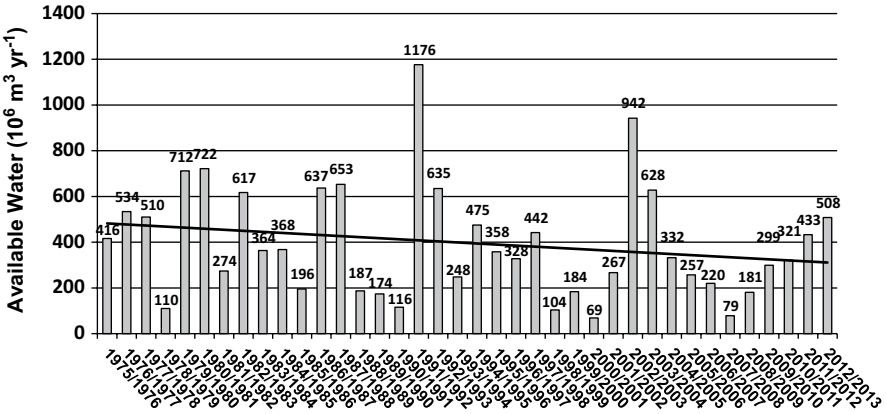

Fig. 31.1 Annual amounts of available water (10^6 m^3) in Lake Kinneret as published by the Israel Hydrological Service. The *black line* represents a linear regression from 1975/1976 to 2012/2013. (Adapted from Weinberger et al. 2012)

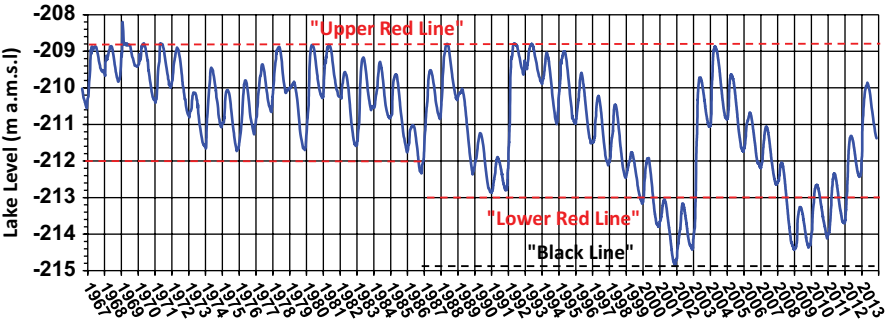

Fig. 31.2 Lake Kinneret daily water levels 1967–2013. (Data source: Israel Hydrological Service)

Because Lake Kinneret is the only surface source of freshwater, openly visible and used for recreation, it is viewed by the public and the media as the "national barometer of the nation's water situation," while in fact the aquifers are a more substantial reservoir and source. The availability of water in the aquifers is affected by anthropogenic pollution above them, rendering substantial volumes unusable except after groundwater remediation and/or treatment of the extracted water. Strict management of the Kinneret watershed over the past 2–3 decades (as reported later in this chapter) has resulted in the ability to maintain ecological health and good water quality for water supply despite substantial population growth and anthropogenic stresses.

31.3 Lake Kinneret as an Operational Reservoir of the National Water Carrier

The National Water Carrier (NWC) originates in Lake Kinneret and carries freshwater to the center and southern parts of the country. It began operating in 1964 and constitutes the central artery of the national water supply system. The NWC is fed along its way by groundwater sources and delivers water to urban and agricultural demand zones. Lake water is pumped vertically some 350 m (from the lake's elevation of ~−210 to ~150 m) through a closed conduit, then open canals, through a holding reservoir and a modern water treatment plant into a 108″ pipeline that goes south. Over the years and until about a decade ago, Lake Kinneret has provided through the NWC annual quantities of water that ranged between 300 and 500×10^6 m^3 year^{-1}. This amount has been reduced in recent years to 150–250×10^6 m^3 year^{-1}. In addition, the lake supplies 25–45×10^6 m^3 year^{-1} of water directly to local consumers around the lake. In accordance with the 1994 Peace Treaty and later agreed adjustments, Israel provides the Hashemite Kingdom of Jordan with 50–55×10^6 m^3 year^{-1} from the outlet of Lake Kinneret, while storing in the lake in winter 10–20×10^6 m^3 from the Yarmouk River that are "returned" to Jordan in summer. The overall consumption from Lake Kinneret is between 230 and 350×10^6 m^3 year^{-1}, balancing the amounts of available water (Table 31.2 and 31.1).

The inflows to the lake vary from year to year. There have been extended periods of low inflow years, while the extractions were driven by demands and have not been adjusted so as to maintain water levels within dictated bounds. As a result, water levels have oscillated within the year and declined from 1 year to the next during long dry spells, as seen in Fig. 31.2. Thus, with the onset of the operation of the NWC in 1964, the amplitude of Lake Kinneret water levels increased. In 1986, the level dropped for the first time below −212 m, reaching −213 m by 1990. During the high rainfall winter of 1991/1992, the water level rose back to the upper red line, but over the next 10 years, the total amount pumped exceeded the available water year after year. The years 1992–2002 and 2004–2009 experienced cumulative declines of lake level by 6 and 5.5 m, respectively. The wet years of 1991–1992 and 2002–2004 produced periodic recoveries, but were soon succeeded by normal and low inflow years that resulted in lowering the lake levels.

This cyclical behavior brought the minimum water level in Lake Kinneret to lower values, as seen in Fig. 31.2. The minimum operational level (the lower red line) in the lake was initially set to −212 m then lowered to −213 m in 1986, following examination of ecological considerations. The considerations for determining the lower red line were mainly a combination of operational needs and experts' evaluation of the negative processes that may be driven by low water levels (mainly salinization and eutrophication). Between 1992 and 2002, the level dropped by 6 m, and reached a minimum of −214.87 m in November 2001. Although the actual level dropped below the prescribed −213 m "lower red line" during the crises of 1999–2001 and 2008–2011, the lower red line was left unchanged. The minimum

level of −214.87 m reached in November 2001 was then set in law as the minimum admissible level and referred to as the "black line" (Fig. 31.2).

One of the major concerns for water quality has been the salinity of Lake Kinneret water, which rose to 380 mg Cl^{-1} L^{-1} in 1964, for which two theories were offered (see Chap. 8 "Salinity"). Concern over high salinity rose primarily because the water delivered from the lake to the center and south of the country carried with it large quantities of salt, up to 100,000 t $year^{-1}$ of chloride, which was deposited on and into the irrigated soils. The salinity further increases while water is used in the urban areas, resulting in high salinity of the treated sewage effluents, which are then used for irrigation. Thus, reduction of Lake Kinneret salinity became a main management objective.

31.4 Lake Kinneret Watershed

Lake Kinneret Watershed is bordered by the Golan Heights on the East, Mount Hermon in the North, and Eastern Galilee to the West. The area of the watershed is 2,730 km^2, of which ca. 75 % is in Israel and the rest in Lebanon. Some 220,000 people live in the Israeli part of the basin, in 6 regional authorities and 27 local and municipalities (Markel 2008). The watershed is primarily used for agriculture, including orchards, field crops, fishponds, cowsheds, and cattle-grazing areas (for more details see Chap. 30 "Social and economic background"). This determines the main pollutants in the watershed: nutrients, herbicides, pesticides, and pathogenic bacteria (Berman 1998; Markel and Shamir 2002). Industrial areas in the basin are few and of small size, hence they produce only a small fraction of the pollution that enters the lake. However, oil and fuel pollution results from leaks in petrol stations in the watershed and boat activity on the lake.

The increased human activities in the watershed over the past 50 years have led to the appearance of various point-and-diffuse sources of pollutants, including sewage effluents, cowshed drainage, agricultural drainage, industrial drainage, and urban drainage. Superimposed on these were the drainage of Lake Hula and its adjacent swamps in the Hula Valley and the diversion of the Jordan River from its historical route in the 1950s (Dimentman et al. 1992; Markel 2000). The Hula area was reclaimed in 1994 through the "peat soil reclamation project" and the creation of a new wetland in order to stabilize groundwater levels, reduce pollution of Lake Kinneret, and generate new income from ecotourism (Markel et al. 1998; Markel 2000).

31.5 Objectives of Lake and Watershed Management

Upon the background presented above, the 2012 National Water Policy assigns to management of the lake two primary objectives, which are prioritized as follows:

1. Lake Kinneret will continue to function as a strategic water source and reservoir for the state of Israel, used mainly for the north of the country, while maintaining its connection to the national supply grid.
2. The lake will serve as a sustainable unique environmental resource for the benefit of the people in the area and the rest of the country.

With the large-scale development of desalination in recent years, the role of the natural sources of water is changing. It might seem that the importance of the natural sources can be reduced, but yet, as stated clearly in the 2012 Plan, Lake Kinneret will continue to be a strategic resource for water supply. The order of priority of the two stated objectives for the lake is: water supply first, while providing ecological services. It is understood that good ecological status of the lake is a necessary condition for both objectives. These prioritized objectives have directed and will continue to direct the monitoring program and management of the lake and watershed, as will be described in the following sections. Both objectives require that the watershed be managed to achieve efficient water uses and to reduce loadings of nutrients and pollutants into the lake.

31.6 Organizational Aspects

The responsibility for managing Lake Kinneret as a water resource (among other national water resources and systems) resides with the director of the Israeli Water Authority (IWA, until 2007 the Water Commission), the senior government official in charge of water in the country. The IWA was established in 2007 as a sequel to the Water Commission, and has taken on the dual roles of regulator and manager of the water resources. It is governed by a board constituted of the directors general of five ministries: Energy and Water (previously National Infrastructure), Environmental Protection, Agriculture, Interior, and Treasury, plus the director of the IWA (chair).

In 1998, the Water Commissioner adopted the recommendation of two professional reports, by an Israeli panel and an international expert, and established the Lake Kinneret and Watershed Unit (LKWU) within the Water Commission. A senior scientist was appointed to head this unit. The major objective of the LKWU has been to establish a coordination and management platform for all monitoring activities in the lake and its watershed (Markel and Shamir 2002).

In 2003, the unit's responsibility was expanded to all management activities in the lake and its watershed. The LKWU, together with a group of experts that functions as its steering committee, constitutes the IWA's arm for supervising activities in Lake Kinneret and its watershed, where several formal and informal entities with different perspectives and responsibilities operate. The LKWU currently coordinates and supervises the monitoring program (described in Chap. 32, "Monitoring"), as well as the lake and its watershed management, and serves in an advisory capacity to the director of IWA. The institutional and organizational setup of the monitoring and management systems of Lake Kinneret and its watershed are

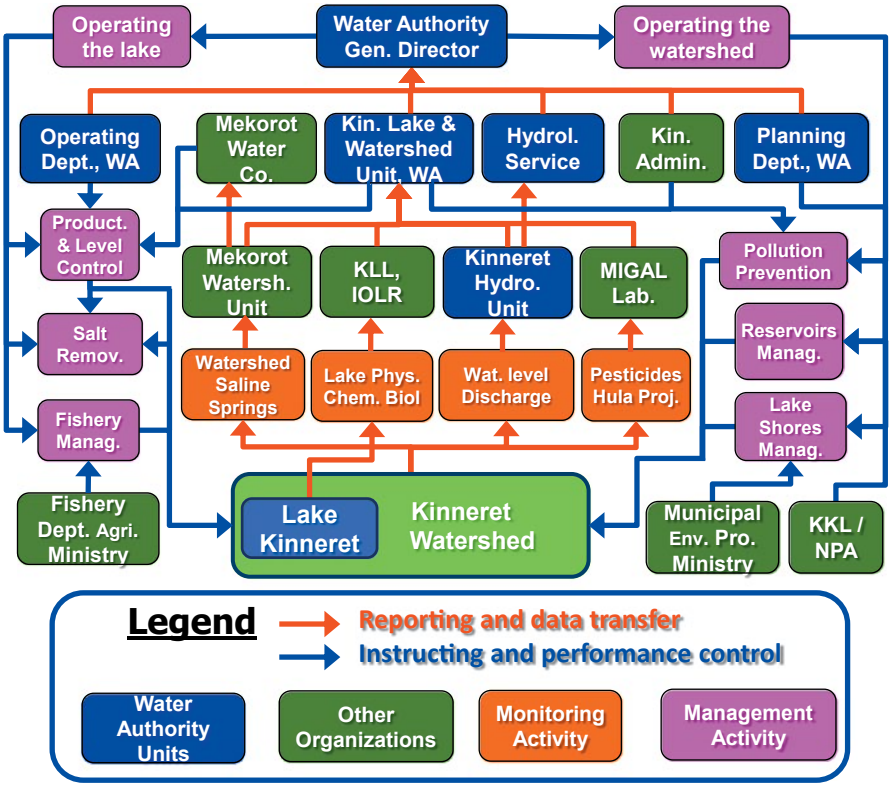

Fig. 31.3 The organizational setup of the Monitoring and Management System of Lake Kinneret and its watershed. Israel Water Authority (IWA) units are in *blue,* other organizations in *green,* monitoring activity in *orange* and management activities in *purple.* Data reporting and transfer are shown by *red arrows* while instructions and performance control are in *blue arrows. KKL* Keren Kayemet Le'Israel, *NPA* Israel Nature and Parks Authority, *WA* Water Authority, *IOLR* Israel Oceanographic and Limnological Research

depicted in Fig. 31.3, which shows that several different organizations take part in the monitoring program:

- The Yigal Alon Kinneret Limnological Laboratory (KLL) of Israel Oceanographic and Limnological Research (IOLR) monitors biological, chemical, physical, and health-related parameters in the lake. KLL produces short- and long-term reports on the state of the ecological balance of the lake.
- The Kinneret Watershed Unit, of the Mekorot Water Company monitors water quality in the watershed's waterways, and in the saline springs. The unit produces a detailed long-term database of the major pollutant loads from the watershed and annual water and salt balances for the lake.
- The Kinneret Hydrometric Unit of the Israel Hydrological Service, which is part of the IWA, measures water levels in the lake and streams, calculates stream discharges, and produces water balances of the lake and its watershed including forecasts of future water balances.

- MIGAL Laboratory, a regional scientific institute of the Galilee, monitors herbicides, pesticides, and organic contamination in the watershed, as well as the water quality of the water bodies in the Hula Project (the reclamation project of the Hula Valley peat soils).
- The Fisheries Department of the Ministry of Agriculture and Rural Development monitors the catch of the commercial fisheries, and jointly with the IWA, it decides on the fish-stocking program in the lake.

Other organizations or units are involved in management of the lake and its watershed (Fig. 31.3). The Operating Department of the IWA assists the IWA general director in decision making on water production from the lake and hence on water level control. Mekorot Water Company assists the Operating Department of the IWA to achieve this goal, as well as the goal of salt removal from the lake. A joint committee composed of the Fishery Department (FD) of the Ministry of Agriculture and the LKWU of the IWA jointly oversees fisheries management. Many organizations are involved with the operation of the lake's shores, including: the Lake Kinneret Administration Unit (LKA, in Hebrew: *Minhelet Hakinneret*), the Kinneret Municipal Council, the Ministry of Environmental Protection, as well as LKWU (Fig. 31.3). The LKA, a nonstatutory unit established in 1969, serves as an arm of the IWA for pollution control and prevention in the watershed. Management in the watershed, including the Hula peat soils reclamation project, involves also the Planning Department of the IWA, Keren Kayemet Le'Israel (KKL), and the Israel Nature and Parks Authority (Fig. 31.3).

31.7 Lake and Watershed Monitoring and Research

31.7.1 Monitoring

The important role of Lake Kinneret as a national water resource and the concern for water quality in the lake have led to the creation of an extensive water quantity and quality-monitoring program in both the lake and watershed (Markel and Shamir 2002). Monitoring the lake and its watershed and the creation of a long-term database are essential for advised managing policy and operational decisions. Therefore, a monitoring program was initiated in 1969, 5 years after initial operation of the NWC.

The monitoring program has been designed and subsequently expanded and improved to provide "optimal" coverage in time and space, with due consideration of the capabilities of manpower and budgetary limitations. The technical monitoring program is described in details in Chap. 32 ("Monitoring"). Since the initiation of the Lake and Watershed Monitoring Unit in 1998, many changes have been introduced to improve the system, in particular its spatial coverage and online real-time monitoring. For example, the introduction of the Mini Bat, which is an undulating towed vehicle carrying instruments for spatial monitoring within the water body, the introduction of the lake Ecoraft in 2002, and the online alarm systems in several watershed stations (see Chap. 32 "Monitoring").

31.7.2 Research

Research of the lake and its watershed provides the scientific basis for the design and operation of the monitoring program and for the decision-making process. The IWA funds research projects that focus on understanding the biogeochemical processes taking place in the lake and the watershed. It has also commissioned and funded development of models and tools to assist decision making regarding management of the lake and watershed, some of which are detailed below.

31.8 Lake and Watershed Management

31.8.1 Lake Management

Prescribing Desired Water Withdrawal Volumes and the Resulting Water Levels Decisions on the volumes of water to be withdrawn during the spring and summer each year are determined primarily based on the forecasted minimum water level that will be reached in December (see Fig. 31.2). The director of the IWA convenes periodically an operations committee, a wide team of experts, to advise him on the withdrawal from the lake and from the main aquifers based on the status of these sources and the forecasted inflows and demands. The Israel Hydrological Service (IHS) recommends a withdrawal plan from all major water sources including Lake Kinneret, with due consideration of their current and forecasted quantity and quality states. The LKWU synthesizes the IHS recommendation with the knowledge and experts' inputs regarding the chemical–biological–ecological state of the lake, and recommends the minimum level that should be reached in the coming fall/winter season. Once the director of the IWA decides upon a withdrawal plan, Mekorot Water Company follows these instructions and adjusts its supply plan accordingly.

In the past 15 years, the LKWU has recommended that if the forecasted minimum level is to be below that of last year, then it should decline by no more than 0.5 m. The level trajectory in Fig. 31.2 indicates that this recommendation was accepted in most of the years, except in 2001 and 2008 when the water crisis was very severe, and the coastal and mountain Aquifers were in even worse situation than Lake Kinneret.

Salinity Control The salinity of Lake Kinneret ranges between 240 and 300 mg Cl^{-} L^{-1}, which causes salt accumulation when its water is delivered to irrigated lands and therefore it is deemed too high for irrigation (Chap. 8 "Salinity"). Therefore, reduction of the lake's salinity is an important management objective. The mechanism of salt entry into the lake was a topic of much professional study and debate for many years. Eventually, an almost universal consensus settled on the "gravity-driven mechanism" (Gvirtzman et al. 1997; Rimmer et al. 1999).

According to this mechanism, the freshwater that flows to the lake from the Eastern Galilee aquifer mixes with the deep brines and discharges into the lake through saline springs. With this understanding of the salinization mechanism, the following actions have been undertaken to reduce salt entry into the lake:

- Since 1967, the waters of some saline springs along the northwest shore of the lake are being diverted (Table 31.3) into a "saline water carrier" that goes along the western shore of the lake and discharges into the Southern Jordan River (see map in Fig. 1.1, Chap. 1). A significant portion of the Nur Springs (ca. 15×10^6 m^3 year^{-1}) is diverted to the saline water carrier, with an average salinity of 2,200 mg Cl^- L^{-1} yielding removal of 33,000 t Cl^- year^{-1}. The very saline spring "Hamey Tveria" which has a salinity of 17,000–18,000 mg Cl^- L^{-1} and a discharge of ca. 0.75×10^6 m^3 year^{-1} is similarly diverted to the saline water carrier and removes another 13,000 t of Cl^- year^{-1} (Berger et al. 2013).
- According to the "gravity-driven mechanism," lowering the water levels in the upper western reaches of the basin, from which water flows underground and emerges in the lake after mixing with brines, will reduce saline flows into the lake. To reduce these water levels, the amount of water that is pumped from the aquifer was increased from 15×10^6 m^3 year^{-1} in the 1990s to 25×10^6 m^3 year^{-1} in the past 2 decades (Berger et al. 2013).
- The annual salt contribution of those saline springs that cannot be monitored, is calculated (by the Mekorot Watershed Unit), using an integrated water–salt–energy mass balance model for the years 1990–2011. The results show that the annual contribution of these sources declined from around 90,000 t Cl^- year^{-1} in the 1990s to 60,000 t Cl^- year^{-1} in the beginning of the 2010s (Fig. 31.4). This reduction is attributed, according to the "gravity-driven mechanism," to the increased pumping from the wells in the Eastern Galilee and decrease in the annual precipitation in the region, that have led to lower freshwater recharge in the saline springs (Berger et al. 2013).
- The subsurface spring Fullia-A that is estimated to contribute between 10,000 and 20,000 t Cl^- year^{-1} has been captured under a 10 m diameter concrete cap with an outlet pipe. After a few years of monitoring the water and salt discharges from the cap, its water will also be diverted to the saline water carrier, thereby removing a further 10–20 % of the salt currently entering the lake.

Regulation of the Fishery The management of fishery is detailed in Chap. 36 "Fisheries Management". Stocking, removal, and other fishery regulations have the potential to modify not only the fish populations but also various other ecosystem components and thus indirectly to affect water quality (Carpenter and Kitchell 1988). Fishery management is used by the IWA as a tool for managing and balancing the lake ecological system. This is achieved by stocking "good" fish and excluding "bad" fish from the lake. The stocking and related programs are controlled jointly by the IWA and by the FD of the Ministry of Agriculture and Rural Development through the "Stocking and Fisheries Management Committee" (see Fig. 31.3). It includes representatives from the Ministry of Agriculture (chair), the IWA (deputy chair), the FD, the KLL, the Lake Kinneret Administration (LKA),

Table 31.3 Major planning and management processes and events in the watershed over the last century, and their consequences

Year/period	Lake and watershed events	Possible impact
1932	The Deganya Dam was built on the Jordan River outflow impounding the lake	Possible manipulation of lake water levels according to dam operation
1951–1958	Drainage of Lake Hula and its adjacent marshes to increase arable land and eradicate malaria	Increased load of TSS and nitrogen to Lake Kinneret
1964	NWC begins operation. Lake Kinneret water is pumped into the NWC at Sapir Site (see Fig. 1.1, Chap. 1)	Increased amplitude of water level fluctuations, possible change in lake currents, changed annual cycle of outflow volumes (more outflow in summer, less in winter)
1967	The saline water carrier (see Fig. 1.1, Chap. 1) begins operation, diversion of saline springs	Decreased salinity of Lake Kinneret
1970–1980	Rapid population increase in the Kinneret watershed, increases in the number of dairy farms and area of irrigated crops and orchards	Reduced flows in the Jordan River and increased loads of dissolved phosphorus and ammonium
1977–1985	Construction of extensive sewage treatment plants in the watershed replacing old septic systems	Initial rise and subsequent decline of P and N loads
1977–1994	Deterioration of the peat soil in the Hula Valley due to rapid decomposing of the organic matter in the soil	Decrease organic nitrogen load and increase nitrate load
1984	Operation of Einan Reservoir to contain and treat effluents from Qiryat Shemona and western Hula basin, to be recycled for local agriculture	Reduced flows of sewage effluents into Lake Kinneret
1986	Legal minimum water level lowered from −212 to −213 m a.m.s.l.	Lake water levels are manipulated to larger amplitudes
1994–1997	Hula Restoration Program. Raising of the groundwater table and creation of Lake Agmon	Decreased peat soil degradation and associated underground fires and peat dust storms; decreased nitrogen release from peat
1999	Agmon water diverted to Einan Reservoir and utilized for irrigation	Decreased nitrogen flow to Lake Kinneret
1999	Diversion of water from the Western Canal to Einan	Decreased pollution leakage from the Western Canal
1998–2000	Deepening of a 3-km section of the Jordan River between the Pkak Bridge and Benot Yaacov Bridge to enhance drainage	Increased water velocity and increased TSS and PP loads in the Jordan River due to increased erosion
2000	Connecting Druze villages in northern Golan Heights to sewage systems, replacing septic systems	Increased pollution to the upper Jordan River
2004	Connecting sewage from Druze villages to a central treatment plant	Decreased pollution to the upper Jordan River through Saar Stream
2010–present	Winter drainage from the peat soils of the Hula Valley is directed to Lake Kinneret instead of to Einan Reservoir	Increased supply of nitrogen and other peat materials to Lake Kinneret

Table 31.3 (continued)

Year/period	Lake and watershed events	Possible impact
2011–2012	According to IWA policy, based on the "Precautionary Principle," IWA allows only limited clearing and removal of the shoreline inundated vegetation	Increase in vegetation habitats for fish and rehabilitation of the fish population, ecological system improvement

TSS total suspended solids, *NWC* national water carrier, *a.m.s.l.* above mean sea level, *IWA* Israeli Water Authority, *PP* particulate phosphorus

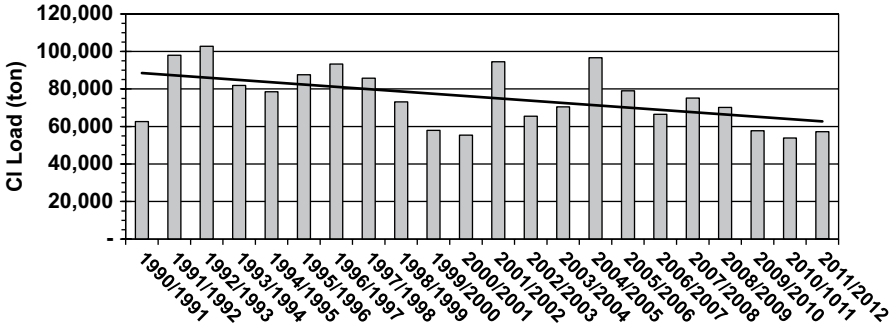

Fig. 31.4 The calculated annual (hydrological years, Oct–Sep) chloride load (ton year^{-1}) of the nonmonitored saline springs (Berger et al. 2013). *Black line* is a linear regression line

fish experts from universities, and a representative of the Kinneret fishermen. Once a decision on a detailed stocking plan had been made, the FD is in charge of rearing or purchase of fingerlings to be stocked, and of monitoring the sizes of the harvested fish and the total mass landed for each species. Supervisors from the FD are responsible for enforcing the fishing regulations, with some assistance from supervisors of the LKA. Fishery management in Lake Kinneret is an important tool that helps to preserve Lake Kinneret as a major water resource in Israel and at the same time serves to supply fishermen a reasonable fish yield (Markel 2012).

Management of the Shores Lake Kinneret water levels have undergone substantial changes between 1990 and 2012 (Fig. 31.2). When the level drops, dense vegetation develops on the exposed shores—mainly *Phragmites australis*, *Tamarix* sp., and *Cyperus* spp. The vegetation may act as a "nutrient pump," by sucking up nutrients from the sediments and later releasing them to the water when it decomposes after being inundated when water levels rise. This may have negative effects of nutrient enrichment. However, this vegetation also serves as an important habitat for fish reproduction and fingerling survival (Chap. 29 "Littoral"). Moreover, according to Tibor et al. (2012), in 2001, the total phosphorus content of the entire mass of vegetation over the full strip of water level fluctuations was only 23 t P. This should be compared to the 600 t of P contained in the uppermost 10 cm sediment layer of the same shore strip (Eckert et al. 2003). Removal of coastal vegetation has the potential of disturbing this layer and releasing phosphorus. If only the labile phosphorus,

which accounts for 20% of total phosphorus of this layer (Eckert et al. 2003), is released into the lake by the vegetation removal, it will be four times as large as the contribution of the decomposed vegetation.

A wide strip of coastal vegetation was flooded in winter 2011/2012 due to a level rise of 2.35 m during that winter. Shore operators and tourism managers demanded that this vegetation should have been cut and removed prior to the water level rise. The IWA policy, based on ecological knowledge and the "precautionary principle," allowed only limited clearing and removal of the vegetation (Table 31.3). This conflict of interests led to a governmental conflict between different ministries which was ultimately resolved by a compromise solution that defined the limited amount of vegetation removal allowed in each type of shore, according to the type and intensity of its use (Markel et al. 2012).

31.9 Management of the Watershed

The watershed contributes water and materials that enter the lake. Management of the watershed is therefore critical in controlling these inputs. Extensive monitoring of inflow volumes and material concentrations throughout the watershed is used to identify pollutant sources and to then determine effective actions that should be taken to control them.

The major anthropogenic changes that took place in the watershed over the decades (Table 31.3) have been: (1) the drainage of Lake Hula and its adjacent swamps between 1951 and 1958, (2) rapid increase in the number of inhabitants, and (3) rapid increase in the number of dairy farms and of irrigated crops and orchards between 1970 and 1980. These developments led to an increase in loads of nutrients and suspended solids to Lake Kinneret (see Chap. 18 "Material Load"). Consequently, a number of management actions were taken to minimize the inflow of pollutants into the lake. Led by the LKWU and supervised by the LKA, these actions are:

- *Preventing sewage flow:* Sewage treatment in the watershed began in the mid-1980s. Since then, the IWA and the LKA acted vigorously to eliminate point source pollution in the Israeli part of the watershed. This does not include the sewage in Lebanon, which accounts for 25% of the total watershed area. Practically, as for now, all of the anthropogenic sewage in the Israeli part of the watershed is treated in treatment plants and then stored in reservoirs for summer irrigation. Since the watershed is mainly rural, most of the treatment plants are extensive plants with an anaerobic pond, aeration ponds, and a treated wastewater reservoir. Advanced sewage treatment plants are operated near the cities of Qiryat Shemona, Zefat, Hazor, and Tiberias, on the Golan Heights and in the Eastern Galilee. The supervisors of the LKA oversee all treatment plants and reservoirs in order to anticipate and remedy leakages and failures of operation. All dairy cowsheds have been refurbished in the last decade so that the winter rain

does not flush the manure to the drained streams and their effluent is transferred to one of the treatment plants of the watershed.

- *Fish pond management:* Many fish ponds were operated in the northern sections of the watershed in the 1960/1970s. In the 1980s, the number of fishponds decreased due to low market price of carp and to the fact that growing tilapia (locally called "Musht") is not possible in the cold water of the Jordan River. Since the 1990s, regulations were set for eliminating pollution from fishponds, by water recycling and filtering of the pond outflows. Currently, the main fish farming still operating in the northern part of the watershed is trout, which is based on the cold high-quality water of the Dan spring. Active drum filters are used since 2000 to remove the fish feces and extra food from the outflows of the trout farms. This management action reduced the total phosphorus emission of the trout farms from 10 t in 2000 to about 4 t in 2010.
- *Minimization of diffuse pollution sources:* The IWA acts to minimize nutrient outflow from irrigated crop and pasture areas through regulations and enforcement. A new project based on cooperation between the IWA, the Ministry of Agriculture and Rural Development, and the Ministry of Environment Protection is planning to remove pasture cows from the vicinity of running streams during the summer. This project will be implemented by introducing watering points far enough from the streams. In addition, the IWA and the Ministry of Environmental Protection enforce and control the amounts, types, and application modes of pesticides and herbicides that are used in the watershed.
- *Prevention of fuel and oil pollution:* Fuel and oil repositories are closely controlled and monitored to prevent the spills that in the past caused substantial pollution. Means have been put in place for dealing with oil spill events on the lake itself, from boats or fueling stations.
- *Management of water resources in the watershed:* Water from the various sources (freshwater, drainage water, and treated sewage) is allocated to different uses and users (domestic, farmers, and ecotourism sites) according to a general plan that considers both quantities and qualities. A large-scale rehabilitation project—the Hula Project—was initiated in 1994, creating some 90 km of regulating canals and the small shallow Lake Agmon, which is a focal point for ecotourism. It also serves for storage and reuse of peat drainage and prevents it from being drained down to Lake Kinneret because of its high nutrient content (Hambright and Zohary 1999; Markel et al. 1998). The LKWU leads the Hula operating team, which includes representatives from LKA, KKL, Israel Nature and Parks Authority, Galilee Water Association, the Peat Farmers Association, and Mekorot Water Company (Fig. 31.3). This team makes operating decisions regarding Agmon water levels, and whether to direct peat drainage water to the Einan Reservoir or to Lake Kinneret.
- *Oversight of development and construction activities in the watershed:* According to the water law, all development and construction plans in the watershed that may affect water quality or pollution loads are subject to scrutiny, approval, and oversight by the LKA according to its authorization from the director of IWA.

31.10 Evaluation of the Impact of Watershed Management on the Material Loads

Rom et al. (Chap. 18 "Material Load" provide a long-term (1970–2012) perspective of the loads from the Jordan River to Lake Kinneret. They conclude that the changes in loadings of nutrients and other materials into Lake Kinneret are clearly correlated with long-term changes in Jordan River discharge volumes and are affected by anthropogenic developments and management actions in the watershed. In the high-rainfall years of 1971, 1981, 1987, 1988, 1992, and 2003, the total suspended solids (TSS), phosphorus, and nitrogen loads were the highest in the record. In the 1970s, an increase in total dissolved phosphorus (TDP), N_{org}, and NH_4 loads was recorded. This was most probably due to the rapid population increase in the Kinneret watershed concomitant with a rapid increase in the number of dairy farms (Table 31.3). In the mid-1980s, a decrease in TDP, N_{org} and NH_4 was observed, possibly as a consequence of the operation of the Einan Reservoir and other reservoirs to treat and contain effluents from Qiryat Shemona and northern Hula basin, to be recycled for local agriculture. The creation of the Agmon wetland in the Hula Valley and initiation of the "Hula Project" in 1994 caused a slight decrease in NO_3 load, although this is hard to detect due to the masking of the load data by the variation of the annual discharge data. Flood protection and improved drainage were installed in 1998–2000, including deepening the channel of the Jordan River in the 3-km stretch between the Pkak and Benot Yaacov bridges (see Fig. 18.1 and Table 18.3 in Chap. 18). It is suggested that this action caused an increase in particulate material load, mainly TSS and particulate phosphorus. While the "Hula Project" in 1994 and the enhanced drainage in 1998–2000 were very important management actions, they led to a decrease in the total nitrogen to total phosphorus (TN to TP) ratio, which favors nitrogen-fixing cyanobacteria in the lake (Zohary 2004; Hadas et al. 2012). Consequently, the Hula Project operation was changed in 2010 to diverting winter flows from the nitrogen-rich Hula peat soils to Lake Kinneret rather than to Einan Reservoir (Table 18.3 in Chap. 18 "Material Loads").

31.11 Conclusions

Lake Kinneret is a central component of the Israeli national water supply system, being its only large surface reservoir. The replenishment of the watershed and lake constitute about one third of the replenishment of all freshwater sources between the Mediterranean Sea and the Jordan River (Table 31.1). This water is used in the watershed itself and is supplied from the lake to the central and southern regions of the country via the NWC, as well as to local consumers around the lake and to the Hashemite Kingdom of Jordan. While water supply is a first priority, the lake is also a major environmental and recreational amenity and an important fisheries resource. Healthy lake ecology is a fundamental condition for fulfilling all these

roles, and strict management of the lake and watershed is exercised to ensure this. To this end, the lake and its watershed command special attention in the management plans of the IWA.

Management objectives and the means for achieving them have been enumerated, described, and discussed in this chapter. They include monitoring programs and tools, as well as the organizational structures for oversight and enforcement. The major lake and watershed management actions that were implemented during the past 4 decades are listed in Table 31.3, with their possible impact on the lake's water quality, which indicate that management of the watershed has a positive impact. In addition, fisheries and shoreline management also supported the ecological state of Lake Kinneret. Ongoing and expanded lake and watershed management, stable water levels, salinity control, and fisheries management are promising means for maintaining a healthy ecological system and improved water quality in Lake Kinneret.

Acknowledgments We thank Prof. Avital Gasith, Prof. Boaz Lazar, and Prof. Eran Friedler for their continued engagement in and contributions to the activities of the Kinneret and Watershed Monitoring Steering Committee that oversees monitoring and management actions in the Lake and its watershed.

References

Berger D, Rom M, Porat R (2013) The water, salt and energy balances of Lake Kinneret, 2011/12. Report submitted by the Mekorot Watershed Unit, 41 p. (in Hebrew)

Berman T (1998) Lake Kinneret and its catchment: international pressures and environmental impacts. Water Policy 1(2):193–207

Carpenter S, Kitchell J (1988) Consumer control of lake productivity. BioScience 38:764–769

Dimentman CH, Bromley HJ, Por FD (1992) Lake Hula, reconstruction of fauna and hydrobiology of a lost lake. The Israeli Academy of Sciences and Humanities, Jerusalem, 170 pp

Eckert W, Didenko J, Uri E, Eldar D (2003) Spatial and temporal variability of particulate phosphorus fractions in seston and sediments of Lake Kinneret under changing loading scenarios. Hydrobiologia 494:223–229

Givati A, Rosenfeld D (2007) Possible impacts of anthropogenic aerosols on water resources of the Jordan River and the Sea of Galilee. Water Resour Res 43(10). W10419. doi:10.1029/2006WR005771, pp 1–15

Gvirtzman H, Garven G, Gvirtzman G (1997) Hydrogeological modeling of the saline hot springs at the Sea of Galilee, Israel. Water Resour Res 33:913–926

Hadas O, Pinkas R, Malinsky-Rushansky N, Nishri A, Kaplan A, Rimmer A, Sukenik A (2012) Appearance and establishment of diazotrophic cyanobacteria in Lake Kinneret, Israel. Freshwat Biol 57:1214–1227

Hambright KD, Zohary T (1999) The Hula Valley (northern Israel) wetlands rehabilitation project. In: Streever W (ed) An international perspective on wetland rehabilitation. Kluwer Academic, The Netherlands, pp 173–180

IWA—Israel Water and Sewage Authority (2012) Long-term master plan for the national water sector—policy document, Ver. 4, approved at the 68th Meeting of the Council of the Government Water and Sewage Authority. http://www.water.gov.il/Hebrew/Planning-and-Development/Planning/MasterPlan/DocLib4/MasterPlan-en-v.4.pdf. Accessed 8 Aug 2012

Markel D (2000) Biogeochemical processes in a reflooded wetland: sulfur and iron cycles in Lake Agmon, Hula Valley, Northern Israel. Report GSI/1/2000, 135 p. (In Hebrew)
Markel D (2008) Monitoring and managing Lake Kinneret and its watershed, Northern Israel, a response to environmental, anthropogenic and political constraints. In: Menon S (ed) Watershed management: case studies. The Icafi University Press, Punjagutta, pp 87–106
Markel D (2012) Fishery regulation in Lake Kinneret as a tool for improved management of the lake. Dayig Umidge 15:1597–1600 (In Hebrew)
Markel D, Shamir U (2002) Monitoring Lake Kinneret and its watershed: forming the basis for management of a water supply lake. In: Rubin H, Nachtnebel P, Furst J, Shamir U (eds) Preserving the quality of our water resources. Springer, Berlin, pp 177–189
Markel D, Sass E, Lazar B, Bein A (1998) The main biogeochemical cycles in the newly created Lake Agmon, Hula Valley, Northern Israel. Wetlands Ecol Manag 6:103–120
Markel D, Zohary T, Gabay E, Gasith A (2012) Finding a conservative solution to the problem of inundated costal vegetation at Lake Kinneret shoreline, while balancing between the needs of the water system and tourism. Ecol Environ 3(3):213–215 (in Hebrew)
Rimmer A, Hurwitz S, Gvirtzman H (1999) Spatial and temporal characteristics of saline springs: Sea of Galilee, Israel. Ground Water 37:663–673
Tibor G, Markel D, Kaplan D, Haramati M, Tal D (2012) A rapid and cost effective method for vegetation mapping and nutrient content evaluation along the receding Lake Kinneret shoreline using oblique airborne video integrated into the GeoSky™ system. Isr J Plant Sci 60:151–159
Weinberger G, Livsitz Y, Givati A, Zilberband M, Tal A, Weiss M, Zurieli A (2012) The natural water resources between the Mediterranean Sea and the Jordan River, Israel Hydrological Service Report. http://www.water.gov.il/Hebrew/ProfessionalInfoAndData/Data-Hidrologeime/DocLib4/water_report-MEDITERRANEAN-SEA-AND-THE-JORDAN.pdf. Accessed 2012
Zohary T (2004) Changes to the phytoplankton assemblage of Lake Kinneret after decades of a predictable, repetitive pattern. Freshw Biol 49(10):1355–1371

Chapter 32
The Monitoring Program

Assaf Sukenik, Tamar Zohary and Doron Markel

Abstract The monitoring program of Lake Kinneret and its watershed was established more than 40 years ago with objectives to follow the quantity and quality of the lake water, to observe and predict long-term changes in water quality, and to identify the processes that determine and affect water quality. This chapter describes the various components of the Kinneret monitoring program, alongside its development and evolution during the past decades. Recent application of early warning monitoring systems and advanced techniques for near-real-time, synoptic, and high-resolution data collection of many water quality parameters are briefly outlined.

Keywords Monitoring · Database · Water quality parameters · Early warning monitoring system · Real-time data collection

32.1 Definitions and Goals

Routine quality assessment of aquatic ecosystems and water resources is essential for water bodies that constitute major sources of drinking water, as is the case for Lake Kinneret. High-quality assessment of aquatic ecosystems and water resources requires extensive operations of monitoring, including sample collection, laboratory analyses, data storage and organization, and data analyses. The design of these operations must take into account short- and long-term objectives and consider many parameters that affect the physical, chemical, and biological nature of the water (Meybeck et al. 1996). The general objectives of the assessment of the quality of the aquatic environment are: (1) assure that the water is suitable for its intended

A. Sukenik (✉) · T. Zohary
The Yigal Allon Kinneret Limnological Laboratory, Israel Oceanographic & Limnological Research, P.O.Box 447, 14950 Migdal, Israel
e-mail: assaf@ocean.org.il

T. Zohary
e-mail: tamarz@ocean.org.il

D. Markel
Lake Kinneret and Watershed Unit, Israel Water Authority,
Z.H.R. Industrial Park, P.O. Box 623, 12000 Rosh Pina, Israel
e-mail: Doronm10@water.gov.il

T. Zohary et al. (eds.), *Lake Kinneret, Ecology and Management,* Aquatic Ecology Series 6,
DOI 10.1007/978-94-017-8944-8_32,

use and (2) identify temporal changes in the quality of the aquatic environment and point out natural and anthropogenic factors that affect these trends. To be able to meet those objectives, a monitoring program for an aquatic environment must be based on long-term, standardized routine measurement and observation of a suite of parameters characterizing the environment.

A monitoring program should be differentiated from other types of aquatic environmental observation programs that are more limited in time, scope, or in targets, such as surveys or surveillances. A survey is an intensive program of a finite duration, designed to measure and observe the quality of the environment for a specific purpose. Surveillance is a system or activity that monitors environmental quality parameters in order to detect and follow pollution concentration in time for remedial measures. Certain standard elements are common to all water quality assessment programs: defined objectives, preliminary surveys, monitoring design, field sampling, laboratory activities, data quality control, data storage treatment and reporting, data interpretation, and water management recommendations (Meybeck et al. 1996).

32.2 An Integrated Monitoring Program for Lake Kinneret and its Watershed

Monitoring of Lake Kinneret has been carried out since 1969 with objectives to follow the quality of the lake water, to observe and predict long-term changes in water quality, and to identify the processes that determine and affect water quality. A year later, in 1970, the monitoring of the Kinneret watershed began, with the objectives to quantify the amounts of water and nutrient loads reaching the lake. The ongoing monitoring of the lake and its watershed is conducted by teams from several organizations, including: the Kinneret Limnological Laboratory (KLL) of the Israel Oceanographic and Limnological Research, the Watershed Unit of Mekorot—the National Water Company, the Israel Hydrological Services of the Israel Water Authority, and the Fisheries Department of the Ministry of Agriculture and Rural Development, with most funding from the Israel Water Authority (see Chap. 31). Over time, the need to integrate the various monitoring programs into a single comprehensive program was realized and a specialized "Kinneret and watershed unit" was set up within the Israel Water Authority to oversee, coordinate, and steer the monitoring activities.

The overall lake and watershed monitoring program has evolved over the past five decades in order to fulfill the general aim of aiding and supporting management of the watershed and the lake towards meeting the lake's role as a system that is used for water supply and provides ecological services. The multidisciplinary and multi-institutional monitoring program is based primarily on sampling water from several fixed locations (sampling stations) within the lake and along the Jordan River and other inflowing streams (KLL and Mekorot). The water samples collected are analyzed for a wide range of parameters (KLL and Mekorot) which reflect the current status of the water in the lake and its watershed, can be used to examine long-term trends in water quantity and quality, and assist in identifying sources

of pollution. In addition, water discharge is measured on the inflowing rivers and saline springs (Hydrological Services). Saline springs around the lake are further sampled for their salt content (Mekorot). Fish catch and fingerling stocking are also monitored (Fisheries Department).

The different organizations participating in the Kinneret monitoring produce monthly and/or annual reports (mostly in Hebrew) in which the data are presented and analyzed, with implications being highlighted (i.e., Berger et al. 2012; Weinberger et al. 2012). Some of those data are also presented on the organizations' websites.

This established monitoring program will continue to be essential in the coming years even though a new source of water, from desalination, has entered the Israeli water budget. Long-term plans of the Israel Water Authority (IWA 2012) confirm that Lake Kinneret will continue to be an important strategic source of freshwater.

32.3 The Monitoring Program for Lake Kinneret

32.3.1 Historical Perspective

Scientific data collection from Lake Kinneret was initiated in 1757 by Hasselquist, a student of Linnaeus, who collected faunal specimens and helped describe *Tilapia galilaea* as an endemic fish of the lake. Subsequently, other scholars such as Tristram (1865), Barrois (1894), and Annandale (1916) studied the lake and its environment, unveiling its flora, fauna, chemical composition, and hydrography, as described by Serruya (1978). Later, intense and targeted surveys were performed in response to specific practical aspects of water productivity and fisheries (Ricardo-Bertram 1944). It was only after the establishment of the State of Israel in 1948, and the planning of the National Water Carrier, making Lake Kinneret Israel's primary water source, first for agriculture and later for drinking water, that intense studies of the Lake Kinneret ecosystem were initiated.

Problems of water quality in Lake Kinneret were first identified with the initial operation of the National Water Carrier in 1964 and were associated with the spring algal bloom that contributed to bad taste of the water (Serruya 1978). Consequently, a multiannual monitoring program, designed to reflect ecosystem variability in time and space, was initiated in 1969. Since then it provides a long-term limnological and hydrological database. The KLL jointly with the Watershed Unit of Mekorot carry out this entire program.

32.3.2 Sampling Stations, Depths, and Frequency

The objectives of the monitoring program for Lake Kinneret, balanced by practical considerations of available resources, dictate the frequency of sampling, the number of sampling sites, and their location in the lake. Furthermore, the physical

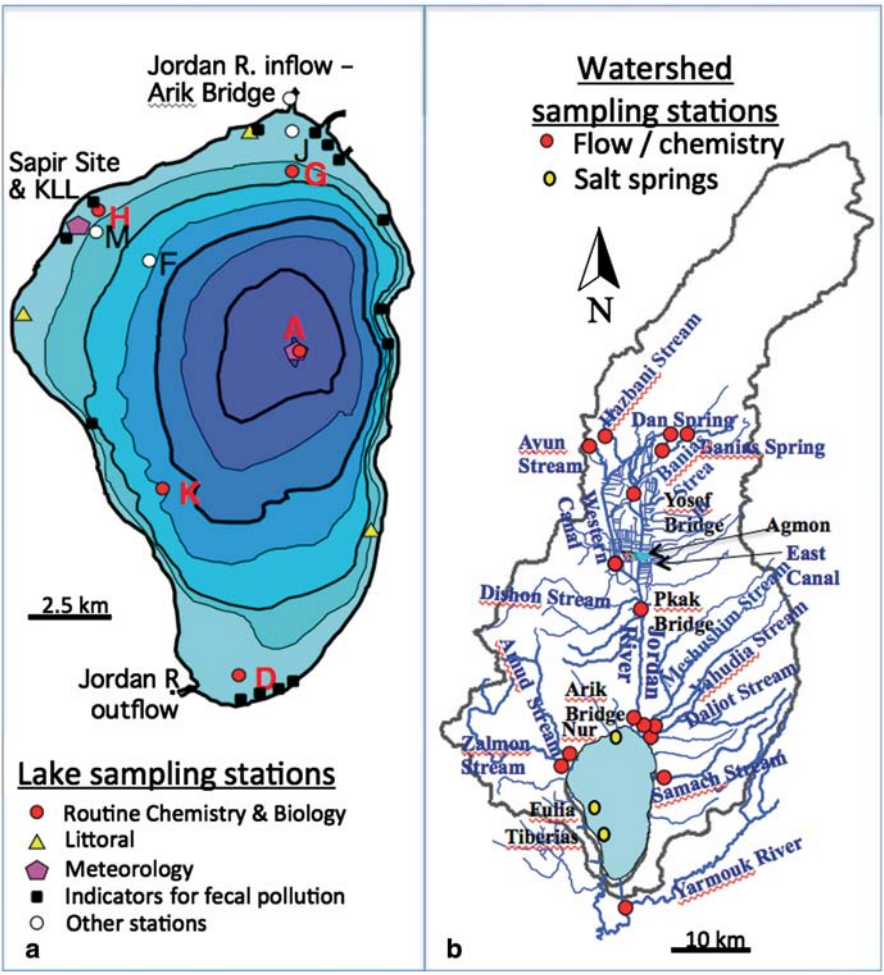

Fig. 32.1 Location maps of monitoring stations in Lake Kinneret and its watershed. **a** Lake Kinneret (symbol legend *below* map). **b** Watershed (symbol legend *above* map). Additional explanations: *KLL*—Kinneret Limnological Laboratory. *Other stations*—stations *F*, *M* are used for sedimentation flux measurements, *J* for occasional biological measurements, and *Arik* for pesticides. *Littoral stations*—shallow water stations for occasional biology and chemistry measurements

dimensions of the lake, its bathymetry, and current regime are used to determine the number of samples collected along the water column at each station and the type of analyses performed on these samples.

The Kinneret sampling stations used for the monitoring of most chemical and biological parameters are presented in Fig. 32.1a. Station (Sta.) A, located near the deepest site in the lake, is the main station. Samples from Sta. A are collected weekly and analyzed for a large number of physical, chemical, and biological parameters (Table 32.1). Stas. G, D, and K, located along a line stretching from north to south,

Table 32.1 The monitoring program of Lake Kinneret: parameters, sampling stations, and sampling frequency. Samples for the chemical and biological parameters are collected from fixed depths along the water column (up to 13 depth samples)

Parameter	Station(s)	Frequency
Meteorology		
Air temperature	A, Ginnosar	10 min
Surface water temperature	A, Ginnosar	10 min
Relative humidity	A, Ginnosar	10 min
Wind (speed and direction)	A, Ginnosar	10 min
Long wave radiation	A, Ginnosar	10 min
Shortwave radiation	A, Ginnosar	10 min
Barometric pressure	A, Ginnosar	10 min
Light radiation (PAR)	Roof of KLL	Continuous
Physics		
Water level	Tiberias	Daily
Temperature profile in water column	A, D, G, H, K 5–15 additional stations	Weekly fortnightly
	A, H	10 min
Secchi depth	A, D, G, H, K	Weekly
Currents	Variable sites	Continuous
Profile of light penetration	A	Every other week
Sedimentation fluxes	A, F, K, M	Every other week
Chemistry (in water column)		
Alkalinity	A, D, G, H, K	Every other week
Chloride	A, D, G, H, K Salt springs	Weekly Weekly
Conductivity	A, D, G, H, K	Weekly
Calcium	A, D, G, H, K	Every other week
Organic carbon (dissolved; particulate)	A	Every other week
Soluble Nitrogen (Kjeldahl)	A,	Weekly
	D, G, H, K	Every other week
Total nitrogen (Kjeldahl)	A, D, G, H, K	Weekly
Ammonia	A, D, G, H, K	Weekly
Nitrite	A, D, G, H, K	Weekly
Nitrate	A, D, G, H, K	Weekly
Oxygen	A	Weekly
	D, G, H, K	Every other week
pH	A, D, G, H, K	Weekly
Total dissolved phosphorous	A	Weekly
Orthophosphate	A, D, H, K	Weekly
Chemistry (in water column)		
Total phosphorous	A, D, G, H, K	Weekly
Silica	A	Every other week
Sulfate	A, D, G, H, K	Every other week
Sulfide	A, D, H, K	Weekly
Total suspended solids	A, D, G, H	Every other week

Table 32.1 (continued)

Parameter	Station(s)	Frequency
Turbidity	A, D, G, H, K	Weekly
Biology		
Phytoplankton species & abundance	A	Every other week
Chlorophyll	A	Every other week
Primary productivity	A	Every other week
Zooplankton species & abundance	A, D, G, H, K	Every other week
Microzooplankton abundance	A	Monthly
Fish abundance	All over the lake	8 surveys per year
Heterotrophic bacterial abundance	A	Monthly
Bacterial production	A	Monthly
Community respiration rates	A	Every other week
Nitrogen fixation rates	A	Monthly
Harvested biomass of commercial fish species	Fish market, fishing harbor	Monthly
Stocked fingerlings	Ginnosar	Annually
Health related		
Pesticides	A, D, G, H, Arik Bridge	Every other week
Cyanotoxins	A Surface scums	Monthly During blooms
Fecal bacteria	14 littoral sites	Monthly
Synoptic & remotely operated monitoring		
Temperature, conductivity, turbidity, chlorophyll (U-TUMS)	Transects over entire lake	Every 2 months
Surface distribution of surface water temperature and chlorophyll (satellite images)	Entire lake	Every 3 days
Water column temperature (T-chain)	A	Every 10 min.
Profiler (O_2, pH, turbidity, ORP, chlorophyll, temperature, conductivity)	A	4 profiles/day

as well as Sta. H, at the inlet of the National Water Carrier, are sampled for fewer parameters and for some parameters at lower frequency (Table 32.1). At these five stations, discrete-depth water samples are collected from depths covering the entire water column, with high depth resolution (1–3 m) near the surface and at 5-m intervals from 10 m to the bottom sediments. During stratification (April through November), three additional samples are collected at Sta. A, one from the middle of the thermocline and two located 1 m above and below it. Other sampling stations marked in Fig. 32.1a and/or sampling depths are employed for parameters that for technical or other reasons are not sampled with the weekly/fortnightly sampling for chemical and biological parameters, as discussed below and in the relevant book chapters (Chaps. 6, 8, 16, 27, and 28, Sects. 33.2 and 33.3).

Additional routine monitoring of salinity and temperature at 5–15 additional sampling stations, depending on season, is conducted fortnightly by Mekorot to

Table 32.2 Instrument and manufacturer details for meteorological and physical parameters measured on Lake Kinneret

Parameter	Instrument	Manufacturer
Wind speed and direction	Wind monitor Model 05103 R M	Young Company, MI, USA
Long-wave and shortwave radiation	CNR 4 net radiometer	Kipp & Zonen, Delft, the Netherlands
Barometric pressure	CS106 Barometric Pressure Sensor	Campbell Scientific, Logan, UT, USA
Air temperature and relative humidity	MP101a—humidity–temperature meteorological probe	ROTRONIC Instrument Corp., NY, USA
Photosynthetically active radiation	LI-190 quantum sensor with a LI-1400 Data logger	LiCor, Lincoln, NE, USA
Light intensity	LI-190 quantum sensor with a LI-250A Light Meter	LiCor, Lincoln, NE, USA
Vertical profiling of water temperature	Oceanographic's MinosX	AML Oceanographic, Sidney, B.C., Canada
Automatic recording of water temperatures	Thermistor chains	PME, Carlsbad, CA, USA

supplement the database for their monthly estimates of salt, heat, and water balances (Assouline 1993; Berger et al. 2012).

32.3.3 Parameters Monitored

The Kinneret monitoring program includes parameters that are meteorological, physical, chemical, biological, and related to public health, as detailed in Table 32.1.

Meteorological data: Are collected continuously from two "meteorological stations" (Fig. 32.1a), at Sta. A, and on the western shore at Ginnosar (which in 2006 replaced a station 1 km offshore the KLL). Each meteorological station is equipped with instruments to measure wind speed and direction, long- and shortwave radiation, barometric pressure, air temperature, and relative humidity (details in Table 32.2 and Chap. 6). Photosynthetically active radiation is also recorded continuously (Table 32.2) on the roof of the KLL.

Physical Data: Lake water level is recorded daily at an offshore station near Tiberias. Full-depth profiles of water temperature (instrument details in Table 32.2) and Secchi depth are taken at each of the five pelagic sampling stations and times. Light penetration is measured every second week with a LiCor light meter (Table 32.2). Sedimentation fluxes are followed using sediment traps (Chap. 27) at ~2-week intervals, and the procedure requires making the sampling on designated boat trips. With technological developments, automatic instruments recording water temperatures by thermistor chains (Table 32.2) were introduced and are now installed at two stations, collecting water column temperature data continuously in addition to the routine weekly profiles.

Chemical Data: A long suite of chemical parameters (Table 32.1) are determined routinely on water samples brought to the laboratory from Stas. A, D, G, H, and K (Fig. 32.1). Water samples are collected by a Vertical Point Water Sampler (Aquatic Research Instruments, Hope, ID, USA). The chemical parameters include nutrient concentrations (all species of N and P), pH, alkalinity, total and dissolved organic C, dissolved oxygen, sulfide and sulfate, silica, chloride, conductivity, total suspended solids (TSS), and turbidity (Table 32.1). All analytical procedures follow standard methods (APHA 2005). In recent years, some of these parameters are also monitored automatically at Sta. A (see below, Ecoraft). In addition, the salinity of the major salt springs within and around the lake perimeter is monitored at weekly intervals.

Biological Parameters: Most of these parameters are determined routinely on samples from a single station (Sta. A) due to the greater time investment required for their analyses as compared to chemical parameters. Both standing-stock and rate parameters are being determined regularly. The standing-stock parameters include phytoplankton (chlorophyll, species composition, species abundance, and biomass), zooplankton (species and abundance), and heterotrophic bacteria (abundance; see methods in Chaps. 10, 13, and 15, respectively). Rate parameters include primary production, bacterial production, community respiration, and nitrogen fixation (see brief description of relevant methodologies in Sects. 24.1, 25.1, and 25.2 and Chap. 22, respectively). Fish abundance is determined separately, in dedicated night surveys, by means of scientific echo sounding equipment (Chap. 16). Harvest estimates of all commercially important species are made monthly, based on catch statistics. The annual amounts of fingerlings stocked in the lake are also documented (Chap. 36).

Public Health Parameters: The need for monitoring public health-related parameters developed over time. As the Kinneret watershed is mostly agricultural, the need to monitor pesticide residues in the lake and its watershed arose and was initiated in 1980 (Sect. 33.2). Similarly, since the lake provides drinking water and is a major recreational site, health standards required that bacterial indicators for fecal contamination be monitored (Sect. 33.3). Since 1987, indicators for fecal pollution are monitored at 14 near-shore stations (Fig. 32.1) representing major water pumping sites, recreational beaches, and inflows of the Jordan River and other streams. With the first appearance and blooming of toxin-producing Nostocalean cyanobacteria in Lake Kinneret in 1994 (Chap. 12), the need to monitor cyanotoxins was identified and initiated (Sect. 33.1).

Data Storage: the Lake Kinneret Database (LKDB) and the Kinneret Data Center The Lake Kinneret Database (LKBD), housed at the KLL, contains all the monitoring information collected by the KLL since 1969, with metadata to describe how the data were collected, organized, and archived. It is a unique source of information due to the quality of the data and its long-term continuity. Much of the data are viewable online at the Kinneret Data Center http://www.ocean.org.il/Eng/KineretDataCenter/ProfileDC.asp

Mekorot, the Hydrological Services, and the Department of Fisheries maintain additional complementary databases. In addition, the Israel Water Authority houses

and maintains a comprehensive database, containing all data from all organizations taking part in the Kinneret monitoring.

32.4 Advanced Near-Real-Time Monitoring Approach: Rationale, Technology, and Examples

The design of the routine monitoring program with several fixed stations and weekly/fortnightly sampling makes it nearly impossible to detect phenomena and processes at higher spatial and temporal resolution, such as patchy distribution of a particular parameter. Intensification of the traditional monitoring scheme by adding stations and increasing sampling frequency could resolve this problem but would require substantial investment in manpower, equipment, and operational costs. On the other hand, ignoring patchy structures and short-lived processes limits our understanding of the organization and functioning of the ecosystem. Several innovative approaches have been implemented in Lake Kinneret to resolve issues of limnological and water quality aspects at high spatial and temporal resolutions. These include: (1) automated sampling, including an unmanned automated monitoring station that profiles and samples the water column several times a day; (2) application of underwater-towed undulating monitoring system (U-TUMS) that is carried behind a boat and can sample within a short time large portions of the lake volume; and (3) remote sensing.

Automated Sampling Equipment– The meteorological parameters (at the two meteorological stations) as well as water temperature (using thermistor chains at two stations) are being monitored by automated equipment that sends real-time or near-real-time data to the laboratory.

An Unmanned Monitoring Platform for Real-Time Monitoring of Water Quality Parameters– The Ecoraft (Fig. 32.2a), an acronym for "ECOlogical monitoring RAFT," was installed in Lake Kinneret in February 2002. The Ecoraft is a 10 × 7-m, 10-ton catamaran-type steel raft anchored at the deepest part of Lake Kinneret (Sta. A), providing a platform for continuous monitoring using automated instrumentation, telecommunication with the shore-based laboratory, and space for additional on-lake monitoring and research activities (Wagner et al. 2005). Solar panels roofing part of the raft attached to a storage battery supply the energy required for uninterrupted operation of the scientific instruments. A cabin provides shelter for sensitive equipment and a bench for sample processing. A fence, protecting from vandalism, was also found essential. The Ecoraft is equipped with the following scientific functions:

- A winch-operated sampler designed and manufactured for the Ecoraft by ISI (Instrumental solutions Inc. Vicksburg, MS, USA). The profiler hosts an upgraded multi-sensor Eureka Manta2 (Eureka Environmental Engineering, Austin, TX, USA), presented in Fig. 32.2b, c, which records depth, temperature, conductivity, pH, dissolved oxygen, chlorophyll, and turbidity. The profiler is programmed

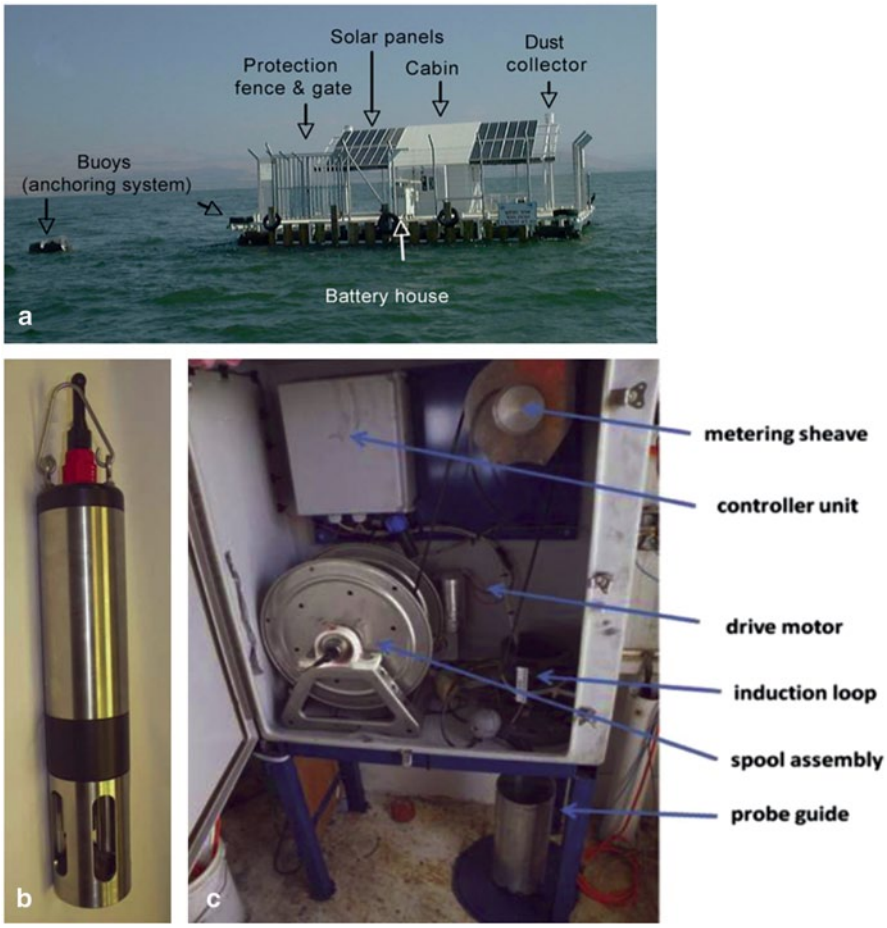

Fig. 32.2 An unmanned monitoring platform for real-time monitoring of Lake Kinneret water quality parameters. **a** The Ecoraft, anchored at Sta. A, equipped with solar panels and batteries to supply local energy requirements, a cabin for housing scientific equipment and for conducting fields work, and dust collectors. **b** An upgraded multi-sensor Eureka Manta2 used in conjunction with **c**. **c** A winch-operated sampler housed inside the cabin

to conduct a depth profile at 0.5-m intervals of those parameters every 6 h and transfer the data to a computer at the laboratory.

- A full meteorological station, installed and maintained by the Israel Meteorological Services.
- Dust collectors for monitoring aeolian nutrient loading.
- A thermistor chain with 40 thermistors spread over the 42-m water column, recording water temperature at 10-min intervals.

With the Ecoraft and the automatic profiler, continuous records of water quality data spanning the entire water column are being collected at full diel cycles, 365 days a

year, including weekends and holidays. Sampling is easily performed during storm conditions that do not allow conventional sampling by boat. Much of the data collected automatically are posted in near real time at the Kinneret Data Center (http://kinneret.ocean.org.il/Default.aspx). Additional sampling and measuring equipment can be installed on the raft, currently an instrument that measures phytoplankton abundance by taxonomic groups and its photosynthetic activity, a PhytoPAM (Walz, Germany), operates on it.

Examples for new insights or features revealed by the automatic profiler on the Ecoraft include fluorometric data demonstrating diel vertical migration in *Peridinium* (Usvyatsov and Zohary 2006), the temporal dynamics of a metalimnetic layer of photosynthetic bacteria (Rimmer et al. 2008), and the temporal dynamics of a layer with residual oxygen in the upper hypolimnion in late spring (Nishri et al. 2011).

Underwater-Towed Undulating Monitoring System– To increase the spatial resolution of several *in situ*-measured limnological parameters (temperature, turbidity, salinity, and chlorophyll), an U-TUMS has been applied over the last decade. The U-TUMS is suitable for studying processes that occur over a large portion of the water body. It is composed of a vehicle (carrier), a set of sensors, and navigation devices (geographic positioning system-GPS, SONAR, and speedometer), which are interconnected and operated via an on-board computer. The U-TUMS vehicle—MiniBAT (GuildLine, Canada) is loaded with fast response sensors that collect measurements while the vehicle is towed behind a boat along chosen transects at a speed of 4 knots and undulates (diving or climbing) at rates of up to 90 cm s^{-1}.

Data collected by the U-TUMS demonstrated strong spatial heterogeneity of water quality parameters during different seasons and at specific locations (Sukenik et al. 2002). Distinctive features, such as thermocline location and tilting, were identified during the stratification period. The river inflow plume and sites of underwater saltwater intrusion were easily detected. A high fluorescence signal of the *Peridinium* bloom was recorded concomitant with high turbidity values during the spring bloom (Ostrovsky and Sukenik 2008; Zohary et al. 2012).

Remote Sensing– The aim of remote sensing of Lake Kinneret is to provide truly synoptic monitoring of water quality parameters. Satellite image-based lake water quality mapping is done using SISCAL (www.siscal.net), a facility developed within a European research program and currently operated by Informus and Israel Oceanographic and Limnological Research. This monitoring is based on two satellites (MODIS Aqua, Terra) with a spatial resolution of 1×1 km and a third (MERIS) satellite with spatial resolution of 300×300 m that passes over the lake every three days. The obtained satellite images are processed using calibrated algorithms and the spatial distribution of surface water temperature, Secchi depth, TSS, and chlorophyll are produced and posted at http://isramar.ocean.org.il/isramar2009/siscal/default.aspx?id=Kinneret. The calculated maps are frequently verified with ground data collected at the monitoring stations.

32.5 The Monitoring Program for the Kinneret Watershed

A monitoring program for the watershed of Lake Kinneret originated in the 1940s with the beginning of discharge measurements on the Jordan River. However, the current coupled quantity–quality approach for this program was initiated only in 1970, a year after the establishment of the monitoring program for the lake. The watershed monitoring program combines continuous discharge measurements with sampling of water for chemical analyses that jointly yield loading estimates. This program is carried out jointly by the Israel Hydrological Services of the Water Authority (discharge measurements) and the Watershed Unit of Mekorot Water Company (sampling and chemical determinations). The main objective is to quantify the loads of particulates and solutes entering Lake Kinneret, focusing on phosphorus and nitrogen species, and to identify their sources. The parameters being determined are chloride, all nitrogen and phosphorus species, alkalinity, sulfate, calcium, and total suspended matter. The locations of the sampling stations (Fig. 32.1b) were chosen to enable quantification of the loads from the main Jordan River tributaries (Dan, Hazbani and Banias), as well as from the Jordan River proper and from other main streams flowing into Lake Kinneret (Meshushim, Yahudia, Daliot, Samach, Amud, and Zalmon). The southernmost monitoring station is located near the intersection of the Yarmouk River with the lower Jordan River. This station monitors the water pumped from the Yarmouk River and discharged into Lake Kinneret according to the 1994 peace agreement between Israel and Jordan.

Discharge at each sampling station is calculated from continuous measurement of the water level with a hydrometric gauge at a calibrated control section of the river. The continuous discharge data are then translated to daily, monthly, and annual volumes of water. Water quality measurements are made on water samples taken next to each hydrometric gauge. Some of the sampling stations contain automatic samplers, which sample the river or stream every 30 min, storing the water samples in a refrigerated bottle that is replaced automatically every 6 h (see Fig. 2 in Chap. 18). Thus, four successive bottles, mixed into one bottle in the laboratory, comprise a time-integrated water sample representing a single day. A series of chemical analyses is then conducted on those daily-integrated samples. Finally, the daily discharge is multiplied by the daily-integrated concentration of each chemical component to get the daily load of this component (Chap. 18). The daily loads are summed up to monthly loads, which are the units reported in the Israel Water Authority Database and used in many related studies. So far, automated sampling was applied at 4 of the 16 watershed stations: Hazbani, Banias, Pkak Bridge, and Meshushim Stream (Fig. 32.1b).

The 12 other watershed stations are being sampled manually once or twice a week. Consequently, due to insufficient sampling frequency, monthly loading estimates from those other stations are inaccurate. In particular, flood events with peak nutrient concentrations may be missed or alternatively overemphasized. Nevertheless, other sources of inaccuracy are associated with the automatic samplers, as

explained in Chap. 18. Therefore, while considering the monthly loads from the Kinneret watershed, one should not ignore these sources of inaccuracy. Moreover, since the automatic sampling stations were installed in the beginning of the 1990s, the long-term record from the water quality measurement stations also requires attention when comparing data from pre- and post-automatic sampling (Chap. 18). Lastly, nutrient loads to Lake Kinneret from the Jordan River are being calculated based on data from the Pkak Bridge Station, ~20 km upstream of the Jordan River entrance into Lake Kinneret. This site was chosen rather than the Arik Bridge, right at the inflow (Fig. 32.1), because for technical reasons discharge estimates at the Arik Bridge are inaccurate.

32.5.1 Advanced Monitoring and Alarm Stations in the Watershed

Since September 11, 2001, the world's attitude regarding water security has changed. This trend led to the development of water security precautions in the water sector of Israel, including the Kinneret watershed monitoring system. As part of that new attitude, some of the water quality measurement stations in the watershed were upgraded to be water quality alarm stations. The purpose of this upgrade was to provide managers with alarms that will make it possible to prevent events of exceptional/severe water contamination. These systems include a set of online electrodes (pH, temperature, conductivity, oxidation reduction potential-ORP, ammonium, and turbidity) that are dipped in a PVC bath. The bath is part of a flow-cell system through which fresh stream water flows continuously (see Fig. 18.2 in Chap. 18). The electrodes in the bath generate online measurements; the data are sent through cellular communication to a data center at Sapir Site (Fig. 32.1a), run by the Watershed Unit of Mekorot.

A real-time control system developed by the Watershed Unit of Mekorot introduced a new dynamic water quality index, designed to explore and alarm of any systematic change in water quality in the watershed. This index weighs and integrates the measurements recorded from all available sensors into a single overall easily tractable index value. The resulting integrated index value is highly sensitive to any simultaneous change recorded in measurements such as deviation from acceptable ranges, a sudden "jump" in recordings, or a continuous (may be even low) increase or decrease in values over time. An alarm message is sent when the overall index deviates from its acceptable range.

In addition to this alarm system, an online bioassay tool was added by Mekorot to provide yet another sensitive alarm for a drastic change in the water quality of the Jordan River or its tributaries. The combination of the hydro-chemical online measurements, a decision support system for announcing an alarm, and a bioassay tool created a comprehensive warning system that allows mangers to decide on drastic steps due to an alarm of acute contamination of the river water. Operational steps that follow include an immediate halting of all pumping of water from Lake

Kinneret, fast and intensive monitoring to identify the exact pollutant, and a series of operational steps that may reduce its impact on water quality.

32.6 Concluding Remarks

The monitoring program for Lake Kinneret and its watershed has produced a database spanning more than four decades that is one of the most detailed long-term records for a natural subtropical lake subjected to a Mediterranean climate. Most of the chapters in this book have relied heavily on data generated as part of this monitoring program. As Lake Kinneret continues to be a strategic source of drinking water for the State of Israel, even in the current situation with desalinated water providing a greater portion of Israel's freshwaters, the monitoring program will continue to generate important data and understanding on the functioning of a stratified subtropical lake.

It is expected that the current effort to establish online real-time monitoring methods will be further implemented in additional monitoring sites and will cover other environmental parameters that represent biological processes (i.e., primary production and respiration) and biological stocks (i.e., phytoplankton, zooplankton, and fish) in addition to various geochemical parameters. Video-assisted classification and enumeration of planktonic organisms has been recently discussed as a viable option using advanced video recording devices of rapid flow of aquatic samples via micrometric flow through capillary (Flow-cytometry, FlowCAM, Fluid Imaging Technologies Ltd.). *In situ* estimation of photosynthetic activity in aquatic ecosystems is currently possible with various fluorescence approaches (FRRF, PAM, delayed fluorescence).

Online monitoring procedures generate huge data sets. These need to be acquired, treated, and processed in ways that are user friendly and easily accessible for interpretation and presentation. Thus, there is room for greater involvement of information technology experts who will contribute to the development and application of software to deal, analyze, and present those large data sets. They will also contribute to communicate those observations and conclusions based on them, to water managers and to the public, using advanced web technologies.

The Lake Kinneret monitoring program has been evolved into its current status over four decades. The conceptual aspects of the monitoring program and its various operational components can be easily implemented in monitoring plans designed for other freshwater and marine ecosystems. Different aspects of the monitoring program should be considered while implemented in other systems. This includes the design of the program, technical details of how to conduct the sampling and the analytical determinations and how to report them, the multi-disciplinary character of the scientists and the organizations involved, the combination of collecting data in conventional ways at low spatial and temporal resolution with automated ways at high resolution, the creation of a database, and the presentation of data online.

References

Annandale N (1916) A report on the biology of the lake of Tiberias. Asian Soc Bengal 11:437–476
APHA—American Public Health Association (2005) Standard methods for the examination of water and wastewater, 25th edn. American Public Health Association, Washington DC
Assouline S (1993) Estimation of lake hydrologic budget terms using the simultaneous solution of water, heat, and salt balances and a Kalman filtering approach—application to Lake Kinneret. Water Resour Res 29(9):3041–3048
Barrois T (1894) Contribution Ã l'étude de quelques lacs de Syrie. Rev Biol Nord 6:224–314
Berger D, Teltsch B, Sarusi F, Rom M (2012) The water, salt and energy balances of Lake Kinneret, 2010/11. Report submitted by the Mekorot Watershed Unit, April 2012, 45 p (in Hebrew)
IWA-Israel Water and Sewage Authority (2012) Long-term master plan for the National Water Sector—policy document, Version 4, Approved at the 68th meeting of the Council of the Government Water and Sewage Authority, August 8 2012 (in Hebrew). http://www.water.gov.il/Hebrew/Planning-and-Development/Planning/MasterPlan/DocLib4/MasterPlan-en-v.4.pdf
Meybeck M, Kuusisto E, Mäkelä A, Mälkki E (1996) Water quality. In: Bartram J, Balance R (eds) Water quality monitoring. E and FN Spon, London, pp 9–33
Nishri A, Rimmer A, Wagner U, Rosentraub Z, Yeates P (2011) Physical controls on spatial variability in decomposition of organic matter in Lake Kinneret, Israel. Aquat Geochem 17(3):195–207
Ostrovsky I, Sukenik A (2008) Spatial heterogeneity of biogeochemical parameters in a subtropical lake. In: Mohanty PK (ed) Monitoring and modeling lakes and coastal environments. Springer, Heidelberg, pp 79–90
Ricardo-Bertram CK (1944) Abridged report on the fish and fishery of Lake Tiberias. Department of agriculture and fisheries of palestine report no. 1944/9, 14 pp
Rimmer A, Ostrovsky I, Yacobi YZ (2008) Light availability for *Chlorobium phaeobacteroides* development in Lake Kinneret. J Plankton Res 30(7):765–776
Serruya C (1978) Lake Kinneret. Monographiae Biologicae. W Junk, The Hague, 501 pp
Sukenik A, Ostrovsky I, Nishri A (2002) Advanced approach for synoptic monitoring of a lake ecosystem—Lake Kinneret as a model. In: Rubin H, Nachtnebel P, Furst J, Shamir U (eds) Water resources quality. Springer, Berlin pp 165–175
Tristram HB (1865) The land of Israel: a journal of travels in Palestine, undertaken with special reference to its physical character. London Society for Promoting Christian Knowledge, London
Usvyatsov S, Zohary T (2006) Lake Kinneret continuous time-depth chlorophyll record highlights major phytoplankton events. Verh internat Verein Limnol 29:1131–1134
Wagner U, Nishri A, Sukenik A, Zohary T (2005) Ecoraft on Lake Kinneret. SIL News 46:8–9
Weinberger G, Livsitz Y, Givati A, Zilberband M, Tal A, Weiss M, Zurieli A (2012) The natural water resources between the Mediterranean sea and the Jordan river, Israel hydrological service report. http://www.water.gov.il/Hebrew/ProfessionalInfoAndData/Data-Hidrologeime/DocLib4/water_report-MEDITERRANEAN-SEA-AND-THE-JORDAN.pdf
Zohary T, Nishri A, Sukenik A (2012) Present–absent: a chronicle of the dinoflagellate *Peridinium gatunense* from Lake Kinneret. Hydrobiologia 698:161–174

Chapter 33
Water Pollutants

Assaf Sukenik, Shmuel Carmeli, Ora Hadas, Edit Leibovici, Nehama Malinsky-Rushansky, Rita Parparov, Rivka Pinkas, Yehudith Viner-Mozzini and David Wynne

Abstract Water pollutants primarily originating from anthropogenic sources impair the ability of lakes and reservoirs to support a human use, such as drinking water, or greatly affect biotic communities, such as fish and other constituents of the food web. Algal blooms and the proliferation of toxic algae and cyanobacteria are also water pollutants that cause major changes in water quality and the ecological status of lentic and lotic ecosystems. Here, we describe two major sources of anthropogenic pollutants in Lake Kinneret: pesticides originated from agricultural activities and fecal indicators originated from domestic and urban pollution. Natural source of in-lake contaminants are toxic compounds produced and excreted by various phytoplankton species. Blooms of toxic species of *Microcystis* and *Aphanizomenon* (Cyanobacteria) were recorded annually since 1994. In this chapter, we bring infor-

A. Sukenik (✉) · O. Hadas · E. Leibovici · N. Malinsky-Rushansky · R. Parparov · R. Pinkas · Y. Viner-Mozzini · D. Wynne
The Yigal Allon Kinneret Limnological Laboratory, Israel Oceanographic & Limnological Research, P.O. Box 447, 14950 Migdal, Israel
e-mail: assaf@ocean.org.il

S. Carmeli
School of Chemistry, Raymond and Beverly Sackler Faculty of Exact Sciences, Tel Aviv University, 69978 Tel Aviv, Israel
e-mail: carmeli@post.tau.ac.il

O. Hadas
e-mail: orah@ocean.org.il

E. Leibovici
e-mail: edit@ocean.org.il

N. Malinsky-Rushansky
e-mail: Hami@ocean.org.il

R. Parparov
e-mail: parpar@ocean.org.il

R. Pinkas
e-mail: rikip@ocean.org.il

Y. Viner-Mozzini
e-mail: diti@ocean.org.il

D. Wynne
e-mail: dwynne@ocean.org.il

T. Zohary et al. (eds.), *Lake Kinneret, Ecology and Management,* Aquatic Ecology Series 6,
DOI 10.1007/978-94-017-8944-8_33,

mation on the type and distribution of anthropogenic and natural pollutants in Lake Kinneret, their multiannual variations, and their implication for water quality.

Keywords Bacterial fecal indicators · Cyanotoxins · Cylindrospermopsin · Herbicides · Microcystin · National Water Carrier · Pesticides · Toxicity index

The major sources of natural and anthropogenic pollutants that affect Lake Kinneret are: 1) pesticides originated from agricultural activities; 2) effluents originated from domestic and urban sewage as reflected by fecal indicators; and 3) blooms of toxic cyanobacteria. In the following sections, we bring information on the type and distribution of anthropogenic and natural pollutants in Lake Kinneret, their occurrence, abundance, multiannual variations, and their impact on water quality.

33.1 Cyanobacterial Toxins

Assaf Sukenik, Yehudith Viner-Mozzini, and Shmuel Carmeli

33.1.1 Introduction

Many species of cyanobacteria produce secondary metabolites, some of which are toxic to other organisms including invertebrates and vertebrates. These substances, frequently referred as "cyanotoxins," show great chemical diversity, ranging from small alkaloids to complex polycyclic compounds and cyclic peptides. While cyanotoxins affect metazoans, it is clear that these are not their original biological target as they evolved much earlier than the appearance of metazoans on earth (Rantala et al. 2004). The biological function of cyanotoxins remains unclear, although recent studies proposed their role in various cellular and population activities like allelopatic effects on algal competitors, iron sequestration, "quorum sensing," intracellular functions, and as intrapopulation or interpopulation infochemicals (Kaplan et al. 2012). Advanced, up-to-date information on the toxicity of cyanobacteria and their worldwide distribution can be found in Pearson et al. (2010) and Paerl and Paul (2011).

33.1.2 Chemical Structures and Toxic Effects

Common cyanotoxins frequently found in Lake Kinneret are the small alkaloid cylindrospermopsin (CYN) and the cyclic peptides, microcystins (MCs). Their chemical structure is presented in Fig. 33.1. MCs consist of a seven-membered peptide ring that is made up of five nonprotein amino acids and two protein amino acids.

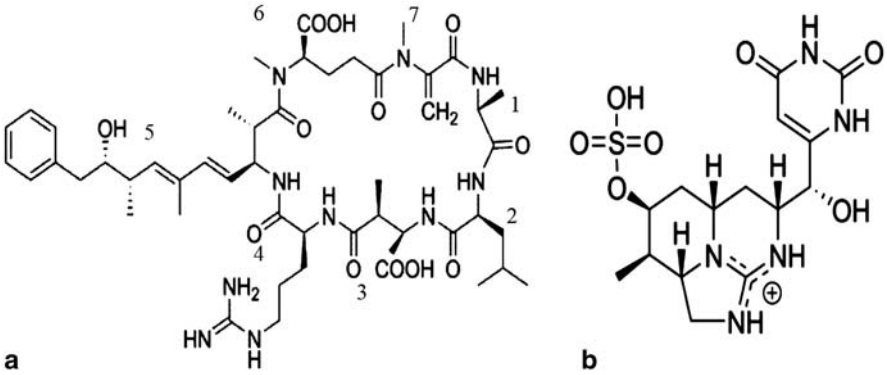

Fig. 33.1 Chemical structure of the main cyanotoxins found in Lake Kinneret. **a** Microcystin-LR (MC-LR)—the numbers indicate the different amino acids that construct this cyclic heptapeptide. **b** Cylindrospermopsin (CYN)

It is these two protein amino acids at positions 2 and 4 (Fig. 33.1a) that distinguish MCs from one another, while the other amino acids are rather constant among variant MCs. Each MC is designated a name depending on the variable amino acids which complete their structure. For example, the most common and potently toxic MC-LR contains the amino acids leucine (L) and arginine (R) in these variable positions 2 and 4, respectively (Fig. 33.1a). CYN is a polycyclic uracil derivative containing guanidino and sulfate groups (Fig. 33.1b). The zwitterionic nature of the molecule makes this toxin highly water soluble.

Cyanotoxins are often classified according to their toxic effects in mammals, creating four main groups: hepatotoxins, neurotoxins, cytotoxins, and dermatotoxins. CYN is toxic to liver and kidney tissue and is thought to inhibit protein synthesis to covalently modify DNA and/or RNA (Humpage and Falconer 2003) and to impose anomalous metabolic responses related to cholesterol metabolism (Reisner et al. 2004). Toxic blooms of cyanobacteria which produce CYN are most commonly found in tropical, subtropical, and arid zone water bodies, and have been reported in Australia, Europe, Israel, Japan, and the USA (Sukenik et al. 2012). MCs are hepatotoxic and can cause serious damage to the liver in humans (Carmichael 2008). There are more than 90 known variants of MC but the most reported variant is MC-LR (Spoof et al. 2010). MCs can also be toxic to plants (McElhiney et al. 2001). They bioaccumulate in the liver of fish, in the hepatopancreas of mussels and crustaceans, including zooplankton (Kinnear 2010).

Interestingly, the crude extracts of MC-producing cyanobacteria have been shown to be more potent than pure MCs themselves (Oberemm et al. 1997; Pietsch et al. 2001), apparently due to other secondary metabolites that usually accompany MCs. These other substances were clustered into five groups of protease inhibitors: micropeptins (128 isolated variants; Okino et al. 1993), anabaenopeptins (34 isolated variants; Harada et al. 1995), aeruginosins (27 isolated variants; Murakami et al. 1994), microginins (25 isolated variants; Ishida et al. 2000), microviridins (15 isolated variants; Reshef and Carmeli 2006), and many other compounds that

do not group together. For example, aeruginosins inhibit trypsin-type proteases and impose a reduction in the activity of enzymes responsible for the detoxification process of MCs in a cyanobacterial grazer. This implies that protease inhibitors that accompany MCs may be involved in detoxification of the MCs in the environment.

Neurotoxic compounds produced by cyanobacteria are anatoxin-a, anatoxin-a(S), and the best-known paralytic shellfish toxin (PST) saxitoxin (STX). These neurotoxins, produced by various species of Nostocales, have not been detected in Lake Kinneret so far.

33.1.3 Type and Distribution of Cyanotoxins in Lake Kinneret

The isolation of various species and strains of cyanobacteria from occasional blooms in Lake Kinneret helped identify several cyanotoxins. CYN and its enantiomer 7-epi-cylindrospermopsin were isolated and characterized from *Aphanizomenon ovalisporum* strain ILC-164 isolated from Lake Kinneret (Banker et al. 1997; Banker et al. 2000). Chlorination of CYN formed nontoxic derivatives and consequently provided an operational tool for detoxification of CYN in water supply systems (Banker et al. 2001). The 2005 bloom of *Cylindrospermopsis raciborskii* in Lake Kinneret suggested the domination of a nontoxic strain, and indeed no CYN was found in the isolated clone which lost the *cyrJ* fragment in the CYN synthetase region (Alster et al. 2010). Recently, an additional strain of *A. ovalisporum* and several species of *Anabaena* were isolated from Lake Kinneret. Not one of these isolates was a producer of CYN; they all lost the *cyrJ* domain (Ballot et al. 2011).

MALDI-TOF-MS analyses of cell extracts from MG-K and MB-K isolates of *Microcystis* were performed in order to characterize the MCs produced by these strains (Schatz et al. 2005). The mass spectrum of extracts from MG-K cells showed the molecular ion clusters of different MCs, among which [Asp3] or [Dha7] MC-RR (*m/z* 1024), MC-RR, and MC-WR, were identified. Cells of MB-K possess three MCs: MC-LR, [Asp3] or [Dha7] MC-YR (*m/z* 1031), and MC-YR as well as the protease inhibitors, micropeptin KT946 and anabaenopeptin KT864 (Beresovsky et al. 2006). A bloom material of a brown-colored strain of *Microcystis* sp. that was collected from Lake Kinneret in March 2005 afforded six new metabolites: micropeptin KT1042, microguanidine KT636, aeruginosin KT608A, KT608B, and KT650, and pseudoaeruginosin KT554, along with the known micropeptins SF909 and HM978, cyanopeptolin S, anabaenopeptin F and the two isomers of planktocyclin-*S*-oxide (Lifshitz and Carmeli 2012). Interestingly, two nontoxic subcultures, MG-J and MB-J, spontaneously succeeded the toxic ones under laboratory conditions as the original strains lost a 34 kb of the *mcy* region, encoding the MC synthetase (Schatz et al. 2005). A multiannual survey of MCs in Lake Kinneret clearly indicates that the isolated strains (MG-K and MB-K) are not the only toxigenic *Microcystis* species/strains that flourish in the lake. Several *Microcystis* species formed different bloom patterns of floating scum as demonstrated in Fig. 12.1 of Chap. 12 and a variety of MCs were recorded during *Microcystis* blooms in Lake Kinneret as presented in Fig. 33.2.

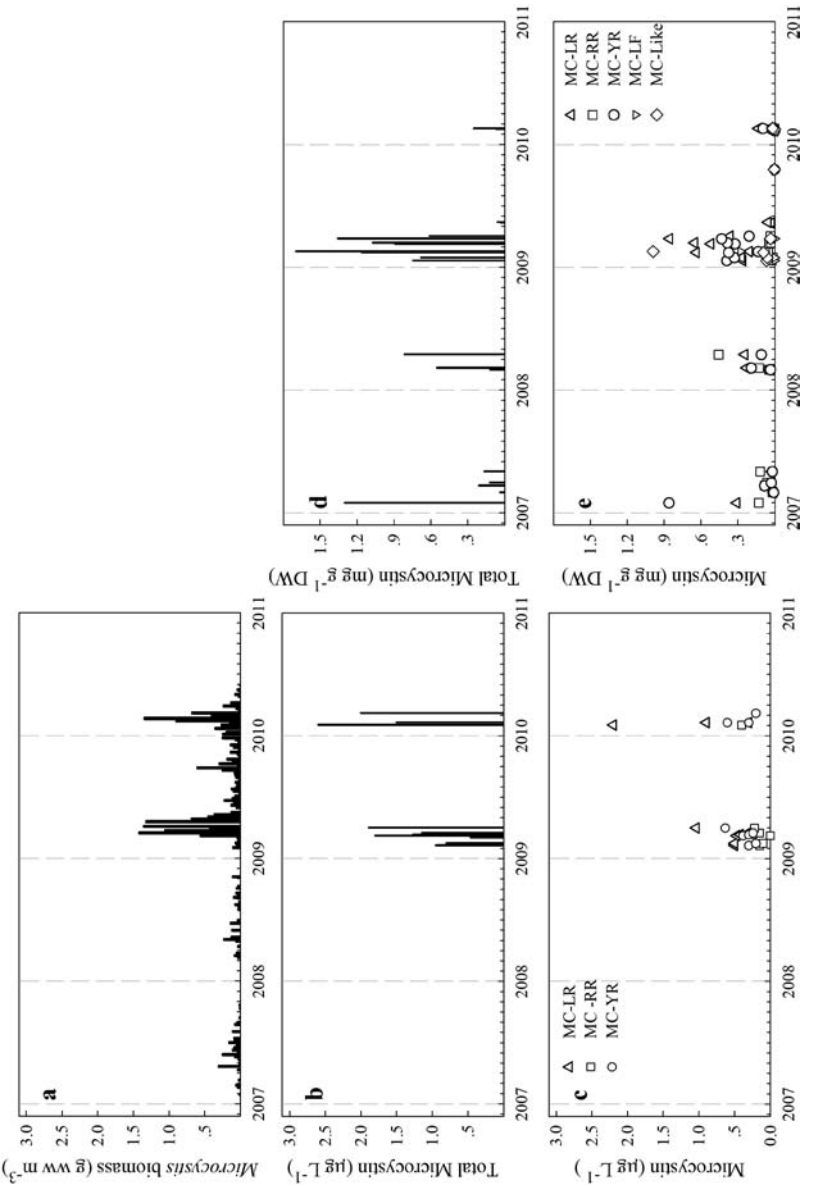

Fig. 33.2 Microcystis (*MC*) biomass (**a**) and microcystins total (**b**) and major (**c**) *MC* derivatives in Lake Kinneret water and total (**d**) and major (**e**) *MC* derivatives in surface scums. Water samples were collected at Sta. A at 1 m depth. *MC* scums were collected at various locations

33.1.4 Multiannual Variations in Cyanotoxin Content and Composition

The qualitative and quantitative monitoring of cyanotoxins in Lake Kinneret is supported by information on the presence/abundance of potentially toxic species, i.e., *A. ovalisporum, Microcystis* spp., and *C. raciborskii*. The analytical procedures are based on published protocols and interlaboratory calibration (Törökné et al. 2004; Lawton et al. 1994). Lake Kinneret water samples were collected once a month at 1-m depth and analyzed for CYN and MCs. Additional samples were collected and analyzed as a population of toxic cyanobacteria were established and occasionally formed floating scums. Analyses were performed by high-performance liquid chromatography integrated with diode array detector (HPLC-DAD) using column and mobile phases suitable for the corresponding toxins. Qualitative verification was performed with authentic standards which are also used for quantification. The standards available for these analyses are CYN (Sigma-Alrich, St. Louis, MO, USA), MC-LR, MC-YR, MC-RR, and MC-LF (Sigma-Alrich, St Louis, MO, USA or Enzo Life Sciences Inc. Farmingdale, NY, USA). In other cases, compounds with spectral characteristics of MC were designated MC-like in association with their elution time (i.e., MC-like-17.5 is a compound eluted at 17.5 min and has a typical spectra of MC in the UV range).

The annual abundance of cyanotoxins in Lake Kinneret generally followed the seasonal pattern of various cyanobacterial species (Figs. 33.2 and 33.3). MC variants were found in the winter and spring (January–April). The winter bloom of *Microcystis* was characterized by relatively low biomass concentrations concomitant with MC concentrations that never exceeded 3 μg L^{-1} (Figs. 33.2b and c). Various MCs could be detected only when *Microcystis* abundance exceeded a certain level (0.5 g ww m^{-3}). Different *Microcystis* species have different cellular MC quota and produce different suites of MCs. Indeed, the variability of the major MC derivatives in the water (MC-LR, MC-YR, and MC-RR, Fig. 33.2c) reflects those variations. The tendency of *Microcystis* colonies to float and to create surface scums ("surface bloom") on calm warm winter mornings (Fig. 12.1, Chap. 12) provided opportunities to assess the toxicity of these populations and to estimate MC content per unit dry weight biomass (Figs. 33.2d and e). Due to the high concentration of *Microcystis* biomass in the floating mats, a strong signal of MCs could be detected and quantified. As a matter of fact, MCs were occasionally detected in the formed floating mats, even when the *Microcystis* concentration in the water column was rather low (compare winters of 2007 and 2008 for total MC concentration in the water column, Fig. 33.2b, with the concentrations measured in floating mats, Fig. 33.2d). Such discrepancies are explained by the fact that MCs in the water column were measured solely at a single location in the lake (Station A) whereas "surface bloom" samples were collected wherever scums were observed, thus do not necessarily represent the *Microcystis* population or concentrations and MC chemotypes found in the water column of station A. Interestingly, the MCs concentrations in all floating mat samples, collected during winter 2010, were rather low

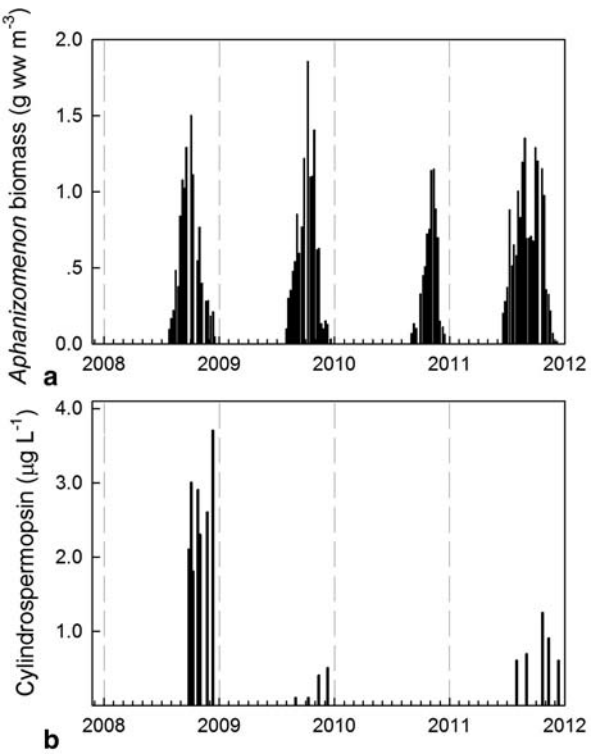

Fig. 33.3 Biomass concentration (wet weight) of *Aphanizomenon ovalisporum* (**a**) and the total (dissolved and particulate) cylindrospermopsin concentration (**b**) in Lake Kinneret, Sta. A, 1 m depth

(Figs. 33.2d and e) and did not reflect the high MC concentration measured in the water column. Such a situation could be explained by differential floating capacity of the various strains with various MC cellular quota and chemotypes, where the less toxic strains have higher floating capacity. Alternatively, variations in the abundance of different *Microcystis* populations within different locations in the lake could be involved.

Since 1994, the summer/autumn population of cyanobacteria in Lake Kinneret has been dominated by Nostocales (*A. ovalisporum* and/or *C. raciborskii*), and the cytotoxic alkaloid, CYN, was frequently measured in the water column (Fig. 33.3). Unlike MCs that are mainly maintained in the producing cell and released to the water upon cell lysis, CYN is continuously released from the cell and a large portion (up to 70%) of the total CYN measured in the water column is of dissolved toxin (Rücker et al. 2007). CYN was identified during the summer and autumn (July–November) and its concentration in the water column roughly follows the abundance of *A. ovalisporum* (Fig. 33.3). Occasionally, traces of CYN were found in Lake Kinneret water weeks after the *A. ovalisporum* population diminished, indicating the chemical stability of this toxin and its slow biodegradation (Wormer et al. 2008). No CYN was detected in Lake Kinneret when *C. raciborskii* dominated (i.e., summer–autumn of 2004, 2005, and 2006), observations which led to a detailed analysis of

the local strain and its characterization as a non-CYN producer, similar to European isolates (Alster et al. 2010). Low CYN concentrations were detected in Lake Kinneret during the summer autumn of 2010 and no CYN signal was measured in 2011 despite the fact that *A. ovalisporum* biomass in these 2 years was at a similar level as in 2008. Such multiannual variations could be explained by variations in the CYN production capacity of the dominant population due to differences in environmental conditions, or by succession of the CYN-producing population with nonproducing strains. The second explanation is more likely as two non-CYN-producing strains of *A. ovalisporum* and other non-CYN producing strains of *Anabaena* were isolated from Lake Kinneret in 2010 (Ballot et al. 2011). This succession process apparently goes in both directions as a toxic population emerged again in summer 2011 (Fig. 33.3).

33.1.5 Implication of Cyanotoxins for Water Quality

Lake Kinneret is used as a major source for water supply, and as such the types and quantities of cyanotoxins are regularly monitored. Water supplied from Lake Kinneret is treated by various technical means to improve its quality. Monitoring of cyanotoxins ensures that the treatment facilities efficiently remove the toxins and that water supplied to consumers is free of cyanotoxins or at least contains substantially reduced concentrations. Advanced filtration techniques efficiently remove *Microcystis* colonies from the pumped water and thereby eliminate most of the MCs associated with the biomass. The removal of soluble CYN requires an alternative approach. An earlier study suggested that water chlorination imposed degradation of the CYN molecule and yielded nontoxic derivatives (Senogles et al. 2000; Banker et al. 2001).

Although many countries adopted the World Health Organization (WHO) provisional standard of MC-LR (1 μg L^{-1}MC-LR) for drinking waters, such a standard has only recently been accepted by the Israeli law. In 2005, a governmental committee reassessed and updated the regulation for the drinking water of Israel. The committee recommended to adopt the WHO provisional standard and to prepare a comprehensive monitoring program to ensure toxin detection in water and to develop an emergency action plan in case cyanotoxins are at a level that creates a health hazard (see page 24 in http://www.health.gov.il/Subjects/Environmental_Health/Documents/water_Adin.pdf). These recommendations were recently approved by a legislative act. A coordinated monitoring activity and information exchange is common practice for the Kinneret Limnological Laboratory (IOLR), the Mekorot Water Company, and other local water utilities that pump water from Lake Kinneret, to assure a cyanotoxin-free water supply at local and national levels.

33.2 Pesticide Residues in the Waters and Fish of Lake Kinneret and the Jordan River

David Wynne, Rita Parparov, Edit Leibowitz

Although Lake Kinneret is used for recreation and tourism, as well as supporting an active fishing industry, its primary role is to supply drinking water to other parts of the country via the National Water Carrier (NWC). The catchment area of Lake Kinneret is a site of intense agricultural practices (see Chap. 30) with the concomitant use of many types and large quantities of pesticides. The term "pesticides" used here is a collective reference to all the different types of toxic chemicals and includes insecticides, herbicides, and fungicides, as listed in Table 33.1. Clearly, the levels of pesticides in the water of a major source of drinking water supply are a matter of vital national concern. Furthermore, since many of these compounds are highly toxic to fish, algae, and other aquatic organisms, their presence may seriously affect the ecology of the lake.

Monitoring of pesticides in Lake Kinneret has been carried out since the late 1970s. Initially, only organochlorine and some organophosphorus compounds were analyzed using a gas chromatograph with electron capture detector, GC-ECD (Wynne 1986). This study showed that Kinneret water (KW) and fish contained many pesticide residues but most of them could not be quantitated with the analytical instrumentation available at the time. The analytical capability of the laboratory was greatly expanded with the upgrade to a high-performance gas chromatograph fitted with a mass-selective detector (GC-MS) in 2000. This chapter summarizes the presence and changes of pesticide residues detected in water samples from Lake Kinneret and the Jordan River and in fish samples from the lake, over the past decade.

Surface water samples were taken regularly from stations A, J, D, and H in the lake and from the Jordan River at the Arik Bridge (station locations in Fig. 1.1 of Chap. 1). From 2007, station K was added and sampling frequency at all stations was increased to bimonthly. Water samples (1 L) were extracted twice with hexane, the combined extracts dried over anhydrous sodium sulfate and reduced in volume on a rotary evaporator. The concentrated extract was then adjusted to a final volume of 1 ml and kept at −20 °C until analyzed. Fish samples were collected from random sampling of fish landings and from the lake to determine "threshold" concentrations of pesticides in Kinneret fish. Additional fish samples from fish kill events were analyzed to determine whether the fish were poisoned. For both types of fish samples, the gills were removed, ground up with anhydrous sodium sulfate, extracted with hexane overnight, then dried, and reduced in volume. Extracts were then cleaned up from substances that might interfere in subsequent analytical procedures by chromatography on a short column of Florisil and the pesticides eluted with a mixture of 15 % (v/v) diethyl ether in petroleum ether. Extracts were then processed as described above for the water samples.

Table 33.1 Pesticide residues detected in water from Lake Kinneret (five stations) and in Jordan River waters (at Arik Bridge). Maximum, average, and standard error (se) for all positive samples (i.e., pesticide detected), and for all samples (including those in which the pesticide was not detected) taken from 2001 to 2011. Also given is the percentage of detected samples in total samples

Compound name, chemical group, and type of pesticide			Lake Kinneret (all stations) 2001–2011 (775 samples)						Jordan River 2001–2011 (97 samples)					
Compound	Chem. group[a]	Pest. type[b]	Positive samples only (ng L^{-1})				All samples (ng L^{-1})		Positive samples only (ng L^{-1})				All samples (ng L^{-1})	
			% Positive	Max	Avg	s.e.	Avg	s.e.	% Positive	Max	Avg	s.e.	Avg	s.e.
Alachlor	OC	H	4	800	78.7	27.9	3.4	6.3	11	330	69.2	34.0	7.8	12.8
Aldrin	OC	I	3	1,600	160	66.9	5.6	13.5	1.0	40	0.0	0.0	0.4	4.1
Ametryn	ONT	H	0.6	30	13.4	6.0	0.1	0.6	3	110	43.0	33.5	1.3	6.5
Amitraz	ON	I	6	3,500	339	103	21.4	28.2	12	2,030	458	195	57.3	79.7
Atrazine	ONT	H	25	1,080	26.7	5.7	6.8	3.0	4	40	22.8	7.0	0.9	2.6
α-HCH	OC	Is	3	120	43.8	5.9	1.4	1.9	2	28	15.0	13.0	0.3	2.0
β-HCH	OC	Is	4	1,100	164	44.4	6.1	10.2	0	n.d.			n.d.	
γ-HCH (lindane)	OC	I	4	210	43.7	9.3	1.6	2.3	2	110	57.0	53.0	1.2	7.9
δ-HCH	OC	Is	2	400	50.3	23.2	1.1	3.8	1.0	10	0.0	0.0	0.1	1.0
Captan	ON, OC	F	4	4,100	449	143	16.8	31.4	2	320	210	110	4.3	24.0
Chlorpyrifos	OP	I	12	3,800	192	58.4	23.6	21.4	23	1,900	147	84.3	33.8	41.8
p, p-DDD	OC	M	4	460	48.7	16.9	2.1	3.8	6	241	47.6	38.9	2.9	10.1
p.p-DDE	OC	M	10	1,200	45.8	16.3	4.7	5.4	12	290	43.3	25.9	5.4	9.7
p, p-DDT	OC	I	4	1,100	138	43.1	6.0	10.1	4	40	16.8	8.7	0.7	2.3
Diazinon	OP	I	16	1,100	32.0	11.0	5.0	4.5	16	500	48.1	31.1	7.9	13.1
Dibrom (naled)	OP	I	4	3,370	424	137.8	16.9	31.0	3	310	220	52.0	6.8	23.3
Dichloroben-zene	OC	I, F	0.3	20	15.0	5.0	0.0	0.6	0	n.d.			n.d.	
Dichlorvos	OP	I	8	1,900	122	37.5	9.5	11.2	12	300	90.1	31.6	11.1	13.7
Dieldrin	OC	I	12	2,580	131	35.8	15.6	13.1	15	1,610	266	125	41.2	53.8

Table 33.1 (continued)

Compound name, chemical group, and type of pesticide			Lake Kinneret (all stations) 2001–2011 (775 samples)						Jordan River 2001–2011 (97 samples)					
Compound	Chem. group[a]	Pest. type[b]	Positive samples only (ng L^{-1})				All samples (ng L^{-1})		Positive samples only (ng L^{-1})				All samples (ng L^{-1})	
			% Positive	Max	Avg	s.e.	Avg	s.e.	% Positive	Max	Avg	s.e.	Avg	s.e.
Dimethoate	OP	I	0.4	290	112	89.3	0.4	6.1	2	2,170	1,145	1,025	23.6	156
Dinocap	ON	F	11	16,200	479	214	55.0	74.0	9	650	248	75.9	23.0	32.6
Diphenyl-amine	ON	I, F	13	770	63.0	11.6	8.1	4.7	21	90	24.8	5.8	5.1	3.4
Disulfaton (disyston)	OP	I	1.3	5,880	680	582	8.8	67.3	0	n.d.			n.d.	
α-Endosulfan	OC	I	9	1,300	191	38.7	16.3	13.0	8	630	162	74.5	13.4	25.6
β-Endosulfan	OC	Is	2	690	113	49.7	2.2	7.8	1.0	73			0.8	7.4
Endosulfan sulfate	OC	M	2	400	97.0	29.4	1.6	5.0	2	6	3.50	2.50	0.07	0.44
Endrin	OC	I	0.3	190	102	88.5	0.3	4.8	1.0	500			5.15	50.8
Endrin aldehyde	OC	M	9	14,600	537	245	48.5	75.5	10	400	202	47.6	20.8	24.3
Ethion	OP	I	0.6	2,120	663	389	4.3	36.7	2	6,500	3,267	3,234	67.4	467
Ethoxyquin	Q	F, P	2	810	150	60.8	3.5	10.5	2	39	23.0	16.0	0.47	2.84
Fenitrothion	OP	I	6	2,500	442	85.3	25.6	25.5	5	310	132	52.3	6.8	16.9
Fenthion	OP	I	3	230	33.4	11.0	1.08	2.26	3	50	24.3	13.1	0.75	3.09
Heptachlor	OC	I	2	510	95.1	34.9	1.84	5.79	0	n.d.			n.d.	
Heptachlor epoxide	OC	M	0.5	780	378	172	1.95	17.3	1.0	62			0.64	6.30
Malathion	OP	I	0.5	540	144	132.0	0.74	9.71	0	n.d.			n.d.	
Methamido-phos	OP	I	3	1,850	197	81.4	6.09	15.7	3	120	43.3	38.3	1.34	7.04
Methidathion	OP	I	1.2	400	59.0	43.2	0.69	4.87	4	120	49.5	25.1	2.04	6.65

Table 33.1 (continued)

Compound name, chemical group, and type of pesticide			Lake Kinneret (all stations) 2001–2011 (775 samples)						Jordan River 2001–2011 (97 samples)					
Compound	Chem. group[a]	Pest. type[b]	Positive samples only (ng L^{-1})				All samples (ng L^{-1})		Positive samples only (ng L^{-1})				All samples (ng L^{-1})	
			% Positive	Max	Avg	s.e.	Avg	s.e.	% Positive	Max	Avg	s.e.	Avg	s.e.
Methoxychlor	OC	I	0.4	2,400	141.7	627	5.48	60.0	2	90	55.0	35.0	1.13	6.60
Monocrotophos	OP	I	4	4,500	433	153	16.8	33.3	9	1,700	355.9	173.4	33.0	60.8
Parathion	OP	I	1.2	670	137	69.5	1.59	8.60	2	410	315.0	95.0	6.5	33.3
Permethrin	Pyr	I	8	3,790	205	82.0	15.6	23.5	8	790	141.4	99.0	11.7	30.1
Phenamiphos	OP	N	0.6	300	188	32.3	0.97	6.34	3	990	369.3	311.8	11.4	58.3
Phorate	OP	I	0.6	500	200	92.8	1.29	9.78	3	7	4.67	1.20	0.14	0.50
Phosdryn	OP	I	5	420	52.4	12.9	2.71	3.42	3	480	236.7	125.7	7.3	29.9
Pirimiphos Me	OP	I	0.4	360	124	118	0.48	7.47						
Prometryn	ON, T	H	3	190	15.2	7.4	0.49	1.41	6	23	15.7	3.4	1.0	1.7
Simazine	ON, T	H	5	2,890	344	105	18.2	26.7	7	810	313.4	128.5	22.6	44.5
Simetryn	ON, T	H	3	770	177	49.5	4.8	10.1	3	84	28.4	27.8	0.88	4.92
Terbuthylazine	ON, T	H	1.4	70	17.4	6.82	0.25	0.99	5	140	34.4	26.5	1.77	6.40
Terbutryne	ON, T	H	19	280	10.8	2.77	2.06	1.26	10	590	67.4	58.1	6.94	19.0
Trichlorobenzene	OC	M	0.1	150			0.19	5.39	1.0	250			2.58	25.4
Trifluralin	ON, OF	H	0.5	40	25.5	8.41	0.13	1.05	1.0	4			0.04	0.41

[a] Chemical group key: *OC* organochlorine, *ON* organonitrogen, *ONT* organonitrogen (triazine), *OP* organophosphorus, *OF* organofluoride, *Pyr* pyrethroid, *Q* quinolone

[b] Pesticide key: *I* insecticide, *F* fungicide, *H* herbicide, *N* nematocide, *M* metabolite, *Is* isomer, *P* plant growth regulator

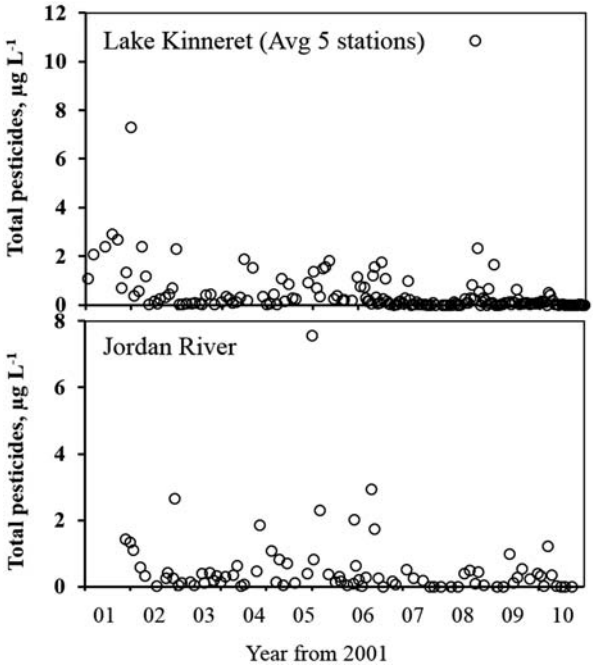

Fig. 33.4 Temporal changes in total pesticide (Tot pests) concentrations (µg L^{-1}) in water from Lake Kinneret (*upper panel*; average of five stations) and from the Jordan River at the Arik Bridge (*lower panel*), 2001–2011

Pesticide residues in the extracts were analyzed on a GC-MS. The pesticides were separated on a capillary column and identified and quantitated based on their retention times and mass spectra, as compared to those of a standard mixture of 58 different pesticides and their breakdown products. The standard mixture includes pesticides and some of their breakdown products currently (and in the past) in use in agriculture in the Upper Galilee (e.g., Bar-Ilan et al. 2002; Melman and Bar-Ilan 2011; Gerstl et al. 2012) and which can be successfully measured by GC-MS. Some pesticides, such as glyphosate (Round-up®), a herbicide used in large quantities in Israel, or the carbamate insecticide aldicarb (Temik®), cannot be analyzed by GC-MS and were, therefore, not included in the standard mixture.

33.2.1 Pesticides in Lake Kinneret and Jordan River Waters

The concentrations of all the pesticide residues detected in Lake Kinneret water were summed to give the total concentration of pesticides for each sampling date (Fig. 33.4). The maximal total pesticide concentration (found at a single sampling station) was 16.5 µg L^{-1}, with an overall average (± standard error, ± s.e.) of 0.4 (±0.048) µg L^{-1}. In Jordan River waters, the maximum pesticide concentration was 7.6 µg L^{-1}, with an average (± s.e.) of 0.5 (±0.11) µg L^{-1}.

The percent of positive samples and the maximum and average concentrations of different pesticide residues detected in KW and Jordan River water at Arik Bridge

(JW), between 2001 and 2011, are shown in Table 33.1. The highest percentage of positive detection in KW was for the herbicide atrazine (25% of all samples); some chemicals (e.g., hexachlorobenzene and methyl parathion) were never detected in KW. Six compounds, the insecticides chlorpyrifos, diazinon, dieldrin, diphenylamine, p, p-dichlorodiphenyldichloroethylene (DDE; a breakdown product of the insecticide dichlorodiphenyltrichloroethane, DDT) and the herbicide terbutryne, were detected in >10% of the KW samples. Some, but not all of these, were also the most commonly detected pesticides in JW; chlorpyrifos and diphenylamine were present in >20% of JW samples (Table 33.1). The maximum concentrations of pesticides in KW were for dinocap (16.2 μg L^{-1}) and endrin aldehyde, a metabolite of endrin (14.6 μg L^{-1}), but these high values occurred only on a single occasion each. Both substances were found in numerous other samples of KW but at much lower concentrations. In KW, the maximum measured concentrations exceeded 1 μg L^{-1} for 23 compounds (aldrin, amitraz, atrazine, β-BHC, captan, chlorpyrifos, DDE, DDT, diazinon, Dibrom, dichlorvos (DDVP), dieldrin, dinocap, disulfaton (disyston), endrin aldehyde, α-endosulfan, ethion, fenitrothion, methamidophos, methoxychlor, monocrotophos, permethrin, simazine). For JW samples, the highest concentration recorded was 6.5 μg L^{-1} for ethion; concentrations of seven compounds (amitraz, chlorpyrifos, dieldrin, dimethoate, ethion, monocrotophos, phenamiphos) exceeded 1 μg L^{-1}. Six compounds (β-BHC, dichlorobenzene, disulfaton, heptachlor, malathion, and methyl pyrimiphos) were not detected in JW but were found in KW samples (Table 33.1). Presumably, these compounds must have entered the lake from sources, presently unknown, other than the Jordan River.

A significant finding of this study was the frequent detection in KW of organochlorinated substances (such as aldrin and dieldrin, isomers of BHC, DDT, and its breakdown products) that have been banned for many years from use in Israel. These chemicals can bind to inert particles in the water column and end up in the sediment from where they may be released again into the lake water. Preliminary studies with sediment cores suggest that this process could have a major role in the recycling of pesticide residues in the lake (Wynne and Parparova 2002; Wynne, unpublished data).

The results presented here were initially based on total pesticide concentrations, averaged over the entire lake (Fig. 33.4). These results were expanded in order to separately include some of the different chemicals in the standard mixture used to calibrate the GC-MS. Concentrations of the organochlorine insecticide, aldrin, and two triazine herbicides, atrazine and terbutryne, in water from stations A and H exhibited strong temporal changes over the study period (Fig. 33.5). Atrazine concentrations were high during spring 2004, then again during summer 2007. Terbutryne showed an additional peak during winter 2010. Aldrin showed a peak at the beginning of the study but was not detected subsequently. Both sampling stations showed similar temporal patterns of these chemicals. It can be surmised that both herbicides were washed into the lake during the winter rainy season. However, Aldrin has been banned from use in Israel for many years and was hardly detected in Jordan River water. Aldrin, like many other organochlorinated compounds, binds strongly to organic material in the lake water and settles in the sediment where

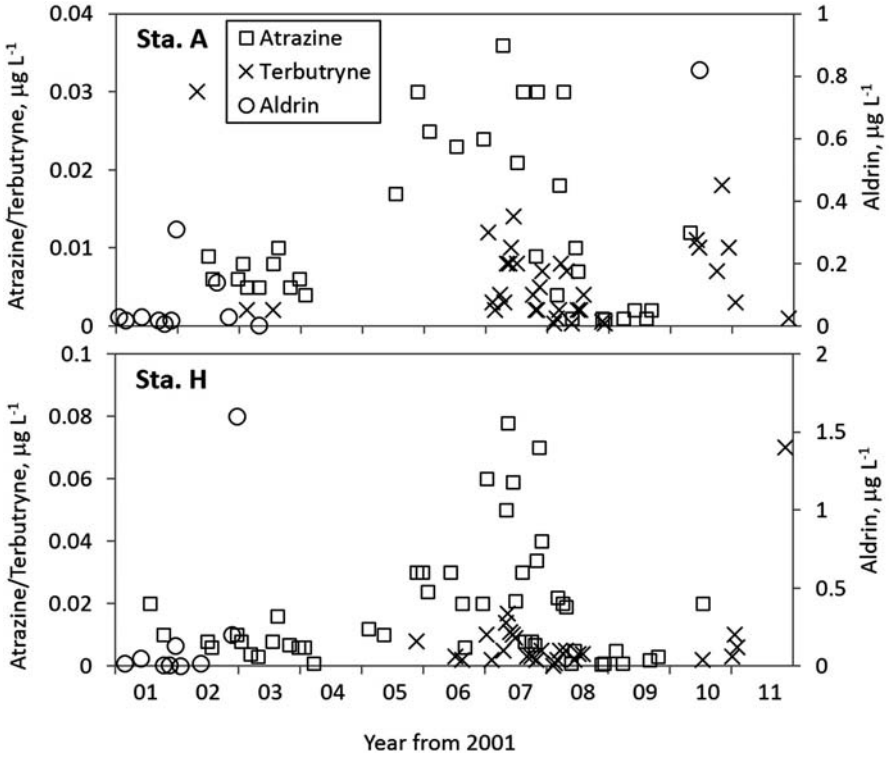

Fig. 33.5 Temporal changes in the concentrations of the organochlorine pesticides aldrin, atrazine, and terbutryne in water from Lake Kinneret at stations A (*upper panel*) and H (*lower panel*). For clarity, only positive values are shown. At Sta. A, the proportion of determinations below detection limit were 93, 75, and 75 % for aldrin, atrazine, and terbutryne. At Sta. H, the proportions were 94, 73, and 78 %, respectively

it may be re-released from the particulate matter, through biological or chemical processes.

33.2.2 Pesticide Toxicity Index

The pesticide toxicity index (PTI), developed by the US Geological Service (Munn and Gilliom 2001), was used to quantitatively assess the degree to which serious pesticide pollution of KW and JR waters may have occurred. The PTI for a given pesticide is determined as:

PTI = Pesticide concentration/Pesticide toxicity

The toxicity was taken as the 96-h 50 % lethal concentration (LD_{50}) measured against the freshwater fish, bluegill (*Lepomis macrochirus*) as the test species. While bluegill does not occur in Lake Kinneret, the toxicities (LD_{50}) of a large num-

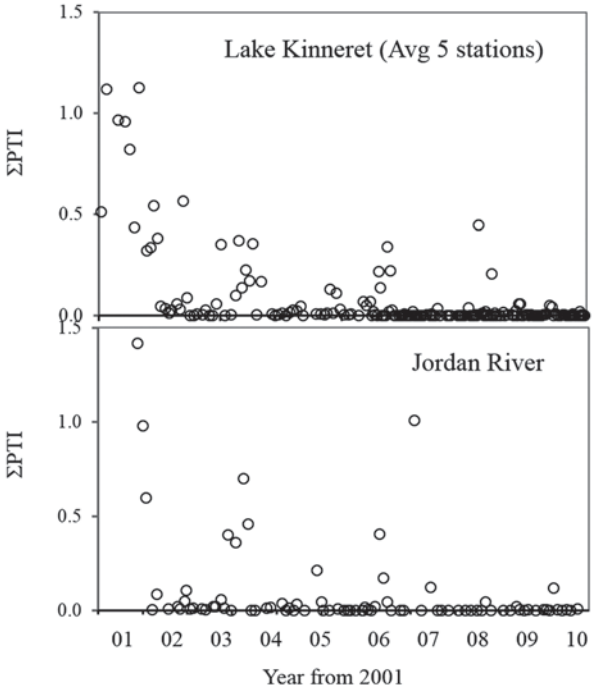

Fig. 33.6 Changes in the total pesticide toxicity index, *ΣPTI* (see text), in water samples from Lake Kinneret (*upper panel*; average of 5 stations) and from the Jordan River (*lower panel*), at the Arik Bridge, 2001–2011

ber of pesticides and related chemicals have been evaluated with this species and are widely available (e.g., Kegley et al. 2010). Although the PTI does not determine whether water in a sample is toxic, it can be used to rank or compare the relative toxicity of samples for use in further analysis or additional assessments. Application of the PTI has several other limitations (Munn and Gilliom 2001), but nevertheless, this index is useful when comparing the potential significance of pesticides at different sampling dates on a common basis; for evaluating relations between pesticide exposure and observed biological conditions, and to indicate where further studies are needed.

The PTI values for all the pesticide residues detected in KW at all stations were summed to give the total PTI value (ΣPTI) for each sampling date (Fig. 33.6). The maximal value of ΣPTI in KW (all sampling stations) was 1.12, with an average (± s.e.) of 0.047 (±0.006). In Jordan River waters, the maximum ΣPTI value was 1.42, with an average (± s.e.) of 0.094 (±0.027). The data in Fig. 33.3 indicate that the levels of pesticide pollution in KW have improved since 2000–2003 and have remained low despite isolated peaks that may result from exceptional events such as spills and poisonings. By contrast, relatively high ΣPTI occurred sporadically in Jordan River waters throughout the study period, although no such events have been recorded since the end of 2008. Only continued monitoring will determine if the low pesticide pollution levels will be maintained in both KW and JR waters. Such a monitoring strategy should include the measurement of pesticide transformation products, where possible, as well as sampling during the first rains of each year when the runoff of pesticides to the rivers would be high.

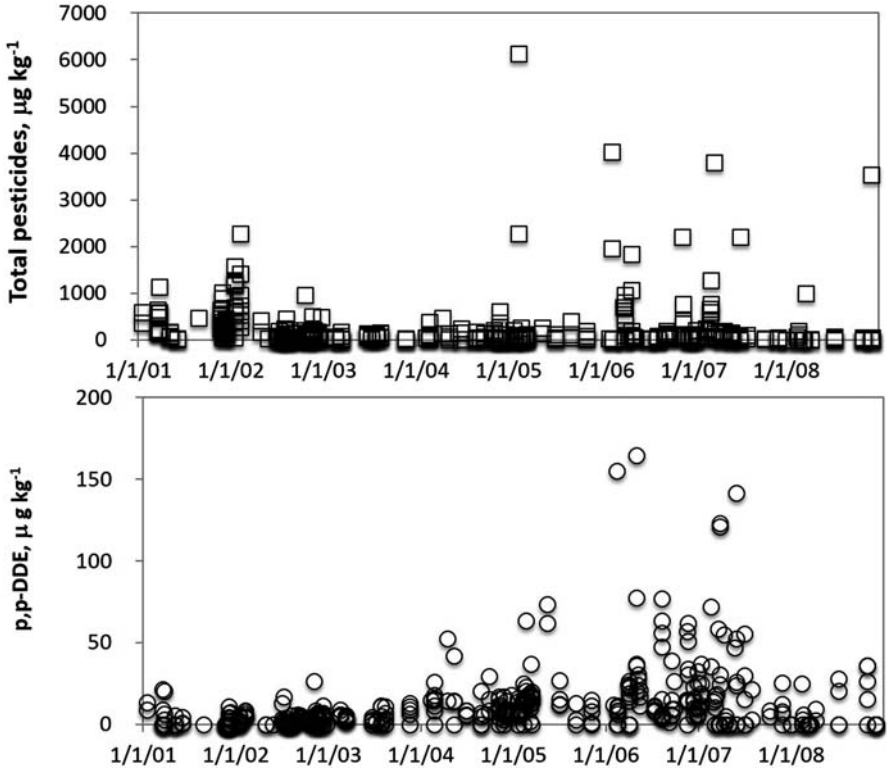

Fig. 33.7 Seasonal changes in total pesticide (Tot pests) concentrations (*upper panel*) and DDE concentrations (*lower panel*) in fish from Lake Kinneret, 2001–2008. Outliers were excluded from the DDE figure

33.2.3 Pesticide Levels in Kinneret Fish

Many suspected cases of accidental or deliberate fish poisonings have occurred in Lake Kinneret since the monitoring of pesticides has began (Table 33.2). DDE, a breakdown product of DDT, was found in 74 % of the fish samples analyzed, reaching DDE concentrations of up to 3,544 µg kg^{-1} (fish tissue) and total pesticides up to 6,000 µg kg^{-1} (Table 33.2, Fig. 33.7).

Two species of fish from Lake Kinneret, *Carasobarbus canis* and *Liza Ramada,* were analyzed to determine "threshold" levels of pesticides (Table 33.3). Nineteen pesticide residues (aldrin, α-BHC, β-BHC, γ-BHC (lindane), dichlorobenzene, dichlorvos, dinocap, endrin aldehyde, ethion, fenitrothion, heptachlor, methidathion, parathion, parathion me, PCNB, phosdryn, prometryn, trichlorobenzene, and trifluralin) were not found in either of the test species and have been omitted from Table 33.3, for clarity. Again, DDE was found in ~50 % of the fish analyzed, the average concentration in all tested fish was of 11.5 and 24.4 µg kg^{-1} in *C. canis* and *L. ramada,* respectively. The organochlorine insecticide α-endosulfan (Thionex®)

Table 33.2 Pesticide residues in fish from Lake Kinneret, 2001−2008 (all fish samples, including events of suspected poisoning, a total of 451 fish tested). % indicates the proportion of all samples that had positive values. Maximum, average, and standard error (se) for all positive samples (i.e., pesticide detected), and for all samples (including those in which the pesticide was not detected) taken from 2001 to 2011

Compound	Positive samples only (μg kg^{-1})				All samples (μg kg^{-1})	
	%	Max	Avg	s.e.	Avg	s.e.
Alachlor	1.3	14.8	8.8	2.7	0.12	0.50
Aldrin	5.3	30.4	8.8	1.8	0.47	0.58
Ametryn	18.6	456	55.2	9.4	10.3	4.70
Amitraz	11.1	443	41.8	11.3	4.60	4.20
Atrazine	4.7	16.1	3.2	0.8	0.15	0.22
α-BHC	4.9	132	14.4	6.7	0.70	1.60
β-BHC	3.8	156	25.4	10.0	0.96	2.20
γ-BHC (lindane)	5.5	36.5	10.5	1.7	0.58	0.62
δ-BHC	2.2	99.9	19.5	9.2	0.43	1.60
Captan	1.6	6,100	1,821	858	28.3	130.6
Chlorpyriphos	6.9	927	52.1	29.7	3.60	8.02
p, p-DDD	10.0	59.6	5.2	1.8	0.52	0.60
p, p-DDE	73.6	3,544	26.1	10.7	19.2	9.20
p, p-DDT	16.4	507	24.3	7.5	4.00	3.20
Diazinon	2.9	6.7	3.1	0.5	0.09	0.17
Dibrom	3.3	161	31.7	10.7	1.06	2.40
Dichlorobenzene	4.9	1,019	211	70.0	10.3	17.96
Dichlorvos	8.4	114	15.8	3.7	1.33	1.29
Dieldrin	31.5	1,900	116.1	23.4	36.60	13.90
Dimethoate	0.2	0.1	0.1		0.00013	0.0028
Dinocap	4.2	133	56.8	7.7	2.40	3.04
Diphenylamine	14.4	3,751	66.9	57.6	9.60	22.0
Disulfoton	4.4	800	251	57.6	11.1	16.5
Endosulfan SO_4	1.1	22.3	7.5	3.8	0.08	0.50
α-Endosulfan	18.2	1,927	203	42.9	36.9	20.2
β-Endosulfan	2.2	275	55.6	29.5	1.20	4.90
Endrin	1.3	36.0	14.5	5.2	0.19	0.87
Endrin ald.	7.3	366	91.8	15.3	6.70	5.80
Ethoxyquin	3.8	32.9	7.5	2.4	0.28	0.57
Fenitrothion	9.3	381	54.0	13.7	5.00	4.80
Fenthion	3.1	30.5	10.1	2.3	0.31	0.62
Heptachlor	2.9	20.8	9.5	1.5	0.28	0.51
Heptachlor epoxide	0.4	1.0	0.7	0.3	0.0032	0.04
Hexachlorobenzene	2.4	48.3	10.0	5.1	0.24	0.89
Malathion	0.9	55.7	23.0	11.3	0.20	1.42
Methamidophos	0.9	228	69.1	53.6	0.61	5.45
Methoxychlor	0.2	1.3	1.3		0.0029	0.06
Methidathion	4.7	32.1	11.1	2.1	0.52	0.68
Monocrotophos	2.2	187	37.8	17.5	0.84	3.03
Parathion	1.3	74	18.8	11.1	0.25	1.46
Parathion Me	0.2	6.8	6.8		0.02	0.32
Permethrin	11.8	182	31.3	5.3	3.70	2.27
Phenamiphos	0.9	25.2	17.0	4.8	0.15	0.89

Table 33.2 (continued)

Compound	Positive samples only (μg kg^{-1})				All samples (μg kg^{-1})	
	%	Max	Avg	s.e.	Avg	s.e.
Phorate	14.4	171	15.1	4.0	2.20	1.64
Phosdryn	3.1	26.4	5.6	2.2	0.17	0.46
Prometryn	0.9	38.6	16.2	8.4	0.14	1.02
Simazine	4.2	204	42.6	14.9	1.80	3.58
Simetryn	6.0	171	39.5	7.6	2.40	2.57
Terbuthylazine	22.4	205	38.4	5.4	8.60	3.00
Terbutryne	0.2	0.4	0.4		0.0009	0.0189
Trichlorobenzene	2.2	46.0	12.5	4.5	0.28	0.86
Trifluralin	0.2	0.5	0.5		0.0011	0.024

has been implicated in many suspected fish poisonings. In the threshold study, this substance was detected in 22 and 18 % of the samples of *C. canis* and *L. ramada,* respectively (Table 33.3), but its average concentrations (1.3–3.8 μg kg^{-1}) were much lower than those found in Kinneret fish after suspected poisoning events.

The data presented here suggest that DDE, DDT, and other organochlorinated pesticides can bind to sediment particles and are then slowly released to the water column by mechanical and/or biological processes. Preliminary data have shown that endosulfan, DDE, DDT, and γ-BHC (lindane) can bind to lake sediments (Wynne and Parparova 2002) but further studies are required in order to understand the factors involved in the binding of these chemicals to particulate matter in the lake and their release back into the aquatic phase.

33.2.4 Summary

- The maximal total pesticide concentration in KW for all the sampling stations was 16.5 μg l^{-1}, with an average (±s.e.) of 0.4 (±0.048) μg l^{-1}. The pattern of annual changes in total pesticide concentrations for all Kinneret stations was similar. In Jordan River waters, the maximum total pesticide concentration was 7.6 μg l^{-1}, with an average (±s.e.) of 0.5 (±0.11) μg l^{-1}.
- Organochlorine substances (such as aldrin and dieldrin, isomers of BHC, DDT, and its breakdown products) that have been banned for many years from use in Israel, were detected frequently in KW. Since these chemicals can bind to inert particles in the water column, they may settle out in the sediment of the lake where they can be released into the lake water by various chemical and/or biological processes. Factors involved in the binding and release of pesticides to particulate matter are still not fully understood
- Studies on potential sources of pesticides into Lake Kinneret need to be expanded, especially by extending sampling and analyses to other areas of the Kinneret watershed.
- ΣPTI values can be a good estimate of the potential toxicity of a particular water sample.

Table 33.3 "Threshold" pesticide concentrations (μg kg^{-1}) in the fish *Liza ramada* ("Buri") and *Carasobarbus canis* from Lake Kinneret, 2007–2009. Maximum, average, and standard error (s.e.) for all positive samples (i.e., pesticide detected), and for all samples (including those in which the pesticide was not detected)

Compound	*L. ramada* (32 fish)						*C. canis* (33 fish)					
	Positive samples only (μg kg^{-1})				All samples (μg kg^{-1})		Positive samples only (μg kg^{-1})				All samples (μg kg^{-1})	
	%	Max	Avg	s.e.	Avg	s.e.	%	Max	Avg	s.e.	Avg	s.e.
Alachlor	3	0.61	0.61		0.02	0.11	0					
Ametryn	3	0.5	0.5		0.02	0.09	0					
Amitraz	3	18	18		0.6	3.18	0				1.9	11.0
Atrazine	0						3	3.2	3.2		0.1	0.6
δ-BHC	6	18.6	11.8	6.8	0.7	2.4	0					
Captan	3	35.7	35.7		1	6.3	0					
Chlorpiriphos	3	14.9	14.9		0.5	2.6	0					
p, p-DDD	16	20.7	8.5	4.6	1.3	2.2	24	60	11.2	7.0	2.7	3.7
p, p-DDE	47	142	24.5	8.8	11.5	6.7	52	123	47.5	7.8	24.4	8.0
p, p-DDT	6	1.2	1	0.2	0.06	0.2	0					
Diazinon	3	1.2	1.2		0.04	0.22	9	4.9	2.9	1.0	0.3	0.5
Dibrom	6	139	75.6	63.2	4.7	17.4	3	57.7	57.7		1.7	10.0
Dieldrin	3	31.8	31.8		1	5.6	6	53.3	32.4	20.9	2.0	6.7
Dimethoate	6	8.4	5.5	3	0.34	1.1	0					
Diphenylamine	9	36.3	21.9	9	2.1	4.4	9	104	36.7	33.6	3.3	10.4
Disulfoton	0						6	10.8	9.5	1.3	0.6	1.6
α–Endosulfan	22	42.7	17.2	6.1	3.8	3.8	18	22.6	7.3	3.5	1.3	1.8
β-Endosulfan	3	11.5	11.5		0.4	2	0					
Endrin	0						12	36	15.1	7.1	1.8	3.3
Ethoxyquin	0						3	30.9	30.9		0.9	5.4
Fenthion	6	1.1	0.8	0.33	0.05	0.15	3	1.4	1.4		0.0	0.2
Heptachlor epoxide	3	1	1		0.03	0.18	3	0.4	0.4		0.0	0.1
Hexachlorobenzene	13	16.6	4.6	4	0.57	1.5	21	48.3	13.0	7.6	2.8	3.9
Malathion	3	55.7	55.7		1.7	9.8	0					
Methamidophos	16	135	41.1	23.9	6.4	10.9	15	60.3	33.0	12.4	5.0	6.9

Table 33.3 (continued)

Compound	*L. ramada* (32 fish)						*C. canis* (33 fish)					
	Positive samples only (μg kg^{-1})				All samples (μg kg^{-1})		Positive samples only (μg kg^{-1})				All samples (μg kg^{-1})	
	%	Max	Avg	s.e.	Avg	s.e.	%	Max	Avg	s.e.	Avg	s.e.
Methoxychlor	3	4.4	4.4		0.14	0.78	3	2	2.0		0.1	0.3
Monocrotophos	3	187	187		5.8	33.1	0					
Pyrimiphos Me	6	87.9	50	39	3.1	11	12	114	64.4	18.7	7.8	12.1
Permethrin	0						3	2.8	2.8		0.1	0.5
Phenamiphos	3	25.2	25.2		0.8	4.5	3	25.2	25.2		0.8	4.4
Phorate	0						6	47.5	25.6	21.9	1.6	5.9
Simazine	6	11.1	10.7	0.4	0.7	1.9	3	10.3	10.3		0.3	1.8
Simetryn	0						3	98.7	98.7		3.0	17.2
Terbuthylazine	6	152	80.7	71	5.0	18.9	12	22.1	10.8	5.6	1.3	2.5
Terbutryne	0						3	0.4	0.4		0.0	0.1

- Threshold studies have shown that when fish kills in the lake are not caused by external poisonings, the average pesticide concentrations in the fish are very low. Such a study needs to be expanded to include all commercially important fish species.

33.3 Fecal Bacterial Indicators

Ora Hadas, Riki Pinkas, Nehama Malinsky-Rushansky

Lake Kinneret serves as the main freshwater reservoir in Israel, besides being a recreational site and supporting a commercial fishery. The main inflow to the lake is the Jordan River, located in the north and draining the northern watershed, which is mainly an agricultural area. Heavy rainfalls over the Kinneret watershed in winter result in floods and storm water runoff picking up fecal contamination from droppings of farm animals and wildlife (Hadas 1988, Bergstein Ben-Dan and Stone 1991). In addition, winter streams from the Golan Heights and Galilee in the north east and west, respectively, overflow from man-made reservoirs containing treated sewage and a recently re-flooded agricultural area (Agmon in the Hula Valley) contribute large amounts of suspended particulate matter, nutrients, and fecal bacteria entering Lake Kinneret. In the south, the Yarmouk River diversion canal is another inlet during winter, transferring excess floodwater into the lake and all constitute potential sources of pollution to Lake Kinneret. Water intakes and bathing beaches are spread along the lake shores serving a large number of users and visitors; therefore, the bacterial quality of the water is of utmost importance.

Good quality drinking water should be devoid of microbial pathogens. However, those pathogens are often difficult to identify and quantify. For this reason, microbial indicators, especially fecal bacterial indicators, which are easier to detect and enumerate, are often used for monitoring the microbial quality of the water rather than the pathogens themselves. In order to indicate the occurrence of a recent contamination by pathogens of fecal origin, the indicator organism should: (1) always be present when the source of the pathogenic microorganism of concern is present, at the same time it should also be absent in clean uncontaminated water, (2) the indicator should be present in large numbers, (3) the indicator should respond to natural environmental conditions and to water and wastewater treatment processes in a manner similar to the pathogens of interest, and (4) the indicator should be easy to isolate, identify, and enumerate. The effectiveness of various key fecal bacterial indicator microorganisms in the assessment of water quality is questioned. Since there is no ideal water quality indicator, it is customary to monitor various indicators in parallel to provide the best information on the water body tested.

The distribution of several different fecal indicators has been monitored at different sites in Lake Kinneret since the 1980s. This monitoring included fecal coliforms, *Escherichia coli,* enterococci, *Clostridium perfringens,* and F male-specific

bacteriophages. *Aeromonas hydrophilla,* even though it is not an enteric bacterium, was monitored during some periods since it is known as a pathogen for fish and humans and it responds to changes in nutrient loads and trophic conditions in the water (Rippey and Cabelli 1980).

In the last decade, the monitoring program was revised, to exclude *C. perfringens* and F male-specific bacteriophages: waterborne transmission is insignificant in the epidemiology of diseases caused by *C. perfringens* (Bisson and Cabelli 1980), and *C. perfringens* was the indicator with the lowest numbers detected. F male-specific bacteriophages showed poor correlation with their potential hosts (*E. coli*), but in cases of acute fecal contamination they still may serve as an additional useful monitoring tool.

33.3.1 The Ongoing Monitoring Program

The monitoring program for the detection of fecal bacterial indicators was applied at 14 sites around the lake representing (1) inflows of the Jordan River and other streams, (2) recreational sites and bathing beaches, and (3) main water intakes (Fig. 33.8). The monitored bacteria were: (1) fecal coliforms, (2) *Escherichia coli,* and (3) enterococci. The membrane-filter (MF) procedure was used for most of the bacterial tests, and counts were expressed as colony-forming units per 100 mL of water, according to standard methods (APHA 2005). During flood events and high turbidity (at the Jordan River entrance to the lake), the most probable number (MPN) method (APHA 2005) was applied.

33.3.2 Jordan River Inlet

The abundance of fecal bacterial indicators at the Jordan River mouth usually ranged between <10 and 2,000, depending on season and rain regime. However, during flood events and after the first heavy rain considerably higher numbers were monitored. The highest bacterial numbers were recorded during a flood event in March 1991, at the Jordan River inlet, with an exceptional maximal value of 26,400 fecal coliforms, 15,400 *E. coli,* and 4,673 enterococci per 100 mL (Fig. 33.9) and water turbidity of 540 NTU. High fecal bacteria numbers usually co-occurred with high turbidity values, as both were usually recorded during winter when heavy rains over the Kinneret watershed resulted in massive storm water runoff, picking particles, and bacteria, indicating that bacteria were attached to particles when entering the lake. Since the late 1990s, due to consecutive drought years and less precipitation with little storm water runoff, less fecal bacterial indicators entered the lake (Fig. 33.9).

In a focused research project (Hadas et al 2000), the distribution of bacteria and river alluvium at the mouth of the Jordan River was related to attenuation in velocity along the jet stream. The main processes occurring at the entrance of the Jordan

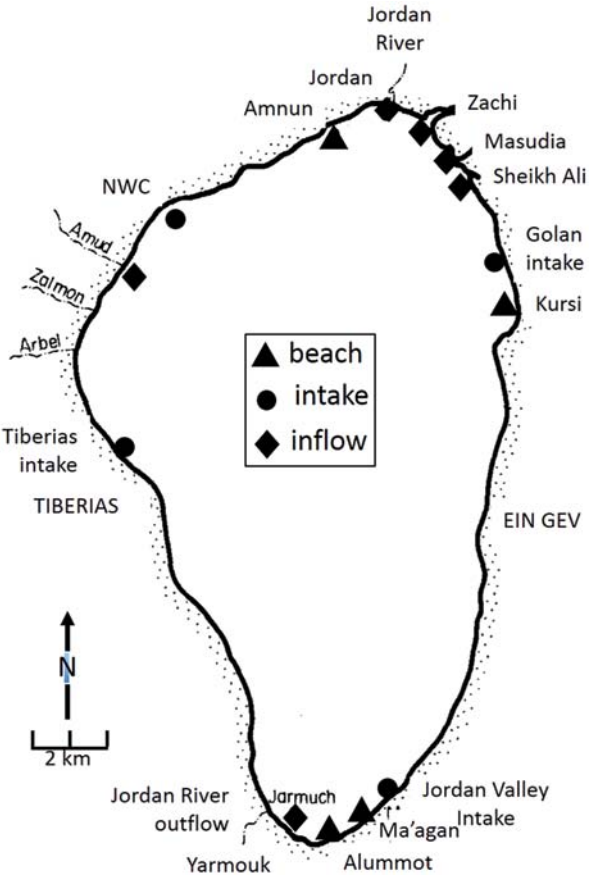

Fig. 33.8 Lake Kinneret sampling sites for fecal bacterial indicators, indicating three types of sampling sites: bathing beaches, water intake sites and river inflows

to the lake are mixing (dilution), sedimentation (deposition), and dispersion of sediments. At the entrance to the lake, flow velocity decreases and sediments are being deposited, forming a barrier bar ~100–200 m from the river mouth. In addition, the lake is more saline than the river (250 and 20 mg chloride L^{-1}, respectively), making it possible to trace the Jordan flow in the lake (Serruya 1974).

The fate of particles brought by the river to the lake was determined by mapping the distribution of (1) natural tracers such as pathogenic bacterial indicators (fecal coliforms), (2) chemical compounds and physical properties (chloride, dry weight), and (3) artificial tracers such as the distribution of fluorescently labeled particles. The strong gradient in salinity indicated rapid mixing and dilution processes near the inflow. The distribution of fecal coliforms, particles (dry weight), and fluorescent tracers showed that bacteria numbers in the water column decreased with distance from the river entrance with the smallest decrease along the southwest direction, suggesting that the flow of the river was strongest at this direction. Fecal coliform distribution was correlated with the particles bacteria are adhered to. When the river flow was slow, sedimentation processes dominated. Larger particles

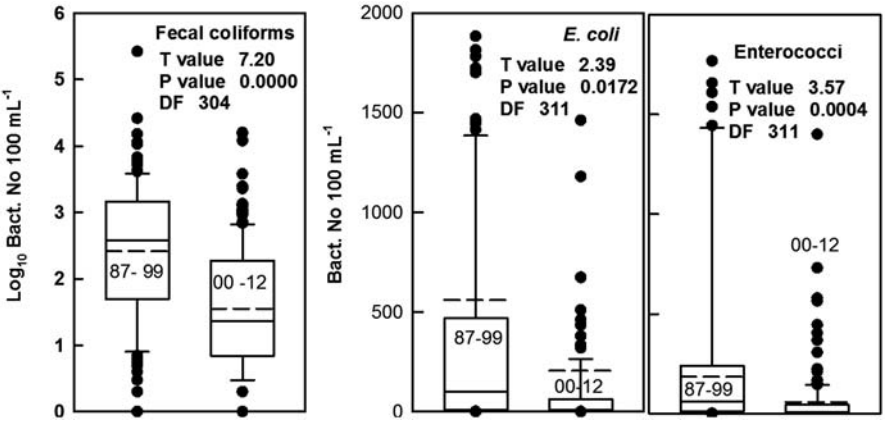

Fig. 33.9 Statistics on the abundance of bacterial fecal indicators at the Jordan River inlet to the lake during 1987–1999 as compared to 2000–2012. Fecal coliforms (Log bacteria No 100 mL^{-1}), *E. coli* and enterococci (Bacteria No 100 mL^{-1}). Box plot shows 5th/95th percentiles (*whisker caps*) and individual outlier points during flood events. Median (*solid line*), mean (*dashed line*)

to which bacteria were attached dropped out closer to the river mouth as compared to smaller particles or free bacteria that were transferred further into the lake. Bacterial distribution was similar to that of the fluorescent tracers, and consistent with current velocity attenuation along the river plume, implying similar physical forces and processes affecting both tracers at the river mouth.

This study has indicated that most of the suspended matter brought by the Jordan River is being deposited at the river mouth area, not more than 500 m from the entrance of the river to the lake. At discharges above 25–30 $m^3\ s^{-1}$, river material is transported southwest along the littoral zone of the western shore toward the intake of the NWC.

33.3.3 The National Water Carrier Intake

Sites of water intake (Fig. 33.8) usually had lower numbers of fecal bacteria indicators than inflows and bathing beaches (Figs. 33.9 and 33.10). The intake to the NWC, located in the northwestern part of the lake (Fig. 33.8) is influenced by the Jordan River inflow in the north (as mentioned above), especially during winter storms. In 1992, with exceptionally heavy rains (781 mm as compared to ~380 mm annual precipitation average), 365 fecal coliforms, 169 *E. coli*, and 555 enterococci per 100 mL were recorded at the NWC intake in February, still much lower numbers than those recorded at the same time at the Jordan River inlet (Figs. 33.9 and 33.10) and at the inflows of other streams (Zachi and Masudia stations, data not presented). These peak bacterial numbers decline within 48 h and numbers in the range of 0–100 per 100 mL were observed at most sampling dates thereafter, although peaks of >100 per 100 mL occurred also in the winters of 1994, 1996, 1998, and 2000 (Fig. 33.10).

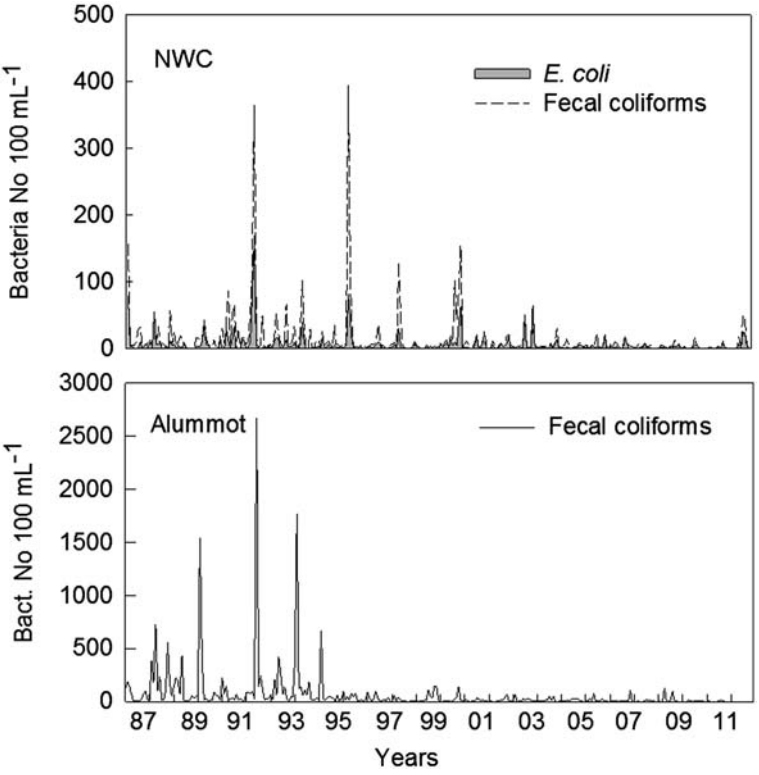

Fig. 33.10 Monthly averages of the abundance of bacterial fecal indicators (bacteria no. 100 mL^{-1}) at the National Water Carrier (*NWC*) and Alummot Beach during 1987–2012

33.3.4 Alummot Beach and Littoral

Alummot Beach at the south of the lake and close to the Yarmouk inlet was chosen as a representative of beach sampling stations. At this station, fecal coliform numbers varied from 0 to 2,668 bacteria 100 mL^{-1} (Fig. 33.10), while highest enterococci numbers, 974 bacteria 100 mL^{-1} were observed during late autumn and winter, after the first rains or as a result of Yarmouk excess water entering the lake nearby (data not shown).

A negative correlation was found between the abundance of fecal bacteria indicators in the littoral zone and the distance from the shoreline. In both water and sediments, higher bacterial numbers were found at sites where streams entered the lake as compared to bathing beaches. This reflects appropriate management of bathing beaches (Bergstein-Ben Dan and Koppel 1992). During the last decade, an effort of the Lake Kinneret Authority, in keeping the beaches around the lake supervised and in good sanitation conditions, resulted in continuously low counts (< 100 bacteria per 100 mL) of fecal indicators in the lake beaches, as seen for the Alummot Beach sampling site (Fig. 33.10).

33.3.5 Models Describing the Distribution of Fecal Bacterial Indicators

The dataset of counts of *E. coli,* enteroccoci, and fecal coliforms at several sites around Lake Kinneret, collected every 2–4 weeks during 1995–2002 showed irregular fluctuations punctuated by aperiodic outbursts of variable magnitude. Such patterns cannot be described by conventional population dynamic models or models derived from chaos theories. They could be described in terms of a probabilistic model, based on the truncated Laplace and extreme value distribution functions, with the counts substituted by their cubic root. The model was tested by comparing the observed frequencies of outbursts exceeding different levels in the second half of each record with those predicted with these two distribution functions, whose parameters had been determined from the data in the first half of the record. Despite the relatively short records and minor violations of the assumptions on which the model is based, there was a reasonable agreement between the estimated and actual frequencies. This demonstrated that it is possible to translate the microbial counts' fluctuation pattern into a set of probabilities or expected frequencies of future outbursts. At least in principle, these can be used to quantify the fecal contamination pattern associated with the water source and as a means to assess the efficacy of preventive measures to reduce it (Hadas et al 2004).

Referring to fecal bacterial pollution, the highest numbers of bacteria indicators studied were observed during the winter rainy season. Much higher numbers of bacteria were detected in the northern part of the lake, than in the south, with highest numbers at the Jordan River inlet. Since most of the fecal bacterial pollution was deposited at the Jordan River mouth and at the other streams entrances into the lake, the quality of Lake Kinneret water is generally good. Exceptions do occur, during flood events or in the case of failures in sewage maintenance of hotels and recreation sites.

Acknowledgments This chapter is based on monitoring and research activities supported by Israel Water Authority, Israel Ministry of Science and Technology (MOST), Israel Ministry of Environmental Protection, and German Ministry of Research and Technology (BMBF). AS would like to acknowledge knowledge sharing with European experts and researchers via the European Cooperation in Science and Technology, COST Action ES 1105.

References

Alster A, Kaplan-Levy R, Sukenik A, Zohary T (2010) Morphology and phylogeny of a non-toxic invasive *Cylindrospermopsis raciborskii* from a Mediterranean Lake. Hydrobiologia 639:115–128

American Public Health Association (2005) Standard methods for the examination of water and wastewater, 25th edn. American Public Health Association, Washington DC

Ballot A, Ramm J, Rundberget T, Kaplan-Levy RN, Hadas O, Sukenik A, Wiedner C (2011) Occurrence of non-cylindrospermopsin-producing *Aphanizomenon ovalisporum* and *Anabaena bergii* in Lake Kinneret (Israel). J Plankton Res 33:1736–1746

Banker R, Carmeli S, Hadas O, Teltsch B, Porat R, Sukenik A (1997) Identification of cylindrospermopsin in *Aphanizomenon ovalisporum* (Cyanophyceae) isolated from Lake Kinneret, Israel. J Phycol 33:613–616

Banker R, Carmeli S, Werman M, Teltsch B, Porat R, Sukenik A (2001) Uracil moiety is required for toxicity of the cyanobacterial hepatotoxin cylindrospermopsin. J Toxicol Environ Health A 62:281–288

Banker R, Teltsch B, Sukenik A, Carmeli S (2000) 7-Epicylindrospermopsin, a toxic minor metabolite of the cyanobacterium *Aphanizomenon ovalisporum* from Lake Kinneret, Israel. J Nat Prod 63:387–389

Bar-Ilan I, Peleg S, Melman G (2002) Organic contaminating compounds in waters of the upper Jordan Basin of Lake Kinneret in 2001. Migal, Kiryat Shmone, 469 pp (in Hebrew)

Beresovsky D, Hadas O, Livne A, Sukenik A, Kaplan A, Carmeli S (2006) Toxins and biologically active secondary metabolites of *Microcystis* sp. isolated from Lake Kinneret. Isr J Chem 46:79–87

Bergstein Ben-Dan T, Stone L (1991) The distribution of fecal pollution indicator bacteria in Lake Kinneret. Water Res 25:263–270

Bergstein-Ben Dan T, Koppel F (1992) Indicator bacteria for fecal pollution in the littoral zone of Lake Kinneret. Water Res 26:1457–1469

Bisson JW, Cabelli VJ (1980) *Clostridium perfringens* as a water pollution indicator. J Water Pollut Control Fed 52:241–248

Carmichael W (2008) A world overview-one-hundred-twenty-seven years of research on toxic cyanobacteria–where do we go from here? In: Hudnell HK (ed) Cyanobacterial harmful algal blooms: state of the science and research needs. Springer, New York. (Adv Exp Med Biol 619:105–126)

Gerstl Z, Nasser A, Lev O (2012) Monitoring of pesticides and organic pollutants in the Kinneret watershed. The Agricultural Research Organization. Bet Dagan and the Hebrew University, Jerusalem, pp 26 (in Hebrew)

Hadas O (1988) Pathogenic indicators in Lake Kinneret. Isr Toxic Assess 3:631–641

Hadas O, Shteinman B, Pinkas R (2000) Distribution of fecal coliforms in the Jordan River mouth originated from anthropogenic activities in the watershed. Water Sci Technol 42:129–133

Hadas O, Corradini MG, Peleg M (2004) Statistical analysis of the fluctuating counts of fecal bacteria in the water of Lake Kinneret. Water Res 38:79–88

Harada K, Fujii K, Shimada T, Suzuki M, Sano H, Adachi K, Carmichael WW (1995) Two cyclic peptides, anabaenopeptins, a third group of bioactive compounds from the cyanobacterium *Anabaena flos aquae* NRC 525-17. Tetrahedron Lett 36:1511–1514

Humpage AR, Falconer IR (2003) Oral toxicity of the cyanobacterial toxin cylindrospermopsin in male Swiss albino mice: determination of no observed adverse effect level for deriving a drinking water guideline value. Environ Toxicol 18:94–103

Ishida K, Kato T, Murakami M, Watanabe M, Watanabe MF (2000) Microginins, zinc metalloproteases inhibitors from the cyanobacterium *Microcystis aeruginosa*. Tetrahedron 56(44):8643–8656

Kaplan A, Harel M, Kaplan-Levy RN, Hadas O, Sukenik A, Dittmann E (2012) The languages spoken in the water body (or the biological role of cyanobacterial toxins). Front Microbiol 3:138. doi:10.3389/fmicb.2012.00138

Kegley SE, Hill BR, Orma S, Choi AH (2010) PAN pesticide database, Pesticide Action Network North America (PANNA), San Fransisco. http://www.pesticideinfo.org

Kinnear S (2010) Cylindrospermopsin: a decade of progress on bioaccumulation research. Mar Drugs 8:542–564

Lawton LA, Edwards C, Codd GA (1994) Extraction and high-performance liquid chromatographic method for the determination of microcystins in raw and treated waters. Analyst 119:1525–1530

Lifshitz M, Carmeli S (2012) Metabolites of *Microcystis aeruginos* a bloom material from Lake Kinneret, Israel. J Nat Prod 75:209–219

McElhiney J, Lawton LA, Leifert C (2001) Investigations into the inhibitory effects of microcystins on plant growth, and the toxicity of plant tissues following exposure. Toxicon 39:1411–1420
Melman G, Bar-Ilan Y (2011) Survey of the use of pesticides in the Kinneret water catchment area, 2010. Migal, Kiryat Shmone, 48 pp (in Hebrew)
Munn MD, Gilliom RJ (2001) Pesticide toxicity index for freshwater aquatic organisms, National Water-Quality Assessment Program, USGS Water-Resources Investigations Report # 01-4077, 61 pp, Water Resources Division, Sacramento, California 95819-6129, USA
Murakami M, Okita Y, Matsuda H, Okino T, Yamaguchi K (1994) Aeruginosin 298-A, a thrombin and trypsin inhibitor from the blue-green alga *Microcystis aeruginosa* (NIES-298). Tetrahedron Lett 35:3129–3132
Oberemm A, Fastner J, Steinberg, CEW (1997) Effects of microcystin-LR and cyanobacterial crude extracts on embryo-larval development of zebrafish (*Danio rerio*). Water Res 31:2918–2921
Okino T, Murakami M, Haraguchi R, Munekata J, Matsuda H, Yamaguchi K (1993) Mieropeptins A and B, plasmin and trypsin inhibitors from the blue-green alga *Microcysis acruginosa*. Tetrahedron Lett 34:8131–8134
Paerl HW, Paul VJ (2011) Climate change: links to global expansion of harmful cyanobacteria. Water Res 46:1349–1363
Pearson L, Mihali T, Moffitt M, Kellmann R, Neilan B (2010) On the chemistry, toxicology and genetics of the cyanobacterial toxins, Microcystin, Nodularin, Saxitoxin and Cylindrospermopsin. Mar Drugs 8:1650–1680
Pietsch C, Wiegand C, Ame MV, Nicklisch A, Wunderlin D, Pflugmacher S (2001) The effects of a cyanobacterial crude extract on different aquatic organisms: evidence for cyanobacterial toxin modulating factors. Environ Toxicol 16:535–542
Rantala A, Fewer DP, Hisbergues M, Rouhiainen L, Vaitomaa J, Börner T, Sivonen K (2004) Phylogenetic evidence for the early evolution of microcystin synthesis. Proc Natl Acad Sci U S A 101:568–573
Reisner M, Carmeli S, Werman M, Sukenik A (2004) The cyanobacterial toxin cylindrospermopsin inhibits pyrimidine nucleotide synthesis and alters cholesterol distribution in mice. Toxicol Sci 82:620–627
Reshef V, Carmeli S (2006) New microviridins from a water bloom of the cyanobacterium *Microcystis* aeruginosa. Tetrahedron 62:7361–7369
Rippey RS, Cabelli VJ (1980) Membrane filter procedure for enumerating *Aeromonas hydrophila* in fresh waters. Appl Environ Microbiol 38:108–113
Rücker J, Stüken A, Nixdorf B, Fastner J, Chorus I, Wiedner C (2007) Concentrations of particulate and dissolved cylindrospermopsin in 21 *Aphanizomenon*-dominated temperate lakes. Toxicon 50:800–809
Schatz D, Keren Y, Hadas O, Carmeli S, Sukenik A, Kaplan A (2005) Ecological implications of the emergence of non-toxic subcultures from toxic *Microcystis* strains. Environ Microbiol 7:798–805
Senogles P, Shaw G, Smith M, Norris R, Chiswell R, Mueller J, Sadler R, Eaglesham G (2000) Degradation of the cyanobacterial toxin cylindrospermopsin, from *Cylindrospermopsis raciborskii*, by chlorination. Toxicon 38:1203–1213
Serruya S (1974) The mixing patterns of the Jordan River in Lake Kinneret. Limnol Oceanogr 19:175–181
Spoof L, Neffling M-R, Meriluoto J (2010) Fast separation of microcystins and nodularins on narrow-bore reversed-phase columns coupled to a conventional HPLC system. Toxicon 55:954–964
Sukenik A, Hadas O, Kaplan A, Quesada A (2012) Invasion of Nostocales (cyanobacteria) to subtropical and temperate freshwater lakes—physiological, regional and global driving forces. Front Microbiol 3:86. doi:10.3389/fmicb.2012.00086
Törökné A, Asztalos M, Bánkiné M, Bickel H, Borbély G, Carmeli S, Codd GA, Fastner J, Huang Q, Humpage A, Metcalf JS, Rábai E, Sukenik A, Surányi G, Vasas G, Weiszfeiler V (2004) Interlaboratory comparison trial on cylindrospermopsin measurement. Anal Biochem 332:280–284

Wormer L, Cirés S, Carrasco D, Quesada A (2008) Cylindrospermopsin is not degraded by co-occurring natural bacterial communities during a 40-day study. Harmful Algae 7:206–213
Wynne D (1986) The potential impact of pesticides on the Kinneret and its watershed, over the period 1980–1984. Environ Pollut (Series A) 42(4):373–386
Wynne D, Parparova R (2002) Pollution of the Kinneret ecosystem 1980–1999: present considerations and future prospects. Verh Int Ver Limnol 28:1709–1712

Chapter 34
Water Quality Assessment

Arkadi Parparov, K David Hambright and Tom Berman

Abstract Water quality in Lake Kinneret was quantified using a system of indices for which water quality parameters and their permissible ranges were identified and defined through a modified Delphi expert panel process. We calculated an aggregate index of water quality (Composite Water Quality Index, CWQI) as a weighted average of rating values for the entire set of water quality indices, in which variable weights for a given index were inversely proportional to the rating value of that index. Since 1991, annual average CWQI showed a trend of deteriorating lake water quality, due mostly to increases in chloride concentration and relative cyanobacteria biomass. Annual variability in CWQI was explained mostly by water level fluctuations, and less so by external nutrient loading. The Lake Kinneret water quality system has demonstrated its effectiveness as a common language for communication between multiple partners in water resource management, as a tool and target for lake management, and as an output of ecological modeling.

Keywords Water quality quantification · Sustainable water resource management · Lake Kinneret · Objective function · Cyanobacteria · Water salinity · Delphi method

34.1 Introduction

Water quality (WQ) is a term used to describe the condition of a water resource, usually with reference to human needs or values, and is therefore likely to have elements of subjectivity related to perceptions and biases of the users of a given water resource (CWA 2002). Progress in WQ assessment has been associated with

A. Parparov (✉) · T. Berman
The Yigal Allon Kinneret Limnological Laboratory, Israel Oceanographic & Limnological Research, P.O. Box 447, 14950, Migdal, Israel
e-mail: parpar@ocean.org.il

K D. Hambright
Department of Biology, University of Oklahoma, 730 Van Vleet Oval, 304 Sutton Hall, Norman, OK 73019, USA
e-mail: dhambright@ou.edu

T. Zohary et al. (eds.), *Lake Kinneret, Ecology and Management,* Aquatic Ecology Series 6,
DOI 10.1007/978-94-017-8944-8_34,

implementation of optimization approaches in the establishment of sustainable management policies based on conservation within desired reference conditions (Jorgensen and Vollenweider 1989; Smith 1990; WFD 2000; Wetzel 2001). The task of water resource management can be formulated (Kalceva et al. 1982; Parparov and Hambright 2007) as optimization of an objective function (Q) of the economic activities (EA) encompassing anthropogenic activities in the lake watershed (quantitatively expressed as nutrient and pollutant loading into the lake) and intensity of water resource use such as water supply, WQ, and economic effectiveness of the management (costs vs. benefits, CB):

$$Q = \Phi(\mathrm{EA}; \mathrm{WQ}; \mathrm{CB}). \tag{34.1}$$

An effective water resource management program based on precise and formal definitions of management criteria and WQ for Lake Kinneret was first proposed in 1996 (Parparov and Hambright 1996). Here, we describe briefly a system of water quality indices (WQIs) developed for Lake Kinneret and summarize results of studies related to quantitative assessment of WQ in the lake carried out since 1996.

34.2 Methodology and Basic Definitions

Parparov et al. (2006) suggested the following principles for the quantification of WQ and its use in lake management:

1. A system of WQIs and their acceptable ranges should be devised and quantified by an expert panel consisting of all partners in lake management.
2. The WQIs and their driving processes must be suitable for mathematical modeling.
3. The WQIs and the model together should serve as a self-organizing tool for lake management.
4. The WQI must be dynamic and sensitive to changes in ecosystem functioning.

Our approach to WQ assessment included the establishment of a WQI system in which important parameters reflective of WQ were identified and their permissible ranges of variation were defined using a modified Delphi expert panel method (Brown et al. 1970; Parparov and Hambright 1996; Parparov et al. 2006). This approach was described in detail in Hambright et al. (2000). Here, we provide a brief overview of the assessment process.

We suggested that the water resources of Lake Kinneret would be managed in order to maintain WQ within the range of a “reference” state based on variability recorded during the period 1969–1992. The rationale for this limitation was based on the consideration that, during this period, lake WQ had been acceptable for all uses, especially for drinking water supply. Long-term monitoring data, including

Table 34.1 Acceptable winter–spring (Jan–Jun) and summer–autumn (Jul–Dec) ranges ($100 \geq$ Rating ≥ 60) for selected water quality indices for conservation of Lake Kinneret water quality

Index	Winter–spring	Summer–autumn
Chloride, mg L^{-1} (Cl)	152–242	153–245
Total suspended solids, mg L^{-1} (TSS)	0.8–8.3	0.3–4.9
Turbidity, NTU (TU)	1.4–5.3	0.8–3.6
Total phosphorus, µg L^{-1} (TP)	7.5–36.7	4.0–27.3
Total nitrogen, mg L^{-1} (TN)	0.38–1.20	0.25–0.98
Chlorophyll, µg L^{-1} (Chl)	4.7–37.7	1.0–10.0
Primary production, g C m^{-2} day^{-1} (PP)	1.13–3.17	0.71–2.32
Cyanobacteria, % total algal biomass (%Cyano)	0–5.1	1–12.3
Biomass of zooplankton, g m^{-3} (ZB)	0.46–3.03	0.55–5.38
Fecal coliforms, No. 100 mL^{-1} (Fcoli)	0–200	0–1,000

frequency distributions, means, and standard deviations of ecological variables in Lake Kinneret from 1969 to 1992, were supplied to an expert panel of limnologists and engineers knowledgeable about Lake Kinneret. The panel was asked to choose about ten parameters most indicative of WQ in the lake. Ten parameters of WQ were chosen as representatives of Kinneret WQ (Table 34.1), and are hence referred to as the indices of WQ. The panel members were then asked to construct rating curves for each parameter spanning the entire range of values observed in the lake. The rating curves represented the relationship (Eq. 34.2) between a given concentration or measurement of the parameter in question (e.g., percentage of cyanobacteria in the total algal biomass, chlorophyll concentration, etc.) and its rating value, R, which ranged from 10 (poor) to 100 (excellent):

$$R = f(\mathrm{WQI}). \tag{34.2}$$

Permissible ranges for each WQI were defined as the range of $60 \leq R \leq 100$, whereas R values < 60 were considered to indicate unacceptable WQ.

The WQ system for Lake Kinneret provides a means for identifying the major water resource uses and environmental threats associated with the use of this water resource

1. *Drinking water supply:* represented by indices of total suspended solids (TSS) and turbidity (TU)
2. *Eutrophication:* represented by the indices total phosphorus (TP), total nitrogen (TN), primary production (PP), chlorophyll (Chl), and percentage of cyanobacteria in the total algal biomass (%Cyano)
3. *Organic pollution:* represented by an index of the number of coliform bacteria (Fcoli)
4. *Nutrition supply for fishes:* represented by the zooplankton biomass (ZB) index
5. *Increase in salinity:* chloride (Cl) concentration index

Following the definition of permissible ranges for each WQI, relationships between various EA (e.g., nutrient loads) and WQ were defined as in Eq. 34.3:

$$\mathrm{WQI} = F(\mathrm{EA}). \tag{34.3}$$

For this step, we applied statistical analyses of the existing Lake Kinneret database, combined with ecological modeling (Gal et al. 2009; Parparov and Gal 2012). We identified external nutrient loading as a proxy for EA in the watershed, and lake water level as a proxy for water withdrawal from the lake. The nutrient loads (as grams per square meter per year) were calculated as a product of the Jordan River water discharge and concentration of the nutrient total forms. It was assumed that water discharge from the Jordan River constituted 70 % of the entire discharge (Gal et al. 2009) and was representative of the total watershed load into the lake. By combining Eqs. 34.2 and 34.3, we established a direct relationship between the quantitative estimates of WQ (as rating values, R, for each WQI) and the EA:

$$R = V(\mathrm{EA}). \tag{34.4}$$

We calculated an aggregate WQI (Composite Water Quality Index, CWQI) as a weighted average of rating values for the entire set of WQIs. The weighting procedure used variable weights inversely proportional to the separate rating values, thus providing extra weight to indices with lower rating values (Parparov and Hambright 2007):

$$\mathrm{CWQI} = \sum \left(\frac{R_\mathrm{i} \cdot (R_0 - R_\mathrm{i})}{\Sigma\,(R_0 - R_\mathrm{i})} \right), \tag{34.5}$$

where R_i are the rating values of the ten WQ indices listed in Table 34.1 and R_0 is a constant = 100. The sensitivity of CWQI to R_0 values and the respective management meanings were discussed in detail in Parparov and Hambright (2007). This weighting approach was found to be more sensitive to, and more reflective of, important changes in ecosystem functioning than approaches using the arithmetic means of multiple WQIs (Parparov and Hambright 2007).

The above-described system provided a direct correspondence between permissible ranges for each WQI and the associated permissible ranges for the various EA:

$$\{\mathrm{WQI}_{\mathrm{LOW}} < \mathrm{WQI} < \mathrm{WQI}_{\mathrm{HIGH}}\} \leftrightarrow \{\mathrm{EA}_{\mathrm{LOW}} < \mathrm{EA} < \mathrm{EA}_{\mathrm{HIGH}}\}, \tag{34.6}$$

where the subscripts LOW and HIGH represent the lower and upper permissible values, respectively, and "↔" infers correspondence. Equation 34.6 provides the limits of management based on criteria of conservation of WQ. When supplemented with the requirements for socioeconomic optimization, this expression may be considered as an operational definition of "sustainable management."

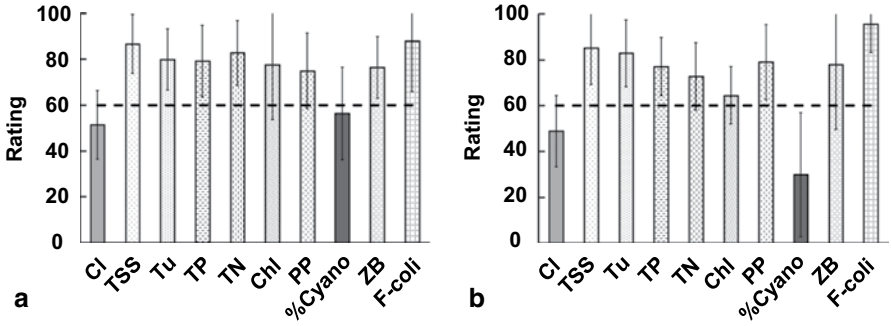

Fig. 34.1 Semiannual rating (multiannual mean ± SD) of the individual WQIs in winter–spring (January–June, *left panel*) and summer–autumn (July–December, *right panel*) during 1991–2011. The *dashed line* (rating = 60) indicates the borderline between acceptable and unacceptable water quality. See Table 34.1 for designations

34.3 Multiannual Dynamics of WQ in Lake Kinneret in 1991–2011

34.3.1 Individual WQIs

Most (eight of ten) of the semiannual average rating values of the individual WQIs during the period 1991–2011 varied within their permissible ranges (i.e., $R > 60$, Fig. 34.1) with some exceptions during episodes of WQ deterioration due to increases in total suspended solids, concentrations of chlorophyll, or fecal coliform bacteria. By contrast, chloride and the percentage of cyanobacteria were below permissible ranges (i.e., $R < 60$) for a substantial portion of the 20-year period. Chloride and percentage of cyanobacteria had lower ratings and therefore they had the strongest impact on the CWQI (Eq. 34.5). The declining trends in annual, average rating values for chloride and percentage of cyanobacteria indicated a deterioration in WQ (Fig. 34.2; $r^2 = 0.50$ and 0.55, respectively; $P < 0.01$) which closely followed trends in lake water levels. There was also a close correlation between the annual average rating value for chloride and lake water level ($r^2 = 0.90$; $P < 0.01$).

34.3.2 Multiannual Dynamics of CWQI

Monthly average CWQI values varied from 27.4 (bad WQ) to 87.3 (excellent WQ). Usually, CWQI was lower in summer–fall, due to increased percentages of cyanobacteria and chloride concentrations (Fig. 34.3a, b). Annual average CWQI showed a significant ($r^2 = 0.40$; $P < 0.01$) downward trend indicative of WQ deterioration (Fig. 34.3c). This trend in declining WQ was driven mostly by chloride and percentage of cyanobacteria rather than by changes in ratings of other

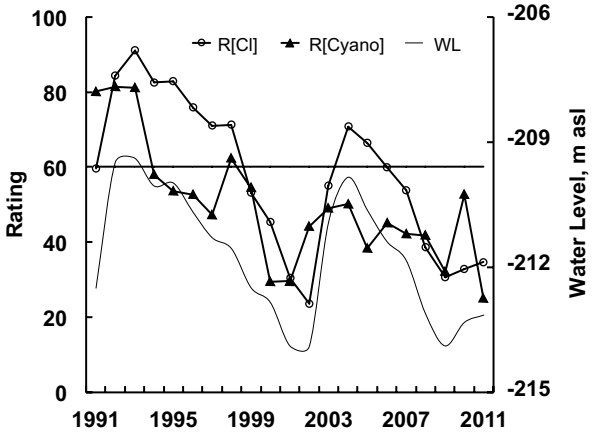

Fig. 34.2 Temporal dynamics of the annual average rating values of chloride and percentage of cyanobacteria (*R[Cl] and R[%Cyano]*, respectively) and lake water level (*WL*), 1991–2011. The *line* set at $R=60$ indicates the borderline between acceptable and unacceptable water quality. (WL data courtesy of the Israel Hydrological Services)

indices, particularly those reflective of the lake trophic status, i.e., TN and TP concentrations, or changes in primary production (see Chaps. 20, 21, 24) [P cycle, N Cycle, PrimProd]. Annual average (1990–2011) chlorophyll did not show any trend. Thus, these data illustrate important conceptual distinctions between the concepts of trophic status and WQ. Estimation of lake trophic status is a task of classification, while WQ assessment contributes solution to the task of qualification (Parparov et al. 2010).

34.4 Use of CWQI as a Tool for Water Resource Management

In most publications concerning aggregate WQIs, the main purpose of the WQI system is to indicate changes in WQ (Cude et al. 2001; Burns et al. 2005). However, the aggregate measure of WQ, such as CWQI, is an argument of the objective function of management (Eq. 34.1) and should be used as a target and a tool for management rather than simply as an indicator of change.

The relationships between ecosystem variables and different environmental effects traditionally are derived from statistical analyses of monitoring data. Water level (WL), used here as a proxy for water withdrawal, showed strong correlations with the rating values for chloride and percentage of cyanobacteria (i.e., the ratings of Cl and %Cyano fell concomitantly with WL). WL accounted for a stronger negative impact on CWQI ($r^2=0.33$, $P<0.01$) compared with the effects of either N or P loading ($r^2=0.08$ and 0.04 for N and P load, respectively) indicating that WQ in Lake Kinneret is more sensitive to water level fluctuations than to changes in nutrient load. The significant relationship between WL and CWQI established a direct link between WQ and an important EA of water withdrawal, enabling the estimation of a threshold value for lake water levels above which acceptable WQ may be maintained (Fig. 34.4, see also Parparov and Hambright 2007).

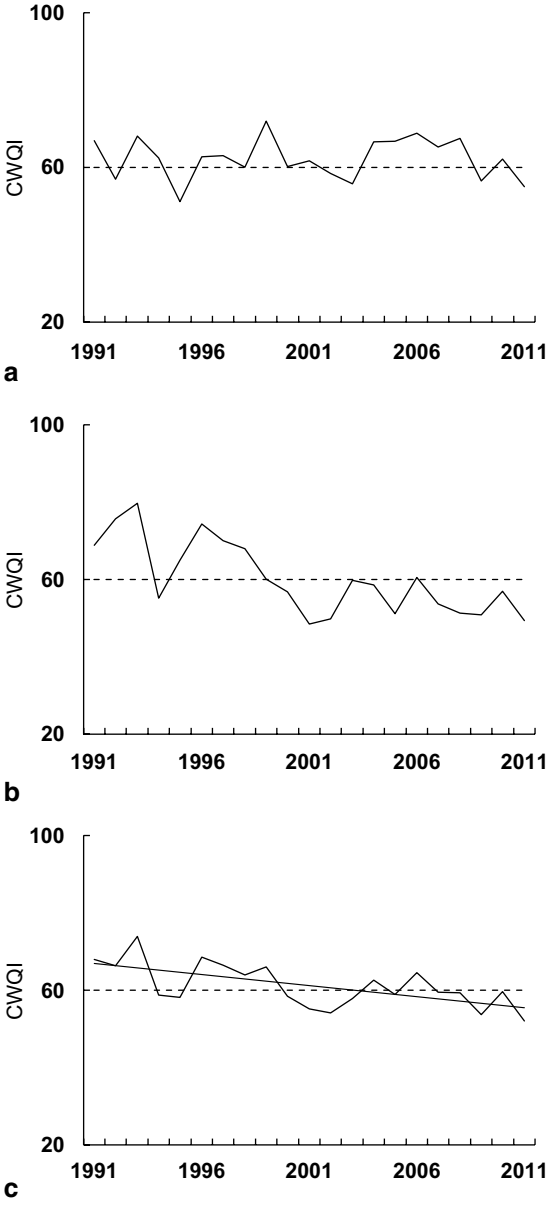

Fig. 34.3 Dynamics of the aggregate water quality (*CWQI*) in 1991–2011. The *dashed lines* set at $R=60$ indicate the borderline between acceptable and unacceptable water quality. **a** First semiannual average (January–June). **b** Second semiannual average (July–December). **c** Annual average. The *solid straight line* represents linear trend ($r^2=0.40$; $P<0.01$)

34.5 Concluding Remarks

Utilization of the system of WQIs for Lake Kinneret over the past 15 years highlighted strengths and weaknesses of this system.

Strengths The WQ system developed for Lake Kinneret has demonstrated its effectiveness as (1) a common language for communication between multiple partners

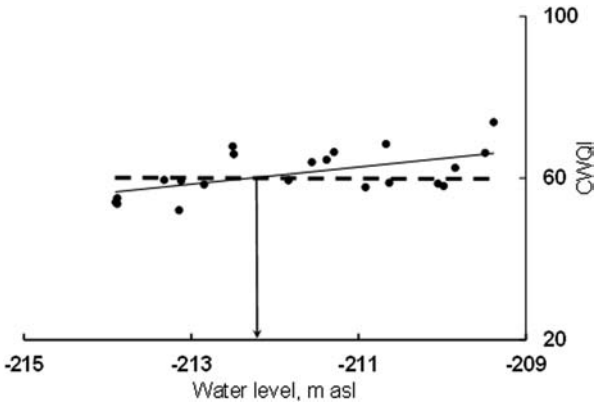

Fig. 34.4 The relationship between lake water level and CWQI, based on Lake Kinneret annual mean values for the period 1991–2011. The *dashed line* set at $R=60$ indicates the borderline between acceptable and unacceptable water quality. The *arrow* indicates a threshold value of water level (~−212.5 m) below which CWQI<60. The *solid line* represents linear regression of CWQI versus water level ($r^2=0.33$, $P<0.01$)

in water resource management and (2) a tool and target for lake management (Parparov et al. 2006), with a specific output of ecological modeling better adopted for the needs of water resource management (Gal et al. 2009).

Weaknesses The principal peculiarity of WQ quantification is its unavoidable conceptual dependence on interaction with water resource users. Almost all basic concepts of WQ assessment, including directions of use for which the WQ system is established, choice of reference period, WQIs and their permissible ranges, and the mode of index aggregation are essentially user defined (Parparov and Hambright 2007). These aspects of water resource management have yet to be adopted and implemented by water policy makers and managers for Lake Kinneret.

The developed system of WQIs is a component of methodological framework that includes the ecological monitoring of lake's WQ, a quantified WQ system, and ecological modeling. Utilization of this framework allowed the outlining of a sustainable management policy for Lake Kinneret (Parparov and Gal 2012). However, the Lake Kinneret WQ system is focused on a single management criterion that could be considered supplementary to the existing hydrological criteria (e.g., quantity of water supplied). We suggest that the subject of sustainable management should be the lake as a socioecological system rather than just an aquatic ecosystem *per se*. Therefore, water resource management should be based on multiple criteria (Eq. 34.1), including economic aspects of the management (O'Riordan 1999; Ludwig 2001; Costanza et al. 2002; Walker et al. 2002; Derissen et al. 2011; Zhu and van Ierland 2012).

References

Brown PM, McClelland NI, Deninger RA, Tozer RG (1970) A water quality index—do we dare? Water Sew Work 11:339–343

Burns N, McIntosh J, Scholes P (2005) Strategies for managing the lakes of the Rotorua District, New Zealand. Lake Reserv Manag 21:61–72

Costanza R, Voinov A, Boumans R et al (2002) Integrated ecological economic modeling of the Patuxent River watershed, Maryland. Ecol Monogr 72(2):203–231
Cude CG (2001) Oregon water quality index: a tool for evaluating water quality management effectiveness. J Am Water Res Assoc 37:125–137
CWA (2002) Federal Water Pollution Control Act [As Amended Through P.L. 107–303, November 27, 2002]
Derissen S, Quaas MF, Baumgärtner S (2011) The relationship between resilience and sustainability of ecological-economic systems. Ecol Econ 70(6):1121–1128
Gal G, Hipsey MR, Parparov A et al (2009) Implementation of ecological modeling as an effective management and investigation tool: Lake Kinneret as a case study. Ecol Model 220:1697–1718
Hambright KD, Parparov A, Berman T (2000) Indices of water quality for sustainable management and conservation of an arid region lake, L. Kinneret (Sea of Galilee), Kinneret. Aquat Conserv Mar Freshw Ecosyst 10:393–406
Jorgensen SE, Vollenweider RA (1989) General introduction. In: Jorgensen SE, Vollenweider RA (eds) Guidelines of lake management, vol 1. Intern. Lake Environment Committee, Shiga, pp 13–18
Kalceva R, Outrata J, Schindler V, Straskraba ZM (1982) An optimization model for the economic control of reservoir eutrophication. Ecol Model 17:121–128
Ludwig D (2001) The Era of management is over. Ecosystems 4(8):758–764
O'Riordan T (1999) Economic challenges for lake management. Hydrobiologia 395–396:13–18
Parparov A, Gal G (2012) Assessment and implementation of a methodological framework for sustainable management: Lake Kinneret as a case study. J Environ Manag 101:111–117
Parparov A, Gal G, Hamilton D, Kasprzak P, Ostapenia A. (2010) Water quality assessment, trophic classification and water resources management. J Water Resour Prot 2:907–915
Parparov A, Hambright KD (1996) A proposed framework for the management of water quality in arid-region lakes. Int Rev Gesamten Hydrobiol 81:435–454
Parparov A, Hambright KD (2007) Composite water quality: evaluation and management feedbacks. Water Qual Res J Can 42:20–25
Parparov A, Hambright KD, Hakanson L, Ostapenia AP (2006) Water quality quantification: basics and implementation. Hydrobiologia 560:227–237
Smith DG (1990) A better water quality indexing system for streams and rivers. Water Res 24:1237–1244
Walker BS, Carpenter S, Anderies J et al. (2002) Resilience management in social-ecological systems: a working hypothesis for a participatory approach. Conserv Ecol 6(1):14. (http://www.consecol.org/vol6/iss1/art14)
Wetzel RG (2001) Limnology. Lake and river ecosystems. 3rd edn. Academic, San Diego, p 1006
WFD (2000) European Water Framework Directive 2000/60/EC of the European Parliament and of the Council of 23 October 2000 establishing a framework for community action in the field of water policy. Official Journal of the European Community L327: 1–72
Zhu X, van Ierland EC (2012) Economic modelling for water quantity and quality management: a welfare program approach. Water Resour Manag 26:2491–2511

Chapter 35
Modeling the Kinneret Ecosystem

Gideon Gal, Arkady Parparov and Natasa Atanasova

Abstract Modeling of the Lake Kinneret ecosystem and its various components has developed greatly since the first effort in 1980. Modeling studies have included a range of approaches, some of which have focused on the entire ecosystem, while others only on certain components. The modeling approaches that have been applied to the Lake Kinneret ecosystem range from statistical approaches, data mining, and machine-learning techniques to flux models, bioenergetics, nutrient–phytoplankton–zooplankton (N–P–Z)-type models, and complete ecosystem models. Models have been used to enhance our understanding of key limnological and food-web processes. The models, however, have also been used as a means for providing resource managers with improved management tools. This has included, in some cases, integrating model output and a quantified water quality (WQ) system as the basis for establishing the relationships between management measures and water quality. Thus, highlighting the role of ecosystem modeling as a critical management tool.

The use of models, especially complex ecosystem models, requires constant updating and ongoing development along with a wide range of information and data. In most cases, the available information and data do not satisfy model needs thereby introducing model uncertainty. In order to improve model reliability, and, as a result, its applicability, it is important to increase the overlap between routine monitoring and model data requirements.

G. Gal (✉) · A. Parparov
The Yigal Allon Kinneret Limnological Laboratory, Israel Oceanographic & Limnological Research, P.O. Box 447, 14950 Migdal, Israel
e-mail: gal@ocean.org.il

A. Parparov
e-mail: parpar@ocean.org.il

N. Atanasova
Centre for Marine and Environmental Research (CIMA) Faro,
University of Algarve, Algarve, Portugal
e-mail: natanaso@gmail.com

T. Zohary et al. (eds.), *Lake Kinneret, Ecology and Management,* Aquatic Ecology Series 6,
DOI 10.1007/978-94-017-8944-8_35,

Keywords Ecosystem model · Statistical model · Water quality · DYCD · Data-driven modeling · Carbon flow · Sensitivity analysis

35.1 Introduction

One of the main advances made in the study of Lake Kinneret since the publication of the 1978 monograph (Serruya 1978) is use of models as a tool for understanding processes and dynamics in the lake ecosystem and as a management tool available to resource managers, i.e., Israeli Water Authority. While early modeling studies of the lake started in 1980, major advances and efforts occurred only a decade, or more, later. The available extensive database and unique limnological conditions such as the physical forcing conditions at the lake (i.e., the daily breeze occurring 4–5 months a year) and regular algal succession through to the mid-1990s have provided the basis for a large number of studies that have attempted to model various aspects of the lake ecosystem or its entirety. In this chapter, we review the outcome of many of the modeling studies conducted since the early 1980s to date. Our chapter focuses on studies in which biological processes are involved. Thus, with the exception of one example, we do not cover models dealing only with physical or hydrological aspects of conservative elements of the ecosystem though much progress has been made in the field of physical modeling of the lake, predominantly by the group at The Centre for Water Research at the University of Western Australia. We divide this chapter into three main sections. We first briefly review many of the modeling approaches and studies that have been conducted on the lake, separating between those that take a holistic ecosystem approach and those that focus on specific aspects or elements of the ecosystem or food web. In this initial section, we do not review the results or outcomes of these studies but rather just the approaches. Results and conclusions of the modeling studies are covered in the following sections. In the second section of the chapter, we provide examples of studies in which the models enhanced our understanding and knowledge of the ecosystem and its underlying processes. The third and final section demonstrates the use of models as a management tool providing examples of studies in which models served as a tool for evaluating management decisions and their impact on the lake ecosystem. We conclude with a brief summary of the benefits and drawbacks of using models.

35.2 Component-Specific Models

Since the first modeling study in 1980 (Serruya et al. 1980), numerous studies have been published on modeling of various aspects of the Lake Kinneret ecosystem (Fig. 35.1). The modeling efforts can be separated into those studies and models that focus on specific segments of the lake ecosystem as opposed to studies that utilize ecosystem models thereby including a wide range of processes typically not included in the more specific models.

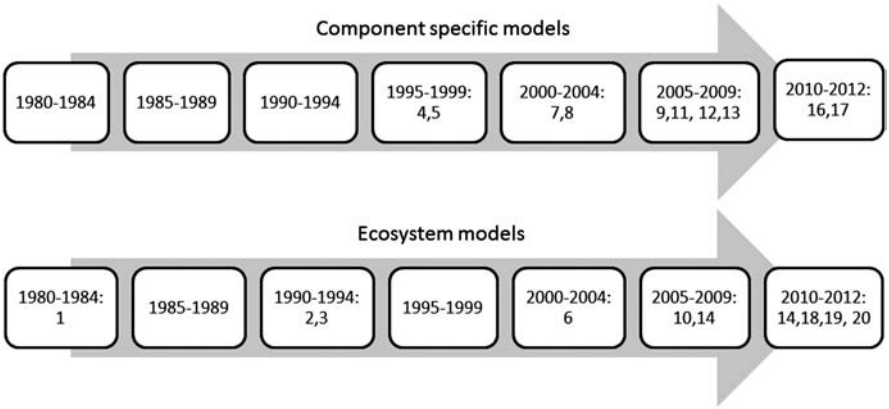

Fig. 35.1 Chronological representation of the modeling experiments in Lake Kinneret, with respect to the model types and modeling goals. Numbers correspond to references in the following list. The year and reference are provided for each study. *1*. Serruya et al. 1980—complete ecosystem; *2*. Stone et al. 1993—complete ecosystem; *3*. Walline et al. 1993—food web; *4*. Nishri et al. 1996—SPM; *5*. Drenner and Hambright 1999—fish; *6*. Hart et al. 2000—complete ecosystem; *7*. Håkanson et al. 2000—SPM; *8*. Hambright et al. 2002—fish; *9*. Ostfeld et al. 2006—phytoplankton; *10*. Bruce et al. 2006—complete ecosystem; *11*. Roelke et al. 2007—phytoplankton; *12*. Atanasova et al. 2008—phytoplankton; *13*. Gilboa et al. 2009—SPM, Chl.; *14*. Gal et al. 2009—complete ecosystem; *15*. Nishri and Hamilton 2010—N cycle; *16*. Gal and Anderson 2010—zooplankton; *17*. Atanasova at al. 2011—phytoplankton; *18*. Makler-Pick et al. 2011a, 2011b—complete ecosystem; *19*. Gal et al. 2012—complete ecosystem; *20*. Li et al. 2012a—complete ecosystem

Component-specific models have included a wide range of food-web elements extending from nutrients and suspended matter up via phytoplankton to zooplankton and fish. Suspended matter and, hence, turbidity are often considered a water quality (WQ) indicator due to their impact on the need for water treatment. Suspended particulate matter (SPM) also indirectly affects the food web due to the impact on light attenuation, which in turn influences primary productivity and heat dispersion. Håkanson et al. (2000) modeled the changes in SPM in the lake by developing within the Stella modeling framework (www.iseesystems.com) a temporally dynamic mathematical model of the monthly cycling of SPM in lakes with variable water levels. The main processes included in the model were inflows, withdrawals, sedimentation, mineralization, mixing, and resuspension. Through the use of Monte Carlo simulations, they examined the main processes leading to changes in SPM. Gilboa et al. (2009) applied a genetic algorithm modeling approach to determine an empirical relationship between SPM concentrations in the lake and light attenuation and chlorophyll concentrations.

Nishri and Hamilton (2010) examined the importance of changes to nitrogen fluxes in the lake using a mass balance approach. The mass balance included the major nitrate and ammonium fluxes such as inflows, withdrawals, phytoplankton, nitrification of ammonium, and denitrification through the application of an inverted Michaelis–Menten equation for dependence on dissolved oxygen (DO) and a first-order dependence on the substrate (NO_3) concentration.

There have only been a limited number of phytoplankton-specific modeling studies, all of which were conducted in recent years using mainly relatively new modeling approaches. Ostfeld et al. (2006) applied a data-driven approach in an attempt to develop a short-term prediction tool for cyanobacteria abundance in the lake. The tool was based on merging a hybrid model tree (MT) with a genetic algorithm to determine key variables affecting the likelihood of a cyanobacteria bloom developing, especially given the changes that have occurred to the lake phytoplankton (Chap. 10). Roelke et al. (2007) applied statistical modeling tools to study the changes that occurred in the lake in the mid-1990s focusing on the disappearance of the *Peridinium*. Ng et al. (2011) used the three-dimensional (3D) hydrodynamic–ecosystem model ELCOM-CAEDYM to examine the evolution of *Peridinium* patch formation in Lake Kinneret. They use the model to show the role physical forcing, at various scales, plays in governing patch dynamics in the lake. Atanasova et al. (2008) used a machine-learning technique, regression trees, to construct a model that would explain the factors influencing the *Peridinium* dynamics and disclose some thresholds in their values that trigger the blooms. These authors also constructed a model that predicts the *Peridinium* concentrations 2 weeks in advance, given the present values of the measured variables. Atanasova et al. (2011) applied a hybrid automated modeling tool (Lagramge[1]) to examine the factors governing the dynamics of dinoflagellates in Lake Kinneret.

Only limited zooplankton or fish-specific modeling work has been conducted for Lake Kinneret. In one effort, a statistical modeling approach was used to examine the large observed changes in the zooplankton population. In that study, Gal and Anderson (2010) used a Markov-switching vector autoregression model in order to determine whether a regime shift had occurred to the predatory zooplankton population in the lake.

Numerous studies have indicated that fish have the ability to impact lake WQ and have often been used as a biomanipulation tool. The results of biomanipulation using fish are, however, not always as predicted (Drenner and Hambright 1999). Hambright et al. (2002) combined experimental work with bioenergetics modeling to examine the impact of *Sarotherodon galilaeus*, a key commercial species, on WQ in Lake Kinneret.

35.3 Ecosystem Models

Complete ecosystem model studies of Lake Kinneret have focused on two main approaches that include modeling carbon flow and fluxes through the ecosystem and construction of an ecosystem model that simulates fluxes or changes in, biomass or, key biochemical cycles. The first series of models attempting to deal with

[1] Lagramge is a deliberate misspelling of its predecessor Lagrange, where “gram” stands for grammar, indicating that this tool uses grammars for representing equations’ search space. More information: http://www-ai.ijs.si/~ljupco/ed/lagrange.html.

an ecosystem were based on simulating carbon flow and fluxes between the various components and separating between seasons. Serruya et al. (1980) examined, on a seasonal basis, the carbon flow between the various internal and external carbon sources and their sinks. They did so by separating between a *Peridinium* year, which was typical at that time, and a less frequent nanoplankton year. The model was based on a combination of experimental data, literature values from other ecosystems, and estimates where information was missing. Only limited information was available, however, for bacterial processes and fish metabolic parameters and biomass. Unfortunately, the authors did not address the impact of the uncertainties on the model outcome. Stone et al. (1993) used linear programming to construct balanced seasonal carbon flowcharts for a lake food web. The model quantified the fluxes between the various compartments comparing between winter–spring and late summer seasons. The flowcharts were constructed based on available standing stock of the various components from bacteria up via Protista, phytoplankton, zooplankton to fish and included ten compartments of biota, including specifically the microbial loop which was lacking in the earlier carbon model (Serruya et al. 1980). Once the model was constructed and tested, the authors evaluated additional pathway scenarios based on alternative hypotheses regarding the reduced role of the microbial food web in Lake Kinneret. They did so by reducing the flows through the microbial loop to 20 % of their original fluxes. They further tested the impact of variability and uncertainty on the balanced flowcharts by allowing a 10 % fluctuation in the various fluxes and not constraining them to constant values. Surprisingly, this limited degree of variability resulted in large changes to the simulated fluxes. An extension to the above model was provided by Hart et al. (2000). Using a mass-balanced carbon flux model and network analysis, they studied the role of protozoa and bacteria in the food web. Their model differed from the original Stone et al. model (1993) in the use of more reliable flux estimates, the addition of a flux from nanophytoplankton to ciliates and alteration of the assumptions on bacterial production and respiration, and application of the model to an extensive period of time. They further used network analysis (Kay et al. 1989) to analyze the role of recycling and the microbial loop in the Lake Kinneret food web.

Walline et al. (1993) also examined the flow of carbon through the food web by constructing a model of Lake Kinneret using the widely accepted Ecopath modeling software (Christensen and Pauly 1992). Ecopath models are mass-balanced snapshots of the food web providing insight into the flows of carbon, or mass, between components. However, the fluxes in Ecopath are balanced through use of generalized matrix inverses in contrast to the linear programming used by Stone et al. (1993). In their model, Walline et al. (1993) examined the importance of the two key food web pathways: the phytoplankton–detritus–protozoa pathway and the phytoplankton–herbivorous zooplankton–carnivorous zooplankton pathway. Based on their model results, they reported on the relative fluxes between the various components of the two pathways. There was, however, no attempt to study the impact of the large degree of uncertainty associated with many of the key parameters thus limiting the validity of their numerical estimates.

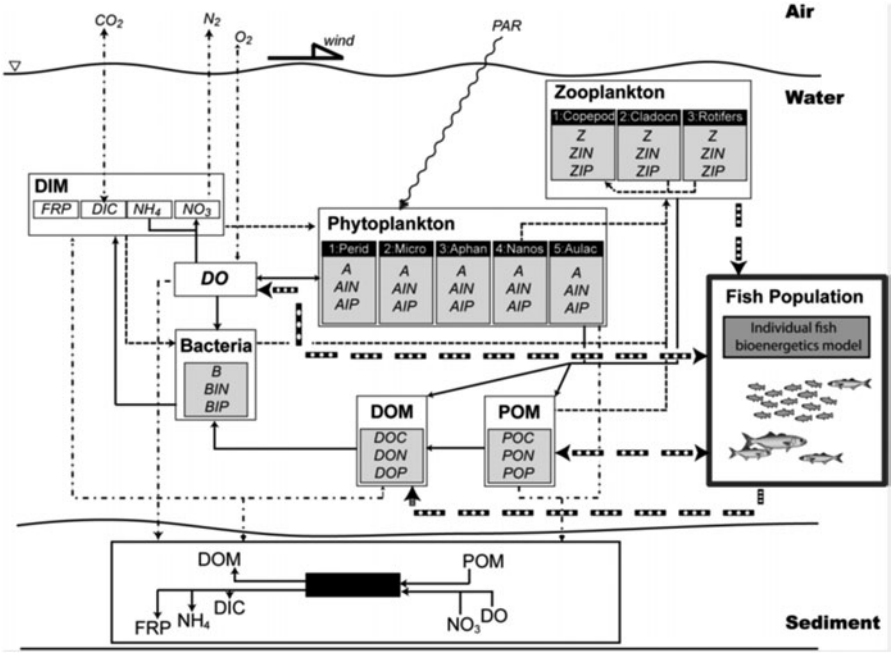

Fig. 35.2 A schematic of the ecosystem components and state variables simulated by DYCD. Phytoplankton biomass (**a**) of five groups is represented in the model: *Peridinium gatunense* (*Perid*), non-N-fixing cyanobacteria such as *Microcystis* (*Micro*), N-fixing cyanobacteria such as *Aphanizomenon* (*Aphan*), Nanoplankton (*Nanos*), and *Aulacoseira* (*Aulac*). In addition, the biomass of three groups of zooplankton (*Z*; *Copepoda, Cladocera, and Rotifera*) and one group of heterotrophic bacteria (**b**) are simulated in the model. *IN* and *IP* refer to internal nitrogen and phosphorus concentrations; *DOM* and *POM* refer to the dissolved and particulate organic cycles (*C, N, P*); *DIM* represents the dissolved inorganic fractions, in the model, for each of the carbon, nitrogen and phosphorus cycles; *DO* dissolved oxygen; *PAR* photosynthetically active radiation. (Adopted from Makler-Pick et al. 2011b with permission from NCR Research Press)

An alternative approach to modeling of the ecosystem is through simulation of the flow of biomass and biogeochemical components through the system. In a series of studies conducted since 2001, the one-dimensional (1D) ecosystem model DYRESM–CAEDYM (dynamic reservoir simulation model–computational aquatic ecosystem dynamics model; DYCD), developed by the Centre for Water Research at the University of Western Australia, has been applied to Lake Kinneret. DYCD comprises the 1D hydrodynamic model DYRESM (Gal et al. 2003; Imberger and Patterson 1981) and the biogeochemical model CAEDYM. DYCD has been applied to numerous lakes around the world (e.g., Burger et al. 2007; Rigosi et al. 2011; Trolle et al. 2008) and in a number of configurations to Lake Kinneret ranging from a simpler food-web structure of three phytoplankton and three zooplankton groups to basic carbon, nitrogen, and phosphorus cycles (Bruce et al. 2006) via a more complex system including bacteria and additional phytoplankton groups (Gal et al. 2009; Li et al. 2012b) and fish (Makler-Pick et al. 2011b, Fig. 35.2). DYCD

is a process-based model that incorporates the important physical processes taking place in a lake leading to changes in temperature and salinity with time and depth. CAEDYM uses a series of ordinary differential equations to describe changes in concentrations of nutrients, detritus, DO, bacteria, phytoplankton, and zooplankton as a function of environmental forcing and ecological interactions for each Lagrangian layer represented by DYRESM. CAEDYM can simulate up to seven phytoplankton groups, five zooplankton groups, heterotrophic bacteria, several groups of benthic organisms (macroalgae, bivalves, and macroinvertebrates), pathogens, geochemistry (heavy metals), organic and inorganic nutrients, the oxygen and carbon cycles, and suspended solids.

In the applications of DYCD to the lake, the model was used to evaluate the impact of changes to various food web and external components on the ecosystem. In addition, DYCD continues to be used as an active tool for assisting resource managers in determining the possible impact of potential management measures on the lake ecosystem. In two recent studies, DYCD was calibrated and applied to the lake in order to evaluate the impact of a number of management actions on the lake ecosystem (Gal et al. 2009; Parparov and Gal 2012). In the two studies, model configuration included the C, N, and P cycles (particulate and dissolved, organic and inorganic), DO, heterotrophic bacteria, five phytoplankton groups, and three zooplankton groups. Through the use of long-term model simulations and scenarios, the authors evaluated the impact of changes in nutrient loads and water level on the ecosystem.

Makler-Pick et al. (2011b) enhanced DYCD by including a fish component to the model (known as DYCD-Fish) in order to examine the role of the dominant planktivorous fish, the bleak, *Mirogrexterraesanctae*, in the lake ecosystem. The fish components were incorporated in a unique way by tracking the fish-specific bioenergetics of a large number of superindividuals, each representing a predefined number of individuals. In order to include variability in the population, the parameters a and b from the length–weight relationship were randomly assigned values from within a predefined range.

Li et al. (2012a) examined a 5-year simulation of the lake in order to determine the relationship between internal nutrient ratios of several phytoplankton functional groups and nutrient ratios within the water column, and to further explore the linkage between the microbial loop and food-web stoichiometry by testing a number of microbial loop configurations.

DYCD is unique in its comprehensive approach providing the user with the ability to simulate a wide range of state variables. This, however, comes with a cost. The large degree of complexity results in a considerable number of parameters requiring an extensive and lengthy calibration process. However, in most cases, information for a large number of parameters is lacking thus affecting the accuracy of the model outcome. Sensitivity analysis (SA) and uncertainty analysis (UA) can assist in increasing model accuracy though there are only a limited number of studies that include the application of an SA or a UA to a comprehensive model such as DYCD. Makler-Pick et al. (2011a) applied a new SA approach to CAEDYM in order to overcome the effect of the large number of parameters and state variables

and managed to provide a list of the parameters to which the model is most sensitive. The analysis results highlighted the importance of particulate organic material in the lake ecosystem and its impact on nutrient budgets. Recently, Gal et al. (2012) adopted the single-model ensemble approach in order to evaluate the impact of model parameter uncertainty on model scenario results. The results indicated that scenario results were relatively robust to parameter uncertainty though phytoplankton variables exhibited increased sensitivity. Nevertheless, trends observed over a wide range of parameter uncertainty matched the trends observed in scenarios based on the calibrated parameter values.

The parallel development of modeling tools and methods and of computing power has increased the number and complexity of modeling approaches used by ecosystem scientists. The progress is also evident in Lake Kinneret modeling studies. The number of studies and the diversity of approaches have increased greatly over the past decade (Fig. 35.1) and undoubtedly will continue to develop. These developments will result in improved models that will offer enhanced accuracy and additional means for examining existing data.

35.4 Implications for Science, Knowledge, and Understanding

Lake ecosystems models have become mainstream research tools that provide a means for exploring processes and interactions within the lake ecosystem and a tool for testing management schemes of the lake itself and of the loads that originate in its watershed. While ecosystem processes and interactions can be examined and studied through lake-based observations or laboratory work, model simulations can provide insight into processes because of the number of variables and processes that can be monitored in the simulated world. Furthermore, it is possible to expose the simulated lake to conditions exceeding the observed historical bounds.

Early application of ecosystem models to the lake served as a means of examining the various food-web pathways. The main focus of these studies was the flux of carbon between the numerous food-web components. Serruya et al. (1980) provided the first major analysis of the carbon fluxes in the lake, separating between *Peridinium* years and non-*Peridinium* years and two major food chains. According to their results, the importance of the two pathways varies between seasons and years with the former dominating the summer–fall and the latter in the winter–spring during years in which *Peridinium* blooms occur. Their model provided insight into the relative fluxes of carbon and indicated a relatively small sedimentation component of typically < 10 % of the total carbon inputs. This can be compared to a contribution of 27 and 70–90 % to the total carbon flux by *Peridinium* and zooplankton, respectively. The model further highlighted the large seasonal differences with a positive carbon balance in the winter–spring but a negative balance in the summer. The authors also concluded that during years in which *Peridinium* are absent, there is a domination of the nanoplankton-grazing pathway due to an increase in the presence of edible algae for the herbivorous zooplankton which can lead to an unbalanced

food web. While the model succeeded in quantifying the carbon fluxes and providing a framework for comparing the relative fluxes, it lacked the microbial loop, a component, the importance of which became clear only following the pivotal paper by Azam et al. (1983).

A major advance in understanding the role of the microbial loop in the lake was provided by Stone et al. (1993) who included it in the carbon flux model they constructed. Their results highlighted the interactions between the zooplankton and microbial components suggesting that during the summer some 45% of the bacterial production is transferred, directly or indirectly, to the zooplankton. As data uncertainty existed in regard to some of the key fluxes, they tested an alternative summer flowchart by altering the microbial fluxes. Though the resulting structure of the chart did not differ greatly from the original version, it did impact the importance of microbial loop in the carbon fluxes in the summer. While the conclusions were in contrast to the original model outcome, they could not be refuted as all values were within acceptable limits.

The extended carbon model developed by Hart et al. (2000) provided a means for examining the role of the microbial loop as a source of carbon for the zooplankton grazers and the degree of recycling of organic compounds. Surprisingly, according to their results, the level of primary productivity did not have a large impact on the flux of carbon from the protozoa up to higher trophic levels. Rather, the flux depended on the amount of fixed carbon originating in the inedible portion of phytoplankton and the efficiency of the microbial loop. The results highlighted and quantified the role of the heterotrophic microorganisms in the carbon budget in the lake. According to the results, the bacteria and protozoa provide nearly 50% of the cladoceran carbon requirements during the winter–spring *Peridinium* blooms. Furthermore, the results suggested that a relationship exists between the contribution of carbon to cladocerans via the microbial loop and the fraction of net phytoplankton productivity. The largest contributions were found to occur during *Peridinium* spring blooms. The efficiency at which bacterial production is transferred up the food web also had a significant impact on the importance of bacteria as a food source for metazoans. The use of the model provided the authors with the ability to quantify recycling of organic material in the system. An alternate approach, to using the model, would have been the difficult task of quantifying these processes based on labor-intensive, and time-consuming, observations and experimental work. The model is however not without fault and suffers from uncertainties especially in parameter values. To overcome this, the authors conducted a sensitivity analysis (SA) in which they varied values of parameters and fluxes such as bacterial production, primary production, bacterial respiration, and fish intake of carbon. They showed that the large changes they made had only limited impact on key model statistics such as metazoan growth efficiency, dependence on particulate organic carbon/dissolved organic carbon (POC/DOC), and Finn's cycling index. The authors thereby concluded that their model outcome and, therefore, their conclusions were robust with the model assumptions (e.g., estimated parameter values).

Results of the Walline et al. (1993) model indicated, as did the Hart et al. (2000) model, that a majority of the herbivorous zooplankton is consumed by predatory zooplankton, while fish consume approximately only 12% of the biomass thus

highlighting the importance of carnivorous zooplankton in controlling the herbivorous zooplankton population. Though the relative predation by fish on herbivorous zooplankton is limited, they do play a role in effecting the zooplankton population by affecting the ratio of carnivorous to herbivorous zooplankton. The results implicitly indicated the role intra-guild predation (IGP) plays in the Lake Kinneret food web.

Using a bioenergetics model of *Sarotherodon galilaeus*, Hambright et al. (2002) concluded that despite their efficient feeding on *Peridinium gatunense* and nanophytoplankton, consumption rates were two orders of magnitude lower than maximum potential plankton growth rates. Thus, they too have limited top-down effect on the food web in general and on phytoplankton, in particular. More recently, machine-learning approaches were used to examine the factors governing *Peridinium* populations (Atanasova et al. 2008, 2011). In both cases, bottom-up control was indicated as the governing force. In the studies, a link to environmental conditions, especially phosphorus and temperature, was highlighted as the main driving factors though the authors do, correctly, point out that it is possible that variables not included in the analysis may play an important role.

An additional top-down versus bottom-up comparison was conducted by Hart (2002) who examined the impact of IGP on top-down processes in the lake with a number of simple models which were constructed based on the Lake Kinneret carbon flux model (Hart et al. 2000). In this study, however, the models were focused on the nano- and picoplankton–zooplankton–bleak part of the food web. Using the models, she explored the impact the IGP has on the ability of planktivorous fish, e.g., bleak, to assert top-down control on the food web. She shows that food webs constructed of small-bodied herbivorous zooplankton, like in Lake Kinneret, are more complex than the traditional large-bodied zooplankton food webs which are typically chain shaped. The additional complexity due to the IGP limits the top-down control in the system.

Our understanding of fluxes within the ecosystem was further enhanced by Bruce et al. (2006) who used DYCD to examine the role of zooplankton in nutrient recycling in the lake. The authors first validated the model and examined the sensitivity of the results to several of the parameters. As expected from a complex, multiparameter model (several hundred), the results were sensitive to a number of the zooplankton parameters examined. Nevertheless, the sensitivity to the parameters did not alter the main conclusions. The model results suggested that zooplankton graze, on average, 51 % of the carbon produced by primary productivity, a value, not dissimilar to the total herbivory by cladocerans of 63 % estimated by Hart et al. (2000). The results further indicated that zooplankton play a key role as a source of biologically available nitrogen and phosphorus in the lake epilimnion, especially throughout the stratified periods, during which there is little influx from external sources. The importance of zooplankton as nutrient recyclers was corroborated by the experimental work conducted by Hambright et al. (2007) and Rachamim (2010).

DYCD has been used in a number of applications including study of the impact of changes to nutrient loading from the watershed (Gal et al. 2009; Parparov and Gal 2012). The results of the long-term scenarios conducted in the two studies allowed the authors to study the relationships between total nitrogen to total phosphorus

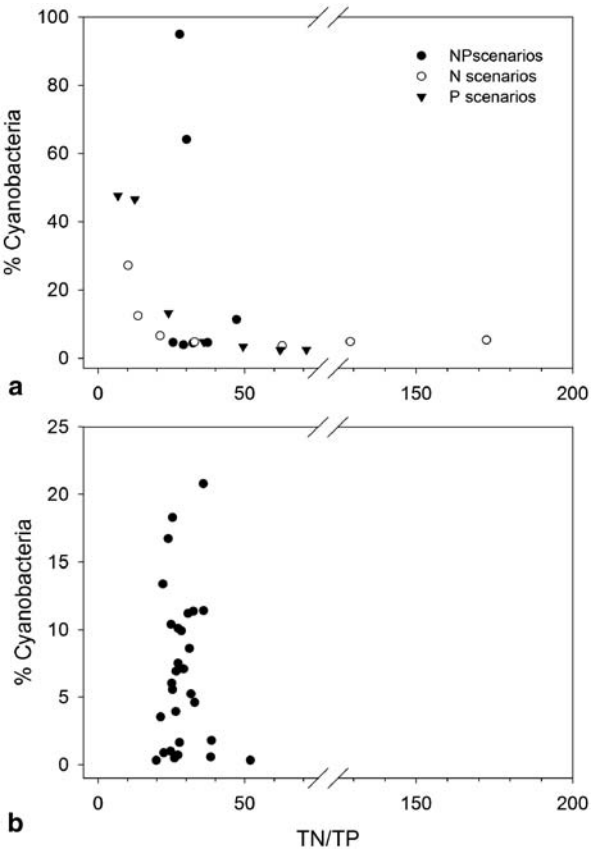

Fig. 35.3 The relationship between percentage of cyanobacteria of total algal biomass and total nitrogen to total phosphorus (*TN/TP*) ratio in the inflows based on model scenarios (**a**) and lake-based data (**b**). Model scenarios included simulations in which N (*N scenarios*) or P (*P scenarios*) or both N and P (*NP scenarios*) were varied, in the inflows, by two orders of magnitude

(TN/TP) ratios in the inflows and the relative contribution of cyanobacteria to the total algal biomass in the lake. Scenario results pointed to a threshold N-to-P ratio, ranging between 15–20, below which a large increase in the relative contribution of cyanobacteria to the total algal biomass occurs (Fig. 35.3). In addition, the results suggested a differential response by the lake to changes in N and P loading with a higher sensitivity and a stronger in-lake TN response in relation to changes in N loading than the in-lake TP response observed in reaction to changes in P loading. These results, latter corroborated by lake-based data, highlighted information on ecosystem processes that were previously undetected.

In recent years, we have witnessed a surge in application of statistical and data-driven methodology as tools for examining key lake ecological issues. The observed abrupt changes to the phytoplankton and zooplankton communities in Lake Kinneret in the mid-1990s (see Chap. 10 "Phytoplankton," Chap. 13 "Metazoan Zooplankton") were the focus of a number of studies. By examining the long-term database, within the framework of alternative states, Roelke et al. (2007) reported a complex triggering mechanism and revealed evidence of system hysteresis. They further tied the changes in the phytoplankton population to fluctuations in other

components of the food web, such as zooplankton and fish. Gal and Anderson (2010) used a free-knot spline mean function estimation method and a Markov-switching vector autoregression model to conclude that a regime shift had occurred in abundance of the predatory zooplankton population during the mid-1990s. They suggested that the regime shift was a result of extremely large bleak (*Mirogrex terraesanctae*) populations after a particularly wet winter characterized by a very rapid increase in water level. A similar outcome was shown via examination of the impact of lake-level change on the zooplankton dynamics under the assumption that large changes in lake level serve as a proxy for high bleak predation rates (Gal et al. 2013). In the study, using the data-driven decision trees approach, the authors statistically linked between the rate of lake-level change during the winter–spring and the size of the zooplankton population. In addition, and in contrast to expectations, they report that bottom-up processes seem to play a role in determining zooplankton abundance.

35.5 Implications for Management

Determining and maintaining lake level are the main management issues facing the Lake Kinneret resource managers. It is therefore not surprising that a number of modeling studies have examined the impact of changes to lake level on the ecosystem. Using a model of the monthly cycling of SPM, Håkanson et al. (2000) pointed to the worst-case (management) scenario, in which the gradual lowering of the lake level by 6 m over 4 years would create very high fluxes of resuspended matter and large changes in SPM. Recognizing the possible weaknesses in the values of some of the parameters, they used a Monte Carlo approach in order to determine which data are required in order to enhance model accuracy. The results suggested that model accuracy will increase following improvement of the modeling parts related to sedimentation and lowering of the wave base. Nishri et al. (1996) also examined the impact of lower lake levels on the ecosystem. According to their model outcomes, the reduction in lake level results in a thinner hypolimnion and, as a consequence, stronger hypolimnetic currents. The enhanced currents, according to the model, lead to increased turbulence, resuspension, and mineralization rates. Both models provided insight into the physical and chemical consequences of changes to lake level and as a result increased the understanding of the impact of lake management strategies on the ecosystem. In both cases, the models were used to study the relationships between various processes and variables, which are difficult to measure and observe in situ. In a more recent study, through the application of DYCD, Parparov and Gal (2012) evaluated the impact of changes of water level on WQ using the composite water quality index (CWQI; Chap. 34 “Water Quality Assessment” by Parparov). Using the combinations of DYCD scenario results and the CWQI, they defined the range of water levels that will allow conservation of the lake WQ within limits that correspond to sustainable management policy. Model output suggested a lake level of −213.5 m (a.s.l) as the lower limit that will allow

conserving water quality. Lake-based data indicated a level of −212.5 m. It is interesting to note the similarity between these results and those indicated by Håkanson et al. (2000). These results also coincide with Nishri et al. (1996) who showed based on their model that lowering lake level to −214 m could potentially impact the ecosystem through increased hypolimnetic currents and a faster hypolimnetic response time to wind stress. They linked stronger currents to changes in SPM and the likely resulting enhancement in mineralization rates.

The ecological aspects of the impact of lake-level management were examined by Makler-Pick et al. (2011b) and Gal et al. (2013). Makler-Pick et al. (2011b) using DYCD-Fish examined the effect of lake-level change on the bleak population and quantified the fish impact on their prey sources. They linked the direct and indirect effects of the bleak on other ecosystem components to changes in lake level, thereby providing information important for resource managers. The study was expanded to examine the intraguild predation interactions between the bleak and zooplankton groups in the lake (Makler-Pick 2010). The results of their model application were in line with insight gained by Hart (2002), that predatory zooplankton are the main controllers of the herbivorous zooplankton population in the lake. This has management implications especially in light of the expensive and fruitless removal program (known as the "dilul") of the bleak, conducted between 1995 and 2006 as a means for increasing herbivorous zooplankton in the lake in order to reduce algal biomass thereby improving water quality. Gal et al. (2013), using decision trees, also demonstrated the importance of relatively large increases in lake level over the course of the winter–spring on the size of the cladoceran and adult copepod populations a year later. However, they clearly indicate that other processes (bottom-up) are also important and control the zooplankton community.

The large temporal variations in the commercial fisheries biomass and catch since the early 2000s including an all-time low in 2008 (details in Chap. 36 "Fisheries Management") have led to a debate regarding fisheries' management in the lake and especially its objectives and effectiveness. As already pointed out above, a number of studies have demonstrated IGP in the lake which results in a dampening of top-down control of zooplankton and algae (Hart 2002; Makler-Pick 2010). *Sarotherodon galilaeus*, commercially the most valuable fish in the lake, has been stocked continuously since the 1950s in order to maintain population size. The reason for this has been the understanding that *S. galilaeus* along with other fish assist in maintaining lake WQ due to consumption of phytoplankton. However, using a bioenergetics model Hambright et al. (2002) showed that the potential for the *S. galilaeus* population in Lake Kinneret to positively affect WQ through algal suppression is low due to their relatively low consumption rate. Results of the Ecopath model constructed by Walline et al. (1993) support this notion and indicate that *S. galilaeus* and silver carp, both of which are stocked into the lake in order to assist in maintaining water quality, have little impact on other components of the food web. While stocking is an acceptable management practice worldwide in order to maintain a commercial stock, it should be recognized that it may not be serving its original purpose in Lake Kinneret.

In the two DYCD studies mentioned above (Gal et al. 2009; Parparov and Gal 2012), the model was applied to the lake and used to evaluate the impact of a number of management actions on the lake ecosystem. Through the use of long-term model simulations and scenarios, the authors evaluated the impact of changes in nutrient loads and water level on the ecosystem. One of the outcomes was the development of a unique framework for defining the permissible ranges of management actions in the context of the Lake Kinneret CWQI (Parparov and Gal 2012). In the study, the authors defined ranges of acceptable limits for each variable (e.g., N load and P load), but rather than providing the range for each variable individually, the ranges were merged to create an area, or polygon, of acceptable ranges of both N and P loading jointly thus also accounting for not only the N-to-P ratios but also the loading values. Thus, the polygon delineates the combined acceptable ranges of nitrogen and phosphorus loading for a given lake level. This approach was later expanded to include definition of the combined acceptable ranges of nutrient loads (nitrogen and phosphorus) and water level (Gilboa- Ben David 2011). Combining the quantified WQ system and an ecosystem model, such as DYCD, provided the authors with a means of establishing and verifying the quantitative relationships between WQ and major management actions, with data obtained from ongoing lake monitoring. The authors were therefore able to establish a direct correspondence between permissible ranges for WQ and permissible ranges for the management actions and thus outline a sustainable management policy for Lake Kinneret water resources. Their approach represents a major step forward in lake management.

35.6 The Benefits and Drawbacks of Modeling

Modeling in general, and ecosystem modeling in particular, offers many advantages to scientists and decision makers providing a means for studying processes and interactions between ecosystem model components. This is extremely beneficial when studying complex ecosystems, such as those found in lakes. These complex systems contain multiple components with various processes affecting each component that also interact with other components. Ecosystem models typically represent a simplified version of reality but nevertheless allow the user to interrogate the ecosystem free of sampling and resource limitations which is not possible when investigating the actual lake. In addition, it is possible to use the ecosystem model to conduct virtual experiments at the ecosystem scale, to study alternative conditions that may affect the questions at hand, and to evaluate the possible impact of conditions beyond those observed historically. This is not possible to do in a real-lake environment and is possible only, to a limited degree, under experimental conditions. Furthermore, conclusions based on model results (or contradictions between model results and expectations or experimental data) can highlight weakness in existing information and assist in focusing research and efforts. Models can guide the monitoring strategies, suggest additional sampling required but also which reductions in effort can be performed thus optimizing the

cost of monitoring. Regardless of whether the model is descriptive, predictive, or prescriptive, the combination of model results with additional utilities such as sensitivity and uncertainty analyses and expert knowledge provides the user with insight and understanding that often cannot be gained through sampling and laboratory experiments.

The use of complex ecosystem models does, however, come with a price. The complexity of the models increases the need for information on parameters and observational data for model input, for calibration, and for model validation. Very rarely are the available data sufficient thereby increasing model uncertainties. Furthermore, enhanced model complexity results in a longer calibration and validation process with increasingly difficulty. Matching and planning monitoring programs and research programs to model needs can reduce much of the uncertainty and assist in the validation process. In addition, as knowledge is gained over time, there is a need to update and modify the available models. This process will reduce model uncertainty and increase its accuracy. However, to achieve this, model development should ideally be an ongoing process. This is often not the case due to the complexity of the model in question and the lengthy process of calibration and validation required following any major changes.

The application of models, in general, and ecosystem models, in particular, to Lake Kinneret research and management has progressed rapidly since 1980 and especially over the last decade. Ecosystem modeling will continue to develop and increasingly become a tool used by limnologists and resource managers alike. Increased understanding of processes occurring in the ecosystem will lead to further modification and enhancement of existing models along with development of new modeling approaches. In addition, application of tools for improving model accuracy and the integration of available real-time data and on-line instruments will result in wider application of models with self-calibration and self-learning capabilities.

References

Atanasova N, Gal G, Kompare B (2008) Modelling dinoflagellate dynamics in Lake Kinneret. Verh Int Verein Limnol 30:100–104

Atanasova N, Gal G, Džeroski S, Todorovski L, Kompare B (2011) Automated discovery of the factors governing Dinoflagellate dynamics in Lake Kinneret. Environ Model Soft 26:658–668

Azam F, Fenchel T, Field JG, Gray JS, Meyer-Reil LA, Thingstad F (1983) The ecological role of water-column microbes in the sea. Mar Ecol Prog Ser 10:257–263

Bruce LC, Hamilton D, Imberger J, Gal G, Gophen M, Zohary T, Hambright KD (2006) A numerical simulation of the role of zooplankton in C, N and P cycling in Lake Kinneret, Israel. Ecol Model 193:412–436

Burger DF, Hamilton DP, Pilditch CA (2007) Modelling the relative importance of internal and external nutrient loads on water column nutrient concentrations and phytoplankton biomass in a shallow polymictic lake. Ecol Model 211:411–423. doi:10.1016/j.ecolmodel.2007.09.028

Christensen V, Pauly D (1992) ECOPATH II—a software for balancing steady-state models and calculating network characteristics. Ecol Model 61:169–185

Drenner RW, Hambright KD (1999) Biomanipulation of fish assemblages as a lake restoration technique. Arch Hydrobiol 146(2):129–165

Gal G, Anderson W (2010) A novel approach to detecting a regime shift in a lake ecosystem. Methods Ecol Evol 1:45–52. doi:10.1111/j.2041–210X.2009.00006.

Gal G, Hipsey MR, Parparov A, Wagner U, Makler V, Zohary T (2009) Implementation of ecological modeling as an effective management and investigation tool: Lake Kinneret as a case study. Ecol Model 220:1697–1718. doi:10.1016/j.ecolmodel.2009.04.010

Gal G, Imberger J, Zohary T, Antenucci J, Anis A, Rosenberg T (2003) Simulating the thermal dynamics of Lake Kinneret. Ecol Model 162:69–86. doi:10.1016/S0304–3800(02)00380–0

Gal G, Makler-Pick V, Shachar N (2012) Dealing with uncertainty in ecosystem model scenarios: application of single-model ensemble approach. Paper presented at the 2012 international congress on environmental modelling and software, Leipzig

Gal G, Skerjanec M, Atanasova N (2013) Dissecting the factors impacting zooplankton community dynamics arising from dramatic changes in water levels: a data-driven modelling approach. Freshw Biol 58:800–816. doi:10.1111/fwb.12087

Gilboa-Ben David Y (2011) Assessing the effects of anthropogenic activities on water quality in Lake Kinneret using an integrated modeling system. PhD disseration, Technion—Israel Institute of Technology, Haifa

Gilboa Y, Friedler E, Gal G (2009) Adapting empirical equations to Lake Kinneret data by using three calibration methods. Ecol Model 220:3291–3300. doi:10.1016/j.ecolmodel.2009.09.007

Håkanson L, Parparov A, Hambright KD (2000) Modelling the impact of water level fluctuations on water quality (suspended particulate matter) in Lake Kinneret, Israel. Ecol Model 128(2–3):101–125. doi:10.1016/S0304–3800(00)00200–3

Hambright KD, Blumenshine SC, Shapiro J (2002) Can filter-feeding fishes improve water quality in lakes? Freshw Biol 47(6):1173–1182

Hambright KD, Zohary T, Gude H (2007) Microzooplankton dominate carbon flow and nutrient cycling in a warm subtropical freshwater lake. Limnol Oceanogr 52:1018–1025

Hart DR (2002) Intraguild predation, invertebrate predators, and trophic cascades in lake food webs. J Theor Biol 218:111–128. doi:10.1006/jtbi.2002.3053

Hart DR, Stone L, Berman T (2000) Seasonal dynamics of the Lake Kinneret food web: the importance of the microbial loop. Limnol Oceanogr 45(2):350–361

Imberger J, Patterson JC (1981) A dynamic reservoir simulation model DYRESM: 5. In: Fischer HB (ed) Transport models for inland and coastal waters. Academic, New York, pp 310–361

Kay JJ, Graham LA, Ulanowicz RE (1989) A detailed guide to network analysis. In: Wulff F, Field JG, Mann KH (eds) Network analysis in marine ecology: methods and applications. Springer, Berlin

Li Y, Waite AM, Gal G, Hipsey MR (2012a) An analysis of the relationship between phytoplankton internal stoichiometry and water column N:P ratios in a dynamic lake environment. Ecol Model 252:196–213. doi:10.1016/j.ecolmodel.2012.06.021

Li Y, Waite AM, Gal G, Hipsey MR (2012b) Do phytoplankton nutrient ratios reflect patterns of water column nutrient ratios? A numerical stoichiometric analysis of Lake Kinneret. Procedia Environ Sci 13:1630–1640. doi:10.1016/j.proenv.2012.01.156

Makler-Pick V (2010) A lake ecosystem model as a research tool for exploring fish impacts on food web dynamics with emphasis on intraguild predation. Technion—Israel Institute of Technology, Haifa

Makler-Pick V, Gal G, Gorfine M, Hipsey MR, Carmel Y (2011a) Sensitivity analysis for complex ecological models—a new approach. Environ Model Soft 26:124–134. doi:10.1016/j.envsoft.2010.06.010

Makler-Pick V, Gal G, Shapiro J, Hipsey MR (2011b) Exploring the role of fish in a lake ecosystem (Lake Kinneret, Israel) by coupling an individual-based fish population model to a dynamic ecosystem model. Can J Fish Aquat Sci 68:1265–1284. doi:10.1139/f2011–051

Ng SMY, Antenucci JP, Hipsey MR, Tibor G, Zohary T (2011) Physical controls on the spatial evolution of a dinoflagellate bloom in a large lake. Limnol Oceanogr 56(6):2265–2281. doi:10.4319/lo.2011.56.6.2265

Nishri A, Hamilton D (2010) A mass balance evaluation of the ecological significance of historical nitrogen fluxes in Lake Kinneret. Hydrobiologia 655(1):109–119. doi:10.1007/s10750–010-0408–3

Nishri A, Herman G, Shlichter M (1996) The response of the sedimentological regime in Lake Kinneret to lower lake levels. Hydrobiologia 339(1–3):149–160

Ostfeld A, Tubaltzev A, Rom M, Kronaveter L (2006) A hybrid model tree (MT)—Genetic Algorithm (GA) scheme for toxic cyanobacteria predictions in Lake Kinneret. World Environment and Water Resoiurce Congress 2006, pp 1–9. doi:10.1061/40856(200)125

Parparov A, Gal G (2012) Assessment and implementation of the methodological framework for sustainable management: Lake Kinneret as a case study. J Environ Manag 101:111–117. doi:10.1016/j.jenvman.2012.01.030

Rachamim T (2010) The role of zooplankton in nutrient recycling in Lake Kinneret (Zooplankton Stoichiometry). PhD dissertation, Bar Ilan University, Ramat Gan, Israel

Rigosi A, Marcé R, Escot C, Rueda FJ (2011) A calibration strategy for dynamic succession models including several phytoplankton groups. Environ Model Soft 26:697–710. doi:10.1016/j.envsoft.2011.01.007

Roelke DL, Zohary T, Hambright KD, Montoya JV (2007) Alternative states in the phytoplankton of Lake Kinneret, Israel (Sea of Galilee). Freshw Biol 52(3):399–411. doi:10.1111/j.1365–2427.2006.01703.x

Serruya C (1978) Lake Kinneret. Monographiae Biologicae, vol 32. Dr. W. Junk, The Hague

Serruya C, Gophen M, Pollingher U (1980) Lake Kinneret: carbon flow patterns and ecosystem management. Arch Hydrobiol 88(3):265–302

Stone L, Berman T, Bonner R, Barry S, Weeks SW (1993) Lake Kinneret: A seasonal model for carbon flux through the planktonic biota. Limnol Oceanogr 38(8):1680–1695

Trolle D, Jørgensena TB, Jeppesen E (2008) Predicting the effects of reduced external nitrogen loading on the nitrogen dynamics and ecological state of deep Lake Ravn, Denmark, using the DYRESM–CAEDYM model. Limnologica 38:220–232. doi:10.1016/j.limno.2008.05.009

Walline P, Pisanty S, Gophen M, Berman T (1993) The ecosystem of Lake Kinneret, Israel. In: Christensen V, Pauly D (eds) Trophic models of aquatic ecosystems. ICLARM, Manila, pp 103–109

Chapter 36
Fisheries Management

Ilia Ostrovsky, Tamar Zohary, James Shapiro, Gregory Snovsky and Doron Markel

Abstract Fish are at the top of aquatic food webs impacting on other biota. Removal of fish by fishing, or stocking the lake with desired fish species has the potential to modify fish populations (their size/age structure, abundance and biomass) and various other ecosystem components and thus affect water quality. Analysis of long-termdata onthe catches of commercially important fish species,stocking of fingerlings,lake water levels,and littoral modifications, allowed revealing the key factors affecting the fish populations, fishing pressure, and mass of landed fish. Long-term decreasesin water level negatively affected reproduction and survival of natural/stocked fingerlings of some cyprinids (*Mirogrex terraesanctae, Hypophthalamichthys molitrix, Cyprinus carpio*) and cichlids(*Sarotherodon galilaeus, Oreochromis aureus*). In contrast, rapid rises in water level vastly enlarged the areas of inundated terrestrial vegetation and stony/rocky littoral and thus positively affected the reproduction and survival of these fish and their landing after a temporallag.Fishing pressure on reproductively active large cichlidswas enhanced at low water levelsdue to exposing these fish at spawning time (spring and summer) to fishermen. Such overfishing resulted in lowering the number of reproductively capable cichlids below a certain critical level, leading to a decrease in the reproductive capacity of the population and the collapse of its standing stock (i.e. "recruitment overfishing"). The endemic bleak, *Mirogrex terraesanctae* is the dominant pelagic zooplanktivore of Lake Kinneret. Large water level fluctuationsimpacted its

I. Ostrovsky (✉) · T. Zohary
The Yigal Allon Kinneret Limnological Laboratory, Israel Oceanographic & Limnological Research, P.O. Box 447, 14950 Migdal, Israel
e-mail: ostrovsky@ocean.org.il

T. Zohary
e-mail: tamarz@ocean.org.il

J. Shapiro · G. Snovsky
Fishery Department, Ministry of Agriculture and Rural Development, 14100 Tiberias, Israel
e-mail: Jamess@moag.gov.il

G. Snovsky
e-mail: gregorys@moag.gov.il

D. Markel
Lake Kinneret and Watershed Unit, Israel Water Authority, Z.H.R. Industrial Park, P.O.Box 623, 12000 Rosh Pina, Israel
e-mail: Doronm10@water.gov.il

T. Zohary et al. (eds.), *Lake Kinneret, Ecology and Management,* Aquatic Ecology Series 6,
DOI 10.1007/978-94-017-8944-8_36,

reproduction and determinedthe abundance of this ecologically important species. Biomanipulation, by mean of subsidized harvesting, implemented to suppress its abundance in critical years, was highly controversial, and was stopped in 2006. Of the stocked grey mullets, *Mugil cephalus* had lower natural mortality rate, higher growth rate, reached larger sizes, and thus had a higher market value than *Liza ramada*. Still, fingerlings of the second species were more readily available, such that *L. ramada* was stocked in larger numbers and was more abundant in the commercial catch.We argue that fish stock management in Lake Kinneret should focus on the restoration of native fish populations and their sustainable fishery.

Keywords Fish stock · Catch · Littoral · Fishery · Water quality · Overfishing · Stocking · Water level fluctuation

36.1 Introduction

Fish are at the top of aquatic food webs impacting on other biota as well as on water quality by grazing on phytoplankton, preying on zooplankton, zoobenthos, and other fish, by feeding on organic matter, by accumulating phosphorus (P) in their skeleton, and by excreting nitrogen (N) and P (Holmlund and Hammer 1999; Carpenter et al. 2001). Removal of fish from the lake by fishing or alternatively stocking the lake with desired fish species has the potential to modify not only the fish populations but also various other ecosystem components and thus to indirectly affect water quality (Carpenter and Kitchell 1988). In contrast, ill-management and poor fishery practices can cause major damage to an ecosystem, some of which could be irreversible. As such, fisheries management is an important tool available to managers in order to preserve a lake ecosystem and its water quality.

The primary goal of fisheries management in Lake Kinneret is to contribute to the stabilization of the ecological system as part of the effort to preserve the lake as a major water resource for the State of Israel (Markel 2008; Markel 2012; Chap. 31). A secondary goal is to improve fishery yield and income by sustaining a fishery for commercial species. However, if these two goals contradict, requiring different actions, the first goal overrules; water quality cannot be compromised for the needs of fishery. Fishery management in the lake consists of multiple components including: (1) regulating fishing practices by instituting laws and regulations, (2) enforcing these laws, and (3) stocking fingerlings of desirable species. An additional practice applied in the past was subsidized commercial harvest aimed at the reduction of zooplanktivory to improve water quality.

Considering each of these points in detail:

1. The laws regarding fishing are designed to ensure that a sufficiently large proportion of the fish reach maturity and have at least one successful year of reproduction, as is common worldwide. Recent investigations show that large, elderly females are far more important than younger fish in maintaining productive fisheries (Berkeley et al. 2004). As such, these laws aim at preventing overfishing and protecting the fish during spawning, by (a) dictating a minimum permissible

net mesh size, to ensure that the largest specimens of each species are harvested, while the smaller individuals are left to grow and reproduce; (b) limiting the number of fishing boats, the length, and number of nets per boat and prohibiting illegal forms of fishing such as poisons, electrofishing, and underwater hunting with harpoons; (c) forbidding fishing in the Beteha lagoons (at the northeast part of the lake) for 2 months in spring, when the cichlid species use this region as their main spawning grounds; and (d) forbidding commercial fishing without a license.

2. The enforcement of these laws in Lake Kinneret has always been limited in its scope due to shortage of enforcement personnel, the prevalence of aggressive behavior of some fishermen, and lenient penalties for violators. As a result, overfishing continues to impair the state of the fish populations, especially that of the commercially valuable tilapias (*Sarotherodon galilaeus* and *Oreochromis aureus*). Illegal fishing, including fishing by poisoning, continues to be a problem.
3. Stocking of fingerlings of a few selected species (tilapia, grey mullets, and silver carp) is practiced in order to increase the catch and fishermen's income, while at the same time making some contribution to the improvement of the lake's water quality by feeding on phytoplankton, bacteria, and detrital organic matter. Regular stocking programs were initiated in the 1950s. The principles underlying fish stocking are (a) native fish can be introduced cautiously, taking into account the possible decrease in the genetic variability of their populations; (b) exotic fish can be introduced only if they are unable to reproduce in the lake and only after a period of observation in ponds; and (c) piscivorous fish should not be introduced, as these may irreversibly affect the Kinneret food web.
4. Overabundant small bleak (*Mirogrex* [syn. *Acanthobrama*] *terraesanctae*) in extreme flood years led to the lowest-ever levels of zooplankton abundance (Ostrovsky and Walline 2001; Chap. 16). To minimize negative impacts down the food chain, subsidized commercial fishing has been used to reduce predation pressure on zooplankton. In practice, the main objective of this management practice (improved water quality) was not obtained by its application, and it was discarded.

Introduction of alien species such as the grey mullets (*Mugil cephalus* and *Liza ramada*) was motivated by the fast growth rates of these species and assessments that their potential food resources were underutilized in Lake Kinneret (Ben Tuvia et al. 1992). Of the stocked alien species, only common carp (*Cyprinus carpio*) is able to reproduce in the lake (e.g., Snovsky et al. 2010), and because of this its intentional stocking was stopped in 1948. The sections below addressing the fisheries of tilapia, grey mullet, and carp also provide details on the stocking of these species.

The stocking programs and fisheries on Lake Kinneret are controlled by the Israel Water Authority and by the Israel Fisheries Department of the Ministry of Agriculture. An intergovernmental committee the "Stocking and Fisheries Management Committee" directs and oversees these management activities. This committee includes representatives from the Ministry of Agriculture (chair), Israel Water Authority (deputy chair), Fisheries Department, Kinneret Limnological Laboratory of IOLR, Kinneret Authority, fish experts from the Israeli universities, and a representative of the Kinneret fishermen. The Fisheries Department is responsible for issuing fishing licenses to fishermen and fishing boats, rearing or purchasing fingerlings to be stocked, and monitoring the size structure of the harvested fish and

the total mass landed for each species. Its officers are also responsible for enforcing the fishing regulations.

The largest fishery on Lake Kinneret in terms of annual fisheries biomass yield has been for many years that of the endemic bleak, *M. terraesanctae,* locally known as lavnun or the "Kinneret sardine." However, the main income to fishermen came from several other, larger-body-size fishes of much higher commercial value. These include the two native tilapias, *S. galilaeus* and *O. aureus,* and four alien stocked species: the grey mullets *M. cephalus and L. ramada,* silver carp *Hypophthalamichthys molitrix,* and common carp *Cyprinus carpio* (that is no longer stocked).

On various occasions, it was proposed to introduce into Lake Kinneret a high-commercial value piscivorous fish that cannot reproduce in the lake, such as the European seabass (*Dicentrarchus labrax*), but such suggestions were always rejected. According to the trophic cascade theory, adding a piscivore to the lake ecosystem may suppress the productivity of planktivorous fish. This may diminish their ability to clean the water by feeding on phytoplankton and organic matter (Hairston et al. 1960; Drenner and Hambright 2002), and as such would contradict the primary goal of the fish introduction program. Furthermore, since the seabass was shown to feed well on *Sarotherodon* sp. (Chervinski and Shapiro 1980), the most valuable native tilapia in Lake Kinneret, its introduction could suppress the tilapia standing stock and reduce its yield, another undesirable likely outcome.

The objective of this chapter is to give an overview of the historical and current thinking with respect to fisheries management in Lake Kinneret.

36.2 The Recent History of Fishery on Lake Kinneret

The history of fishery on Lake Kinneret dates back to prehistoric civilizations ~5,000 years ago, with archeological evidence especially from Beit Yerach, an ancient city on the southern shore of the lake by the Jordan River outflow (Nun 1977). Stories of this fishery at the times of Jesus comprise an integral part of the New Testament. Nun (1977) provides a detailed account of the history of fishing on Lake Kinneret. This chapter is restricted to fisheries practices and its management in recent times.

During the eighteenth and nineteenth centuries, under the Ottoman rule, fishery on Lake Kinneret was low; commercial fishing was revived in 1920, when the British abolished the practice of renting fishing rights and levying a fishing tax and permitted unlimited fishery by all licensed fishermen (Nun 1977). During 1935–1945, the number of licensed fisherman on the lake was 180–204, the number of small fishing boats was 36–57, and the yield was about 400 t of fish annually (A Survey of Palestine 1946). Fish biologists analyzing the Kinneret fisheries suggested that the unlimited fishery policy since 1920 resulted in overfishing (A Survey of Palestine 1946). As such, strict rules and fishery regulations were invoked leading to improvement of the harvest by the early 1940s (Nun 1977). For comparison, in 2011, the number of licensed small fishing boats on Lake Kinneret was 65, with 284 licensed fishermen (C Angiuni, Department of Fisheries, personal communication).

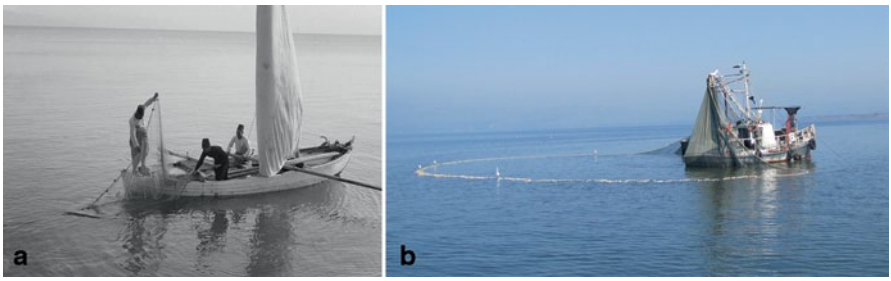

Fig. 36.1 Fishermen on Lake Kinneret in the 1940s (*left*, photo by G. Eric Matson, the Library of Congress) and in 2013, using a purse seine (*right*, photo by I. Ostrovsky)

Between 1950 and 1970, the fish catch gradually increased, from ~400 to 1,500–2,000 t annually, as a result of the combined effect of (1) improved fishing gear, (2) increased fishing effort, and (3) intensive stocking of fingerlings (Ben Tuvia et al. 1992). The improvement in fishing gear (Fig. 36.1) included more powerful boat engines, introduction of multispecies nets, replacement of coarse mesh cotton nets by fine monofilament nets, use of fish-finding echo sounders, mechanization of purse seine units, and introduction of laborsaving devices for packing and storage of large catches. All these resulted in a large increase in the fishing effort.

In the early 1970s, the total catch reached a plateau of 1,500–2,000 t, which lasted until 1999–2000. From then on, the catch declined, reaching an all-time minimum in 2008, with only moderate recovery since then (Fig. 36.2). The decline was attributed mainly to overfishing of commercially valuable fish (Zohary et al. 2008; Ostrovsky et al. 2013), concurrent with a sharp decrease in market demand for bleak. Other possible factors that could affect the fish populations and their landings are discussed below and in Chap. 16.

Gill and trammel nets and purse seining are the two main methods of fishing used currently. In the 1970s, 6–9-m-deep trammel monofilament nets were introduced. In the early 1980s, 90 small (4–6 m) fishing boats were employed, deploying multiple floating and sinking gill and trammel nets (Bar Ilan 1985). Purse seining was introduced as early as 1939 (Ben Tuvia et al. 1992) and used mostly for fishing bleak in the pelagic waters. By the 1980s, this method was employed by seven 10–12-m boats. With a sharp decline in the market for bleak, purse seining has nearly stopped since ~2005, with only one boat operating a purse seine on the lake in 2012.

36.3 Subsidized Harvesting of the Endemic Bleak, *Mirogrex terraesanctae*

As the dominant pelagic fish and a zooplanktivore, the bleak plays an important role in trophic interactions in Lake Kinneret. Despite its relatively low commercial value, a canning industry supported the bleak fishery so that its annual catch increased from ~200 t in the 1940s to ~1,000 t at the beginning of the 1970s through

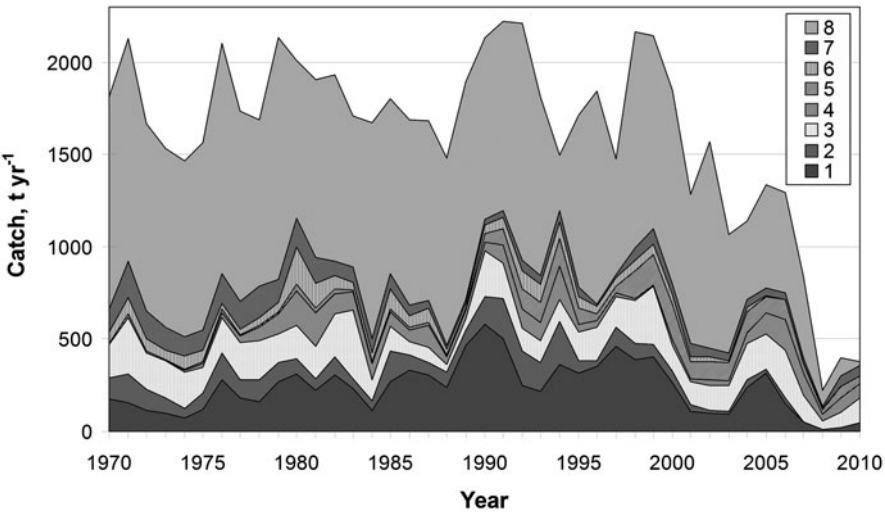

Fig. 36.2 Annual catches of the main fish species in Lake Kinneret, 1970–2010. *1 Sarotherodon galilaeus*, *2 Oreochromis aureus*, *3* Mugilids (*Liza ramada* and *Mugil cephalus*), *4 Hypophthalmichthys molitrix*, *5 Cyprinus carpio*, *6 Tristramella simonis*, *7 Barbus* spp., *8* Mirogrex terraesanctae. (Source: Ministry of Agriculture and Rural Development, Department of Fisheries and Agriculture)

the early 1990s (Fig. 36.2), contributing on average 50–60 % of all landed fish by mass. The situation changed in the early 1990s, when extreme fluctuations in water level took place as a result of increased abstraction in response to a rising demand for freshwater, concomitant with a long-term decline of inflow volumes (Zohary and Ostrovsky 2011; Chap. 7). Large rises in water level (>4 m, in comparison with a natural amplitude of ~1.5 m, Hambright et al. 1997) in exceptionally wet winters were followed by a huge reproductive success and enormous increases in bleak abundance, as recorded by acoustic surveys (Ostrovsky and Walline 2001; Ostrovsky et al. 2013). Excessive abundance and therefore excessive food requirements of this zooplanktivorous fish in the following 2–3 years suppressed zooplankton biomass and eventually led to a population of almost only sub-commercial-sized fish and the collapse of the bleak fishery (Chaps. 13 and 16). In an attempt to reduce fish predation pressure on zooplankton, increase the biomass of herbivorous zooplankton, improve water quality, and to revive the purse seine fishery, a subsidized harvest of the bleak was initiated and funded by the Israel Water Authority. The so-called bleak culling program was implemented to supplement the commercial fishery. Starting in winter 1994–1995, fishermen were paid to harvest bleak of all sizes and particularly fish smaller than commercial size. These fish were subsequently dumped outside the lake drainage basin. The fishermen were required to use regular purse seine nets with an added panel of smaller than regular mesh net (bunt) for retaining small fish. In practice, such a net design was implemented during the first 2 years, whereas later, the fishermen caught fish with standard nets only in order to have the flexibility to sell the larger fish commercially. The culling program

removed a total ~6,000 t of bleak from 1994 to 2006; at the same time, the bleak commercial fishery removed an additional total of ~4,000 t (Shapiro 2009).

The bleak-thinning program was controversial from the start of its implementation, with contrasting expert opinions regarding the reasons for the fishery collapse and different predictions regarding the likely outcome of subsidizing the harvest of sub-commercial-sized fish (Hambright and Shapiro 1997; Gophen et al. 1999). Hambright and Shapiro (1997) suggested that the fishing collapse in 1993 was due to a decade-long shift in harvested fish size and two consecutive fishing seasons of severe overharvest. Ostrovsky et al. (2013) argued that the fishery collapse was a result of the high mortality of large post-spawning individuals following years of unusually high reproductive success. This reproductive success was attributed to major water level rises and caused a deficiency of zooplankton food resulting from excessive predation pressure on zooplankton (Chap. 16). Blumenshine and Hambright (2003) compared potential predation pressure on Kinneret herbivorous zooplankton by bleak to that by the other major zooplankton predators, the cyclopoid copepods. They concluded that copepods accounted for a greater portion of the predation mortality on herbivorous zooplankton than bleak. These authors suggested that reduction in bleak predation pressure (by a subsidized harvest) may have led to increases in cyclopoid copepod abundance and thereby a net increase in predation pressure on herbivorous zooplankton, i.e., the opposite of the desired outcome. Walline et al. (2000) used data from acoustic measurements of fish populations and a spatially explicit bioenergetic model to calculate the potential consumption of zooplankton by fish. Their calculations indicated that the culling program reduced the potential for consumption of zooplankton by bleak and that targeting smaller fish in the removal program could have had a greater effect than that achieved by using commercial-size mesh nets.

Looking back, it is now possible to summarize the pros and cons of the bleak-thinning program, as conducted on Lake Kinneret during 1994–2006. The objectives of the thinning program were only partially accomplished. While fish predation pressure on zooplankton was apparently reduced, it remains unclear whether the subsidized bleak removal led to an increase in the biomass of herbivorous zooplankton and to an increased cleaning of the water by those herbivores. Certainly, there was no direct evidence to an improvement of water quality resulting from this program. The two most intensive ever blooms of harmful cyanobacteria on Lake Kinneret, in summer 1994 and again in summer 2005 (Chap. 12), both occurred despite subsidized harvest, within 2 years after a major rise in water level (Zohary and Ostrovsky 2011). It also remains inconclusive whether the thinning program contributed significantly to the observed eventual recovery of the bleak population. Management of the lake water levels within a narrower range of seasonal fluctuations could naturally prevent the unwanted changes in the bleak population, making the subsidized harvest unnecessary.

Irrespective of the thinning program, since 2006 the commercial fishery of the bleak has dwindled down to less than 100 t annually (Fig. 36.2), due to a sharp decline in market demand for this species, as a result of the closure of the market in Gaza and closure of three of the four local sardine-canning factories.

36.4 The Native Tilapias, Sarotherodon *galilaeus* (*amnun hagalil*) and *Oreochromis aureus* (*amnun hayarden*): Stocking and Overfishing

S. galilaeus (also known as *St. Peter's fish* in English, *musht abiad* in Arabic, or *amnun hagalil* in Hebrew) was the most commercially valuable fish in Lake Kinneret until 1999 when catches began to decline significantly. *O. aureus* (*musht lubbad* in Arabic or *amnun hayarden* in Hebrew) is another commercially important tilapia species. Intensive stocking of these indigenous cichlids was motivated by their high economic contribution to the local fishery, as well as their being considered major players in the Kinneret food web by feeding primarily on the bloom-forming dinoflagellate, *Peridinium gatunense* and on zooplankton (Zohary et al. 1994). It was believed that the lake ecosystem was capable of supporting much higher standing stocks of these tilapia species, which could not be attained naturally due to the shortage of suitable spawning grounds and/or high natural mortality of fry (Bar Ilan 1985).

The stocking of native tilapia *S. galilaeus* was initiated in 1951 and has continued since (Table 36.1). A brood stock kept at the Fisheries Department Station at Ginnosar, on the western shore of Lake Kinneret, produces fingerlings grown in ponds until their release to the lake, usually in August–September each year. Stocking of *O. aureus* began in 1958, but was stopped in 1984, as *O. aureus* was assumed to compete for food with *S. galilaeus,* the latter having higher commercial value and considered better for water quality as it fed more on *Peridinium* and less on zooplankton (Gophen et al. 1983; Zohary et al. 1994). While the stocking of *O. aureus* was followed by a remarkable increase in its catches (Reich 1976), no increase of landing was associated with stocking of *S. galilaeus* (Serruya and Leventer 1984). Moreover, at certain times, an increase in *S. galilaeus* stocking coincided with a decrease in its catch in the following years (Reich 1976 and Fig. 36.3b). In the mid-1980s, the stocking of *S. galilaeus* was intensified, reaching a maximum of six million fingerlings annually from 1999 to 2002 (Table 36.1). However, the assertion of Bar Ilan (1985) that a million stocked *S. galilaeus* fingerlings would lead to an additional 80–90 t of landed fish was not confirmed. Overall, no significant correlation was found between the number of stocked fish and their annual catch 2 years later, when the stocked fish should have reached the minimum commercial length of 20 cm. Moreover, an unexpected but highly significant negative correlation coefficient ($R = -0.79$) was observed between the number of *S. galilaeus* fingerlings introduced during years of increasing stocking effort (Fig. 36.3a), and the catch 2 years later (Fig. 36.3b). It could be that this is an artifact associated with two concurrent but independent trends. One trend is increased tilapia stocking in an attempt to compensate for the "insufficient" natural reproduction. The other trend of decreasing catch resulted from an extended period of gradually declining water levels, from 1995 to 2002. In the earlier years of this period, insufficient fishery control led to notably high catches as the fish had little refuge (see below). But, as a result, the stock became very small and catch decreased markedly in the later years. This demonstrates that the lack of fishery control can negate the expected

Table 36.1 Annual stocking (number of fingerlings · 10^6) of commercially important fish species in Lake Kinneret. (Source: Ministry of Agriculture and Rural Development, Department of Fisheries and Agriculture)

Year	S. gal	O. aur	Mug.	H. mol	Year	S. gal	O. aur	Mug.	H. mol
1970	0.70	2.45	3.62	0.02	1991	2.70	0.00	0.00	0.16
1971	2.15	1.09	0.63	0.00	1992	1.50	0.27	0.39	0.20
1972	2.13	1.04	0.01	0.02	1993	3.00	0.00	0.70	0.20
1973	1.54	0.25	0.03	0.63	1994	2.80	0.00	0.85	0.20
1974	1.87	3.19	0.00	1.33	1995	3.50	0.00	1.00	0.20
1975	1.27	3.85	0.57	0.67	1996	3.50	0.00	0.74	0.20
1976	1.75	0.44	1.36	1.04	1997	4.00	0.00	1.00	0.03
1977	1.64	3.22	0.85	1.86	1998	4.00	0.00	1.02	0.20
1978	2.25	0.00	0.77	1.10	1999	6.00	0.00	0.70	0.20
1979	2.00	0.00	1.10	1.20	2000	6.02	0.00	1.03	0.20
1980	1.80	0.40	1.20	1.70	2001	6.02	0.00	1.00	0.20
1981	1.80	0.95	0.90	1.50	2002	6.00	0.00	0.49	0.20
1982	1.70	1.50	0.20	0.60	2003	4.00	0.00	1.64	0.20
1983	2.36	0.17	0.03	0.56	2004	3.00	0.00	0.49	0.20
1984	4.63	0.03	1.20	0.00	2005	2.50	0.00	1.20	0.40
1985	5.50	0.00	1.23	0.00	2006	2.50	0.00	0.69	0.40
1986	3.00	0.00	0.14	0.00	2007	2.50	0.00	0.85	0.19
1987	3.50	0.00	1.40	0.02	2008	1.20	0.00	0.71	0.50
1988	3.50	0.10	1.50	0.07	2009	0.73	0.00	0.82	0.38
1989	2.80	0.00	1.00	0.07	2010	0.77	0.00	0.40	0.42
1990	2.85	0.00	0.97	0.26	2011	0.77	0.00	1.01	0.37

S. gal – Sarotherodon galilaeus, *O. aur – Oreochromis aureus*, *Mug – Mugilids*, *H. mol – Hypophthalmichthys molitrix*

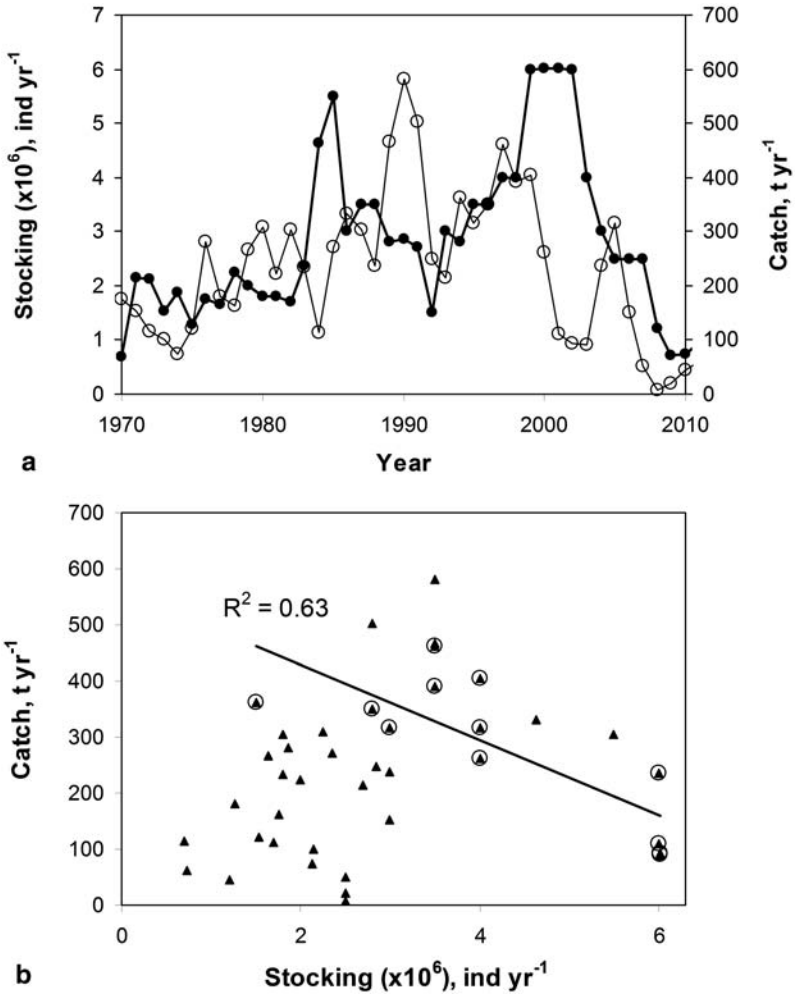

Fig. 36.3 Annual stocking and catch of *S. galilaeus* in Lake Kinneret. **a** The temporal dynamics; fish stocked are shown in *filled circles*; catches are shown in *empty circles*. **b** The relationship between the number of fingerlings stocked and their catch 2 years later; fish stocked between 1970 and 2009 are shown in *small triangles* ($R^2 = 0.032$, $n = 40$, $p > 0.05$); fish stocked between 1992 and 2003 are *circled* ($R^2 = 0.63$, $n = 12$, $p < 0.01$). (Source: Ministry of Agriculture and Rural Development, Department of Fisheries and Agriculture)

benefits of stocking. Consequently, the stocking strategy was changed. From 2008, a smaller number (~one million) of larger-size fry with higher chances of survival have been stocked.

In fact, it remains unknown whether and how much stocking has contributed to the catch of *S. galilaeus*. Current research focuses on finding a suitable means of marking the stocked fingerlings of *S. galilaeus* by a physical tag, dye, or molecular

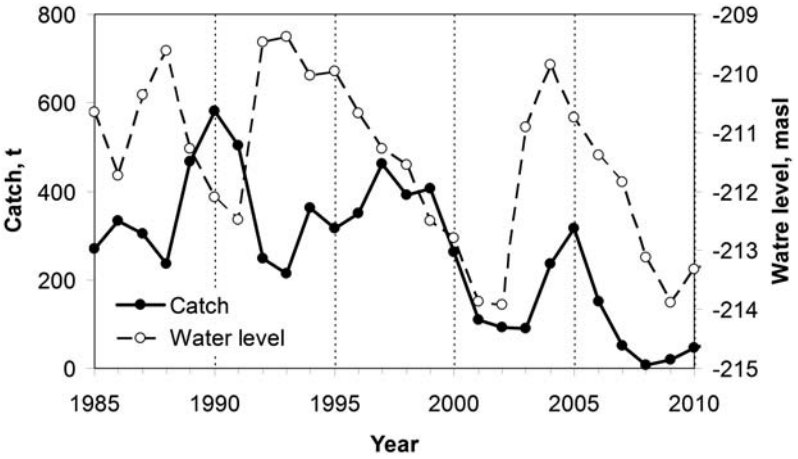

Fig. 36.4 Changes in annual catches of tilapia *S. galileus* (*full circles*) in relation to the mean annual water level (*empty circles*). A negative correlation between *S. galilaeus* annual catch and annual mean water level was observed until 1998. Since 1999, the catch covaried with the water level, until the virtual disappearance of *S. galilaeus* in the catches of 2007–2011. Water level is presented in meters above sea level (*masl*). (Data sources: Catch—Ministry of Agriculture and Rural Development, Department of Fisheries and Agriculture; water level—Israel Hydrological Services)

marker, so that in the future, it will be possible to estimate directly the contribution of stocked fish to the catch.

Long-term production of fingerlings from a genetically limited brood stock may, over time, lead to a decline in the genetic variability of the entire population of *S. galilaeus* in the lake. Surprisingly, Shitenberg (2006) has revealed particularly small genetic variability of *S. galilaeus* from native populations of all over Israel in comparison with the genetic variability of this species in native populations in Ghana. The low natural genetic variability in Israel may be attributed to Israel being at the northernmost tip of the biogeographic distribution of this African fish. Probably, the entire population in Israel stems from a small number of founding parents. Thus, further limiting the genetic variability of the Kinneret *S. galilaeus* by long-term stocking is a definite concern.

A time series of Lake Kinneret water levels and the annual catches of *S. galilaeus* (Fig. 36.4) shows apparent relationships between these two variables. A strong negative correlation ($R = -0.84$, $p < 0.01$) between the tilapia catch and water level was recorded from 1985 through 1998; subsequently, the two variables were positively correlated. A possible explanation for the negative correlation is that during 1985 to 1998, low water levels made it easier to catch the fish at the lake periphery; at lower lake levels, the proportion of sandy littoral areas progressively increases at the expense of stony and rocky substrates, the latter providing better refuge for fish (Gasith and Gafny 1990). Furthermore, at declining water levels, the sandy littoral was devoid of vegetation, (Chap. 29). Thus, at lower water levels, *S. galilaeus*

had less refuge, especially during the spawning season (April–July) when the fish congregate in shallow water and are easy to harvest. Eventually, the average size of landed fish (length and weight per individual) declined (Ostrovsky 2005; Ostrovsky et al. 2013), as is typical for fish subjected to strong fishing pressure.

From 1998 onwards, the correlation between water level and *S. galilaeus* harvest became positive. With an impoverished population depleted of its larger individuals, especially its maternal stock, low water levels no longer provided opportunities for easy fishing, as the large fish simply did not exist. The high rainfall winter of 2002–2003, with its rapid rise in water level, provided a "window of opportunity" for fish reproduction (sensu Gasith and Gafny 1998; Chap. 29). The dense shoreline vegetation that had developed on the exposed beaches during the previous years of low water levels was inundated by the rising waters, providing refuge and shelter from predators and fishermen, abundant food in the form of algae and invertebrates, suitable spawning grounds, and excellent growth conditions for the young-of-year. This winter was followed by improved catch in the following 2–3 years.

From 1997 through 2002, years with a steady decline of the mean water level, an unusually high increase in fishing mortality caused a large rise in the proportion of sub-commercial size *S. galilaeus* (<20 cm total length) in the catch, from 43 % in 1997 to ~80 % in 2002 (Ostrovsky 2005). The observed increase in fishing pressure, decline in the mean size of caught fish, and concurrent drop in the mass of landed *S. galilaeus* indicated intense overfishing. Continued intensive fishing on *S. galilaeus* during the years with declining water levels from 2005 onwards caused a collapse of the tilapia fishery by 2008 (Fig. 36.2). Venturelli et al. (2009) showed a direct link between population age structure and reproductive rate, consistent with strong effects of maternal quality on population dynamics. They concluded that a population of older, larger individuals has a higher maximum reproductive rate than a population of the same number of younger, smaller individuals and that this difference increases with the reproductive lifespan of the population. In Lake Kinneret, the observed collapse of the most commercially important fish was probably caused by removal of the older female fish by intensive fishing (Ostrovsky, unpublished results).

Predation by the piscivorous Great Cormorant *Phalacrocorax carbo* may have influenced the abundance of some fish species over the past years. The numbers of these birds have increased over the last decade and presently flocks of thousands of cormorants populate the northern part of Lake Kinneret in winter (Shy et al. 2003). While on the lake, they consume mostly bleak and cichlids (about 50 % of each species, Artzi 2011). Still, the proportion of *S. galilaeus* out of the total cichlids in cormorant diet has not been estimated and thus it is currently impossible to conclude definitely if these birds affect the *S. galilaeus* catch.

Several other factors may have contributed to the 2008 collapse of the *S. galilaeus* fishery and the Kinneret fishery in general, as summarized by Zohary et al. (2008). These included the lack of *Peridinium gatunense,* the main food item of *S. galilaeus* as this species failed to bloom in most (10 out of 16) of the years between

1996 and 2011 (Zohary et al. 2012); illegal fishing with pesticides causing fish kills (Chap. 33.2); and possible predation of fingerlings by catfish, *Clarias lazera*. However, solid data to support any of these suggestions are lacking.

36.5 *Hypophthalamichthys Molitrix* (Silver Carp)

The silver carp was first introduced and stocked in the lake in 1969. While its commercial value per mass is relatively small compared to tilapia and grey mullets, its large body mass makes it commercially valuable. Because these fish graze on phytoplankton and other small organic particles, it was assumed that the silver carp would contribute to cleaning the water. For a decade between 1973 and 1983, about one million fingerlings of this species, raised at the Nir David Station of the Department of Fisheries and Agriculture, were stocked annually (Table 36.1). Silver carp grows in Lake Kinneret at extremely fast rates, similar to that in fishponds (Shefler and Reich 1977; Snovsky 2000). It is an obligate filter-feeding planktivore, consuming anything suspended in the water (Shapiro 1985; Spataru and Gophen 1985). In the early 1980s, concern was raised that *H. molitrix* competed with *S. galilaeus* and *O. aureus* for zooplankton (Sparatu 1976; Gophen and Pollinger 1985; Sparatu and Gophen 1985). Because of this, its stocking was stopped in 1984. Due to recurrent requests from fishermen, the understanding that this species does not reproduce in Lake Kinneret or its inflowing rivers and that this fish at low densities will not have adverse impacts on the ecosystem, stocking was reinstated in 1988, at a reduced amount of 200,000 fingerlings annually, which was increased to 400,000 fingerlings in 2005 (Table 36.1). Currently, the stocking of silver carp in Lake Kinneret is being reconsidered, and in the meantime the amount stocked in 2012 was 300,000. The primary concern with regard to silver carp stems from the bad experience with this species in the USA, where silver carp and related species are considered some of the worst alien species to have invaded their lakes and rivers (Chick and Pegg 2001). Moreover, since a proportion of the silver carp's diet comes from zooplankton, it catalyzes nutrient turnover and availability and thus usually causes an increase rather than decrease in phytoplankton biomass (Zhang et al. 2008). Hence, this species should not be used for biomanipulation in mesotrophic lakes (Radke and Kahl 2002).

Shortly after the initiation of stocking, during the period 1976–1988, the catch of silver carp followed closely the number of fingerlings stocked 3 years earlier (Fig. 36.5a), as expected for a species that cannot reproduce in the lake or its catchment, and a significant correlation ($R=0.83$, $p<0.01$) was found between the two variables (Fig. 36.5b). However, since 1989–1990, the correlation between the catch and number of stocked fish disappeared, and from then on the harvest was not related to the number of fingerlings stocked (Fig. 36.5). Since this species cannot reproduce in the lake or its catchment, we suggested that survival of the fingerlings varied from year to year, with changes in water level and the availability of inun-

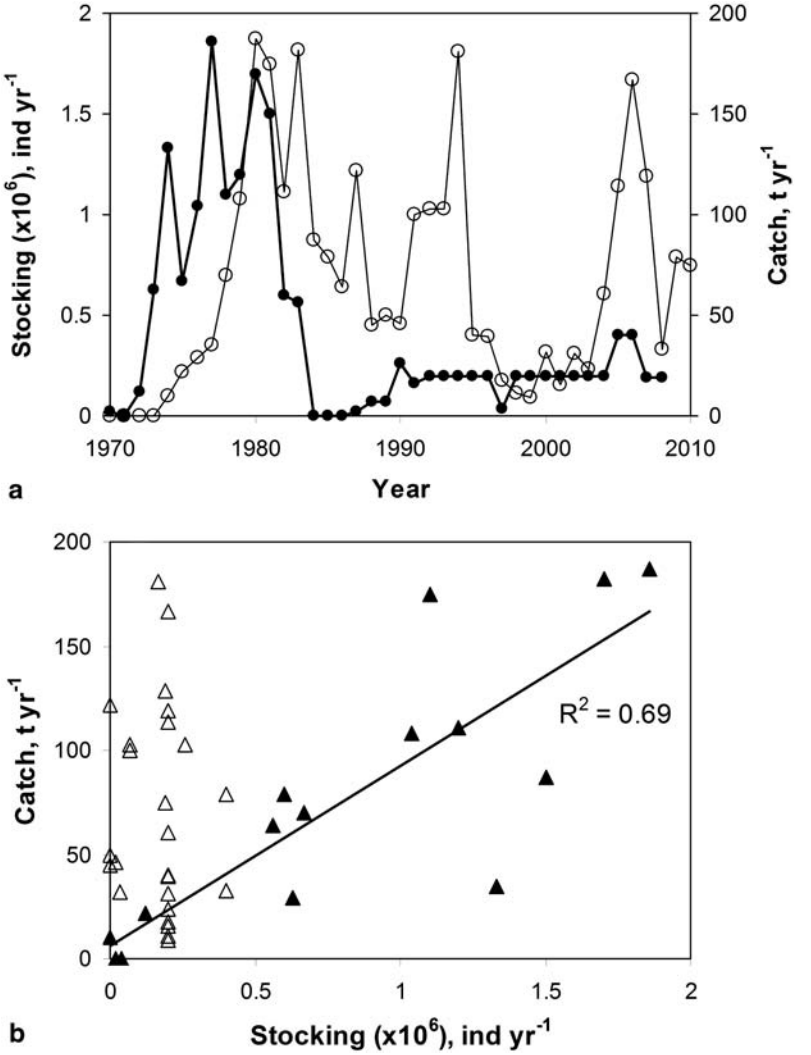

Fig. 36.5 Stocking and annual catch of *H. molitrix* in Lake Kinneret, 1969–2011. **a** Temporal dynamics; fish stocked are shown in *filled circles*; catches are shown in *empty circles*. **b** The relationships between the number of stocked fish and their catch 3 years later, when they first reached commercial size; fish stocked between 1969 and 1983 are shown in *filled triangles* ($R^2=0.69$, $n=15$, $p<0.001$); fish stocked between 1984 and 2008 are shown in *empty triangles* ($R^2=0.0035$, $n=25$, $p>0.05$). (Source: Ministry of Agriculture and Rural Development, Department of Fisheries and Agriculture)

dated vegetation in the littoral zone (Chap. 29). Other possible factors leading to the observed lack of correlation since the early 1990s could be parameters related to the size and health of fingerlings, conditions at the time of stocking, and changes in phytoplankton species composition.

36.6 *Cyprinus carpio* (Common Carp): Stocking and Catch

Stocking of *C. carpio* was intentional only in 1948; later, large numbers of fingerlings and adults escaped from fishponds in the watershed and populated the lake. In spite of this and the low ability of this species to reproduce in Lake Kinneret, prior to the early 1990s, the catch of common carp has remained low, averaging 13.5 t year^{-1} (Fig. 36.2). This led Reich (1976) to conclude that the conditions in Lake Kinneret were not optimal for its growth and breeding. However, this seems to have changed over time. Since 1990, carp catches increased to ~ 100 t year^{-1}, even though carp farming in the Kinneret watershed was stopped in the early 1990s. These changes occurred concurrently with low lake water levels and increased lake level fluctuations that in wet winters created large littoral areas with flooded shoreline vegetation, which probably could serve as suitable spawning grounds of carp and habitat for the growth and survival of its fingerlings.

36.7 *M. cephalus and L. ramada* (Grey Mullets, Buri): Stocked Aliens that do not Reproduce in Lake Kinneret

Two species of alien grey mullets (*M. cephalus, L. ramada*) have been introduced to the lake annually since 1958. These marine species cannot reproduce in the freshwater lake. The small (<0.1 g) fry are collected from December to March in the Mediterranean estuaries, acclimated, and then released into Lake Kinneret. Stocking of grey mullets is efficient due to high growth rate and low mortality rate. The return rate of the stocked fish in the commercial catch is assessed at ~30% (Snovsky 1993). Of the two species, *M. cephalus* has higher growth rate, reaches larger sizes, and thus has higher market value, so was considered more desirable than *L. ramada* (Snovsky and Ostrovsky 2014). However, *L. ramada* fry are usually more available than those of *M. cephalus,* and the price per fingerling is considerably lower. Therefore, on average since 1995, ~90% of the stocked grey mullets were *L. ramada*.

Currently, grey mullets have the highest value per kilogram of any commercial fish caught in Lake Kinneret. During the years following the collapse of the tilapia fishery in 2008, grey mullets comprised the primary income-generating commercial catch.

Grey mullets are bottom feeders, consuming the lake sediments and sieving out organic matter and living organisms, so they are assumed not to compete with the native tilapias for food. Still, since benthivorous species may cause recurrent resuspension of bottom sediments and thus stimulate upward nutrient flux to the water column (Katz et al. 2012), the actual ecological role of grey mullets should be carefully investigated, and the amount of stocked fingerlings needs to be reassessed accordingly. At present, the number of stocked fry is limited to one million fingerlings of both species combined per year.

36.8 Conclusions and Recommendations

1. *Reduction of overfishing:* The extensive overfishing that has been observed in the lake (Ostrovsky 2005) suggests that fish standing stocks and landings can be increased by optimization of the amount of fishing effort through catch and effort controls (e.g., introduction of fishing quotas, moratoria), by enforcing the established minimum fish size limits, by regulating the gear and fishing methods used (net mesh size, number, and length of nets per fishing boat), and by regulating when and where fishing is permitted or prohibited. Furthermore, the authorities should monitor the mass, size, and age of the catch (FAO 1997) and enforce the fishing laws in response to the observed status of the fishery. Some of these control measures are already part of the Kinneret Fishing Law and the activities of the Department of Fisheries. However, due to limited law enforcement and lack of fast feedback from the fishery monitoring program, fish continue to be harvested at an average size that is smaller than that which would produce the maximum yield per recruit (i.e., "growth overfishing").
2. *Maintenance of native fish stocks:* Fish stock management in Lake Kinneret should focus on the *restoration* of native fish populations and their sustainable fishery. These species are evolutionarily adapted to the natural ambient conditions. The maintenance of native fish stocks at productive levels requires an adequate abundance of reproductively mature adults (spawners) and suitable habitats for successfully passing through the different stages in the life history. Overfishing results in lowering the number of reproductively capable individuals below a certain critical level, leading to a decrease in the reproductive capacity of the population and the collapse of its standing stock (i.e., "recruitment overfishing"). To resolve this, the spawning stock biomass should be restored to sustainable levels. In particular, fishing in the littoral zone, or at least in some parts of the littoral zone, must be restricted during the spawning and nesting periods. Such restrictions are already implemented in the Beteha region on the northeastern lakeshore for 2 months in spring each year, but their enforcement is limited. The restrictions should be fully enforced and expanded to the littoral zone around the entire lake. Concurrently, the stocking policy of alien species should be reassessed.
3. *Water level fluctuations:* Water level fluctuations and the mean annual water level strongly affect the littoral habitats, fish reproduction, and fingerling survival. Fishing pressure on large individuals, which are reproductively active, is linked to the mean water level. Therefore, restricting water level fluctuations to the range to which native Kinneret fishes have been evolutionarily adapted should be an important stabilizing measure for sustainable management of fish resources. This recommendation has been accepted by the water authority, and in accordance with the new master plan for the water system of Israel, the Lake Kinneret water level will be kept in the future above the "red line" of −213 m.
4. *Technology transfer and public education:* Overfishing and usage of illegal fishing methods, together with unintentional introduction of alien species, have fre-

quently led to the destruction of aquatic ecosystems and fisheries (Pauly et al. 2002). Often, the damaging actions are due to the lack of understanding by those conducting them. An urgent need exists to develop the means to educate fishermen and residents of the Kinneret region about sustainable fisheries and ecosystem management so that they will take part in the conservation of the lake rather than harming it unintentionally.

5. *A sound fisheries biology program:* This chapter highlights many areas where our knowledge is limited, and further research and monitoring are urgently needed in order to improve the management of Lake Kinneret fish populations and its fisheries. Examples of current knowledge gaps include monitoring data on the actual standing stocks of the different species, maximum sustainable yields for the commercial species, the contribution of stocked *S. galilaeus* to the harvest, the role of silver carp and grey mullets in the food web, effort and catch impacts, the role of catfish as top predators, and competition for food resources between native and alien species. Such studies require multiinstitutional and multidisciplinary efforts, special funding and equipment, and dedicated personnel.

References

A Survey of Palestine (1946) Prepared in December 1945 and January 1946 for the information of the Anglo-American Committee of Inquiry. Jerusalem: Government Printer (1946–1947)

Artzi Y (2011) Large cormorant feeding in Lake Kinneret in winter 2010–2011. Israel nature and parks board internal report (In Hebrew)

Bar Ilan M (1985) Fisheries management of Lake Kinneret. FAO Fish Rep 289(3):391–398

Ben Tuvia A, Davidoff EB, Shapiro J, Shefler D (1992) Biology and management of Lake Kinneret fisheries. Bamigdeh 44(2):48–65

Berkeley SA, Chapman C, Sogard SM (2004) Maternal age as a determinant of larval growth and survival in a marine fish, *Sebastes melanops*. Ecology 85:1258–1264

Blumenshine SC, Hambright KD (2003) Top-down control in pelagic systems: a role for invertebrate predation. Hydrobiologia 491:347–356

Carpenter SR, Kitchell J (1988) Consumer control of lake productivity. Bioscience 38:764–769

Carpenter SR, Cole J, Hodgson J et al (2001) Trophic cascades, nutrients, and lake productivity: whole lake experiments. Ecol Monogr 71:163–186

Chervinski J, Shapiro J (1980) Additional experiments on the growth of juveniles and fingerlings of the European sea bass (*Dicentrarchus labrax* L.). Bamigdeh 32(3):78–85

Chick JH, Pegg MA (2001) Invasive carp in the Mississippi River Basin. Science 292(5525): 2250–2251

Drenner RW, Hambright KD (2002) Piscivores, trophic cascades and lake management. Sci World 2:284–307

FAO Technical Guidelines for Responsible Fisheries (1997) Fisheries Management 4. Food and Agriculture Organization of the United Nations, Rome, p 82

Gasith A, Gafny S (1990) Effects of water level fluctuation on the structure and function of the littoral zone. In: Tilzer MM, Serruya C (eds) Large lakes: ecological structure and function. Springer, Berlin, pp 156–171

Gasith A, Gafny S (1998) Importance of physical structures in lakes: the case of Lake Kinneret and general implications. In: Jeppesen E, Sondergaard M, Sondegaard M, Christoffersen K (eds) Structuring role of submeged macrophytes in lakes. Springer, Berlin, pp 331–338

Gophen M, Pollingher U (1985) Relationships between food availability, fish predation and the abundance of the herbivorous zooplankton community in Lake Kinneret. Arch Hydrobiol Beih Ergebn Limnol 21:397–405

Gophen M, Drenner RW, Vinyard GG (1983) Fish introductions into Lake Kinneret—call for concern. Fish Manag 14(1):43–45

Gophen M, Walline P, Ostrovsky I, Azoulay B, Easton J (1999) Water quality and fishery management in Lake Kinneret, Israel. In: Tundisi JG, Straskraba M (eds) Theoretical reservoir ecology and its applications. Backhuys, Sao Carlos, pp 493–503

Hairston NG, Smith FE, Slobodkin LB (1960) Community structure, population control, and competition. Am Nat 94:421–425

Hambright KD, Shapiro J (1997) The 1993 collapse of the Lake Kinneret commercial bleak fishery. Fish Manag Ecol 4:275–283

Hambright KD, Zohary T, Eckert W (1997) Potential influence of low water levels on Lake Kinneret: re-appraisal and modification of an early hypothesis. Limnologica 27(2):149–155

Holmlund CM, Hammer M (1999) Ecosystem services generated by fish populations. Ecol Econ 29:253–268

Jackson JBC, Kirby MX, Berger WH, Bjorndal KA, Botsford LW, Bourque BJ, Bradbury RH, Cooke R, Erlandson J, Estes JA, Hughes TP, Kidwell S, Lange CB, Lenihan HS, Pandolfi JM, Peterson CH, Steneck RS, Tegner MJ, Warner RR (2001) Historical overfishing and the recent collapse of coastal ecosystems. Science 293(5530):629–637

Katz T, Yahel G, Reidenbach M, Tunnicliffe V, Herut B, Crusius J, Whitney F, Snelgrove PVR, Lazar B (2012) Resuspension by fish facilitates the transport and redistribution of coastal sediments. Limnol Oceanogr 57:945–958

Markel D (2008) Monitoring and managing Lake Kinneret and its Watershed, Northern Israel, a response to environmental, anthropogenic and political constraints. In: Menon S (ed) Watershed management: case studies. The Icafi University Press, Punjagutta, pp 87–106

Markel D (2012) Fishery regulation in Lake Kinneret as a tool for improved management of the lake. Dayig Umidge 15:1597–1600 (In Hebrew)

Nun M (1977) Sea of Kinneret. Hakibbutz Hameuchad Publisher, Tel Aviv, p 260 (In Hebrew)

Ostrovsky I (2005) Assessing mortality changes from size-frequency curves. J Fish Biol 66(6):1624–1632

Ostrovsky I, Walline P (2001) Multiannual changes in the pelagic fish *Acanthobrama terraesanctae* in Lake Kinneret (Israel) in relation to food sources. Verh Int Ver Theor Angewandte Limnol 27:2090–2094

Ostrovsky I, Rimmer A, Yacobi YZ, Nishri A, Sukenik A, Hadas O, Zohary T (2013) Long-term changes in the Lake Kinneret ecosystem: the effects of climate change and anthropogenic factors. In: Goldman CR, Kumagai M, Robarts RD (eds) Climate change and inland waters: impacts and mitigation approaches for ecosystems and society. Wiley-Blackwell, Hoboken, pp 271–293

Pauly D, Christensen V, Guénette S, Pitcher TJ, Sumaila UR, Walters CJ, Watson R, Zeller D (2002) Towards sustainability in world fisheries. Nature 418:689–695

Radke RJ, Kahl U (2002) Effects of a filter-feeding fish [silver carp, *Hypophthalmichthys molitrix* (Val.)] on phyto- and zooplankton in a mesotrophic reservoir: results from an enclosure experiment. Freshw Biol 47:2337–2344

Reich K (1976) Problems of fisheries research in Lake Kinneret. Bamigdeh 28(1/2):3–11

Serruya C, Leventer H (1984) Lakes and reservoirs in Israel. In: Taub FB (ed) Lake and reservoirs. Elsevier Science, Amsterdam, pp 357–383

Shapiro J (1985) Food and intestinal contents of the silver carp, *Hypothalmichthys molitrix* (Val), in Lake Kinneret between 1982–1984. Bamigdeh 37(1):3–18

Shapiro J (2009) The fisheries and aquaculture of Israel 2007. State of Israel, Ministry of Agriculture and Rural Development, Department of Fisheries and Agriculture, p 48 (In Hebrew)

Shefler D, Reich K (1977) Growth of silver carp (*Hypophthalmichthys molitrix*) in Lake Kinneret in 1969–1975. Bamigdeh 29(1):3–16

Shitenberg A (2006) The phylogeography of three Israeli Tilapiinae (Cichlidae) species. MSc thesis, Tel Aviv University
Shy E, Geva A, Goren M (2003) Resolving the conflict between Great Cormorants *Phalacrocorax carbo* and aquaculture in Israel: efficiency and cost-benefit analysis of methods, use of alternative feeding sites and presumed Cormorant impact on water quality of the national reservoir. Vogelwelt 124 (Suppl):355–367
Snovsky G (1993) Biological aspects and fishery of grey mullets in Lake Kinneret. Fish Aquac Isr 1:33–50 (In Hebrew)
Snovsky G (2000) Biology and fishery of the silver carp. Fish Aquac Isr 1:108–117 (In Hebrew)
Snovsky G, Ostrovsky I (2014) The grey mullets in Lake Kinneret: the success of introduction and possible effect on water quality. Water and Irrigation 35–533:32 (In Hebrew)
Snovsky G, Shapiro J, Sonin O (2010) Trends of carp fishing in the Sea of Galilee. Fish Fish Feed Isr 3–4:1457–1462 (In Hebrew)
Spataru P (1976) The feeding habits of *Tilapia galilaea* (Artedi) in Lake Kinneret (Israel). Aquaculture 9:47–59
Spataru P, Gophen M (1985) Feeding behaviour of silver carp *Hypophthalmichthys molitrix* Val. and its impact on the food web in Lake Kinneret, Israel. Hydrobiologia 120(1):53–61
Venturelli PA, Shuter BJ, Murphy CA (2009) Evidence for harvest-induced maternal influences on the reproductive rates of fish populations. Proc Biol Sci 276(1658):919–924
Walline PD, Tyler JA, Brandt SB, Ostrovsky I, Jech JM (2000) Lavnun abundance: how changes may affect consumption of Lake Kinneret zooplankton. Arch Hydrobiol 55:493–511
Zhang X, Xie P, Huang X (2008) A review of nontraditional biomanipulation. Sci World J 8:1184–1196
Zohary T, Erez J, Gophen M, Berman-Frank I, Stiller M (1994) Seasonality of stable carbon isotopes with Lake Kinneret pelagic food web. Limnol Oceanogr 39(5):1030–1043
Zohary T, Nishri A, Sukenik A (2012) Present-absent: a chronicle of the dinoflagellate *Peridinium gatunense* from Lake Kinneret. Hydrobiologia 698:161–174
Zohary T, Gasith A, Markel D, Ostrovsky I (2008) The collapse of the Saint Peter's fish fishery in Lake Kinneret. Fish Fish Breed Isr 39:1214–1224 (in Hebrew)
Zohary T, Ostrovsky I (2011) Ecological impacts of excessive water level fluctuations in stratified freshwater lake. Inland Waters 1:47–59

Part VII
Overview

Chapter 37
Lake Kinneret: Current Understanding and Future Perspectives

Tamar Zohary, Assaf Sukenik and Ami Nishri

Abstract This chapter is an overview of the current state of knowledge on Lake Kinneret and the understanding of how this ecosystem functions, as reflected in the chapters of this book.

Keywords Hydrodynamic regime · Nutrient cycling · Food web · Trophic state · Water level fluctuations

37.1 Introduction

Since the publication of the monograph on Lake Kinneret (Serruya 1978), there has been a steady, in some cases substantial, progress in understanding the driving forces in Lake Kinneret and their effects on the functioning of this ecosystem. Modern instruments and methodologies, enhanced computational power, extended long-term biological and geochemical databases, as well as developments in limnological theory, all contributed to our current understanding of this dynamic ecosystem. Here, we summarize the current state of knowledge of one of Israel's major sources of freshwater, Lake Kinneret, as reflected in the chapters of this book.

37.2 Location, Morphological, and Climatic Setting

Lake Kinneret is a relatively large (169 km^2), moderately deep (42 m maximum depth) mountain-enclosed lake of relatively simple topography and morphometry (Fig. 1.1, Chap. 1), located in the semiarid (direct annual rainfall: ~400 mm)

T. Zohary (✉) · A. Sukenik · A. Nishri
The Yigal Allon Kinneret Limnological Laboratory, Israel Oceanographic & Limnological Research, P.O. Box 447, 14950, Migdal, Israel
e-mail: tamarz@ocean.org.il

A. Sukenik
e-mail: assaf@ocean.org.il

A. Nishri
e-mail: nishri@ocean.org.il

T. Zohary et al. (eds.), *Lake Kinneret, Ecology and Management,* Aquatic Ecology Series 6,
DOI 10.1007/978-94-017-8944-8_37,

northern part of the Syrian–African Rift Valley. The lake is a regional exception, as there are no other natural freshwater lakes of substantial size in Israel or its neighboring Middle East countries, including Cyprus, Egypt, Jordan, Syria, Lebanon, and the entire Arab peninsula. The lake, located within the Dead Sea tectonic depression, has exceptionally low elevation of more than 200 m below sea level. In fact, its elevation is the lowest on Earth for a freshwater lake. These geographic and topographic locations lead to predominantly hot weather with summer air temperatures often exceeding 40 °C and winter lows rarely declining below 10 °C.

The Mediterranean climate brings rainfall only in the cool winters while the summers are dry and hot. Consequently, riverine inflows, nutrient loads, and lake water levels are also highly seasonal, being high in winter–spring and low in summer–fall. This seasonal pattern of air temperature and inflows plays a major role in the lake's physical and biogeochemical processes. The relatively deep water column and the spring–summer warm air temperatures allow for stable stratification in the summer, whereby the strong westerly winds every afternoon maintain a well-mixed epilimnion, of ~15-m thickness in August–September, a sharp thermocline, and induce strong internal wave activity that imposes boundary mixing. The cool winters are characterized by periods of extended relatively calm and sunny weather that are interrupted occasionally by rainstorms coming from the Mediterranean, or by "sharakiya" storms of strong easterly winds coming from the surrounding deserts and usually lasting several days.

Circulation of surface water in the lake is mostly in two, uneven gyres that are seen in images acquired by Landsat satellites: a large counterclockwise gyre in the northern and central parts of the lake and a small clockwise gyre in its southern part.

37.3 Water Balance

The Jordan River is the major source of water, solutes, and allochthonous particles to Lake Kinneret, contributed by the river tributaries as well as through leaching and erosion of soils and leakage of effluents. The Jordan River supplies about 70% of the total inflowing water, ~90% of the total nitrogen, and ~80% of the total phosphorus loads from riverine sources. Additional inflows are from several seasonal streams of variable sizes, some of which flow only during flood events. The discharge of the Jordan River decreased from $\sim 500 \cdot 10^6$ m^3 year^{-1} in the 1970s to $\sim 400 \cdot 10^6$ m^3 year^{-1} in the 2010s (Chap. 7). This 20% decrease was attributed to combined impacts of a decrease in effective rain at the northern part of the watershed and an increase in water consumption upstream of the lake. A volume of $\sim 250 \times 10^6$ m^3 evaporates annually, this outflux has remained stable over time. The water residence time in the lake used to be 8 years in the 1970s and 1980s. With gradually declining inflow volumes and stable evaporation, the current residence time has increased to 10 years.

The natural outflow from Lake Kinneret was solely to the southern Jordan River, with peak flow in spring declining to low flow levels in the summer–fall. Since the

construction of the Deganya Dam on the southern Jordan in 1932, the outflow has been controlled. For the past five decades, the National Water Carrier, inaugurated in 1964, comprises the main outflow route for Kinneret water, through pumping at Sapir site (see map in Fig. 1.1 of Chap. 1). Since 1964, outflow through the southern Jordan occurred only when water levels rose close to the upper red line, mostly in exceptionally wet winters (Chaps. 7 and 31). The seasonal regime of outflow has also changed from a strongly seasonal natural pattern to a managed outflow regime via the national water carrier, with reduced seasonal variations (Hambright et al. 2004).

37.4 Salinity and the Mechanism of Salinization

The salinity of Lake Kinneret water, 190–290 mg Cl^{-1} L^{-1}, is considerably higher than the salinity of the inflowing rivers (e.g., Jordan River water contains 15–20 mg Cl^{-1} L^{-1}), and is unusually high for freshwater lakes. This elevated salinity is attributed to the region's geological history, whereby seawater infiltrating the Dead Sea Rift Valley was evaporated and the brines formed interacted with the surrounding Ca-carbonate rock formations through a dolomitization process, thus forming $CaCl_2$ brines. These brines can now be found in deep groundwater bodies at the vicinity of the current site of Lake Kinneret (Chap. 8). The mechanism of salt entry into the lake was controversial for many years. The current understanding is that fresh groundwater in aquifers located at some distance west of the lake induce hydraulic pressure on the brines, resulting in an upward flow of mixtures containing both brines and freshwater. These mixtures seep through fractures and emerge through onshore and offshore saline springs (Chap. 8). Today's management strategy (see Chap. 31) of lowering saline water inflows is by lowering fresh groundwater levels in the eastern Galilee aquifer to reduce the driving force of saline flows into the lake.

37.5 The Annual Cycle of Major Hydrodynamic, Chemical, and Biological Processes

Our current understanding of hydrodynamic processes in Lake Kinneret was advanced substantially by the dedicated studies of Imberger and coworkers (Chap. 9 and references therein). They identified five distinct hydrodynamic regimes in the annual cycle. Those five phases are detailed below, each with the major biogeochemical processes associated with it:

1. In January, the water column is fully mixed over its entire depth such that the vertical distribution of solutes and particles is homogeneous and the entire water column is oxygenated. Water turbulence is energized by wind shear. Convective

mixing and bottom drag due to topographic gyres are dominant processes. These conditions are suitable for blooms of the filamentous diatom *Aulacoseira granulata* that requires turbulence to remain in suspension. Ammonium, originally from hypolimnion but now mixed in the entire water column, is nitrified to nitrate.

2. In February and March, radiative heating stabilizes the water column and turbulence is faded, leading to the onset of thermal stratification in March and providing suitable conditions for the growth of motile dinoflagellates and buoyant cyanobacteria such as *Microcystis* that compete against each other.
3. By April, the lake is thermally stratified, with a well-mixed epilimnion of ~12-m thickness, a distinct metalimnion layer of ~5 m in thickness overlying the hypolimnion. April to July is a period of progressive heating and increasing winds during which a near-perfect balance between Coriolis, buoyancy, and wind forces is maintained. Between March and May, the annual maximum phytoplankton biomass and production are attained, usually in the form of a bloom of *Peridinium gatunense* although since the mid-1990s on some years other species dominated in spring. By June, the spring bloom populations crash as nutrients are exhausted. During this period, a benthic boundary layer develops near the sediments, of ~<1–9-m thickness, depending on location and on wind-induced water motions above the sediments. Most of the biogeochemical activities in the deeper water take place in the benthic boundary layer, while the hypolimnion above it is relatively stagnant, with minimal vertical mixing. Basin-scale internal waves persist and support both gentle horizontal mixing in the surface layer and a flux in the benthic boundary layer of the sublittoral zone that maintains a supply of NH_4 to the plankton in the surface layer. With the onset of stratification, oxygen is depleted initially from the benthic boundary layer and subsequently from the entire hypolimnion, to its complete elimination below the thermocline within 4–6 weeks. The nitrate content of the deepwater is consumed within a few weeks. Biodegradation through sulfate reduction follows in the deepwater and the uppermost part of the bed sediments; methanogenesis predominates deeper in the sediments. Spring is also the time of the highest water levels and reproduction of the different cichlid species in the littoral zone.
4. August and September are characterized by thermal equilibrium, with stable thermocline at ~15–17-m depth and occasional vertical mode-two waves homogenizing deep-water parcels with upper water layers. Limited availability of phosphorus dictates low phytoplankton standing stocks in the epilimnion. The summer assemblage of phytoplankton is dominated by filamentous and elongated morphotypes belonging to the cyanobacteria, chlorophytes, and diatoms. If N availability becomes limiting, N_2-fixing cyanobacteria predominate (Chap. 22). Concomitantly, dense populations of anoxygenic photosynthetic bacteria are found in the metalimnion, where ~0.1–1 % of the incident light is still available (Sect. 15.2). In the benthic boundary layer, anaerobic decomposition continues and its products (PO_4, H_2S, NH_4, CO_2, methane) accumulate.
5. From October to December, cool air and natural convection gradually restore Lake Kinneret to a cold homogeneous water body. At this time, nutrients (NH_4^+

and soluble P) previously stored in the lake pelagic benthic boundary layer are being gradually introduced to the epilimnion. The summer assemblage of phytoplankton is maintained. Despite the addition of nutrients, algal productivity is usually at its annual minimum. Possible reasons are shorter day length, deeper epilimnion (so less time in the photic zone), and declining water temperatures. The deepening of the thermocline is probably associated with massive resuspension of sediments containing organic matter, which are focused toward the lake center. Upon settling down to the pelagic hypolimnion these are degraded, enriching the dissolved nutrient pools (Chap. 28)—which will get dispersed in the water column by turnover. As the thermocline sinks, chemosynthetic bacteria become active primary producers at oxic–anoxic interfaces, using energy obtained from the chemical oxidation of simple inorganic compounds to synthesize carbohydrate from carbon dioxide and water (Sect. 24.2). Turnover is usually completed by the end of December or early in January.

37.6 Nutrient Sources and Recycling

Three major sources provide nutrients to the Kinneret ecosystem: (1) Riverine, mainly via the Jordan River (Chap. 18). Riverine nutrient loads are high in winter–spring and low in summer–fall. (2) Internal sources originating from the pool of nutrients accumulated in the hypolimnion during stratification, due to the decomposition of sedimented organic matter from the photic zone. The accumulated nutrients become available to the productive upper layer upon destratification but mostly at turnover. (3) Dry and wet atmospheric deposition (as dust and rain) directly precipitated on the lake. This external source is the dominant source in summer (Chap. 19). Remineralization of nutrients (by microorganisms and zooplankton) is an additional source, important in the summer when N and P concentrations are low. Remineralization does not provide new nutrients (as do the external sources) but allows sequential, multiple use of nutrient already present in the system, by fast recycling. An additional, occasional, minor source of nutrients is the decomposition of littoral vegetation in the spring of wet years with a substantial increase of water level.

Phosphorus is considered the main limiting nutrient in Lake Kinneret, most of the year. Its availability places an upper limit to the standing stock biomass of the phytoplankton. Soluble reactive P concentrations in the photic waters are typically at about 2–3 μg L^{-1} with a short peak of 6 μg L^{-1} in February; total P concentrations are ~30 μg L^{-1} in the winter–spring and half of that in the summer–fall. In the lower water mass, orthophosphate accumulates over time as a result of decomposition of settling organic matter, reaching about 150 μg L^{-1} in the benthic boundary layer just before turnover. At turnover, this stored PO_4 is dispersed throughout the entire water column and part of it becomes available to the biota in the photic layers. Riverine inflows are another major source of P to the biota in winter and spring. In the summer, the contribution of both riverine

flows and internally recycled sources decline and dust becomes the main external source of P. The annual load of P from dust is ~40 ton year^{-1}, most of it in the summer months, compared to the riverine P load of ~85 ton year^{-1}, most of which enters the lake in winter–spring. Since nearly all P in dust is bioavailable to the biota whereas only about one third of the P of riverine sources is bioavailable, the contribution from dust is an important one. The biologically available P is primarily assimilated by phytoplankton. This leads to low SRP levels in the epilimnion, particularly in summer–fall. Remineralization of P in the epilimnion by zooplankton, especially microzooplankton, contributes to maintaining the low, but rather uniform level of primary and secondary production during the summer. When P is available, it is rapidly assimilated by phytoplankton species with intrinsic capacity for luxury uptake of phosphate and its deposition as internal storage in polyphosphate bodies. Dominant Kinneret species such as *P. gatunense* and *Aphanizomenon ovalisporum* are capable of such luxury P uptake and storage. When P becomes depleted and internal P pools are exhausted, alkaline phosphatase activity increases to allow scavenging of organic P.

Dissolved inorganic N (DIN) concentrations in the epilimnion fluctuate between summer–fall lows and spring highs (range 5 –1,000 μg L^{-1}). The two main sources of inorganic N are turnover and riverine inputs. Turnover enriches the upper waters with NH_4; riverine inflows contribute mostly NO_3 and to a lesser extent organic N. An additional significant source of N is direct rain, which is rich in nitrate of European origin. All these sources are mostly limited to the winter–spring. Unlike the case for P, dust is N-poor and does not constitute a significant source of N, so in the summer external sources of N are minor. Thus, in summer internal sources become important, especially transfer of NH_4 from deeper water through boundary mixing in the sublittoral zone. Without major external inputs, from March–April onwards epilimnetic DIN concentrations decline gradually, mostly due to uptake by phytoplankton and bacteria. Blooms of N_2-fixing cyanobacteria usually developed in years with a rapid decline of DIN (from April to June) and especially if a critically low DIN level (of ~20 μg L^{-1}) was reached early enough in the summer (Hadas et al. 2012).

As the lake stratifies, below the thermocline, organic nitrogen is gradually decomposed to ammonium, whereas confined nitrate is reduced to nitrite, which immediately reacts with ammonium via anaerobic ammonium oxidation (anammox), releasing N_2 gas that escapes to the atmosphere. Upon the extinction of the nitrate, the nitrite diminishes and the anammox process ceases. Consequently, NH_4 accumulates over time in the lower water mass, reaching concentrations of ~1.5 mg L^{-1} just before overturn.

Dissolved inorganic carbon. The photic waters of Lake Kinneret are typically of high pH (8.2–9) and alkalinity (~2.5 mM). Under these conditions, most of the inorganic C is in the form of HCO_3^- while $CO_{2(aq)}$ concentrations are low (~10 μM). Many algal species and particularly the dinoflagellate *P. gatunense* preferentially take up CO_2, as opposed to bicarbonate. In March–April, when the typical Kinneret spring bloom develops and peaks, CO_2 supply through gas exchange at the air–water interphase is negligible due to low winds. Intensive photosynthesis at this

time causes the pH to increase above 9 and massive calcite precipitation occurs. For each mole of calcite precipitated, a mole of CO_2 is released and is available for algal uptake. This additional, previously unaccounted for source of CO_2, probably further supports the *P. gatunense* bloom. In recent years, when *P. gatunense* did not bloom, no other phytoplankton species reached its peak spring biomass, despite the fact that calcite precipitation was noticed, although to a lower extent. These observations indicate the adaptability of *P. gatunense* to the local environment.

Calcite precipitation and the associated CO_2 production end more or less concurrently with the crash of the *P. gatunense* bloom, giving advantage to algal species that preferentially and readily assimilate bicarbonate (e.g., *Peridiniopsis* spp., *Aphanizomenon ovalisporum*). The summer blooms of the toxic cyanobacterium *A. ovalisporum* occurred during periods of high pH values with low ambient concentrations of dissolved CO_2 (Hadas et al. 1999).

Silica. The photic waters of Lake Kinneret typically contain abundant silica (2–3 mg Si L^{-1}), such that Si availability does not limit diatom growth. Nevertheless, diatom blooms are always associated with declines in epilimnetic Si concentrations, and the extent of those blooms can be estimated from the decline in Si.

Trace elements. Several trace elements are considered important to the growth and photosynthesis of the phytoplankton of Lake Kinneret; the most important ones are iron, molybdenum, and selenium. Iron, essential for photosynthesis, occurs in the epilimnion as Fe(II) at concentrations that are ~30 times higher than expected thermodynamically and are sufficient to support seasonal algal blooms (Shaked et al. 2002). Similarly, soluble molybdenum, needed for nitrate assimilation, occurs at sufficiently high concentrations (Chap. 28). Selenium (Se) was found to be an essential microelement for the growth of *P. gatunense* (Chap. 11). Its primary source is the Hula peats. It was hypothesized that the re-flooding of the Hula Valley in 1994 and the associated reduction in the amount of Hula peat water reaching the lake is associated with the lack of *Peridinium* blooms on some years.

37.7 Dynamics of the Phytoplankton Community

The phytoplankton of Lake Kinneret is best represented by a single bloom-forming species, the dinoflagellate *P. gatunense*. Until the mid-1990s, *P. gatunense* bloomed between March and May each year, reaching wet weight biomass of 150–250 g m^{-2} and comprising >95% of total phytoplankton biomass, thus effectively excluding other species. By May–June, the bloom declined due to the lack of CO_2 and the summer had a diverse assemblage of nanoplanktonic species, mostly chlorophytes, diatoms, and cyanobacteria, with a low total biomass. Since the mid-1990s, the spring *Peridinium* bloom occurred only in high-rainfall years, whereas the spring phytoplankton assemblage in low-rainfall years was different from year to year. On some of those "non-*Peridinium* years," spring blooms of the invasive filamentous chlorophyte *Mougeotia* sp. or of the toxic cyanobacterium *Microcystis* sp.

developed, but these blooms never attained the biomass and the degree of dominance obtained by *Peridinium*.

Since the mid-1990s, cyanobacterial biomass has increased, and cyanobacteria of the Nostocales order have dominated the summer phytoplankton community. The domination of nostocalean species was attributed to: (1) their N_2-fixing capability which gives them an advantage under N-depleted conditions that developed in early summer in recent years and (2) temporal variations in regional climatic and limnological conditions such as increased water temperatures and changes in the wind regime that affect physical mixing processes and water turbulence (Sukenik et al. 2012, Hadas et al. 2012).

37.8 The Zooplankton and Fish

The metazoan zooplankton populations are dominated by small species of cladocerans and copepods, with abundant rotifers (Chap. 13). The small size is thought to be related to high predation pressure by the dominant pelagic fish, the endemic bleak (*Mirogrex terraesanctae*), which is planktivorous and constitutes ~90 % of the fish in the pelagic zone (Chap. 16). The microzooplankton, composed of protozoan unicellular grazers (ciliates, flagellates) as well as rotifers and the naupiar stages of the copepods, are important major components in the microbial loop. Zooplankton are major mineralizers of nutrients, the microzooplankton are more effective than the crustacean. Fish also contribute to nutrient remineralization, but at rates that are an order of magnitude lower than that of the larger zooplankton.

Lake Kinneret is home to 19 native species of fish plus a few alien species, some of which are stocked (Chap. 16). Most of the fish species spend at least part of their life in the littoral zone, many depend on littoral resources (stones, inundated vegetation) for reproduction. The "flagship" fish species, the cichlid *Sarotherodon galilaeus* (St. Peter's fish), that also has a high commercial value, feeds primarily on *Peridinium*; in non-*Peridinium,* low-rainfall years, its commercial harvest crashed due to overfishing, shortage of suitable nesting and nursing habitats, and probably also due to the lack of *Peridinium,* its main food.

37.9 The Food Web

The food web of Lake Kinneret was perceived in the 1970s as being made of two food chains: the classical phytoplankton–zooplankton–zooplanktivorous fish food chain, mostly active in the summer, and a second *Peridinium* food chain, active in the winter and spring. This perception reflected the ecological theory accepted at the time. Today, trophic interactions within an ecosystem are described by complex food webs rather than linear food chains. This new perception supported by the application of new methodologies led to our current understating of the food

web in Lake Kinneret, as outlined in Chap. 17. The current, complex food web now incorporates additional primary producers previously unaccounted for such as chemosynthetic bacteria (Sect. 24.2) and anoxygenic photosynthetic bacteriaphotosynthetic pigments (Sect. 15.2), the role of the microbial loop and micrograzers as major nutrient remineralizers (Chap. 14), and intra-guild predation. This complexity was further investigated and verified using stable isotope studies and ecosystem modeling (Chap. 35).

37.10 Decomposition of Particulate Organic Matter

Lake surface water primary production (annual average of 1.7 g C m^{-2} day^{-1}; Chap. 24) is sufficiently high to allow for large sedimentation fluxes of biodegradable organic matter (annual average of ~0.30 g C m^{-2} day^{-1}; Chap. 27). Upon stratification, within 6–8 weeks aerobic decomposition processes consume all the oxygen below the thermocline. The rest of the organic matter that settles from above (about half) is either decomposed under anoxic conditions in the lower water mass and sediments or buried in the sediments. Initially, decomposition proceeds via nitrate reduction, but only a small proportion of the organic matter is decomposed in this way. After all nitrogen is consumed, sulfate reduction prevails in the hypolimnion and the sediment–water interface, leading to the decomposition of about two third of the remaining organic matter. The primary source of sulfate is gypsum dissolution in the drainage basin (Triassic formations in the Hermon Mountain and in the dried peat soils of the Hula Valley). Another path for organic matter breakdown is through methanogenesis (Sect. 25.4), which predominates in the deeper sediments, where SO_4 is absent.

37.11 The Lake's Trophic Status

The strong seasonality of the meteorological and hydrological forcing factors and in the external loads of nutrients is reflected also in the trophic status of the lake, which alternates between being eutrophic in winter–spring and mesotrophic in summer–fall. The winter–spring eutrophic state is expressed by a major bloom each year, with epilimnetic chlorophyll concentrations often >30 μg L^{-1}, primary production rates exceeding 2 g C m^{-2} day^{-1}, and Secchi depth of ~2.5 m. In the mesotrophic summer–fall season, primary production and algal biomass are maintained at lower levels while cyanobacteria predominate. Epilimnetic chlorophyll concentrations are usually below 10 μg L^{-1}, primary production ranges 1–1.8 g C m^{-2} day^{-1}, and Secchi transparency often exceeds 3.5 m (Sect. 24.1). A long-term trend of increasing phytoplankton biomass, Chl *a* and primary production in summer–fall was recorded, with increasing contribution of cyanobacteria and higher frequency of toxic blooms, thus the current status in the summers is more eutrophic than in the past.

37.12 Water Level Fluctuations and Littoral Resources

Lake Kinneret is different from many other naturally clear-water lakes in that macrophytic vegetation does not develop in its shallow water zone—the littoral. The main reason for the lack of macrophytes is the strong wind action that uproots new seedlings. Superimposed are water level fluctuations considerably greater than natural that cause the regions of macrophyte growth to alternate between in and out of the water (Chap. 29). Macrophytes occur in the littoral zone mostly only if they germinate on dry shores and later get inundated by rising water levels. Consecutive years of drought and negative water balance result in declining water levels and exposure of shore areas on which shore vegetation develops. On rainy years, water level rapidly increases and the shore vegetation is inundated, presenting a window of opportunity for the littoral zone biota.

The littoral zone is the part of the lake where impacts of water level fluctuations are most evident (Chap. 29). This zone changes its physical location and characteristics as water levels fluctuate seasonally and interannually. Abiotic (sand, stones) and biotic (vegetation) substrates form littoral habitats of varying complexity that change markedly on both spatial and temporal scales. Most fish and macroinvertebrates use littoral habitats for at least part of their life cycle. Many use littoral resources (substrate for attachment, refuge, food) for reproduction and growth. Water level fluctuations influence the availability of littoral resources and result in cascading impact on population size, with top-down food web effects. Upon inundation of shore vegetation, fish and invertebrates take advantage of the temporarily available vegetative resources for reproduction (e.g., cichlids) and refuge for their fingerlings (e.g., cichlids, bleak). Likewise, drawdown of the lake results in the loss of inundated vegetation and rocky substrates, i.e., loss of refuge, spawning, and nursery sites, thus limiting the fish and invertebrates that depend on the availability of such habitats. The reproduction success and population size of the main zooplanktivore fish, *Mirogrex terraesanctae,* are directly related to the availability of rocky littoral habitat (used for spawning) and inundated vegetation (nursery).

The case of Lake Kinneret underscores that water level fluctuations can act as a major environmental factor influencing habitat structure and availability, and related interactions. With global warming and predictions that extreme droughts and flood events will be more frequent than in the past, this factor may become increasingly important in subtropical lakes presently experiencing stable water levels.

37.13 Lake Stability

A stable ecosystem is an ecosystem that maintains a constant character in the presence of forces, which threaten to disturb it, i.e., it is resistant to change. During the 1970s and 1980s, Lake Kinneret was considered to be a stable aquatic ecosystem. A remarkable year-to-year stability of the annual phytoplankton succession pattern was reported, in Pollingher's (1981) words: "The annual succession at the species

level has been an almost constant event in the lake for many years." A long-term (1972–1993) analysis of phytoplankton biomass, primary production, chlorophyll concentrations, Secchi depth, and total suspended solids by Berman et al. (1995) has shown that there were no significant trends in the dynamics of all these parameters. They concluded that Lake Kinneret has shown remarkable stability over 22 years despite considerable environmental changes, population growth, and intense economic development.

Schindler (1987) suggested that among the earliest responses of lake ecosystems to stress would be changes in species composition of small, rapidly reproducing organisms with wide dispersal powers, such as phytoplankton, and the disappearance of sensitive organisms from aquatic communities. Using Schindler's criteria, it becomes evident that since the mid-1990s Lake Kinneret gives signs of ecosystem deterioration and that its stability as an ecosystem has diminished. The previously recorded year-to-year stability in the phytoplankton seasonal succession has disappeared (Zohary 2004). Since 1996, *Peridinium* blooms became irregular; in 10 out of the 17 years between 1996 and 2012, *Peridinium* did not bloom. In "non-*Peridinium* years," other species dominated in spring, but without a repeatable pattern (Zohary et al. 2012). Out of the 7 "*Peridinium* years," 5 had exceptionally intense blooms, such that the amplitude of annual peak phytoplankton biomass has increased considerably compared to that recorded before 1994. The summer phytoplankton assemblage has also undergone major changes in species composition: elongated morphotypes became dominant (as opposed to small rounded cells and coenobia dominating before 1994) and cyanobacteria increased in both their relative and absolute abundance. A severe decline was recorded in the phytoplankton species diversity, as well as a major shift in the dominant and common species: 18 of the 47 species that Pollingher (1978) listed as being common are no longer common, an additional six species were not recorded even once since 2006 (Sect. 10.1). Several alien species invaded the lake and became established, in particular filamentous species such as the cyanobacteria *Aphanizomenon ovalisporum* and *Cylindrospermopsis raciborskii* and the chlorophyte *Mougeotia* sp.

Not only the phytoplankton but also the zooplankton exhibited a regime shift in the mid-1990s (Gal and Anderson 2010). The zooplankton population of Lake Kinneret crashed to very low abundance levels in 1993, after which it recovered but then crashed again in 2003. These crashes were attributed to population explosions of the bleak, the major Kinneret zooplanktivore. Those population explosions were associated with the exceptional water level rises of winter 1991/1992 and again of winter 2002/2003 (Chap. 16), which instigated exceptional reproductive success of the bleak (Zohary and Ostrovsky 2011). Other indications for reduced ecosystem stability include the invasion and establishment of an alien snail, *Pseudoplotia scabra,* to near extinction of the native snail fauna (Heller et al. 2014) and the collapse of the Kinneret fishery in 2008 (Chap. 36).

The factors causing ecosystem destabilization remain obscure. We propose that the extreme changes to the water level regime comprised a key destabilizing factor. Over the past few decades, Lake Kinneret was managed to maximize its storage capacity. This was attained by pumping out water in excess of the "available water"

(see Chap. 7) in low-rainfall years, to "make room" for filling the lake in high-rainfall years. Specifically, two extreme events of >4-m rise in water level in a single exceptionally wet winter (1991/1992 and 2002/2003), each following a series of years with continuously declining water levels (Chap. 7, Fig. 7.5), proved as disturbances to ecosystem stability to which the lake's resilience was insufficient. Other water level-related features that may have contributed to ecosystem destabilization were much greater than the natural amplitude of water level fluctuations, and the particularly low water levels on some years.

Another likely destabilizing factor is the hydrological changes in the Hula Valley beginning in 1993–1994 as a result of the re-flooding of the peat soils and creation of the Agmon wetland. This led to a reduction in the amounts of nitrate, sulfate, selenium, and possibly other important dissolved organic compounds of Hula peat origin. Other man-induced changes in the Kinneret catchment are listed in Table 1.2 of Chap. 1, their direct or synergistic effects are still unclear. Although Berman et al. (1995) argued that during 22 years, man-induced changes did not impact Lake Kinneret, the following 20 years of additional anthropogenic impacts certainly left their mark on ecosystem stability. Lake Kinneret requires careful and scientifically supported management that takes into consideration its current, more sensitive, and less stable ecological state.

37.14 Prospects for the Future

The current understanding of the Lake Kinneret ecosystem and its complexity reflects a major advancement gained by continuous dedicated research and monitoring programs. This acquired knowledge has been constantly integrated into the environmental planning policy and management activities aimed at maintaining a sustainable aquatic ecosystem that will provide diverse system services for generations to come.

As in many other complex ecosystems, Lake Kinneret is affected by temporal variations occurring at regional and global scales. Prediction of the potential responses of this ecosystem to such changes requires fundamental understanding of its complexity and the intricate interactions between its physical, geochemical, and biological components. In this respect, several general limnological and local issues need further attention, insight, and development.

Lake Kinneret continues to be a major source of freshwater for drinking and irrigation. Hence, its relatively high salinity (for a freshwater lake) is of major concern. Furthermore, the observed long-term decline in the volumes of water entering the lake from the catchment suggest that the salinity of Lake Kinneret will continue to increase—unless actions taken today and in the future will successfully reduce the influx of saline water (Chaps. 7, 8, and 31). Little is known about the likely response of the Kinneret biota to higher than current salinities; this knowledge gap requires intensive research. Unmonitored sources of salinity to Lake Kinneret account for about half of the current Cl inputs. These sources should be found and explored.

The findings that dust constitutes a major external source of P, especially in summer, and that the source of the phosphorus in the dust is probably from agricultural fertilization has major implications for many water bodies in similar and drier climates (Chap. 19). These findings from Lake Kinneret must be further substantiated (with data from additional sampling stations) and if confirmed—will require thinking on how to minimize the transfer of P from fertilized soils to dust.

Improved spatial resolution of hydrodynamic data is needed, including current measurements and additional thermistor chains. These are needed for studies such as sediment transport fluxes, phytoplankton patchiness, and management of pumping sites to avoid pumping hypolimnetic water.

The current identification of phytoplankton and zooplankton species relies on morphology-based classical taxonomy. Again and again this taxonomy proves to be insufficient and requires supplementation of modern molecular tools. DNA bar coding of all the phytoplankton and zooplankton species occurring in Lake Kinneret is ongoing. There is scope to expand this bar-coding initiative to include all Kinneret biota, from the primary producers to the top predators. DNA bar coding will have diverse applications in future research such as estimation of species abundance, trophic interaction studies, ability to track the origin and dispersal patterns of alien species, and life cycle studies.

New insights into the N cycle of Lake Kinneret were introduced in Chaps. 21 and 22, which suggested that several microbial processes occur that were not studied experimentally in Lake Kinneret, including anammox, DNRN, and DNRA.

The dissolved organic nitrogen (DON) is yet an insufficiently explored component of the dissolved organic matter (DOM) and potentially an important contributor to the nitrogen budget and certainly associated with nitrogen recycling processes. Technical constrains to chemically define this component are awaiting analytical breakthrough and hinder advancement in understanding the role of DON in the system. The assimilation of amino acids and simple amino sugars was demonstrated for some representative species of the Kinneret phytoplankton (Berman and Chava 1999). Nevertheless, the DON fraction is more complex and needs further attention by both chemists and microbiologists.

The degradation of DOM is generally attributed to aerobic and anaerobic bacteria whose diverse origin can be unveiled by metagenomic analyses. The dynamics of these microbial communities are affected not only by environmental conditions but also by the coexisting planktonic populations, e.g., cyanobacteria and algae. Similarly, the microbial community may affect the phytoplankton assemblage via interpopulation “chemical talk” and allelopathic interactions.

Certain phytoplankton species may benefit from available DOM via mixotrophic activity. This metabolic strategy, that complements photosynthetic carbon assimilation, requires detailed studies to elucidate its contribution to the primary producers as an additional source either of carbon and energy or of other major nutrients.

The persistence of cyanobacteria populations in Lake Kinneret in recent years attracted the attention of the scientific community as well as of authorities and water managers. The desire to control and minimize bloom events of toxic cyanobacteria calls for deeper understanding of cyanobacterial responses to the environmental

conditions and their physiological and biochemical mechanisms that support their domination. Toxic substances and many other secondary metabolites whose biological role is unknown are among the rich arsenal of substances that provide cyanobacteria their ecological advantages.

Further emphasis is needed on studies of the biology and ecology of the Kinneret fish, under the recent ecological conditions that prevail in the lake since the mid-1990s. This includes studies of the population genetics, food sources, feeding behavior, reproduction behavior, survival of the young of year, interspecies competition for food (e.g., the native St. Peter's fish vs. the stocked silver carp), susceptibility to pollutants, and the role of catfish as top predators, to name a few. Since most Kinneret fish species rely on littoral sources (e.g., for food, refuge) at least during part of their life cycle, it is important to also study processes taking place in the littoral zone.

The one-dimensional (1D) ecosystem model DYCD (short for DYRESM–CAEDYM, dynamic reservoir simulation model–computational aquatic ecosystem dynamics model; Chap. 35) is currently being used for exploration of scientific questions, and as a management support tool that enables long-term scenario testing. It is expected that in the future, management will rely even heavier on modeling, so there is scope for further development and improvement of DYCD and similar models. For example, modeling is the only available tool today to forecast the likely consequences of climate change. Advanced ecosystem modeling, including 3D modeling capabilities for physical, chemical and biological processes, is needed to allow scenario testing and exploration of problems associated with short timescales but high spatial variability. The development of ensemble modeling capabilities will provide means to solidify model predictions by comparing model outcome of several independent models. Merging of climatic and ecosystem models will enhance 3D modeling capabilities. Integration of on-line real-time monitoring into the modeling system will enable to auto-calibrate the models and to run scenarios at real-time. The monitoring program and experimental activities should be revised from time to time to fill in gaps identified by ecosystem modeling.

References

Berman T, Chava S (1999) Algal growth on organic compounds as nitrogen sources. J Plankton Res 21:1423–1437

Berman T, Stone L, Yacobi YZ, Kaplan B, Shlichter M, Nishri A, Pollingher U (1995) Primary production and phytoplankton in Lake Kinneret: a long-term record (1972–1993). Limnol Oceanogr 40(6):1064–1076

Gal G, Anderson W (2010) A novel approach to detecting a regime shift in a lake ecosystem. Method Ecol Evol 1:45–52

Hadas O, Pinkas R, Delphine E, Vardi A, Kaplan A, Sukenik A (1999) Limnological and ecophysiological aspects of *Aphanizomenon ovalisporum* bloom in Lake Kinneret, Israel. J Plankton Res 21(8):1439–1453

Hadas O, Pinkas R, Malinsky-Rushansky N, Nishri A, Kaplan A, Rimmer A, Sukenik A (2012) Appearance and establishment of diazotrophic cyanobacteria in Lake Kinneret, Israel. Freshwater Biol 57(6):1214–1227

Hambright KD, Eckert W, Leavitt PR, Schelske CL (2004) Effects of historical lake level and land use on sediment and phosphorus accumulation rates in Lake Kinneret. Environ Sci Technol 38:6460–6467

Heller J, Dolev A, Zohary T, Gal G (2014) Invasion dynamics of the snail *Pseudoplotia scabra* in Lake Kinneret. Biol Invasions 16:7–12

Pollingher U (1978) The phytoplankton of Lake Kinneret. In: Serruya C (ed) Lake Kinneret: Monographiae Biologicae, vol 32. Dr. Junk, The Hague, pp 229–242

Pollingher U (1981) The structure and dynamics of the phytoplankton assemblages in Lake Kinneret, Israel. J Plank Res 3 (1):93–105

Schindler DW (1987) Detecting ecosystem responses to anthropogenic stress. Can J Fish Aquatic Sci 44:6–25

Serruya, C (ed) (1978) Lake Kinneret: Monographiae Biologicae. Dr. Junk, The Hague, p 501

Shaked Y, Erel Y, Sukenik A (2002) Phytoplankton-mediated redox cycle of iron in the epilimnion of Lake Kinneret. Environ Sci Technol 36: 460–467

Sukenik A, Hadas O, Kaplan A, Quesada A (2012) Invasion of Nostocales (cyanobacteria) to subtropical and temperate freshwater lakes? Physiological, regional and global driving forces. Front Microbio 3:86. doi:10.3389/fmicb.2012.00086

Zohary T (2004) Changes to the phytoplankton assemblage of Lake Kinneret after decades of a predictable, repetitive pattern. Freshwat Biol 49:1355–1371

Zohary T, Nishri A, Sukenik A (2012) Present-absent: a chronicle of the dinoflagellate *Peridinium gatunense* from Lake Kinneret. Hydrobiologia 698: 161–174

Zohary T, Ostrovsky I (2011) Ecological impacts of excessive water level fluctuations in stratified freshwater lake. Inland Waters 1: 47–59

Index

Symbols
^{3}H-thymidine method, 440
^{13}C signature, 461
^{14}C-tracer method, 418
β-carotene (β-car), 492
γ-proteobacteria, 260
δ^{13}C in fractionation, 410
δ^{13}C-POM analysis, 435
δ^{13}C signature, 298, 435

A
Abiotic substrate, 520
Abundance, 162, 175, 234, 247, 251, 259, 262, 265, 280, 282, 300, 348, 479, 602, 628, 646
  heterotrophic nanoflagellates, 298
  in Lake Kinneret, 192, 214
  inter-annual variation in, 243
  of *A. ovalisporum* heterocysts, 388
  of copepod, 236
  of fecal bacterial indicators, 599
  of *Microcystis*, 222, 582, 583
  of *M. terraesanctae,* 282, 284
  of native molluscs, 525
  of *Peridinium* 197, 200, 207
  of picophytoplankton and micro-grazers, 295
  of plankton, 179
  of polyphosphate bodies, 220
  of zooplankton, 233, 238, 243, 287, 637
  patterns, 180, 250, 264
Acanthobrama lissneri, 317
Acanthobrama terraesanctae, 274, 295
Acinetobacter sp., 260
Active faults, 21
Aeolian phosphorous, 360
Aeolian transport, 336, 345
Aeromonas veronii, 260
Aeruginosins, 579
Agmon, 557, 598, 668
Agriculture, 75, 89, 114, 536, 542, 548, 549, 563, 589
Air temperature, 7, 86, 89, 90, 94, 399, 401, 567, 658
Akinete, 214, 216, 221, 223
Alien fish, 649
Alkalinity (Alk), 323, 401, 403–405, 407, 408, 410, 488, 500, 502, 507, 568, 572, 662
Allochthonous, 296
  phosphorous load, 348, 350, 351, 352, 357, 361
Alummot beach, 602
Ammonia, 249, 260, 383, 387, 393, 430
Ammonia oxidation, 383, 387, 392
Ammonium (NH_4), 9, 315, 321, 323, 324, 345, 349, 358, 367, 370, 372, 375, 389, 430, 431, 500, 504, 573, 619, 660
  excretion of, 255
  in algal nitrogen nutrition, 385
  in anaerobic metabolism, 435
  in natural ecosystems, 387
  source of, 368, 373
  to nitrite conversion, 377, 383
Amud, 572
Anabaenopeptin, 579, 580
Anaerobic oxidation of methane (AOM), 459, 461
Analytical, 126, 259, 361, 568, 574, 582, 585, 669
Anammox, 371, 373–375, 378, 383, 387, 407
Anguilla anguilla, 274
Anoxic, 255, 264, 268, 284, 335, 367, 371, 372, 373, 386, 399, 406–408, 502, 665

T. Zohary et al. (eds.), *Lake Kinneret, Ecology and Management,* Aquatic Ecology Series 6, 673
DOI 10.1007/978-94-017-8944-8, © Springer Science+Business Media Dordrecht 2014

Anthropogenic, 99, 109, 310, 320, 323, 330, 332, 391, 494, 546, 556, 558, 562, 668
Antimony (Sb), 500, 506
Anuraeopsis fissa, 234, 240
Aphanizomenon, 214, 215, 221, 370
Aphanizomenon ovalisporum, 171, 172, 217, 222, 302, 388, 389, 393, 405, 412, 667
Aquifer, 47, 72, 75, 100, 101, 113, 119, 125, 126, 334, 365, 546
Archaea, 247, 260, 262, 383, 430, 459, 460
Artesian flow, 116
Arylsulfatase, 453
Assimilation, 217, 220, 221, 298, 330, 381, 385, 393, 403, 406, 418, 425, 669
Assimilation number (A.N.), 424, 425
Astatotilapia flaviijosephi, 278, 528
Asticcacaulis sp, 260
Atmospheric deposition, 344, 366, 381, 390, 661
Atrazine, 590
Aulacoseira granulata, 177, 180, 302, 452, 456, 458, 493, 660
Autochthonous, 60, 296, 340, 390, 401, 413, 464, 466, 468, 481, 489, 519
Automatic sampling, 311, 313, 314, 316, 317, 323, 573
Autotrophy, 429
Available water, 103, 104, 545, 547, 667
Avdat group, 125
Ayun, 101, 109

B

Bacteria, 242, 247–249, 252, 255, 265, 268, 293, 299, 301, 302, 383, 387, 389, 392, 430, 435, 440, 442, 451, 468
  abundance, 263
  molecular characterization of, 383
  photosynthesis, 268
Bacterial carbon demand (BCD), 468
Bacterial community, 259, 260, 386, 445
Bacterial count, 263
Bacteriophage, 443, 599
Balance, 146
  energy, 90, 93, 95, 102
  mass, 349, 350, 356, 360, 361, 373, 450, 619
  solute, 115, 119, 120, 127
  water, 90, 93, 102, 104, 107, 109, 542, 658, 666
Banias, 99, 105, 108, 330, 332, 335, 337, 572
Barbel, 280
Barbus longiceps, 4, 280
Baseflow, 74
Basin-scale, 144, 146, 150
Bathymetry, 22, 23, 63, 65, 66, 564
Beggiatoa, 430, 434
Beit Tzeida, 123
Benthic boundary layer (BBL), 137, 149, 150, 350, 358, 361, 367, 375, 376, 387, 400, 401, 408, 409, 459, 508
Bias control, 317
Bioavailable Phosphorous, 202, 348
Biodegradation, 374, 400, 407, 408, 412, 502, 504, 507, 511, 583, 660
Biomanipulation, 620, 647
Biomass, 137, 171, 179, 180, 192, 194, 199, 204, 217
  total, 172, 175, 179
  wet-weight, 162, 170, 194, 231, 404, 421, 663
Bleak, 13, 233, 278, 279, 280, 282, 287, 302, 527, 623, 628, 629, 638, 639, 640, 641, 646, 664, 667
Bloom, 9, 179, 180, 193, 194, 200, 202, 206, 222
  Peridinium, 6, 180, 182, 194, 197, 198, 201, 203–205, 207, 208, 221, 262, 297, 368, 384, 385, 399
  spring, 9, 179, 180, 191, 208, 216, 217, 263, 369, 372, 375, 398, 404, 411, 427
Borehole, 47, 116
Bosmina longirostris, 234
Brevundimonas aurantica, 260
Brine, 55
  Ca-chloride, 48
Buoyancy, 137, 142, 144, 147, 149, 152, 368, 370, 378, 503, 510, 511, 660
  mixing, 400
Burger number, 146, 147
Burial rate, 486

C

C:P ratio, 202
Ca-chloride brine, 42, 44, 47, 51, 53, 121
CaCO3, 403, 412, 488, 489
CAEDYM, 622, 623
Calcite, 48
  precipitation, 199, 315, 354, 398, 401, 403, 404, 405, 406, 408, 411, 412, 663
  primary, 51, 53
Calcium (Ca), 323, 339, 572
Capoeta damascina, 280
Carasobarbus canis, 280, 593

Carbon, 138, 205, 242, 248, 256, 268, 297, 298, 299, 348, 398, 404, 418, 429, 435, 448, 475, 621, 624, 625
cycle, 392, 418, 430, 459, 461, 623
demand, 446
fixation, 251, 391, 392, 431, 432, 434, 435, 468
flux, 248, 297, 428, 621, 624, 626
isotopes, 410, 434
Carmel fault, 20
Catch, 280, 629, 639, 642, 645
annual, 340, 360, 639, 642
of *Sarotherodon galilaeus,* 300, 646
Caulobacter sp., 260
Cell specific carbon uptake, 442, 443
Ceratium hirundinella, 172, 180, 193, 384
Chemoautotrophic bacteria, 251, 298, 391, 430, 435, 464
Chemoautotrophs, 430
Chemoclines, 386, 387, 392, 430, 431, 434
Chemotypes, 582, 583
Chloride (Cl), 500, 568, 611, 612
concentration, 114, 116, 125, 126, 137, 501, 609
Chlorobium limicola, 264
Chlorophyll a (Chl a), 183, 213, 265, 268, 418, 421, 435, 492
Chlorophyll b (Chl b), 493
Chlorophyll c (Chl c), 493
Chlorophyll (Chl), 9, 198–200, 202, 204, 263, 385, 389, 418, 441, 510, 568, 571, 611, 619, 665
degradation pigments, 200, 213
Chlorophyta, 177, 463
Chlorophytes, 163, 171, 177, 179, 180, 297, 425, 447, 493, 660, 663
Chrysosporum, 174
Chytrid, 207
Ciliates, 207, 228, 242, 247, 250, 251, 252, 255, 268, 297–299, 302, 435, 463, 621, 664
Clarias gariepinus, 300, 529
Clearance, 75, 249, 253, 298
Climatic categories, 83
Clostridium perfringens, 598
CO2 user, 412
Coastal, 66, 102, 114, 279, 555
Cobalt (Co), 500, 504
Cold nights, 87
Coleps, 255, 435
Colored dissolved organic matter (CDOM), 421
Colpoda steinii, 255
Common carp, 529, 637, 638, 649
Community respiration (CR), 441, 443, 447, 449, 464, 475, 482, 568
Complete mixing (CM), 127, 502
Conceptual, 117, 125, 574, 612, 614
Conductance, 126
Confined, 117, 124, 126, 139, 234, 240
Conservative ions, 121
Coriolis
effect, 65
force, 142, 145, 146
Cover basalt, 20
Craters, 62, 66
Crystallization, 403, 412
Cultivated land, 13, 536
Cyanobacteria, 163, 171, 172, 175, 180, 213, 215, 218, 219, 221, 243, 252, 293, 301, 302, 366, 412, 425, 478, 492, 494, 524, 558, 568, 579, 582, 611, 612, 620, 627, 641, 660, 662, 663, 665, 667, 669
diazotrophic, 388
isolation of, 219
nitrogen fixation in, 223, 368, 370, 388, 393, 394, 447
toxin production in, 222
transparent exopolymer particles production in, 480
Cyclidium, 250, 435
Cycling, 445, 462, 468, 474, 480, 481, 486, 509, 619, 628
Cyclotella, 177
Cylindrospermopsin (CYN), 218, 220, 578, 580, 582, 583
Cylindrospermopsis, 389, 393
Cylindrospermopsis raciborskii, 171, 175, 214, 215, 217 222, 302, 388, 393, 667
Cyperus alopecuroides, 521
Cyprinus carpio, 529, 637, 649
Cyprus lows, 84, 88
Cyst, 172, 195
Cytophaga sp., 260

D

Dalyot, 101
Dan, 44, 99, 105, 108, 264, 330, 332
Dan stream, 99, 332
Data-driven modeling, 243
decision trees, 628
hybrid model tree, 620
lagramge, 620
regression trees, 620

DDT, 590, 593, 595
Dead Sea fault, 20, 21, 23, 30–33, 60, 66
Dead Sea Rift (DSR), 55, 122, 659
  brines, 121
Dead Sea Transform (DST), 39, 42, 44, 60
Decomposition, 12, 184, 204, 206, 249, 295, 297, 324, 330, 331, 334, 345, 366, 368, 376, 400, 434, 446, 452, 460, 478, 493, 661, 665
Deepening, 100, 136, 137, 153, 240, 251, 325, 368, 400, 435, 491, 500, 501, 507, 511, 558, 661
Degania dam, 10, 12, 102, 103, 119
Degree of solution saturation, 403
Delphi method, 608
Denitrification, 10, 332, 371, 372, 383, 386, 387, 393, 400, 430, 619
Desalination, 14, 544, 549, 563
  plants, 544
Detritus, 44, 48, 249, 301, 421, 623
Deuterium, 123
Diatoms, 163, 171, 177, 266, 425, 493, 524, 660, 663
Diffuse pollution sources, 557
Diffusion, 124, 358, 367, 376, 377, 409, 412, 502
Dinoflagellates, 162, 163, 172, 180, 183, 191–194, 197–199, 202–204, 206, 207, 264, 266, 297, 301, 302, 349, 398, 405, 412, 425, 478, 479, 493
Dinophyta, 182
Direct watershed, 97, 102, 108, 119
Dir Hana formation, 118
Discharge, 12, 42, 44, 47, 75, 93, 116, 119, 124, 126, 310, 312, 321, 331, 572, 658
  effect, 323
Dishon river, 73, 101
Disribution
  vertical, 183, 200, 215, 228, 238, 240, 299, 358, 419
Dissimilatory nitrate reduction (DNRA), 387, 388, 669
Dissimilatory nitrate reduction to nitrite (DNRN), 373, 374, 376, 378, 407, 669
Dissolved inorganic carbon (DIC), 398, 405, 406, 408, 409, 410, 412
Dissolved inorganic nitrogen (DIN), 222, 330, 332, 333, 344, 366, 368, 372, 375, 378, 381, 388, 389, 393, 394, 662
Dissolved oxygen (DO), 9, 367, 375, 376, 400, 401, 431, 432, 502, 619, 623
Distribution, 85, 138, 182, 187, 193, 204, 217, 234, 235, 240, 247, 284, 317, 335, 351, 357, 578, 598, 599, 603, 645
  patchiness, 201
DNA barcode, 163
Drainage, 49, 73, 100, 321, 324, 325, 331, 335, 336, 345, 357, 509, 548, 558
Dry weight, 202, 221, 343, 344, 371, 403, 451, 474, 475, 478, 487, 582, 600
Dust, 42, 44, 48, 330, 336, 337, 341, 343, 344, 360, 402, 464, 468, 505, 662, 669
Dust collector, 342, 343
DYCD, 622, 626, 628, 630, 670
DYRESM, 622

E
East canal, 100
Eastern Galilee mountains, 98–101, 117, 126
Eastern marginal fault, 21, 29
Echinenone, 493
Echo sounder, 283, 286, 639
Ecological services, 549, 562
Ecopath, 621, 629
Ecoraft, 551, 568–570
Ecosystem model, 242, 300, 618, 620, 624, 630, 670
Education, 538
Effluents, 13, 76, 114, 324, 357, 542, 548, 558
Einan, 101, 324, 325, 357, 557, 558
End member, 122, 507
Endosulphan, 595
Enterococci, 598, 599, 601
Epilimnion, 9, 200, 248, 250, 268, 330, 366, 367, 370, 375, 377, 381, 388, 393, 399, 401, 402, 412, 421, 426, 456, 464, 487, 492, 493, 501, 508, 510, 626, 660, 661, 662, 663
Erosion, 63, 65, 72, 75, 76, 324, 325, 337, 355, 378, 511, 658
Errors, 121, 312
Escherichia coli, 599, 601
Euglenophyta, 182
Euphotic, 183, 251, 375, 384, 391, 394, 398, 399, 419, 431, 432, 433, 434, 435, 467, 481, 491, 493, 510, 518
Evaporation, 9, 10, 14, 42, 47, 49, 90, 93, 95, 101, 102, 103, 107, 121, 127, 128, 129, 338, 342, 402, 545
Evapotranspiration, 545
Evolution, 375, 459, 460, 620
Excretion, 220, 242, 243, 255, 296, 344, 366, 391, 443
Export ratio (ER), 490

F
Fault system, 20, 23, 30, 60, 66
Fecal
  coliforms, 598, 599, 601
  indicators, 598, 602
  pollution, 568
Feeding experiments, 294
Ferric iron, 458
Fingerlings, 281, 282, 300, 301, 529, 555, 568, 636, 637, 639, 642, 644, 647, 649, 666
Fish, 13, 14, 222, 278, 279, 281, 284, 293, 299, 300, 434, 465, 527, 553, 585, 619, 621, 628, 629, 637, 638, 639, 641, 642, 647, 650, 666
  biology, 274, 278
  pelagic, 283
  predation, 233, 236, 240
  respiration, 451
  species, 528, 636, 646, 664, 670
Fishery, 287, 553, 638, 639, 650
  commercial, 13, 280, 598, 636, 640, 641
Fishery regulation, 553, 638
Fishing practice, 636
Fishpond management, 557
Fish stock, 650
Flagellum, 193, 200, 208
Fluorescent tracers, 600
Food, 171, 179, 248, 252, 255, 282, 298, 302, 518, 528, 641, 649, 670
  chain, 294, 295, 301, 624, 664
  web, 223, 247, 268, 280, 288, 293, 294, 297, 301, 302, 434, 435, 618, 621, 625, 626, 628, 636, 642, 664, 666
Forestry, 536
Fractures, 117, 124, 126, 659
Fucoxanthin, 493
Functional groups, 228, 234, 302, 623

G
Gambusia affinis, 274
Garra rufa, 278
Gas
  ebullition, 460
  exchange, 9, 398, 400, 405, 662
Gas chromatography–mass spectrometry (GC-MS), 585, 589, 590
Genetic algorithm, 619
Geochemical composition, 115
Geological groups, 125
Geology, 31, 69
Geomorphology, 69, 188
Global warming, 109, 134, 223, 666
Golan heights, 12, 21, 29, 44, 53, 73, 74, 82, 98, 100, 102, 105, 108, 109, 332, 536, 548, 556, 598
Gravity, 22, 24, 139, 144, 147, 205, 455
Gravity-driven flow, 118
Grazing, 76, 205, 207, 223, 242, 247, 248, 251, 252, 256, 296, 297, 366, 536, 636
Green algae, 524
Grey mullet, 280, 302, 637, 647, 649
Gross primary production (GPP), 428, 429, 441, 443, 445, 449, 464, 465, 467, 468
Gross sedimentation rate (GSR), 486, 487
Ground surface temperature, 86
Ground water, 100, 119, 124, 324, 332, 335, 542
Growth, 142, 202, 218, 222, 249, 278, 286, 384, 404, 430, 447, 508, 520, 521, 649, 663, 666
  factors, 182, 208
  rate, 197, 208, 219, 249, 626, 649
Gyres, 137, 139, 140, 658

H
H_2S oxidation, 298, 394, 430
Habitat, 53, 54, 150, 200, 278, 279, 281, 518, 520, 527, 555, 649, 666
Habitat complexity, 518, 527
Harrat Ash-Shaam, 21, 24
Hatzor, 101
Hazbaya, 99
Hazor stream, 73
HCO_3^- consumer, 398
Health, 538, 568, 648
Heat flow, 22
Heinrich events, 49
Hemigrammocapoeta nana, 278
Herbicide, 589, 590
Herbivore, 242, 281, 299
Hermon Range, 99
Heterocyst, 214, 388
Heterotrophic bacteria, 206, 249, 293, 297, 301, 302, 385, 387, 440, 445, 447, 449, 463, 467, 524, 568, 623
Heterotrophic nanoflagellates (HNAN), 248, 249, 297, 298
Heterotrophy, 430, 467
High-frequency, 144, 147, 148
History, 194, 274, 475, 521, 618, 638, 650
Holocene, 44, 48, 54
Horizontal dispersion, 137, 150
HPLC-DAD, 582

Hula valley, 598, 663, 665, 668
Hydrodynamic regime, 659
Hydrological modeling, 107
  reservoir approach, 108
  spatially distributed, 109
  statistical, 108
  water management, 109
Hydrological year, 311, 320, 321
Hydrometric gauge, 312, 572
Hypolimnetic accumulation, 350
Hypolimnetic Cl-, 9, 123
Hypolimnion, 137, 144, 150, 248, 250, 251, 252, 260, 262, 270, 284, 349, 356, 359, 367, 375, 376, 381, 383, 386, 388, 392, 393, 400, 408, 427, 431, 434, 442, 452, 456, 458, 459, 486, 490, 491, 510, 571, 628, 660, 661, 665
Hypophthalamichthys molitrix, 638, 647
Hypsographic curve, 102

I
Inertial period, 139, 142, 147
Inflows, 9, 14, 42, 88, 93, 102, 375, 389, 425, 465, 474, 482, 487, 547, 601, 619, 658
  water, 62, 102, 115, 121, 127, 659
Inorganic
  matter, 481, 488
  reduced compounds, 430
Insecticide, 589, 590, 593
Intensity—Duration—Probability (IDP), 85
Internal loading, 348, 349, 359, 360
Internal P loading, 353, 358
Internal waves, 141, 144, 146, 147, 154, 399, 432, 491, 660
Intra-guild predation (IGP), 296, 300, 626, 629
Invasion, 216, 218, 287, 335, 401, 412, 458
Invertebrates, 279, 295, 518, 525, 526, 578, 646, 666
Iron, 24, 339, 430, 451, 499, 508, 578, 663
Irrigation, 12, 72, 76, 113, 324, 335, 336, 338, 539, 548, 552, 556, 668
Isotopic
  composition, 123, 335, 338, 344, 393, 394, 409, 410
  fractionation, 393, 394, 411
Israeli Hydrological Service (IHS), 102, 108, 115, 312
Israel Oceanographic and Limnological Research (IOLR), 6, 538, 584, 637
Israel Water Authority (IWA), 14, 562, 563, 568, 572, 637, 640
Iyyon river, 72

J
Jordan Gorge, 73, 74
Jordan Rift Valley, 72, 85, 97
Jordan River, 12, 13, 44, 48, 52, 53, 60, 72, 88, 99–101, 106–109, 119, 123, 127, 186, 208, 260, 278, 310–312, 320, 321, 323, 325, 332, 335, 336, 337, 338, 351–353, 359, 365, 381, 383, 389, 394, 429, 455, 457, 475, 477, 489, 545, 557, 568, 572, 573, 585, 589, 590, 592, 598, 599, 658
  southern, 10, 12, 49, 102, 103, 115, 375, 465
  tributaries of, 72, 99, 572
Judea, 44, 125
Judea group, 101, 117, 125

K
Karst, 73, 99, 108
Kc—partial attenuation coefficient, 420
Kd—light attenuation coefficient, 419, 420
Kelvin, 144, 147, 149, 150
Kendal test, 320
Keratella cochlearis, 240
Kezinim, 99
Kibbutz Degania, 2
Kibbutz Massada, 86, 89
Kinarot basin, 117
Kinarot valley, 20, 24, 30
Kinneret basin, 10, 20, 26, 29–32, 34, 75, 76, 97, 137, 537, 538
Kinneret bleak, 279, 295, 525, 527, 529
Kinneret Limnological Laboratory (KLL), 550, 562
Koppen method, 83
Korazim heights, 21, 30, 73
Kurnub, 125

L
Lake
  bathymetry, 6, 60, 62, 63, 518, 519
  level, 2, 48, 66, 74, 88, 89, 106, 115, 124, 126, 127, 129, 133, 243, 520, 521, 547, 628, 630, 649
  management, 552, 608, 614, 628, 630
  salinity, 114, 115, 127
  stability, 180, 666
  water level, 14, 74, 119, 134, 545, 567, 610
Lake Agmon, 13, 357, 557
Lake Hula, 10, 100, 107, 330, 335, 337, 338, 548, 556
Lake Kinneret, 1, 4, 5, 6, 7, 10, 12, 13, 14, 20, 22, 23, 24, 30, 33, 34, 42, 43, 44, 45
  Valley, 82, 85

watershed, 82, 97, 103, 104, 107, 127, 324, 330, 344, 509, 545, 548
Lake Kinneret and Watershed Unit (LKWU), 549, 551, 556, 557
Lake Kinneret Database (LKDB), 356, 360, 568
Lake Lisan, 42, 43, 48, 49, 53, 117
Land degradation, 75, 76
LandSat, 187, 658
Landscape, 75, 76
Land use, 69, 73, 536
Larvae, 279, 283, 284, 525, 526
Last glacial, 43, 44, 48, 51, 53
Leaching ratio, 115
Life cycle, 192, 194, 216, 518, 527, 666, 670
Light extinction coefficient, 133, 136
Limiting factor, 218, 325, 447
Linear
change, 128
interpolation, 315
Lisan, 39, 48
Lithology, 28, 50, 73, 74
Littoral, 184, 207, 268, 279, 280, 281, 286, 287, 356, 358, 370, 464, 487, 518, 519, 528, 666
zone, 63, 340, 368, 399, 401, 434, 520, 521, 524, 527, 529, 602, 648, 650, 664, 666
Liza ramada, 639
Long-term dynamics, 231
Loss on ignition (LI), 474, 476
Loss process, 387
Lower cretaceous, 118
Lower Water Mass (LWM), 330, 366, 368, 398, 406, 431, 500, 661, 662, 665
Lutein, 493

M

Macrophytes, 518, 519, 524, 666
emergent, 520, 522
submerged, 520
Magnetics, 22
MALDI-TOF-MS, 580
Management, 90, 223, 535
actions, 321, 323, 324, 556, 557, 558, 623, 630
objective, 552
Manganese, 451
Mango tilapia, 278
Manual sampling, 311, 312, 314–316, 323
Marshes, 331, 344
Measurements, 24, 67, 90, 182, 185, 193, 287, 312, 360, 393, 406, 418, 420, 424, 443, 448, 449, 464, 475, 487, 489, 494, 571, 572, 573, 669
Mediterranean Basin, 84
Mediterranean climate, 83, 106, 658
Mediterranean Sea Breeze (MSB), 88, 91
Mekorot, 102, 115, 120, 562, 566
Melanoides tuberculata, 525
Melanopsis costata, 525
MERIS FR, 65, 187
Meshushim, 30, 101, 345, 572
Mesocyclops ogunnus, 233
Metalimnion, 134, 137, 147, 150, 151, 240, 251, 262, 264, 265, 268, 284, 298, 367, 375, 376, 392, 432, 460, 465, 474, 476, 491, 502, 511, 660
Meteorological station, 86, 89, 91, 567
Methane, 63, 430, 435, 459, 461
Methanogenesis, 406, 408, 409, 451, 458, 459, 461, 665
Methanogenic bacteria (MB), 458
Methanotrophy, 459, 461
Microbial grazers, 242
Microbial loop, 247, 295, 297, 298, 299, 381, 446, 621, 623, 625, 664, 665
Microcystins (MCs), 218, 578, 579, 582
Microcystis, 176, 204, 208, 214, 215, 216, 218, 222, 393, 478, 580, 582, 584, 660, 663
Microginins, 579
Microviridins, 579
Microzooplankton, 228, 234, 242, 249, 256, 299, 302, 443, 662, 664
Mirogrex [syn. *Acanthobrama*] *terraesanctae,* 637
Mixing zone, 126
Mixotrophic flagellates, 248
Molar ratio of Mg/Cl−, 123
Molecular analysis, 265, 460
Molecular diffusion, 9, 123
Molibdenum (Mo), 500, 506, 508, 663
Monitoring, 6, 102, 184, 187, 223, 228, 294, 310, 312, 330, 348, 361, 584
program, 351, 425, 474, 549, 551, 559, 562, 563, 567, 569, 572, 574, 584, 599, 631, 650
Monte Carlo, 619, 628
Monthly loads, 312, 315, 572, 573
Morpholineaments, 23, 66
Motility, 195, 208
Mougeotia sp., 171, 179, 180, 187, 302, 393, 431, 467, 663, 667
MSL/ASL, 315, 316
Mt. Hermon, 44, 69, 71, 72, 99, 100, 109, 330, 332, 338, 548, 665
Mugil cephalus, 637, 649
Mullet, 284

Multiannual variations, 582, 584
Multi-beam, 59, 62, 66

N
N:P ratio, 222, 330, 627, 630
Nanoplankton, 202, 204, 299, 385, 621
National Water Carrier (NWC), 4, 6, 12, 102, 113, 464, 465, 468, 547, 551, 563, 566, 585, 601, 659
National Water Master Plan, 650
Nesting, 279, 528, 664
Net-autotrophic, 467
Net-heterotrophic, 467
Neurotoxic, 580
Nitrate (NO_3), 9, 186, 255, 321, 331, 383, 386, 660, 668
Nitrite, 377, 383, 386
Nitrobacter, 383
Nitrogen, 214, 242, 249, 344, 365, 366, 372, 626
  compounds, 321
  cycling, 377
  fixation, 218, 388, 389, 394, 568
  flux, 375, 619
  uptake, 203, 242, 385
Nitrosomonas, 383
Nitrosospira, 383, 392
Non-linear steepening, 147, 151
Non-Peridinium, 171, 179, 180, 295, 449, 624, 663, 667
Northern sub-basin, 26, 29, 30, 32, 34
Nostocales, 172, 214–216, 222, 223, 388, 580, 583, 664
Numerical, 126, 140, 150, 621
Nutrient concentrations, 494, 623
Nutrient cycling, 206, 248, 297
Nutrient loads, 7, 223, 323, 324, 330, 487, 562, 573, 599, 610, 623, 630, 658, 661
Nutrient recycling, 242, 255, 491, 626

O
Objective function, 608, 612
Ohalo-II, 48, 50–53, 55
Operational management, 127, 542
Optimal depth, 424, 425
Oreochromis aureus, 207, 295, 528, 637, 642
Organic carbon (Corg), 251, 337, 358, 429, 430, 435, 440, 441, 449, 456
  dissovled, 296, 445, 459, 461, 474
  labile, 476, 478
  particulate, 404, 412, 466, 474
  total, 474
Organic matter, 208, 335, 373, 406, 456
  dissolved, 330, 474, 480, 669
  particulate, 249, 298, 457, 474, 476, 492
Organic matter sedimentation rate (OMSR), 490
Organic nitrogen (Norg), 315, 321, 324, 331, 369, 373
Organizational aspects, 549
Osmotrophs, 296, 301, 302
Ostracods, 48, 51, 53, 54
Outflows, 93, 94, 102, 115, 119, 127, 129, 370, 464, 557
Overfishing, 638, 639, 646, 650, 664
Overlap study period, 313
Oxic-anoxic interface, 367, 430, 431
Oxidative stress, 205, 206
Oxy-anions, 507
Oxy-hydroxides, 505, 507, 508
Oxynoemacheilus tigris, 278
Ozone, 335

P
Paralytic shellfish toxin (PST), 580
Particulate organic matter (POM), 393, 394, 487, 489, 491
Patchiness, 669
P-burial, 361
P-diagenesis, 356, 357
Peat, 13, 324, 331, 335, 336–338, 344, 509, 551, 557, 668
Pelagic zone, 123, 279, 283, 286, 287, 340, 518, 519, 529, 664
Peridinin, 193, 200, 493
Peridiniopsis, 172, 193, 412
Peridinium, 137, 142, 179, 180, 184, 191–194
Peridinium gatunense, 162, 172, 183, 191–194, 200, 204, 263, 301, 302, 368, 369, 386, 393, 398, 412, 418, 431, 433, 509, 646, 660, 662, 663
Pesticide, 589
  residues, 568, 585, 589, 592
P-exchange, 358
Phlyctochytrium, 207
Phosphate, 203, 217, 219, 221, 222, 348, 349, 354, 357, 662
Phosphorous, 242, 491
  mass balance, 343
Phosphorus
  Ca-bound, 339
  dissolved, 321, 324
  fractions, 321, 339
Photosynthetically active radiation (PAR), 419, 426

Photosynthetic bacteria, 179, 259, 298, 302, 431, 434, 435, 571, 660, 665
Photosynthetic pigments, 213, 492, 665
Phototactic, 200
Phragmites australis, 458, 521, 523, 524, 555
Phreatic, 117, 125, 332, 334, 335
Phycocyanin, 221
Phycoerythrin, 221
Phylogenetic diversity, 260
Phytobenthos, 524
Phytoplankton, 9, 162, 163, 171, 172, 177, 179, 180, 183, 184, 186, 188, 191, 198, 201, 221, 222, 233, 236, 252, 256, 268, 280, 287, 294, 297, 300–302, 349, 384, 385
Phytoplankton biomass, 163, 171, 172, 177, 180, 183, 194, 208, 218, 233, 263, 301, 418, 427, 441, 449, 452, 456, 467, 481, 492, 647, 667
Phytoplankton pigments, 492
Phytoplankton primary production, 457
Picoeukaryotes, 253, 297
Picophytoplankton, 247, 296–298, 302, 403
Pigment indices (PI), 492
Pkak Bridge, 310, 312–314, 320, 325, 336, 338, 572, 573
PlanktoMetrix, 163
P-mineralization, 356
Poincare, 144, 146, 148, 150
Polyglucan, 202
Polyphosphate bodies, 208, 219, 221, 412, 662
Polysaccharide, 206, 248, 297, 481
Pore water (PW), 9, 123, 371, 375, 452, 456
P-partitioning, 353, 355, 360
Predator-prey interactions, 234
Primary production, 185, 398, 403, 405, 418, 463, 486, 490, 511, 568, 625
  net, 428, 449
Profiler, 200, 375, 569, 571
Programmed cell death (PCD), 205, 206
Prosthecochloris aestuaris, 264
Protista, 449, 468, 621
Protistan, 443
Protozoa, 247, 249, 252, 255, 297, 621, 625
P-sedimentation, 356, 361
Pseudomonas anguilliseptica, 260
Pseudomonas pavonanceae, 260
Pseudophoxinus kervillei, 278
Pseudoplotia scabra, 525, 526, 667
Public education, 650
Public health, 567, 568
Pumping, 12, 102, 113, 118, 119, 126, 332, 342, 343, 370, 371, 378, 573, 659, 667, 669

Q
Quaternary, 31, 39

R
Rain, 84, 85, 88, 320, 332, 334, 335, 338, 341, 344, 545
Rainfall, 73, 76, 82, 83, 85, 99, 117, 124, 339
Rainfall-runoff, 101, 107, 108
Rain shadow, 85
Real-time, 573
Redfield ratio, 202
Red line, 106, 117, 118, 119, 544, 650
Redox gradient, 511
Reducing bacteria
  sulphate, 430, 452, 453, 456, 458, 505, 511
Reduction of Iron oxide, 502
Refuge, 13, 14, 281, 282, 284, 301, 518, 519, 528, 642, 646, 666, 670
Remineralization, 242, 249, 255, 299, 661
Remote sensing, 187, 571
Replenishment, 9, 544, 545, 558
Residence time, 127, 315, 324, 658
Respiration, 199, 337, 398, 429, 446
  production, 568, 574
  quotient, 448, 450
Resuspension, 284, 356, 431, 434, 482, 487, 489, 491, 628, 649
Rheinheimera sp., 260
River mouth, 600, 601
Robust, 311, 317, 624, 625
  regression line, 317, 320
Rokad, 100
Rubisco, 410, 411, 412
Running median, 317, 321

S
Sa'ar, 99, 100
Salaria fluviatilis, 278
Saline springs, 47, 53, 102, 115–117, 119, 120, 122, 550, 553, 563, 659
Saline water carrier (SWC), 115, 553
Salinity control, 552, 559
Sampling, 228
  mix, 228, 234
  profile, 228, 230, 234, 236, 238
Sarotherodon galilaeus, 528, 620, 626, 637, 642
Satellite image, 66
Satellite Information System on Coastal area and Lakes (SISCAL), 187, 571
Saxitoxin (STX), 580
Scenarios, 621, 623, 624, 630
Sea of Galilee, 2, 4, 39, 42, 43

Secchi depth, 420, 567, 571, 665, 667
Sediment accumulation rate, 452
Sedimentation, 348, 600, 619, 624, 628
Sedimentation rate, 27, 60, 66, 206, 355
Sedimentation trap, 486, 487, 488
Sediment transport, 65, 669
Sediment trap, 206, 360, 401
Sediment-water interface (SWI), 356, 358, 371, 386, 392, 394, 408, 431, 462, 465, 502, 505, 511, 665
Seiche, 66, 242, 368, 399, 432
Seiching, 268, 399, 487, 494
Seismicity, 22, 31, 32, 34
Seismic reflection, 22, 27
Selenium (Se), 196, 208, 331, 336, 499, 509, 663, 668
Sensitivity analysis (SA), 623, 625
Sequential P extraction, 351, 353
Seston, 268, 355, 358, 361, 371, 451, 474–479, 481
Settling flux, 355, 356, 358, 361
Sewage, 12, 76, 324, 357, 537, 538, 548, 556, 598
Shewanella putrefaciens, 260
Shores management, 555
Shore vegetation, 521, 666
Side springs, 101, 108
Silver carp, 280, 302, 629, 637, 647, 651, 670
Si'on, 99
Sloppy feeding, 296, 443
Smoothers, 317
Snir, 70, 99, 108
Snow, 109, 332, 334
Solute, 102
Southern sub-basin, 26, 30, 31, 34
Spatial distribution, 85, 125, 183, 185, 187, 188, 201, 268, 283, 430, 571
Spatial variability, 670
Spawning, 14, 279, 281, 282, 286, 301, 303, 519, 528, 641, 642, 646, 649, 650, 666
Species richness, 182, 524
Sphingomonas, 260
Springs, 279, 332
Station A, 54, 90, 162, 185, 230, 236, 262, 263, 433, 440, 442, 564, 582
Statistical modeling, 620
Staurastrum manfeldtii, 171, 179, 302
Stella, 619
Step reduction, 115, 128
Stochastic, 129
Stocked fish, 642, 647, 649
Stocking, 13, 280, 553, 642
Stoichiometry, 371, 373, 623
St. Peter's fish, 4, 182, 274, 301, 302, 642, 664, 670
Stratification, 9, 133, 137, 141, 142, 194, 240, 251, 372, 373, 378, 386, 399, 409, 425, 665
Streams, 44, 53, 60, 88, 100, 102, 108, 109, 123, 127, 557, 602, 658
Structure, 6, 20, 23, 30, 31, 72, 125, 133, 134, 141, 146, 250, 260, 349, 425, 427, 460, 518, 527, 578, 622, 666
Stylonichia, 255
Sub-littoral, 355, 358, 368, 660
Subsidized harvest, 300, 640, 641
Sulfate, 10, 323, 325, 336, 374, 503, 665, 668
Sulfate reduction, 388, 406, 407, 408, 431, 434, 451, 452, 455, 456, 457, 458, 462, 665
Sulfide, 388, 391, 431, 434, 435, 453, 459, 460, 503, 568
Surface layer, 134, 137, 141, 142, 144, 149, 150–153, 406, 413, 660
Surface runoff, 99, 101, 115, 128
Suspended matter, 351, 457, 477, 572, 601, 619
Suspended particles, 337
Sustainable water resources management, 614
Synedra, 177
Synoptic, 571

T

Tabgha, 91, 116, 122, 124–126
Tahal, 6, 23, 60, 102, 115
Tamarix jordanis, 458, 521
Tectonics, 27
Tel Bet Yerach, 2, 40, 48, 50–53
Temporal changes, 32, 562, 590
Teo, 101
Thecae, 193, 195, 197, 202, 206, 297, 446, 447
Theil-Sen estimator, 317
Thermal structure, 134, 183, 425, 427
Thermocline, 500, 501, 507, 510, 511, 566, 571, 660, 661, 665
Thermocline deepening, 136, 501, 511
Thiocapsa roseopersicina, 264
Tilapia zillii, 278
TN/TP ratio, 321, 325, 558, 627
Topographic gyres, 140, 660
Top predators, 300, 302, 651, 669, 670
Torrential rains, 85
Total dissolved phosphorus (TDP), 315, 321, 324, 325, 339, 349, 350, 359, 558
Total nitrogen (TN), 321, 325, 612, 627

Total phosphorus (TP), 222, 315, 321, 323, 324, 325, 338, 341, 349, 350, 352
Total suspended solids (TSS), 313, 315, 321, 339, 353, 474, 475, 568, 571, 611, 667
Tourism, 537, 556, 585
Toxicity index, 591
  organochlorine, 595
Toxins, 222, 582, 584
Transparent exopolymer particles (TEP), 391, 480
Transverse faults, 29, 34
Trap-to-water ratio (TWR), 492
Trend, 62, 89, 128, 186, 234, 236, 317, 342, 349, 352, 357, 427, 446, 573, 642, 665
Trend analysis, 317
Tristramella sacra, 317
Tristramella simonis, 278, 317, 639
Trophic level, 162, 242, 249, 296, 297, 299, 301
Turbulent kinetic energy (TKE), 137, 142, 197
Turnover time, 442, 476
Two-layer stratification, 142, 152
Typha angustata, 521

U
Ubadiya, 1
Uncertainty, 621, 624, 625, 631
Underwater-towed undulating monitoring system (U-TUMS), 569, 571
Upper catchments of the Jordan River, 97
Uptake, 221, 406
Uptake rate, 202, 204, 384, 524
Upwelling, 2, 31, 47, 100, 142, 150, 443
Uranium (U), 500, 506, 508

V
Vertical distribution, 183, 187
Vertical migration, 198, 200, 201, 208, 240, 571
Vibrio-like bacteria, 262
von Bertalanffy growth equation, 317

W
Water Authority, 310, 650
Water Commission, 549
Water-energy-solute balance, 102
Water level, 106, 487, 518, 520, 524, 528, 529
Water level fluctuations, 14, 48, 106, 107, 109, 281, 282, 287, 427, 487, 495, 519, 527, 528, 555, 612, 650, 666
Water quality, 6, 114, 174, 180, 187, 222, 544, 551, 636
  aggregated, 627
  quantification, 608, 614
  system, 630
Water quality indices (WQI), 608, 609, 610, 628
Water quality monitoring station (WQMS), 312, 313, 314
Water resources management, 109, 614
Watershed, 103, 104, 109, 311, 320
  management, 310, 311, 321, 549, 559
Water supply, 12, 182, 281, 468, 544, 547, 549, 562, 584
Water temperature, 7, 55, 144, 194, 199, 217, 222, 223, 279, 426, 501, 567, 569, 571, 661, 664
Wazani, 99
Wedderburn number, 137, 144, 151
Weighted average, 312, 610
Weight-length relationship, 278
West Canal, 100
Western marginal fault, 29
Wind direction, 138, 142, 144, 151, 152
Wind speed, 90, 94, 136, 138, 394, 491, 567

X
Xiphophorus hellerii, 274

Y
Yarmouk, 51, 100, 602
Yehudia, 101

Z
Zalmon, 101, 572
Zefat, 74, 536–538, 556
Zooplanktivore, 284, 287, 302, 527, 639, 666, 667
Zooplankton, 640, 641, 647
  cladocera, 302, 443, 451
  copepods, 233, 238, 243, 299, 300, 302, 443, 451
  herbivorous, 641
  microzooplankton, 662
  nauplii, 299, 302
  predatory, 232–234, 300, 302, 620, 625, 628, 629
  rotifera, 443, 451